

C–H Activation by Nickel and Iron Catalysis

Dissertation

for the award of the degree

“Doctor rerum naturalium”

of the Georg-August-University of Göttingen



within the doctoral program of chemistry

of the Georg-August-University School of Science (GAUSS)

submitted by

Thomas Müller

from Donaueschingen

Göttingen, 2019

Thesis Committee

Prof. Dr. Lutz Ackermann, Institute of Organic and Biomolecular Chemistry,
Göttingen

Prof. Dr. Konrad Koszinowski, Institute of Organic and Biomolecular Chemistry,
Göttingen

Examination Board

Reviewer: Prof. Dr. Lutz Ackermann, Institute of Organic and Biomolecular Chemistry

Second Reviewer: Prof. Dr. Konrad Koszinowski, Institute of Organic and
Biomolecular Chemistry

Further Members of the Examination Board

Prof. Dr. Ricardo Mata, Institute of Physical Chemistry

Dr. Sebastian Kruss, Institute of Physical Chemistry

Dr. Shoubhik Das, Institute of Organic and Biomolecular Chemistry

Dr. Michael John, Institute of Organic and Biomolecular Chemistry

Date of the Oral Examination: 26.06.2019

Acknowledgment

Zuallererst gilt an dieser Stelle mein großer Dank meinem Doktorvater Professor Lutz Ackermann für die Möglichkeit die vorliegende Arbeit unter seiner Anleitung anzufertigen. Neben der stets freundlichen und fachlich inspirierenden Arbeitsatmosphäre ist es mir besonders wichtig zu erwähnen, dass mir immerzu alle Freiheiten gewährt wurden, mich neben der Forschung in vollem Umfang meinen Kindern und meiner Familie zu widmen, was nicht selbstverständlich zu sein scheint. Dafür möchte ich an dieser Stelle meinen großen Dank aussprechen!

Des Weiteren danke ich Professor Konrad Koszinowski für die Betreuung dieser Arbeit im Rahmen des GAUSS Promotionsprogramms und der damit einhergehenden Übernahme des Zweitgutachtens. Ebenso bedanke ich mich bei Prof. Ricardo Mata, Dr. Sebastian Kruss, Dr. Shoubhik Das und Dr. Michael John für die Teilnahme im Rahmen der Prüfungskommission.

Auch der analytischen Abteilung des Institutes für deren schnelles und gewissenhaftes Bearbeiten jeglicher Art an Messaufträgen gilt mein besonderer Dank, da ohne dessen Support oftmals ein so reibungsloser Arbeitsablauf nicht möglich wäre.

Ebenso wenig wäre ein so gelungenes Arbeitsumfeld innerhalb des Arbeitskreises möglich ohne die grandiose Unterstützung von Karsten, Stefan und Gabi. Würde von euch nicht das nötige „Werkzeug“ bereitgestellt werden, seien es Equipment, Chemikalien, die Wartung aller technischen Geräte, Laborjournale etc., würde wahrscheinlich ein heilloses Chaos ausbrechen.

Das ganze hätte nicht halb so viel Spass bereitet, wären da nicht all die Arbeitskollegen und neuen Freunde, mit denen ich während der letzten 4 Jahre einen großen Teil meiner Zeit verbringen durfte. Besonders bedanken muss ich mich dabei bei Alex B., der mit mir gemeinsam den Weg „PhD“ angefangen hat und mit dem ich von Anfang an eine echte Freundschaft verbunden habe. Vielen Dank auch an Julian, mit dem ich, so glaube ich, auf einer „Wellenlänge“ liege und über alles Chemische und Nicht-Chemische reden könnte. Nicht vergessen und vor allem bedanken möchte ich mich bei Marc, Nicolas, Svenja, Torben und Alex S., diejenigen die (gefühlte) von Anfang an da waren und die Zeit im Labor (und auch außerhalb) sehr angenehm gemacht haben.

Weiterhin möchte ich mich bei Joachim Loup, Nikolaos Kaplaneris, Tjark Meyer, Dr. Lars Finger, Ralf Steinbock, Leonardo Massignan and Jiayu Mo bedanken, die wesentlich am Gelingen dieser Arbeit durch deren gründliches Korrekturlesen beigetragen haben. Auch meinem ehemaligen Labor 308, und dabei vor allem Joachim Loup und Gianpiero Cera, bedanke ich mich für deren stete Hilfsbereitschaft in jeglichen chemischen Problemstellungen. Auch Dr. João C. A. Oliveira und Jiayu Mo bedanke ich mich für die Kollaboration an diversen Projekten.

Mein besonderer Dank geht an Marc, Nicolas, Alex B., Julian, Alex S., Ralf, Torben, João, Alan, Max und Nate für die überraschend unterhaltsamen Kegelabende, Grillfeiern und sonstigen Unternehmungen, welche die letzten vier Jahre hier in Göttingen sehr lebenswert gemacht haben.

Während meiner Studienzeit in Freiburg lernte ich, was, so glaub ich zumindest, einen großen Teil eines guten Chemikers ausmacht, nämlich das „Handwerk“ Chemie im Labor in Form des „Kochens“ zu beherrschen. Daher danke ich meinen ehemaligen Bachelor- und Master-Betreuern, Dr. Simon Allmendinger und Dr. Alex Haydl, für deren Hingabe, Sorgfalt und Geduld dieses „Handwerk“ zu lernen und zu optimieren.

Zu guter Letzt gebührt mein größter Dank jedoch meinen Eltern, und mehr noch Katja und meinen Kindern Lara und Jannis. Euer bedingungslose Liebe, euer Rückhalt und Unterstützung haben all das erst möglich gemacht!

Göttingen, Juni 2019

Thomas Müller

Contents

1	Introduction	1
1.1	Transition Metal-Catalyzed C–H Activation	2
1.2	Nickel-Catalyzed C–H Activation	6
1.2.1	Nickel-Catalyzed C–H Arylation, Alkynylation and Alkylation.....	8
1.2.2	Nickel-Catalyzed C–S Bond Formation.....	17
1.2.3	Nickel-Catalyzed Hydroarylation of Alkynes and Alkenes	19
1.3	Iron-Catalyzed C–H Activation	27
1.3.1	Iron-Catalyzed C–H Activation with Organometallic Reagents	31
1.3.2	Iron-Catalyzed C–H Activation with Organic Electrophiles.....	34
1.3.3	Iron-Catalyzed Hydroarylation of C–C Multiple Bonds	37
2	Objectives	40
3	Results and Discussion	44
3.1	Nickel(II)-Catalyzed C–H Chalcogenation of Anilines.....	44
3.1.1	Optimization Studies	44
3.1.2	Scope of the Nickel-Catalyzed C–H Thiolation of Anilines.....	51
3.1.3	Scope of the Nickel-Catalyzed C–H Selenation of Anilines.	58
3.1.4	Mechanistic Studies	64
3.2	Nickel(0)-Catalyzed C–H Activation of Heteroarenes with Allenes	68
3.2.1	Optimization Studies	68
3.2.2	Scope of the Nickel-Catalyzed C–H Allylation of Imidazoles and Purines.....	73
3.2.3	Scope of the Nickel-Catalyzed C–H Alkenylation of Imidazoles and Purines.....	77
3.2.4	Mechanistic Studies	81

3.3	Iron-Catalyzed C–H/N–H Allene Annulation	86
3.3.1	Optimization Studies	87
3.3.2	Scope of the Iron-Catalyzed C–H/N–H Annulation	88
3.3.3	Mechanistic Studies	94
3.4	Iron-Catalyzed Annulation Reaction using Propargyl Acetates	98
3.4.1	Optimization	98
3.4.2	Scope of the Iron-Catalyzed C–H Annulation.....	102
3.4.3	Mechanistic Studies	110
4	Summary and Outlook	119
5	Experimental Part	124
5.1	General Remarks	124
5.2	General Procedures	127
5.3	Nickel-Catalyzed C–H Thiolation/Selenylation of Pyrimidyl Anilines.....	130
5.3.1	Experimental Procedures and Analytical Data - Thiolation	130
5.3.2	Experimental Procedures and Analytical Data - Selenylation	152
5.3.3	Experimental Procedures and Analytical Data – Removal of the Directing Group.....	169
5.3.4	Mechanistic Studies	172
5.4	Nickel-Catalyzed C–H Allylation of Imidazole and Purine Derivatives.....	176
5.4.1	Experimental Procedures and Analytical Data – Nickel-catalyzed C–H Allylation	176
5.4.2	Experimental Procedures and Analytical Data – Nickel-catalyzed C–H Alkenylation	189
5.4.3	Mechanistic Studies	203

5.5	Iron-Catalyzed C–H/N–H Annulation with Allenyl Acetates	207
5.5.1	Experimental Procedures and Analytical Data – Allenyl Acetates.....	207
5.5.2	Experimental Procedures and Analytical Data – TAH Benzamides	217
5.5.3	Mechanistic Studies	223
5.6	Iron-Catalyzed C–H/N–H Annulation with Propargyl Acetates	226
5.6.1	Experimental Procedures and Analytical Data – TAH Benzamides	226
5.6.2	Experimental Procedures and Analytical Data – Propargyl Acetates..	245
5.6.3	Mechanistic Studies	252
6	References	263
7	Appendix	277

List of Abbreviations

Ac	acetyl
acac	acetyl acetonate
Ad	adamantyl
Alk	alkyl
AMLA	ambiphilic metal ligand activation
aq	aqueous
AQ	8-aminoquinoline
Ar	aryl
atm	atmospheric pressure
BDMAE	bis(2-dimethylaminoethyl)ether
BHT	2,6-di- <i>tert</i> -butyl-4-methylphenol
BIES	base-assisted internal electrophilic substitution
Bn	benzyl
<i>n</i> Bu	<i>n</i> -butyl
calc.	calculated
<i>cat.</i>	catalytic
CMD	concerted metalation deprotonation
cod	1,5-cyclooctadiene
Cy	cyclohexyl
δ	Chemical shift
d	doublet
DCB	dichlorobenzene
DCIB	dichloroisobutane
dcype	1,2-bis(dicyclohexylphosphino)ethane
dd	doublet of doublets
DG	directing group
dme	dimethoxyethane
DMF	<i>N,N</i> -dimethylformamide
DMSO	dimethylsulfoxide
dppbz	1,2-bis(diphenylphosphino)benzene
dppe	1,2-bis(diphenylphosphino)ethane
dppen	1,2-bis(diphenylphosphino)ethene
dppf	1,1'-bis(diphenylphosphino)ferrocene
dt	doublet of triplets

DtBEAD	di- <i>tert</i> -butyl ethylenediamine
dtbpy	di- <i>tert</i> -butyl-2,2'-bipyridine
EI	electron ionization
equiv	equivalent
ESI	electrospray ionization
Et	ethyl
g	gram
GC	gas chromatography
h	hour
hept	heptyl
hex	hexyl
HRMS	high resolution mass spectrometry
Hz	Hertz
<i>i</i>	<i>iso</i>
IES	intermolecular electrophilic substitution
IMes	1,3-bis(2,4,6-trimethylphenyl)imidazole-2-ylidene
IPr	1,3-bis(2,6- <i>iso</i> -propylphenyl)imidazole-2-ylidene
^{Me} IPr	1,3-bis(2,6- <i>iso</i> -propylphenyl)-4,5-dimethyl-imidazole-2-ylidene
IPr ^{OMe}	1,3-bis(2,6-di- <i>iso</i> -propyl-4-methoxyphenyl)-imidazole-2-ylidene
IPr*	1,3-bis(2,6-dibenzhydryl-4-methylphenyl)-imidazole-2-ylidene
IPr* ^{OMe}	1,3-bis(2,6-dibenzhydryl-4-methoxyphenyl)-imidazole-2-ylidene
IR	infrared spectroscopy
<i>J</i>	coupling constant
KIE	kinetic isotope effect
L	ligand
LA	Lewis acid
<i>m</i>	<i>meta</i>
m	multiplet
M	molar
[M] ⁺	molecular ion peak
MAD	methylaluminium bis(2,6-di- <i>tert</i> -butyl-4-methylphenoxide)
Me	methyl
Mes	mesityl
mg	milligram
MHz	megahertz
min	minute

mL	mililiter
mmol	milimole
MOM	methoxymethyl acetal
M. p.	melting point
MS	mass spectrometry
<i>m/z</i>	mass to charge ratio
napht	naphthenate
NHC	N-heterocyclic carbene
NMR	nuclear magnetic resonance
<i>o</i>	<i>ortho</i>
OLED	organic light emitting diode
<i>p</i>	<i>para</i>
pent	pentyl
Ph	phenyl
PIP	(2-pyridin-2-yl)isopropylamine
Piv	pivaloyl
ppm	parts per million
Pr	propyl
py(m)	pyridyl or pyrimidyl
q	quartett
RT	room temperature
s	singlet and second
SET	single electron transfer
SPS	solvent purification system
<i>t</i>	<i>tert</i>
t	triplet
<i>T</i>	temperature
TAM	triazolyldimethylmethyl
TEMPO	2,2,6,6-tetramethylpiperidine- <i>N</i> -oxide
THF	tetrahydrofurane
TLC	thin layer chromatography
TM	transition metal
TMEDA	<i>N,N,N',N'</i> -tetramethylethylenediamine
TMS	trimethylsilyl
TS	transition state
X	(pseudo-)halide

1 Introduction

„Es ist also erwiesen, dass viele, sowohl einfache als zusammengesetzte Körper, sowohl in fester als in aufgelöster Form, die Eigenschaft besitzen, auf zusammengesetzte Körper einen, von der gewöhnlichen chemischen Verwandtschaft ganz verschiedenen Einfluss auszuüben, indem sie dabei in dem Körper eine Umsetzung der Bestandtheile in anderen Verhältnissen bewirken, ohne dass sie dabei mit ihren Bestandtheilen nothwendig selbst Theil nehmen“

(Berzelius, 1835)^[1]

In the early 19th century, BERZELIUS was the first to propose a “new force”, which he described as an omnipresent phenomenon in nature, and called it “*catalysis*”.^[2] The word *catalysis* is derived from the ancient Greek words *kata*, meaning *down* and *lyein*, meaning *loosen*. From a present point of view, this description seems to be an extremely unfortunate choice, because catalytic reactions are in most cases highly productive processes.

The definition of *catalysis* that lasts until now goes back to OSTWALD: “*a catalyst accelerates a chemical reaction without affecting the position of the equilibrium*”.^[3] From that date, almost 200 years ago, catalysis has raised to one of the most important fields of research in chemistry. Groundbreaking technologies based on catalysis, such as the HABER-BOSCH process^[4] for the synthesis of ammonia from elementary nitrogen and hydrogen, or the ZIEGLER-NATTA polymerization^[5] for the mass production of polymers, represent milestones for industrial processes, and further caused changes in society.

Due to the growing demand for chemical products for a plethora of applications in pharmaceutical and agrochemical industry, polymer science and many other areas, the development of new organic transformations is indispensable. Obviously, the accessibility of new compounds provided by these technologies represents a huge benefit for the life of many people. However, a number of drawbacks are associated with their synthesis, for example the production of toxic waste, the consumption of non-renewable natural resources and the high energy demand.

Therefore, catalytic transformations are important techniques, as implied within the *12 Principles of Green Chemistry*,^[6] and nowadays, more than 85% of all produced chemicals pass through at least one catalytical process.^[7]

1.1 Transition Metal-Catalyzed C–H Activation

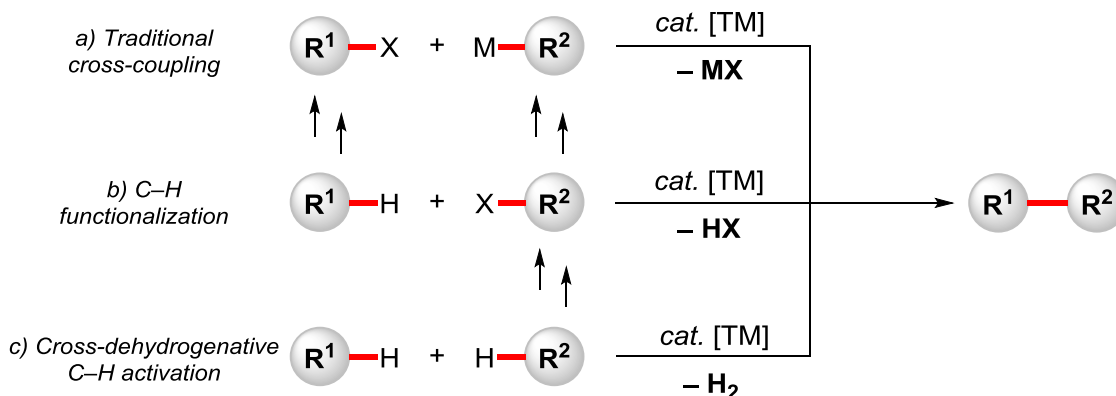
The defined construction of molecular building blocks for the development of various functionalized materials and pharmaceuticals posed major challenges to organic chemists for centuries. Therefore, the discovery of catalytic processes set the stage for the selective formation of carbon–carbon (C–C) and carbon–heteroatom (C–Het) bonds, which constituted one of the most important developments for organic syntheses.

Early works by GLASER,^[8] ULLMANN,^[9] as well as GOLDBERG^[10] indicated the potential of these catalytic methods. In particular, the copper-catalyzed formation of new C–C bonds, especially on arene C(sp²)–H bonds, enabled the synthesis of biaryl motifs, an omnipresent scaffold in natural occurring compounds, which are otherwise hard to access.^[11] Indeed, this method suffered from harsh reaction conditions, low selectivities and moderate yields and, therefore, its applications was found to be limited. A major breakthrough in the field of selective C–C/C–Het coupling was achieved with the development of palladium-catalyzed cross-coupling reactions, processes that tremendously expanded the toolbox of modern organic synthesis.^[12] In this context, a range of well-known named reactions, such as the KUMADA-CORRIU,^[13] NEGISHI,^[14] MIGITA-KOSUGI-STILLE,^[14a, 15] SUZUKI-MIYAURA^[16] and HIYAMA^[17] cross-couplings enabled the highly efficient and selective synthesis of biaryls, while the MIZOROKI-HECK^[18] reaction allowed for the selective alkenylation of aryl halides, and the SONOGASHIRA-HAGIHARA^[19] reaction represents a unique alkynylation strategy. These methods have found widespread applications in the pharmaceutical, agrochemical and chemical industry and, moreover, this research was recognized with the Nobel Prize in 2010 awarded to A. Suzuki, E.-i. Negishi and R. Heck.^[20]

Indisputably, these remarkable achievements changed the world of organic chemists, but still significant drawbacks are directly linked to cross-coupling reactions. Thus, prefunctionalizations of the starting materials are necessary. Besides the organic (pseudo)halides, the employed organic nucleophiles, such as Grignard reagents,

1 Introduction

organozinc and toxic organotin compounds, require multistep syntheses and, in addition, these compounds are often difficult to handle and store. Therefore, the development of alternative methodologies such as C–H activation is highly desirable.^[21]



Scheme 1.1: Comparison of traditional cross-coupling vs. C–H activation.

While cross-dehydrogenative C–H activation strategies in principle constitute the most efficient approach, which formally only generate hydrogen as by-product, stoichiometric oxidants are needed, resulting in additional waste generation (Scheme 1.1c).^[21] Traditional cross-coupling, although very efficient, does not only require an electrophilic coupling partner, but also an additional nucleophilic organometallic reagent, which leads to the formation of stoichiometric amounts of partially toxic waste (Scheme 1.1a).

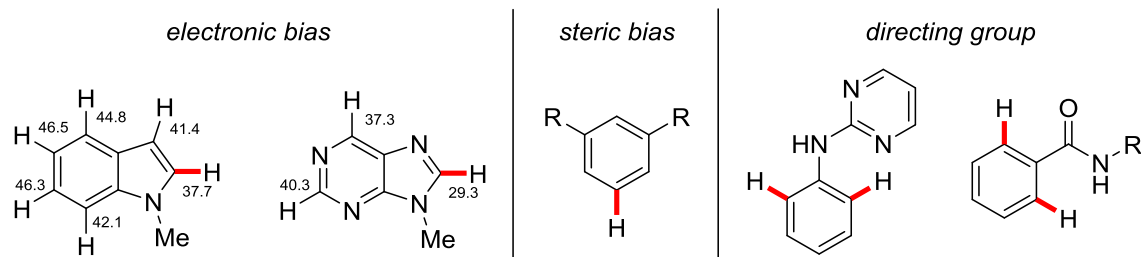
Therefore, the direct functionalization of C–H bonds is extremely desirable in terms of step- and atom-economy,^[22] and bears great potential for the construction of C–C and C–Het bonds without the requirement of any prefunctionalization steps (Scheme 1.1b).^[23]

Thus, C–H activation would provide the most favourable access for the synthesis of highly-functionalized organic molecules, but some key challenges have to be addressed. Whereas, in traditional cross-coupling reactions the regioselectivity of the C–C or C–Het bond forming step is clearly defined by the substitution pattern of the electrophile and nucleophile, for direct C–H functionalization reactions the control of selectivity is of major importance.

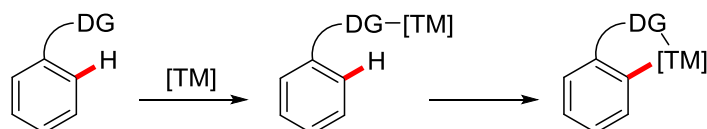
1 Introduction

As C–H bonds are omnipresent in organic molecules, exhibiting almost identical bond dissociation energies, there are mainly three ways how to control the selectivity: *i*) the electronic distinction of C–H bonds caused by the differences in kinetic acidity, *ii*) the use of bulky substituents, that are blocking adjacent positions and thereby resulting in a steric control (Scheme 1.2a), and *iii*) the introduction of Lewis-basic directing groups to coordinate transition metal complexes in close proximity to the C–H bond to be activated (Scheme 1.2b).^[23b] Furthermore, the introduction of directing groups generates a huge variety of different substrate classes, and in many cases the directing group can be removed after the desired transformation, even in a traceless fashion.

a) Differentiation of C–H bonds



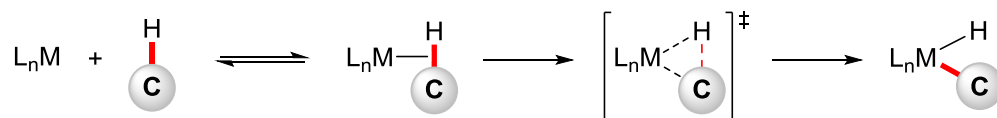
b) Influence of the directing group



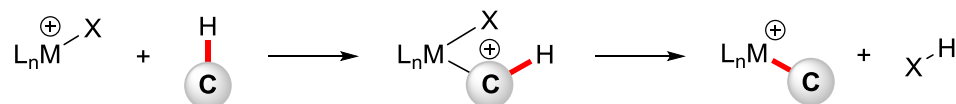
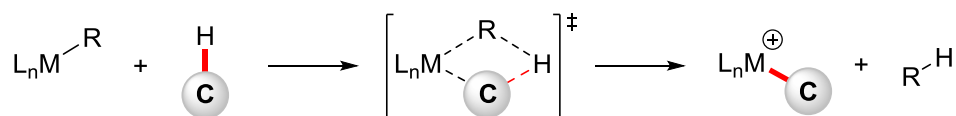
Scheme 1.2: Strategies for site-selectivity in C–H activation.

While the achievements in the field of C–H activation grew rapidly within the last decades, extensive investigations on the nature of the key-step, the initial C–H bond cleavage, have been conducted.^[24] Therefore, excluding radical-type outer-sphere mechanisms,^[25] five different pathways for the C–H bond dissociation, depending on the nature of the metal catalyst and oxidation state, have been identified (Scheme 1.3): *a*) oxidative addition for electron-rich late transition metals in low oxidation states, such as ruthenium(0), rhodium(I) and palladium(0),^[24a] *b*) electrophilic substitution in case of late transition metals in higher oxidation states,^[24c] *c*) σ -bond metathesis for early transition metals and lanthanoids,^[24b] *d*) 1,2-addition to unsaturated M=X bonds, such as metal imido complexes, and *e*) base-assisted metalation.^[24a]

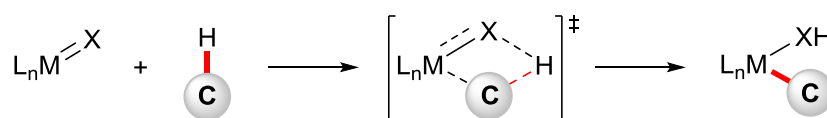
a) Oxidative addition



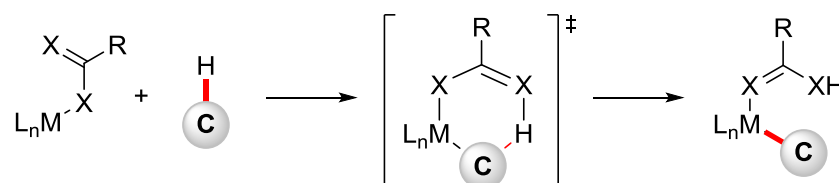
b) Electrophilic substitution

c) σ -bond metathesis

d) 1,2-Addition

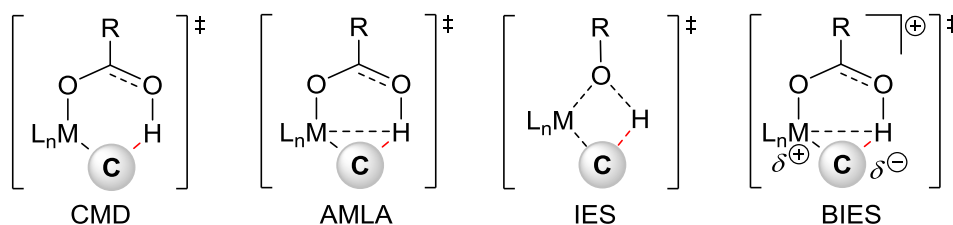


e) Base-assisted metalation



Scheme 1.3: Different modes for organometallic C–H activation.

The base-assisted C–H cleavage was further investigated in detail and upon intensive research in this area several transition states were proposed, describing the activation mode of C–H activation events more precisely (Scheme 1.4).^[24a]



Scheme 1.4: Transition state models for base-assisted C–H activation events.

The *concerted metalation-deprotonation* (CMD)^[26] and *ambiphilic metal-ligand activation* (AMLA)^[27] were independently disclosed and describe the interaction of the metal center, carboxylate-ligand and the C–H bond *via* a six-membered transition

state. These activation modes are especially used to describe C–H activation events of electron-deficient substrates with relative high kinetic acidity. In contrast, the *intermolecular electrophilic substitution* (IES)^[28] proceeds *via* a strained four-membered transition state and has been proposed for C–H activation mechanisms relying on alkoxide bases. On the other hand, *base-assisted internal substitution* (BIES)^[29] has been proposed to explain the preferred reactivity of electron-rich substrates.

1.2 Nickel-Catalyzed C–H Activation

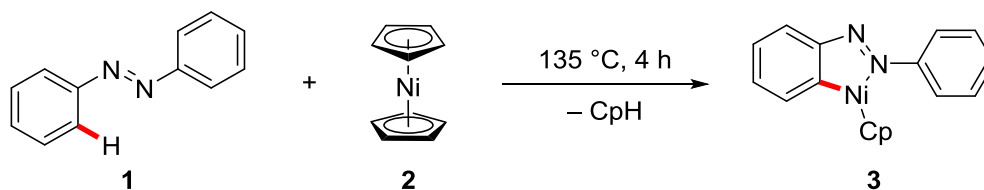
Transition metal-catalyzed C–H activation has become one of the most viable and powerful tools for a broad range of chemical transformations. Especially, the noble 4d and 5d metals, namely rhodium, iridium, palladium and ruthenium, contributed to major achievements in this field of research.^[30] However, due to the relatively high costs and low natural abundance of these metals, more sustainable resources for metal catalysts are needed. Therefore, metal catalysts based on earth-abundant 3d metals have gained significant attention throughout the last years.^[31]

In particular, nickel showcases many benefits, as it is less expensive than the precious transition metals and less toxic than the commonly used palladium catalysts.^[32] Moreover, nickel exhibits specific properties, contrasting with palladium, that needs to be pointed out. For instance, nickel is a relatively electropositive transition metal. Therefore, it undergoes oxidative addition more readily and allows for the use of electrophiles in cross-coupling reactions^[33] that would be considerably less reactive under palladium catalysis such as phenol derivatives.^[34] In addition, nickel can exhibit a number of readily available oxidation states, allowing for different modes of reactivity, which enable the development of innovative transformations based on single electron transfer (SET).^[35]

To this end, a wide range of transformations have been developed employing nickel catalysis, such as KUMADA^[36] and NEGISHI^[37] cross-coupling reactions, reduction of multiple bonds and other functional groups employing Raney nickel, HECK-type^[32b] reactions, and C–H functionalizations, among others.

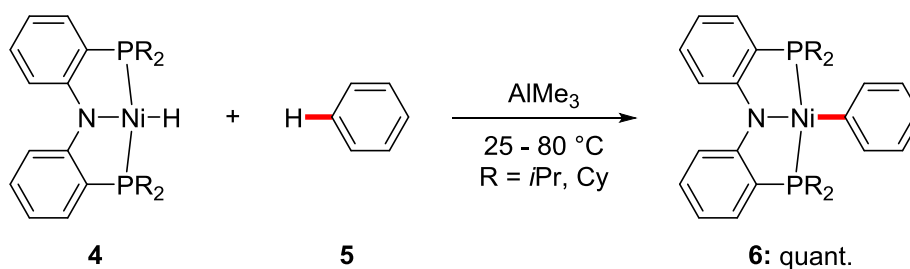
1 Introduction

One of the first and important contributions to nickel-catalyzed C–H activation was reported in the early 1960s by DUBECK (Scheme 1.5).^[38] In this report diazobenzene (**1**) was reacted with stoichiometric amounts of nickelocene (**2**) at elevated temperatures and the product **3** could be isolated and characterized. This example highlights the strength of nickel in being capable to undergo C–H nickelation at the *ortho* C–H bond of diazoarenes **1** by using the diazo moiety as directing group.



Scheme 1.5: C–H cyclometalation of diazobenzene **1**.

After this seminal observation, research came to a standstill for almost 50 years, until 2006, when LIANG disclosed that the nickel(II) pincer complex **4** could react with benzene (**5**) to provide complex **6** *via* oxidative addition into the C–H bond of benzene without any directing group (Scheme 1.6).^[39] This example is of particular interest, highlighting the remarkable reactivity of inexpensive nickel(II) catalysts as compared to the commonly used 4d and 5d metals.

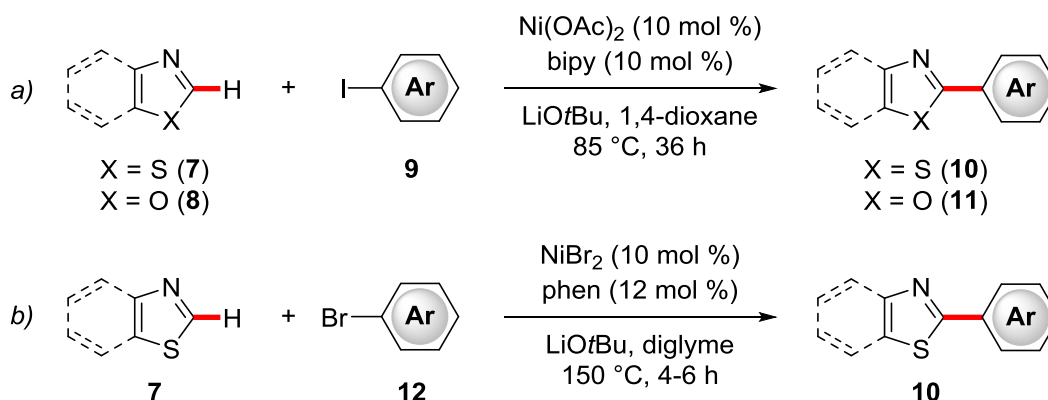


Scheme 1.6: Stoichiometric arene C–H activation with nickel(II) pincer complex **4**.

Subsequently, the use of nickel catalysis to achieve C–H activation was investigated in more detail by the groups of NAKAO/HIYAMA, MIURA, ITAMI, HU and ACKERMANN, among others.^[40] In this context, the development of new methodologies for C–H activation, including direct arylation, alkynylation and alkylation reactions, hydroarylation-type reactions and annulations strategies^[41] were mainly focused on the use of electronically-biased azoles and related heterocycles.

1.2.1 Nickel-Catalyzed C–H Arylation, Alkynylation and Alkylation

In 2009, the first examples of C–H arylation of the electronically activated azole derivatives **7** and **8** with simple aryl halides **9/12** were concurrently reported by MIURA and ITAMI (Scheme 1.7).^[40d, 40e] In both reactions, simple nickel(II) salts in the presence of bidentate nitrogen-based ligands enabled the synthesis of arylated azoles **10-11** in high yields.



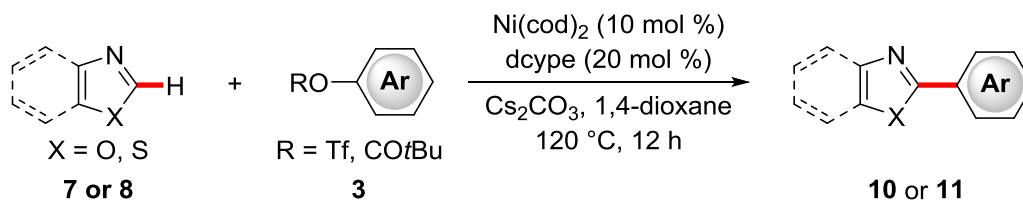
Scheme 1.7: Nickel-catalyzed C–H arylation of azoles.

The outcome of the reaction was strongly dependent on the nature of the base and hence, solely LiOtBu was efficient to achieve the desired transformation. Later, the protocol developed by ITAMI could be improved by using the less expensive base Mg(OtBu)₂ as an alternative to LiOtBu.^[42] With these new conditions in hand, also electron-deficient haloarenes were suitable substrates for the C–H arylation reactions.

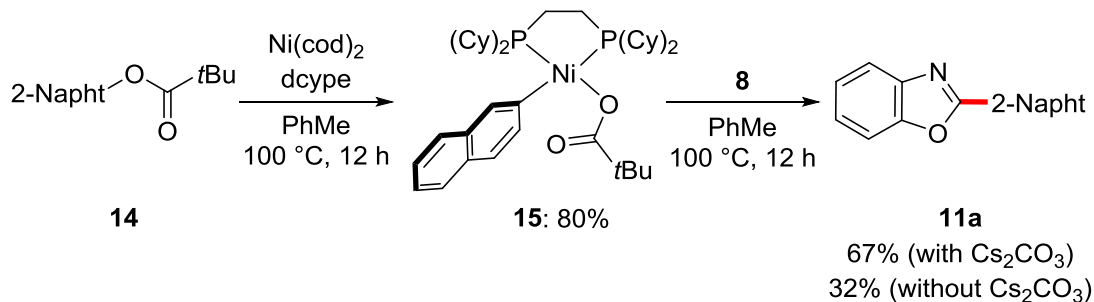
In addition to aryl halides, readily available and inexpensive phenol derivatives could also be employed as arylating reagents. The group of ITAMI developed the nickel-catalyzed C–H/C–O coupling of 1,3-azoles **7** and **8** with aryl pivalates or triflates **13**, featuring an effective Ni(cod)₂/dcype catalyst system (Scheme 1.8a).^[40a] In addition to aryl pivalates and triflates, also aryl carbonates, sulfamates, tosylates, and mesylates proved to be viable substrates.^[43]

1 Introduction

a) Nickel-catalyzed C–H arylation of azoles with aryl pivalates and triflates



b) Mechanistic studies on the nickel-catalyzed C–H/C–O biaryl coupling



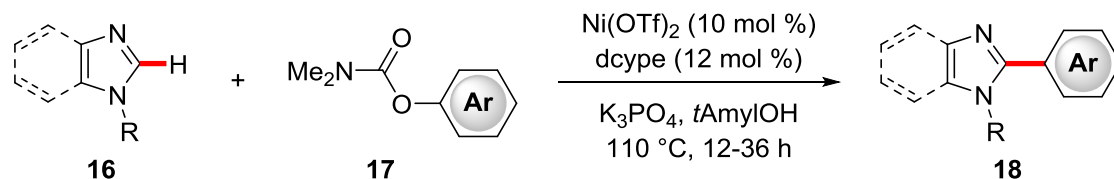
Scheme 1.8: a) Nickel-catalyzed C–H arylation of azoles **7** and **8** with phenol derivatives, b) mechanistic investigations.

Importantly, the use of dcype (**22**) as the ligand was crucial to obtain good results, while other ligands, such as triphenyl phosphine, dppe or N-heterocyclic carbenes did not perform well in the envisioned reaction. Detailed mechanistic studies by ITAMI revealed a pronounced ligand effect, since complex **15**, generated *via* oxidative addition into the C–O bond of naphthyl pivalate **14**, could be isolated only in presence of dcype. Furthermore, complex **15** was able to release the arylated product **11a** when treated with **8** in a stoichiometric fashion (Scheme 1.8b).^[44]

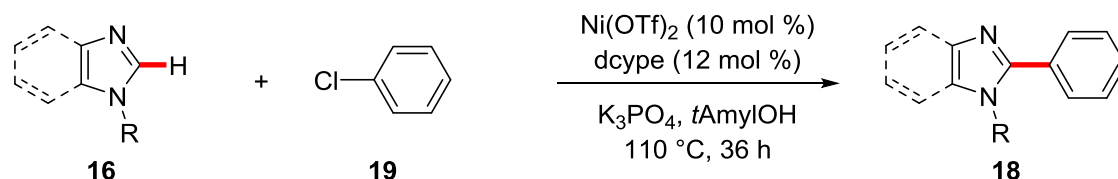
Whereas benzothiazoles **7** and benzoxazoles **8** mostly react smoothly in nickel-catalyzed C–H arylation reactions, benzimidazoles and imidazoles had previously not been viable substrates in this kind of transformations. However, ITAMI and YAMAGUCHI were able to employ aryl carbamates **17** and rarely used chlorobenzene **19** for the C–H arylation of challenging (benz)imidazole derivatives **16** (Scheme 1.9a and b).^[45] Interestingly, the envisioned reaction showed a strong dependence on the solvent used, whereby only tertiary alcohols, especially *tert*-amyl alcohol, allowed for the efficient C–H arylation. Furthermore, by changing the ligand from dcype, utilized for the arylation protocol, to dcyp_t (**23**), enol derivatives such as vinyl carbamate **20** could be used as coupling partner to achieve the C–H alkenylation of benzimidazoles, as well as other azole derivatives (Scheme 1.9c).^[45]

1 Introduction

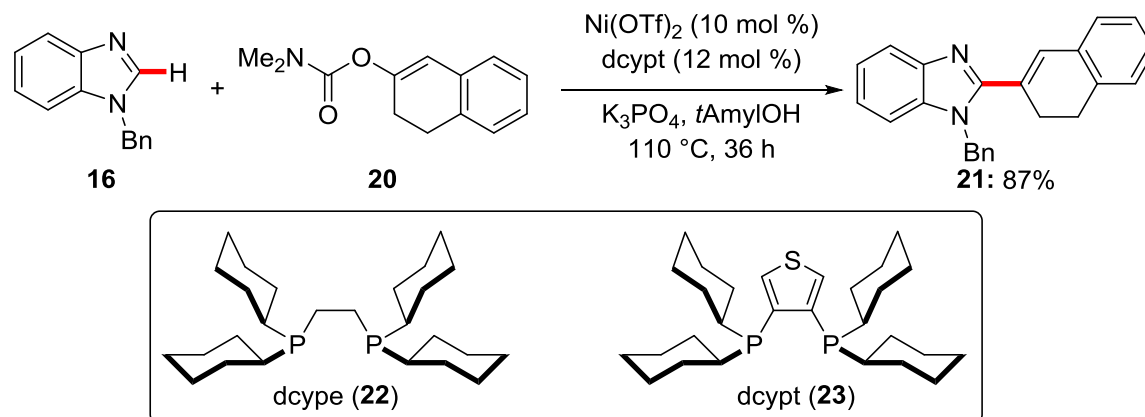
a) Arylation of (benz)imidazoles with aryl carbamates



b) Arylation of (benz)imidazoles with chlorobenzene



c) Alkenylation of benzimidazoles with vinyl carbamate

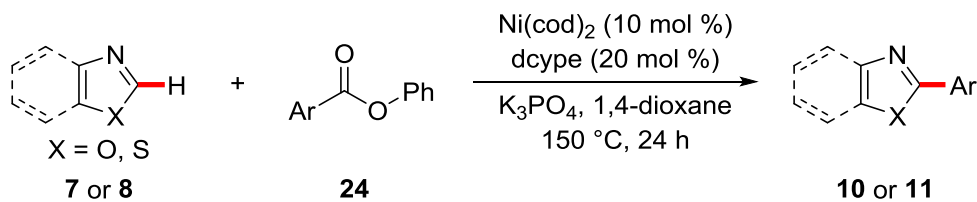


Scheme 1.9: Nickel-catalyzed C–H arylation and alkenylation of (benz)imidazole derivatives.

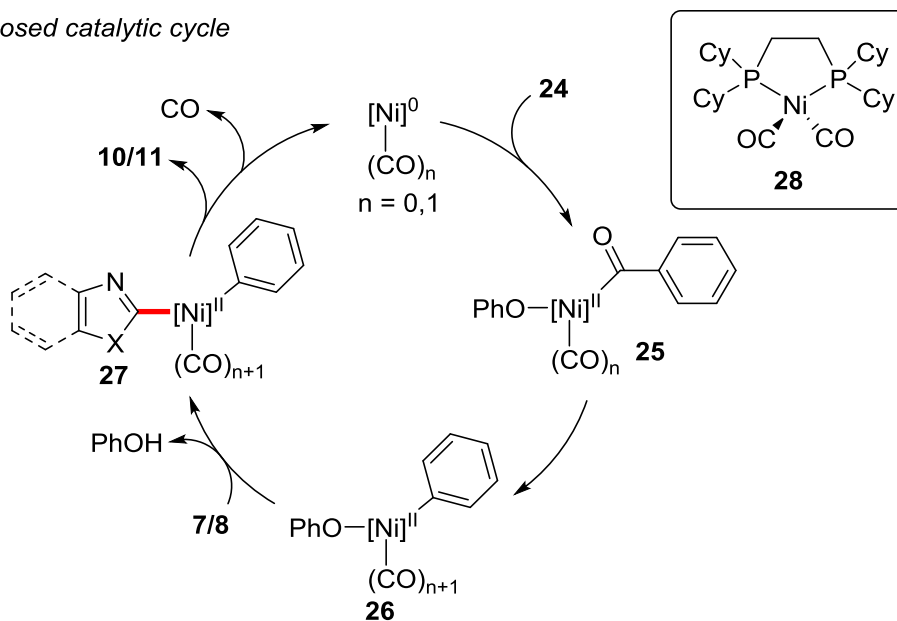
In 2012, ITAMI disclosed a further approach to achieve biaryl formation *via* a decarbonylative coupling of azoles **7** or **8** with aryl esters **24**.^[46] Here, the $\text{Ni}(\text{cod})_2/\text{dcyce}$ catalytic system, similar to the C–H/C–O coupling of aryl carbamates, enabled the synthesis of various (hetero)arylated azole derivatives **10** or **11** (Scheme 1.10a).

A mechanistic proposal rationalized that nickel(0) complex **28** could be an intermediate within a plausible catalytic cycle, involving a nickel(0)/nickel(II) redox system (Scheme 1.10b). Later on, the group of GADE supported the presence of intermediate **28** by the formation and characterization of a related complex.^[47] Furthermore, HOUK and LU reported more detailed investigations by computational studies for the decarbonylation step.^[48]

a) Nickel-catalyzed decarbonylative arylation of azoles with aryl esters



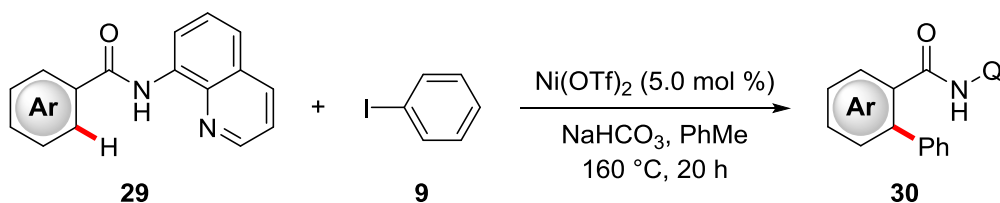
b) Proposed catalytic cycle



Scheme 1.10: a) Decarbonylative arylation of azoles **7** and **8**; b) proposed catalytic cycle.

While a majority of reported methods for the direct C–H arylation were restricted to the use of activated C–H bonds in heteroaromatic substrates, such as pyridines, perfluorinated arenes or azole derivatives,^[49] in which an acidic C–H bond is functionalized, examples for the catalytic functionalization of unactivated C–H bonds in arenes remain comparatively scarce. Inspired by the pioneering work of DAUGULIS introducing the *N,N'*-bidentate directing groups 8-aminoquinoline (8-AQ) for palladium-catalyzed C–H functionalizations,^[50] the group of CHATANI developed a nickel-catalyzed C–H arylation of aromatic amides **29** containing 8-AQ as the directing group (Scheme 1.11).^[51]

1 Introduction

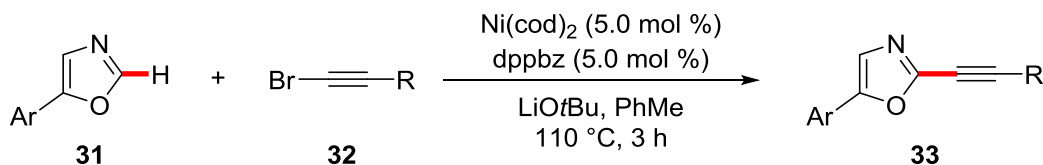


Scheme 1.11: Nickel-catalyzed C–H arylation of benzamides **29** with iodobenzene **9**.

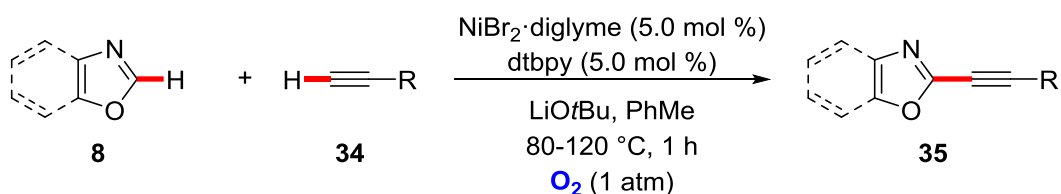
Nickel-catalyzed C–H functionalizations are not limited to arylation reactions of electronically-biased hetero(aromatic) substrates or arenes bearing bidentate auxiliaries. Subsequently, numerous protocols for the corresponding nickel-catalyzed alkyne annulation, alkynylation and alkylation reactions of inert C–H bonds under bidentate chelate-assistance and substrates with activated C–H bonds have been developed, which have been summarized in selected reviews.^[31a, 49c]

It is noteworthy that the introduction of alkynes *via* transition metal-catalyzed C–H activation has been identified as a powerful alternative to the conventional SONOGASHIRA-HAGIHARA coupling.^[52] An early protocol for the nickel-catalyzed alkynylation of 5-aryloxazoles **31** with alkynyl bromides **32** was described by MIURA in 2009 (Scheme 1.12a).^[53] Here, the catalytic system consisted of Ni(cod)₂ as the catalyst and 1,2-bis(diphenylphosphino)benzene (dppbz) as the ligand. One year later, in 2010, the same group was able to achieve a similar C–H alkynylation of azoles **8** with terminal alkynes **34**, such as simple acetylenes, in an oxidative fashion, utilizing environmentally benign O₂ as the sacrificial oxidant (Scheme 1.12b).^[54]

a) Alkynylation of azoles with bromoalkynes



b) Oxidative alkynylation of azoles with terminal alkynes

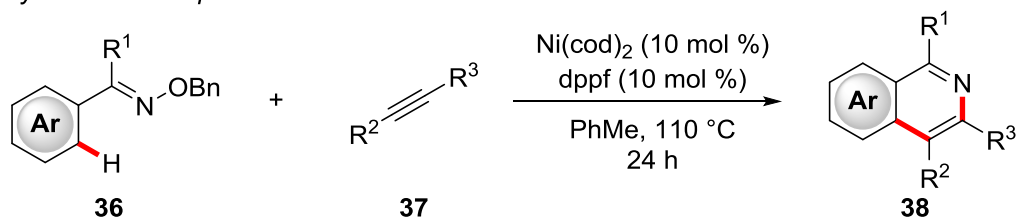


Scheme 1.12: Nickel-catalyzed (oxidative) alkynylation of oxazoles **31** and **8**.

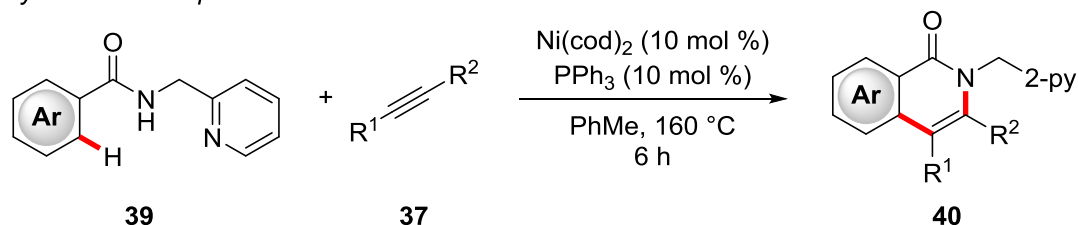
1 Introduction

Furthermore, the use of monodentate and bidentate directing groups enabled a wide variety of strategies, employing alkynes as coupling partners, either achieving alkynylation reactions or annulations reactions.^[41, 55] As highlighted in Scheme 1.13, nickel-catalyzed C–H/N–H annulation reactions can be applied for the construction of various N-heterocyclic structures.

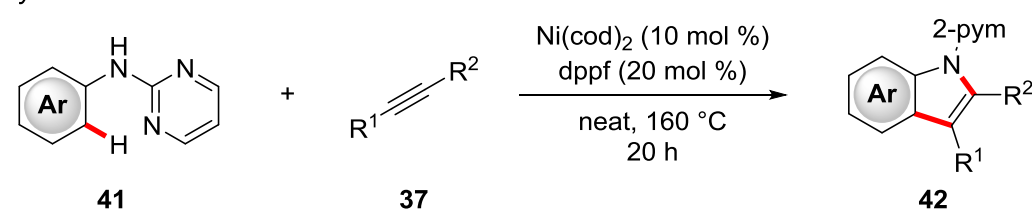
a) Synthesis of isoquinolines



b) Synthesis of isoquinolinones



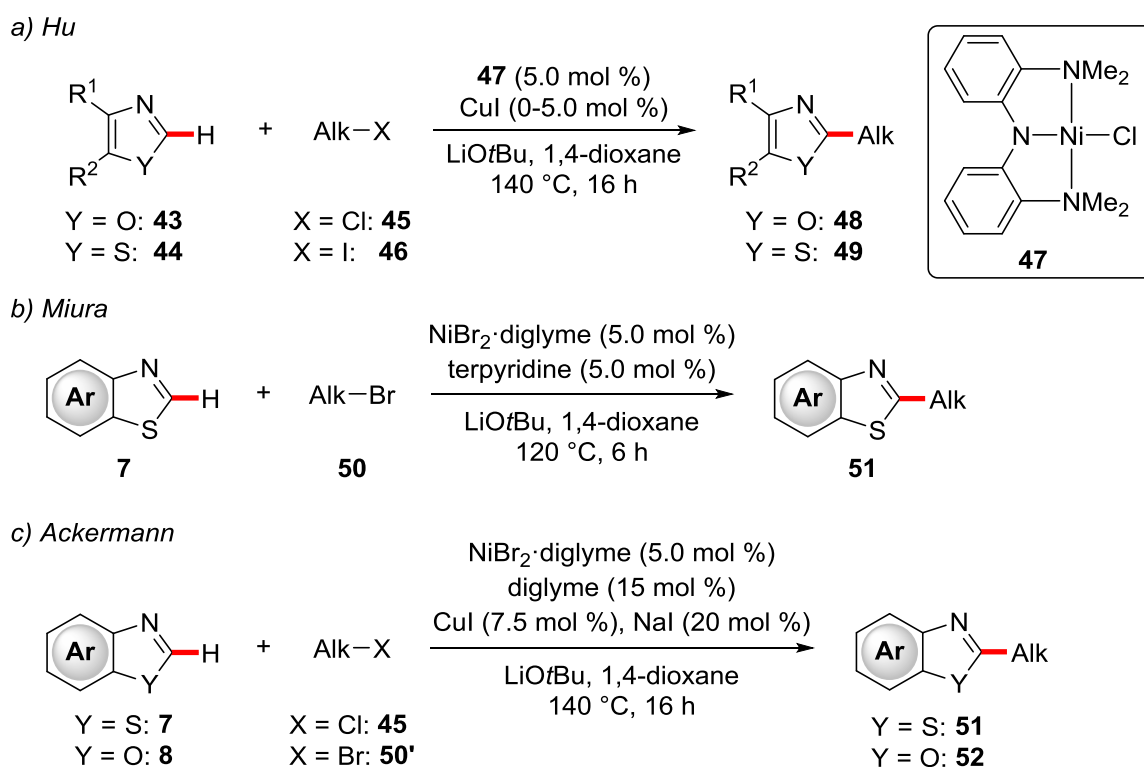
c) Synthesis of indoles



Scheme 1.13: Synthesis of N-heterocyclic structures *via* nickel-catalyzed alkyne annulations.

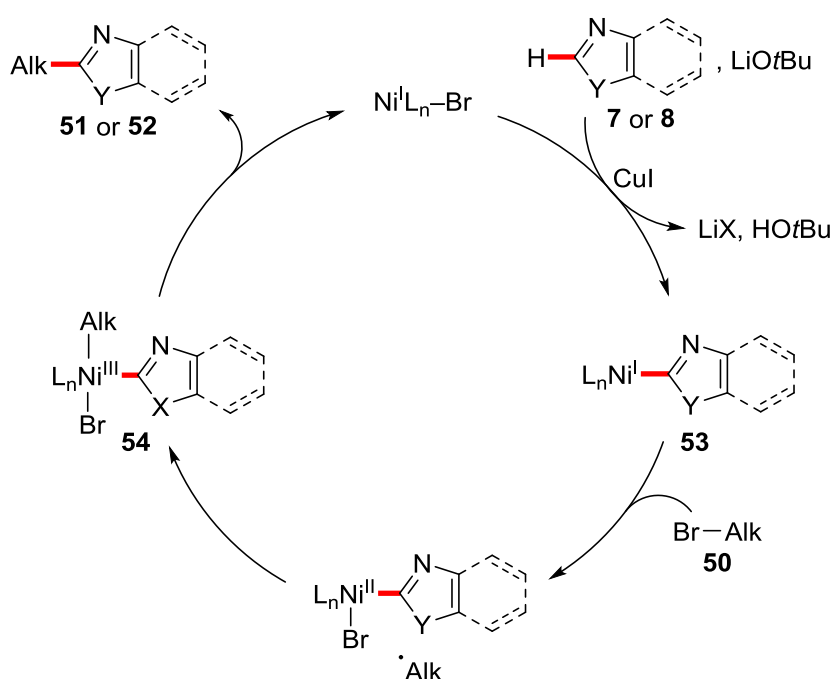
For example, KURAHASHI and MATSUBARA developed an alkyne annulation of ketoximes **36** for the synthesis of isoquinolines **38** (Scheme 1.13a),^[56] whereas CHATANI developed a protocol for the construction of substituted isoquinolinones **40** by reacting benzamides **39**, bearing a bidentate directing group, with internal alkynes under similar conditions (Scheme 1.13b).^[57] In contrast, ACKERMANN could achieve the synthesis of indoles^[58] **42** from N-pyrimidyl anilines **41** and alkynes **37** *via* nickel-catalyzed C–H/N–H annulation (Scheme 1.13c).^[55b] Noteworthy, this C–H/N–H bond activation protocol proceeds in the absence of any metal oxidants and with excellent chemo- and regio-selectivities. Furthermore, numerous other alkynylation and annulations reactions utilizing terminal alkynes under oxidative conditions^[55c, 59] or direct alkynylations using bromo alkynes^[60] were developed.

In addition to arylation and alkynylation reactions, methods for the introduction of alkyl groups are highly desirable transformations. Regarding transition metal-catalyzed C–H alkylations, two general approaches have been commonly followed, *i*) the hydroarylation of alkenes, which will be discussed later, and *ii*) the use of electrophilic alkyl halides for the direct C–H activation. However, the use of alkyl halides in direct C–H alkylation suffers from several limitations. Thus, the oxidative addition of alkyl halides to transition metal complexes is an unfavourable process and the corresponding alkylmetal complexes tend to undergo β -hydride elimination.^[61] In 2010, HU^[40c], MIURA^[62] and ACKERMANN^[40b] independently reported on the nickel-catalyzed C–H alkylation of azoles with alkyl halides (Scheme 1.14). The catalytic system, reported by HU was comprised of the nickel-pincer complex **47** and additional copper(I) salts for facile transmetalation. Also, ACKERMANN made use of similar copper(I) salts. Under those conditions, a broad substrate scope with various alkyl iodides, bromides, and alkyl chlorides proved to be applicable in the transformation.



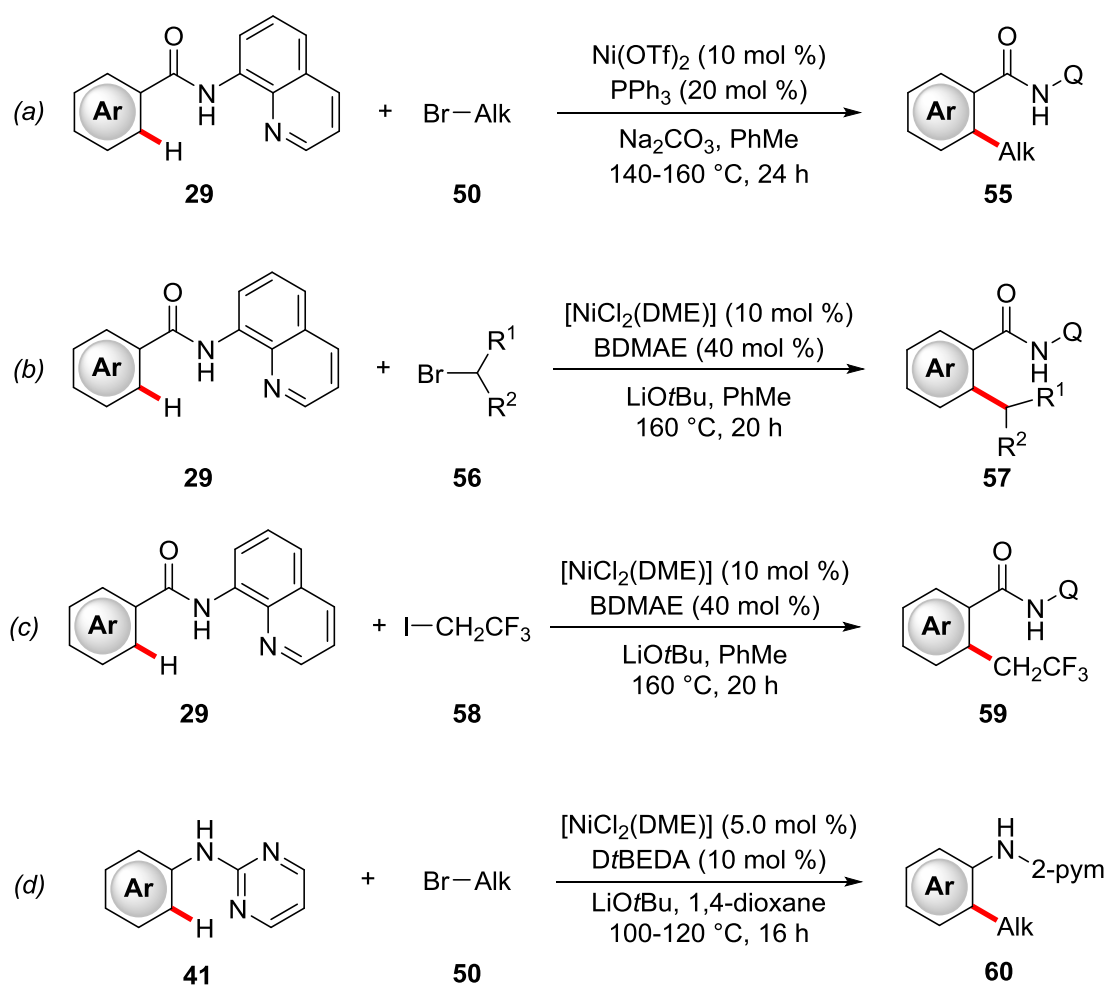
Scheme 1.14: Nickel-catalyzed C–H alkylations of azoles.

To gain insights into the mode of action of the nickel-catalyzed alkylation, MIURA and ACKERMANN independently performed detailed mechanistic studies. To this end, radical clock experiments provided strong support for radical intermediates to be involved, and therefore a plausible catalytic cycle was proposed (Scheme 1.15). After initial C–H metalation of azole **7/8**, the alkyl halide **50** is activated by single electron transfer, followed by a radical recombination to generate nickel(III) intermediate **54**. Then, reductive elimination releases the desired product **51/52** and regenerates the catalytically active nickel(I) species.



Scheme 1.15: Plausible catalytic cycle for the nickel-catalyzed C–H alkylation of azoles.

In 2013, CHATANI reported on the chelation-assisted nickel-catalyzed C–H alkylation of aromatic amides **29** with alkyl bromides **50** (Scheme 1.16a).^[63] Interestingly, among various tested directing groups, only the bidentate 8-aminoquinoline auxiliary provided efficient reactivity to give the desired alkylated products **55**. Furthermore, the addition of NaI allowed for the use of alkyl chlorides as electrophile.



Scheme 1.16: Nickel-catalyzed C–H alkylations under chelate-assistance.

Subsequently, ACKERMANN enabled the use of challenging secondary alkyl halides **56** (Scheme 1.16b and c), and trifluoroethyl iodide (**58**) also proved to be a viable substrate for the first time.^[64] Furthermore, the protocol could be applied to aniline derivatives **41** being for the first time devoid of a bidentate directing group (Scheme 1.16d).^[65] Thus, the monodentate pyrimidine directing group enabled access to alkylated aniline derivatives **60**.

Additionally, various protocols for the installation of alkyl,^[66] benzyl,^[66b, 67] and allyl^[66b, 68] groups were developed by means of nickel-catalyzed C–H functionalization with alkyl halides or pseudohalides.

1.2.2 Nickel-Catalyzed C–S Bond Formation

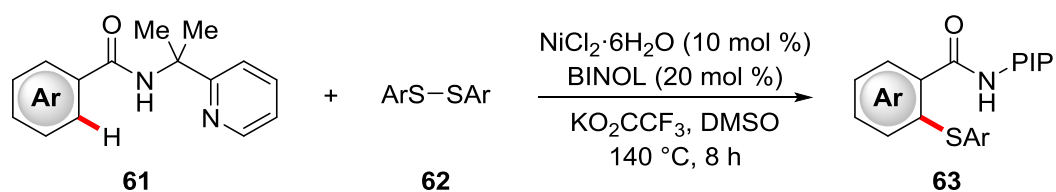
Organosulfur compounds are useful building blocks in organic synthesis. Among these compounds, aryl sulfides represent an important structural motif found in a huge variety of biologically and pharmaceutically active compounds, e. g. for the treatment of diabetes, immune or Alzheimer's disease, among others.^[69] Furthermore, dibenzothiophene, the fused form of diarylsulfides, represent one of the most important subunits for optoelectronic devices such as semiconducting polymers or OLEDs.^[70]

Commonly applied strategies for the formation of C–S bonds have been devoted to direct cross-coupling reactions of aryl halides with thiols or the addition of thiols to unsaturated C–C bonds.^[71] Nonetheless, the use of expensive aryl halides, high catalyst loadings due to sulfide poisoning, or the addition of superstoichiometric amounts of additives and harsh reaction conditions translate into significant limitations.

To improve the synthetic access to sulfur-containing compounds, transformations *via* transition metal-catalyzed C–H functionalizations have emerged as a rapidly expanding field of research on C–S bond formation.^[69a, 70a, 70b, 71] Worth mentioning is the pioneering work on C–S bond formation through the use of palladium(II)-based catalysts by INAMOTO in 2008.^[72]

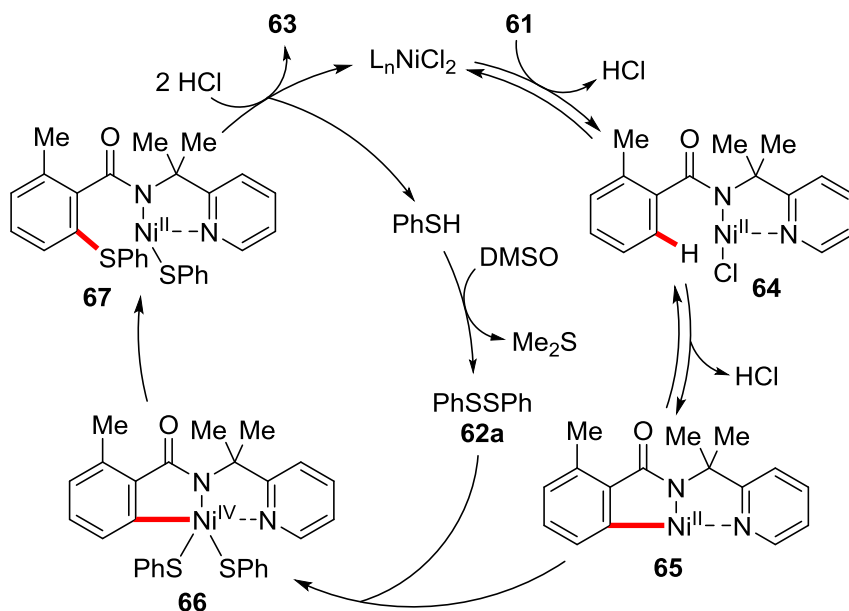
In the following years, numerous protocols for the construction of sulfur-containing heterocycles by means of intramolecular palladium-catalyzed C–H activation were developed.^[73] Furthermore, copper-based catalysts significantly expanded the field of C–S bond formation reactions, enabling the formation of diaryl sulfides and benzothiazoles, among others.^[69a] However, these methods required the use of expensive second-row transition metals and/or stoichiometric copper(II) or silver(I) salts as cocatalytic oxidants. With regard to this, an approach employing nickel-catalyzed C–H activation for the formation of C–S bonds would be a useful alternative. SHI reported the first nickel-catalyzed C–H thiolation reaction employing bidentate chelate-assistance (Scheme 1.17).^[74] In the absence of silver(I) additives, 2-(pyridine-2-yl)isopropyl- (*N*-PIP) benzamides **61** could be converted into the desired *ortho*-thiolated products **63** using diaryldisulfides **62**.

1 Introduction



Scheme 1.17: Nickel-catalyzed C–H thiolation of benzamides **61** with disulfides **62**.

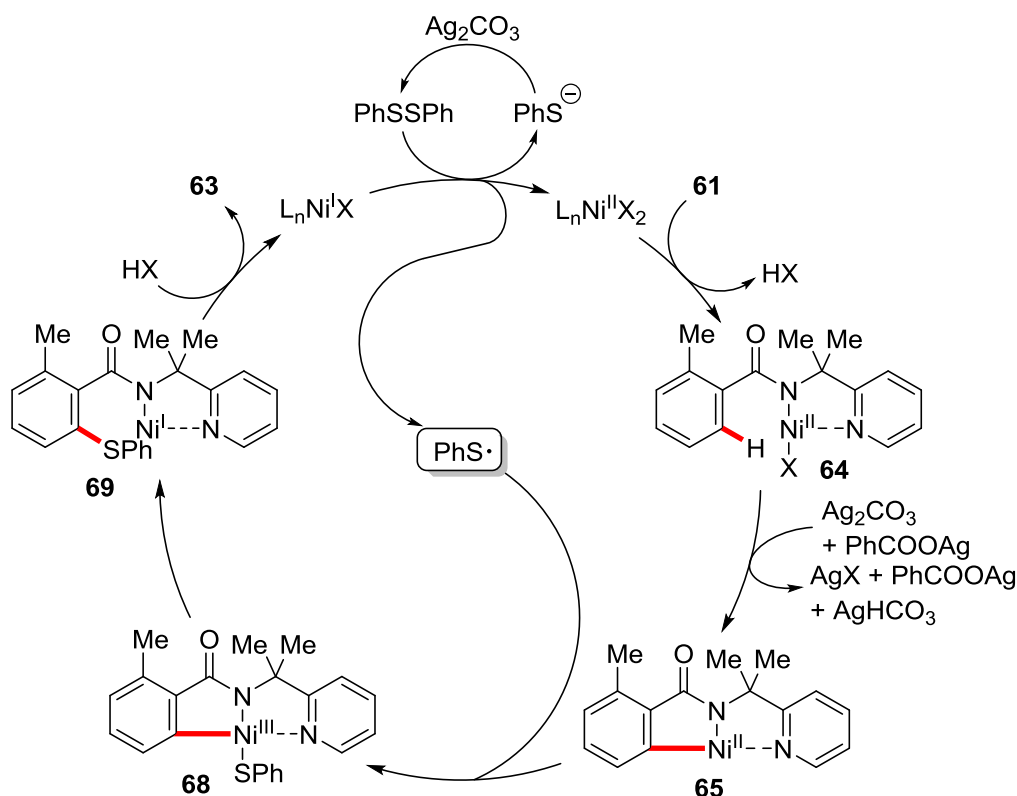
The proposed mechanism includes a nickel(II)/nickel(IV) catalytic cycle involving oxidative addition of the disulfide to the nickel(II)-pincer complex **65**, followed by reductive elimination to **67** (Scheme 1.18). Subsequently, protonation releases the desired product **63** and thiophenol, with regeneration of the active catalyst.



Scheme 1.18: Proposed catalytic cycle.

In contrast, LU independently reported on a related direct thioarylation procedure of similar PIP-protected benzamides **61** using NiCl_2 as the catalyst and benzoic acid as the ligand of choice.^[75] Here, using the same PIP-derived benzamides **61** and diaryl disulfides **62** in the presence of stoichiometric amounts of Ag_2CO_3 as oxidant provided an efficient access to valuable aryl sulfides.

Whereas Shi proposed a Ni(II)/Ni(IV) catalytic cycle by oxidative addition of the disulfide,^[74] Lu suggested a SET-type process *via* a phenyl sulfide radical to generate the nickel(III) intermediate **68** (Scheme 1.19). Subsequent reductive elimination of **68** followed by protodemetalation generates the *ortho*-thiolated product **63** and a nickel(I) species, which is then reoxidized to the catalytically active nickel(II) species and a phenyl sulfide radical.



Scheme 1.19. Proposed Ni(I)/Ni(III) catalytic cycle for the direct *ortho*-thiolation of aromatic amides.

Additionally, various protocols for the direct thioetherification of acryl amides^[76] and aliphatic amides^[77] utilizing diaryl disulfides or thiophenols, as well as protocols for the synthesis of sulfones, utilizing sulfonyl chlorides,^[78] have been developed.

1.2.3 Nickel-Catalyzed Hydroarylation of Alkynes and Alkenes

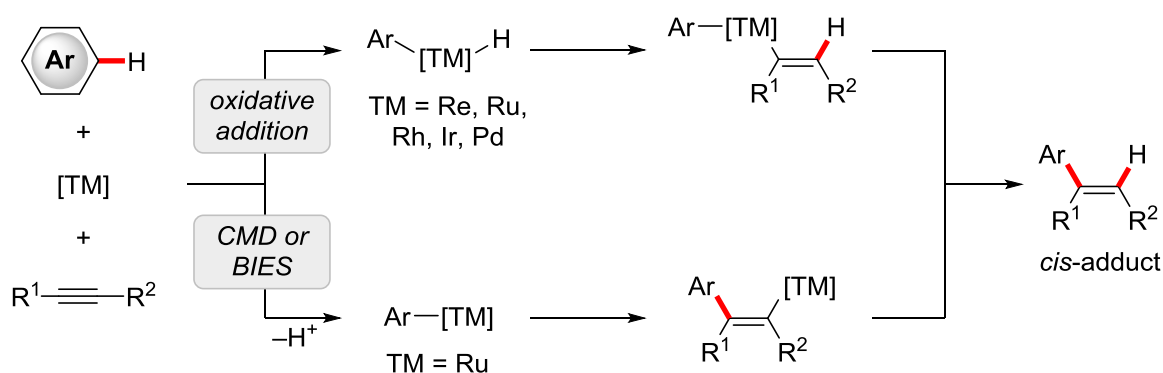
Hydroarylation reactions of multiple C–C bonds are among the most popular synthetic tools in transition metal catalysis for the selective introduction of alkyl or alkenyl groups at aromatic or heteroaromatic compounds.^[79]

In general, these methods provide a more selective access to various structural scaffolds compared to complementary transformations such as FRIEDEL-CRAFTS

1 Introduction

alkylations^[80] or HECK- and FUJIWARA-MORITANI^[81] reactions. For instance, in the case of FRIEDEL-CRAFTS alkylations, halogenated precursors, strongly acidic reactants and/or harsh reaction conditions are usually required. Furthermore, stoichiometric amounts of waste products are often generated in these processes and undesired overalkylations can occur. Similarly, HECK- and related cross-coupling reactions also rely on pre-functionalized starting materials, at the cost of stoichiometric waste formation. Therefore, more atom- and step economic hydroarylation reactions represent an environmentally benign alternative to these traditional methodologies.

In general, two mechanistic pathways for the hydroarylation of alkynes are possible, either through alkyne activation or (hetero)arene activation.^[41a] In the latter case, the arene C–H bond can be activated either by oxidative addition, by LLHT, CMD or BIES, among others (Scheme 1.20). Subsequently, the alkyne can undergo a migratory insertion into the corresponding [TM]–C or the [TM]–H bond to give an arylmetal species or an alkenylated metal species, respectively. Finally, the adduct is selectively formed either *via* protodemetalation or C–C bond forming reductive elimination.

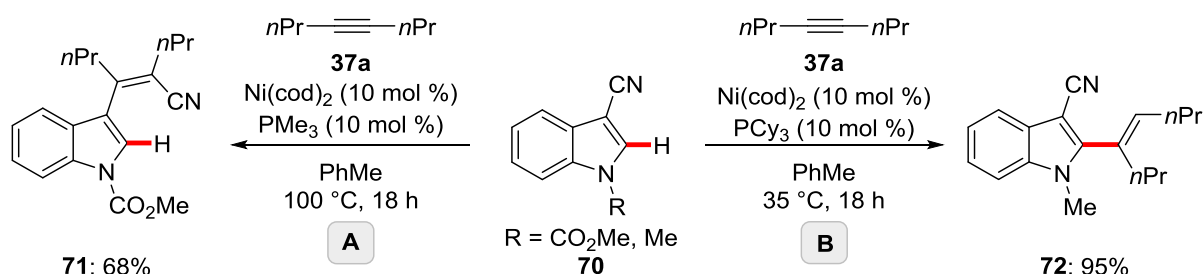


Scheme 1.20: Mechanistic pathways for alkyne hydroarylation.

In the last decade, nickel-catalyzed hydroarylation reactions of alkynes and alkenes have experienced a tremendous progress.^[41b] In 2006, NAKAO and HIYAMA made a notable observation during their investigations on an attempted nickel(0)-catalyzed arylation of indole **70** with 4-octyne **37a**.^[82] Besides the desired product **71**, arising from the arylation reaction (Scheme 1.21; **A**), small amounts of a compound resulting from the insertion of the alkyne into the C–H bond at the C-2 position from **70** were isolated. This switch in selectivity, from arylation to

1 Introduction

hydroarylation, could further be optimized by changing the ligand from PMe_3 to PCy_3 and the *N*-protecting group on the indole (Scheme 1.21; **B**), allowing for the selective synthesis of alkenylated indole derivatives **72**.

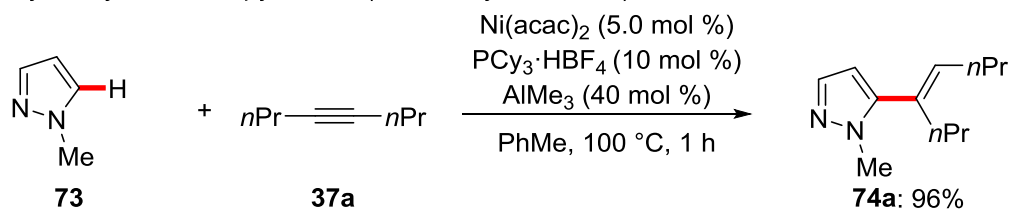


Scheme 1.21: Nickel-catalyzed arylocyanation (path A) or hydroarylation (path B) of alkynes.

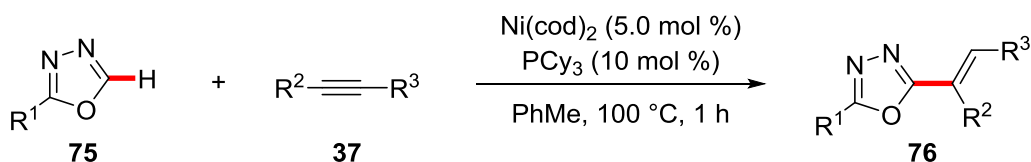
In addition, various five-membered heteroarenes, including benzimidazole, caffeine, purine, benzoxazole, benzofurane, benzothiazole, and thiazole, also participated in the envisioned hydroarylation with alkyne **37a**, affording the corresponding alkenyl heteroarenes with high regioselectivity for the C-2 position.^[82] Subsequently, the groups of NAKAO/HIYAMA, and MIURA applied similar nickel/phosphine catalysts for the nickel-catalyzed hydroarylation of five-membered heteroarenes, such as pyrazoles **73**,^[83] oxadiazoles **75**,^[84] and imidazoles **77**^[85] (Scheme 1.22).

1 Introduction

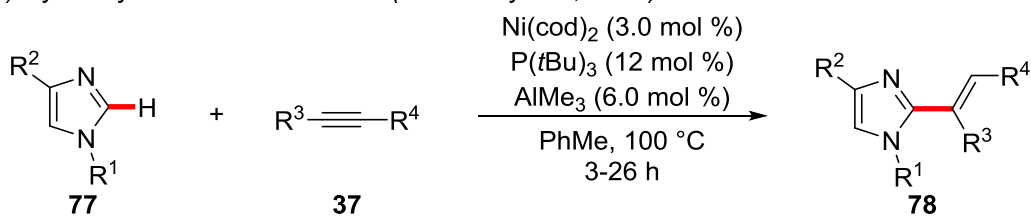
a) *Hydroarylation with pyrazoles (Nakao/Hiyama, 2007)*



b) *Hydroarylation with oxadiazoles (Miura, 2009)*



c) *Hydroarylation with imidazoles (Nakao/Hiyama, 2009)*

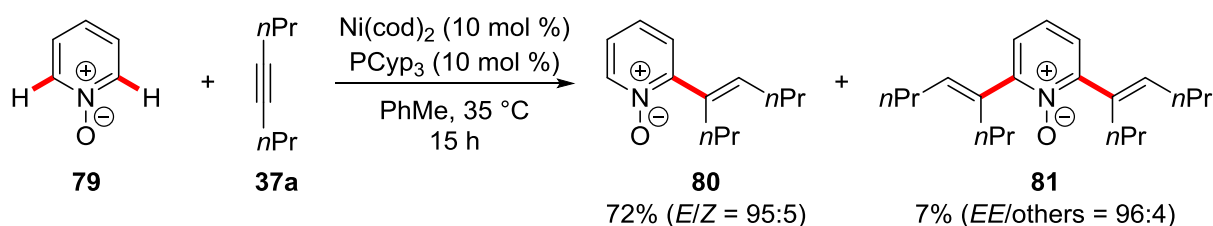


Scheme 1.22: Nickel-catalyzed hydroarylation of alkynes **37** with five-membered heteroarenes.

1 Introduction

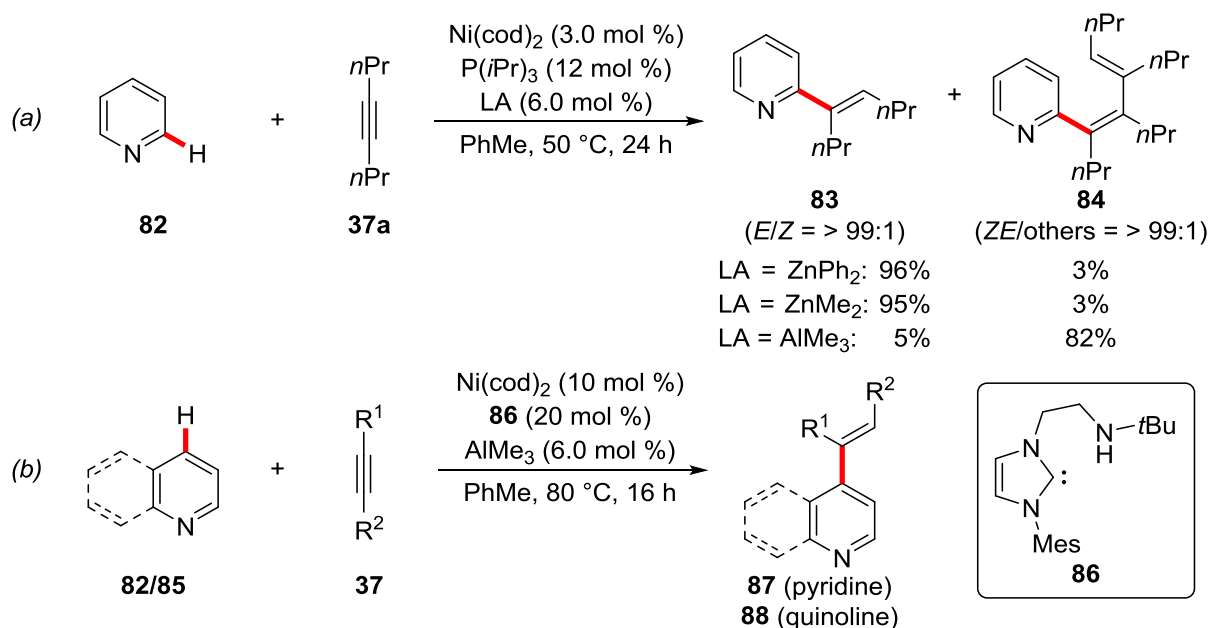
HIYAMA reported a catalytic system using bench-stable $\text{Ni}(\text{acac})_2$ for the hydroarylation of alkynes **37**. Here, the catalytically active nickel(0) species is formed by the action of AlMe_3 as the reducing agent (Scheme 1.22a). Furthermore, MIURA reported a $\text{Ni}(\text{cod})_2/\text{PCy}_3$ system, which allowed the efficient conversion of oxadiazoles **75** (Scheme 1.22b), and NAKAO and HIYAMA reported on a C-2 selective hydroarylation procedure for imidazoles **77** using AlMe_3 as the additive (Scheme 1.22c). However, when imidazoles bearing a substituent in the C-2 position were used, regioselective hydroarylation in C-5 position occurred, leading to alkenylated imidazoles **78** with high *E/Z* ratios.

Also electron-deficient six-membered heteroarenes **79** proved to be viable substrates in nickel-catalyzed hydroarylation reactions. In 2007, NAKAO and HIYAMA showed that pyridine *N*-oxides **79** were suitable substrates, affording the desired 2-alkenylated products **80x3** with exclusive C-2 selectivity and high *E/Z* ratios (Scheme 1.23).^[86]



Scheme 1.23: Nickel-catalyzed hydroarylation with pyridine *N*-oxides **79**.

Furthermore, simple pyridines **82** could be employed in the hydroarylation of alkynes **37** through cooperative nickel/Lewis acid catalysis. NAKAO and HIYAMA developed a regioselective C-2 alkenylation of pyridines employing ZnPh_2 or ZnMe_2 as Lewis acids (Scheme 1.24a).^[87] Whereas ONG devised a catalytic system utilizing $\text{Ni}(\text{cod})_2$ as the catalyst precursor and the amino-linked bidentate NHC ligand **86** along with the Lewis acid AlMe_3 for the unusual *para*-functionalization of pyridines **82** and quinolines **85** (Scheme 1.24b).^[88]



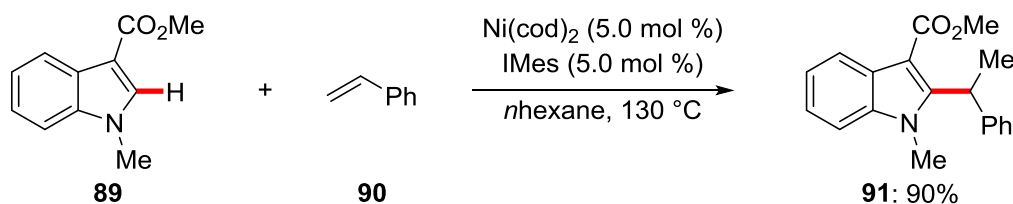
Scheme 1.24: Nickel/Lewis acid-catalyzed C2-selective (a) or C-4-selective (b) hydroarylation with pyridines **82** and quinolines **85**.

Nickel-catalyzed hydroarylation reactions are not only applicable to alkynes, but also to alkenes. In particular, nickel catalysts with NHC ligands have proven to be efficient catalytic systems for the alkylation of various heteroarenes.

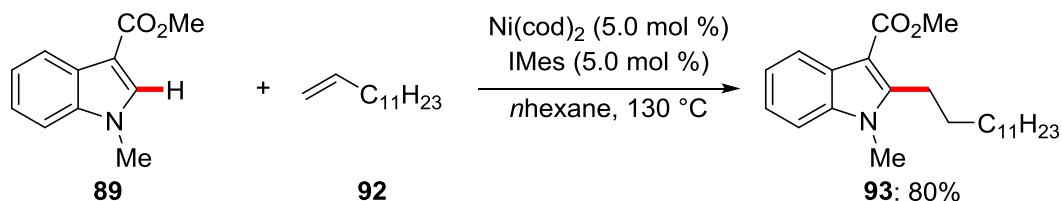
In this context, the group of NAKAO and HIYAMA developed a procedure for the hydroheteroarylation of alkenes. Here, the NHC ligand IMes along with Ni(cod)₂ as the precatalyst enabled the efficient C-2 selective functionalization of indoles **89**. Interestingly, this occurred with a switch in selectivity depending on the nature of the alkenes (Scheme 1.25).^[89]

Activated alkene derivatives such as vinyl arenes (e.g. styrene (**90**)) reacted at the C-2 position to selectively afford the branched alkylated indole **91** (Scheme 1.25a), whereas unactivated olefins, such as simple 1-tridecene (**92**), gave the linear product **93** in high selectivity and good yields (Scheme 1.25b).

a) Hydroarylation of styrene (**90**) (branched selectivity)



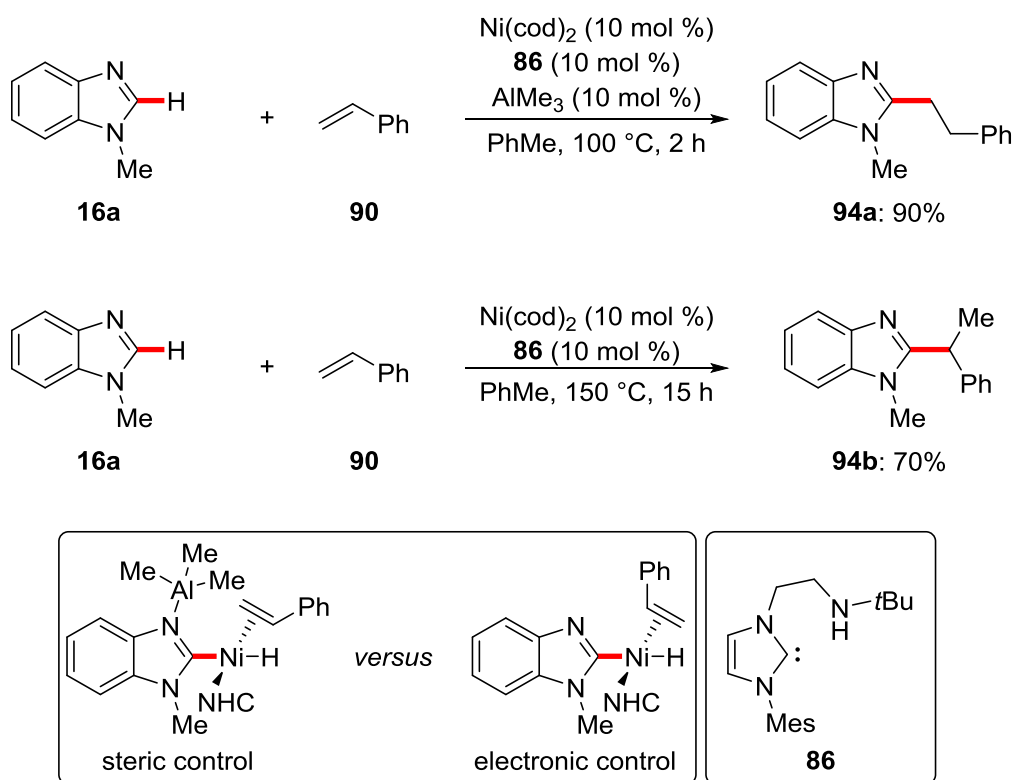
b) Hydroarylation of unactivated 1-tridecene (**92**) (linear selectivity)



Scheme 1.25: Switch in selectivity in nickel-catalyzed hydroheteroarylation of terminal alkenes.

Subsequently, ONG developed a protocol for the hydroheteroarylation of vinylarenes **90** employing $\text{Ni}(\text{cod})_2$ and the amino-NHC ligand **86**, where the regioselectivity towards branched and linear alkylated products could be controlled by slight changes in the reaction conditions (Scheme 1.26).^[90] Hence, the selectivity switched from branched to linear in the presence of the Lewis acid AlMe_3 due to dative binding of AlMe_3 by the benzimidazole nitrogen atom. Thus, the coordination of styrene to the nickel-hydride species (Scheme 1.26) and the subsequent insertion into the Ni–H bond is controlled by sterics over electronics, and therefore solely delivering the linear product **94a**. In absence of AlMe_3 , electronic control favoured the insertion of the hydride in β -position of the vinylarene **90**, which enabled the formation of the branched product **94b**.

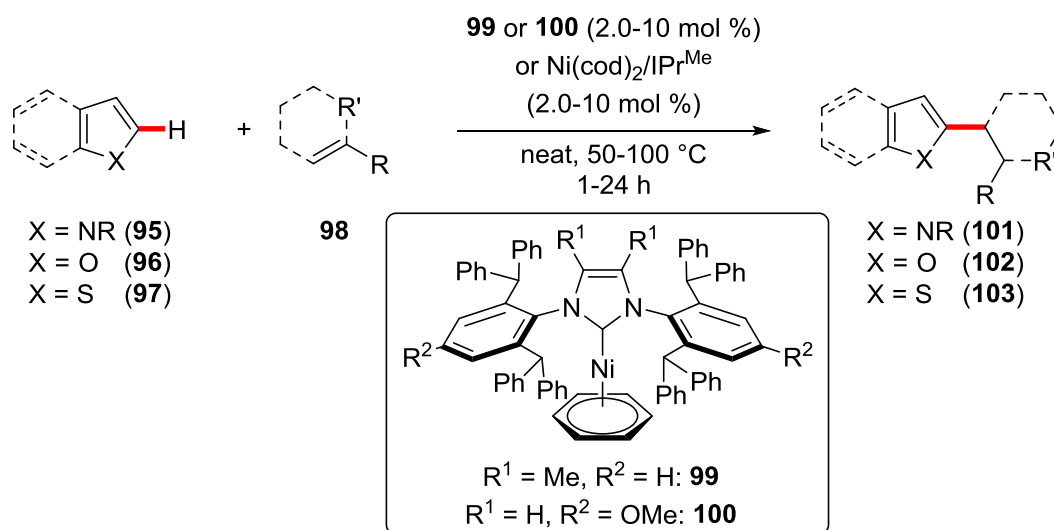
Furthermore, the use of cooperative nickel/Lewis acid catalytic systems was expanded to other substrate classes, such as the C-4 selective alkylation of pyridines employing the bulky Lewis acid MAD,^[91] hydroarylations of simple alkenes with pyridones,^[92] or the use of allylarenes as coupling partners, in which olefin isomerization gave rise to either branched and linear alkylated benzimidazoles and otherazole derivatives, respectively.^[93]



Scheme 1.26: Switch in selectivity in the nickel-catalyzed hydroarylation of styrenes with benzimidazoles.

Despite the enhanced selectivities and reactivities observed in synergistic^[94] nickel/Lewis acid-catalyzed hydroarylations governed by the judicious choice of aluminium-based Lewis acids, several reports highlighted the importance of the utilized NHC ligands^[95] to achieve hydroarylation reactions with new types of ligand-controlled selectivities.

An elegant approach for rational ligand design to achieve hydroarylation reactions with high *anti*-Markovnikov selectivities towards the linear alkylated heteroarene products **101-103** was reported by NAKAO and HARTWIG (Scheme 1.27).^[96] Within these studies, a nickel catalyst generated *in situ* from Ni(cod)₂ and the sterically hindered NHC ligand IPr^{Me} or the well-defined nickel(NHC)(arene) complexes **99/100** were used. The envisioned hydroarylation reaction was not only applicable to unactivated terminal and internal alkenes, also various heteroarene substrates, such as indoles **95**, pyrroles **96a**, benzofurans **96b** and thiazoles **97** proved to be suitable substrates.



Scheme 1.27: Nickel-catalyzed hydroheteroarylation using well-defined Ni(NHC)(arene) complexes.

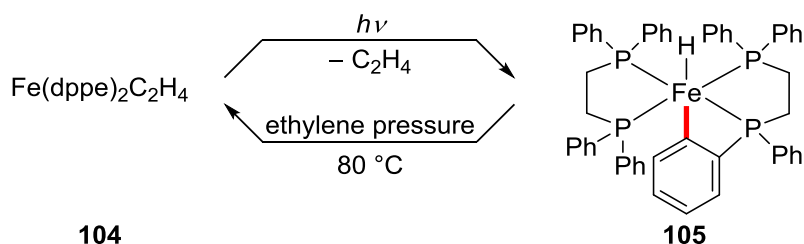
1.3 Iron-Catalyzed C–H Activation

The use of transition metals in catalytic transformations grew up to one of the most important techniques to assemble molecular frameworks. As discussed before, major contributions were achieved by the use of precious metals, such as rhodium, palladium or platinum, among others. Nevertheless, the use of iron complexes as catalysts has many attractive benefits over the use of “expensive alternatives” in transition metal-catalyzed C–H functionalizations.^[97]

First, iron is the most abundant transition metal in the Earth’s crust and therefore much cheaper than the precious late transition metals. Second, due to its low toxicity, iron compounds are tolerated or even incorporated in various biological systems, such as cytochrome P450, the food industry and cosmetics. Furthermore, iron can occupy various oxidation states ranging from -2 to +5, enabling plenty of reactivities to be operative.^[97b, 98] For C–H activations, these reactivities can be grouped into two main categories, *i*) outer-sphere activation, and *ii*) inner-sphere, organometallic activation. Thus, iron complexes in high oxidation states preferentially proceeds through radical pathways *via* hydrogen abstraction^[99] or C–H insertion with iron oxo/imido species.^[100] Here, the weakest C–H bonds, such as benzylic or allylic C–H bonds, are usually functionalized.

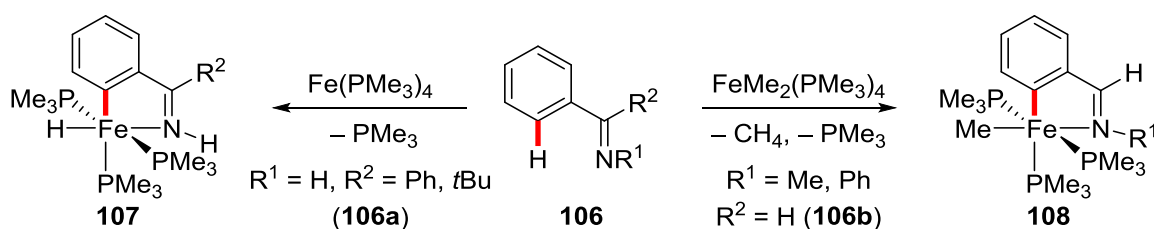
On the other hand, iron in low oxidation states may be operative as an iron-centered nucleophile and is capable to catalyze different reaction types such as nucleophilic substitutions, hydrogenations, cycloisomerizations or traditional cross-coupling reactions, among others.^[101]

Due to various different C–H activation modes, including iron-mediated radical reactions, FRIEDEL-CRAFTS-type electrophilic substitutions, or cross-dehydrogenative coupling reactions, low valent iron species have proven to be viable catalysts for the direct C–H functionalizations that involve the participation of an organoiron species in the C–H bond activation step.^[97b, 98, 102] In 1968, HATA reported on an early example of stoichiometric organometallic C–H activation upon irradiation of the 1,2-bis(diphenyl-phosphino)ethane-ligated iron(0) ethylene complex **104** (Scheme 1.28).^[103]



Scheme 1.28: Stoichiometric C–H activation of a well-defined iron complex **104**.

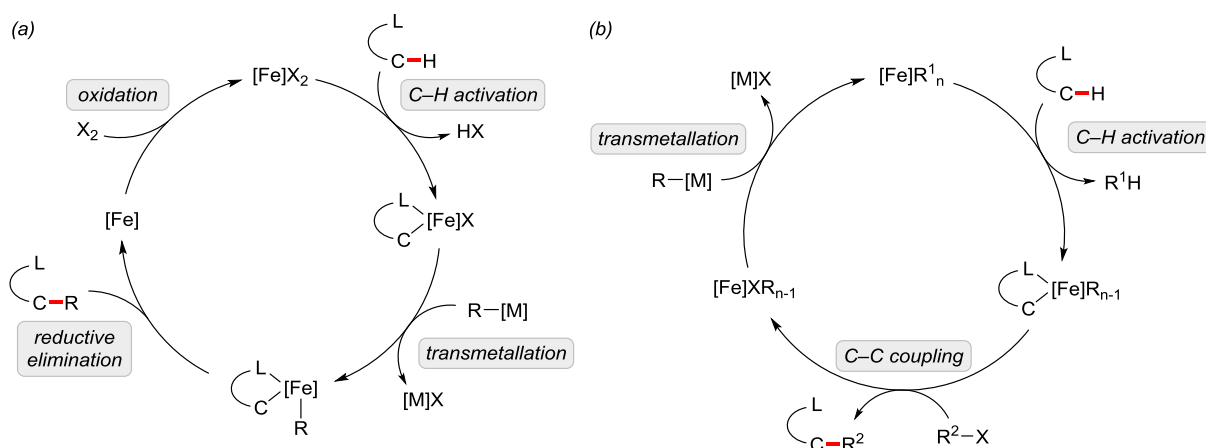
The *ortho*-C–H bond of one of the phenyl groups is oxidatively added to the iron(0) center to form the cyclometallated iron(II) hydride complex **105**. Under ethylene pressure, this complex can convert back to the initial iron(0) species. Subsequently, stoichiometric cyclometalation reactions utilizing iron complexes were described. For example, KLEIN disclosed the stoichiometric reaction of aryl imines using the iron monophosphine complexes $\text{Fe}(\text{PMe}_3)_4$ and $\text{FeMe}_2(\text{PMe}_3)_4$ in cyclometalation reactions, which are representative of the reactivity of this kind of complexes (Scheme 1.29).^[104]



Scheme 1.29: Stoichiometric cyclometalation of aryl imines with iron phosphine complexes.

The reaction of ketimine **106a** with $\text{Fe}(\text{PMe}_3)_4$ proceeds *via* nitrogen-assisted C–H oxidative addition. In contrast, when applying the complex $\text{FeMe}_2(\text{PMe}_3)_4$ to a stoichiometric reaction with benzaldimine **106b**, C–H activation was proposed to proceed *via* σ -bond metathesis.

The observation that stoichiometric C–H activation in the *ortho*-position of simple arenes can occur under directed chelate-assistance set the stage for the development of iron-catalyzed directing group-assisted C–H activation methodologies. Here, two possible reaction manifolds can be differentiated, a) C–H activation utilizing organometallic reagents, along with external oxidants, or b) C–H activation by the reaction of nucleophilic iron intermediates with organic electrophiles. In Scheme 1.30, hypothetical catalytic cycles with the key elementary steps are depicted for each of the two concepts.^[98b]

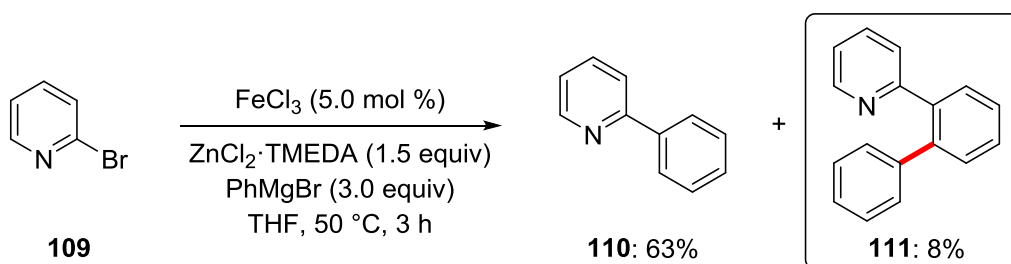


Scheme 1.30: Proposed mechanisms for iron-catalyzed C–H functionalizations with a) organometallic reagents, or with b) organic electrophiles.

1.3.1 Iron-Catalyzed C–H Activation with Organometallic Reagents

Typically, C–H functionalizations employing organometallic reagents are initiated by cyclometallation of low-valent organoiron(II) species or organoiron(III) species, followed by transmetallation with *in situ* generated aryl zinc reagents. Subsequently, oxidation-induced reductive elimination is forming the thermodynamically stable C–C bond (Scheme 1.30a). In general, this catalytic cycle is related to palladium-catalyzed direct C–H alkylations using organotin or organoboron reagents.^[105]

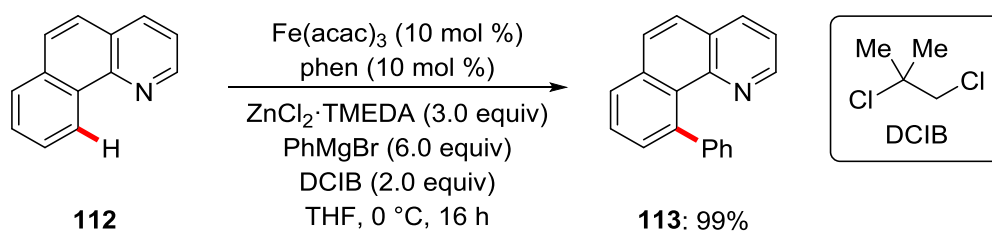
An early example of iron-catalyzed oxidative C–H activation was reported by NAKAMURA based on a serendipitous observation during their studies on the iron-catalyzed cross-coupling of 2-bromopyridine **109** with Grignard reagents (Scheme 1.31).^[106] In addition to the expected 2-phenylpyridine product **110**, small amounts of a second, C–C coupled product **111** were produced in 8% yield. Noteworthily, product **111** had to arise from an iron-catalyzed C–H activation of the initially generated 2-phenylpyridine **110**.



Scheme 1.31: Early example of directed iron-catalyzed C–H arylation.

On the basis of further extensive studies, NAKAMURA made several conclusions in order to develop a general methodology for directed iron-catalyzed C–H arylation reactions: *i*) 2,2'-bipyridyl, the homo-coupled byproduct, served as indispensable ligand for iron, *ii*) an oxidant was required to facilitate catalytic turnover, *iii*) diphenyl zinc *in situ* formed from $\text{ZnCl}_2 \cdot \text{TMEDA}$ and PhMgBr likely served as proper coupling partner. Thus, NAKAMURA reported an optimized protocol for the iron-catalyzed C–H arylation of benzo[*h*]quinoline **112** using phenanthroline as bidentate ligand and dichloroisobutane (DCIB) as the oxidant of choice (Scheme 1.32).^[107] The same conditions had previously been used for iron-catalyzed homo-coupling reactions of Grignard reagents.^[108]

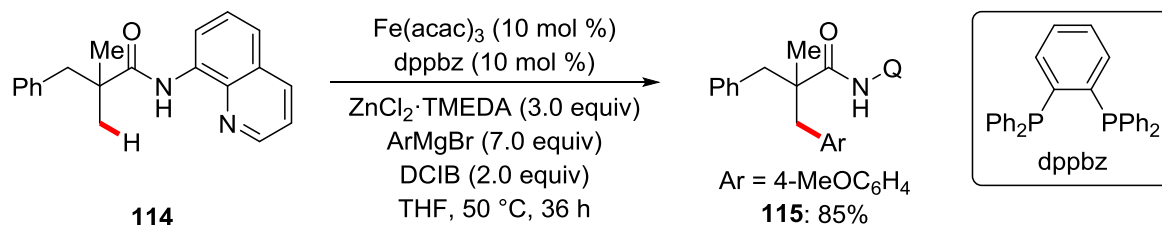
1 Introduction



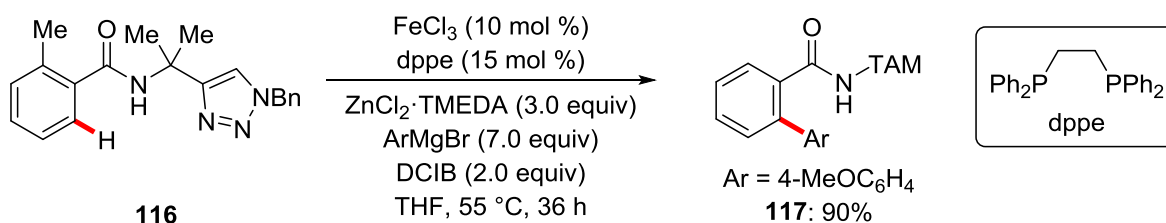
Scheme 1.32: Direct iron-catalyzed C–H arylation of benzo[*h*]quinoline **112**.

Subsequently, iron-catalyzed C–H arylation reactions could be extended to other substrate classes such as (hetero)aryl imines,^[109] *N*-methyl benzamides^[110] and alkenes.^[111]

Major progress in the field of low-valent iron-catalyzed C–H activation was achieved by the development of direct arylation protocols of unactivated C(sp³)–H and C(sp²)–H bonds using bidentate directing groups.^[50b, 112] In particular, NAKAMURA^[113] reported on the direct arylation of aliphatic amides derived from 8-AQ (**114**) with aryl zinc reagents (Scheme 1.33a), whereas ACKERMANN^[114] developed a powerful method using the triazolyl dimethylmethyl (TAM) group as a highly effective bidentate directing group for the direct arylation of aliphatic as well as aromatic amides **116** (Scheme 1.33b).

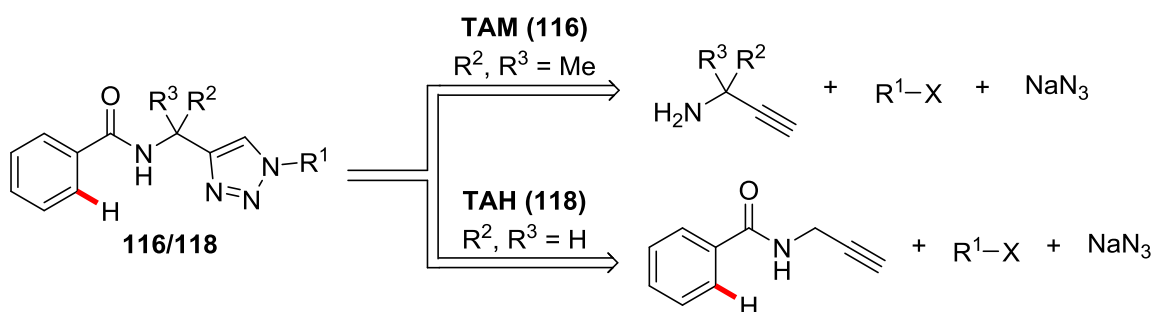


(b) Ackermann



Scheme 1.33: Iron-catalyzed arylation of aliphatic and aromatic C–H bonds.

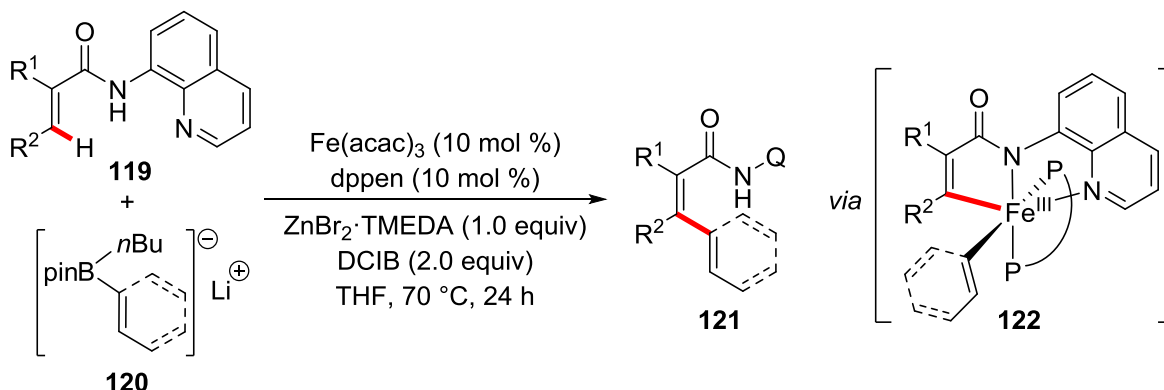
Noteworthy, the family of triazole-based TAM and TAH directing groups, developed by ACKERMANN, are easily accessible by the copper-catalyzed click 1,3-dipolar cycloaddition in a highly modular manner (Scheme 1.34).^[98b, 114-115]



Scheme 1.34: Retrosynthetic analysis for the synthesis of the TAM and TAH directing group.

In general, contrary to the protocols employing monodentate directing groups, bidentate phosphine ligands, such as dppbz or dppe, were found to be crucial to promote the desired C–H arylation, while bidentate nitrogen-based ligands proved ineffective.

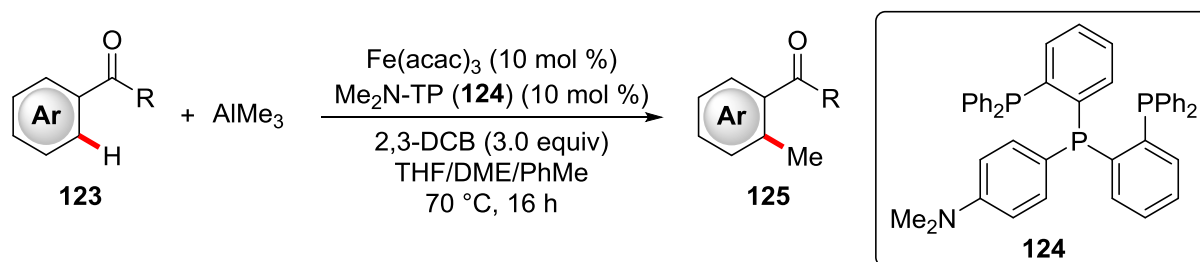
Although the use of Grignard reagents as arylating reagents allowed for efficient C–H arylations, significant limitations with respect to functional group tolerance arose. In particular, the formation of aryl–alkenyl or alkenyl–alkenyl C–C bonds led to undesired alkene isomerization, due to strong interactions of the metal center with the π -bond of alkenes.^[116] Therefore, NAKAMURA developed a protocol to overcome these limitations by employing organoboron reagents for the C–H arylation and alkenylation of (hetero)aromatic and olefinic amides under chelate-assistance. For example, the alkenyl amide **119** was efficiently converted to well-defined 1,3-dienes **121** using alkenyl boronates **120** (Scheme 1.35).^[117]



Scheme 1.35: C–H arylation/alkenylation using organoboron compounds.

Furthermore, the use of zinc additives was mandatory to achieve the desired C–H functionalization. The zinc salt is indeed considered to mediate the transmetalation of the aryl/alkenyl group from the boronate to an iron(III) species. Hence, after transmetalation the octahedral coordinated key ferracycle intermediate **122** was proposed to be generated.^[118]

In addition to arylation and alkenylation reactions, C–H alkylation reactions^[119] using *in situ* generated alkylzinc reagents were also accomplished *via* bidentate chelate-assistance, with major contributions by NAKAMURA^[120] and ACKERMANN,^[121] respectively. Furthermore, NAKAMURA reported on a selective C–H methylation of arenes **123** bearing weakly coordinating carbonyl groups (e.g. carboxylic acid, ester, ketone), using AlMe₃ as methyl source under oxidative conditions.^[122] Noteworthy, a significant ligand effect was observed. While the tridentate ligand Me₂N-TP (**124**) gave the best results, commonly used bidentate ligands such as dppen, dppbz, and dtbpy fell short in providing the desired methylation products **125** (Scheme 1.36).



Scheme 1.36: Iron-catalyzed methylation of arenes bearing carbonyl directing groups.

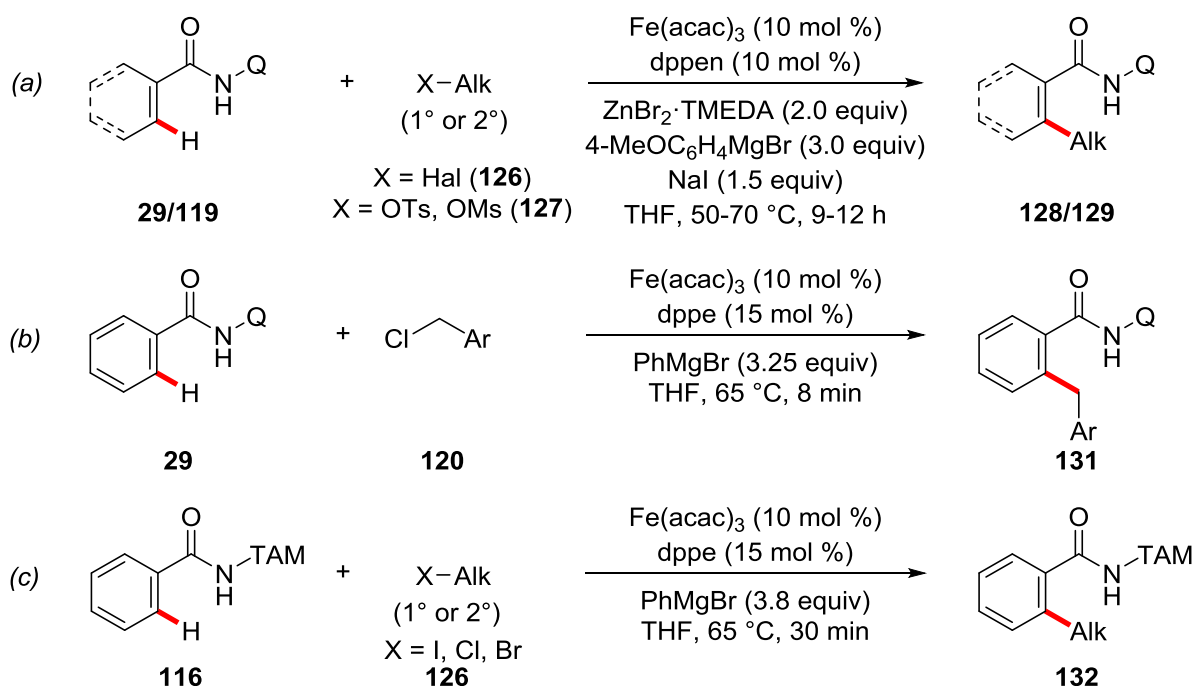
1.3.2 Iron-Catalyzed C–H Activation with Organic Electrophiles

Iron-catalyzed C–H activations utilizing organometallic reagents as nucleophilic coupling partners typically require the presence of an oxidant to achieve the desired transformation.^[123] In contrast, an external oxidant is not needed, when using electrophiles as coupling partners in iron-catalyzed C–H activations. Instead, an appropriate base for the deprotonation of the C–H bond is used, which does not react with the electrophile itself. In this context, various electrophiles were employed for the formation of C–C bonds, including coupling reactions with alkyl electrophiles,^[124] alkynyl electrophiles,^[125] or allylic electrophiles,^[124a, 126] among others.

1 Introduction

In 2014, NAKAMURA reported an early example of iron-catalyzed C–H alkylation reactions of alkenes **119** and (hetero)arenes **29** bearing the bidentate 8-AQ directing group (Scheme 1.37a).^[124c] Here, the use of an organometallic Grignard reagent is still required as the base, since side reactions, such as arylation or methylation, were observed in the presence of organozinc reagents. Also, the use of an excess of NaI and of the conjugated bidentate phosphine ligand dppen appeared to be crucial for the developed reaction in order to suppress undesired C–H arylations.

Besides primary and secondary alkyl tosylates, mesylates and halides proved to be viable electrophiles for the transformation. It is noteworthy, that detailed mechanistic studies revealed the radical nature of the key C–X cleavage step by performing radical-clock experiments. This observation was further supported by inhibition of the catalytic efficiency in presence of TEMPO as radical scavenger.



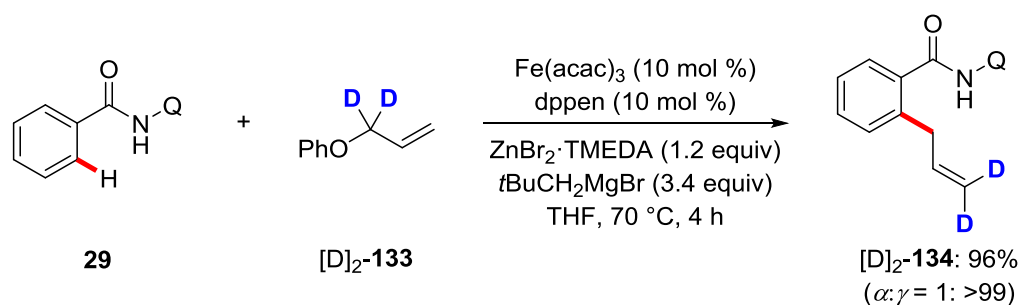
Scheme 1.37: Iron-catalyzed alkylation (1° and 2°) and benzylation of amides with tosylates, mesylates and halides.

A similar protocol using benzyl (**130**) and secondary alkyl halides as coupling partners (Scheme 1.37b),^[124b] and in addition, an analogous C–H alkylation protocol using primary alkyl bromides^[124d] were described by COOK. Interestingly, slow addition of PhMgBr was mandatory to achieve efficient conversions, enabling the alkylation of a variety of aryl, heteroaryl and alkenyl amides.

1 Introduction

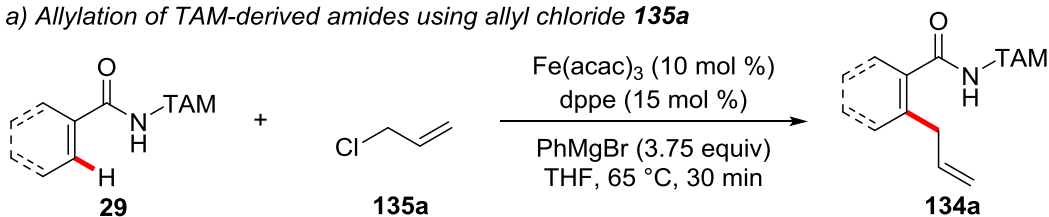
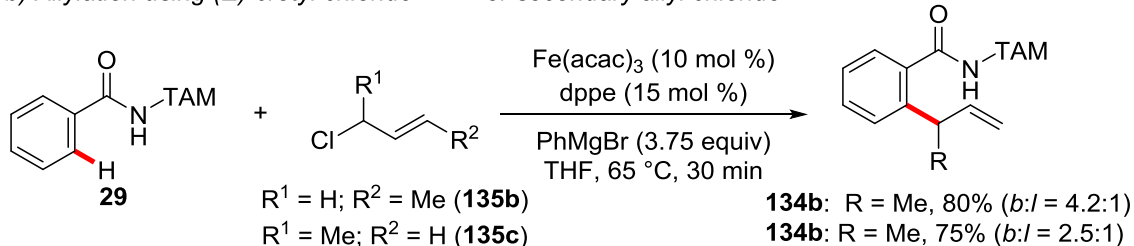
Due to the short reaction times of less than 10 minutes, the authors suggested that a phenyliron species, formed by transmetalation from PhMgBr, immediately undergoes turnover-limiting binding of the amide substrate, followed by rapid and irreversible C–H cleavage.

In contrast, ACKERMANN described an alkylation approach utilizing the modular click-triazole-based TAM. Their optimal catalytic system for the conversion of secondary and primary alkyl bromides **126** was consisting of Fe(acac)₃/dppe as catalyst and PhMgBr as the base (Scheme 1.37c).^[124a] Here, various (hetero)aromatic amides **116** were alkylated in short reaction times, delivering the desired products **132** in good yields. Furthermore, NAKAMURA reported on the iron-catalyzed C–H allylation reaction using allyl phenyl ether **133** as allylating reagent, which represents the first example of iron-catalyzed activation utilizing organic electrophiles as coupling partners for the allylation of quinolineamides **29** (Scheme 1.38).^[126b]



Scheme 1.38: Iron-catalyzed allylation of arenes under chelate-assistance.

Interestingly, a reaction conducted in the presence of the deuterium-labelled allyl phenyl ether **[D]₂-133** selectively afforded the γ -deuterated product **[D]₂-134**, which is suggestive of an S_N2'-type mechanism to be operative (Scheme 1.38). Furthermore, user-friendly allyl chlorides **135** proved to be viable allylating reagents in iron-catalyzed C–H allylation reactions of amides, making use of the modular triazole-containing TAM group as reported by ACKERMANN (Scheme 1.39).^[124a] Under the optimized reaction conditions employing Fe(acac)₃, dppe as the ligand and PhMgBr as the base, a variety of aromatic, heteroaromatic, and olefinic C–H bonds could be allylated in moderate to good yields. Notably, with (*E*)-crotyl chloride **135b** or the secondary allyl chloride **135c**, the branched allylated product (*b*) was formed in both cases with preferential regioselectivity as compared to the linear product (*l*), providing support for the formation of a η^3 -allyl intermediate.

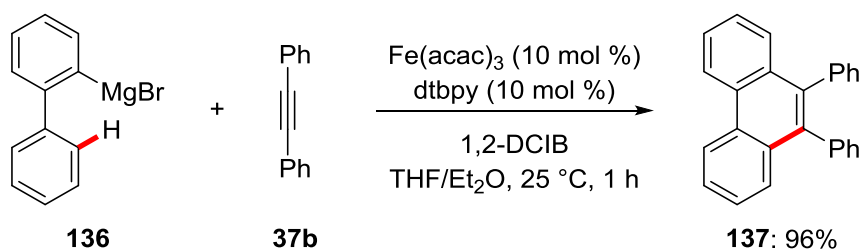
a) Allylation of TAM-derived amides using allyl chloride **135a**b) Allylation using (*E*)-crotyl chloride **135b** or secondary allyl chloride **135c**

Scheme 1.39: Iron-catalyzed C–H allylation of triazole-based amides.

1.3.3 Iron-Catalyzed Hydroarylation of C–C Multiple Bonds

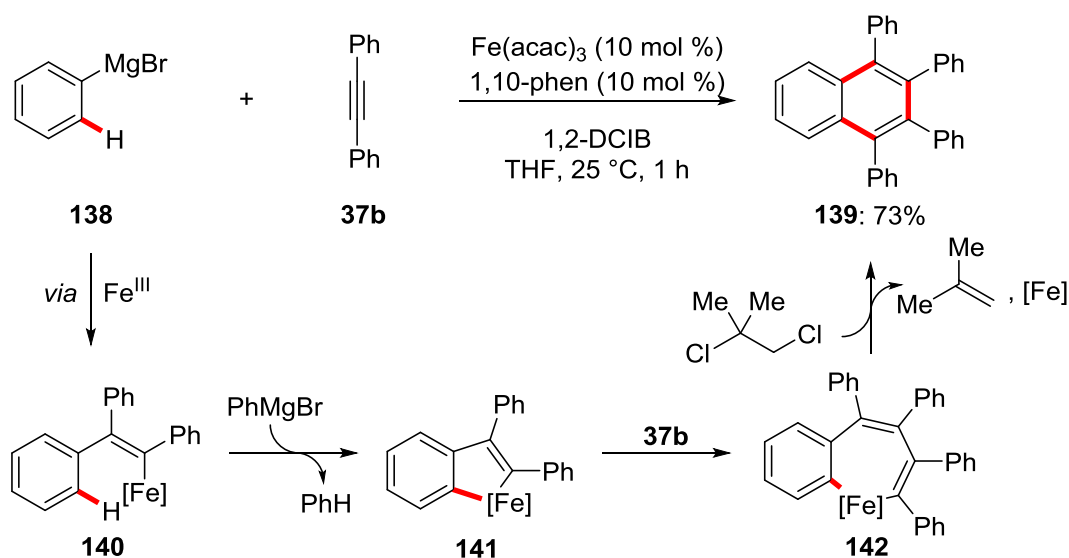
The addition of C–H bonds to unsaturated C–C bonds such as alkenes and alkynes *via* transition metal-catalyzed C–H activation represents an atom-economical approach for the introduction of synthetically meaningful alkyl or alkenyl groups.^[127] In this context, low-valent iron species and their corresponding ferracycle intermediates are able to be coordinated by π -systems, such as alkynes and alkenes.^[128] Here, besides alkylation and alkenylation reactions, C–H activation/annulations strategies could be exploited for the synthesis of polyaromatic structures and *N*-heterocycles.

NAKAMURA disclosed the synthesis of phenanthrene derivatives **137** through [4+2] benzannulation between alkyne **37b** and biaryl Grignard reagents **136** under oxidative conditions (Scheme 1.40).^[129] A catalytic system comprising of $\text{Fe}(\text{acac})_3/\text{dtbpy}$ as catalyst and DCIB as an oxidant allowed the synthesis of various 9-substituted or 9,10-disubstituted phenanthrenes.

Scheme 1.40: Synthesis of phenanthrene derivatives **137** *via* iron-catalyzed [4+2] benzannulation.

1 Introduction

Furthermore, NAKAMURA reported on the synthesis of polysubstituted naphthalene derivatives **139** by slightly changing the reaction conditions.^[130] An oxidative [2+2+2] annulation of aryl Grignard reagents **138** with two molecules of alkyne **37b** was enabled by a combination of Fe(acac)₃ as catalyst and 1,10-phen as the ligand, together with DCIB as external oxidant (Scheme 1.41).



Scheme 1.41: Iron-catalyzed oxidative [2+2+2] annulations.

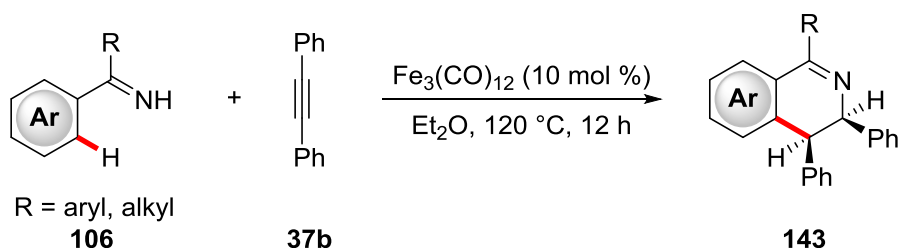
As to the reaction mechanism, the reaction is proposed to proceed through an iron-catalyzed carbometalation of the alkyne with an aryl Grignard reagent. The thus formed alkenyliron species **140** undergoes intramolecular C–H activation to form the five-membered ferracycle **141**. Thereafter, insertion of a second molecule of alkyne, followed by reductive elimination and oxidation by DCIB, forms the desired annulated naphthalene derivative **139** and regenerates the active iron catalyst.

A related protocol developed by YOSHIKAI made use of arylindium reagents to achieve [2+2+2] annulation reactions.^[131] Here, using a simple iron(III)/bisphosphine catalytic system enabled the synthesis of polysubstituted naphthalene derivatives from various alkyl- and aryl-substituted alkynes without the need of an additional external oxidant.

Besides the construction of polyaromatic structures, such as phenanthrenes or naphthalenes, the synthesis of *N*-heteroaromatic molecules was achieved by means of iron-catalyzed C–H activation/annulation strategies using substrates bearing *N*-containing Lewis-basic directing groups.

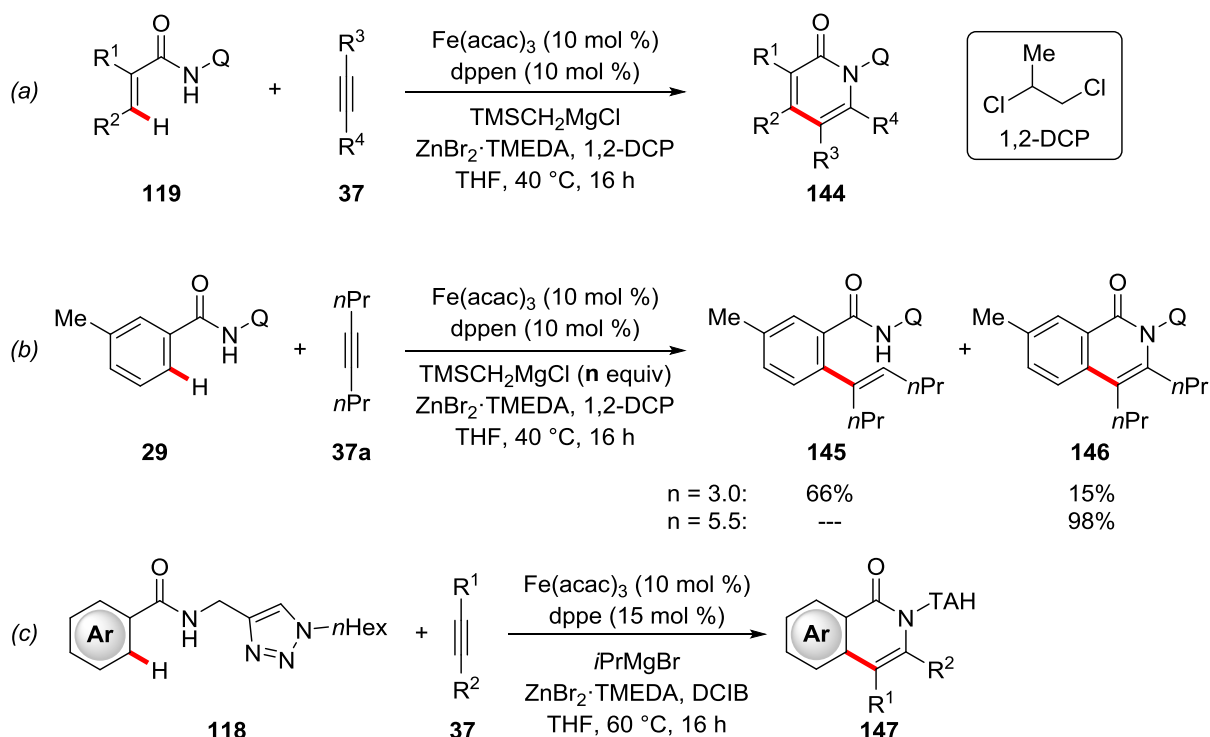
1 Introduction

Based on the seminal work of REED on iron(0)-mediated imine cyclometalations,^[132] WANG developed a redox-neutral [4+2] cyclization reaction between aromatic imines **106** and internal alkynes **37b** using $\text{Fe}_3(\text{CO})_{12}$ as catalyst to produce 3,4-dihydroisoquinoline derivatives **143** (Scheme 1.42).^[133]



Scheme 1.42: Iron-catalyzed redox-neutral [4+2] annulations of imines and internal alkynes.

In contrast, NAKAMURA^[134] and ACKERMANN^[135] achieved the synthesis of pyridone and isoquinolone derivatives by the use of alkynes and aromatic amides bearing the well-established 8-AQ or the modular triazole-based TAH bidentate groups, respectively (Scheme 1.43).



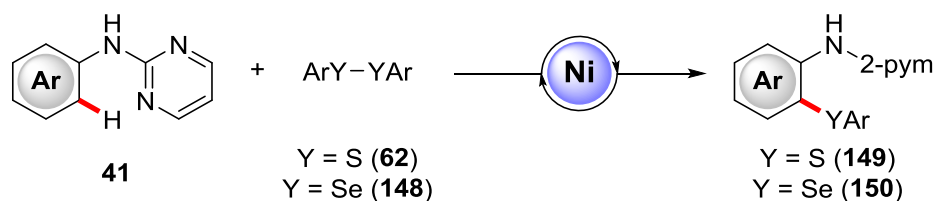
Scheme 1.43: Iron-catalyzed alkyne annulation for the synthesis of pyridines **144** and isoquinolones **146-147**.

2 Objectives

C–H activation has significantly improved the resource economy of organic synthesis,^[136] not only through the development of new methodologies for the construction of important organic scaffolds, but also by providing a more powerful and more sustainable approach for the functionalization of various different substrate classes.^[23a, 137] In particular, during the last decade, considerable progress has been made for the use of earth-abundant and cost-effective 3d metal catalysts as alternatives to the frequently used precious 4d and 5d metals. In this context, the development of new transformations utilizing nickel catalysts is of particular interest, because nickel exhibits unique reactivity profiles, making nickel complexes straightforward and environmentally friendly synthetic tools for the formation of new C–C and C–Het bonds.

For instance, the development of general methods for the synthesis of biaryl sulfides has received significant attention in the pharmaceutical industry, because the C–S bond is indispensable in various biologically active compounds. Therefore, several protocols using nickel catalysts for the formation of C–S bonds are known in the literature. However, the known procedures are largely restricted to the direct thiolation of electron-deficient benzamides bearing bidentate auxiliaries.

In stark contrast, the group of ACKERMANN was able to utilize electron-rich aniline derivatives **41** bearing a pyrimidyl moiety as an efficient monodentate directing group for nickel-catalyzed C–H alkylations using secondary alkyl bromides.^[65, 138] Based on these results, a new approach for the direct nickel-catalyzed C–H thiolation and selenylation of electron-rich 2-pyrimidyl anilines **41** with diaryl dichalcogenides **62/148** was investigated (Scheme 2.1).



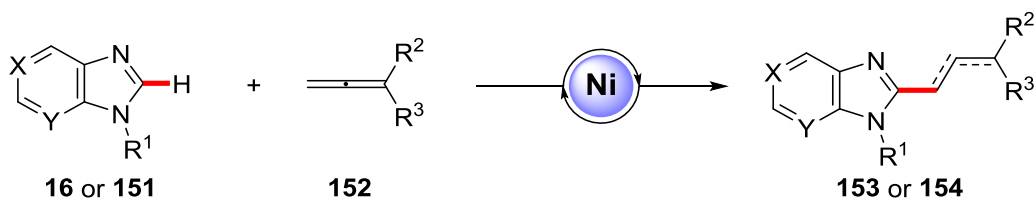
Scheme 2.1: Nickel-catalyzed C–H chalcogenation of pyrimidyl anilines **41**.

2 Objectives

The thus obtained 2-aminothiophenols **149** and seleno-analogs **150** are important structural motifs found in numerous biologically active compounds. Furthermore, they are useful precursors in the synthesis of various drug molecules such as phenothiazines, dibenzothiazepines and benzothiazoles.

The formation of C–C bonds *via* transition metal-catalyzed C–H activation has emerged as powerful platform for synthetic chemists. In particular, hydroarylation-type C–H functionalizations represent an expedient access for the introduction of alkyl and alkenyl groups. In this regard, the use of nickel catalysts for the addition of C–H bonds onto unsaturated substrates, such as alkynes and alkenes is well-established.^[31a, 41, 112a] In stark contrast, the use of allenes in the field of transition metal-catalyzed C–H functionalization is comparatively under-explored.

Several examples utilizing allenes for hydroarylation reactions through C–H activation have been developed by rhodium,^[139] ruthenium,^[140] cobalt,^[141] and manganese catalysis,^[142] but the use of nickel catalysts remained unprecedented. To address these limitations, a user-friendly Ni(cod)₂/NHC catalytic system for the C–H activation/hydroarylation of allenes **152** with benzimidazoles **16** and purine derivatives **151** was developed in collaboration with S. Nakanowatari (Scheme 2.2).



Scheme 2.2: Nickel-catalyzed hydroheteroarylation of allenes **152**.

However, the control of selectivity to obtain either allylated or alkenylated hydroarylation products **153** or **154**, respectively, represented a major issue that needed to be addressed. Therefore, the question arose which reaction conditions could offer a selective access to the desired products. The development of a versatile protocol for the selective functionalization of various heteroaromatic substrates was hence in high demand.

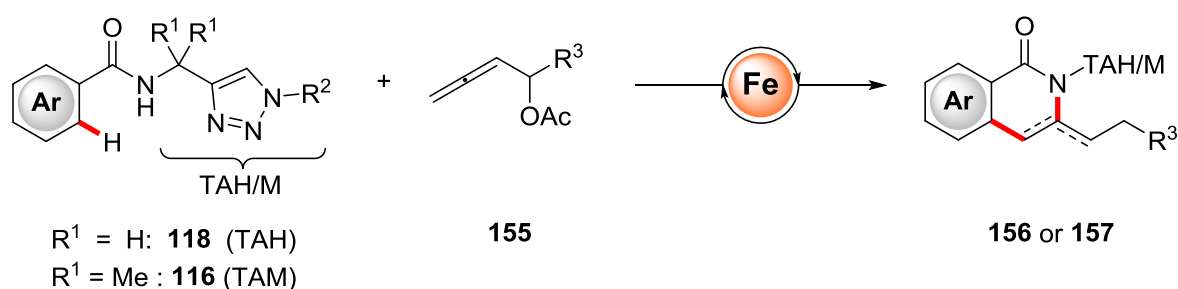
2 Objectives

Compared to nickel complexes, the use of iron compounds as catalysts in C–C bond forming reactions is even more desirable. In particular, reactions that involve inner-sphere C–H activation assisted by coordinating directing groups have gained significant attention throughout the last years, and have been mainly dominated by the use of the 8-AQ auxiliary.^[50c]

Major advances in the field of iron-catalyzed C–H functionalizations were accomplished by ACKERMANN who introduced a novel class of bidentate directing groups based on the triazole moiety, namely the modular triazolylmethylmethyl (TAM) directing group family.^[115]

With this easily accessible triazole-based directing groups in hand, ACKERMANN developed various C–H transformations, such as arylation,^[114] alkylation,^[121, 124a] and alkynylation^[125] reactions of benzamides. Furthermore, TAM-derived benzamides could be applied for the synthesis of *N*-heterocycles using internal alkynes.^[135]

However, iron-catalyzed C–H annulation reactions remained a challenging transformation, and rather complicated reaction conditions are necessary to achieve satisfactory results. Thus, in the case of oxidative C–H annulations, a huge excess of Grignard reagents and the use of an external oxidants, such as 1,2-DCIB, are crucial for an efficient conversion. Therefore, J. Mo identified allenyl acetates **155** as suitable coupling partner in an iron-catalyzed annulation reaction using TAH-derived benzamides **118** under external oxidant-free conditions. In this context, an iron-catalyzed protocol for the synthesis of isoquinolone derivatives **156** or **157**, respectively, depending on the modular nature of the triazole-derived directing group, was to be developed (Scheme 2.3).

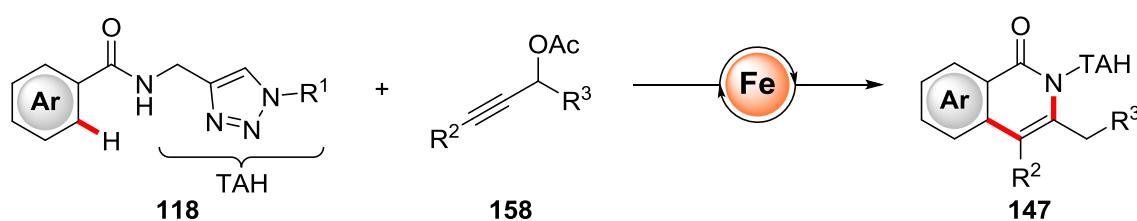


Scheme 2.3: Iron-catalyzed C–H/N–H annulations with allenyl acetates **155**.

2 Objectives

Furthermore, detailed mechanistic investigations using isotopically-labelled substrates were supposed to give unprecedented insights into the iron-catalyzed C–H activation manifold.

Finally, a similar approach for the synthesis of various isoquinolone derivatives **147** using propargyl acetates **158** as coupling partners was probed (Scheme 2.4). Here, detailed mechanistic studies, including computation and Mössbauer spectroscopy should provide insights into the oxidation states of the key organoiron species, which allows for a better understanding of the catalyst's mode of action.



Scheme 2.4: Envisioned iron-catalyzed C–H/N–H annulations with propargyl acetates **158**.

3 Results and Discussion

3.1 Nickel(II)-Catalyzed C–H Chalcogenation of Anilines

Based on the initial studies of LU^[75] and SHI,^[74] who used diaryl disulfides **62** for the *ortho*-thiolation of benzamides, various procedures for the formation of C–S bonds via C–H activation were reported. Mainly bidentate directing groups, such as PIP or 8-AQ were required to enable efficient C–H thiolation reactions.^[76-78]

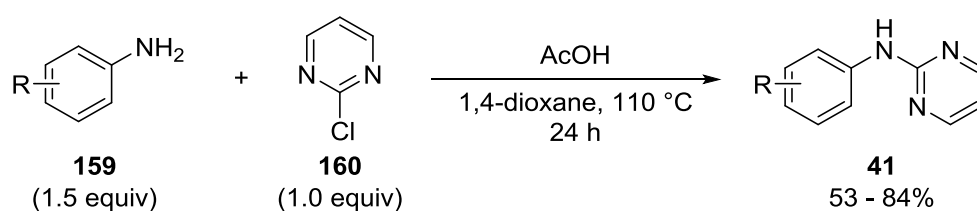
Furthermore, efficient transformations required complex reaction conditions including silver salts or organic oxidizing reagents, strong bases and in some instance additional ligands.

In sharp contrast, the use of monodentate directing groups would illustrate an alternative, more atom economic approach. The practical use of the monodentate pyrimidyl group was previously demonstrated by ACKERMANN for the nickel-catalyzed synthesis of indole derivatives and the *ortho*-alkylation of electron-rich aniline derivatives.^[55a, 55b, 65] To this end, the synthesis of thiolated aryl motifs, derived from other substrate classes than benzamides using *N*-pyrimidyl anilines would be a favourable approach for the formation of heteroatom-containing aryl thioethers.

3.1.1 Optimization Studies

The catalytic system composed of (DME)NiCl₂, Di-*tert*BEDA and LiOtBu, which was based on a previous study by our group on the nickel(II)-catalyzed alkylation of anilines,^[65] was chosen as a starting point to test the envisioned nickel-catalyzed C–H chalcogenation of electron-rich anilines. For the synthesis of the desired aniline derivatives, a generally applicable methodology was used (Scheme 3.1). Thus, a nucleophilic aromatic substitution, using commercially available anilines **159** and 2-chloro pyrimidine (**160**) was employed, delivering the desired *N*-pyrimidyl anilines **41** in moderate to good yields.

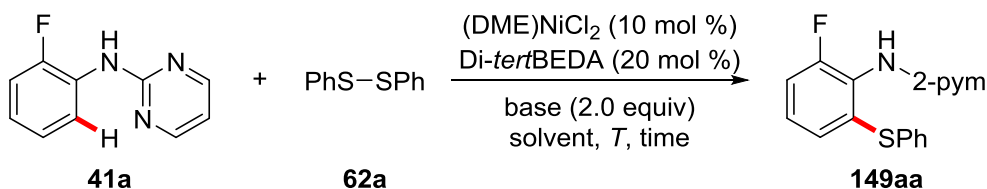
3 Results and Discussion



Scheme 3.1: General method for the synthesis of 2-pyrimidyl anilines **41**.

Preliminary studies conducted by Z. Ruan, employing *N*-pyrimidylaniline **41a** with diphenyl disulfide **62a** as coupling partner in toluene as solvent (entry 1) showed promising results, delivering the desired *ortho*-thiolated *N*-pyrimidyl aniline **149aa** in 28% yield (Table 3.1).

Table 3.1: Exploring of solvents and bases for the nickel-catalyzed thiolation of *N*-pyrimidyl aniline **41a**.^[a]



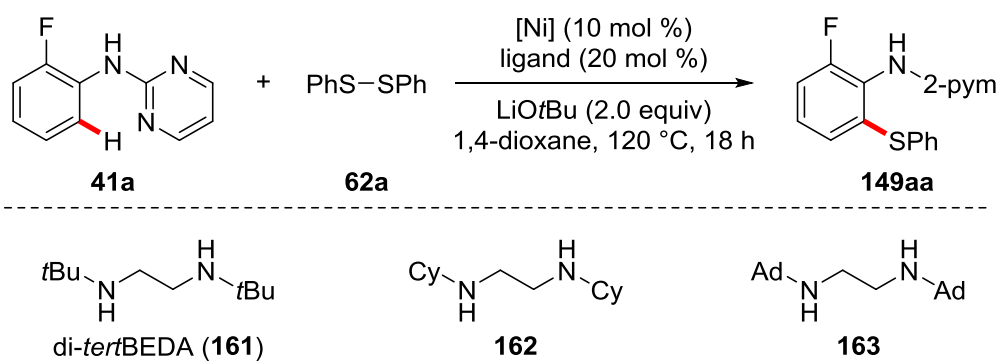
Entry	Base	Solvent	T / °C	t / h	Yield / %
1	LiOtBu	PhMe	100	18	28
2	LiOtBu	DCE	120	16	9
3	LiOtBu	DMF	120	16	traces
4	LiOtBu	THF	60	18	4
5	LiOtBu	DMSO	120	18	---
6	LiOtBu	<i>m</i> -Xylene	120	18	20
7	LiOtBu	1,4-Dioxane	120	18	31
8	KOtBu	1,4-Dioxane	120	18	22
9	Na ₂ CO ₃	1,4-Dioxane	120	18	---
10	Cs ₂ CO ₃	1,4-Dioxane	120	18	---
11	NaOAc	1,4-Dioxane	120	18	---

^[a] Reaction conditions: **41a** (0.50 mmol), **62a** (1.00 mmol), (DME)NiCl₂ (10 mol %), Di-*tert*BEDA (**161**) (20 mol %), base (2.0 equiv), solvent (1.5 mL), *T*, 16-18 h.

3 Results and Discussion

Based on this result, various other solvents, such as DCE, DMF, THF or DMSO, were tested, showing that compared to toluene the reaction was shut down or did not lead to improved yields (entries 2 to 5). Only *m*-xylene (entry 6) gave significant product formation. 1,4-Dioxane was superior to toluene (entry 7), and 1,4-dioxane was used as the solvent of choice. Probing of other bases, such as Na₂CO₃, Cs₂CO₃ or NaOAc (entry 9 and 11), could not improve the reactivity and the use of KO^tBu as strong base gave slightly lower yields, compared to LiO^tBu. Therefore, LiO^tBu was chosen as base for further investigations.

Table 3.2: Testing of nickel catalysts and ligands for the catalytic thiolation of *N*-pyrimidyl aniline **41a**.^[a]



Entry	[Ni]	ligand	Yield / %
1	(DME)NiCl ₂	Di- <i>tert</i> BEDA (161)	31
2	(DME)NiCl ₂	161	35 ^[b]
3	Ni(OTf) ₂	161	31
4	Ni(acac) ₂	161	14
5	NiCl ₂	161	24
6	(DME)NiCl ₂	PPh ₃	26
7	(DME)NiCl ₂	162	11
8	(DME)NiCl ₂	163	23
9	(DME)NiCl ₂	dppe	---
10	(DME)NiCl ₂	dppp	---

3 Results and Discussion

Entry	[Ni]	ligand	Yield / %
11	(DME)NiCl ₂	dppf	13
12	(DME)NiCl ₂	1,10-phen	6

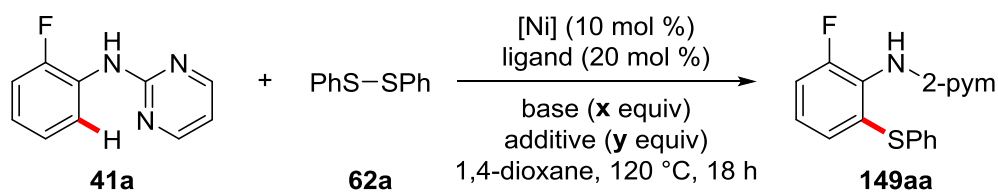
^[a] Reaction conditions: **41a** (0.50 mmol), **62a** (1.00 mmol), [Ni] (10 mol %), ligand (20 mol %), LiOtBu (2.0 equiv), 1,4-dioxane (1.5 mL), 120 °C, 18 h, yields of isolated products. ^[b] [Ni] (20 mol %) and Di-*tert*BEDA (40 mol %).

The evaluation of nickel catalysts (Table 3.2) established that common nickel(II) catalysts in presence of the bidentate nitrogen based ligand di-*tert*BEDA (**161**) were all competent catalyst precursors. Ni(OTf)₂ showed comparable results to (DME)NiCl₂ delivering the desired product in 31% yield. Ni(OAc)₂ and NiCl₂ gave slightly lower yields. The test of various ligands unraveled that a similar set of bidentate nitrogen ligands (**162/163**) and 1,10-phenanthroline led to reduced yields (entry 7, 8 and 12). Triphenyl phosphine as monodentate phosphine ligand gave comparable results to **161** (entry 6), but the use of bidentate phosphine ligands such as dppe and dppp was not effective. Only dppf (entry 11) proved to be efficient, affording the desired *ortho*-thiolated product **149aa** with low yield.

To further optimize the reaction, the effect of different silver(I) and copper(II) salts as additives was evaluated (Table 3.3), as they were known to facilitate thiolation reactions.^[143] Various nickel(II) precursors in the presence of **161** or PPh₃ were tested, showing that common silver(I) salts, such as Ag₂CO₃ or Ag₂O with LiOtBu or KTFA as base (entry 1 and 2), could not improve the yields. The use of substoichiometric amounts of copper(II) salts for the first time was effective to improve the yields significantly (entries 3-5). Reaction conditions composed of (DME)NiCl₂, **161**, LiOtBu and 0.2 equivalents of CuCl₂ considerably promoted the reaction, yielding 51% of the desired product (entry 3). Other copper(II) salts in combination with Ni(OTf)₂ as the catalyst also proved suitable. The slightly increased yields can be explained by higher amounts of the copper(II) salts (entry 4 to 8). The use of 0.5 equivalents of CuCl₂ (entry 9) seemed to be optimal, yielding the desired product in 81% yield, whereas the use of PPh₃ had no significant impact on the reaction, compared to the use of **161**. A control experiment in the absence of the nickel catalyst showed a conversion to the product of only 39% (entry 10).

3 Results and Discussion

Table 3.3: Probing additives for the nickel-catalyzed thiolation of *N*-pyrimidyl aniline **41a**.^[a]



Entry	[Ni]	Ligand	Base / <i>x</i>	Additive / <i>y</i>	Yield / %
1	(DME)NiCl ₂	161	LiOtBu / 2.0	Ag ₂ CO ₃ / 2.0	24
2	(DME)NiCl ₂	161	KTFA / 2.0	Ag ₂ O / 1.0	25
3	(DME)NiCl ₂	161	LiOtBu / 2.0	CuCl ₂ / 0.2	51
4	Ni(OTf) ₂	161	LiOtBu / 2.0	CuCl ₂ / 0.2	56
5	Ni(OTf) ₂	161	LiOtBu / 2.0	Cu(OAc) ₂ / 0.2	53
6	Ni(OTf) ₂	PPh ₃	LiOtBu / 2.0	CuCl ₂ / 0.2	58
7	Ni(OTf) ₂	161	LiOtBu / 2.0	CuCl ₂ / 0.5	60
8	Ni(OTf) ₂	161	LiOtBu / 2.0	CuBr ₂ / 0.5	68
9	Ni(OTf) ₂	PPh ₃	LiOtBu / 2.0	CuCl ₂ / 0.5	81
10	---	PPh ₃	LiOtBu / 2.0	CuCl ₂ / 0.5	39

^[a] Reaction conditions: **41a** (0.50 mmol), **62a** (1.00 mmol), [Ni] (10 mol %), ligand (20 mol %), base (2.0 equiv), additive, 1,4-dioxane (1.5 mL), 120 °C, 18 h.

In view of reports by YU, QING and FUKUZAWA on copper-mediated/-catalyzed thiolation reactions of (hetero)arenes using stoichiometric or catalytic amounts of copper(II) salts,^[144] the observed background reaction in the absence of the nickel catalyst (entry 10) is caused by the presence of copper. Therefore, alternative additives were explored, which are unable to promote a competing copper- or silver-mediated thiolation reactions. To this end, various possible metal salt were screened (Table 3.4) in order to replace copper(II) or silver(I) additives.

Highly promising results were achieved, employing Zn(OTf)₂ as an additive, delivering the desired *ortho*-thiolated *N*-pyrimidyl-aniline **149aa** in 50% isolated yield (entry 1). Next, a variety of first-row metal salts, such as vanadium(V) oxide, iron(III) chloride and manganese(IV) oxide were tested (entries 4–6).

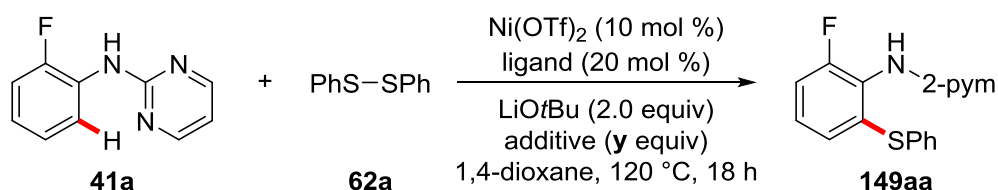
3 Results and Discussion

Among these, solely manganese(IV) oxide showed good conversions, affording the desired product **149aa** in 65% or 73% yield, employing the ligands di-*tert*BEDA or PPh₃ (entries 6 and 7), respectively. By increasing the amount of MnO₂ to 1.0 equivalent, the yield could be improved to 91% (entry 8).

To our surprise, in the absence of a ligand (entry 11) and in the presence of MnO₂ as oxidant, the reaction resulted in almost quantitative turnover, delivering **149aa** in 96% yield. In addition, a decreased catalyst loading of 2.5 mol % yielded the desired product with 89% (entry 12).

To ensure the catalytic nature of the envisioned reaction, again a control experiment in absence of nickel catalyst was performed. Here, no product was formed, confirming the necessity of catalytic amounts of nickel to achieve the desired transformation.

Table 3.4: Probing oxidants for the nickel-catalyzed thiolation of *N*-pyrimidyl aniline **41a**.^[a]



Entry	Ligand	Additive / <i>y</i>	Yield / %
1	161	Zn(OTf) ₂ / 0.5	50
2	PPh ₃	Zn(OTf) ₂ / 0.5	35
3	161	Zn(OTf) ₂ / 1.0	11
4	PPh ₃	V ₂ O ₅ / 0.5	24
5	PPh ₃	FeCl ₃ / 0.5	18
6	161	MnO ₂ / 0.5	65
7	PPh ₃	MnO ₂ / 0.5	73
8	PPh ₃	MnO ₂ / 1.0	91
9	PCy ₃	MnO ₂ / 1.0	68
10	PPh ₃	MnO ₂ / 1.0	--- ^[b]

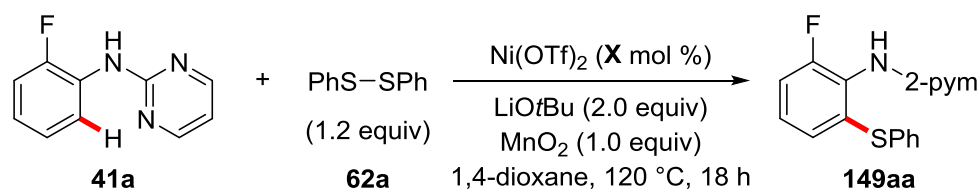
3 Results and Discussion

Entry	Ligand	Additive / y	Yield / %
11	---	MnO ₂ / 1.0	96
12	---	MnO ₂ / 1.0	89 ^[c]
13	---	MnO ₂ / 1.0	--- ^[b]

^[a] Reaction conditions: **41a** (0.50 mmol), **62a** (0.60 mmol), Ni(OTf)₂ (10 mol %), ligand (20 mol %), LiOtBu (2.0 equiv), additive, 1,4-dioxane (1.5 mL), 120 °C, 18 h; ^[b] without [Ni]; ^[c] Ni(OTf)₂ (2.5 mol %).

With the optimized reaction conditions in hand, the influence of the catalyst loading on the outcome of the C–H thiolation reaction was investigated (Table 3.5). To our delight, even low catalyst loadings of 1.0 mol % delivered **149aa** with a very good yield of 88%. Also, performing a gram scale reaction starting with 5 mmol *N*-pyrimidylaniline **41a**, yielded the desired product in synthetically meaningful yields of 76%.

Table 3.5: Effect of catalyst loading on the nickel-catalyzed thiolation of aniline **41a**.^[a]

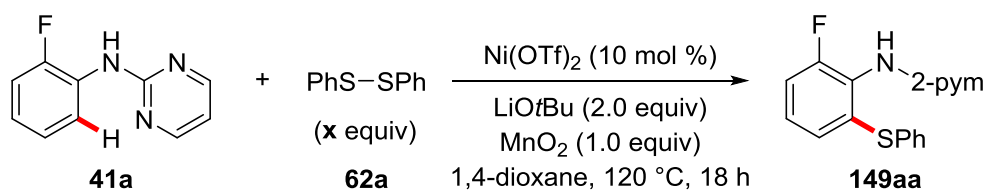


Entry	Loading / X	Yield / %
1	10	96, 76 ^[b]
2	7.5	94
3	5.0	90
4	2.5	89
5	1.0	88

^[a] Reaction conditions: **41a** (0.50 mmol), **62a** (0.60 mmol), Ni(OTf)₂ (X mol %), LiOtBu (2.0 equiv), MnO₂ (1.0 equiv), 1,4-dioxane (1.5 mL), 120 °C, 18 h; ^[b] gram scale reaction using 5 mmol **41a**.

Furthermore, the effect of the amount of the thiolating reagent diphenyl disulfide **62a** was probed (Table 3.6). As was shown in Table 3.5, 1.2 equivalents of **62a** gave optimal results, delivering the desired product **149aa** in 96% yield. Interestingly, lowering the amount of **62a** to 0.6 or 0.3 equivalents, yielded in 90% and 54% **149aa**, respectively. This result is a hint, that both sulfur motifs of the diphenyl disulfide were incorporated in the product.

Table 3.6: Amount of diphenyl disulfide **62a**.^[a]



Entry	62a / x equiv	Yield / %
1	2.0	92
2	1.2	96
3	0.6	90
4	0.3	54

^[a] Reaction conditions: **41a** (0.50 mmol), **62a** (x equiv), Ni(OTf)₂ (10 mol %), LiOtBu (2.0 equiv), MnO₂ (1.0 equiv), 1,4-dioxane (1.5 mL), 120 °C, 18 h.

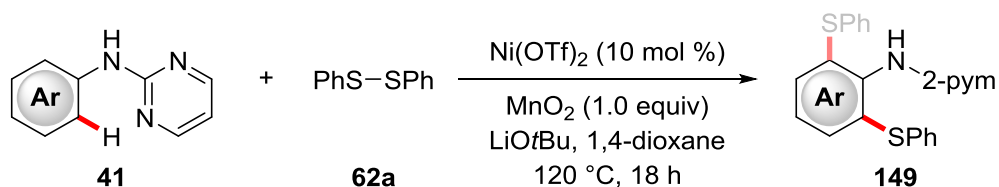
3.1.2 Scope of the Nickel-Catalyzed C–H Thiolation of Anilines

With the optimized reaction conditions in hand, we next explored the applicability of the C–H thiolation protocol towards differently substituted *N*-pyrimidyl anilines **41** (Table 3.7). With regard to 2-substituted *N*-pyrimidyl anilines, electron-rich as well as electron-deficient aniline derivatives were converted to the corresponding thiolated products **149aa-149ga** with high levels of positional selectivity. Here, phenyl-, *tert*-butyl, methoxy- and even methyl thioether-substituted anilines were well-tolerated, the latter one with a somewhat reduced yield of 49%. Unfortunately, bromo- and methyl-substituents in 2-position (entry 6 and 7) were not tolerated in the desired reaction. C–H thiolations on *meta*-decorated arenes **41n-41r** preferentially proceeded at the less congested C–H bond. In case of *para*-substituted arenes, valuable electrophilic functional groups, such as chloro, bromo, and iodo, were well-tolerated

3 Results and Discussion

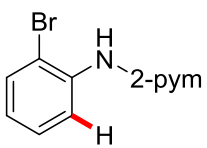
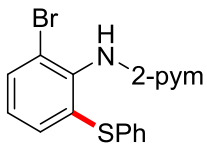
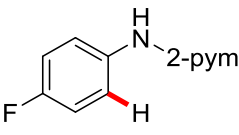
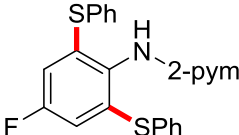
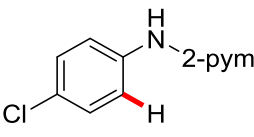
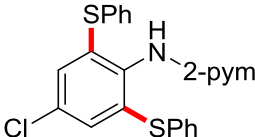
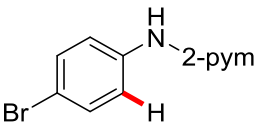
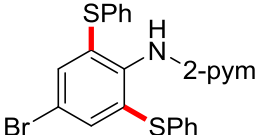
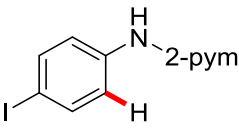
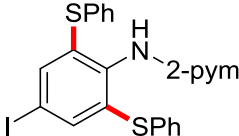
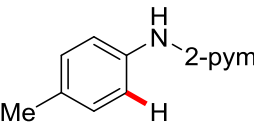
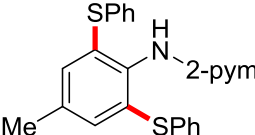
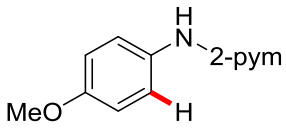
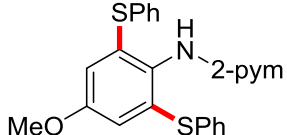
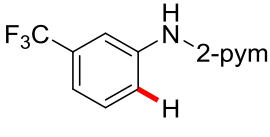
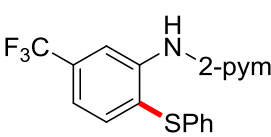
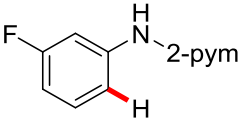
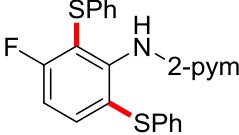
(entry 9–11), delivering the desired di-thiolated products **149ha-149ma** in moderate yields. Furthermore, a variety of di- and tri-substituted aniline derivatives **41s-41x** delivered the desired products in good to excellent yields (entry 19–24).

Table 3.7: Scope of the nickel-catalyzed C–H thiolation of anilines with diphenyl disulfide.^[a]

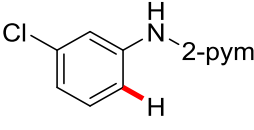
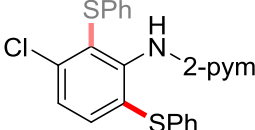
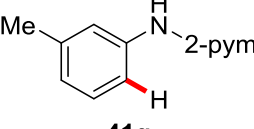
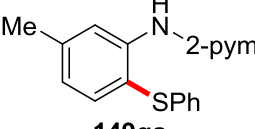
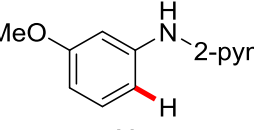
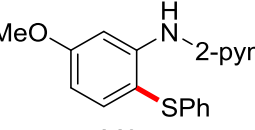
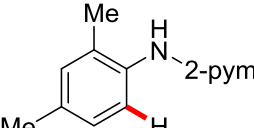
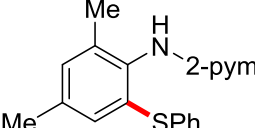
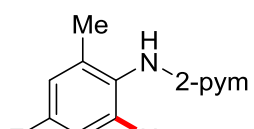
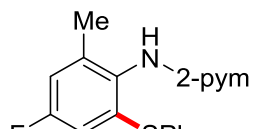
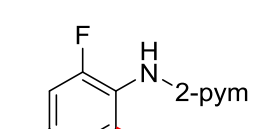
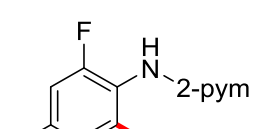
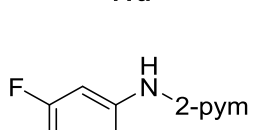
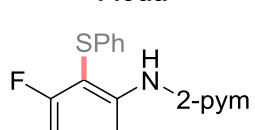
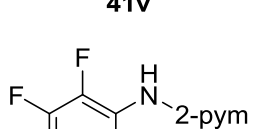
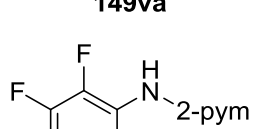
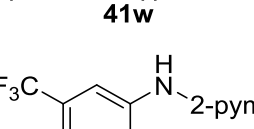
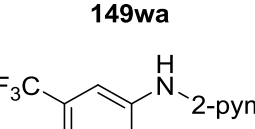


Entry	41	149	Yield / %
1			96
2			91
3			66
4			80
5			49
6			---

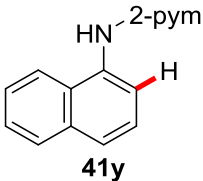
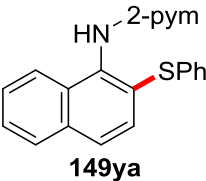
3 Results and Discussion

Entry	41	149	Yield / %
7	 41g	 149ga	---
8	 41h	 149ha	52 (1:4.4) ^[c]
9	 41i	 149ia	53 ^[b]
10	 41j	 149ja	55 ^[b]
11	 41k	 149ka	35 ^[b]
12	 41l	 149la	39 (1:5.4) ^[c]
13	 41m	 149ma	44 (1:4.2) ^[c]
14	 41n	 149na	76
15	 41o	 149oa	56 ^[b]

3 Results and Discussion

Entry	41	149	Yield / %
16	 <p>41p</p>	 <p>149pa</p>	71 (2.4:1) ^[c]
17	 <p>41q</p>	 <p>149qa</p>	43
18	 <p>41r</p>	 <p>149ra</p>	30
19	 <p>41s</p>	 <p>149sa</p>	74
20	 <p>41t</p>	 <p>149ta</p>	93
21	 <p>41u</p>	 <p>149ua</p>	94
22	 <p>41v</p>	 <p>149va</p>	57 (1:3.1) ^[c]
23	 <p>41w</p>	 <p>149wa</p>	85
24	 <p>41x</p>	 <p>149xa</p>	12

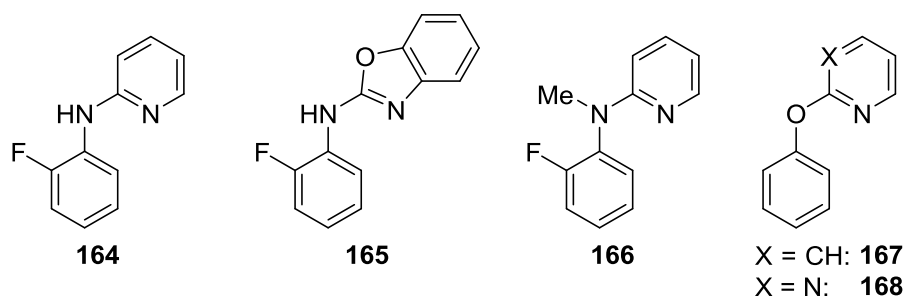
3 Results and Discussion

Entry	41	149	Yield / %
25			87

^[a] Reaction conditions: **41** (0.50 mmol), **62** (0.60 mmol), Ni(OTf)₂ (10 mol %), LiOtBu (2.0 equiv), MnO₂ (1.0 equiv), 1,4-dioxane (1.5 mL), 120 °C, 18 h; ^[b] only di-thiolation; ^[c] combined yields of isolated products, ratio of mono- and di-selectivity of the C–H thiolation in parantheses.

In addition, substrates exhibiting *ortho*-fluoro substituents were chemoselectively functionalized at the *ortho* C–H bond, while the C–F bond^[145] stayed intact. When using the naphthalene derivative **41y** (entry 25), C–H thiolation occurred site-selectively at the β -position, while the *peri*-C–H bond remained unaffected.

During the examination of the reaction scope, various other modifications on the aniline substrate (**164–168**) were investigated (Scheme 3.2). After changing the nature of the directing group from pyrimidyl to pyridine (**164**) or benzoxazole (**165**), no product formation was observed. Hence, the presence of the pyrimidyl group is crucial for the outcome of the reaction. Furthermore, the free *NH* in the aniline is essential, as methylation of the amine moiety (**166**) completely shuts down the reaction completely. Using similar *O*-pyrimidyl or –pyridyl derived phenol substrates (**167** or **168**) did not lead to any product formation.

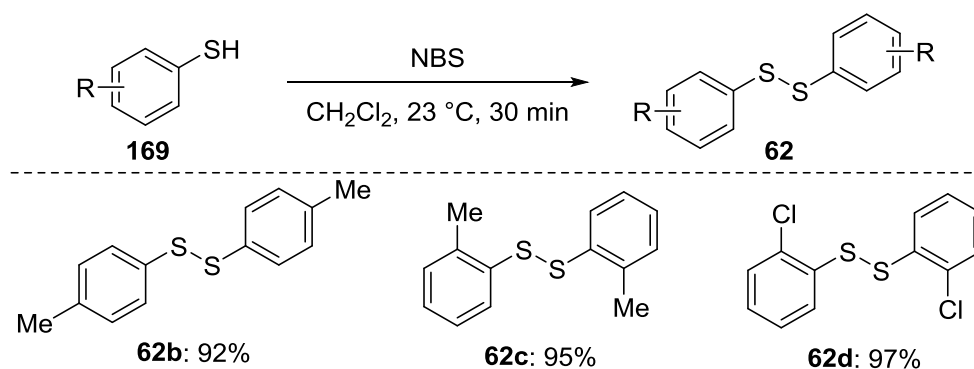


Scheme 3.2: Various aniline and phenol derivatives unsuccessfully tested in the nickel-catalyzed C–H thiolation.

Besides numerous aniline derivatives, a variety of diaryl disulfides **62** were tested in the nickel-catalyzed C–H thiolation reaction. If not commercially available, diaryl disulfides can be easily prepared by reacting the corresponding thiols under oxidative conditions using *N*-bromosuccine imide (NBS).^[146]

3 Results and Discussion

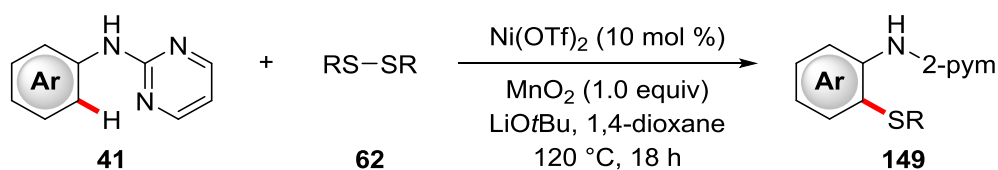
Both, electron-rich as well as electron-deficient diaryl disulfides bearing either a methyl- or a chloro-substituent in the *para*-position, or even in the more sterically congested *ortho*-position could be synthesized, using thiols **169** and NBS as oxidant (Scheme 3.3).



Scheme 3.3: Synthesis of diaryl disulfides **62**.

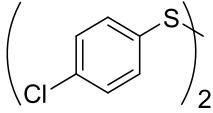
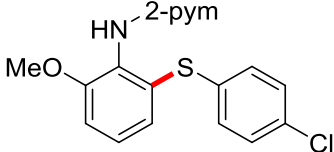
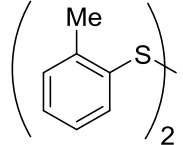
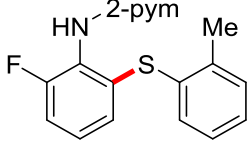
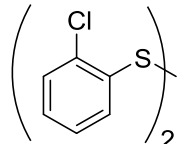
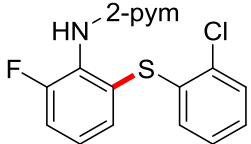
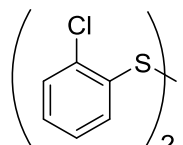
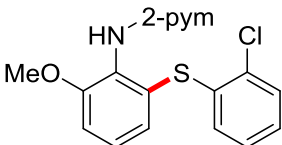
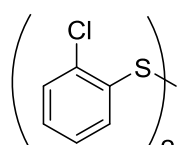
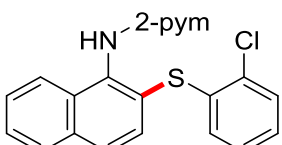
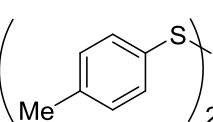
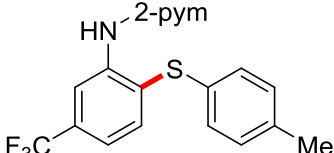
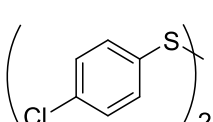
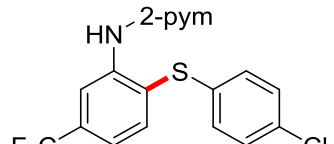
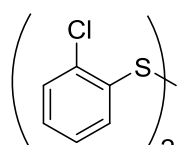
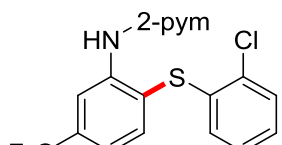
With several diaryl disulfides **62** in hand, differently substituted *N*-pyrimidyl anilines **41** could be converted to the desired thioether products in moderate to very good yields. Moreover, the challenging pyridyl disulfide **62f** was a viable substrate, delivering **149af** in a moderate yield of 55%, despite its capability to act as a bidentate ligand.

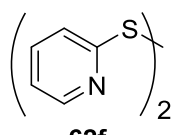
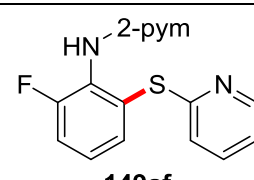
Table 3.8: Scope of the nickel-catalyzed C–H thiolation with disulfides **62**.^[a]



Entry	62	149	Yield / %
1			94
2			96

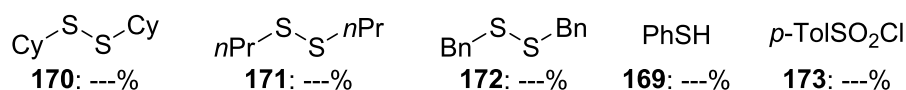
3 Results and Discussion

Entry	62	149	Yield / %
3	 62e	 149de	53
4	 62c	 149ac	93
5	 62d	 149ad	94
6	 62d	 149dd	37
7	 62d	 149yd	82
8	 62b	 149nb	57
9	 62e	 149ne	55
10	 62d	 149nd	72

Entry	62	149	Yield / %
11			55

^[a] Reaction conditions: **41** (0.50 mmol), **62** (0.60 mmol), Ni(OTf)₂ (10 mol %), LiOtBu (2.0 equiv), MnO₂ (1.0 equiv), 1,4-dioxane (1.5 mL), 120 °C, 18 h.

Unfortunately, under the optimized reaction conditions dialkyl- (**170/171**) or dibenzyl- (**172**) disulfides (Scheme 3.4) fell short in providing the C–H thiolated product.



Scheme 3.4: Unsuccessful coupling partners.

Based on the reports by SHI, CHATANI and KAMBE, who employed thiophenols and aryl sulfonylchlorides in nickel-catalyzed sulfenylation and sulfonylation reactions of aromatic amides,^[78, 147] we also tested thiophenol (**169**) and *para*-toluene sulfonylchloride (**173**) as coupling partner, but they did not lead to any *ortho*-functionalized aniline derivatives.

3.1.3 Scope of the Nickel-Catalyzed C–H Selenation of Anilines.

With the excellent versatility towards differently substituted *N*-pyrimidyl anilines **41** and various diaryl disulfides **62**, we next became interested to probe whether this protocol could also be exploited for the challenging nickel-catalyzed selenylation reaction.

Indeed, this could be illustrated by employing diphenyl diselenide **148a** under otherwise identical reaction conditions. Thus, a variety of aniline derivatives **41**, comparable to the scope of the C–H thiolation reaction, were efficiently converted to the desired 2-aminoselenophenols **150** (Table 3.9). The C–H selenylation proceeded with a high positional selectivity and functional group tolerance. In case of anilines **41** with substitution at the C-2 and C-3 position, the desired products were afforded in moderate to good yields (entries 2–6 and 10–14).

3 Results and Discussion

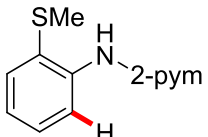
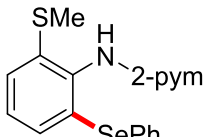
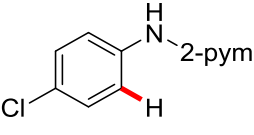
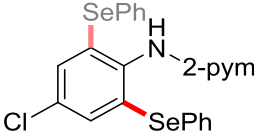
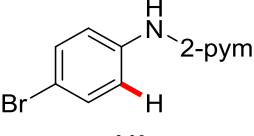
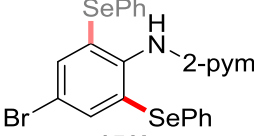
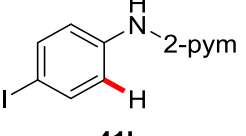
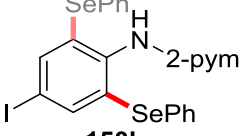
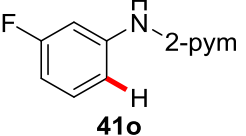
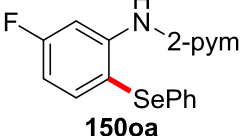
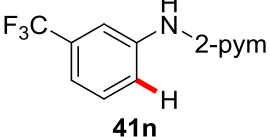
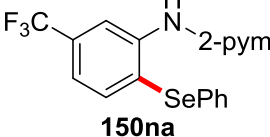
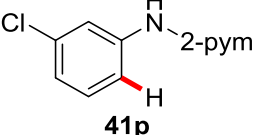
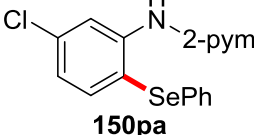
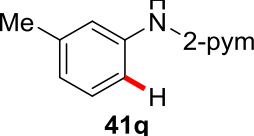
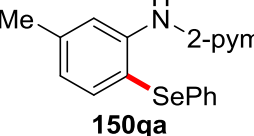
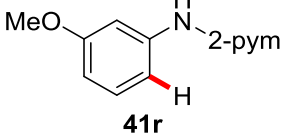
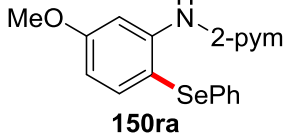
Using the unsubstituted *N*-pyrimidyl aniline **41z** or anilines with substituents in 4-position **41i-k** resulted in mixtures of both mono- and di-selenylated products, in which the mono-selenylated 2-aminoselenophenol is generated in slightly higher amounts (entries 1 and 7–9). Moreover, various di- and tri-substituted *N*-pyrimidyl anilines, bearing methyl and/or fluoro groups as well as the naphthyl aniline **41y** delivered the desired products **150ta-150wa** and **150ya** in moderate to very good yields.

Table 3.9: Scope of the nickel-catalyzed C–H selenation of anilines **41** with diphenyl diselenides **148**.^[a]

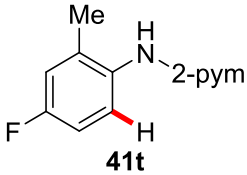
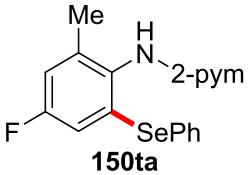
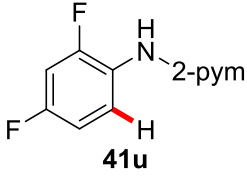
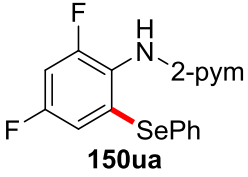
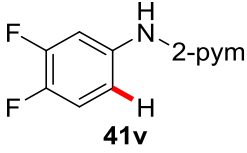
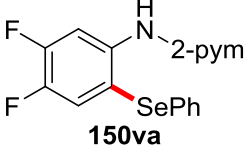
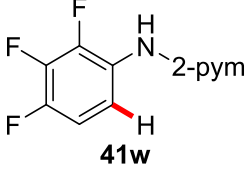
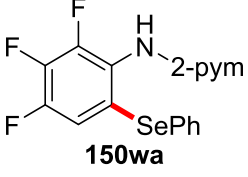
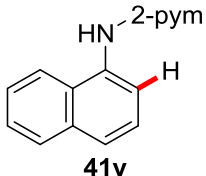
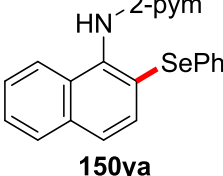
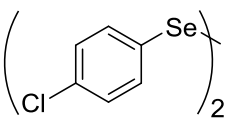
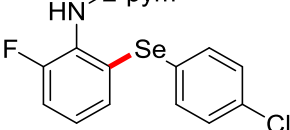
Reaction scheme: Aniline **41** (Ar group) + PhSe–SePh (**148a**) $\xrightarrow[\text{LiOtBu, 1,4-dioxane, 120 °C, 18 h}]{\text{Ni(OTf)}_2 \text{ (10 mol \%), MnO}_2 \text{ (1.0 equiv)}}$ Product **150** (Ar group, 2-pym, SePh)

Entry	41	150	Yield / %
1			39 (1.1:1) ^[b]
2			74
3			82
4			45
5			65

3 Results and Discussion

Entry	41	150	Yield / %
6	 41e	 150ea	52
7	 41i	 150ia	58 (1.7:1) ^[b]
8	 41j	 150ja	54 (1.7:1) ^[b]
9	 41k	 150ka	59 (1.8:1) ^[b]
10	 41o	 150oa	48
11	 41n	 150na	56
12	 41p	 150pa	58
13	 41q	 150qa	32
14	 41r	 150ra	41

3 Results and Discussion

Entry	41	150	Yield / %
15			84
16			52
17			49
18			52
19			78
20			74

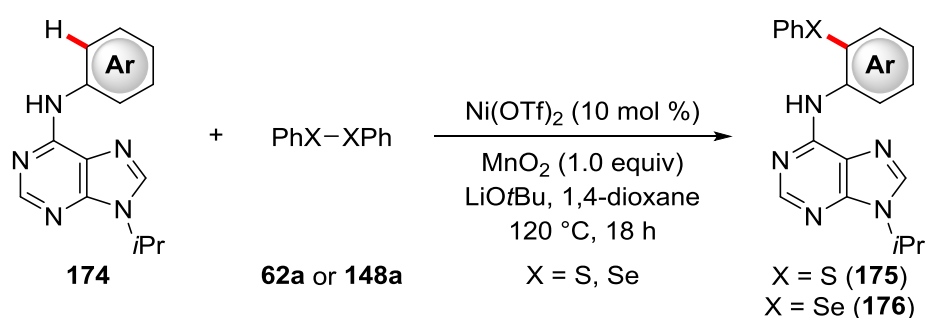
^[a] Reaction conditions: **41** (0.50 mmol), **148** (0.60 mmol), Ni(OTf)₂ (10 mol %), LiOtBu (2.0 equiv), MnO₂ (1.0 equiv), 1,4-dioxane (1.5 mL), 120 °C, 18 h; ^[b] combined yields of isolated products, ratio of mono- and disselectivity of the C–H selenation in parantheses.

In addition to the aniline derivatives shown in the scope, various other *N*-pyrimidyl anilines were tested. However, more sensitive functional groups, such as nitro, ketone or ester, were not tolerated in the nickel(II)-catalyzed C–H functionalization reaction. Employing diphenyl ditelluride was not suitable as a coupling partner.

A structural motif that is often found in pharmaceuticals and bioactive compounds is the purine scaffold. Nickel-catalyzed C–H activation strategies are largely limited to benzamide substrates bearing a *N,N*-bidentate directing groups and the number of protocols that can employ purines as substrate is scarce. Based on the work of our group, regarding nickel-catalyzed C–H alkylation reaction of *N*-pyrimidyl anilines,^[65] C–H alkylations also were achieved employing purine nucleosides.^[148] Building on those results, nickel-catalyzed C–H thiolation and C–H selenylation reactions using purine **174** and diphenyl disulfide/diselenide **62a/148a** could be achieved. Under otherwise identical reaction conditions, a representative set of purines **174a-174b** was reacted with **62a** or **148a** to deliver the desired products **175/176** in good to excellent yields with a high level of position-selectivity.

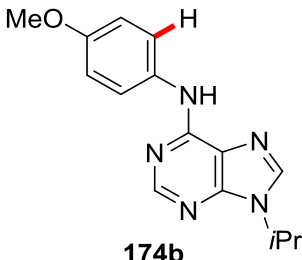
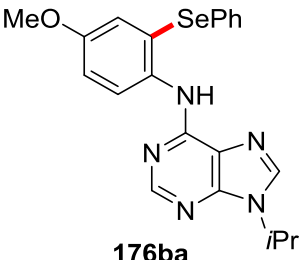
The purine **174b**, bearing a *para*-methoxy substituent on the aryl moiety afforded product **176ba** in 20% yield, possibly as a result of an electronic effect.

Table 3.10: Nickel-catalyzed chalcogenation of purine derivatives **174**.^[a]



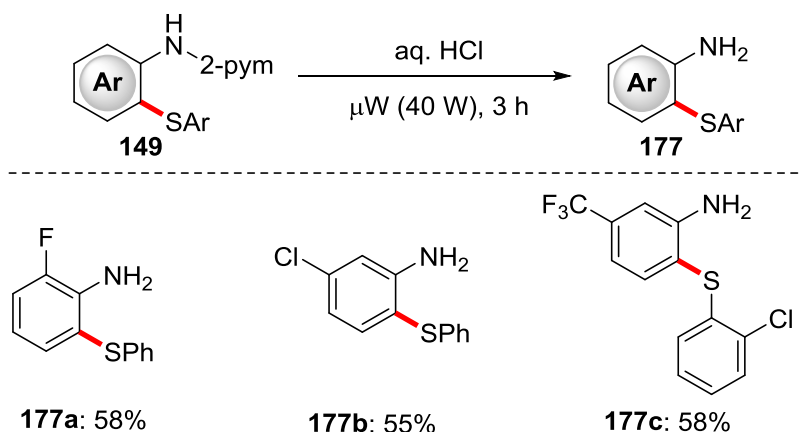
Entry	174	175/176	Yield / %
1			92
2			82

3 Results and Discussion

Entry	174	175/176	Yield / %
3	 <p>174b</p>	 <p>176ba</p>	20

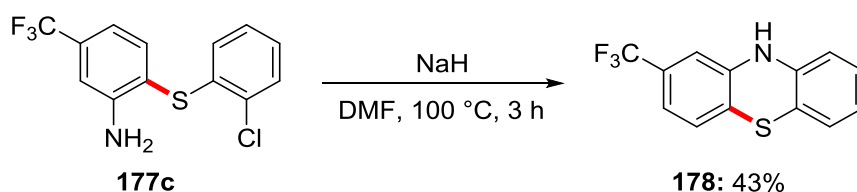
^[a] Reaction conditions: **174** (0.50 mmol), **62a** or **148a** (0.60 mmol), Ni(OTf)₂ (10 mol %), LiOtBu (2.0 equiv), MnO₂ (1.0 equiv), 1,4-dioxane (1.5 mL), 120 °C, 18 h.

To further highlight the practical utility of the nickel-catalyzed C–H chalcogenation strategy, the directing group was removed in a traceless fashion (Scheme 3.5). Here, the products **149** of the thiolation reaction were successfully converted to the desired 2-amino thiophenols **177** *via* microwave irradiation in aqueous HCl solution. Unfortunately, the deprotection procedure was not suitable for the corresponding selenophenols **150**.



Scheme 3.5: Removal of the pyrimidyl directing group.

2-Amino thiophenols represent useful precursors for the synthesis of phenothiazines, a structural class of highly potent drugs, which exerts diverse biological activities, such as neuroleptic action, antimicrobial and antitumor effects.^[149] Thus, using the 2-amino thiophenol **177c**, bearing a chloro-substituent in 2-position of the arene ring, we were pleased to provide step-economical access to the phenothiazine **178** *via* a nucleophilic aromatic substitution of the halogen, by heating **177c** in dimethyl formamide at 100 °C in presence of sodium hydride in 43% yield (Scheme 3.6).^[150]

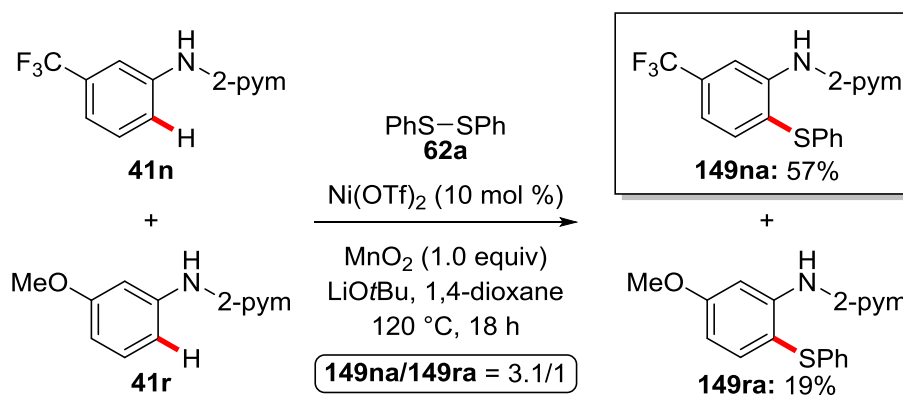


Scheme 3.6: Synthesis of phenothiazine **178** from 2-amino thiophenol **177c**.

3.1.4 Mechanistic Studies

After investigation of the scope of the nickel-catalyzed C–H chalcogenation, detailed mechanistic experiments were conducted to gain detailed insights into its mode of action.

We initiated these studies by performing intermolecular competition experiments between the electron-deficient aniline **41n** and the electron-rich aniline **41r** (Scheme 3.7). In this experiment, a clear preference for the electron-deficient aniline **41n** was detected, being suggestive of an assisted electrophilic mode of action not to be operative.



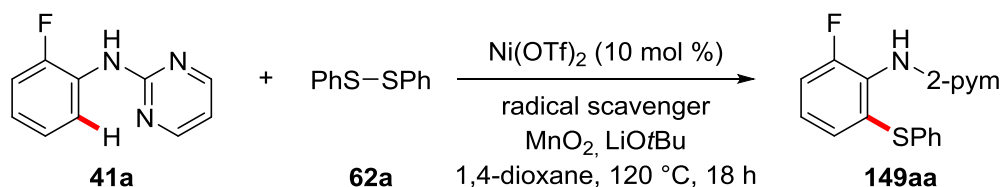
Scheme 3.7: Intermolecular competition experiment between electron-deficient and electron-rich pyrimidyl anilines.

Next, to examine whether any radical species are involved in the C–H chalcogenation, reactions in the presence of radical scavengers were conducted (Table 3.11). Hence, overstoichiometric amounts of BHT and galvinoxyl completely stopped the reaction (entries 3 and 4). By running the reaction in the presence of TEMPO as radical scavenger the yield was decreased from 96% (standard conditions, entry 1) to only 6% (entry 2). However, it should be taken into account that TEMPO can also interact in many ways with the nickel catalyst, enabling side-reactions such as coordination with the catalyst or oxidation reactions.

3 Results and Discussion

Nevertheless, the assumption that this transformation involves a radical pathway seems reasonable, particularly in comparison to similar nickel-catalyzed C–H thiolation reactions.^[75]

Table 3.11: Influence of radical scavengers in the nickel-catalyzed thiolation.^[a]

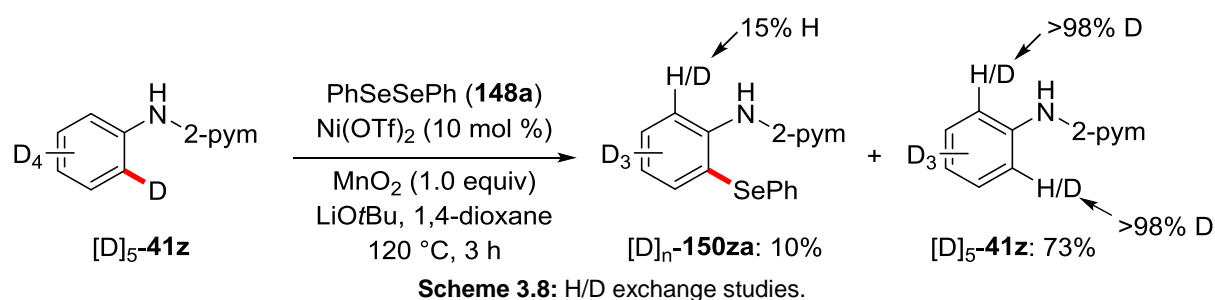


Entry	Radical Scavenger	Equiv	Yield / %
1	---	---	96
2	TEMPO	2.0	6
3	BHT	2.0	---
4	galvinoxyl	2.0	---

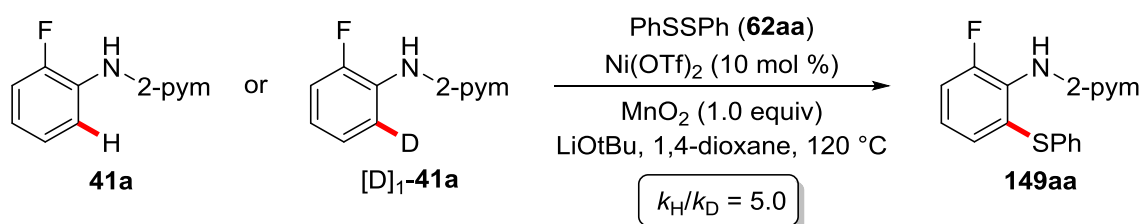
^[a] Reaction conditions: **41a** (0.50 mmol), **62a** (0.60 mmol), Ni(OTf)₂ (10 mol %), LiOtBu (2.0 equiv), MnO₂ (1.0 equiv), radical scavenger (2.0 equiv), 1,4-dioxane (1.5 mL), 120 °C.

Subsequently, a reaction using the isotopically-labelled *N*-pyrimidyl aniline [D]₅-**41z** and diphenyl diselenide **148a** was performed under the standard conditions (Scheme 3.8). After 3 h, the reaction yielded the selenylated *N*-pyrimidyl aniline **150za** in 10% together with unreacted starting material **41z** in 73%. Whereas no H/D scrambling was determined in the reisolated starting material, the 2-aminoselenophenol **150za** slightly showed H/D scrambling in the other *ortho* position with 15% proton incorporation.

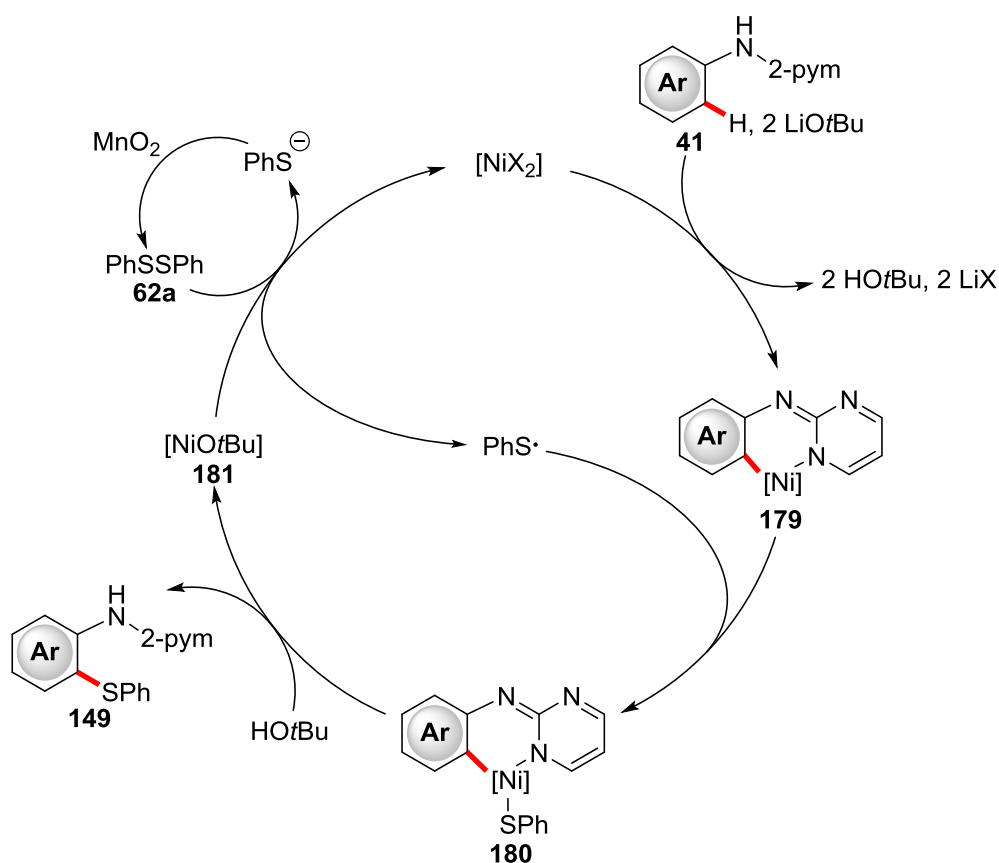
3 Results and Discussion



Finally, an experiment to determine the KIE, using substrate **41a** and isotopically-labelled $[D]_1\text{-41a}$, respectively, (Scheme 3.9) revealed a KIE of $k_H/k_D = 5.0$, indicating a rate-determining C–H activation manifold. Noteworthy, the observed significant primary KIE is in accordance with the result obtained by the H/D exchange experiment, highlighting the possibly irreversible nature of the initial C–H activation manifold.



Thus, based on these results a catalytic cycle was proposed, which initiates by a rate-determining and irreversible C–H nickelation of **41** to generate nickelacycle **179** (Scheme 3.10). Then, oxidation by a sulfenyl radical generates the nickel(III) species **180** via a SET-type process. Subsequently, reductive elimination follows and results in the formation of *ortho*-sulfenylated product **149** and nickel(I) species **181**. The active nickel(II) catalyst is proposed to be regenerated by the action of disulfide **62**, which itself is formed by the oxidant MnO_2 .



Scheme 3.10: Plausible catalytic cycle.

In summary, a versatile and robust method to access *ortho*-sulfenylated or -selenylated *N*-pyrimidyl anilines has been developed. A simple ligand-free $Ni(OTf)_2$ catalyst enabled the synthesis of *ortho*-sulfenylated/selenylated *N*-pyrimidyl anilines with high levels of positional control and good chemoselectivity. In addition, the traceless removal of the directing group allowed for the synthesis of 2-amino thiophenols, which are used as key building blocks for the synthesis of various antipsychotic, antidepressant and immunosuppressive agents,^[151] as clearly demonstrated with their applicability to the synthesis of phenothiazines as important drug molecules. Furthermore, the applicability of the nickel-catalyzed C–H chalcogenation method to purine derivatives highlights the importance of this transformation gaining access to a biologically important substrate class.

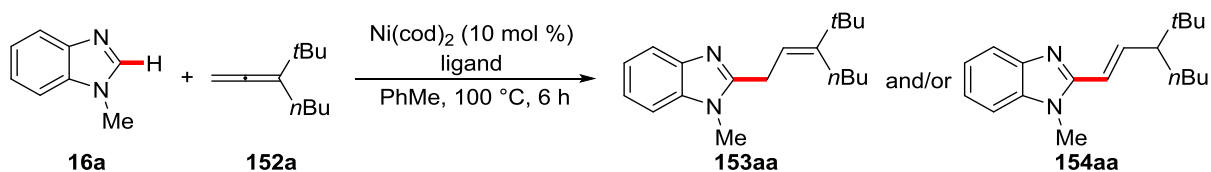
3.2 Nickel(0)-Catalyzed C–H Activation of Heteroarenes with Allenes

Nickel-catalyzed C–H functionalization processes for the formal hydroarylation of C–C multiple bonds have been rarely utilized until recently.^[41a, 112a] Consequently, during the last decade reports on nickel-catalyzed hydroarylation strategies of unsaturated compounds such as alkynes and alkenes using (hetero)arenes have been developed. In contrast to these achievements, C–H functionalizations employing more challenging allenes were thus far not accomplished by nickel catalysis. A general approach using allenes for nickel-catalyzed hydroarylation processes would considerably expand the chemist's toolbox and is therefore highly desirable.

3.2.1 Optimization Studies

Given the numerous examples by NAKAO/HIYAMA, ONG and others employing various heteroarenes such as indoles, benzofuranes and benzimidazoles for nickel-catalyzed hydroarylation reactions of alkynes and alkenes, we became interested to develop a novel nickel-catalyzed hydroarylation methodology of allenes using heteroarenes.^[152] Nickel/phosphine and nickel/NHC catalytic systems are well-known to facilitate this kind of transformations. Therefore, an alternative route that employs allenes **152** as versatile coupling partners for the synthesis of alkenylated or alkylated heteroarenes would indeed be highly desirable.

The study was commenced by S. Nakanowatari probing various reaction conditions for the envisioned hydroarylation-type C–H functionalization using *N*-methyl benzimidazole **16a** and 1,1-disubstituted allene **152a** (Scheme 3.11) as the model substrates.



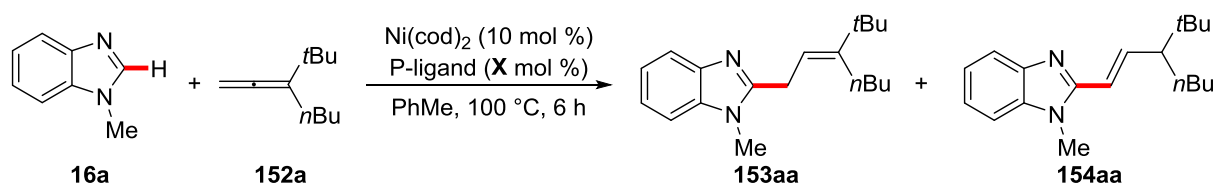
Scheme 3.11: Nickel(0)-catalyzed hydroarylation C–H functionalization of 1,1-disubstituted allene **152a**.

3 Results and Discussion

Promising results were obtained, using Ni(cod)₂ as source of nickel(0) in toluene as solvent affording alkenylated and/or allylated *N*-methyl benzimidazoles **153aa** and/or **154aa**, respectively. Typically, elevated reaction temperatures of at least 100 °C were required to achieve satisfactory results. Further, various reaction conditions with different phosphine ligands were investigated (Table 3.12).

Here, commonly employed phosphine ligands, such as PPh₃, PCy₃ or bidentate phosphines (entries 3-6), did not lead to significant conversions, yielding only undesired dimers and trimers of allene **152a**.

Table 3.12: Test of phosphine ligands for the nickel(0)-catalyzed hydroarylation of allene **152a**.^[a]



Entry	Ligand / X	Yield / %	
		153aa	154aa
1	PPh ₃ / 20	---	---
2	PCy ₃ / 20	1 ^[b]	---
3	dppe / 10	---	---
4	dppf / 10	---	---
5	XPhos / 10	---	---
6	SPhos / 10	---	---

^[a] Reaction conditions: **16a** (0.50 mmol), **152a** (0.80 mmol), [Ni(cod)₂] (10 mol %), ligand (X mol %), toluene (1.5 mL), 100 °C, 6 h; yields of the isolated products; ^[b] GC-conversion using *n*-dodecane as the internal standard.

Since the catalyst consisting of Ni(cod)₂/phosphines catalytic system were not applicable to the envisioned C–H allylation/alkenylation reaction, various *N*-heterocyclic carbenes were tested (Scheme 3.12). Those ligands are similar to electron-rich phosphine ligands in their electronic properties. Furthermore, NHC ligands were shown to be efficient ligands for similar hydroarylation reactions using nickel catalysts.^[88, 90c, 91, 96, 153]

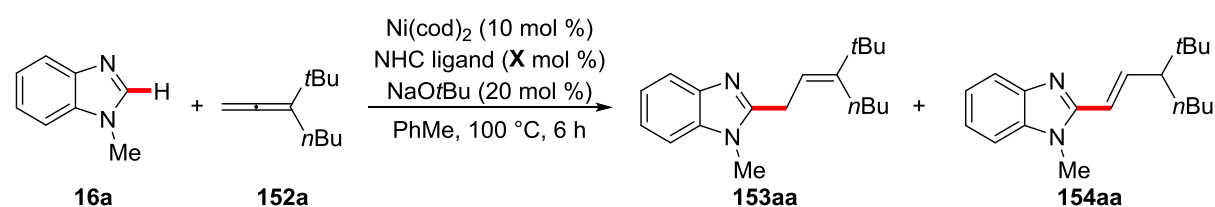
3 Results and Discussion

Using the easily accessible azolium salts, NaOtBu was chosen as a base to generate *in situ* the free carbene ligand. The imidazolium-based carbenes ICy and IMes (entries 2 and 7) gave moderate to good yields of the allylated product **153aa**, respectively. Less bulky ligands, such as IMe or ItBu (entries 1 and 3), resulted in significantly lower conversions. Moving from imidazolium to benzimidazolium salts (entries 4-6) did not improve the efficacy of the transformation. The bulkier IPr ligand provided better conversion, yielding the desired allylated benzimidazole **153aa** in 87% (entry 10). More electron-rich ligands, such as ^{Me}IPr (entry 13) or IPr^{OMe} (entry 14), and the congested ligands IPr* (entry 15) and IPr*^{OMe} (entry 16) did not improve the efficacy. Notably, the use of those types of NHC ligands led to the formation of a side product, namely the alkenylated benzimidazole **154aa**.

Furthermore, more specialized NHC ligands, such NHC ligands with benzothiazole or triazole cores (entries 17 and 18), cyclopropylidene (entry 19) and bidentate NHCs (entries 20-22) were tested, which led to no or very low conversions.

Because the commonly used imidazolium salts require a strong base to generate the free carbene ligand *in situ*, hydroarylation reactions employing the free carbene ligand IPr (entry 11) in the absence of an additional base were probed. The reaction led to a comparable result, affording the desired product **153aa** in 85% yield. This result clearly showed that the base or the *in situ* generated alcohol is not essential for the C–H activation step. Furthermore, the deliberate addition of tBuOH had no significant impact on the outcome of the standard reaction.

Table 3.13: Screening of NHC ligands for the nickel(0)-catalyzed hydroarylation of allene **152a**.^[a]



Entry	NHC ligand / X	Yield / %	
		153aa	154aa
1	IMe·HI / 10	25	---
2	ICy·HCl / 10	61	---

3 Results and Discussion

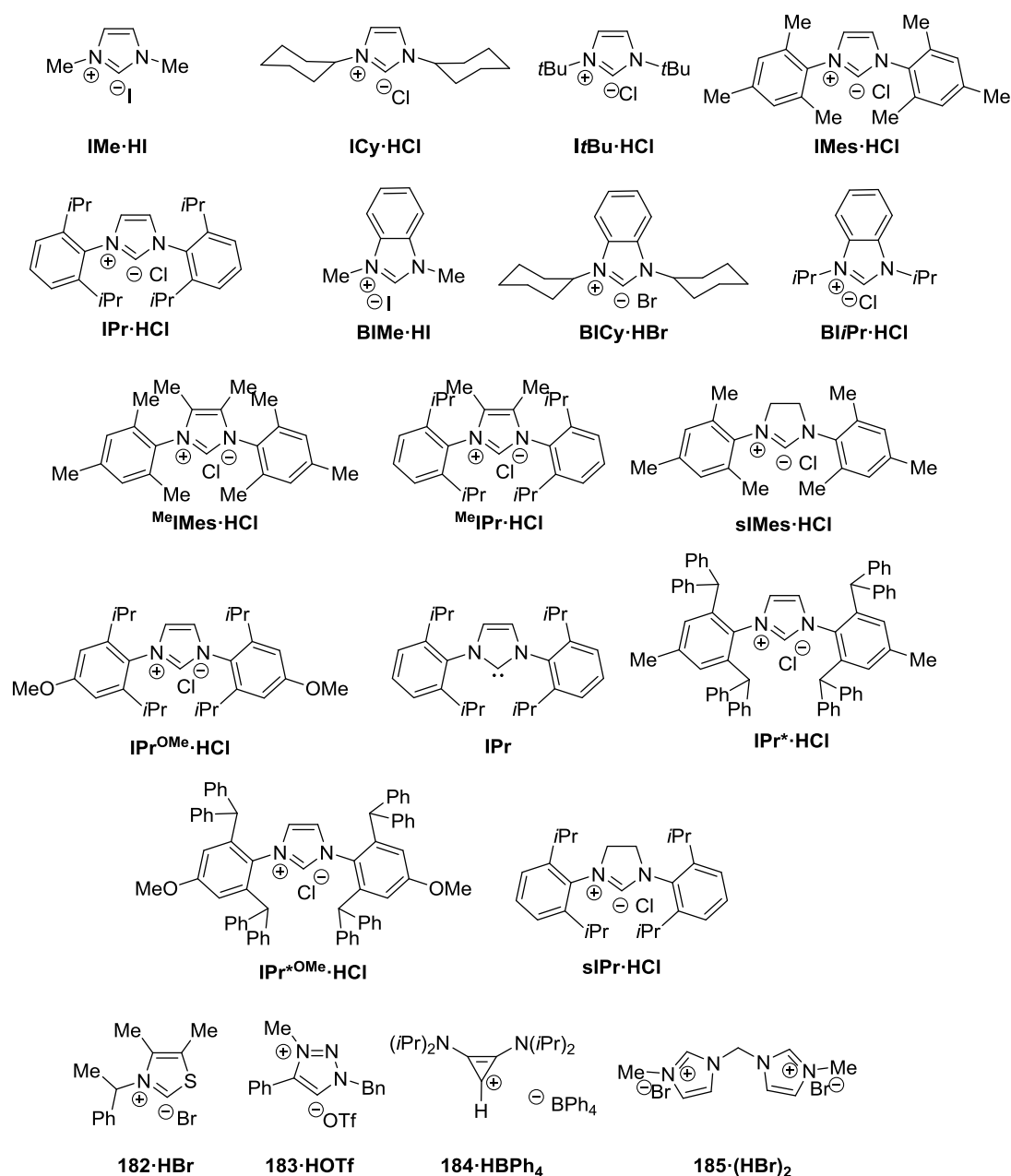
Entry	NHC ligand / X	Yield / %	
		153aa	154aa
3	ItBu·HCl / 10	---	---
4	BIMe·HI / 10	1 ^[b]	---
5	BICy·HBr / 10	---	---
6	BI <i>i</i> Pr·HCl / 10	36	---
7	IMes·HCl / 10	72	---
8	sIMes·HCl / 10	48	---
9	^{Me} IMes·HCl / 10	73	---
10	IPr·HCl / 10	87	---
11	IPr / 10	85^[c]	---
12	sIPr·HCl / 10	---	---
13	^{Me} IPr·HCl / 10	52	27
14	IPr ^{OMe} ·HCl / 10	49	---
15	IPr [*] ·HCl / 10	20	16
16	IPr ^{*OMe} ·HCl / 10	54	34
17	182 ·HBr / 10	---	---
18	183 ·HOTf / 10	3 ^[b]	---
19	184 ·HBPh ₃ / 10	---	---
20	185 (HBr) ₂ / 5	1 ^[b]	---

^[a] Reaction conditions: **16a** (0.50 mmol), **152a** (0.80 mmol), [Ni(cod)₂] (10 mol %), ligand (**X** mol %), NaOtBu (20 mol %), solvent (1.5 mL), 100 °C, 6 h; yields of the isolated products; ^[b] ¹H NMR yield using *n*-dodecane as the internal standard; ^[c] without NaOtBu.

In the course of the optimization of the NHC ligands a major side product besides the desired allylated product **153aa** was represented by the formation of the isomeric alkenylated hydroarylation product **154aa**. Since the reaction using free IPr delivered

3 Results and Discussion

chemoselectively the allylated benzimidazole (Table 3.14, entry 1), we became interested in the selective formation of the alkenylated product **154aa**.



Scheme 3.12: Different NHC ligands tested.

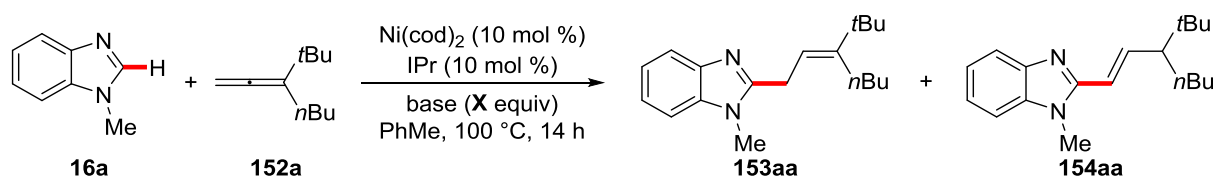
Thus, we continued our study in regard of the targeted synthesis of **154aa**. Using the free carbene IPr in presence of NaOtBu, we could observe the formation of both, the allylated and alkenylated product **153** and **154**. Starting with 0.2 or 0.5 equivalents NaOtBu (entries 2 and 3), respectively, mixtures of both products were formed, whereas when using stoichiometric amounts of the base, the alkenylated product **154aa** was obtained selectively in a high yield of 82% (Table 3.14, entry 4). In

3 Results and Discussion

summary, two sets of conditions were developed for the selective synthesis of allylated and alkenylated *N*-methyl benzimidazoles.

However, when we employed NaO*t*Pr as the base (entry 5) a lower selectivity was observed, delivering a mixture of **153aa** and **154aa** with 42% and 57% yield, respectively. In contrast, NaOMe solely provided the allylated product **153aa**.

Table 3.14: Effect of the base on the chemoselectivity of the nickel-catalyzed hydroarylation of allene **152a**.^[a]



Entry	Base / X	Yield / %	
		153aa	154aa
1	---	85	---
2	NaO <i>t</i> Bu / 0.2	37	63
3	NaO <i>t</i> Bu / 0.5	26	72
4	NaO <i>t</i> Bu / 1.0	---	82
5	NaO <i>t</i> Bu / 2.0	---	81
6	---	--- ^[b]	--- ^[b]
7	NaO <i>t</i> Pr / 1.0	42	57
8	NaOMe / 1.0	63	---

^[a] Reaction conditions: **16a** (0.50 mmol), **152a** (0.80 mmol), [Ni(cod)₂] (10 mol %), IPr (10 mol %), base (X mol %), solvent (1.5 mL), 100 °C, 14 h; yields of the isolated products; ^[b] without Ni(cod)₂.

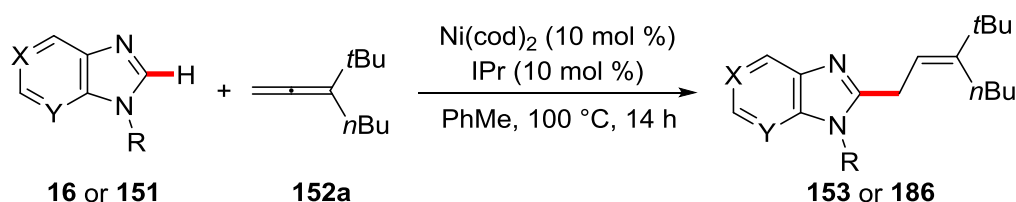
3.2.2 Scope of the Nickel-Catalyzed C–H Allylation of Imidazoles and Purines

With the optimized reaction conditions in hand, the applicability of the envisioned C–H hydroarylation of allenes **152** using a variety of decorated heteroarenes **16/151** was examined. The scope for the nickel(0)-catalyzed allylation reaction is shown in Table 3.15.

3 Results and Discussion

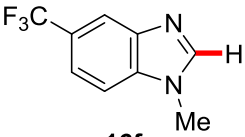
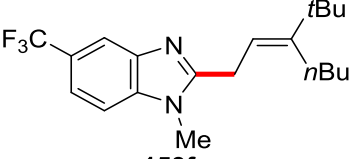
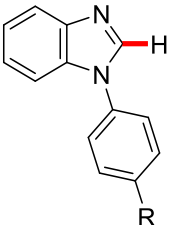
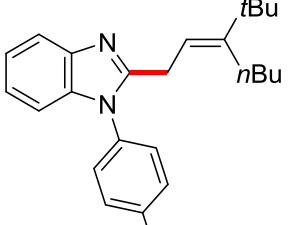
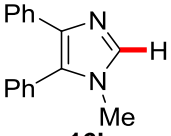
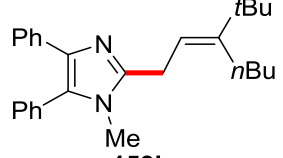
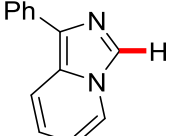
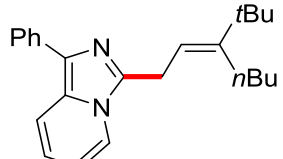
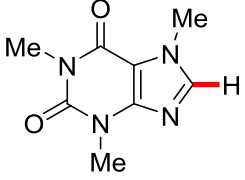
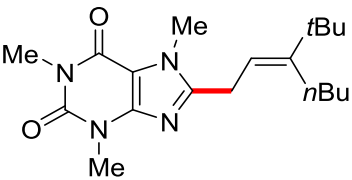
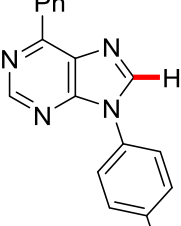
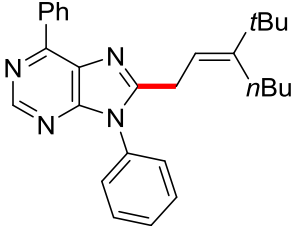
To our delight, the protocol was found to be broadly applicable to differently substituted benzimidazole **16** and purine derivatives **151**. As for the substituents on the nitrogen of the benzimidazole derivatives, methyl (entry 1), *n*-butyl, benzyl, and the MOM group (entry 2) succeeded in the reaction, delivering the desired products in moderate to good yields. Substitution on the benzimidazole was successfully tested, bearing the electron-donating methoxy (entry 3) or the electron-withdrawing trifluoromethyl group (entry 4) in C-5 position with good yields. Also, *N*-aryl benzimidazoles **16g-16h**, 4,5-diphenyl imidazole **16i** as well as imidazo-[1,5-*a*]pyridine **16j** were well-tolerated, thereby delivering the allylated products **153ga-153ja**. Furthermore, various 6-aryl purine derivatives, including caffeine **16k**, reacted successfully, affording the C-8 allylated products **153ka** and **186aa-186da** in good to excellent yields (entries 8-10) with high levels of positional selectivity for the C-8 position. Unfortunately, other heteroaromatic compounds, such as benzoxazole, benzothiazole or indole derivatives, were no suitable substrates for the nickel(0)-catalyzed C–H allylation protocol.

Table 3.15: Scope of the nickel-catalyzed C–H allylation reaction.^[a]

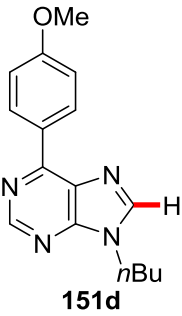
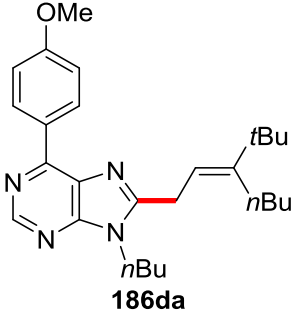


Entry	16 or 151	153 or 186	Yield / %
1			85
2			R = <i>n</i> Bu (153ba): 62 R = Bn (153ca): 84 R = MOM (153da): 50
3			82

3 Results and Discussion

Entry	16 or 151	153 or 186	Yield / %
4	 <p>16f</p>	 <p>153fa</p>	65
5	 <p>16g-h</p>	 <p>153ga-h</p>	R = H (153ga): 62 R = OMe (153ha): 77
6	 <p>16i</p>	 <p>153ia</p>	57
7	 <p>16j</p>	 <p>153ja</p>	64
8	 <p>16k</p>	 <p>153ka</p>	90
9	 <p>151a-c</p>	 <p>186a-c</p>	R = H (186aa): 92 R = OMe (186ba): 72 R = CF ₃ (186ca): 79

3 Results and Discussion

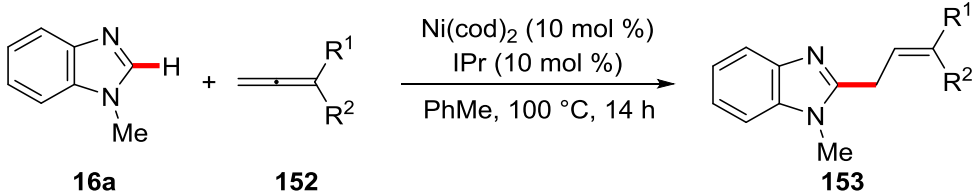
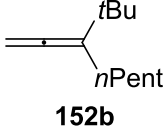
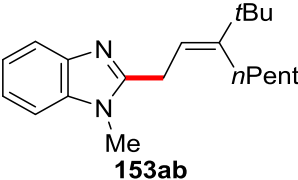
Entry	16 or 151	153 or 186	Yield / %
10	 <p>151d</p>	 <p>186da</p>	94

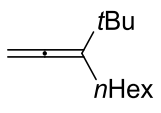
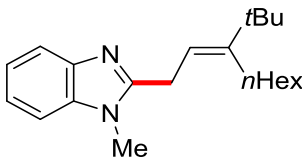
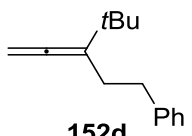
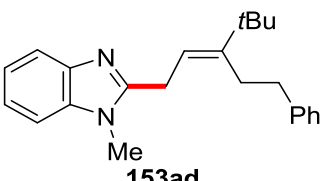
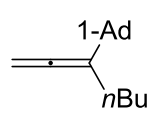
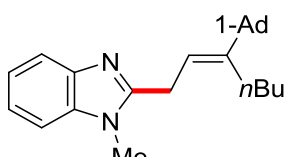
^[a] Reaction conditions: **16/151** (0.50 mmol), **152a** (0.80 mmol), [Ni(cod)₂] (10 mol %), IPr (10 mol %), PhMe (1.5 mL), 100 °C, 14 h.

Next, the scope of the viable allenes **152** was examined (Table 3.16). The substitution pattern of the allenes turned out to be crucial for the outcome of the reaction. Therefore, allenes with a defined substitution pattern were needed. First, 1,1-disubstituted allenes **152** were suitable coupling partners, while 1,3-disubstituted allenes did not react. Second, one of the substituents needed to have a quaternary carbon center, such as *tert*-butyl or adamantyl, while the other one should preferentially feature a primary carbon center, such as *n*-butyl, *n*-pentyl, *n*-hexyl or ethylbenzene.

Various allenes **152** were thus examined for their applicability. To our delight, the tested allenes led to high yields (77–98%) for the allylated products **153ab-153ae**.

Table 3.16: Scope of the nickel-catalyzed C–H allylation using different 1,1-disubstituted allenes **152**.^[a]

 <p>16a + 152 $\xrightarrow[\text{PhMe, 100 °C, 14 h}]{\text{Ni(cod)}_2 \text{ (10 mol \%), IPr (10 mol \%)}}$ 153</p>			
Entry	152	153	Yield / %
1	 <p>152b</p>	 <p>153ab</p>	77

Entry	152	153	Yield / %
2	 152c	 153ac	87
3	 152d	 153ad	91
4	 xx152e	 153ae	98

^[a] Reaction conditions: **16a** (0.50 mmol), **152** (0.80 mmol), [Ni(cod)₂] (10 mol %), IPr (10 mol %), PhMe (1.5 mL), 100 °C, 14 h.

3.2.3 Scope of the Nickel-Catalyzed C–H Alkenylation of Imidazoles and Purines.

Furthermore, with the protocol for the nickel(0)-catalyzed C–H alkenylation in hand, we subsequently also tested its versatility (Table 3.17). The desired C–H functionalization proceeded efficiently in the presence of 1.0 equivalent NaOtBu with excellent regioselectivity, delivering solely the corresponding alkenylated product (*E*)-**154**. Similar to the C–H allylation reaction (see Table 3.15) variously substituted benzimidazoles **16a–g**, purines **151** and 4,5-diphenyl imidazole **16i** were competent substrates.

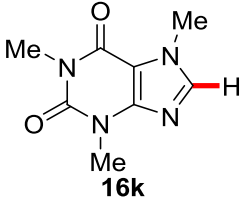
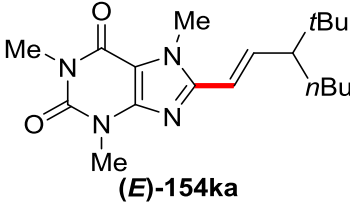
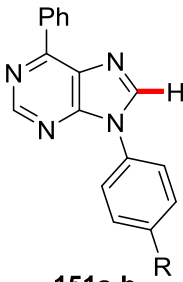
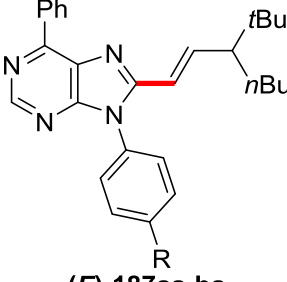
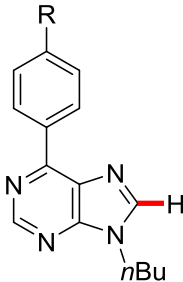
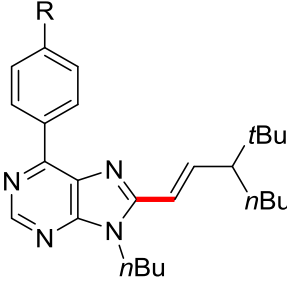
It is worth mentioning the reactions using purine derivatives, as these substrates are of great interest in the medicinal and pharmaceutical chemistry.^[154] The corresponding alkenylated purines **187aa–187ea** could be isolated in good to excellent yields of 63 to 95% (entries 7–9).

3 Results and Discussion

Table 3.17: Scope for the nickel-catalyzed C–H alkenylation.^[a]

Entry	16/151	154/187	Yield / %
1			82
2			R = <i>n</i> Bu (154ba): 72 R = Bn (154ca): 73
3			78
4			87
5			R = H (154ga): 58 R = CF ₃ (154la): 85
6			63

3 Results and Discussion

Entry	16/151	154/187	Yield / %
7	 <p>16k</p>	 <p>(E)-154ka</p>	86
8	 <p>151a-b</p>	 <p>(E)-187aa-ba</p>	R = H (187aa): 63 R = OMe (187ba): 87
9	 <p>151d-e</p>	 <p>(E)-187da-ea</p>	R = H (187da): 95 R = OMe (187ea): 79

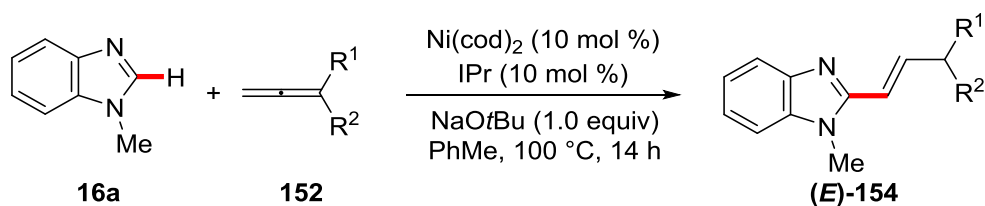
^[a] Reaction conditions: **16/151** (0.50 mmol), **152a** (0.80 mmol), [Ni(cod)₂] (10 mol %), IPr (10 mol %), NaOtBu (1.0 equiv), PhMe (1.5 mL), 100 °C, 14 h.

Likewise, the scope of allenes was investigated for the direct C–H alkenylation (Table 3.18). Indeed, as was the case for the C–H allylation (*vide supra*), only 1,1-disubstituted allenes **152** were suitable substrates, delivering the corresponding alkenylated products **154ab–af** with good yields ranging from 71–86%.

At that time, A. Bigot synthesized several allenes during an internship within his Bachelor studies. Therein, several allenes were synthesized, including allene **152f** bearing a cyclopropyl substituent. With this allene as valuable substrates in hand, we were able to perform the desired C–H alkenylation reaction affording the desired product **154af** with 26% yield without ring-opening of the sensitive cyclopropane motif.

3 Results and Discussion

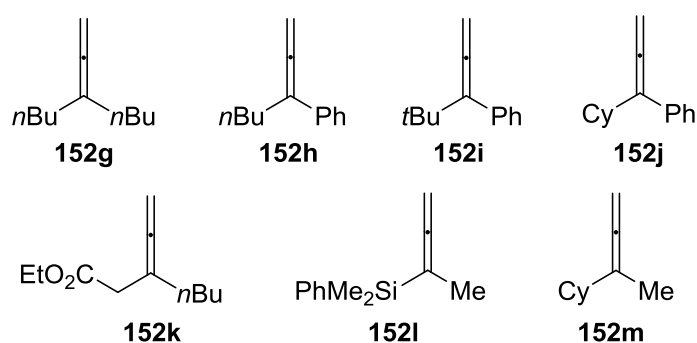
Table 3.18: Nickel-catalyzed C–H alkenylation using different 1,1-disubstituted allenes **152**.^[a]



Entry	152	154	Yield / %
1			80
2			84
3			86
4			71
5			26

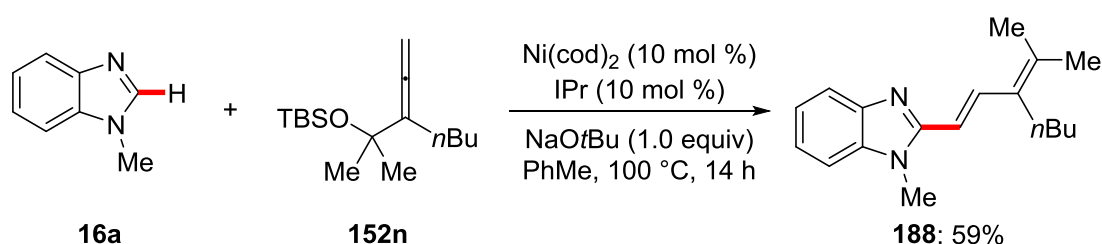
^[a] Reaction conditions: **16a** (0.50 mmol), **152** (0.80 mmol), [Ni(cod)₂] (10 mol %), IPr (10 mol %), NaOtBu (1.0 equiv), PhMe (1.5 mL), 100 °C, 14 h.

In addition, several other 1,1-disubstituted allenes **152g-m** (Scheme 3.13) were synthesized and employed for the developed nickel(0)-catalyzed C–H allylation/alkenylation reaction, albeit with thus far limited success.



Scheme 3.13: Failed examples for 1,1-disubstituted allenes.

Moreover, the nickel(0)-catalyzed C–H alkenylation protocol could be applied to the dienylative C–H activation and concurrent C–O cleavage under otherwise identical reaction conditions (Scheme 3.14). Thus, the use of (*tert*-butyldimethylsilyl)ether substituted allene **152n** delivered the dienylated benzimidazole **188** as the sole product in 59% yield with high levels of chemo- and stereo-selectivity.



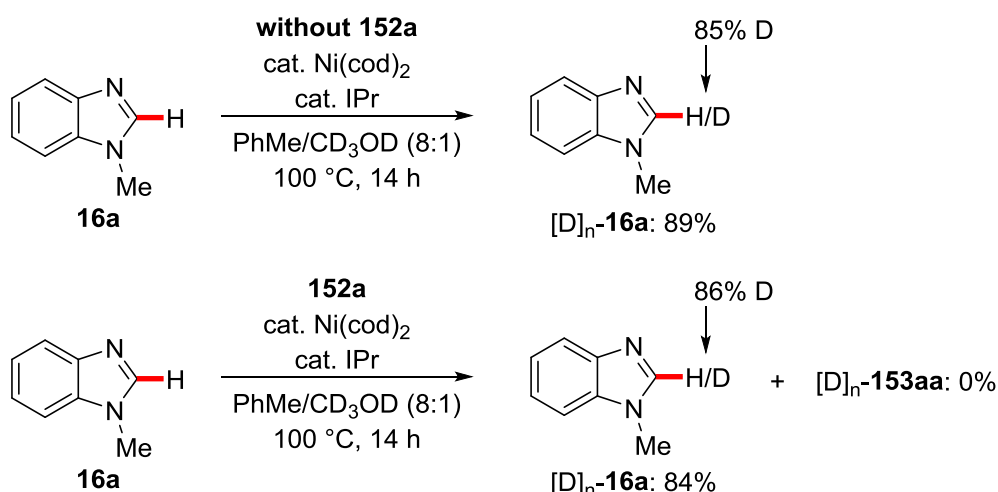
Scheme 3.14: Nickel-catalyzed dienylation using allene **152n**.

3.2.4 Mechanistic Studies

After the investigation of the versatility of the nickel(0)-catalyzed C–H allylation and C–H alkenylation reactions, detailed mechanistic experiments were conducted to gain insights into its mode of action.

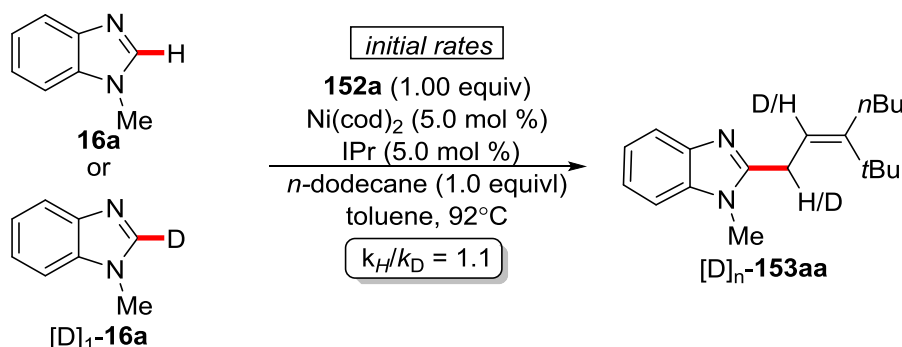
First, deuteration studies in the presence of CD₃OD as co-solvent were conducted (Scheme 3.15). Here, performing the reaction in the absence of allene **152a** revealed a significant H/D scrambling with 85% deuterium incorporation at the C-2 position. The same holds true, when the reaction was performed in the presence of the allene **152a**. The reisolated starting material also showed a significant H/D scrambling with 86% deuterium incorporation.

3 Results and Discussion



Scheme 3.15: H/D exchange with isotopically labeled co-solvent.

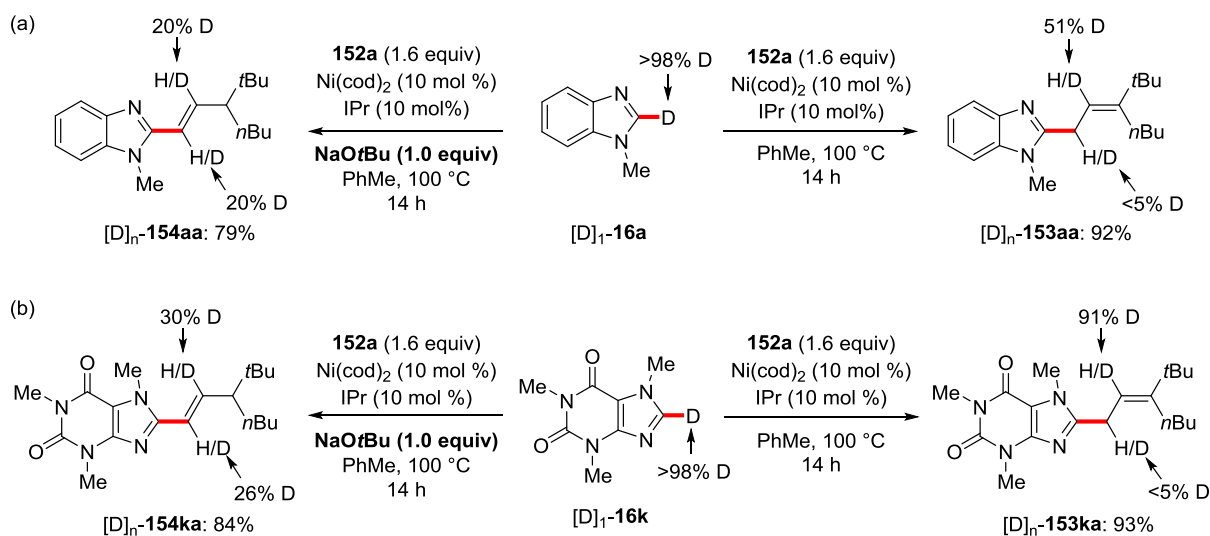
These findings are indicative that the C-2 position of the benzimidazole **16** is activated in a reversible fashion. Additionally, a KIE experiment was conducted by S. Nakanowatari comparing the initial rates of the deuterated benzimidazole [D]₁-**16a** and the standard substrate **16a** in independent reactions. A minor KIE of $k_H/k_D = 1.1$ suggested again a facile C–H activation, providing support that the C–H scission is not the turnover-limiting step of the overall transformation (Scheme 3.16).



Scheme 3.16: Kinetic isotope effect.

Moreover, C–H activations with the isotopically-labelled benzimidazole [D]₁-**16a** and caffeine [D]₁-**16k**, respectively, were performed (Scheme 3.17). Here, under the reaction conditions allylated products [D]_n-**153aa** and [D]_n-**153ka** were obtained with high deuterium incorporations at the olefinic position of the allyl moiety. In the alkenylated products [D]_n-**154aa** and [D]_n-**154ka**, deuterium incorporation was observed on both sides of the olefin in the range of 20-30%.

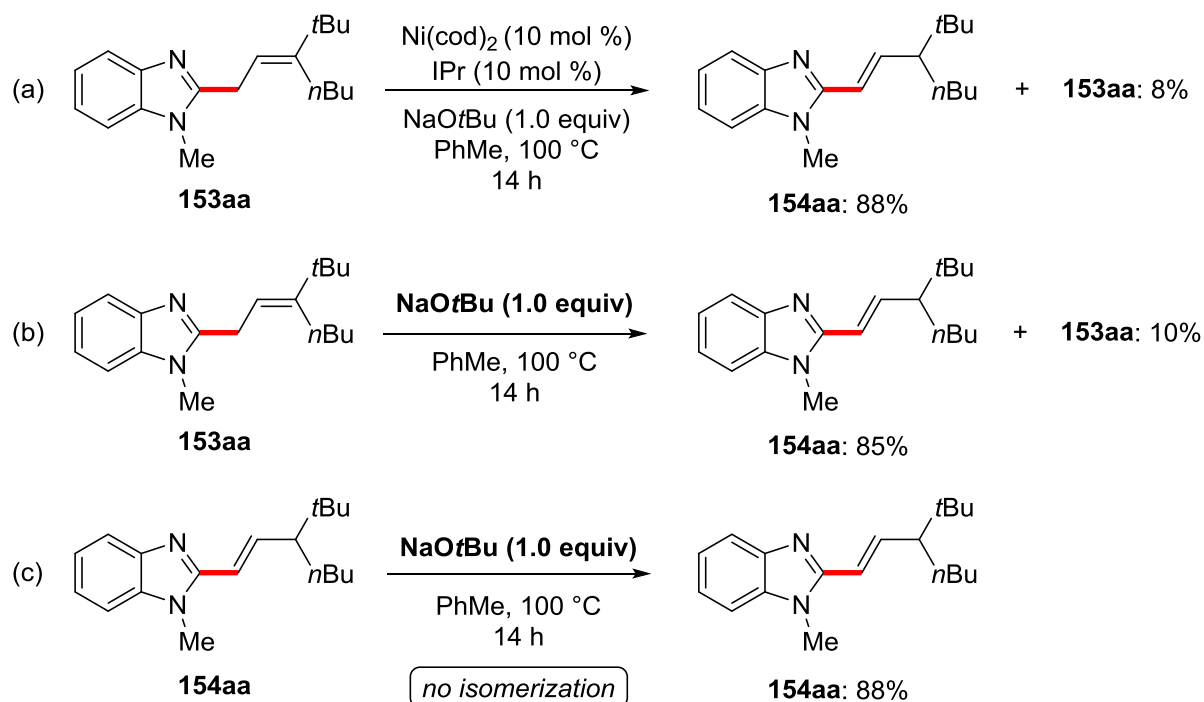
3 Results and Discussion



Since the formation of the alkenylated products likely occurred through an isomerization process originated from the allyl group, several test reactions were performed to get detailed insights into the reaction mechanism (Scheme 3.18). When the allylated product **153aa** was subjected to the standard reaction conditions using NaOtBu as the base in presence of the nickel catalyst (Scheme 3.18a), the isomerized product **154aa** could be isolated in 88% yield. A similar result could be achieved, when **153aa** and 1.0 equivalent of NaOtBu were heated in toluene at 100 °C (Scheme 3.18b). Here, the alkenylated product **154aa** was isolated in 85% yield.

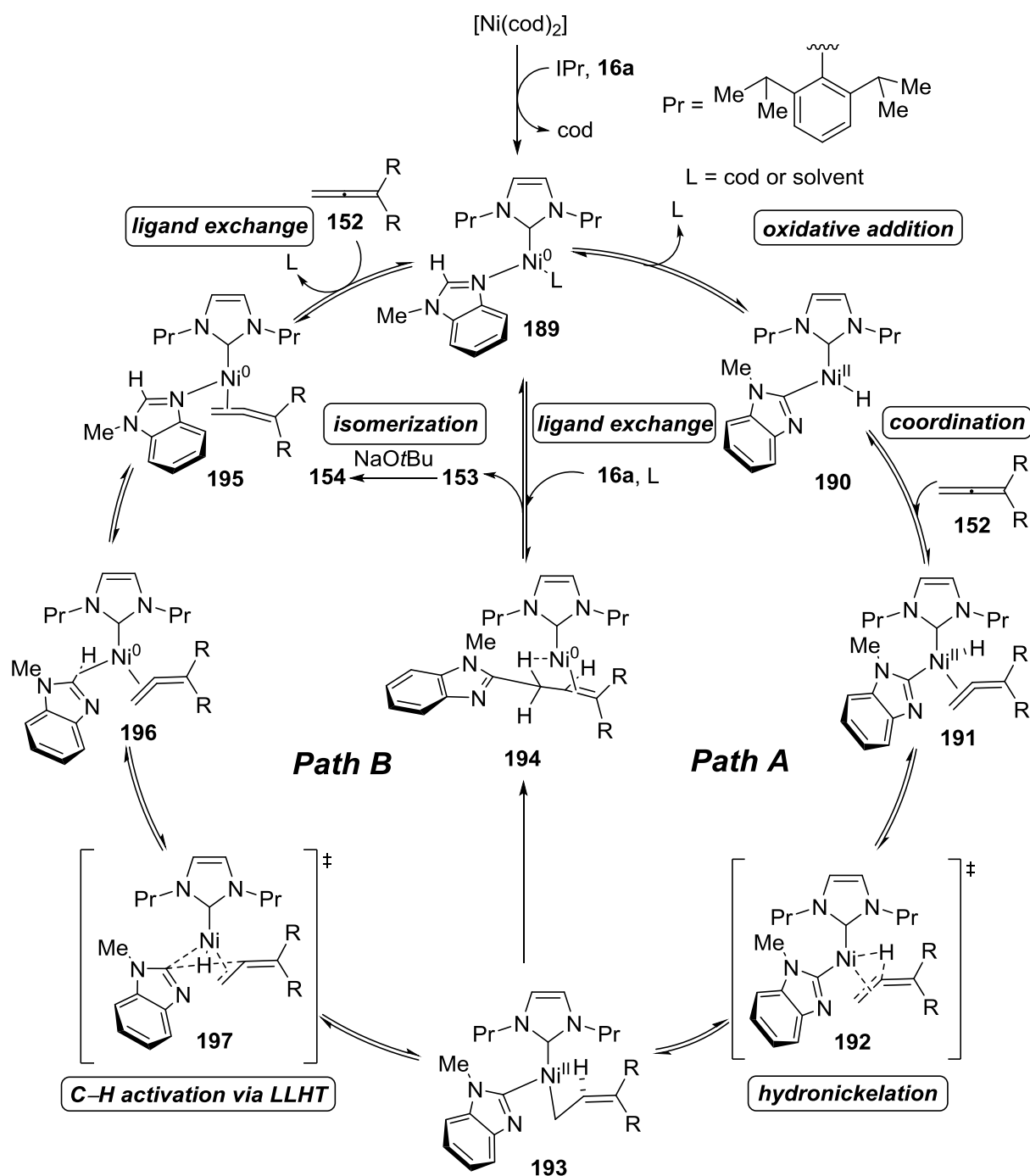
Importantly, no isomerization was observed, carrying out the same reaction starting with the alkenylated benzimidazole **154aa** (Scheme 3.18c). These results are in agreement with observations achieved by an *in operando* ^1H NMR study in $[\text{D}]_8$ -toluene (performed by S. Nakanowatari) and computational DFT studies (performed by Dr. J. C. A. Oliveira). It could be shown that the allylated product **153aa** isomerized to the thermodynamically more stable alkenylated product (**E**)-**154aa** in the presence of the base.

3 Results and Discussion



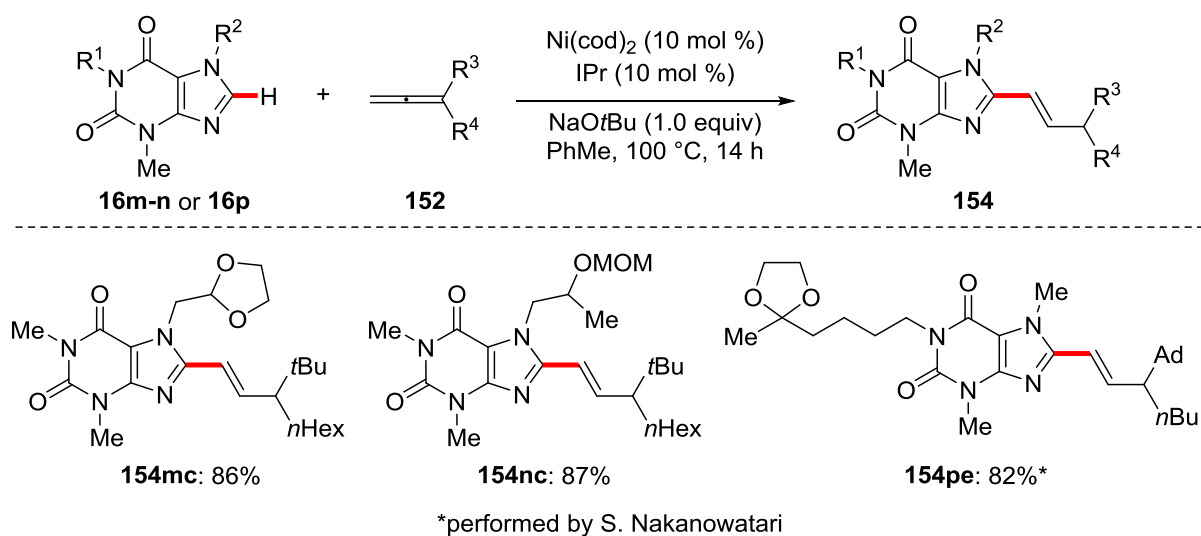
Scheme 3.18: Isomerization studies.

Based on the obtained results and previous reports on nickel(0)-catalyzed hydroarylation reactions of alkynes and alkenes,^[41] a catalytic cycle was proposed, which initiates with a ligand exchange, and the *in situ* generation of the [NHC-Ni⁰L_n] complex **189** (Scheme 3.19). This complex then undergoes oxidative addition with the C–H bond of benzimidazole to form the activated nickel complex **190** (path A). Subsequently, coordination of the allene **152** (**191**), followed by hydronickelation (**192**) forms the allylated nickel complex **193**. Upcoming C–C forming reductive elimination will generate the product-nickel complex **194**. Finally, ligand exchange will regenerate the active complex **189** and release the desired allylated product **153**, which, in the presence of base, will isomerize to the alkenylated product **154**. An alternative route (path B) also starts from the active complex **189**. Here, after coordination of allene substrate **152** intermediate **195** is formed. Complex **195** further undergoes agostic interaction (**196**), and C–H activation through ligand-to-ligand-hydrogen transfer (LLHT) to form the key intermediate **193**.



Scheme 3.19: Plausible catalytic cycle.

Finally, the synthetic utility of the envisioned transformation was highlighted by the late-stage diversification of caffeine-derived diphosphodiesterase inhibitor natural products **16m-n** and **16p** (Scheme 3.20). Here, we were able to access the C–H alkenylated products in synthetically useful yields of 82–87%.



Scheme 3.20: Late-stage C–H alkenylation of diphosphodiesterase inhibitors.

In summary, a powerful nickel(0)-catalyzed C–H activation with allenes has been developed. The C–H activation/hydroarylation features excellent control of the chemo- and region-selectivity. Furthermore, the switchable selectivity enabled the introduction of either allyl or alkenyl groups, thereby providing a general access to synthetically meaningful imidazole and purine derivatives.

3.3 Iron-Catalyzed C–H/N–H Allene Annulation

The development of methods that utilize iron catalysts for C–H activation reactions is a highly attractive approach due to its beneficial features in terms of earth-abundance, cost-effectiveness and low toxicities. Especially, the use of low-valent iron species has been intensively investigated, because they are found to be competent for the activation of thermodynamically stable C(sp²)–H as well as C(sp³)–H bonds under mild reaction conditions, providing a step- and atom-economical approach for the construction of new C–C bonds.

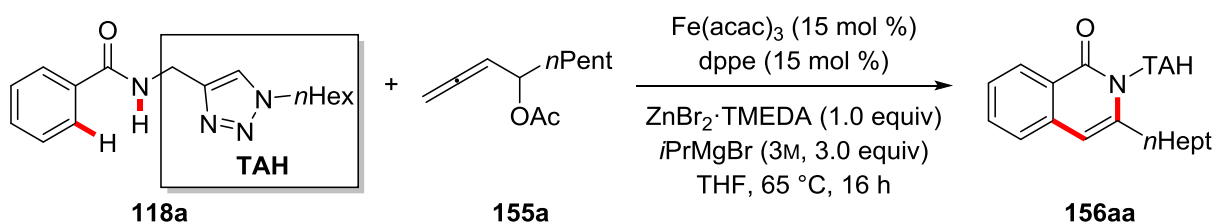
In particular, a number of methods for the alkylation and alkenylation through hydroarylation of alkenes or alkynes have been reported using low-valent iron catalysts.^[106, 128a] Furthermore, C–H annulation methodologies utilizing alkynes were developed for the synthesis of polyaromatic structures and *N*-heterocycles. One major drawback of those annulation procedures is the necessity of stoichiometric amounts of an oxidizing reagent, such as 1,2-DCIB or 1,2-DCP, which often limits the functional group tolerance of these transformations.

The use of bidentate directing groups in iron-catalyzed C–H activations has emerged as a powerful approach for establishing novel C–C forming processes.^[98, 102] Especially, the directing group derived from 8-AQ, developed by DAUGULIS,^[50c] enabled various transformations with important contributions by COOK^[124B, 124D] and NAKAMURA.^[120a, 124c, 126b] But the 8-AQ auxiliary is quite tedious to access in a modular fashion and its removal usually requires harsh reaction conditions, such as concentrated HCl at high reaction temperatures. Therefore, alternative bidentate auxiliaries are highly desirable.

ACKERMANN recently introduced a new family of triazole-based directing groups, the so called TAM group.^[114] These kind of directing groups are easily accessible and the traceless removal can be achieved under much milder reaction conditions, compared to other bidentate auxiliaries.

3.3.1 Optimization Studies

Based on those major contributions in the field of iron catalysis achieved by ACKERMANN, my colleague J. Mo in the ACKERMANN group has developed a strategy for the iron-catalyzed C–H/N–H annulations of TAH benzamide **118a**, using allenyl acetate **155a** for the synthesis of isoquinolone **156aa** under external oxidant-free conditions (Scheme 3.21).^[155]

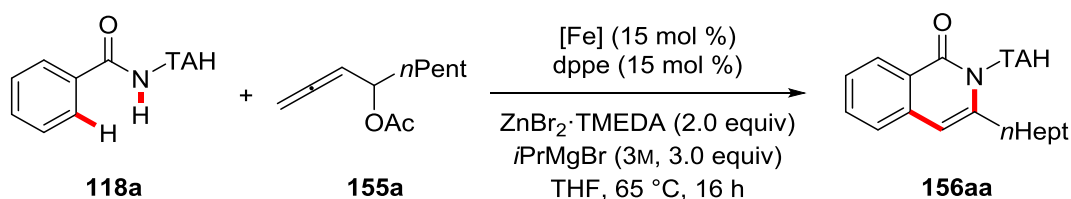


Scheme 3.21: Optimized reaction conditions of the iron-catalyzed C–H/N–H annulation of benzamide **xx** with allenyl acetate **xx** for the synthesis of isoquinolone **xx**.

The optimal catalytic system consisted of the cheap and commercially available iron(III) salt Fe(acac)₃, dppe as the ligand, ZnBr₂·TMEDA and *i*PrMgBr in THF at 65 °C. It is noteworthy that stoichiometric amounts of the zinc salt proved to be mandatory for promoting the envisioned C–H functionalization, and among a variety of tested bidentate phosphine ligands, dppe was identified as being optimal.

Furthermore, the use of an excess of Grignard was mandatory, first, to deprotonate the amide and therefore making it more nucleophilic, and second to undergo the transmetalation with the zinc salt in order to form an organometallic zinc reagent. Among testing different iron sources, the iron(III) compounds $\text{Fe}(\text{dbm})_3$ and FeCl_3 as well as FeCl_2 provided excellent conversions to the annulated isoquinolone **156aa** in 86-94% yield (Table 3.19).

Table 3.19: Screening of iron catalysts for the annulation reaction.^[a]



Entry	[Fe]	Yield / %
1	$\text{Fe}(\text{acac})_3$	91
2	$\text{Fe}(\text{dbm})_3$	86
3	FeCl_3	88
4	FeCl_2	94

^[a] Reaction conditions: **118a** (0.30 mmol), **155a** (0.90 mmol), [Fe] (15 mol %), dppe (15 mol %), $\text{ZnBr}_2 \cdot \text{TMEDA}$ (0.60 mmol), $i\text{PrMgBr}$ (3M, 0.90 mmol), THF (0.40 mL), 65 °C, 16 h.

3.3.2 Scope of the Iron-Catalyzed C–H/N–H Annulation

With the optimized reaction conditions in hand, we next explored the applicability towards differently substituted TAH benzamides **118**.

A representative scope with TAH benzamides was established by J. Mo.^[155] In addition, the scope of suitable benzamides **118** could be extended to those bearing a methyl- or fluoro-substituent at the 2-position, yielding the desired products **156ba** and **156ca** in moderate amounts of 50% and 58%, respectively (Table 3.20). Benzamides bearing a substituent at the 3-position (**118d-f**) reacted in a regioselective fashion, delivering the products in very good yields, even tolerating synthetically useful bromo substituents.

3 Results and Discussion

Table 3.20: Scope of the iron-catalyzed C–H/N–H annulations using different TAH benzamides **118**.^[a]

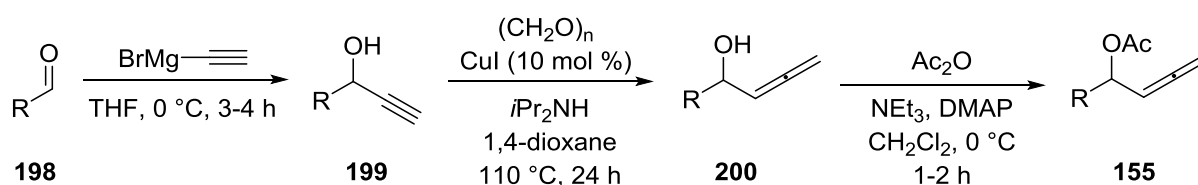
Entry	118	156	Yield / %
1	 118b	 156ba	50
2	 118c	 156ca	58
3	 118d	 156da	82
4	 118e	 156ea	87 (3.6:1) ^[b]
5	 118f	 156fa	86

^[a] Reaction conditions: **118** (0.30 mmol), **155a** (0.90 mmol), Fe(acac)₃ (15 mol %), dppe (15 mol %), ZnBr₂·TMEDA (0.60 mmol), *i*PrMgBr (3M, 0.90 mmol), THF (0.40 mL), 65 °C, 16 h, ^[b] ratio of regio isomers, combined yield of isolated products.

After establishing the scope with different benzamides **118**, various allenyl acetates **155** were investigated for their use in the iron-catalyzed C–H/N–H annulation reaction (Table 3.21).

3 Results and Discussion

In general, the synthesis of these allenes (Scheme 3.22) was accomplished, beginning with a 1,2-addition of ethynylmagnesium bromide to the corresponding aldehydes **198** forming the propargylic alcohols **199**. Thereafter, a copper-catalyzed Crabbé homologation to form the allene **200**,^[156] and acetate protection of the alcohol delivers the desired allenyl acetates **155** in overall good yields.



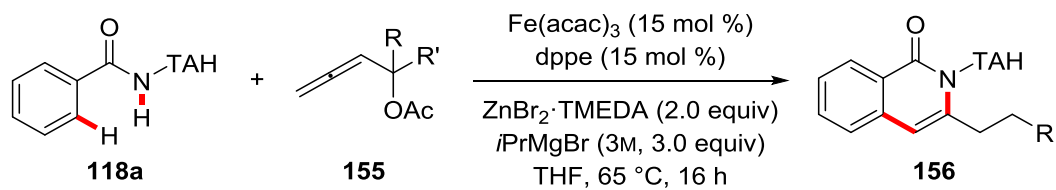
Scheme 3.22: General synthesis of allenes **xx2**.

As shown in Table 3.21, various decorated allenes were amenable substrates. Allenyl acetates **155** bearing alkyl groups with different chain-lengths and also α -cyclohexyl- or benzyl groups were efficiently converted, delivering the corresponding isoquinolones **156aa-ae** with very good yields (entries 1-5). Furthermore, allenes bearing a benzylether moiety (**155f**, entry 6) or reactive alkyl chloride (**155g**, entry 7) efficiently reacted to the desired products with excellent yields. Aryl-substituted allenyl acetates **155h-j** (entry 8-10) were also selectively converted, tolerating the synthetically meaningful aryl chloride. With allenes containing a quaternary carbon center in α -position, such as allene **155k** and **155l** (entries 11 and 12), lower yields were observed, delivering the desired products **156ak** and **156al** in 40% and 25% yield, respectively.

The inherently decreased reactivity of this kind of allenyl acetates, exhibiting an additional substituent at the acetate leaving group may be due to the increased steric bulk of these substrates.

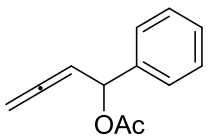
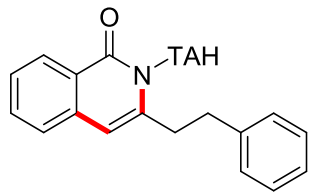
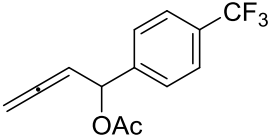
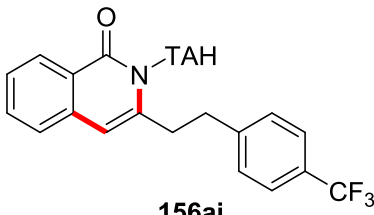
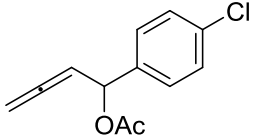
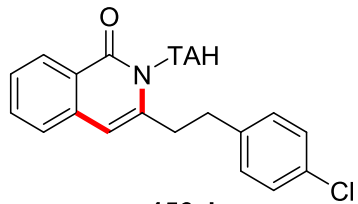
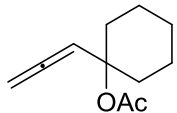
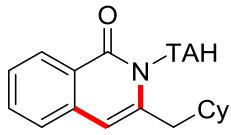
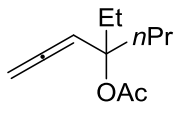
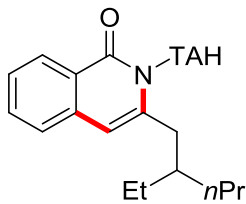
3 Results and Discussion

Table 3.21: Scope of the iron-catalyzed C–H/N–H annulations using different allenyl acetates **155**.^[a]



Entry	155	156	Yield / %
1			91
2			93
3			86
4			87
5			85
6			94
7			91

3 Results and Discussion

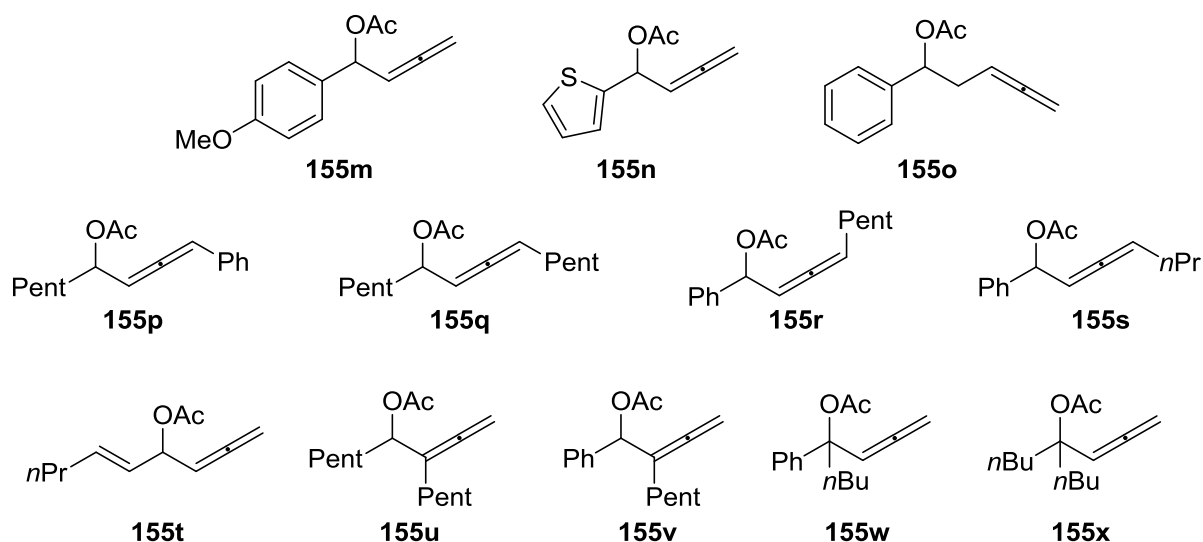
Entry	155	156	Yield / %
8	 155h	 156ah	53
9	 155i	 156ai	56
10	 155j	 156aj	67
11	 155k	 156ak	40
12	 155l	 156al	25

^[a] Reaction conditions: **118a** (0.30 mmol), **155** (0.90 mmol), Fe(acac)₃ (15 mol %), dppe (15 mol %), ZnBr₂·TMEDA (0.60 mmol), *i*PrMgBr (3M, 0.90 mmol), THF (0.40 mL), 65 °C, 16 h.

Besides the allenyl acetates **155a-l** shown in Table 3.21, a series of differently substituted allenes **155m-x** were synthesized to investigate what the limitations of this transformation are (Scheme 3.23). To this end, allenyl acetates bearing electron-rich (hetero)aryl groups, such as the 4-methoxyphenyl (**155m**) or thiophenyl (**155n**) substituents fell short in the reaction, only giving low conversions of <10%.

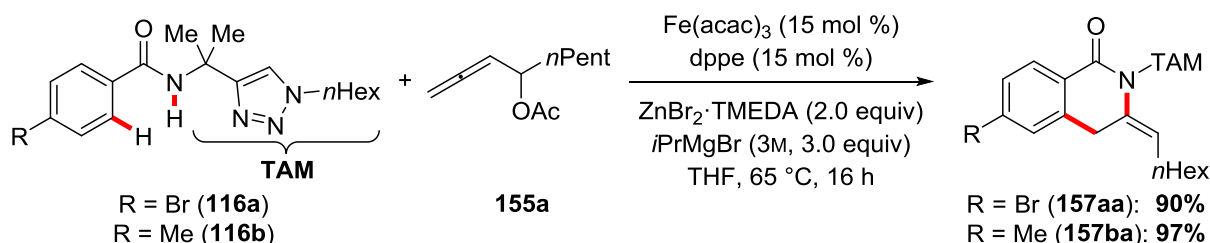
3 Results and Discussion

The homoallenyl acetate **155o**, and various 1,1- and 1,3-disubstituted allenyl acetates did not react under the optimized reaction conditions. Also, allenes having two substituents in the α -position to the acetate leaving group failed in the desired transformation.



Scheme 3.23: Unsuccessful allenyl acetates.

Interestingly, changing the modular nature of the triazole group from the triazolylmethyl amide (TAH) to the *gem*-dimethyl substituted TAM directing group enabled the synthesis of non-aromatic *exo*-methylene dihydroisoquinolones **157** (Scheme 3.24). A representative scope with TAM benzamides **116** was established by J. Mo.^[155] Benzamides bearing a methyl- (**116b**) or a bromo-substituent (**116a**) in the 4-position, delivered the desired products **157aa** and **157ba** in excellent yields.



Scheme 3.24: Iron-catalyzed C-H/N-H annulations with TAM benzamides **116**.

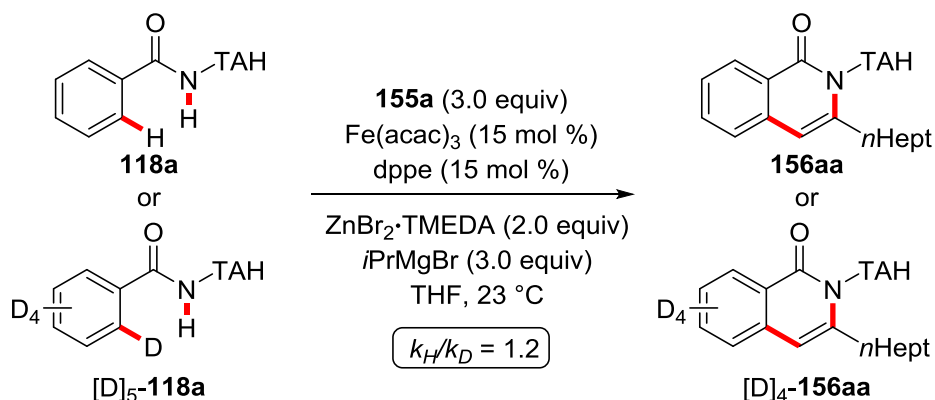
3.3.3 Mechanistic Studies

To gain a better understanding of the reaction, mechanistic experiments were performed by J. Mo, including *i*) intermolecular competition experiments between electron-rich and electron-deficient TAH benzamides, *ii*) reactions with the isotopically-labelled TAH substrate [D]₅-**118a** and allene **155a**, and *iii*) the determination of a kinetic isotope effect (KIE) by independent reactions using *in situ* React-IR measurement or an intermolecular KIE by performing a one-pot reaction.

These experiments showed that

- electron-deficient benzamides react preferentially as compared to electron-rich ones,
- when performing the reaction with isotopically-labelled [D]₅-**118a**, no deuterium was transposed from the former *ortho*-position onto the allene coupling partner,
- an intermolecular KIE of 1.2 was determined by independent reactions using *in situ* React-IR measurement and an intermolecular KIE of 1.5 by one-pot reaction.

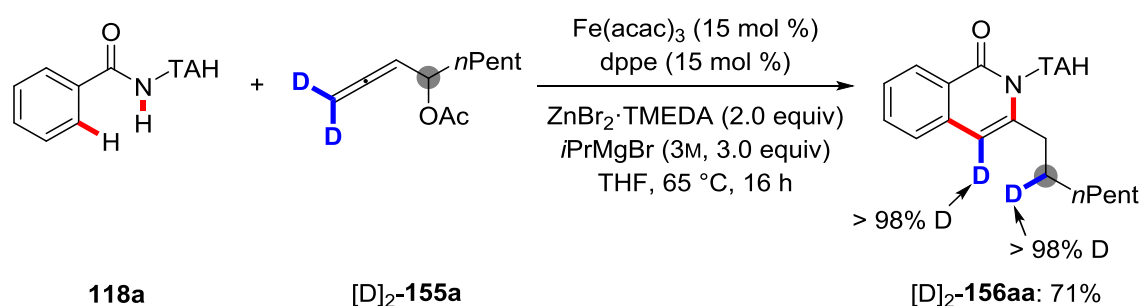
A similar kinetic isotope effect was studied by a comparison of the deuterated benzamide [D]₅-**118a** and the standard substrate **118a** in independent reactions, which were analyzed by ¹H NMR spectroscopy. Here, a minor KIE of $k_H/k_D = 1.2$ was observed, suggesting a facile C–H activation, which is not the rate-determining step of the overall reaction (Scheme 3.25).



Scheme 3.25: Intermolecular Kinetic Isotope Effect (KIE) by independent reactions.

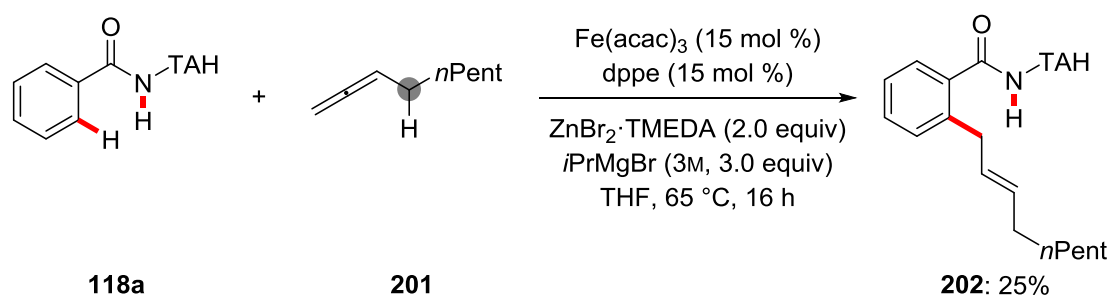
3 Results and Discussion

To gain more insight into the elementary steps of the reaction mechanism, we subjected the isotopically-labelled allene **[D]₂-155a** to the standard reaction conditions (Scheme 3.26). This reaction resulted in site-selective deuterium incorporation in the product **[D]₂-156aa**, in which a single deuterium was selectively transposed to the α -position of the acetate leaving group of allenyl acetate **155**. The same holds true, when reacting TAM benzamide **116** with **[D]₂-155a** as performed by J. Mo. Also here, deuterium incorporation, with >98% deuterium content, could be observed in the α -position of the allenyl acetate.^[155]



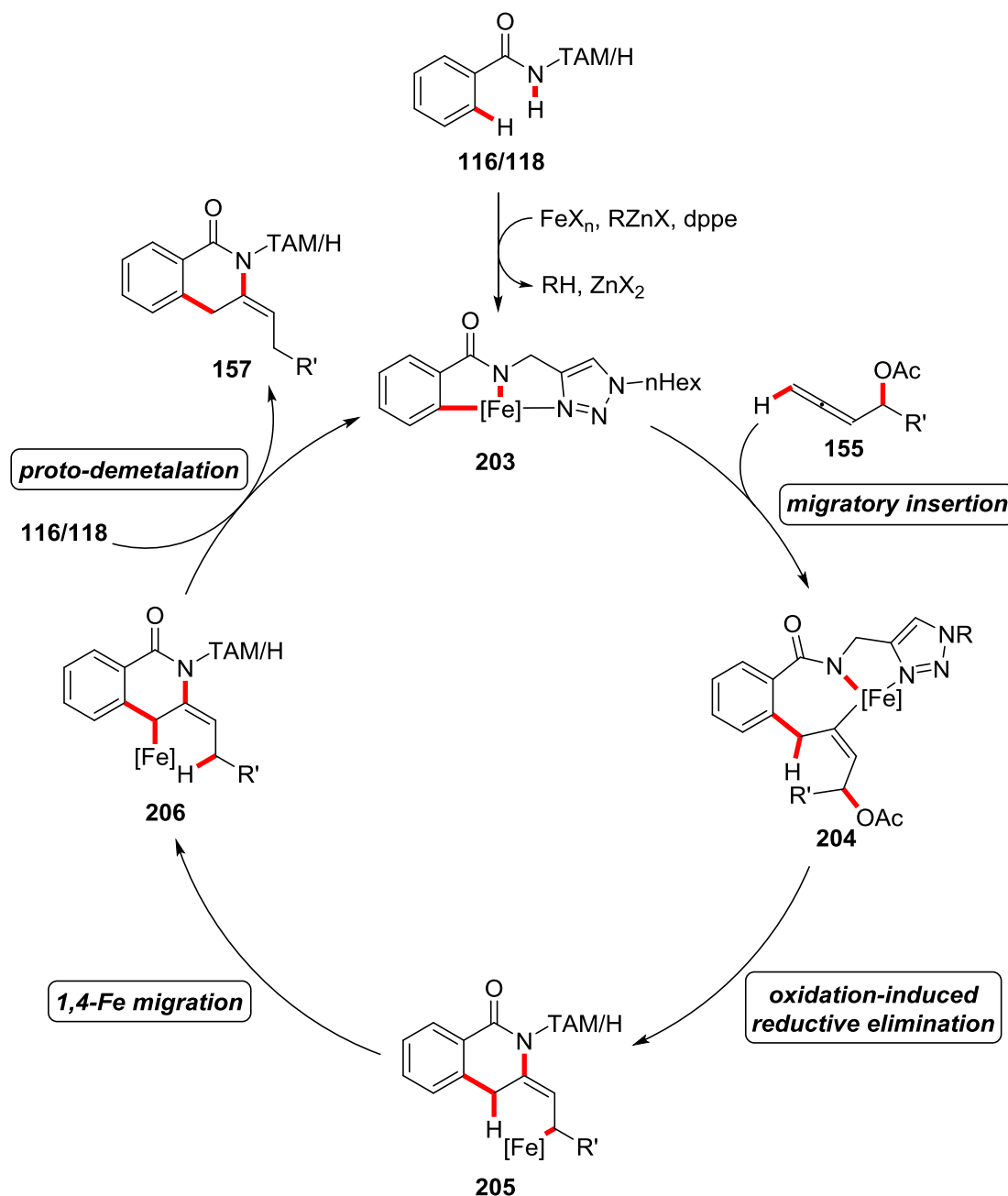
Scheme 3.26: Reaction of TAH benzamide **118** with the isotopically-labeled allene **[D]₂-155a**.

This observation highlights the key role of the C–O cleavage of the acetate within the external-oxidant-free allene annulation reaction. Furthermore, the importance of the acetate for the C–H/N–H annulation process was shown, when reacting the terminal allene **201** being devoid of the acetate leaving group (Scheme 3.27). Here, the reaction under otherwise identical reaction conditions led to the corresponding hydroarylation product **202**, in albeit low yield of 25%. Both findings are suggestive of an oxidation-induced reductive elimination being operative within the mechanistic pathway.



Scheme 3.27: Allene hydroarylation.

Finally, based on our mechanistic studies a catalytic cycle was proposed as depicted in Scheme 3.28.



Scheme 3.28: Plausible catalytic cycle.

The reaction is initiated by the facile C–H metalation to generate the iron species **203**. Subsequent allene coordination and migratory insertion leads to the formation of a key cyclometalated species **204**. Thereafter, oxidation-induced reductive elimination is proposed to yield the iron allyl complex **205**.

Based on the mechanistic findings, achieved by the reactions using allenyl acetate [D]₂-**155a**, where selective deuterium transposition was observed, we propose that the iron allyl complex **205** then undergoes a unique intramolecular C–H activation by 1,4-iron migration as the key step to generate the stabilized allylic-benzylic iron intermediate **206**. Finally, proto-demetalation with the amide motif either of TAM amide **116** or TAH amide **118** delivers the *exo*-methylene-3,4-dihydroisoquinolone **157**, which undergoes isomerization to **156**.

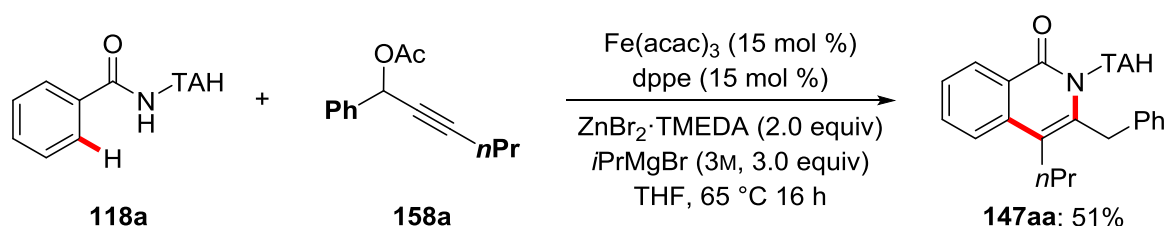
In summary, we have developed a powerful C–H/N–H annulation strategy using triazole-derived benzamides **116/118** and easily accessible allenyl acetates **155** for the expedient synthesis of differently substituted isoquinolones. Furthermore, the modular nature of the triazole group set the stage for the selective synthesis of *exo*-methylene 3,4-dihydroisoquinolones by using the removable TAM directing group. In addition, mechanistic studies enabled detailed insights into the catalyst's mode of action, as an unprecedented 1,4-iron migration was revealed to be operative within the catalytic cycle.

3.4 Iron-Catalyzed Annulation Reaction using Propargyl Acetates

The iron-catalyzed C–H/N–H annulation strategy using allenyl acetates (Chapter 3.3) highlighted the necessity of the acetate leaving group to serve as an internal oxidant. Therefore, in comparison to recent reports on iron-catalyzed annulation reactions, for the first time additional oxidants were not required to enable highly efficient C–H activation/annulation. Throughout the studies of this unique reactivity, we were pleased to find out that not only allenyl acetates **155**, but also propargyl acetates **158** served as suitable substrates to achieve a similar transformation being devoid of any external oxidants.^[157]

3.4.1 Optimization

Throughout the investigation of the C–H/N–H annulations reaction using allenyl acetates **155**, we also tested other unsaturated coupling partners. Hence, differently substituted propargyl acetates **158** were found to be suitable coupling partners for the synthesis of 3,4-disubstituted isoquinolones (Scheme 3.29).



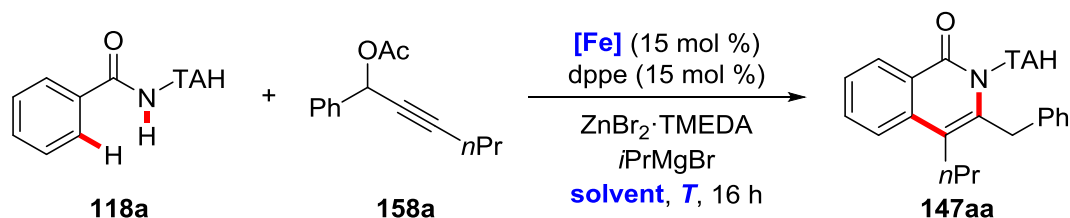
Scheme 3.29: Iron-catalyzed C–H/N–H annulation using propargyl acetate **158a**.

Hence, we commenced our studies by using propargyl acetate **158a** and TAH benzamide **118a** for the iron-catalyzed C–H/N–H annulation reaction for the synthesis of the 3,4-disubstituted isoquinolone **147aa** (Table 3.22). With the same conditions shown for the previous annulation protocol utilizing allenyl acetates, already promising conversions were observed (entry 1). We further optimized the C–H activation by testing various iron catalysts at different reaction temperatures. Conducting the reaction in the presence of Fe(acac)₃ at 40 °C or even at room temperature (entries 2 and 3) increased the yields to 73% and 64%, respectively. Also the biomass-derived^[31a, 158] solvent 2-MeTHF performed well in the reaction, delivering the desired product **147aa** in 60% yield (entry 4).

3 Results and Discussion

Furthermore, probing simple iron(II) and iron(III) sources revealed that all of them are active catalysts under the reaction conditions (entries 5–7). The best results were obtained with iron(II) chloride at ambient temperature (entry 7), affording product **147aa** with 81% yield (entry 4). This result could further be improved by lowering the amount of propargyl acetate from 3.0 to 2.0 equivalents, yielding the isoquinolone **147aa** with 85% (entry 8). In contrast, when performing the reaction within four hours (entry 9) or with a lower catalyst loading of 10 mol % (entry 10) decreased yields were observed. Lastly, no reaction took place in the absence of an iron catalyst (entry 14).

Table 3.22: Optimization of iron-catalyzed C–H activation with propargyl acetate **158a**.^[a]



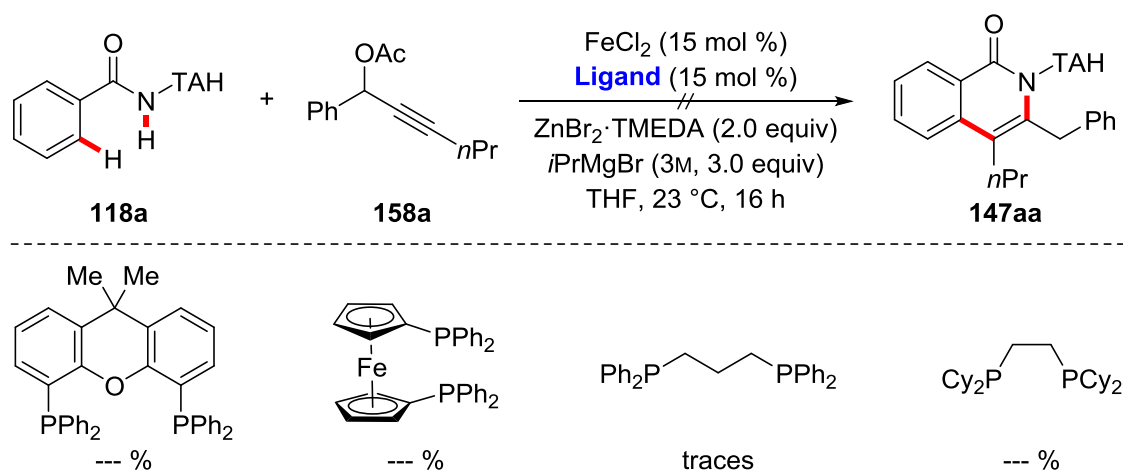
Entry	[Fe]	Solvent	<i>T</i> / °C	Yield / %
1	Fe(acac) ₃	THF	65	51
2	Fe(acac) ₃	THF	40	73
3	Fe(acac) ₃	THF	23	64 ^[b]
4	Fe(acac) ₃	2-MeTHF	23	60
5	Fe(dbm) ₃	THF	23	58
6	FeCl ₃	THF	23	69
7	FeCl ₂	THF	23	81
8	FeCl ₂	THF	23	85 ^[c]
9	FeCl ₂	THF	23	58 ^[d]
10	FeCl ₂	THF	23	42 ^[e]

3 Results and Discussion

Entry	[Fe]	Solvent	T / °C	Yield / %
11	FeCl ₂	THF	40	80
12	FeCl ₂	THF	65	75
13	FeCl ₂	2-MeTHF	23	56
14	---	THF	23	--- ^[f]

^[a] Reaction conditions: **118a** (0.30 mmol), **158a** (0.90 mmol), [Fe] (15 mol %), dppe (15 mol %), ZnBr₂·TMEDA (0.60 mmol), *i*PrMgBr (3M, 0.90 mmol), THF (0.80 mL), T, 16 h, ^[b] 24 h; ^[c] 2.0 equiv **158a** instead of 3.0; ^[d] 4 h; ^[e] FeCl₂ (10 mol %); ^[f] without [Fe].

As the use of dppe as the ligand was mandatory to achieve reasonable conversion in the iron-catalyzed C–H/N–H annulation reaction using allenyl acetates,^[155] we again reinvestigated the role of the ligand (Scheme 3.30). Unfortunately, when other phosphorous-based bidentate ligands, such as xantphos, dppf, dppp or dcype were employed, no reaction was observed, proving the importance of dppe as the ligand of choice.



Scheme 3.30: Tested bidentate phosphine ligands.

Further aspects that needed to be considered included the role of the zinc salt and the Grignard reagent, as those can have distinct effects on the reaction. As shown in earlier reports on iron-catalyzed C–H arylation reactions by NAKAMURA^[107, 109c, 110] and YOSHIKAI,^[109b] Ph₂Zn generated *in situ* from PhMgBr and ZnCl₂·TMEDA was suggested to be important to achieve the C–H transformation, while other organometallic additives proved to be ineffective.

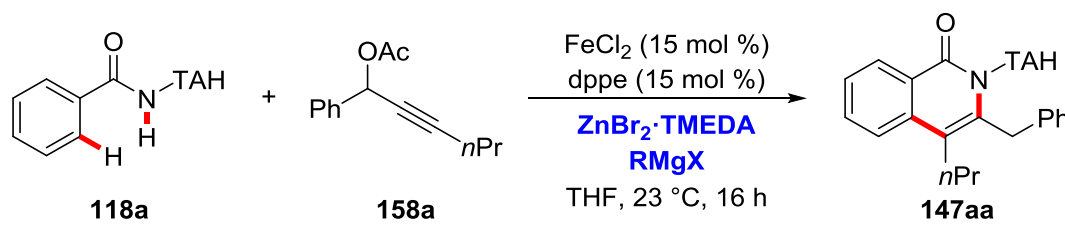
3 Results and Discussion

Also, the use of Grignard reagent as a reducing agent to generate low-valent iron species or organometallic species is possible.

Therefore, we tried to investigate to what extent those two additives are necessary to achieve an effective C–H transformation (Table 3.23). Lowering the amount of zinc salt led to a slightly decreased yield of the desired product (entry 2). More importantly, lowering the amount of the Grignard *i*PrMgBr from 3.0 to 1.5 equivalents, resulted in poor conversions, where only 21% of product **147aa** could be isolated (entry 3). This result seems plausible, due to the fact that probably 1.0 equivalent of *i*PrMgBr is needed for the deprotonation of the acidic amide N–H bond. Therefore, there is not enough PhMgBr left, required for the formation of Ph₂Zn.

The use of zinc salts lacking the additional TMEDA ligand, such as ZnBr₂ and ZnCl₂, also performed well in the reaction, affording the desired product **147aa** in 67% and 70%, respectively (entries 4 and 5). Interestingly, when employing the zinc additive in substoichiometric amounts (entries 6 and 7), that is with 0.2 or 0.5 equivalents, the yields dropped dramatically. Apparently, it is necessary to use equal amounts of the zinc salt, in order to generate stoichiometric amounts of an organometallic zinc species, which facilitates the reaction. Nevertheless, the exact role of the zinc additive as well as the Grignard reagent is not yet understood exactly. For the Grignard reagent, also other reagents, such as CyMgCl, showed comparable results to *i*PrMgBr, and high yields of **147aa** were obtained (entry 8).

Table 3.23: Test of zinc salts and Grignard reagents.^[a]



Entry	[Zn] / equiv	RMgX / equiv	Yield / %
1	ZnBr ₂ ·TMEDA / 2.0	<i>i</i> PrMgBr / 3.0	85
2	ZnBr ₂ ·TMEDA / 1.0	<i>i</i> PrMgBr / 3.0	70
3	ZnBr ₂ ·TMEDA / 1.0	<i>i</i> PrMgBr / 1.5	21
4	ZnBr ₂ / 2.0	<i>i</i> PrMgBr / 3.0	67

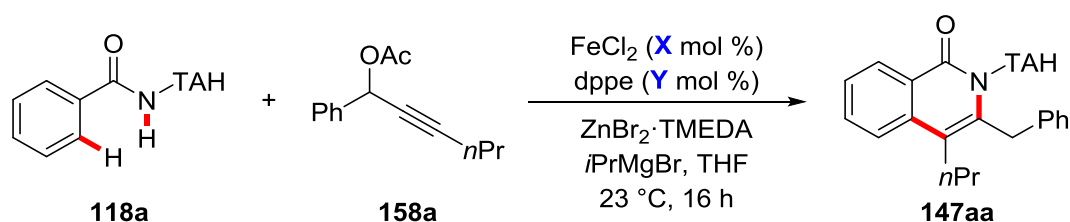
3 Results and Discussion

Entry	[Zn] / equiv	RMgX / equiv	Yield / %
5	ZnCl ₂ / 2.0	<i>i</i> PrMgBr / 3.0	70
6	ZnBr ₂ ·TMEDA / 0.5	<i>i</i> PrMgBr / 3.0	38
7	ZnBr ₂ ·TMEDA / 0.2	<i>i</i> PrMgBr / 3.0	16
8	ZnBr ₂ ·TMEDA / 2.0	CyMgCl / 3.0	86

^[a] Reaction conditions: **118a** (0.30 mmol), **158a** (0.60 mmol), FeCl₂ (15 mol %), dppe (15 mol %), [Zn], Grignard, THF (0.80 mL), 23 °C, 16 h.

Next, a job plot analysis regarding the metal-to-ligand ratio was conducted in detail (Table 3.24). A ratio of [Fe]:L of 1:1 seemed to perform best in the desired C–H activation, as for other metal-to-ligand ratios slightly decreased yields were observed.

Table 3.24: Investigation of the metal-to-ligand ratio.



Entry	X	Y	[Fe]:L ratio	Yield / %
1	15	7.5	2:1 (1:0.5)	74
2	15	15	1:1	85
3	15	30	1:2	70
4	15	60	1:4	72

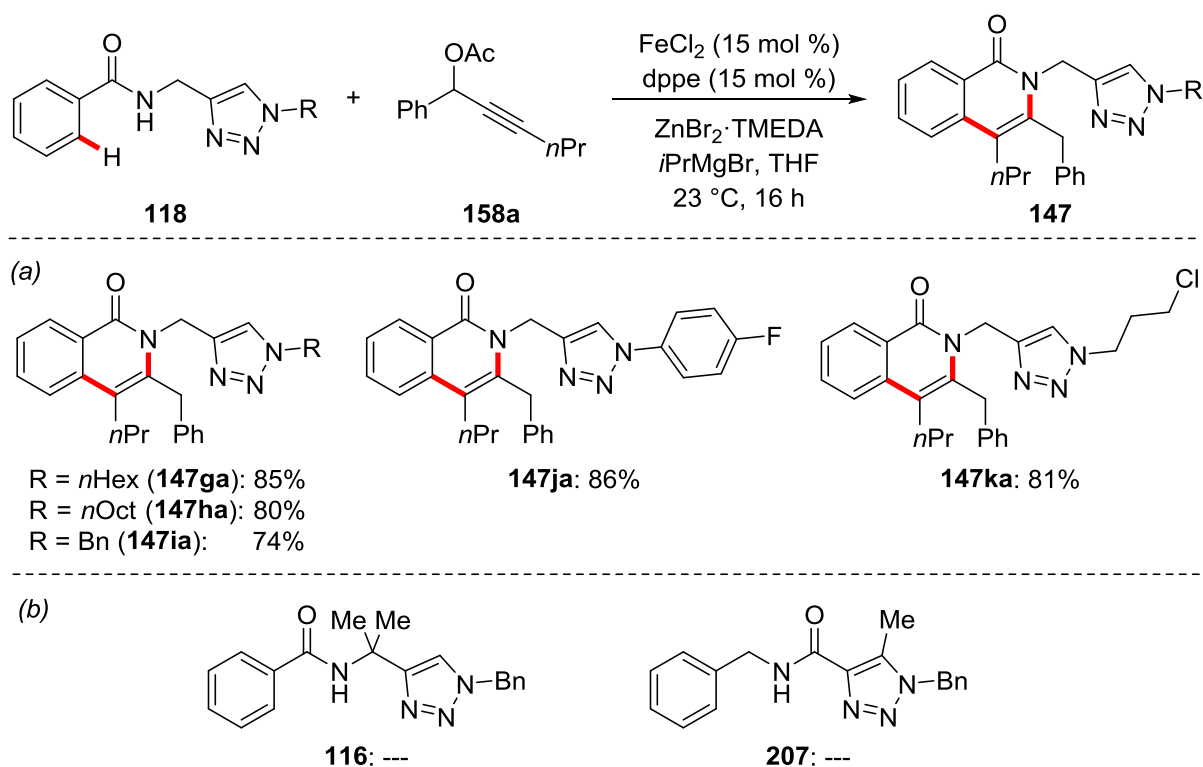
^[a] Reaction conditions: **118a** (0.30 mmol), **158a** (0.60 mmol), FeCl₂ (**X** mol %), dppe (**Y** mol %), ZnBr₂·TMEDA (2.0 equiv), *i*PrMgBr (3.0 M in 2-MeTHF, 0.90 mmol), THF (0.80 mL), 23 °C, 16 h.

3.4.2 Scope of the Iron-Catalyzed C–H Annulation

With the optimized reaction conditions in hand, we tested its applicability regarding the triazole-derived TAH benzamide substrates **118**, bearing different *N*-substituents on the triazole moiety.

3 Results and Discussion

We were pleased to find that structural variations, such as alkyl-, benzyl-, aryl- and even the reactive alkyl chloride group, were well tolerated, delivering the desired isoquinolones **147ga-ka** in very good yields (Scheme 3.31a). Unfortunately, the *gem*-dimethyl triazole-based TAM benzamide **116** and the tri-substituted 1,2,3-triazole-based TST benzamide **207** were not suitable substrates. Also amides bearing the 8-AQ auxiliary delivered the corresponding isoquinolone only in small amounts.



Scheme 3.31: Impact of the *N*-substituent of triazole moiety on the annulations reaction; Reaction conditions: **118** (0.30 mmol), **158a** (0.60 mmol), FeCl₂ (15 mol %), dppe (15 mol %), ZnBr₂·TMEDA (2.0 equiv), *i*PrMgBr (3.0 M in 2-MeTHF, 0.90 mmol), THF (0.80 mL), 23 °C, 16 h.

Thereafter, we explored the scope with differently decorated benzamides (Table 3.25). To our delight, the developed catalyst was applicable to a variety of decorated amides **118**, delivering the desired products **147** in overall high yields. Besides the unsubstituted TAH benzamide **118a** (entry 1), which was smoothly converted, various *para*-, *meta*- and *ortho*-substituted benzamides were tested. Having a substituent in *para*-position, a wide range of electron-withdrawing and electron-donating groups, including thioether, methoxy as well as dimethyl amino (entries 2-7), were well-tolerated.

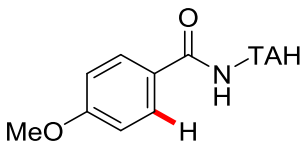
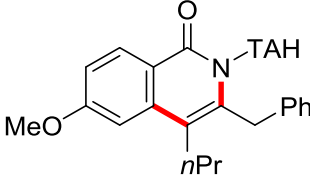
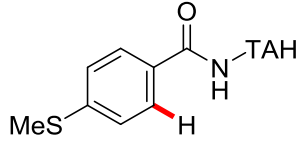
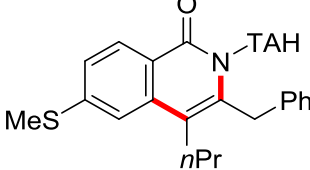
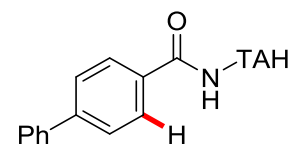
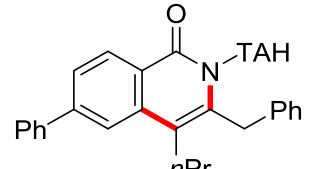
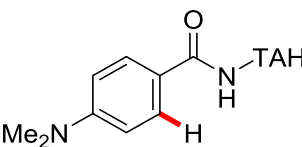
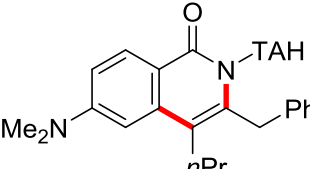
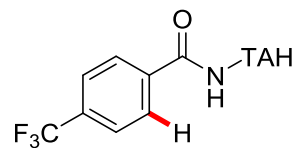
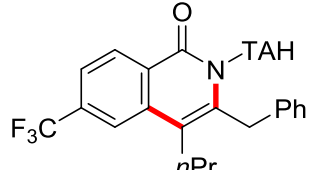
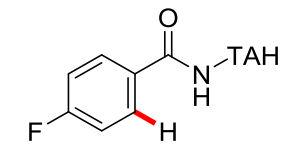
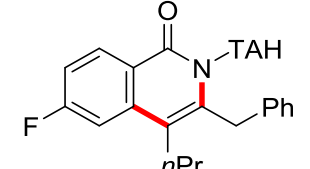
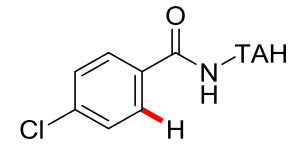
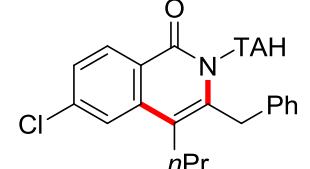
3 Results and Discussion

Likewise, halides in the 4-position were efficiently converted with moderate to excellent yields, giving rise to synthetically useful isoquinolones **147ra-ua** (entries 8-11). Having a fluoro substituent in 2-position, the reaction afforded the desired product **147ca** in a moderate yield of 56%, whereas the 2-methyl benzamide **118b** did not perform well in the reaction, presumably due to the increased steric bulk in the *ortho*-position of the starting material (entries 12 and 13). Good yields with a high level of regioselectivity could be observed for the *meta*-substituted benzamides **118d-f** and **118v-w**. Only with a fluoro group in the 3-position, we observed a mixture of regioisomers (entry 15). Furthermore, thiophenyl- (**118x**) and naphthyl- (**118y**) derived benzamides were suitable substrates in the present transformation, yielding the desired products in moderate yield (entries 19 and 20). To our delight, the olefinic C(sp²)-H bond of cyclohexene carboxamide **118z** was identified to be reactive under the optimized reaction conditions (entry 21), showing that also non-aromatic alkenyl amides can be suitable substrates for the iron-catalyzed C-H/N-H annulation reactions.

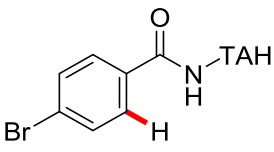
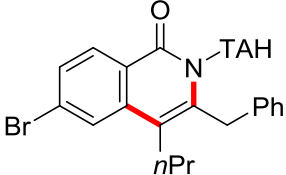
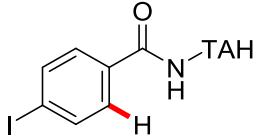
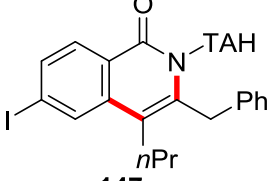
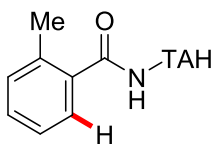
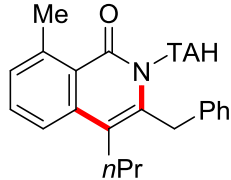
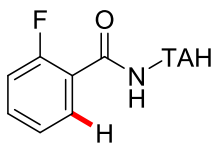
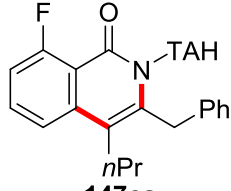
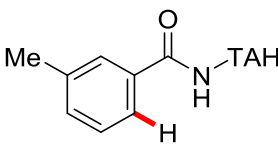
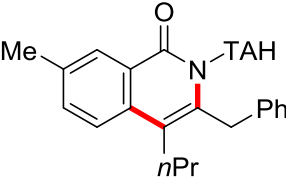
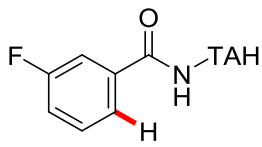
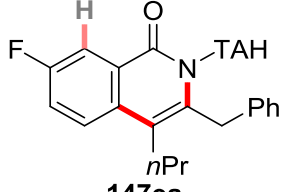
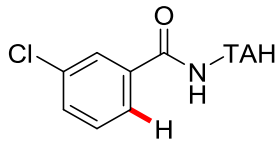
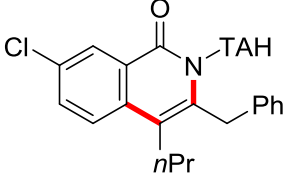
Table 3.25: Scope of benzamides **118** for the iron-catalyzed C-H/N-H alkyne annulations.^[a]

Entry	118	147	Yield / %
1	 118a	 147aa	85
2	 118l	 147la	75

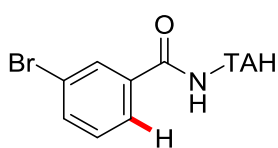
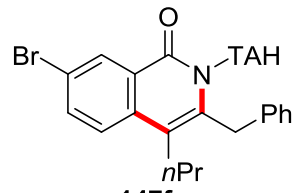
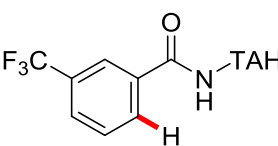
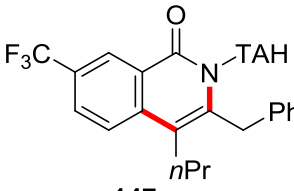
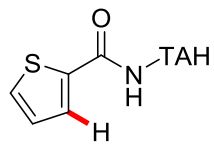
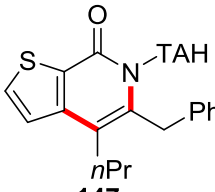
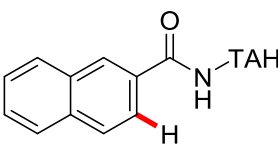
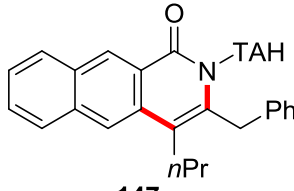
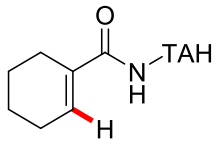
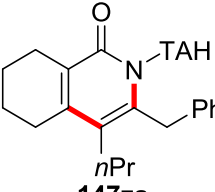
3 Results and Discussion

Entry	118	147	Yield / %
3	 <p>118m</p>	 <p>147ma</p>	81
4	 <p>118n</p>	 <p>147na</p>	80
5	 <p>118o</p>	 <p>147oa</p>	68
6	 <p>118p</p>	 <p>147pa</p>	66
7	 <p>118q</p>	 <p>147qa</p>	87
8	 <p>118r</p>	 <p>147ra</p>	73
9	 <p>118s</p>	 <p>147sa</p>	74

3 Results and Discussion

Entry	118	147	Yield / %
10	 <p>118t</p>	 <p>147ta</p>	71
11	 <p>118u</p>	 <p>147ua</p>	59
12	 <p>118b</p>	 <p>147ba</p>	34
13	 <p>118c</p>	 <p>147ca</p>	58
14	 <p>118d</p>	 <p>147da</p>	78
15	 <p>118e</p>	 <p>147ea</p>	79 (1.1:1) ^[b]
16	 <p>118v</p>	 <p>147va</p>	55

3 Results and Discussion

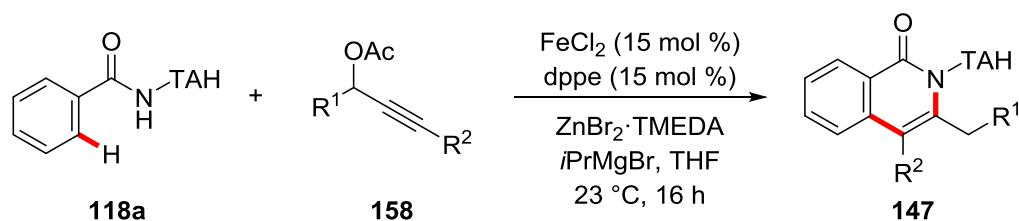
Entry	118	147	Yield / %
17	 <p>118f</p>	 <p>147fa</p>	72
18	 <p>118w</p>	 <p>147wa</p>	66
19	 <p>118x</p>	 <p>147xa</p>	48
20	 <p>118y</p>	 <p>147ya</p>	56
21	 <p>118z</p>	 <p>147za</p>	22

^[a] Reaction conditions: **118** (0.30 mmol), **158a** (0.60 mmol), FeCl₂ (15 mol %), dppe (15 mol %), ZnBr₂·TMEDA (2.0 equiv), *i*PrMgBr (3M, 3.0 equiv), THF (0.80 mL), 23 °C, 16 h; ^[b] ratio of regio isomers, combined yield of isolated products.

With this broad applicability towards differently substituted benzamides in hand, we became interested in exploring the scope regarding the propargyl acetates **155** (Table 3.26).

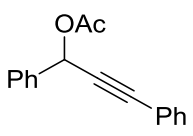
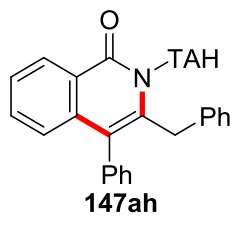
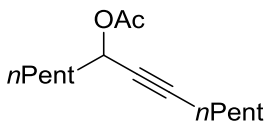
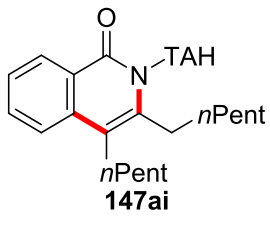
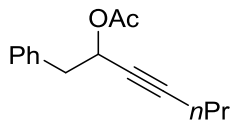
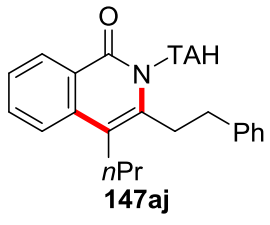
3 Results and Discussion

Table 3.26: Scope of propargyl acetates **158** for the iron-catalyzed C–H/N–H alkyne annulations.^[a]



Entry	158	147	Yield / %
1	<p>158b</p>	<p>Ar = 4-MeC₆H₄: 147ab</p>	86
2	<p>158c</p>	<p>Ar = 4-CF₃C₆H₄: 147ac</p>	53
3	<p>158d</p>	<p>Ar = 4-ClC₆H₄: 147ad</p>	78
4	<p>158e</p>	<p>Ar = 4-BrC₆H₄: 147ae</p>	88
5	<p>158f</p>	<p>147af</p>	35
6	<p>158g</p>	<p>147ag</p>	58

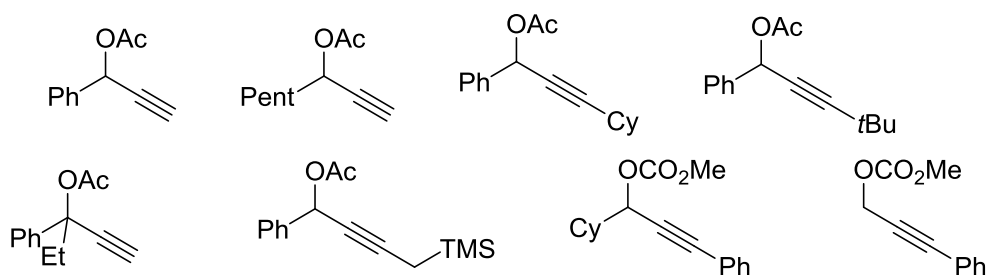
3 Results and Discussion

Entry	158	147	Yield / %
7	 <p>158h</p>	 <p>147ah</p>	78
8	 <p>158i</p>	 <p>147ai</p>	64
9	 <p>158j</p>	 <p>147aj</p>	39

^[a] Reaction conditions: **118a** (0.30 mmol), **158** (0.60 mmol), FeCl₂ (15 mol %), dppe (15 mol %), ZnBr₂·TMEDA (2.0 equiv), *i*PrMgBr (3M, 3.0 equiv), THF (0.80 mL), 23 °C, 16 h.

The reaction proceeded well for all employed substrates shown in Table 3.26. Propargyl acetates, bearing a substituent in the 4-position of the aryl moiety (entries 1-4), such as methyl, trifluoromethyl, chloro or bromo, were efficiently converted to the desired isoquinolones **147ab-ae** with 53-88% yield. Substitution of the phenyl by cyclohexyl substituent afforded the isoquinolone **147a** with a moderate yield of 58% (entry 6). Otherwise, different substitution pattern on the propargyl acetate, e.g. diphenyl or di-*n*-pentyl (entries 7 and 8) proved to be applicable, giving good conversions. Substitution of the phenyl group by a benzyl group in α -position of the acetate led to a decreased yield of 39% (entry 9).

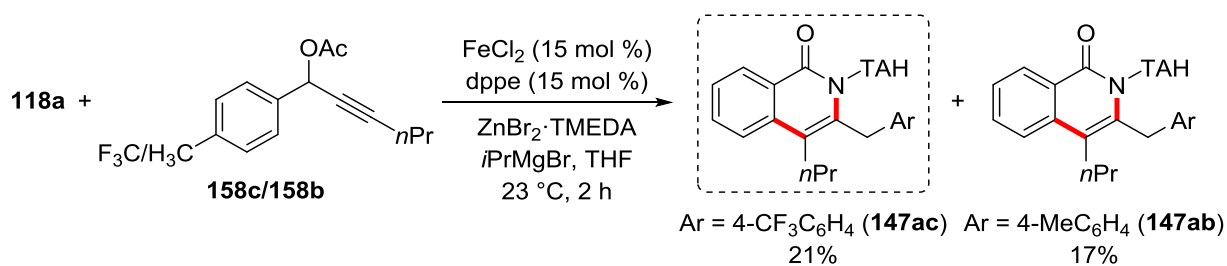
As shown in Scheme 3.32, a number of different propargyl acetates and carbonates were tested in the iron-catalyzed annulation reaction, which gave less satisfactory results.



Scheme 3.32: Unsuccessful alkyne substrates.

3.4.3 Mechanistic Studies

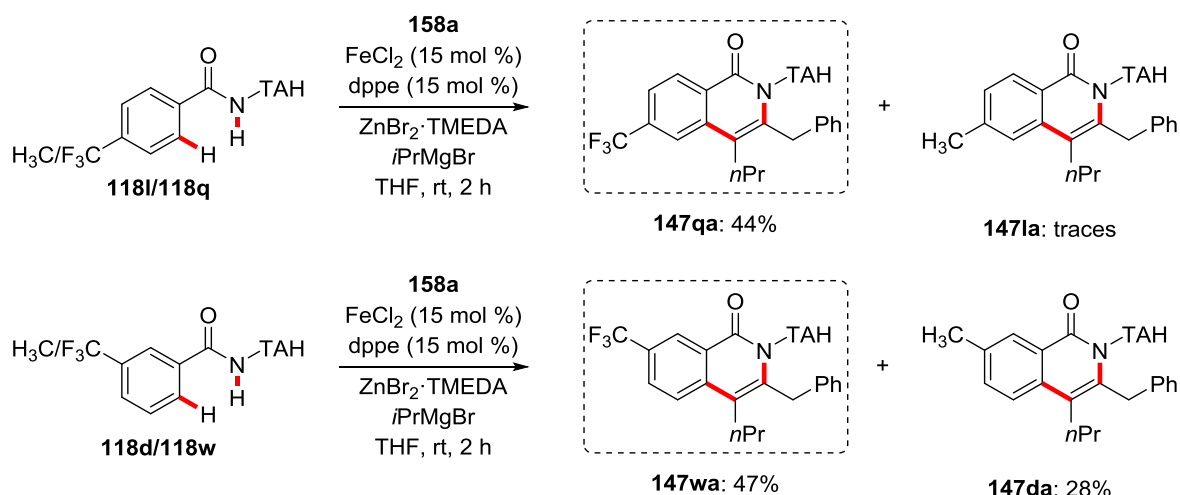
After establishing the scope and limitations of the iron-catalyzed C–H/N–H annulations of TAH benzamides **118**, mechanistic studies were conducted to gain insights into the mode of action. Competition experiments between the electron-rich and electron-deficient propargyl acetates **158b** and **158c** were conducted (Scheme 3.33). Here, no preference for one over the other alkyne substrates could be observed, showing that the electronic nature of the alkyne substrates **158** on the reaction is negligible.



Scheme 3.33: Competition experiments between electron-rich and electron-deficient propargyl acetates **158**.

However, intermolecular competition experiments highlighted the inherently higher reactivity of the electron-deficient arenes **118q** and **118w**, either with an electron-withdrawing group in *para*- or *meta*-position (Scheme 3.34), which can be rationalized by a ligand-to-ligand hydrogen transfer (LLHT) mechanism to be operative.^[29b, 159]

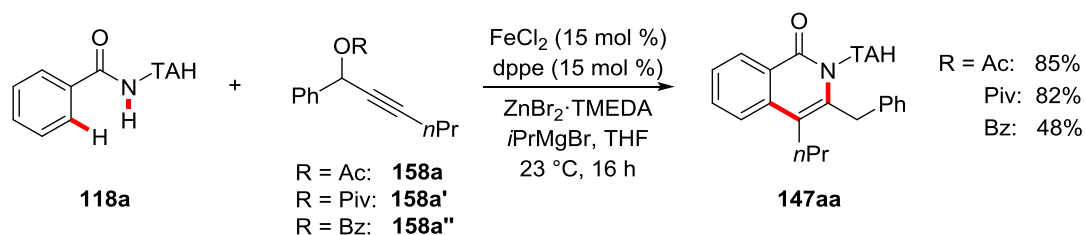
3 Results and Discussion



Scheme 3.34: Competition experiments between electron-rich and electron-deficient benzamides **118**.

Since during the course of the reaction the acetate C–O bond of the propargyl acetate needs to be cleaved, we investigated the effect of the leaving group on the reaction. Therefore, we tested various propargyl alcohol derivatives **158**, bearing different carboxyl leaving groups, such as acetate, pivalate and benzoate (Scheme 3.35).

Whereas the aliphatic carboxylates acetate and pivalate gave comparable results yielding the desired product **147aa** in 85% and 82%, respectively, the benzoate-derived alkyne was less effective, affording **147aa** in moderate yield of 48%.



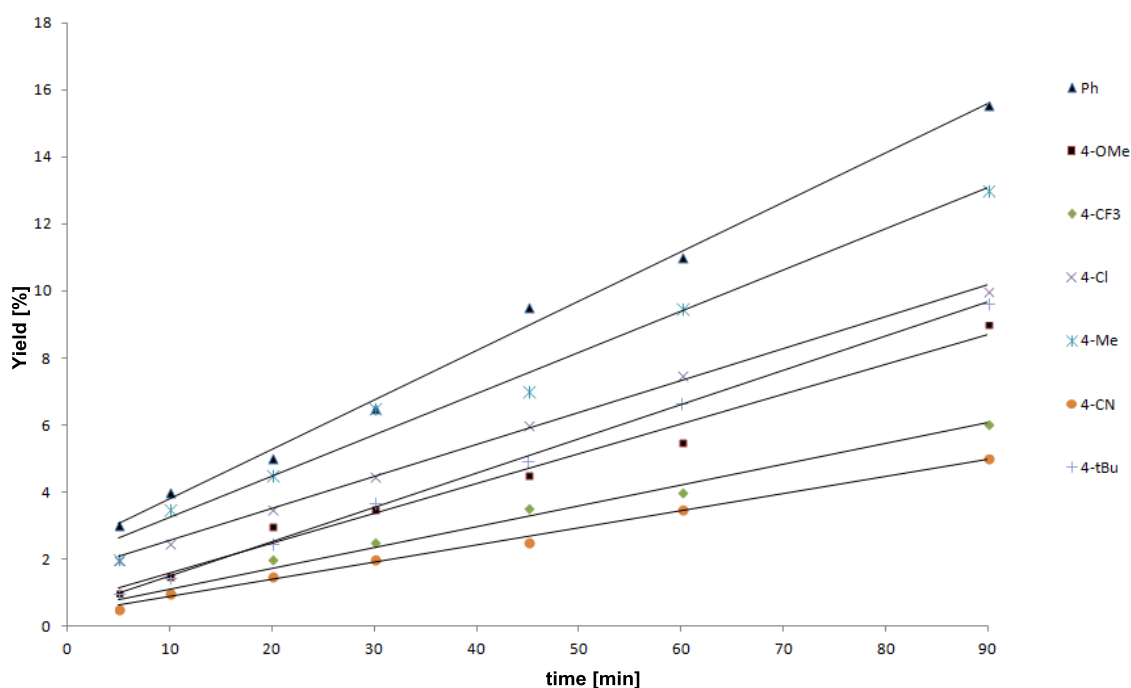
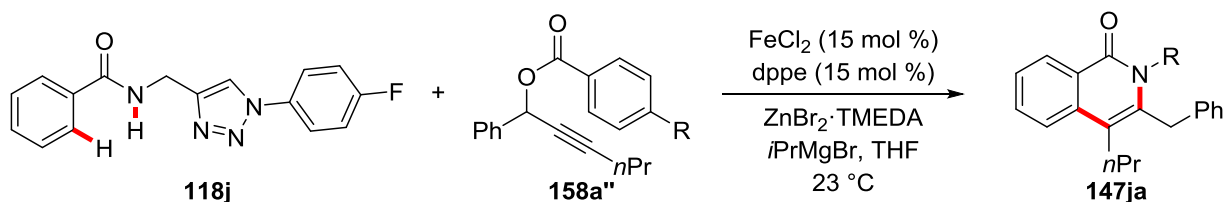
Scheme 3.35: Effect of the leaving group for the iron-catalyzed C–H/N–H annulations.

Obviously, there is a significant difference, whether aliphatic carboxylates or the benzoate served as the internal oxidant. Here, either steric or electronic factors could potentially play a major role with regard to the leaving group abilities.

To gain further insights into the electronic effect of the benzoate-derived alkynes, an initial rate analysis for the reaction of TAH benzamide **118j** with alkynes **158a''**, bearing different substituents in the *para*-position of the benzoyl group was conducted (Scheme 3.36).

3 Results and Discussion

In general, electron-rich benzoates are showing higher initial rates than the electron-deficient ones. The results obtained, were not fully conclusive because e.g. the substrate with the more electron-withdrawing chloro group is reacting faster than the ones with electron-donating methoxy and *tert*-butyl groups.



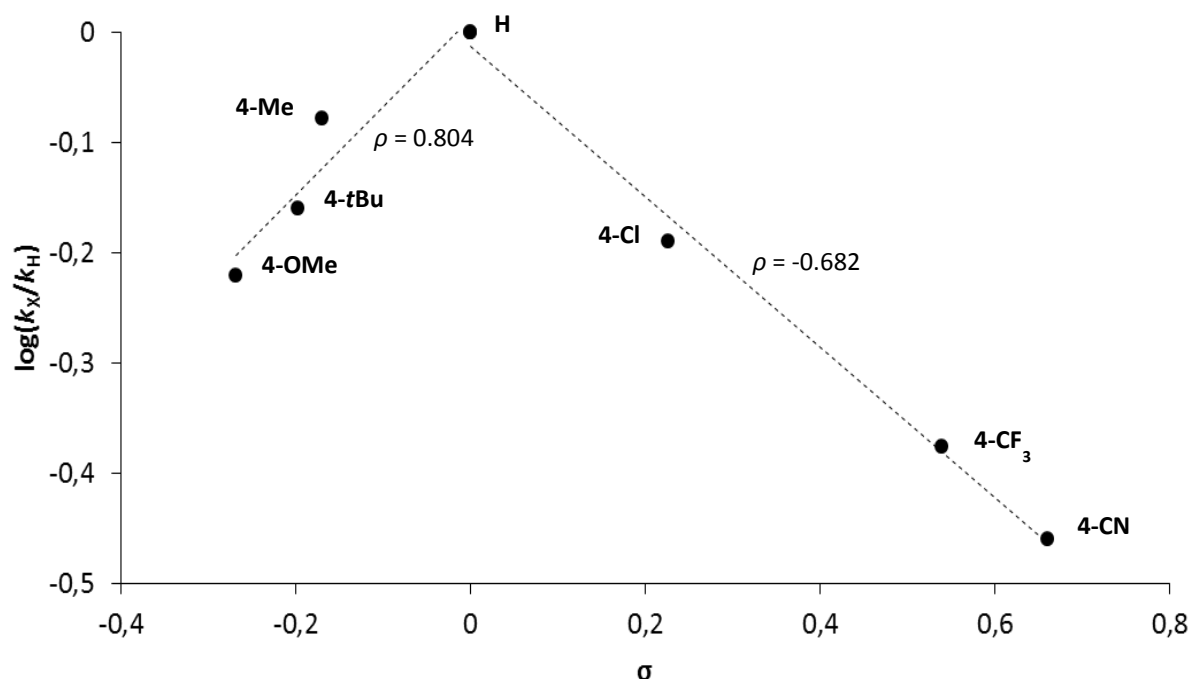
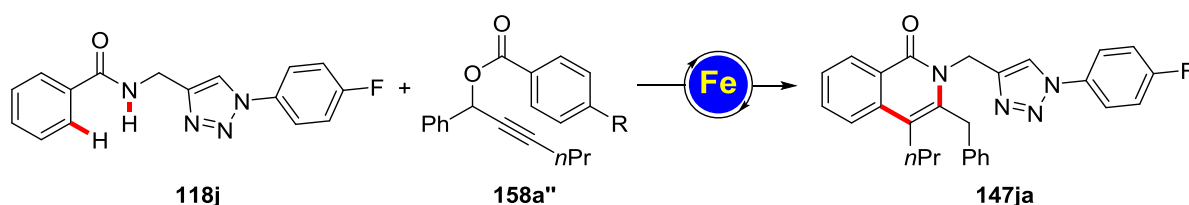
Scheme 3.36: Initial rates for the iron-catalyzed C–H/N–H alkyne annulations using differently *para*-substituted propargyl benzoates.

In order to elucidate electronic effects on the iron-catalyzed C–H/N–H annulation, a Hammett-type analysis was done (Scheme 3.37). The initial rates $\log(k_X/k_H)$ of the employed propargyl benzoates relative to the unsubstituted alkyne, given by the reaction of **118j** with **158a''** are correlated with the *sigma* values of the *para*-substituents of the benzoyl moiety on the alkyne.^[160]

Here, a concave downwards deviation was observed, showing a positive slope for electron-donating substituents exhibiting negative sigma values and a negative slope for electron-withdrawing substituents exhibiting positive sigma values.

3 Results and Discussion

These results indicate a change in the rate-limiting step, depending on the electronic nature of substituent, whereas the inherent mechanism should not change throughout the reaction.^[160-161] However, not only inductive electronic effects should be considered, also other factors causing secondary effects on the reaction kinetics such as steric or mesomeric effects can affect the course or kinetics of the reaction.

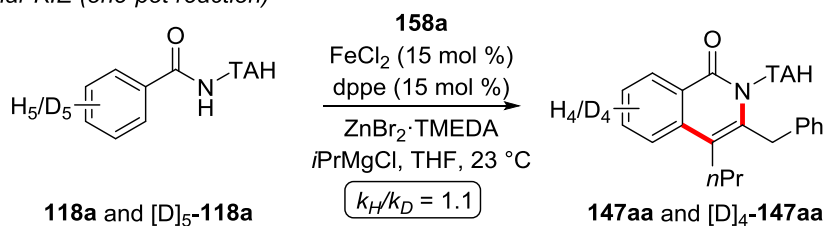


Scheme 3.37: Hammett-plot correlation for the iron-catalyzed C–H/N–H alkyne annulations using differently *para*-substituted propargyl benzoates.

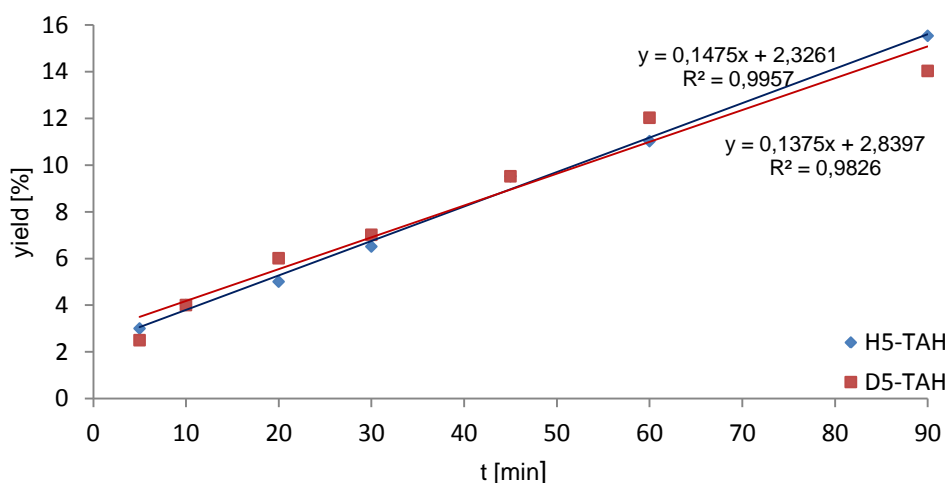
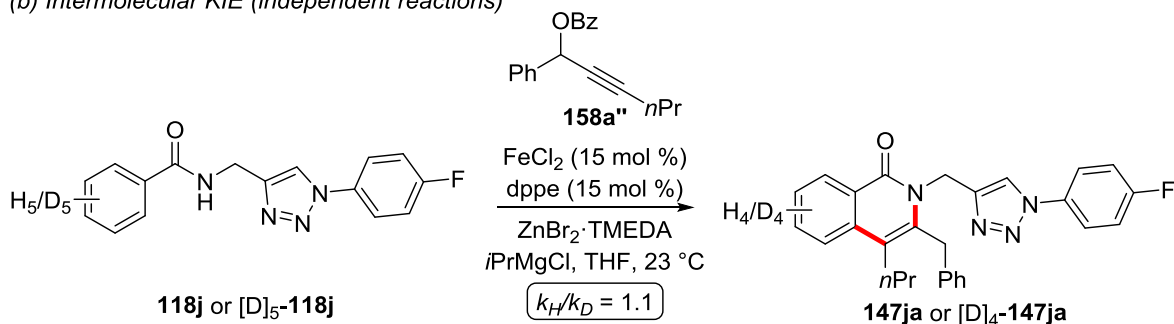
Intermolecular kinetic isotope effects were conducted to figure out if the C–H activation event is the rate-determining step. The comparison of the inherent reactivity of [D]₅-**118a** and **118** in a one-pot reaction revealed a KIE of $k_H/k_D = 1.1$ (Scheme 3.38a). In addition, a further KIE experiment was conducted, using [D]₅-**118j** or **118j** and alkyne **158''** in independent reactions (Scheme 3.38b). Also here, a minor primary KIE of $k_H/k_D = 1.1$ was observed. Both findings indicate that the C–H bond cleavage is not the rate-determining step of this reaction; rather an elementary step that includes the involvement of the alkyne substrate, such as the migratory insertion or reductive elimination steps that should be rate-determining.

3 Results and Discussion

(a) Intermolecular KIE (one-pot reaction)



(b) Intermolecular KIE (independent reactions)



Scheme 3.38: Kinetic isotope effect studies.

In addition, detailed computational studies were conducted by Dr. J.C.A. de Oliveira to gain further insights into the reaction mechanism, which will be discussed later on by a plausible catalytic cycle.

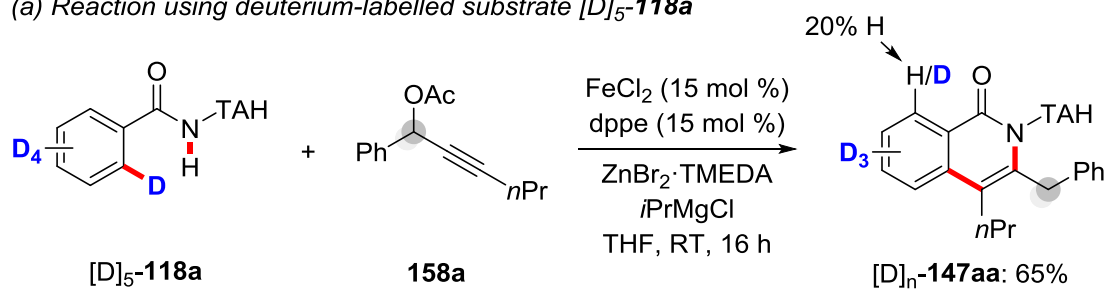
Within the recently presented external-oxidant-free allene annulation process (see Chapter 3.3),^[155] studies with deuterium-labelled $[D]_2$ -**155a** revealed that a single deuterium was selectively transposed to the α -position of the allenyl acetate **155**, thereby highlighting the key role of the C–O/C–H cleavage in the course of an oxidative-induced reductive elimination.

Intrigued by this result and further investigations on the mechanism of the iron-catalyzed C–H/N–H annulations, we became interested to elucidate the source of protons for the C–O cleavage of the acetates leaving group in propargyl acetates **158** (Scheme 3.39).

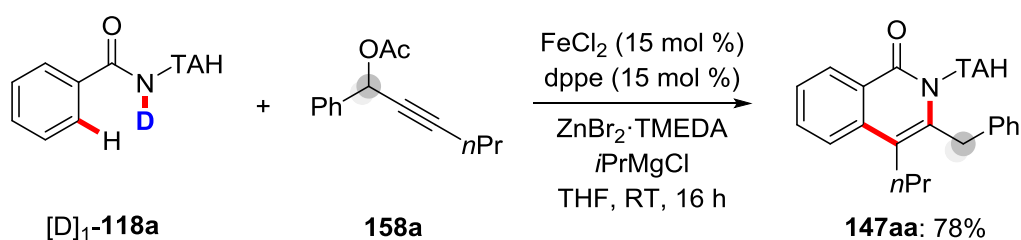
To find out what a possible source of protons could be, several reactions using isotopically-labelled substrates were conducted. First, running the reaction with the deuterium-labelled TAH benzamide [D]₅-**118a** under otherwise identical conditions, 65% of [D]_n-**147aa** could be isolated (Scheme 3.39a). Here, no deuterium was incorporated in the benzylic position, the position where the acetate leaving group was attached to. However, H/D scrambling (~20%) at the *ortho*-position of the corresponding isoquinolone [D]_n-**147aa** could be observed, illustrating the reversible nature of the C–H activation event. When the specifically labelled N–D amide [D]₁-**118a** was used, again no deuterium incorporation was observed (Scheme 3.39b), likely because this proton is readily removed by the Grignard reagent. Also, when the standard reaction was conducted in the presence of isotopically-labelled Grignard [D]₆-*i*PrMgBr (Scheme 3.39c), [D]₈-THF (Scheme 3.39d) or [D]₂₀-dppe (Scheme 3.39e), no deuterium was transposed to the product. To finally elucidate where the proton for the terminal proto-demetalation step originates from, it is necessary to perform further studies.

3 Results and Discussion

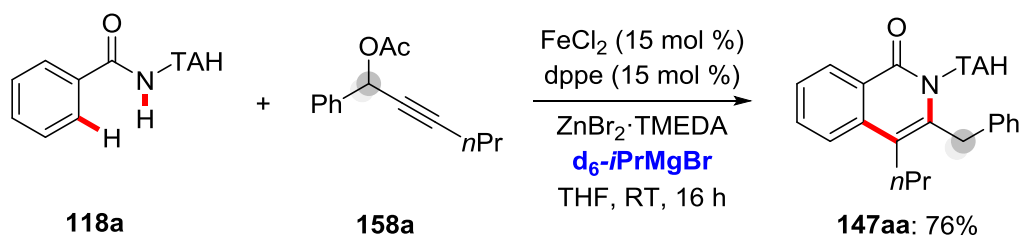
(a) Reaction using deuterium-labelled substrate $[D]_5$ -**118a**



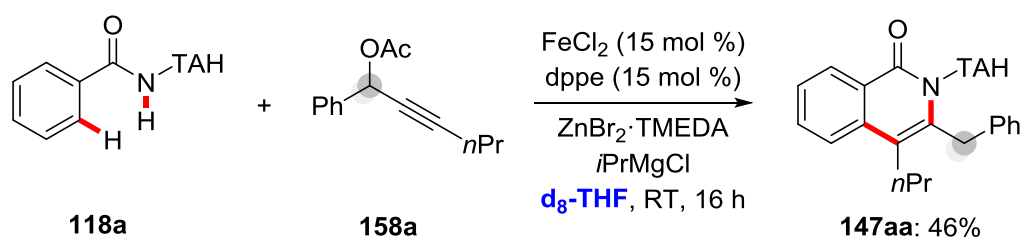
(b) Reaction using deuterium-labelled substrate $[D]_1$ -**118a**



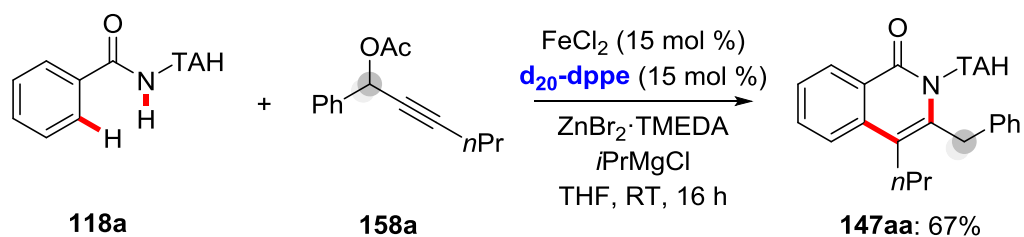
(c) Reaction using deuterium-labelled Grignard reagent d_6 -*iPrMgBr*



(d) Reaction using deuterium-labelled solvent d_8 -THF

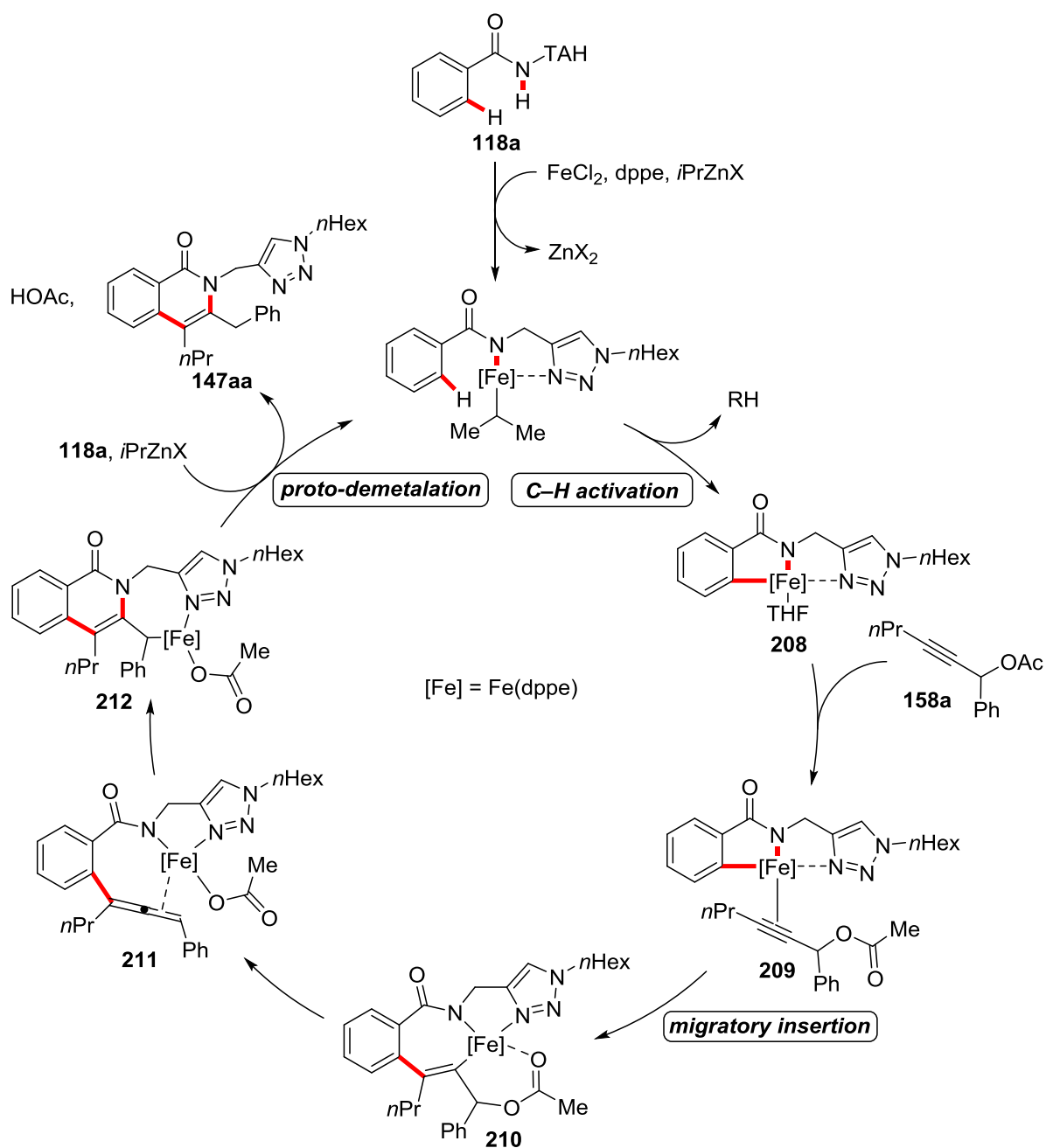


(e) Reaction using deuterium-labelled ligand d_{20} -dppe



Scheme 3.39: Mechanistic studies using isotopically-labelled substrates.

Finally, based on these findings and detailed computational analysis a plausible catalytic cycle is shown in Scheme 3.40. Here, the iron(II)-catalyzed C–H/N–H annulation sequence is proposed to be initiated by facile C–H activation *via* LLHT to generate the cyclometalated iron species **208** (Scheme 8). After coordination of substrate **158a**, intermediate **209** undergoes fast migratory insertion to deliver complex **210**, which then forms the energetically favourable allene intermediate complex **211** in an exergonic pathway by cleavage of the C–O bond of the acetate leaving group. Thereafter, insertion of the allene moiety into the N–Fe bond forms the annulated iron complex **212** and, finally proto-demetalation releases the desired isoquinolone product **147aa** and regenerates the active iron catalyst.



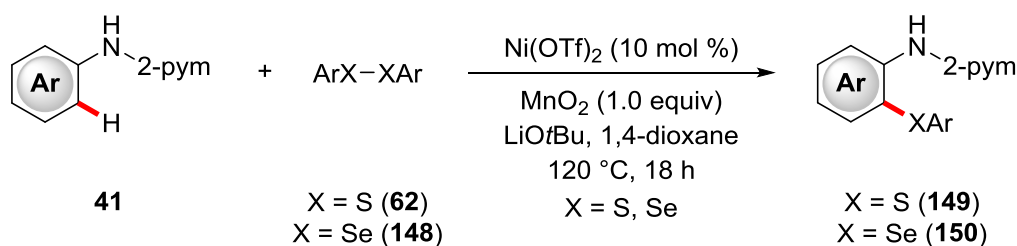
Scheme 3.40: Plausible catalytic cycle.

In summary, we have reported on a C-H activation/annulation strategy using propargyl acetates **158** with the aid of a catalyst based on earth-abundant iron at ambient temperature and in the absence of any external oxidants. The versatile iron catalyst provided expedient access to differently substituted isoquinolones **147**. Furthermore, detailed mechanistic studies using DFT computation, supported by unprecedented Mössbauer spectroscopy provided key insights into the catalysts mode of action, highlighting the importance of high spin iron(II) complexes to be involved as the crucial intermediates in the developed C-H functionalization manifold.

4 Summary and Outlook

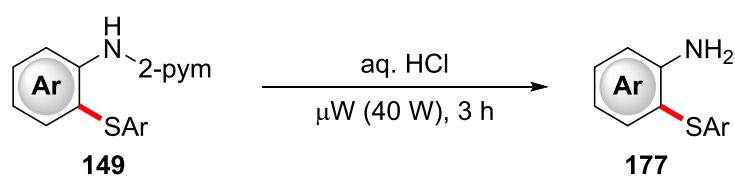
During the last decade, transition metal-catalyzed C–H functionalizations have emerged as a powerful and reliable tool for the efficient construction of C–C and C–Het bonds, which allowed for novel sustainable and cost-efficient syntheses of key structural motifs for material science, medicinal chemistry and crop protection. Within this thesis, investigations have been devoted to the development of new methodologies for powerful C–H functionalizations based on sustainable, earth-abundant 3d transition metal catalysts.

In the first project, the nickel-catalyzed C–H chalcogenation of aniline derivatives **41** with diaryl dichalcogenides **62/148** was examined (Scheme 4.1). In contrast to the previously described protocols for the direct C–H thiolation employing bidentate directing groups, here a versatile nickel(II) catalyst set the stage for a robust strategy for C–H chalcogenations of electron-rich anilines bearing the monodentate pyrimidyl group.



Scheme 4.1: Nickel-catalyzed C–H chalcogenation of *N*-pyrimidyl anilines **41**.

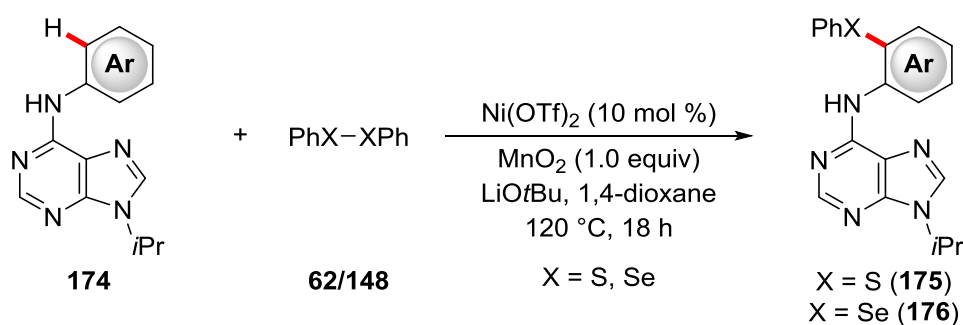
Thus, easily accessible diaryl disulfides and diselenides allowed for the efficient synthesis of *ortho*-thiolated and -selenylated 2-pyrimidyl anilines **149** and **150**. Due to the outstanding robustness of the nickel(II) catalyst high levels of chemo- and site-selectivity were achieved, which was further reflected by tolerating various functional groups, such as sensitive halides. Furthermore, the traceless removal of the pyrimidyl directing group enabled the synthesis of 2-aminothiophenols **177**, which represent important key scaffolds for various drug molecules (Scheme 4.2).



Scheme 4.2: Removal of the pyrimidyl group.

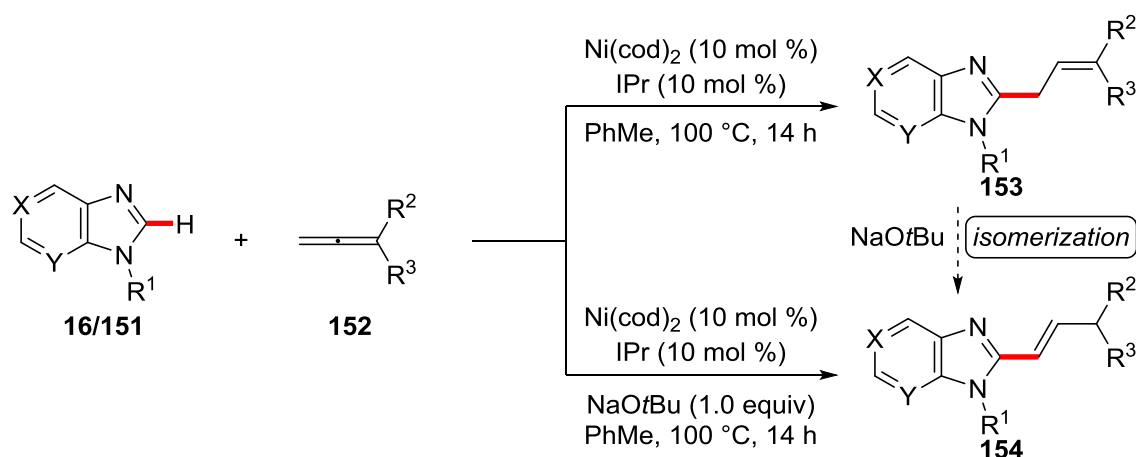
Mechanistic studies revealed the C–H activation step to be rate-determining and provided strong evidence for a SET-type process to be involved in the catalytic cycle.

The C–H activation was not restricted to *N*-pyrimidyl anilines, but could also be extended to purine derivatives. Thus, a small set of purine derivatives **174** were efficiently converted to their thiolated and selenylated analogs **175/176**, showing the importance of the envisioned C–H chalcogenation reaction, allowing access to biologically important substrate classes (Scheme 4.3).



Scheme 4.3: Nickel-catalyzed C–H chalcogenation of purine derivatives **174**.

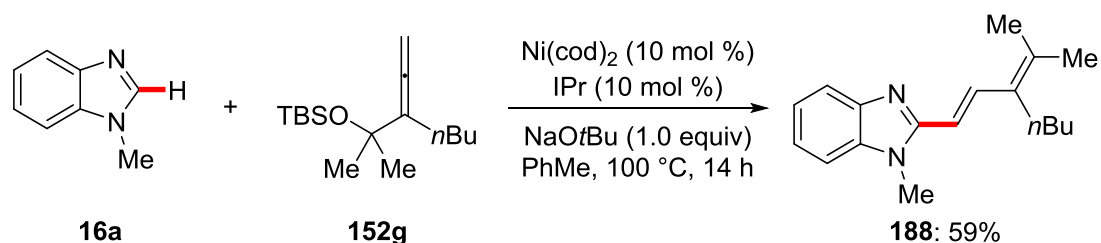
In the second project, we developed the first nickel(0)-catalyzed hydroheteroarylation of allenes **152** using biologically relevant heterocycles (Scheme 4.4). Thus, a full control in regio- and chemo-selectivity allowed for the synthesis of a variety of allylated and alkenylated imidazole and purine derivatives **153** and **154**.



Scheme 4.4: Nickel-catalyzed hydroheteroarylation of allenes.

Initial investigations on a catalyst consisting of $\text{Ni}(\text{cod})_2$ and the N-heterocyclic carbene ligand IPr enabled the highly efficient C–H allylation of imidazole and purine derivatives **16** or **151**, respectively. Interestingly, in the presence of NaOtBu as the base a switch in selectivity from allylation to alkenylation was observed, highlighting the versatile hydroarylation protocol for the introduction of either allyl or alkenyl groups. This result was further confirmed by the base-mediated isomerization of **153** to the thermodynamically more stable alkenylated imidazole **154**, which is in full agreement with computational DFT studies.

With a versatile nickel catalyst in hand, the nickel(0)-catalyzed C–H alkenylation protocol could further be applied to dienylation through C–H activation and concurrent C–O cleavage (Scheme 4.5) and the late-stage diversification of caffeine-derived diphosphodiesterase inhibitors.

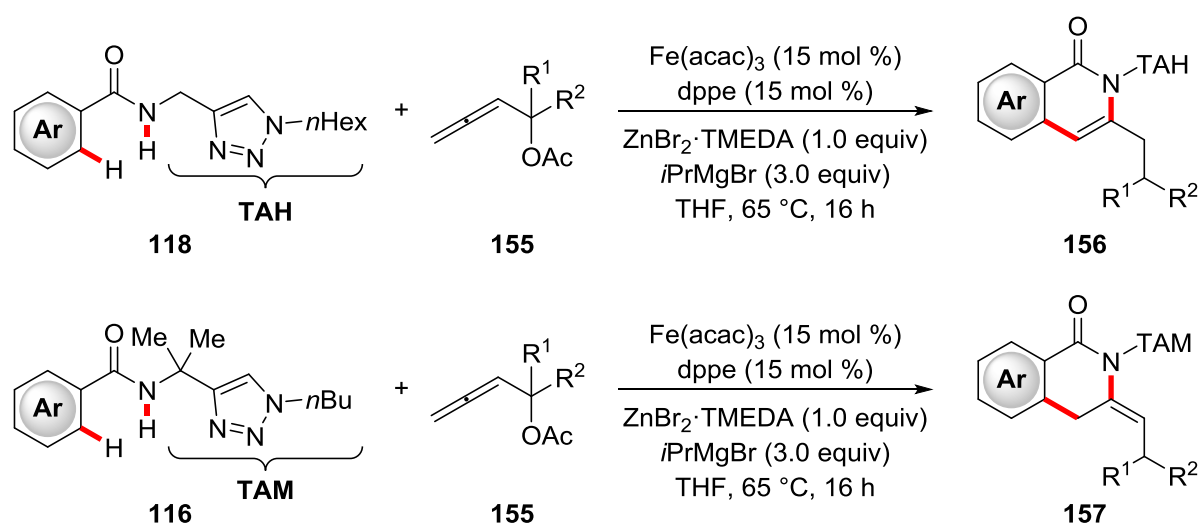


Scheme 4.5: Nickel-catalyzed dienylation of *N*-methyl benzimidazole **16a**.

Overall, this protocol represents a useful method for the C–H allylation, alkenylation, and dienylation of biologically relevant and synthetically meaningful imidazole and purine derivatives.

4 Summary and Outlook

In the third project, an iron-catalyzed C–H/N–H annulations strategy for the synthesis of isoquinolones **156** or *exo*-methylene isoquinolones **157** with triazole-derived benzamides **118/116** using allenyl acetates **155** was realized (Scheme 4.6). While other protocols relied on the use of external oxidants, such as expensive DCIB or DCP, to achieve efficient reactions, the envisioned methodology represents the first oxidative iron-catalyzed C–H activation/annulation under external oxidant-free reaction conditions.

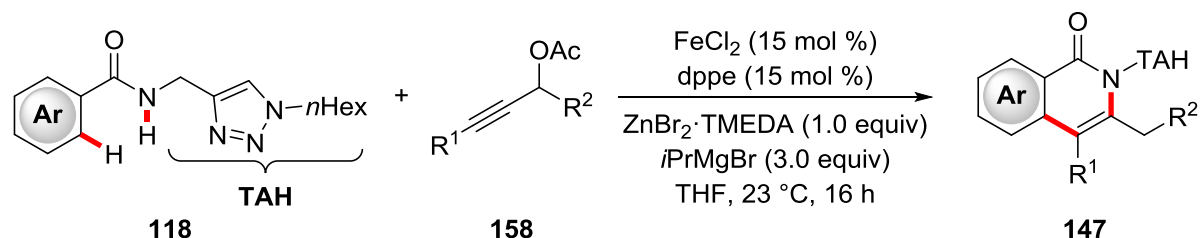


Scheme 4.6: Iron-catalyzed C–H/N–H annulations with allenyl acetates **155**.

After considerable investigations on the reaction conditions, the modular nature of the triazole group enabled the synthesis of isoquinolones **156** and *exo*-methylene isoquinolones **157**, respectively. Thus, differently decorated allenes **155** as well as aromatic TAH/M amides **118/116** delivered the desired products with high levels of positional selectivity control, fully tolerating reactive functional groups, including synthetically meaningful aryl and alkyl chlorides. Furthermore, the versatile C–H activation/annulation proceeded through facile C–H cleavage even at room temperature, and the modular nature of the triazole group allowed for the synthesis of *NH*-free isoquinolones. Additionally, detailed mechanistic studies, including H/D-exchange experiments, KIE studies, competition experiments and reactions using isotopically-labelled allenyl acetates were conducted, revealing an unprecedented 1,4-iron migration to be involved in the C–H activation manifold.

4 Summary and Outlook

Within the last project, we developed an iron-catalyzed C–H activation/annulations with propargyl acetates **158** for the synthesis of 3,4-disubstituted isoquinolones **147** (Scheme 4.7). Here, we became interested in delineating its catalytic nature in more detail by extensive theoretical and experimental analysis.



Scheme 4.7: Iron-catalyzed C–H/N–H annulations with alkynes **158**.

To this end, mechanistic studies, including competition experiments, KIE studies and DFT computation were conducted, revealing a plausible catalytic C–H activation manifold. Furthermore, Mössbauer spectroscopic analysis, conducted by my colleagues provided detailed mechanistic insights into the catalyst's mode of action, supporting the presence of high spin iron(II) species as crucial intermediates in the C–H functionalization manifold.

5 Experimental Part

5.1 General Remarks

All reactions involving moisture- or air-sensitive reagents or products were performed under an inert atmosphere of nitrogen using pre-dried glassware and standard Schlenk techniques. If not otherwise noted yields refer to isolated compounds, estimated to be >95% pure as determined by ^1H NMR and GC analysis.

Vacuum

A Vacuubrand RZ 6 vacuum pump was used throughout the course of this thesis. The pressure was measured to be 0.7 mbar (uncorrected value).

Melting Points

Melting points were measured on a Stuart[®] Melting Point Apparatus SMP3 from Barloworld Scientific. Values are uncorrected.

Chromatography

Analytical thin layer chromatography (TLC) was performed on silica gel 60 F₂₅₄ aluminium sheets from MERCK. Plates were either visualized under irradiation at 254 nm or 365 nm or developed by treatment with a potassium permanganate solution followed by careful warming. Chromatographic purification was accomplished by flash column chromatography on MERCK Geduran[®] silica gel, grade 60 (40–63 μm , 70–230 mesh ASTM).

Gas Chromatography

Monitoring of reaction process *via* gas chromatography or coupled gas chromatography-mass spectrometry was performed using a 7890 GC-system with/without mass detector 5975C (Triple-Axis-Detector) or a 7890B GC-system coupled with a 5977A mass detector, both from Agilent Technologies[®].

Infrared Spectroscopy

Infrared (IR) spectra were recorded using a Bruker[®] Alpha-P ATR spectrometer. Liquid samples were measured as film and solid samples neat. Spectra were recorded in the range from 4000 to 400 cm^{-1} . Analysis of the spectral data were carried out using Opus 6. Absorption is given in wave numbers (cm^{-1}).

Nuclear Magnetic Resonance Spectroscopy

Nuclear magnetic resonance (NMR) spectra were recorded on Mercury Plus 300, VNMRS 300, Inova 500 and 600 from Varian[®], or Avance 300, Avance III 300 and 400, Avance III HD 400 and 500 from Bruker[®]. Chemical shifts are reported in δ -values in ppm relative to the residual proton peak or carbon peak of the deuterated solvent.

	¹ H NMR	¹³ C NMR
CDCl ₃	7.26	77.16
DMSO-d ₆	2.50	39.52

The following abbreviations are used to describe the observed multiplicities: s (singlet), d (doublet), t (triplet), q (quartet), p (pentet), h (hexet), hept (heptet), m (multiplet) or analogous representations. The coupling constants *J* are reported in Hertz (Hz). Analysis of the recorded spectra was carried out using MestReNova 10 software.

Mass Spectrometry

Electron ionization (EI) and EI high resolution mass spectra (HRMS) were measured on a time-of-flight mass spectrometer AccuTOF from JOEL. Electrospray ionization (ESI) mass spectra were recorded on an Io-Trap mass spectrometer LCQ from Finnigan, a quadrupole time-of-flight maXis from Bruker Daltonic or on a time-of-flight mass spectrometer microTOF from Bruker Daltonic. ESI-HRMS spectra were recorded on a Bruker Apex IV or Bruker Daltonic 7T, fourier transform ion cyclotron resonance (FTICR) mass spectrometer. The ratios of mass to charge (*m/z*) are indicated, intensities relative to the base peak (*I* = 100) are given in parentheses.

Solvents

Solvents for column chromatography were purified via distillation under reduced pressure prior to their use. All solvents for reactions involving moisture-sensitive reagents were dried, distilled and stored under inert atmosphere (Ar or N₂) according to following standard procedures:

Purified by solvent purification system (SPS-800, M. Braun): CH₂Cl₂, toluene, tetrahydrofuran, dimethylformamide, diethylether.

Dried and distilled over sodium/benzophenone: 1,4-dioxane, *o*-, *m*-, *p*-xylene, methanol.

Dried and distilled over CaH₂: 1,2-Dichloroethane.

Chemicals

Chemicals obtained from commercial sources with a purity >95% were used as received without further purification. The following compounds were known from the literature and were synthesized according to the previously known methods:

N-(pyrimidine-2-yl)anilines **41**,^[162] [D]₅-**41z**,^[163] disulfides **62b-d**,^[164] 1,2-dipropyl-disulfane **171**,^[164] *N*-methyl benzimidazoles **16e-f**,^[165] benzimidazoles **16b-d**,^[166] *N*-aryl benzimidazoles **16g-h** and **16l**,^[167] purines **151a-e**,^[168] 1-phenylimidazo[1,5-*a*]pyridine **16j**,^[169] 1-methyl-4,5-diphenyl-1*H*-imidazole **16i**,^[170] [D]₁-caffeine **16k**,^[171] 1,1-disubstituted allenes **152a-e**,^[172] 1,1-disubstituted allene **152g**,^[173] the NHC ligands IPr,^[174] IPr*,^[175] and IPr*OMe,^[176] TAM- and TAH benzamides **116** and **118**,^[125, 135] allenyl acetates **155a-155l**,^[177] propargyl acetates **158a-j**.^[178]

5.2 General Procedures

General Procedure A: Nickel(II)-Catalyzed C–H Thiolation of Pyrimidyl Anilines

Anilines **41** (0.5 mmol, 1.0 equiv.), disulfides **62** (0.6 mmol, 1.2 equiv.), Ni(OTf)₂ (17.8 mg, 10.0 mol %), MnO₂ (43.5 mg, 0.5 mmol, 1.0 equiv) and LiOtBu (80.0 mg, 1.0 mmol, 2.0 equiv) were placed in a 25 ml Schlenk tube and equipped with a septum. The tube was degassed and purged with N₂ three times. 1,4-Dioxane (1.5 ml 0.33 M) was added, and the tube was then placed into an oil bath and the mixture was stirred at 120 °C for 18 h. At ambient temperature, EtOAc (5 ml) was added and the reaction mixture was filtrated through a small pad of silica. The filtrate was concentrated under reduced pressure and purified by flash column chromatography (*n*hexane/EtOAc) to afford the desired product **149**.

General Procedure B: Nickel(II)-Catalyzed C–H Selenylation of Pyrimidyl Anilines

Anilines **41** (0.5 mmol, 1.0 equiv.), diselenides **148** (0.6 mmol, 1.2 equiv.), Ni(OTf)₂ (17.8 mg, 10.0 mol %), MnO₂ (43.5 mg, 0.5 mmol, 1.0 equiv) and LiOtBu (80.0 mg, 1.0 mmol, 2.0 equiv) were placed in a 25 ml Schlenk tube and equipped with a septum. The tube was degassed and purged with N₂ three times. 1,4-Dioxane (1.5 ml) was added, and the tube was then placed into an oil bath and the mixture was stirred at 120 °C for 18 h. At ambient temperature, EtOAc (5 ml) was added and the reaction mixture was filtrated through a small pad of silica. The filtrate was concentrated under reduced pressure and purified by flash column chromatography (*n*hexane/EtOAc) to afford the desired product **150**.

General Procedure C: Cleavage of the Pyrimidyl Group

ortho-Thiolated *N*-pyrimidyl anilines **149** were dissolved in aqueous HCl (37%; 1.0 mL per 0.2 mmol substrate) in a microwave vial. The vial was capped and heated up to 150 °C (40 W) for 3 h in the microwave oven. The reaction mixture was allowed to cool to ambient temperature and poured into EtOAc (10–40 mL), and saturated aqueous Na₂CO₃ solution was added until the pH was adjusted to 7. The aqueous layer was extracted with EtOAc (3 × 40 mL), the combined organic layers were dried over Na₂SO₄ and concentrated under reduced pressure. Purification by flash column chromatography (*n*hexane/EtOAc) afforded the desired product **177**.

General Procedure D: Nickel(0)-Catalyzed Hydroarylation of Allenes with Allyl-Selectivity

A suspension of heteroarene **16/151** (0.50 mmol, 1.0 equiv), allene **152** (0.80 mmol, 1.6 equiv), Ni(cod)₂ (13.8 mg, 50 μmol, 10.0 mol %) and IPr (19.4 mg, 50 μmol, 10.0 mol %) in toluene (1.5 mL) was stirred at 100 °C for 14 h under a nitrogen atmosphere. At ambient temperature, EtOAc (5 mL) was added. The solvent was removed *in vacuo* and the remaining residue was purified by column chromatography on silica gel to afford the desired product **153/186**.

General Procedure E: Nickel(0)-Catalyzed Hydroarylation of Allenes with Alkenyl-Selectivity

A suspension of heteroarene **16/151** (0.50 mmol, 1.0 equiv), allene **152** (0.80 mmol, 1.6 equiv), Ni(cod)₂ (13.8 mg, 50 μmol, 10.0 mol %), IPr (19.4 mg, 50 μmol, 10.0 mol %) and NaOtBu (0.50 mmol, 1.0 equiv) in toluene (1.5 mL) was stirred at 100 °C for 14 h under a nitrogen atmosphere. At ambient temperature, EtOAc (5 mL) was added. The solvent was removed under reduced pressure and the remaining residue was purified by column chromatography on silica gel to afford the desired product **154/187**.

General Procedure F: Iron(II)-Catalyzed C–H/N–H Allene Annulation

To a stirred solution of **118/116** (0.30 mmol), ZnBr₂·TMEDA (206 mg, 0.60 mmol) and dppe (17.9 mg, 15 mol %) in THF (0.20 mL) *i*PrMgBr (3M in 2-MeTHF, 300 μL, 0.90 mmol) was added in one portion and the reaction mixture was stirred for 5 min at ambient temperature. Fe(acac)₃ (15.9 mg, 15 mol %) was added in a single portion. After stirring the solution for additional 5 min, allene **155** (0.90 mmol, 3.0 equiv) was added as a solution in THF (0.20 mL) in one portion. The mixture was placed in a pre-heated oil bath at 65 °C. After stirring for 16 h, sat. aqueous NH₄Cl (2.0 mL) was added to the reaction mixture, which was then extracted with CH₂Cl₂ (3 × 15 mL). The combined organic extracts were dried over Na₂SO₄, filtered and concentrated. The crude product was purified by column chromatography on silica gel to afford the desired product **156**.

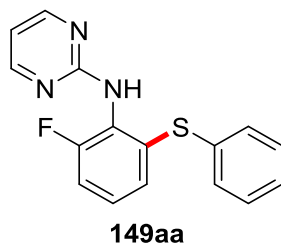
General Procedure G: Iron-Catalyzed C–H/N–H Alkyne Annulation.

To a stirred solution of **118** (0.30 mmol), ZnBr₂·TMEDA (205 mg, 0.60 mmol, 2.0 equiv) and dppe (17.9 mg, 15 mol %) in THF (0.40 mL) *i*PrMgBr (3.0M in 2-MeTHF, 300 μL, 0.90 mmol) was added in one portion and the reaction mixture was stirred for 5 min at ambient temperature. Then, FeCl₂ (5.7 mg, 15 mol %) was added in a single portion. After stirring the solution for additional 5 min, alkyne **158** (0.90 mmol, 3.0 equiv) was added as a solution in THF (0.40 mL). Then, the mixture was stirred at ambient temperature. After stirring for 16 h, sat. aqueous NH₄Cl (3.0 mL) was added to the reaction mixture, which was extracted with CH₂Cl₂ (3 × 15 mL). The combined organic extracts were dried over Na₂SO₄, filtered and concentrated under reduced pressure. The crude product was purified by column chromatography on silica gel to afford the desired product **147**.

5.3 Nickel-Catalyzed C–H Thiolation/Selenylation of Pyrimidyl Anilines

5.3.1 Experimental Procedures and Analytical Data - Thiolation

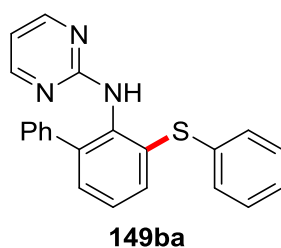
N-[2-Fluoro-6-(phenylthio)phenyl]pyrimidin-2-amine (**149aa**)



The general procedure **A** was followed using substrate **41a** (94.6 mg, 0.50 mmol) and diphenyl disulfide **62a** (131 mg, 0.60 mmol). Purification by column chromatography (*n*hexane/EtOAc: 5/1) yielded **149aa** (142 mg, 96%) as a colorless solid.

M.p. 145–147 °C. $^1\text{H NMR}$ (300 MHz, CDCl_3): δ = 8.31 (d, J = 4.8 Hz, 2H), 7.33–7.00 (m, 8H), 6.94 (br s, 1H), 6.65 (t, J = 4.8 Hz, 1H). $^{13}\text{C NMR}$ (76 MHz, CDCl_3): δ = 160.8 (C_q), 158.5 (d, $^1J_{\text{C-F}}$ = 251.8 Hz, C_q), 158.2 (2C, CH), 134.9 (C_q), 134.3 (C_q), 131.4 (CH), 129.4 (CH), 127.7 (d, $^4J_{\text{C-F}}$ = 3.3 Hz, CH), 127.5 (CH), 127.1 (d, $^3J_{\text{C-F}}$ = 8.7 Hz, CH), 126.7 (d, $^2J_{\text{C-F}}$ = 13.1 Hz, C_q), 115.6 (d, $^2J_{\text{C-F}}$ = 20.8 Hz, CH), 112.9 (CH). $^{19}\text{F NMR}$ (282 MHz, CDCl_3): δ = -115.87 (dd, J = 9.1, 5.1 Hz). **IR** (ATR): 3206, 3150, 3920, 1578, 1442, 1412, 897, 752, 687, 503 cm^{-1} . **MS** (EI) m/z (relative intensity): 297 (18) $[\text{M}]^+$, 276 (10), 205 (20), 188 (100), 168 (8). **HR-MS** (EI) m/z calcd for $\text{C}_{16}\text{H}_{12}\text{FN}_3\text{S}$, $[\text{M}]^+$ 297.0736, found 297.0732.

N-[3-(Phenylthio)-(1,1'-biphenyl)-2-yl]pyrimidin-2-amine (**149ba**)

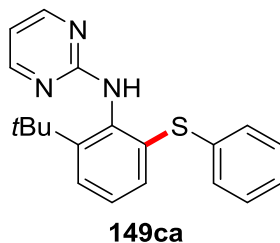


The general procedure **A** was followed using substrate **41b** (124 mg, 0.50 mmol) and diphenyl disulfide **62a** (131 mg, 0.60 mmol). Purification by column chromatography (*n*hexane/EtOAc: 5/1) yielded **149ba** (161 mg, 91%) as a colorless solid.

5 Experimental Part

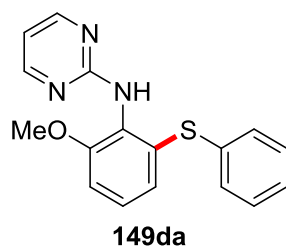
M.p. 132–135 °C. **¹H NMR** (300 MHz, CDCl₃): δ = 8.17 (d, *J* = 4.8 Hz, 2H), 7.41–7.33 (m, 4H), 7.33–7.17 (m, 9H), 6.80 (br s, 1H), 6.50 (t, *J* = 4.8 Hz, 1H). **¹³C NMR** (126 MHz, CDCl₃): δ = 161.0 (C_q), 158.0 (CH), 140.4 (C_q), 139.9 (C_q), 135.4 (C_q), 135.1 (C_q), 135.0 (C_q), 131.9 (CH), 131.2 (CH), 129.9 (CH), 129.4 (CH), 128.8 (CH), 128.2 (CH), 127.5 (CH), 127.3 (CH), 127.2 (CH), 112.1 (CH). **IR** (ATR): 3209, 3055, 1584, 1514, 1438, 1401, 793, 753, 740, 696 cm⁻¹. **MS** (EI) *m/z* (relative intensity): 355 (7) [M]⁺, 246 (100), 167 (4), 109.0 (6), 77.0 (5). **HR-MS** (EI) *m/z* calcd for C₂₂H₁₇N₃S, [M]⁺ 355.1143, found 355.1136.

***N*-[2-(*tert*-Butyl)-6-(phenylthio)phenyl]pyrimidin-2-amine (149ca)**



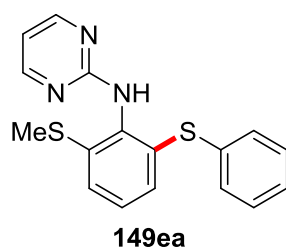
The general procedure **A** was followed using substrate **41c** (114 mg, 0.50 mmol) and diphenyl disulfide **62a** (131 mg, 0.60 mmol). Purification by column chromatography (*n*hexane/EtOAc: 4/1) yielded **149ca** (110 mg, 66%) as a bright yellow solid.

M.p. 149–152 °C. **¹H NMR** (300 MHz, CDCl₃): δ = 8.34 (d, *J* = 4.8 Hz, 2H), 7.37 (dd, *J* = 8.0, 1.5 Hz, 1H), 7.35–7.20 (m, 5H), 7.16 (dd, *J* = 7.9, 7.9 Hz, 1H), 7.04 (dd, *J* = 7.8, 1.5 Hz, 1H), 6.75 (br s, 1H), 6.61 (t, *J* = 4.8 Hz, 1H), 1.40 (s, 9H). **¹³C NMR** (76 MHz, CDCl₃): δ = 162.4 (C_q), 158.4 (CH), 149.4 (C_q), 140.3 (C_q), 135.3 (C_q), 135.0 (C_q), 132.8 (CH), 129.3 (CH), 129.2 (CH), 128.1 (CH), 127.6 (CH), 125.7 (CH), 111.8 (CH), 35.8 (C_q), 31.1 (CH₃). **IR** (ATR): 3196, 2956, 1584, 1519, 1445, 1406, 794, 738, 688, 479 cm⁻¹. **MS** (ESI) *m/z* (relative intensity): 336 (100) [M+H]⁺, 288 (11), 280 (23). **HR-MS** (ESI) *m/z* calcd for C₂₀H₂₂N₃S, [M+H]⁺ 336.1529, found 336.1531.

***N*-[2-Methoxy-6-(phenylthio)phenyl]pyrimidin-2-amine (149da)**

The general procedure **A** was followed using substrate **41d** (101 mg, 0.50 mmol) and diphenyl disulfide **62a** (131 mg, 0.60 mmol). Purification by column chromatography (*n*hexane/EtOAc: 4/1) yielded **149da** (124 mg, 80%) as a colorless solid.

M.p. 210–212 °C. **¹H NMR** (300 MHz, CDCl₃): δ = 8.33 (d, *J* = 4.8 Hz, 2H), 7.36–7.29 (m, 2H), 7.27–7.17 (m, 3H), 7.13 (dd, *J* = 8.1, 8.1 Hz, 1H), 6.91–6.84 (m, 2H), 6.75 (br s, 1H), 6.63 (t, *J* = 4.8 Hz, 1H), 3.81 (s, 3H). **¹³C NMR** (126 MHz, CDCl₃): δ = 161.6 (C_q), 158.1 (CH), 155.3 (C_q), 135.6 (C_q), 135.5 (C_q), 131.8 (CH), 129.2 (CH), 127.2 (CH), 127.2 (CH), 124.0 (CH), 112.4 (CH), 110.4 (CH), 56.0 (CH₃). **IR** (ATR): 3208, 2963, 1572, 1527, 1445, 1410, 1258, 1036, 757, 692 cm⁻¹. **MS** (EI) *m/z* (relative intensity): 309 (15) [M]⁺, 278 (82), 200 (100), 185 (50), 157 (12), 43 (30). **HR-MS** (EI) *m/z* calcd for C₁₇H₁₅N₃OS, [M]⁺ 309.0936, found 309.0946.

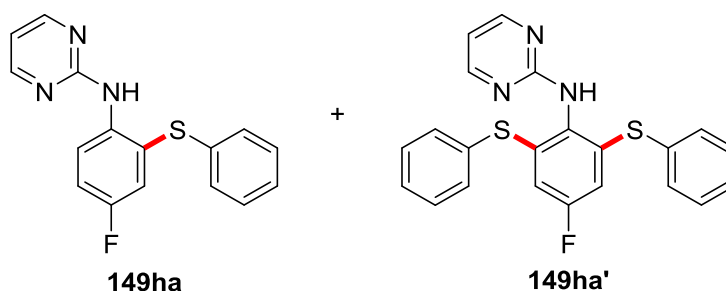
***N*-[2-(Methylthio)-6-(phenylthio)phenyl]pyrimidin-2-amine (149ea)**

The general procedure **A** was followed using substrate **41e** (109 mg, 0.50 mmol) and diphenyl disulfide **62a** (131 mg, 0.60 mmol). Purification by column chromatography (*n*hexane/EtOAc: 4/1) yielded **149ea** (80.2 mg, 49%) as a yellow solid.

M.p. 169–172 °C. **¹H NMR** (300 MHz, CDCl₃): δ = 8.34 (d, *J* = 4.8 Hz, 2H), 7.36–7.30 (m, 2H), 7.28–7.20 (m, 3H), 7.20–7.14 (m, 2H), 7.03 (dd, *J* = 6.2, 3.0 Hz, 1H), 6.79 (br s, 1H), 6.64 (t, *J* = 4.8 Hz, 1H), 2.40 (s, 3H). **¹³C NMR** (76 MHz, CDCl₃): δ = 161.4 (C_q), 158.4 (CH), 139.5 (C_q), 136.7 (C_q), 134.6 (C_q), 134.5 (C_q), 132.2 (CH),

129.3 (CH), 128.0 (CH), 127.9 (CH), 127.6 (CH), 124.5 (CH), 112.6 (CH), 15.8 (CH₃). **IR** (ATR): 3204, 3143, 2917, 1580, 1523, 1438, 1404, 743, 689, 453 cm⁻¹. **MS** (EI) *m/z* (relative intensity): 325 (19) [M]⁺, 278 (92), 216 (100), 201 (70), 200 (50), 169 (23). **HR-MS** (EI) *m/z* calcd for C₁₇H₁₅N₃S₂, [M]⁺ 325.0707, found 325.0715.

***N*-[4-Fluoro-2-(phenylthio)phenyl]pyrimidin-2-amine (149ha) and *N*-[4-Fluoro-2,6-bis(phenylthio)phenyl]pyrimidin-2-amine (149ha')**



The general procedure **A** was followed using substrate **41h** (94.6 mg, 0.50 mmol) and diphenyl disulfide **62a** (131 mg, 0.60 mmol). Purification by column chromatography (*n*hexane/EtOAc: 4/1) yielded **149ha** (14.2 mg, 10%) as a bright yellow solid and **149ha'** (85.9 mg, 42%) as a colorless solid.

***N*-[4-Fluoro-2-(phenylthio)phenyl]pyrimidin-2-amine (149ha):**

M.p. 88–90 °C. **¹H NMR** (300 MHz, CDCl₃): δ = 8.46 (dd, *J* = 9.1, 5.4 Hz, 1H), 8.39 (d, *J* = 4.8 Hz, 2H), 7.90 (br s, 1H), 7.29–7.16 (m, 6H), 7.13 (ddd, *J* = 9.1, 8.0, 3.0 Hz, 1H), 6.72 (t, *J* = 4.8 Hz, 1H). **¹³C NMR** (126 MHz, CDCl₃): δ = 159.9 (C_q), 158.0 (CH), 157.8 (d, ¹*J*_{C-F} = 244.4 Hz, C_q), 137.0 (d, ⁴*J*_{C-F} = 2.7 Hz, C_q), 135.0 (C_q), 129.4 (CH), 128.8 (CH), 126.9 (CH), 123.5 (d, ³*J*_{C-F} = 7.8 Hz, C_q), 121.8 (d, ³*J*_{C-F} = 7.6 Hz, CH), 121.6 (d, ²*J*_{C-F} = 23.1 Hz, CH), 116.8 (d, ²*J*_{C-F} = 21.8 Hz, CH), 113.15 (CH). **¹⁹F NMR** (282 MHz, CDCl₃): δ = -119.68 (ddd, *J* = 8.1, 8.1, 5.4 Hz). **IR** (ATR): 3350, 3053, 1580, 1526, 1448, 1406, 793, 737, 690, 541 cm⁻¹. **MS** (ESI) *m/z* (relative intensity): 336 (13) [M+K]⁺, 320 (31) [M+Na]⁺, 298 (100) [M+H]⁺, 206 (7), 189 (13). **HR-MS** (ESI) *m/z* calcd for C₁₆H₁₃FN₃S, [M+H]⁺ 298.0809, found 298.0810.

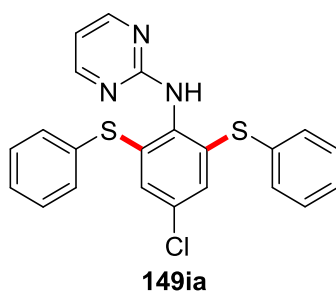
***N*-[4-Fluoro-2,6-bis(phenylthio)phenyl]pyrimidin-2-amine (149ha'):**

M.p. 129–131 °C. **¹H NMR** (400 MHz, CDCl₃): δ = 8.37 (d, *J* = 4.8 Hz, 2H), 7.46–7.40 (m, 4H), 7.36–7.30 (m, 6H), 6.91 (br s, 1H), 6.68 (t, *J* = 4.8 Hz, 1H), 6.53 (d, *J* = 8.8 Hz, 2H). **¹³C NMR** (101 MHz, CDCl₃): δ = 161.4 (d, ¹*J*_{C-F} = 249.4 Hz, C_q),

5 Experimental Part

161.4 (C_q), 158.4 (CH), 141.1 (d, ³J_{C-F} = 8.9 Hz, C_q), 134.0 (CH), 132.5 (C_q), 129.7 (CH), 129.4 (d, ⁴J_{C-F} = 3.0 Hz, C_q), 128.8 (CH), 113.8 (d, ²J_{C-F} = 25.4 Hz, CH), 112.7 (CH). ¹⁹F NMR (376 MHz, CDCl₃): δ = -112.76 (dd, J = 8.7, 8.7 Hz). IR (ATR): 3184, 2912, 1582, 1439, 1404, 1196, 793, 742, 641, 417 cm⁻¹. MS (EI) *m/z* (relative intensity): 405 (7) [M]⁺, 313 (8), 297 (18), 296 (100), 218 (51), 187 (12), 109 (18). HR-MS (EI) *m/z* calcd for C₂₂H₁₆FN₃S₂, [M]⁺ 405.0770, found 405.0763.

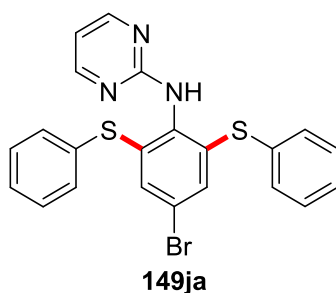
N-[4-Chloro-2,6-bis(phenylthio)phenyl]pyrimidin-2-amine (**149ia**):



The general procedure **A** was followed using substrate **41i** (103 mg, 0.50 mmol) and diphenyl disulfide **62a** (131 mg, 0.60 mmol). Purification by column chromatography (*n*hexane/EtOAc: 4/1) yielded **149ia** (100 mg, 47%) as a colorless solid.

M.p. 139–142 °C. ¹H NMR (400 MHz, CDCl₃): δ = 8.35 (d, J = 4.8 Hz, 2H), 7.42–7.36 (m, 4H), 7.34–7.27 (m, 6H), 7.05 (br s, 1H), 6.90 (s, 2H), 6.67 (t, J = 4.8 Hz, 1H). ¹³C NMR (101 MHz, CDCl₃): δ = 161.1 (C_q), 158.3 (CH), 139.6 (C_q), 133.3 (CH), 133.3 (C_q), 133.2 (C_q), 133.0 (C_q), 129.7 (CH), 128.5 (CH), 127.9 (CH), 112.8 (CH). IR (ATR): 3319, 3058, 1580, 1476, 1439, 1392, 787, 742, 688, 476 cm⁻¹. MS (ESI) *m/z* (relative intensity): 444 (10) [M+Na]⁺ (³⁵Cl), 422 (100) [M+H]⁺ (³⁵Cl). HR-MS (ESI) *m/z* calcd for C₂₂H₁₇N₃³⁵ClS₂, [M+H]⁺ 422.0547, found 422.0545.

N-[4-Bromo-2,6-bis(phenylthio)phenyl]pyrimidin-2-amine (**149ja**)

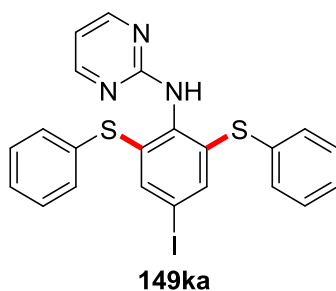


5 Experimental Part

The general procedure **A** was followed using substrate **41j** (125 mg, 0.50 mmol) and diphenyl disulfide **62a** (131 mg, 0.60 mmol). Purification by column chromatography (*n*hexane/EtOAc: 4/1) yielded **149ja** (129 mg, 55%) as a colorless solid.

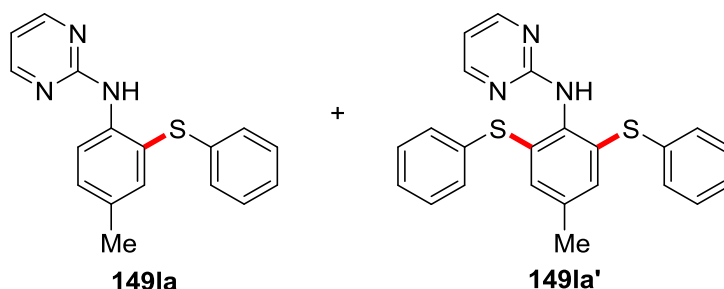
M.p. 148–152 °C. **¹H NMR** (300 MHz, CDCl₃): δ = 8.32 (d, *J* = 4.8 Hz, 2H), 7.38–7.23 (m, 10H), 7.06 (s, 2H), 6.95 (br s, 1H), 6.65 (t, *J* = 4.8 Hz, 1H). **¹³C NMR** (76 MHz, CDCl₃): δ = 161.0 (C_q), 158.3 (CH), 139.6 (C_q), 134.1 (C_q), 133.2 (C_q), 133.1 (CH), 131.0 (CH), 129.7 (CH), 128.4 (CH), 121.0 (C_q), 112.9 (CH). **IR** (ATR): 3057, 2909, 1583, 1520, 1407, 794, 741, 683, 645, 464 cm⁻¹. **MS** (EI) *m/z* (relative intensity): 467 (5) [M]⁺, 358 (100) (⁸¹Br), 356 (98) (⁷⁹Br), 280 (50) (⁸¹Br), 278 (49) (⁷⁹Br), 199 (28), 109 (17). **HR-MS** (EI) *m/z* calcd for C₂₂H₁₆N₃S₂⁷⁹Br, [M]⁺ 464.9969, found 464.9954.

N-[4-Iodo-2,6-bis(phenylthio)phenyl]pyrimidin-2-amine (**149ka**)



The general procedure **A** was followed using substrate **41k** (149 mg, 0.50 mmol) and diphenyl disulfide **62a** (131 mg, 0.60 mmol). Purification by column chromatography (*n*hexane/EtOAc: 4/1) yielded **149ka** (89.6 mg, 35%) as a yellow solid.

M.p. 150–152 °C. **¹H NMR** (300 MHz, CDCl₃): δ = 8.31 (d, *J* = 4.8 Hz, 2H), 7.36–7.22 (m, 12H), 6.87 (br s, 1H), 6.64 (t, *J* = 4.8 Hz, 1H). **¹³C NMR** (126 MHz, CDCl₃): δ = 160.9 (C_q), 158.1 (CH), 138.9 (C_q), 137.7 (CH), 135.6 (C_q), 133.4 (C_q), 132.6 (CH), 129.5 (CH), 128.2 (CH), 112.9 (CH), 92.1 (C_q). **IR** (ATR): 3186, 2909, 1579, 1439, 1405, 793, 742, 687, 638, 458 cm⁻¹. **MS** (EI) *m/z* (relative intensity): 513 (10) [M]⁺, 420 (8), 404 (100), 326 (22), 277 (14), 199 (8), 168 (7). **HR-MS** (EI) *m/z* calcd for C₂₂H₁₆IN₃S₂, [M]⁺ 512.9830, found 512.9836.

***N*-[4-Methyl-2-(phenylthio)phenyl]pyrimidin-2-amine (149la) and *N*-[4-Methyl-2,6-bis(phenylthio)phenyl]pyrimidin-2-amine (149la')**

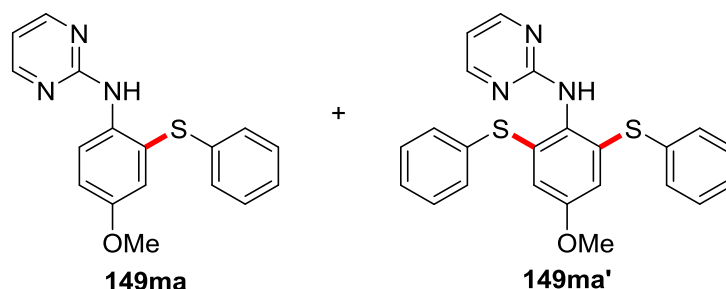
The general procedure **A** was followed using substrate **41I** (92.6 mg, 0.50 mmol) and diphenyl disulfide **62a** (131 mg, 0.60 mmol). Purification by column chromatography (*n*hexane/EtOAc: 5/1) yielded **149la** (9.00 mg, 6%) as a yellow solid and **149la'** (66.7 mg, 33%) as a colorless solid.

***N*-[4-Methyl-2-(phenylthio)phenyl]pyrimidin-2-amine (149la):**

M.p. 100–102 °C. **¹H NMR** (300 MHz, CDCl₃): δ = 8.43 (d, *J* = 8.4 Hz, 1H), 8.38 (d, *J* = 4.8 Hz, 2H), 8.06 (br s, 1H), 7.42 (d, *J* = 1.5 Hz, 1H), 7.26 (dd, *J* = 8.3, 1.8 Hz, 1H), 7.23–7.15 (m, 2H), 7.15–7.05 (m, 3H), 6.69 (t, *J* = 4.8 Hz, 1H), 2.32 (s, 3H). **¹³C NMR** (76 MHz, CDCl₃): δ = 160.1 (C_q), 158.0 (CH), 139.1 (C_q), 137.2 (CH), 136.7 (C_q), 132.6 (C_q), 131.4 (CH), 129.2 (CH), 127.4 (CH), 126.0 (CH), 120.1 (CH), 120.0 (C_q), 112.9 (CH), 20.7 (CH₃). **IR** (ATR): 3353, 2916, 1579, 1516, 1438, 1394, 831, 791, 742, 689 cm⁻¹. **MS** (ESI) *m/z* (relative intensity): 216 (26) [M+Na]⁺, 294 (100) [M+H]⁺, 185 (16). **HR-MS** (ESI) *m/z* calcd for C₁₇H₁₆N₃S, [M+H]⁺ 294.1059, found 294.1061.

***N*-[4-Methyl-2,6-bis(phenylthio)phenyl]pyrimidin-2-amine (149la')**

M.p. 142–144 °C. **¹H NMR** (400 MHz, CDCl₃): δ = 8.29 (d, *J* = 4.8 Hz, 2H), 7.34–7.30 (m, 4H), 7.27–7.18 (m, 6H), 6.99 (d, *J* = 0.6 Hz, 2H), 6.91 (br s, 1H), 6.60 (t, *J* = 4.8 Hz, 1H), 2.17 (s, 3H). **¹³C NMR** (101 MHz, CDCl₃): δ = 161.4 (C_q), 158.1 (CH), 137.6 (C_q), 135.9 (C_q), 135.0 (C_q), 134.6 (C_q), 131.8 (CH), 131.7 (CH), 129.3 (CH), 127.4 (CH), 112.5 (CH), 21.1 (CH₃). **IR** (ATR): 3138, 2914, 1580, 1516, 1442, 1406, 799, 755, 685, 415 cm⁻¹. **MS** (EI) *m/z* (relative intensity): 401 (6) [M]⁺, 292 (100), 214 (37), 182 (10). **HR-MS** (EI) *m/z* calcd for C₂₃H₁₉N₃S₂, [M]⁺ 401.1020, found 401.1018.

***N*-[4-Methoxy-2-(phenylthio)phenyl]pyrimidin-2-amine (149ma) and *N*-[4-Methoxy-2,6-bis(phenylthio)phenyl]pyrimidin-2-amine (149ma')**

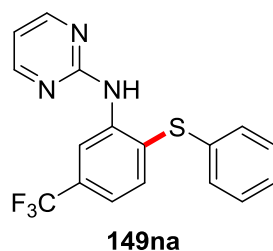
The general procedure **A** was followed using substrate **41m** (101 mg, 0.50 mmol) and diphenyl disulfide **62a** (131 mg, 0.60 mmol). Purification by column chromatography (*n*hexane/EtOAc: 5/1) yielded **149ma** (13 mg, 8%) as a yellow oil and **149ma'** (74 mg, 36%) as a colorless solid.

***N*-[4-Methoxy-2-(phenylthio)phenyl]pyrimidin-2-amine (149ma):**

¹H NMR (300 MHz, CDCl₃) δ = 8.35 (d, *J* = 4.8 Hz, 2H), 8.31 (d, *J* = 9.0 Hz, 1H), 7.74 (br s, 1H), 7.25–7.08 (m, 6H), 7.00 (dd, *J* = 9.0, 3.0 Hz, 1H), 6.66 (t, *J* = 4.8 Hz, 1H), 3.78 (s, 3H). ¹³C NMR (76 MHz, CDCl₃): δ = 160.3 (C_q), 158.1 (CH), 155.4 (C_q), 135.9 (C_q), 134.4 (C_q), 129.3 (CH), 128.2 (CH), 126.4 (CH), 123.2 (C_q), 122.5 (CH), 120.5 (CH), 116.2 (CH), 112.7 (CH), 55.8 (CH₃). IR (ATR): 3360, 2931, 1579, 1513, 1445, 1403, 1276, 1207, 1036, 740 cm⁻¹. MS (ESI) *m/z* (relative intensity): 332 (43) [M+Na]⁺, 310 (100) [M+H]⁺, 201 (19). HR-MS (ESI) *m/z* calcd for C₁₇H₁₆N₃OS, [M+H]⁺ 310.1009, found 310.1009.

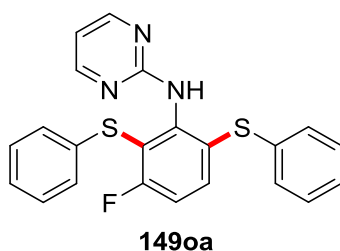
***N*-[4-Methoxy-2,6-bis(phenylthio)phenyl]pyrimidin-2-amine (149ma')**

M.p. 126–128 °C. ¹H NMR (300 MHz, CDCl₃): δ = 8.32 (d, *J* = 4.8 Hz, 2H), 7.41–7.36 (m, 4H), 7.32–7.22 (m, 6H), 6.66 (br s, 1H), 6.62 (t, *J* = 4.8 Hz, 1H), 6.55 (s, 2H), 3.55 (s, 3H). ¹³C NMR (76 MHz, CDCl₃): δ = 161.7 (C_q), 158.5 (C_q), 158.3 (CH), 138.9 (C_q), 133.8 (C_q), 133.0 (CH), 129.5 (CH), 128.3 (C_q), 128.0 (CH), 114.4 (CH), 112.4 (CH), 55.5 (CH₃). IR (ATR): 3188, 2961, 2911, 1517, 1439, 1407, 1224, 753, 735, 686 cm⁻¹. MS (ESI) *m/z* (relative intensity): 440 (20) [M+Na]⁺, 418 (100) [M+H]⁺. HR-MS (ESI) *m/z* calcd for C₂₃H₂₀N₃OS₂, [M+H]⁺ 418.1042, found 418.1041.

***N*-[2-(Phenylthio)-5-(trifluoromethyl)phenyl]pyrimidin-2-amine (149na)**

The general procedure **A** was followed using substrate **41n** (120 mg, 0.50 mmol) and diphenyl disulfide **62a** (131 mg, 0.60 mmol). Purification by column chromatography (*n*hexane/EtOAc: 4/1) yielded **149na** (133 mg, 76%) as a colorless solid.

M.p. 116–118 °C. **¹H NMR** (300 MHz, CDCl₃): δ = 9.03 (d, *J* = 1.7 Hz, 1H), 8.46 (d, *J* = 4.8 Hz, 2H), 8.29 (br s, 1H), 7.64 (d, *J* = 8.1 Hz, 1H), 7.30–7.13 (m, 6H), 6.80 (t, *J* = 4.8 Hz, 1H). **¹³C NMR** (126 MHz, CDCl₃): δ = 159.6 (C_q), 158.1 (CH), 141.5 (C_q), 136.2 (CH), 134.8 (C_q), 132.2 (q, ²*J*_{C-F} = 32.4 Hz, C_q), 129.6 (CH), 128.7 (CH), 127.0 (CH), 124.6 (q, ⁴*J*_{C-F} = 1.2 Hz, C_q), 124.1 (q, ¹*J*_{C-F} = 272.7 Hz, C_q), 118.7 (q, ³*J*_{C-F} = 3.8 Hz, CH), 116.2 (q, ³*J*_{C-F} = 4.0 Hz, CH), 113.9 (CH). **¹⁹F NMR** (282 MHz, CDCl₃): δ = -63.21 (s). **IR** (ATR): 3340, 1568, 1523, 1439, 1400, 1329, 1118, 1078, 794, 743 cm⁻¹. **MS** (ESI) *m/z* (relative intensity): 348 (100) [M+H]⁺, 279 (6), 223 (5), 173 (7). **HR-MS** (ESI) *m/z* calcd for C₁₇H₁₃N₃SF₃, [M+H]⁺ 348.0777, found 348.0782.

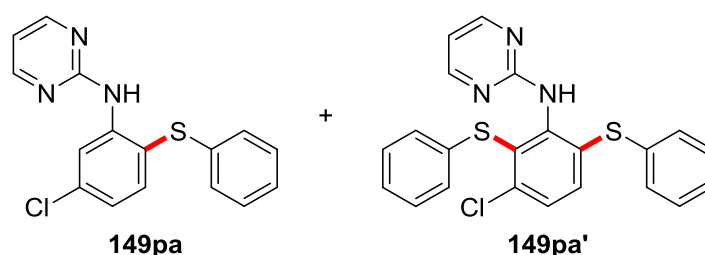
***N*-[3-Fluoro-2,6-bis(phenylthio)phenyl]pyrimidin-2-amine (149oa)**

The general procedure **A** was followed using substrate **41o** (94.6 mg, 0.50 mmol) and diphenyl disulfide **62a** (131 mg, 0.60 mmol). Purification by column chromatography (*n*hexane/EtOAc: 4/1) yielded **149oa** (83.3 mg, 56%) as a colorless solid.

M.p. 113–115 °C. **¹H NMR** (400 MHz, CDCl₃): δ = 8.26 (d, *J* = 4.8 Hz, 2H), 7.43 (dd, *J* = 8.7, 5.9 Hz, 1H), 7.29 (br s, 1H), 7.25–7.05 (m, 10H), 6.99 (dd, *J* = 8.7, 8.0 Hz,

1H), 6.64 (t, $J = 4.8$ Hz, 1H). $^{13}\text{C NMR}$ (101 MHz, CDCl_3): $\delta = 162.9$ (d, $^1J_{\text{C-F}} = 249.9$ Hz, C_q), 160.9 (C_q), 157.9 (CH), 142.7 (d, $^4J_{\text{C-F}} = 2.7$ Hz, C_q), 135.9 (C_q), 135.6 (C_q), 135.2 (d, $^3J_{\text{C-F}} = 9.5$ Hz, CH), 130.6 (CH), 129.3 (CH), 129.0 (CH), 128.9 (d, $^3J_{\text{C-F}} = 3.6$ Hz, C_q), 128.7 (CH), 127.2 (CH), 126.4 (CH), 120.2 (d, $^2J_{\text{C-F}} = 19.0$ Hz, C_q), 114.3 (d, $^2J_{\text{C-F}} = 24.2$ Hz, CH), 113.3 (CH). $^{19}\text{F NMR}$ (376 MHz, CDCl_3): $\delta = -101.62$ (dd, $J = 7.9, 6.1$ Hz). **IR** (ATR): 3209, 3059, 1584, 1437, 1401, 1023, 794, 737, 687, 469 cm^{-1} . **MS** (EI) m/z (relative intensity): 405 (11) $[\text{M}]^+$, 312 (12), 296 (100), 218 (62), 187 (12), 109 (10), 77 (8). **HR-MS** (EI) m/z calcd for $\text{C}_{22}\text{H}_{16}\text{FN}_3\text{S}_2$, $[\text{M}]^+$ 405.0770, found 405.0778.

***N*-[5-Chloro-2-(phenylthio)phenyl]pyrimidin-2-amine (149pa) and *N*-[3-Chloro-2,6-bis(phenylthio)phenyl]pyrimidin-2-amine (149pa')**



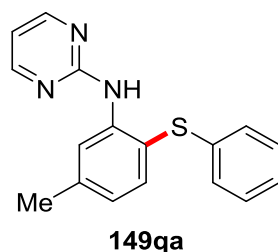
The general procedure **A** was followed using substrate **41p** (103 mg, 0.50 mmol) and diphenyl disulfide **62a** (131 mg, 0.60 mmol). Purification by column chromatography (*n*hexane/ EtOAc: 4/1) yielded **149pa** (80.0 mg, 51%) as a colorless solid and **149pa'** (45.0 mg, 21%) as a colorless solid.

***N*-[5-Chloro-2-(phenylthio)phenyl]pyrimidin-2-amine (149pa):**

M.p. 136–138 °C. $^1\text{H NMR}$ (300 MHz, CDCl_3): $\delta = 8.82$ (d, $J = 2.3$ Hz, 1H), 8.42 (d, $J = 4.8$ Hz, 2H), 8.30 (br s, 1H), 7.51 (d, $J = 8.2$ Hz, 1H), 7.26–7.16 (m, 2H), 7.14–7.07 (m, 3H), 6.99 (dd, $J = 8.3, 2.3$ Hz, 1H), 6.75 (t, $J = 4.8$ Hz, 1H). $^{13}\text{C NMR}$ (126 MHz, CDCl_3): $\delta = 159.5$ (C_q), 158.0 (CH), 142.6 (C_q), 137.9 (CH), 136.9 (C_q), 136.0 (C_q), 129.4 (CH), 127.4 (CH), 126.3 (CH), 122.4 (CH), 119.1 (CH), 117.5 (C_q), 113.8 (CH). **IR** (ATR): 3345, 3117, 1574, 1557, 1513, 1435, 939, 791, 740, 467 cm^{-1} . **MS** (ESI) m/z (relative intensity): 740 (27), 381 (100), 353 (8) $[\text{M}+\text{K}]^+$, 336 (14) $[\text{M}+\text{Na}]^+$ (^{35}Cl), 314 (45) $[\text{M}+\text{H}]^+$ (^{35}Cl), 279 (25). **HR-MS** (ESI) m/z calcd for $\text{C}_{16}\text{H}_{13}\text{N}_3\text{S}^{35}\text{Cl}$, $[\text{M}+\text{H}]^+$ 314.0513, found 314.0506.

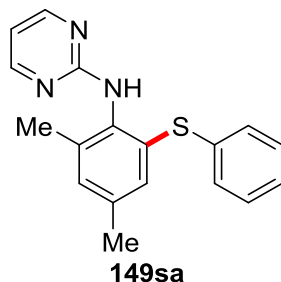
***N*-[3-Chloro-2,6-bis(phenylthio)phenyl]pyrimidin-2-amine (149pa')**

M.p. 117–120 °C. **¹H NMR** (300 MHz, CDCl₃): δ = 8.24 (d, *J* = 4.8 Hz, 2H), 7.34–7.17 (m, 8H), 7.15–6.98 (m, 5H), 6.61 (t, *J* = 4.8 Hz, 1H). **¹³C NMR** (126 MHz, CDCl₃): δ = 160.9 (C_q), 158.0 (CH), 142.0 (C_q), 139.0 (C_q), 135.9 (C_q), 135.0 (C_q), 134.7 (C_q), 133.2 (CH), 132.2 (CH), 131.0 (C_q), 129.5 (CH), 129.1 (CH), 128.2 (CH), 128.2 (CH), 127.9 (CH), 126.2 (CH), 113.1 (CH). **IR** (ATR): 3203, 3058, 1581, 1445, 1401, 1387, 795, 737, 628, 491 cm⁻¹. **MS** (ESI) *m/z* (relative intensity): 444 (14) [M+Na]⁺ (³⁵Cl), 422 (100) [M+H]⁺ (³⁵Cl). **HR-MS** (ESI) *m/z* calcd for C₂₂H₁₇N₃S₂³⁵Cl, [M+H]⁺ 422.0547, found 422.0541.

***N*-[5-Methyl-2-(phenylthio)phenyl]pyrimidin-2-amine (149qa)**

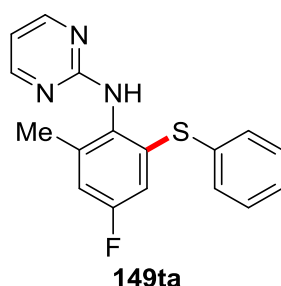
The general procedure **A** was followed using substrate **41q** (92.6 mg, 0.50 mmol) and diphenyl disulfide **62a** (131 mg, 0.60 mmol). Purification by column chromatography (*n*hexane/ EtOAc: 4/1) yielded **149qa** (63.3 mg, 43%) as a white solid.

M.p. 110–112 °C. **¹H NMR** (300 MHz, CDCl₃): δ = 8.47 (s, 1H), 8.41 (d, *J* = 4.8 Hz, 2H), 8.22 (br s, 1H), 7.50 (d, *J* = 7.8 Hz, 1H), 7.23–7.14 (m, 2H), 7.14–7.04 (m, 3H), 6.90–6.85 (m, 1H), 6.72 (t, *J* = 4.8 Hz, 1H), 2.45 (s, 3H). **¹³C NMR** (76 MHz, CDCl₃): δ = 159.9 (C_q), 158.0 (CH), 141.6 (C_q), 141.4 (C_q), 137.1 (CH), 137.1 (C_q), 129.2 (CH), 127.0 (CH), 125.8 (CH), 123.8 (CH), 120.1 (CH), 116.2 (C_q), 113.1 (CH), 22.1 (CH₃). **IR** (ATR): 3347, 2917, 1575, 1528, 1438, 1392, 791, 740, 690, 625, 469 cm⁻¹. **MS** (EI) *m/z* (relative intensity): 293.1 (16) [M]⁺, 184.1 (100), 169.1 (6), 109.0 (5), 77.0 (5). **HR-MS** (EI) *m/z* calcd for C₁₇H₁₅N₃S, [M]⁺ 293.0987, found 293.0988.

***N*-[2,4-Dimethyl-6-(phenylthio)phenyl]pyrimidin-2-amine (149sa)**

The general procedure **A** was followed using substrate **41s** (99.6 mg, 0.50 mmol) and diphenyl disulfide **62a** (131 mg, 0.60 mmol). Purification by column chromatography (*n*hexane/EtOAc: 4/1) yielded **149sa** (114 mg, 74%) as a colorless solid.

M.p. 137–139 °C. **¹H NMR** (300 MHz, CDCl₃): δ = 8.26 (d, *J* = 4.8 Hz, 2H), 7.25–7.20 (m, 2H), 7.19–7.08 (m, 3H), 7.06 (s, 2H), 6.77 (br s, 1H), 6.56 (t, *J* = 4.8 Hz, 1H), 2.27 (s, 3H), 2.23 (s, 3H). **¹³C NMR** (76 MHz, CDCl₃): δ = 161.5 (C_q), 158.2 (CH), 137.5 (C_q), 137.1 (C_q), 135.6 (C_q), 134.8 (C_q), 132.9 (C_q), 131.7 (CH), 131.3 (CH), 130.6 (CH), 129.1 (CH), 126.8 (CH), 111.9 (CH), 21.1 (CH₃), 19.0 (CH₃). **IR** (ATR): 3206, 2919, 1583, 1516, 1439, 1410, 798, 738, 686, 473 cm⁻¹. **MS** (ESI) *m/z* (relative intensity): 308 (100) [M+H]⁺, 199 (16). **HR-MS** (ESI) *m/z* calcd for C₁₈H₁₈N₃S, [M+H]⁺ 308.1216, found 308.1212.

***N*-[4-Fluoro-2-methyl-6-(phenylthio)phenyl]pyrimidin-2-amine (149ta)**

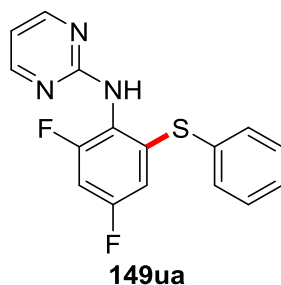
The general procedure **A** was followed using substrate **41t** (102 mg, 0.50 mmol) and diphenyl disulfide **62a** (131 mg, 0.60 mmol). Purification by column chromatography (*n*hexane/EtOAc: 4/1) yielded **149ta** (145 mg, 93%) as a colorless solid.

M.p. 157–159 °C. **¹H NMR** (300 MHz, CDCl₃): δ = 8.31 (d, *J* = 4.8 Hz, 2H), 7.40–7.33 (m, 2H), 7.32–7.22 (m, 3H), 6.89–6.83 (m, 2H), 6.67 (dd, *J* = 8.7, 2.9 Hz, 1H), 6.62 (t,

5 Experimental Part

$J = 4.8$ Hz, 1H), 2.25 (s, 3H). **^{13}C NMR** (126 MHz, CDCl_3): $\delta = 161.4$ (C_q), 161.1 (d, $^1J_{\text{C-F}} = 247.0$ Hz, C_q), 158.3 (CH), 139.9 (d, $^3J_{\text{C-F}} = 8.7$ Hz, C_q), 138.3 (d, $^3J_{\text{C-F}} = 8.9$ Hz, C_q), 133.0 (C_q), 133.0 (CH), 131.4 (d, $^4J_{\text{C-F}} = 2.9$ Hz, C_q), 129.5 (CH), 128.2 (CH), 115.8 (d, $^2J_{\text{C-F}} = 22.2$ Hz, CH), 114.5 (d, $^2J_{\text{C-F}} = 24.7$ Hz, CH), 112.2 (CH), 19.2 (CH_3). **^{19}F NMR** (282 MHz, CDCl_3): $\delta = -114.69$ (dd, $J = 9.0, 9.0$ Hz). **IR** (ATR): 3208, 2915, 1575, 1510, 1439, 1412, 850, 799, 752, 688 cm^{-1} . **MS** (EI) m/z (relative intensity): 311 (9) [M^+], 202 (100). **HR-MS** (EI) m/z calcd for $\text{C}_{17}\text{H}_{14}\text{FN}_3\text{S}$, [M^+] 311.0892, found 311.0887.

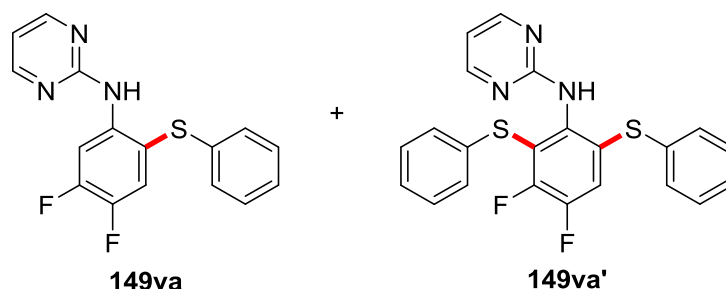
N-[2,4-Difluoro-6-(phenylthio)phenyl]pyrimidin-2-amine (**149ua**)



The general procedure **A** was followed using substrate **41u** (104 mg, 0.50 mmol) and diphenyl disulfide **62a** (131 mg, 0.60 mmol). Purification by column chromatography (*n*hexane/EtOAc: 4/1) yielded **149ua** (148 mg, 94%) as a colorless solid.

M.p. 145–147 °C. **^1H NMR** (300 MHz, CDCl_3): $\delta = 8.35$ (d, $J = 4.8$ Hz, 2H), 7.45–7.39 (m, 2H), 7.37–7.28 (m, 4H), 6.81–6.72 (m, 1H), 6.68 (t, $J = 4.8$ Hz, 1H), 6.63–6.53 (m, 1H). **^{13}C NMR** (75 MHz, CDCl_3): $\delta = 161.1$ (C_q), 160.8 (dd, $^{1/3}J_{\text{C-F}} = 249.1, 12.7$ Hz, C_q), 158.9 (dd, $^{1/3}J_{\text{C-F}} = 253.0, 13.3$ Hz, C_q), 158.3 (CH), 130.0 (dd, $J = 9.9, 2.4$ Hz, C_q), 133.7 (CH), 131.9 (C_q), 129.8 (CH), 128.9 (CH), 121.1 (dd, $J = 14.3, 4.0$ Hz, C_q), 112.8 (CH), 111.7 (dd, $^{2/4}J_{\text{C-F}} = 24.8, 3.4$ Hz, CH), 102.7 (dd, $^2J_{\text{C-F}} = 26.5, 25.0$ Hz, CH). **^{19}F NMR** (282 MHz, CDCl_3): $\delta = -111.36$ (dd, $J = 16.0, 8.4$ Hz), -112.72 (m). **IR** (ATR): 3205, 2972, 1577, 1441, 1407, 1112, 997, 789, 743, 495 cm^{-1} . **MS** (ESI) m/z (relative intensity): 651 (36), 314 (100) [M-H^+], 283 (58), 255 (61). **HR-MS** (ESI) m/z calcd for $\text{C}_{16}\text{H}_{10}\text{N}_3\text{F}_2\text{S}$, [M-H^+] 314.0569, found 314.0562.

***N*-[4,5-Difluoro-2-(phenylthio)phenyl]pyrimidin-2-amine (149va) and *N*-[3,4-Difluoro-2,6-bis(phenylthio)phenyl]pyrimidin-2-amine (149va')**



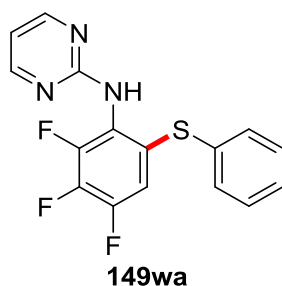
The general procedure **A** was followed using substrate **41v** (104 mg, 0.50 mmol) and diphenyl disulfide **62a** (131 mg, 0.60 mmol). Purification by column chromatography (*n*hexane/EtOAc: 4/1) yielded **149va** (21.3 mg, 14%) as a sticky oil and **149va'** (90.0 mg, 42%) as a colorless solid.

***N*-[4,5-Difluoro-2-(phenylthio)phenyl]pyrimidin-2-amine (149va):**

¹H NMR (300 MHz, CDCl₃): δ = 8.71 (dd, *J* = 13.6, 8.0 Hz, 1H), 8.41 (d, *J* = 4.8 Hz, 2H), 8.19 (br s, 1H), 7.41 (dd, *J* = 9.2 Hz, 1H), 7.27–7.08 (m, 5H), 6.76 (t, *J* = 4.8 Hz, 1H). ¹³C NMR (75 MHz, CDCl₃): δ = 159.4 (C_q), 158.0 (CH), 151.5 (dd, ^{1/2}*J*_{C-F} = 248.7, 12.7 Hz, C_q), 144.9 (dd, ^{1/2}*J*_{C-F} = 246.5, 13.6 Hz, C_q), 138.8 (d, ³*J*_{C-F} = 10.3 Hz, C_q), 135.5 (C_q), 129.5 (CH), 127.6 (CH), 126.7 (CH), 124.7 (dd, ^{2/3}*J*_{C-F} = 18.1, 1.9 Hz, CH), 114.7 (C_q), 113.8 (CH), 108.6 (d, ²*J*_{C-F} = 24.4 Hz, CH).

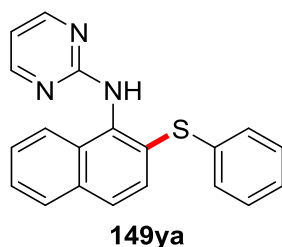
***N*-[3,4-Difluoro-2,6-bis(phenylthio)phenyl]pyrimidin-2-amine (149va'):**

M.p. 108–110 °C. ¹H NMR (300 MHz, CDCl₃): δ = 8.27 (d, *J* = 4.8 Hz, 2H), 7.38–7.26 (m, 4H), 7.23–7.10 (m, 6H), 7.09 (br s, 1H), 7.03 (dd, *J* = 10.1, 8.2 Hz, 1H), 6.65 (t, *J* = 4.8 Hz, 1H). ¹³C NMR (126 MHz, CDCl₃): δ = 161.0 (C_q), 157.9 (CH), 150.0 (dd, ^{1/2}*J*_{C-F} = 249.3, 13.5 Hz, C_q), 149.1 (dd, ^{1/2}*J*_{C-F} = 252.2, 14.9 Hz, C_q), 135.9 (d, ³*J*_{C-F} = 3.1 Hz, C_q), 134.8 (C_q), 133.4 (C_q), 132.6 (CH), 132.2 (dd, *J*_{C-F} = 5.9, 4.0 Hz, C_q), 129.6 (CH), 129.4 (CH), 129.1 (CH), 128.3 (CH), 126.9 (CH), 123.5 (d, ²*J*_{C-F} = 15.0 Hz, C_q), 119.6 (d, ²*J*_{C-F} = 19.7 Hz, CH), 113.1 (CH). ¹⁹F NMR (282 MHz, CDCl₃): δ = -126.57 (dd, *J* = 24.0, 8.2 Hz), -136.19 (dd, *J* = 24.0, 10.1 Hz). **IR** (ATR): 3211, 3070, 2919, 1581, 1523, 1439, 918, 795, 686, 490 cm⁻¹. **MS** (EI) *m/z* (relative intensity): 423 (10) [M]⁺, 331 (12), 315 (19), 314 (100), 236(58), 205 (9), 43 (15). **HR-MS** (EI) *m/z* calcd for C₂₂H₁₅F₂N₃S₂, [M]⁺ 423.0675, found 423.0669.

***N*-[2,3,4-Trifluoro-6-(phenylthio)phenyl]pyrimidin-2-amine (149wa)**

The general procedure **A** was followed using substrate **41w** (113 mg, 0.50 mmol) and diphenyl disulfide **62a** (131 mg, 0.60 mmol). Purification by column chromatography (*n*hexane/EtOAc: 4/1) yielded **149wa** (142 mg, 85%) as a yellow solid.

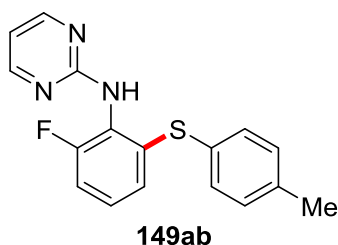
M.p. 126–128 °C. **¹H NMR** (300 MHz, CDCl₃): δ = 8.33 (d, *J* = 4.8 Hz, 2H), 7.36–7.22 (m, 5H), 6.98 (br s, 1H), 6.87 (ddd, *J* = 10.1, 7.6, 2.3 Hz, 1H), 6.72 (t, *J* = 4.8 Hz, 1H). **¹³C NMR** (126 MHz, CDCl₃): δ = 160.4 (C_q), 158.2 (CH), 149.2 (ddd, ¹*J*_{C-F} = 250.5, ²*J*_{C-F} = 10.3, ³*J*_{C-F} = 3.7 Hz, C_q), 148.1 (ddd, ¹*J*_{C-F} = 253.9 Hz, ²*J*_{C-F} = 10.8 Hz, ³*J*_{C-F} = 4.5 Hz, C_q), 139.7 (ddd, ¹*J*_{C-F} = 251.8, ²*J*_{C-F} = 15.2, 15.2 Hz, C_q), 132.7 (C_q), 132.1 (CH), 130.0 (dd, *J*_{C-F} = 7.1, 3.3 Hz, C_q), 129.7 (CH), 128.3 (CH), 123.8 (dd, *J*_{C-F} = 10.8, 3.7 Hz, C_q), 113.8 (dd, ²*J*_{C-F} = 19.8 Hz, ³*J*_{C-F} = 3.4 Hz, CH), 113.3 (CH). **¹⁹F NMR** (282 MHz, CDCl₃): δ = -133.8 (ddd, *J* = 20.8, 6.5, 2.3 Hz), -135.99 (ddd, *J* = 21.4, 10.2, 6.5 Hz), -158.53 (ddd, *J* = 21.1, 7.6 Hz). **IR** (ATR): 3165, 2973, 2922, 1580, 1489, 1439, 1012, 742, 686, 484 cm⁻¹. **MS** (EI) *m/z* (relative intensity): 333 (24) [M]⁺, 314 (11), 256 (6), 241 (18), 224 (100), 77 (6), 43 (13). **HR-MS** (EI) *m/z* calcd for C₁₆H₁₀F₃N₃S, [M]⁺ 333.0548, found 333.0551.

***N*-[2-(Phenylthio)naphthalen-1-yl]pyrimidin-2-amine (149ya)**

The general procedure **A** was followed using substrate **41y** (111 mg, 0.50 mmol) and diphenyl disulfide **62a** (131 mg, 0.60 mmol). Purification by column chromatography (*n*hexane/EtOAc: 4/1) yielded **149ya** (144 mg, 87%) as a pale yellow solid.

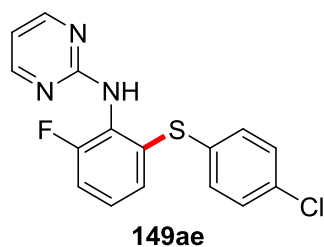
M.p. 163–165 °C. **¹H NMR** (400 MHz, CDCl₃): δ = 8.29 (d, *J* = 4.5 Hz, 2H), 8.01–7.95 (m, 1H), 7.86–7.81 (m, 1H), 7.71 (d, *J* = 8.7 Hz, 1H), 7.61 (br s, 1H), 7.51–7.44 (m, 2H), 7.39 (d, *J* = 8.7 Hz, 1H), 7.37–7.32 (m, 2H), 7.28–7.16 (m, 3H), 6.62 (t, *J* = 4.8 Hz, 1H). **¹³C NMR** (101 MHz, CDCl₃): δ = 162.3 (C_q), 158.4 (CH), 135.3 (C_q), 134.3 (C_q), 133.7 (C_q), 131.8 (C_q), 131.6 (C_q), 131.6 (CH), 129.3 (CH), 129.0 (CH), 128.4 (CH), 127.9 (CH), 127.3 (CH), 126.9 (CH), 126.4 (CH), 124.1 (CH), 112.3 (CH). **IR** (ATR): 3196, 3058, 2920, 1579, 1444, 1375, 788, 743, 690, 515 cm⁻¹. **MS** (EI) *m/z* (relative intensity): 329 (6) [M]⁺, 221 (17), 220 (100), 192 (4), 140 (7), 115 (7). **HR-MS** (EI) *m/z* calcd for C₂₀H₁₅N₃S, [M]⁺ 329.0987, found 329.0993.

***N*-[2-Fluoro-6-(*p*-tolylthio)phenyl]pyrimidin-2-amine (149ab)**



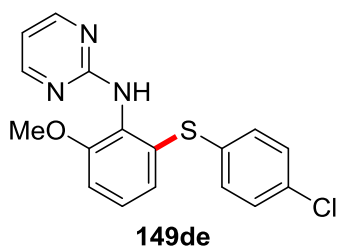
The general procedure **A** was followed using substrate **41a** (94.6 mg, 0.50 mmol) and disulfide **62b** (148 mg, 0.60 mmol). Purification by column chromatography (*n*hexane/EtOAc: 4/1) yielded **149ab** (147 mg, 94%) as a colorless solid.

M.p. 178–180 °C. **¹H NMR** (300 MHz, CDCl₃): δ = 8.34 (d, *J* = 4.8 Hz, 2H), 7.25 (d, *J* = 8.6 Hz, 2H), 7.15–6.96 (m, 5H), 6.77 (br s, 1H), 6.68 (t, *J* = 4.8 Hz, 1H), 2.30 (s, 3H). **¹³C NMR** (126 MHz, CDCl₃): δ = 160.9 (C_q), 158.5 (d, ¹*J*_{C-F} = 251.5 Hz, C_q), 158.2 (CH), 138.1 (C_q), 136.4 (C_q), 132.5 (CH), 130.3 (CH), 130.0 (C_q), 127.2 (d, ³*J*_{C-F} = 8.7 Hz, CH), 126.5 (d, ⁴*J*_{C-F} = 3.3 Hz, CH), 125.8 (d, ³*J*_{C-F} = 13.4 Hz, C_q), 114.9 (d, ²*J*_{C-F} = 20.9 Hz, CH), 112.8 (CH), 21.3 (CH₃). **¹⁹F NMR** (282 MHz, CDCl₃): δ = -116.54 (dd, *J* = 9.3, 5.5 Hz). **IR** (ATR): 3207, 2927, 1581, 1523, 1443, 1410, 899, 776, 672, 509 cm⁻¹. **MS** (EI) *m/z* (relative intensity): 311 (20) [M]⁺, 290 (9), 205 (28), 188 (100). **HR-MS** (EI) *m/z* calcd for C₁₇H₁₄FN₃S, [M]⁺ 311.0892, found 311.0888.

***N*-2-[(4-Chlorophenyl)thio]-6-fluorophenyl}pyrimidin-2-amine (149ae)**

The general procedure **A** was followed using substrate **41a** (94.6 mg, 0.50 mmol) and disulfide **62e** (172 mg, 0.60 mmol). Purification by column chromatography (*n*hexane/EtOAc: 4/1) yielded **149ae** (159 mg, 96%) as a colorless solid.

M.p. 214–215 °C. **¹H NMR** (300 MHz, *d*₆-DMSO): δ = 8.91 (br s, 1H), 8.31 (d, *J* = 4.8 Hz, 2H), 7.39 (d, *J* = 8.8 Hz, 2H), 7.31 (d, *J* = 8.7 Hz), 7.29–7.15 (m, 2H), 6.97–6.91 (m, 1H), 6.74 (t, *J* = 4.8 Hz, 1H). **¹³C NMR** (75 MHz, *d*₆-DMSO): δ = 161.1 (C_q), 158.7 (d, ¹*J*_{C-F} = 248.4 Hz, C_q), 157.9 (CH), 137.0 (C_q), 133.4 (CH), 132.9 (C_q), 132.5 (C_q), 129.4 (CH), 127.8 (d, ³*J*_{C-F} = 8.9 Hz, CH), 126.7 (d, ²*J*_{C-F} = 14.3 Hz, C_q), 126.2 (d, ⁴*J*_{C-F} = 3.2 Hz, CH), 114.7 (d, ²*J*_{C-F} = 21.2 Hz, CH), 112.0 (CH). **¹⁹F NMR** (282 MHz, *d*₆-DMSO): δ = -112.83 (m). **IR** (ATR): 3200, 2923, 1583, 1443, 1410, 896, 788, 774, 504, 487 cm⁻¹. **MS** (ESI) *m/z* (relative intensity): 332 (100) [M+H]⁺ (³⁵Cl). **HR-MS** (ESI) *m/z* calcd for C₁₆H₁₂³⁵ClFN₃S, [M+H]⁺ 332.0421, found 332.0419.

***N*-{2-[(4-Chlorophenyl)thio]-6-methoxyphenyl}pyrimidin-2-amine (149de)**

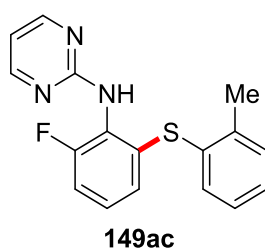
The general procedure **A** was followed using substrate **41d** (101 mg, 0.50 mmol) and disulfide **62e** (172 mg, 0.60 mmol). Purification by column chromatography (*n*hexane/EtOAc: 3/1) yielded **149de** (91.0 mg, 53%) as a yellow solid.

M.p. 161–163 °C. **¹H NMR** (500 MHz, *d*₆-DMSO): δ = 8.55 (s, 1H), 8.25 (d, *J* = 4.8 Hz, 1H), 7.37 (d, *J* = 8.6 Hz, 2H), 7.28 (d, *J* = 8.6 Hz, 2H), 7.18 (t, *J* = 8.1 Hz,

5 Experimental Part

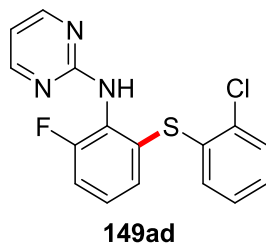
1H), 6.99 (dd, $J = 8.3, 0.9$ Hz, 1H), 6.68 (dd, $J = 8.4, 1.0$ Hz, 1H), 6.66 (t, $J = 4.8$ Hz, 1H), 3.71 (s, 3H). **^{13}C NMR** (126 MHz, $\text{d}_6\text{-DMSO}$): $\delta = 161.7$ (C_q), 157.9 (CH), 156.3 (C_q), 136.2 (C_q), 134.2 (C_q), 133.2 (CH), 132.2 (C_q), 129.4 (CH), 127.7 (CH), 127.6 (C_q), 122.5 (CH), 111.5 (CH), 110.9 (CH), 55.8 (CH_3). **IR** (ATR): 3197, 2921, 1569, 151, 1443, 1407, 1039, 821, 796, 767 cm^{-1} . **MS** (ESI) m/z (relative intensity): 366 (35) $[\text{M}+\text{Na}]^+$ (^{35}Cl), 344 (100) $[\text{M}+\text{H}]^+$ (^{35}Cl), 201 (6), 170 (13). **HR-MS** (ESI) m/z calcd for $\text{C}_{17}\text{H}_{14}^{35}\text{ClN}_3\text{OS}$, $[\text{M}+\text{H}]^+$ 344.0619, found 344.0620.

***N*-[2-Fluoro-6-(*o*-tolylthio)phenyl]pyrimidin-2-amine (149ac)**



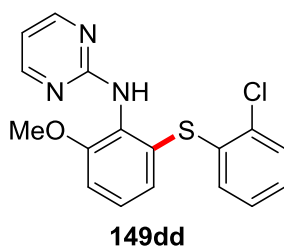
The general procedure **A** was followed using substrate **41a** (94.6 mg, 0.50 mmol) and disulfide **62c** (148 mg, 0.60 mmol). Purification by column chromatography (*n*hexane/EtOAc: 4/1) yielded **149ac** (145 mg, 94%) as a colorless solid.

M.p. 153–155 °C. **^1H NMR** (300 MHz, CDCl_3): $\delta = 8.35$ (d, $J = 4.8$ Hz, 2H), 7.28–7.14 (m, 3H), 7.14–7.00 (m, 3H), 6.88–6.82 (m, 2H), 6.69 (t, $J = 4.8$ Hz, 1H), 2.34 (s, 3H). **^{13}C NMR** (76 MHz, CDCl_3): $\delta = 160.9$ (C_q), 158.6 (d, $^1J_{\text{C-F}} = 251.5$ Hz, C_q), 158.3 (CH), 140.3 (C_q), 135.7 (d, $^3J_{\text{C-F}} = 1.2$ Hz, C_q), 133.2 (CH), 132.5 (C_q), 130.9 (CH), 128.4 (CH), 127.3 (d, $^3J_{\text{C-F}} = 8.8$ Hz, CH), 127.0 (CH), 125.9 (d, $^4J_{\text{C-F}} = 3.3$ Hz, CH), 125.7 (C_q), 114.7 (d, $^2J_{\text{C-F}} = 20.9$ Hz, CH), 112.9 (CH), 20.7 (CH_3). **^{19}F NMR** (283 MHz, CDCl_3): $\delta = -116.13$ (dd, $J = 9.1, 5.8$ Hz). **IR** (ATR): 3204, 2925, 1579, 1523, 1442, 1408, 896, 776, 750, 514 cm^{-1} . **MS** (ESI) m/z (relative intensity): 312 (100) $[\text{M}+\text{H}]^+$, 297 (6), 170 (7). **HR-MS** (ESI) m/z calcd for $\text{C}_{17}\text{H}_{15}\text{N}_3\text{FS}$, $[\text{M}+\text{H}]^+$ 312.0965, found 312.0967.

***N*-{2-[(2-Chlorophenyl)thio]-6-fluorophenyl}pyrimidin-2-amine (149ad)**

The general procedure **A** was followed using substrate **41a** (94.6 mg, 0.50 mmol) and disulfide **62d** (172 mg, 0.60 mmol). Purification by column chromatography (*n*hexane/EtOAc: 4/1) yielded **149ad** (156 mg, 96%) as a colorless solid.

M.p. 145–146 °C. **¹H NMR** (400 MHz, CDCl₃): δ = 8.32 (d, *J* = 4.8 Hz, 2H), 7.34–7.32 (m, 1H), 7.23–7.15 (m, 3H), 7.10–7.05 (m, 1H), 7.03–7.00 (m, 2H), 6.96 (br s, 1H), 6.67 (t, *J* = 4.8 Hz, 1H). **¹³C NMR** (101 MHz, CDCl₃): δ = 160.6 (C_q), 158.4 (d, ¹*J*_{C-F} = 252.4 Hz, C_q), 158.1 (CH), 134.3 (d, ²*J*_{C-F} = 23.1 Hz, C_q), 131.6 (C_q), 131.6 (C_q), 131.0 (CH), 130.0 (CH), 129.4 (d, ⁴*J*_{C-F} = 3.3 Hz, CH), 128.2 (d, ³*J*_{C-F} = 12.8 Hz, C_q), 128.0 (CH), 127.4 (CH), 127.2 (d, ³*J*_{C-F} = 8.6 Hz, CH), 116.9 (d, ²*J*_{C-F} = 20.9 Hz, CH), 113.1 (CH). **¹⁹F NMR** (282 MHz, CDCl₃): δ = -116.43 (dd, *J* = 9.3, 5.5 Hz). **IR** (ATR): 3202, 3060, 1581, 1567, 1442, 1409, 901, 786, 754, 690 cm⁻¹. **MS** (ESI) *m/z* (relative intensity): 332 (100) [M+H]⁺ (³⁵Cl), 203 (9), 170 (8). **HR-MS** (ESI) *m/z* calcd for C₁₆H₁₂N₃F³⁵ClS, [M+H]⁺ 332.0419, found 332.0422.

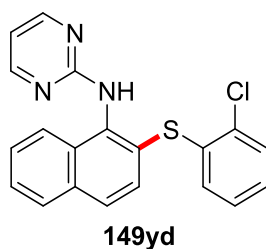
***N*-{2-[(2-Chlorophenyl)thio]-6-methoxyphenyl}pyrimidin-2-amine (149dd)**

The general procedure **A** was followed using substrate **41d** (101 mg, 0.50 mmol) and disulfide **62d** (172 mg, 0.60 mmol). Purification by column chromatography (*n*hexane/EtOAc: 4/1) yielded **149dd** (63.6 mg, 37%) as a pale-yellow oil.

¹H NMR (500 MHz, CDCl₃): δ = 8.38 (s, 2H), 7.33–7.30 (m, 1H), 7.18 (d, *J* = 8.1, 8.1 Hz, 1H), 7.10–7.01 (m, 3H), 6.98–6.94 (m, 2H), 6.84 (s, 1H), 6.66 (s, 1H), 3.82 (s,

3H). ^{13}C NMR (126 MHz, CDCl_3): δ = 161.6 (C_q), 157.8 (CH), 155.3 (C_q), 135.7 (C_q), 134.4 (C_q), 132.4 (C_q), 131.6 (CH), 129.8 (CH), 128.8 (C_q), 127.7 (CH), 127.7 (CH), 127.3 (CH), 127.2 (CH), 125.6 (CH), 111.6 (CH), 56.0 (CH_3). **MS** (ESI) m/z (relative intensity): 366 (32) $[\text{M}+\text{Na}]^+$ (^{35}Cl), 344 (100) $[\text{M}+\text{H}]^+$ (^{35}Cl). **HR-MS** (ESI) m/z calcd for $\text{C}_{17}\text{H}_{15}\text{N}_3^{35}\text{ClOS}$, $[\text{M}+\text{H}]^+$ 344.0619, found 344.0614.

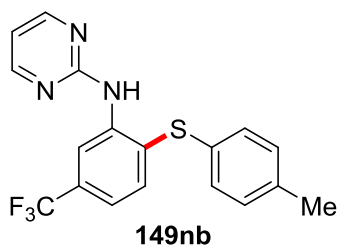
***N*-{2-[(2-Chlorophenyl)thio]naphthalen-1-yl}pyrimidin-2-amine (149yd)**



The general procedure **A** was followed using substrate **41y** (110 mg, 0.50 mmol) and disulfide **62d** (148 mg, 0.60 mmol). Purification by column chromatography (*n*hexane/EtOAc: 4/1) yielded **149yd** (148 mg, 82%) as a colorless oil.

^1H NMR (500 MHz, CDCl_3): δ = 8.43 (s, 2H), 7.99 (d, J = 8.1 Hz, 1H), 7.86 (dd, J = 8.0, 0.9 Hz, 1H), 7.75 (d, J = 8.6 Hz, 1H), 7.66 (s, 1H), 7.54–7.46 (m, 2H), 7.43 (d, J = 8.6 Hz, 1H), 7.34 (dd, J = 8.3, 1.2 Hz, 1H), 7.10–7.06 (m, 2H), 7.03–6.98 (m, 1H), 6.73 (s, 1H). ^{13}C NMR (126 MHz, CDCl_3): δ = 158.0 (C_q), 136.1 (C_q), 135.3 (C_q), 134.4 (C_q), 134.2 (C_q), 131.6 (CH), 131.5 (C_q), 130.0 (CH), 129.9 (CH), 128.8 (C_q), 128.4 (CH), 128.0 (CH), 127.8 (CH), 127.3 (CH), 126.9 (CH), 126.9 (CH), 124.5 (CH). **MS** (ESI) m/z (relative intensity): 386 (26) $[\text{M}+\text{Na}]^+$ (^{35}Cl), 364 (100) $[\text{M}+\text{H}]^+$ (^{35}Cl), 221 (11). **HR-MS** (ESI) m/z calcd for $\text{C}_{20}\text{H}_{15}\text{N}_3^{35}\text{ClIS}$, $[\text{M}+\text{H}]^+$ 364.0670, found 364.0665.

***N*-[2-(*p*-Tolylthio)-5-(trifluoromethyl)phenyl]pyrimidin-2-amine (149nb)**

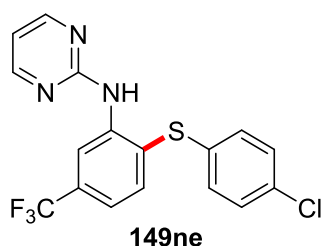


5 Experimental Part

The general procedure **A** was followed using substrate **41n** (120 mg, 0.50 mmol) and disulfide **62b** (148 mg, 0.60 mmol). Purification by column chromatography (*n*hexane/EtOAc: 4/1) yielded **149nb** (103 mg, 57%) as a colorless solid.

M.p. 93–95 °C. **¹H NMR** (500 MHz, CDCl₃): δ = 8.97 (d, *J* = 1.4 Hz, 1H), 8.47 (d, *J* = 4.8 Hz, 2H), 8.25 (br s, 1H), 7.57 (d, *J* = 8.0 Hz, 1H), 7.21 (dd, *J* = 8.1, 1.4 Hz, 1H), 7.16 (d, *J* = 8.2 Hz, 2H), 7.08 (d, *J* = 8.0 Hz, 2H), 6.80 (t, *J* = 4.8 Hz, 1H), 2.29 (s, 3H). **¹³C NMR** (126 MHz, CDCl₃): δ = 159.7 (C_q), 158.1 (CH), 140.9 (C_q), 137.5 (C_q), 135.4 (CH), 131.7 (q, ²*J*_{C-F} = 32.3 Hz, C_q), 130.7 (C_q), 130.4 (CH), 129.8 (CH), 126.1 (C_q), 124.1 (q, ¹*J*_{C-F} = 272.6 Hz, C_q), 118.8 (q, ³*J*_{C-F} = 3.8 Hz, CH), 116.3 (q, ³*J*_{C-F} = 4.0 Hz, CH), 113.8 (CH), 21.2 (CH₃). **¹⁹F NMR** (471 MHz, CDCl₃): δ = -62.72 (s). **IR** (ATR): 3347, 1577, 1522, 1430, 1327, 1157, 1140, 1077, 792, 483 cm⁻¹. **MS** (ESI) *m/z* (relative intensity): 384 (24) [M+Na]⁺, 362 (100) [M+H]⁺. **HR-MS** (ESI) *m/z* calcd for C₁₈H₁₄N₃F₃S, [M+H]⁺ 362.0933, found 362.0934.

N-{2-[(4-Chlorophenyl)thio]-5-(trifluoromethyl)phenyl}pyrimidin-2-amine (**149ne**)

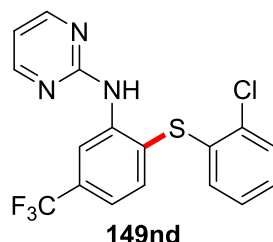


The general procedure **A** was followed using substrate **41n** (120 mg, 0.50 mmol) and disulfide **62e** (172 mg, 0.60 mmol). Purification by column chromatography (*n*hexane/EtOAc: 4/1) yielded **149ne** (105 mg, 55%) as a colorless solid.

M.p. 105–106 °C. **¹H NMR** (500 MHz, d₆-DMSO): δ = 8.93 (s, 1H), 8.46 (d, *J* = 4.8 Hz, 2H), 8.24 (d, *J* = 1.3 Hz, 1H), 7.48–7.43 (m, 2H), 7.41 (d, *J* = 8.7 Hz, 2H), 7.30 (d, *J* = 8.7 Hz, 2H), 6.90 (t, *J* = 4.8 Hz, 1H). **¹³C NMR** (126 MHz, d₆-DMSO): δ = 160.0 (C_q), 158.4 (CH), 139.8 (C_q), 133.6 (CH), 132.7 (C_q), 132.7 (C_q), 132.5 (C_q), 132.4 (CH), 129.8 (CH), 129.0 (q, ²*J*_{C-F} = 32.0 Hz, C_q), 124.0 (q, ¹*J*_{C-F} = 272.4 Hz, C_q), 120.8 (q, ³*J*_{C-F} = 3.7 Hz, CH), 119.9 (d, ³*J*_{C-F} = 3.9 Hz, CH), 113.6 (CH). **¹⁹F NMR** (471 MHz, d₆-DMSO): δ = -61.22 (s). **IR** (ATR): 3347, 1576, 1519, 1428, 1396, 1325, 1127, 1078, 799, 484 cm⁻¹. **MS** (ESI) *m/z* (relative intensity): 420 (4)

$[M+K]^+$ (^{35}Cl), 382 (100) $[M+H]^+$ (^{35}Cl), 288 (4). **HR-MS** (ESI) m/z calcd for $\text{C}_{17}\text{H}_{12}\text{N}_3\text{F}_3^{35}\text{ClS}$, $[M+H]^+$ 382.0387, found 382.0384.

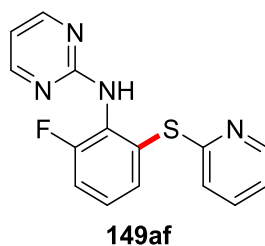
***N*-{2-[(2-Chlorophenyl)thio]-5-(trifluoromethyl)phenyl}pyrimidin-2-amine (149nd)**



The general procedure **A** was followed using substrate **41n** (478 mg, 2.00 mmol) and disulfide **62d** (689 mg, 2.40 mmol). Purification by column chromatography (*n*hexane/EtOAc: 4/1) yielded **149nd** (552 mg, 72%) as a colorless solid.

M.p. 150–152 °C. $^1\text{H NMR}$ (300 MHz, CDCl_3): δ = 9.12 (d, J = 1.7 Hz, 1H), 8.47 (d, J = 4.8 Hz, 2H), 8.26 (br s, 1H), 7.67 (d, J = 8.1 Hz, 1H), 7.39 (dd, J = 7.5, 1.8 Hz, 1H), 7.31–7.25 (m, 1H), 7.14–7.02 (m, 2H), 6.82 (t, J = 4.8 Hz, 1H), 6.72 (dd, J = 7.6, 1.9 Hz, 1H). $^{13}\text{C NMR}$ (75 MHz, CDCl_3): δ = 159.5 (C_q), 158.1 (CH), 142.4 (C_q), 137.3 (CH), 134.5 (C_q), 133.1 (q, $^2J_{\text{C-F}}$ = 32.4 Hz, C_q), 132.5 (C_q), 130.1 (CH), 127.9 (CH), 127.7 (CH), 127.5 (CH), 124.0 (q, $^1J_{\text{C-F}}$ = 272.9 Hz, C_q), 122.0 (d, $^4J_{\text{C-F}}$ = 1.3 Hz, C_q), 118.9 (q, $^3J_{\text{C-F}}$ = 3.8 Hz, CH), 116.2 (q, $^3J_{\text{C-F}}$ = 4.1 Hz, CH), 114.1 (CH). $^{19}\text{F NMR}$ (282 MHz, CDCl_3): δ = -62.94 (s). **IR** (ATR): 3366, 1576, 1524, 1430, 1398, 1325, 1157, 1119, 1081, 748 cm^{-1} . **MS** (ESI) m/z (relative intensity): 404 (31) $[M+\text{Na}]^+$ (^{35}Cl), 382 (100) $[M+H]^+$ (^{35}Cl). **HR-MS** (ESI) m/z calcd for $\text{C}_{17}\text{H}_{12}\text{N}_3\text{S}^{35}\text{ClF}_3$, $[M+H]^+$ 382.0387, found 382.0384.

***N*-[2-Fluoro-6-(pyridin-2-ylthio)phenyl]pyrimidin-2-amine (149af)**



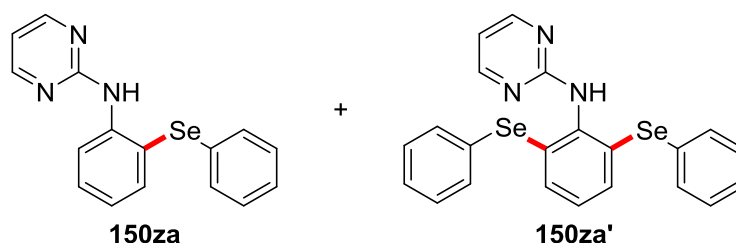
5 Experimental Part

The general procedure **A** was followed using substrate **41a** (94.6 mg, 0.50 mmol) and disulfide **62f** (132 mg, 0.60 mmol). Purification by column chromatography (*n*hexane/EtOAc: 2/1) yielded **149af** (81.9 mg, 55%) as a yellow liquid.

¹H NMR (300 MHz, CDCl₃): δ = 8.50 (d, *J* = 4.8 Hz, 2H), 7.82 (d, *J* = 8.2 Hz, 1H), 7.78–7.69 (m, 1H), 7.56 (d, *J* = 8.1 Hz, 1H), 7.51–7.44 (m, 1H), 7.38 (d, *J* = 8.1 Hz, 1H), 7.31 (td, *J* = 8.2, 5.4 Hz, 1H), 7.12–7.00 (m, 2H), 6.88 (t, *J* = 4.8 Hz, 1H). **¹³C NMR** (75 MHz, CDCl₃): δ = 161.1 (C_q), 159.7 (d, ¹*J*_{C-F} = 252.1 Hz, C_q), 159.6 (C_q), 158.3 (CH), 154.7 (C_q), 148.4 (CH), 138.3 (C_q), 137.4 (CH), 129.3 (d, ³*J*_{C-F} = 8.6 Hz, CH), 122.4 (d, ⁴*J*_{C-F} = 3.3 Hz, CH), 120.9 (CH), 119.7 (CH), 119.4 (CH), 114.8 (d, ²*J*_{C-F} = 20.5 Hz, CH), **¹⁹F NMR** (282 MHz, CDCl₃): δ = -120.24 (dd, *J* = 8.9, 5.5 Hz). **IR** (ATR): 3196, 2943, 1593, 1446, 1418, 876, 776, 765, 514, 497 cm⁻¹. **MS** (ESI) *m/z* (relative intensity): 297 (100) [M+H]⁺, 265 (5), 203 (3). **HR-MS** (ESI) *m/z* calcd for C₁₅H₁₂FN₄S, [M+H]⁺ 299.0564, found 299.0586.

5.3.2 Experimental Procedures and Analytical Data - Selenylation

***N*-[2-(Phenylselanyl)phenyl]pyrimidin-2-amine (150za)** and ***N*-[2,6-Bis(phenylselanyl)phenyl]pyrimidin-2-amine (150za')**



The general procedure **A** was followed using substrate **41z** (85.6 mg, 0.50 mmol) and diphenyl diselenide **148a** (187 mg, 0.60 mmol). Purification by column chromatography (*n*hexane/EtOAc: 4/1) yielded **150za** (33.5 mg, 21%) as a colorless oil and **150za'** (43.9 mg, 18%) as a colorless solid.

***N*-[2-(Phenylselanyl)phenyl]pyrimidin-2-amine (150za):**

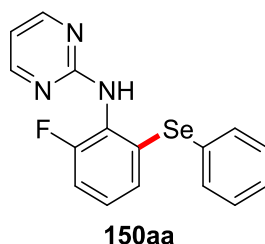
¹H NMR (300 MHz, CDCl₃): δ = 8.54 (dd, *J* = 8.3, 1.2 Hz, 1H), 8.40 (d, *J* = 4.8 Hz, 2H), 8.16 (br s, 1H), 7.72 (dd, *J* = 7.7, 1.6 Hz, 1H), 7.48–7.41 (m, 1H), 7.33–7.27 (m, 2H), 7.22–7.11 (m, 3H), 7.03–6.96 (m, 1H), 6.71 (t, *J* = 4.8 Hz, 1H). **¹³C NMR** (76 MHz, CDCl₃): δ = 160.1 (C_q), 158.0 (CH), 141.2 (C_q), 137.9 (CH), 131.4 (C_q),

130.6 (CH), 130.4 (CH), 129.5 (CH), 126.8 (CH), 123.2 (CH), 120.0 (CH), 119.0 (C_q), 113.1 (CH). **IR** (ATR): 3336, 3049, 1572, 1512, 1431, 1397, 1303, 1020, 795, 753, 735, 689 cm⁻¹. **MS** (ESI) *m/z* (relative intensity): 328 (100) [M+H]⁺, 170 (83). **HR-MS** (ESI) *m/z* calcd for C₁₆H₁₄N₃Se, [M+H]⁺ 328.0348, found 328.0350.

***N*-[2,6-Bis(phenylselanyl)phenyl]pyrimidin-2-amine (150za')**:

M.p. 141–143 °C. **¹H NMR** (300 MHz, CDCl₃): δ = 8.32 (d, *J* = 4.8 Hz, 2H), 7.50–7.45 (m, 4H), 7.27–7.18 (m, 8H), 7.01 (br s, 1H), 6.95 (dd, *J* = 7.8 Hz, 1H), 6.65 (t, *J* = 4.8 Hz, 1H). **¹³C NMR** (76 MHz, CDCl₃): δ = 161.4 (C_q), 158.3 (CH), 137.4 (C_q), 134.4 (CH), 133.4 (C_q), 132.2 (CH), 130.3 (C_q), 129.5 (CH), 128.0 (CH), 127.9 (CH), 112.8 (CH). **IR** (ATR): 3194, 1573, 1429, 1394, 795, 777, 740, 718, 690, 462 cm⁻¹. **MS** (ESI) *m/z* (relative intensity): 506 (18) [M+Na]⁺, 484 (100) [M+H]⁺, 381 (34), 353 (23), 170 (84). **HR-MS** (ESI) *m/z* calcd for C₂₂H₁₈N₃Se₂, [M+H]⁺ 483.9830, found 483.9821.

***N*-[2-Fluoro-6-(phenylselanyl)phenyl]pyrimidin-2-amine (150aa)**

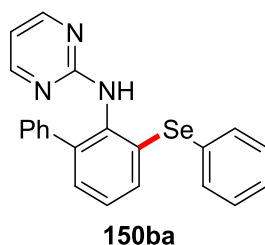


The general procedure **B** was followed using substrate **41a** (94.6 mg, 0.50 mmol) and diphenyl diselenide **148a** (187 mg, 0.60 mmol). Purification by column chromatography (*n*hexane/EtOAc: 4/1) yielded **150aa** (128 mg, 74%) as a colorless solid.

M.p. 146–148 °C. **¹H NMR** (300 MHz, CDCl₃): δ = 8.36 (d, *J* = 4.8 Hz, 2H), 7.54–7.45 (m, 2H), 7.28–7.20 (m, 3H), 7.19–7.03 (m, 4H), 6.70 (t, *J* = 4.8 Hz, 1H). **¹³C NMR** (126 MHz, CDCl₃): δ = 160.9 (C_q), 158.2 (d, ¹*J*_{C-F} = 251.6 Hz, C_q), 158.1 (CH), 134.1 (CH), 133.0 (C_q), 129.7 (C_q), 129.5 (CH), 128.4 (d, ⁴*J*_{C-F} = 3.4 Hz, CH), 128.0 (CH), 127.5 (d, ³*J*_{C-F} = 8.3 Hz, CH), 126.7 (d, ²*J*_{C-F} = 13.1 Hz, C_q), 115.3 (d, ²*J*_{C-F} = 20.9 Hz, CH), 112.8 (CH). **¹⁹F NMR** (282 MHz, CDCl₃): δ = -116.54 (dd, *J* = 9.3, 5.5 Hz). **IR** (ATR): 3209, 3152, 2923, 1582, 1525, 1443, 770, 748, 643, 487 cm⁻¹. **MS**

(EI) m/z (relative intensity): 345 (11) $[M]^+$, 253 (4), 188 (100), 168 (8), 141 (6). **HR-MS** (EI) m/z calcd for $C_{16}H_{12}N_3Se$, $[M]^+$ 345.0180, found 345.0172.

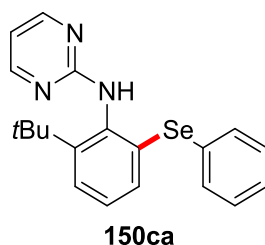
***N*-[3-(Phenylselanyl)-(1,1'-biphenyl)-2-yl]pyrimidin-2-amine (150ba)**



The general procedure **B** was followed using substrate **41b** (124 mg, 0.50 mmol) and diphenyl diselenide **148a** (187 mg, 0.60 mmol). Purification by column chromatography (*n*hexane/EtOAc: 4/1) yielded **150ba** (166 mg, 82%) as a colorless solid.

M.p. 143–146 °C. 1H NMR (400 MHz, $CDCl_3$): δ = 8.23 (d, J = 4.8 Hz, 2H), 7.57–7.53 (m, 2H), 7.36–7.32 (m, 2H), 7.32–7.22 (m, 8H), 7.17 (dd, J = 7.7, 7.7 Hz, 1H), 6.85 (br s, 1H), 6.55 (t, J = 4.8 Hz, 1H). ^{13}C NMR (101 MHz, $CDCl_3$): δ = 161.3 (C_q), 158.1 (CH), 140.2 (C_q), 139.7 (C_q), 135.1 (C_q), 134.8 (CH), 133.8 (C_q), 132.1 (CH), 130.4 (C_q), 129.7 (CH), 129.5 (CH), 128.9 (CH), 128.3 (CH), 128.0 (CH), 127.5 (CH), 127.4 (CH), 112.2 (CH). **IR** (ATR): 3194, 2919, 1580, 1519, 1441, 1406, 750, 692, 662, 637 cm^{-1} . **MS** (ESI) m/z (relative intensity): 426 (46) $[M+Na]^+$, 404 (100) $[M+H]^+$, 236 (16), 103 (29). **HR-MS** (ESI) m/z calcd for $C_{22}H_{18}N_3Se$, $[M+H]^+$ 404.0661, found 404.0660.

***N*-[2-(*tert*-Butyl)-6-(phenylselanyl)phenyl]pyrimidin-2-amine (150ca)**

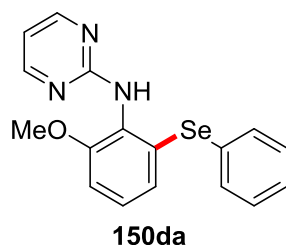


The general procedure **B** was followed using substrate **41c** (114 mg, 0.50 mmol) and diphenyl diselenide **148a** (187 mg, 0.60 mmol). Purification by column chromatography (*n*hexane/EtOAc: 4/1) yielded **150ca** (86.7 mg, 45%) as a colorless solid.

5 Experimental Part

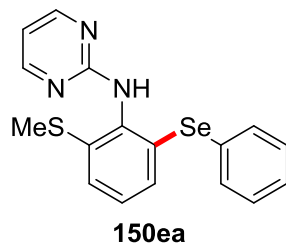
M.p. 154–156 °C. **¹H NMR** (300 MHz, CDCl₃): δ = 8.36 (s, 2H), 7.54–7.48 (m, 2H), 7.37 (dd, J = 6.1, 3.4 Hz, 1H), 7.32–7.24 (m, 3H), 7.11–7.08 (m, 2H), 6.87 (br s, 1H), 6.63 (t, J = 4.8 Hz, 1H), 1.39 (s, 9H). **¹³C NMR** (126 MHz, CDCl₃): δ = 162.1 (C_q), 158.4 (CH), 149.1 (C_q), 138.1 (C_q), 135.3 (C_q), 135.2 (CH), 130.3 (CH), 130.2 (C_q), 129.4 (CH), 128.2 (CH), 128.0 (CH), 125.9 (CH), 111.8 (CH), 35.9 (C_q), 31.3 (CH₃). **IR** (ATR): 3197, 2962, 1576, 1442, 1401, 798, 781, 736, 691, 641 cm⁻¹. **MS** (EI) m/z (relative intensity): 383 (2) [M]⁺, 326 (20), 248 (9), 226 (100), 210 (47), 196 (9), 169 (8), 77 (11). **HR-MS** (ESI) m/z calcd for C₂₀H₂₁N₃Se, [M+H]⁺ 384.0974, found 384.0976.

***N*-[2-Methoxy-6-(phenylselanyl)phenyl]pyrimidin-2-amine (150da)**



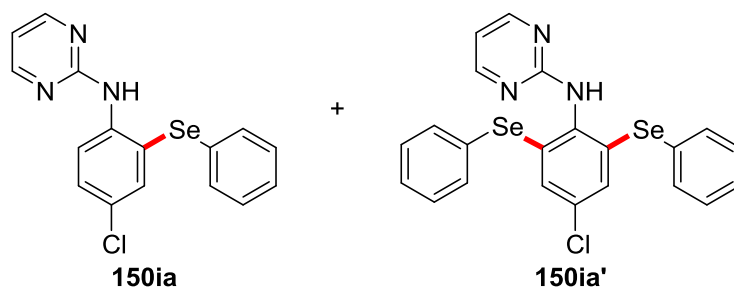
The general procedure **B** was followed using substrate **41d** (101 mg, 0.50 mmol) and diphenyl diselenide **148a** (187 mg, 0.60 mmol). Purification by column chromatography (*n*hexane/EtOAc: 4/1) yielded **150da** (115 mg, 65%) as a off-white solid.

M.p. 198–201 °C. **¹H NMR** (300 MHz, CDCl₃): δ = 8.33 (d, J = 4.8 Hz, 2H), 7.54–7.41 (m, 2H), 7.27–7.19 (m, 3H), 7.04 (t, J = 8.0 Hz, 1H), 6.92–6.78 (m, 3H), 6.64 (t, J = 4.8 Hz, 1H), 3.78 (s, 3H). **¹³C NMR** (75 MHz, CDCl₃): δ = 161.7 (C_q), 158.2 (CH), 154.7 (C_q), 134.6 (CH), 133.3 (C_q), 131.2 (C_q), 129.4 (CH), 127.8 (CH), 127.4 (C_q), 127.3 (CH), 124.9 (CH), 112.6 (CH), 110.0 (CH), 56.0 (CH₃). **IR** (ATR): 3193, 2921, 1571, 1436, 1412, 1023, 763, 749, 691, 643 cm⁻¹. **MS** (ESI) m/z (relative intensity): 380 (31) [M+Na]⁺, 358 (100) [M+H]⁺, 201 (45), 140 (93). **HR-MS** (ESI) m/z calcd for C₁₇H₁₆N₃OSe, [M+H]⁺ 358.0454, found 358.0460.

***N*-[2-(Methylthio)-6-(phenylselanyl)phenyl]pyrimidin-2-amine (150ea)**

The general procedure **B** was followed using substrate **41e** (109 mg, 0.50 mmol) and diphenyl diselenide **148a** (187 mg, 0.60 mmol). Purification by column chromatography (*n*hexane/EtOAc: 4/1) yielded **150ea** (97.3 mg, 52%) as a colorless solid.

M.p. 155–156 °C. **¹H NMR** (400 MHz, CDCl₃): δ = 8.36 (d, *J* = 4.8 Hz, 2H), 7.54–7.46 (m, 2H), 7.32–7.21 (m, 3H), 7.16 (dd, *J* = 7.7, 1.8 Hz, 1H), 7.11 (dd, *J* = 7.6 Hz, 1H), 7.06 (dd, *J* = 7.6, 1.8 Hz, 1H), 6.87 (br s, 1H), 6.66 (t, *J* = 4.8 Hz, 1H), 2.39 (s, 3H). **¹³C NMR** (101 MHz, CDCl₃): δ = 161.5 (C_q), 158.5 (CH), 138.9 (C_q), 134.9 (CH), 134.8 (C_q), 134.6 (C_q), 130.1 (C_q), 129.5 (CH), 129.1 (CH), 128.1 (CH), 128.1 (CH), 124.8 (CH), 112.6 (CH), 15.8 (CH₃). **IR** (ATR): 3179, 3048, 2905, 1575, 1511, 1435, 1401, 746, 694, 642 cm⁻¹. **MS** (ESI) *m/z* (relative intensity): 396 (9) [M+Na]⁺, 374 (100) [M+H]⁺, 217 (30), 170 (77). **HR-MS** (ESI) *m/z* calcd for C₁₇H₁₆N₃SeS, [M+H]⁺ 374.0225, found 374.0233.

***N*-[4-Chloro-2-(phenylselanyl)phenyl]pyrimidin-2-amine (150ia) and *N*-[4-Chloro-2,6-bis(phenylselanyl)phenyl]pyrimidin-2-amine (150ia')**

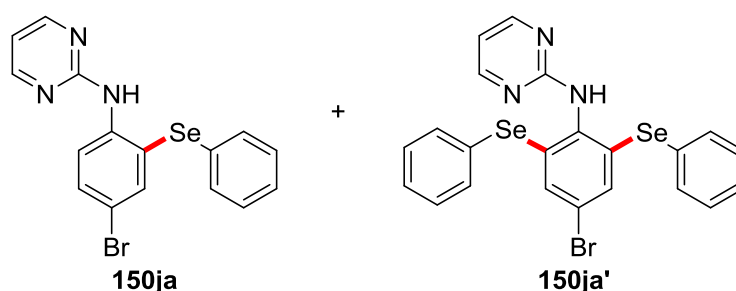
The general procedure **B** was followed using substrate **41i** (103 mg, 0.50 mmol) and diphenyl diselenide **148a** (187 mg, 0.60 mmol). Purification by column chromatography (*n*hexane/EtOAc: 4/1) yielded **150ia** (66.6 mg, 37%) as a colorless solid and **150ia'** (55.2 mg, 21%) as a yellow solid.

***N*-[4-Chloro-2-(phenylselanyl)phenyl]pyrimidin-2-amine (150ia):**

M.p. 97–99 °C. $^1\text{H NMR}$ (300 MHz, CDCl_3): δ = 8.50 (d, J = 8.9 Hz, 1H), 8.40 (d, J = 4.8 Hz, 2H), 8.07 (br s, 1H), 7.67 (d, J = 2.5 Hz, 1H), 7.38 (dd, J = 8.9, 2.5 Hz, 1H), 7.35–7.30 (m, 2H), 7.25–7.15 (m, 3H), 6.74 (t, J = 4.8 Hz, 1H). $^{13}\text{C NMR}$ (76 MHz, CDCl_3): δ = 159.9 (C_q), 158.1 (CH), 139.7 (C_q), 136.6 (CH), 131.0 (CH), 130.5 (C_q), 130.3 (CH), 129.7 (CH), 127.4 (CH), 127.3 (C_q), 121.0 (CH), 120.6 (C_q), 113.4 (CH). **IR** (ATR): 3332, 3052, 1573, 1519, 1444, 1396, 795, 732, 690, 593 cm^{-1} . **MS** (ESI) m/z (relative intensity): 383 (78) $[\text{M}+\text{Na}]^+$ (^{35}Cl), 362 (100) $[\text{M}+\text{H}]^+$ (^{35}Cl). **HR-MS** (ESI) m/z calcd for $\text{C}_{16}\text{H}_{13}^{35}\text{ClN}_3\text{Se}$, $[\text{M}+\text{H}]^+$ 361.9956, found 361.9956.

***N*-{4-Chloro-2,6-bis(phenylselanyl)phenyl}pyrimidin-2-amine (150ia'):**

M.p. 166–168 °C. $^1\text{H NMR}$ (300 MHz, CDCl_3): δ = 8.35 (d, J = 4.8 Hz, 2H), 7.55–7.48 (m, 4H), 7.36–7.24 (m, 6H), 7.03 (s, 2H), 6.94 (br s, 1H), 6.69 (t, J = 4.8 Hz, 1H). $^{13}\text{C NMR}$ (126 MHz, CDCl_3): δ = 161.1 (C_q), 158.3 (CH), 135.8 (C_q), 135.1 (CH), 134.9 (C_q), 133.5 (C_q), 130.2 (CH), 129.7 (CH), 128.9 (C_q), 128.6 (CH), 112.9 (CH). **IR** (ATR): 3133, 2902, 1582, 1507, 1405, 1373, 796, 733, 687, 462 cm^{-1} . **MS** (ESI) m/z (relative intensity): 518 (100) $[\text{M}+\text{H}]^+$ (^{35}Cl). **HR-MS** (ESI) m/z calcd for $\text{C}_{22}\text{H}_{17}^{35}\text{ClN}_3\text{Se}_2$, $[\text{M}+\text{H}]^+$ 517.9435, found 517.9443.

***N*-[4-Bromo-2-(phenylselanyl)phenyl]pyrimidin-2-amine (150ja) and *N*-[4-Bromo-2,6-bis(phenylselanyl)phenyl]pyrimidin-2-amine (150ja')**

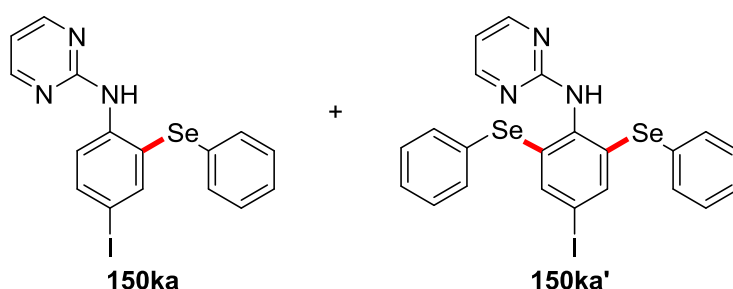
The general procedure **B** was followed using substrate **41j** (125 mg, 0.50 mmol) and diphenyl diselenide **148a** (187 mg, 0.60 mmol). Purification by column chromatography (*n*hexane/EtOAc: 5/1) yielded **150ja** (68.3 mg, 34%) as a colorless solid and **150ja'** (55.8 mg, 20%) as a colorless solid.

***N*-[4-Bromo-2-(phenylselanyl)phenyl]pyrimidin-2-amine (150ja):**

M.p. 91–93 °C. $^1\text{H NMR}$ (300 MHz, CDCl_3): δ = 8.47 (d, J = 8.9 Hz, 1H), 8.41 (d, J = 4.8 Hz, 2H), 8.10 (br s, 1H), 7.82 (d, J = 2.4 Hz, 1H), 7.51 (dd, J = 8.9, 2.4 Hz, 1H), 7.36–7.30 (m, 2H), 7.25–7.17 (m, 3H), 6.74 (t, J = 4.8 Hz, 1H). $^{13}\text{C NMR}$ (126 MHz, CDCl_3): δ = 159.7 (C_q), 157.9 (CH), 140.1 (C_q), 139.4 (CH), 133.2 (CH), 130.9 (CH), 130.4 (C_q), 129.6 (CH), 127.3 (CH), 121.2 (CH), 120.8 (C_q), 114.6 (C_q), 113.4 (CH). **IR** (ATR): 3351, 3332, 1576, 1511, 1444, 1393, 1379, 1297, 793, 734 cm^{-1} . **MS** (ESI) m/z (relative intensity): 406 (100) $[\text{M}+\text{H}]^+$, 327 (3), 249 (31). **HR-MS** (ESI) m/z calcd for $\text{C}_{16}\text{H}_{13}\text{N}_3\text{Se}^{79}\text{Br}$, $[\text{M}+\text{H}]^+$ 405.9450, found 405.9443.

***N*-[4-Bromo-2,6-bis(phenylselanyl)phenyl]pyrimidin-2-amine (150ja'):**

M.p. 156–158 °C. $^1\text{H NMR}$ (400 MHz, CDCl_3): δ = 8.34 (d, J = 4.8 Hz, 2H), 7.52–7.48 (m, 4H), 7.32–7.25 (m, 6H), 7.20 (s, 2H), 6.96 (br s, 1H), 6.68 (t, J = 4.8 Hz, 1H). $^{13}\text{C NMR}$ (101 MHz, CDCl_3): δ = 161.1 (C_q), 158.4 (CH), 136.0 (C_q), 135.6 (C_q), 135.0 (CH), 133.3 (CH), 129.8 (CH), 129.1 (C_q), 128.6 (CH), 121.5 (C_q), 113.0 (CH). **IR** (ATR): 3136, 2903, 1581, 1508, 1442, 1405, 1369, 732, 688, 445 cm^{-1} . **MS** (ESI) m/z (relative intensity): 584 (7) $[\text{M}+\text{Na}]^+$ (^{79}Br), 562 (100) $[\text{M}+\text{H}]^+$ (^{79}Br), 399 (7), 117 (30). **HR-MS** (ESI) m/z calcd for $\text{C}_{22}\text{H}_{17}\text{N}_3^{79}\text{BrSe}_2$, $[\text{M}+\text{H}]^+$ 561.8929, found 561.8932.

***N*-[4-Iodo-2-(phenylselanyl)phenyl]pyrimidin-2-amine (150ka) and *N*-[4-Iodo-2,6-bis(phenylselanyl)phenyl]pyrimidin-2-amine (150ka')**

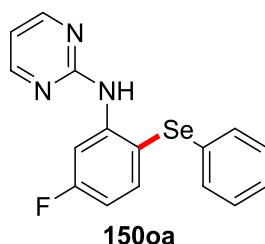
The general procedure **B** was followed using substrate **41k** (149 mg, 0.50 mmol) and diphenyl diselenide **148a** (187 mg, 0.60 mmol). Purification by column chromatography (*n*hexane/EtOAc: 4/1) yielded **150ka** (84.4 mg, 38%) as a yellow solid and **150ka'** (63.8 mg, 21%) as a colorless solid.

***N*-[4-Iodo-2-(phenylselanyl)phenyl]pyrimidin-2-amine (150ka):**

M.p. 119–121 °C. $^1\text{H NMR}$ (300 MHz, CDCl_3): δ = 8.40 (d, J = 4.8 Hz, 2H), 8.32 (d, J = 8.8 Hz, 1H), 8.23 (br s, 1H), 8.01 (d, J = 2.2 Hz, 1H), 7.69 (dd, J = 8.8, 2.2 Hz, 1H), 7.35–7.27 (m, 2H), 7.25–7.14 (m, 3H), 6.75 (t, J = 4.8 Hz, 1H). $^{13}\text{C NMR}$ (75 MHz, CDCl_3): δ = 159.5 (C_q), 158.0 (CH), 145.3 (CH), 140.7 (C_q), 139.2 (CH), 130.9 (CH), 130.6 (C_q), 129.7 (CH), 127.3 (CH), 121.9 (CH), 121.4 (C_q), 113.4 (CH), 85.2 (C_q). **IR** (ATR): 3344, 3321, 1575, 1555, 1507, 1476, 1440, 1392, 792, 739 cm^{-1} . **MS** (ESI) m/z (relative intensity): 454 (100) $[\text{M}+\text{H}]^+$, 329 (25), 297 (25), 171 (20). **HR-MS** (ESI) m/z calcd for $\text{C}_{16}\text{H}_{13}\text{N}_3\text{SeI}$, $[\text{M}+\text{H}]^+$ 453.9315, found 453.9310.

***N*-[4-Iodo-2,6-bis(phenylselanyl)phenyl]pyrimidin-2-amine (150ka'):**

M.p. 145–147 °C. $^1\text{H NMR}$ (400 MHz, CDCl_3): δ = 8.33 (d, J = 4.6 Hz, 2H), 7.50–7.46 (m, 4H), 7.45 (s, 2H), 7.30–7.23 (m, 6H), 6.97 (br s, 1H), 6.68 (t, J = 4.8 Hz, 1H). $^{13}\text{C NMR}$ (101 MHz, CDCl_3): δ = 161.0 (C_q), 158.3 (CH), 139.7 (CH), 136.8 (C_q), 135.7 (C_q), 134.7 (CH), 129.8 (CH), 129.4 (C_q), 128.5 (CH), 113.0 (CH), 92.9 (C_q). **IR** (ATR): 3187, 3045, 1581, 1443, 1404, 848, 737, 688, 669, 472 cm^{-1} . **MS** (ESI) m/z (relative intensity): 610 (100) $[\text{M}+\text{H}]^+$ (^{80}Se), 483 (15), 452 (48), 308 (14), 172 (8). **HR-MS** (ESI) m/z calcd for $\text{C}_{22}\text{H}_{17}\text{N}_3\text{ISe}_2$, $[\text{M}+\text{H}]^+$ 609.8796, found 609.8791.

***N*-[5-Fluoro-2-(phenylselanyl)phenyl]pyrimidin-2-amine (150oa)**

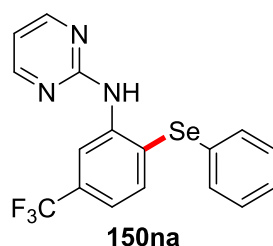
The general procedure **B** was followed using substrate **41o** (94.6 mg, 0.50 mmol) and diphenyl diselenide **148a** (187 mg, 0.60 mmol). Purification by column chromatography (*n*hexane/EtOAc: 4/1) yielded **150oa** (82.2 mg, 48%) as a colorless solid.

M.p. 133–135 °C. $^1\text{H NMR}$ (300 MHz, CDCl_3): δ = 8.59 (dd, J = 12.2, 2.8 Hz, 1H), 8.44 (d, J = 4.8 Hz, 2H), 8.40 (br s, 1H), 7.73 (dd, J = 8.5, 6.6 Hz, 1H), 7.29–7.14 (m, 5H), 6.77 (t, J = 4.8 Hz, 1H), 6.71 (ddd, J = 8.5, 7.9, 2.8 Hz, 1H). $^{13}\text{C NMR}$ (75 MHz, CDCl_3): δ = 164.5 (d, $^1J_{\text{C-F}}$ = 246.5 Hz, C_q), 159.6 (C_q), 158.0 (CH), 143.2 (d, $^3J_{\text{C-F}}$ =

5 Experimental Part

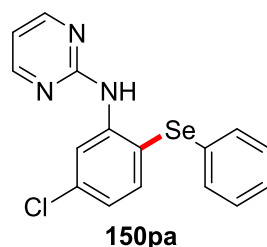
12.8 Hz, C_q), 139.7 (d, ³J_{C-F} = 9.7 Hz, CH), 131.5 (C_q), 129.8 (CH), 129.6 (CH), 126.8 (CH), 113.7 (CH), 112.3 (d, ⁴J_{C-F} = 3.3 Hz, C_q), 109.5 (d, ²J_{C-F} = 22.0 Hz, CH), 106.5 (d, ²J_{C-F} = 29.0 Hz, CH). **¹⁹F NMR** (282 MHz, CDCl₃): δ = -107.95 (m). **IR** (ATR): 3331, 1568, 1520, 1435, 1393, 861, 790, 736, 616, 582 cm⁻¹. **MS** (ESI) *m/z* (relative intensity): 384 (20) [M+K]⁺, 362 (64) [M+NH₄]⁺, 346 (100) [M+H]⁺, 189 (72), 173 (38). **HR-MS** (ESI) *m/z* calcd for C₁₆H₁₃FN₃Se, [M+H]⁺ 346.0254, found 346.0250.

***N*-[2-(Phenylselanyl)-5-(trifluoromethyl)phenyl]pyrimidin-2-amine (150na)**



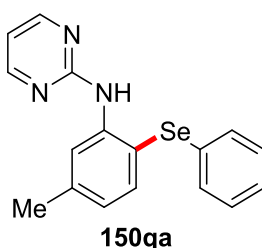
The general procedure **B** was followed using substrate **41n** (120 mg, 0.50 mmol) and diphenyl diselenide **148a** (187 mg, 0.60 mmol). Purification by column chromatography (*n*hexane/EtOAc: 4/1) yielded **150na** (110 mg, 56%) as a colorless solid.

M.p. 97–100 °C. **¹H NMR** (300 MHz, CDCl₃): δ = 8.93 (d, *J* = 1.6 Hz, 1H), 8.45 (d, *J* = 4.8 Hz, 2H), 8.22 (br s, 1H), 7.76 (d, *J* = 8.0 Hz, 1H), 7.40–7.29 (m, 2H), 7.27–7.16 (m, 4H), 6.79 (t, *J* = 4.8 Hz, 1H). **¹³C NMR** (126 MHz, CDCl₃): δ = 159.6 (C_q), 158.0 (CH), 141.3 (C_q), 137.4 (CH), 132.2 (q, ²J_{C-F} = 32.3 Hz, C_q), 131.4 (CH), 130.0 (C_q), 129.7 (CH), 127.5 (CH), 124.1 (q, ¹J_{C-F} = 272.2 Hz, C_q C_q), 123.3 (C_q), 119.0 (q, ³J_{C-F} = 3.7 Hz, CH), 116.3 (q, ³J_{C-F} = 4.0 Hz, CH), 113.7 (CH). **¹⁹F NMR** (282 MHz, CDCl₃): δ = -62.81 (s). **IR** (ATR): 3325, 1569, 1524, 1437, 1426, 1328, 1119, 794, 737, 604 cm⁻¹. **MS** (ESI) *m/z* (relative intensity): 434 (27) [M+K]⁺, 412 (100), 396 (39) [M+H]⁺, 353 (11), 238 (14). **HR-MS** (ESI) *m/z* calcd for C₁₇H₁₃F₃N₃Se, [M+H]⁺ 396.0222, found 396.0227.

***N*-[5-Chloro-2-(phenylselanyl)phenyl]pyrimidin-2-amine (150pa)**

The general procedure **B** was followed using substrate **41p** (103 mg, 0.50 mmol) and diphenyl diselenide **148a** (187 mg, 0.60 mmol). Purification by column chromatography (*n*hexane/EtOAc: 4/1) yielded **150pa** (104 mg, 58%) as a colorless solid.

M.p. 133–135 °C. **¹H NMR** (300 MHz, CDCl₃): δ = 8.77 (d, *J* = 2.3 Hz, 1H), 8.44 (d, *J* = 4.8 Hz, 2H), 8.27 (br s, 1H), 7.65 (d, *J* = 8.2 Hz, 1H), 7.32–7.24 (m, 2H), 7.23–7.12 (m, 3H), 6.97 (dd, *J* = 8.2, 2.3 Hz, 1H), 6.77 (t, *J* = 4.8 Hz, 1H). **¹³C NMR** (75 MHz, CDCl₃): δ = 159.6 (C_q), 158.1 (CH), 142.4 (C_q), 138.9 (CH), 136.7 (C_q), 131.0 (C_q), 130.3 (CH), 129.6 (CH), 127.0 (CH), 122.7 (CH), 119.2 (CH), 116.2 (C_q), 113.7 (CH). **IR** (ATR): 3331, 1574, 1557, 1515, 1434, 1410, 1391, 790, 737, 620 cm⁻¹. **MS** (EI) *m/z* (relative intensity): 361 (7) [M]⁺ (³⁵Cl), 206 (32), 204 (100), 169 (20). **HR-MS** (ESI) *m/z* calcd for C₁₆H₁₃³⁵ClN₃Se, [M+H]⁺ 361.9930, found 361.9946.

***N*-[5-Methyl-2-(phenylselanyl)phenyl]pyrimidin-2-amine (150qa)**

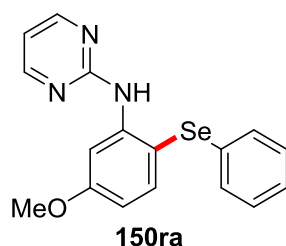
The general procedure **B** was followed using substrate **41q** (92.6 mg, 0.50 mmol) and diphenyl diselenide **148a** (187 mg, 0.60 mmol). Purification by column chromatography (*n*hexane/EtOAc: 4/1) yielded **150qa** (54.7 mg, 32%) as a colorless solid.

M.p. 106–108 °C. **¹H NMR** (300 MHz, CDCl₃): δ = 8.40 (d, *J* = 4.8 Hz, 1H), 8.37 (d, *J* = 1.2 Hz, 2H), 8.16 (br s, 1H), 7.61 (d, *J* = 7.8 Hz, 1H), 7.29–7.23 (m, 2H), 7.20–

5 Experimental Part

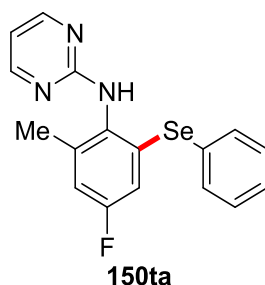
7.09 (m, 3H), 6.83 (dd, $J = 7.8, 1.3$ Hz, 1H), 6.71 (t, $J = 4.8$ Hz, 1H), 2.43 (s, 3H). ^{13}C NMR (126 MHz, CDCl_3): $\delta = 159.9$ (C_q), 157.9 (CH), 141.1 (C_q), 137.9 (CH), 131.8 (C_q), 123.0 (CH), 129.4 (CH), 126.5 (CH), 124.1 (CH), 120.4 (CH), 115.4 (C_q), 112.9 (CH), 22.10 (CH_3). IR (ATR): 3333, 1574, 1527, 1437, 1392, 1020, 790, 736, 625, 610, 452 cm^{-1} . MS (ESI) m/z (relative intensity): 358 (98), 342 (88) $[\text{M}+\text{H}]^+$, 185 (100). HR-MS (ESI) m/z calcd for $\text{C}_{17}\text{H}_{16}\text{N}_3\text{Se}$, $[\text{M}+\text{H}]^+$ 342.0505, found 342.0508.

N-[5-Methoxy-2-(phenylselanyl)phenyl]pyrimidin-2-amine (**150ra**)



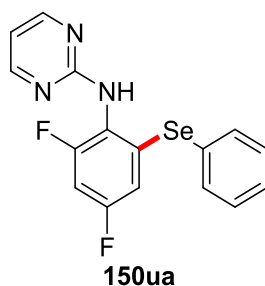
The general procedure **B** was followed using substrate **41r** (101 mg, 0.50 mmol) and diphenyl diselenide **148a** (187 mg, 0.60 mmol). Purification by column chromatography (*n*hexane/EtOAc: 4/1) yielded **150ra** (63.4 mg, 41%) as a colorless solid.

M.p. 85–87 °C. ^1H NMR (300 MHz, CDCl_3): $\delta = 8.42$ (d, $J = 4.8$ Hz, 2H), 8.41 (d, $J = 2.5$ Hz, 1H), 8.34 (br s, 1H), 7.67 (d, $J = 8.5$ Hz, 1H), 7.25–7.08 (m, 5H), 6.72 (t, $J = 4.8$ Hz, 1H), 6.58 (dd, $J = 8.5, 2.8$ Hz, 1H), 3.89 (s, 3H). ^{13}C NMR (76 MHz, CDCl_3): $\delta = 162.0$ (C_q), 159.9 (C_q), 158.0 (CH), 142.9 (C_q), 139.6 (CH), 132.4 (C_q), 129.4 (CH), 129.3 (CH), 126.4 (CH), 113.2 (CH), 108.5 (C_q), 108.3 (CH), 105.2 (CH), 55.6 (CH_3). IR (ATR): 3335, 2953, 1562, 1446, 1258, 1166, 859, 733, 632, 455 cm^{-1} . MS (ESI) m/z (relative intensity): 396 (20) $[\text{M}+\text{K}]^+$, 374 (76), 358 (61) $[\text{M}+\text{H}]^+$, 201 (100), 173 (22). HR-MS (ESI) m/z calcd for $\text{C}_{17}\text{H}_{16}\text{N}_3\text{OSe}$, $[\text{M}+\text{H}]^+$ 358.0454, found 358.0445.

***N*-[4-Fluoro-2-methyl-6-(phenylselanyl)phenyl]pyrimidin-2-amine (150ta)**

The general procedure **B** was followed using substrate **41t** (102 mg, 0.50 mmol) and diphenyl diselenide **148a** (187 mg, 0.60 mmol). Purification by column chromatography (*n*hexane/EtOAc: 4/1) yielded **150ta** (150 mg, 84%) as a colorless solid.

M.p. 143–145 °C. **¹H NMR** (300 MHz, CDCl₃): δ = 8.32 (d, *J* = 4.8 Hz, 2H), 7.55–7.50 (m, 2H), 7.33–7.24 (m, 3H), 6.86 (dd, *J* = 8.9, 2.8 Hz, 1H), 6.74 (br s, 1H), 6.70 (dd, *J* = 8.5, 3.0 Hz, 1H), 6.64 (t, *J* = 4.8 Hz, 1H), 2.24 (s, 3H). **¹³C NMR** (75 MHz, CDCl₃): δ = 161.3 (C_q), 161.3 (d, ¹*J*_{C-F} = 248.4 Hz, C_q), 158.4 (CH), 139.5 (d, ³*J*_{C-F} = 8.4 Hz, C_q), 136.0 (d, ³*J*_{C-F} = 8.1 Hz, C_q), 135.3 (CH), 131.5 (d, ⁴*J*_{C-F} = 2.9 Hz, C_q), 129.6 (CH), 128.5 (CH), 128.3 (C_q), 115.8 (d, ²*J*_{C-F} = 22.4 Hz, CH), 115.45 (d, ²*J*_{C-F} = 24.3 Hz, CH), 112.1 (CH), 18.9 (CH₃). **¹⁹F NMR** (282 MHz, CDCl₃): δ = -114.62 (t, *J* = 8.7 Hz). **IR** (ATR): 3208, 3060, 1573, 1505, 1437, 1411, 799, 744, 690, 541 cm⁻¹. **MS** (ESI) *m/z* (relative intensity): 773 (30), 398 (100) [M+K]⁺, 382 (24) [M+Na]⁺, 376 (99) [M+NH₄]⁺, 360 (16) [M+H]⁺, 203 (19). **HR-MS** (ESI) *m/z* calcd for C₁₇H₁₅FN₃Se, [M+H]⁺ 360.0410, found 360.0416.

***N*-[2,4-Difluoro-6-(phenylselanyl)phenyl]pyrimidin-2-amine (150ua)**

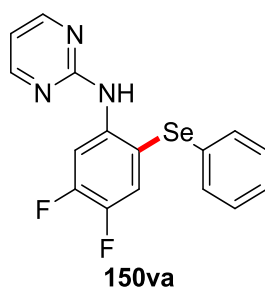
The general procedure **B** was followed using substrate **41u** (104 mg, 0.50 mmol) and diphenyl diselenide **148a** (187 mg, 0.60 mmol). Purification by column

5 Experimental Part

chromatography (*n*hexane/EtOAc: 4/1) yielded **150ua** (95.0 mg, 52%) as a yellow solid.

M.p. 137–140 °C. **¹H NMR** (300 MHz, CDCl₃): δ = 8.36 (d, *J* = 4.8 Hz, 2H), 7.58–7.54 (m, 2H), 7.37–7.28 (m, 3H), 7.07 (br s, 1H), 6.78 (ddd, *J* = 9.5, 8.4, 2.8 Hz, 1H), 6.70 (t, *J* = 4.8 Hz, 1H), 6.64 (ddd, *J* = 8.4, 2.7, 1.6 Hz, 1H). **¹³C NMR** (75 MHz, CDCl₃): δ = 161.6 (dd, ¹*J*_{C-F} = 183.7 Hz, ³*J*_{C-F} = 12.4 Hz, C_q), 161.2 (C_q), 158.4 (CH), 158.2 (dd, ¹*J*_{C-F} = 187.2, ³*J*_{C-F} = 12.5 Hz, C_q), 137.2 (d, *J* = 7.9 Hz, C_q), 135.8 (CH), 130.0 (CH), 129.1 (CH), 127.9 (C_q), 121.7 (dd, ²*J*_{C-F} = 13.8, ⁴*J*_{C-F} = 4.0 Hz, C_q), 113.3 (dd, ²*J*_{C-F} = 24.3, ²*J*_{C-F} = 3.6 Hz, CH), 112.9 (CH), 102.9 (dd, ²*J*_{C-F} = 26.5, 24.8 Hz, CH). **¹⁹F NMR** (282 MHz, CDCl₃): δ = -111.28 (dd, *J* = 15.6, 8.2 Hz), -113.20 (m). **IR** (ATR): 3203, 2921, 1583, 1523, 1443, 1410, 997, 832, 745, 690 cm⁻¹. **MS** (ESI) *m/z* (relative intensity): 402 (6) [M+K]⁺, 380 (30), 364 (100) [M+H]⁺. **HR-MS** (ESI) *m/z* calcd for C₁₆H₁₂F₂N₃Se, [M+H]⁺ 364.0160, found 364.0162.

N[4,5-Difluoro-2-(phenylselanyl)phenyl]pyrimidin-2-amine (**150va**)



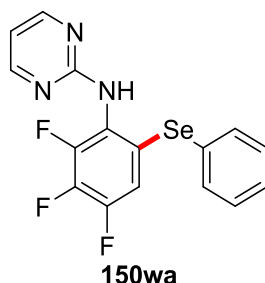
The general procedure **B** was followed using substrate **41v** (104 mg, 0.50 mmol) and diphenyl diselenide **148a** (187 mg, 0.60 mmol). Purification by column chromatography (*n*hexane/EtOAc: 4/1) yielded **150va** (89.3 mg, 49%) as a colorless solid.

M.p. 117–119 °C. **¹H NMR** (300 MHz, CDCl₃): δ = 8.65 (dd, *J* = 13.6, 7.8 Hz, 1H), 8.43 (d, *J* = 4.8 Hz, 2H), 8.15 (br s, 1H), 7.54 (dd, *J* = 9.4, 8.8 Hz, 1H), 7.34–7.27 (m, 2H), 7.25–7.16 (m, 3H), 6.77 (t, *J* = 4.8 Hz, 1H). **¹³C NMR** (126 MHz, CDCl₃): δ = 159.4 (C_q), 157.9 (CH), 151.2 (dd, ¹*J*_{C-F} = 247.8 Hz, ³*J*_{C-F} = 12.8 Hz, C_q), 145.0 (dd, ¹*J*_{C-F} = 246.9 Hz, ³*J*_{C-F} = 13.4 Hz, C_q), 138.2 (dd, ²*J*_{C-F} = 10.0 Hz, ³*J*_{C-F} = 2.5 Hz, CH), 130.6 (CH), 130.5 (C_q), 129.6 (CH), 127.3 (CH), 125.5 (dd, ²*J*_{C-F} = 18.1 Hz, ³*J*_{C-F} = 1.6 Hz, CH), 113.6 (CH), 112.9 (C_q), 108.7 (d, ²*J*_{C-F} = 24.0 Hz, CH).

5 Experimental Part

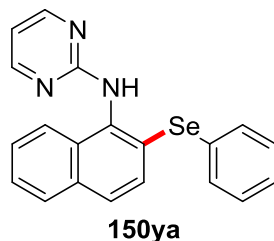
¹⁹F NMR (282 MHz, CDCl₃): δ = -132.6 (dddd, J = 22.3, 13.6, 8.8, 1.3 Hz), -144.6 (ddd, J = 22.2, 9.5, 7.9 Hz). **IR** (ATR): 3354, 3050, 1569, 1446, 1396, 881, 742, 690, 568, 452 cm⁻¹. **MS** (ESI) m/z (relative intensity): 386 (8) [M+Na]⁺, 381 (88), 364 (100) [M+H]⁺, 353 (44), 221 (11), 207 (75). **HR-MS** (ESI) m/z calcd for C₁₆H₁₂F₂N₃Se, [M+H]⁺ 364.0160, found 364.0155.

***N*-[2,3,4-Trifluoro-6-(phenylselanyl)phenyl]pyrimidin-2-amine (150wa)**



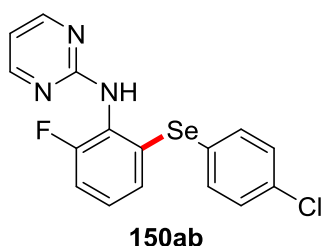
The general procedure **B** was followed using substrate **41w** (113 mg, 0.50 mmol) and diphenyl diselenide **148a** (187 mg, 0.60 mmol). Purification by column chromatography (*n*hexane/EtOAc: 4/1) yielded **150wa** (98.7 mg, 52%) as a yellow solid.

M.p. 118–119 °C. **¹H NMR** (300 MHz, CDCl₃): δ = 8.35 (d, J = 4.8 Hz, 2H), 7.52–7.46 (m, 2H), 7.35–7.23 (m, 3H), 7.20 (br s, 1H), 6.88 (ddd, J = 9.9, 7.7, 2.3 Hz, 1H), 6.73 (t, J = 4.8 Hz, 1H). **¹³C NMR** (126 MHz, CDCl₃): δ = 160.6 (C_q), 158.2 (CH), 149.5 (ddd, ¹ J_{C-F} = 251.5 Hz, ² J_{C-F} = 10.4 Hz, ³ J_{C-F} = 3.2 Hz, C_q), 147.9 (ddd, ¹ J_{C-F} = 254.7 Hz, ² J_{C-F} = 10.6 Hz, ³ J_{C-F} = 4.0 Hz, C_q), 139.5 (ddd, ¹ J_{C-F} = 251.8 Hz, ² J_{C-F} = 15.4 Hz, C_q), 134.8 (CH), 129.8 (CH), 128.7 (CH), 128.3 (C_q), 127.4 (dd, ³ J_{C-F} = 6.2 Hz, ⁴ J_{C-F} = 3.8 Hz, C_q), 123.8 (dd, ² J_{C-F} = 10.7 Hz, ³ J_{C-F} = 3.7 Hz, C_q), 114.6 (dd, ² J_{C-F} = 19.5 Hz, ³ J_{C-F} = 3.5 Hz, CH), 113.3 (CH). **¹⁹F NMR** (282 MHz, CDCl₃): δ = -134.66 (ddd, J = 20.6, 6.4, 2.3 Hz), -135.65 (ddd, J = 21.1, 9.9, 6.4 Hz), -158.80 (ddd, J = 20.9, 20.9, 7.7 Hz). **IR** (ATR): 3196, 2972, 1579, 1489, 1439, 1408, 1008, 735, 686, 465 cm⁻¹. **MS** (ESI) m/z (relative intensity): 382 (100) [M+H]⁺, 236 (34), 159 (13). **HR-MS** (ESI) m/z calcd for C₁₆H₁₁N₃F₃Se, [M+H]⁺ 382.0065, found 382.0067.

***N*-[2-(Phenylselanyl)naphthalen-1-yl]pyrimidin-2-amine (150ya)**

The general procedure **B** was followed using substrate **41y** (111 mg, 0.50 mmol) and diphenyl diselenide **148a** (187 mg, 0.60 mmol). Purification by column chromatography (*n*hexane/EtOAc: 4/1) yielded **150ya** (148 mg, 78%) as a yellow solid.

M.p. 144–146 °C. **¹H NMR** (300 MHz, CDCl₃): δ = 8.31 (d, *J* = 4.8 Hz, 2H), 7.98–7.91 (m, 1H), 7.86–7.78 (m, 1H), 7.65 (d, *J* = 8.7 Hz, 1H), 7.55–7.49 (m, 2H), 7.49–7.44 (m, 2H), 7.41 (d, *J* = 8.6 Hz, 1H), 7.40 (br s, 1H), 7.29–7.20 (m, 3H), 6.64 (t, *J* = 4.8 Hz, 1H). **¹³C NMR** (126 MHz, CDCl₃): δ = 162.1 (C_q), 158.4 (CH), 134.4 (CH), 133.8 (C_q), 133.7 (C_q), 131.6 (C_q), 130.2 (C_q), 130.2 (C_q), 129.7 (CH), 129.5 (CH), 128.4 (CH), 127.9 (CH), 127.9 (CH), 126.9 (CH), 126.2 (CH), 123.6 (CH), 112.3 (CH). **IR** (ATR): 3223, 3058, 1577, 1561, 1441, 1384, 817, 791, 738, 691 cm⁻¹. **MS** (ESI) *m/z* (relative intensity): 400 (16) [M+Na]⁺, 378 (67) [M+H]⁺, 221 (100). **HR-MS** (ESI) *m/z* calcd for C₂₀H₁₆N₃Se, [M+H]⁺ 378.0505, found 378.0507.

***N*-{2-[(4-Chlorophenyl)selanyl]-6-fluorophenyl}pyrimidin-2-amine (150ab)**

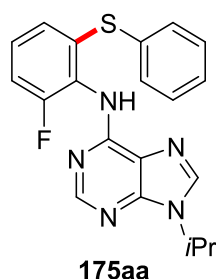
The general procedure **B** was followed using substrate **41a** (94.6 mg, 0.50 mmol) and diselenide **148b** (191 mg, 0.60 mmol). Purification by column chromatography (*n*hexane/EtOAc: 4/1) yielded **150ab** (140 mg, 74%) as a yellow solid.

M.p. 210–212 °C. **¹H NMR** (300 MHz, d₆-DMSO): δ = 8.99 (s, 1H), 8.33 (d, *J* = 4.8 Hz, 2H), 7.48 (d, *J* = 8.6 Hz, 2H), 7.39 (d, *J* = 8.6 Hz, 2H), 7.22–7.12 (m, 2H),

5 Experimental Part

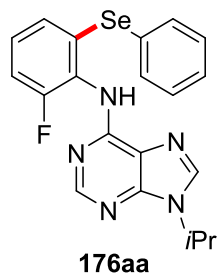
6.97–6.88 (m, 1H), 6.76 (t, $J = 4.8$ Hz, 1H). $^{13}\text{C NMR}$ (75 MHz, d_6 -DMSO): $\delta = 161.2$ (C_q), 158.4 (d, $^1J_{\text{C-F}} = 249.1$ Hz, C_q), 158.0 (CH), 136.1 (CH), 135.0 (C_q), 133.2 (C_q), 129.6 (CH), 128.0 (d, $^3J_{\text{C-F}} = 8.6$ Hz, CH), 128.0 (C_q), 126.9 (d, $^4J_{\text{C-F}} = 3.4$ Hz, CH), 126.7 (d, $^3J_{\text{C-F}} = 14.1$ Hz, C_q), 114.5 (d, $^2J_{\text{C-F}} = 21.1$ Hz, CH), 112.1 (CH). $^{19}\text{F NMR}$ (282 MHz, d_6 -DMSO): $\delta = -113.03$ (m). **IR** (ATR): 3195, 2966, 1580, 1520, 1441, 1408, 1086, 789, 774, 483 cm^{-1} . **MS** (ESI) m/z (relative intensity): 402 (6) $[\text{M}+\text{Na}]^+$, 381 (100) $[\text{M}+2\text{H}]^+$, 353 (49), 279 (7), 190 (8), 170 (8). **HR-MS** (ESI) m/z calcd for $\text{C}_{16}\text{H}_{12}^{35}\text{ClFN}_3\text{Se}$, $[\text{M}+\text{H}]^+$ 379.9861, found 379.9855.

N-[2-Fluoro-6-(phenylthio)phenyl]-9-isopropyl-9*H*-purin-6-amine (**175aa**)



The general procedure **A** was followed using substrate **174a** (136 mg, 0.50 mmol) and diphenyl disulfide **62a** (131 mg, 0.60 mmol). Purification by column chromatography (*n*hexane/EtOAc: 1/1) yielded **175aa** (175 mg, 92%) as a yellow oil.

$^1\text{H NMR}$ (300 MHz, CDCl_3): $\delta = 8.41$ (s, 1H), 7.86 (s, 1H), 7.48 (br s, 1H), 7.32–7.26 (m, 2H), 7.21–7.07 (m, 6H), 4.84 (sept, $J = 6.8$ Hz, 1H), 1.61 (d, $J = 6.8$ Hz, 6H). $^{13}\text{C NMR}$ (76 MHz, CDCl_3): $\delta = 158.7$ (d, $^1J_{\text{C-F}} = 252.1$ Hz, C_q), 153.0 (C_q), 152.6 (CH), 149.9 (C_q), 138.5 (CH), 136.2 (C_q), 133.9 (C_q), 132.0 (CH), 129.3 (CH), 127.9 (d, $^3J_{\text{C-F}} = 8.6$ Hz, CH), 127.6 (CH), 127.3 (d, $^4J_{\text{C-F}} = 3.3$ Hz, CH), 125.5 (d, $^2J_{\text{C-F}} = 13.8$ Hz, C_q), 120.8 (C_q), 115.35 (d, $^2J_{\text{C-F}} = 20.8$ Hz, CH), 47.2 (CH), 22.9 (CH_3). $^{19}\text{F NMR}$ (283 MHz, CDCl_3): $\delta = -115.55$ (dd, $J = 9.0, 5.6$ Hz). **IR** (ATR) = 3382, 1607, 1575, 1470, 1450, 1003, 896, 750, 694, 649 cm^{-1} . **MS** (EI) m/z (relative intensity): 379 (10) $[\text{M}]^+$, 360 (9), 287 (30), 270 (69), 228 (100), 201 (8). **HR-MS** (EI) m/z calcd for $\text{C}_{20}\text{H}_{18}\text{FN}_5\text{S}$, $[\text{M}]^+$ 379.1267, found 379.1263.

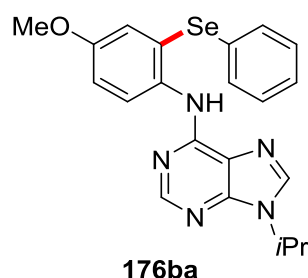
***N*-[2-Fluoro-6-(phenylselanyl)phenyl]-9-isopropyl-9*H*-purin-6-amine (176aa)**

The general procedure **B** was followed using substrate **174a** (136 mg, 0.50 mmol) and diphenyl diselenide **148a** (187 mg, 0.60 mmol). Purification by column chromatography (*n*hexane/EtOAc: 1/1) yielded **176aa** (175 mg, 82%) as a yellow oil.

¹H NMR (400 MHz, CDCl₃): δ = 8.41 (s, 1H), 7.86 (s, 1H), 7.68 (br s, 1H), 7.46–7.42 (m, 2H), 7.18–7.07 (m, 6H), 4.85 (sept, *J* = 6.8 Hz, 1H), 1.61 (d, *J* = 6.8 Hz, 6H).

¹³C NMR (101 MHz, CDCl₃): δ = 158.5 (d, ¹*J*_{C-F} = 252.4 Hz, C_q), 153.2 (C_q), 152.5 (CH), 149.9 (C_q), 138.5 (CH), 134.4 (CH), 133.8 (C_q), 129.6 (C_q), 129.4 (CH), 128.5 (d, ⁴*J*_{C-F} = 3.4 Hz, CH), 128.3 (d, ³*J*_{C-F} = 8.2 Hz, CH), 128.0 (CH), 125.8 (d, ²*J*_{C-F} = 13.6 Hz, C_q), 120.7 (C_q), 115.3 (d, ²*J*_{C-F} = 20.8 Hz, CH), 47.3 (CH), 22.8 (CH₃).

¹⁹F NMR (376 MHz, CDCl₃): δ = -116.20– -116.25 (m). **IR** (ATR) = 3156, 2972, 1609, 1574, 1463, 1261, 1222, 881, 745, 693 cm⁻¹. **MS** (EI) *m/z* (relative intensity): 427 (8) [M]⁺, 335 (6), 270 (73), 228 (100), 201 (7). **HR-MS** (ESI) *m/z* calcd for C₂₀H₁₉FN₅Se, [M+H]⁺ 428.0785, found 428.0781.

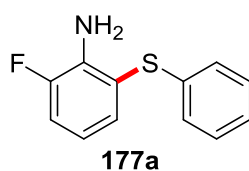
***N*-[4-methoxy-2-(phenylselanyl)phenyl]-9-isopropyl-9*H*-purin-6-amine (176ba)**

The general procedure **B** was followed using substrate **174b** (142 mg, 0.50 mmol) and diphenyl diselenide **148a** (187 mg, 0.60 mmol). Purification by column chromatography (*n*hexane/EtOAc: 1/1) yielded **176ba** (42.8 mg, 20%) as a yellow oil.

¹H NMR (300 MHz, CDCl₃): δ = 8.45 (s, 1H), 8.32 (d, *J* = 8.9 Hz, 1H), 8.27 (br s, 1H), 7.86 (s, 1H), 7.42–7.36 (m, 2H), 7.17 (d, *J* = 2.9 Hz, 1H), 7.16–7.10 (m, 3H), 6.99 (dd, *J* = 9.0, 3.0 Hz, 1H), 4.84 (sept, *J* = 6.8 Hz, 1H), 3.77 (s, 3H), 1.61 (d, *J* = 6.8 Hz, 6H). **¹³C NMR** (76 MHz, CDCl₃): δ = 156.2 (C_q), 152.6 (C_q), 152.5 (CH), 149.3 (C_q), 138.3 (CH), 132.8 (C_q), 132.1 (CH), 130.6 (C_q), 129.4 (CH), 127.3 (CH), 124.1 (C_q), 124.1 (CH), 121.2 (CH), 120.9 (C_q), 115.4 (CH), 55.7 (CH₃), 47.2 (CH), 22.9 (CH₃).

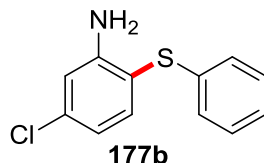
5.3.3 Experimental Procedures and Analytical Data – Removal of the Directing Group

2-Fluoro-6-(phenylthio)aniline (177a)



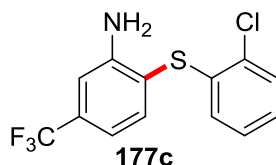
The general procedure **C** was followed using substrate **149aa** (59.6 mg, 0.20 mmol) in aqueous HCl (37%, 1.0 mL). Purification by column chromatography (*n*hexane/EtOAc: 5/1) yielded **177a** (25.3 mg, 58%) as a colorless oil.

¹H NMR (400 MHz, CDCl₃): δ = 7.27–7.26 (m, 1H), 7.26–7.22 (m, 2H), 7.18–7.14 (m, 1H), 7.14–7.10 (m, 2H), 7.08 (ddd, *J* = 10.8, 8.2, 1.4 Hz, 1H), 6.68 (ddd, *J* = 8.0, 5.4, 5.4 Hz, 1H), 4.32 (br s, 2H). **¹³C NMR** (76 MHz, CDCl₃): δ = 151.6 (d, ¹*J*_{C-F} = 241.6 Hz, C_q), 137.8 (d, ²*J*_{C-F} = 12.3 Hz, C_q), 136.1 (C_q), 132.4 (d, ⁴*J*_{C-F} = 3.1 Hz, CH), 129.2 (CH), 127.0 (CH), 125.9 (CH), 117.4 (d, ³*J*_{C-F} = 7.7 Hz, CH), 116.8 (d, ³*J*_{C-F} = 3.0 Hz, C_q), 116.5 (d, ²*J*_{C-F} = 18.7 Hz, CH). **¹⁹F NMR** (283 MHz, CDCl₃): δ = -132.24 (dd, *J* = 10.7, 5.3 Hz). **IR** (ATR): 3479, 3372, 3060, 1616, 1568, 1473, 1196, 739, 722, 690 cm⁻¹. **MS** (EI) *m/z* (relative intensity) 219 (82) [M]⁺, 204 (17), 186 (14), 86 (17), 84 (28), 58 (35), 43 (100). **HR-MS** (EI) *m/z* calcd for C₁₂H₁₀FNS [M]⁺ 219.0518, found 219.0512.

5-Chloro-2-(phenylthio)aniline (177b)

The general procedure **C** was followed using substrate **149pa** (157 mg, 0.50 mmol) in aqueous HCl (37%, 2.0 mL). Purification by column chromatography (*n*hexane/EtOAc: 5/1) yielded **177b** (65.0 mg, 55%) as a yellow solid.

M.p. 62–64 °C. **¹H NMR** (300 MHz, CDCl₃): δ = 7.38 (d, *J* = 8.2 Hz, 1H), 7.27–7.20 (m, 2H), 7.16–7.05 (m, 3H), 6.78 (d, *J* = 2.2 Hz, 1H), 6.73 (dd, *J* = 8.2, 2.2 Hz, 1H), 4.37 (br s, 2H). **¹³C NMR** (76 MHz, CDCl₃): δ = 149.8 (C_q), 138.6 (CH), 137.0 (C_q), 136.4 (C_q), 129.2 (CH), 126.6 (CH), 125.8 (CH), 118.9 (CH), 115.0 (CH), 113.0 (C_q). **IR** (ATR): 3477, 3371, 1598, 1579, 1473, 1254, 1074, 784, 737, 685 cm⁻¹. **MS** (EI) *m/z* (relative intensity) 235 (100) [M]⁺ (³⁵Cl), 220 (10), 200 (13), 167 (23), 158 (12). **HR-MS** (EI) *m/z* calcd for C₁₂H₁₀³⁵ClNS [M]⁺ 235.0222, found 235.0222.

2-[(2-Chlorophenyl)thio]-5-(trifluoromethyl)aniline (177c)

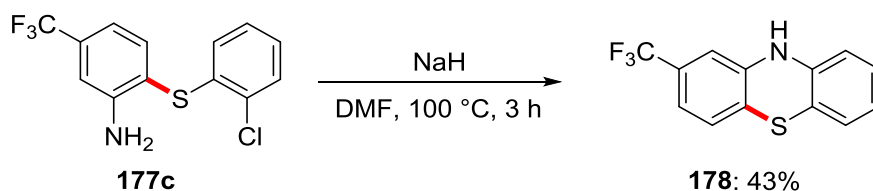
The general procedure **C** was followed using substrate **149nd** (382 mg, 1.00 mmol) in aqueous HCl (37%, 5.0 mL). Purification by column chromatography (*n*hexane/EtOAc: 4/1) yielded **177c** (157 mg, 52%) as a yellow oil.

¹H NMR (300 MHz, CDCl₃): δ = 7.55 (d, *J* = 7.9 Hz, 1H), 7.41–7.34 (m, 1H), 7.14–7.05 (m, 2H), 7.05–6.97 (m, 2H), 6.72–6.64 (m, 1H), 4.48 (br s, 2H). **¹³C NMR** (126 MHz, CDCl₃): δ = 149.1 (C_q), 138.0 (CH), 134.6 (C_q), 133.5 (q, ²*J*_{C-F} = 32.2 Hz, C_q), 131.9 (C_q), 129.9 (CH), 127.4 (CH), 127.0 (CH), 126.8 (CH), 123.9 (d, ¹*J*_{C-F} = 271.9 Hz, C_q), 117.0 (C_q), 115.1 (q, ³*J*_{C-F} = 3.8 Hz, CH), 111.8 (q, ³*J*_{C-F} = 3.9 Hz, CH). **¹⁹F NMR** (283 MHz, CDCl₃): δ = -63.28 (s). **IR** (ATR): 3480, 3380, 1613, 1450, 1432, 1335, 1249, 1167, 1121, 747 cm⁻¹. **MS** (EI) *m/z* (relative intensity) 303 (77) [M]⁺

5 Experimental Part

(^{35}Cl), 284 (9) (^{35}Cl), 268 (100), 247 (18), 235 (24), 199 (55). **HR-MS** (EI) m/z calcd for $\text{C}_{13}\text{H}_9^{35}\text{ClF}_3\text{NS}$ [M] $^+$ 303.0096, found 303.0094.

Synthesis of 2-(trifluoromethyl)-10*H*-phenothiazine **178**

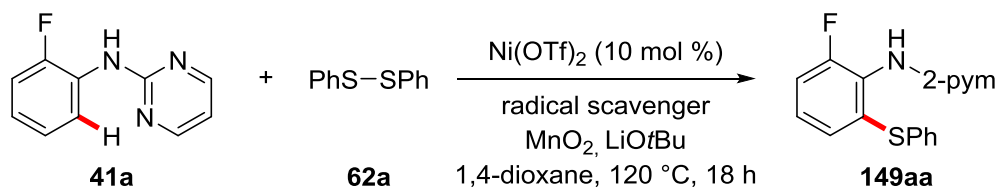


2-Amino thiophenol **177c** (145 mg, 0.48 mmol, 1.0 equiv) was dissolved in dry DMF (1.0 mL) and heated to 100 °C under a nitrogen atmosphere. Then, a suspension of NaH (60% in mineral oil, 40.0 mg, 0.96 mmol, 2.0 equiv) in DMF (1.0 mL) was slowly added. After complete addition, the reaction mixture was stirred for 3 h at 100 °C. After complete reaction, the mixture was cooled to 0 °C and carefully diluted with water (~5 mL). The aqueous phase was extracted with CH_2Cl_2 (3 \times 30 mL), the combined organic layers washed with brine and dried over Na_2SO_4 . The solvent was removed under reduced pressure and the residue was purified by flash column chromatography (SiO_2 , 100% *n*pentane) to afford the desired product **178** (55.4 mg, 0.21 mmol, 43%) as pale yellow solid.

M.p. 187–189 °C. $^1\text{H NMR}$ (300 MHz, CDCl_3): δ = 7.56 (d, J = 8.0 Hz, 1H), 7.39 (dd, J = 8.0, 1.4 Hz, 1H), 7.36–7.34 (m, 1H), 7.25–7.15 (m, 2H), 7.02–6.95 (m, 2H), 6.91 (s, 1H). $^{13}\text{C NMR}$ (126 MHz, CDCl_3): δ = 144.1 (C_q), 137.5 (C_q), 136.4 (CH), 133.2 (q, $^2J_{\text{C-F}}$ = 32.5 Hz, C_q), 130.4 (CH), 127.7 (CH), 126.8 (q, $^3J_{\text{C-F}}$ = 1.7 Hz, C_q), 125.0 (C_q), 123.6 (CH), 123.6 (q, $^1J_{\text{C-F}}$ = 272.5 Hz, C_q), 119.0 (CH), 117.3 (q, $^2J_{\text{C-F}}$ = 3.7 Hz, CH), 112.4 (q, $^2J_{\text{C-F}}$ = 3.7 Hz, CH). $^{19}\text{F NMR}$ (283 MHz, CDCl_3): δ = -63.20 (s). **MS** (EI) m/z (relative intensity) 267 (100) [M] $^+$, 247 (16), 235 (14), 222 (5), 199 (7), 154 (4). **HR-MS** (EI) m/z calcd for $\text{C}_{13}\text{H}_8\text{F}_3\text{NS}$ [M] $^+$ 267.0330, found 267.0330. The analytical data correspond with those reported in literature.^[179]

5.3.4 Mechanistic Studies

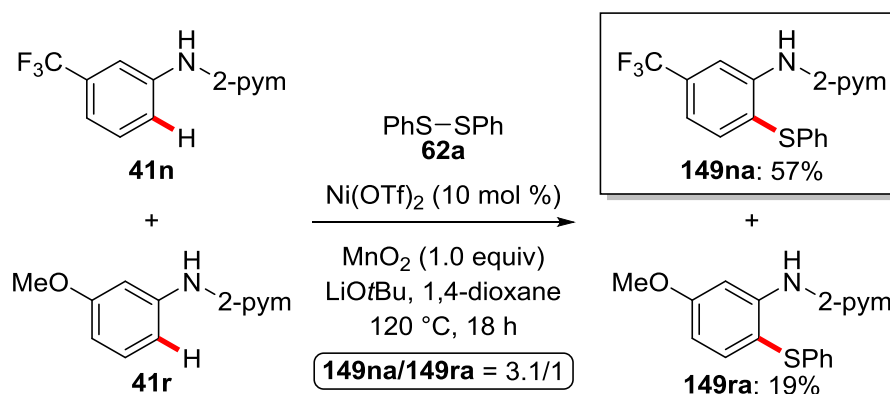
Reactions with Radical Scavengers



Entry	Radical Scavenger	Equiv	Yield / %
1	---		96
2	TEMPO	2.0	6
3	BHT	2.0	---
4	galvinoxyl	2.0	---

The general procedure **A** was followed using pyrimidyl aniline **41a** (94.6 mg, 0.50 mmol, 1.0 equiv), diphenyl disulfide **62a** (131 mg, 0.6 mmol, 1.2 equiv) and a radical scavenger (2.0 equiv). For TEMPO, the reaction mixture was purified by column chromatography (*n*hexane/EtOAc: 5/1) to yield the desired product **149aa** (8.9 mg, 6%) as a colorless solid. For BHT and galvinoxyl, no product formation was observed by GC-MS and ¹H NMR analysis of the crude reaction mixture.

Intermolecular Competition Experiments

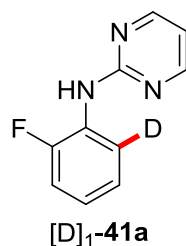


5 Experimental Part

N-[3-(Trifluoromethyl)phenyl]pyrimidin-2-amine (**41n**) (120 mg, 0.50 mmol), *N*-(3-methoxyphenyl)pyrimidin-2-amine (**41r**) (101 mg, 0.50 mmol), diphenyl disulfide **62a** (131 mg, 0.60 mmol) Ni(OTf)₂ (17.8 mg, 10 mol %), MnO₂ (43.5 mg, 0.50 mmol) and LiOtBu (80.0 mg, 1.00 mmol) were placed in a 25 mL Schlenk-tube. The tube was degassed and purged with N₂ for three times. Then, dry 1,4-dioxane (1.5 mL) was added, and the mixture was stirred at 120 °C for 18 h. At ambient temperature, EtOAc (5.0 ml) was added, and the reaction mixture was filtered through a small plug of silica. The filtrate was concentrated under reduced pressure and purified by flash column chromatography on silica gel (*n*hexane/EtOAc: 5/1) to afford **149na** (98.9 mg, 57%) as the major product and **149ra** (28.9 mg, 19%) as the minor product.

Kinetic Isotope Effect Experiments

Synthesis of [D]₁-41a

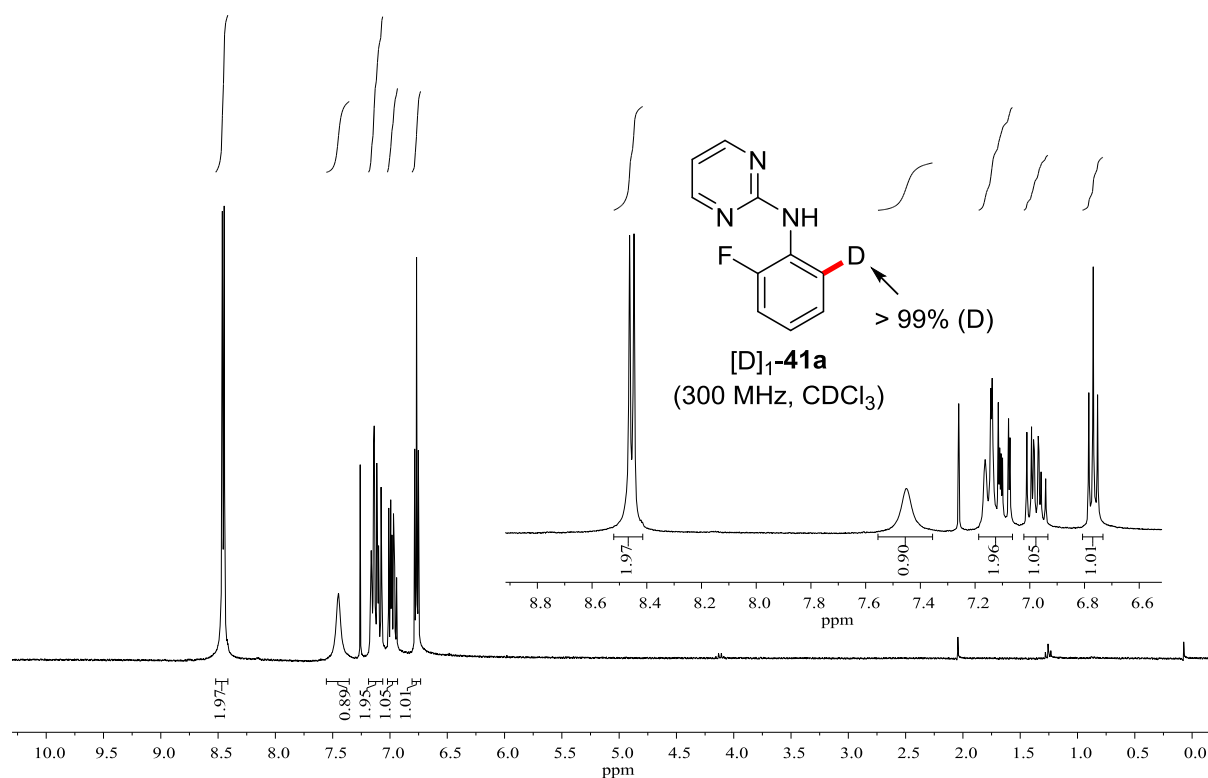


Pyrimidyl aniline **41a** (1.14 g, 6.00 mmol), [RuCl₂(*p*-cymene)] (73.5 mg, 2.0 mol %), KOAc (58.9 mg, 10.0 mol %) and D₂O (1.1 mL, 10.3 equiv) were placed in a 25 mL Schlenk-tube under a nitrogen atmosphere. Then, PhMe (3.0 mL) was added and the mixture was stirred at 80 °C for 24 h. After cooling to ambient temperature, the reaction mixture was extracted with EtOAc (3 × 10 mL). The combined organic layers were dried over Na₂SO₄ and concentrated under reduced pressure. With the crude product the same procedure was repeated again. Following the same work-up procedure, the crude product was purified by column chromatography (*n*hexane/EtOAc: 5/1) to give the *ortho*-deuterated product [D]₁-**41a** (1.11 g) as a colorless solid. ¹H NMR analysis showed >95% deuterium incorporation in the *ortho*-position.

¹H NMR (300 MHz, CDCl₃): δ = 8.45 (d, *J* = 4.8 Hz, 2H), 7.45 (s, 1H), 7.19–7.06 (m, 2H), 6.98 (ddd, *J* = 8.2, 7.4, 4.8 Hz, 1H), 6.77 (dd, *J* = 4.8, 4.8 Hz, 1H). ¹³C NMR (101 MHz, CDCl₃): δ = 160.1 (C_q), 158.1 (CH), 152.8 (d, ¹*J*_{C-F} = 243.0 Hz, C_q), 128.0

5 Experimental Part

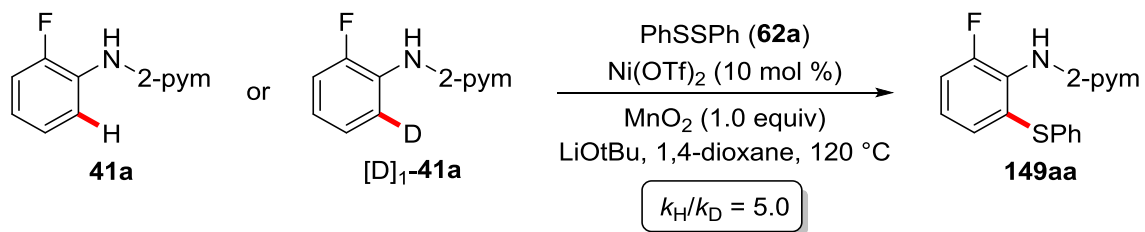
(d, $^2J_{C-F} = 9.8$ Hz, C_q), 124.3 (d, $^4J_{C-F} = 3.7$ Hz, CH), 122.6 (d, $^3J_{C-F} = 7.6$ Hz, CH), 120.6 (t, $^1J_{C-D} = 25.2$ Hz, C_q), 114.9 (d, $^2J_{C-F} = 19.3$ Hz, CH), 113.2 (CH). ^{19}F NMR (376 MHz, $CDCl_3$): $\delta = -131.25 - -131.33$ (m). **MS** (EI) m/z (relative intensity) 190 (36) $[M]^+$, 172 (15), 171 (100), 137 (4), 84 (11). **HR-MS** (EI) m/z calcd for $C_{10}H_7DFN_3$ $[M]^+$ 190.0765, found 190.0757.



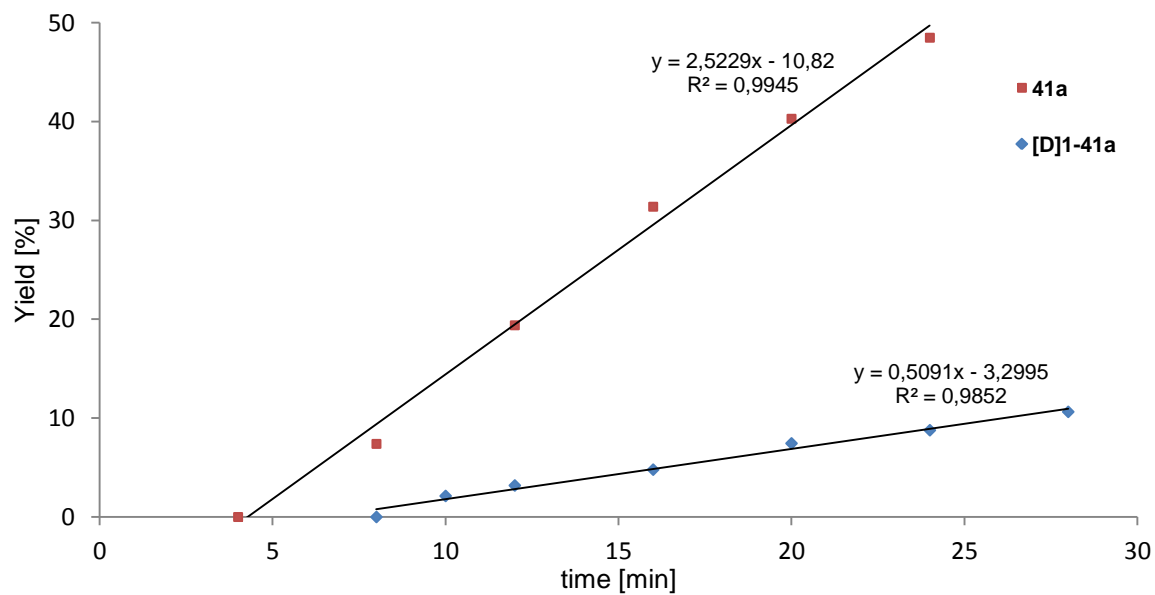
1) Parallel Experiments

Two independent reactions with **41a** and $[D]_1\text{-41a}$ under the standard conditions were performed: Following the general procedure **A**, **41a** (189 mg, 1.0 mmol) or $[D]_1\text{-41a}$ (190 mg, 1.0 mmol), diphenyl disulfide **62a** (262 mg, 1.2 mmol), $Ni(OTf)_2$ (35.7 mg, 10.0 mol %), MnO_2 (86.9 mg, 1.0 mmol), $LiOtBu$ (160 mg, 2.0 mmol) and internal standard 1-fluorononane (36.6 mg, 0.25 mmol) in 1,4-dioxane (3.0 mL) were stirred at 120 °C. After the reaction times indicated below, aliquots of 0.1 mL were taken out of the reaction mixture. The aliquots were filtered over a short plug of silica gel and diluted with $CDCl_3$ (0.5 mL). Yields of products were determined by ^{19}F NMR spectroscopy.

5 Experimental Part



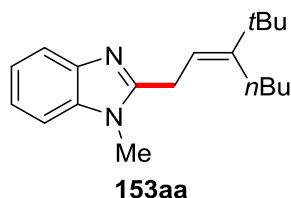
t [min]	2	4	5	8	10	12	16	20	24	28
41a [%]	-	0	-	7.4	-	19.4	31.4	40.3	48.5	-
[D] ₁ -41a [%]	0	-	0	0	2.1	3.2	4.8	7.5	8.8	10.6



5.4 Nickel-Catalyzed C–H Allylation of Imidazole and Purine Derivatives

5.4.1 Experimental Procedures and Analytical Data – Nickel-catalyzed C–H Allylation

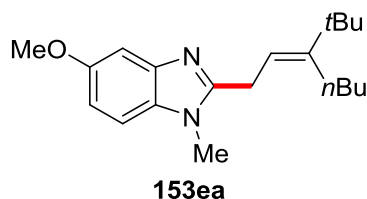
(*E*)-2-[3-(*tert*-Butyl)hept-2-en-1-yl]-1-methyl-1*H*-benzo[*d*]imidazole (153aa)



The general procedure **D** was followed using benzimidazole **16a** (66.1 mg, 0.50 mmol) and allene **152a** (122 mg, 0.80 mmol). Purification by column chromatography on silica gel (*n*hexane/EtOAc: 5/1) yielded **153aa** (121 mg, 85%) as a white solid.

M.p. = 84–86 °C. **¹H NMR** (500 MHz, CDCl₃): δ = 7.75–7.70 (m, 1H), 7.31–7.26 (m, 1H), 7.25–7.21 (m, 2H), 5.38 (t, *J* = 6.5 Hz, 1H), 3.68 (d, *J* = 6.3 Hz, 2H), 3.68 (s, 3H), 2.22–2.16 (m, 2H), 1.49–1.38 (m, 4H), 1.05 (s, 9H), 0.96 (t, *J* = 7.1 Hz, 3H). **¹³C NMR** (126 MHz, CDCl₃): δ = 154.9 (C_q), 151.0 (C_q), 142.7 (C_q), 136.2 (C_q), 122.1 (CH), 121.9 (CH), 119.4 (CH), 115.8 (CH), 108.9 (CH), 37.0 (C_q), 32.4 (CH₂), 29.9 (CH₃), 29.4 (CH₃), 28.7 (CH₂), 27.8 (CH₂), 23.7 (CH₂), 14.1 (CH₃). **IR** (ATR): 2951, 1650, 1461, 1287, 982, 735, 547, 442 cm⁻¹. **MS** (EI) *m/z* (relative intensity): 284 (19) [M]⁺, 269 (35), 241 (28), 227 (100), 199 (8), 185 (22), 146 (25), 131 (9), 77 (6), 41 (9). **HR-MS** (EI) *m/z* calcd for C₁₉H₂₈N₂ [M]⁺ 284.2252, found 284.2245.

(*E*)-2-[3-(*tert*-Butyl)hept-2-en-1-yl]-5-methoxy-1-methyl-1*H*-benzo[*d*]imidazole (153ea)

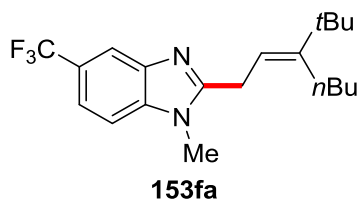


The general procedure **D** was followed using benzimidazole **16e** (81.1 mg, 0.50 mmol) and allene **152a** (122 mg, 0.80 mmol). Purification by column

chromatography on silica gel (*n*hexane/EtOAc: 5/1) yielded **153ea** (129 mg, 82%) as a white solid.

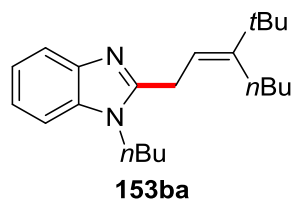
M.p. = 86–88 °C. **¹H NMR** (500 MHz, CDCl₃): δ = 7.22 (d, *J* = 2.3 Hz, 1H), 7.15 (d, *J* = 8.7 Hz, 1H), 6.89 (dd, *J* = 8.7, 2.4 Hz, 1H), 5.37 (t, *J* = 6.5 Hz, 1H), 3.85 (s, 3H), 3.65 (s, 3H), 3.65 (d, *J* = 6.3 Hz, 2H), 2.20–2.15 (m, 2H), 1.47–1.37 (m, 4H), 1.04 (s, 9H), 0.96 (t, *J* = 7.1 Hz, 3H). **¹³C NMR** (126 MHz, CDCl₃): δ = 156.1 (C_q), 155.1 (C_q), 150.9 (C_q), 143.3 (C_q), 130.8 (C_q), 115.9 (CH), 111.8 (CH), 109.3 (CH), 102.0 (CH), 56.0 (CH₃), 37.0 (C_q), 32.5 (CH₂), 30.0 (CH₃), 29.5 (CH₃), 28.7 (CH₂), 27.8 (CH₂), 23.7 (CH₂), 14.1 (CH₃). **IR** (ATR): 2953, 2869, 1489, 1433, 1274, 1199, 1154, 1028, 825, 795 cm⁻¹. **MS** (ESI) *m/z* (relative intensity) 315 (100) [M+H]⁺. **HR-MS** (ESI) *m/z* calcd for C₂₀H₃₁N₂O [M+H]⁺ 315.2431, found 315.2431.

(*E*)-2-[3-(*tert*-Butyl)hept-2-en-1-yl]-1-methyl-5-(trifluoromethyl)-1*H*-benzo[*d*]imidazole (153fa)



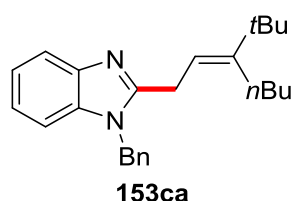
The general procedure **D** was followed using benzimidazole **16f** (100 mg, 0.50 mmol) and allene **152a** (122 mg, 0.80 mmol). Purification by column chromatography on silica gel (*n*hexane/EtOAc: 5/1) yielded **153fa** (115 mg, 65%) as a white solid.

M.p. = 98–100 °C. **¹H NMR** (500 MHz, CDCl₃): δ = 7.99 (s, 1H), 7.49 (dd, *J* = 8.4, 1.1 Hz, 1H), 7.35 (d, *J* = 8.4 Hz, 1H), 5.39 (t, *J* = 6.5 Hz, 1H), 3.73 (s, 3H), 3.70 (d, *J* = 6.5 Hz, 2H), 2.22–2.17 (m, 2H), 1.47–1.39 (m, 4H), 1.06 (s, 9H), 0.96 (t, *J* = 7.0 Hz, 3H). **¹³C NMR** (126 MHz, CDCl₃): δ = 156.9 (C_q), 151.7 (C_q), 142.2 (C_q), 138.1 (C_q), 125.0 (q, ¹*J*_{C-F} = 271.1 Hz, C_q), 124.4 (q, ²*J*_{C-F} = 32.1 Hz, C_q), 119.1 (q, ³*J*_{C-F} = 3.5 Hz, CH), 117.0 (q, ³*J*_{C-F} = 3.9 Hz, CH), 115.2 (CH), 109.2 (CH), 37.2 (C_q), 32.5 (CH₂), 30.3 (CH₃), 29.6 (CH₃), 28.8 (CH₂), 27.9 (CH₂), 23.8 (CH₂), 14.1 (CH₃). **¹⁹F NMR** (282 MHz, CDCl₃): δ = -60.51 (s). **IR** (ATR): 2958, 2868, 1323, 1224, 1108, 1046, 891, 808, 713, 663 cm⁻¹. **MS** (ESI) *m/z* (relative intensity): 353 (100) [M+H]⁺. **HR-MS** (ESI) *m/z* calcd for C₂₀H₂₈N₂F₃ [M+H]⁺ 353.2199, found 353.2206.

(E)-1-Butyl-2-[3-(*tert*-butyl)hept-2-en-1-yl]-1*H*-benzo[*d*]imidazole (153ba)

The general procedure **D** was followed using benzimidazole **16b** (87.1 mg, 0.50 mmol) and allene **152a** (122 mg, 0.80 mmol). Purification by column chromatography on silica gel (*n*hexane/EtOAc: 4/1) yielded **153ba** (101 mg, 62%) as a white solid.

M.p. = 147–149 °C. **¹H NMR** (500 MHz, CDCl₃): δ = 7.75–7.71 (m, 1H), 7.32–7.28 (m, 1H), 7.24–7.20 (m, 2H), 5.40 (t, *J* = 6.4 Hz, 1H), 4.07–4.04 (m, 2H), 3.68 (d, *J* = 6.4 Hz, 2H), 2.20–2.15 (m, 2H), 1.81–1.73 (m, 2H), 1.47–1.38 (m, 6H), 1.04 (s, 9H), 0.98–0.94 (m, 6H). **¹³C NMR** (126 MHz, CDCl₃): δ = 154.6 (C_q), 150.6 (C_q), 142.8 (C_q), 135.4 (C_q), 122.0 (CH), 121.8 (CH), 119.4 (CH), 116.5 (CH), 109.4 (CH), 43.8 (CH₂), 37.0 (C_q), 32.4 (CH₂), 32.1 (CH₂), 29.4 (CH₃), 28.7 (CH₂), 27.8 (CH₂), 23.7 (CH₂), 20.5 (CH₂), 14.0 (CH₃), 13.9 (CH₃). **IR** (ATR): 3093, 2959, 2870, 1454, 1415, 1365, 1330, 1153, 988, 744 cm⁻¹. **MS** (ESI) *m/z* (relative intensity): 327 (100) [M+H]⁺, 285 (5). **HR-MS** (ESI) *m/z* calcd for C₂₂H₃₅N₂ [M+H]⁺ 327.2795, found 327.2808.

(E)-1-Benzyl-2-[3-(*tert*-butyl)hept-2-en-1-yl]-1*H*-benzo[*d*]imidazole (153ca)

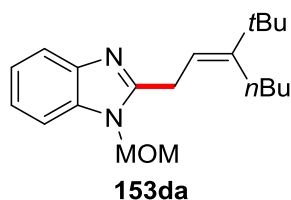
The general procedure **D** was followed using benzimidazole **16c** (104 mg, 0.50 mmol) and allene **152a** (122 mg, 0.80 mmol). Purification by column chromatography on silica gel (*n*hexane/EtOAc: 4/1) yielded **153ca** (152 mg, 84%) as an off-white solid.

M.p. = 54–55 °C. **¹H NMR** (600 MHz, CDCl₃): δ = 7.78 (d, *J* = 8.0 Hz, 1H), 7.30–7.23 (m, 4H), 7.19–7.17 (m, 2H), 7.02–6.99 (m, 2H), 5.37 (t, *J* = 6.4 Hz, 1H), 5.32 (s, 2H),

5 Experimental Part

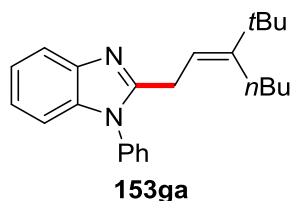
3.66 (d, $J = 6.5$ Hz, 2H), 2.08–2.03 (m, 2H), 1.37–1.29 (m, 4H), 0.95 (s, 9H), 0.88 (t, $J = 7.0$ Hz, 3H). ^{13}C NMR (126 MHz, CDCl_3): $\delta = 155.0$ (C_q), 151.1 (C_q), 142.7 (C_q), 136.2 (C_q), 135.8 (C_q), 129.0 (CH), 127.9 (CH), 126.2 (CH), 122.5 (CH), 122.1 (CH), 119.5 (CH), 115.9 (CH), 109.7 (CH), 47.1 (CH_2), 36.9 (C_q), 32.3 (CH_2), 29.3 (CH_3), 28.5 (CH_2), 27.9 (CH_2), 23.6 (CH_2), 13.9 (CH_3). IR (ATR): 2958, 2869, 1495, 1452, 1406, 1348, 985, 913, 726, 695 cm^{-1} . MS (ESI) m/z (relative intensity): 361 (100) $[\text{M}+\text{H}]^+$, 317 (5), 130 (4). HR-MS (ESI) m/z calcd for $\text{C}_{25}\text{H}_{33}\text{N}_2$ $[\text{M}+\text{H}]^+$ 361.2638, found 361.2649.

(*E*)-2-[3-(*tert*-Butyl)hept-2-en-1-yl]-1-(methoxymethyl)-1*H*-benzo[*d*]imidazole (153da)



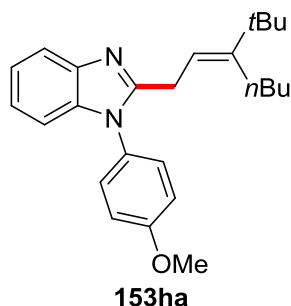
The general procedure **D** was followed using benzimidazole **16d** (80.6 mg, 0.50 mmol) and allene **152a** (122 mg, 0.80 mmol). Purification by column chromatography on silica gel (*n*hexane/EtOAc: 4/1) yielded **153da** (78.6 mg, 50%) as a yellow oil.

^1H NMR (300 MHz, CDCl_3): $\delta = 7.74$ – 7.70 (m, 1H), 7.42–7.39 (m, 1H), 7.26–7.23 (m, 2H), 5.42 (s, 2H), 5.29 (t, $J = 6.5$ Hz, 1H), 3.73 (d, $J = 6.5$ Hz, 2H), 3.28 (s, 3H), 2.26–2.09 (m, 2H), 1.47–1.35 (m, 4H), 1.03 (s, 9H), 0.98–0.90 (m, 3H). ^{13}C NMR (126 MHz, CDCl_3): $\delta = 154.9$ (C_q), 150.9 (C_q), 142.2 (C_q), 135.4 (C_q), 122.6 (CH), 122.4 (CH), 119.3 (CH), 115.7 (CH), 109.3 (CH), 74.3 (CH_2), 56.3 (CH_2), 36.9 (C_q), 32.4 (CH_2), 29.4 (CH_3), 28.5 (CH_2), 26.7 (CH_3), 23.6 (CH_2), 14.0 (CH_3). IR (ATR): 2956, 1704, 1455, 1362, 1153, 1120, 1097, 916, 744 cm^{-1} . MS (ESI) m/z (relative intensity) 315 (100) $[\text{M}+\text{H}]^+$. HR-MS (ESI) m/z calcd for $\text{C}_{20}\text{H}_{29}\text{N}_2\text{O}$ $[\text{M}+\text{H}]^+$ 313.2274, found 313.2276.

(E)-2-[3-(tert-Butyl)hept-2-en-1-yl]-1-phenyl-1H-benzo[d]imidazole (153ga)

The general procedure **D** was followed using benzimidazole **16g** (97.1 mg, 0.50 mmol) and allene **152a** (122 mg, 0.80 mmol). Purification by column chromatography on silica gel (*n*hexane/EtOAc: 4/1) yielded **153ga** (107 mg, 62%) as a yellow oil.

¹H NMR (500 MHz, CDCl₃): δ = 7.79 (d, *J* = 8.0 Hz, 1H), 7.56–7.48 (m, 3H), 7.36–7.34 (m, 2H), 7.29–7.26 (m, 1H), 7.21–7.18 (m, 1H), 7.09 (d, *J* = 8.0 Hz, 1H), 5.31 (t, *J* = 6.6 Hz, 1H), 3.57 (d, *J* = 6.6 Hz, 2H), 1.77–1.70 (m, 2H), 1.24–1.13 (m, 4H), 0.93 (s, 9H), 0.82 (t, *J* = 7.1 Hz, 3H). **¹³C NMR** (126 MHz, CDCl₃): δ = 154.8 (C_q), 150.2 (C_q), 142.6 (C_q), 136.8 (C_q), 136.1 (C_q), 129.8 (CH), 128.9 (CH), 127.6 (CH), 122.6 (CH), 122.4 (CH), 119.3 (CH), 116.5 (CH), 110.0 (CH), 36.9 (CH₂), 32.4 (C_q), 29.4 (CH₃), 28.1 (CH₂), 27.9 (CH₂), 23.6 (CH₂), 14.0 (CH₃). **IR** (ATR): 2953, 2868, 1596, 1498, 1454, 1393, 1266, 760, 741, 696 cm⁻¹. **MS** (ESI) *m/z* (relative intensity): 347 (100) [M+H]⁺, 303 (7). **HR-MS** (ESI) *m/z* calcd for C₂₄H₃₁N₂ [M+H]⁺ 347.2482, found 347.2482.

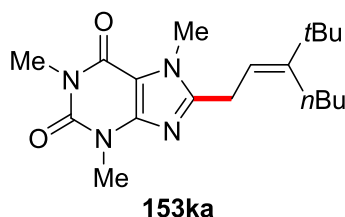
(E)-2-[3-(tert-Butyl)hept-2-en-1-yl]-1-(4-methoxyphenyl)-1H-benzo[d]imidazole (153ha)

The general procedure **D** was followed using benzimidazole **16h** (112 mg, 0.50 mmol) and allene **152a** (122 mg, 0.80 mmol). Purification by column

chromatography on silica gel (*n*hexane/EtOAc: 4/1) yielded **153ha** (145 mg, 77%) as a yellow solid.

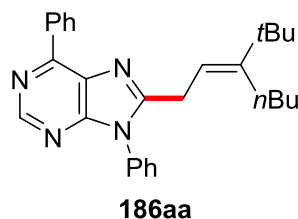
M.p. = 57–58 °C. **¹H NMR** (500 MHz, CDCl₃): δ = 7.78 (d, *J* = 8.0 Hz, 1H), 7.28–7.23 (m, 3H), 7.18 (ddd, *J* = 8.2, 7.3, 1.1 Hz, 1H), 7.06 (d, *J* = 7.9 Hz, 1H), 7.05–7.01 (m, 2H), 5.32 (t, *J* = 6.6 Hz, 1H), 3.89 (s, 3H), 3.54 (d, *J* = 6.7 Hz, 2H), 1.78–1.73 (m, 2H), 1.26–1.13 (m, 4H), 0.95 (s, 9H), 0.83 (t, *J* = 7.1 Hz, 3H). **¹³C NMR** (126 MHz, CDCl₃): δ = 159.9 (C_q), 155.3 (C_q), 150.1 (C_q), 142.6 (C_q), 137.2 (C_q), 128.9 (CH), 128.7 (C_q), 122.6 (CH), 122.3 (CH), 119.2 (CH), 116.6 (CH), 115.0 (CH), 110.1 (CH), 55.8 (CH₃), 36.8 (C_q), 32.3 (CH₂), 29.3 (CH₃), 28.0 (CH₂), 27.8 (CH₂), 23.5 (CH₂), 13.9 (CH₃). **IR** (ATR): 2954, 2869, 1488, 1433, 1195, 1150, 1028, 825, 794, 623 cm⁻¹. **MS** (ESI) *m/z* (relative intensity): 393 (5) [M+NH₄]⁺, 377 (100) [M+H]⁺, 333 (9). **HR-MS** (ESI) *m/z* calcd for C₂₅H₃₃N₂O [M+H]⁺ 377.2587, found 377.2590.

(*E*)-8-[3-(*tert*-Butyl)hept-2-en-1-yl]-1,3,7-trimethyl-3,7-dihydro-1*H*-purine-2,6-dione (153ka)



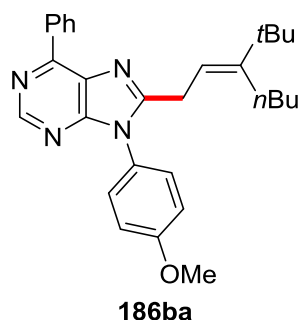
The general procedure **D** was followed using caffeine **16k** (97.1 mg, 0.50 mmol) and allene **152a** (122 mg, 0.80 mmol). Purification by column chromatography on silica gel (*n*hexane/EtOAc: 4/1) yielded **153ka** (157 mg, 90%) as an off-white solid.

M.p. = 108–110 °C. **¹H NMR** (500 MHz, CDCl₃): δ = 5.26 (t, *J* = 6.5 Hz, 1H), 3.86 (s, 3H), 3.56 (s, 3H), 3.50 (d, *J* = 6.5 Hz, 2H), 3.38 (s, 3H), 2.16–2.10 (m, 2H), 1.41–1.35 (m, 4H), 1.03 (s, 9H), 0.93 (t, *J* = 7.0 Hz, 3H). **¹³C NMR** (126 MHz, CDCl₃): δ = 155.4 (C_q), 153.8 (C_q), 152.1 (C_q), 151.8 (C_q), 148.0 (C_q), 114.4 (CH), 107.7 (C_q), 37.1 (C_q), 32.4 (CH₂), 31.9 (CH₃), 29.8 (CH₃), 29.4 (CH₃), 28.6 (CH₂), 28.0 (CH₃), 27.0 (CH₂), 23.6 (CH₂), 14.0 (CH₃). **IR** (ATR): 2952, 2869, 1708, 1653, 1546, 1442, 1219, 1038, 979, 743 cm⁻¹. **MS** (ESI) *m/z* (relative intensity): 715 (64) [2M+Na]⁺, 369 (25) [M+Na]⁺, 347 (100) [M+H]⁺. **HR-MS** (ESI) *m/z* calcd for C₁₉H₃₁N₄O₂ [M+H]⁺ 347.2442, found 347.2449.

(E)-8-[3-(tert-Butyl)hept-2-en-1-yl]-6,9-diphenyl-9H-purine (186aa)

The general procedure **D** was followed using purine **151a** (136 mg, 0.50 mmol) and allene **152a** (122 mg, 0.80 mmol). Purification by column chromatography on silica gel (*n*hexane/EtOAc: 4/1) yielded **186aa** (195 mg, 92%) as a pale yellow solid.

M.p. = 61–63 °C. **¹H NMR** (500 MHz, CDCl₃): δ = 8.94 (s, 1H), 8.86 (ddd, *J* = 8.3, 2.4 Hz, 2H), 7.61–7.52 (m, 6H), 7.43–7.39 (m, 2H), 5.30 (t, *J* = 6.7 Hz, 1H), 3.67 (d, *J* = 6.7 Hz, 2H), 1.81–1.75 (m, 2H), 1.29–1.17 (m, 4H), 0.95 (s, 9H), 0.86 (t, *J* = 7.0 Hz, 3H). **¹³C NMR** (126 MHz, CDCl₃): δ = 157.0 (C_q), 155.0 (C_q), 153.5 (C_q), 152.4 (CH), 151.4 (C_q), 136.1 (C_q), 134.1 (C_q), 130.9 (CH), 130.7 (C_q), 130.0 (CH), 129.9 (CH), 129.7 (CH), 128.8 (CH), 127.8 (CH), 115.4 (CH), 36.9 (C_q), 32.3 (CH₂), 29.3 (CH₃), 28.4 (CH₂), 28.1 (CH₂), 23.6 (CH₂), 14.0 (CH₃). **IR** (ATR): 2955, 2869, 1585, 1561, 1502, 1454, 1324, 764, 690, 664 cm⁻¹. **MS** (EI) *m/z* (relative intensity): 424 (100) [M]⁺, 409 (96), 381 (87), 367 (52), 325 (64), 285 (80). **HR-MS** (ESI) *m/z* calcd for C₂₈H₃₃N₄ [M+H]⁺ 425.2700, found 425.2696.

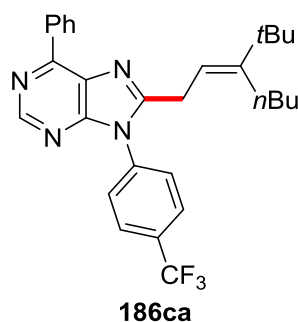
(E)-8-[3-(tert-Butyl)hept-2-en-1-yl]-9-(4-methoxyphenyl)-6-phenyl-9H-purine (186ba)

The general procedure **D** was followed using purine **151b** (151 mg, 0.50 mmol) and allene **152a** (122 mg, 0.80 mmol). Purification by column chromatography on silica gel (*n*hexane/EtOAc: 4/1) yielded **186ba** (164 mg, 72%) as an off-white solid.

5 Experimental Part

M.p. = 103–105 °C. **¹H NMR** (600 MHz, CDCl₃): δ = 8.93 (s, 1H), 8.87–8.84 (m, 2H), 7.60–7.55 (m, 2H), 7.54–7.50 (m, 1H), 7.32–7.29 (m, 2H), 7.09–7.06 (m, 2H), 5.32 (t, *J* = 6.7 Hz, 1H), 3.88 (s, 3H), 3.65 (d, *J* = 6.7 Hz, 2H), 1.84–1.79 (m, 2H), 1.31–1.19 (m, 4H), 0.97 (s, 9H), 0.87 (t, *J* = 7.1 Hz, 3H). **¹³C NMR** (126 MHz, CDCl₃): δ = 160.4 (C_q), 157.2 (C_q), 155.2 (C_q), 153.3 (C_q), 152.2 (CH), 151.2 (C_q), 136.1 (C_q), 130.7 (CH), 130.6 (C_q), 129.8 (CH), 128.9 (CH), 128.7 (CH), 126.5 (C_q), 115.5 (CH), 115.2 (CH), 55.9 (CH₃), 37.0 (C_q), 32.4 (CH₂), 29.4 (CH₃), 28.4 (CH₂), 28.2 (CH₂), 23.7 (CH₂), 14.1 (CH₃). **IR** (ATR): 2960, 2862, 1562, 1515, 1321, 1256, 838, 765, 692, 614 cm⁻¹. **MS** (EI) *m/z* (relative intensity): 454 (78) [M]⁺, 439 (100), 411 (87), 397 (47), 355 (45), 316 (69). **HR-MS** (EI) *m/z* calcd for C₂₉H₃₄N₄O [M]⁺ 454.2733, found 454.2732.

(*E*)-8-[3-(*tert*-Butyl)hept-2-en-1-yl]-6-phenyl-9-[4-(trifluoromethyl)phenyl]-9H-purine (**186ca**)



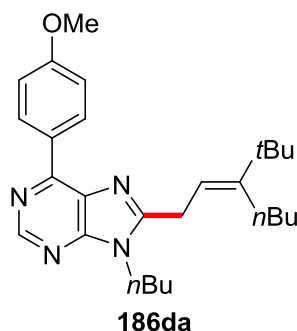
The general procedure **D** was followed using purine **151c** (170 mg, 0.50 mmol) and allene **152a** (122 mg, 0.80 mmol). Purification by column chromatography on silica gel (*n*hexane/EtOAc: 4/1) yielded **186ca** (195 mg, 79%) as a white solid.

M.p. = 93–95 °C. **¹H NMR** (600 MHz, CDCl₃): δ = 8.94 (s, 1H), 8.87–8.84 (m, 2H), 7.86 (d, *J* = 8.4 Hz, 2H), 7.61–7.57 (m, 4H), 7.56–7.52 (m, 1H), 5.27 (t, *J* = 6.7 Hz, 1H), 3.70 (d, *J* = 6.7 Hz, 2H), 1.84–1.78 (m, 2H), 1.30–1.20 (m, 4H), 0.94 (s, 9H), 0.86 (t, *J* = 7.1 Hz, 3H). **¹³C NMR** (126 MHz, CDCl₃): δ = 156.2 (C_q), 154.7 (C_q), 153.8 (C_q), 152.4 (CH), 151.8 (C_q), 137.3 (C_q), 135.8 (C_q), 131.70 (q, ²*J*_{C-F} = 33.0 Hz, C_q), 131.0 (CH), 130.6 (C_q), 129.9 (CH), 128.7 (CH), 128.1 (CH), 127.05 (q, ³*J*_{C-F} = 3.5 Hz, CH), 123.6 (q, ¹*J*_{C-F} = 272.2 Hz, C_q), 115.1 (CH), 37.0 (C_q), 32.3 (CH₂), 29.3 (CH₃), 28.5 (CH₂), 28.3 (CH₂), 23.6 (CH₂), 14.0 (CH₃). **¹⁹F NMR** (282 MHz, CDCl₃): δ = -62.84 (s). **IR** (ATR): 2958, 2871, 1586, 1322, 1167, 1124,

5 Experimental Part

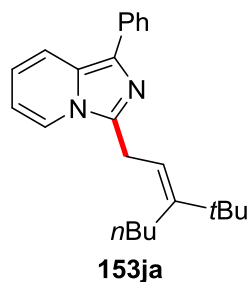
1066, 767, 693, 623 cm^{-1} . **MS** (EI) m/z (relative intensity): 492 (73) $[\text{M}]^+$, 477 (100), 449 (82), 435 (42), 393 (62), 353 (77). **HR-MS** (ESI) m/z calcd for $\text{C}_{29}\text{H}_{32}\text{N}_4\text{F}_3$ $[\text{M}+\text{H}]^+$ 493.2574, found 493.2576.

(*E*)-9-Butyl-8-[3-(*tert*-butyl)hept-2-en-1-yl]-6-(4-methoxyphenyl)-9*H*-purine (186da)



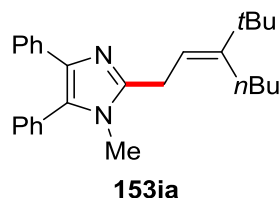
The general procedure **D** was followed using purine **151d** (141 mg, 0.50 mmol) and allene **152a** (122 mg, 0.80 mmol). Purification by column chromatography on silica gel (*n*hexane/EtOAc: 4/1) yielded **186da** (204 mg, 94%) as a yellow oil.

^1H NMR (500 MHz, CDCl_3): δ = 8.90 (s, 1H), 8.85–8.81 (m, 2H), 7.08–7.04 (m, 2H), 5.45 (t, J = 6.5 Hz, 1H), 4.21–4.16 (m, 2H), 3.89 (s, 3H), 3.75 (d, J = 6.5 Hz, 2H), 2.22–2.17 (m, 2H), 1.87–1.79 (m, 2H), 1.52–1.36 (m, 6H), 1.07 (s, 9H), 0.99–0.95 (m, 6H). **^{13}C NMR** (126 MHz, CDCl_3): δ = 161.8 (C_q), 156.3 (C_q), 154.0 (C_q), 152.7 (C_q), 151.7 (C_q), 151.5 (C_q), 131.5 (CH), 130.2 (C_q), 115.5 (CH), 114.1 (CH), 55.5 (CH), 42.9 (CH_2), 37.1 (C_q), 32.4 (CH_2), 32.1 (CH_2), 30.5 (CH_3), 29.4 (CH_3), 28.7 (CH_2), 28.2 (CH_2), 23.7 (CH_2), 20.3 (CH_2), 14.1 (CH_3), 13.8 (CH_3). **IR** (ATR): 2957, 2871, 1703, 1577, 1513, 1251, 1172, 1030, 842, 805 cm^{-1} . **MS** (EI) m/z (relative intensity): 434 (69) $[\text{M}]^+$, 419 (100), 391 (95), 377 (62), 335(45), 281 (48), 254 (37), 240 (41). **HR-MS** (EI) m/z calcd for $\text{C}_{27}\text{H}_{38}\text{N}_4\text{O}$ $[\text{M}]^+$ 434.3046, found 434.3037.

(E)-3-[3-(*tert*-Butyl)hept-2-en-1-yl]-1-phenylimidazo[1,5-a]pyridine (153ja)

The general procedure **D** was followed using imidazole **16j** (97.1 mg, 0.50 mmol) and allene **152a** (122 mg, 0.80 mmol). Purification by column chromatography on silica gel (*n*hexane/EtOAc: 4/1) yielded **153ja** (111 mg, 64%) as a brown oil.

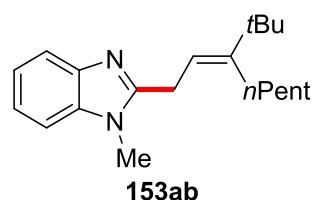
¹H NMR (300 MHz, CDCl₃): δ = 7.91–7.86 (m, 2H), 7.78 (ddd, *J* = 9.3, 1.1 Hz, 1H), 7.67 (ddd, *J* = 7.2, 1.0 Hz, 1H), 7.48–7.41 (m, 2H), 7.30–7.22 (m, 1H), 6.72 (ddd, *J* = 9.3, 6.4, 0.8 Hz, 1H), 6.56–6.50 (m, 1H), 5.41 (t, *J* = 6.4 Hz, 1H), 3.86 (d, *J* = 6.4 Hz, 2H), 2.30–2.21 (m, 2H), 1.55–1.39 (m, 4H), 1.07 (s, 9H), 0.98 (t, *J* = 6.1 Hz, 3H). **¹³C NMR** (126 MHz, CDCl₃): δ = 151.3 (C_q), 138.2 (C_q), 135.3 (C_q), 130.0 (C_q), 128.7 (CH), 126.8 (C_q), 126.5 (CH), 126.2 (CH), 121.4 (CH), 119.1 (CH), 118.8 (CH), 115.6 (CH), 112.4 (CH), 37.1 (C_q), 32.6 (CH₂), 29.6 (CH₃), 28.9 (CH₂), 27.1 (CH₂), 23.8 (CH₂), 14.2 (CH₃). **IR** (ATR): 2953, 2868, 1601, 1519, 1474, 1327, 1065, 957, 768, 695 cm⁻¹. **MS** (EI) *m/z* (relative intensity): 346 (62) [M]⁺, 289 (75), 245 (16), 207 (40), 194 (100), 167 (29). **HR-MS** (EI) *m/z* calcd for C₂₄H₃₀N₂ [M]⁺ 346.2409, found 346.2414.

(E)-2-[3-(*tert*-Butyl)hept-2-en-1-yl]-1-methyl-4,5-diphenyl-1*H*-imidazole (153ia)

The general procedure **D** was followed using imidazole **16i** (117 mg, 0.50 mmol) and allene **152a** (122 mg, 0.80 mmol). Purification by column chromatography on silica gel (*n*hexane/EtOAc: 4/1) yielded **153ia** (111 mg, 57%) as a yellow oil.

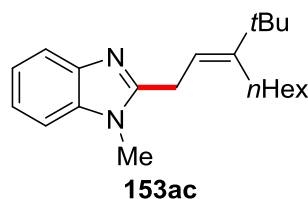
¹H NMR (600 MHz, CDCl₃): δ = 7.49–7.41 (m, 5H), 7.35–7.32 (m, 2H), 7.20–7.16 (m, 2H), 7.13–7.09 (m, 1H), 5.44 (t, *J* = 6.4 Hz, 1H), 3.61 (d, *J* = 6.4 Hz, 2H), 3.33 (s, 3H), 2.20–2.14 (m, 2H), 1.48–1.37 (m, 4H), 1.07 (s, 9H), 0.96 (t, *J* = 7.0 Hz, 3H). **¹³C NMR** (126 MHz, CDCl₃): δ = 150.3 (C_q), 147.9 (C_q), 136.3 (C_q), 135.0 (C_q), 131.6 (C_q), 131.0 (CH), 129.2 (C_q), 129.0 (CH), 128.5 (CH), 128.1 (CH), 126.8 (CH), 126.1 (CH), 116.8 (CH), 37.0 (C_q), 32.4 (CH₂), 31.1 (CH₃), 29.5 (CH₃), 28.7 (CH₂), 27.8 (CH₂), 23.7 (CH₂), 14.1 (CH₃). **IR** (ATR): 2957, 2870, 1601, 1505, 1441, 1395, 965, 917, 770, 694 cm⁻¹. **MS** (EI) *m/z* (relative intensity): 386 (9) [M]⁺, 371 (5), 329 (100), 299 (6), 285 (17), 247 (7). **HR-MS** (EI) *m/z* calcd for C₂₇H₃₄N₂ [M]⁺ 386.2722, found 386.2719.

(E)-2-[3-(*tert*-Butyl)oct-2-en-1-yl]-1-methyl-1*H*-benzo[*d*]imidazole (153ab)



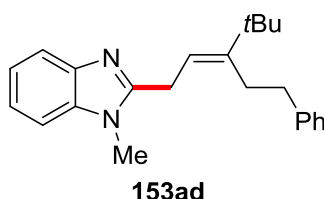
The general procedure **D** was followed using benzimidazole **16a** (66.1 mg, 0.50 mmol) and allene **152b** (133 mg, 0.80 mmol). Purification by column chromatography on silica gel (*n*hexane/EtOAc: 4/1) yielded **153ab** (115 mg, 77%) as a white solid.

M.p. = 76–78 °C. **¹H NMR** (600 MHz, CDCl₃): δ = 7.74–7.70 (m, 1H), 7.29–7.26 (m, 1H), 7.26–7.21 (m, 2H), 5.38 (t, *J* = 6.5 Hz, 1H), 3.68 (d, *J* = 6.5 Hz, 2H), 3.68 (s, 3H), 2.22–2.15 (m, 2H), 1.50–1.43 (m, 2H), 1.41–1.33 (m, 4H), 1.05 (s, 9H), 0.94–0.91 (m, 3H). **¹³C NMR** (126 MHz, CDCl₃): δ = 154.8 (C_q), 151.0 (C_q), 142.6 (C_q), 136.1 (C_q), 122.0 (CH), 121.8 (CH), 119.3 (CH), 115.8 (CH), 108.9 (CH), 37.1 (C_q), 32.9 (CH₂), 30.1 (CH₂), 30.0 (CH₃), 29.6 (CH₃), 29.0 (CH₂), 27.9 (CH₂), 22.7 (CH₂), 14.3 (CH₃). **IR** (ATR): 2934, 2855, 1650, 1494, 1458, 1398, 1305, 1285, 980, 734 cm⁻¹. **MS** (ESI) *m/z* (relative intensity): 299 (100) [M+H]⁺. **HR-MS** (ESI) *m/z* calcd for C₂₀H₃₁N₂ [M+H]⁺ 299.2482, found 299.2483.

(E)-2-(3-(tert-Butyl)non-2-en-1-yl)-1-methyl-1H-benzo[d]imidazole (153ac)

The general procedure **D** was followed using benzimidazole **16a** (66.1 mg, 0.50 mmol) and allene **152c** (144 mg, 0.80 mmol). Purification by column chromatography on silica gel (*n*hexane/EtOAc: 4/1) yielded **153ac** (142 mg, 87%) as a white solid.

M.p. = 77–79 °C. **¹H NMR** (500 MHz, CDCl₃): δ = 7.74–7.70 (m, 1H), 7.31–7.27 (m, 1H), 7.25–7.21 (m, 2H), 5.38 (t, *J* = 6.5 Hz, 1H), 3.68 (s, 3H), 3.68 (d, *J* = 6.5 Hz, 2H), 2.21–2.16 (m, 2H), 1.49–1.36 (m, 4H), 1.36–1.29 (m, 4H), 1.05 (s, 9H), 0.91 (t, *J* = 6.9 Hz, 3H). **¹³C NMR** (126 MHz, CDCl₃): δ = 154.9 (C_q), 151.1 (C_q), 142.7 (C_q), 136.2 (C_q), 122.1 (CH), 121.9 (CH), 119.4 (CH), 115.8 (CH), 109.0 (CH), 37.0 (C_q), 31.8 (CH₂), 30.3 (CH₂), 30.3 (CH₂), 30.0 (CH₃), 29.5 (CH₃), 29.0 (CH₂), 27.8 (CH₂), 22.8 (CH₂), 14.2 (CH₃). **IR** (ATR): 2952, 2928, 2853, 1508, 1463, 1439, 1396, 1330, 767, 743 cm⁻¹. **MS** (ESI) *m/z* (relative intensity): 313 (100) [M+H]⁺. **HR-MS** (ESI) *m/z* calcd for C₂₁H₃₃N₂ [M+H]⁺ 313.2638, found 313.2640.

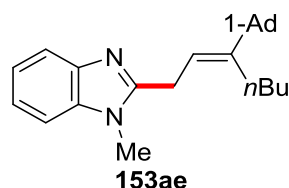
(E)-2-(4,4-Dimethyl-3-phenethylpent-2-en-1-yl)-1-methyl-1H-benzo[d]imidazole (153ad)

The general procedure **D** was followed using benzimidazole **16a** (66.1 mg, 0.50 mmol) and allene **152d** (160 mg, 0.80 mmol). Purification by column chromatography on silica gel (*n*hexane/EtOAc: 4/1) yielded **153ad** (151 mg, 91%) as a white solid.

M.p. = 84–85 °C. **¹H NMR** (500 MHz, CDCl₃): δ = 7.76–7.72 (m, 1H), 7.35–7.21 (m, 8H), 5.51 (t, *J* = 6.5 Hz, 1H), 3.71 (d, *J* = 6.5 Hz, 2H), 3.68 (s, 3H), 2.80–2.75 (m,

2H), 2.55–2.50 (m, 2H), 1.13 (s, 9H). ^{13}C NMR (126 MHz, CDCl_3): δ = 154.6 (C_q), 149.9 (C_q), 142.6 (C_q), 142.4 (C_q), 136.1 (C_q), 128.7 (CH), 128.4 (CH), 126.2 (CH), 122.2 (CH), 122.0 (CH), 119.4 (CH), 116.9 (CH), 109.0 (CH), 37.2 (C_q), 36.3 (CH_2), 31.2 (CH_2), 29.9 (CH_3), 29.5 (CH_3), 27.7 (CH_2). IR (ATR): 2962, 2868, 1497, 1474, 1393, 1286, 750, 718, 705, 462 cm^{-1} . MS (ESI) m/z (relative intensity): 333 (100) $[\text{M}+\text{H}]^+$. HR-MS (ESI) m/z calcd for $\text{C}_{23}\text{H}_{29}\text{N}_2$ $[\text{M}+\text{H}]^+$ 333.2325, found 333.2325.

2-(*E*)-3-(Adamantan-2-yl)hept-2-en-1-yl)-1-methyl-1*H*-benzo[*d*]imidazole (153ae)

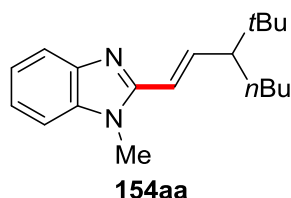


The general procedure **D** was followed using benzimidazole **16a** (66.1 mg, 0.50 mmol) and allene **152e** (184 mg, 0.80 mmol). Purification by column chromatography on silica gel (*n*hexane/EtOAc: 4/1) yielded **153ae** (178 mg, 98%) as a white solid.

M.p. = 151–153 °C. ^1H NMR (500 MHz, CDCl_3): δ = 7.74–7.70 (m, 1H), 7.30–7.26 (m, 1H), 7.26–7.21 (m, 2H), 5.30 (t, J = 6.5 Hz, 1H), 3.69 (d, J = 6.5 Hz, 2H), 3.68 (s, 3H), 2.20–2.14 (m, 2H), 1.98 (br s, 3H), 1.73–1.59 (m, 12H), 1.46–1.36 (m, 4H), 0.96 (t, J = 6.9 Hz, 3H). ^{13}C NMR (126 MHz, CDCl_3): δ = 155.0 (C_q), 151.6 (C_q), 142.7 (C_q), 136.2 (C_q), 122.1 (CH), 121.8 (CH), 119.4 (CH), 116.0 (CH), 108.9 (CH), 41.2 (CH_2), 38.6 (C_q), 37.0 (CH_2), 32.7 (CH_2), 30.0 (CH_3), 28.7 (CH), 27.8 (CH_2), 27.5 (CH_2), 23.7 (CH_2), 14.1 (CH_3). IR (ATR): 2896, 2845, 1512, 1471, 1443, 1332, 1239, 1006, 767, 744 cm^{-1} . MS (EI) m/z (relative intensity): 362 (18) $[\text{M}]^+$, 319 (38), 306 (17), 227 (100), 146 (36), 135 (32). HR-MS (EI) m/z calcd for $\text{C}_{25}\text{H}_{34}\text{N}_2$ $[\text{M}]^+$ 362.2722, found 362.2724.

5.4.2 Experimental Procedures and Analytical Data – Nickel-catalyzed C–H Alkenylation

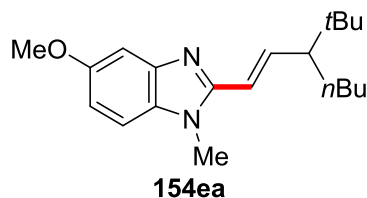
(*E*)-2-[3-(*tert*-Butyl)hept-1-en-1-yl]-1-methyl-1*H*-benzo[*d*]imidazole (154aa)



The general procedure **E** was followed using benzimidazole **16a** (66.1 mg, 0.50 mmol) and allene **152a** (122 mg, 0.80 mmol). Purification by column chromatography on silica gel (*n*hexane/EtOAc: 5/1) yielded **154aa** (117 mg, 82%) as a pale yellow oil.

¹H NMR (500 MHz, CDCl₃): δ = 7.76–7.72 (m, 1H), 7.30–7.26 (m, 1H), 7.26–7.20 (m, 2H), 6.91 (dd, *J* = 15.4, 10.4 Hz, 1H), 6.38 (d, *J* = 15.4 Hz, 1H), 3.78 (s, 3H), 1.90 (td, *J* = 10.6, 2.3 Hz, 1H), 1.65–1.57 (m, 1H), 1.40–1.21 (m, 4H), 1.16–1.08 (m, 1H), 0.95 (s, 9H), 0.86 (t, *J* = 7.2 Hz, 3H). **¹³C NMR** (126 MHz, CDCl₃): δ = 151.2 (C_q), 143.9 (CH), 143.0 (C_q), 135.9 (C_q), 122.4 (CH), 122.3 (CH), 119.3 (CH), 117.0 (CH), 109.1 (CH), 55.4 (CH), 33.5 (C_q), 30.9 (CH₂), 29.9 (CH₃), 28.7 (CH₂), 28.1 (CH₃), 22.9 (CH₂), 14.2 (CH₃). **IR** (ATR): 2952, 1649, 1461, 1287, 1005, 735, 547, 442 cm⁻¹. **MS** (EI) *m/z* (relative intensity): 284 (24) [M]⁺, 227 (100), 197 (16), 185 (94), 170 (18), 146 (19), 57 (18). **HR-MS** (EI) *m/z* calcd for C₁₉H₂₈N₂ [M]⁺ 284.2252, found 284.2253.

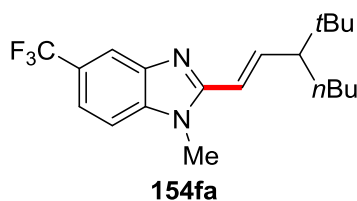
(*E*)-2-[3-(*tert*-Butyl)hept-1-en-1-yl]-5-methoxy-1-methyl-1*H*-benzo[*d*]imidazole (154ea)



The general procedure **E** was followed using benzimidazole **16e** (81.1 mg, 0.50 mmol) and allene **152a** (122 mg, 0.80 mmol). Purification by column chromatography on silica gel (*n*hexane/EtOAc: 5/1) yielded **154ea** (123 mg, 78%) as a white solid.

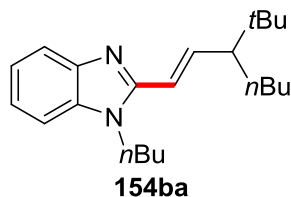
M.p. = 117–119 °C. **¹H NMR** (600 MHz, CDCl₃): δ = 7.23 (d, *J* = 2.4 Hz, 1H), 7.14 (d, *J* = 8.7 Hz, 1H), 6.87 (dd, *J* = 8.7, 2.3 Hz, 1H), 6.86 (dd, *J* = 15.6, 10.2 Hz, 1H), 6.33 (d, *J* = 15.3 Hz, 1H), 3.83 (s, 3H), 3.73 (s, 3H), 1.88 (td, *J* = 10.7, 2.3 Hz, 1H), 1.64–1.56 (m, 1H), 1.38–1.21 (m, 4H), 1.14–1.06 (m, 1H), 0.94 (s, 9H), 0.85 (t, *J* = 7.2 Hz, 3H). **¹³C NMR** (126 MHz, CDCl₃): δ = 156.4 (C_q), 151.3 (C_q), 143.7 (C_q), 143.3 (CH), 130.5 (C_q), 117.0 (CH), 112.2 (CH), 109.4 (CH), 101.5 (CH), 55.9 (CH), 55.4 (CH₃), 33.6 (C_q), 31.0 (CH₂), 30.0 (CH₃), 28.8 (CH₂), 28.2 (CH₃), 23.0 (CH₂), 14.3 (CH₃). **IR** (ATR): 2964, 2946, 2867, 1489, 1453, 1191, 1153, 980, 835, 798 cm⁻¹. **MS** (EI) *m/z* (relative intensity): 314 (14) [M]⁺, 257 (100), 243 (3), 215 (32), 200 (9), 176 (8). **HR-MS** (EI) *m/z* calcd for C₂₀H₃₀N₂O [M]⁺ 314.2358, found 314.2352.

(E)-2-[3-(*tert*-Butyl)hept-1-en-1-yl]-1-methyl-5-(trifluoromethyl)-1*H*-benzo[d]-imidazole (154fa)



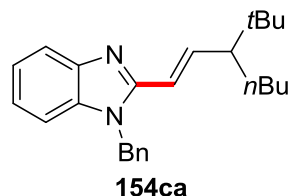
The general procedure **E** was followed using benzimidazole **16f** (100 mg, 0.50 mmol) and allene **152a** (122 mg, 0.80 mmol). Purification by column chromatography on silica gel (*n*hexane/EtOAc: 4/1) yielded **154fa** (154 mg, 87%) as a pale yellow solid.

M.p. = 81–83 °C. **¹H NMR** (600 MHz, CDCl₃): δ = 8.00 (s, 1H), 7.46 (dd, *J* = 8.5, 1.3 Hz, 1H), 7.34 (d, *J* = 8.5 Hz, 1H), 6.97 (dd, *J* = 15.4, 10.4 Hz, 1H), 6.39 (d, *J* = 15.4 Hz, 1H), 3.80 (s, 3H), 1.92 (td, *J* = 10.7, 2.4 Hz, 1H), 1.66–1.58 (m, 1H), 1.38–1.23 (m, 4H), 1.16–1.07 (m, 1H), 0.95 (s, 9H), 0.86 (t, *J* = 7.1 Hz, 3H). **¹³C NMR** (126 MHz, CDCl₃): δ = 153.0 (C_q), 145.6 (CH), 142.5 (C_q), 137.8 (C_q), 125.0 (q, ¹*J*_{C-F} = 271.5 Hz, C_q), 124.8 (q, ²*J*_{C-F} = 32.1 Hz, C_q), 119.1 (q, ³*J*_{C-F} = 3.6 Hz, CH), 116.9 (q, ³*J*_{C-F} = 4.2 Hz, CH), 116.5 (CH), 109.4 (CH), 55.5 (CH), 33.6 (C_q), 31.0 (CH₂), 30.2 (CH₃), 28.8 (CH₂), 28.2 (CH₃), 23.0 (CH₂), 14.3 (CH₃). **¹⁹F NMR** (376 MHz, CDCl₃): δ = -60.63 (s). **IR** (ATR): 2957, 2867, 1450, 1327, 1226, 1113, 1047, 931, 885, 803 cm⁻¹. **MS** (EI) *m/z* (relative intensity): 352 (7) [M]⁺, 337 (6), 296 (53), 253 (100), 251 (19), 239 (10), 214 (14), 57 (20). **HR-MS** (EI) *m/z* calcd for C₂₀H₂₇N₂F₃ [M]⁺ 352.2126, found 352.2113.

(E)-1-Butyl-2-[3-(tert-butyl)hept-1-en-1-yl]-1H-benzo[d]imidazole (154ba)

The general procedure **E** was followed using benzimidazole **16b** (87.1 mg, 0.50 mmol) and allene **152a** (122 mg, 0.80 mmol). Purification by column chromatography on silica gel (*n*hexane/EtOAc: 4/1) yielded **154ba** (118 mg, 72%) as a colorless oil.

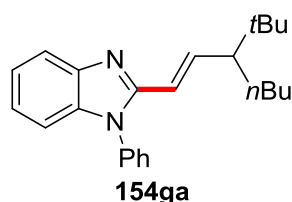
¹H NMR (500 MHz, CDCl₃): δ = 7.77–7.72 (m, 1H), 7.31–7.27 (m, 1H), 7.25–7.19 (m, 2H), 6.92 (dd, *J* = 15.4, 10.4 Hz, 1H), 6.35 (d, *J* = 15.4 Hz, 1H), 4.16 (t, *J* = 7.2 Hz, 2H), 1.90 (td, *J* = 10.7, 2.3 Hz, 1H), 1.81–1.72 (m, 2H), 1.66–1.57 (m, 1H), 1.40–1.21 (m, 6H), 1.16–1.06 (m, 1H), 0.95 (s, 9H), 0.93 (t, *J* = 7.4 Hz, 3H), 0.86 (t, *J* = 7.1 Hz, 3H). **¹³C NMR** (126 MHz, CDCl₃): δ = 150.8 (C_q), 143.6 (CH), 143.1 (C_q), 135.3 (C_q), 122.3 (CH), 122.2 (CH), 119.4 (CH), 117.3 (CH), 109.4 (CH), 55.4 (CH), 43.3 (CH₂), 33.6 (C_q), 32.4 (CH₂), 30.9 (CH₂), 28.7 (CH₂), 28.1 (CH₃), 22.9 (CH₂), 20.3 (CH₂), 14.2 (CH₃), 13.9 (CH₃). **IR** (ATR): 2955, 2932, 2862, 1650, 1453, 1405, 1329, 1284, 975, 739 cm⁻¹. **MS** (EI) *m/z* (relative intensity): 326 (17) [M]⁺, 269 (100), 227 (46), 213 (15), 183 (12), 173 (13), 169 (22), **HR-MS** (EI) *m/z* calcd for C₂₂H₃₄N₂ [M]⁺ 326.2722, found 326.2733.

(E)-1-Benzyl-2-[3-(tert-butyl)hept-1-en-1-yl]-1H-benzo[d]imidazole (154ca)

The general procedure **E** was followed using benzimidazole **16c** (104 mg, 0.50 mmol) and allene **152a** (122 mg, 0.80 mmol). Purification by column chromatography on silica gel (*n*hexane/EtOAc: 4/1) yielded **154ca** (132 mg, 73%) as an off-white solid.

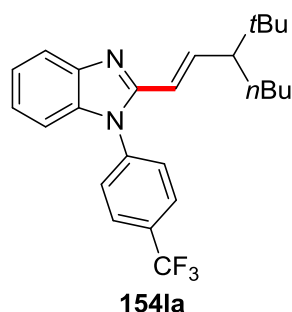
M.p. = 73–75 °C. **¹H NMR** (600 MHz, CDCl₃): δ = 7.84–7.71 (m, 1H), 7.31–7.13 (m, 6H), 7.12–6.97 (m, 2H), 6.89 (dd, *J* = 15.4, 10.3 Hz, 1H), 6.32 (d, *J* = 15.4 Hz, 1H), 5.35 (s, 2H), 1.80 (td, *J* = 10.3, 2.6 Hz, 1H), 1.62–1.48 (m, 1H), 1.30–1.18 (m, 4H), 1.00 (m, 1H), 0.87 (s, 9H), 0.83–0.77 (m, 3H). **¹³C NMR** (126 MHz, CDCl₃): δ = 151.0 (C_q), 143.9 (CH), 143.0 (C_q), 136.1 (C_q), 135.3 (C_q), 128.8 (CH), 127.8 (CH), 126.2 (CH), 122.4 (CH), 122.4 (CH), 119.3 (CH), 117.1 (CH), 109.3 (CH), 55.1 (CH), 46.7 (CH₂), 33.3 (C_q), 30.6 (CH₂), 28.5 (CH₂), 27.8 (CH₃), 22.7 (CH₂), 14.0 (CH₃). **IR** (ATR): 2957, 1651, 1495, 1453, 1366, 1251, 975, 734, 703, 444 cm⁻¹. **MS** (EI) *m/z* (relative intensity): 360 (12) [M]⁺, 303 (67), 261 (38), 169 (17), 91 (100). **HR-MS** (EI) *m/z* calcd for C₂₅H₃₂N₂ [M]⁺ 360.2565, found 360.2566.

(E)-2-[3-(*tert*-Butyl)hept-1-en-1-yl]-1-phenyl-1*H*-benzo[*d*]imidazole (154ga)



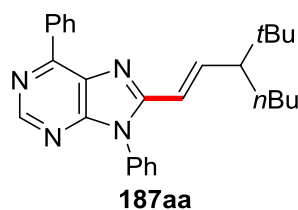
The general procedure **E** was followed using benzimidazole **16g** (97.1 mg, 0.50 mmol) and allene **152a** (122 mg, 0.80 mmol). Purification by column chromatography on silica gel (*n*hexane/EtOAc: 4/1) yielded **154ga** (101 mg, 58%) as a colorless oil.

¹H NMR (600 MHz, CDCl₃): δ = 7.81 (d, *J* = 8.1 Hz, 1H), 7.61–7.56 (m, 2H), 7.54–7.51 (m, 1H), 7.41–7.38 (m, 2H), 7.28 (ddd, *J* = 8.2, 7.0, 1.3 Hz, 1H), 7.20–7.17 (m, 1H), 7.16–7.14 (m, 1H), 6.84 (dd, *J* = 15.5, 10.4 Hz, 1H), 6.12 (d, *J* = 15.7 Hz, 1H), 1.76 (td, *J* = 10.7, 2.3 Hz, 1H), 1.57–1.51 (m, 1H), 1.33–1.20 (m, 4H), 1.07–1.01 (m, 1H), 0.89 (s, 9H), 0.84 (t, *J* = 7.2 Hz, 3H). **¹³C NMR** (126 MHz, CDCl₃): δ = 150.8 (C_q), 143.7 (C_q), 136.4 (C_q), 136.0 (C_q), 129.8 (CH), 128.8 (CH), 127.6 (CH), 122.9 (CH), 122.8 (CH), 119.3 (CH), 118.1 (CH), 110.1 (CH), 55.1 (CH), 33.6 (C_q), 30.9 (CH₂), 28.8 (CH₂), 28.1 (CH₃), 22.9 (CH₂), 14.3 (CH₃). **IR** (ATR): 2955, 2864, 1595, 1498, 1450, 1388, 978, 759, 739, 695 cm⁻¹. **MS** (EI) *m/z* (relative intensity): 346 (15) [M]⁺, 289 (100), 259 (14), 247 (58), 232 (15), 207 (12). **HR-MS** (EI) *m/z* calcd for C₂₄H₃₀N₂ [M]⁺ 346.2409, found 346.2413.

(E)-2-[3-(tert-Butyl)hept-1-en-1-yl]-1-(4-(trifluoromethyl)phenyl)-1H-benzo[d]imidazole (154la)

The general procedure E was followed using benzimidazole **16I** (131 mg, 0.50 mmol) and allene **152a** (122 mg, 0.80 mmol). Purification by column chromatography on silica gel (*n*hexane/EtOAc: 4/1) yielded **154la** (177 mg, 85%) as a yellow oil.

¹H NMR (500 MHz, CDCl₃): δ = 7.87 (d, *J* = 8.2 Hz, 2H), 7.82 (d, *J* = 8.1 Hz, 1H), 7.55 (d, *J* = 8.2 Hz, 2H), 7.31 (ddd, *J* = 8.2, 7.2, 1.2 Hz, 1H), 7.22 (ddd, *J* = 8.2, 7.2, 1.1 Hz, 1H), 7.16 (d, *J* = 8.0 Hz, 1H), 6.90 (dd, *J* = 15.5, 10.4 Hz, 1H), 6.10 (d, *J* = 15.5 Hz, 1H), 1.79 (td, *J* = 10.4, 2.4 Hz, 1H), 1.61–1.52 (m, 1H), 1.33–1.19 (m, 4H), 1.09–1.00 (m, 1H), 0.90 (s, 9H), 0.85 (t, *J* = 7.1 Hz, 3H). **¹³C NMR** (126 MHz, CDCl₃): δ = 150.5 (C_q), 144.8 (CH), 143.2 (C_q), 139.2 (C_q), 135.9 (C_q), 130.9 (q, ²*J*_{C-F} = 33.0 Hz, C_q), 128.0 (CH), 127.2 (q, ³*J*_{C-F} = 3.6 Hz, CH), 123.8 (q, ¹*J*_{C-F} = 272.4 Hz, C_q), 123.5 (CH), 123.3 (CH), 119.6 (CH), 117.6 (CH), 109.8 (CH), 55.2 (CH), 33.6 (C_q), 30.8 (CH₂), 28.6 (CH₂), 28.0 (CH₃), 22.8 (CH₂), 14.2 (CH₃). **¹⁹F NMR** (471 MHz, CDCl₃): δ = -62.55 (s). **IR** (ATR): 2957, 2867, 1609, 1451, 1319, 1127, 1066, 844, 739, 446 cm⁻¹. **MS** (EI) *m/z* (relative intensity): 414 (12) [M]⁺, 357 (100), 327 (15), 315 (90), 313 (31), 300 (14), 276 (10). **HR-MS** (EI) *m/z* calcd for C₂₅H₂₉N₂F₃ [M]⁺ 414.2283, found 414.2291.

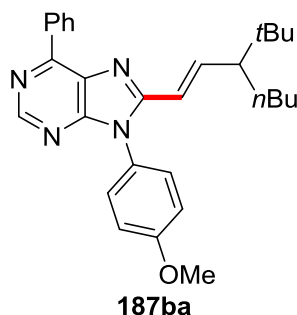
(E)-8-[3-(tert-Butyl)hept-1-en-1-yl]-6,9-diphenyl-9H-purine (187aa)

5 Experimental Part

The general procedure **E** was followed using purine **151a** (136 mg, 0.50 mmol) and allene **152a** (122 mg, 0.80 mmol). Purification by column chromatography on silica gel (*n*hexane/EtOAc: 4/1) yielded **187aa** (135 mg, 63%) as a colorless oil.

¹H NMR (600 MHz, CDCl₃): δ = 8.93 (s, 1H), 8.92–8.90 (m, 2H), 7.65–7.52 (m, 6H), 7.48–7.45 (m, 2H), 7.00 (dd, *J* = 15.6, 10.4 Hz, 1H), 6.25 (d, *J* = 15.6 Hz, 1H), 1.83 (td, *J* = 10.6, 2.4 Hz, 1H), 1.63–1.55 (m, 1H), 1.34–1.22 (m, 4H), 1.10–1.03 (m, 1H), 0.92 (s, 9H), 0.87 (t, *J* = 7.1 Hz, 3H). **¹³C NMR** (126 MHz, CDCl₃): δ = 154.6 (C_q), 153.1 (C_q), 152.2 (C_q), 152.1 (CH), 146.8 (CH), 136.1 (C_q), 134.0 (C_q), 131.2 (C_q), 130.8 (CH), 129.9 (CH), 129.9 (CH), 129.4 (CH), 128.7 (CH), 127.7 (CH), 117.8 (CH), 55.2 (CH), 33.8 (C_q), 30.9 (CH₂), 28.7 (CH₂), 28.1 (CH₃), 22.9 (CH₂), 14.3 (CH₃). **IR** (ATR): 2955, 2866, 1575, 1560, 1502, 1325, 908, 765, 731, 693 cm⁻¹. **MS** (EI) *m/z* (relative intensity): 424 (15) [M]⁺, 409 (15), 368 (74), 325 (100), 299 (16), 286 (40). **HR-MS** (ESI) *m/z* calcd for C₂₈H₃₃N₄ [M+H]⁺ 425.2700, found 425.2698.

(*E*)-8-[3-(*tert*-Butyl)hept-1-en-1-yl]-9-(4-methoxyphenyl)-6-phenyl-9*H*-purine (**187ba**)



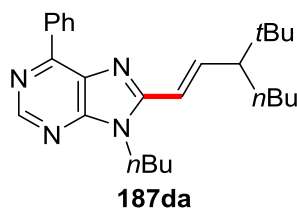
The general procedure **E** was followed using purine **151b** (151 mg, 0.50 mmol) and allene **152a** (122 mg, 0.80 mmol). Purification by column chromatography on silica gel (*n*hexane/EtOAc: 4/1) yielded **187ba** (197 mg, 87%) as a white solid.

M.p. = 118–121 °C. **¹H NMR** (600 MHz, CDCl₃): δ = 8.92 (s, 1H), 8.91–8.89 (m, 2H), 7.61–7.58 (m, 2H), 7.55–7.51 (m, 1H), 7.38–7.35 (m, 2H), 7.13–7.10 (m, 2H), 7.00 (dd, *J* = 15.6, 10.4 Hz, 1H), 6.24 (d, *J* = 15.6 Hz, 1H), 3.91 (s, 3H), 1.83 (td, *J* = 10.6, 2.4 Hz, 1H), 1.62–1.55 (m, 1H), 1.34–1.21 (m, 4H), 1.10–1.04 (m, 1H), 0.92 (s, 9H), 0.86 (t, *J* = 7.0 Hz, 3H). **¹³C NMR** (126 MHz, CDCl₃): δ = 160.3 (C_q), 155.0 (C_q), 153.1 (C_q), 152.6 (C_q), 152.2 (CH), 146.8 (CH), 136.2 (C_q), 131.2 (C_q), 130.8 (CH), 130.0 (CH), 128.9 (CH), 128.8 (CH), 126.4 (C_q), 117.8 (CH), 115.2 (CH), 55.8 (CH₃),

5 Experimental Part

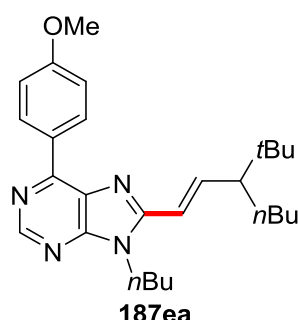
55.2 (CH), 33.7 (C_q), 30.8 (CH₂), 28.6 (CH₂), 28.1 (CH₃), 22.8 (CH₂), 14.2 (CH₃). **IR** (ATR): 2952, 2866, 1585, 1514, 1250, 837, 763, 686, 651, 596 cm⁻¹. **MS** (EI) *m/z* (relative intensity): 454 (33) [M]⁺, 439 (23), 411 (17), 398 (100), 355 (98), 316 (28), 57 (28). **HR-MS** (EI) *m/z* calcd for C₂₉H₃₄N₄O [M]⁺ 454.2733, found 454.2716.

(E)-9-Butyl-8-[3-(*tert*-butyl)hept-1-en-1-yl]-6-phenyl-9*H*-purine (187da)



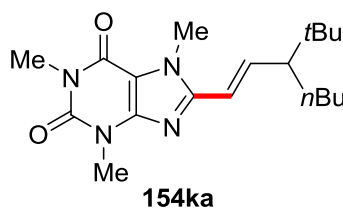
The general procedure **E** was followed using purine **151d** (127 mg, 0.50 mmol) and allene **152a** (122 mg, 0.80 mmol). Purification by column chromatography on silica gel (*n*hexane/EtOAc: 4/1) yielded **187da** (193 mg, 95%) as a colorless oil.

¹H NMR (600 MHz, CDCl₃): δ = 8.93 (s, 1H), 8.88–8.86 (m, 2H), 7.58–7.55 (m, 2H), 7.52–7.48 (m, 1H), 7.15 (dd, *J* = 15.3, 10.4 Hz, 1H), 6.43 (d, *J* = 15.3 Hz, 1H), 4.33 (t, *J* = 7.4 Hz, 2H), 1.97 (td, *J* = 10.4, 2.3 Hz, 1H), 1.85–1.79 (m, 2H), 1.70–1.62 (m, 1H), 1.43–1.23 (m, 6H), 1.19–1.10 (m, 1H), 0.99 (s, 9H), 0.96 (t, *J* = 7.4 Hz, 3H), 0.88 (t, *J* = 7.1 Hz, 3H). **¹³C NMR** (126 MHz, CDCl₃): δ = 153.9 (C_q), 152.6 (C_q), 152.3 (C_q), 151.3 (CH), 146.4 (CH), 136.2 (C_q), 131.3 (C_q), 130.6 (CH), 129.9 (CH), 128.6 (CH), 117.0 (CH), 55.5 (CH), 42.3 (CH₂), 33.8 (CH₂), 32.5 (CH₂), 31.0 (CH₂), 28.7 (C_q), 28.2 (CH₃), 23.0 (CH₂), 20.2 (CH₂), 14.3 (CH₃), 13.9 (CH₃). **IR** (ATR): 2956, 2867, 1583, 1456, 1393, 1323, 1160, 975, 760, 724 cm⁻¹. **MS** (ESI) *m/z* (relative intensity): 405 (100) [M+H]⁺. **HR-MS** (ESI) *m/z* calcd for C₂₆H₃₇N₄ [M+H]⁺ 405.3013, found 405.3013.

(E)-9-Butyl-8-[3-(*tert*-butyl)hept-1-en-1-yl]-6-(4-methoxyphenyl)-9H-purine (187ea)

The general procedure **E** was followed using purine **151e** (141 mg, 0.50 mmol) and allene **152a** (122 mg, 0.80 mmol). Purification by column chromatography on silica gel (*n*hexane/EtOAc: 4/1) yielded **187ea** (171 mg, 79%) as a colorless oil.

¹H NMR (600 MHz, CDCl₃): δ = 8.88–8.85 (m, 3H), 7.11 (dd, *J* = 15.4, 10.5 Hz, 1H), 7.08–7.05 (m, 2H), 6.40 (d, *J* = 15.3 Hz, 1H), 4.29 (t, *J* = 7.3 Hz, 1H), 3.88 (s, 3H), 1.95 (td, *J* = 10.6, 2.1 Hz, 1H), 1.84–1.75 (m, 3H), 1.68–1.61 (m, 1H), 1.42–1.29 (m, 7H), 0.97 (s, 9H), 0.94 (t, *J* = 7.3 Hz, 3H), 0.86 (t, *J* = 6.9 Hz, 3H). **¹³C NMR** (126 MHz, CDCl₃): δ = 161.7 (C_q), 161.7 (C_q), 153.6 (C_q), 151.3 (C_q), 146.0 (CH), 131.6 (CH), 131.5 (C_q), 130.6 (C_q), 117.1 (CH), 114.1 (CH), 114.1 (CH), 55.5 (OCH₃), 55.5 (CH), 42.3 (CH₂), 33.8 (CH₂), 32.5 (CH₂), 31.0 (CH₂), 28.8 (C_q), 28.2 (CH₃), 23.0 (CH₂), 20.2 (CH₂), 14.3 (CH₃), 13.9 (CH₃). **IR** (ATR): 2954, 2932, 2867, 1577, 1512, 1439, 1251, 1173, 842, 805 cm⁻¹. **MS** (EI) *m/z* (relative intensity): 434 (41) [M]⁺, 377 (100), 335 (92), 321 (37), 281 (40), 254 (28), 240 (32). **HR-MS** (EI) *m/z* calcd for C₂₇H₃₈N₄O [M]⁺ 434.3046, found 434.3063.

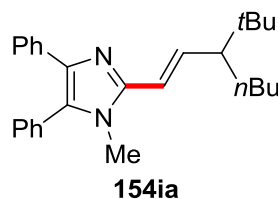
(E)-8-[3-(*tert*-butyl)hept-1-en-1-yl]-1,3,7-trimethyl-3,7-dihydro-1H-purine-2,6-dione (154ka)

5 Experimental Part

The general procedure **E** was followed using caffeine (**16k**) (97.1 mg, 0.50 mmol) and allene **152a** (122 mg, 0.80 mmol). Purification by column chromatography on silica gel (*n*hexane/EtOAc: 4/1) yielded **154ka** (149 mg, 86%) as a white solid.

M.p. = 151–153 °C. **¹H NMR** (500 MHz, CDCl₃): δ = 6.79 (dd, *J* = 15.3, 10.5 Hz, 1H), 6.19 (d, *J* = 15.3 Hz, 1H), 3.95 (s, 3H), 3.58 (s, 3H), 3.38 (s, 3H), 1.86 (td, *J* = 10.5, 2.4 Hz, 1H), 1.65–1.55 (m, 1H), 1.36–1.22 (m, 4H), 1.12–1.03 (m, 1H), 0.92 (s, 9H), 0.86 (t, *J* = 7.1 Hz, 3H). **¹³C NMR** (126 MHz, CDCl₃): δ = 155.4 (C_q), 151.9 (C_q), 145.0 (C_q), 148.6 (C_q), 145.3 (CH), 115.5 (CH), 107.4 (C_q), 55.3 (CH), 33.6 (C_q), 31.6 (CH₃), 30.9 (CH₂), 29.9 (CH₃), 28.6 (CH₂), 28.1 (CH₃), 28.0 (CH₃), 22.9 (CH₂), 14.2 (CH₃). **IR** (ATR): 2952, 2861, 1698, 1655, 1544, 1433, 1224, 1039, 980, 742 cm⁻¹. **MS** (EI) *m/z* (relative intensity): 346 (14) [M]⁺, 331 (4), 289 (100), 247 (52), 233(15), 207 (21), 57 (13). **HR-MS** (EI) *m/z* calcd for C₁₉H₃₀N₄O₂ [M]⁺ 346.2369, found 346.2373.

(*E*)-2-[3-(*tert*-Butyl)hept-1-en-1-yl]-1-methyl-4,5-diphenyl-1*H*-imidazole (**154ia**)

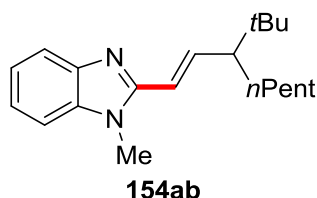


The general procedure **E** was followed using imidazole **16i** (117 mg, 0.50 mmol) and allene **152a** (122 mg, 0.80 mmol). Purification by column chromatography on silica gel (*n*hexane/EtOAc: 4/1) yielded **154ia** (123 mg, 63%) as a brown solid.

M.p. = 86–89 °C. **¹H NMR** (600 MHz, CDCl₃): δ = 7.50–7.46 (m, 2H), 7.46–7.40 (m, 3H), 7.34–7.31 (m, 2H), 7.21–7.17 (m, 2H), 7.15–7.10 (m, 1H), 6.63 (dd, *J* = 15.5, 10.2 Hz, 1H), 6.27 (d, *J* = 15.5 Hz, 1H), 3.45 (s, 3H), 1.84 (td, *J* = 10.7, 2.2 Hz, 1H), 1.65–1.57 (m, 1H), 1.45–1.23 (m, 5H), 0.96 (s, 9H), 0.88 (t, *J* = 7.2 Hz, 3H). **¹³C NMR** (126 MHz, CDCl₃): δ = 145.6 (C_q), 138.7 (CH), 137.8 (C_q), 135.0 (C_q), 131.3 (C_q), 131.1 (CH), 129.4 (C_q), 129.0 (CH), 128.5 (CH), 128.2 (CH), 127.3 (CH), 126.3 (CH), 117.8 (CH), 55.3 (CH), 33.5 (C_q), 31.3 (CH₃), 31.0 (CH₂), 28.9 (CH₂), 28.2 (CH₃), 23.0 (CH₂), 14.3 (CH₃). **IR** (ATR): 2953, 2863, 1600, 1453, 1363, 1071, 967, 772, 713, 694 cm⁻¹. **MS** (EI) *m/z* (relative intensity): 386 (69) [M]⁺, 371 (58), 343 (64), 329

(100), 287 (35), 247 (71). **HR-MS** (ESI) m/z calcd for $C_{27}H_{35}N_2$ $[M+H]^+$ 387.2795, found 387.2805.

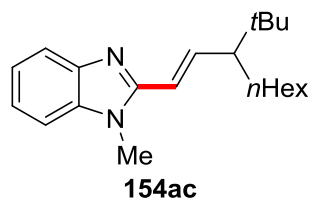
(E)-2-[3-(tert-Butyl)oct-1-en-1-yl]-1-methyl-1H-benzo[d]imidazole (154ab)



The general procedure **E** was followed using benzimidazole **16a** (66.1 mg, 0.50 mmol) and allene **152b** (133 mg, 0.80 mmol). Purification by column chromatography on silica gel (*n*hexane/EtOAc: 4/1) yielded **154ab** (119 mg, 80%) as an off-white solid.

M.p. = 75–77 °C. **¹H NMR** (600 MHz, $CDCl_3$): δ = 7.76–7.72 (m, 1H), 7.29–7.26 (m, 1H), 7.25–7.21 (m, 2H), 6.91 (dd, J = 15.4, 10.4 Hz, 1H), 6.38 (d, J = 15.4 Hz, 1H), 3.76 (s, 3H), 1.90 (td, J = 10.7, 2.3 Hz, 1H), 1.63–1.56 (m, 1H), 1.41–1.33 (m, 1H), 1.33–1.20 (m, 5H), 1.17–1.10 (m, 1H), 0.95 (s, 9H), 0.87–0.84 (m, 3H). **¹³C NMR** (126 MHz, $CDCl_3$): δ = 151.0 (C_q), 143.8 (CH), 142.9 (C_q), 135.8 (C_q), 122.3 (CH), 122.2 (CH), 119.2 (CH), 117.0 (CH), 109.1 (CH), 55.5 (CH), 33.6 (CH_2), 32.2 (CH_2), 29.9 (CH_3), 29.1 (CH_2), 28.4 (C_q), 28.2 (CH_3), 22.8 (CH_2), 14.4 (CH_3). **IR** (ATR): 2934, 2855, 1650, 1494, 1458, 1398, 1305, 1285, 980, 734 cm^{-1} . **MS** (ESI) m/z (relative intensity): 597 (6) $[2M+H]^+$, 299 (100) $[M+H]^+$, 243 (4), 185 (3). **HR-MS** (ESI) m/z calcd for $C_{20}H_{31}N_2$ $[M+H]^+$ 299.2482, found 299.2484.

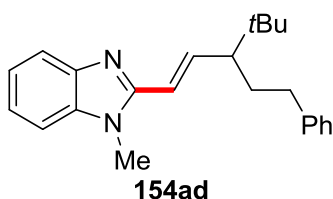
(E)-2-[3-(tert-Butyl)non-1-en-1-yl]-1-methyl-1H-benzo[d]imidazole (154ac)



The general procedure **E** was followed using benzimidazole **16a** (66.1 mg, 0.50 mmol) and allene **152c** (144 mg, 0.80 mmol). Purification by column chromatography on silica gel (*n*hexane/EtOAc: 4/1) yielded **154ac** (138 mg, 84%) as a pale yellow solid.

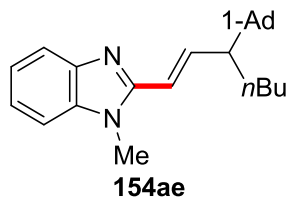
M.p. = 66–68 °C. **¹H NMR** (500 MHz, CDCl₃): δ = 7.76–7.71 (m, 1H), 7.30–7.26 (m, 1H), 7.25–7.20 (m, 2H), 6.90 (dd, *J* = 15.4, 10.4 Hz, 1H), 6.38 (d, *J* = 15.4 Hz, 1H), 3.77 (s, 3H), 1.90 (td, *J* = 10.6, 2.2 Hz, 1H), 1.63–1.56 (m, 1H), 1.41–1.19 (m, 8H), 1.17–1.08 (m, 1H), 0.95 (s, 9H), 0.85 (t, *J* = 7.0 Hz, 3H). **¹³C NMR** (126 MHz, CDCl₃): δ = 151.2 (C_q), 143.9 (CH), 143.1 (C_q), 135.9 (C_q), 122.4 (CH), 122.3 (CH), 119.3 (CH), 117.0 (CH), 109.1 (CH), 55.4 (CH), 33.5 (C_q), 32.0 (CH₂), 29.8 (CH₃), 29.6 (CH₂), 29.0 (CH₂), 28.7 (CH₂), 28.1 (CH₃), 22.8 (CH₂), 14.2 (CH₃). **IR** (ATR): 2934, 2858, 1650, 1493, 1458, 1398, 1305, 1284, 979, 734 cm⁻¹. **MS** (EI) *m/z* (relative intensity): 312 (17) [M]⁺, 255 (100), 197 (12), 185 (77), 183 (25), 170 (13), 159 (14), 146 (22). **HR-MS** (EI) *m/z* calcd for C₂₁H₃₂N₂ [M]⁺ 312.2565, found 312.2555.

(*E*)-2-(4,4-Dimethyl-3-phenethylpent-1-en-1-yl)-1-methyl-1*H*-benzo[*d*]-imidazole (154ad)



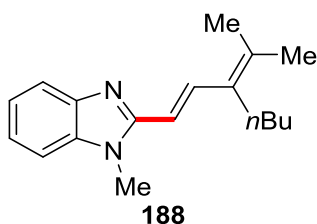
The general procedure **E** was followed using benzimidazole **16a** (66.1 mg, 0.50 mmol) and allene **152d** (160 mg, 0.80 mmol). Purification by column chromatography on silica gel (*n*hexane/EtOAc: 4/1) yielded **154ad** (144 mg, 86%) as a yellow oil.

¹H NMR (300 MHz, CDCl₃): δ = 7.81–7.74 (m, 1H), 7.34–7.24 (m, 5H), 7.21–7.14 (m, 3H), 7.01 (dd, *J* = 15.5, 10.3 Hz, 1H), 6.42 (d, *J* = 15.5 Hz, 1H), 3.80 (s, 3H), 2.81–2.70 (m, 1H), 2.44 (ddd, *J* = 13.7, 9.9, 6.9 Hz, 1H), 2.06–1.92 (m, 2H), 1.76–1.60 (m, 1H), 0.96 (s, 9H). **¹³C NMR** (126 MHz, CDCl₃): δ = 150.8 (C_q), 143.1 (CH), 142.9 (C_q), 142.4 (C_q), 135.8 (C_q), 128.5 (CH), 128.4 (CH), 125.8 (CH), 122.5 (CH), 122.4 (CH), 119.3 (CH), 117.6 (CH), 109.2 (CH), 54.9 (CH), 34.8 (CH₂), 33.7 (C_q), 30.9 (CH₂), 29.9 (CH₃), 28.2 (CH₃). **IR** (ATR): 2948, 2864, 1495, 1460, 1396, 1325, 976, 908, 738, 699 cm⁻¹. **MS** (ESI) *m/z* (relative intensity): 333 (100) [M+H]⁺. **HR-MS** (ESI) *m/z* calcd for C₂₃H₂₉N₂ [M+H]⁺ 333.2325, found 333.2326.

2-[(*E*)-3-(Adamantan-2-yl)hept-1-en-1-yl]-1-methyl-1*H*-benzo[*d*]imidazole (154ae)

The general procedure **E** was followed using benzimidazole **16a** (66.1 mg, 0.50 mmol) and allene **152e** (184 mg, 0.80 mmol). Purification by column chromatography on silica gel (*n*hexane/EtOAc: 4/1) yielded **154ae** (129 mg, 71%) as a white solid.

M.p. = 156–159 °C. **¹H NMR** (600 MHz, CDCl₃): δ = 7.76–7.72 (m, 1H), 7.30–7.27 (m, 1H), 7.26–7.21 (m, 2H), 6.93 (dd, *J* = 15.4, 10.5 Hz, 1H), 6.36 (d, *J* = 15.5 Hz, 1H), 3.78 (s, 3H), 1.96 (br s, 3H), 1.74 (td, *J* = 10.8, 2.2 Hz, 1H), 1.71–1.53 (m, 13H), 1.38–1.21 (m, 4H), 1.12–1.04 (m, 1H), 0.86 (t, *J* = 7.2 Hz, 3H). **¹³C NMR** (126 MHz, CDCl₃): δ = 151.1 (C_q), 143.4 (CH), 143.0 (C_q), 135.8 (C_q), 122.3 (CH), 122.2 (CH), 119.3 (CH), 117.1 (CH), 109.1 (CH), 56.3 (CH), 40.6 (CH₂), 37.5 (CH₂), 35.5 (C_q), 30.9 (CH₂), 29.9 (CH₃), 29.1 (CH), 27.0 (CH₂), 23.0 (CH₂), 14.3 (CH₃). **IR** (ATR): 2901, 2848, 1650, 1460, 1398, 1324, 1285, 969, 740, 437 cm⁻¹. **MS** (EI) *m/z* (relative intensity): 362 (19) [M]⁺, 319 (45), 291 (52), 227 (14), 183 (16), 135 (100), 93 (23). **HR-MS** (EI) *m/z* calcd for C₂₅H₃₄N₂ [M]⁺ 362.2722, found 362.2717.

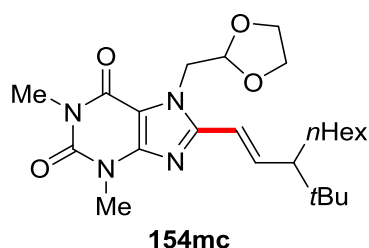
(*E*)-1-Methyl-2-[3-(propan-2-ylidene)hept-1-en-1-yl]-1*H*-benzo[*d*]imidazole (188)

The general procedure **E** was followed using benzimidazole **16a** (66.1 mg, 0.50 mmol) and allene **152g** (215 mg, 0.80 mmol). Purification by column chromatography on silica gel (*n*hexane/EtOAc: 5/1) yielded **188** (79.4 mg, 59%) as a pale brownish solid.

5 Experimental Part

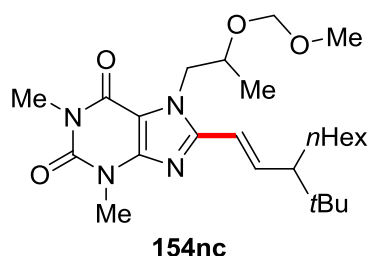
M.p. = 100–103 °C. **¹H NMR** (500 MHz, CDCl₃): δ = 8.00 (d, *J* = 15.6 Hz, 1H), 7.74–7.72 (m, 1H), 7.28–7.19 (m, 3H), 6.45 (d, *J* = 15.6 Hz, 1H), 3.76 (s, 3H), 2.41–2.36 (m, 2H), 2.02 (s, 3H), 1.90 (s, 3H), 1.48–1.37 (m, 4H), 0.96 (t, *J* = 7.1 Hz, 3H). **¹³C NMR** (126 MHz, CDCl₃): δ = 152.6 (C_q), 143.4 (C_q), 138.3 (C_q), 136.1 (C_q), 136.0 (CH), 131.6 (C_q), 122.3 (CH), 122.1 (CH), 119.1 (CH), 110.2 (CH), 109.0 (CH), 31.2 (CH₂), 29.8 (CH₃), 28.1 (CH₂), 23.1 (CH₂), 22.3 (CH₃), 21.2 (CH₃), 14.2 (CH₃). **IR** (ATR): 2952, 2857, 1618, 1458, 1434, 1392, 1330, 1290, 964, 740 cm⁻¹. **MS** (EI) *m/z* (relative intensity): 268 (17) [M]⁺, 253 (100), 225 (14), 210 (27), 195 (10), 146 (5). **HR-MS** (EI) *m/z* calcd for C₁₈H₂₄N₂ [M]⁺ 268.1939, found 268.1938.

(*E*)-7-[(1,3-Dioxolan-2-yl)methyl]-8-[3-(*tert*-butyl)non-1-en-1-yl]-1,3-dimethyl-3,7-dihydro-1*H*-purine-2,6-dione (**154mc**)



The general procedure **E** was followed using caffeine derivative **16m** (133 mg, 0.50 mmol) and allene **152c** (144 mg, 0.80 mmol). Purification by column chromatography on silica gel (*n*hexane/EtOAc: 2/1) yielded **154mc** (193 mg, 86%) as a white solid.

M.p. = 112–114 °C. **¹H NMR** (400 MHz, CDCl₃): δ = 6.82 (dd, *J* = 15.3, 10.4 Hz, 1H), 6.30 (d, *J* = 15.3 Hz, 1H), 5.22 (t, *J* = 3.6 Hz, 1H), 4.58 (d, *J* = 3.6 Hz, 2H), 3.83 (s, 4H), 3.59 (s, 3H), 3.39 (s, 3H), 1.88 (td, *J* = 10.6, 2.3 Hz, 1H), 1.64–1.54 (m, 1H), 1.33–1.19 (m, 8H), 1.16–1.05 (m, 1H), 0.93 (s, 9H), 0.86 (t, *J* = 6.9 Hz, 3H). **¹³C NMR** (101 MHz, CDCl₃): δ = 155.3 (C_q), 151.9 (C_q), 150.6 (C_q), 148.6 (C_q), 144.7 (CH), 116.5 (CH), 107.4 (C_q), 101.8 (CH), 65.4 (CH₂), 55.1 (CH), 46.5 (CH₂), 33.7 (CH₂), 32.0 (CH₂), 29.9 (CH₃), 29.5 (CH₂), 29.0 (C_q), 28.6 (CH₂), 28.1 (CH₃), 28.0 (CH₃), 22.8 (CH₃), 14.2 (CH₃). **IR** (ATR): 2950, 1702, 1654, 1543, 1469, 1413, 1223, 977, 745, 503 cm⁻¹. **MS** (ESI) *m/z* (relative intensity): 915 (53) [2M+Na]⁺, 827 (13), 447 (100) [M+H]⁺. **HR-MS** (ESI) *m/z* calcd for C₂₄H₃₉N₄O₄ [M+H]⁺ 447.2966, found 447.2957.

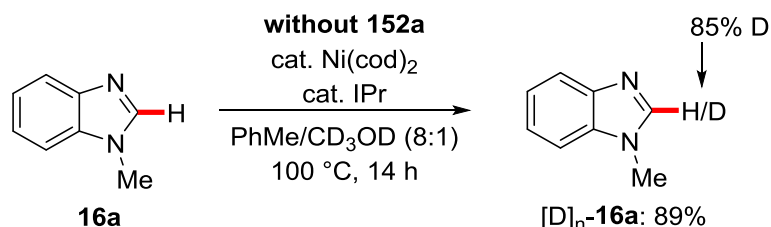
(E)-8-[3-(tert-Butyl)non-1-en-1-yl]-7-[2-(methoxymethoxy)propyl]-1,3-dimethyl-3,7-dihydro-1H-purine-2,6-dione (154nc)

The general procedure **E** was followed using caffeine derivative **16n** (141 mg, 0.50 mmol) and allene **152c** (144 mg, 0.80 mmol). Purification by column chromatography on silica gel (*n*hexane/EtOAc: 2/1) yielded **154nc** (202 mg, 87%) as a colorless oil.

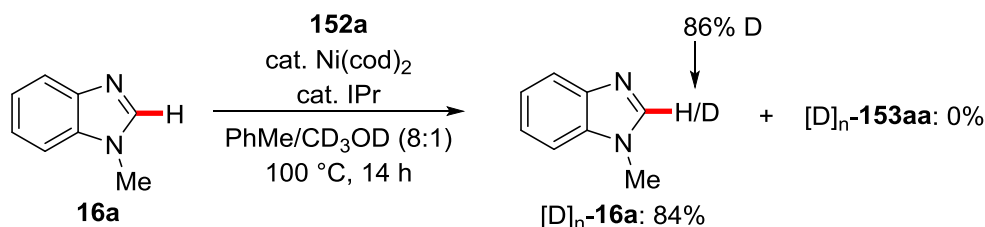
¹H NMR (300 MHz, CDCl₃): δ = 6.79 (dd, *J* = 15.4, 10.6 Hz, 1H), 6.31 (ddd, *J* = 15.4, 1.3, 0.6 Hz, 1H), 4.53 (dd, *J* = 6.9, 1.8 Hz, 1H), 4.43 (dt, *J* = 13.7, 3.3 Hz, 1H), 4.31 (dd, *J* = 6.9, 1.0 Hz, 1H), 4.18–4.10 (m, 1H), 4.07–4.01 (m, 1H), 3.56 (s, 3H), 3.37 (s, 3H), 3.05 (s, 3H), 1.86 (td, *J* = 10.6, 2.5 Hz, 1H), 1.30–1.21 (m, 11H), 1.12–1.03 (m, 1H), 0.90 (s, 9H), 0.83 (t, *J* = 6.9 Hz, 3H). **¹³C NMR** (126 MHz, CDCl₃): δ = 154.9 (C_q), 151.7 (C_q), 150.4 (C_q), 148.6 (C_q), 144.4 (CH), 144.4 (CH), 116.4 (CH), 106.6 (C_q), 95.0 (C_q), 72.8 (CH), 55.2 (CH₃), 55.0 (CH₃), 50.2 (CH₂), 33.6 (CH₂), 32.0 (CH₂), 29.9 (CH₃), 28.9 (CH₂), 28.6 (CH₂), 28.0 (CH₂), 27.9 (CH₃), 22.7 (CH₂), 18.0 (CH₃), 14.1 (CH₃). **IR** (ATR): 2932, 1698, 1654, 1542, 1469, 1411, 1223, 1031, 917, 729 cm⁻¹. **MS** (ESI) *m/z* (relative intensity): 462 (52) [M]⁺, 417 (100), 373 (21), 194 (37), 45 (57). **HR-MS** (ESI) *m/z* calcd for C₂₅H₄₃N₄O₄ [M+H]⁺ 463.3284, found 463.3277.

5.4.3 Mechanistic Studies

H/D Exchange experiments

In absence of allene **152**

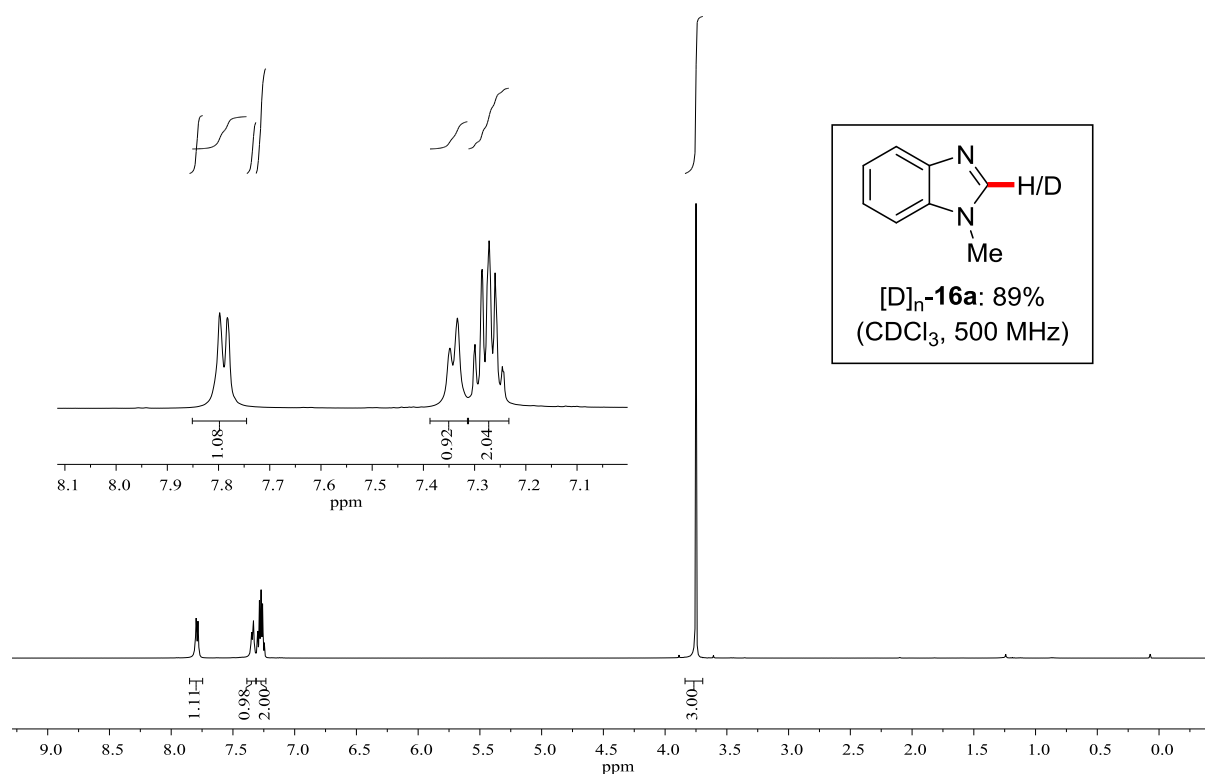
To an oven-dried Schlenk tube were added 1-methyl-1*H*-benzo[*d*]imidazole **16a** (0.50 mmol, 1.0 equiv), Ni(cod)₂ (13.8 mg, 50.0 μmol, 10 mol %), IPr (19.4 mg, 50.0 μmol, 10 mol %), toluene (1.5 mL) and CD₃OD (0.2 mL) under a nitrogen atmosphere. The mixture was stirred at 100 °C for 14 h. At ambient temperature, the solvent was removed under reduced pressure and the remaining residue was purified by column chromatography on silica gel (EtOAc) to afford [D]_n-**16a** (58.9 mg, 89%). The deuterium incorporation was estimated by ¹H-NMR spectroscopy.

In presence of allene **152a**

To an oven-dried Schlenk tube were added 1-methyl-1*H*-benzo[*d*]imidazole **16a** (0.50 mmol, 1.0 equiv), allene **152a** (0.80 mmol, 1.6 equiv), Ni(cod)₂ (13.8 mg, 50.0 μmol, 10 mol %), IPr (19.4 mg, 50.0 μmol, 10 mol %), toluene (1.5 mL) and CD₃OD (0.2 mL) under a nitrogen atmosphere.

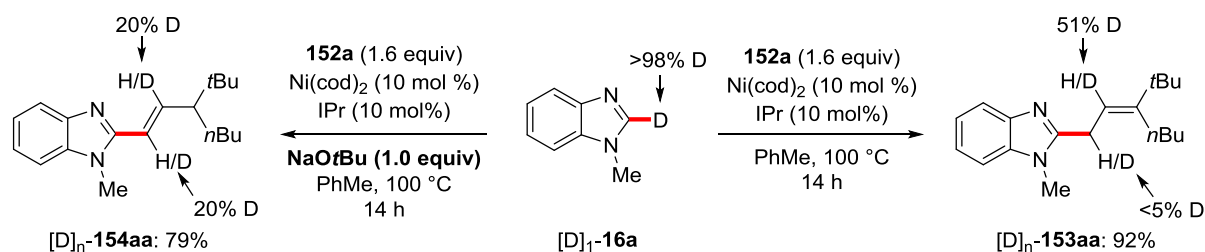
5 Experimental Part

The mixture was stirred at 100 °C for 14 h. At ambient temperature, the solvent was removed under reduced pressure and the remaining residue was purified by column chromatography on silica gel (100 % EtOAc) to afford $[D]_n$ -**16a** (55.5 mg, 84%). The deuterium incorporation was estimated by $^1\text{H-NMR}$ spectroscopy.



Reaction using isotopically-labelled substrates

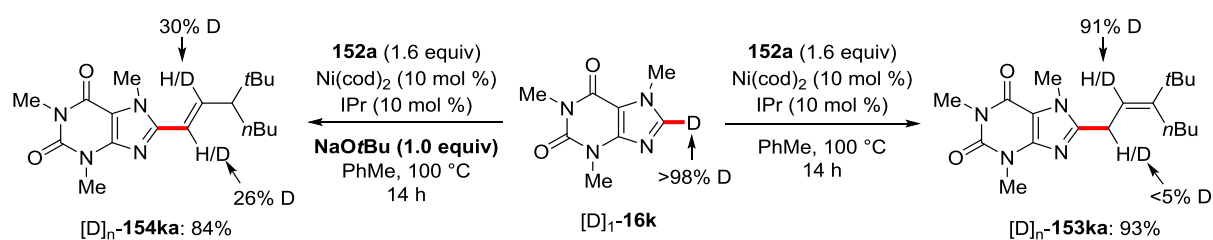
Reaction with of isotopically-labelled $[D]_1$ -**16a** with allene **152a**



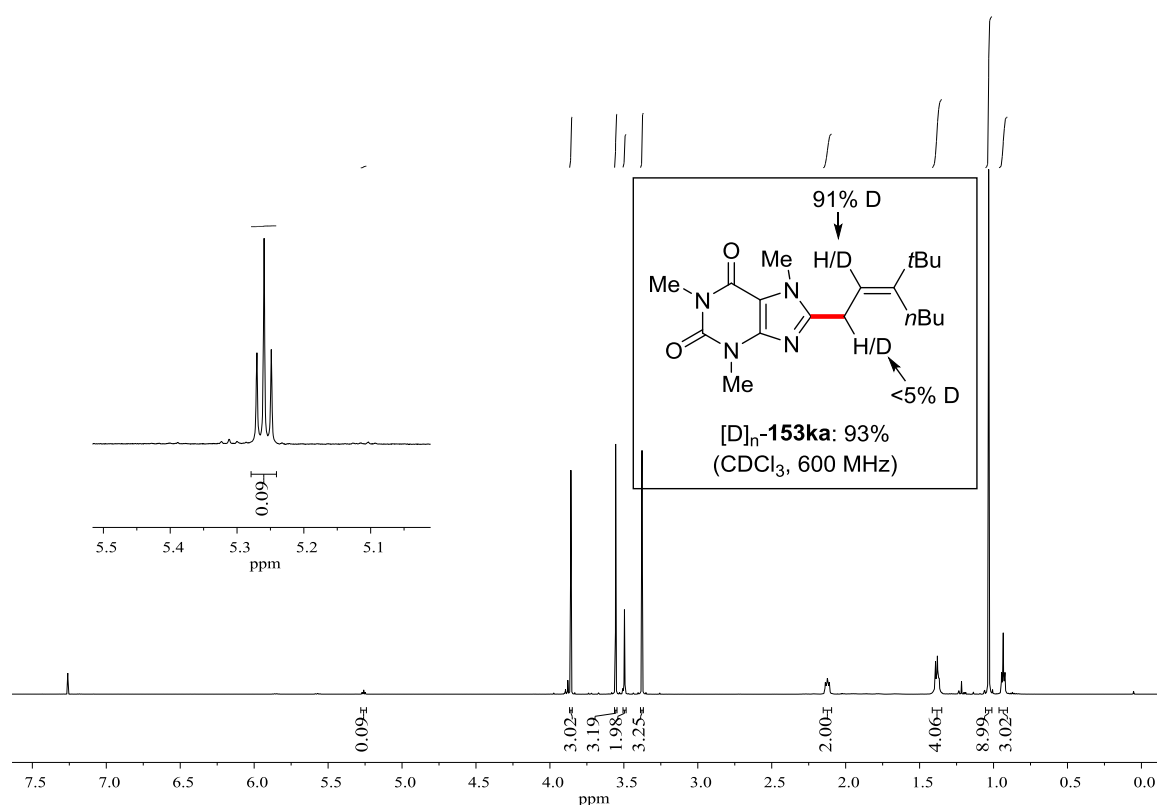
A solution of $[D]_1$ -**16a** (66.6 mg, 0.50 mmol, 1.0 equiv), allene **152a** (122 mg, 0.80 mmol, 1.6 equiv), $\text{Ni}(\text{cod})_2$ (13.8 mg, 50.0 μmol , 10.0 mol %), IPr (19.4 mg, 50.0 μmol , 10.0 mol %) with or without NaOtBu (48.1 mg, 0.50 mmol, 1.0 equiv) in toluene (1.5 mL) was stirred at 100 °C for 14 h.

5 Experimental Part

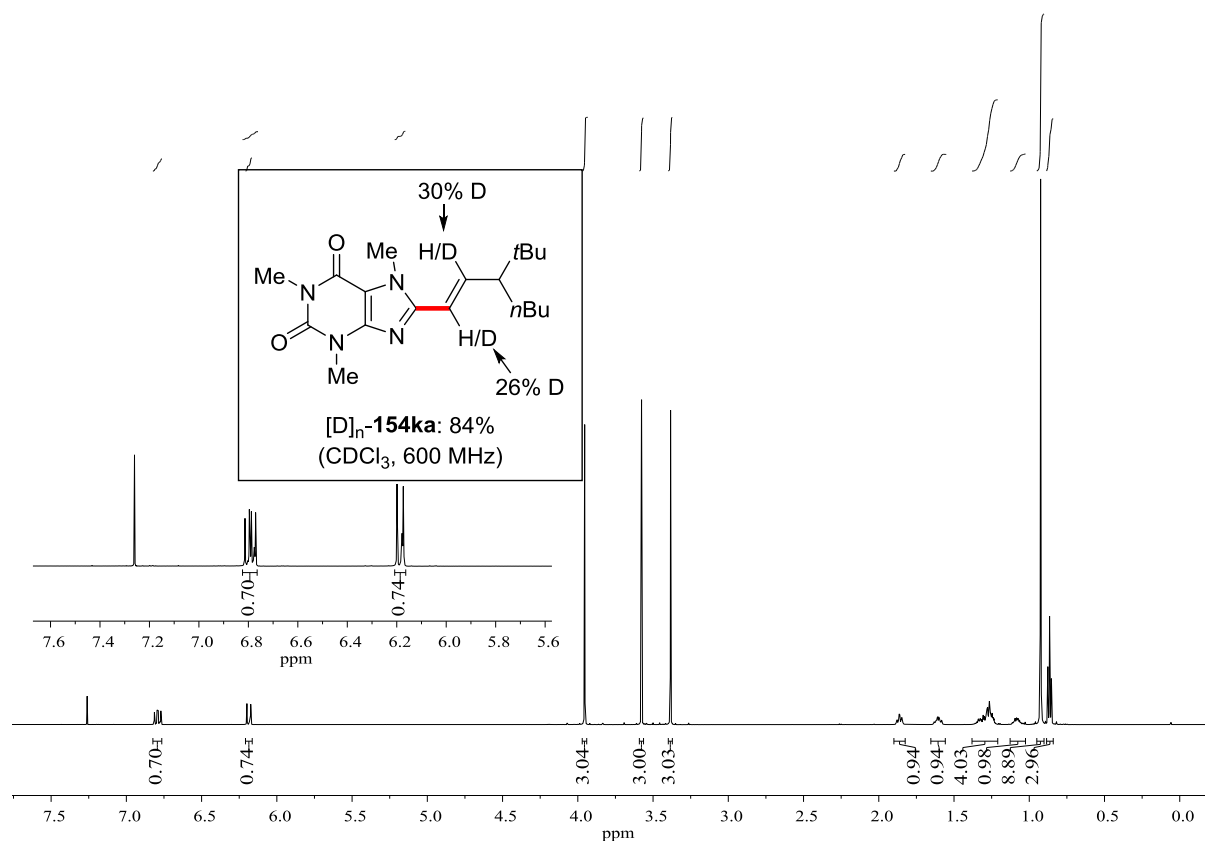
At ambient temperature, the solvent was removed under reduced pressure and the remaining residue was purified by column chromatography on silica gel (*n*hexane/EtOAc: 8/1 to 100% EtOAc) to afford the desired products [D]_n-**154aa** (112 mg, 79%) or [D]_n-**153aa** (131 mg, 92%), respectively. The deuterium incorporation was estimated by ¹H-NMR spectroscopy.



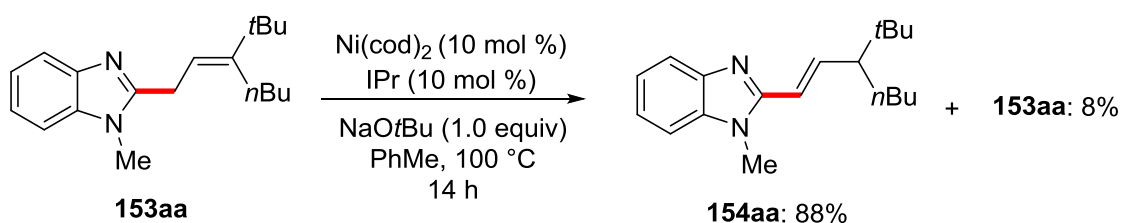
A solution of [D]₁-**16k** (97.6 mg, 0.50 mmol, 1.0 equiv), allene **152a** (122 mg, 0.80 mmol, 1.6 equiv), Ni(cod)₂ (13.8 mg, 50.0 μmol, 10.0 mol %), IPr (19.4 mg, 50.0 μmol, 10.0 mol %) with or without NaOtBu (48.1 mg, 0.50 mmol, 1.0 equiv) in toluene (1.5 mL) was stirred at 100 °C for 14 h. At ambient temperature, the solvent was removed under reduced pressure and the remaining residue was purified by column chromatography on silica gel (*n*hexane/EtOAc: 5/1) to afford [D]_n-**153ka** (162 mg, 93%) or [D]_n-**154ka** (146 mg, 84%), respectively. The deuterium incorporation was estimated by ¹H-NMR spectroscopy.



5 Experimental Part

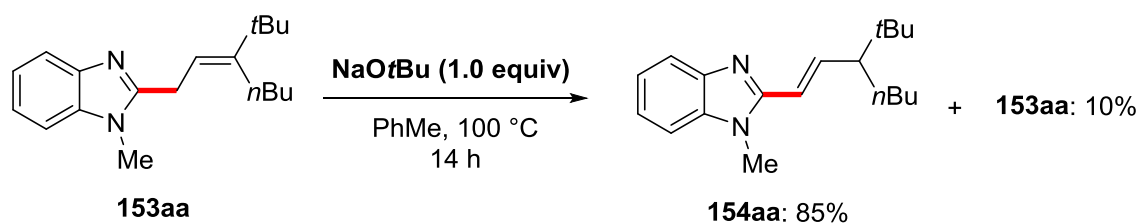


Isomerization Experiments

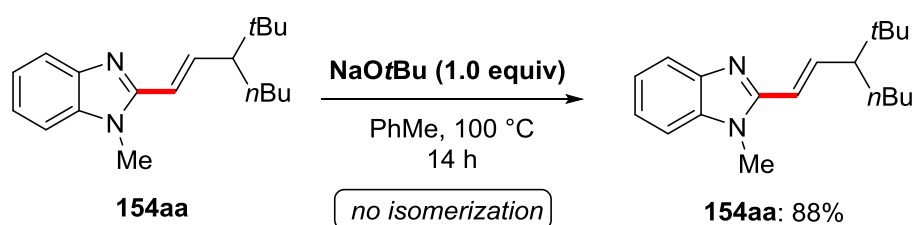


A solution of **153aa** (142 mg, 0.50 mmol, 1.0 equiv), Ni(cod)₂ (13.8 mg, 50.0 μmol, 10.0 mol %), IPr (19.4 mg, 50.0 μmol, 10.0 mol %) and NaOtBu (48.1 mg, 0.50 mmol, 1.0 equiv) in toluene (1.5 mL) was stirred at 100 °C for 14 h. At ambient temperature, the solvent was removed under reduced pressure and the remaining residue was purified by column chromatography on silica gel (*n*hexane/EtOAc: 5/1) to afford the isomerized product **154aa** (124.7 mg, 88%) and reisolated **153aa** (11.4 mg, 8%).

5 Experimental Part



A solution of **153aa** (142 mg, 0.50 mmol, 1.0 equiv) and NaOtBu (48.1 mg, 0.50 mmol, 1.0 equiv) in toluene (1.5 mL) was stirred at 100 °C for 14 h. At ambient temperature, the solvent was removed under reduced pressure and the remaining residue was purified by column chromatography on silica gel (*n*-hexane/EtOAc: 5/1) to afford the isomerized product **154aa** (121 mg, 85%) and reisolated **153aa** (14.1 mg, 10%).

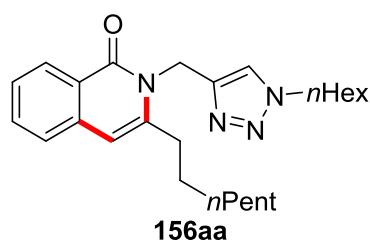


A solution of **154aa** (142 mg, 0.50 mmol, 1.0 equiv) and NaOtBu (48.1 mg, 0.50 mmol, 1.0 equiv) in toluene (1.5 mL) was stirred at 100 °C for 14 h. At ambient temperature, the solvent was removed under reduced pressure and the remaining residue was purified by column chromatography on silica gel (*n*-hexane/EtOAc: 5/1) to reisolate the non-isomerized starting material **154aa** (125 mg, 88%).

5.5 Iron-Catalyzed C–H/N–H Annulation with Allenyl Acetates

5.5.1 Experimental Procedures and Analytical Data – Allenyl Acetates

3-*n*-Heptyl-2-[(1-*n*-hexyl-1*H*-1,2,3-triazol-4-yl)methyl]isoquinolin-1(2*H*)-one (156aa)

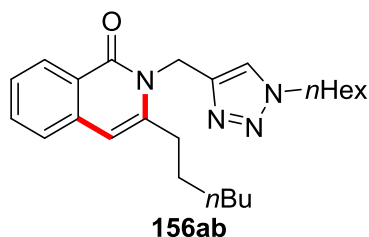


5 Experimental Part

The general procedure **F** was followed using **118a** (85.9 mg, 0.30 mmol) and allene **155a** (164 mg, 0.90 mmol). Purification by column chromatography (*n*hexane/EtOAc: 4/1) yielded **156aa** (112 mg, 91%) as a white solid.

M.p. = 76–78 °C. **¹H NMR** (600 MHz, CDCl₃): δ = 8.35 (d, *J* = 8.0 Hz, 1H), 7.70 (s, 1H), 7.60–7.56 (m, 1H), 7.43–7.38 (m, 2H), 6.34 (s, 1H), 5.38 (s, 2H), 4.24 (t, *J* = 7.3 Hz, 2H), 2.98 (t, *J* = 7.7 Hz, 2H), 1.86–1.80 (m, 2H), 1.71 (dt, *J* = 15.4, 7.7 Hz, 2H), 1.48 (dt, *J* = 15.3, 7.3 Hz, 2H), 1.40–1.34 (m, 2H), 1.32–1.23 (m, 10H), 0.89 (t, *J* = 6.9 Hz, 3H), 0.83 (t, *J* = 7.0 Hz, 3H). **¹³C NMR** (126 MHz, CDCl₃): δ = 163.3 (C_q), 144.1 (C_q), 143.6 (C_q), 136.9 (C_q), 132.3 (CH), 127.7 (CH), 125.9 (CH), 125.4 (CH), 124.3 (C_q), 123.8 (CH), 105.2 (CH), 50.5 (CH₂), 39.2 (CH₂), 33.2 (CH₂), 31.9 (CH₂), 31.3 (CH₂), 30.3 (CH₂), 29.4 (CH₂), 29.3 (CH₂), 28.9 (CH₂), 26.3 (CH₂), 22.8 (CH₂), 22.6 (CH₂), 14.3 (CH₃), 14.1 (CH₃). **IR** (ATR): 2926, 2853, 1643, 1618, 1593, 1413, 1052, 801, 756, 690 cm⁻¹. **MS** (EI) *m/z* (relative intensity): 408 (70) [M]⁺, 337 (53), 324 (47), 295 (63), 242 (48), 172 (39), 159 (91), 43 (100). **HR-MS** (EI) *m/z* calcd for C₂₅H₃₆N₄O [M]⁺ 408.2889, found 408.2879.

3-*n*-Hexyl-2-[(1-*n*-hexyl-1*H*-1,2,3-triazol-4-yl)methyl]isoquinolin-1(2*H*)-one (156ab)

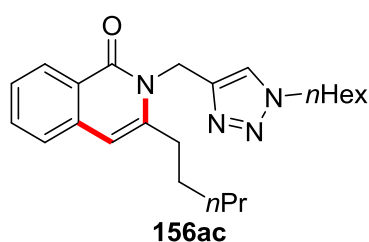


The general procedure **F** was followed using **118a** (85.9 mg, 0.30 mmol) and allene **155b** (151 mg, 0.90 mmol). Purification by column chromatography (*n*hexane/EtOAc: 4/1) yielded **156ab** (112 mg, 93%) as a white solid.

M.p. = 79–81 °C. **¹H NMR** (600 MHz, CDCl₃): δ = 8.34 (d, *J* = 8.1 Hz, 1H), 7.70 (s, 1H), 7.59–7.56 (m, 1H), 7.40–7.38 (m, 2H), 6.34 (s, 1H), 5.38 (s, 2H), 4.24 (t, *J* = 7.3 Hz, 2H), 2.98 (t, *J* = 7.7 Hz, 2H), 1.87–1.81 (m, 2H), 1.71 (dt, *J* = 15.5, 7.7 Hz, 2H), 1.52–1.45 (m, 2H), 1.37–1.31 (m, 4H), 1.29–1.22 (m, 6H), 0.90 (t, *J* = 7.1 Hz, 3H), 0.83 (t, *J* = 7.0 Hz, 3H). **¹³C NMR** (126 MHz, CDCl₃): δ = 163.3 (C_q), 144.1 (C_q), 143.6 (C_q), 136.9 (C_q), 132.3 (CH), 127.7 (CH), 125.9 (CH), 125.4 (CH), 124.3 (C_q),

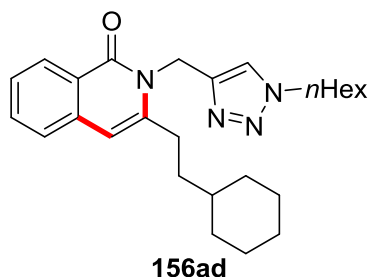
123.8 (CH), 105.2 (CH), 50.5 (CH₂), 39.2 (CH₂), 33.2 (CH₂), 31.9 (CH₂), 31.3 (CH₂), 30.3 (CH₂), 29.1 (CH₂), 28.9 (CH₂), 26.3 (CH₂), 22.8 (CH₂), 22.6 (CH₂), 14.3 (CH₃), 14.1 (CH₃). **IR** (ATR): 3149, 2953, 2929, 2858, 1646, 1619, 1595, 1047, 754, 673 cm⁻¹. **MS** (EI) *m/z* (relative intensity): 394 (82) [M]⁺, 337 (60), 324 (47), 295 (31), 281 (56), 228 (53), 159 (100). **HR-MS** (EI) *m/z* calcd for C₂₄H₃₄N₄O [M]⁺ 394.2733, found 394.2723.

2-[(1-*n*-Hexyl-1*H*-1,2,3-triazol-4-yl)methyl]-3-*n*-pentylisoquinolin-1(2*H*)-one (156ac)



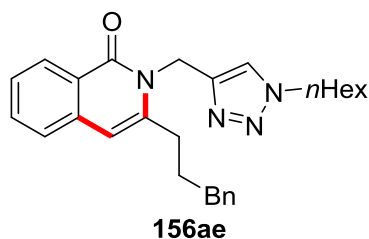
The general procedure **F** was followed using **118a** (85.9 mg, 0.30 mmol) and allene **155c** (139 mg, 0.90 mmol). Purification by column chromatography (*n*hexane/EtOAc: 3/1) yielded **156ac** (98.5 mg, 86%) as a white solid.

M.p. = 75–77 °C. **¹H NMR** (600 MHz, CDCl₃): δ = 8.34 (d, *J* = 8.0 Hz, 1H), 7.70 (s, 1H), 7.58 (ddd, *J* = 8.1, 7.2, 1.3 Hz, 1H), 7.43–7.38 (m, 2H), 6.34 (s, 1H), 5.38 (s, 2H), 4.24 (t, *J* = 7.3 Hz, 2H), 2.98 (t, *J* = 7.7 Hz, 2H), 1.87–1.81 (m, 2H), 1.72 (dt, *J* = 15.4, 7.6 Hz, 2H), 1.50–1.44 (m, 2H), 1.43–1.36 (m, 2H), 1.29–1.23 (m, 6H), 0.92 (t, *J* = 7.2 Hz, 3H), 0.85–0.82 (m, 3H). **¹³C NMR** (126 MHz, CDCl₃): δ = 163.3 (C_q), 144.1 (C_q), 143.6 (C_q), 136.9 (C_q), 132.3 (CH), 127.7 (CH), 125.9 (CH), 125.4 (CH), 124.3 (C_q), 123.8 (CH), 105.2 (CH), 50.5 (CH₂), 39.2 (CH₂), 33.1 (CH₂), 31.6 (CH₂), 31.3 (CH₂), 30.3 (CH₂), 28.6 (CH₂), 26.3 (CH₂), 22.7 (CH₂), 22.6 (CH₂), 14.2 (CH₃), 14.1 (CH₃). **IR** (ATR): 2950, 2932, 2857, 1648, 1619, 1593, 1438, 1169, 1042, 734 cm⁻¹. **MS** (EI) *m/z* (relative intensity): 380 (100) [M]⁺, 337 (61), 324 (43), 267 (59), 214 (50), 159 (98), 138 (33). **HR-MS** (EI) *m/z* calcd for C₂₃H₃₂N₄O [M]⁺ 380.2576, found 380.2566.

3-(2-Cyclohexylethyl)-2-[(1-*n*-hexyl-1*H*-1,2,3-triazol-4-yl)methyl]isoquinolin-1(2*H*)-one (156ad)

The general procedure **F** was followed using **118a** (85.9 mg, 0.30 mmol) and allene **155d** (175 mg, 0.90 mmol). Purification by column chromatography (*n*hexane/EtOAc: 3/2) yielded **156ad** (110 mg, 87%) as a white solid.

M.p. = 106–107 °C. **¹H NMR** (600 MHz, CDCl₃): δ = 8.34 (d, *J* = 8.0 Hz, 1H), 7.70 (s, 1H), 7.59–7.56 (m, 1H), 7.42–7.38 (m, 2H), 6.34 (s, 1H), 5.37 (s, 2H), 4.24 (t, *J* = 7.3 Hz, 2H), 3.02–2.97 (m, 2H), 1.85–1.81 (m, 4H), 1.76–1.70 (m, 2H), 1.69–1.64 (m, 1H), 1.61–1.57 (m, 2H), 1.47–1.39 (m, 1H), 1.29–1.23 (m, 8H), 1.21–1.13 (m, 1H), 1.00 (qd, *J* = 12.4, 3.2 Hz, 2H), 0.84 (t, *J* = 7.0 Hz, 3H). **¹³C NMR** (126 MHz, CDCl₃): δ = 163.3 (C_q), 144.1 (C_q), 144.1 (C_q), 137.0 (C_q), 132.3 (CH), 127.7 (CH), 125.9 (CH), 125.4 (CH), 124.2 (C_q), 123.8 (CH), 105.0 (CH), 50.5 (CH₂), 39.2 (CH₂), 37.7 (CH), 36.8 (CH₂), 33.5 (CH₂), 31.3 (CH₂), 30.7 (CH₂), 30.3 (CH₂), 26.8 (CH₂), 26.5 (CH₂), 26.3 (CH₂), 22.6 (CH₂), 14.1 (CH₃). **IR** (ATR): 2923, 2851, 1647, 1617, 1593, 1412, 1047, 831, 778, 755 cm⁻¹. **MS** (EI) *m/z* (relative intensity): 420 (60) [M]⁺, 337 (83), 324 (100), 254 (35), 172 (32), 159 (70), 138 (28). **HR-MS** (EI) *m/z* calcd for C₂₆H₃₆N₄O [M]⁺ 420.2889, found 420.2890.

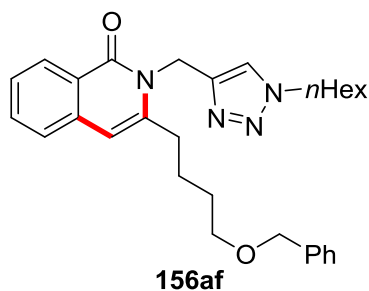
2-[(1-*n*-Hexyl-1*H*-1,2,3-triazol-4-yl)methyl]-3-(3-phenylpropyl)isoquinolin-1(2*H*)-one (156ae)

5 Experimental Part

The general procedure **F** was followed using **118a** (85.9 mg, 0.30 mmol) and allene **155e** (182 mg, 0.90 mmol). Purification by column chromatography (*n*hexane/EtOAc: 3/2) yielded **156ae** (109 mg, 85%) as a white solid.

M.p. = 100–102 °C. **¹H NMR** (300 MHz, CDCl₃): δ = 8.35 (d, *J* = 8.1 Hz, 1H), 7.70 (s, 1H), 7.60–7.56 (m, 1H), 7.42–7.39 (m, 2H), 7.32–7.29 (m, 2H), 7.29–7.19 (m, 3H), 6.34 (s, 1H), 5.37 (s, 2H), 4.27 (t, *J* = 7.3 Hz, 2H), 3.08 (t, *J* = 7.5 Hz, 2H), 2.84 (t, *J* = 7.6 Hz, 2H), 2.08–2.03 (m, 2H), 1.87–1.81 (m, 2H), 1.30–1.24 (m, 6H), 0.84 (t, *J* = 7.0 Hz, 3H). **¹³C NMR** (126 MHz, CDCl₃): δ = 163.2 (C_q), 144.0 (C_q), 143.0 (C_q), 141.6 (C_q), 136.8 (C_q), 132.4 (CH), 128.5 (CH), 128.5 (CH), 127.7 (CH), 126.1 (CH), 126.0 (CH), 125.4 (CH), 124.3 (C_q), 123.8 (CH), 105.2 (CH), 50.5 (CH₂), 39.2 (CH₂), 35.6 (CH₂), 32.7 (CH₂), 31.3 (CH₂), 30.5 (CH₂), 30.3 (CH₂), 26.3 (CH₂), 22.6 (CH₂), 14.1 (CH₃). **IR** (ATR): 2925, 2859, 1645, 1620, 1594, 1410, 1047, 752, 698, 675 cm⁻¹. **MS** (EI) *m/z* (relative intensity): 428 (14) [M]⁺, 337 (100), 324 (18), 172 (19), 159 (67), 138 (30), 91 (38). **HR-MS** (EI) *m/z* calcd for C₂₇H₃₂N₄O [M]⁺ 428.2576, found 428.2564.

3-[4-(Benzyloxy)-*n*-butyl]-2-[(1-*n*-hexyl-1*H*-1,2,3-triazol-4-yl)methyl]isoquinolin-1(2*H*)-one (**156af**)



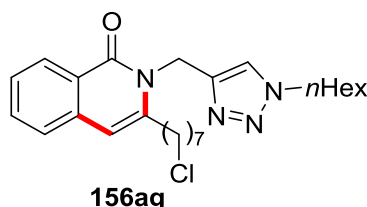
The general procedure **F** was followed using **118a** (85.9 mg, 0.30 mmol) and allene **155f** (222 mg, 0.90 mmol). Purification by column chromatography (*n*hexane/EtOAc: 3/1) yielded **156af** (133 mg, 94%) as a white solid.

M.p. = 68–69 °C. **¹H NMR** (600 MHz, CDCl₃): δ = 8.35 (d, *J* = 8.4 Hz, 1H), 7.71 (s, 1H), 7.60–7.56 (m, 1H), 7.42–7.39 (m, 2H), 7.35–7.31 (m, 4H), 7.29–7.25 (m, 1H), 6.35 (s, 1H), 5.37 (s, 2H), 4.52 (s, 2H), 4.26–4.22 (m, 2H), 3.58 (t, *J* = 5.8 Hz, 2H), 3.02 (t, *J* = 7.2 Hz, 2H), 1.87–1.80 (m, 6H), 1.30–1.24 (m, 6H), 0.84 (t, *J* = 6.9 Hz, 3H). **¹³C NMR** (126 MHz, CDCl₃): δ = 163.3 (C_q), 144.0 (C_q), 143.2 (C_q), 138.6 (C_q),

5 Experimental Part

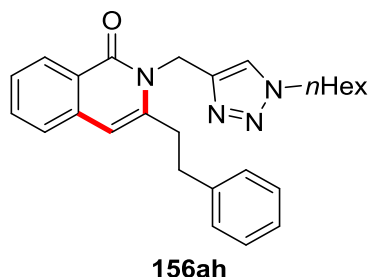
136.9 (C_q), 132.3 (CH), 128.4 (CH), 127.7 (CH), 127.7 (CH), 127.6 (CH), 126.0 (CH), 125.4 (CH), 124.3 (C_q), 123.8 (CH), 105.3 (CH), 73.1 (CH₂), 69.9 (CH₂), 50.5 (CH₂), 39.1 (CH₂), 32.8 (CH₂), 31.3 (CH₂), 30.3 (CH₂), 29.4 (CH₂), 26.3 (CH₂), 25.5 (CH₂), 22.6 (CH₂), 14.1 (CH₃). **IR** (ATR): 2951, 2927, 2855, 1644, 1619, 1594, 1411, 1118, 727, 692 cm⁻¹. **MS** (EI) *m/z* (relative intensity): 472 (28) [M]⁺, 381 (28), 367 (19), 200 (67), 167 (40), 91 (100). **HR-MS** (EI) *m/z* calcd for C₂₉H₃₆N₄O₂ [M]⁺ 472.2838, found 472.2844.

3-(7-Chloro-*n*-heptyl)-2-[(1-*n*-hexyl-1*H*-1,2,3-triazol-4-yl)methyl]isoquinolin-1(2*H*)-one (156ag)



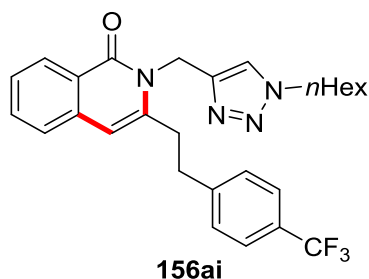
The general procedure **F** was followed using **118a** (85.9 mg, 0.30 mmol) and allene **155g** (195 mg, 0.90 mmol). Purification by column chromatography (*n*hexane/EtOAc: 3/2) yielded **156ag** (121 mg, 91%) as a white solid.

M.p. = 62–63 °C. **¹H NMR** (300 MHz, CDCl₃): δ = 8.35 (dd, *J* = 8.0, 1.2 Hz, 1H), 7.72 (s, 1H), 7.59 (ddd, *J* = 8.1, 6.9, 1.4 Hz, 1H), 7.47–7.34 (m, 2H), 6.34 (s, 1H), 5.38 (s, 2H), 4.25 (t, *J* = 7.3 Hz, 2H), 3.54 (t, *J* = 6.7 Hz, 2H), 3.05–2.94 (m, 2H), 1.92–1.64 (m, 6H), 1.58–1.36 (m, 6H), 1.32–1.21 (m, 6H), 0.90–0.78 (m, 3H). **¹³C NMR** (126 MHz, CDCl₃): δ = 163.3 (C_q), 144.0 (C_q), 143.4 (C_q), 136.9 (C_q), 132.4 (CH), 127.7 (CH), 126.0 (CH), 125.4 (CH), 124.3 (C_q), 123.8 (CH), 105.2 (CH), 50.5 (CH₂), 45.2 (CH₂), 39.2 (CH₂), 33.1 (CH₂), 32.7 (CH₂), 31.3 (CH₂), 30.3 (CH₂), 29.3 (CH₂), 28.9 (CH₂), 28.7 (CH₂), 27.0 (CH₂), 26.3 (CH₂), 22.6 (CH₂), 14.1 (CH₃). **IR** (ATR): 2929, 2857, 1650, 1621, 1596, 1410, 1167, 1046, 755, 728 cm⁻¹. **MS** (EI) *m/z* (relative intensity): 442 (66) [³⁵Cl, M]⁺, 407 (52), 337 (72), 324 (58), 276 (31), 172 (35), 159 (100), 138 (40). **HR-MS** (EI) *m/z* calcd for C₂₅H₃₅³⁵ClN₄O [M]⁺ 442.2499, found 442.2514.

2-[(1-*n*-Hexyl-1*H*-1,2,3-triazol-4-yl)methyl]-3-phenethylisoquinolin-1(2*H*)-one (156ah)

The general procedure **F** was followed using **118a** (85.9 mg, 0.30 mmol) and allene **155h** (169 mg, 0.9 mmol). Purification by column chromatography (*n*hexane/EtOAc: 3/1) yielded **156ah** (66.1 mg, 53%) as a white solid.

M.p. = 67-69 °C. **¹H NMR** (300 MHz, CDCl₃): δ = 8.36 (d, *J* = 7.4 Hz, 1H), 7.72 (s, 1H), 7.62–7.56 (m, 1H), 7.45–7.38 (m, 2H), 7.33–7.21 (m, 5H), 6.35 (s, 1H), 5.39 (s, 2H), 4.30–4.21 (m, 2H), 3.39–3.30 (m, 2H), 3.10–3.02 (m, 2H), 1.90–1.79 (m, 2H), 1.32–1.23 (m, 6H), 0.89–0.80 (m, 3H). **¹³C NMR** (126 MHz, CDCl₃): δ = 163.2 (C_q), 143.9 (C_q), 142.6 (C_q), 140.2 (C_q), 136.8 (C_q), 132.4 (CH), 128.6 (CH), 128.5 (CH), 127.7 (CH), 126.5 (CH), 126.1 (CH), 125.5 (CH), 124.4 (C_q), 123.8 (CH), 105.7 (CH), 50.5 (CH₂), 39.2 (CH₂), 35.2 (CH₂), 34.7 (CH₂), 31.3 (CH₂), 30.3 (CH₂), 26.3 (CH₂), 22.6 (CH₂), 14.1 (CH₃). **IR** (ATR): 2953, 2925, 1646, 1621, 1592, 1338, 1169, 830, 764, 697 cm⁻¹. **MS** (EI) *m/z* (relative intensity): 414 (100) [M⁺], 323 (17), 301 (46), 248 (60), 158 (45), 91 (67). **HR-MS** (EI) *m/z* calcd for C₂₆H₃₀N₄O [M]⁺ 414.2420, found 414.2418.

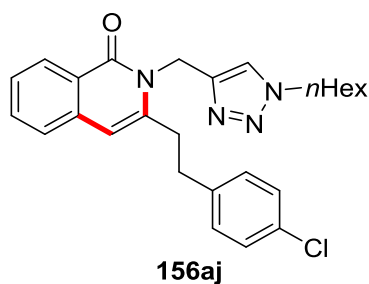
2-[(1-*n*-Hexyl-1*H*-1,2,3-triazol-4-yl)methyl]-3-[4-(trifluoromethyl)phenethyl]-isoquinolin-1(2*H*)-one (156ai)

5 Experimental Part

The general procedure **F** was followed using **118a** (85.9 mg, 0.30 mmol) and allene **155i** (231 mg, 0.90 mmol). Purification by column chromatography (*n*hexane/EtOAc: 3/1) yielded **156ai** (81.3 mg, 56%) as a pale yellow solid.

M.p. = 108–109 °C. **¹H NMR** (300 MHz, CDCl₃): δ = 8.40–8.33 (m, 1H), 7.76 (s, 1H), 7.62–7.54 (m, 3H), 7.46–7.37 (m, 4H), 6.32 (s, 1H), 5.39 (s, 2H), 4.26 (t, *J* = 7.3 Hz, 2H), 3.38 (t, *J* = 7.4 Hz, 2H), 3.12 (t, *J* = 7.3 Hz, 2H), 1.91–1.79 (m, 2H), 1.34–1.21 (m, 6H), 0.90–0.78 (m, 3H). **¹³C NMR** (126 MHz, CDCl₃): δ = 163.2 (C_q), 144.3 (C_q), 143.8 (C_q), 141.9 (C_q), 136.6 (C_q), 132.5 (CH), 128.9 (CH), 128.9 (q, ²*J*_{C-F} = 32.3 Hz, C_q), 127.7 (CH), 126.3 (CH), 125.6 (q, ³*J*_{C-F} = 3.7 Hz, CH), 125.5 (CH), 124.4 (C_q), 124.3 (q, ¹*J*_{C-F} = 271.4 Hz, C_q), 124.0 (CH), 105.8 (CH), 50.6 (CH₂), 39.2 (CH₂), 34.8 (CH₂), 34.3 (CH₂), 31.3 (CH₂), 30.3 (CH₂), 26.3 (CH₂), 22.6 (CH₂), 14.1 (CH₃). **¹⁹F NMR** (282 MHz, CDCl₃): δ = -62.41 (s). **IR** (ATR): 2933, 2860, 1649, 1617, 1597, 1323, 1158, 1111, 1066, 753 cm⁻¹. **MS** (EI) *m/z* (relative intensity): 482 (100) [M]⁺, 369 (43), 323 (27), 317 (42), 295 (22), 158 (57), 138 (23). **HR-MS** (ESI) *m/z* calcd for C₂₇H₃₀F₃N₄O [M+H]⁺ 483.2366, found 483.2369.

3-(4-Chlorophenethyl)-2-[(1-*n*-hexyl-1*H*-1,2,3-triazol-4-yl)methyl]isoquinolin-1(2*H*)-one (**156aj**)



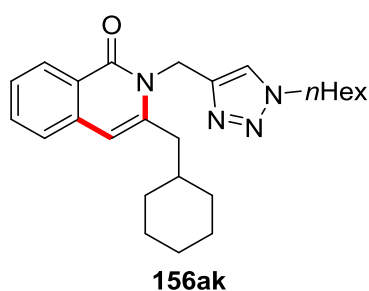
The general procedure **F** was followed using **118a** (85.9 mg, 0.30 mmol) and allene **155j** (200 mg, 0.90 mmol). Purification by column chromatography (*n*hexane/EtOAc: 3/2) yielded **156aj** (89.9 mg, 67%) as a pale yellow solid.

M.p. = 92–94 °C. **¹H NMR** (600 MHz, CDCl₃): δ = 8.36 (d, *J* = 8.0 Hz, 1H), 7.74 (s, 1H), 7.59 (ddd, *J* = 8.2, 7.2, 1.3 Hz, 1H), 7.42 (ddd, *J* = 8.2, 7.2, 1.1 Hz, 1H), 7.40 (d, *J* = 7.9 Hz, 1H), 7.28–7.25 (m, 2H), 7.22–7.19 (m, 2H), 6.31 (s, 1H), 5.38 (s, 2H), 4.26 (t, *J* = 7.3 Hz, 2H), 3.33 (t, *J* = 7.7 Hz, 2H), 3.03 (t, *J* = 7.5 Hz, 2H), 1.88–1.82 (m, 2H), 1.31–1.23 (m, 6H), 0.86–0.82 (m, 3H). **¹³C NMR** (126 MHz, CDCl₃): δ = 163.2 (C_q), 143.9 (C_q), 142.2 (C_q), 138.6 (C_q), 136.7 (C_q), 132.5 (CH), 132.2 (C_q),

5 Experimental Part

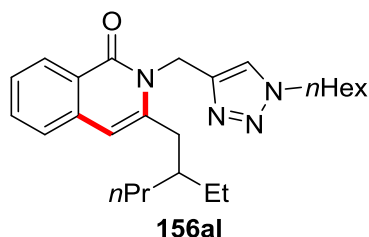
129.9 (CH), 128.8 (CH), 127.7 (CH), 126.2 (CH), 125.5 (CH), 124.4 (C_q), 123.9 (CH), 105.8 (CH), 50.5 (CH₂), 39.2 (CH₂), 34.5 (CH₂), 34.4 (CH₂), 31.3 (CH₂), 30.3 (CH₂), 26.3 (CH₂), 22.6 (CH₂), 14.1 (CH₃). **IR** (ATR): 2959, 2927, 2857, 1649, 1622, 1592, 1490, 1169, 1092, 764 cm⁻¹. **MS** (ESI) *m/z* (relative intensity): 919 (53) [³⁵Cl, 2M+Na]⁺, 471 (40) [³⁵Cl, M+Na]⁺, 449 (100) [³⁵Cl, M+H]⁺. **HR-MS** (ESI) *m/z* calcd for C₂₆H₃₀N₄O³⁵Cl [M+H]⁺ 449.2103, found 449.2100.

3-(Cyclohexylmethyl)-2-[(1-*n*-hexyl-1*H*-1,2,3-triazol-4-yl)methyl]isoquinolin-1(2*H*)-one (156ak)



The general procedure **F** was followed using **118a** (85.9 mg, 0.30 mmol) and allene **155k** (163 mg, 0.90 mmol). Purification by column chromatography (*n*hexane/EtOAc: 3/2) yielded **156ak** (49.2 mg, 40%) as a brownish oil.

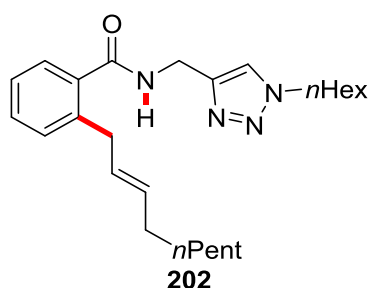
¹H NMR (300 MHz, CDCl₃): δ = 8.37–8.32 (m, 1H), 7.67 (s, 1H), 7.59 (ddd, *J* = 8.1, 6.9, 1.4 Hz, 1H), 7.44–7.36 (m, 2H), 6.29 (s, 1H), 5.37 (s, 2H), 4.24 (t, *J* = 7.3 Hz, 2H), 2.83 (d, *J* = 6.9 Hz, 2H), 1.92–1.78 (m, 4H), 1.79–1.57 (m, 4H), 1.35–1.16 (m, 9H), 1.14–0.96 (m, 2H), 0.89–0.78 (m, 3H). **¹³C NMR** (126 MHz, CDCl₃): δ = 163.4 (C_q), 144.1 (C_q), 141.7 (C_q), 136.7 (C_q), 132.3 (CH), 127.7 (CH), 125.9 (CH), 125.4 (CH), 124.3 (C_q), 123.7 (CH), 107.0 (CH), 50.5 (CH₂), 41.3 (CH₂), 39.6 (CH₂), 37.4 (CH), 33.4 (CH₂), 31.3 (CH₂), 30.3 (CH₂), 26.5 (CH₂), 26.4 (CH₂), 26.3 (CH₂), 22.5 (CH₂), 14.1 (CH₃). **IR** (ATR): 2922, 2851, 1646, 1622, 1592, 1419, 1340, 1168, 1043, 766 cm⁻¹. **MS** (ESI) *m/z* (relative intensity): 835 (35) [2M+Na]⁺, 813 (8) [2M+H]⁺, 429 (19) [M+Na]⁺, 407 (100) [M+H]⁺. **HR-MS** (ESI) *m/z* calcd for C₂₅H₃₅N₄O [M+H]⁺ 407.2805, found 407.2805.

3-(2-Ethylpentyl)-2-[(1-hexyl-1*H*-1,2,3-triazol-4-yl)methyl]isoquinolin-1(2*H*)-one (156al)

The general procedure **F** was followed using **118a** (85.9 mg, 0.30 mmol) and allene **155I** (164 mg, 0.90 mmol). Purification by column chromatography (*n*hexane/EtOAc: 3/2) yielded **156al** (30.2 mg, 25%) as a yellow oil.

¹H NMR (600 MHz, CDCl₃): δ = 8.35 (d, *J* = 8.2 Hz, 1H), 7.68 (s, 1H), 7.58 (ddd, *J* = 8.2, 7.1, 1.3 Hz, 1H), 7.43–7.38 (m, 2H), 6.30 (s, 1H), 5.38 (s, 2H), 4.26–4.20 (m, 2H), 2.89 (s, 2H), 1.86–1.80 (m, 2H), 1.76–1.69 (m, 1H), 1.48–1.35 (m, 6H), 1.29–1.23 (m, 6H), 0.93 (t, *J* = 7.5 Hz, 3H), 0.89 (t, *J* = 6.8 Hz, 3H), 0.83 (t, *J* = 7.0 Hz, 3H).

¹³C NMR (126 MHz, CDCl₃): δ = 163.4 (C_q), 144.1 (C_q), 142.3 (C_q), 136.8 (C_q), 132.3 (CH), 127.7 (CH), 125.9 (CH), 125.4 (CH), 124.3 (C_q), 123.7 (CH), 107.1 (CH), 50.5 (CH₂), 39.4 (CH₂), 38.4 (CH), 38.1 (CH₂), 35.3 (CH₂), 31.3 (CH₂), 30.3 (CH₂), 26.3 (CH₂), 25.8 (CH₂), 22.6 (CH₂), 19.9 (CH₂), 14.6 (CH₃), 14.1 (CH₃), 10.9 (CH₃).

(*E*)-*N*-[(1-*n*-Hexyl-1*H*-1,2,3-triazol-4-yl)methyl]-2-(*non*-2-en-1-yl)benzamide (202)

The general procedure **F** was followed using **118a** (85.9 mg, 0.30 mmol) and allene **201** (112 mg, 0.90 mmol). Purification by column chromatography (*n*hexane/EtOAc: 1/1) yielded **202** (62.2 mg, 25%) as a colorless oil.

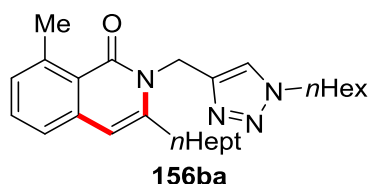
¹H NMR (600 MHz, CDCl₃): δ = 7.61 (s, 1H), 7.34–7.29 (m, 2H), 7.23 (d, *J* = 7.9 Hz, 1H), 7.17 (dd, *J* = 7.5, 7.5 Hz, 1H), 6.62 (s, 1H), 5.49–5.41 (m, 2H), 4.65 (d, *J* = 5.6 Hz, 2H), 4.31 (t, *J* = 7.3 Hz, 2H), 3.53 (d, *J* = 5.6 Hz, 2H), 2.13–2.05 (m, 2H),

5 Experimental Part

1.92–1.84 (m, 2H), 1.40–1.22 (m, 14H), 0.90–0.84 (m, 6H). ^{13}C NMR (126 MHz, CDCl_3): δ = 170.0 (C_q), 144.5 (C_q), 139.5 (C_q), 135.7 (C_q), 131.4 (CH), 130.2 (CH), 130.0 (CH), 127.7 (CH), 127.1 (CH), 126.0 (CH), 122.1 (CH), 50.6 (CH_2), 35.6 (CH_2), 32.0 (CH_2), 31.3 (CH_2), 31.1 (CH_2), 30.4 (CH_2), 29.8 (CH_2), 29.2 (CH_2), 27.5 (CH_2), 26.3 (CH_2), 22.8 (CH_2), 22.6 (CH_2), 14.3 (CH_3), 14.1 (CH_3). IR (ATR): 3286, 2925, 2855, 1656, 1594, 1436, 1240, 767, 749, 695 cm^{-1} . MS (EI) m/z (relative intensity): 410 (25) $[\text{M}]^+$, 325 (18), 311 (34), 157 (31), 144 (100), 138 (30). HR-MS (EI) m/z calcd for $\text{C}_{25}\text{H}_{38}\text{N}_4\text{O}$ $[\text{M}]^+$ 410.3046, found 410.3053.

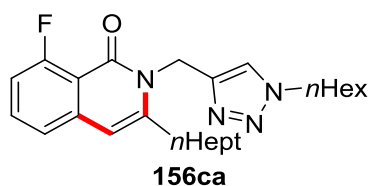
5.5.2 Experimental Procedures and Analytical Data – TAH Benzamides

3-*n*-Heptyl-2-[(1-*n*-hexyl-1*H*-1,2,3-triazol-4-yl)methyl]-8-methylisoquinolin-1(2*H*)-one (156ba)



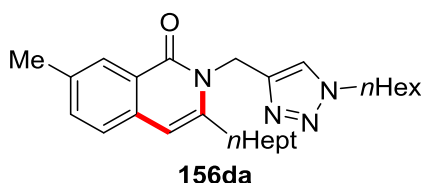
The general procedure **F** was followed using **118b** (90.1 mg, 0.30 mmol) and allene **155a** (164 mg, 0.90 mmol). Purification by column chromatography (*n*hexane/EtOAc: 4/1) yielded **156ba** (63.5 mg, 50%) as a white solid.

M.p. = 76–78 °C. ^1H NMR (600 MHz, CDCl_3): δ = 7.67 (s, 1H), 7.40 (dd, J = 7.6, 7.6 Hz, 1H), 7.23 (d, J = 7.6 Hz, 1H), 7.14 (d, J = 7.6 Hz, 1H), 6.26 (s, 1H), 5.32 (s, 2H), 4.25 (t, J = 7.3 Hz, 2H), 2.93–2.90 (m, 5H), 1.88–1.82 (m, 2H), 1.72–1.65 (m, 2H), 1.49–1.42 (m, 2H), 1.38–1.33 (m, 2H), 1.32–1.25 (m, 10H), 0.89 (t, J = 7.0 Hz, 3H), 0.86–0.83 (m, 3H). ^{13}C NMR (126 MHz, CDCl_3): δ = 164.0 (C_q), 144.4 (C_q), 143.3 (C_q), 141.5 (C_q), 138.6 (C_q), 131.6 (CH), 129.0 (CH), 123.8 (CH), 123.7 (CH), 122.9 (C_q), 105.5 (CH), 50.5 (CH_2), 39.2 (CH_2), 33.1 (CH_2), 31.9 (CH_2), 31.3 (CH_2), 30.3 (CH_2), 29.4 (CH_2), 29.4 (CH_2), 28.9 (CH_2), 26.3 (CH_2), 24.1 (CH_3), 22.8 (CH_2), 22.6 (CH_2), 14.3 (CH_3), 14.1 (CH_3). IR (ATR): 2953, 2931, 2857, 1651, 1608, 1460, 1291, 1043, 821, 807 cm^{-1} . MS (EI) m/z (relative intensity): 422 (100) $[\text{M}]^+$, 351 (41), 338 (42), 309 (48), 256 (65), 173 (90), 43 (94). HR-MS (EI) m/z calcd for $\text{C}_{26}\text{H}_{38}\text{N}_4\text{O}$ $[\text{M}]^+$ 422.3046, found 422.3056.

8-Fluoro-3-*n*-heptyl-2-[(1-*n*-hexyl-1*H*-1,2,3-triazol-4-yl)methyl]isoquinolin-1(2*H*)-one (156ca)

The general procedure **F** was followed using **118c** (91.3 mg, 0.30 mmol) and allene **155a** (164 mg, 0.90 mmol). Purification by column chromatography (*n*hexane/EtOAc: 4/1) yielded **156ca** (74.2 mg, 58%) as a white solid.

M.p. = 134–136 °C. **¹H NMR** (500 MHz, CDCl₃): δ = 7.81 (s, 1H), 7.48 (ddd, *J* = 8.0, 8.0, 4.8 Hz, 1H), 7.16 (d, *J* = 7.9 Hz, 1H), 7.00 (ddd, *J* = 11.7, 8.0, 0.7 Hz, 1H), 6.29 (s, 1H), 5.31 (s, 2H), 4.25 (t, *J* = 7.3 Hz, 2H), 3.00 (t, *J* = 7.7 Hz, 2H), 1.87–1.82 (m, 2H), 1.73–1.68 (m, 2H), 1.51–1.45 (m, 2H), 1.40–1.34 (m, 2H), 1.32–1.24 (m, 10H), 0.88 (t, *J* = 7.0 Hz, 3H), 0.85–0.82 (m, 3H). **¹³C NMR** (126 MHz, CDCl₃): δ = 162.4 (d, ¹*J*_{C-F} = 262.7 Hz, C_q), 160.6 (d, ³*J*_{C-F} = 4.6 Hz, C_q), 145.0 (C_q), 143.6 (C_q), 139.7 (C_q), 133.1 (d, ³*J*_{C-F} = 10.1 Hz, CH), 124.4 (CH), 121.3 (d, ⁴*J*_{C-F} = 4.4 Hz, CH), 113.5 (d, ³*J*_{C-F} = 5.3 Hz, C_q), 112.5 (d, ²*J*_{C-F} = 21.9 Hz, CH), 104.5 (d, ⁴*J*_{C-F} = 2.2 Hz, CH), 50.6 (CH₂), 38.9 (CH₂), 33.2 (CH₂), 31.9 (CH₂), 31.3 (CH₂), 30.3 (CH₂), 29.4 (CH₂), 29.3 (CH₂), 28.8 (CH₂), 26.3 (CH₂), 22.8 (CH₂), 22.6 (CH₂), 14.3 (CH₃), 14.1 (CH₃). **¹⁹F NMR** (282 MHz, CDCl₃): δ = -111.95 (ddd, *J* = 11.8, 4.9, 2.1 Hz). **IR** (ATR): 2927, 2855, 1646, 1619, 1604, 1420, 1158, 1055, 819, 684 cm⁻¹. **MS** (ESI) *m/z* (relative intensity): 875 (27) [2M+Na]⁺, 853 (16) [2M+H]⁺, 449 (14) [M+Na]⁺, 427 (100) [M+H]⁺. **HR-MS** (ESI) *m/z* calcd for C₂₅H₃₆N₄OF [M+H]⁺ 427.2868, found 427.2870.

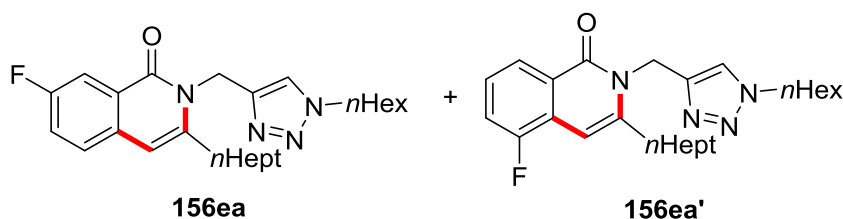
3-*n*-Heptyl-2-[(1-*n*-hexyl-1*H*-1,2,3-triazol-4-yl)methyl]-7-methylisoquinolin-1(2*H*)-one (156da)

5 Experimental Part

The general procedure **F** was followed using **118d** (90.1 mg, 0.30 mmol) and allene **155a** (164 mg, 0.90 mmol). Purification by column chromatography (*n*hexane/EtOAc: 3/2) yielded **156da** (104 mg, 82%) as a white solid.

M.p. = 74–75 °C. **¹H NMR** (500 MHz, CDCl₃): δ = 8.15 (s, 1H), 7.70 (s, 1H), 7.41 (dd, *J* = 8.1, 1.8 Hz, 1H), 7.33 (d, *J* = 8.1 Hz, 1H), 6.32 (s, 1H), 5.38 (s, 2H), 4.24 (t, *J* = 7.3 Hz, 2H), 2.96 (t, *J* = 7.7 Hz, 2H), 2.46 (s, 3H), 1.87–1.80 (m, 2H), 1.74–1.66 (m, 2H), 1.50–1.44 (m, 2H), 1.40–1.33 (m, 2H), 1.32–1.23 (m, 10H), 0.89 (t, *J* = 6.9 Hz, 3H), 0.85–0.82 (m, 3H). **¹³C NMR** (126 MHz, CDCl₃): δ = 163.4 (C_q), 144.3 (C_q), 142.6 (C_q), 136.0 (C_q), 134.7 (C_q), 134.0 (CH), 127.2 (CH), 125.4 (CH), 124.2 (C_q), 123.8 (CH), 105.1 (CH), 50.4 (CH₂), 39.1 (CH₂), 33.0 (CH₂), 31.9 (CH₂), 31.2 (CH₂), 30.2 (CH₂), 29.4 (CH₂), 29.3 (CH₂), 28.8 (CH₂), 26.2 (CH₂), 22.7 (CH₂), 22.5 (CH₂), 21.5 (CH₃), 14.2 (CH₃), 14.0 (CH₃). **IR** (ATR): 2954, 2924, 2856, 1645, 1598, 1208, 1052, 830, 799, 531 cm⁻¹. **MS** (EI) *m/z* (relative intensity): 422 (100) [M]⁺, 351 (49), 338 (42), 309 (67), 256 (66), 186 (36), 173 (90). **HR-MS** (EI) *m/z* calcd for C₂₆H₃₈N₄O [M]⁺ 422.3046, found 422.3048.

7-Fluoro-3-*n*-heptyl-2-[(1-*n*-hexyl-1*H*-1,2,3-triazol-4-yl)methyl]isoquinolin-1(2*H*)-one (156ea) and 5-Fluoro-3-*n*-heptyl-2-[(1-*n*-hexyl-1*H*-1,2,3-triazol-4-yl)methyl]isoquinolin-1(2*H*)-one (156ea')



The general procedure **F** was followed using **118e** (91.3 mg, 0.30 mmol) and allene **155a** (164 mg, 0.90 mmol). Purification by column chromatography (*n*hexane/EtOAc: 4/1) yielded **156ea** (86.9 mg, 68%) and **156ea'** (24.6 mg, 19%) as white solids.

7-Fluoro-3-*n*-heptyl-2-[(1-*n*-hexyl-1*H*-1,2,3-triazol-4-yl)methyl]isoquinolin-1(2*H*)-one (156ea):

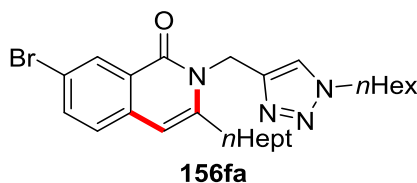
M.p. = 127–129 °C. **¹H NMR** (600 MHz, CDCl₃): δ = 7.97 (dd, *J* = 9.4, 2.7 Hz, 1H), 7.70 (s, 1H), 7.41 (dd, *J* = 8.6, 5.1 Hz, 1H), 7.31 (ddd, *J* = 8.6, 8.5, 2.7 Hz, 1H), 6.33 (s, 1H), 5.36 (s, 2H), 4.25 (t, *J* = 7.3 Hz, 2H), 3.00–2.95 (m, 2H), 1.87–1.81 (m, 2H),

5 Experimental Part

1.70 (dt, $J = 15.4, 7.7$ Hz, 2H), 1.51–1.44 (m, 2H), 1.40–1.34 (m, 2H), 1.32–1.23 (m, 10H), 0.88 (t, $J = 6.9$ Hz, 3H), 0.85–0.81 (m, 3H). **^{13}C NMR** (126 MHz, CDCl_3): $\delta = 162.5$ (d, $^4J_{\text{C-F}} = 3.7$ Hz, C_q), 160.9 (d, $^1J_{\text{C-F}} = 245.8$ Hz, C_q), 143.8 (C_q), 142.9 (d, $^4J_{\text{C-F}} = 2.5$ Hz, C_q), 133.6 (C_q), 127.7 (d, $^3J_{\text{C-F}} = 7.7$ Hz, CH), 125.6 (d, $^3J_{\text{C-F}} = 7.9$ Hz, C_q), 123.8 (CH), 121.3 (d, $^2J_{\text{C-F}} = 23.8$ Hz, CH), 112.6 (d, $^2J_{\text{C-F}} = 22.6$ Hz, CH), 104.5 (CH), 50.5 (CH_2), 39.3 (CH_2), 33.1 (CH_2), 31.9 (CH_2), 31.3 (CH_2), 30.3 (CH_2), 29.4 (CH_2), 29.3 (CH_2), 28.9 (CH_2), 26.3 (CH_2), 22.8 (CH_2), 22.6 (CH_2), 14.3 (CH_3), 14.1 (CH_3). **^{19}F NMR** (282 MHz, CDCl_3): $\delta = -114.34$ (m). **IR** (ATR): 2928, 2854, 1646, 1596, 1493, 1428, 1053, 893, 845, 797 cm^{-1} . **MS** (EI) m/z (relative intensity): 426 (64) $[\text{M}]^+$, 355 (42), 342 (40), 260 (26), 190 (32), 177 (100), 138 (32). **HR-MS** (EI) m/z calcd for $\text{C}_{25}\text{H}_{35}\text{FN}_4\text{O}$ $[\text{M}]^+$ 426.2795, found 426.2792.

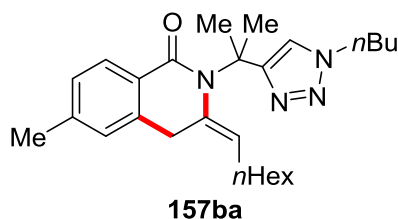
5-Fluoro-3-*n*-heptyl-2-[(1-*n*-hexyl-1*H*-1,2,3-triazol-4-yl)methyl]isoquinolin-1(2*H*)-one (156ea'):

M.p. = 123-124 °C. **^1H NMR** (600 MHz, CDCl_3): $\delta = 8.12$ (d, $J = 7.9$ Hz, 1H), 7.70 (s, 1H), 7.32 (ddd, $J = 7.9, 7.9, 5.2$ Hz, 1H), 7.29–7.27 (m, 1H), 6.55 (s, 1H), 5.37 (s, 2H), 4.25 (t, $J = 7.4$ Hz, 2H), 3.03–2.99 (m, 2H), 1.87–1.82 (m, 2H), 1.73 (dt, $J = 15.4, 7.7$ Hz, 2H), 1.51–1.46 (m, 2H), 1.38 (dt, $J = 14.7, 7.1$ Hz, 2H), 1.32–1.23 (m, 10H), 0.89 (t, $J = 6.9$ Hz, 3H), 0.84 (t, $J = 6.9$ Hz, 3H). **^{13}C NMR** (126 MHz, CDCl_3): $\delta = 162.4$ (d, $^4J_{\text{C-F}} = 2.9$ Hz, C_q), 157.2 (d, $^1J_{\text{C-F}} = 250.3$ Hz, C_q), 144.6 (C_q), 143.8 (C_q), 126.5 (d, $^2J_{\text{C-F}} = 16.7$ Hz, C_q), 126.0 (d, $^3J_{\text{C-F}} = 4.2$ Hz, C_q), 125.9 (d, $^3J_{\text{C-F}} = 7.6$ Hz, CH), 123.8 (CH), 123.4 (d, $^4J_{\text{C-F}} = 3.8$ Hz, CH), 117.0 (d, $^2J_{\text{C-F}} = 19.6$ Hz, CH), 97.4 (d, $^3J_{\text{C-F}} = 5.5$ Hz, CH), 50.5 (CH_2), 39.3 (CH_2), 33.5 (CH_2), 31.9 (CH_2), 31.3 (CH_2), 30.3 (CH_2), 29.4 (CH_2), 29.3 (CH_2), 28.9 (CH_2), 26.3 (CH_2), 22.8 (CH_2), 22.6 (CH_2), 14.3 (CH_3), 14.1 (CH_3). **^{19}F NMR** (282 MHz, CDCl_3): $\delta = -123.54$ (dd, $J = 9.5, 5.5$ Hz). *NMR contains 8% of regioisomer **156ea'**. **IR** (ATR): 2925, 2854, 1624, 1465, 1284, 1053, 893, 809, 722, 552 cm^{-1} . **MS** (EI) m/z (relative intensity): 426 (96) $[\text{M}]^+$, 355 (63), 342 (60), 260 (38), 177 (100), 167 (39), 138 (32). **HR-MS** (EI) m/z calcd for $\text{C}_{25}\text{H}_{35}\text{FN}_4\text{O}$ $[\text{M}]^+$ 426.2795, found 426.2799.

7-Bromo-3-*n*-heptyl-2-[(1-*n*-hexyl-1*H*-1,2,3-triazol-4-yl)methyl]isoquinolin-1(2*H*)-one (156fa)

The general procedure **F** was followed using **118f** (110 mg, 0.30 mmol) and allene **155a** (164 mg, 0.90 mmol). Purification by column chromatography (*n*hexane/EtOAc: 3/2) yielded **156fa** (126 mg, 86%) as a white solid.

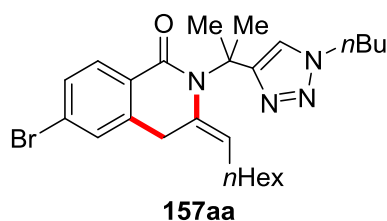
M.p. = 72–73 °C. **¹H NMR** (500 MHz, CDCl₃): δ = 8.48 (d, *J* = 2.1 Hz, 1H), 7.71 (s, 1H), 7.65 (dd, *J* = 8.4, 2.1 Hz, 1H), 7.29 (d, *J* = 8.4 Hz, 1H), 6.30 (s, 1H), 5.36 (s, 2H), 4.25 (t, *J* = 7.4 Hz, 2H), 2.98 (t, *J* = 7.7 Hz, 2H), 1.88–1.80 (m, 2H), 1.74–1.67 (m, 2H), 1.51–1.44 (m, 2H), 1.41–1.34 (m, 2H), 1.31–1.24 (m, 10H), 0.89 (t, *J* = 6.9 Hz, 3H), 0.84 (t, *J* = 7.0 Hz, 3H). **¹³C NMR** (126 MHz, CDCl₃): δ = 162.2 (C_q), 144.4 (C_q), 143.8 (C_q), 135.6 (C_q), 135.6 (CH), 130.4 (CH), 127.3 (CH), 125.6 (C_q), 123.9 (CH), 119.5 (C_q), 104.6 (CH), 50.5 (CH₂), 39.2 (CH₂), 33.2 (CH₂), 31.9 (CH₂), 31.2 (CH₂), 30.2 (CH₂), 29.4 (CH₂), 29.3 (CH₂), 28.7 (CH₂), 26.2 (CH₂), 22.7 (CH₂), 22.5 (CH₂), 14.2 (CH₃), 14.0 (CH₃). **IR** (ATR): 2951, 2929, 2858, 1645, 1618, 1588, 1467, 1276, 799, 533 cm⁻¹. **MS** (EI) *m/z* (relative intensity): 486 (63) [⁷⁹Br, M]⁺, 415 (35), 373 (25), 320 (24), 236 (55), 138 (47), 43 (100). **HR-MS** (EI) *m/z* calcd for C₂₅H₃₅⁷⁹BrN₄O [M]⁺ 486.1994, found 486.1980.

(*E*)-2-[2-(1-*n*-Butyl-1*H*-1,2,3-triazol-4-yl)propan-2-yl]-3-heptylidene-6-methyl-3,4-dihydroisoquinolin-1(2*H*)-one (157ba)

The general procedure **F** was followed using **116b** (45.1 mg, 0.15 mmol) and allene **155a** (82.0 mg, 0.45 mmol). Purification by column chromatography (*n*hexane/EtOAc: 3/1) yielded **157ba** (63.4 mg, 97%) as a colorless oil.

¹H NMR (600 MHz, C₆D₆): δ = 8.32 (d, J = 7.9 Hz, 1H), 7.50 (s, 1H), 6.81 (dd, J = 7.9, 1.7, 1H), 6.63 (s, 1H), 5.58 (t, J = 7.7 Hz, 1H), 3.65 (t, J = 7.3 Hz, 2H), 3.43 (s, 2H), 2.17 (s, 6H), 2.00 (s, 3H), 1.93 (dt, J = 7.4 Hz, 2H), 1.39–1.30 (m, 2H), 1.21–1.10 (m, 8H), 0.98–0.91 (m, 2H), 0.84 (t, J = 7.1 Hz, 3H), 0.62 (t, J = 7.4 Hz, 3H). **¹³C NMR** (126 MHz, C₆D₆): δ = 164.9 (C_q), 153.7 (C_q), 141.8 (C_q), 139.0 (C_q), 135.8 (C_q), 129.2 (CH), 129.0 (C_q), 127.7 (CH), 127.0 (CH), 122.8 (CH), 122.0 (CH), 57.9 (C_q), 49.6 (CH₂), 32.9 (CH₂), 32.5 (CH₂), 32.1 (CH₂), 30.2 (CH₂), 30.1 (CH₃), 29.5 (CH₂), 27.6 (CH₂), 23.2 (CH₂), 21.5 (CH₃), 20.1 (CH₂), 14.5 (CH₃), 13.6 (CH₃). **IR** (ATR): 2957, 2930, 2871, 1648, 1457, 1378, 1163, 1046, 835, 498 cm⁻¹. **MS** (ESI) m/z (relative intensity): 868 (100) [2M+Na]⁺, 445 (94) [M+Na]⁺, 423 (93) [M+H]⁺, 407 (100) [M+H]⁺. **HR-MS** (ESI) m/z calcd for C₂₆H₃₉N₄O [M+H]⁺ 423.3118, found 423.3114.

(E)-6-Bromo-2-[2-(1-*n*-butyl-1*H*-1,2,3-triazol-4-yl)propan-2-yl]-3-heptylidene-3,4-dihydro-isoquinolin-1(2*H*)-one (157aa)



The general procedure **F** was followed using **116a** (110 mg, 0.30 mmol) and allene **155a** (164 mg, 0.90 mmol). Purification by column chromatography (*n*hexane/EtOAc: 3/1) yielded **157aa** (131 mg, 90%) as a colorless oil.

¹H NMR (300 MHz, C₆D₆): δ = 8.03 (d, J = 8.3 Hz, 1H), 7.38 (s, 1H), 7.06 (dd, J = 8.3, 2.0 Hz, 1H), 6.96 (s, 1H), 5.56 (t, J = 7.8 Hz, 1H), 3.64 (t, J = 7.3 Hz, 2H), 3.23 (s, 2H), 2.09 (s, 6H), 1.90–1.76 (m, 2H), 1.42–1.26 (m, 2H), 1.24–1.08 (m, 8H), 1.01–0.83 (m, 5H), 0.62 (t, J = 7.3 Hz, 3H). **¹³C NMR** (126 MHz, C₆D₆): δ = 163.9 (C_q), 153.4 (C_q), 140.9 (C_q), 134.8 (C_q), 130.7 (CH), 130.3 (C_q), 130.2 (CH), 129.4 (CH), 126.2 (C_q), 123.8 (CH), 121.7 (CH), 58.1 (C_q), 49.7 (CH₂), 32.5 (CH₂), 32.5 (CH₂), 32.1 (CH₂), 30.1 (CH₂), 29.8 (CH₃), 29.5 (CH₂), 27.6 (CH₂), 23.2 (CH₂), 20.0 (CH₂), 14.5 (CH₃), 13.6 (CH₃). **IR** (ATR): 2956, 2927, 2855, 1649, 1590, 1321, 1167, 1045, 766, 498 cm⁻¹. **MS** (ESI) m/z (relative intensity): 509 (16) [⁷⁹Br, 2M+Na]⁺, 487

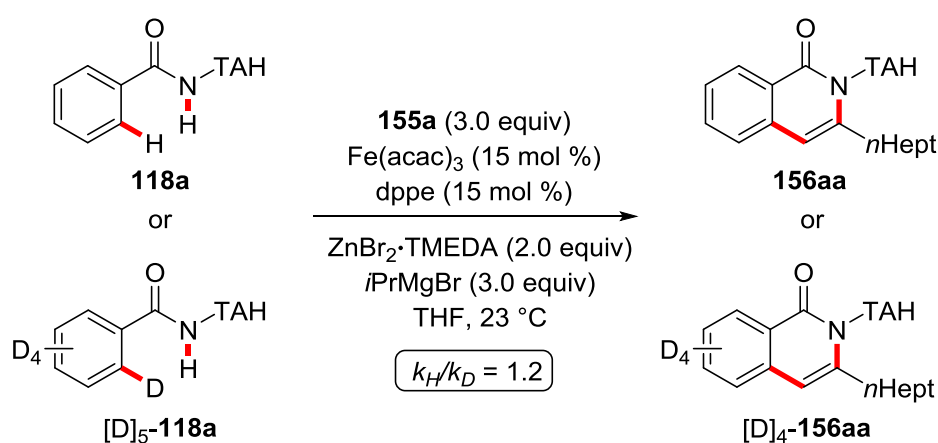
5 Experimental Part

(34) [^{79}Br , $\text{M}+\text{H}$] $^+$, 166 (100). **HR-MS** (ESI) m/z calcd for $\text{C}_{25}\text{H}_{36}^{79}\text{BrN}_4\text{O}$ [$\text{M}+\text{H}$] $^+$ 487.2067, found 487.2071.

5.5.3 Mechanistic Studies

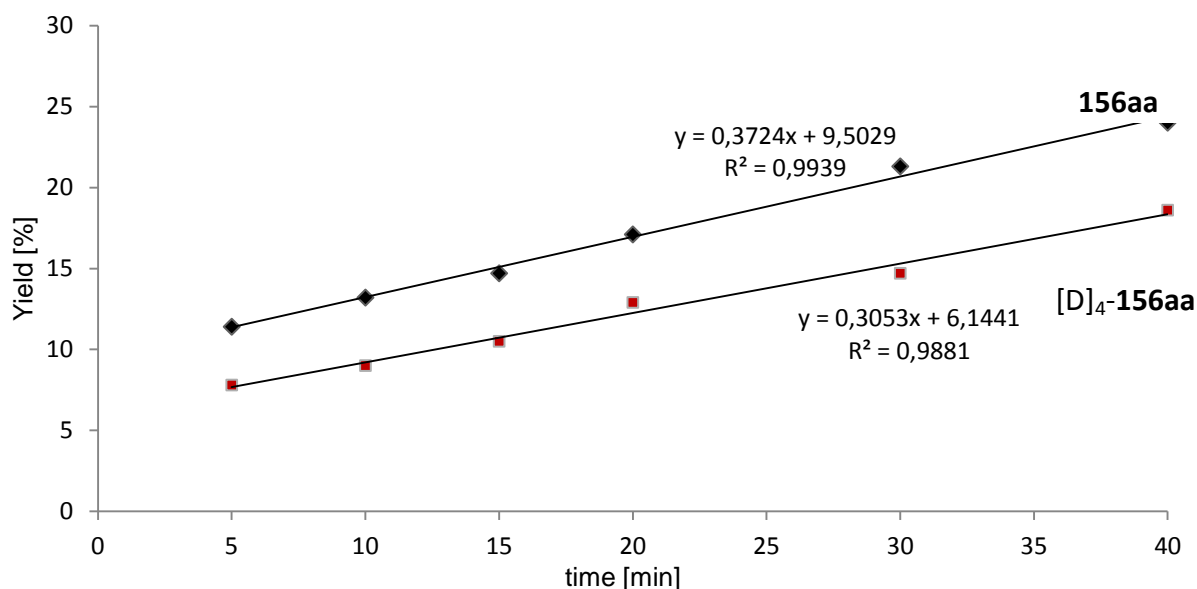
Intermolecular Kinetic Isotope Effect (KIE) Measurement (independent reactions)

To a stirred solution of **118a** (85.9 mg, 0.30 mmol) or $[\text{D}]_5\text{-118a}$ (87.4 mg, 0.30 mmol), $\text{ZnBr}_2\cdot\text{TMEDA}$ (206 mg, 0.60 mmol), dppe (17.9 mg, 15 mol %) in THF (0.6 mL) $i\text{PrMgBr}$ (3.0M in 2-MeTHF, 300 μL , 0.90 mmol) was added in one portion and the reaction mixture was stirred for 5 min at ambient temperature. Then, $\text{Fe}(\text{acac})_3$ (15.9 mg, 15 mol %) was added in a single portion. After stirring the solution for additional 5 min, a solution of allene **155a** (164 mg, 0.90 mmol) in THF (0.6 mL) was added in one portion. The mixture was stirred at ambient temperature and quenched after the reaction times indicated below by addition of sat. aqueous NH_4Cl (2 mL) and EtOAc (5 mL). The samples were extracted with CH_2Cl_2 (4 \times 5 mL). The combined organic layers were dried over Na_2SO_4 and the solvent was removed under reduced pressure. Yields of products were determined by ^1H NMR spectroscopy, using 1,3,5-trimethoxybenzene as internal standard.

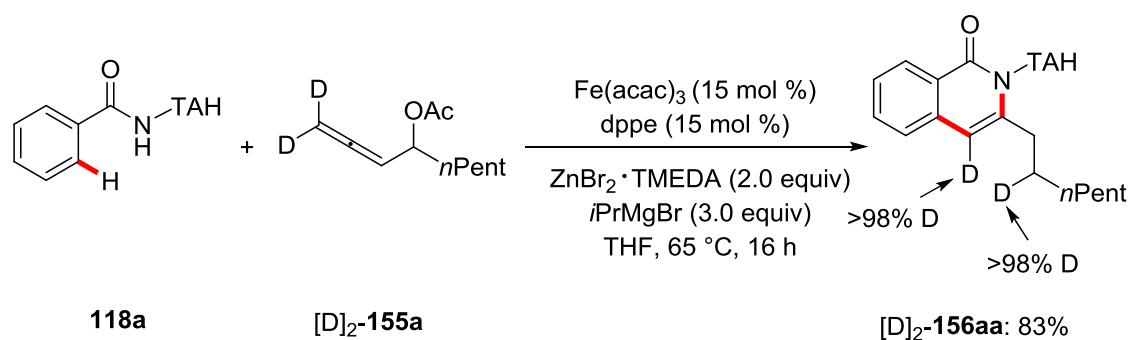


t [min]	5	10	15	20	30	40
156aa [%]	11.4	13.2	14.7	17.1	21.3	24.0
$[\text{D}]_4\text{-156aa}$ [%]	7.8	9.0	10.5	12.9	14.7	18.6

5 Experimental Part

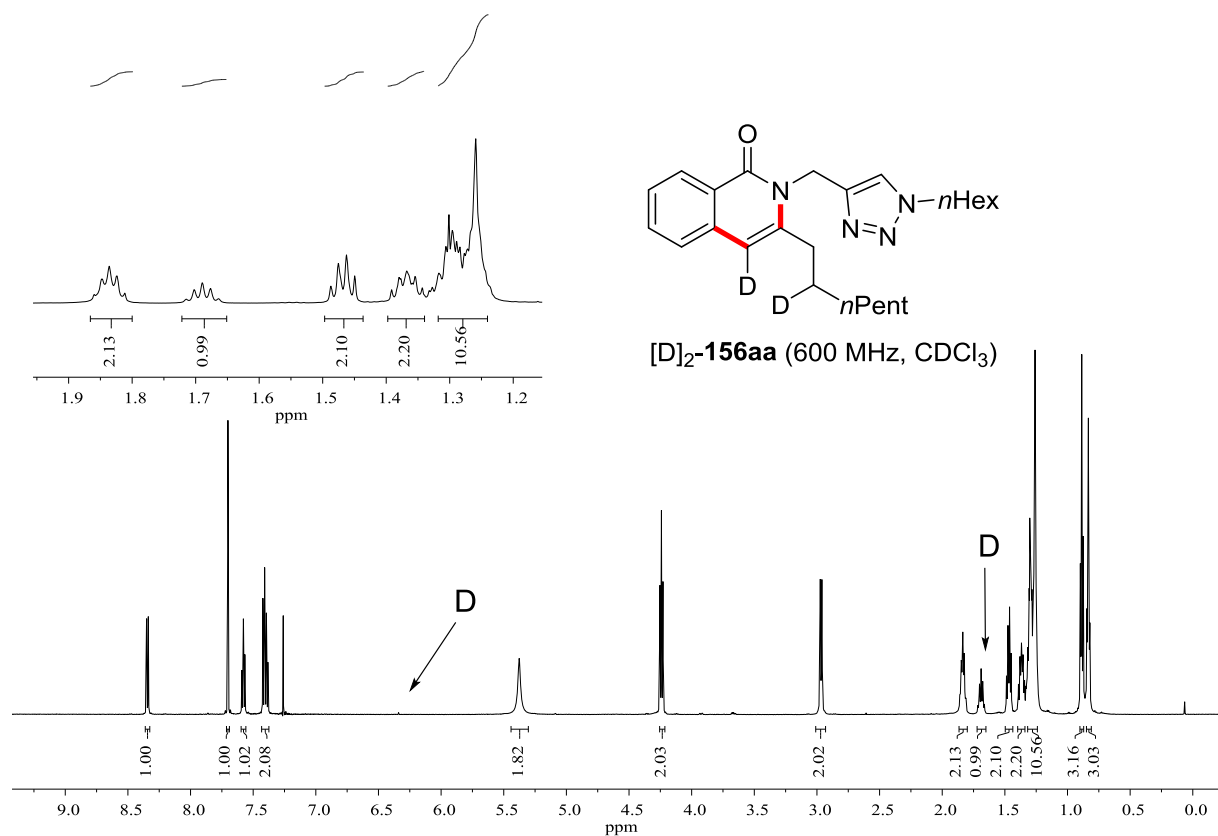
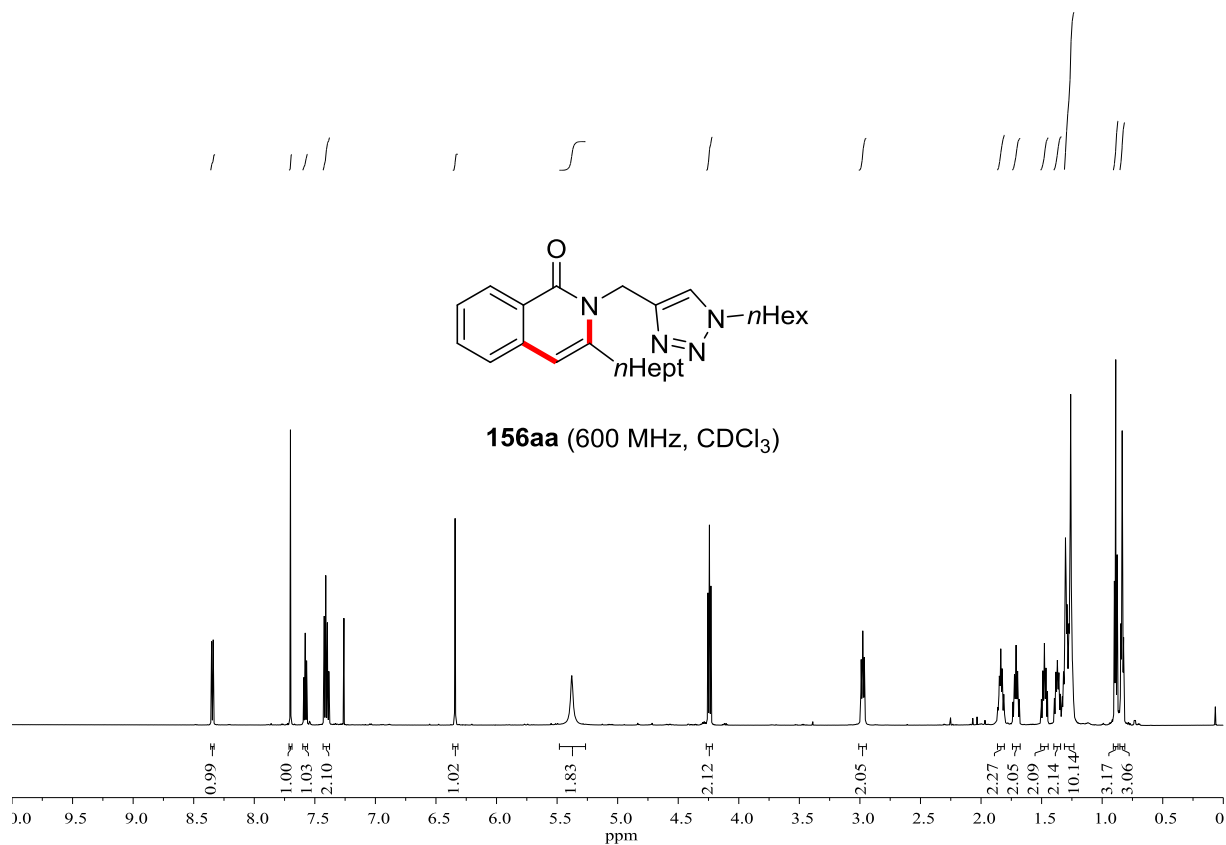


C–H/N–H/C–O/C–H Functionalizations with Isotopically-labelled Substrates



To a stirred solution of **118a** (85.9 mg, 0.30 mmol), $\text{ZnBr}_2 \cdot \text{TMEDA}$ (206 mg, 0.60 mmol), dppe (17.9 mg, 15 mol %) in THF (0.20 mL), $i\text{PrMgBr}$ (3.0M in 2-MeTHF, 300 μL , 0.90 mmol) was added in one portion and the reaction mixture was stirred for 5 min at ambient temperature. Then, Fe(acac)_3 (15.9 mg, 15 mol %) was added in a single portion. After stirring the solution for additional 5 min, a solution of allene $[\text{D}]_2\text{-155a}$ (166 mg, 0.90 mmol) in THF (0.20 mL) was added in one portion. The mixture was placed in a pre-heated oil bath at 65 $^\circ\text{C}$. After stirring for 16 h, sat. aqueous NH_4Cl (2.0 mL) was added to the reaction mixture, which was extracted with CH_2Cl_2 (3 \times 15 mL). The combined organic extracts were dried over Na_2SO_4 , filtered and concentrated. Purification by column chromatography (*n*hexane/EtOAc: 3/1) yielded $[\text{D}]_2\text{-156aa}$ (102 mg, 83%) as a white solid. **HR-MS** (ESI) m/z calcd for $\text{C}_{25}\text{H}_{35}\text{N}_4\text{OD}_2$ $[\text{M}+\text{H}]^+$ 411.3087, found 411.3090.

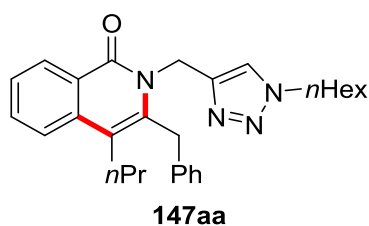
5 Experimental Part



5.6 Iron-Catalyzed C–H/N–H Annulation with Propargyl Acetates

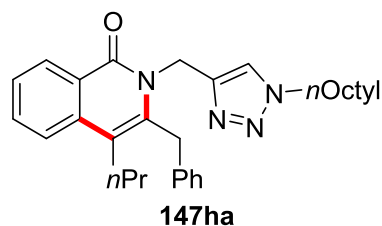
5.6.1 Experimental Procedures and Analytical Data – TAH Benzamides

3-Benzyl-2-[(1-*n*-hexyl-1*H*-1,2,3-triazol-4-yl)methyl]-4-*n*-propylisoquinolin-1(2*H*)-one (147aa)



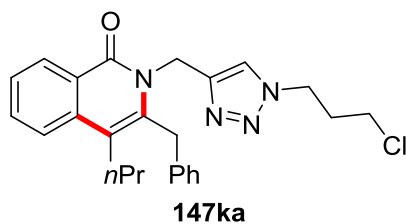
The general procedure **G** was followed using **118a** (85.9 mg, 0.30 mmol) and propargyl acetate **158a** (130 mg, 0.60 mmol). Purification by column chromatography (*n*hexane/EtOAc: 3/2) yielded **147aa** (112 mg, 85%) as a white solid.

M.p. = 97–98 °C. **¹H NMR** (600 MHz, CDCl₃): δ = 8.49 (d, *J* = 8.0 Hz, 1H), 7.74–7.68 (m, 3H), 7.48 (t, *J* = 7.3 Hz, 1H), 7.33 (t, *J* = 7.7 Hz, 2H), 7.28 – 7.24 (m, 3H), 5.19 (br s, 2H), 4.61 (s, 2H), 4.26 (t, *J* = 7.3 Hz, 2H), 2.77–2.71 (m, 2H), 1.89–1.82 (m, 2H), 1.61–1.53 (m, 2H), 1.32–1.23 (m, 6H), 0.99 (t, *J* = 7.3 Hz, 3H), 0.84 (t, *J* = 6.7 Hz, 3H). **¹³C NMR** (126 MHz, CDCl₃): δ = 162.7 (C_q), 144.2 (C_q), 137.4 (C_q), 137.1 (C_q), 136.7 (C_q), 132.4 (CH), 129.1 (CH), 128.3 (CH), 128.0 (CH), 126.9 (CH), 126.2 (CH), 125.3 (C_q), 124.0 (CH), 123.1 (CH), 116.4 (C_q), 50.5 (CH₂), 40.0 (CH₂), 35.0 (CH₂), 31.3 (CH₂), 30.4 (CH₂), 30.3 (CH₂), 26.3 (CH₂), 23.6 (CH₂), 22.6 (CH₂), 14.6 (CH₃), 14.1 (CH₂). **IR** (ATR): 3122, 2952, 2931, 1650, 1610, 1313, 1063, 776, 732, 715 cm⁻¹. **MS** (EI) *m/z* (relative intensity): 442 (72) [M]⁺, 329 (32), 276 (86), 248 (100), 242 (47), 112 (64). **HR-MS** (EI) *m/z* calcd for C₂₈H₃₄N₄O [M]⁺ 442.2733, found 442.2722.

3-Benzyl-2-[(1-*n*-octyl-1*H*-1,2,3-triazol-4-yl)methyl]-4-*n*-propylisoquinolin-1(2*H*)-one (147ha)

The general procedure **G** was followed using **118h** (94.3 mg, 0.30 mmol) and propargyl acetate **158a** (130 mg, 0.60 mmol). Purification by column chromatography (*n*hexane/EtOAc: 3/2) yielded **147ha** (113 mg, 80%) as an off-white solid.

M.p. = 112–113 °C. **¹H NMR** (600 MHz, CDCl₃): δ = 8.49 (dd, *J* = 8.1, 0.9 Hz, 1H), 7.74–7.68 (m, 3H), 7.48 (ddd, *J* = 8.0, 6.7, 1.4 Hz, 1H), 7.33 (dd, *J* = 7.6, 7.6 Hz, 2H), 7.27–7.24 (m, 3H), 5.19 (br s, 2H), 4.61 (s, 2H), 4.26 (t, *J* = 7.3 Hz, 2H), 2.76–2.71 (m, 2H), 1.90–1.81 (m, 2H), 1.62–1.53 (m, 2H), 1.32–1.18 (m, 10H), 0.99 (t, *J* = 7.3 Hz, 3H), 0.85 (t, *J* = 7.1 Hz, 3H). **¹³C NMR** (126 MHz, CDCl₃): δ = 162.7 (C_q), 144.2 (C_q), 137.4 (C_q), 137.1 (C_q), 136.7 (C_q), 132.4 (CH), 129.1 (CH), 128.3 (CH), 128.0 (CH), 126.9 (CH), 126.2 (CH), 125.3 (C_q), 124.1 (CH), 123.1 (CH), 116.4 (C_q), 50.6 (CH₂), 40.0 (CH₂), 35.0 (CH₂), 31.9 (CH₂), 30.4 (CH₂), 30.3 (CH₂), 29.2 (CH₂), 29.1 (CH₂), 26.7 (CH₂), 23.6 (CH₂), 22.8 (CH₂), 14.6 (CH₃), 14.3 (CH₃). **IR** (ATR): 3153, 2924, 1640, 1592, 1333, 1044, 773, 751, 714, 698 cm⁻¹. **MS** (EI) *m/z* (relative intensity): 470 (90) [M]⁺, 329 (36), 276 (100), 270 (44), 248 (99), 140 (74). **HR-MS** (ESI) *m/z* calcd for C₃₀H₃₉N₄O [M+H]⁺ 471.3118, found 471.3114.

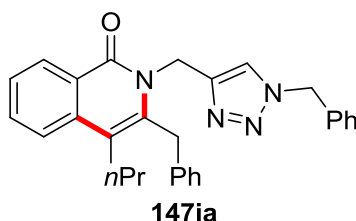
3-Benzyl-2-[[1-(3-chloropropyl)-1*H*-1,2,3-triazol-4-yl]methyl]-4-*n*-propylisoquinolin-1(2*H*)-one (147ka)

5 Experimental Part

The general procedure **G** was followed using **118k** (83.6 mg, 0.30 mmol) and propargyl acetate **158a** (130 mg, 0.60 mmol). Purification by column chromatography (*n*hexane/EtOAc: 3/2) yielded **147ka** (106 mg, 81%) as a yellow oil.

¹H NMR (600 MHz, CDCl₃): δ = 8.48 (d, *J* = 7.7 Hz, 1H), 7.78 (s, 1H), 7.74–7.68 (m, 2H), 7.50–7.47 (m, 1H), 7.36–7.32 (m, 2H), 7.27–7.25 (m, 3H), 5.19 (s, 2H), 4.60 (s, 2H), 4.46 (t, *J* = 6.7 Hz, 2H), 3.51 (t, *J* = 6.1 Hz, 2H), 2.76–2.72 (m, 2H), 2.37–2.33 (m, 2H), 1.61–1.54 (m, 2H), 1.00 (t, *J* = 7.3 Hz, 3H). **¹³C NMR** (126 MHz, CDCl₃): δ = 162.7 (C_q), 144.3 (C_q), 137.3 (C_q), 137.0 (C_q), 136.7 (C_q), 132.5 (CH), 129.1 (CH), 128.3 (CH), 127.9 (CH), 126.9 (CH), 126.2 (CH), 125.3 (C_q), 124.7 (CH), 123.2 (CH), 116.5 (C_q), 47.3 (CH₂), 41.4 (CH₂), 39.9 (CH₂), 35.0 (CH₂), 32.7 (CH₂), 30.5 (CH₂), 23.6 (CH₂), 14.62 (CH₃). **IR** (ATR): 2957, 2870, 1639, 1590, 1337, 1314, 1045, 770, 710, 698 cm⁻¹. **MS** (EI) *m/z* (relative intensity): 434 (50) [³⁵Cl, M]⁺, 329 (39), 276 (68), 248 (100), 234 (66), 91 (43). **HR-MS** (ESI) *m/z* calcd for C₂₅H₂₈³⁵ClN₄O [M+H]⁺ 435.1946, found 435.1944.

3-Benzyl-2-[(1-benzyl-1*H*-1,2,3-triazol-4-yl)methyl]-4-*n*-propylisoquinolin-1(2*H*)-one (**147ia**)



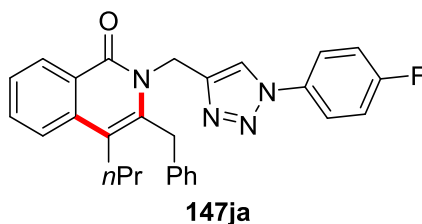
The general procedure **G** was followed using **118i** (57.7 mg, 0.20 mmol) and propargyl acetate **158a** (86.5 mg, 0.40 mmol). Purification by column chromatography (*n*hexane/EtOAc: 3/2) yielded **147ia** (65.0 mg, 74%) as a white solid.

M.p. = 156–157 °C. **¹H NMR** (600 MHz, CDCl₃): δ = 8.46 (d, *J* = 8.0 Hz, 1H), 7.73–7.68 (m, 3H), 7.47 (ddd, *J* = 8.1, 6.7, 1.4 Hz, 1H), 7.35–7.31 (m, 5H), 7.27–7.24 (m, 5H), 5.44 (s, 2H), 5.17 (br s, 2H), 4.61 (s, 2H), 2.76–2.71 (m, 2H), 1.61–1.53 (m, 2H), 0.99 (t, *J* = 7.3 Hz, 3H). **¹³C NMR** (126 MHz, CDCl₃): δ = 162.7 (C_q), 144.7 (C_q), 137.3 (C_q), 137.1 (C_q), 136.7 (C_q), 134.5 (C_q), 132.4 (CH), 129.1 (CH), 128.7 (CH), 128.3 (CH), 128.2 (CH), 127.9 (CH), 126.9 (CH), 126.1 (CH), 125.3 (C_q), 124.2 (CH), 123.1 (CH), 116.4 (C_q), 54.3 (CH₂), 39.9 (CH₂), 35.0 (CH₂), 30.4 (CH₂), 23.6 (CH₂),

5 Experimental Part

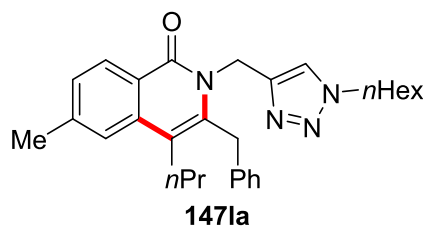
14.6 (CH₃). **IR** (ATR): 3134, 2958, 1644, 2594, 1340, 1054, 804, 713, 693, 454 cm⁻¹. **MS** (EI) *m/z* (relative intensity): 448 (19) [M]⁺, 329 (23), 276 (22), 248 (43), 91 (100), 43 (70). **HR-MS** (ESI) *m/z* calcd for C₂₉H₂₉N₄O [M+H]⁺ 449.2336, found 449.2332.

3-Benzyl-2-{[1-(4-fluorophenyl)-1*H*-1,2,3-triazol-4-yl]methyl}-4-*n*-propylisoquinolin-1(2*H*)-one (147ja)



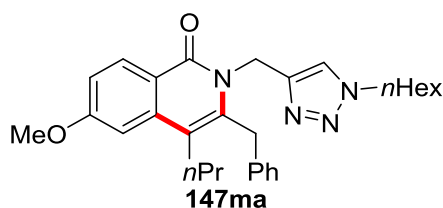
The general procedure **G** was followed using **118j** (88.9 mg, 0.30 mmol) and propargyl acetate **158a** (130 mg, 0.60 mmol). Purification by column chromatography (*n*hexane/EtOAc: 3/2) yielded **147ja** (117 mg, 86%) as a white solid.

M.p. = 94–96 °C. **¹H NMR** (600 MHz, CDCl₃): δ = 8.49 (d, *J* = 8.1 Hz, 1H), 8.17 (s, 1H), 7.75–7.70 (m, 2H), 7.70–7.67 (m, 2H), 7.51–7.48 (m, 1H), 7.36 (dd, *J* = 7.6, 7.6 Hz, 2H), 7.30–7.26 (m, 3H), 7.19–7.15 (m, 2H), 5.27 (s, 2H), 4.64 (s, 2H), 2.78–2.73 (m, 2H), 1.63–1.54 (m, 2H), 1.01 (t, *J* = 7.3 Hz, 3H). **¹³C NMR** (126 MHz, CDCl₃): δ = 162.8 (C_q), 162.4 (d, ¹*J*_{C-F} = 248.8 Hz, C_q), 145.1 (C_q), 137.3 (C_q), 136.9 (C_q), 136.7 (C_q), 133.3 (d, ⁴*J*_{C-F} = 2.8 Hz, C_q), 132.5 (CH), 129.2 (CH), 128.3 (CH), 128.0 (CH), 127.0 (CH), 126.3 (CH), 125.2 (C_q), 123.2 (CH), 122.6 (CH), 122.5 (d, ³*J*_{C-F} = 8.6 Hz, CH), 116.7 (d, ²*J*_{C-F} = 23.2 Hz, CH), 116.7 (C_q), 39.9 (CH₂), 35.1 (CH₂), 30.5 (CH₂), 23.7 (CH₂), 14.6 (CH₃). **¹⁹F NMR** (282 MHz, CDCl₃): δ = -112.24 – -112.34 (m). **IR** (ATR): 2957, 1640, 1590, 1514, 1337, 1232, 1041, 836, 769, 703 cm⁻¹. **MS** (EI) *m/z* (relative intensity): 452 (41) [M]⁺, 424 (50), 276 (40), 248 (100), 148 (71), 43 (81). **HR-MS** (EI) *m/z* calcd for C₂₈H₂₆FN₄O [M+H]⁺ 453.2085, found 453.2082.

3-Benzyl-2-[(1-*n*-hexyl-1*H*-1,2,3-triazol-4-yl)methyl]-6-methyl-4-*n*-propylisoquinolin-1(2*H*)-one (147la)

The general procedure **G** was followed using **118l** (90.1 mg, 0.30 mmol) and propargyl acetate **158a** (130 mg, 0.60 mmol). Purification by column chromatography (*n*hexane/EtOAc: 3/2) yielded **147la** (103 mg, 75%) as a white solid.

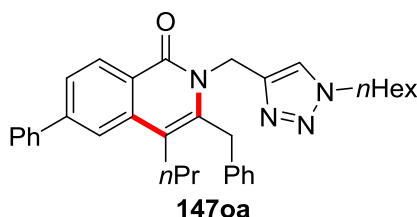
M.p. = 93–94 °C. **¹H NMR** (600 MHz, CDCl₃): δ = 8.37 (d, *J* = 8.2 Hz, 1H), 7.72 (s, 1H), 7.48 (s, 1H), 7.34–7.30 (m, 3H), 7.27–7.24 (m, 3H), 5.17 (br s, 2H), 4.59 (br s, 2H), 4.25 (t, *J* = 7.4 Hz, 2H), 2.74–2.68 (m, 2H), 2.52 (s, 3H), 1.88–1.82 (m, 2H), 1.61–1.52 (m, 2H), 1.31–1.23 (m, 6H), 1.00 (t, *J* = 7.3 Hz, 3H), 0.84 (t, *J* = 7.0 Hz, 3H). **¹³C NMR** (126 MHz, CDCl₃): δ = 162.7 (C_q), 144.4 (C_q), 142.8 (C_q), 137.5 (C_q), 137.2 (C_q), 136.9 (C_q), 129.1 (CH), 128.3 (CH), 1280 (CH), 127.8 (CH), 126.9 (CH), 124.0 (CH), 123.1 (C_q), 122.9 (CH), 116.2 (C_q), 50.5 (CH₂), 39.9 (CH₂), 35.0 (CH₂), 31.3 (CH₂), 30.4 (CH₂), 30.3 (CH₂), 26.4 (CH₂), 23.6 (CH₂), 22.6 (CH₂), 22.5 (CH₃), 14.6 (CH₃), 14.1 (CH₃). **IR** (ATR): 3133, 2958, 2917, 1649, 1614, 1336, 1055, 830, 723, 467 cm⁻¹. **MS** (EI) *m/z* (relative intensity): 456 (100) [M]⁺, 343 (45), 290 (98), 262 (89), 242 (37), 112 (51). **HR-MS** (EI) *m/z* calcd for C₂₉H₃₆N₄O [M]⁺ 456.2889, found 456.2883.

3-Benzyl-2-[(1-*n*-hexyl-1*H*-1,2,3-triazol-4-yl)methyl]-6-methoxy-4-*n*-propylisoquinolin-1(2*H*)-one (147ma)

The general procedure **G** was followed using **118m** (94.9 mg, 0.30 mmol) and propargyl acetate **158a** (130 mg, 0.60 mmol). Purification by column chromatography (*n*hexane/EtOAc: 3/2) yielded **147ma** (115 mg, 81%) as a white solid.

M.p. = 108–110 °C. **¹H NMR** (600 MHz, CDCl₃): δ = 8.42–8.40 (m, 1H), 7.72 (s, 1H), 7.35–7.31 (m, 2H), 7.27–7.23 (m, 3H), 7.09–7.05 (m, 2H), 5.16 (br s, 2H), 4.58 (br s, 2H), 4.25 (t, *J* = 7.3 Hz, 2H), 3.93 (s, 3H), 2.71–2.67 (m, 2H), 1.88–1.82 (m, 2H), 1.61–1.52 (m, 2H), 1.31–1.24 (m, 6H), 0.99 (t, *J* = 7.3 Hz, 3H), 0.84 (t, *J* = 7.0 Hz, 3H). **¹³C NMR** (126 MHz, CDCl₃): δ = 162.9 (C_q), 162.4 (C_q), 144.4 (C_q), 138.7 (C_q), 137.8 (C_q), 137.4 (C_q), 130.4 (CH), 129.1 (CH), 128.0 (CH), 126.9 (CH), 124.0 (CH), 119.3 (C_q), 115.9 (C_q), 114.7 (CH), 105.3 (CH), 55.6 (CH₃), 50.5 (CH₂), 39.8 (CH₂), 35.1 (CH₂), 31.3 (CH₂), 30.6 (CH₂), 30.3 (CH₂), 26.4 (CH₂), 23.4 (CH₂), 22.6 (CH₂), 14.7 (s CH₃), 14.1 (CH₃). **IR** (ATR): 2950, 2929, 1646, 1612, 1597, 1235, 1031, 840, 791, 724 cm⁻¹. **MS** (ESI) *m/z* (relative intensity): 967 (30) [2M+Na]⁺, 945 (13) [2M+H]⁺, 495 (17) [M+Na]⁺, 473 (100) [M+H]⁺. **HR-MS** (ESI) *m/z* calcd for C₂₉H₃₇N₄O₂ [M+H]⁺ 473.2911, found 473.2902.

3-Benzyl-2-[(1-*n*-hexyl-1*H*-1,2,3-triazol-4-yl)methyl]-6-phenyl-4-*n*-propylisoquinolin-1(2*H*)-one (147oa)



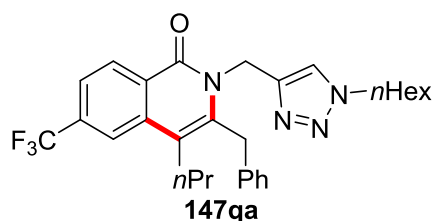
The general procedure **G** was followed using **118o** (109 mg, 0.30 mmol) and propargyl acetate **158a** (130 mg, 0.60 mmol). Purification by column chromatography (*n*hexane/EtOAc: 3/2) yielded **147oa** (106 mg, 68%) as a pale yellow solid.

M.p. = 90–92 °C. **¹H NMR** (600 MHz, CDCl₃): δ = 8.55 (d, *J* = 8.3 Hz, 1H), 7.89 (d, *J* = 1.5 Hz, 1H), 7.75 (s, 1H), 7.72 (dd, *J* = 8.3, 1.6 Hz, 1H), 7.70–7.67 (m, 2H), 7.54–7.50 (m, 2H), 7.45–7.42 (m, 1H), 7.37–7.33 (m, 2H), 7.30–7.25 (m, 3H), 5.21 (br s, 2H), 4.64 (br s, 2H), 4.27 (t, *J* = 7.3 Hz, 2H), 2.83–2.79 (m, 2H), 1.90–1.83 (m, 2H), 1.68–1.58 (m, 2H), 1.33–1.24 (m, 6H), 1.01 (t, *J* = 7.3 Hz, 3H), 0.85 (t, *J* = 7.0 Hz, 3H). **¹³C NMR** (126 MHz, CDCl₃): δ = 162.6 (C_q), 145.3 (C_q), 144.2 (C_q), 140.9 (C_q), 137.6 (C_q), 137.3 (C_q), 137.1 (C_q), 129.1 (CH), 129.1 (CH), 128.9 (CH), 128.2 (CH), 128.0 (CH), 127.6 (CH), 126.9 (CH), 125.5 (CH), 124.2 (C_q), 124.0 (CH), 121.6 (CH), 116.5 (C_q), 50.5 (CH₂), 40.0 (CH₂), 35.1 (CH₂), 31.3 (CH₂), 30.4 (CH₂), 30.3 (CH₂), 26.4 (CH₂), 23.7 (CH₂), 22.6 (CH₂), 14.7 (CH₃), 14.1 (CH₃). **IR** (ATR): 2954, 2928,

5 Experimental Part

2868, 1640, 1614, 1452, 1314, 1046, 761, 696 cm^{-1} . **MS** (ESI) m/z (relative intensity): 1059 (63) $[2\text{M}+\text{Na}]^+$, 841 (16), 519 (100) $[\text{M}+\text{H}]^+$, 323 (73). **HR-MS** (ESI) m/z calcd for $\text{C}_{34}\text{H}_{39}\text{N}_4\text{O}$ $[\text{M}+\text{H}]^+$ 519.3118, found 519.3104.

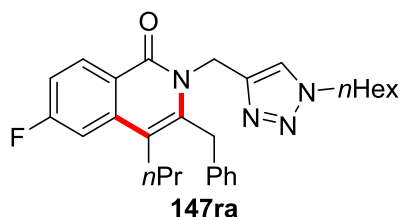
3-Benzyl-2-[(1-*n*-hexyl-1*H*-1,2,3-triazol-4-yl)methyl]-4-*n*-propyl-6-(trifluoromethyl)-isoquinolin-1(2*H*)-one (147qa)



The general procedure **G** was followed using **118q** (106 mg, 0.30 mmol) and propargyl acetate **158a** (130 mg, 0.60 mmol). Purification by column chromatography (*n*hexane/EtOAc: 3/2) yielded **147qa** (133 mg, 87%) as a white solid.

M.p. = 133–134 °C. **^1H NMR** (600 MHz, CDCl_3): δ = 8.59 (d, J = 8.4 Hz, 1H), 7.96 (s, 1H), 7.73 (s, 1H), 7.67 (dd, J = 8.4, 1.3 Hz, 1H), 7.35 (dd, J = 7.6, 7.6 Hz, 2H), 7.29–7.24 (m, 3H), 5.19 (br s, 2H), 4.66 (br s, 2H), 4.27 (t, J = 7.3 Hz, 2H), 2.79–2.74 (m, 2H), 1.90–1.83 (m, 2H), 1.62–1.53 (m, 2H), 1.32–1.24 (m, 6H), 1.01 (t, J = 7.3 Hz, 3H), 0.84 (t, J = 7.0 Hz, 3H). **^{13}C NMR** (126 MHz, CDCl_3): δ = 161.9 (C_q), 143.7 (C_q), 139.0 (C_q), 136.9 (C_q), 136.8 (C_q), 134.01 (q, $^2J_{\text{C-F}}$ = 32.1 Hz, C_q), 129.4 (CH), 129.2 (CH), 127.9 (CH), 127.3 (C_q), 127.1 (CH), 124.1 (CH), 124.0 (q, $^1J_{\text{C-F}}$ = 272.7 Hz, C_q), 122.1 (q, $^3J_{\text{C-F}}$ = 3.1 Hz, CH), 120.5 (q, $^3J_{\text{C-F}}$ = 4.0 Hz, CH), 116.2 (C_q), 50.6 (CH_2), 40.2 (CH_2), 35.1 (CH_2), 31.3 (CH_2), 30.3 (CH_2), 26.3 (CH_2), 23.6 (CH_2), 22.6 (CH_2), 14.5 (CH_3), 14.1 (CH_3). **^{19}F NMR** (282 MHz, CDCl_3): δ = -62.93 (s). **IR** (ATR): 2955, 2873, 1651, 1360, 1315, 1125, 1074, 795, 724, 696 cm^{-1} . **MS** (ESI) m/z (relative intensity): 1043 (31) $[2\text{M}+\text{Na}]^+$, 511 (100) $[\text{M}+\text{H}]^+$. **HR-MS** (ESI) m/z calcd for $\text{C}_{29}\text{H}_{34}\text{F}_3\text{N}_4\text{O}$ $[\text{M}+\text{H}]^+$ 511.2679, found 511.2678.

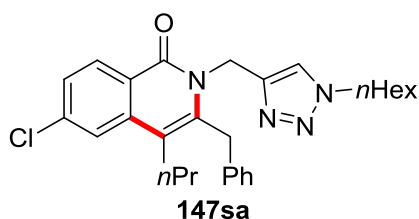
3-Benzyl-6-fluoro-2-[(1-*n*-hexyl-1*H*-1,2,3-triazol-4-yl)methyl]-4-*n*-propylisoquinolin-1(2*H*)-one (147ra)



The general procedure **G** was followed using **118r** (91.3 mg, 0.30 mmol) and propargyl acetate **158a** (130 mg, 0.60 mmol). Purification by column chromatography (*n*hexane/EtOAc: 3/2) yielded **147ra** (100 mg, 73%) as a white solid.

M.p. = 135–137 °C. **¹H NMR** (600 MHz, CDCl₃): δ = 8.48 (dd, *J* = 8.9, 6.1 Hz, 1H), 7.72 (s, 1H), 7.36–7.30 (m, 3H), 7.28–7.24 (m, 3H), 7.18 (ddd, *J* = 8.4, 8.4, 2.3 Hz, 1H), 5.16 (br s, 2H), 4.61 (br s, 2H), 4.26 (t, *J* = 7.3 Hz, 2H), 2.70–2.64 (m, 2H), 1.89–1.82 (m, 2H), 1.59–1.51 (m, 2H), 1.32–1.24 (m, 6H), 0.99 (t, *J* = 7.3 Hz, 3H), 0.84 (t, *J* = 6.8 Hz, 3H). **¹³C NMR** (126 MHz, CDCl₃): δ = 165.6 (d, ¹*J*_{C-F} = 250.9 Hz, C_q), 162.0 (C_q), 144.0 (C_q), 139.2 (d, ³*J*_{C-F} = 9.7 Hz, C_q), 138.7 (C_q), 137.1 (C_q), 131.5 (d, ³*J*_{C-F} = 10.1 Hz, CH), 129.2 (CH), 127.9 (CH), 127.0 (CH), 124.0 (CH), 121.9 (C_q), 115.9 (d, ⁴*J*_{C-F} = 3.3 Hz, C_q), 114.8 (d, ²*J*_{C-F} = 23.4 Hz, CH), 108.4 (d, ²*J*_{C-F} = 22.8 Hz, CH), 50.5 (CH₂), 39.9 (CH₂), 35.1 (CH₂), 31.3 (CH₂), 30.6 (CH₂), 30.3 (CH₂), 26.4 (CH₂), 23.4 (CH₂), 22.6 (CH₂), 14.6 (CH₃), 14.1 (CH₃). **¹⁹F NMR** (282 MHz, CDCl₃): δ = -105.94 – -106.06 (m). **IR** (ATR): 2952, 2929, 2868, 1650, 1601, 1342, 1165, 787, 724, 699 cm⁻¹. **MS** (ESI) *m/z* (relative intensity): 943 (100) [2M+Na]⁺, 921 (8) [2M+H]⁺, 483 (36) [M+Na]⁺, 461 (94) [M+H]⁺. **HR-MS** (ESI) *m/z* calcd for C₂₈H₃₄FN₄O [M+H]⁺ 461.2711, found 461.2705.

3-Benzyl-6-chloro-2-[(1-*n*-hexyl-1*H*-1,2,3-triazol-4-yl)methyl]-4-*n*-propylisoquinolin-1(2*H*)-one (147sa)

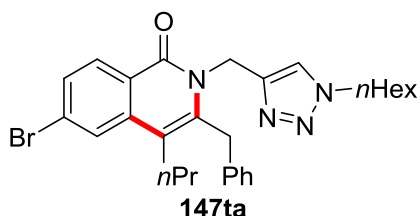


5 Experimental Part

The general procedure **G** was followed using **118s** (96.2 mg, 0.30 mmol) and propargyl acetate **158a** (130 mg, 0.60 mmol). Purification by column chromatography (*n*hexane/EtOAc: 3/2) yielded **147sa** (118 mg, 80%) as a pale yellow solid.

M.p. = 146–147 °C. **¹H NMR** (600 MHz, CDCl₃): δ = 8.40 (d, *J* = 8.6 Hz, 1H), 7.71 (s, 1H), 7.66 (d, *J* = 1.9 Hz, 1H), 7.42 (dd, *J* = 8.6, 1.9 Hz, 1H), 7.34 (dd, *J* = 7.6, 7.6 Hz, 2H), 7.28–7.23 (m, 3H), 5.16 (s, 2H), 4.61 (s, 2H), 4.26 (t, *J* = 7.3 Hz, 2H), 2.71–2.66 (m, 2H), 1.89–1.83 (m, 2H), 1.59–1.52 (m, 2H), 1.31–1.25 (m, 6H), 1.00 (t, *J* = 7.3 Hz, 3H), 0.84 (t, *J* = 7.0 Hz, 3H). **¹³C NMR** (126 MHz, CDCl₃): δ = 162.1 (C_q), 143.9 (C_q), 139.1 (C_q), 138.8 (C_q), 138.1 (C_q), 137.0 (C_q), 130.1 (CH), 129.2 (CH), 127.9 (CH), 127.0 (CH), 126.6 (CH), 124.0 (CH), 123.6 (C_q), 122.7 (CH), 115.6 (C_q), 50.5 (CH₂), 40.0 (CH₂), 35.1 (CH₂), 31.3 (CH₂), 30.4 (CH₂), 30.3 (CH₂), 26.4 (CH₂), 23.5 (CH₂), 22.6 (CH₂), 14.6 (CH₃), 14.1 (CH₃). **IR** (ATR): 3134, 2949, 2918, 1648, 1600, 1335, 1055, 831, 787, 723 cm⁻¹. **MS** (EI) *m/z* (relative intensity): 476 (83) [³⁵Cl, M]⁺, 310 (89), 282 (89), 242 (80), 112 (100), 85 (88). **HR-MS** (EI) *m/z* calcd for C₂₈H₃₃³⁵ClN₄O [M]⁺ 476.2343, found 476.2343.

3-Benzyl-6-bromo-2-[(1-*n*-hexyl-1*H*-1,2,3-triazol-4-yl)methyl]-4-*n*-propylisoquinolin-1(2*H*)-one (**147ta**)

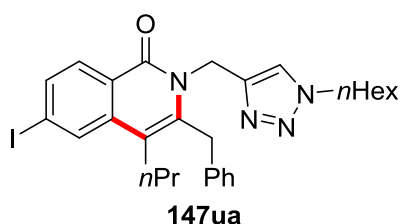


The general procedure **G** was followed using **118t** (110 mg, 0.30 mmol) and propargyl acetate **158a** (130 mg, 0.60 mmol). Purification by column chromatography (*n*hexane/EtOAc: 3/2) yielded **147ta** (112 mg, 71%) as a white solid.

M.p. = 144–145 °C. **¹H NMR** (600 MHz, CDCl₃): δ = 8.32 (d, *J* = 8.6 Hz, 1H), 7.83 (d, *J* = 1.6 Hz, 1H), 7.71 (s, 1H), 7.57 (dd, *J* = 8.6, 1.6 Hz, 1H), 7.34 (dd, *J* = 7.6, 7.6 Hz, 2H), 7.27–7.23 (m, 3H), 5.15 (br s, 2H), 4.61 (br s, 2H), 4.26 (t, *J* = 7.3 Hz, 2H), 2.71–2.65 (m, 2H), 1.89–1.81 (m, 2H), 1.59–1.51 (m, 2H), 1.32–1.23 (m, 6H), 1.00 (t, *J* = 7.3 Hz, 3H), 0.84 (t, *J* = 6.8 Hz, 3H). **¹³C NMR** (126 MHz, CDCl₃): δ = 162.2 (C_q), 143.9 (C_q), 138.8 (C_q), 138.3 (C_q), 137.0 (C_q), 130.1 (CH), 129.4 (CH), 129.2 (CH), 127.9 (CH), 127.9 (C_q), 127.0 (CH), 125.9 (CH), 124.0 (CH), 123.9 (C_q), 115.5 (C_q),

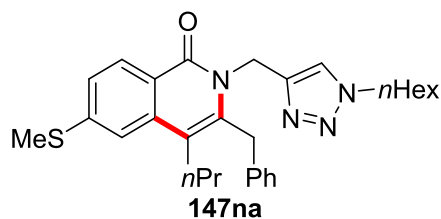
50.5 (CH₂), 40.0 (CH₂), 35.1 (CH₂), 31.3 (CH₂), 30.3 (CH₂), 30.3 (CH₂), 26.3 (CH₂), 23.5 (CH₂), 22.6 (CH₂), 14.6 (CH₃), 14.1 (CH₃). **IR** (ATR): 3134, 2949, 2917, 1647, 1598, 1377, 1055, 821, 786, 722 cm⁻¹. **MS** (EI) *m/z* (relative intensity): 522 (55) [⁸¹Br, M]⁺, 354 (54), 326 (58), 242 (80), 112 (100), 85 (75). **HR-MS** (EI) *m/z* calcd for C₂₈H₃₃⁸¹BrN₄O [M]⁺ 522.1817, found 522.1803.

3-Benzyl-2-[(1-*n*-hexyl-1H-1,2,3-triazol-4-yl)methyl]-6-iodo-4-*n*-propylisoquinolin-1(2*H*)-one (147ua)



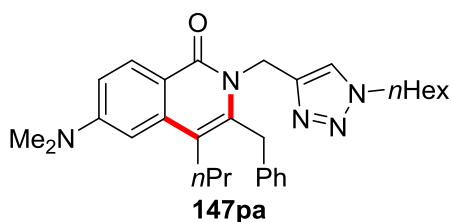
The general procedure **G** was followed using **118u** (124 mg, 0.30 mmol) and propargyl acetate **158a** (130 mg, 0.60 mmol). Purification by column chromatography (*n*hexane/EtOAc: 3/2) yielded **147ua** (100 mg, 59%) as a white solid.

M.p. = 131–133 °C. **¹H NMR** (600 MHz, CDCl₃): δ = 8.15 (d, *J* = 8.5 Hz, 1H), 8.06 (d, *J* = 1.5 Hz, 1H), 7.77 (dd, *J* = 8.4, 1.5 Hz, 1H), 7.71 (s, 1H), 7.34 (dd, *J* = 7.5, 7.5 Hz, 2H), 7.28–7.22 (m, 3H), 5.15 (br s, 2H), 4.60 (br s, 2H), 4.26 (t, *J* = 7.4 Hz, 2H), 2.71–2.65 (m, 2H), 1.89–1.82 (m, 2H), 1.59–1.50 (m, 2H), 1.31–1.24 (m, 6H), 0.99 (t, *J* = 7.3 Hz, 3H), 0.84 (t, *J* = 7.0 Hz, 3H). **¹³C NMR** (126 MHz, CDCl₃): δ = 162.4 (C_q), 143.9 (C_q), 138.6 (C_q), 138.3 (C_q), 137.0 (C_q), 135.1 (CH), 132.3 (CH), 129.9 (CH), 129.2 (CH), 127.9 (CH), 127.0 (CH), 124.4 (C_q), 124.0 (CH), 115.2 (C_q), 100.8 (C_q), 50.5 (CH₂), 40.1 (CH₂), 35.1 (CH₂), 31.3 (CH₂), 30.3 (CH₂), 30.2 (CH₂), 26.4 (CH₂), 23.6 (CH₂), 22.6 (CH₂), 14.6 (CH₃), 14.1 (CH₃). **IR** (ATR): 2949, 2915, 1647, 1596, 1583, 1377, 1174, 1055, 786, 722 cm⁻¹. **MS** (ESI) *m/z* (relative intensity): 1159 (64) [2M+Na]⁺, 591 (31) [M+Na]⁺, 569 (100) [M+H]⁺, 263 (41). **HR-MS** (ESI) *m/z* calcd for C₂₈H₃₄IN₄O [M+H]⁺ 569.1772, found 569.1771.

3-Benzyl-2-[(1-*n*-hexyl-1*H*-1,2,3-triazol-4-yl)methyl]-6-(methylthio)-4-*n*-propylisoquinolin-1(2*H*)-one (147na)

The general procedure **G** was followed using **118n** (99.7 mg, 0.30 mmol) and propargyl acetate **158a** (130 mg, 0.60 mmol). Purification by column chromatography (*n*hexane/EtOAc: 3/2) yielded **147na** (118 mg, 80%) as a white solid.

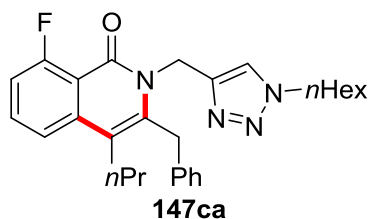
M.p. = 111–112 °C. **¹H NMR** (600 MHz, CDCl₃): δ = 8.36 (d, *J* = 8.5 Hz, 1H), 7.73 (s, 1H), 7.46 (d, *J* = 1.6 Hz, 1H), 7.35–7.32 (m, 3H), 7.27–7.24 (m, 3H), 5.17 (s, 2H), 4.60 (s, 2H), 4.26 (t, *J* = 7.3 Hz, 2H), 2.73–2.69 (m, 2H), 2.58 (s, 3H), 1.89–1.82 (m, 2H), 1.61–1.54 (m, 2H), 1.31–1.25 (m, 6H), 1.00 (t, *J* = 7.3 Hz, 3H), 0.85 (t, *J* = 6.9 Hz, 3H). **¹³C NMR** (126 MHz, CDCl₃): δ = 162.4 (C_q), 144.7 (C_q), 144.1 (C_q), 138.0 (C_q), 137.2 (C_q), 137.1 (C_q), 129.1 (CH), 128.6 (CH), 127.9 (CH), 126.9 (CH), 124.1 (CH), 123.9 (CH), 122.2 (C_q), 118.7 (CH), 115.7 (C_q), 50.6 (CH₂), 39.9 (CH₂), 35.0 (CH₂), 31.3 (CH₂), 30.4 (CH₂), 30.3 (CH₂), 26.3 (CH₂), 23.5 (CH₂), 22.6 (CH₂), 15.3 (CH₃), 14.6 (CH₃), 14.1 (CH₃). **IR** (ATR): 3125, 2949, 2921, 1645, 1601, 1587, 1178, 834, 787, 722 cm⁻¹. **MS** (EI) *m/z* (relative intensity): 488 (100) [M]⁺, 375 (50), 322 (81), 294 (74), 242 (42), 112 (72). **HR-MS** (ESI) *m/z* calcd for C₂₉H₃₇N₄OS [M+H]⁺ 489.2683, found 489.2680.

3-Benzyl-6-(dimethylamino)-2-[(1-*n*-hexyl-1*H*-1,2,3-triazol-4-yl)methyl]-4-*n*-propyl-isoquinolin-1(2*H*)-one (147pa)

The general procedure **G** was followed using **118p** (95.8 mg, 0.30 mmol) and propargyl acetate **158a** (130 mg, 0.60 mmol). Purification by column chromatography (*n*hexane/EtOAc: 3/2) yielded **147pa** (95.8 mg, 66%) as an off-white solid.

M.p. = 118–120 °C. **¹H NMR** (600 MHz, CDCl₃): δ = 8.33 (d, *J* = 9.0 Hz, 1H), 7.71 (s, 1H), 7.34–7.30 (m, 2H), 7.27–7.22 (m, 3H), 6.95 (dd, *J* = 9.0, 1.8 Hz, 1H), 6.78 (s, 1H), 5.15 (s, 2H), 4.54 (s, 2H), 4.24 (t, *J* = 7.4 Hz, 2H), 3.11 (s, 6H), 2.71–2.66 (m, 2H), 1.88–1.81 (m, 2H), 1.62–1.55 (m, 2H), 1.31–1.24 (m, 6H), 0.98 (t, *J* = 7.4 Hz, 3H), 0.86–0.83 (m, 3H). **¹³C NMR** (126 MHz, CDCl₃): δ = 162.5 (C_q), 152.7 (C_q), 144.8 (C_q), 138.2 (C_q), 137.6 (C_q), 137.3 (C_q), 129.7 (CH), 129.0 (CH), 128.0 (CH), 126.7 (CH), 123.9 (CH), 115.9 (C_q), 112.6 (CH), 112.6 (CH), 103.0 (C_q), 50.5 (CH₂), 40.6 (CH₃), 40.6 (CH₃), 39.6 (CH₂), 35.1 (CH₂), 31.3 (CH₂), 30.6 (CH₂), 30.3 (CH₂), 26.3 (CH₂), 23.2 (CH₂), 22.6 (CH₂), 14.8 (CH₃), 14.1 (CH₃). **IR** (ATR): 2952, 2927, 1633, 1609, 1579, 1395, 1187, 826, 792, 698 cm⁻¹. **MS** (EI) *m/z* (relative intensity): 485 (57) [M]⁺, 457 (38), 372 (100), 319 (63), 291 (83), 91 (34). **HR-MS** (ESI) *m/z* calcd for C₃₀H₄₀N₅O [M+H]⁺ 486.3227, found 486.3224.

3-Benzyl-8-fluoro-2-[(1-*n*-hexyl-1*H*-1,2,3-triazol-4-yl)methyl]-4-*n*-propylisoquinolin-1(2*H*)-one (147ca)



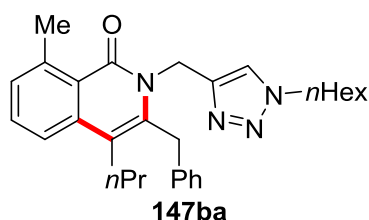
The general procedure **G** was followed using **118c** (91.3 mg, 0.30 mmol) and propargyl acetate **158a** (130 mg, 0.60 mmol). Purification by column chromatography (*n*hexane/EtOAc = 3/2) yielded **147ca** (80.2 mg, 58%) as a white solid.

M.p. = 133–135 °C. **¹H NMR** (600 MHz, CDCl₃): δ = 7.83 (s, 1H), 7.61 (ddd, *J* = 8.1, 8.1, 5.1 Hz, 1H), 7.48 (d, *J* = 8.3 Hz, 1H), 7.34 (dd, *J* = 7.6, 7.6 Hz, 2H), 7.26 (dd, *J* = 7.6, 7.6 Hz, 3H), 7.11 (dd, *J* = 11.5, 8.0 Hz, 1H), 5.12 (br s, 2H), 4.65 (br s, 2H), 4.26 (t, *J* = 7.3 Hz, 2H), 2.73–2.67 (m, 2H), 1.89–1.82 (m, 2H), 1.59–1.50 (m, 2H), 1.32–1.24 (m, 6H), 0.98 (t, *J* = 7.3 Hz, 3H), 0.84 (t, *J* = 7.0 Hz, 3H). **¹³C NMR** (126 MHz, CDCl₃): δ = 162.9 (d, ¹*J*_{C-F} = 262.9 Hz, C_q), 160.0 (d, ³*J*_{C-F} = 4.8 Hz, C_q), 143.9 (C_q), 139.6 (C_q), 138.7 (C_q), 137.1 (C_q), 133.0 (d, ³*J*_{C-F} = 10.3 Hz, CH), 129.1 (CH), 127.9 (CH), 127.0 (CH), 124.5 (CH), 118.9 (d, ⁴*J*_{C-F} = 4.4 Hz, CH), 115.5 (d, ⁵*J*_{C-F} = 1.9 Hz, C_q), 114.6 (d, ³*J*_{C-F} = 4.1 Hz, C_q), 113.0 (d, ²*J*_{C-F} = 22.1 Hz, CH), 50.5 (CH₂), 39.8 (CH₂), 35.1 (CH₂), 31.3 (CH₂), 30.9 (CH₂), 30.3 (CH₂), 26.4 (CH₂), 23.4

5 Experimental Part

(CH₂), 22.6 (CH₂), 14.6 (CH₃), 14.1 (CH₃). ¹⁹F NMR (282 MHz, CDCl₃): δ = -110.53 (dd, *J* = 11.7, 5.1 Hz). IR (ATR): 3130, 2957, 2928, 1645, 1596, 1306, 1051, 811, 768, 708 cm⁻¹. MS (EI) *m/z* (relative intensity): 460 (55) [M]⁺, 347 (24), 294 (100), 266 (63), 242 (28), 112 (34). HR-MS (EI) *m/z* calcd for C₂₈H₃₃FN₄O [M]⁺ 460.2638 found 460.2620.

3-Benzyl-2-[(1-*n*-hexyl-1*H*-1,2,3-triazol-4-yl)methyl]-8-methyl-4-*n*-propylisoquinolin-1(2*H*)-one (147ba)



The general procedure **G** was followed using **118b** (90.1 mg, 0.30 mmol) and propargyl acetate **158a** (130 mg, 0.60 mmol). Purification by column chromatography (*n*hexane/EtOAc: 3/2) yielded **147ba** (46.3 mg, 34%) as a pale yellow solid.

M.p. = 101–102 °C. ¹H NMR (600 MHz, CDCl₃): δ = 7.71 (s, 1H), 7.57 (d, *J* = 8.1 Hz, 1H), 7.54–7.51 (m, 1H), 7.35–7.32 (m, 2H), 7.27–7.23 (m, 4H), 5.14 (br s, 2H), 4.56 (br s, 2H), 4.27 (t, *J* = 7.3 Hz, 2H), 2.97 (s, 3H), 2.73–2.67 (m, 2H), 1.89–1.82 (m, 2H), 1.59–1.52 (m, 2H), 1.31–1.25 (m, 6H), 0.98 (t, *J* = 7.3 Hz, 3H), 0.85 (t, *J* = 7.0 Hz, 3H). ¹³C NMR (126 MHz, CDCl₃): δ = 163.4 (C_q), 144.6 (C_q), 142.1 (C_q), 138.3 (C_q), 137.5 (C_q), 137.1 (C_q), 131.5 (CH), 129.5 (CH), 129.1 (CH), 128.0 (CH), 126.8 (CH), 124.0 (C_q), 123.9 (CH), 121.3 (CH), 116.0 (C_q), 50.5 (CH₂), 40.0 (CH₂), 35.1 (CH₂), 31.3 (CH₂), 30.9 (CH₂), 30.3 (CH₂), 26.4 (CH₂), 24.9 (CH₃), 23.4 (CH₂), 22.6 (CH₂), 14.6 (CH₃), 14.1 (CH₃). IR (ATR): 2956, 2928, 2869, 1770, 1644, 1600, 1305, 1049, 785, 697 cm⁻¹. MS (EI) *m/z* (relative intensity): 456 (96) [M]⁺, 343 (22), 290 (100), 262 (91), 242 (42), 112 (50). HR-MS (EI) *m/z* calcd for C₂₉H₃₆N₄O [M]⁺ 456.2889, found 456.2896.

(*n*hexane/EtOAc: 3/2) yielded **147ea** (51.5 mg, 37%) and **147ea'** (58.2 mg, 42%) as white solids.

3-Benzyl-7-fluoro-2-[(1-*n*-hexyl-1*H*-1,2,3-triazol-4-yl)methyl]-4-*n*-propylisoquinolin-1(2*H*)-one (147ea):

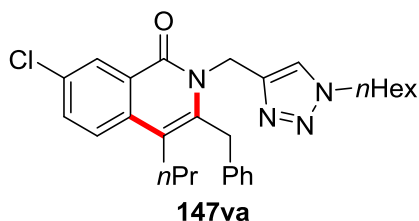
M.p. = 141–143 °C. **¹H NMR** (600 MHz, CDCl₃): δ = 8.11 (dd, *J* = 9.3, 2.9 Hz, 1H), 7.73 (s, 1H), 7.71 (dd, *J* = 9.1, 5.0 Hz, 1H), 7.42 (ddd, *J* = 8.9, 8.1, 2.9 Hz, 1H), 7.34 (dd, *J* = 7.5, 7.5 Hz, 2H), 7.28–7.25 (m, 3H), 5.17 (br s, 2H), 4.61 (br s, 2H), 4.27 (t, *J* = 7.3 Hz, 2H), 2.75–2.70 (m, 2H), 1.89–1.82 (m, 2H), 1.59–1.51 (m, 2H), 1.32–1.24 (m, 6H), 0.99 (t, *J* = 7.3 Hz, 3H), 0.84 (t, *J* = 7.0 Hz, 3H). **¹³C NMR** (126 MHz, CDCl₃): δ = 161.9 (d, ⁴*J*_{C-F} = 3.4 Hz, C_q), 161.0 (d, ¹*J*_{C-F} = 246.7 Hz, C_q), 144.0 (C_q), 137.3 (C_q), 136.4 (d, ⁵*J*_{C-F} = 2.4 Hz, C_q), 133.4 (C_q), 129.1 (CH), 127.9 (CH), 127.0 (CH), 126.9 (d, ³*J*_{C-F} = 7.9 Hz, C_q), 125.7 (d, ³*J*_{C-F} = 7.6 Hz, CH), 124.0 (CH), 121.1 (d, ²*J*_{C-F} = 23.3 Hz, CH), 116.0 (C_q), 113.2 (d, ²*J*_{C-F} = 22.4 Hz, CH), 50.5 (CH₂), 40.1 (CH₂), 34.9 (CH₂), 31.3 (CH₂), 30.6 (CH₂), 30.3 (CH₂), 26.4 (CH₂), 23.7 (CH₂), 22.6 (CH₂), 14.6 (CH₃), 14.1 (CH₃). **¹⁹F NMR** (282 MHz, CDCl₃): δ = -114.57 (ddd, *J* = 9.3, 8.1, 5.0 Hz). **IR** (ATR): 2954, 2920, 1648, 1600, 1493, 1346, 1057, 825, 725, 542 cm⁻¹. **MS** (EI) *m/z* (relative intensity): 460 (83) [M]⁺, 294 (92), 266 (100), 242 (61), 112 (62), 85 (48). **HR-MS** (EI) *m/z* calcd for C₂₈H₃₃FN₄O [M]⁺ 460.2638, found 460.2639.

3-Benzyl-5-fluoro-2-[(1-*n*-hexyl-1*H*-1,2,3-triazol-4-yl)methyl]-4-*n*-propylisoquinolin-1(2*H*)-one (147ea'):

M.p. = 142–144 °C. **¹H NMR** (600 MHz, CDCl₃): δ = 8.32 (dd, *J* = 7.9, 1.4 Hz, 1H), 7.73 (s, 1H), 7.41 (ddd, *J* = 7.9, 7.9, 4.6 Hz, 1H), 7.38–7.33 (m, 3H), 7.29–7.26 (m, 3H), 5.17 (br s, 2H), 4.61 (br s, 2H), 4.27 (t, *J* = 7.3 Hz, 2H), 2.81 (s, 2H), 1.89–1.82 (m, 2H), 1.60–1.52 (m, 2H), 1.33–1.24 (m, 6H), 0.97 (t, *J* = 7.3 Hz, 3H), 0.85 (t, *J* = 7.0 Hz, 3H). **¹³C NMR** (126 MHz, CDCl₃): δ = 161.6 (d, ⁴*J*_{C-F} = 3.0 Hz, C_q), 158.5 (d, ¹*J*_{C-F} = 252.6 Hz, C_q), 143.9 (C_q), 138.0 (C_q), 137.2 (C_q), 129.1 (CH), 127.9 (CH), 127.8 (d, ³*J*_{C-F} = 3.9 Hz, C_q), 127.0 (CH), 126.6 (d, ³*J*_{C-F} = 9.1 Hz, CH), 126.3 (d, ³*J*_{C-F} = 9.9 Hz, C_q), 124.5 (d, ⁴*J*_{C-F} = 3.5 Hz, CH), 124.0 (CH), 119.4 (d, ²*J*_{C-F} = 25.1 Hz, CH), 114.4 (d, ⁴*J*_{C-F} = 5.8 Hz, C_q), 50.5 (CH₂), 40.4 (CH₂), 34.6 (CH₂), 32.4 (d, ⁴*J*_{C-F} = 12.2 Hz, CH₂), 31.3 (CH₂), 30.3 (CH₂), 26.4 (CH₂), 24.6 (d, ⁵*J*_{C-F} = 3.7 Hz, CH₂), 22.6 (CH₂), 14.6 (CH₃), 14.1 (CH₃). **¹⁹F NMR** (282 MHz, CDCl₃): δ = -114.13 (ddd, *J* = 4.2, 2.9, 1.6 Hz). **IR** (ATR): 2957, 2930, 1649, 1594, 1228, 1063, 1007, 782,

755, 726 cm^{-1} . **MS** (EI) m/z (relative intensity): 460 (75) $[\text{M}]^+$, 294 (82), 266 (100), 242 (58), 112 (61), 85 (47). **HR-MS** (EI) m/z calcd for $\text{C}_{28}\text{H}_{33}\text{FN}_4\text{O}$ $[\text{M}]^+$ 460.2638, found 460.2641.

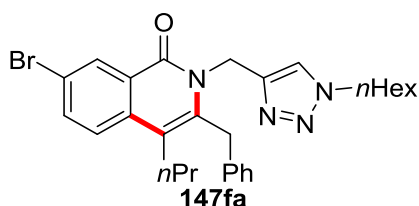
3-Benzyl-7-chloro-2-[(1-*n*-hexyl-1*H*-1,2,3-triazol-4-yl)methyl]-4-*n*-propylisoquinolin-1(2*H*)-one (147va)



The general procedure **G** was followed using **118v** (96.2 mg, 0.30 mmol) and propargyl acetate **158a** (130 mg, 0.60 mmol). Purification by column chromatography (*n*hexane/EtOAc: 3/2) yielded **147va** (78.9 mg, 55%) as an off-white solid.

M.p. = 138–139 °C. **^1H NMR** (600 MHz, CDCl_3): δ = 8.45 (d, J = 2.3 Hz, 1H), 7.72 (s, 1H), 7.66–7.61 (m, 2H), 7.36–7.32 (m, 2H), 7.28–7.23 (m, 3H), 5.17 (s, 2H), 4.61 (s, 2H), 4.26 (t, J = 7.3 Hz, 2H), 2.73–2.69 (m, 2H), 1.89–1.83 (m, 2H), 1.58–1.51 (m, 2H), 1.31–1.25 (m, 6H), 0.98 (t, J = 7.3 Hz, 3H), 0.85 (t, J = 7.0 Hz, 3H). **^{13}C NMR** (126 MHz, CDCl_3): δ = 161.7 (C_q), 143.9 (C_q), 137.6 (C_q), 137.1 (C_q), 135.1 (C_q), 132.8 (CH), 132.2 (C_q), 129.2 (CH), 127.9 (CH), 127.7 (CH), 127.0 (CH), 126.4 (C_q), 125.0 (CH), 124.1 (CH), 116.0 (C_q), 50.5 (CH_2), 40.1 (CH_2), 35.0 (CH_2), 31.3 (CH_2), 30.5 (CH_2), 30.3 (CH_2), 26.4 (CH_2), 23.6 (CH_2), 22.6 (CH_2), 14.6 (CH_3), 14.1 (CH_3). **IR** (ATR): 3134, 2953, 2923, 1648, 1595, 1304, 1055, 823, 724, 669 cm^{-1} . **MS** (EI) m/z (relative intensity): 476 (61) $[\text{M}]^+$, 310 (80), 282 (86), 242 (71), 112 (97), 69 (100). **HR-MS** (EI) m/z calcd for $\text{C}_{28}\text{H}_{33}^{35}\text{ClN}_4\text{O}$ $[\text{M}]^+$ 476.2343, found 476.2345.

3-Benzyl-7-bromo-2-[(1-*n*-hexyl-1*H*-1,2,3-triazol-4-yl)methyl]-4-*n*-propylisoquinolin-1(2*H*)-one (147fa)

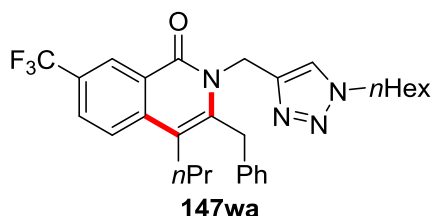


5 Experimental Part

The general procedure **G** was followed using **118f** (110 mg, 0.30 mmol) and propargyl acetate **158a** (130 mg, 0.60 mmol). Purification by column chromatography (*n*hexane/EtOAc: 3/2) yielded **147fa** (113 mg, 72%) as a white solid.

M.p. = 143–144 °C. **¹H NMR** (600 MHz, CDCl₃): δ = 8.61 (d, *J* = 2.2 Hz, 1H), 7.76 (dd, *J* = 8.8, 2.2 Hz, 1H), 7.72 (s, 1H), 7.58 (d, *J* = 8.8 Hz, 1H), 7.34 (dd, *J* = 7.5, 7.5 Hz, 2H), 7.28–7.23 (m, 3H), 5.17 (br s, 2H), 4.61 (br s, 2H), 4.26 (t, *J* = 7.3 Hz, 2H), 2.73–2.68 (m, 2H), 1.89–1.82 (m, 2H), 1.58–1.49 (m, 2H), 1.32–1.25 (m, 6H), 0.98 (t, *J* = 7.3 Hz, 3H), 0.85 (t, *J* = 7.0 Hz, 3H). **¹³C NMR** (126 MHz, CDCl₃): δ = 161.7 (C_q), 143.9 (C_q), 137.9 (C_q), 137.1 (C_q), 135.6 (CH), 135.5 (C_q), 130.9 (CH), 129.2 (CH), 128.0 (CH), 127.1 (CH), 126.7 (C_q), 125.2 (CH), 124.2 (CH), 120.1 (C_q), 116.1 (C_q), 50.5 (CH₂), 40.1 (CH₂), 34.9 (CH₂), 31.2 (CH₂), 30.3 (CH₂), 30.2 (CH₂), 26.3 (CH₂), 23.5 (CH₂), 22.5 (CH₂), 14.5 (CH₃), 14.0 (CH₃). **IR** (ATR): 2949, 2916, 1647, 1596, 1583, 1377, 1055, 813, 786, 722 cm⁻¹. **MS** (ESI) *m/z* (relative intensity): 1065 (44) [⁸¹Br, 2M+Na]⁺, 523 (100) [⁸¹Br, M+H]⁺. **HR-MS** (EI) *m/z* calcd for C₂₈H₃₄⁸¹BrN₄O [M+H]⁺ 523.1892, found 523.1890.

3-Benzyl-2-[(1-*n*-hexyl-1*H*-1,2,3-triazol-4-yl)methyl]-4-*n*-propyl-7-(trifluoromethyl) isoquinolin-1(2*H*)-one (**147wa**)



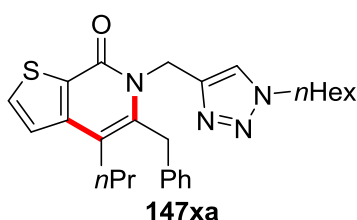
The general procedure **G** was followed using **118w** (106 mg, 0.30 mmol) and propargyl acetate **158a** (130 mg, 0.60 mmol). Purification by column chromatography (*n*hexane/EtOAc: 3/2) yielded **147wa** (102 mg, 66%) as a white solid.

M.p. = 116–117 °C. **¹H NMR** (300 MHz, CDCl₃): δ = 8.77 (s, 1H), 7.90–7.79 (m, 2H), 7.75 (s, 1H), 7.38–7.31 (m, 2H), 7.31–7.22 (m, 3H), 5.19 (s, 2H), 4.67 (s, 2H), 4.27 (t, *J* = 7.3 Hz, 2H), 2.80–2.71 (m, 2H), 1.92–1.80 (m, 2H), 1.65–1.49 (m, 2H), 1.36–1.20 (m, 6H), 1.01 (t, *J* = 7.3 Hz, 3H), 0.88–0.81 (m, 3H). **¹³C NMR** (126 MHz, CDCl₃): δ = 162.1 (C_q), 143.7 (C_q), 139.9 (C_q), 139.1 (C_q), 136.8 (C_q), 129.2 (CH), 128.4 (q, ³*J*_{C-F} = 3.2 Hz, CH), 128.2 (C_q), 127.9 (CH), 127.1 (CH), 126.1 (q, ³*J*_{C-F} = 3.6 Hz, CH), 125.0 (C_q), 124.2 (CH), 124.1 (CH), 124.1 (q, ¹*J*_{C-F} = 271.5 Hz, C_q), 116.0 (C_q), 50.6

5 Experimental Part

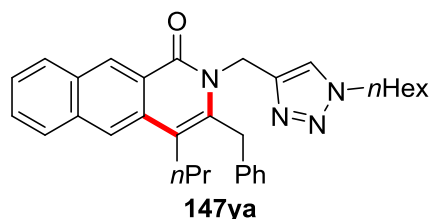
(CH₂), 40.1 (CH₂), 35.2 (CH₂), 31.3 (CH₂), 30.4 (CH₂), 30.3 (CH₂), 26.4 (CH₂), 23.6 (CH₂), 22.6 (CH₂), 14.6 (CH₃), 14.1 (CH₃). **¹⁹F NMR** (282 MHz, CDCl₃). δ = -62.38 (s). **IR** (ATR): 2931, 2872, 1655, 1622, 1323, 1297, 1130, 1030, 830, 714 cm⁻¹. **MS** (EI) *m/z* (relative intensity): 510 (63) [M]⁺, 344 (72), 316 (76), 242 (57), 112 (88), 85 (70), 43 (100). **HR-MS** (ESI) *m/z* calcd for C₂₉H₃₄F₃N₄O [M+H]⁺ 511.2679, found 511.2676.

5-Benzyl-6-[(1-*n*-hexyl-1*H*-1,2,3-triazol-4-yl)methyl]-4-*n*-propylthieno[2,3-*c*]pyridin-7(6*H*)-one (147xa)



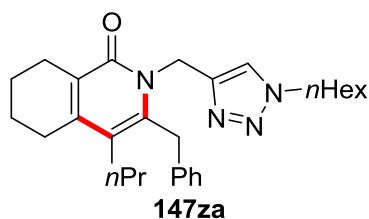
The general procedure **G** was followed using **118x** (87.7 mg, 0.30 mmol) and propargyl acetate **158a** (130 mg, 0.60 mmol). Purification by column chromatography (*n*hexane/EtOAc: 3/2) yielded **147xa** (64.6 mg, 48%) as an off-white solid.

M.p. = 100–102 °C. **¹H NMR** (600 MHz, CDCl₃): δ = 7.76 (s, 1H), 7.70 (d, *J* = 5.3 Hz, 1H), 7.35–7.31 (m, 2H), 7.29 (d, *J* = 5.3 Hz, 1H), 7.27–7.25 (m, 1H), 7.24–7.21 (m, 2H), 5.19 (s, 2H), 4.60 (s, 2H), 4.26 (t, *J* = 7.4 Hz, 2H), 2.72–2.67 (m, 2H), 1.88–1.82 (m, 2H), 1.59–1.52 (m, 2H), 1.31–1.24 (m, 6H), 0.95 (t, *J* = 7.3 Hz, 3H), 0.85 (t, *J* = 6.9 Hz, 3H). **¹³C NMR** (126 MHz, CDCl₃): δ = 158.9 (C_q), 146.2 (C_q), 144.0 (C_q), 138.4 (C_q), 137.4 (C_q), 133.1 (CH), 129.1 (CH), 128.7 (C_q), 127.9 (CH), 126.9 (CH), 124.2 (CH), 123.3 (CH), 116.4 (C_q), 50.5 (CH₂), 39.7 (CH₂), 34.5 (CH₂), 32.3 (CH₂), 31.3 (CH₂), 30.3 (CH₂), 26.4 (CH₂), 24.0 (CH₂), 22.6 (CH₂), 14.5 (CH₃), 14.1 (CH₃). **IR** (ATR): 2930, 2866, 1646, 1576, 1450, 1131, 787, 718, 694, 457 cm⁻¹. **MS** (ESI) *m/z* (relative intensity): 919 (81) [2M+Na]⁺, 897 (13) [2M+H]⁺, 471 (45) [M+Na]⁺, 449 (100) [M+H]⁺. **HR-MS** (ESI) *m/z* calcd for C₂₆H₃₃N₄OS [M+H]⁺ 449.2370, found 449.2377.

3-Benzyl-2-[(1-*n*-hexyl-1*H*-1,2,3-triazol-4-yl)methyl]-4-*n*-propylbenzo[*g*]isoquinolin-1(2*H*)-one (147ya)

The general procedure **G** was followed using **118y** (101 mg, 0.30 mmol) and propargyl acetate **158a** (130 mg, 0.60 mmol). Purification by column chromatography (*n*hexane/EtOAc: 3/2) yielded **147ya** (82.4 mg, 56%) as a yellow solid.

M.p. = 155–157 °C. **¹H NMR** (600 MHz, CDCl₃): δ = 9.09 (s, 1H), 8.15 (s, 1H), 8.05 (d, *J* = 8.3 Hz, 1H), 7.98 (d, *J* = 8.3 Hz, 1H), 7.75 (s, 1H), 7.59 (ddd, *J* = 8.1, 6.9, 1.0 Hz, 1H), 7.51 (ddd, *J* = 7.9, 6.9, 1.0 Hz, 1H), 7.36–7.30 (m, 4H), 7.28–7.25 (m, 1H), 5.21 (s, 2H), 4.63 (s, 2H), 4.26 (t, *J* = 7.3 Hz, 2H), 2.89–2.83 (m, 2H), 1.89–1.82 (m, 2H), 1.71–1.63 (m, 2H), 1.31–1.24 (m, 6H), 1.06 (t, *J* = 7.3 Hz, 3H), 0.84 (t, *J* = 7.0 Hz, 3H). **¹³C NMR** (126 MHz, CDCl₃): δ = 163.3 (C_q), 144.3 (C_q), 137.5 (C_q), 135.8 (C_q), 135.5 (C_q), 132.8 (C_q), 131.4 (C_q), 129.4 (CH), 129.2 (CH), 129.1 (CH), 128.1 (CH), 128.1 (CH), 128.0 (CH), 126.9 (CH), 126.0 (CH), 124.0 (CH), 124.0 (C_q), 121.6 (CH), 116.3 (C_q), 50.6 (CH₂), 39.8 (CH₂), 35.1 (CH₂), 31.3 (CH₂), 30.7 (CH₂), 30.3 (CH₂), 26.3 (CH₂), 23.5 (CH₂), 22.6 (CH₂), 14.7 (CH₃), 14.1 (CH₃). **IR** (ATR): 2926, 1641, 1619, 1380, 1218, 1047, 882, 795, 728, 477 cm⁻¹. **MS** (EI) *m/z* (relative intensity): 492 (69) [M]⁺, 401 (17), 326 (75), 298 (69), 112 (33), 91 (53). **HR-MS** (EI) *m/z* calcd for C₃₂H₃₆N₄O [M]⁺ 492.2889, found 492.2889.

3-Benzyl-2-[(1-*n*-hexyl-1*H*-1,2,3-triazol-4-yl)methyl]-4-*n*-propyl-5,6,7,8-tetrahydroisoquinolin-1(2*H*)-one (147za)

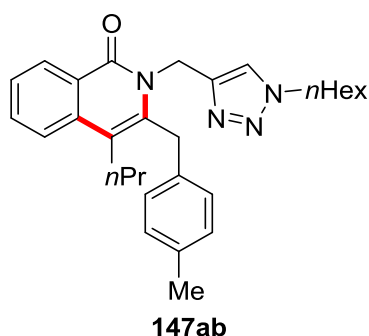
5 Experimental Part

The general procedure **G** was followed using **118z** (87.1 mg, 0.30 mmol) and propargyl acetate **158a** (130 mg, 0.60 mmol). Purification by column chromatography (*n*hexane/EtOAc: 3/2) yielded **147za** (29.7 mg, 22%) as a yellow oil.

¹H NMR (600 MHz, CDCl₃): δ = 7.75 (s, 1H), 7.32 (dd, *J* = 7.6, 7.6 Hz, 2H), 7.24 (dd, *J* = 7.3, 7.3 Hz, 1H), 7.18 (d, *J* = 7.3 Hz, 2H), 5.08 (s, 2H), 4.50 (s, 2H), 4.25 (t, *J* = 7.4 Hz, 2H), 2.58 (q, *J* = 6.5 Hz, 4H), 2.37–2.32 (m, 2H), 1.88–1.82 (m, 2H), 1.79–1.72 (m, 4H), 1.41–1.34 (m, 2H), 1.31–1.26 (m, 6H), 0.90 (t, *J* = 7.3 Hz, 3H), 0.85 (t, *J* = 7.0 Hz, 3H). **¹³C NMR** (126 MHz, CDCl₃): δ = 162.2 (C_q), 147.0 (C_q), 143.9 (C_q), 139.3 (C_q), 137.4 (C_q), 129.0 (CH), 127.9 (CH), 126.8 (CH), 125.7 (C_q), 124.3 (CH), 119.7 (C_q), 50.5 (CH₂), 40.0 (CH₂), 34.7 (CH₂), 31.3 (CH₂), 30.3 (CH₂), 30.3 (CH₂), 27.1 (CH₂), 26.3 (CH₂), 24.7 (CH₂), 24.0 (CH₂), 22.7 (CH₂), 22.6 (CH₂), 22.1 (CH₂), 14.6 (CH₃), 14.1 (CH₃). **IR** (ATR): 2951, 2923, 1644, 1591, 1484, 1302, 1302, 1056, 723, 657 cm⁻¹. **MS** (EI) *m/z* (relative intensity): 446 (57) [M]⁺, 418 (35), 333 (95), 280 (100), 252 (40), 91 (46). **HR-MS** (EI) *m/z* calcd for C₂₈H₃₈N₄O [M]⁺ 446.3046, found 446.3045.

5.6.2 Experimental Procedures and Analytical Data – Propargyl Acetates

2-[(1-*n*-Hexyl-1*H*-1,2,3-triazol-4-yl)methyl]-3-(4-methylbenzyl)-4-*n*-propylisoquinolin-1(2*H*)-one (**147ab**)

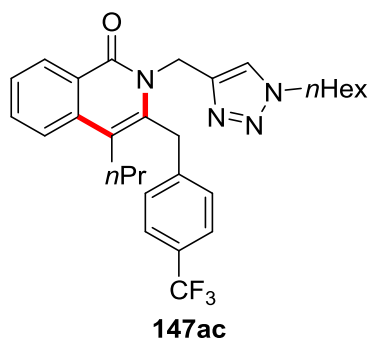


The general procedure **G** was followed using **118a** (85.9 mg, 0.30 mmol) and propargyl acetate **158b** (138 mg, 0.60 mmol). Purification by column chromatography (*n*hexane/EtOAc: 3/2) yielded **147ab** (118 mg, 86%) as a colorless oil.

¹H NMR (300 MHz, CDCl₃): δ = 8.48 (d, *J* = 7.8 Hz, 1H), 7.75–7.66 (m, 3H), 7.48 (ddd, *J* = 8.1, 6.0, 2.1 Hz, 1H), 7.14 (s, 4H), 5.19 (s, 2H), 4.56 (s, 2H), 4.26 (t, *J* = 7.3 Hz, 2H), 2.77–2.69 (m, 2H), 2.33 (s, 3H), 1.91–1.80 (m, 2H), 1.64–1.50 (m,

2H), 1.33–1.22 (m, 6H), 0.99 (t, $J = 7.3$ Hz, 3H), 0.84 (t, $J = 6.8$ Hz, 3H). ^{13}C NMR (75 MHz, CDCl_3): $\delta = 162.8$ (C_q), 144.3 (C_q), 137.4 (C_q), 136.9 (C_q), 136.6 (C_q), 134.3 (C_q), 132.5 (CH), 129.8 (CH), 128.3 (CH), 127.9 (CH), 126.2 (CH), 125.3 (C_q), 124.1 (CH), 123.2 (CH), 116.4 (C_q), 50.5 (CH_2), 39.9 (CH_2), 34.5 (CH_2), 31.2 (CH_2), 30.4 (CH_2), 30.2 (CH_2), 26.3 (CH_2), 23.6 (CH_2), 22.5 (CH_2), 21.2 (CH_3), 14.5 (CH_3), 14.0 (CH_3). IR (ATR): 2955, 2928, 2869, 1641, 1610, 1590, 1336, 1047, 772, 729 cm^{-1} . MS (EI) m/z (relative intensity): 456 (100) $[\text{M}]^+$, 343 (24), 290 (88), 262 (50), 256 (84), 112 (53), 85 (50). HR-MS (EI) m/z calcd for $\text{C}_{29}\text{H}_{36}\text{N}_4\text{O}$ $[\text{M}]^+$ 456.2889, found 456.2885.

2-[(1-*n*-Hexyl-1*H*-1,2,3-triazol-4-yl)methyl]-4-*n*-propyl-3-[4-(trifluoromethyl)benzyl]-isoquinolin-1(2*H*)-one (147ac)



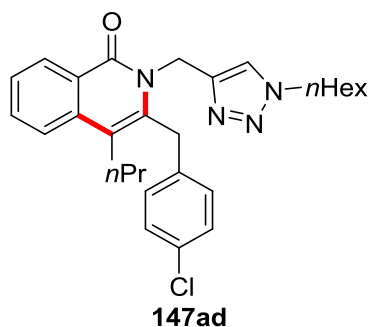
The general procedure **G** was followed using **118a** (85.9 mg, 0.30 mmol) and propargyl acetate **158c** (171 mg, 0.60 mmol). Purification by column chromatography (*n*hexane/EtOAc: 3/2) yielded **147ac** (81.3 mg, 53%) as a sticky yellow oil.

^1H NMR (300 MHz, CDCl_3): $\delta = 8.49$ (d, $J = 8.0$ Hz, 1H), 7.77–7.70 (m, 3H), 7.60 (d, $J = 8.1$ Hz, 2H), 7.50 (ddd, $J = 8.1, 5.0, 3.2$ Hz, 1H), 7.39 (d, $J = 8.0$ Hz, 2H), 5.13 (s, 2H), 4.69 (s, 2H), 4.26 (t, $J = 7.3$ Hz, 2H), 2.76–2.67 (m, 2H), 1.91–1.80 (m, 2H), 1.6–1.49 (m, 2H), 1.32–1.22 (m, 6H), 1.00 (t, $J = 7.2$ Hz, 3H), 0.84 (t, $J = 6.8$ Hz, 3H). ^{13}C NMR (126 MHz, CDCl_3): $\delta = 162.6$ (C_q), 143.9 (C_q), 141.7 (C_q), 136.6 (C_q), 136.1 (C_q), 132.6 (CH), 129.4 (q, $^2J_{\text{C-F}} = 32.4$ Hz, C_q), 128.3 (CH), 128.3 (CH), 126.5 (CH), 126.0 (q, $^3J_{\text{C-F}} = 3.7$ Hz, CH), 125.4 (C_q), 124.2 (q, $^1J_{\text{C-F}} = 271.5$ Hz, C_q), 124.2 (CH), 123.2 (CH), 116.8 (C_q), 50.6 (CH_2), 40.0 (CH_2), 34.9 (CH_2), 31.3 (CH_2), 30.5 (CH_2), 30.3 (CH_2), 26.3 (CH_2), 23.6 (CH_2), 22.6 (CH_2), 14.6 (CH_3), 14.1 (CH_2). ^{19}F NMR (282 MHz, CDCl_3): $\delta = -62.47$ (s). IR (ATR): 2957, 2931, 1643, 1611, 1592, 1322, 1162, 1121, 1066, 772 cm^{-1} . MS (ESI) m/z (relative intensity): 1043 (86) $[2\text{M}+\text{Na}]^+$,

5 Experimental Part

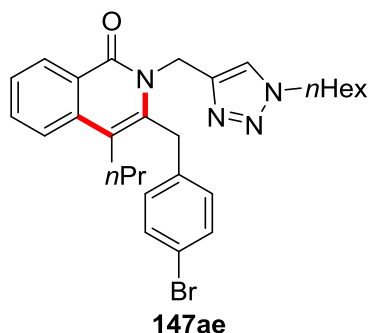
901 (5), 777 (3), 511 (100) $[M+H]^+$. **HR-MS** (ESI) m/z calcd for $C_{29}H_{34}F_3N_4O$ $[M+H]^+$ 511.2679, found 511.2674.

3-(4-Chlorobenzyl)-2-[(1-*n*-hexyl-1*H*-1,2,3-triazol-4-yl)methyl]-4-*n*-propylisoquinolin-1(2*H*)-one (147ad)



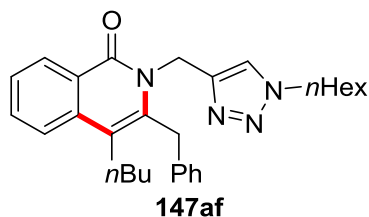
The general procedure **G** was followed using **118a** (85.9 mg, 0.30 mmol) and propargyl acetate **158d** (150 mg, 0.60 mmol). Purification by column chromatography (*n*hexane/EtOAc: 3/2) yielded **147ad** (111 mg, 78%) as a yellow oil.

1H NMR (600 MHz, $CDCl_3$): δ = 8.48 (d, J = 7.9 Hz, 1H), 7.74 (s, 1H), 7.73–7.68 (m, 2H), 7.49 (ddd, J = 8.1, 6.0, 2.1 Hz, 1H), 7.30 (d, J = 8.4 Hz, 2H), 7.19 (d, J = 8.4 Hz, 2H), 5.15 (s, 2H), 4.58 (s, 2H), 4.26 (t, J = 7.3 Hz, 2H), 2.73–2.68 (m, 2H), 1.88–1.82 (m, 2H), 1.59–1.52 (m, 2H), 1.31–1.24 (m, 6H), 0.99 (t, J = 7.3 Hz, 3H), 0.84 (t, J = 6.9 Hz, 3H). **^{13}C NMR** (126 MHz, $CDCl_3$): δ = 162.7 (C_q), 144.0 (C_q), 136.6 (C_q), 136.6 (C_q), 135.9 (C_q), 132.8 (C_q), 132.5 (CH), 129.3 (CH), 129.2 (CH), 128.3 (CH), 126.3 (CH), 125.3 (C_q), 124.1 (CH), 123.2 (CH), 116.6 (C_q), 50.6 (CH_2), 39.9 (CH_2), 34.4 (CH_2), 31.3 (CH_2), 30.4 (CH_2), 30.3 (CH_2), 26.3 (CH_2), 23.6 (CH_2), 22.6 (CH_2), 14.6 (CH_3), 14.1 (CH_3). **IR** (ATR): 3120, 2956, 2927, 1643, 1589, 1489, 1340, 1091, 769, 482 cm^{-1} . **MS** (ESI) m/z (relative intensity): 975 (61) $[2M+Na]^+$, 833 (5), 727 (5), 477 (100) $[M+H]^+$. **HR-MS** (ESI) m/z calcd for $C_{28}H_{34}^{35}ClN_4O$ $[M+H]^+$ 477.2416, found 477.2410.

3-(4-Bromobenzyl)-2-[(1-*n*-hexyl-1*H*-1,2,3-triazol-4-yl)methyl]-4-*n*-propylisoquinolin-1(2*H*)-one (147ae)

The general procedure **G** was followed using **118a** (85.9 mg, 0.30 mmol) and propargyl acetate **158e** (177 mg, 0.60 mmol). Purification by column chromatography (*n*hexane/EtOAc: 3/2) yielded **147ae** (137 mg, 88%) as a white solid.

M.p. = 51–53 °C. **¹H NMR** (300 MHz, CDCl₃): δ = 8.48 (d, *J* = 8.0 Hz, 1H), 7.77–7.66 (m, 3H), 7.54–7.41 (m, 3H), 7.14 (d, *J* = 8.1 Hz, 2H), 5.14 (s, 2H), 4.56 (s, 2H), 4.26 (t, *J* = 7.3 Hz, 2H), 2.76–2.64 (m, 2H), 1.92–1.79 (m, 2H), 1.63–1.48 (m, 2H), 1.28 (s, 6H), 0.99 (t, *J* = 7.3 Hz, 3H), 0.84 (t, *J* = 6.0 Hz, 3H). **¹³C NMR** (75 MHz, CDCl₃): δ = 162.8 (C_q), 144.1 (C_q), 136.7 (C_q), 136.6 (C_q), 136.5 (C_q), 132.6 (CH), 132.3 (CH), 129.8 (CH), 128.4 (CH), 126.4 (CH), 125.4 (C_q), 124.2 (CH), 123.2 (CH), 120.9 (C_q), 116.6 (C_q), 50.5 (CH₂), 39.9 (CH₂), 34.4 (CH₂), 31.2 (CH₂), 30.4 (CH₂), 30.2 (CH₂), 26.3 (CH₂), 23.6 (CH₂), 22.5 (CH₂), 14.5 (CH₃), 14.0 (CH₃). **IR** (ATR): 2954, 2928, 2869, 1641, 1590, 1486, 1010, 770, 727, 699 cm⁻¹. **MS** (EI) *m/z* (relative intensity): 522 (67) [⁸¹Br, M]⁺, 356 (47), 320 (50), 246 (100), 112 (61), 85 (60). **HR-MS** (EI) *m/z* calcd for C₂₈H₃₃⁸¹BrN₄O [M]⁺ 522.1824, found 522.1829.

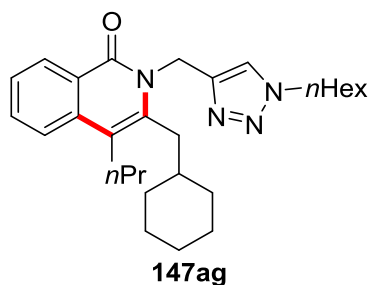
3-Benzyl-4-*n*-butyl-2-[(1-*n*-hexyl-1*H*-1,2,3-triazol-4-yl)methyl]isoquinolin-1(2*H*)-one (147af)

5 Experimental Part

The general procedure **G** was followed using **118a** (85.9 mg, 0.30 mmol) and propargyl acetate **158f** (138 mg, 0.60 mmol). Purification by column chromatography (*n*hexane/EtOAc: 3/2) yielded **147af** (48.5 mg, 35%) as an off-white solid.

M.p. = 97–99 °C. **¹H NMR** (400 MHz, CDCl₃): δ = 8.49 (d, *J* = 7.9 Hz, 1H), 7.75–7.68 (m, 3H), 7.48 (ddd, *J* = 8.1, 6.4, 1.7 Hz, 1H), 7.36–7.31 (m, 2H), 7.29–7.23 (m, 3H), 5.19 (s, 2H), 4.61 (s, 2H), 4.26 (t, *J* = 7.3 Hz, 2H), 2.79–2.72 (m, 2H), 1.90–1.82 (m, 2H), 1.57–1.48 (m, 2H), 1.46–1.36 (m, 2H), 1.32–1.24 (m, 6H), 0.91 (t, *J* = 7.2 Hz, 3H), 0.87–0.82 (m, 3H). **¹³C NMR** (101 MHz, CDCl₃): δ = 162.8 (C_q), 144.3 (C_q), 137.5 (C_q), 137.1 (C_q), 136.8 (C_q), 132.5 (CH), 129.2 (CH), 128.4 (CH), 128.1 (CH), 127.0 (CH), 126.2 (CH), 125.4 (C_q), 124.1 (CH), 123.2 (CH), 116.6 (C_q), 50.5 (CH₂), 39.9 (CH₂), 34.9 (CH₂), 32.5 (CH₂), 31.2 (CH₂), 30.2 (CH₂), 28.0 (CH₂), 26.3 (CH₂), 23.2 (CH₂), 22.5 (CH₃), 14.0 (CH₃). **IR** (ATR): 2954, 2928, 2858, 1650, 1597, 1313, 1031, 764, 714, 696 cm⁻¹. **MS** (ESI) *m/z* (relative intensity): 935 (80) [2M+Na]⁺, 779 (6), 489 (20) [M+Na]⁺, 457 (100) [M+H]⁺. **HR-MS** (ESI) *m/z* calcd for C₂₉H₃₇N₄O [M+H]⁺ 457.2962, found 457.2953.

3-(Cyclohexylmethyl)-2-[(1-*n*-hexyl-1*H*-1,2,3-triazol-4-yl)methyl]-4-*n*-propylisoquinolin-1(2*H*)-one (**147ag**)



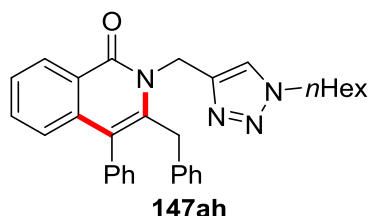
The general procedure **G** was followed using **118a** (85.9 mg, 0.30 mmol) and propargyl acetate **158g** (133 mg, 0.60 mmol). Purification by column chromatography (*n*hexane/EtOAc: 3/2) yielded **147ag** (78.2 mg, 58%) as white solid.

M.p. = 126–128 °C. **¹H NMR** (600 MHz, CDCl₃): δ = 8.44 (d, *J* = 8.0 Hz, 1H), 7.65–7.63 (m, 3H), 7.42 (ddd, *J* = 8.0, 4.9, 3.2 Hz, 1H), 5.45 (s, 2H), 4.23 (t, *J* = 7.3 Hz, 2H), 2.97 (s, 2H), 2.76–2.70 (m, 2H), 1.88–1.80 (m, 4H), 1.77–1.72 (m, 2H), 1.69–1.61 (m, 2H), 1.56–1.48 (m, 2H), 1.28–1.23 (m, 6H), 1.23–1.13 (m, 5H), 1.00 (t, *J* = 7.3 Hz, 3H), 0.85–0.81 (m, 3H). **¹³C NMR** (126 MHz, CDCl₃): δ = 162.8 (C_q),

5 Experimental Part

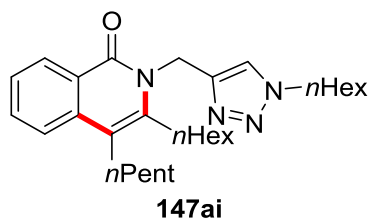
144.4 (C_q), 138.5 (C_q), 136.7 (C_q), 132.2 (CH), 128.2 (CH), 125.7 (CH), 124.9 (C_q), 123.7 (CH), 123.1 (CH), 115.5 (C_q), 50.5 (CH₂), 40.2 (CH₂), 39.4 (CH), 36.3 (CH₂), 33.4 (CH₂), 31.3 (CH₂), 30.4 (CH₂), 30.3 (CH₂), 26.8 (CH₂), 26.5 (CH₂), 26.3 (CH₂), 23.5 (CH₂), 22.6 (CH₂), 14.6 (CH₃), 14.1 (CH₃). **IR** (ATR): 2925, 2851, 1639, 1608, 1588, 1451, 1382, 1043, 768, 699 cm⁻¹. **MS** (EI) *m/z* (relative intensity): 448 (79) [M]⁺, 366 (72), 282 (100), 254 (55), 200 (56), 172 (70). **HR-MS** (ESI) *m/z* calcd for C₂₈H₄₁N₄O [M+H]⁺ 449.3275, found 449.3274.

3-Benzyl-2-[(1-*n*-hexyl-1*H*-1,2,3-triazol-4-yl)methyl]-4-phenylisoquinolin-1(2*H*)-one (147ah)



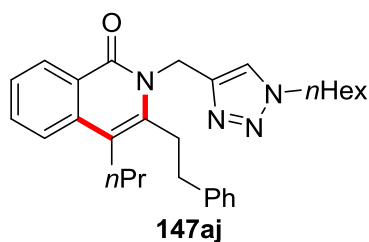
The general procedure **G** was followed using **118a** (85.9 mg, 0.30 mmol) and propargyl acetate **158h** (150 mg, 0.60 mmol). Purification by column chromatography (*n*hexane/EtOAc: 3/2) yielded **147ah** (117 mg, 83%) as a yellow oil.

¹H NMR (300 MHz, CDCl₃): δ = 8.55 (d, *J* = 7.9 Hz, 1H), 7.65 (s, 1H), 7.61–7.46 (m, 3H), 7.45–7.41 (m, 2H), 7.32–7.27 (m, 2H), 7.26–7.12 (m, 4H), 7.09–7.00 (m, 2H), 5.12 (s, 2H), 4.28 (t, *J* = 7.3 Hz, 2H), 3.85 (s, 2H), 1.94–1.82 (m, 2H), 1.36–1.26 (m, 6H), 0.88 (t, *J* = 6.8 Hz, 3H). **¹³C NMR** (126 MHz, CDCl₃): δ = 162.4 (C_q), 143.9 (C_q), 142.3 (C_q), 140.3 (C_q), 136.8 (C_q), 134.3 (C_q), 132.5 (CH), 129.9 (CH), 129.3 (CH), 128.8 (CH), 128.4 (CH), 128.2 (CH), 127.8 (CH), 126.6 (CH), 126.0 (CH), 125.8 (C_q), 124.5 (CH), 123.6 (CH), 113.2 (C_q), 50.4 (CH₂), 42.4 (CH₂), 34.8 (CH₂), 31.3 (CH₂), 30.3 (CH₂), 26.3 (CH₂), 22.6 (CH₂), 14.1 (CH₃). **IR** (ATR): 2929, 2857, 1644, 1589, 1485, 1320, 1047, 762, 696, 524 cm⁻¹. **MS** (EI) *m/z* (relative intensity): 476 (96) [M]⁺, 377 (25), 363 (53), 311 (100), 234 (46), 232 (44). **HR-MS** (ESI) *m/z* calcd for C₃₁H₃₃N₄O [M+H]⁺ 477.2649, found 477.2648.

3-*n*-Hexyl-2-[(1-*n*-hexyl-1*H*-1,2,3-triazol-4-yl)methyl]-4-*n*-pentylisoquinolin-1(2*H*)-one (147ai)

The general procedure **G** was followed using **118a** (85.9 mg, 0.30 mmol) and propargyl acetate **158i** (143 mg, 0.60 mmol). Purification by column chromatography (CH₂Cl₂/MeOH: 95/5) yielded **147ai** (88.6 mg, 64%) as a colorless oil.

¹H NMR (600 MHz, CDCl₃): δ = 8.44 (d, *J* = 7.9 Hz, 1H), 7.71 (s, 1H), 7.66–7.61 (m, 2H), 7.42 (ddd, *J* = 8.0, 6.0, 2.0 Hz, 1H), 5.40 (s, 2H), 4.25 (t, *J* = 7.3 Hz, 2H), 3.03 (s, 2H), 2.71–2.66 (m, 2H), 1.87–1.81 (m, 2H), 1.68–1.62 (m, 2H), 1.58–1.51 (m, 4H), 1.46–1.34 (m, 8H), 1.28–1.23 (m, 6H), 0.94–0.90 (m, 6H), 0.84 (t, *J* = 6.9 Hz, 3H). **¹³C NMR** (126 MHz, CDCl₃): δ = 162.7 (C_q), 144.4 (C_q), 140.2 (C_q), 136.9 (C_q), 132.3 (CH), 128.2 (CH), 125.7 (CH), 124.9 (C_q), 123.9 (CH), 122.8 (CH), 114.5 (C_q), 50.5 (CH₂), 40.0 (CH₂), 32.5 (CH₂), 31.8 (CH₂), 31.3 (CH₂), 30.3 (CH₂), 30.3 (CH₂), 30.1 (CH₂), 29.7 (CH₂), 29.7 (CH₂), 27.9 (CH₂), 26.3 (CH₂), 22.8 (CH₂), 22.7 (CH₂), 22.6 (CH₂), 14.3 (CH₃), 14.3 (CH₃), 14.1 (CH₃). **IR** (ATR): 2953, 2923, 2856, 1642, 1589, 1463, 1337, 1046, 772, 730 cm⁻¹. **MS** (ESI) *m/z* (relative intensity): 951 (100) [2M+Na]⁺, 929 (31), 895 (9), 781 (10), 465 (92) [M+H]⁺, 317 (15). **HR-MS** (ESI) *m/z* calcd for C₂₉H₄₅N₄O [M+H]⁺ 465.3588, found 465.3575.

2-[(1-*n*-Hexyl-1*H*-1,2,3-triazol-4-yl)methyl]-3-phenethyl-4-*n*-propylisoquinolin-1(2*H*)-one (147aj)

5 Experimental Part

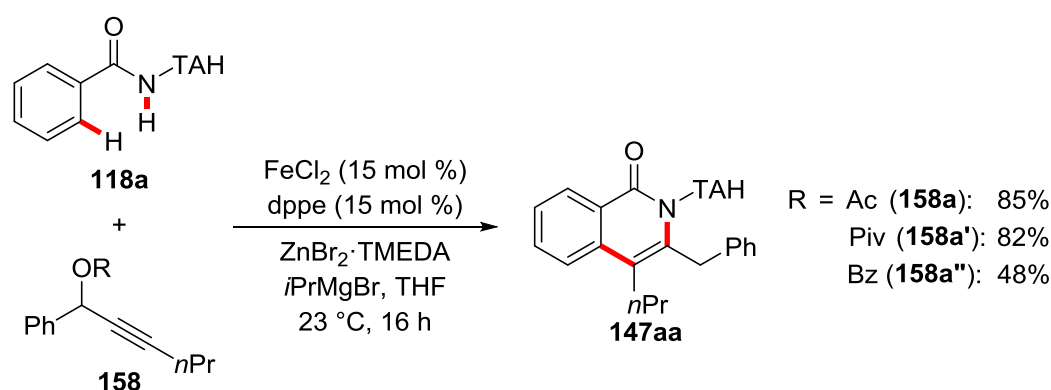
The general procedure **G** was followed using **118a** (85.9 mg, 0.30 mmol) and propargyl acetate **158j** (138 mg, 0.60 mmol). Purification by column chromatography (*n*hexane/EtOAc: 3/2) yielded **147aj** (53.8 mg, 39%) as off-white solid.

M.p. = 106–108 °C. **¹H NMR** (600 MHz, CDCl₃): δ = 8.47 (d, *J* = 7.8 Hz, 1H), 7.72 (s, 1H), 7.68–7.64 (m, 2H), 7.45 (ddd, *J* = 8.1, 6.2, 1.9 Hz, 1H), 7.36–7.32 (m, 4H), 7.27–7.23 (m, 1H), 5.46 (s, 2H), 4.25 (t, *J* = 7.3 Hz, 2H), 3.39 (s, 2H), 3.00–2.96 (m, 2H), 2.71–2.67 (m, 2H), 1.88–1.82 (m, 2H), 1.62–1.54 (m, 2H), 1.30–1.24 (m, 6H), 1.04 (t, *J* = 7.3 Hz, 3H), 0.84 (t, *J* = 7.0 Hz, 3H). **¹³C NMR** (126 MHz, CDCl₃): δ = 162.7 (C_q), 144.3 (C_q), 140.3 (C_q), 139.0 (C_q), 136.8 (C_q), 132.3 (CH), 128.8 (CH), 128.4 (CH), 128.3 (CH), 126.6 (CH), 125.9 (CH), 125.0 (C_q), 123.9 (CH), 123.0 (CH), 115.1 (C_q), 50.5 (CH₂), 40.1 (CH₂), 36.1 (CH₂), 31.5 (CH₂), 31.3 (CH₂), 30.3 (CH₂), 30.0 (CH₂), 26.3 (CH₂), 23.8 (CH₂), 22.6 (CH₂), 14.7 (CH₃), 14.1 (CH₃). **IR** (ATR): 2958, 2928, 2859, 1632, 1581, 1327, 1057, 772, 749, 694 cm⁻¹. **MS** (ESI) *m/z* (relative intensity): 935 (100) [2M+Na]⁺, 913 (22) [2M+H]⁺, 479 (36) [M+Na]⁺, 457 (89) [M+H]⁺. **HR-MS** (ESI) *m/z* calcd for C₂₉H₃₇N₄O [M+H]⁺ 457.2962, found 457.2946.

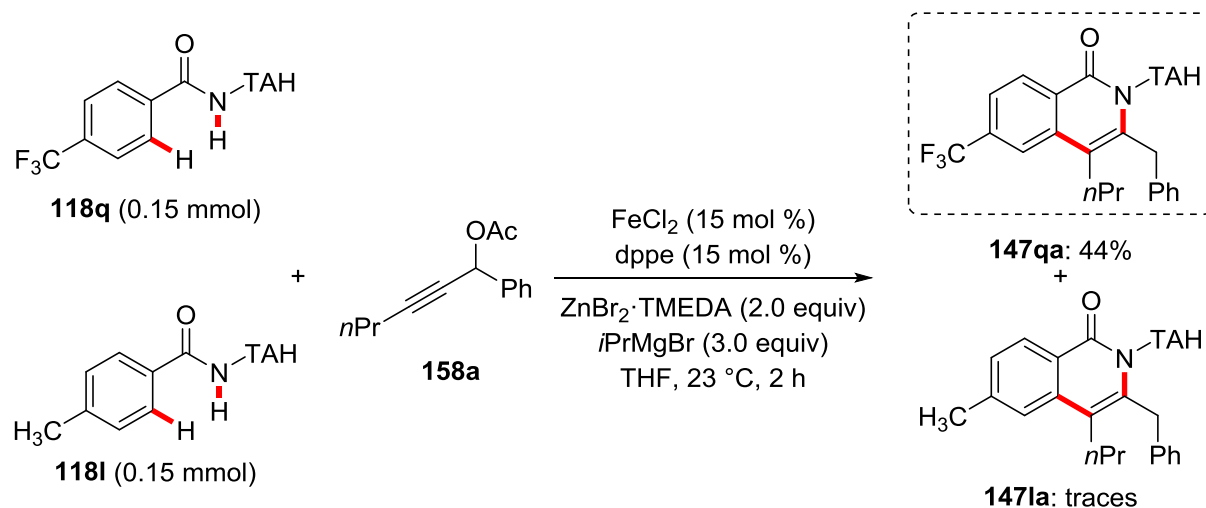
5.6.3 Mechanistic Studies

Effect of the Leaving Group

The general procedure **G** was followed using **118a** (85.9 mg, 0.30 mmol) and propargyl acetates **158a-a''** (0.60 mmol). Purification by column chromatography (*n*hexane/EtOAc: 3/2) yielded **147aa** as off-white solids with the corresponding yields indicated inside the Scheme.

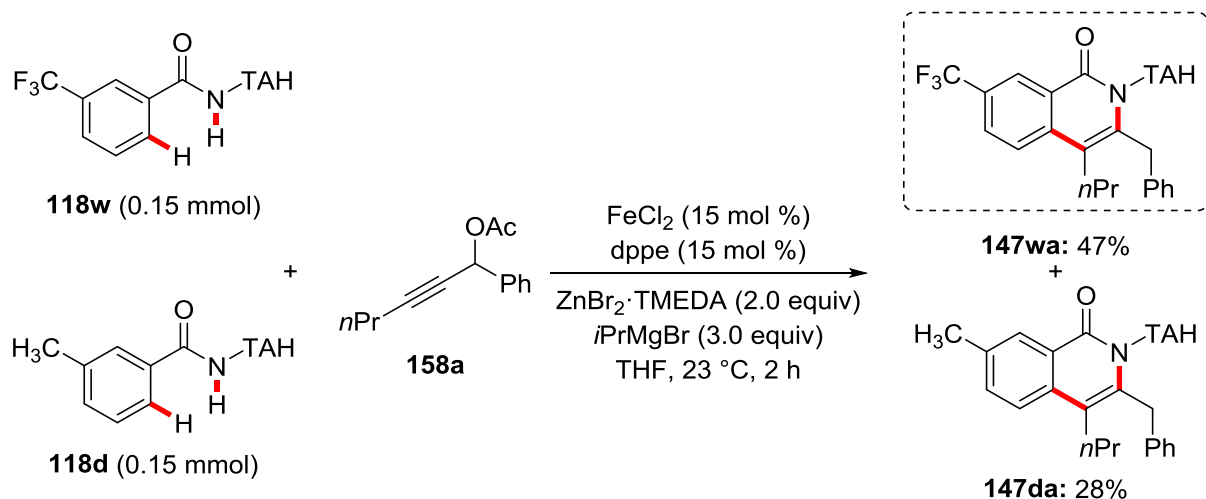


Intermolecular Competition Experiments

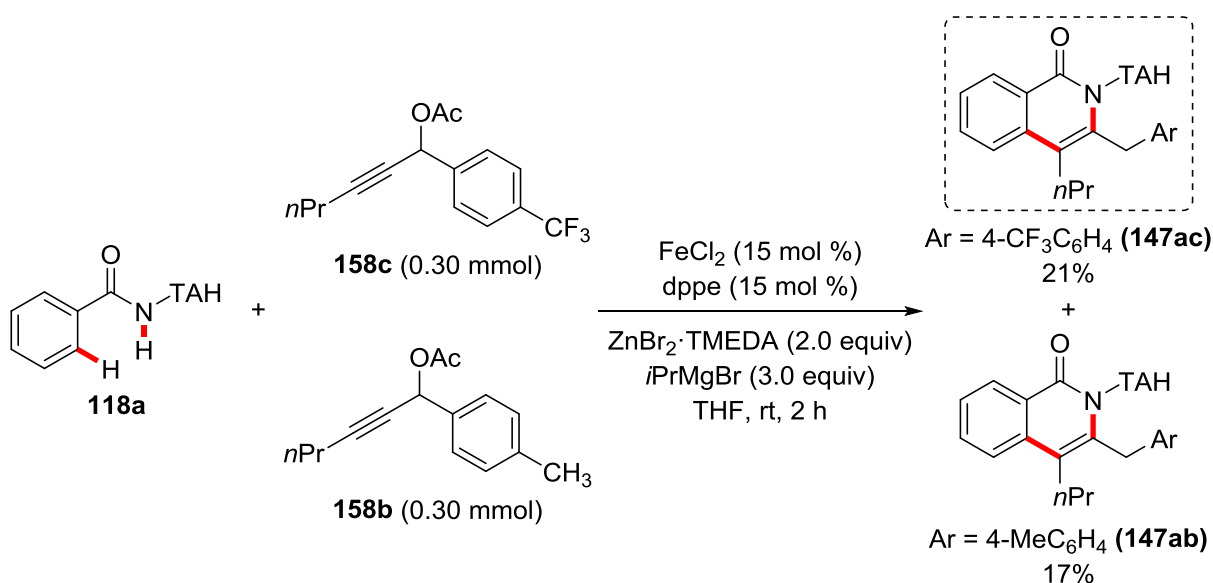


To a stirred solution of **118l** (45.1 mg, 0.15 mmol), **118q** (53.2 mg, 0.15 mmol), $\text{ZnBr}_2 \cdot \text{TMEDA}$ (205 mg, 0.60 mmol) and dppe (17.9 mg, 15 mol %) in THF (0.4 mL), *i*PrMgBr (3.0 M in 2-MeTHF, 300 μL , 0.90 mmol) was added in one portion and the reaction mixture was stirred for 5 min at ambient temperature. Then, FeCl_2 (5.7 mg, 15 mol %) was added in a single portion. After stirring for additional 5 min, a solution of propargyl acetate **158a** (130 mg, 0.60 mmol) in THF (0.40 mL) was added in one portion. The reaction mixture was stirred at ambient temperature. After 2 h, sat. aqueous NH_4Cl (3.0 mL) was added and the reaction mixture was extracted with CH_2Cl_2 (3×15 mL). The combined organic extracts were dried over Na_2SO_4 , filtered and concentrated. Purification by column chromatography (*n*hexane/EtOAc: 3/2) yielded **147qa** (66.7 mg, 44%) as the sole product.

5 Experimental Part



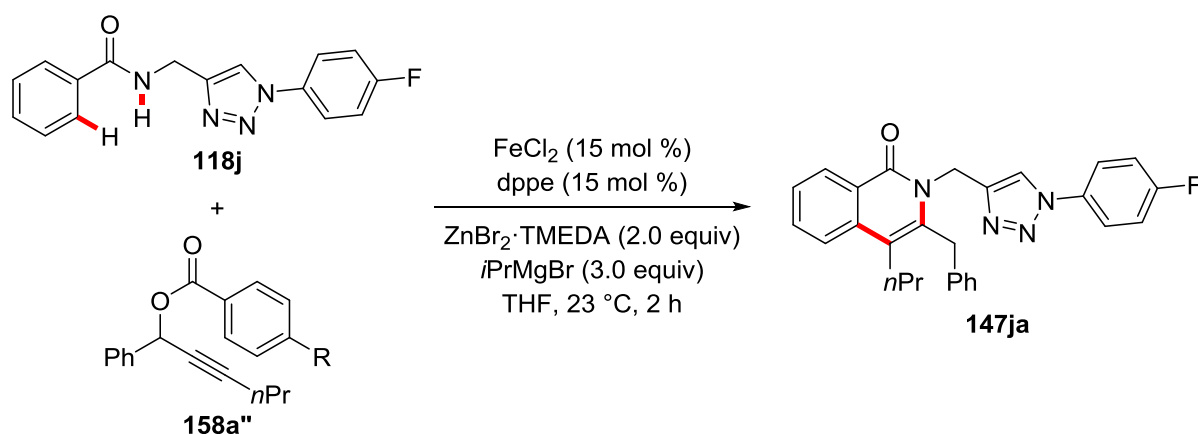
To a stirred solution of **118d** (45.1 mg, 0.15 mmol), **118w** (53.2 mg, 0.15 mmol), $\text{ZnBr}_2 \cdot \text{TMEDA}$ (205 mg, 0.60 mmol) and dppe (17.9 mg, 15 mol %) in THF (0.4 mL), $i\text{PrMgBr}$ (3.0 M in 2-MeTHF, 300 μL , 0.90 mmol) was added in one portion and the reaction mixture was stirred for 5 min at ambient temperature. Then, FeCl_2 (5.7 mg, 15 mol %) was added in a single portion. After stirring for additional 5 min, a solution of propargyl acetate **158a** (130 mg, 0.60 mmol) in THF (0.40 mL) was added in one portion. The reaction mixture was stirred at ambient temperature. After 2 h, sat. aqueous NH_4Cl (3.0 mL) was added and the reaction mixture was extracted with CH_2Cl_2 (3×15 mL). The combined organic extracts were dried over Na_2SO_4 , filtered and concentrated. Purification by column chromatography (*n*hexane/EtOAc: 3/2) yielded **147wa** (71.9 mg, 47%) and **147da** (37.9 mg, 28%).



5 Experimental Part

To a stirred solution of **118a** (85.9 mg, 0.30 mmol), ZnBr₂·TMEDA (205 mg, 0.60 mmol) and dppe (17.9 mg, 15 mol %) in THF (0.4 mL), *i*PrMgBr (3.0 M in 2-MeTHF, 300 μL, 0.90 mmol) was added in one portion and the reaction mixture was stirred for 5 min at ambient temperature. Then, FeCl₂ (5.7 mg, 15 mol %) was added in a single portion. After stirring for additional 5 min, a solution of propargyl acetate **158b** (69.0 mg, 0.30 mmol) and **158c** (85.3 mg, 0.30 mmol) in THF (0.40 mL) was added in one portion. The reaction mixture was stirred at ambient temperature. After 2 h, sat. aqueous NH₄Cl (3.0 mL) was added and the reaction mixture was extracted with CH₂Cl₂ (3 × 15 mL). The combined organic extracts were dried over Na₂SO₄, filtered and concentrated. Purification by column chromatography (*n*hexane/EtOAc: 3/2) afforded a mixture of both products. The yields of **147ac** (21%) and **147ab** (17%) were determined by ¹H-NMR spectroscopy with 1,3,5-trimethoxybenzene as internal standard.

Hammett-Plot with *para*-Substituted Propargyl Benzoates



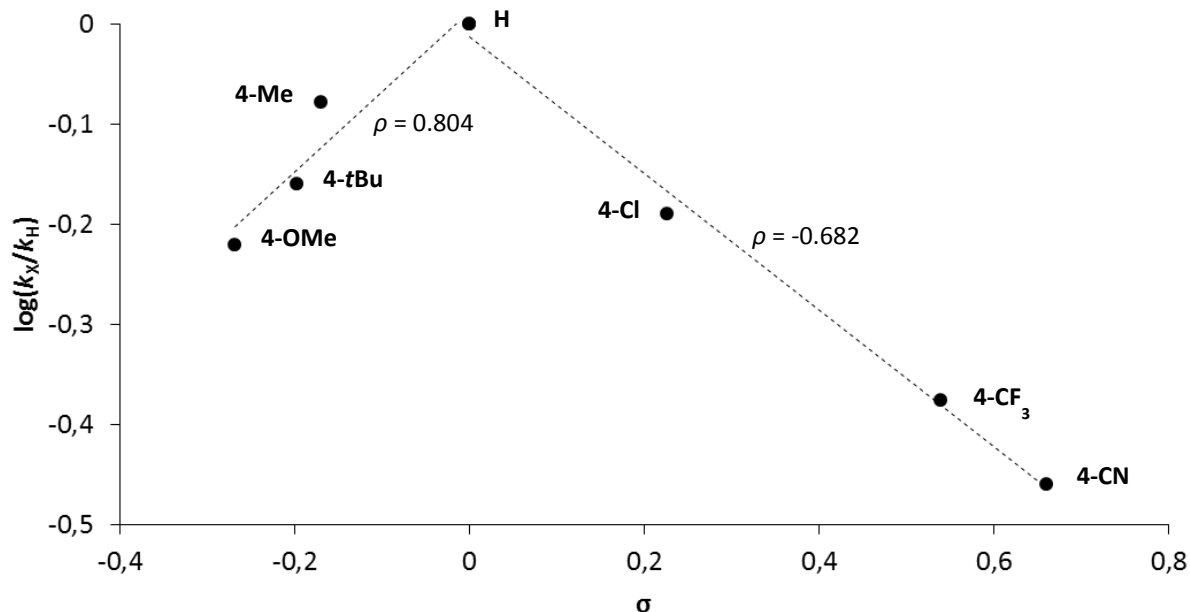
To a stirred solution of **118j** (296 mg, 1.00 mmol), ZnBr₂·TMEDA (603 mg, 2.00 mmol) and dppe (59.8 mg, 15 mol %) and *n*-nonanyl fluoride (73.1 mg, 0.50 mmol, 0.5 equiv) in THF (1.3 mL), *i*PrMgBr (3.0 M in 2-MeTHF, 1.0 mL, 3.00 mmol) was added in one portion and the reaction mixture was stirred for 5 min at ambient temperature. Then, FeCl₂ (19.0 mg, 15 mol %) was added in a single portion. After stirring for additional 5 min, a solution of propargyl acetate **158a''** (2.00 mmol, 2.0 equiv) in THF (1.3 mL) was added in one portion. The reaction mixture was stirred at ambient temperature. After the times indicated below, aliquots of 0.1 mL were taken out of the reaction mixture. The aliquots were filtered over a

5 Experimental Part

short plug of silica gel and diluted with CDCl_3 (1.0 mL). Yields of products were determined by ^{19}F NMR spectroscopy using *n*-nonanyl fluoride as internal standard.

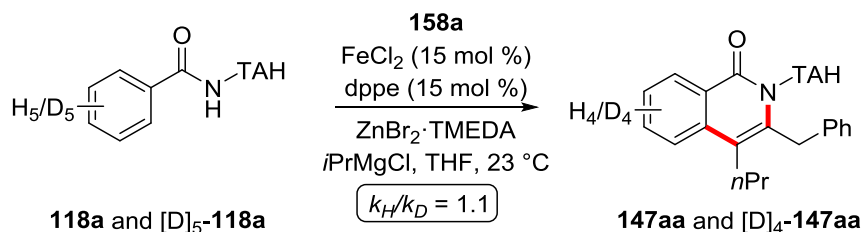
time [min]	5	10	20	30	45	60	90
4-OMe [%]	1.00	1.50	3.00	3.50	4.50	5.50	9.00
4- <i>t</i> Bu [%]	0.99	1.49	2.48	3.71	4.95	6.68	9.65
4-Me [%]	2.00	3.50	4.50	6.50	7.00	9.50	13.00
H [%]	3.01	4.01	5.01	6.52	9.52	11.03	15.54
4-Cl [%]	2.00	2.50	3.50	4.50	6.00	7.50	10.00
4-CF ₃ [%]	0.50	1.00	2.00	2.50	3.50	4.00	6.00
4-CN [%]	0.50	1.00	1.50	2.00	2.50	3.50	5.00

R	rate [1/min]	σ_p	rate [M/s]	k_x/k_H	$\log(k_x/k_H)$
4-OMe	0.0887	-0.268	0,00041065	0,601355932	-0,2208684
4-<i>t</i>Bu	0.1021	-0.197	0,00047269	0,69220339	-0,159766278
4-Me	0.1231	-0,170	0,00056991	0,834576271	-0,078533967
H	0.1475	0.00	0,00068287	1	0
4-Cl	0.0952	0.227	0,00044074	0,645423729	-0,190155072
4-CF₃	0.062	0.54	0,00028704	0,420338983	-0,376400331
4-CN	0.0511	0.66	0,00023657	0,346440678	-0,46037112



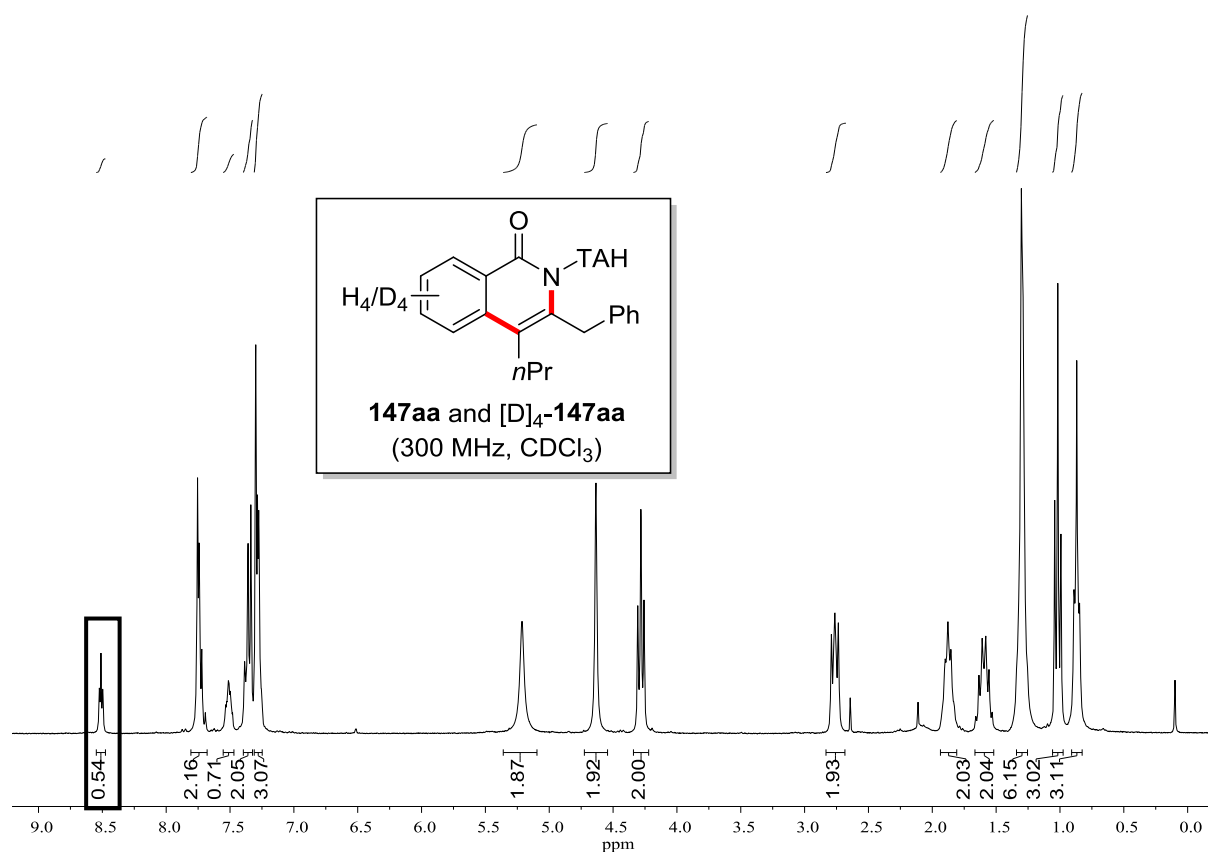
Kinetic Isotope Effects (KIE)

1) Intermolecular KIE (One-Pot Reaction)

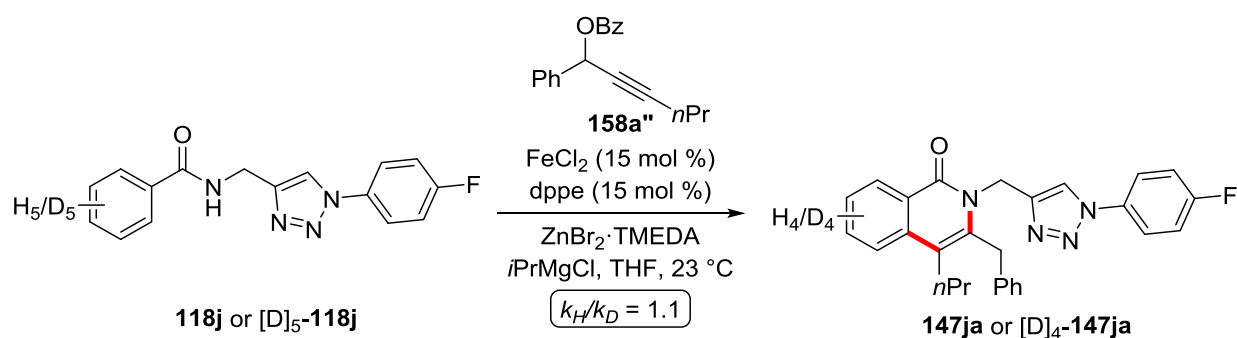


To a stirred solution of **118a** (43.0 mg, 0.15 mmol), $[\text{D}]_5$ -**118a** (43.7 mg, 0.15 mmol) $\text{ZnBr}_2 \cdot \text{TMEDA}$ (205 mg, 0.60 mmol) and dppe (17.9 mg, 15 mol %) in THF (0.4 mL), $n\text{PrMgBr}$ (3.0 M in 2-MeTHF, 300 μL , 0.90 mmol) was added in one portion and the reaction mixture was stirred for 5 min at ambient temperature. Then, FeCl_2 (5.7 mg, 15 mol %) was added in a single portion. After stirring for additional 5 min, a solution of propargyl acetate **158a** (130 mg, 0.60 mmol) in THF (0.4 mL) was added in one portion. After stirring 1 h at ambient temperature, sat. aqueous NH_4Cl (3.0 mL) was added and the reaction mixture was extracted with CH_2Cl_2 (3×15 mL). The combined organic extracts were dried over Na_2SO_4 , filtered and concentrated under reduced pressure. Purification by column chromatography ($n\text{hexane}/\text{EtOAc}$: 3/2) afforded a mixture of both products. The ratio of **147aa** to $[\text{D}]_4$ -**147aa** was determined by ^1H NMR analysis.

5 Experimental Part



2) Intermolecular KIE (Parallel Experiments)

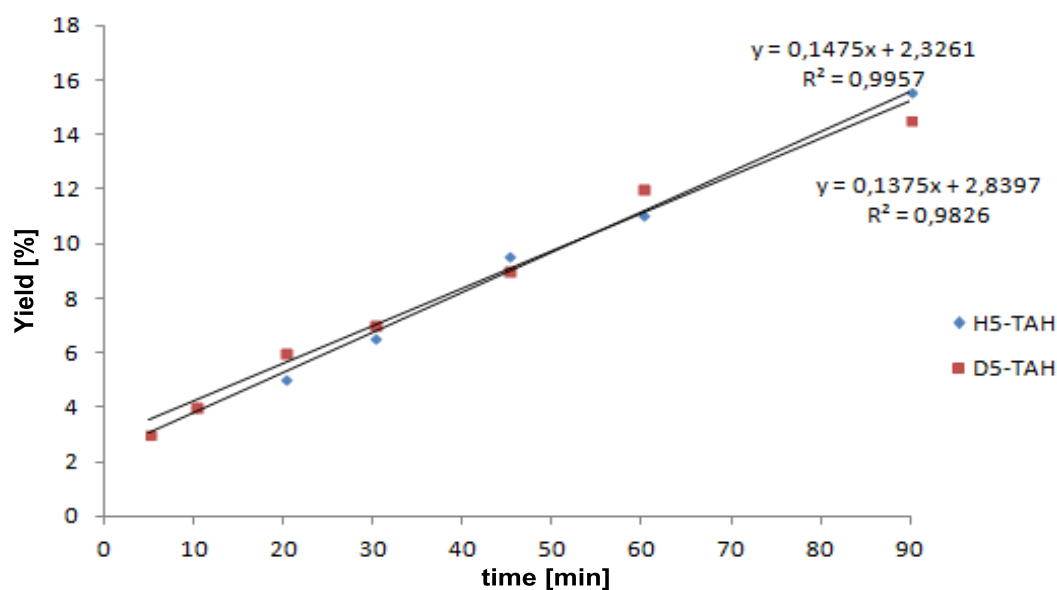


Two independent reactions using either **118j** or [D]₅-**118j** were conducted. To a stirred solution of **118j** (148.0 mg, 0.50 mmol) or [D]₅-**118j** (151 mg, 0.50 mmol) ZnBr₂·TMEDA (341 mg, 1.00 mmol), dppe (29.9 mg, 15 mol %) and *n*-nonanyl fluoride (36.6 mg, 0.25 mmol) in THF (0.65 mL), *i*PrMgBr (3.0 M in 2-MeTHF, 500 μL, 1.50 mmol) was added in one portion and the reaction mixture was stirred for 5 min at ambient temperature. Then, FeCl₂ (9.5 mg, 15 mol %) was added in a single portion. After stirring for additional 5 min, a solution of propargyl acetate **158a''** (216 mg, 1.00 mmol) in THF (0.65 mL) was added in one portion. The reaction mixture was stirred at ambient temperature. After the reaction times indicated below,

5 Experimental Part

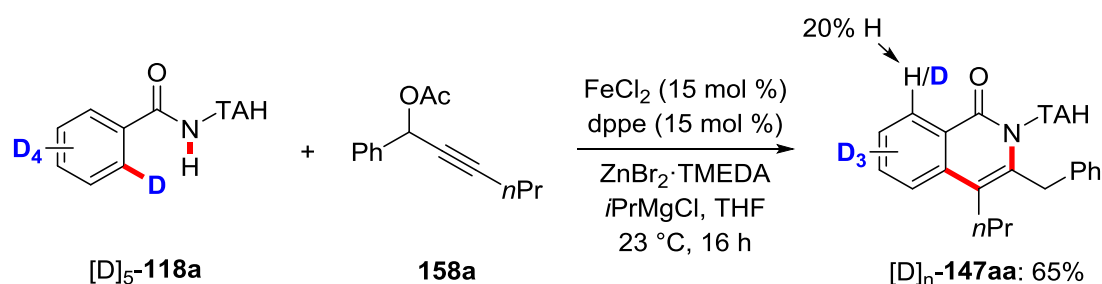
aliquots of 0.1 mL were taken out of the reaction mixture. The aliquots were filtered over a short plug of silica gel and diluted with CDCl₃ (1.0 mL). Yields of products were determined by ¹⁹F NMR spectroscopy using *n*-nonanyl fluoride as internal standard.

time [min]	5	10	20	30	45	60	90
147ja [%]	3.01	4.01	5.01	6.52	9.52	11.03	15.54
[D] ₅ - 147ja [%]	3.01	4.01	6.01	7.02	9.02	12.03	14.53



Reactions using Isotopically-Labelled Substrates

Reaction using deuterium-labelled substrate [D]₅-118a

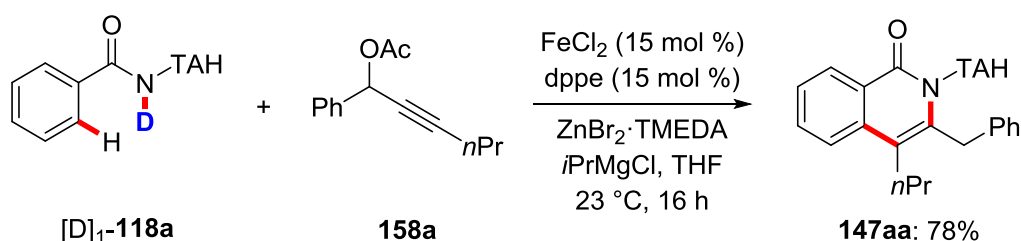


To a stirred solution of [D]₅-118a (87.4 mg, 0.30 mmol), ZnBr₂·TMEDA (205 mg, 0.60 mmol) and dppe (17.9 mg, 15 mol %) in THF (0.4 mL), *i*PrMgBr (3.0 M in 2-MeTHF, 300 μL, 0.90 mmol) was added in one portion and the reaction mixture was stirred for 5 min at ambient temperature. Then, FeCl₂ (5.7 mg, 15 mol %) was added in a single portion. After stirring for additional 5 min, a solution of propargyl

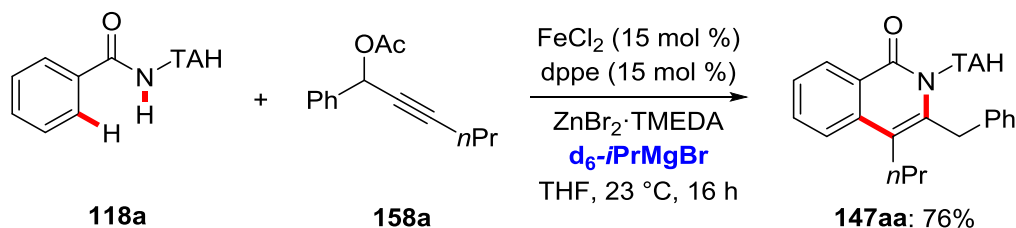
5 Experimental Part

acetate **158a** (130 mg, 0.60 mmol) in THF (0.4 mL) was added in one portion. The reaction mixture was stirred at ambient temperature. After 16 h, sat. aqueous NH_4Cl (3.0 mL) was added and the reaction mixture was extracted with CH_2Cl_2 (3×15 mL). The combined organic extracts were dried over Na_2SO_4 , filtered and concentrated. Purification by column chromatography (*n*hexane/EtOAc: 3/2) yielded the annulated isoquinolone $[\text{D}]_n$ -**147aa** (86.8 mg, 65%) as a white solid. The amount of deuterium incorporation was determined by ^1H NMR spectroscopy.

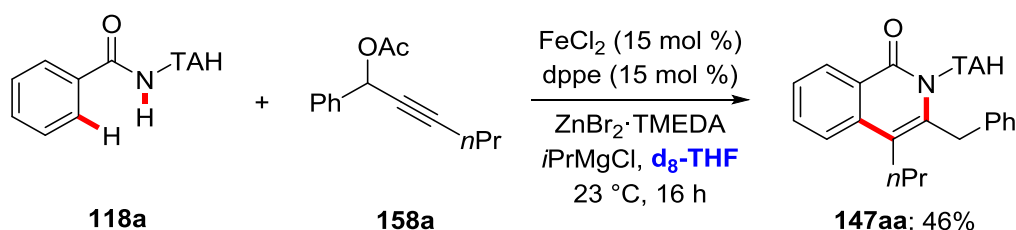
Reaction using deuterium-labelled substrate $[\text{D}]_1$ -**118a**



To a stirred solution of $[\text{D}]_1$ -**118a** (86.2 mg, 0.30 mmol), $\text{ZnBr}_2 \cdot \text{TMEDA}$ (205 mg, 0.60 mmol) and dppe (17.9 mg, 15 mol %) in THF (0.4 mL), *i*PrMgBr (3.0 M in 2-MeTHF, 300 μL , 0.90 mmol) was added in one portion and the reaction mixture was stirred for 5 min at ambient temperature. Then, FeCl_2 (5.7 mg, 15 mol %) was added in a single portion. After stirring for additional 5 min, a solution of propargyl acetate **158a** (130 mg, 0.60 mmol) in THF (0.4 mL) was added in one portion. The reaction mixture was stirred at ambient temperature. After 16 h, sat. aqueous NH_4Cl (3.0 mL) was added and the reaction mixture was extracted with CH_2Cl_2 (3×15 mL). The combined organic extracts were dried over Na_2SO_4 , filtered and concentrated. Purification by column chromatography (*n*hexane/EtOAc: 3/2) yielded the annulated isoquinolone **147aa** (103 mg, 78%) as a white solid. No deuterium incorporation could be observed by ^1H NMR spectroscopy.

Reaction using deuterium-labelled Grignard Reagent d_6 -*i*PrMgBr

To a stirred solution of **118a** (85.9 mg, 0.30 mmol), $ZnBr_2 \cdot TMEDA$ (205 mg, 0.60 mmol) and dppe (17.9 mg, 15 mol %) in THF (0.4 mL), d_6 -*i*PrMgBr (2.0 M in THF, 450 μ L, 0.90 mmol) was added in one portion and the reaction mixture was stirred for 5 min at ambient temperature. Then, $FeCl_2$ (5.7 mg, 15 mol %) was added in a single portion. After stirring for additional 5 min, a solution of propargyl acetate **158a** (130 mg, 0.60 mmol) in THF (0.4 mL) was added in one portion. The reaction mixture was stirred at ambient temperature. After 16 h, sat. aqueous NH_4Cl (3.0 mL) was added and the reaction mixture was extracted with CH_2Cl_2 (3×15 mL). The combined organic extracts were dried over Na_2SO_4 , filtered and concentrated. Purification by column chromatography (*n*hexane/EtOAc: 3/2) yielded the annulated isoquinolone **147aa** (100 mg, 76%) as a white solid. No deuterium incorporation could be observed by 1H NMR spectroscopy.

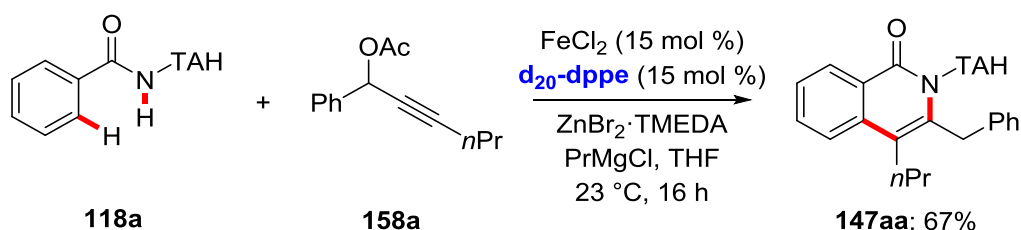
Reaction using deuterium-labelled solvent d_8 -THF

To a stirred solution of **118** (85.9 mg, 0.30 mmol), $ZnBr_2 \cdot TMEDA$ (205 mg, 0.60 mmol) and dppe (17.9 mg, 15 mol %) in d_8 -THF (0.4 mL), *i*PrMgBr (3.0 M in 2-MeTHF, 300 μ L, 0.90 mmol) was added in one portion and the reaction mixture was stirred for 5 min at ambient temperature. Then, $FeCl_2$ (5.7 mg, 15 mol %) was added in a single portion. After stirring for additional 5 min, a solution of propargyl acetate **158a** (130 mg, 0.60 mmol) in d_8 -THF (0.4 mL) was added in one portion. The

5 Experimental Part

reaction mixture was stirred at ambient temperature. After 16 h, sat. aqueous NH_4Cl (3.0 mL) was added and the reaction mixture was extracted with CH_2Cl_2 (3×15 mL). The combined organic extracts were dried over Na_2SO_4 , filtered and concentrated. Purification by column chromatography (*n*hexane/EtOAc: 3/2) yielded the annulated isoquinolone **147aa** (61.5 mg, 46%) as a white solid. No deuterium incorporation could be observed by ^1H NMR spectroscopy.

Reaction using deuterium-labelled ligand d_{20} -dppe



To a stirred solution of **118a** (85.9 mg, 0.30 mmol), $\text{ZnBr}_2 \cdot \text{TMEDA}$ (205 mg, 0.60 mmol) and $\text{d}_{20}\text{-dppe}$ (18.8 mg, 15 mol %) in THF (0.4 mL), $i\text{PrMgBr}$ (3.0 M in 2-MeTHF, 300 μL , 0.90 mmol) was added in one portion and the reaction mixture was stirred for 5 min at ambient temperature. Then, FeCl_2 (5.7 mg, 15 mol %) was added in a single portion. After stirring for additional 5 min, a solution of propargyl acetate **158a** (130 mg, 0.60 mmol) in THF (0.4 mL) was added in one portion. The reaction mixture was stirred at ambient temperature. After 16 h, sat. aqueous NH_4Cl (3.0 mL) was added and the reaction mixture was extracted with CH_2Cl_2 (3×15 mL). The combined organic extracts were dried over Na_2SO_4 , filtered and concentrated. Purification by column chromatography (*n*hexane/EtOAc: 3/2) yielded the annulated isoquinolone **147aa** (89.3 mg, 67%) as a white solid. No deuterium incorporation could be observed by ^1H NMR spectroscopy.

6 References

- [1] J. Berzelius, *Jahresber. Chem.* **1836**, *15*, 242.
- [2] H. B. Kagan, *Comprehensive Asymmetric Catalysis* **1999**, Springer-Verlag, Berlin, 9-33.
- [3] W. Ostwald, *Z. Phys. Chem.* **1894**, *15*, 705-706.
- [4] a) N. Cherkasov, A. O. Ibhaddon, P. Fitzpatrick, *Chemical Engineering and Processing: Process Intensification* **2015**, *90*, 24-33; b) T. Kandemir, M. E. Schuster, A. Senyshyn, M. Behrens, R. Schlögl, *Angew. Chem. Int. Ed.* **2013**, *52*, 12723-12726.
- [5] J. J. Eisch, *Organometallics* **2012**, *31*, 4917-4932.
- [6] a) P. T. Anastas, M. M. Kirchhoff, *Acc. Chem. Res.* **2002**, *35*, 686-694; b) P. T. Anastas, J. C. Warner, *Oxford Universal Press, Oxford* **1998**.
- [7] J. Hagen, in *Technische Katalyse*, Wiley-VCH, Weinheim, **1996**.
- [8] C. Glaser, *Ber. Dtsch. Chem. Ges.* **1869**, *2*, 422-424.
- [9] a) P. E. Fanta, *Synthesis* **1974**, *1974*, 9-21; b) F. Ullmann, J. Bielecki, *Ber. Dtsch. Chem. Ges.* **1901**, *34*, 2174-2185.
- [10] I. Goldberg, *Chem. Ber.* **1906**, *39*, 1691-1692.
- [11] I. Capanec, *Elsevier Science Ltd, Oxford* **2004**.
- [12] a) K. C. Nicolaou, P. G. Bulger, D. Sarlah, *Angew. Chem. Int. Ed.* **2005**, *44*, 4442-4489; b) C. C. C. Johansson Seechurn, M. O. Kitching, T. J. Colacot, V. Snieckus, *Angew. Chem. Int. Ed.* **2012**, *51*, 5062-5085.
- [13] a) R. J. P. Corriu, J. P. Masse, *J. Chem. Soc., Chem. Commun.* **1972**, 144a-144a; b) K. Tamao, K. Sumitani, M. Kumada, *J. Am. Chem. Soc.* **1972**, *94*, 4374-4376.
- [14] a) E. Negishi, A. O. King, N. Okukado, *J. Org. Chem.* **1977**, *42*, 1821-1823; b) A. O. King, N. Okukado, E.-i. Negishi, *J. Chem. Soc., Chem. Commun.* **1977**, 683-684.
- [15] a) J. K. Stille, *Angew. Chem. Int. Ed.* **1986**, *25*, 508-524; b) D. Milstein, J. K. Stille, *J. Am. Chem. Soc.* **1979**, *101*, 4992-4998; c) D. Milstein, J. K. Stille, *J. Am. Chem. Soc.* **1978**, *100*, 3636-3638; d) K. Masanori, S. Yutaka, M. Toshihiko, *Chem. Lett.* **1977**, *6*, 1423-1424; e) K. Masanori, S. Kazuo, S. Yutaka, M. Toshihiko, *Chem. Lett.* **1977**, *6*, 301-302.

6 References

- [16] a) N. Miyaura, A. Suzuki, *Chem. Rev.* **1995**, *95*, 2457-2483; b) N. Miyaura, K. Yamada, A. Suzuki, *Tetrahedron Lett.* **1979**, *20*, 3437-3440; c) N. Miyaura, A. Suzuki, *J. Chem. Soc., Chem. Commun.* **1979**, 866-867.
- [17] a) T. Hiyama, *J. Organomet. Chem.* **2002**, *653*, 58-61; b) Y. Hatanaka, T. Hiyama, *J. Org. Chem.* **1988**, *53*, 918-920.
- [18] a) R. F. Heck, J. P. Nolley, *J. Org. Chem.* **1972**, *37*, 2320-2322; b) M. Tsutomu, M. Kunio, O. Atsumu, *Bull. Chem. Soc. Jpn.* **1971**, *44*, 581-581.
- [19] a) K. Sonogashira, *J. Organomet. Chem.* **2002**, *653*, 46-49; b) K. Sonogashira, Y. Tohda, N. Hagihara, *Tetrahedron Lett.* **1975**, *16*, 4467-4470.
- [20] a) The Nobel prize in Chemistry 2010 - Press Release https://www.nobelprize.org/nobel_prizes/chemistry/laureates/2010/press.html accessed 22.05.2019; b) A. Suzuki, *Angew. Chem. Int. Ed.* **2011**, *50*, 6722-6737; c) E.-i. Negishi, *Angew. Chem. Int. Ed.* **2011**, *50*, 6738-6764.
- [21] L. Ackermann, R. Vicente, A. R. Kapdi, *Angew. Chem. Int. Ed.* **2009**, *48*, 9792-9826.
- [22] B. Trost, *Science* **1991**, *254*, 1471-1477.
- [23] a) R. G. Bergman, *Nature* **2007**, *446*, 391; b) L. Ackermann, in *Directed Metallation* (Ed.: N. Chatani), Springer Berlin, Heidelberg, **2007**, pp. 35-60.
- [24] a) L. Ackermann, *Chem. Rev.* **2011**, *111*, 1315-1345; b) D. Balcells, E. Clot, O. Eisenstein, *Chem. Rev.* **2010**, *110*, 749-823; c) J. A. Labinger, J. E. Bercaw, *Nature* **2002**, *417*, 507.
- [25] a) H. Yi, G. Zhang, H. Wang, Z. Huang, J. Wang, A. K. Singh, A. Lei, *Chem. Rev.* **2017**, *117*, 9016-9085; b) J.-T. Yu, C. Pan, *Chem. Commun.* **2016**, *52*, 2220-2236.
- [26] a) S. I. Gorelsky, D. Lapointe, K. Fagnou, *J. Am. Chem. Soc.* **2008**, *130*, 10848-10849; b) D. García-Cuadrado, A. A. C. Braga, F. Maseras, A. M. Echavarren, *J. Am. Chem. Soc.* **2006**, *128*, 1066-1067; c) L.-C. Campeau, M. Parisien, A. Jean, K. Fagnou, *J. Am. Chem. Soc.* **2006**, *128*, 581-590; d) L.-C. Campeau, M. Parisien, M. Leblanc, K. Fagnou, *J. Am. Chem. Soc.* **2004**, *126*, 9186-9187.
- [27] a) Y. Boutadla, D. L. Davies, S. A. Macgregor, A. I. Poblador-Bahamonde, *Dalton Trans.* **2009**, 5887-5893; b) Y. Boutadla, D. L. Davies, S. A. Macgregor, A. I. Poblador-Bahamonde, *Dalton Trans.* **2009**, 5820-5831.

-
- [28] J. Oxgaard, W. J. Tenn, R. J. Nielsen, R. A. Periana, W. A. Goddard, *Organometallics* **2007**, *26*, 1565-1567.
- [29] a) K. Naksomboon, J. Poater, F. M. Bickelhaupt, M. A. Fernandez-Ibanez, *J. Am. Chem. Soc.* **2019**, *141*, 6719–6725; b) E. Tan, O. Quinonero, M. Elena de Orbe, A. M. Echavarren, *ACS Catal.* **2018**, *8*, 2166-2172; c) D. Zell, M. Bursch, V. Müller, S. Grimme, L. Ackermann, *Angew. Chem. Int. Ed.* **2017**, *56*, 10378-10382; d) H. Wang, M. Moselage, M. J. González, L. Ackermann, *ACS Catal.* **2016**, *6*, 2705-2709; e) D. Santrač, S. Cella, W. Wang, L. Ackermann, *Eur. J. Org. Chem.* **2016**, *2016*, 5429-5436; f) R. Mei, J. Loup, L. Ackermann, *ACS Catal.* **2016**, *6*, 793-797; g) W. Ma, R. Mei, G. Tenti, L. Ackermann, *Chem. Eur. J.* **2014**, *20*, 15248-15251.
- [30] a) B. Ye, N. Cramer, *Acc. Chem. Res.* **2015**, *48*, 1308-1318; b) L. Ackermann, *Acc. Chem. Res.* **2014**, *47*, 281-295; c) S. R. Neufeldt, M. S. Sanford, *Acc. Chem. Res.* **2012**, *45*, 936-946; d) N. Kuhl, M. N. Hopkinson, J. Wencel-Delord, F. Glorius, *Angew. Chem. Int. Ed.* **2012**, *51*, 10236-10254.
- [31] a) P. Gandeepan, T. Müller, D. Zell, G. Cera, S. Warratz, L. Ackermann, *Chem. Rev.* **2018**; b) M. Moselage, J. Li, L. Ackermann, *ACS Catal.* **2016**, *6*, 498-525; c) W. Liu, L. Ackermann, *ACS Catal.* **2016**, *6*, 3743-3752; d) B. Su, Z.-C. Cao, Z.-J. Shi, *Acc. Chem. Res.* **2015**, *48*, 886-896; e) L. Ackermann, *J. Org. Chem.* **2014**, *79*, 8948-8954.
- [32] a) K. S. Egorova, V. P. Ananikov, *Angew. Chem. Int. Ed.* **2016**, *55*, 12150-12162; b) Lin, L. Liu, Y. Fu, S.-W. Luo, Q. Chen, Q.-X. Guo, *Organometallics* **2004**, *23*, 2114-2123.
- [33] T. Takahashi, K.-i. Kanno, in *Modern Organonickel Chemistry* (Ed.: Y. Tamaru), Wiley-VCH, Weinheim, **2005**, pp. 41-55.
- [34] a) T. Mesganaw, N. K. Garg, *Organic Process Research & Development* **2013**, *17*, 29-39; b) B. M. Rosen, K. W. Quasdorf, D. A. Wilson, N. Zhang, A.-M. Resmerita, N. K. Garg, V. Percec, *Chem. Rev.* **2011**, *111*, 1346-1416.
- [35] S. Z. Tasker, E. A. Standley, T. F. Jamison, *Nature* **2014**, *509*, 299-309.
- [36] A. N. Vedernikov, *ChemCatChem* **2014**, *6*, 2490-2492.
- [37] X. Hu, *Chem. Sci.* **2011**, *2*, 1867-1886.
- [38] J. P. Kleiman, M. Dubeck, *J. Am. Chem. Soc.* **1963**, *85*, 1544-1545.
- [39] L.-C. Liang, P.-S. Chien, J.-M. Lin, M.-H. Huang, Y.-L. Huang, J.-H. Liao, *Organometallics* **2006**, *25*, 1399-1411.

-
- [40] a) K. Muto, J. Yamaguchi, K. Itami, *Journal of the American Chemical Society* **2012**, *134*, 169-172; b) L. Ackermann, B. Punji, W. Song, *Adv. Synth. Catal.* **2011**, *353*, 3325-3329; c) O. Vechorkin, V. Proust, X. Hu, *Angew. Chem. Int. Ed.* **2010**, *49*, 3061-3064; d) H. Hachiya, K. Hirano, T. Satoh, M. Miura, *Org. Lett.* **2009**, *11*, 1737-1740; e) J. Canivet, J. Yamaguchi, I. Ban, K. Itami, *Org. Lett.* **2009**, *11*, 1733-1736; f) L. Ackermann, A. Althammer, S. Fenner, *Angew. Chem. Int. Ed.* **2009**, *48*, 201-204.
- [41] a) Y. Nakao, *Chem. Rec.* **2011**, *11*, 242-251; b) Y. Nakao, in *Catalytic Hydroarylation of Carbon-Carbon Multiple Bonds* (Eds.: L. Ackermann, T. B. Gunnoe, L. Goj Habgood), Wiley-VCH, Weinheim, **2017**, pp. 175-192.
- [42] T. Yamamoto, K. Muto, M. Komiyama, J. Canivet, J. Yamaguchi, K. Itami, *Chem. Eur. J.* **2011**, *17*, 10113-10122.
- [43] L. Ackermann, S. Fenner, *Chem. Commun.* **2011**, *47*, 430-432.
- [44] K. Muto, J. Yamaguchi, A. Lei, K. Itami, *J. Am. Chem. Soc.* **2013**, *135*, 16384-16387.
- [45] K. Muto, T. Hatakeyama, J. Yamaguchi, K. Itami, *Chem. Sci.* **2015**, *6*, 6792-6798.
- [46] K. Amaike, K. Muto, J. Yamaguchi, K. Itami, *J. Am. Chem. Soc.* **2012**, *134*, 13573-13576.
- [47] A. Kruckenberg, H. Wadehohl, L. H. Gade, *Organometallics* **2013**, *32*, 5153-5170.
- [48] X. Hong, Y. Liang, K. N. Houk, *J. Am. Chem. Soc.* **2014**, *136*, 2017-2025.
- [49] a) G. Pototschnig, N. Maulide, M. Schnürch, *Chem. Eur. J.* **2017**, *23*, 9206-9232; b) J. Yamaguchi, K. Muto, K. Itami, *Top. Curr. Chem.* **2016**, *374*, 55; c) N. Chatani, *Vol. 56*, **2015**, pp. 19-46.
- [50] a) M. Corbet, F. De Campo, *Angew. Chem. Int. Ed.* **2013**, *52*, 9896-9898; b) O. Daugulis, J. Roane, L. D. Tran, *Acc. Chem. Res.* **2015**, *48*, 1053-1064; c) V. G. Zaitsev, D. Shabashov, O. Daugulis, *J. Am. Chem. Soc.* **2005**, *127*, 13154-13155.
- [51] A. Yokota, Y. Aihara, N. Chatani, *J. Org. Chem.* **2014**, *79*, 11922-11932.
- [52] a) R. Chinchilla, C. Nájera, *Chem. Soc. Rev.* **2011**, *40*, 5084-5121; b) R. Chinchilla, C. Nájera, *Chem. Rev.* **2007**, *107*, 874-922.
- [53] N. Matsuyama, K. Hirano, T. Satoh, M. Miura, *Org. Lett.* **2009**, *11*, 4156-4159.

6 References

- [54] N. Matsuyama, M. Kitahara, K. Hirano, T. Satoh, M. Miura, *Org. Lett.* **2010**, *12*, 2358-2361.
- [55] a) Z. Ruan, S. Lackner, L. Ackermann, *ACS Catal.* **2016**, *6*, 4690-4693; b) W. Song, L. Ackermann, *Chem. Commun.* **2013**, *49*, 6638-6640; c) X.-X. Zheng, C. Du, X.-M. Zhao, X. Zhu, J.-F. Suo, X.-Q. Hao, J.-L. Niu, M.-P. Song, *J. Org. Chem.* **2016**, *81*, 4002-4011.
- [56] Y. Yoshida, T. Kurahashi, S. Matsubara, *Chem. Lett.* **2011**, *40*, 1140-1142.
- [57] H. Shiota, Y. Ano, Y. Aihara, Y. Fukumoto, N. Chatani, *J. Am. Chem. Soc.* **2011**, *133*, 14952-14955.
- [58] L. Ackermann, *Synlett* **2007**, *2007*, 0507-0526.
- [59] a) F.-X. Luo, Z.-C. Cao, H.-W. Zhao, D. Wang, Y.-F. Zhang, X. Xu, Z.-J. Shi, *Organometallics* **2017**, *36*, 18-21; b) C. Lin, J. Zhang, Z. Chen, Y. Liu, Z. Liu, Y. Zhang, *Adv. Synth. Catal.* **2016**, *358*, 1778-1793; c) Y.-H. Liu, Y.-J. Liu, S.-Y. Yan, B.-F. Shi, *Chem. Commun.* **2015**, *51*, 11650-11653.
- [60] a) V. G. Landge, C. H. Shewale, G. Jaiswal, M. K. Sahoo, S. P. Midya, E. Balaraman, *Catal. Sci. Technol.* **2016**, *6*, 1946-1951; b) J. Yi, L. Yang, C. Xia, F. Li, *J. Org. Chem.* **2015**, *80*, 6213-6221; c) Y.-J. Liu, Y.-H. Liu, S.-Y. Yan, B.-F. Shi, *Chem. Commun.* **2015**, *51*, 6388-6391.
- [61] a) E. Shirakawa, D. Ikeda, S. Masui, M. Yoshida, T. Hayashi, *J. Am. Chem. Soc.* **2012**, *134*, 272-279; b) M. D. Greenhalgh, S. P. Thomas, *J. Am. Chem. Soc.* **2012**, *134*, 11900-11903; c) L. Ackermann, *Chem. Commun.* **2010**, *46*, 4866-4877; d) L. Ackermann, P. Novak, R. Vicente, N. Hofmann, *Angew. Chem. Int. Ed.* **2009**, *48*, 6045-6048; e) A. Fürstner, R. Martin, H. Krause, G. Seidel, R. Goddard, C. W. Lehmann, *J. Am. Chem. Soc.* **2008**, *130*, 8773-8787.
- [62] T. Yao, K. Hirano, T. Satoh, M. Miura, *Chem. Eur. J.* **2010**, *16*, 12307-12311.
- [63] Y. Aihara, N. Chatani, *J. Am. Chem. Soc.* **2013**, *135*, 5308-5311.
- [64] W. Song, S. Lackner, L. Ackermann, *Angew. Chem. Int. Ed.* **2014**, *53*, 2477-2480.
- [65] Z. Ruan, S. Lackner, L. Ackermann, *Angew. Chem. Int. Ed.* **2016**, *55*, 3153-3157.
- [66] a) T. Uemura, M. Yamaguchi, N. Chatani, *Angew. Chem. Int. Ed.* **2016**, *55*, 3162-3165; b) Y. Aihara, J. Wuelbern, N. Chatani, *Bull. Chem. Soc. Jpn.* **2015**, *88*, 438-446; c) X. Wu, Y. Zhao, H. Ge, *J. Am. Chem. Soc.* **2014**, *136*, 1789-1792.

6 References

- [67] J. Li, Z. Zheng, T. Xiao, P.-F. Xu, H. Wei, *Asian J. Org. Chem.* **2018**, *7*, 133-136.
- [68] X. Cong, Y. Li, Y. Wei, X. Zeng, *Org. Lett.* **2014**, *16*, 3926-3929.
- [69] a) C. Shen, P. Zhang, Q. Sun, S. Bai, T. S. A. Hor, X. Liu, *Chem. Soc. Rev.* **2015**, *44*, 291-314; b) N. V. Orlov, *ChemistryOpen* **2015**, *4*, 682-697; c) M. M. Kandeel, *Phosphorus Sulfur Silicon Relat Elem.* **2005**, *180*, 217-282.
- [70] a) J. Zhang, L. J. Kang, T. C. Parker, S. B. Blakey, C. K. Luscombe, S. R. Marder, *Molecules (Basel, Switzerland)* **2018**, *23*, 922; b) S. Shome, S. P. Singh, *Chem. Commun.* **2018**, *54*, 7322-7325; c) A. R. Murphy, J. M. J. Fréchet, *Chem. Rev.* **2007**, *107*, 1066-1096.
- [71] R. Mohammadi, A. Hosseinian, K. Didehban, L. Edjlali, *J. Sulfur Chem.* **2018**, *39*, 443-463.
- [72] a) K. Inamoto, C. Hasegawa, K. Hiroya, T. Doi, *Org. Lett.* **2008**, *10*, 5147-5150; b) K. Inamoto, Y. Arai, K. Hiroya, T. Doi, *Chem. Commun.* **2008**, 5529-5531.
- [73] a) K. Inamoto, K. Nozawa, Y. Kondo, *Synlett* **2012**, *23*, 1678-1682; b) R. Samanta, A. P. Antonchick, *Angew. Chem. Int. Ed.* **2011**, *50*, 5217-5220; c) J. Zhu, Z. Chen, H. Xie, S. Li, Y. Wu, *Org. Lett.* **2010**, *12*, 2434-2436; d) K. Inamoto, C. Hasegawa, J. Kawasaki, K. Hiroya, T. Doi, *Adv. Synth. Catal.* **2010**, *352*, 2643-2655; e) L. L. Joyce, R. A. Batey, *Org. Lett.* **2009**, *11*, 2792-2795.
- [74] S.-Y. Yan, Y.-J. Liu, B. Liu, Y.-H. Liu, B.-F. Shi, *Chem. Commun.* **2015**, *51*, 4069-4072.
- [75] K. Yang, Y. Wang, X. Chen, A. A. Kadi, H.-K. Fun, H. Sun, Y. Zhang, H. Lu, *Chem. Commun.* **2015**, *51*, 3582-3585.
- [76] C. Lin, D. Li, B. Wang, J. Yao, Y. Zhang, *Org. Lett.* **2015**, *17*, 1328-1331.
- [77] a) C. Lin, W. Yu, J. Yao, B. Wang, Z. Liu, Y. Zhang, *Org. Lett.* **2015**, *17*, 1340-1343; b) X. Wang, R. Qiu, C. Yan, V. P. Reddy, L. Zhu, X. Xu, S.-F. Yin, *Org. Lett.* **2015**, *17*, 1970-1973; c) S.-Y. Yan, Y.-J. Liu, B. Liu, Y.-H. Liu, Z.-Z. Zhang, B.-F. Shi, *Chem. Commun.* **2015**, *51*, 7341-7344; d) X. Ye, J. L. Petersen, X. Shi, *Chem. Commun.* **2015**, *51*, 7863-7866.
- [78] a) V. P. Reddy, R. Qiu, T. Iwasaki, N. Kambe, *Org. Biomol. Chem.* **2015**, *13*, 6803-6813; b) Z. Wu, H. Song, X. Cui, C. Pi, W. Du, Y. Wu, *Org. Lett.* **2013**, *15*, 1270-1273.

6 References

- [79] L. Ackermann, *Catalytic Hydroarylation of Carbon-Carbon Multiple Bonds*, Wiley-VCH, Weinheim, **2017**.
- [80] a) M. Rueping, B. J. Nachtsheim, *Beilstein J. Org. Chem.* **2010**, *6*, 6; b) N. O. Calloway, *Chem. Rev.* **1935**, *17*, 327-392.
- [81] a) Y. Fujiwara, I. Moritani, S. Danno, R. Asano, S. Teranishi, *J. Am. Chem. Soc.* **1969**, *91*, 7166-7169; b) I. Moritani, Y. Fujiwara, *Tetrahedron Lett.* **1967**, *8*, 1119-1122.
- [82] Y. Nakao, K. S. Kanyiva, S. Oda, T. Hiyama, *J. Am. Chem. Soc.* **2006**, *128*, 8146-8147.
- [83] K. S. Kanyiva, Y. Nakao, T. Hiyama, *ChemInform* **2007**, *38*.
- [84] T. Mukai, K. Hirano, T. Satoh, M. Miura, *J. Org. Chem.* **2009**, *74*, 6410-6413.
- [85] K. S. Kanyiva, F. Löbermann, Y. Nakao, T. Hiyama, *Tetrahedron Lett.* **2009**, *50*, 3463-3466.
- [86] K. S. Kanyiva, Y. Nakao, T. Hiyama, *Angew. Chem. Int. Ed.* **2007**, *46*, 8872-8874.
- [87] Y. Nakao, K. S. Kanyiva, T. Hiyama, *J. Am. Chem. Soc.* **2008**, *130*, 2448-2449.
- [88] C.-C. Tsai, W.-C. Shih, C.-H. Fang, C.-Y. Li, T.-G. Ong, G. P. A. Yap, *J. Am. Chem. Soc.* **2010**, *132*, 11887-11889.
- [89] Y. Nakao, N. Kashihara, K. S. Kanyiva, T. Hiyama, *Angew. Chem. Int. Ed.* **2010**, *49*, 4451-4454.
- [90] a) Y.-X. Wang, M. Ye, *Sci China Chem.* **2018**, *61*, 1004-1013; b) W.-C. Lee, W.-C. Shih, T.-H. Wang, Y. Liu, G. P. A. Yap, T.-G. Ong, *Tetrahedron* **2015**, *71*, 4460-4464; c) W.-C. Shih, W.-C. Chen, Y.-C. Lai, M.-S. Yu, J.-J. Ho, G. P. A. Yap, T.-G. Ong, *Org. Lett.* **2012**, *14*, 2046-2049.
- [91] Y. Nakao, Y. Yamada, N. Kashihara, T. Hiyama, *J. Am. Chem. Soc.* **2010**, *132*, 13666-13668.
- [92] R. Tamura, Y. Yamada, Y. Nakao, T. Hiyama, *Angew. Chem. Int. Ed.* **2012**, *51*, 5679-5682.
- [93] W.-C. Lee, C.-H. Wang, Y.-H. Lin, W.-C. Shih, T.-G. Ong, *Org. Lett.* **2013**, *15*, 5358-5361.
- [94] M. M. Lorion, K. Maindan, A. R. Kapdi, L. Ackermann, *Chem. Soc. Rev.* **2017**, *46*, 7399-7420.

6 References

- [95] a) E. Peris, *Chem. Rev.* **2018**, *118*, 9988-10031; b) Y. Wang, D. Wei, Y. Wang, W. Zhang, M. Tang, *ACS Catal.* **2016**, *6*, 279-289.
- [96] Y. Schramm, M. Takeuchi, K. Semba, Y. Nakao, J. F. Hartwig, *J. Am. Chem. Soc.* **2015**, *137*, 12215-12218.
- [97] a) A. Fürstner, *ACS Cent. Sci.* **2016**, *2*, 778-789; b) I. Bauer, H.-J. Knölker, *Chem. Rev.* **2015**, *115*, 3170-3387; c) K. Junge, K. Schröder, M. Beller, *Chem. Commun.* **2011**, *47*, 4849-4859; d) B. B. Eike, *Curr. Org. Chem.* **2008**, *12*, 1341-1369.
- [98] a) N. Yoshikai, *Isr. J. Chem.* **2017**, *57*, 1117-1130; b) G. Cera, L. Ackermann, *Top. Curr. Chem.* **2016**, *374*, 57.
- [99] a) P. R. Ortiz de Montellano, *Chem. Rev.* **2010**, *110*, 932-948; b) M. S. Chen, M. C. White, *Science* **2010**, *327*, 566-571; c) M. S. Chen, M. C. White, *Science* **2007**, *318*, 783-787; d) P. A. MacFaul, D. D. M. Wayner, K. U. Ingold, *Acc. Chem. Res.* **1998**, *31*, 159-162.
- [100] a) S. M. Paradine, M. C. White, *J. Am. Chem. Soc.* **2012**, *134*, 2036-2039; b) Z. Wang, Y. Zhang, H. Fu, Y. Jiang, Y. Zhao, *Org. Lett.* **2008**, *10*, 1863-1866.
- [101] a) E. McNeill, T. Ritter, *Acc. Chem. Res.* **2015**, *48*, 2330-2343; b) A. Fürstner, R. Martin, K. Majima, *J. Am. Chem. Soc.* **2005**, *127*, 12236-12237.
- [102] R. Shang, L. Ilies, E. Nakamura, *Chem. Rev.* **2017**, *117*, 9086-9139.
- [103] G. Hata, H. Kondo, A. Miyake, *J. Am. Chem. Soc.* **1968**, *90*, 2278-2281.
- [104] a) S. Camadanli, R. Beck, U. Flörke, H.-F. Klein, *Organometallics* **2009**, *28*, 2300-2310; b) H.-F. Klein, S. Camadanli, R. Beck, D. Leukel, U. Flörke, *Angew. Chem. Int. Ed.* **2005**, *44*, 975-977.
- [105] a) X. Chen, J.-J. Li, X.-S. Hao, C. E. Goodhue, J.-Q. Yu, *J. Am. Chem. Soc.* **2006**, *128*, 78-79; b) X. Chen, C. E. Goodhue, J.-Q. Yu, *J. Am. Chem. Soc.* **2006**, *128*, 12634-12635.
- [106] E. Nakamura, N. Yoshikai, *J. Org. Chem.* **2010**, *75*, 6061-6067.
- [107] J. Norinder, A. Matsumoto, N. Yoshikai, E. Nakamura, *J. Am. Chem. Soc.* **2008**, *130*, 5858-5859.
- [108] a) T. Nagano, T. Hayashi, *Org. Lett.* **2005**, *7*, 491-493; b) G. Cahiez, C. Chaboche, F. Mahuteau-Betzer, M. Ahr, *Org. Lett.* **2005**, *7*, 1943-1946.
- [109] a) J. J. Sirois, R. Davis, B. DeBoef, *Org. Lett.* **2014**, *16*, 868-871; b) N. Yoshikai, S. Asako, T. Yamakawa, L. Ilies, E. Nakamura, *Chem. Asian J.*

- 2011**, 6, 3059-3065; c) N. Yoshikai, A. Matsumoto, J. Norinder, E. Nakamura, *Angew. Chem. Int. Ed.* **2009**, 48, 2925-2928.
- [110] L. Ilies, E. Konno, Q. Chen, E. Nakamura, *Asian J. Org. Chem.* **2012**, 1, 142-145.
- [111] L. Ilies, S. Asako, E. Nakamura, *J. Am. Chem. Soc.* **2011**, 133, 7672-7675.
- [112] a) L. C. M. Castro, N. Chatani, *Chem. Lett.* **2015**, 44, 410-421; b) G. Rouquet, N. Chatani, *Angew. Chem. Int. Ed.* **2013**, 52, 11726-11743.
- [113] R. Shang, L. Ilies, A. Matsumoto, E. Nakamura, *J. Am. Chem. Soc.* **2013**, 135, 6030-6032.
- [114] Q. Gu, H. H. Al Mamari, K. Graczyk, E. Diers, L. Ackermann, *Angew. Chem. Int. Ed.* **2014**, 53, 3868-3871.
- [115] H. H. Al Mamari, E. Diers, L. Ackermann, *Chem. Eur. J.* **2014**, 20, 9739-9743.
- [116] a) S. Ueno, N. Chatani, F. Kakiuchi, *J. Org. Chem.* **2007**, 72, 3600-3602; b) M. Wasa, K. S. L. Chan, J.-Q. Yu, *Chem. Lett.* **2011**, 40, 1004-1006; c) R. Waterman, *Organometallics* **2013**, 32, 7249-7263.
- [117] R. Shang, L. Ilies, S. Asako, E. Nakamura, *J. Am. Chem. Soc.* **2014**, 136, 14349-14352.
- [118] a) R. B. Bedford, P. B. Brenner, E. Carter, J. Clifton, P. M. Cogswell, N. J. Gower, M. F. Haddow, J. N. Harvey, J. A. Kehl, D. M. Murphy, E. C. Neeve, M. L. Neidig, J. Nunn, B. E. R. Snyder, J. Taylor, *Organometallics* **2014**, 33, 5767-5780; b) R. B. Bedford, N. J. Gower, M. F. Haddow, J. N. Harvey, J. Nunn, R. A. Okopie, R. F. Sankey, *Angew. Chem. Int. Ed.* **2012**, 51, 5435-5438; c) R. B. Bedford, M. A. Hall, G. R. Hodges, M. Huwe, M. C. Wilkinson, *Chem. Commun.* **2009**, 6430-6432.
- [119] L. Ackermann, *Chem. Commun.* **2010**, 46, 4866-4877.
- [120] a) L. Ilies, S. Ichikawa, S. Asako, T. Matsubara, E. Nakamura, *Adv. Synth. Catal.* **2015**, 357, 2175-2179; b) R. Shang, L. Ilies, E. Nakamura, *J. Am. Chem. Soc.* **2015**, 137, 7660-7663.
- [121] a) K. Graczyk, T. Haven, L. Ackermann, *Chem. Eur. J.* **2015**, 21, 8812-8815; b) Z. Shen, G. Cera, T. Haven, L. Ackermann, *Org. Lett.* **2017**, 19, 3795-3798.
- [122] R. Shang, L. Ilies, E. Nakamura, *J. Am. Chem. Soc.* **2016**, 138, 10132-10135.
- [123] W. Shi, C. Liu, A. Lei, *Chem. Soc. Rev.* **2011**, 40, 2761-2776.
- [124] a) G. Cera, T. Haven, L. Ackermann, *Angew. Chem. Int. Ed.* **2016**, 55, 1484-1488; b) E. R. Fruchey, B. M. Monks, S. P. Cook, *J. Am. Chem. Soc.* **2014**,

- 136, 13130-13133; c) L. Ilies, T. Matsubara, S. Ichikawa, S. Asako, E. Nakamura, *J. Am. Chem. Soc.* **2014**, *136*, 13126-13129; d) B. M. Monks, E. R. Fruchey, S. P. Cook, *Angew. Chem. Int. Ed.* **2014**, *53*, 11065-11069.
- [125] G. Cera, T. Haven, L. Ackermann, *Chem. Eur. J.* **2017**, *23*, 3577-3582.
- [126] a) S. Asako, J. Norinder, L. Ilies, N. Yoshikai, E. Nakamura, *Adv. Synth. Catal.* **2014**, *356*, 1481-1485; b) S. Asako, L. Ilies, E. Nakamura, *J. Am. Chem. Soc.* **2013**, *135*, 17755-17757.
- [127] a) L. Ackermann, T. B. Gunnoe, L. G. Habgood, *Catalytic Hydroarylation of Carbon-Carbon Multiple Bonds*, Wiley-VCH: Weinheim, Germany, **2017**; b) F. Kakiuchi, S. Murai, *Acc. Chem. Res.* **2002**, *35*, 826-834; c) N. Kimura, T. Kochi, F. Kakiuchi, *J. Am. Chem. Soc.* **2017**, *139*, 14849-14852; d) L. N. Lewis, J. F. Smith, *J. Am. Chem. Soc.* **1986**, *108*, 2728-2735; e) S. Murai, F. Kakiuchi, S. Sekine, Y. Tanaka, A. Kamatani, M. Sonoda, N. Chatani, *Nature* **1993**, *366*, 529-531; f) M. Y. Wong, T. Yamakawa, N. Yoshikai, *Org. Lett.* **2015**, *17*, 442-445.
- [128] a) M. D. Greenhalgh, A. S. Jones, S. P. Thomas, *ChemCatChem* **2015**, *7*, 190-222; b) B. D. Sherry, A. Fürstner, *Acc. Chem. Res.* **2008**, *41*, 1500-1511.
- [129] A. Matsumoto, L. Ilies, E. Nakamura, *J. Am. Chem. Soc.* **2011**, *133*, 6557-6559.
- [130] L. Ilies, A. Matsumoto, M. Kobayashi, N. Yoshikai, E. Nakamura, *Synlett* **2012**, *23*, 2381-2384.
- [131] L. Adak, N. Yoshikai, *Tetrahedron* **2012**, *68*, 5167-5171.
- [132] M. M. Bagga, P. L. Pauson, F. J. Preston, R. I. Reed, *Chem. Commun.* **1965**, 543-544.
- [133] T. Jia, C. Zhao, R. He, H. Chen, C. Wang, *Angew. Chem. Int. Ed.* **2016**, *55*, 5268-5271.
- [134] T. Matsubara, L. Ilies, E. Nakamura, *Chem. Asian J.* **2016**, *11*, 380-384.
- [135] G. Cera, T. Haven, L. Ackermann, *Chem. Commun.* **2017**, *53*, 6460-6463.
- [136] T. H. Meyer, L. H. Finger, P. Gandeepan, L. Ackermann, *Trends Chem.* **2019**, *1*, 63-76.
- [137] a) L. Ackermann, *Modern Arylation Methods*, Wiley-VCH, Weinheim, **2009**; b) T. G. Saint-Denis, R.-Y. Zhu, G. Chen, Q.-F. Wu, J.-Q. Yu, *Science* **2018**, *359*, 4798; c) W. Ma, P. Gandeepan, J. Li, L. Ackermann, *Org. Chem. Frontiers* **2017**, *4*, 1435-1467; d) Y. Segawa, T. Maekawa, K. Itami, *Angew. Chem. Int.*

- Ed.* **2015**, *54*, 66-81; e) J. Wencel-Delord, F. Glorius, *Nat. Chem.* **2013**, *5*, 369; f) L. McMurray, F. O'Hara, M. J. Gaunt, *Chem. Soc. Rev.* **2011**, *40*, 1885-1898; g) O. Baudoin, *Chem. Soc. Rev.* **2011**, *40*, 4902-4911.
- [138] D. Ghorai, L. H. Finger, G. Zanoni, L. Ackermann, *ACS Catal.* **2018**, *8*, 11657-11662.
- [139] a) Z.-J. Jia, C. Merten, R. Gontla, C. G. Daniliuc, A. P. Antonchick, H. Waldmann, *Angew. Chem. Int. Ed.* **2017**, *56*, 2429-2434; b) R. Zeng, J. Ye, C. Fu, S. Ma, *Adv. Synth. Catal.* **2013**, *355*, 1963-1970; c) B. Ye, N. Cramer, *J. Am. Chem. Soc.* **2013**, *135*, 636-639; d) R. Zeng, C. Fu, S. Ma, *J. Am. Chem. Soc.* **2012**, *134*, 9597-9600.
- [140] S. Nakanowatari, L. Ackermann, *Chem. Eur. J.* **2015**, *21*, 16246-16251.
- [141] S. Nakanowatari, R. Mei, M. Feldt, L. Ackermann, *ACS Catal.* **2017**, *7*, 2511-2515.
- [142] a) S.-Y. Chen, Q. Li, X.-G. Liu, J.-Q. Wu, S.-S. Zhang, H. Wang, *ChemSusChem* **2017**, *10*, 2360-2364; b) S.-Y. Chen, X.-L. Han, J.-Q. Wu, Q. Li, Y. Chen, H. Wang, *Angew. Chem. Int. Ed.* **2017**, *56*, 9939-9943.
- [143] a) Y. Li, Y. Liu, B.-F. Shi, *Adv. Synth. Catal.* **2017**, *359*, 4117-4121; b) C. Zhang, J. McClure, C. J. Chou, *J. Org. Chem.* **2015**, *80*, 4919-4927; c) L. Yang, Q. Wen, F. Xiao, G.-J. Deng, *Org. Biomol. Chem.* **2014**, *12*, 9519-9523; d) P.-F. Wang, X.-Q. Wang, J.-J. Dai, Y.-S. Feng, H.-J. Xu, *Org. Lett.* **2014**, *16*, 4586-4589; e) R. Das, D. Chakraborty, *Tetrahedron Lett.* **2012**, *53*, 7023-7027; f) S. Ranjit, R. Lee, D. Heryadi, C. Shen, J. E. Wu, P. Zhang, K.-W. Huang, X. Liu, *J. Org. Chem.* **2011**, *76*, 8999-9007; g) S. Zhang, P. Qian, M. Zhang, M. Hu, J. Cheng, *J. Org. Chem.* **2010**, *75*, 6732-6735.
- [144] a) L. Chen, P. Liu, J. Wu, B. Dai, *Tetrahedron* **2018**, *74*, 1513-1519; b) P. Peng, J. Wang, C. Li, W. Zhu, H. Jiang, H. Liu, *RSC Adv.* **2016**, *6*, 57441-57445; c) L. Zhu, X. Cao, R. Qiu, T. Iwasaki, V. P. Reddy, X. Xu, S.-F. Yin, N. Kambe, *RSC Adv.* **2015**, *5*, 39358-39365; d) L. Chu, X. Yue, F.-L. Qing, *Org. Lett.* **2010**, *12*, 1644-1647; e) X. Chen, X.-S. Hao, C. E. Goodhue, J.-Q. Yu, *J. Am. Chem. Soc.* **2006**, *128*, 6790-6791.
- [145] a) Y. A. Ho, M. Leiendecker, X. Liu, C. Wang, N. Alandini, M. Rueping, *Org. Lett.* **2018**, *20*, 5644-5647; b) X. Yang, H. Sun, S. Zhang, X. Li, *J. Org. Chem.* **2013**, *723*, 36-42; c) L. Ackermann, R. Born, J. H. Spatz, D. Meyer, *Angew. Chem. Int. Ed.* **2005**, *44*, 7216-7219.

6 References

- [146] H. Ghafari, M. M. Hashemi, *J. Sulfur Chem.* **2009**, *30*, 578-580.
- [147] A. Yokota, N. Chatani, *Chem. Lett.* **2015**, *44*, 902-904.
- [148] Z. Ruan, D. Ghorai, G. Zanoni, L. Ackermann, *Chem. Commun.* **2017**, *53*, 9113-9116.
- [149] a) B. Varga, A. Csonka, A. Csonka, J. Molnar, L. Amaral, G. Spengler, *Anticancer Res.* **2017**, *37*, 5983-5993; b) A. Jaszczyszyn, K. Gasiorowski, P. Swiatek, W. Malinka, K. Cieslik-Boczula, J. Petrus, B. Czarnik-Matusiewicz, *Pharmacol. Rep.* **2012**, *64*, 16-23.
- [150] C. Marivingt-Mounir, Y. Mettey, J.-M. Vierfond, *J. Heterocycl. Chem.* **1998**, *35*, 843-845.
- [151] a) J. J. Gugger, M. Cassagnol, *Am. J. Addiction* **2008**, *17*, 454-455; b) T. A. Ban, *Neuropsychiatr. Dis. Treat.* **2007**, *3*, 495-500; c) M. E. Scheetz, D. G. Carlson, M. R. Schinitsky, *Infect. Immun.* **1977**, *15*, 145-148; d) E. A. Nodiff, S. Ina, N. Oda, T. Hayazaki, S. Nishibe, T. Kohno, M. Hausman, A. A. Manian, *J. Heterocycl. Chem.* **1967**, *4*, 239-245.
- [152] S. Nakanowatari, T. Müller, J. C. A. Oliveira, L. Ackermann, *Angew. Chem. Int. Ed.* **2017**, *56*, 15891-15895.
- [153] M.-S. Yu, W.-C. Lee, C.-H. Chen, F.-Y. Tsai, T.-G. Ong, *Org. Lett.* **2014**, *16*, 4826-4829.
- [154] a) S. Sahil, M. Samir, K. Sunil, S. Jagjeet, M. S. B. Preet, N. Kunal, *Recent Pat. Anticancer Drug Discov.* **2015**, *10*, 308-341; b) A. Nayak, G. Chandra, I. Hwang, K. Kim, X. Hou, H. O. Kim, P. K. Sahu, K. K. Roy, J. Yoo, Y. Lee, M. Cui, S. Choi, S. M. Moss, K. Phan, Z.-G. Gao, H. Ha, K. A. Jacobson, L. S. Jeong, *J. Med. Chem.* **2014**, *57*, 1344-1354; c) M. Legraverend, D. S. Grierson, *Bioorg. Med. Chem.* **2006**, *14*, 3987-4006; d) L.-L. Gundersen, J. Nissen-Meyer, B. Spilsberg, *J. Med. Chem.* **2002**, *45*, 1383-1386.
- [155] J. Mo, T. Müller, J. C. A. Oliveira, L. Ackermann, *Angew. Chem. Int. Ed.* **2018**, *57*, 7719-7723.
- [156] P. Crabbé, H. Fillion, D. André, J.-L. Luche, *J. Chem. Soc., Chem. Commun.* **1979**, 859-860.
- [157] J. Mo, T. Müller, J. C. A. Oliveira, S. Demeshko, F. Meyer, L. Ackermann, *Angew. Chem. Int. Ed.* **2019**, *58*, DOI:10.1002/anie.201904110.

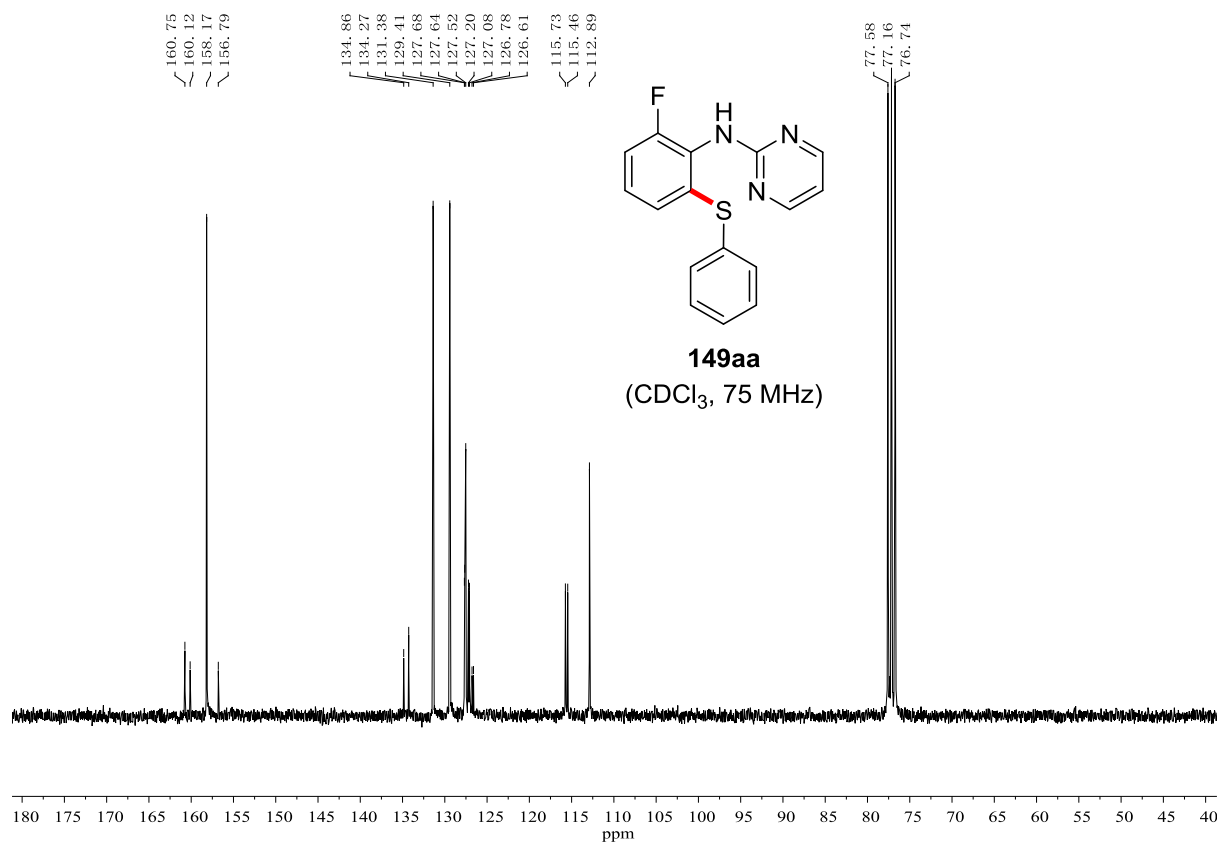
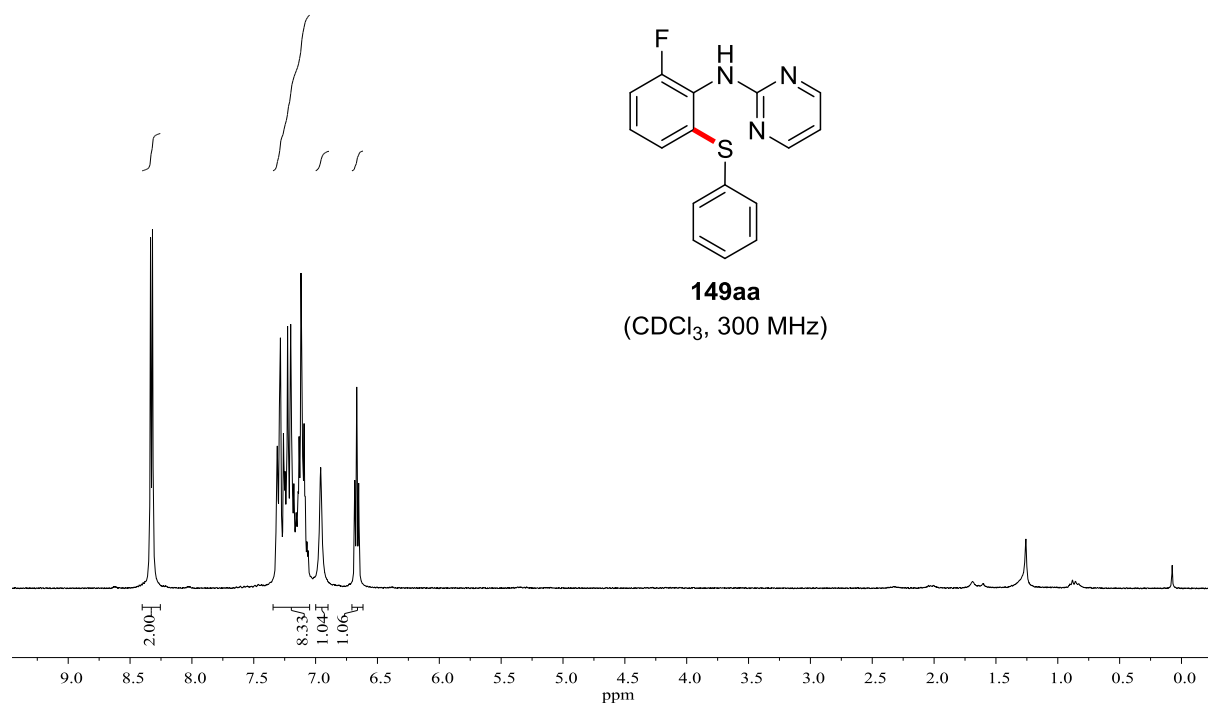
6 References

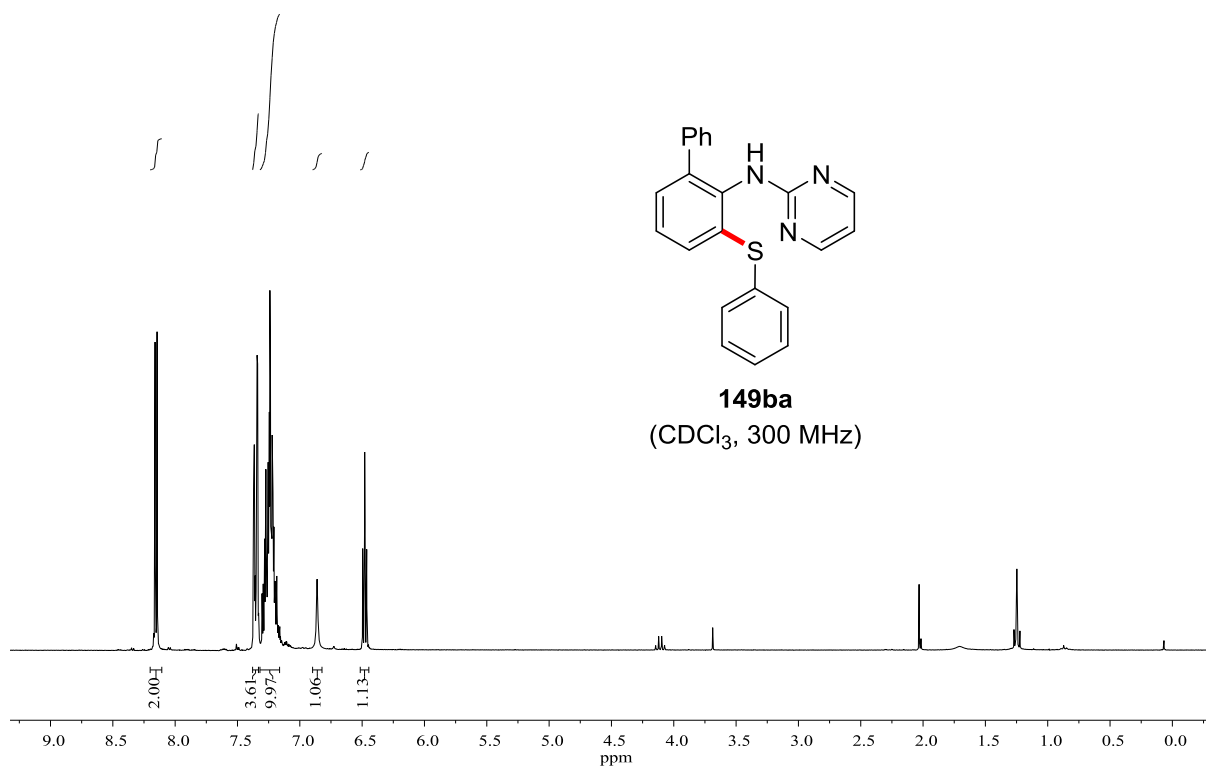
- [158] P. Gandeepan, N. Kaplaneris, S. Santoro, L. Vaccaro, L. Ackermann, *ACS Sustainable Chem. Eng.* **2019**, *7*, 8023-8040.
- [159] O. Eisenstein, J. Milani, R. N. Perutz, *Chem. Rev.* **2017**, *117*, 8710-8753.
- [160] E. K. Anslyn, D. A. Dougherty, *Modern Physical Organic Chemistry*, University Science Books: Sausalito, CA, **2006**.
- [161] a) A. Rana, M. E. Cinar, D. Samanta, M. Schmittel, *Org. Lett.* **2016**, *18*, 84-87; b) Y. Aihara, N. Chatani, *Chem. Sci.* **2013**, *4*, 664-670.
- [162] L. Ackermann, A. V. Lygin, *Org. Lett.* **2012**, *14*, 764-767.
- [163] Y. Liu, Y. Bai, J. Zhang, Y. Li, J. Jiao, X. Qi, *Eur. J. Org. Chem.* **2007**, 6084-6088.
- [164] M. Kirihaara, Y. Asai, S. Ogawa, T. Noguchi, Y. Hirai, *Synthesis* **2007**, *21*, 3286-3289.
- [165] Y. Hang, C. Kui, (Ed.: P. I. Appl.), **2015**.
- [166] a) O. Nacham, K. D. Clark, J. L. Anderson, *RSC Adv.* **2016**, *6*, 11109-11117; b) Q.-X. Liu, W. Zhang, X.-J. Zhao, Z.-X. Zhao, M.-C. Shi, X.-G. Wang, *Eur. J. Org. Chem.* **2013**, 1253-1261.
- [167] H. Yang, Z. Miao, R. Chen, *Lett. Org. Chem.* **2011**, *8*, 325-331.
- [168] a) S. Allu, K. C. Kumara Swamy, *Adv. Synth. Catal.* **2015**, *357*, 2665-2680; b) K. Hiroya, S. Itoh, T. Sakamoto, *J. Org. Chem.* **2004**, *69*, 1126-1136; c) A. K. Bakkestuen, L.-L. Gundersen, *Tetrahedron Lett.* **2003**, *44*, 3359-3362.
- [169] a) M. Mihorianu, H. Franz, P. G. Jones, M. Freytag, G. Kelter, H.-H. Fiebig, M. Tamm, I. Neda, *Appl. Organometal. Chem.* **2016**, *30*, 581-589; b) M.-S. Yu, W.-C. Lee, C.-H. Chen, F.-Y. Tsai, T.-G. Ong, *Org. Lett.* **2014**, *16*, 4826-4829; c) F. Shibahara, Y. Dohke, T. Murai, *J. Org. Chem.* **2012**, *77*, 5381-5388.
- [170] P. C. Kunz, I. Thiel, A. L. Noffke, G. J. Reiß, F. Mohr, B. Spingler, *J. Organomet. Chem.* **2012**, *697*, 33-40.
- [171] R. D. Baxter, D. G. Blackmond, *Tetrahedron* **2013**, *69*, 5604-5608.
- [172] T. Kippo, T. Fukuyama, I. Ryu, *Org. Lett.* **2011**, *13*, 3864-3867.
- [173] A. Köpfer, B. Breit, *Angew. Chem. Int. Ed.* **2015**, *54*, 6913-6917.
- [174] W. Desens, T. Werner, *Adv. Synth. Catal.* **2016**, *358*, 622-630.
- [175] G. Berthon-Gelloz, M. A. Siegler, A. L. Spek, B. Tinant, J. N. H. Reek, I. E. Markó, *Dalton Trans.* **2010**, *39*, 1444-1446.
- [176] S. Meiries, K. Speck, D. B. Cordes, A. M. Z. Slawin, S. P. Nolan, *Organometallics* **2013**, *32*, 330-339.

6 References

- [177] a) W. Li, Z. Lin, L. Chen, X. Tian, Y. Wenig, S.-H. Huang, R. Hong, *Tetrahedron Lett.* **2016**, *57*, 603-606; b) H. Luo, S. Ma, *Eur. J. Org. Chem.* **2013**, 3041-3048; c) L. Zhang, X. Li, Y. Liu, D. Zhang, *Chem. Commun.* **2015**, *51*, 6633-6636; d) Q. Li, C. Fu, S. Ma, *Angew. Chem. Int. Ed.* **2012**, *51*, 11783-11786.
- [178] a) T. Schwier, M. Rubin, V. Gevorgyan, *Org. Lett.* **2004**, *6*, 1999-2001; b) R. Ugajin, S. Kikuchi, T. Yamada, *Synlett* **2014**, *25*, 1178-1180.
- [179] a) D. Ma, Q. Geng, H. Zhang, Y. Jiang, *Angew. Chem. Int. Ed.* **2010**, *49*, 1291-1294; b) N. L. Smith, *J. Org. Chem.* **1950**, *15*, 1125-1130.

7 Appendix



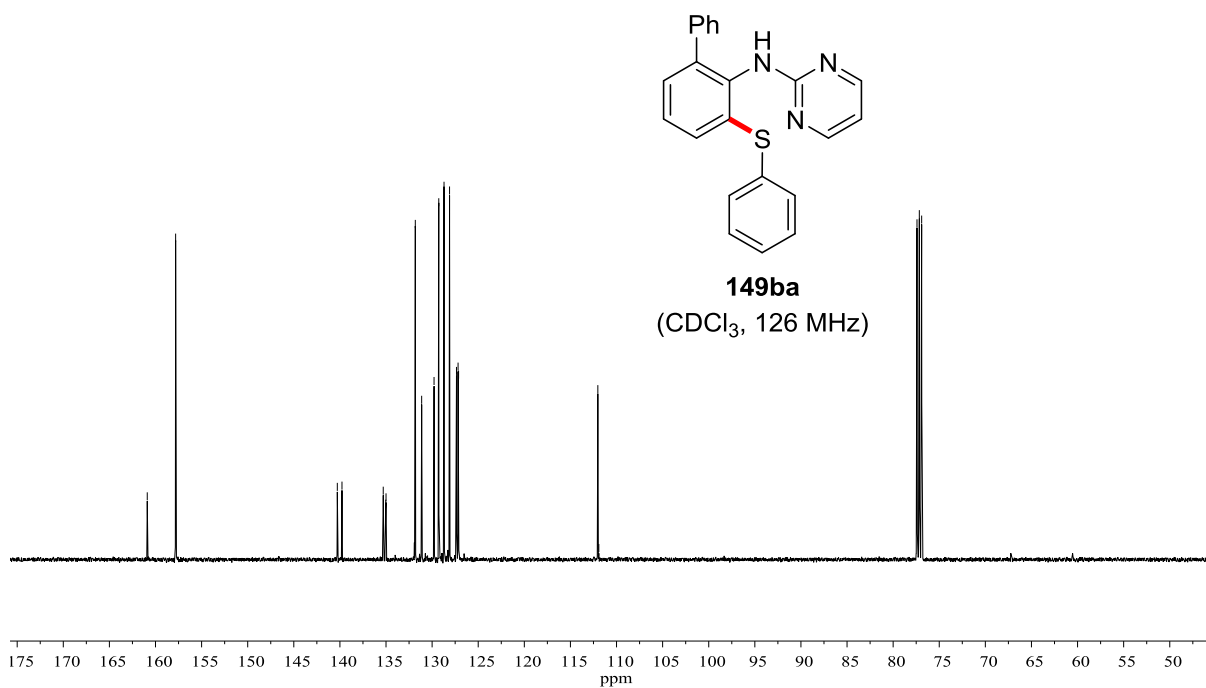


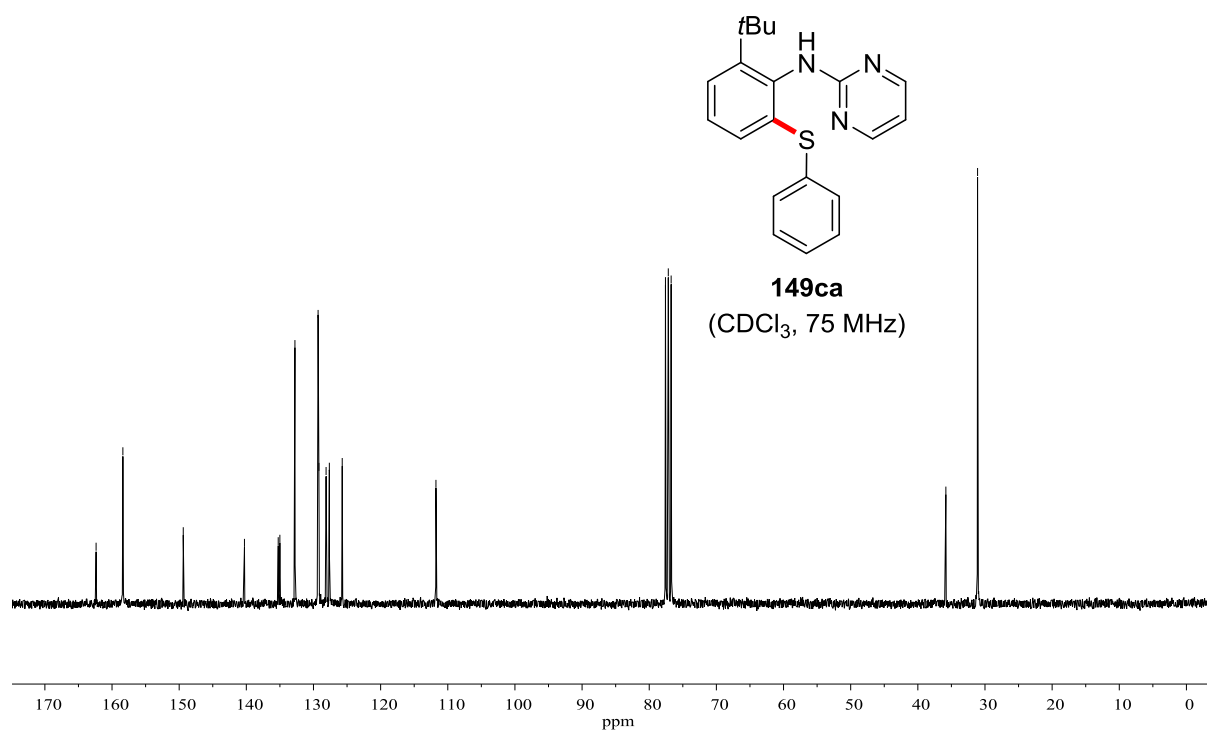
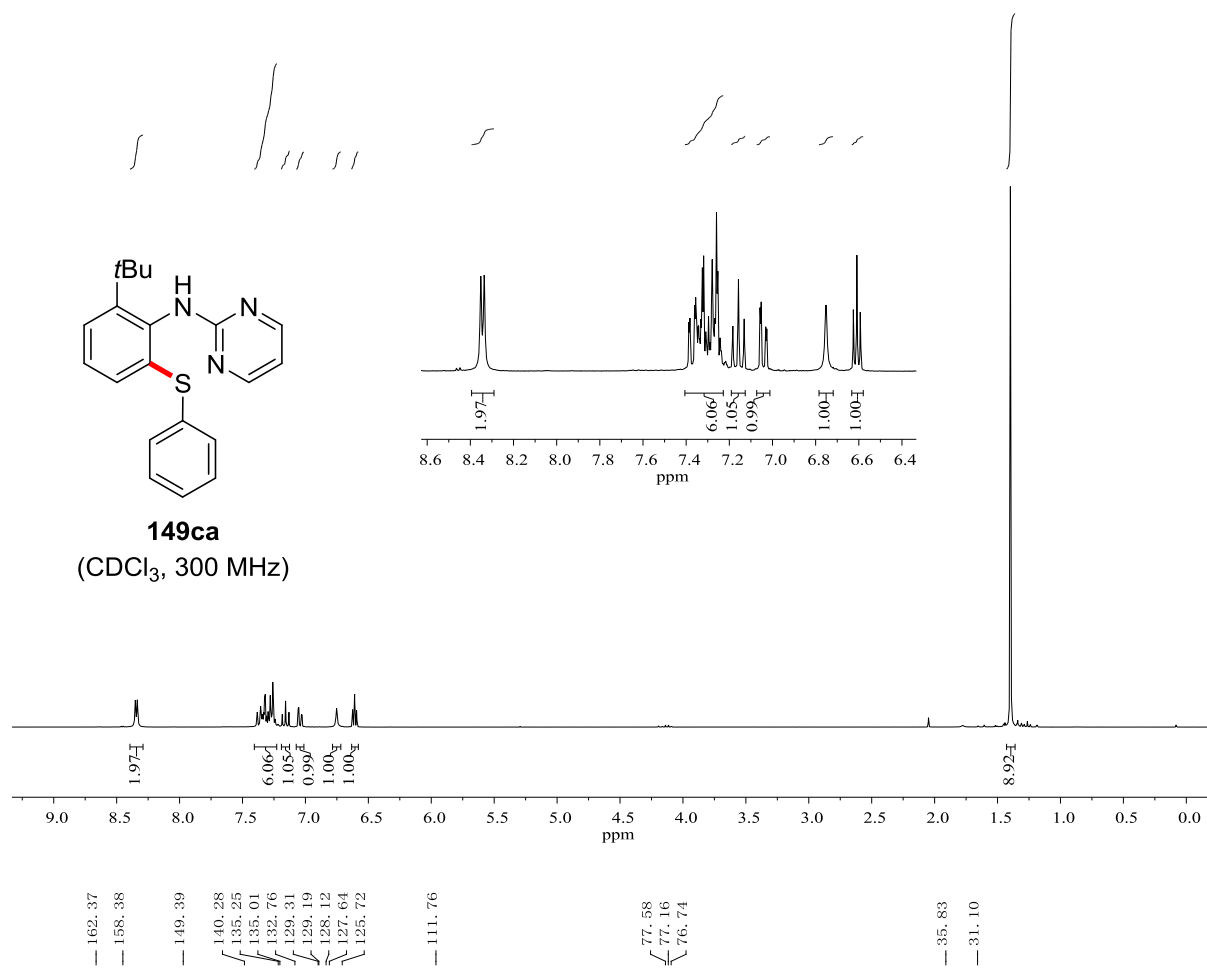
160.89
157.82

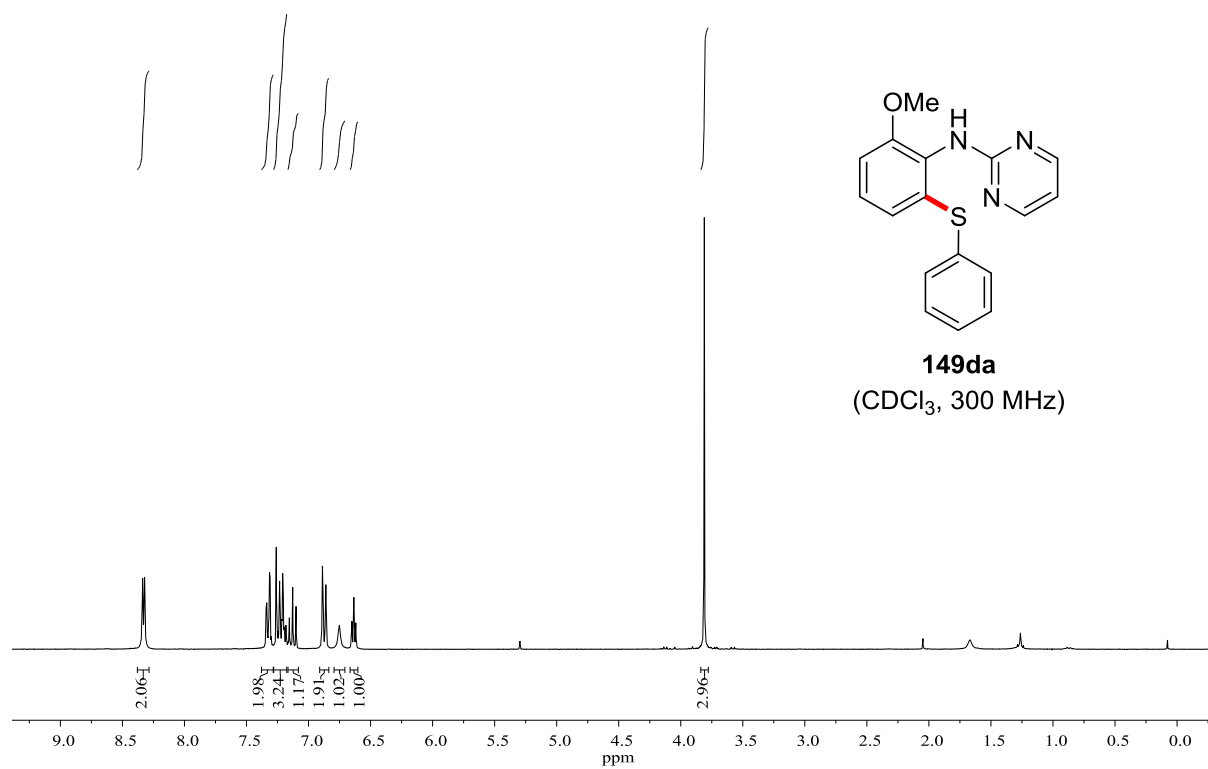
140.28
139.78
135.30
135.03
135.00
131.82
131.13
129.79
129.28
128.71
128.11
127.36
127.18
127.13

112.03
111.92

77.41
77.16
76.91







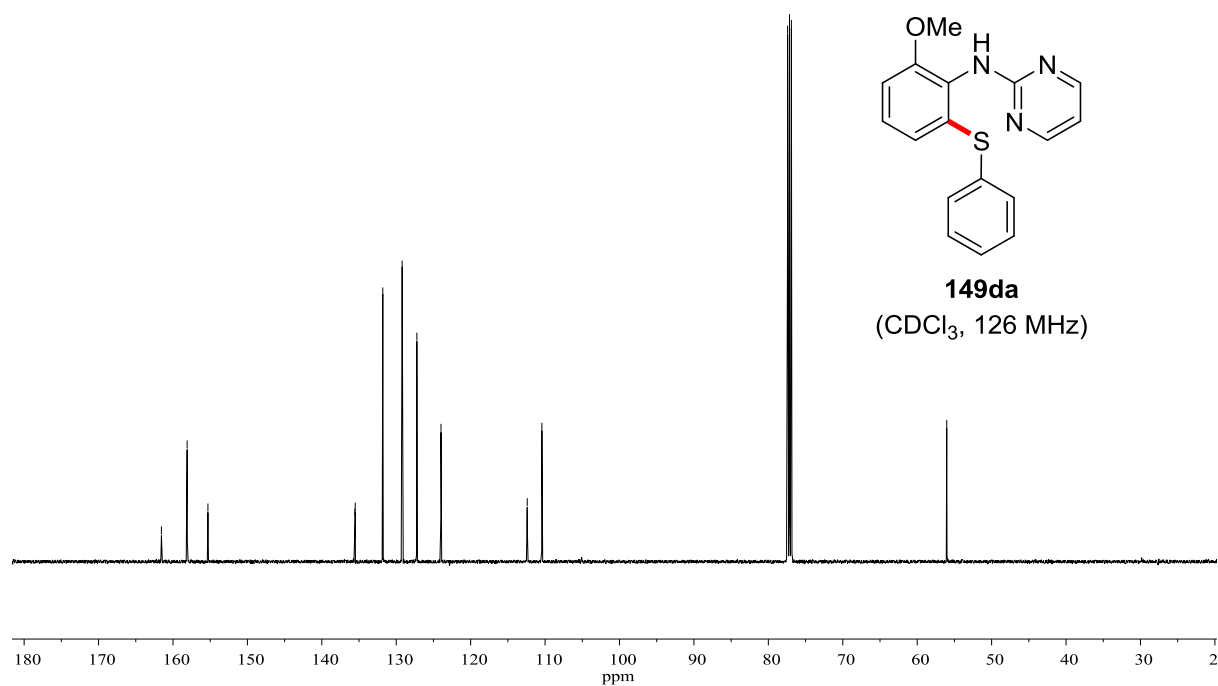
161.55
158.10
155.30

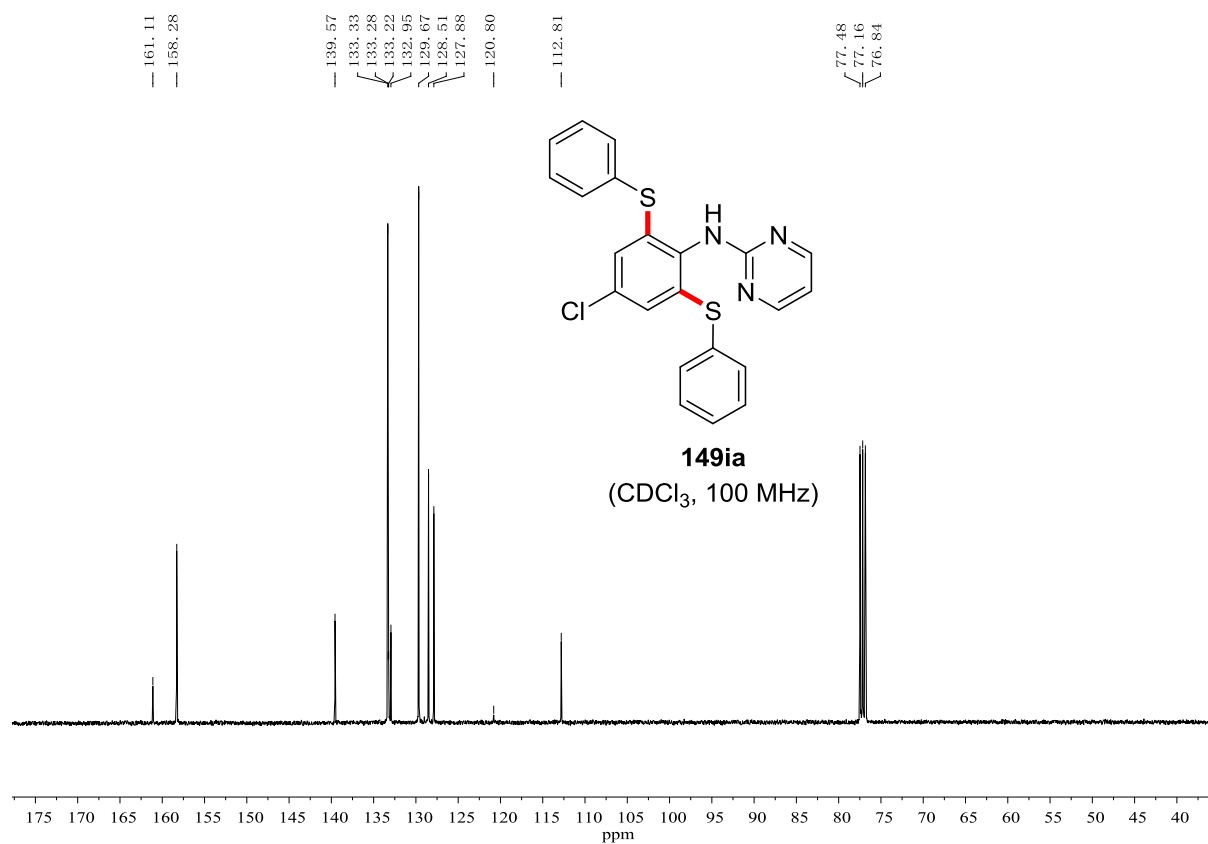
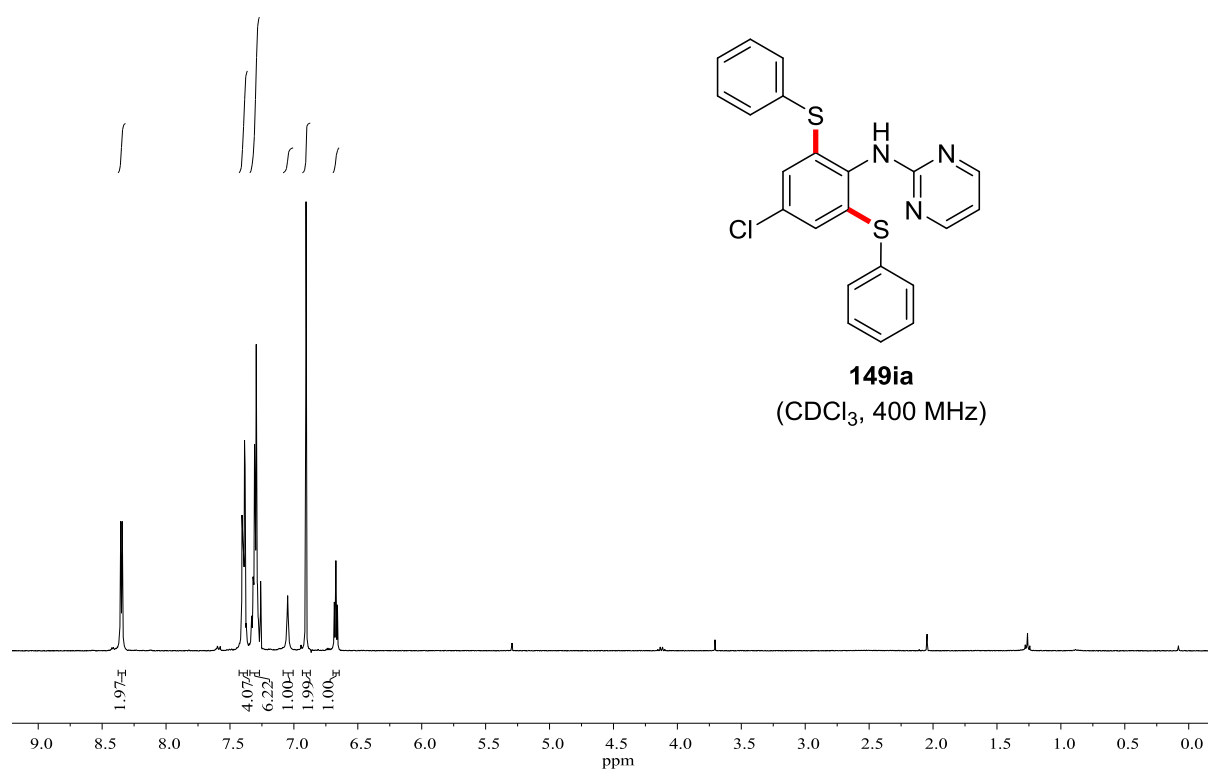
135.56
135.51
131.81
129.21
127.23
123.99

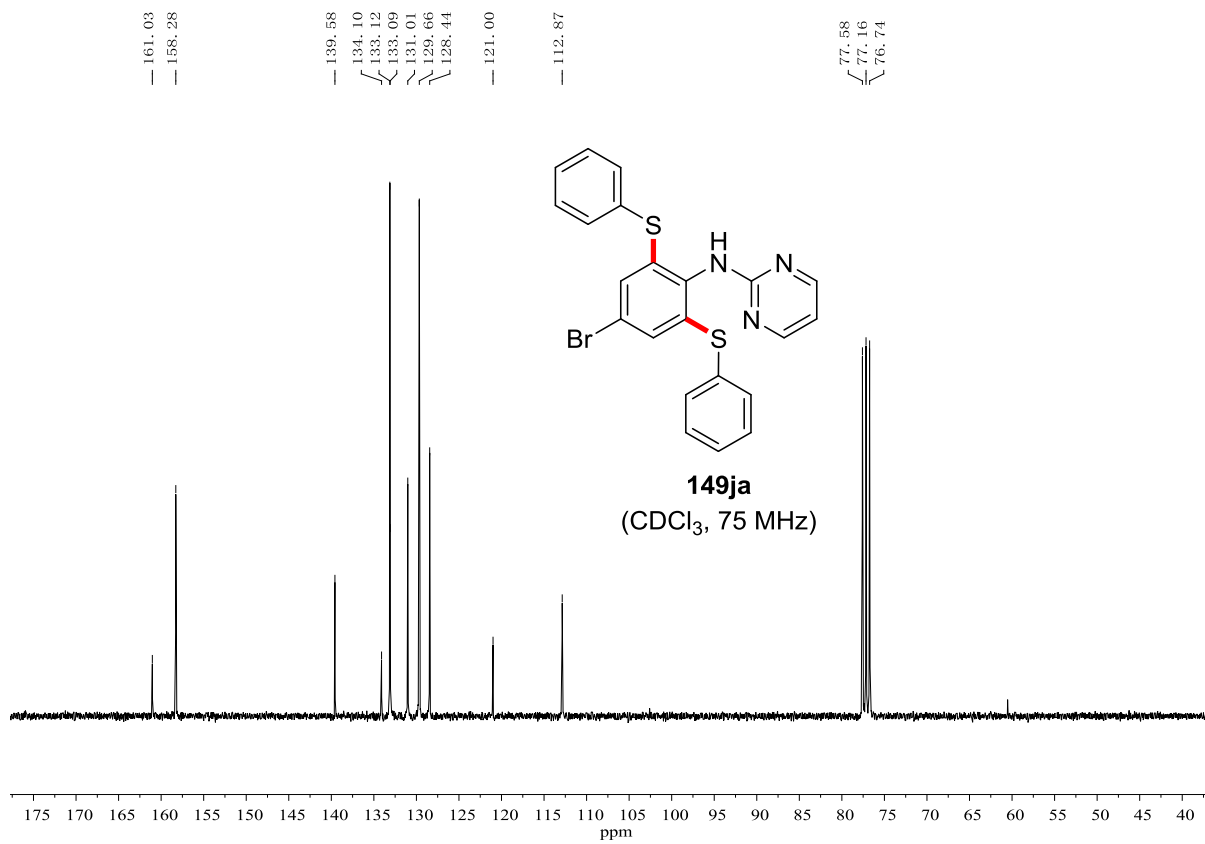
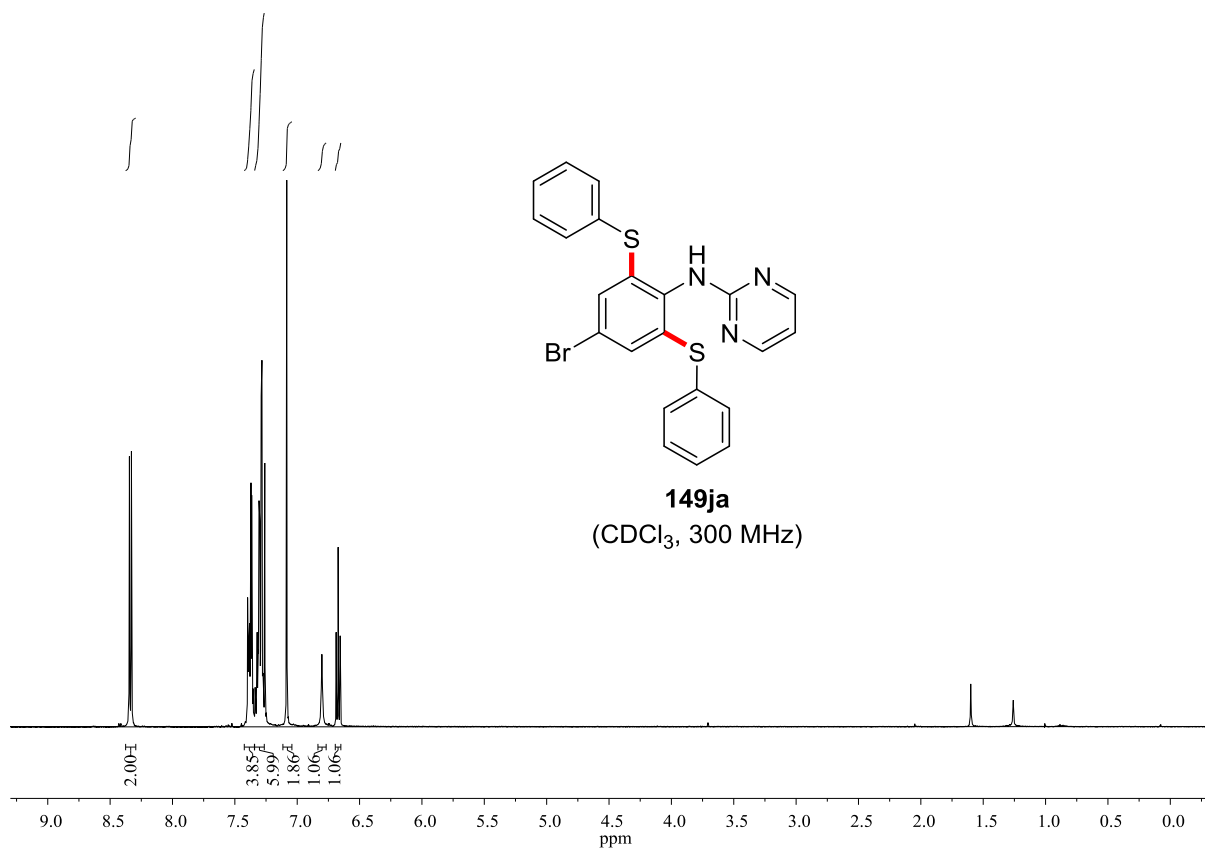
112.40
110.43

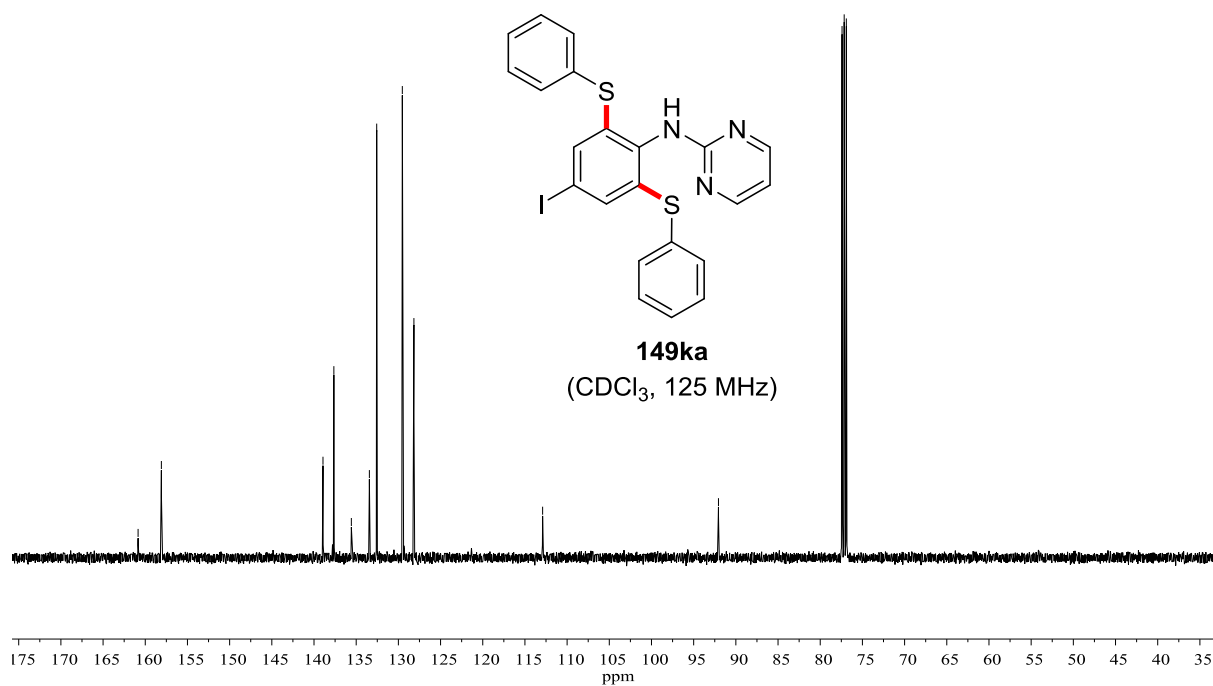
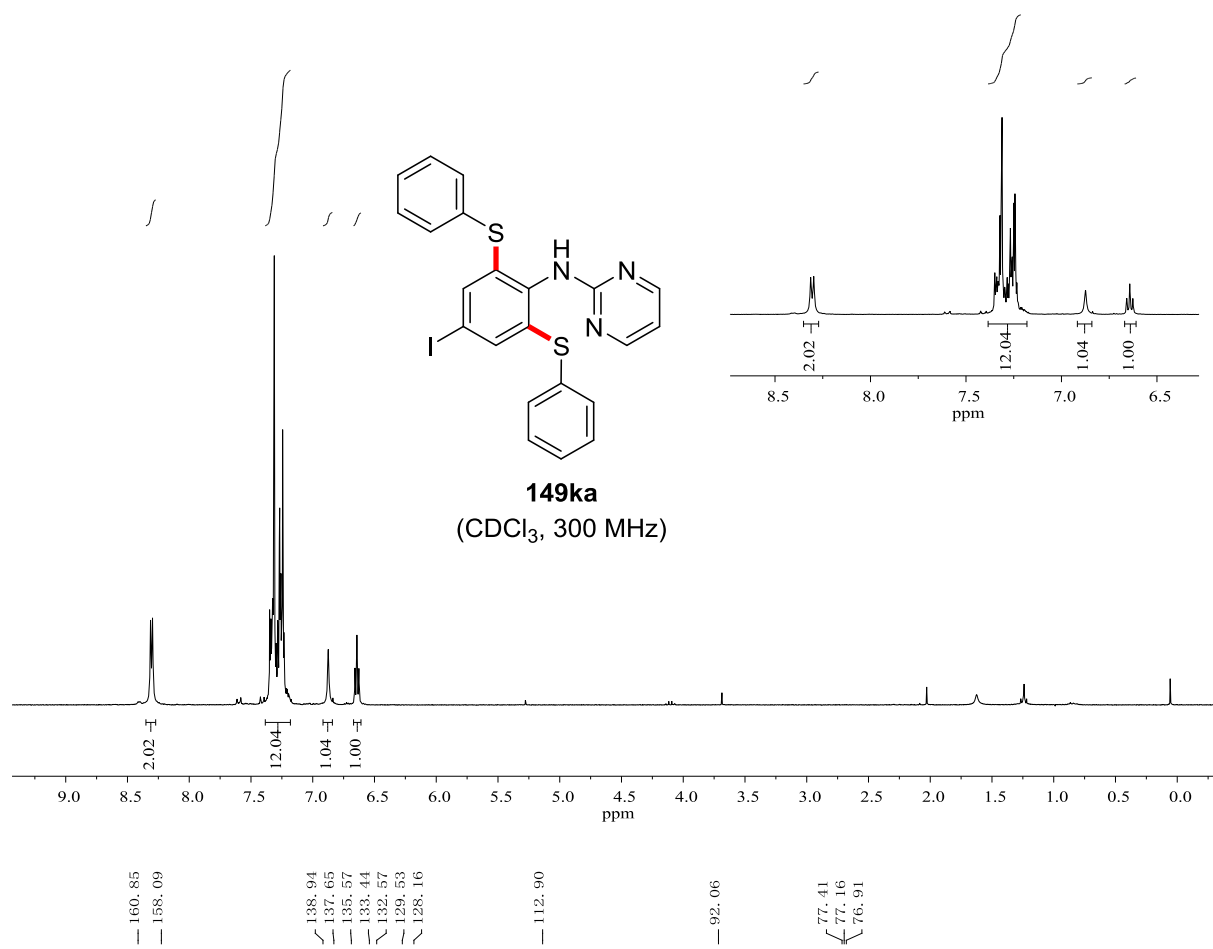
77.41
77.16
76.91

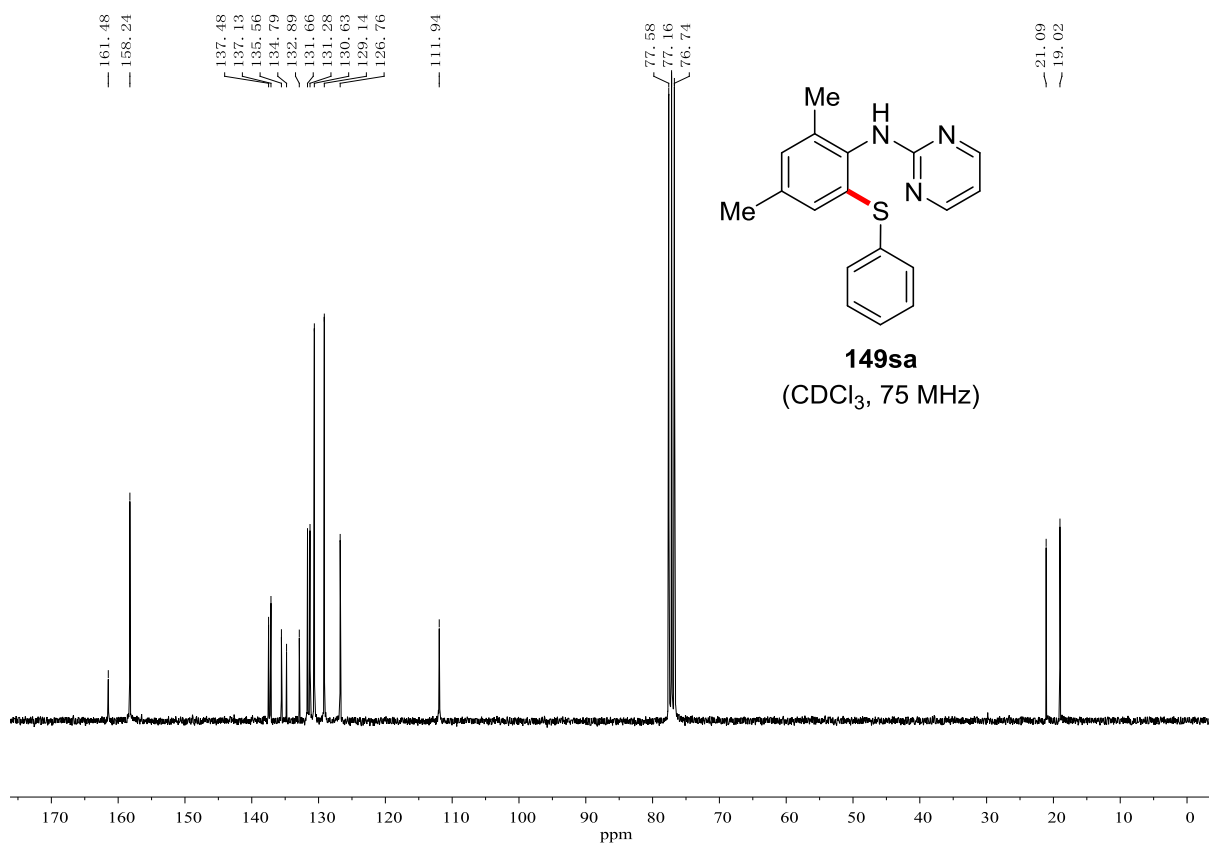
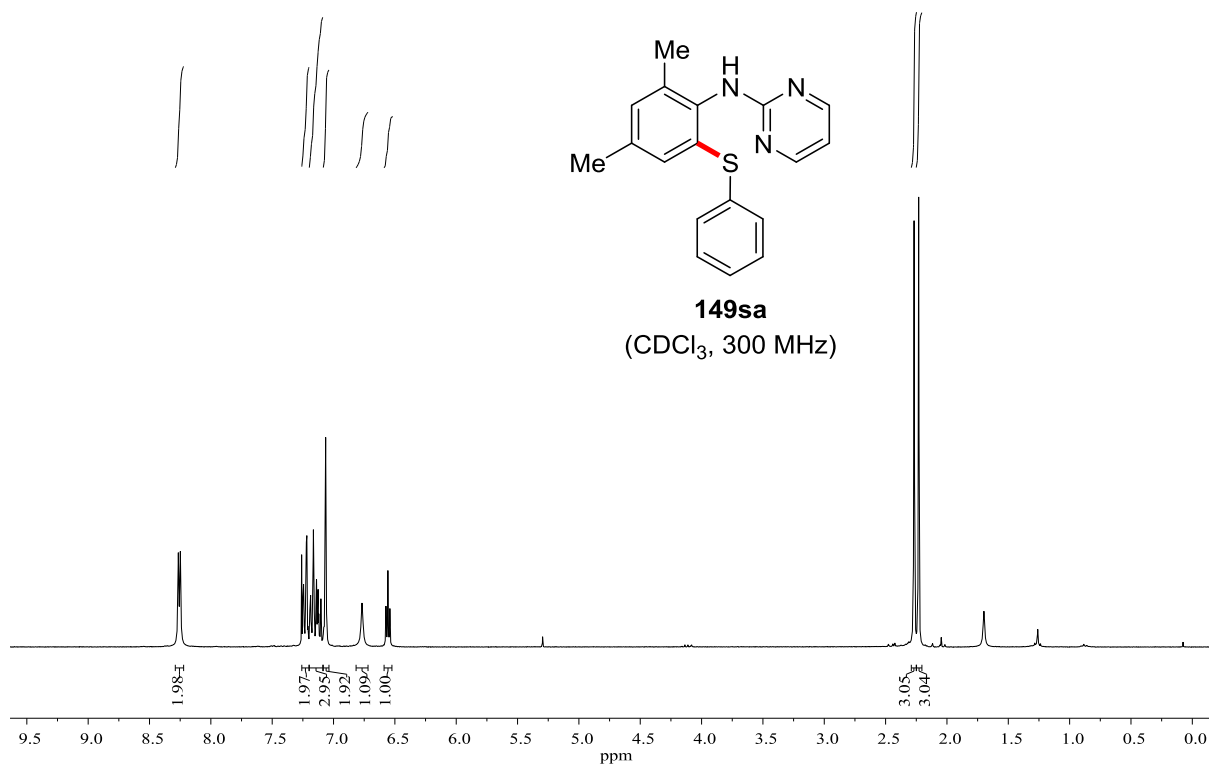
56.03

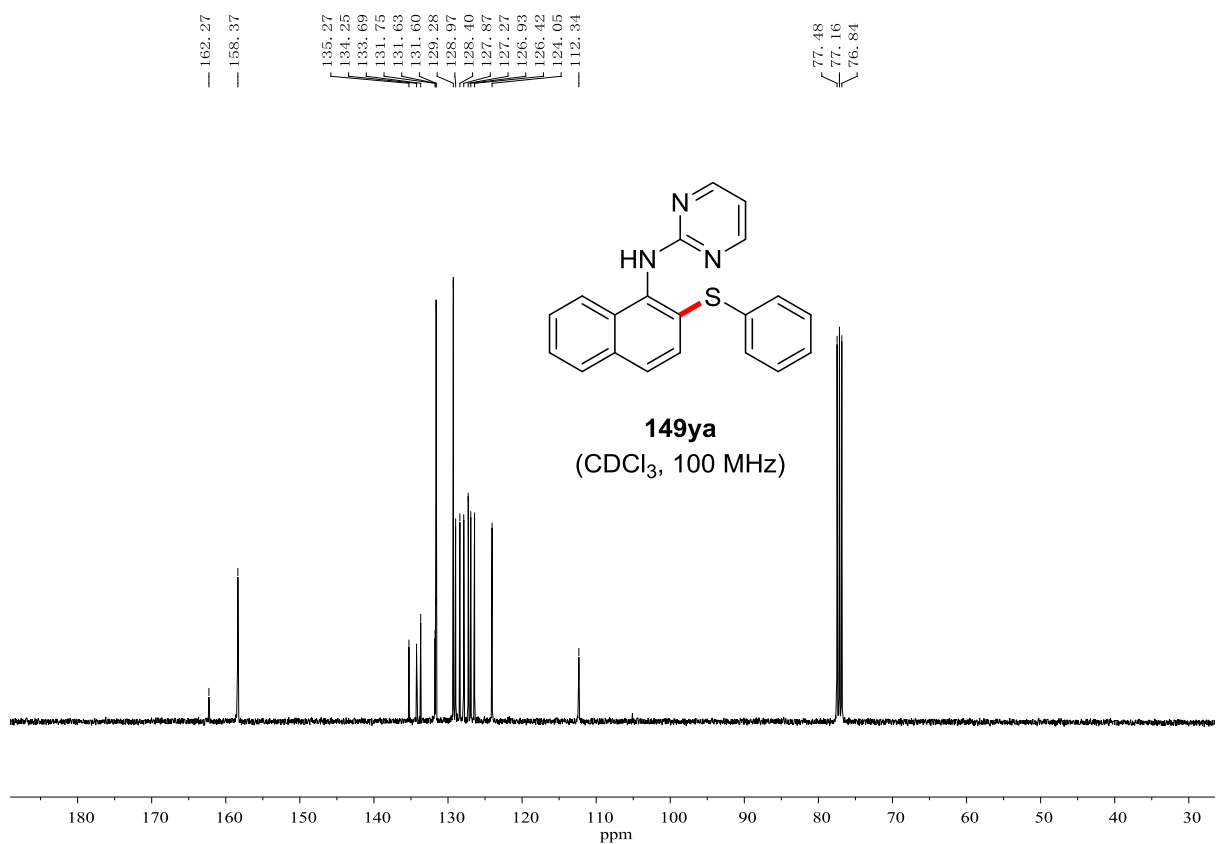
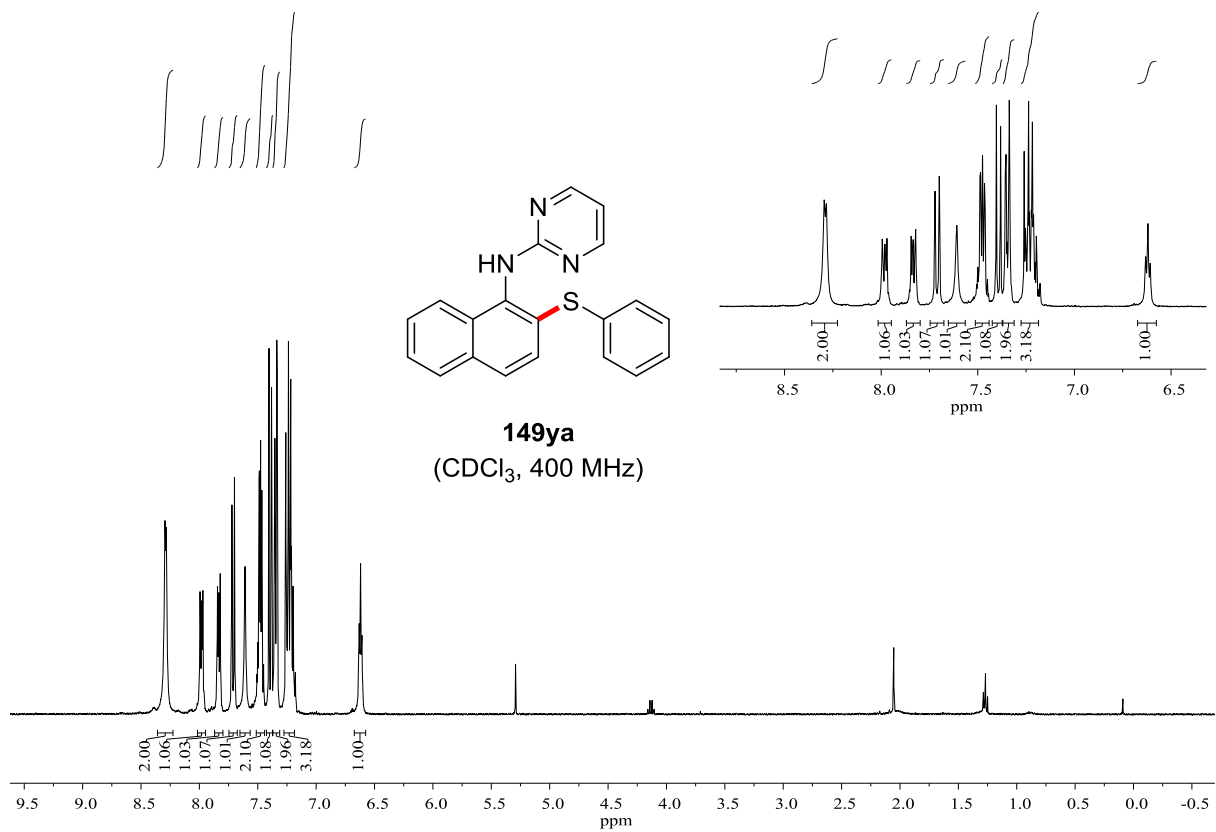


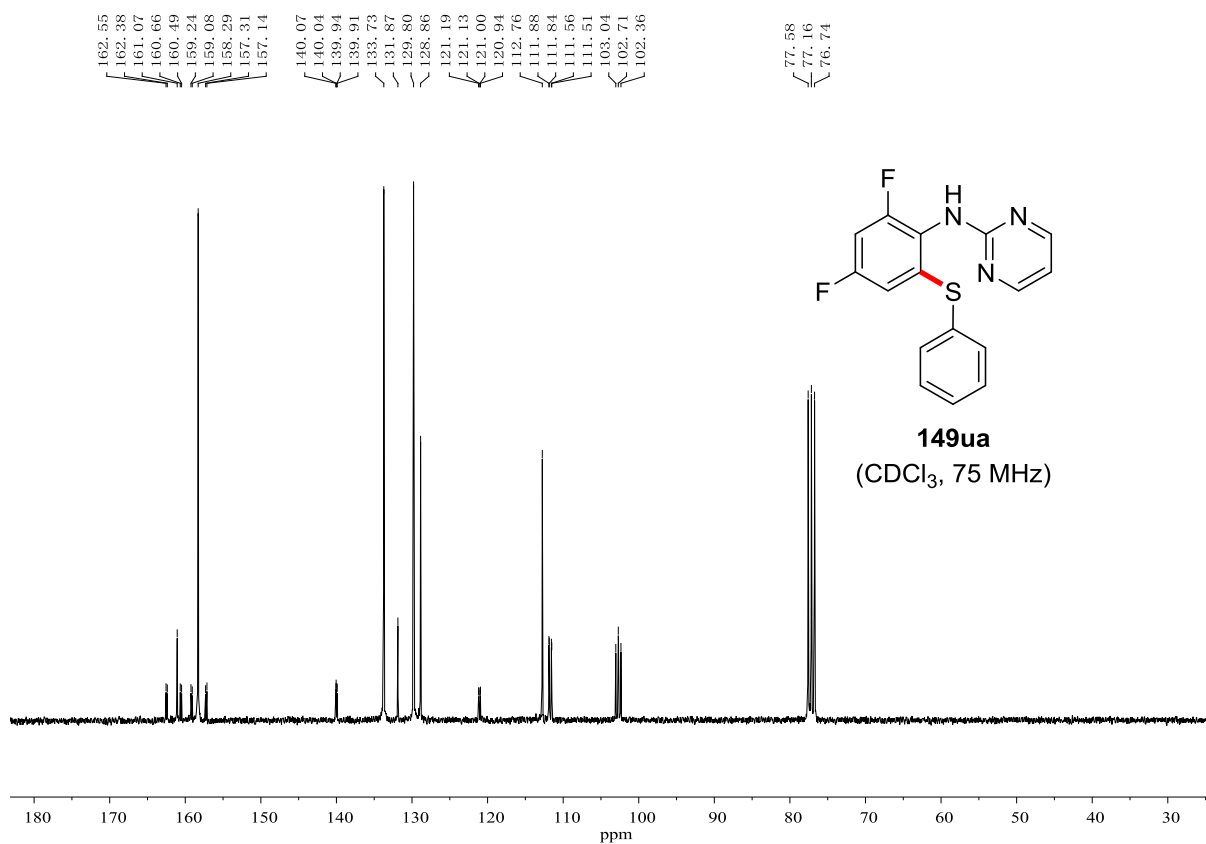
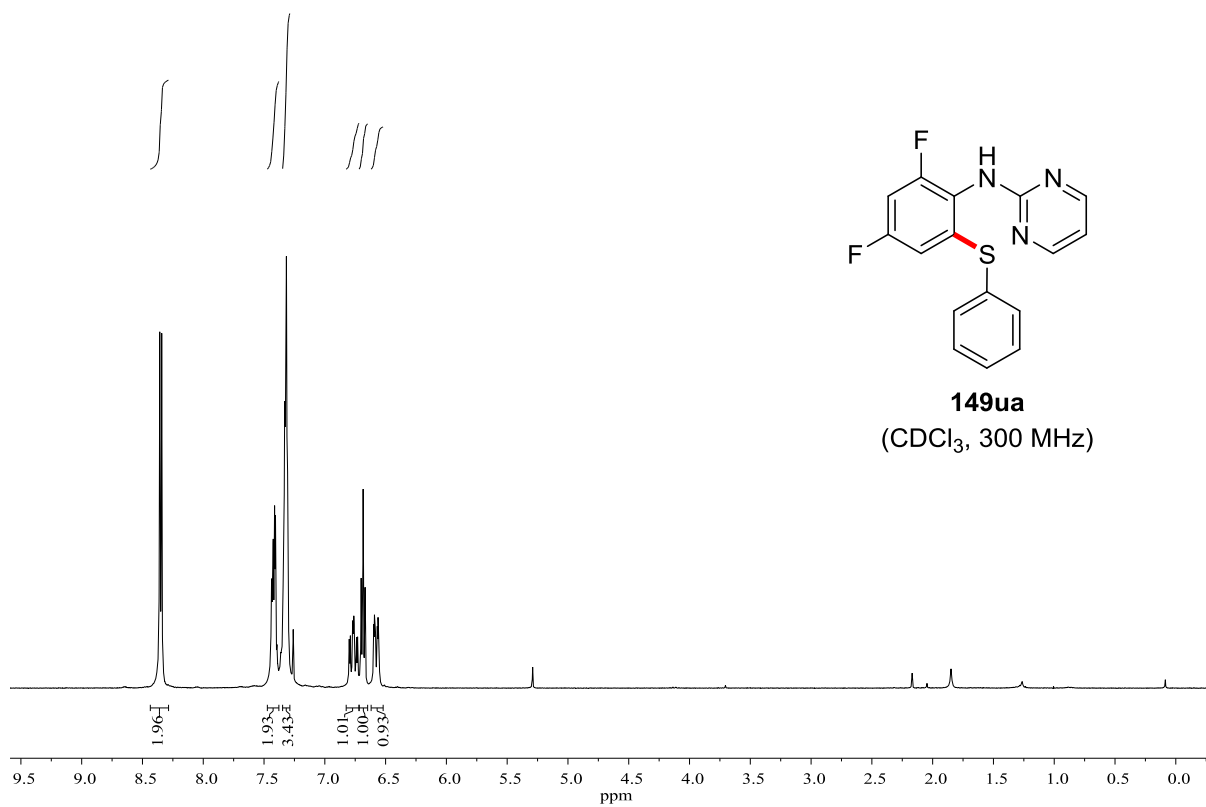


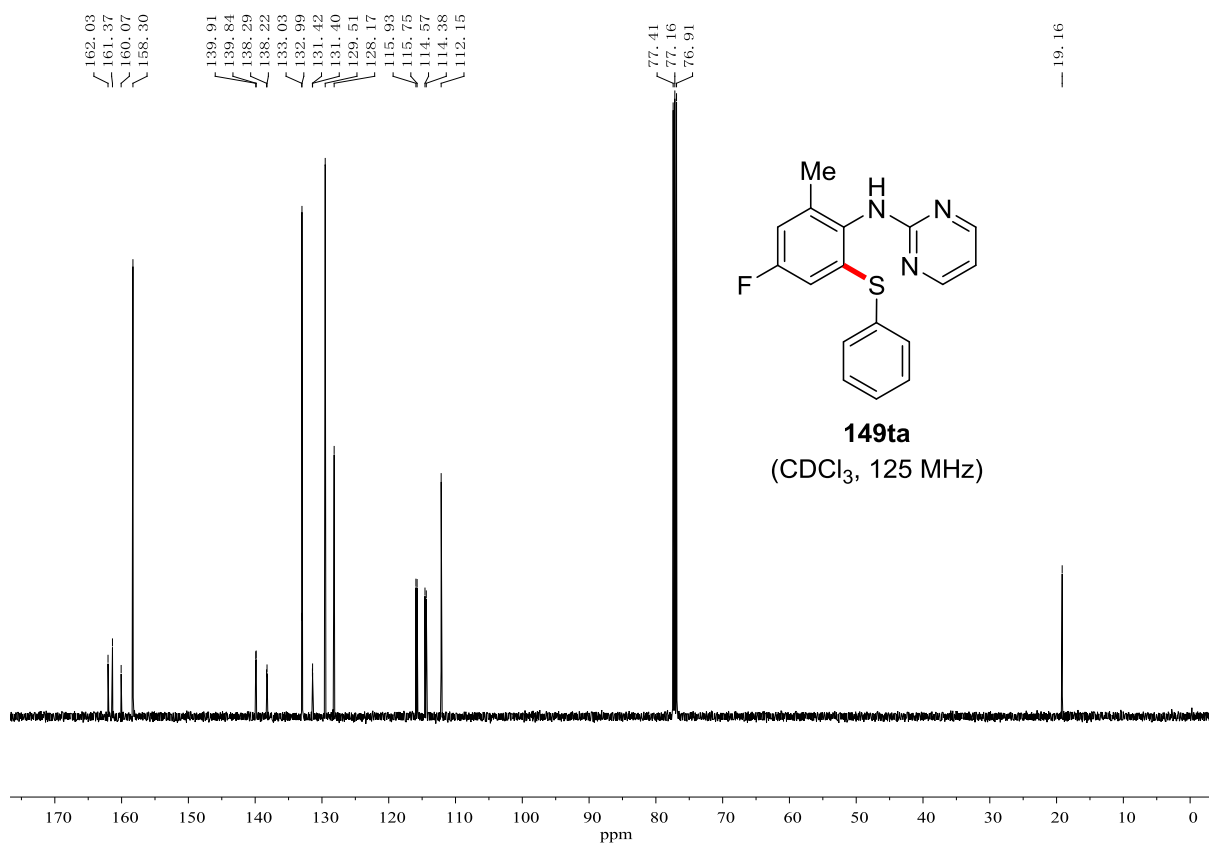
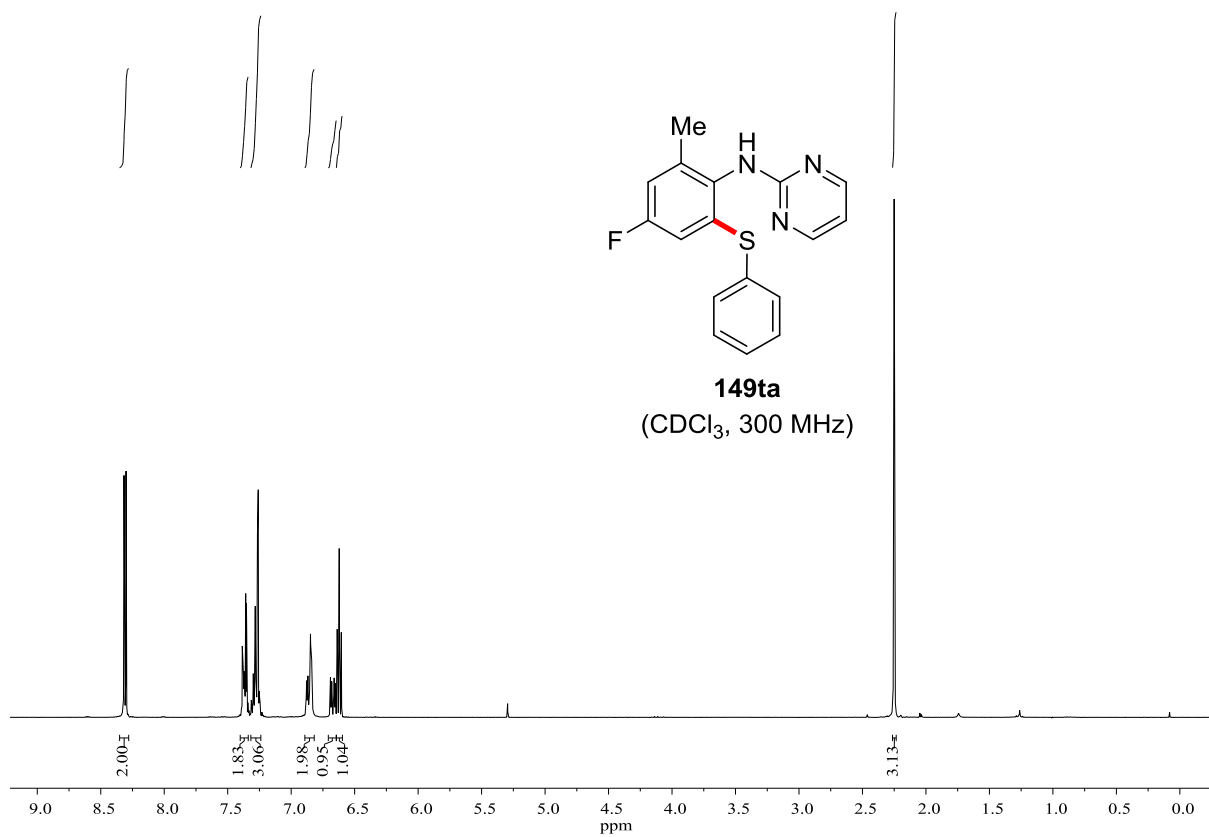


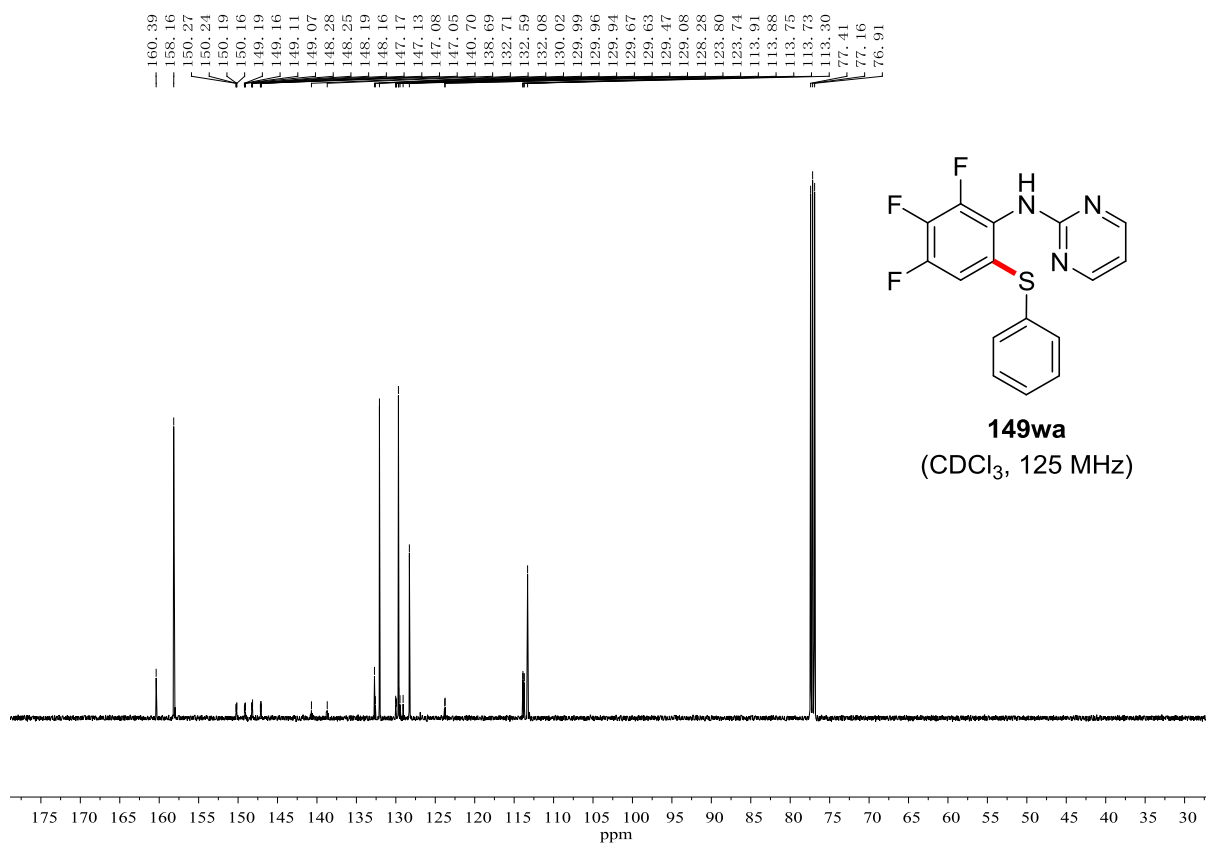
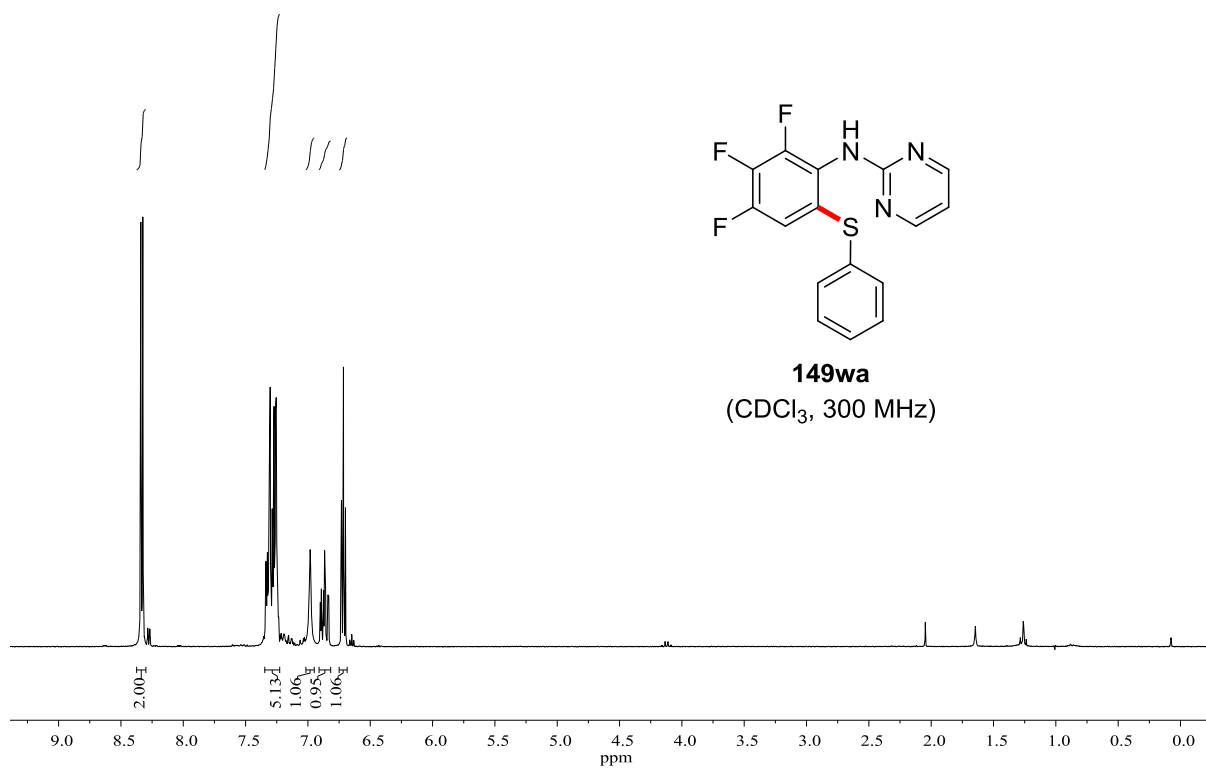


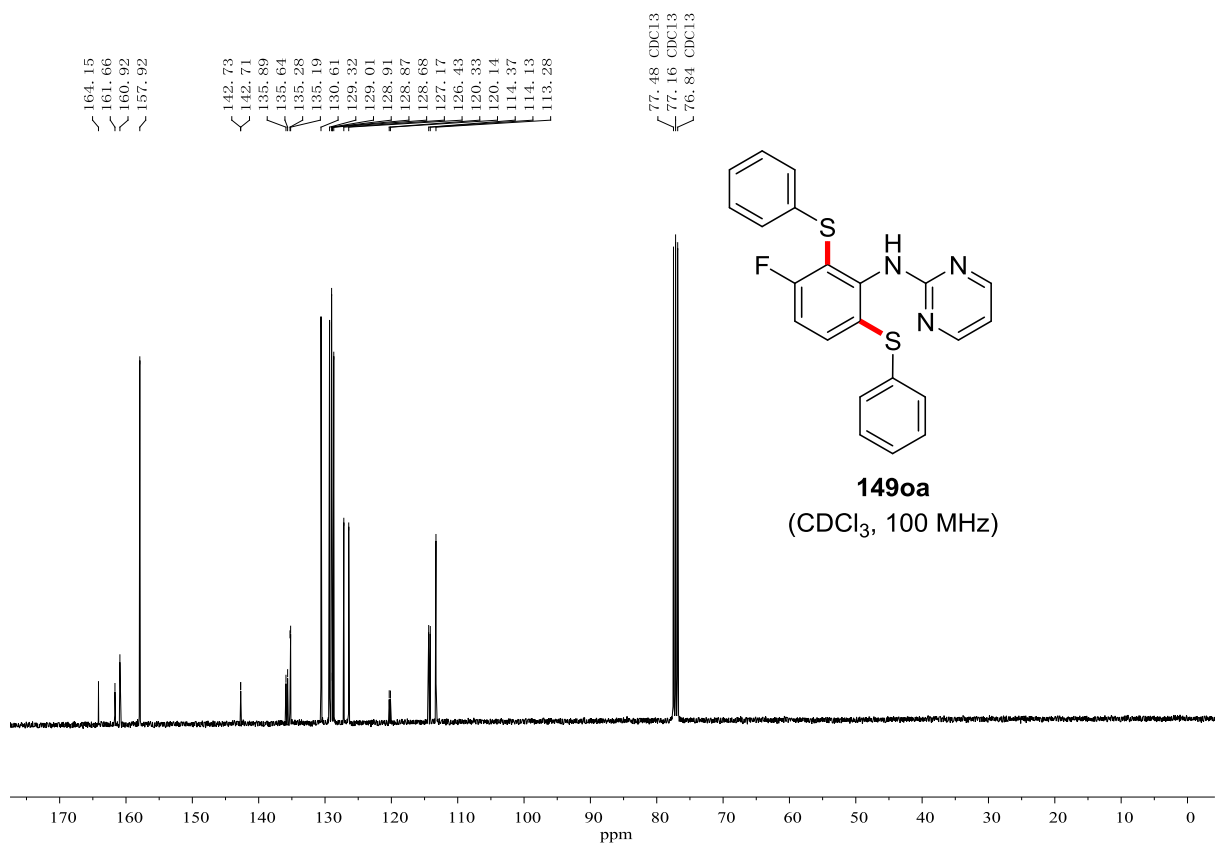
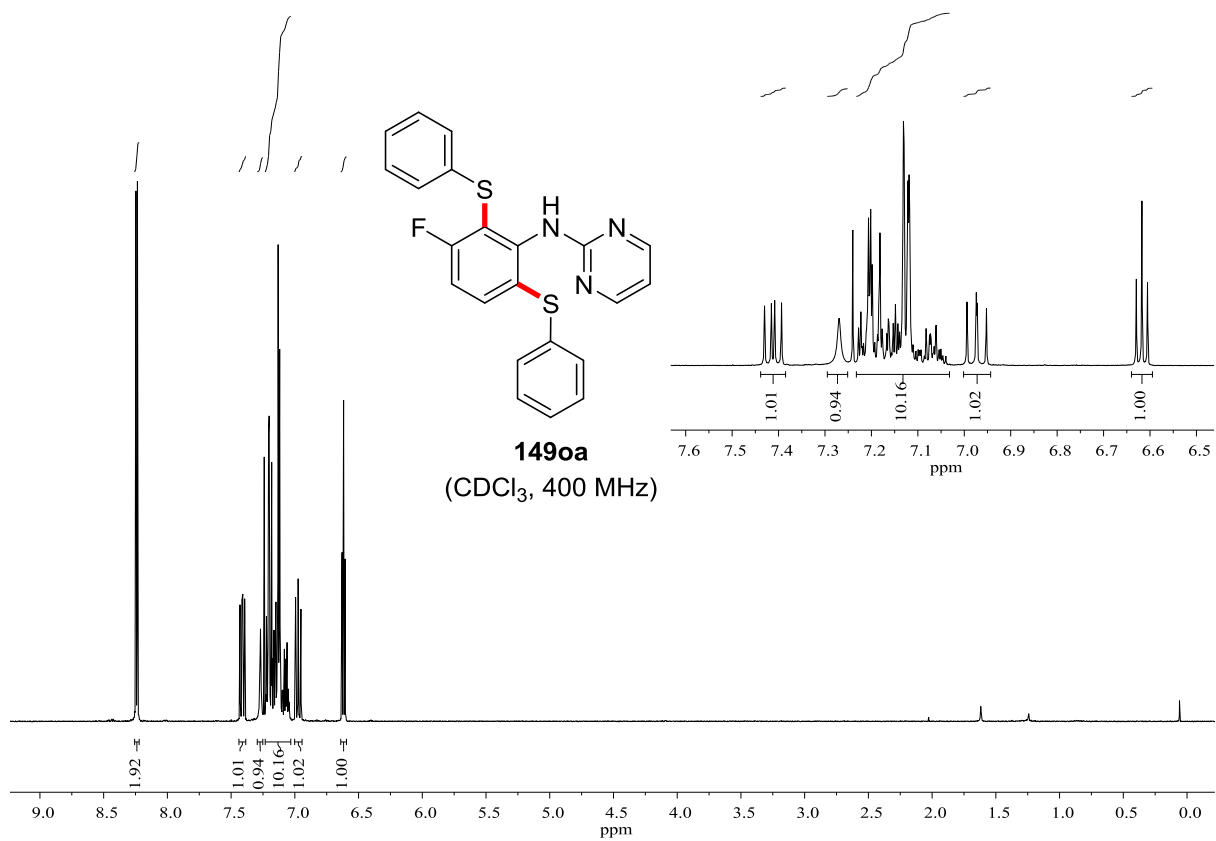


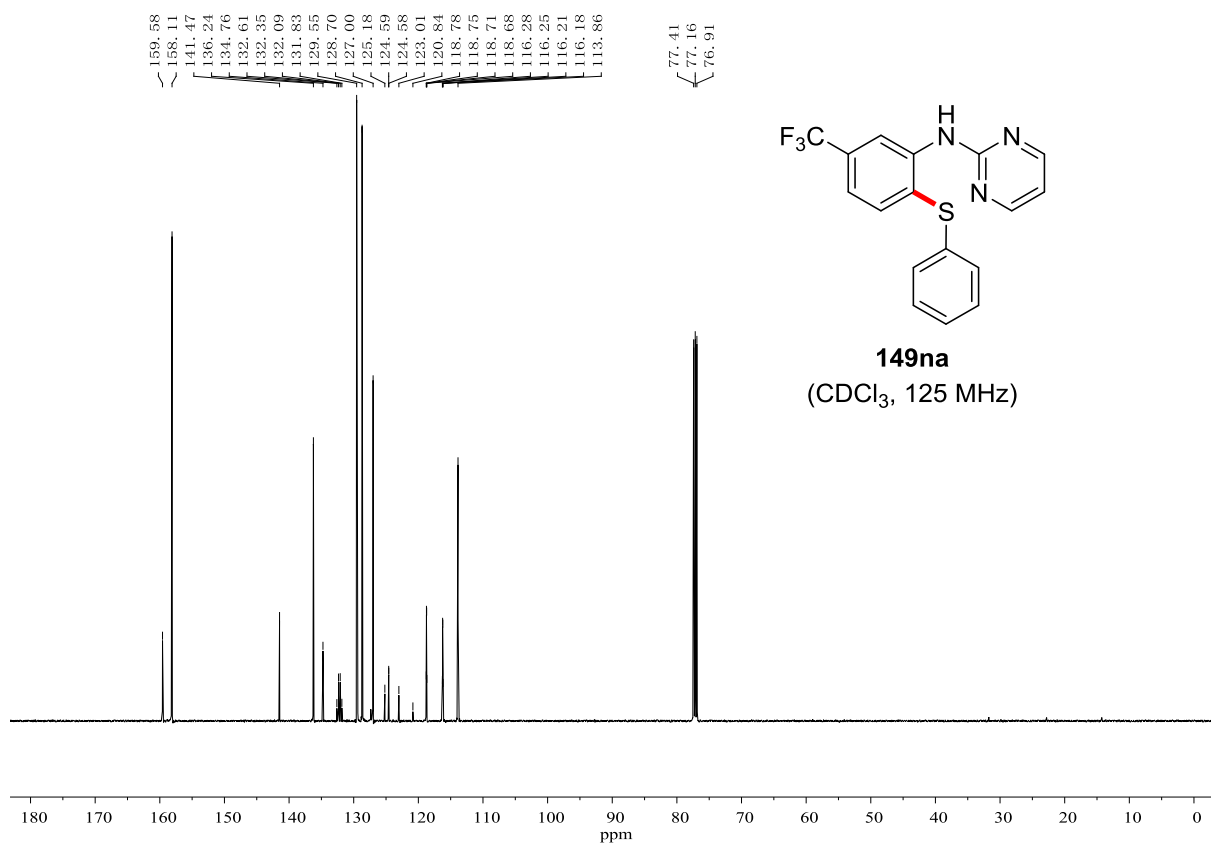
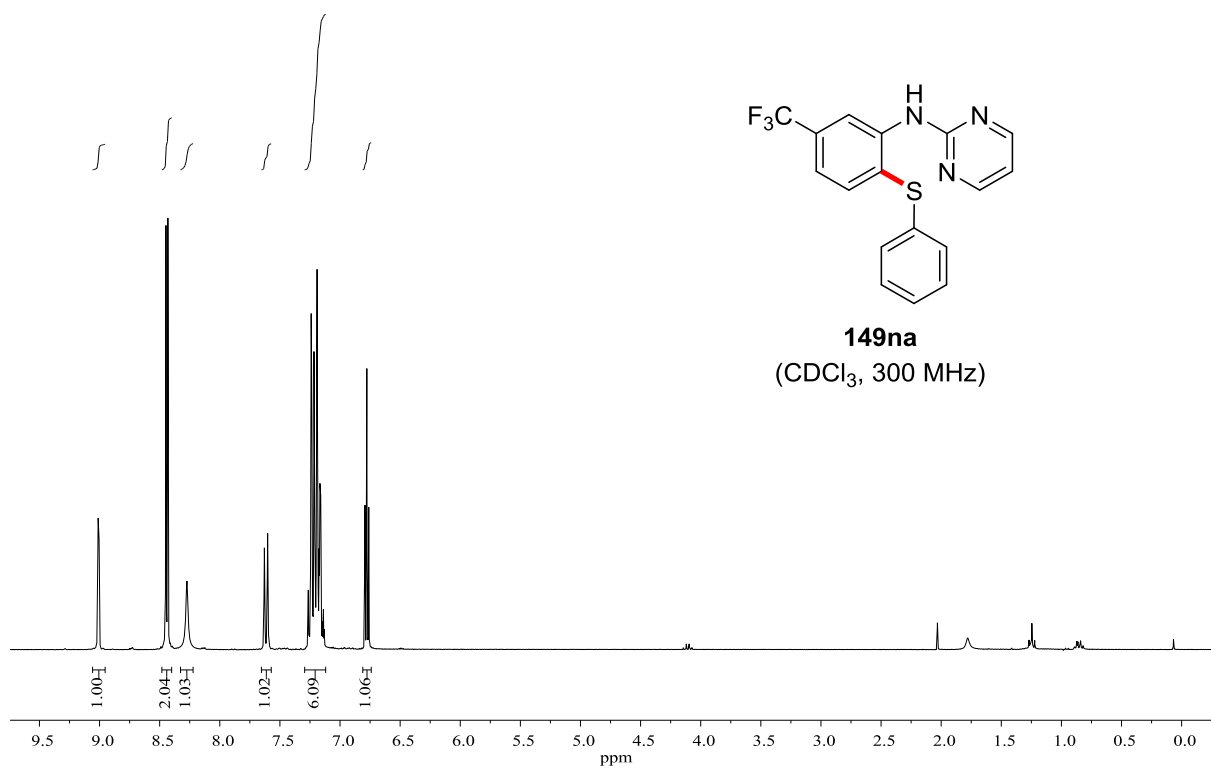


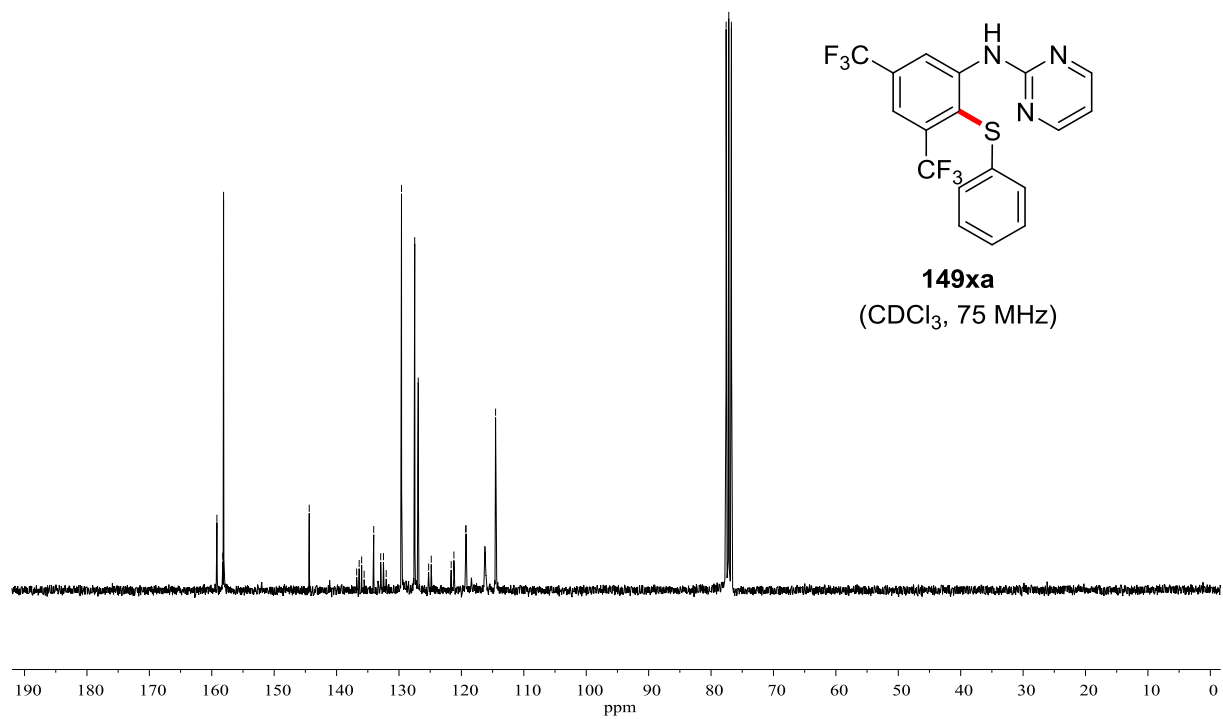
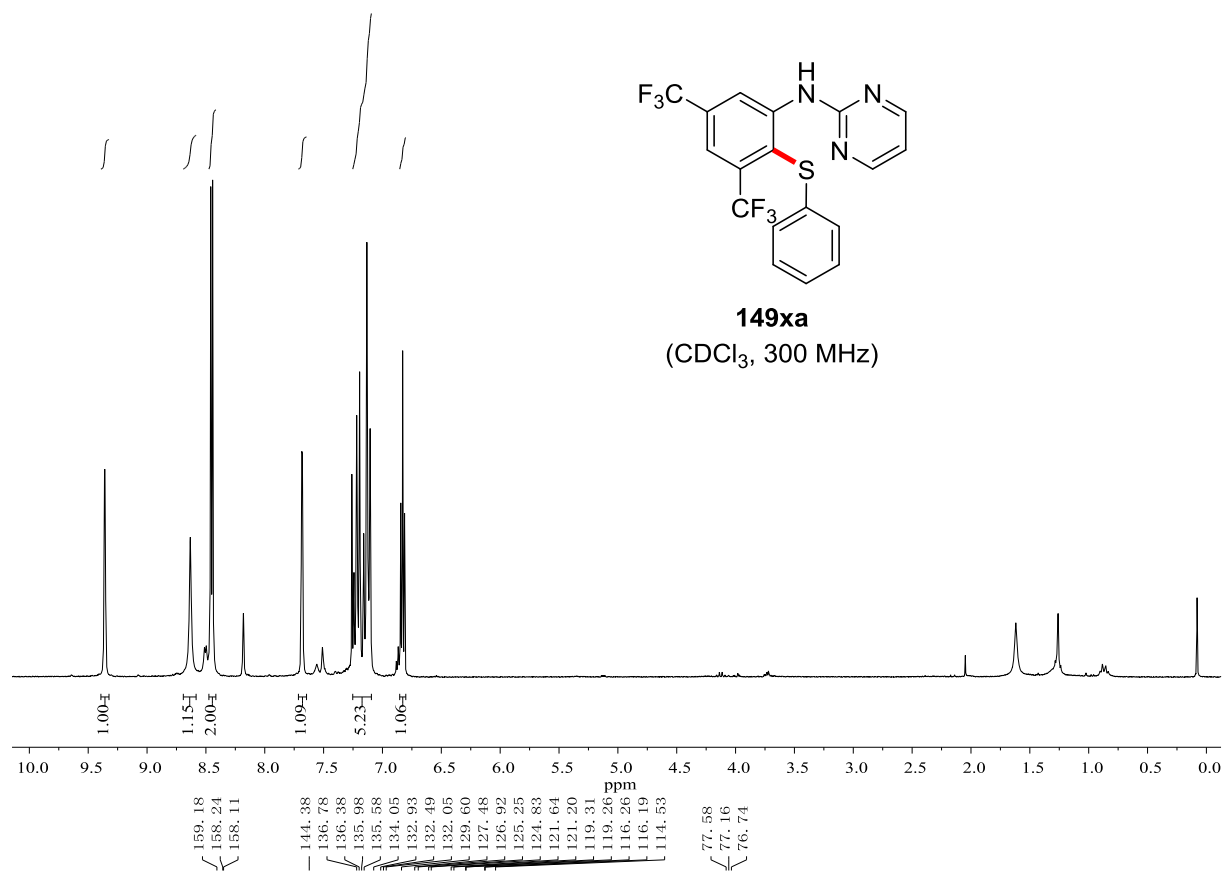


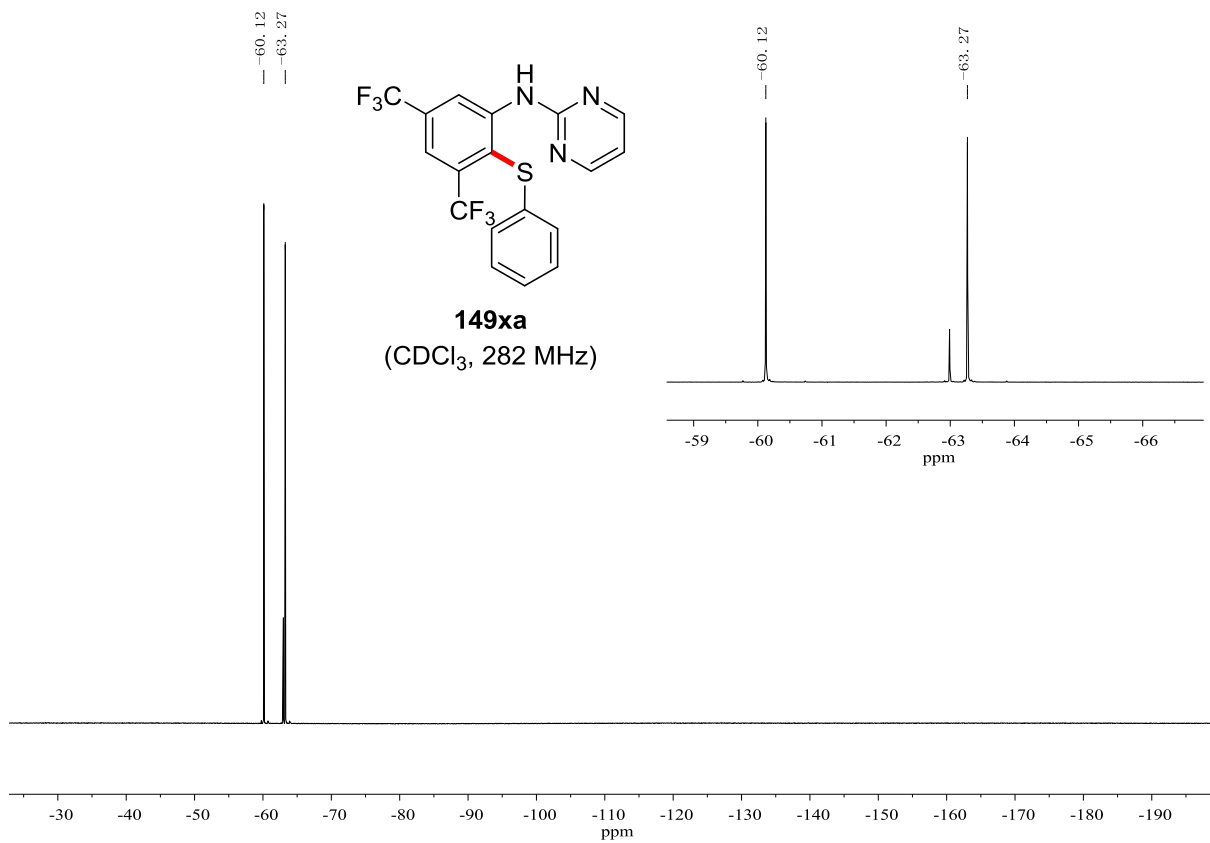


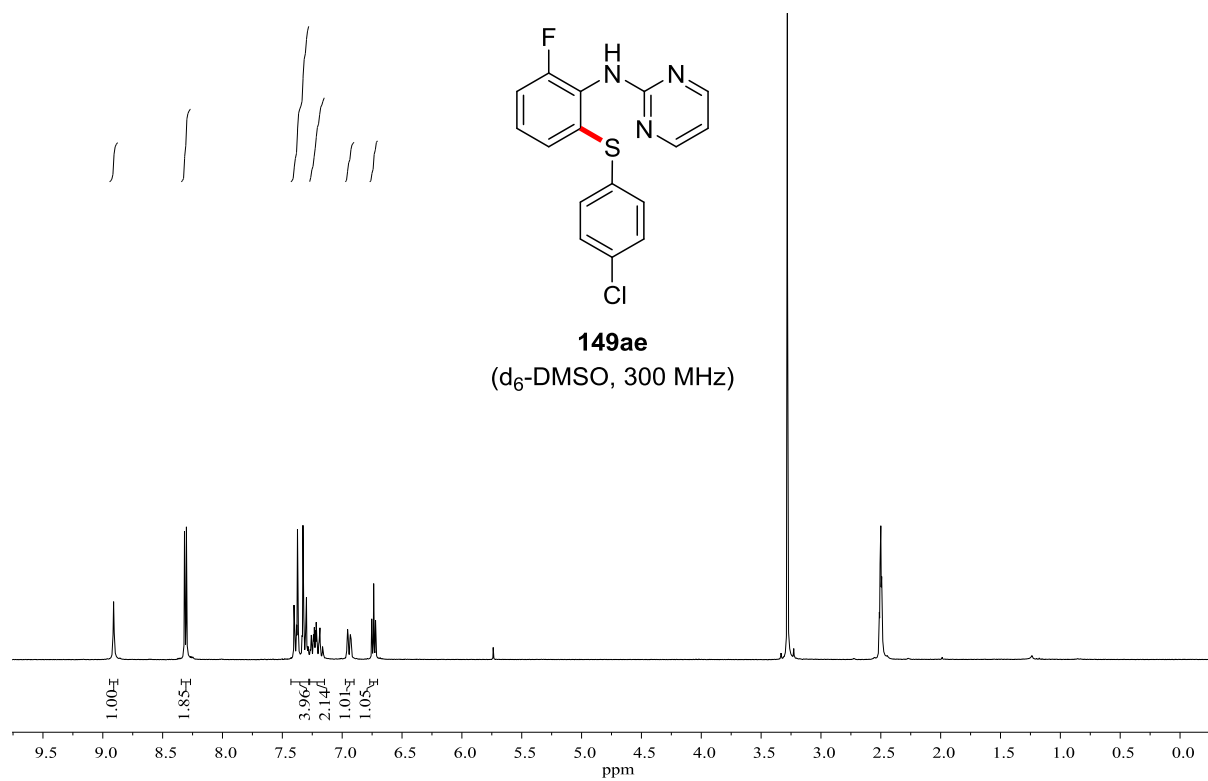




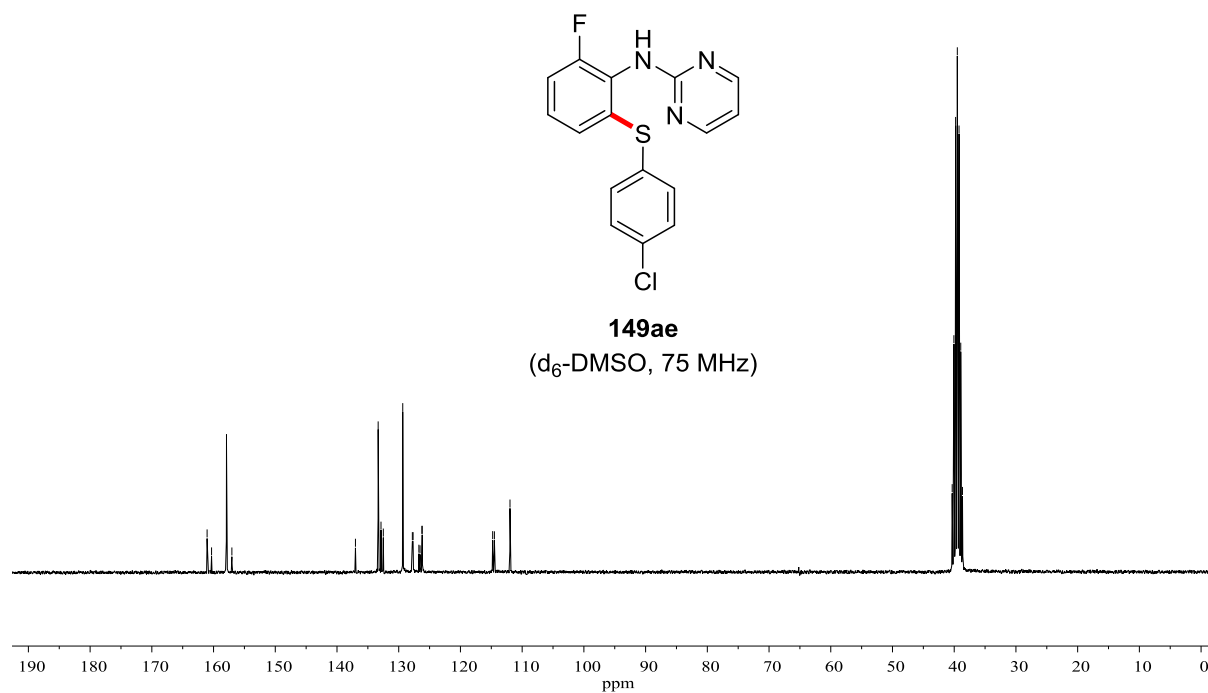


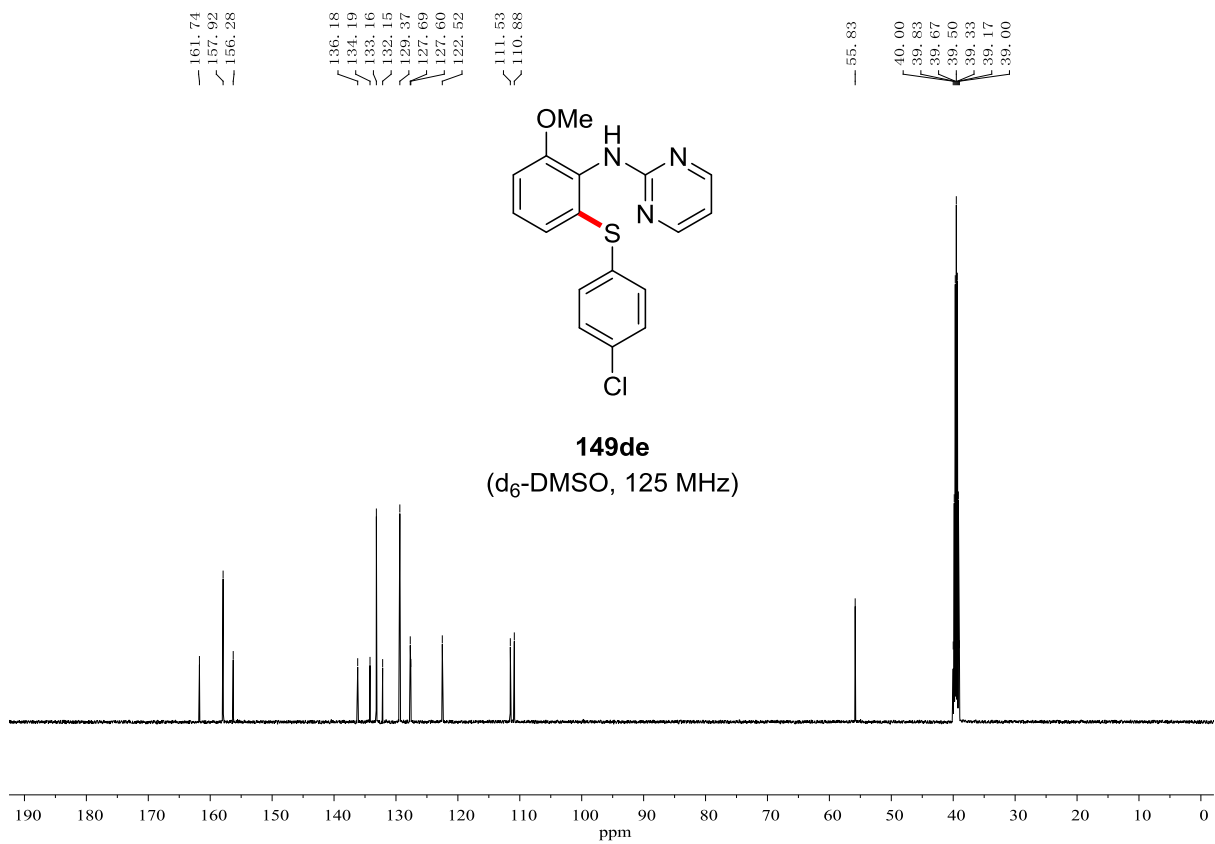
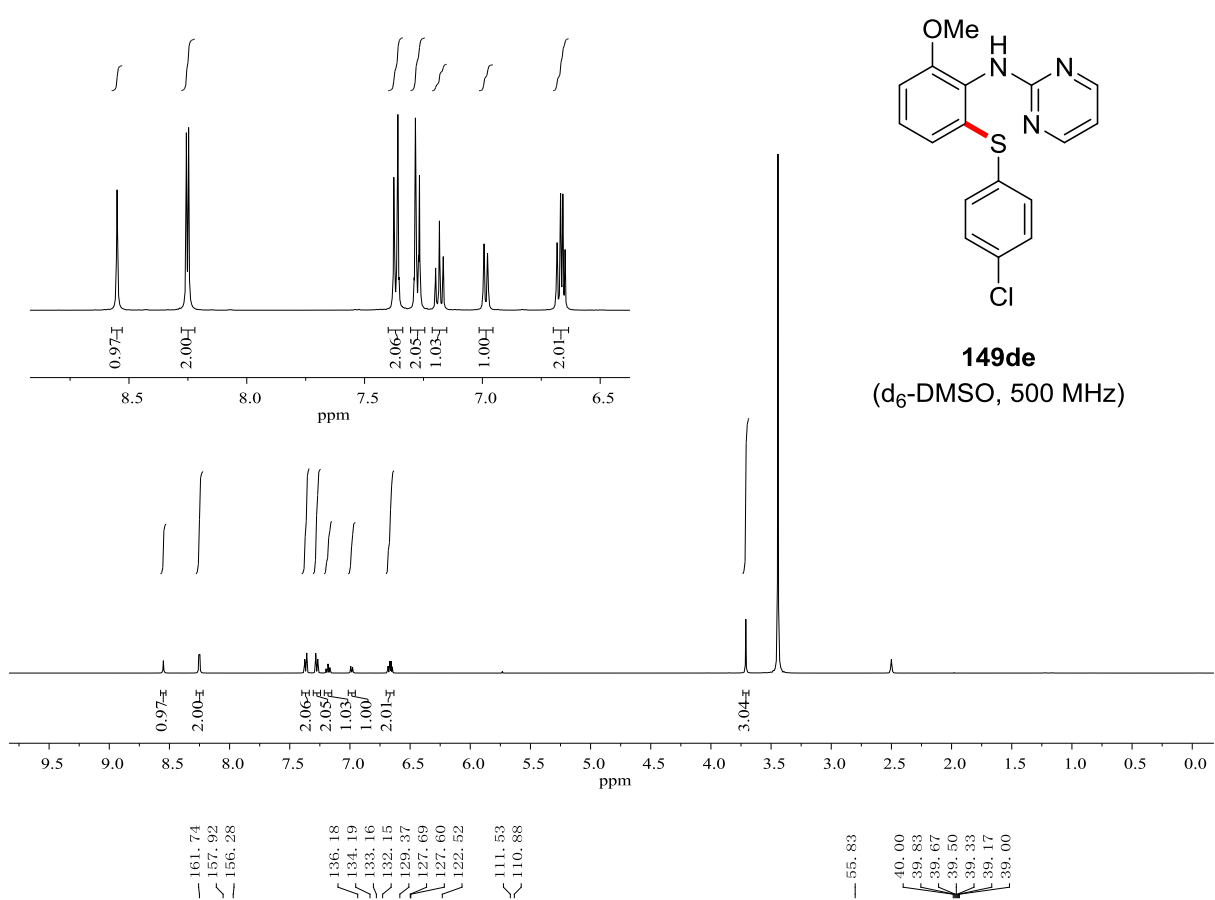


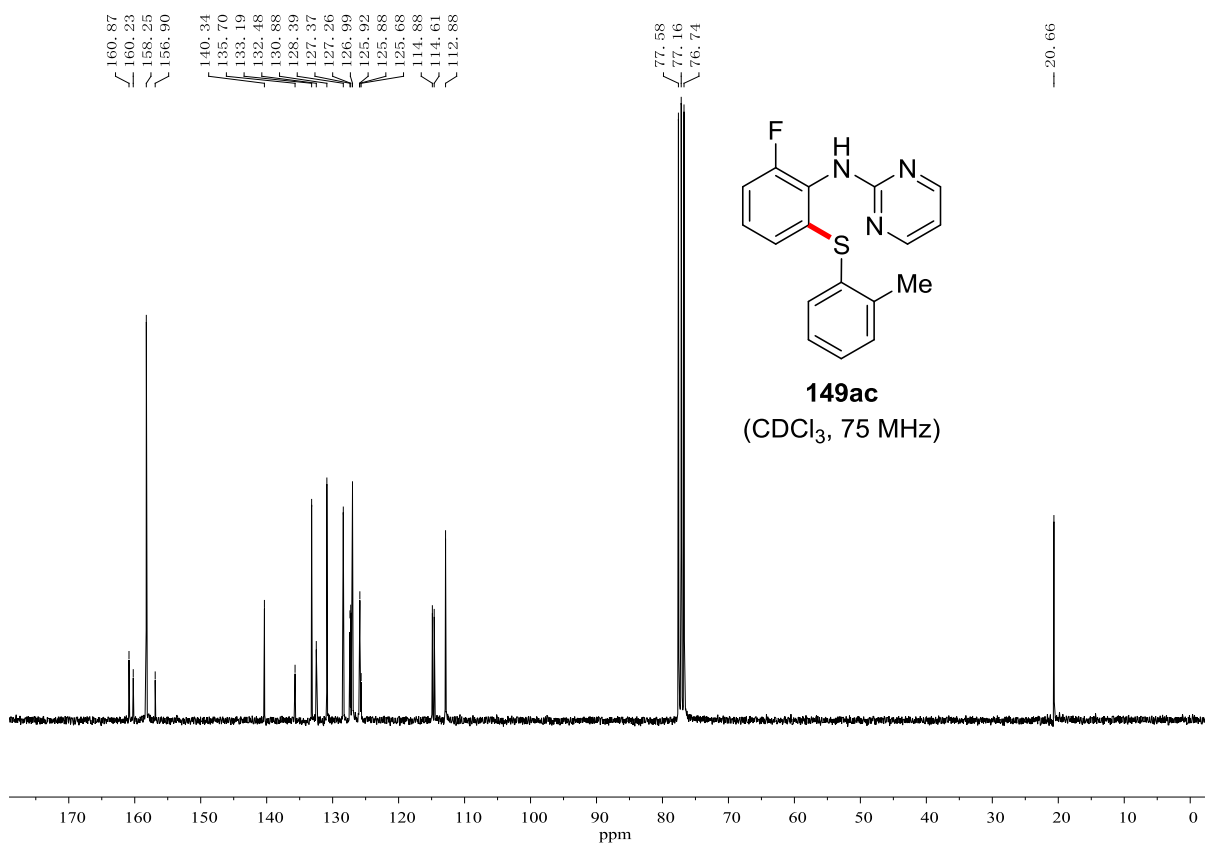
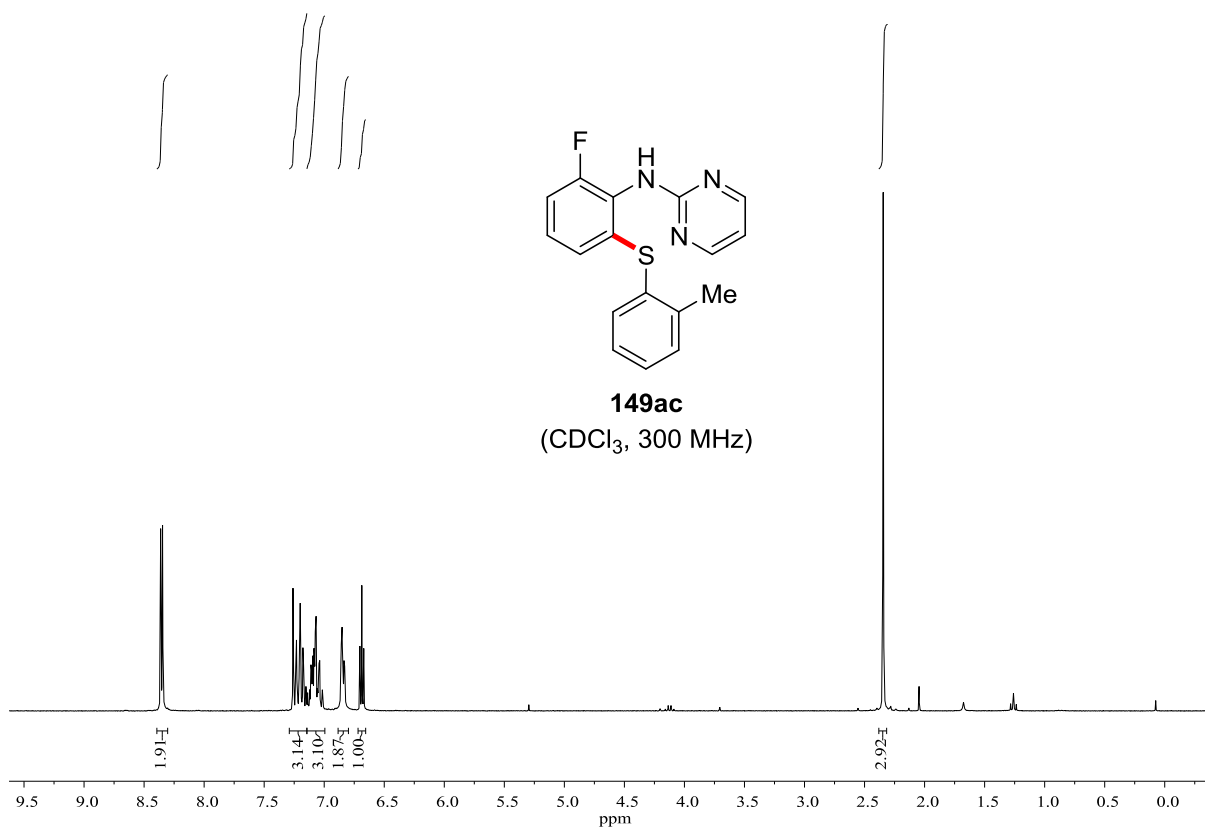


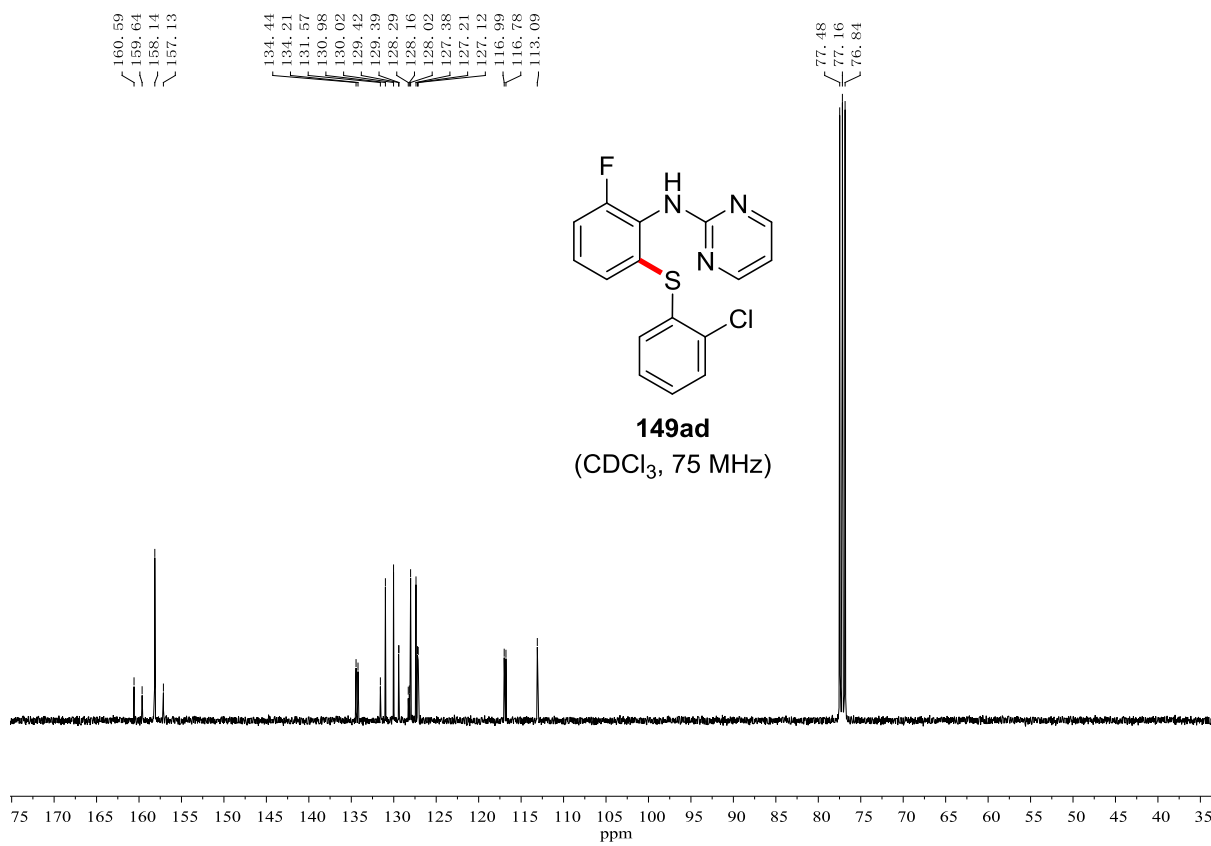
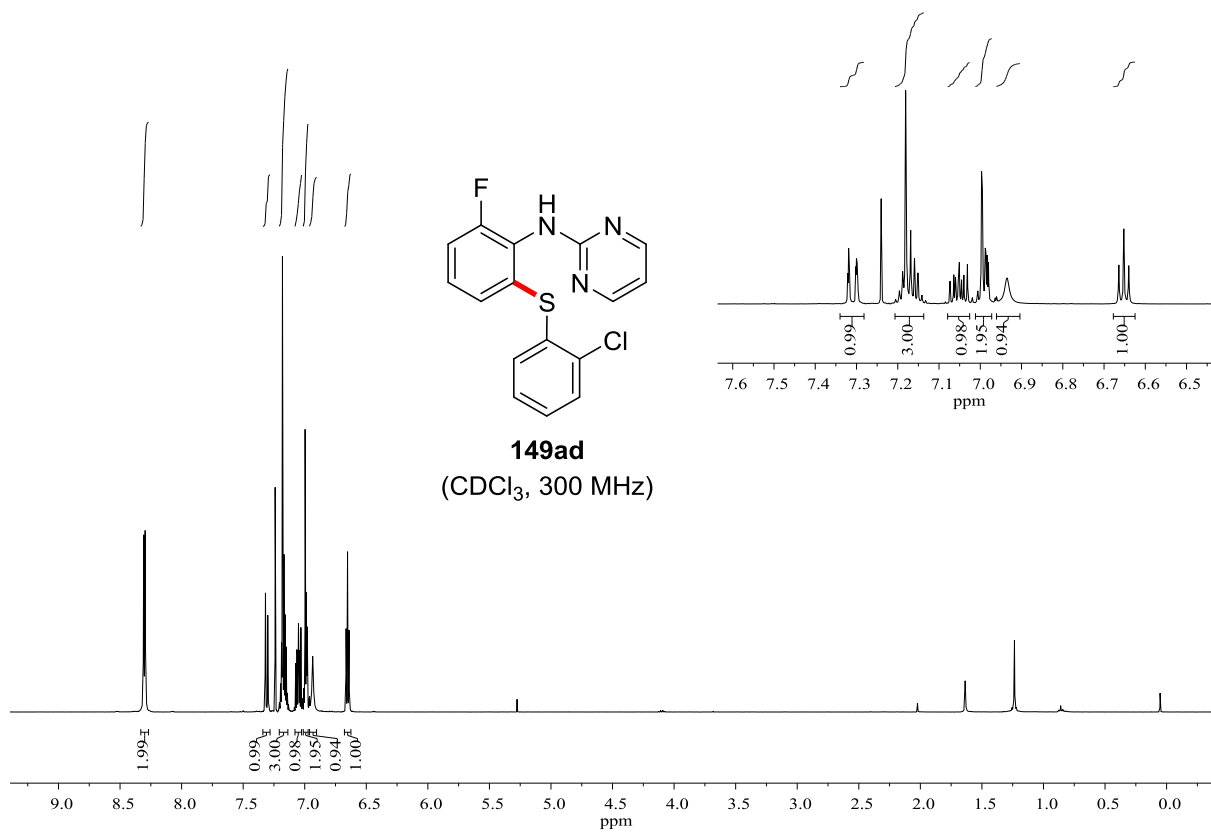


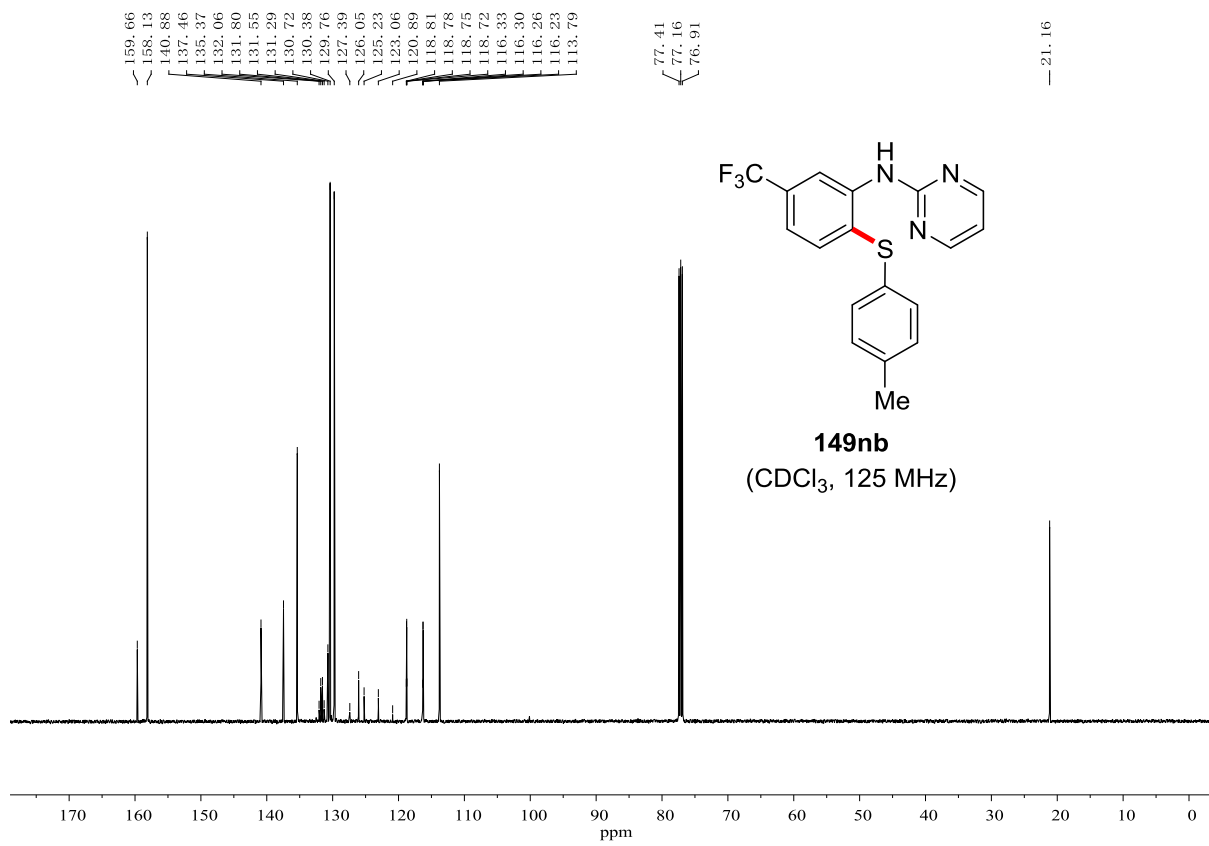
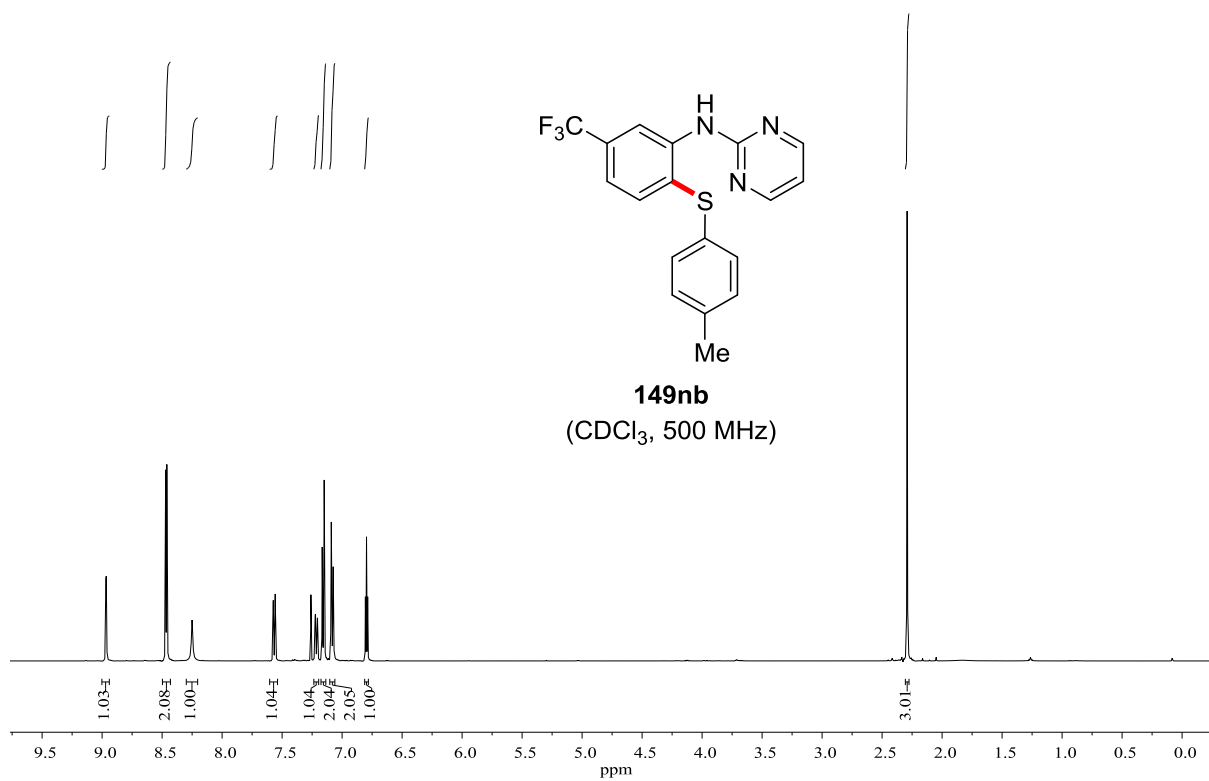
161.05
160.32
157.90
157.03
137.01
133.33
132.87
132.49
129.35
127.79
127.67
126.73
126.54
126.24
126.20
114.78
111.50
111.97
40.33
40.05
39.77
39.49
39.22
38.94
38.66

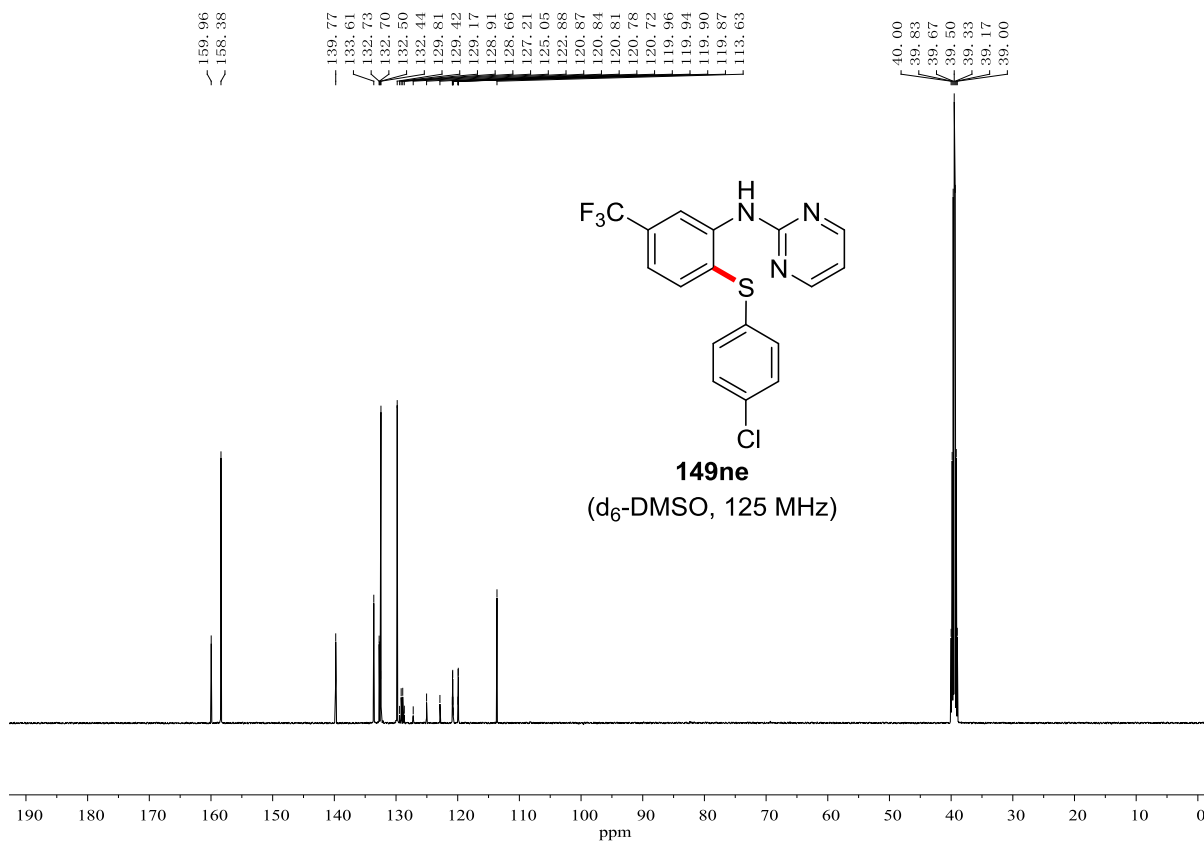
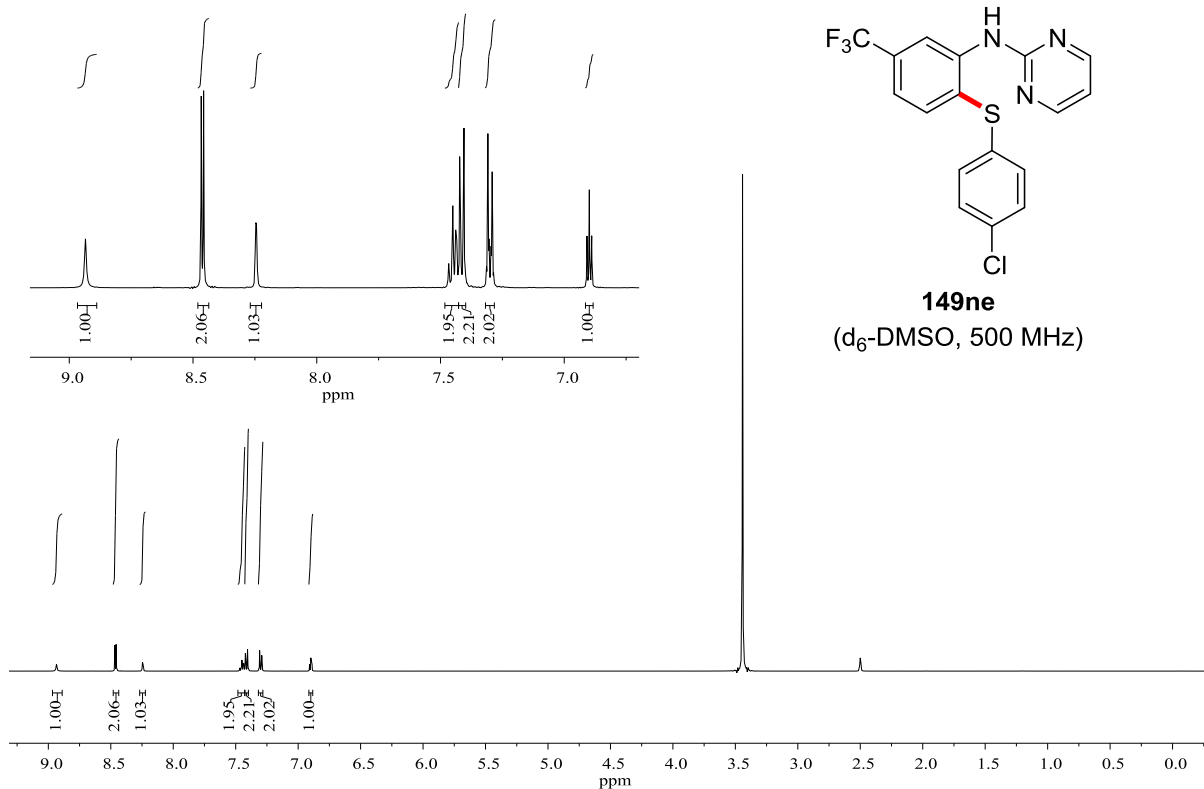


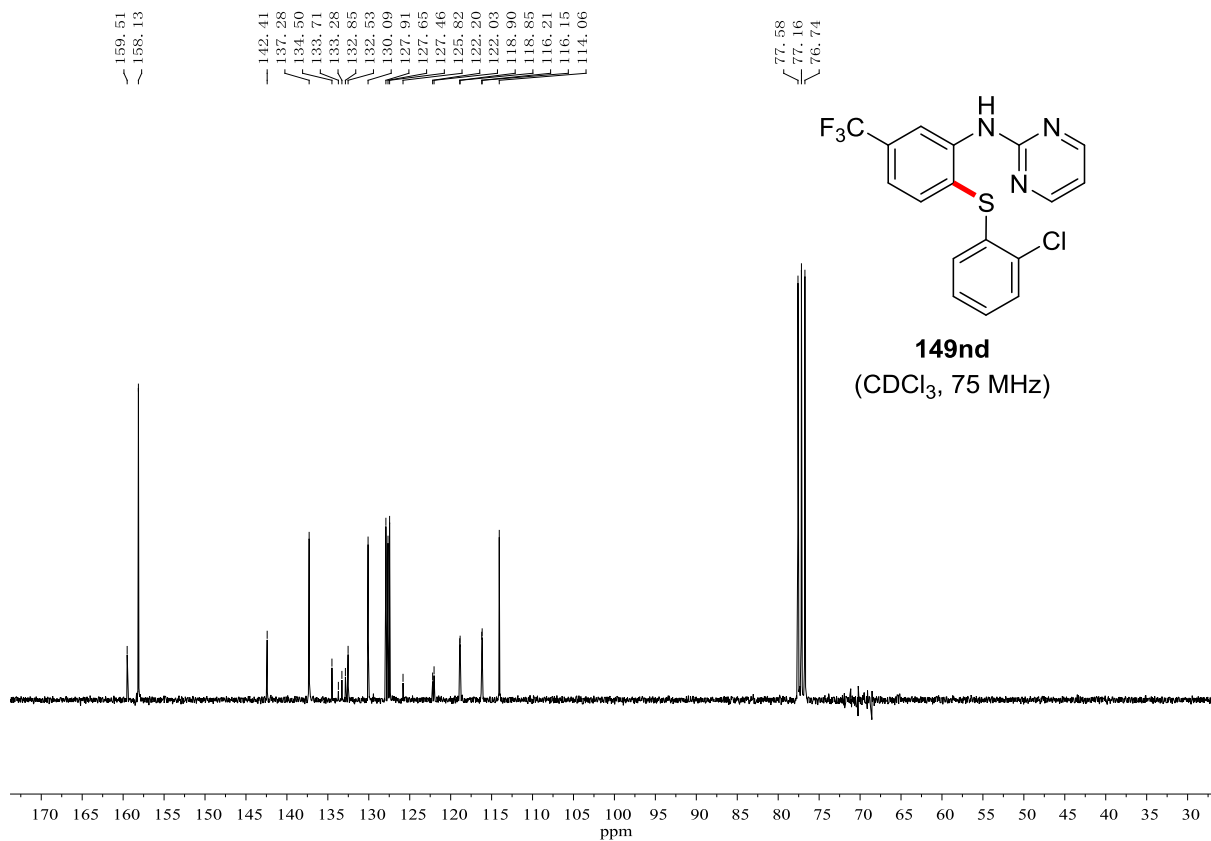
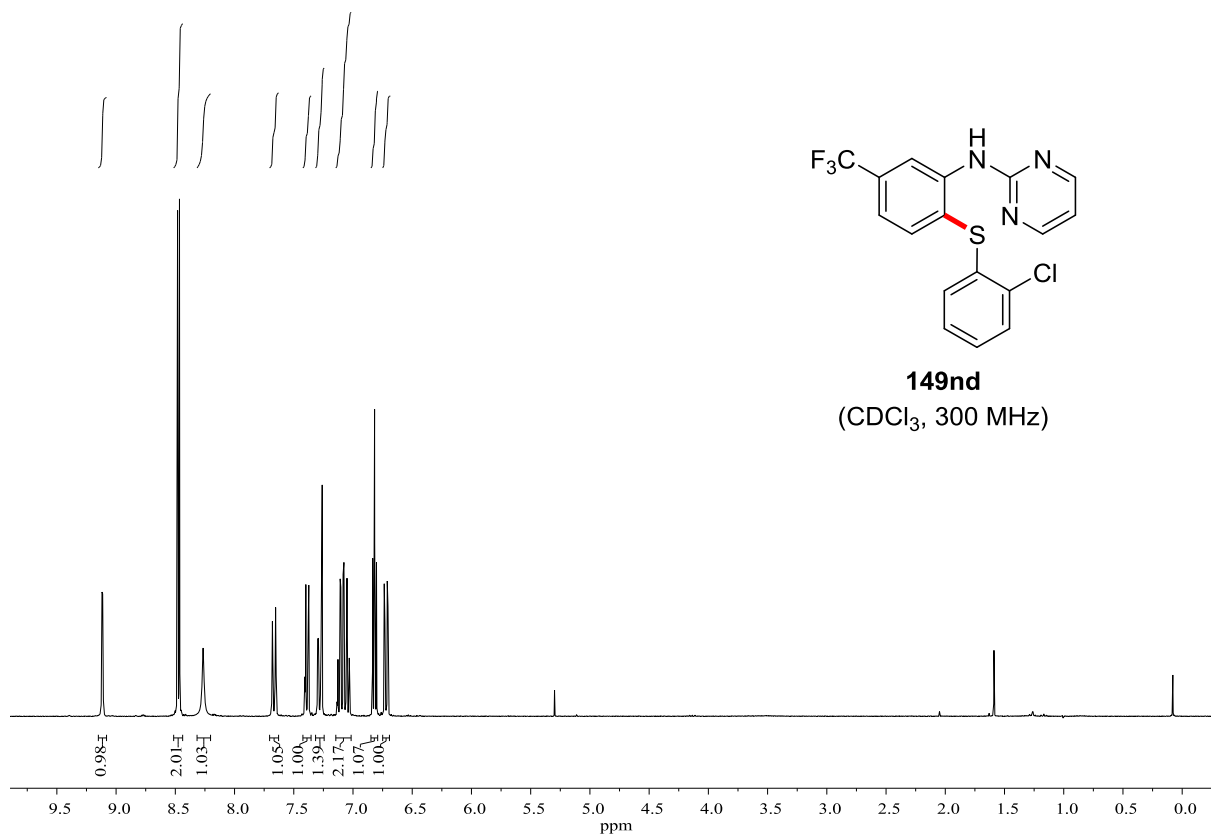


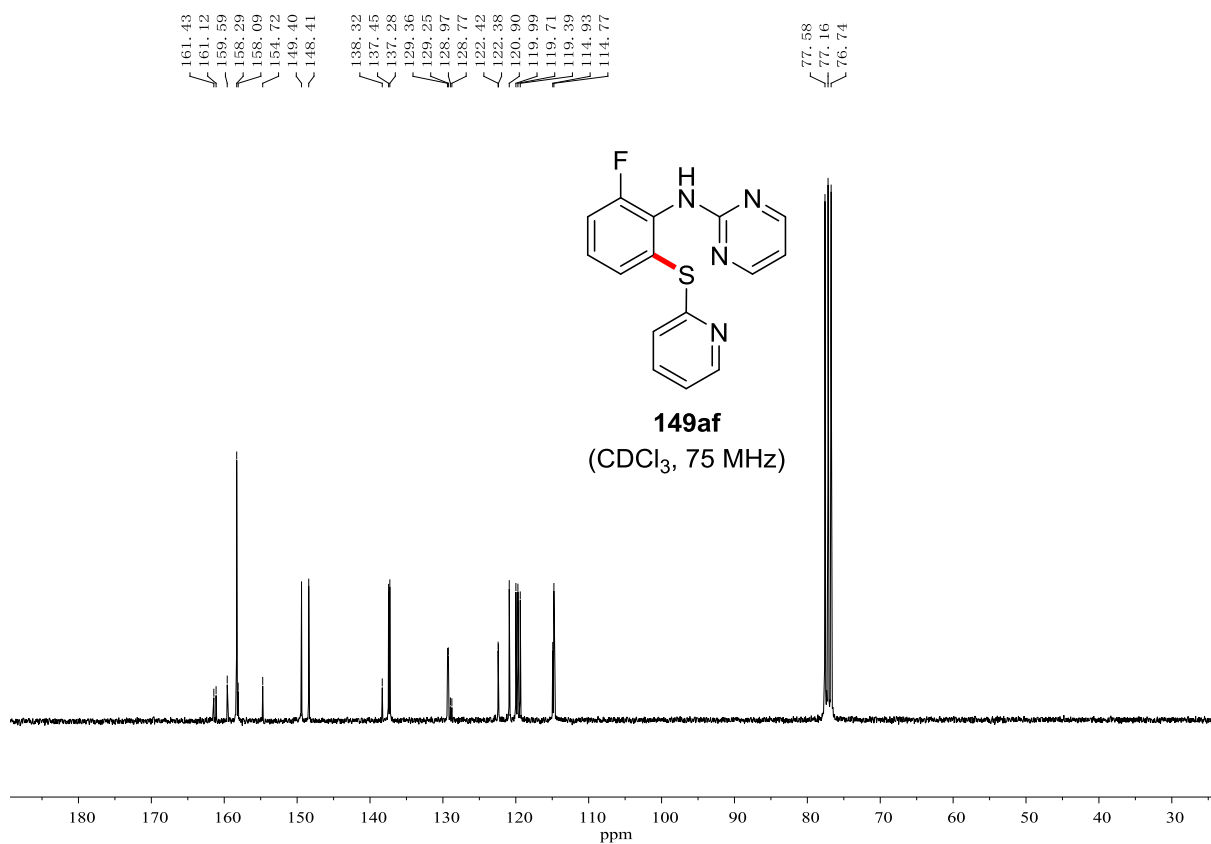
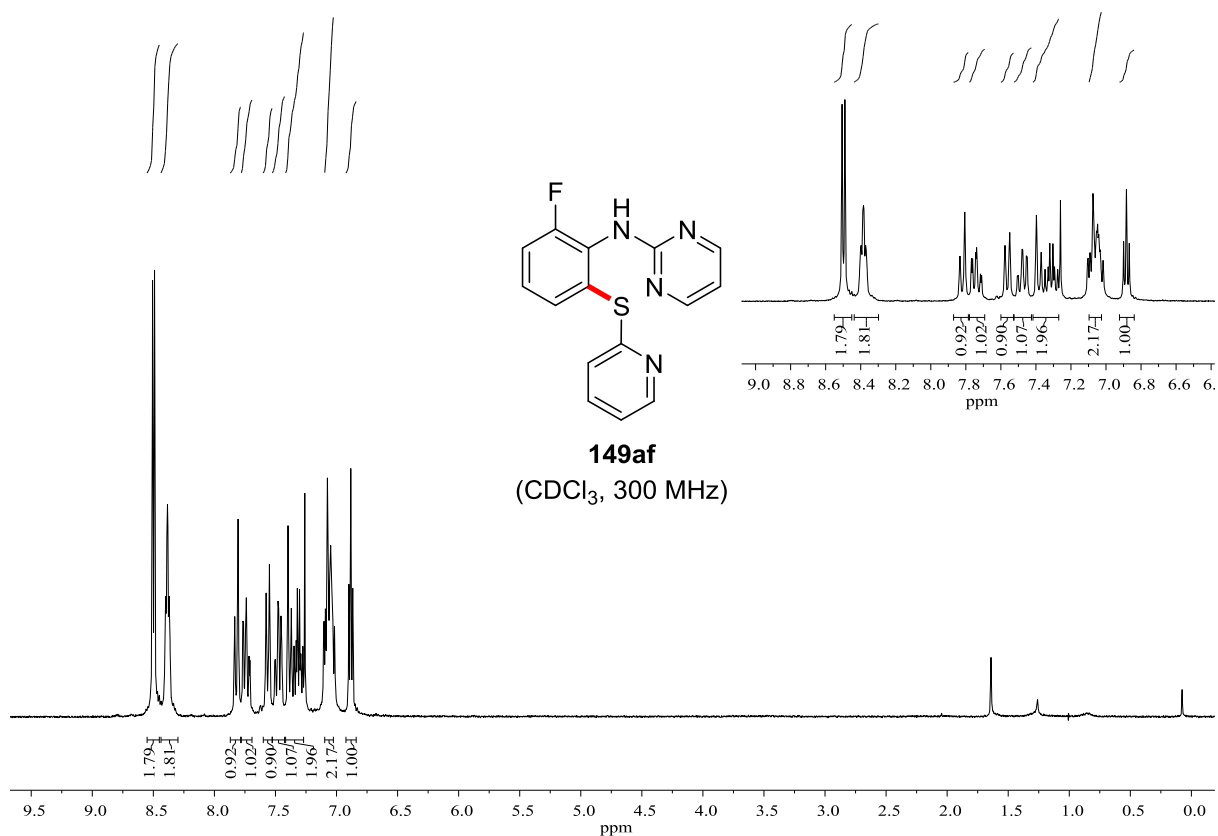


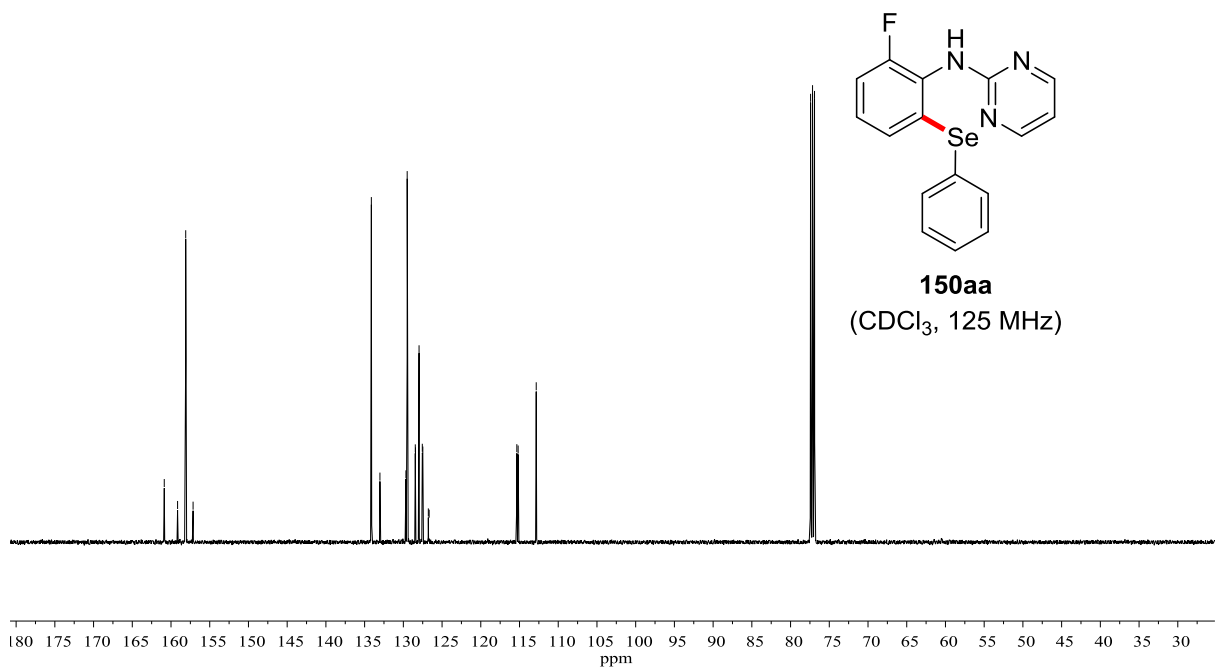
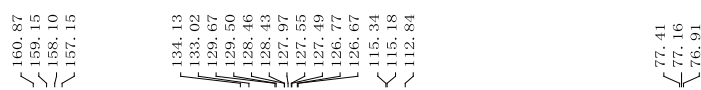
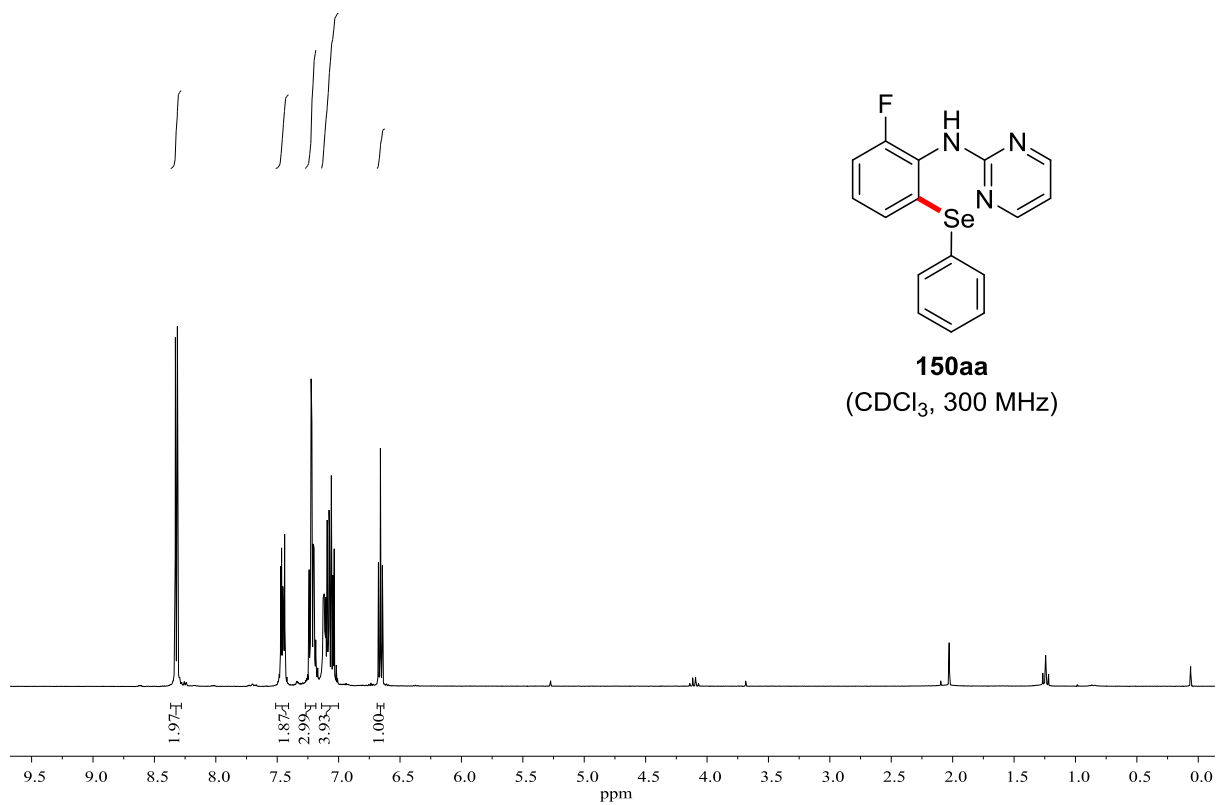


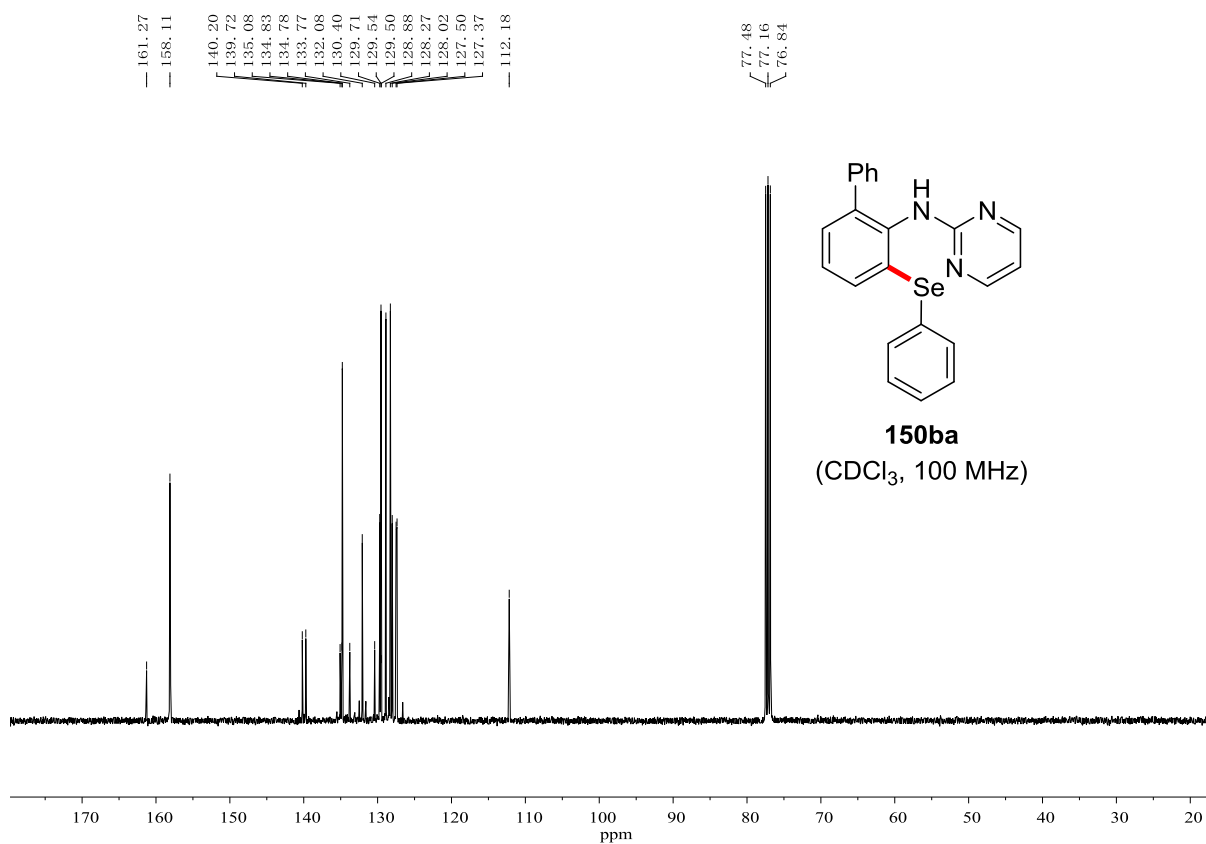
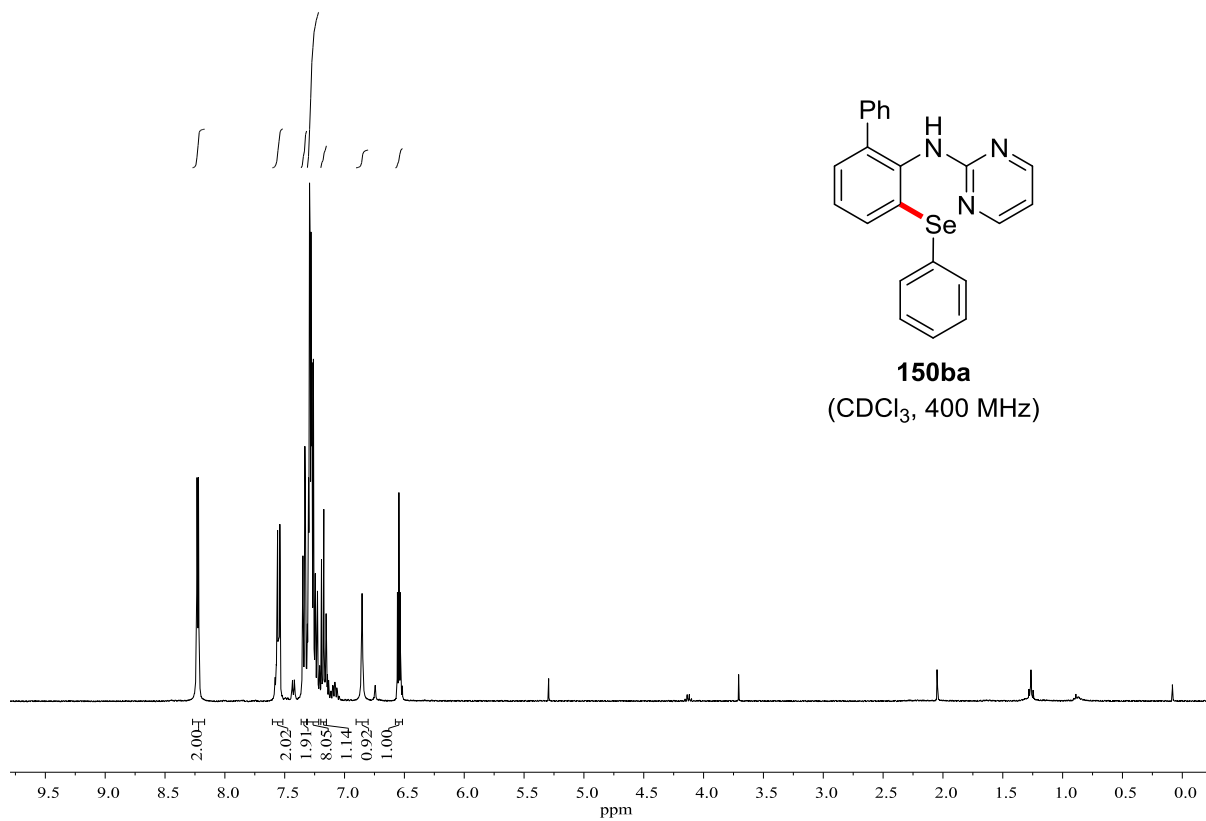


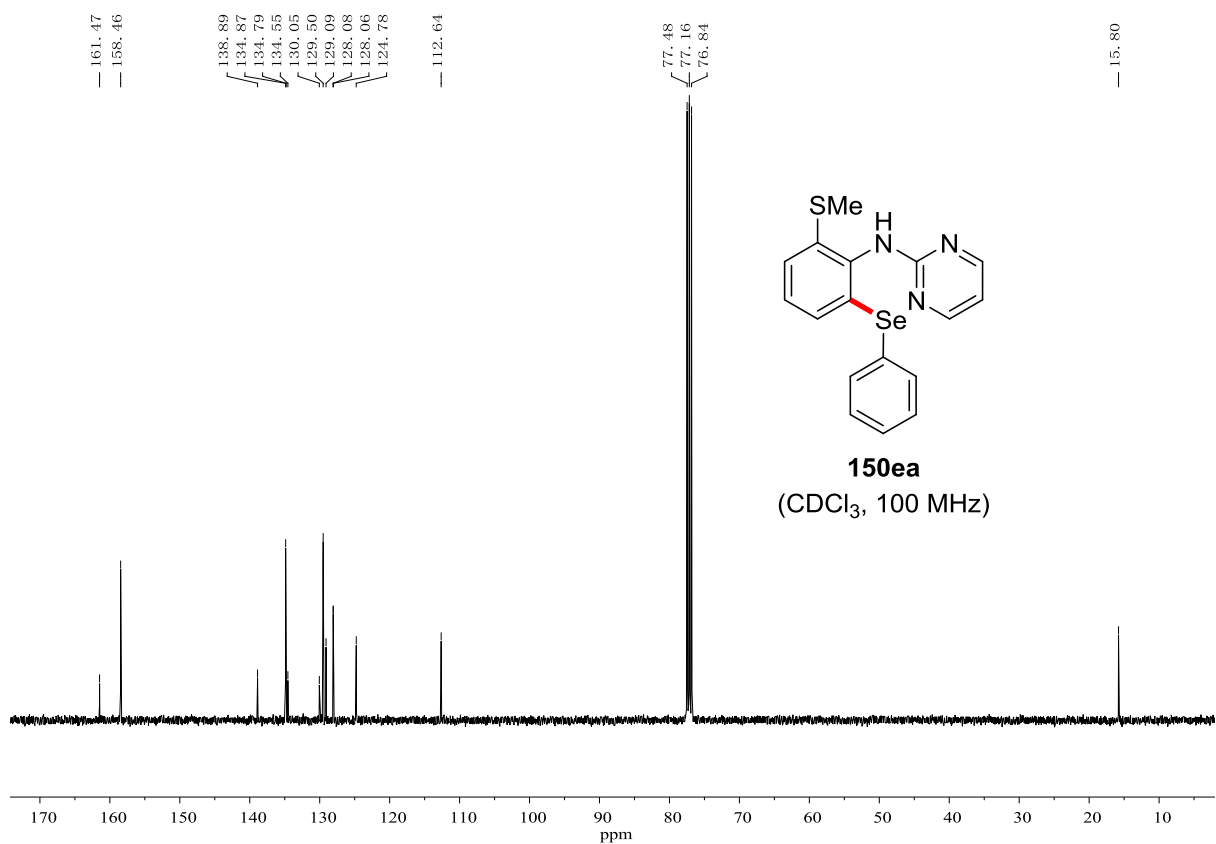
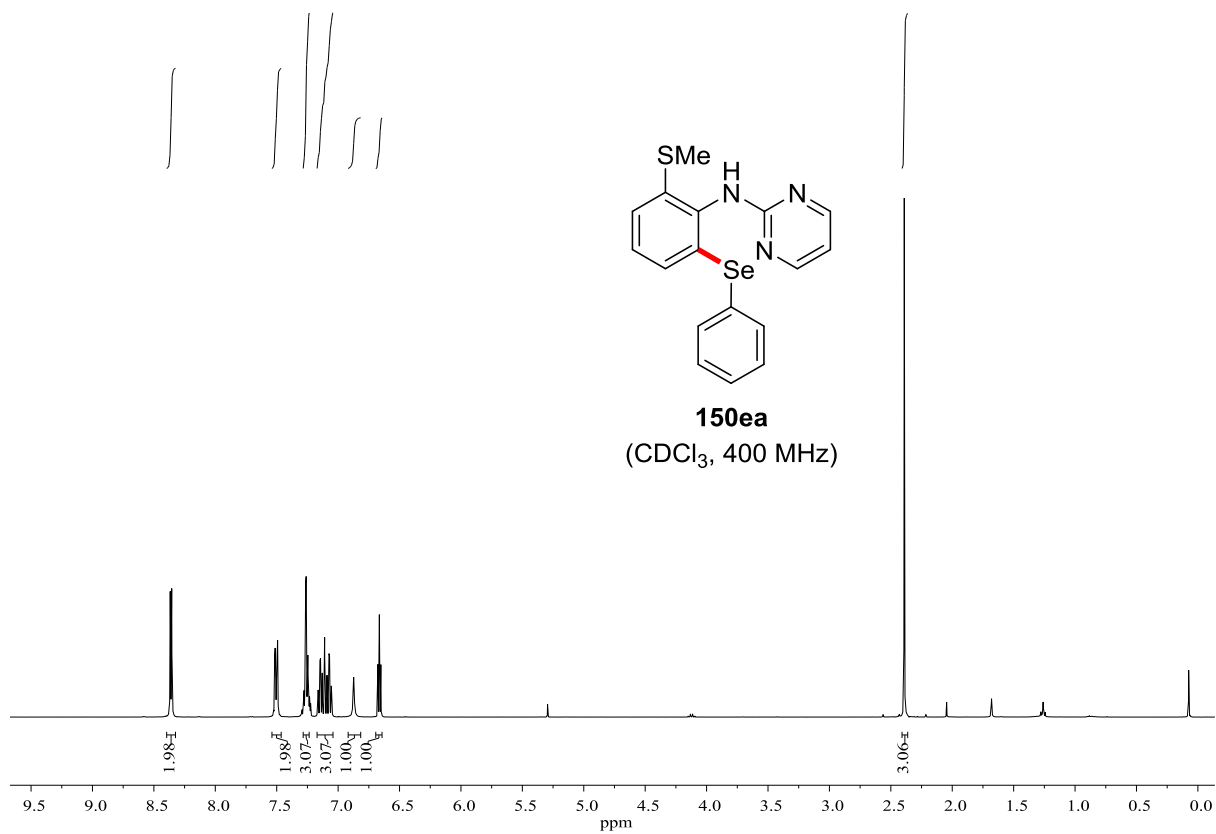


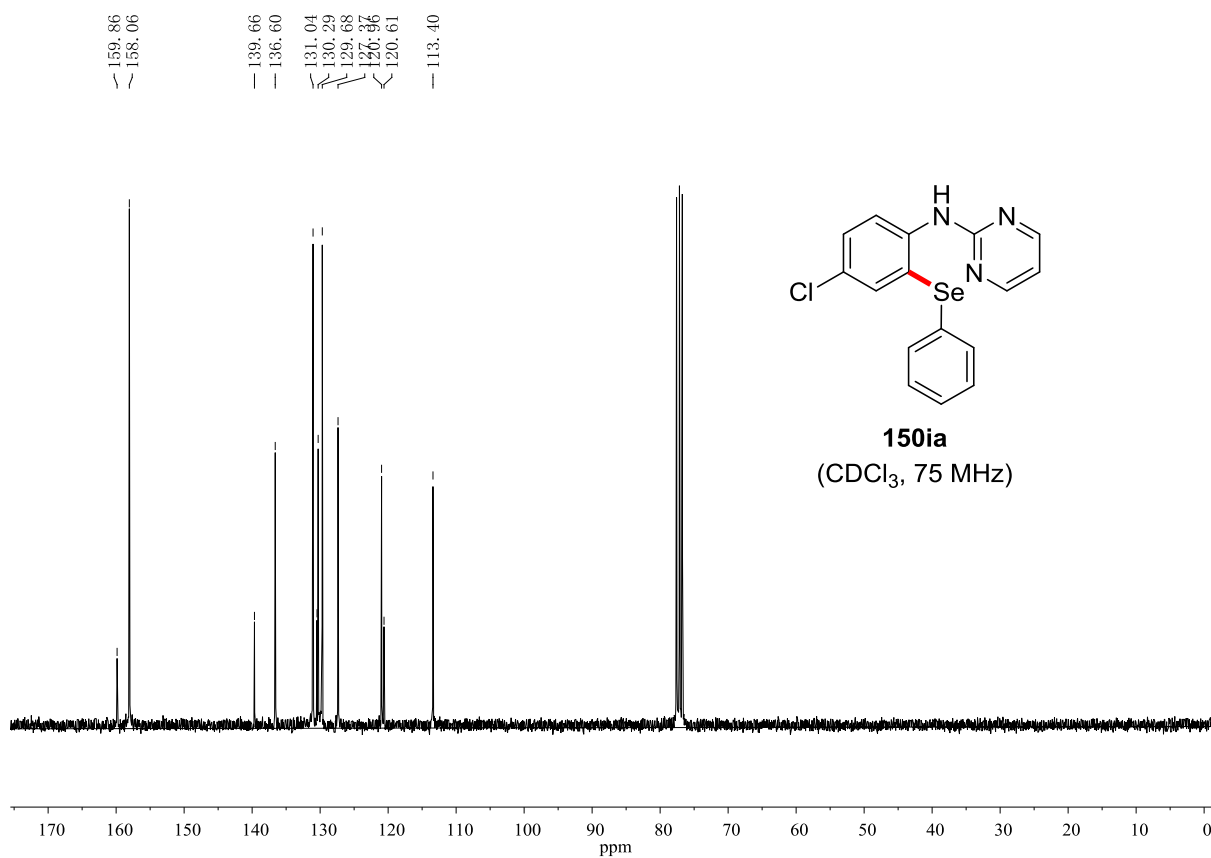
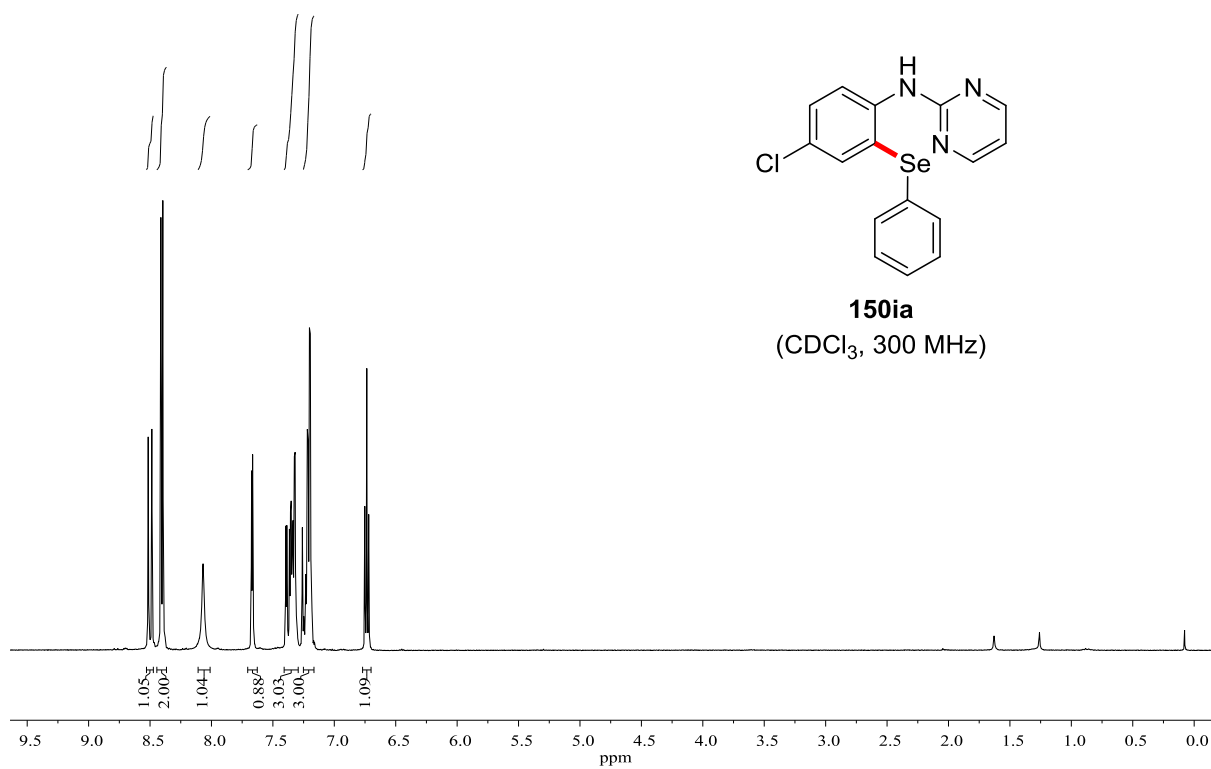


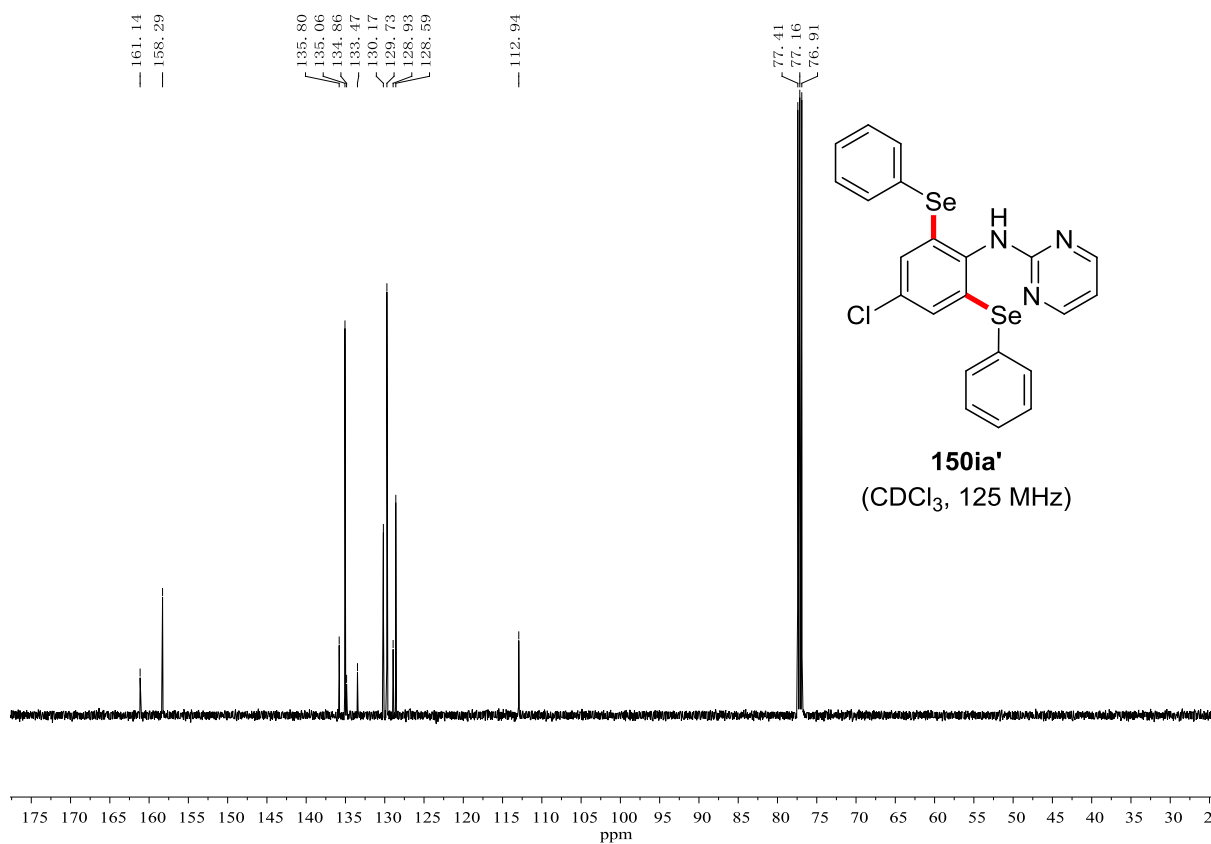
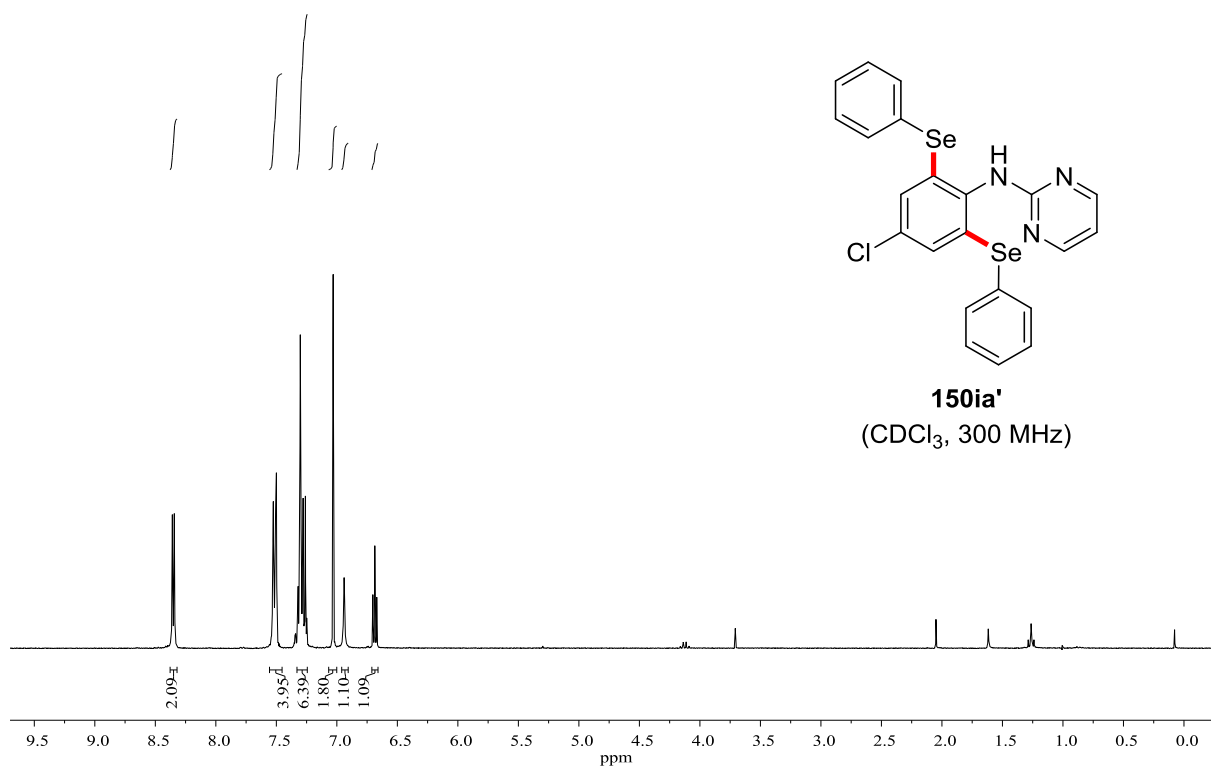


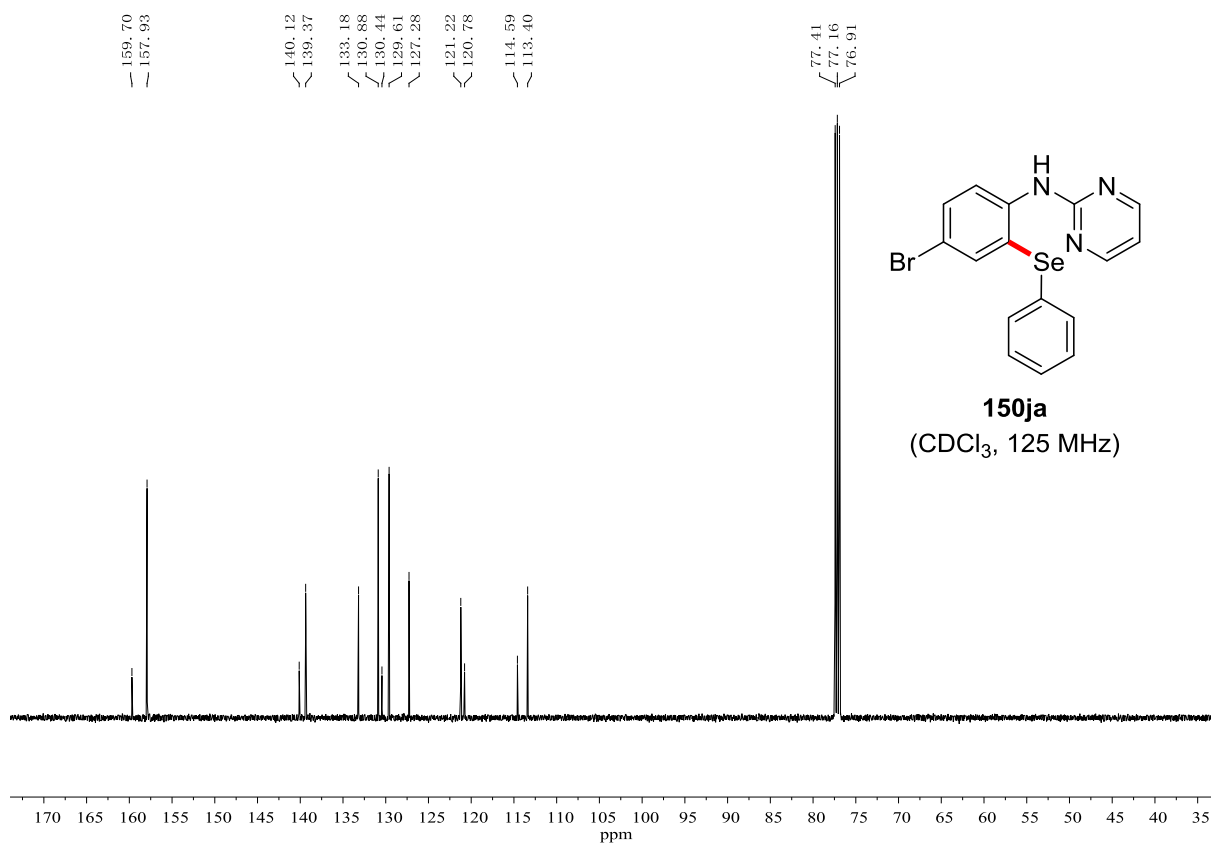
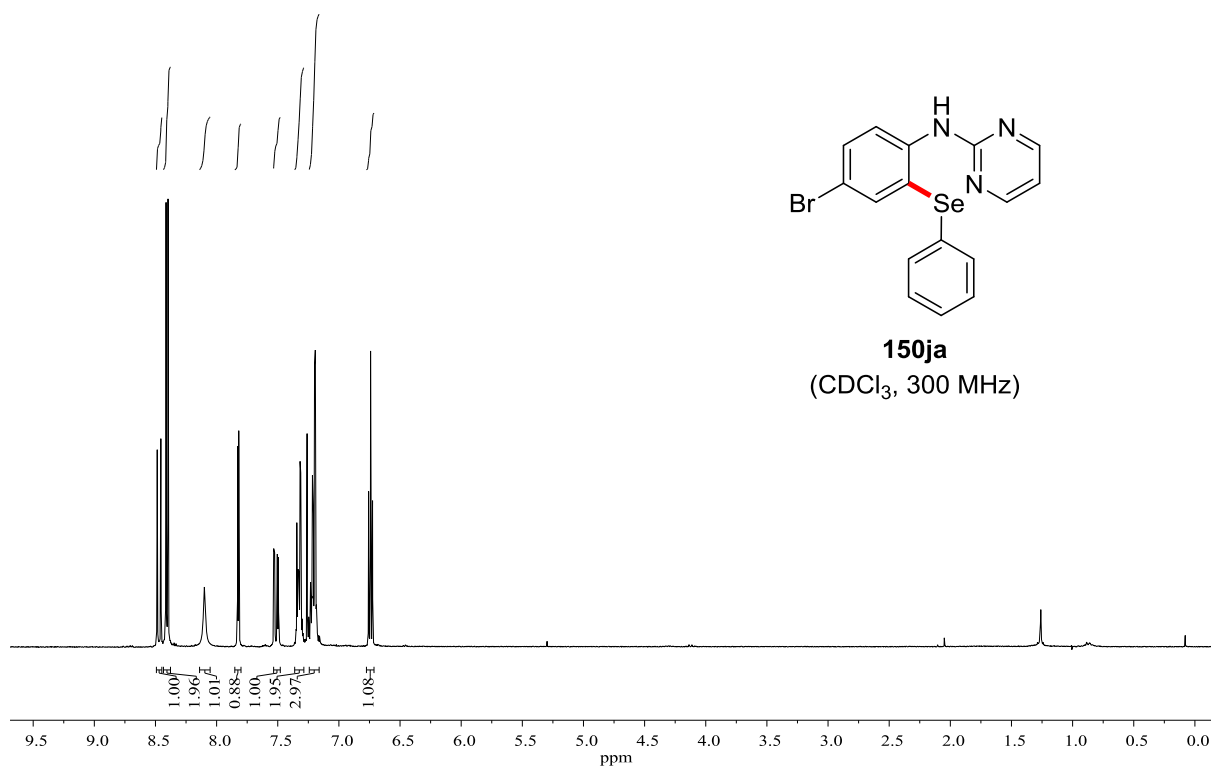


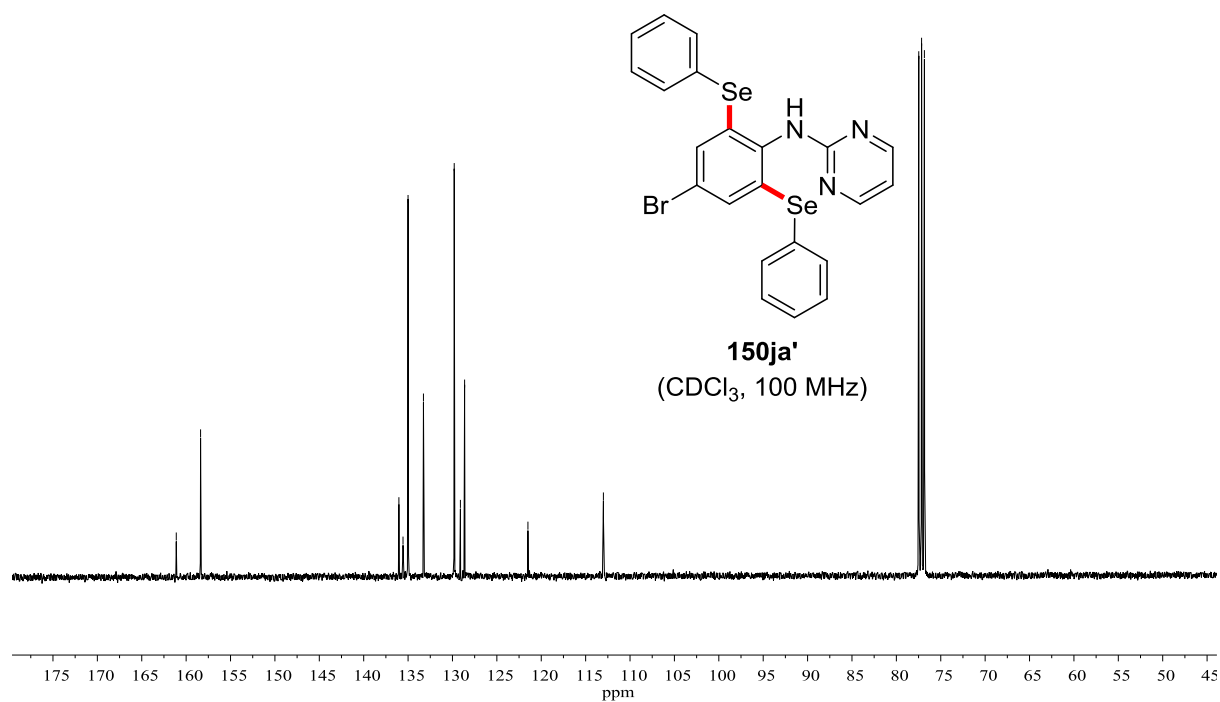
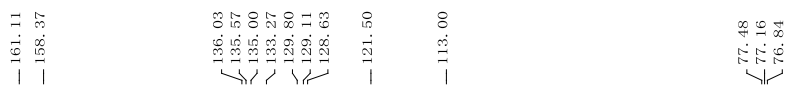
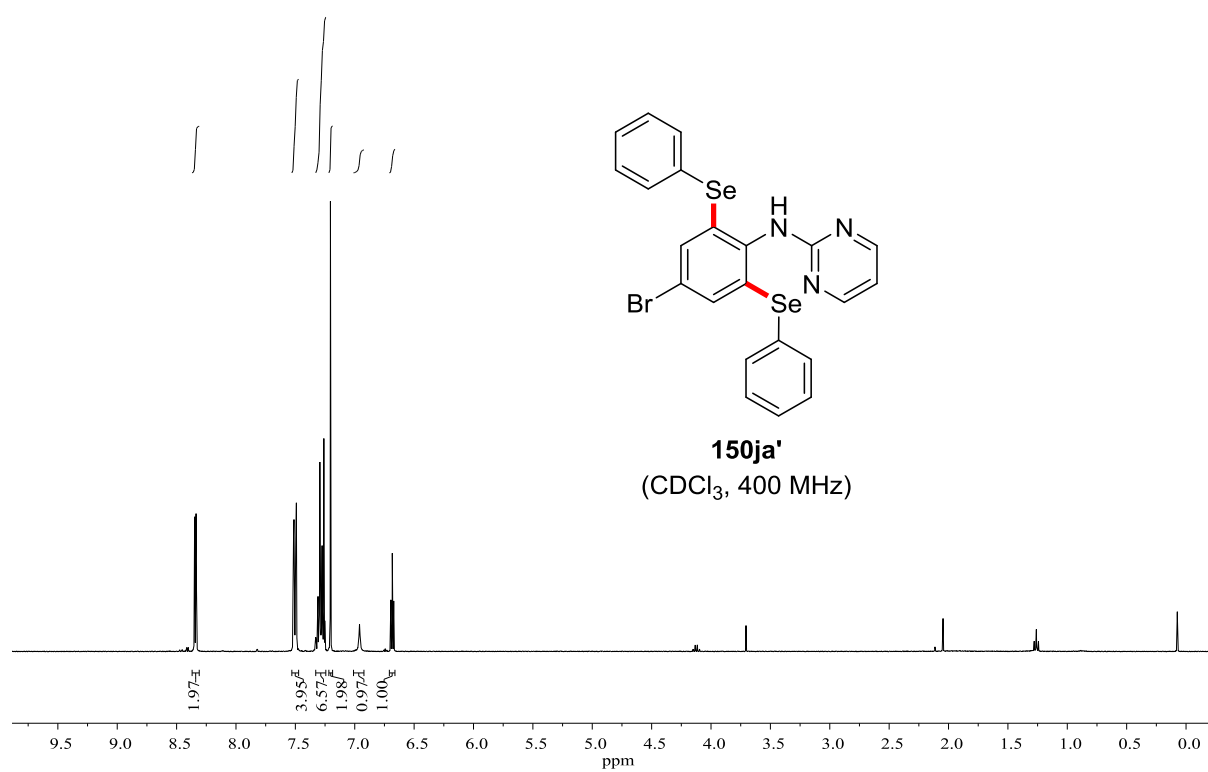


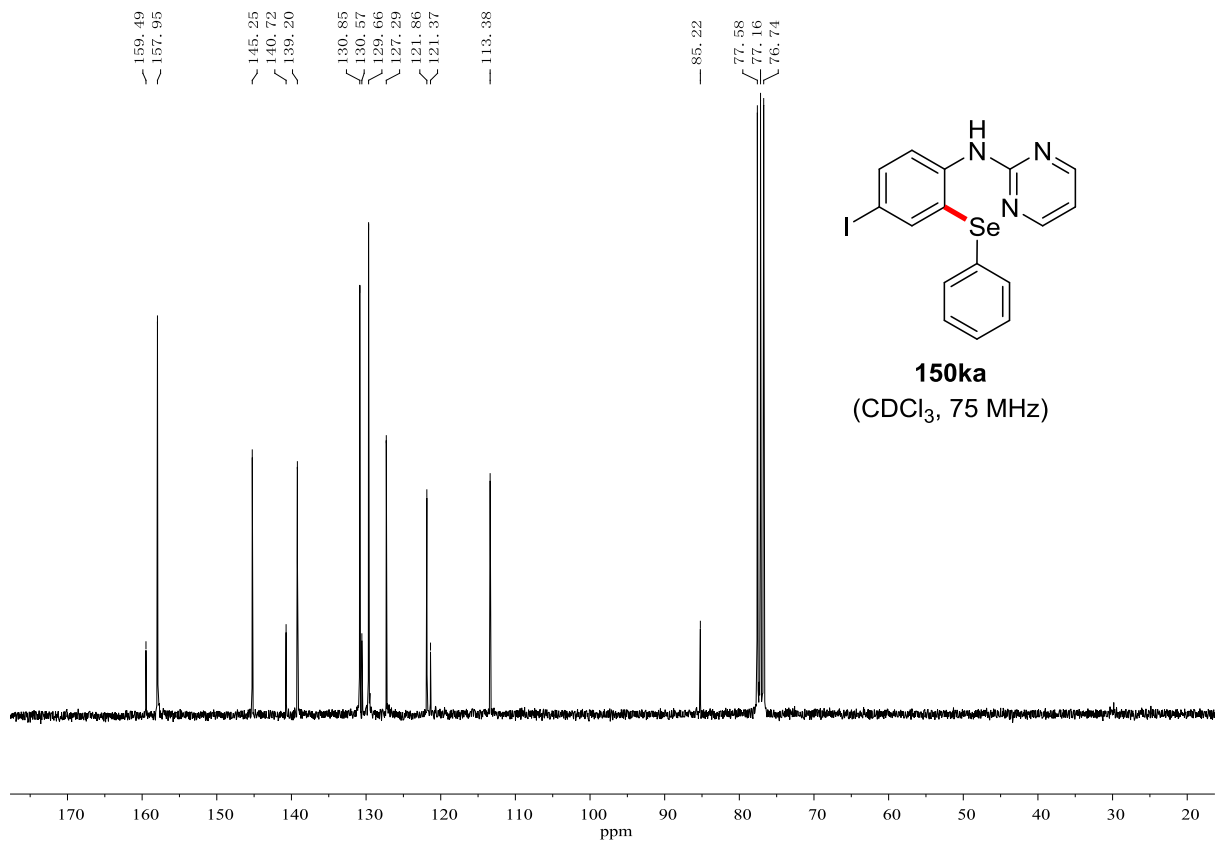
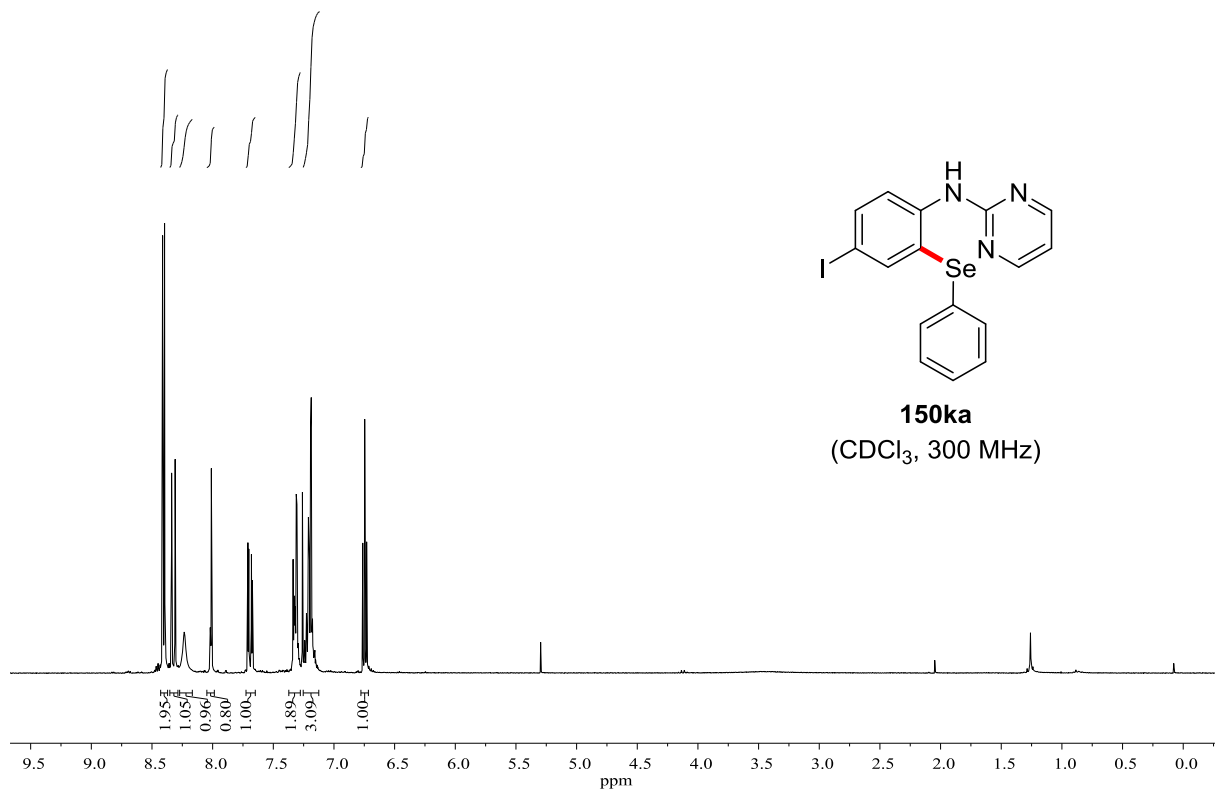


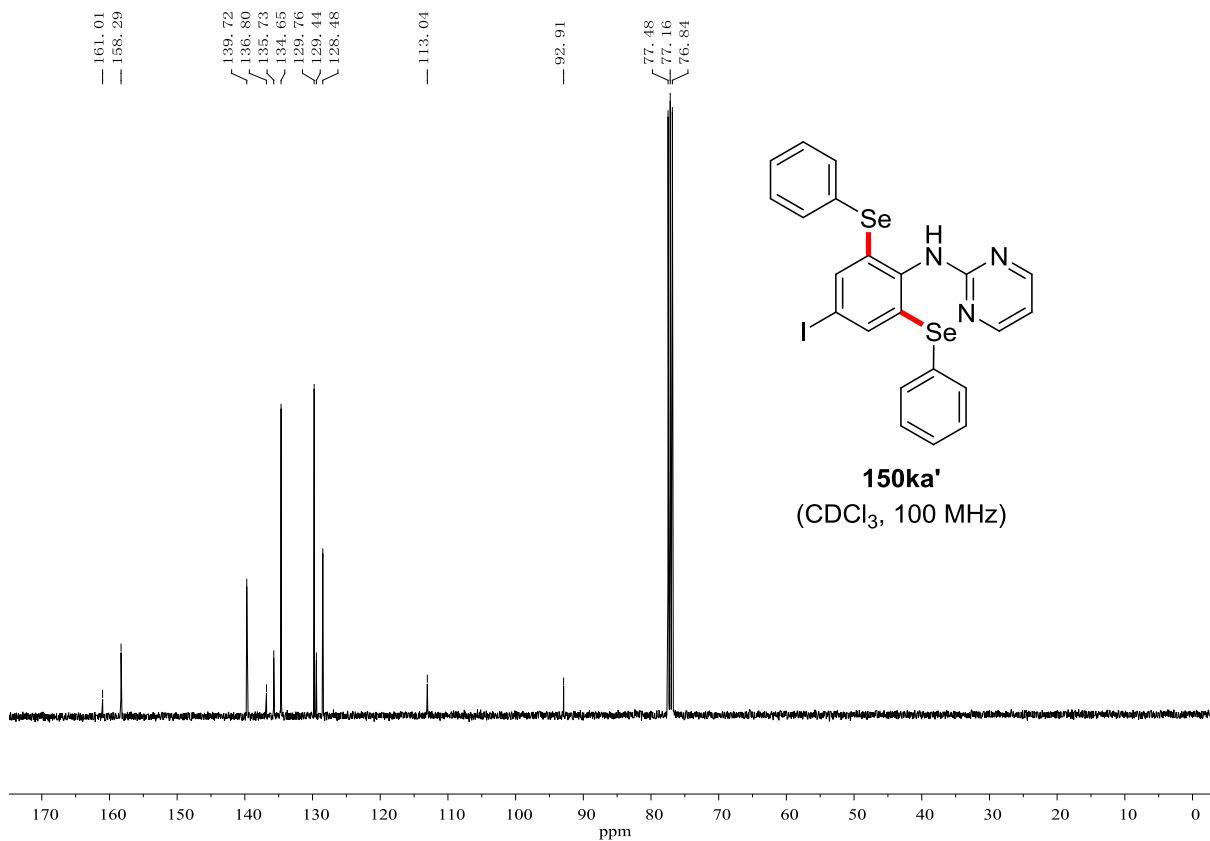
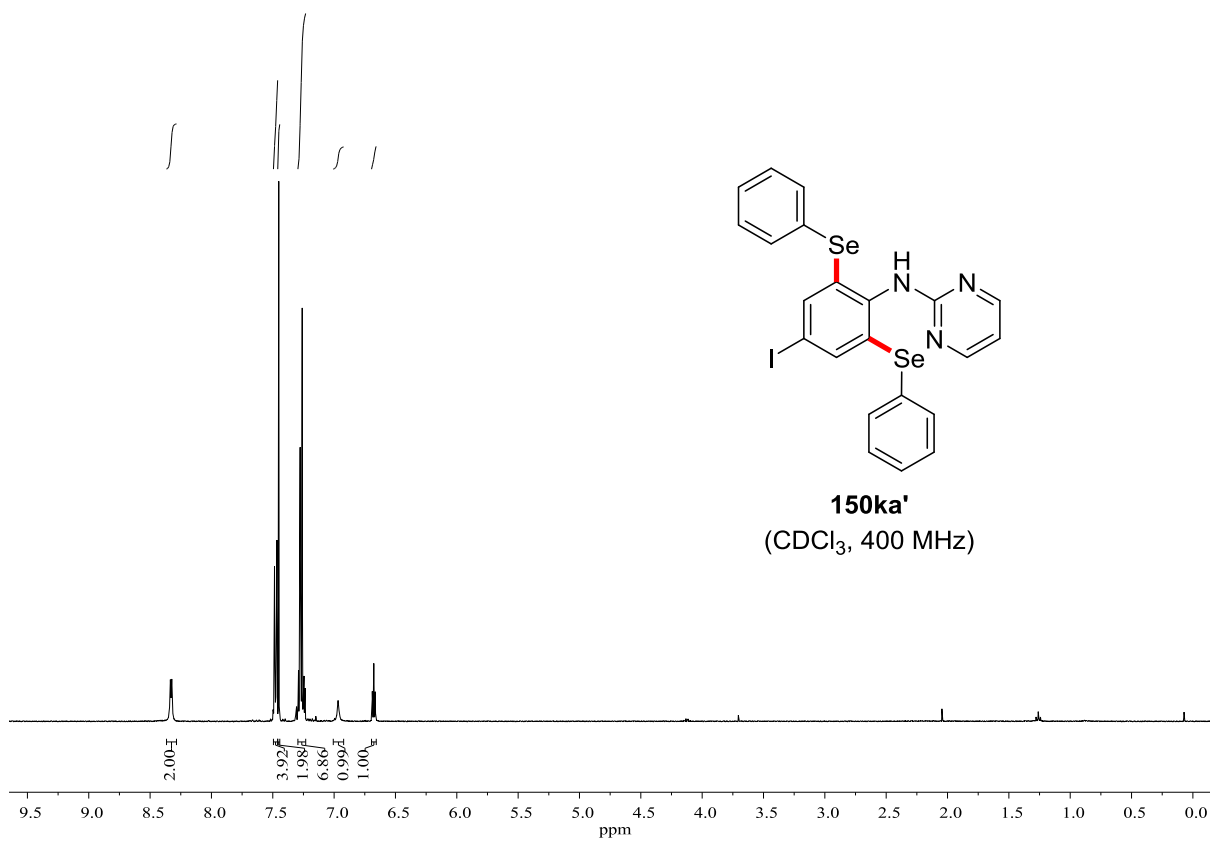


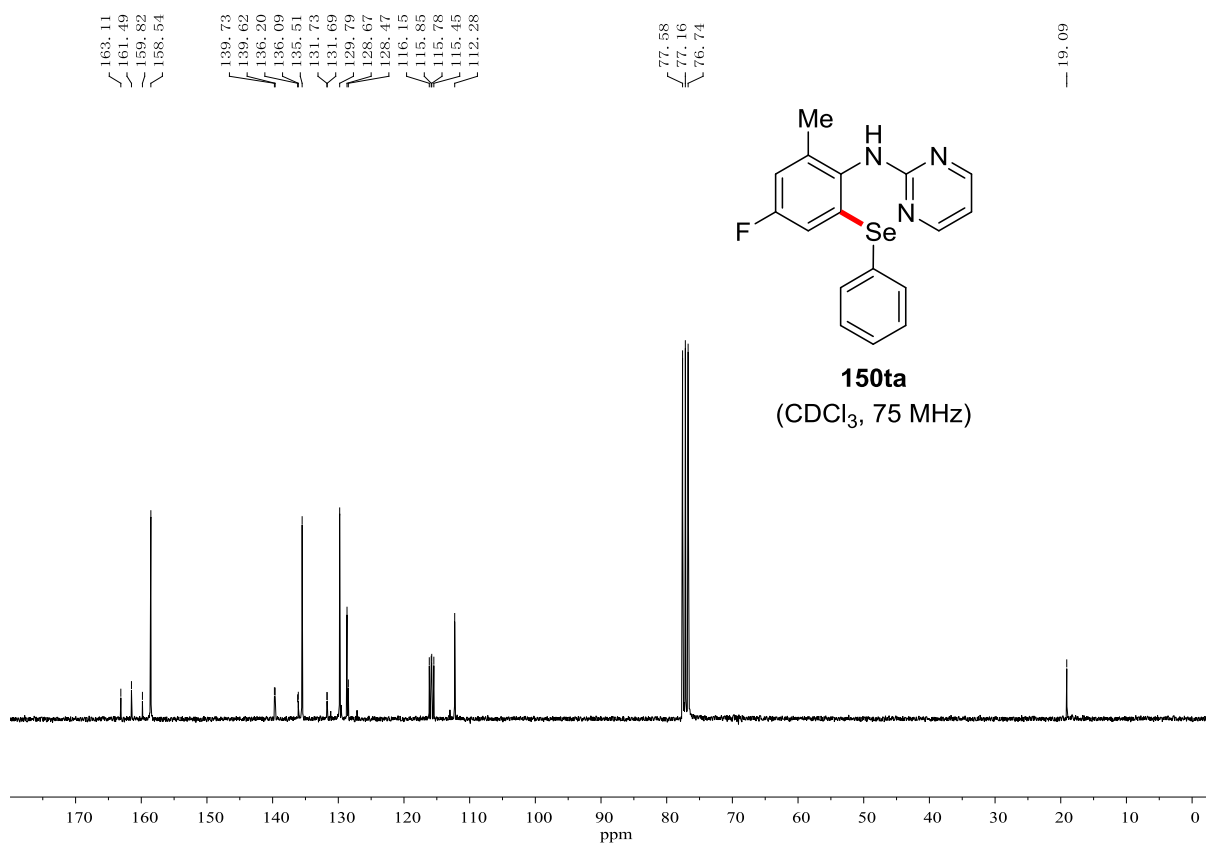
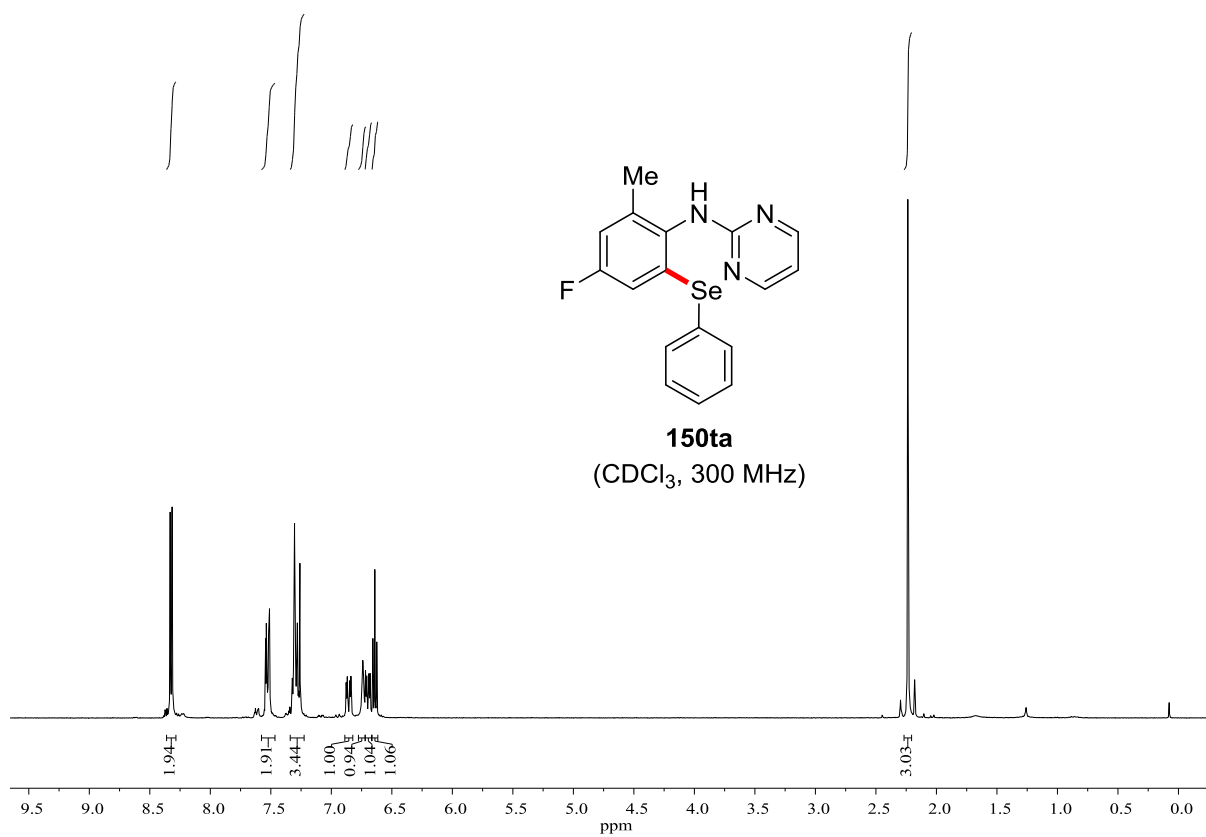


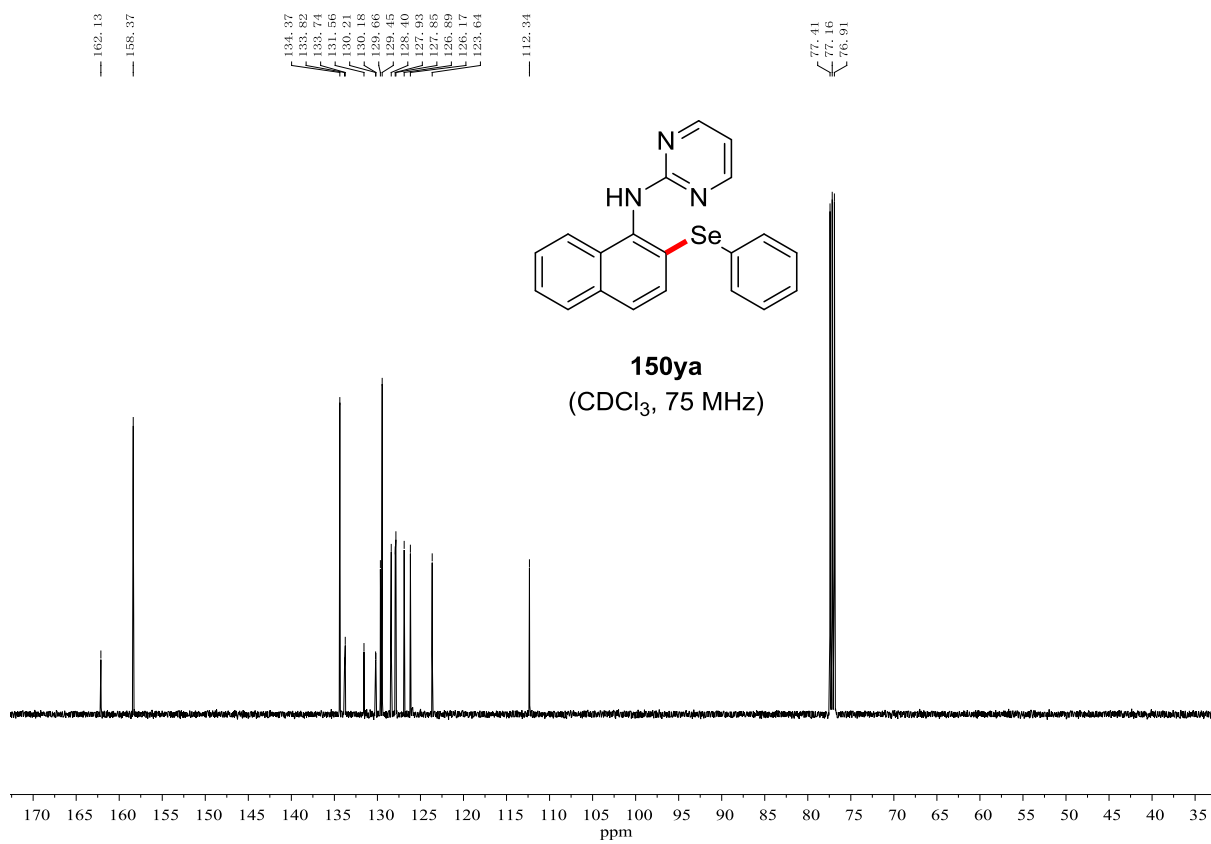
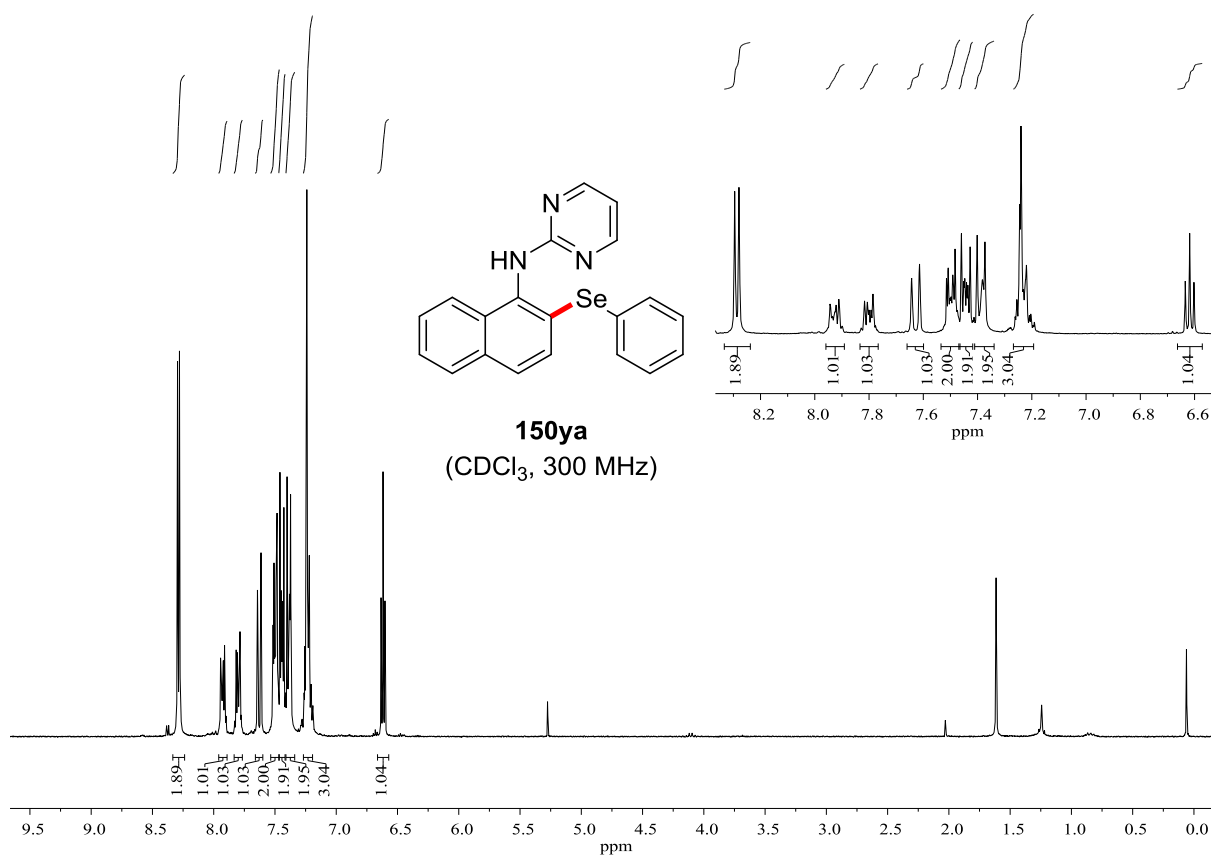


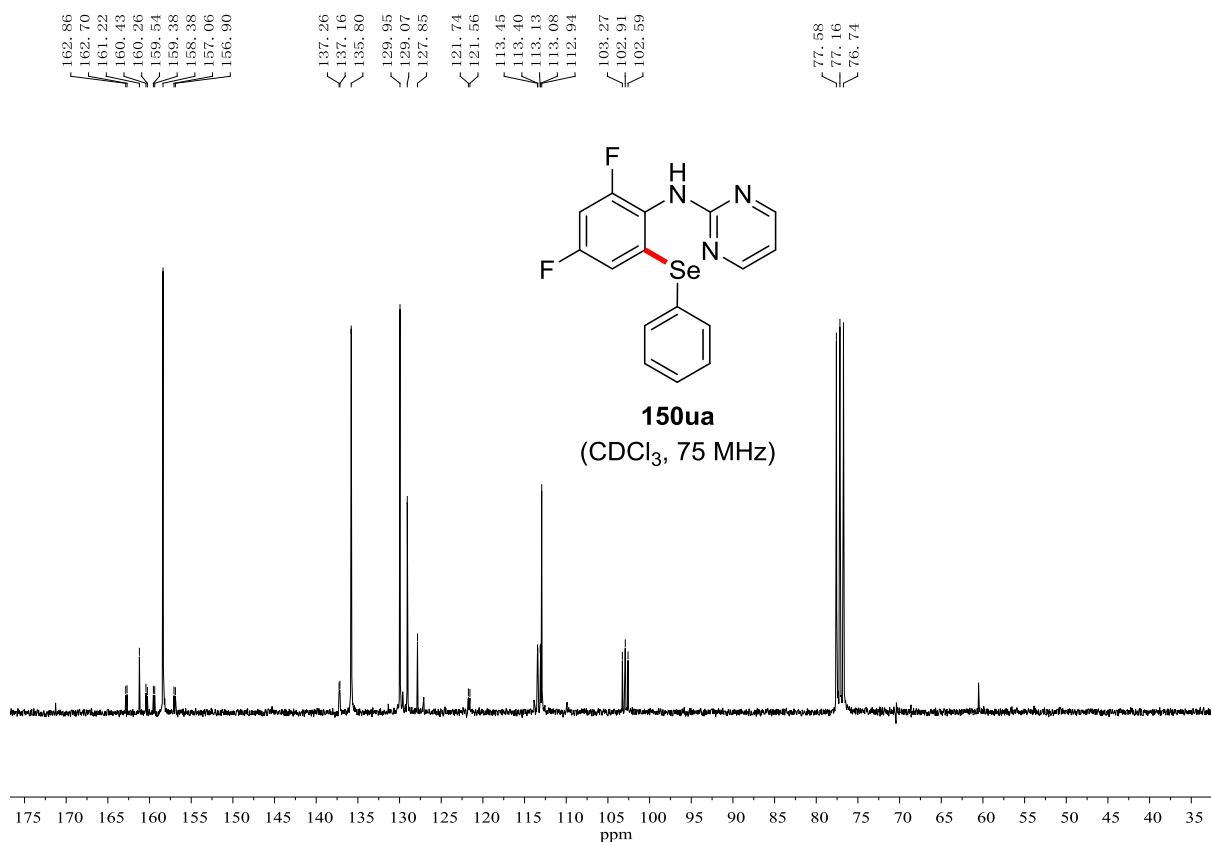
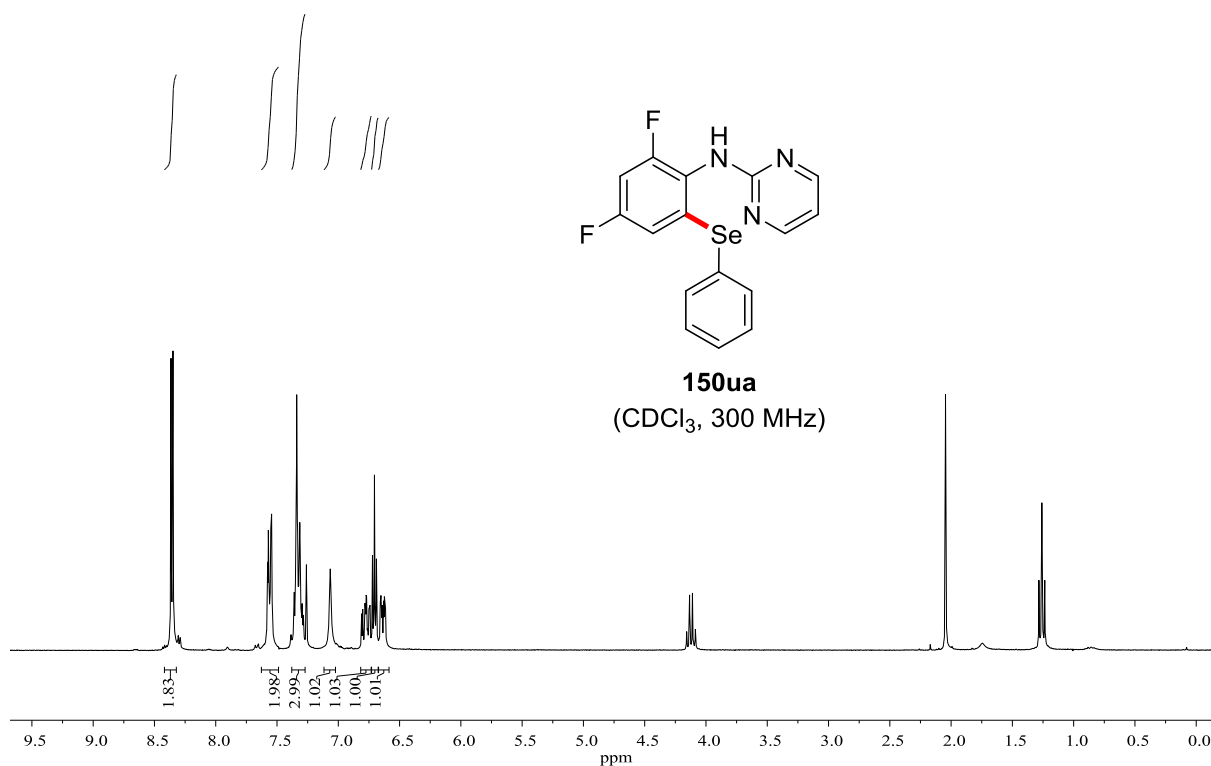


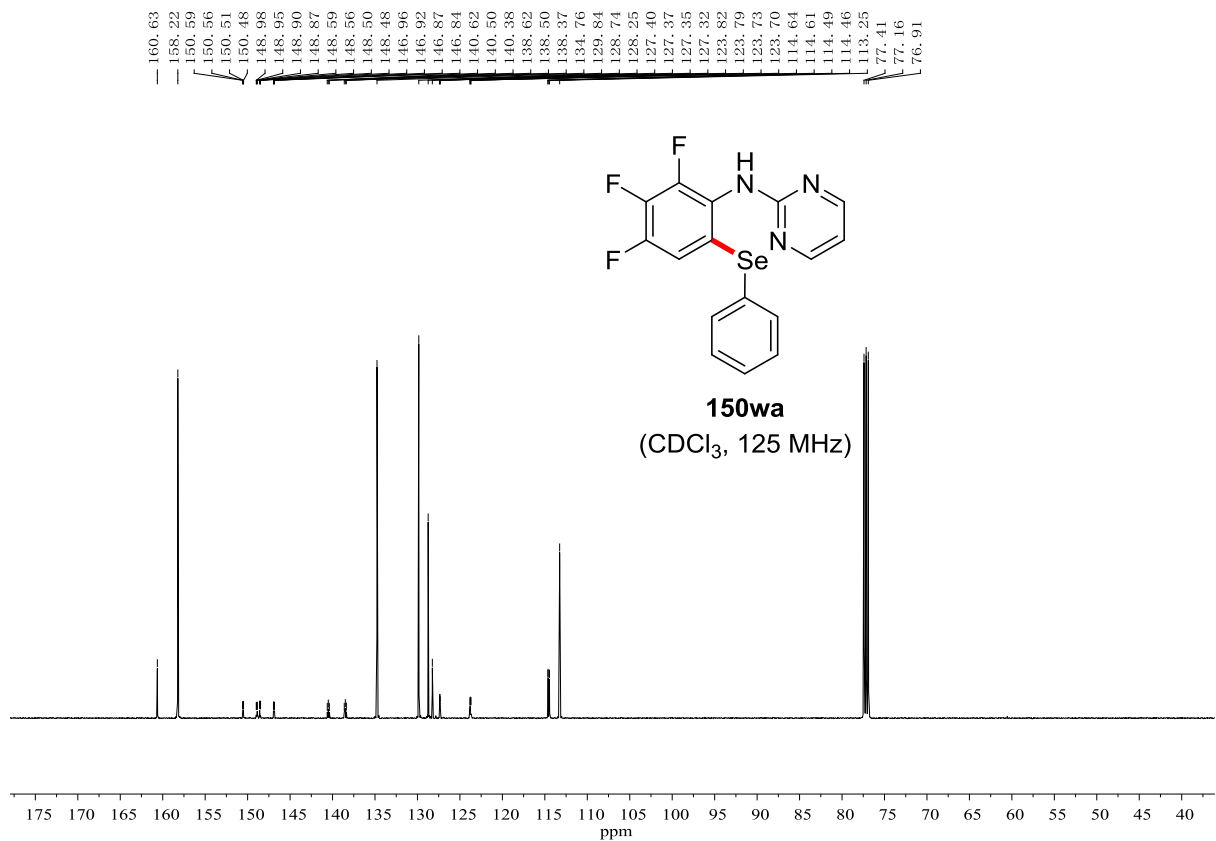
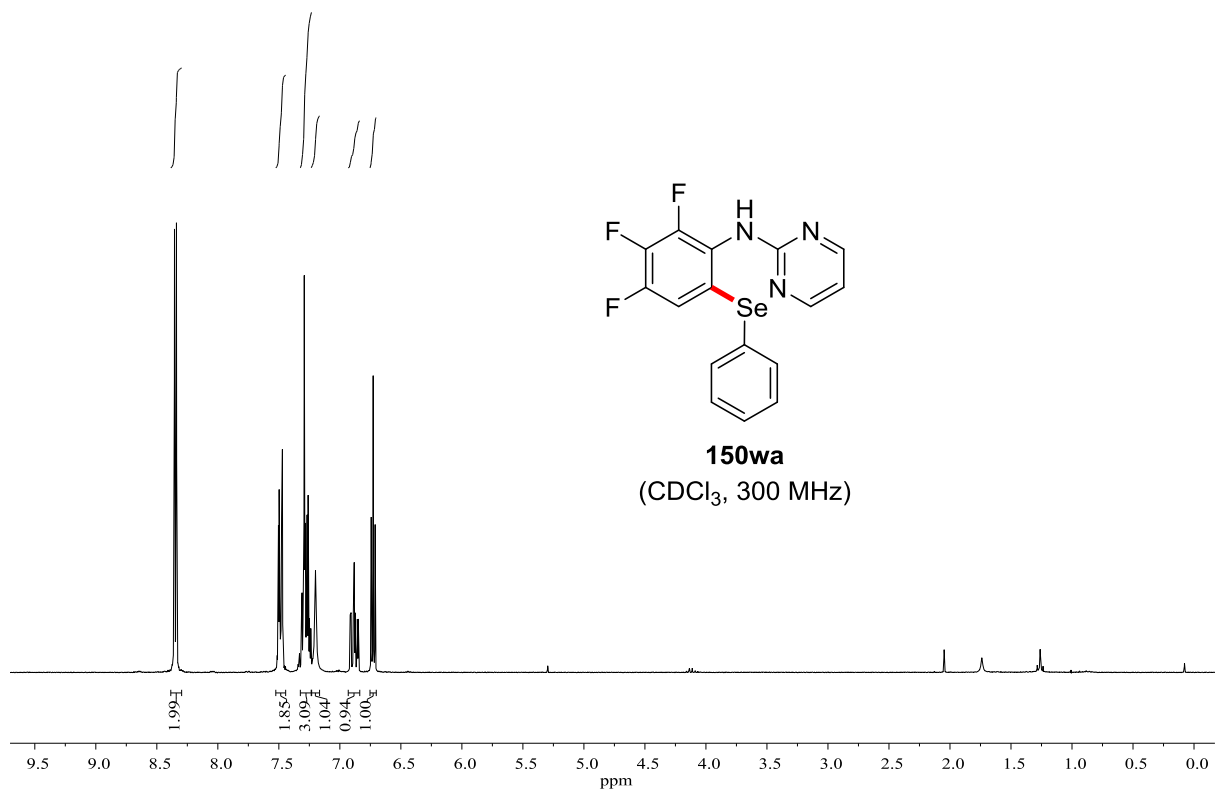


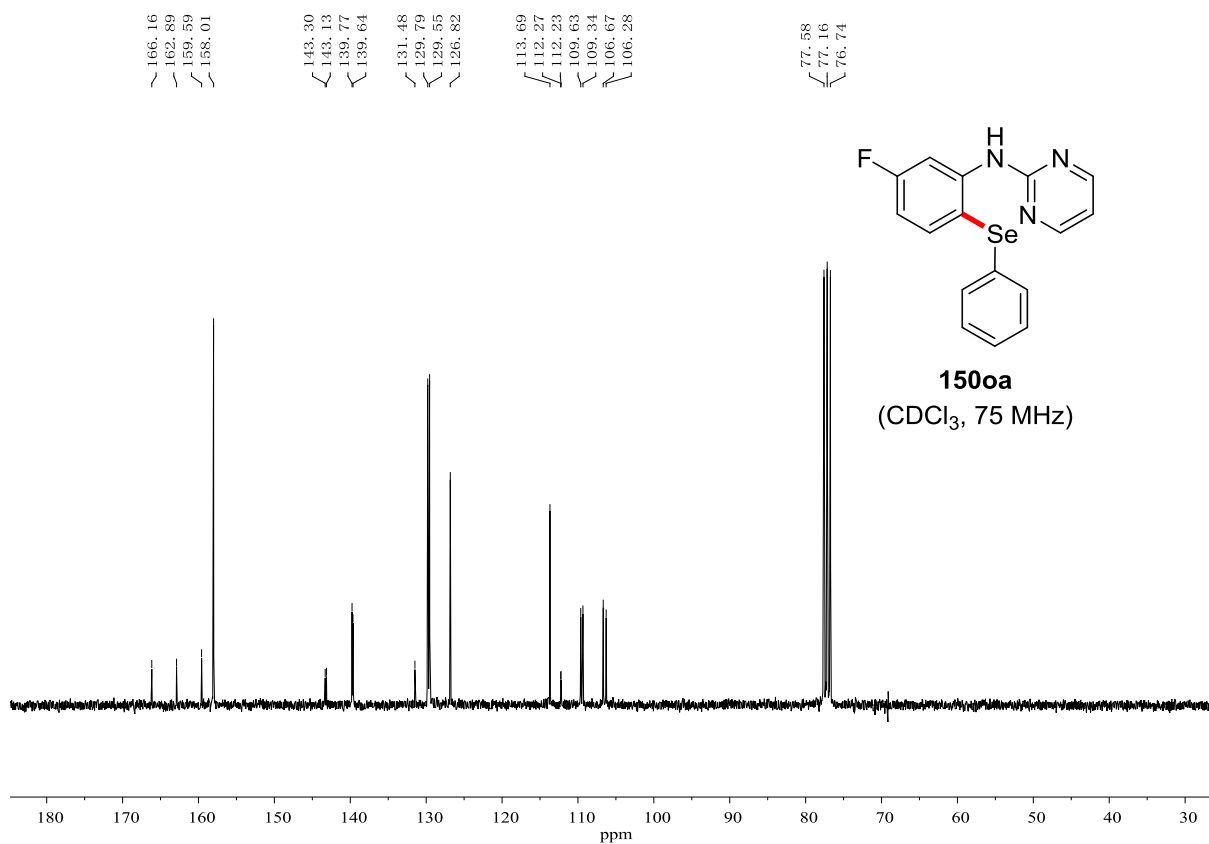
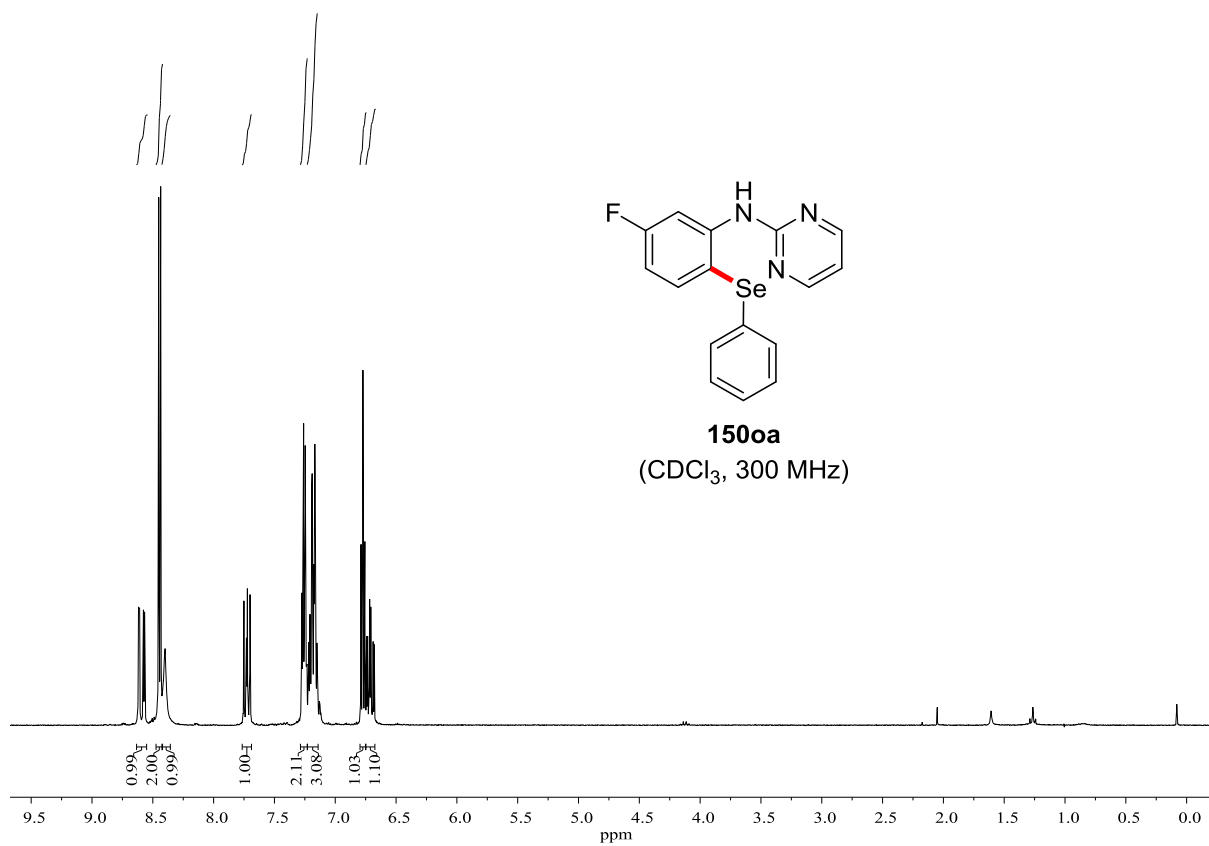


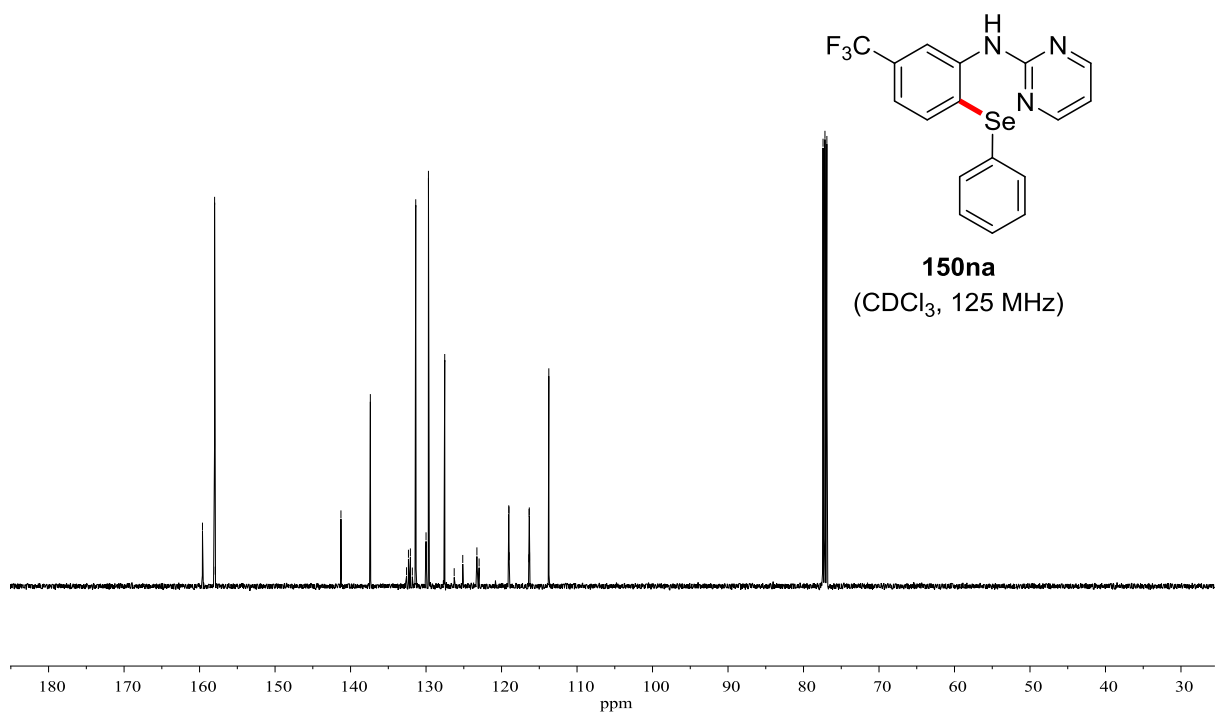
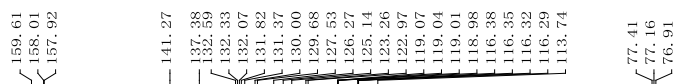
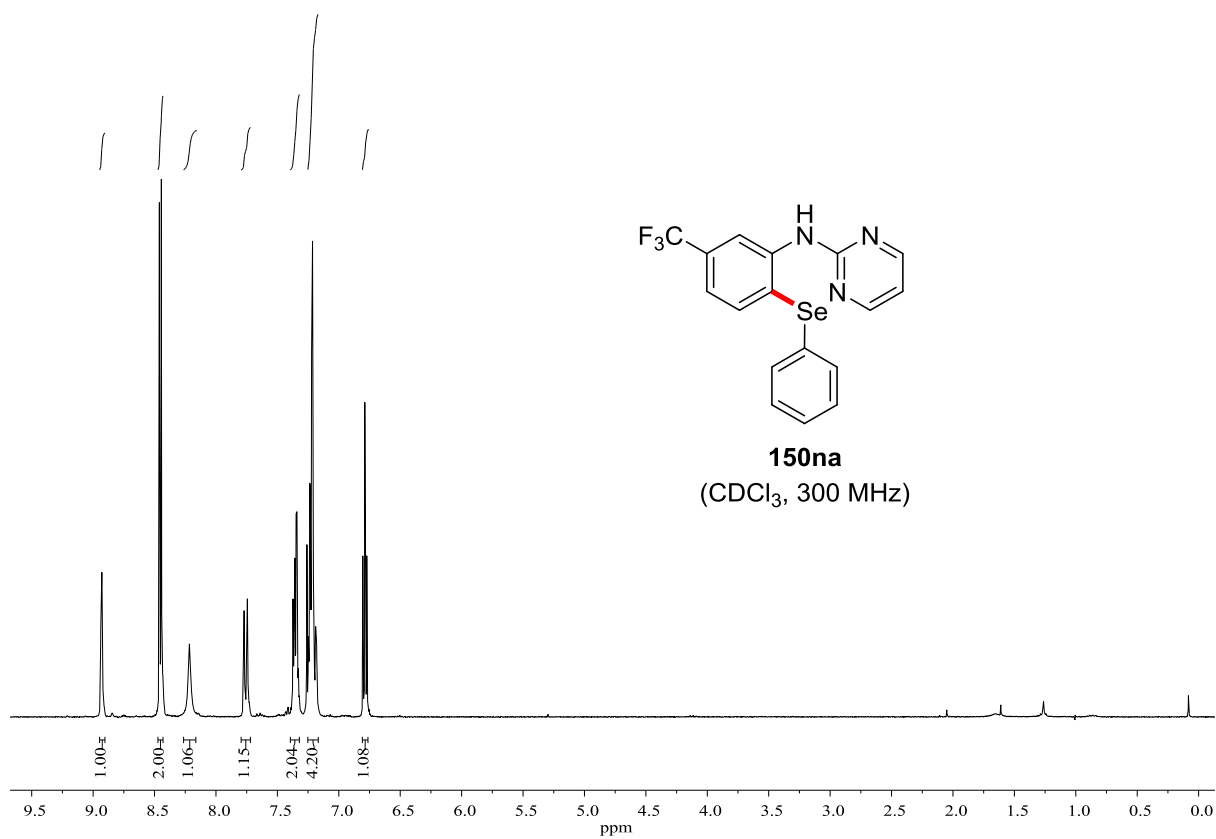


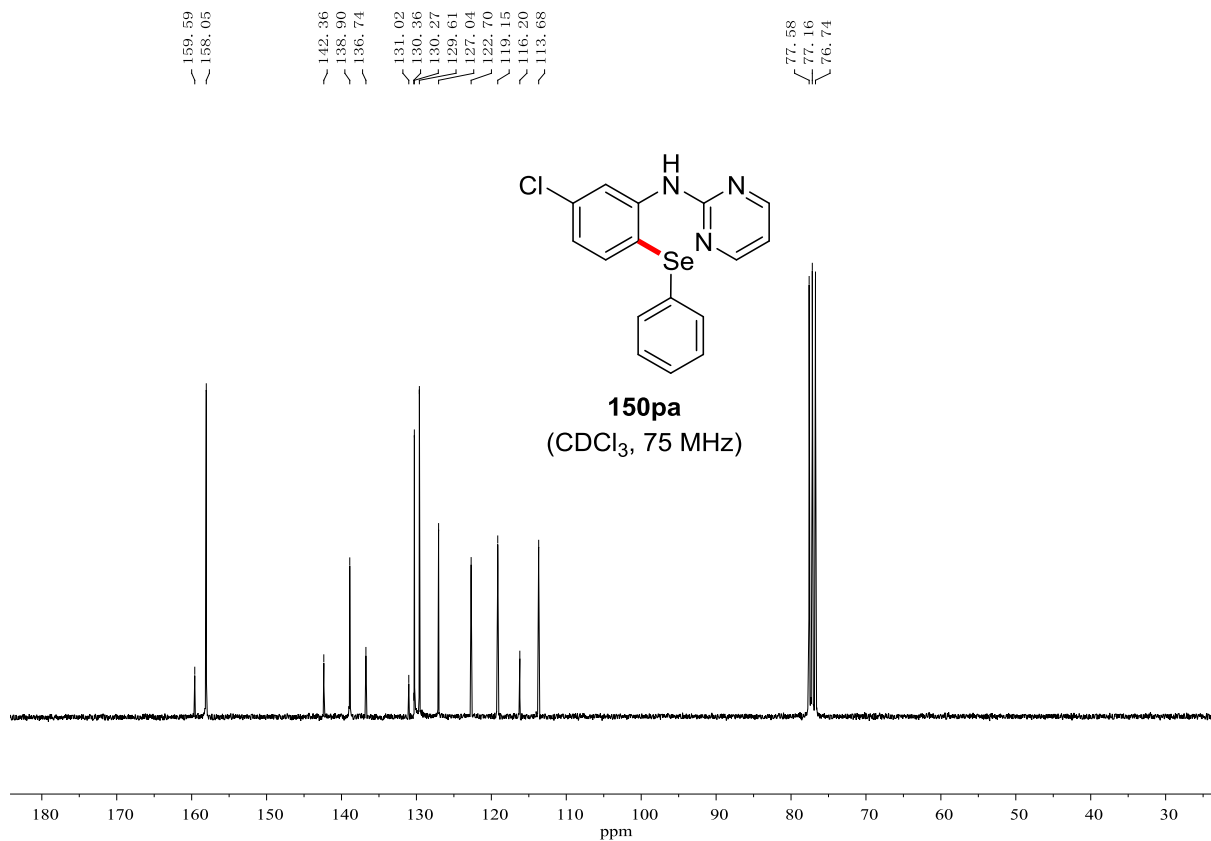
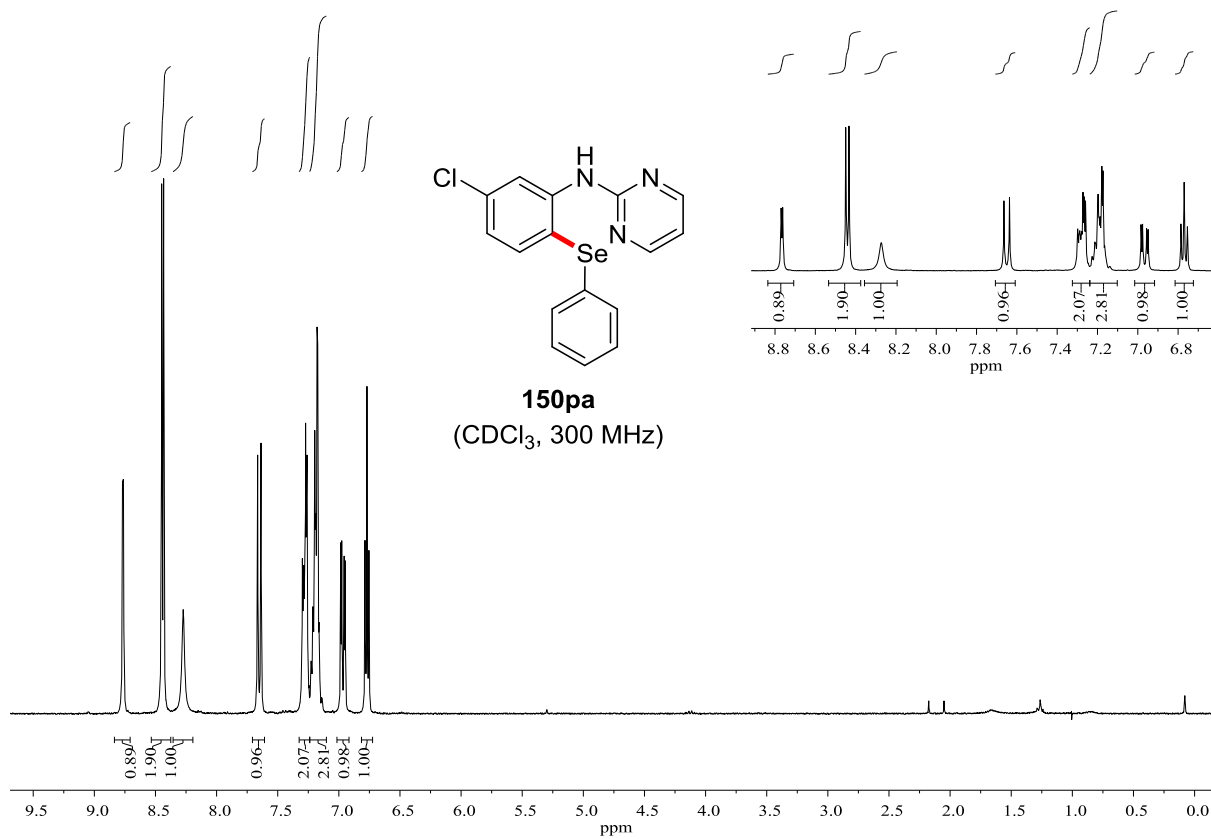


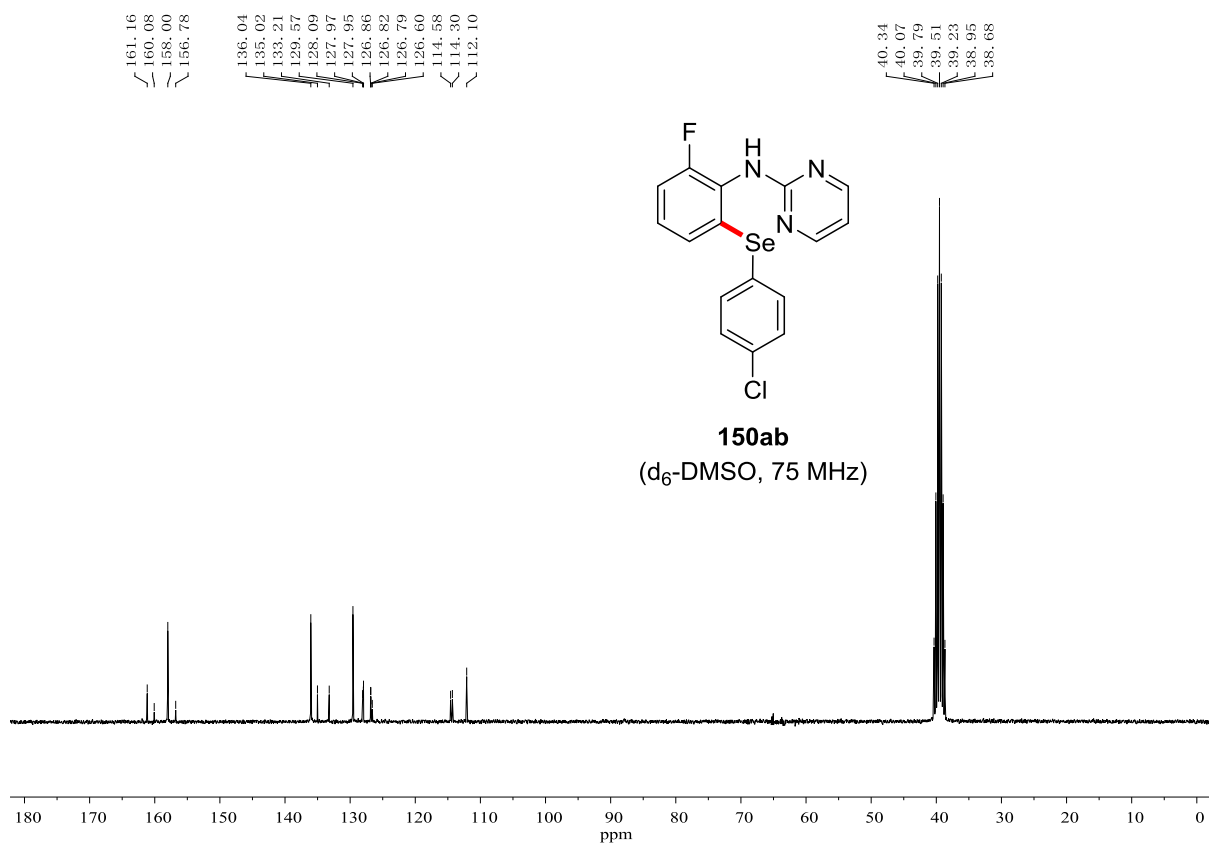
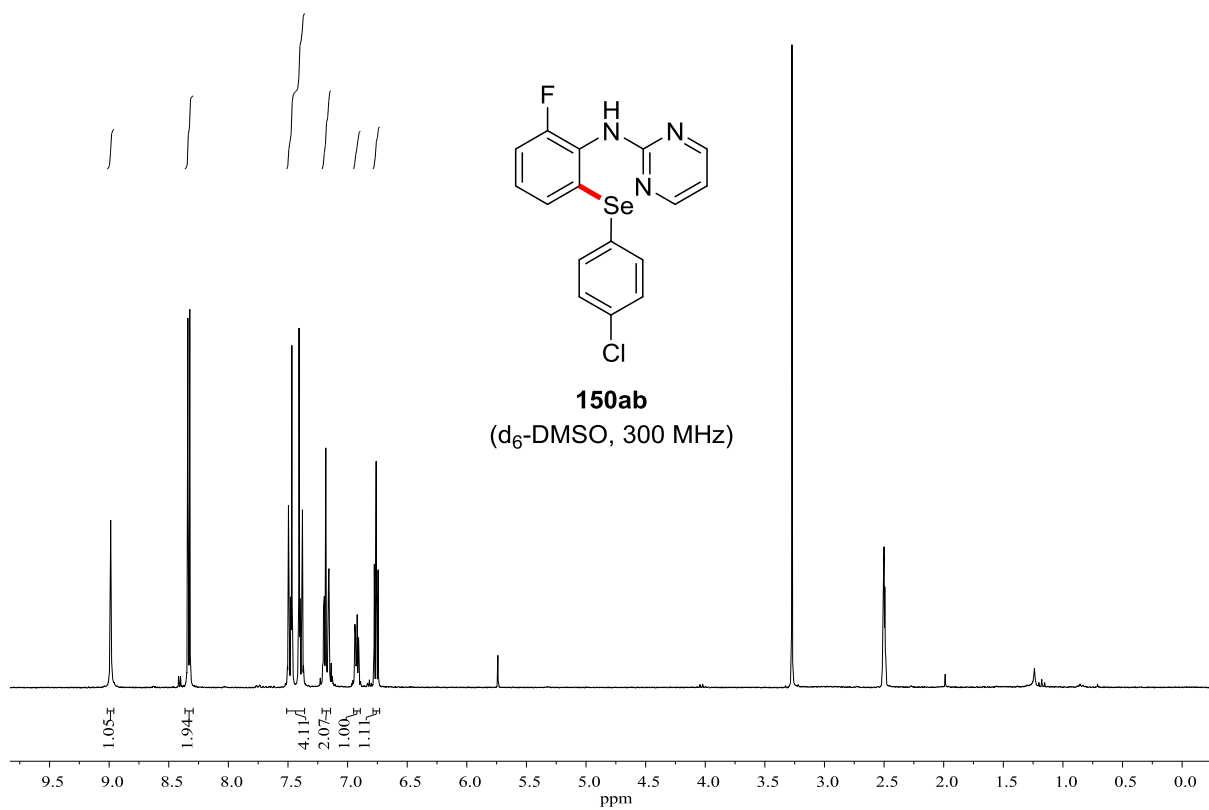


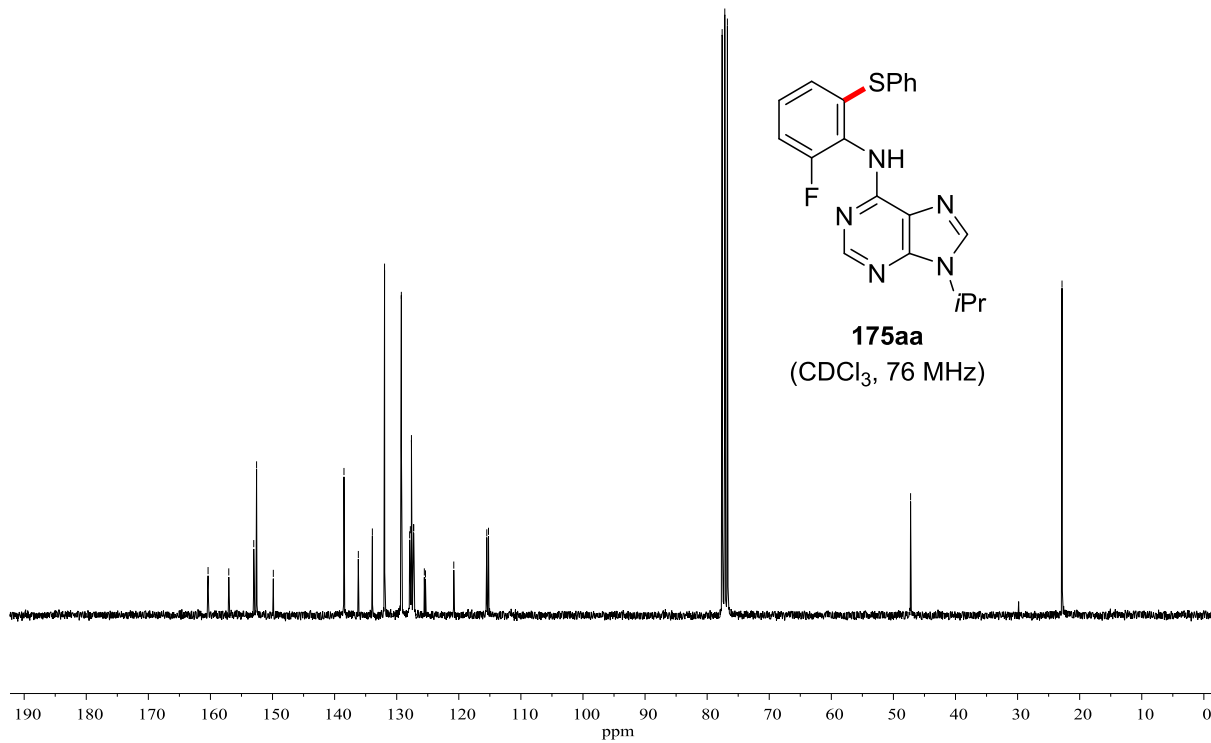
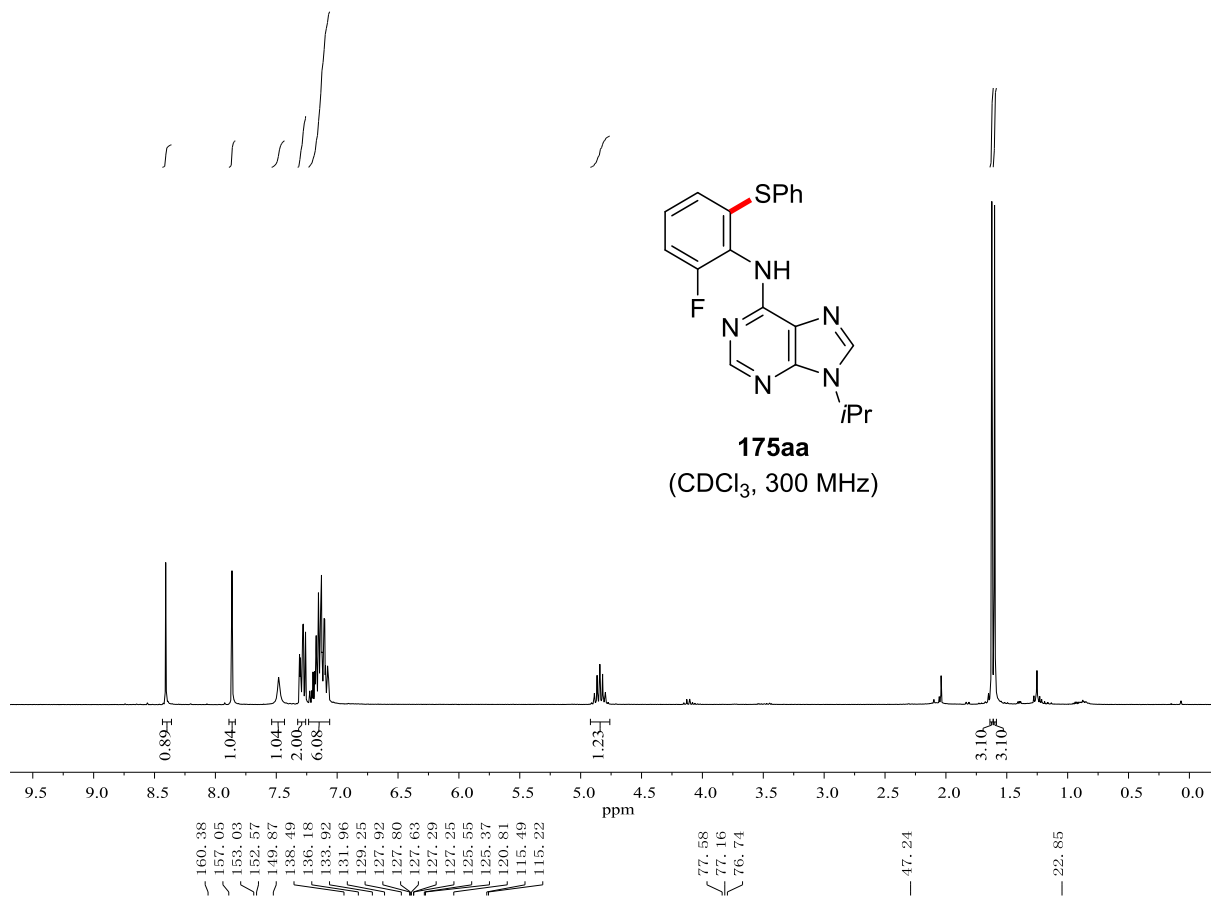


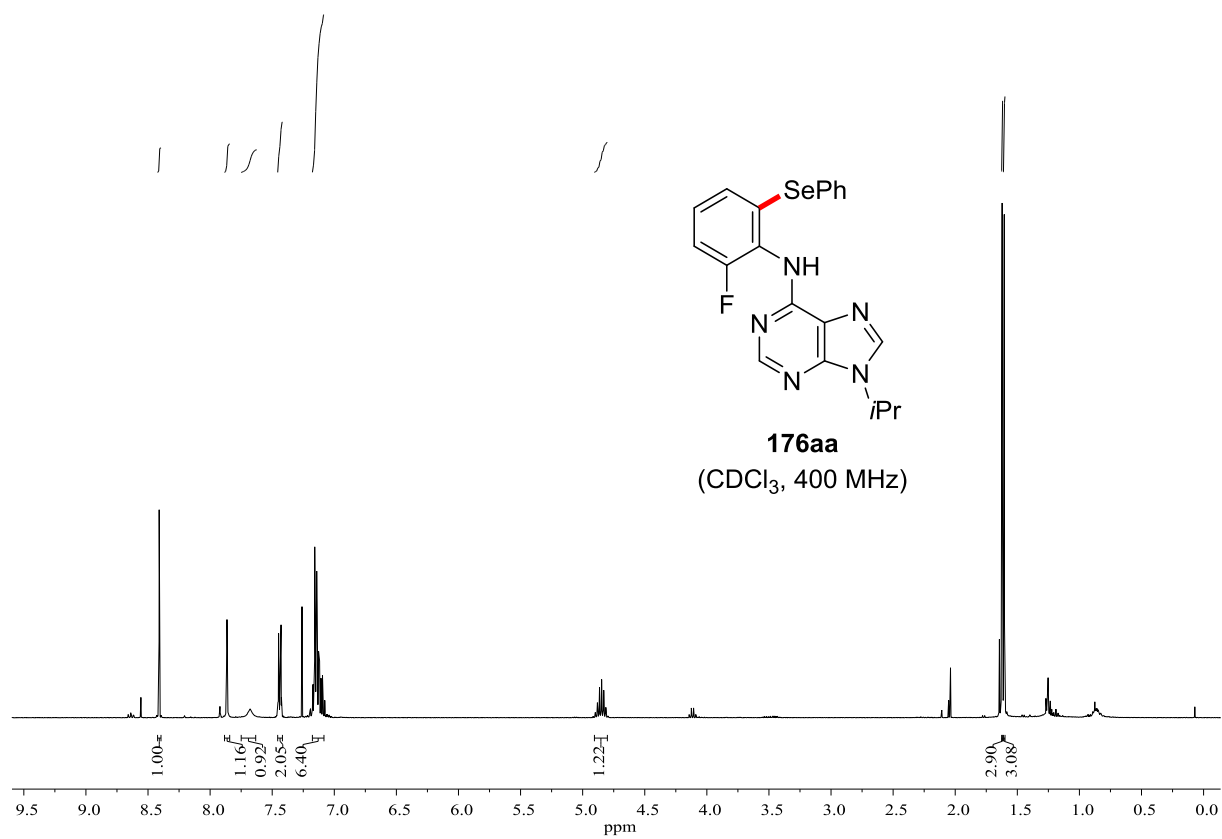
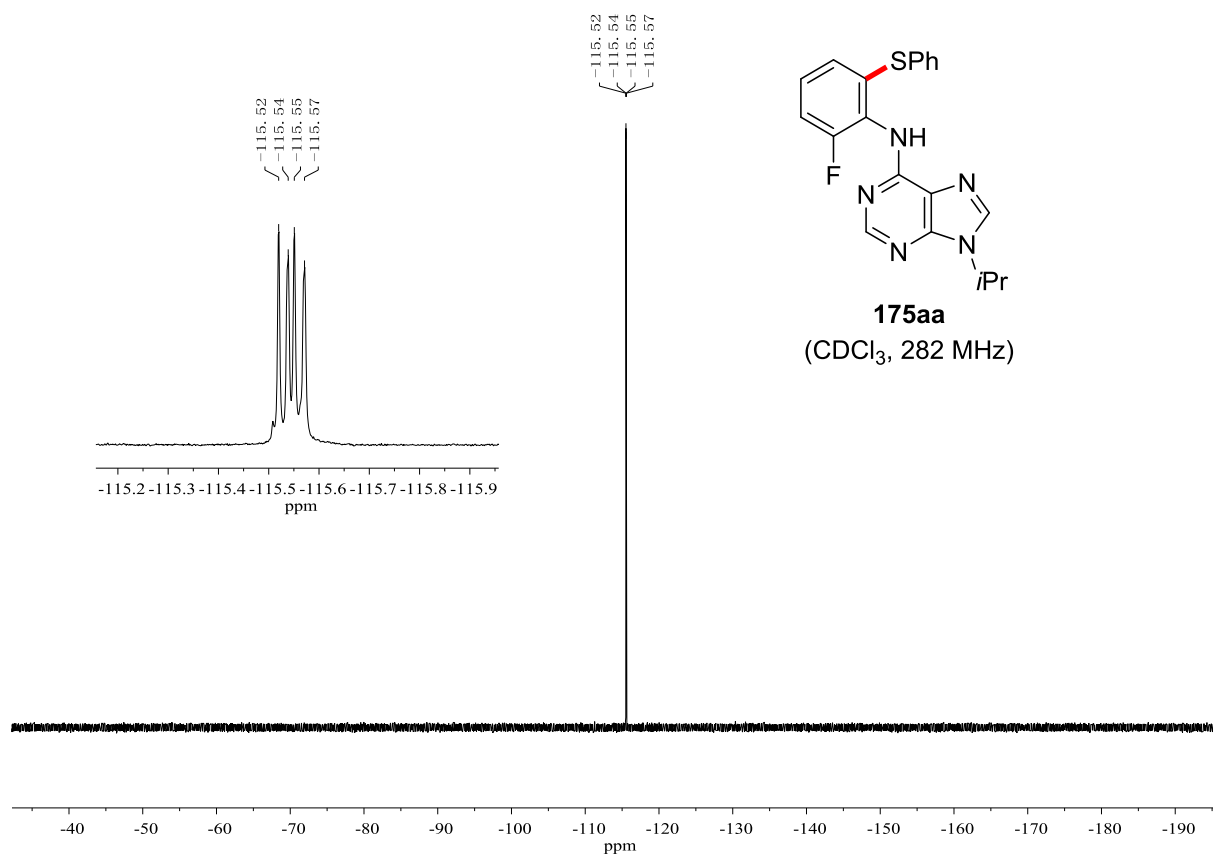


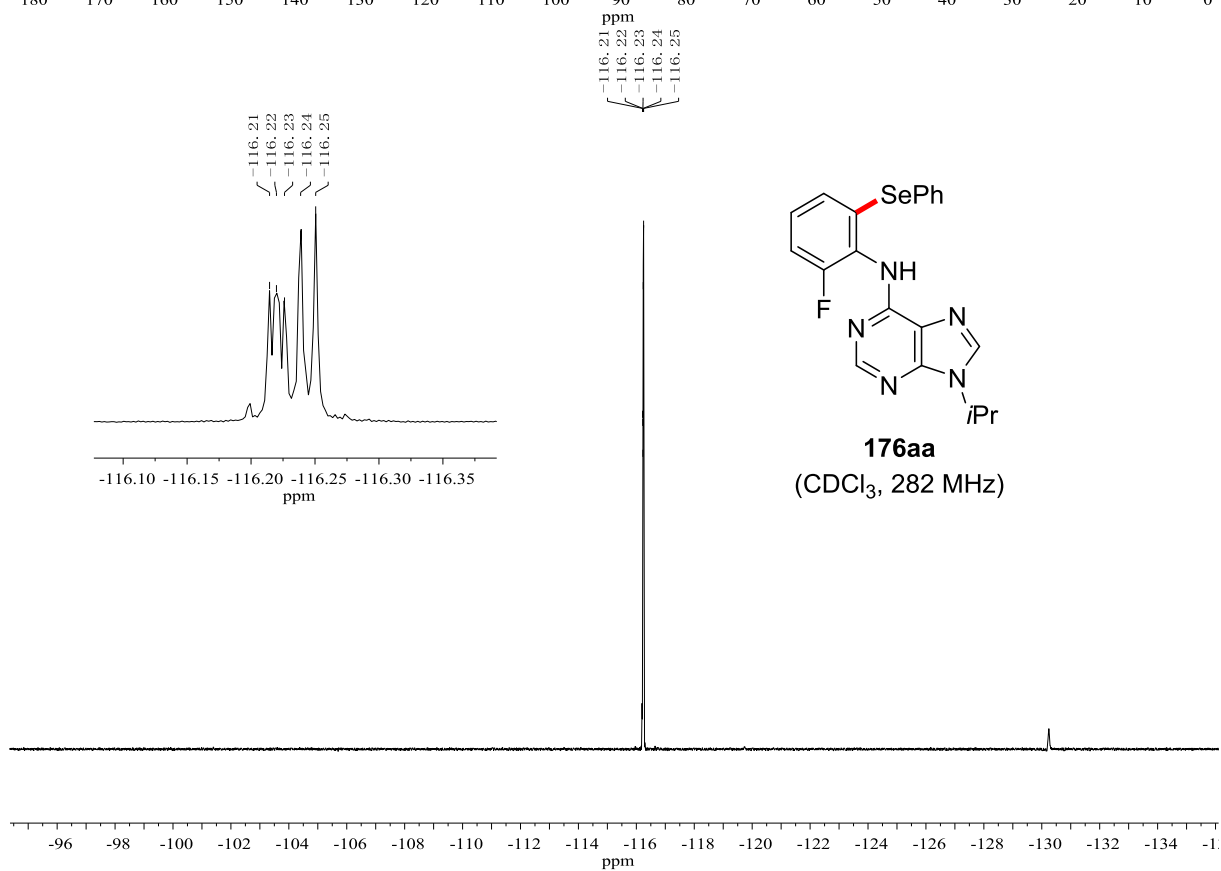
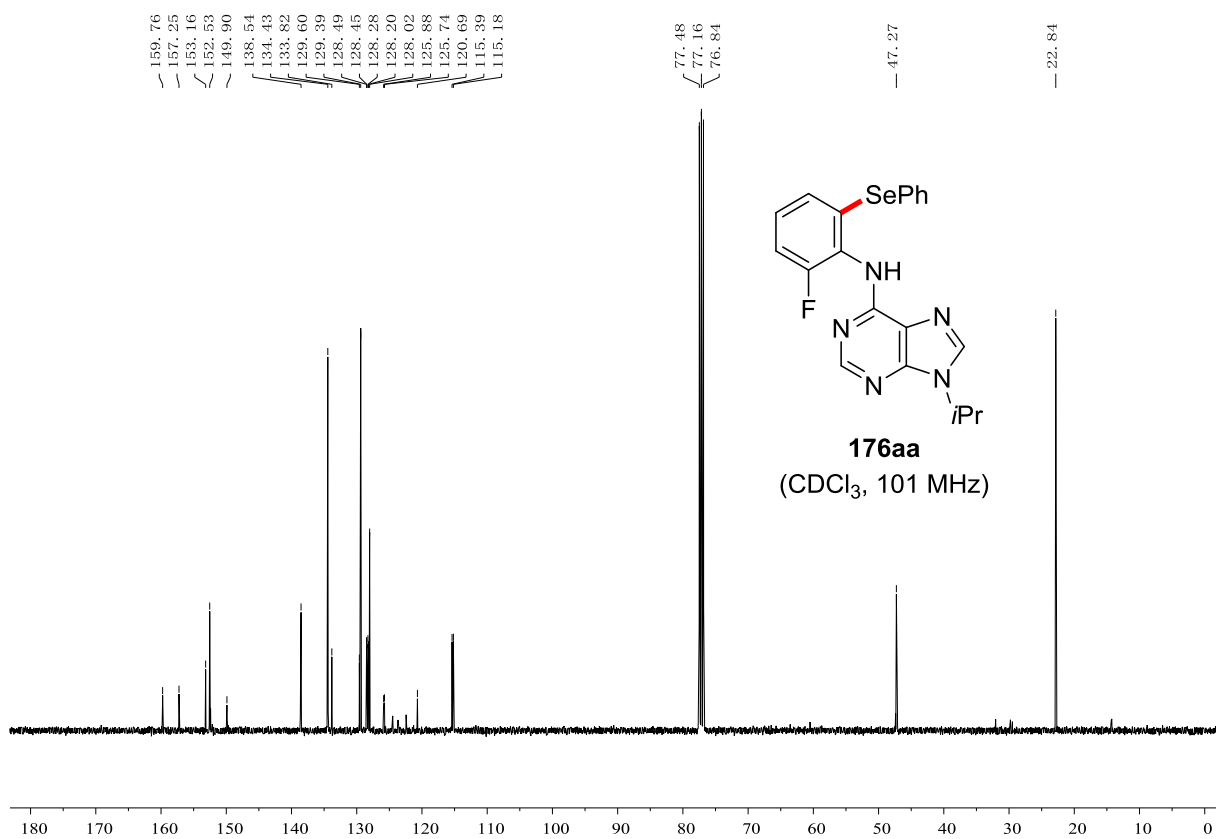


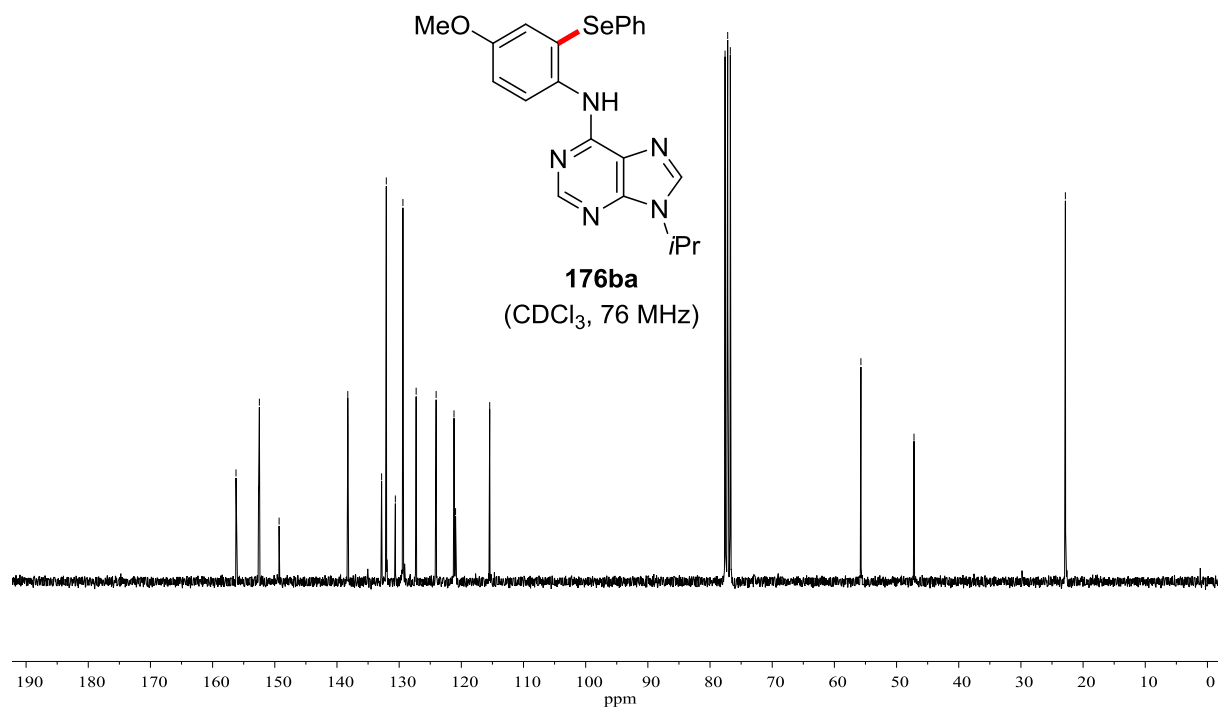
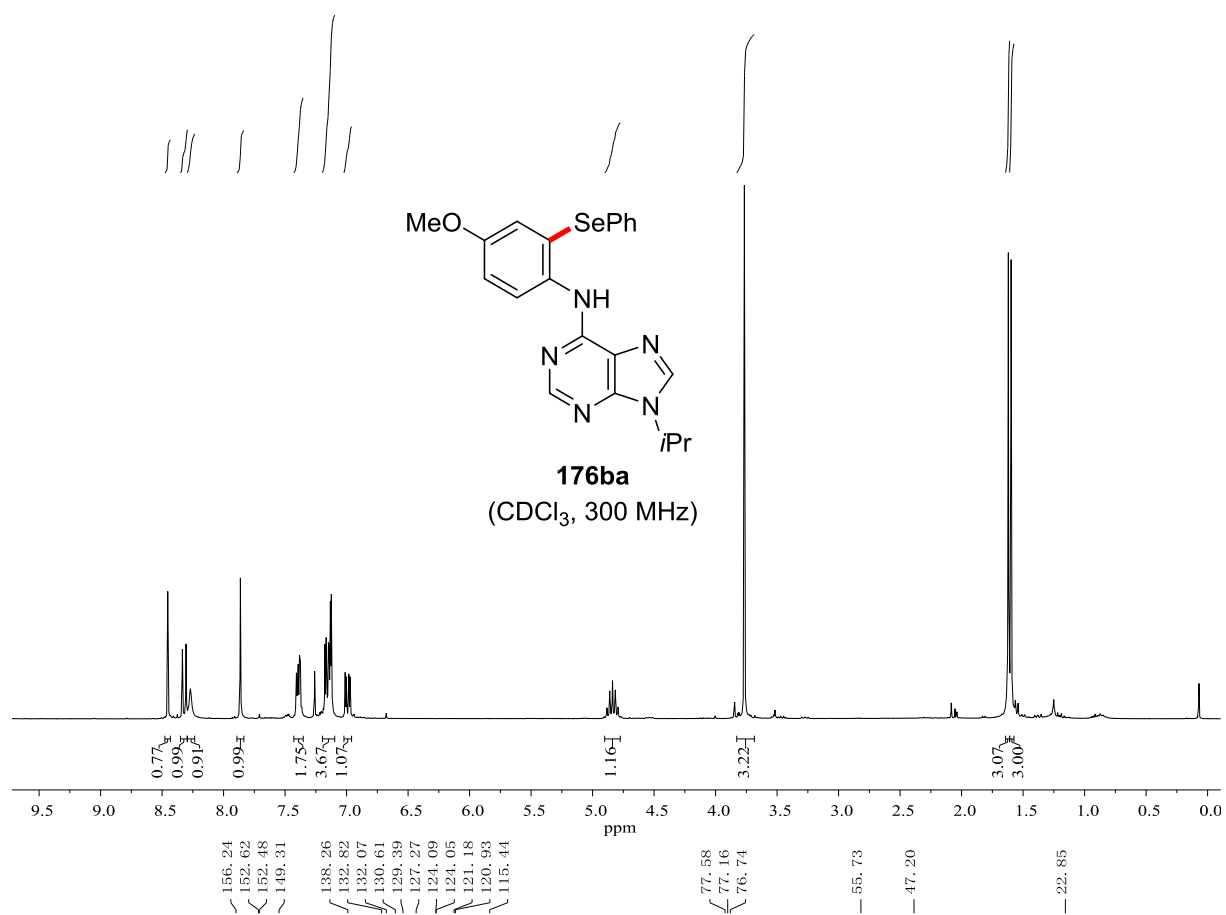


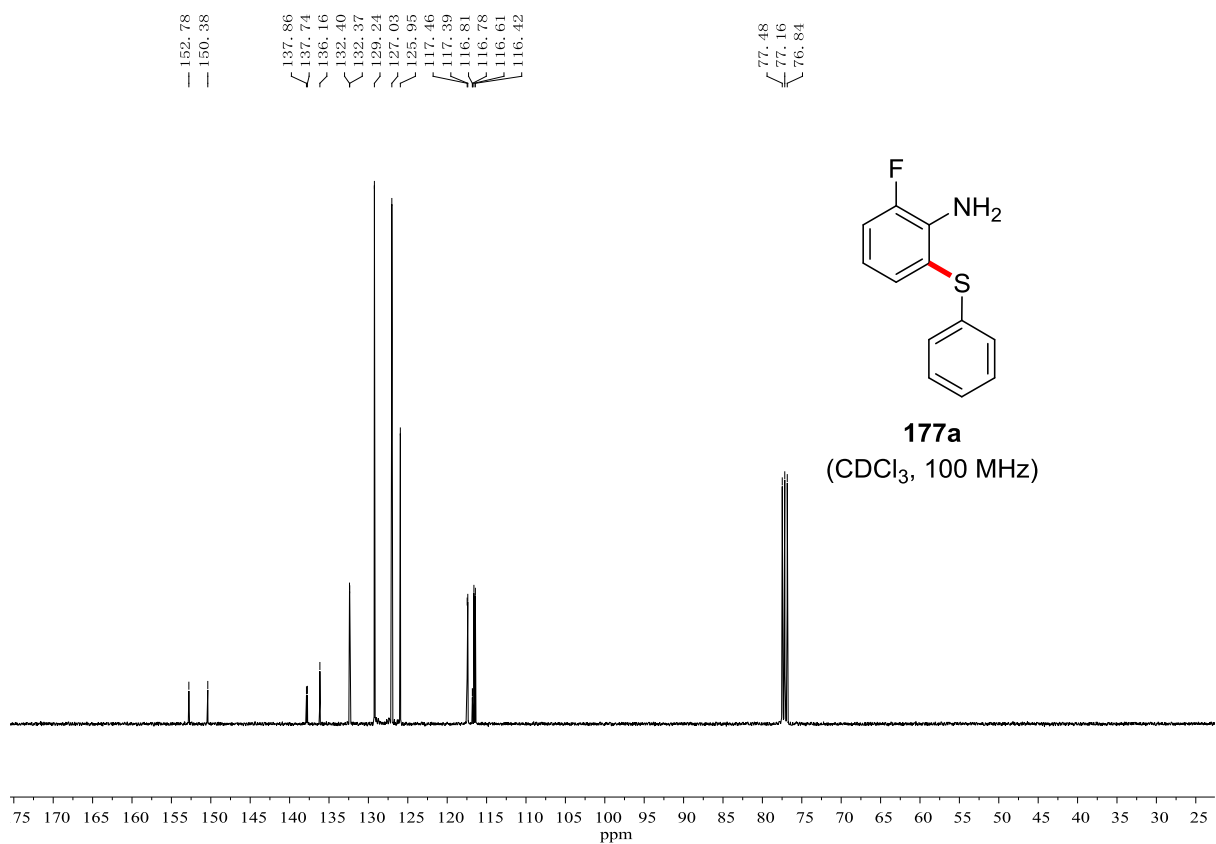
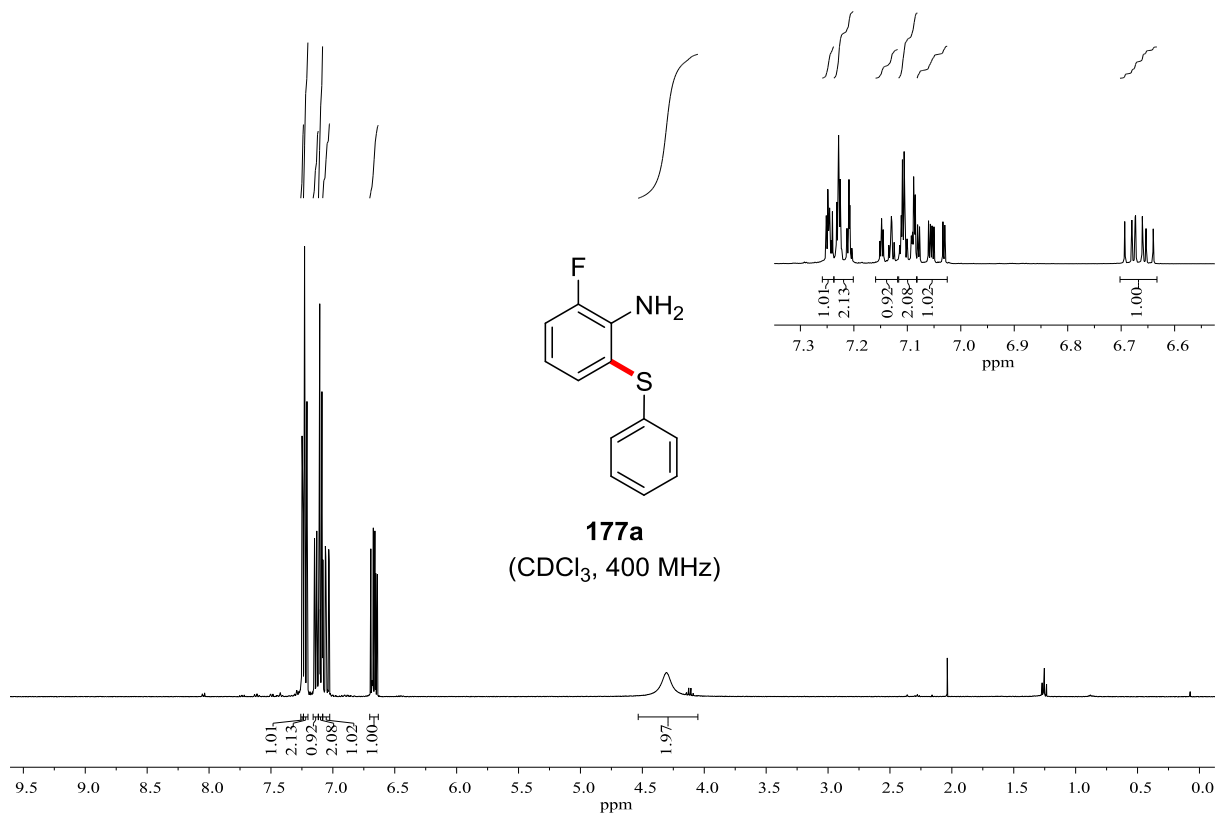


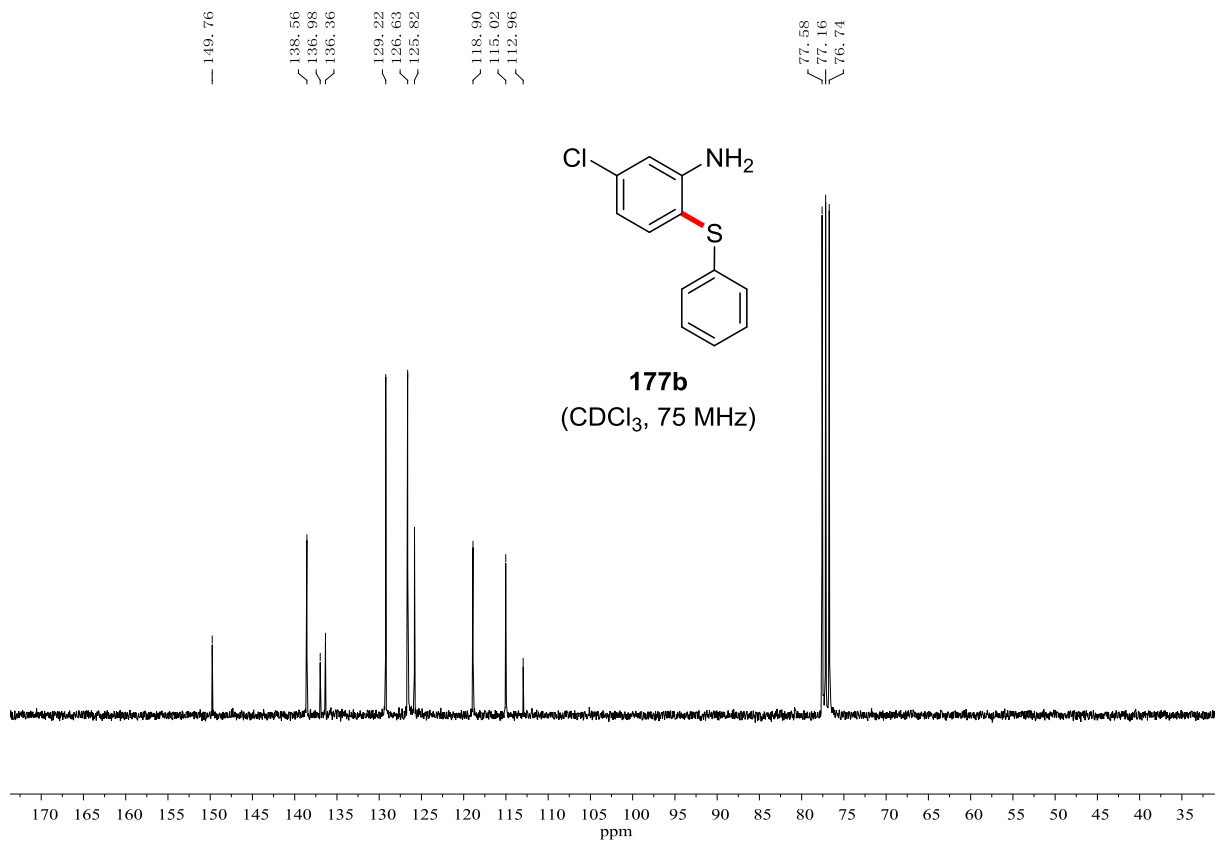
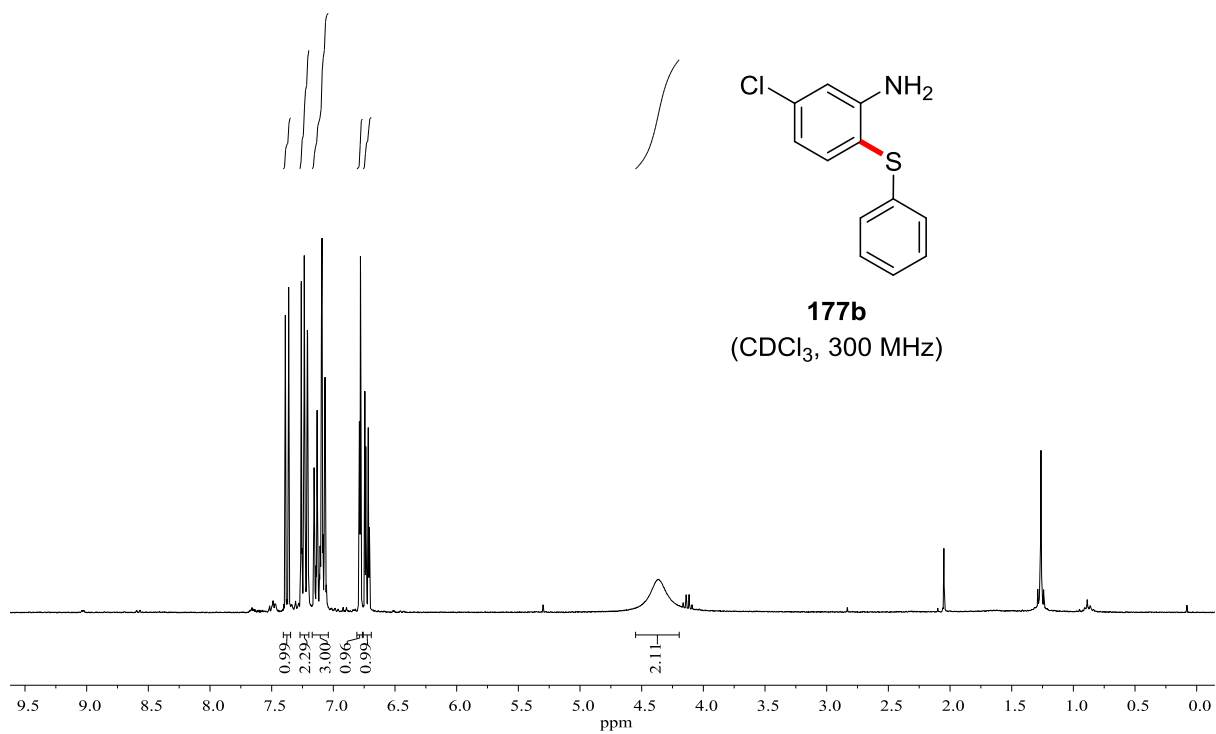


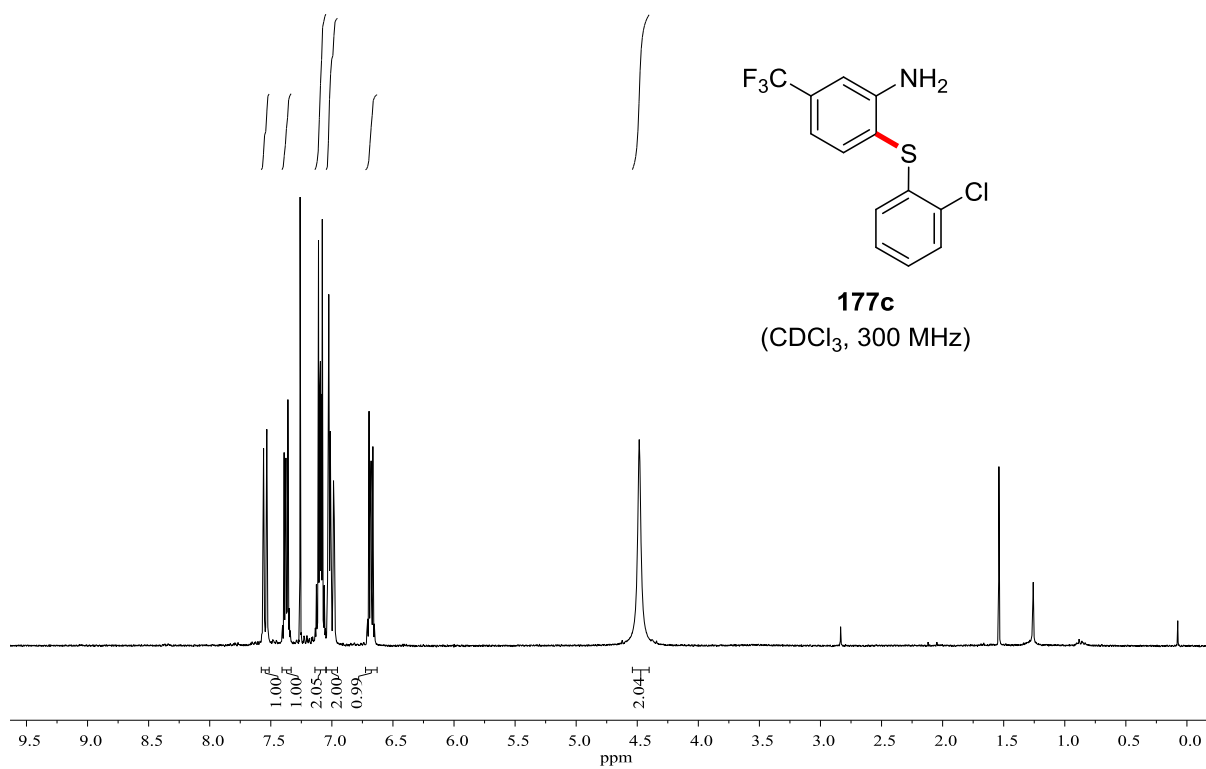




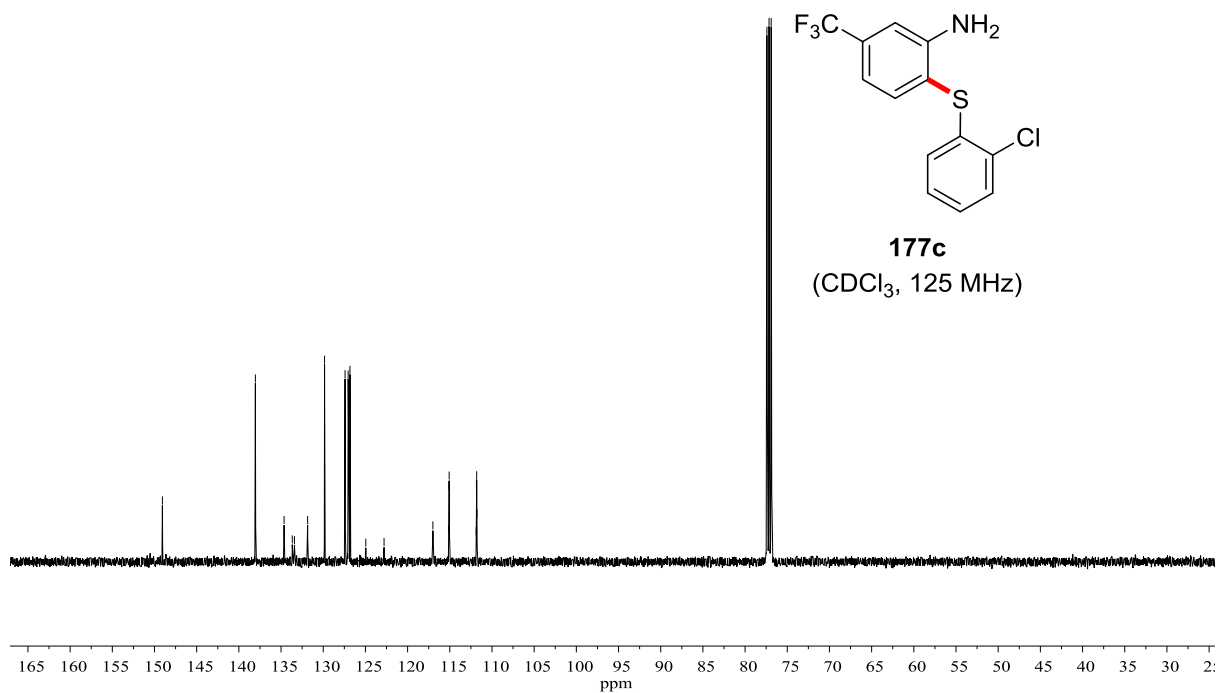


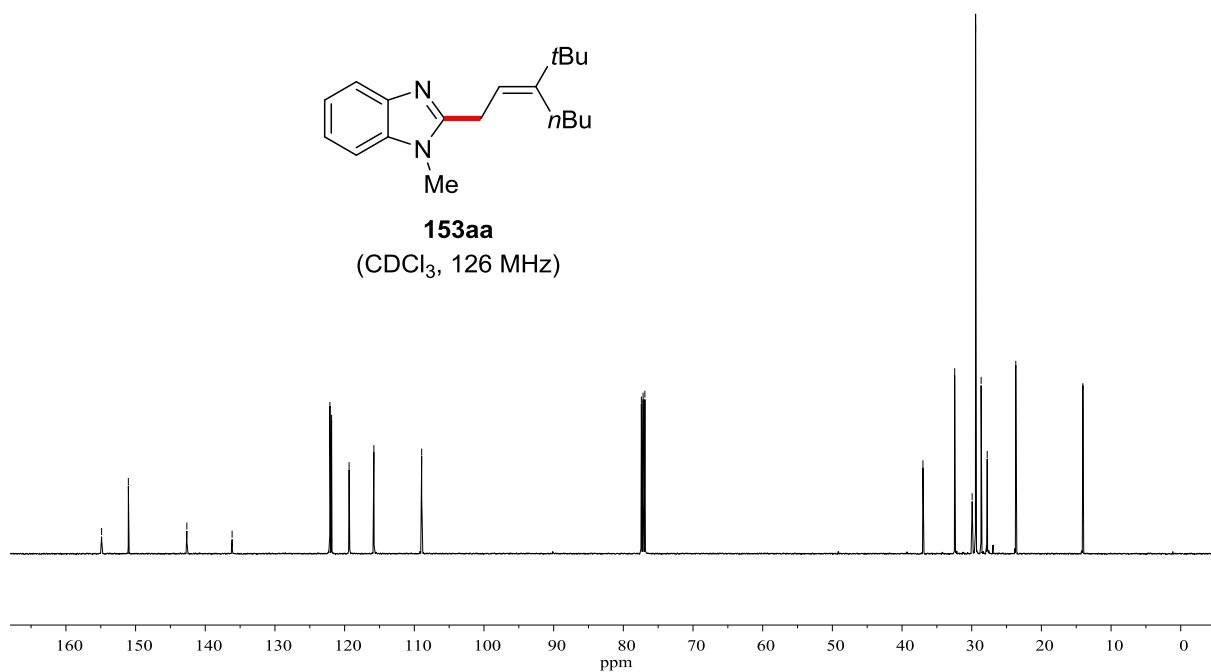
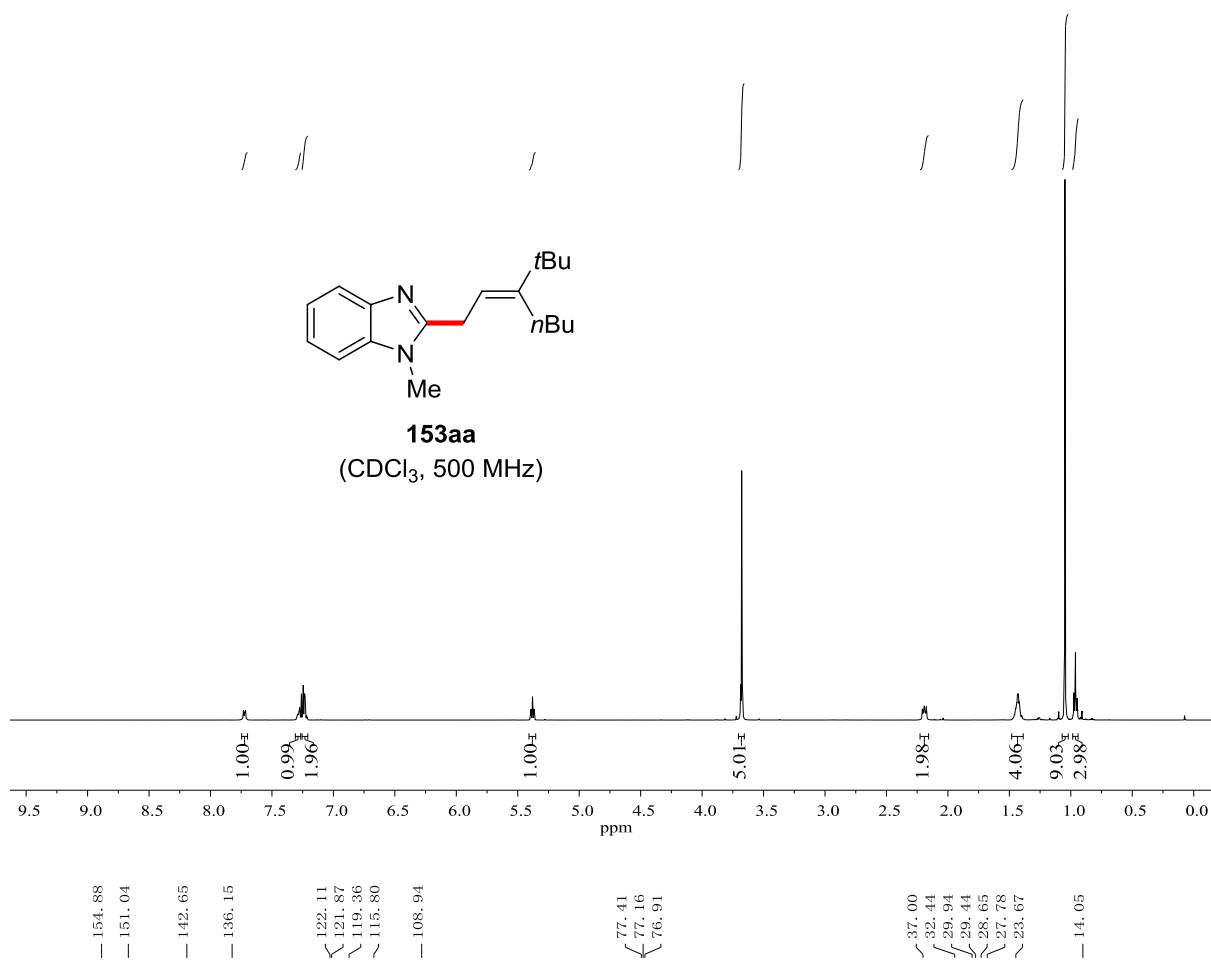


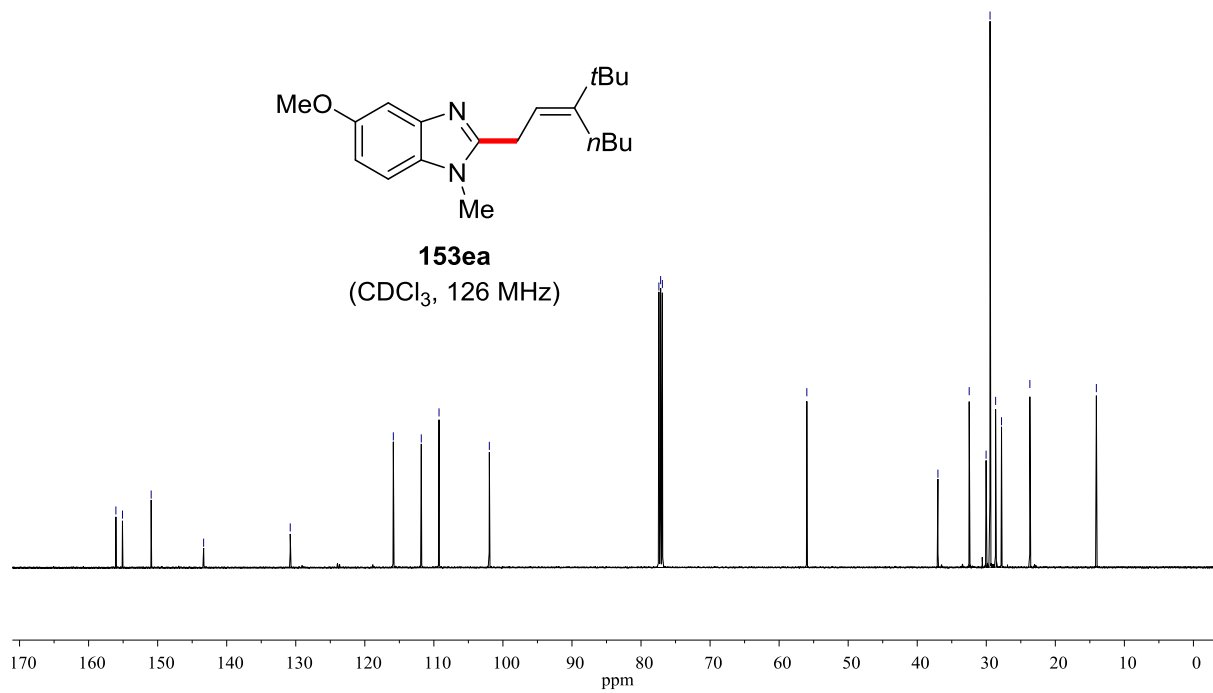
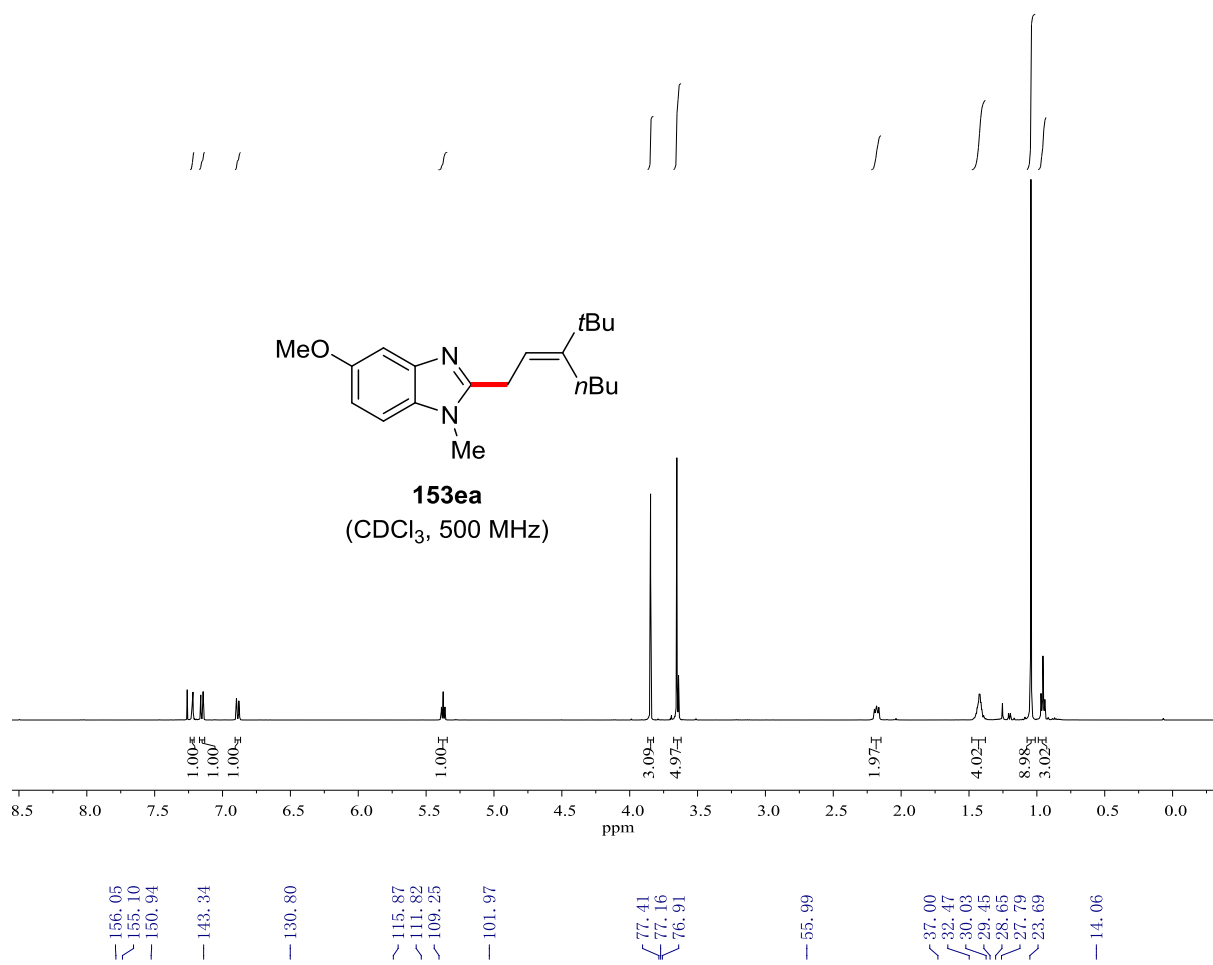


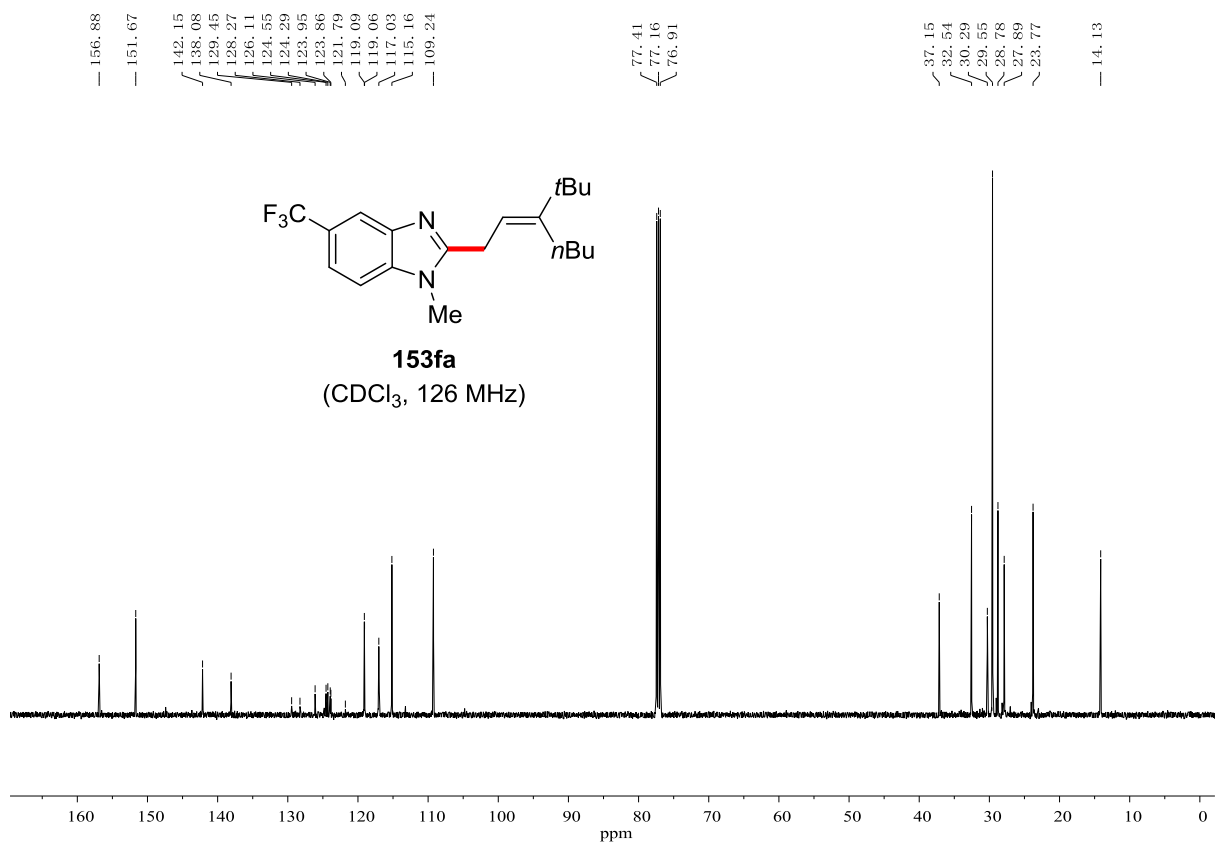
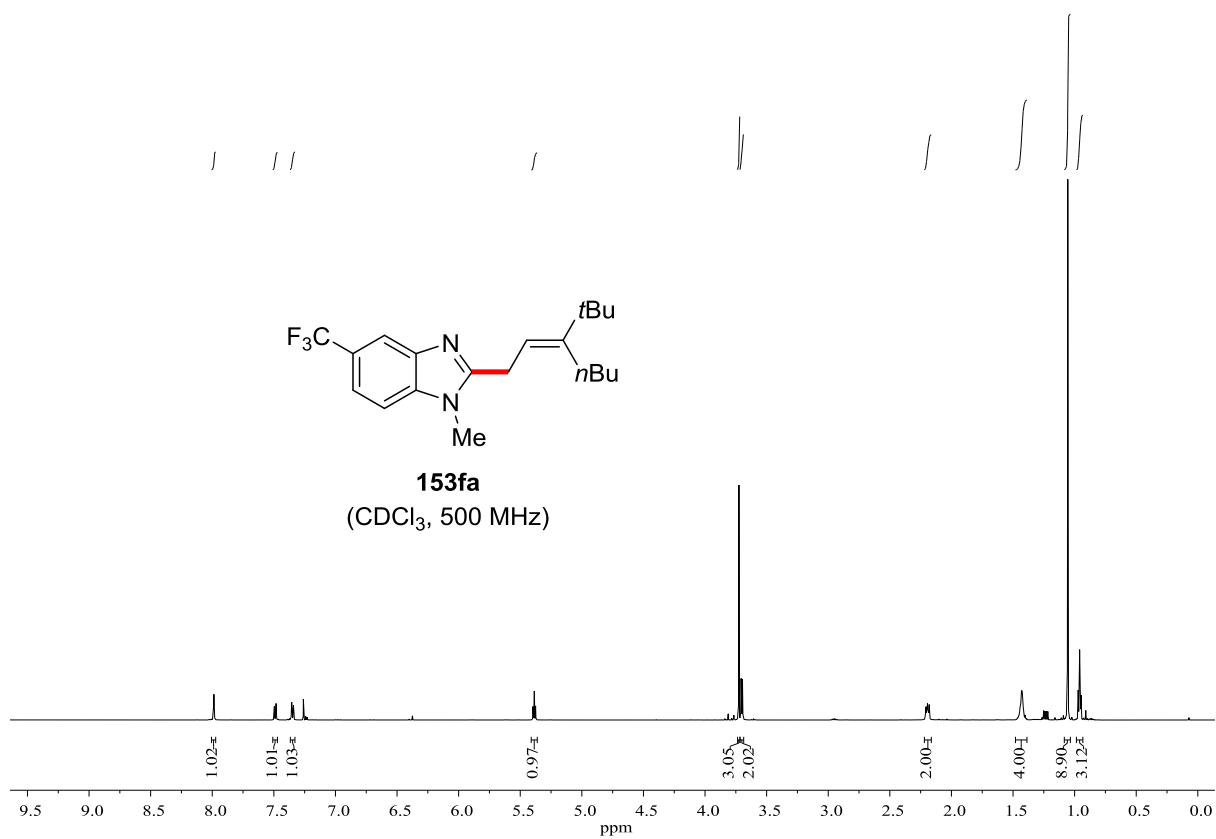


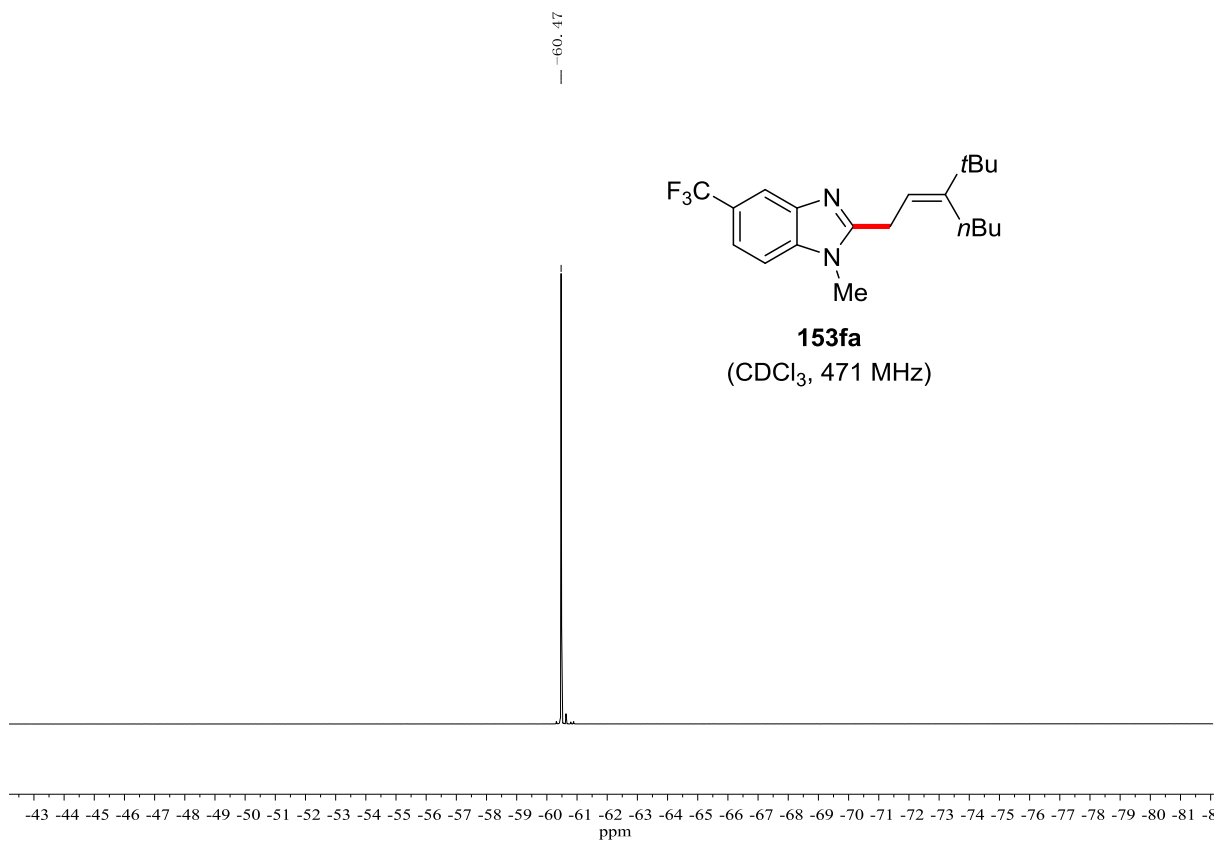
149.06
 138.04
 134.64
 133.67
 133.41
 131.85
 129.85
 127.41
 127.04
 126.83
 124.95
 122.79
 117.00
 115.13
 115.10
 115.07
 115.05
 111.87
 111.84
 111.81
 111.78
 77.41
 77.16
 76.91

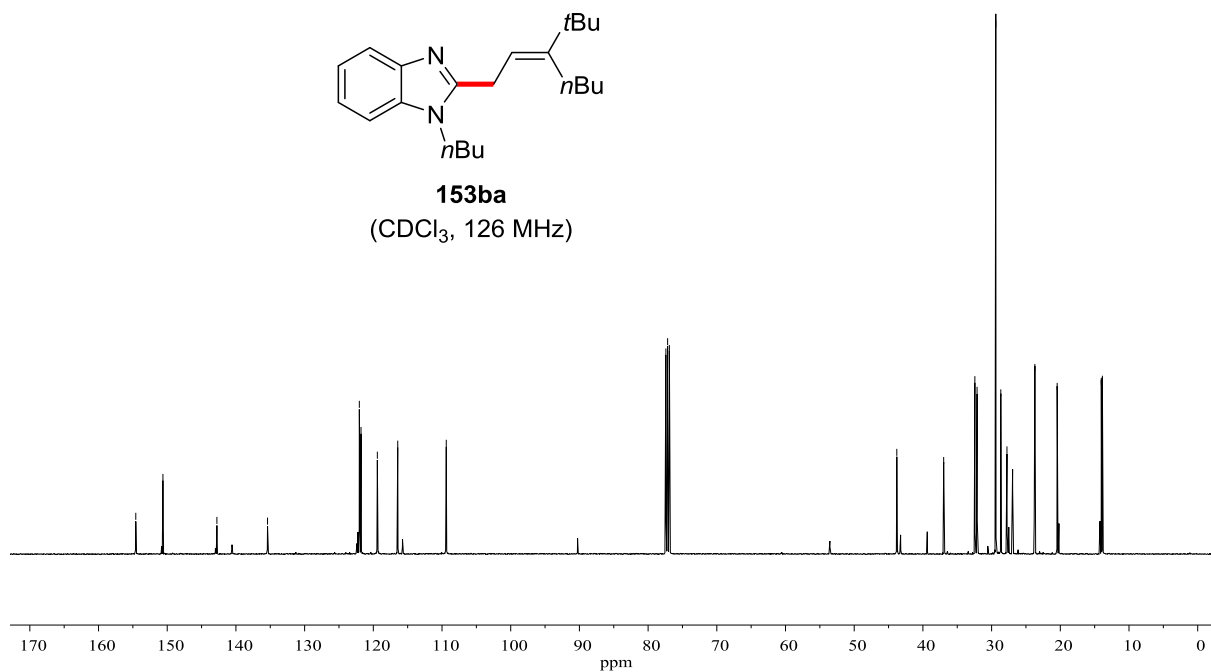
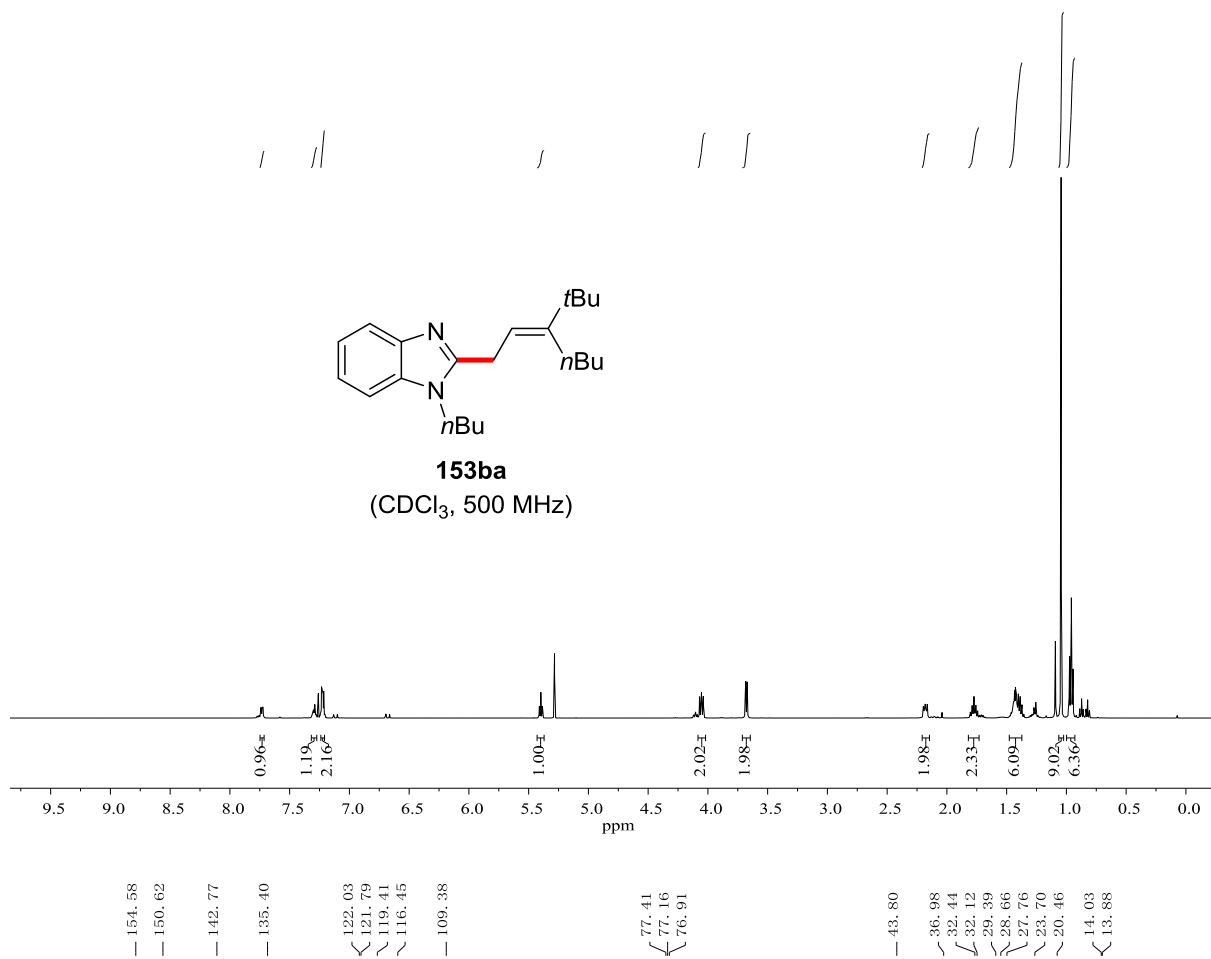


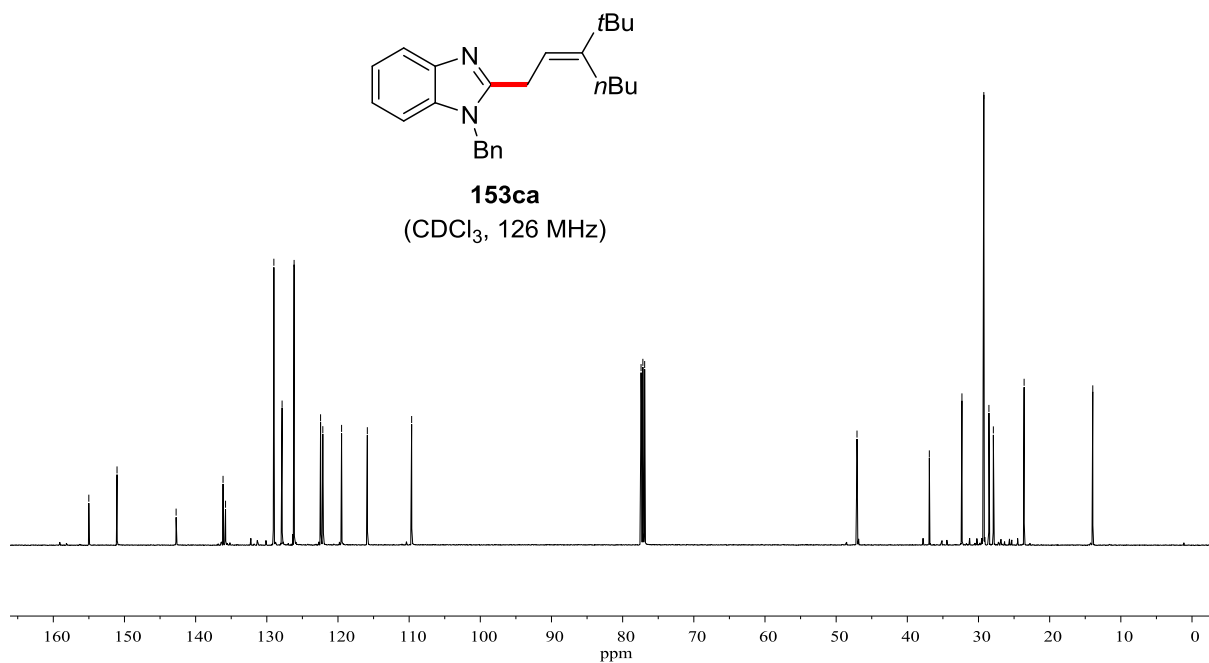
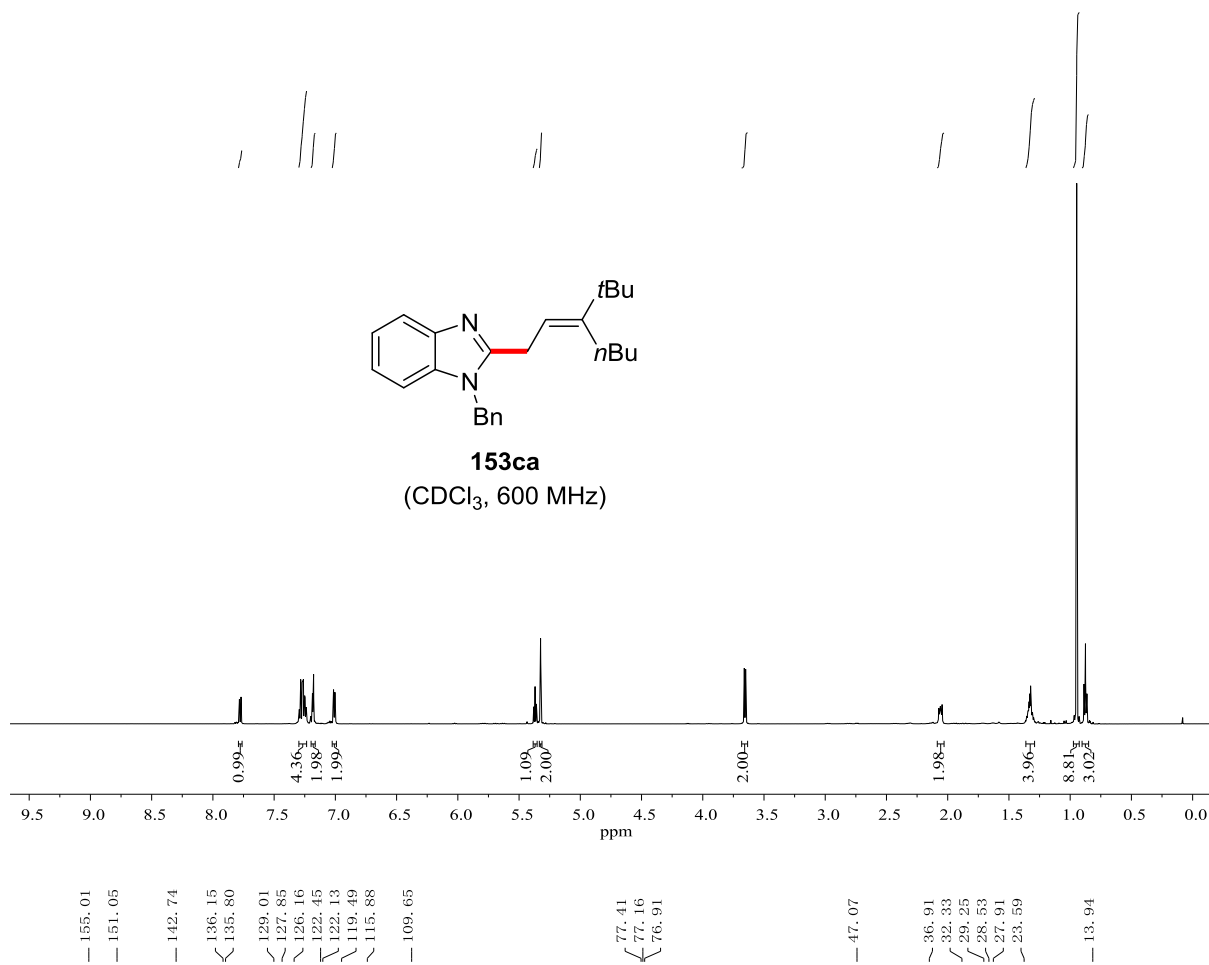


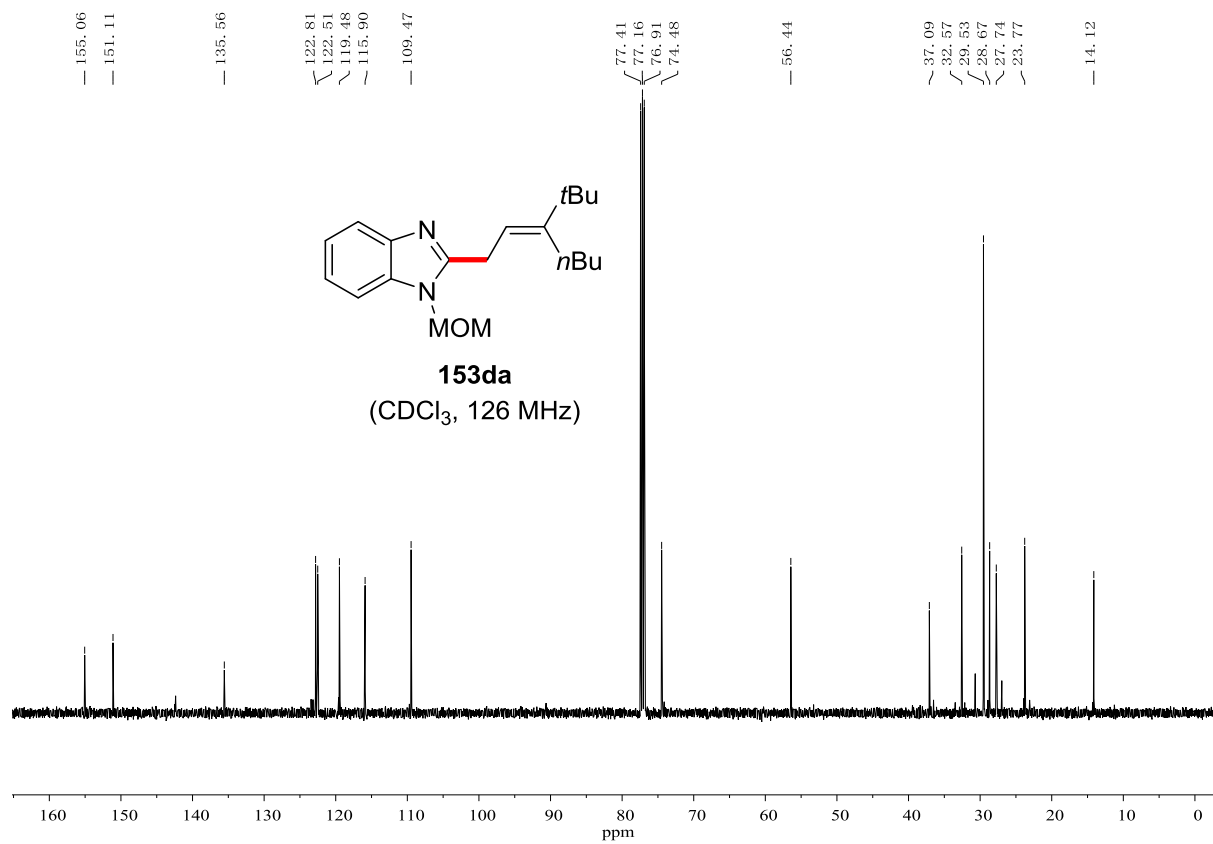
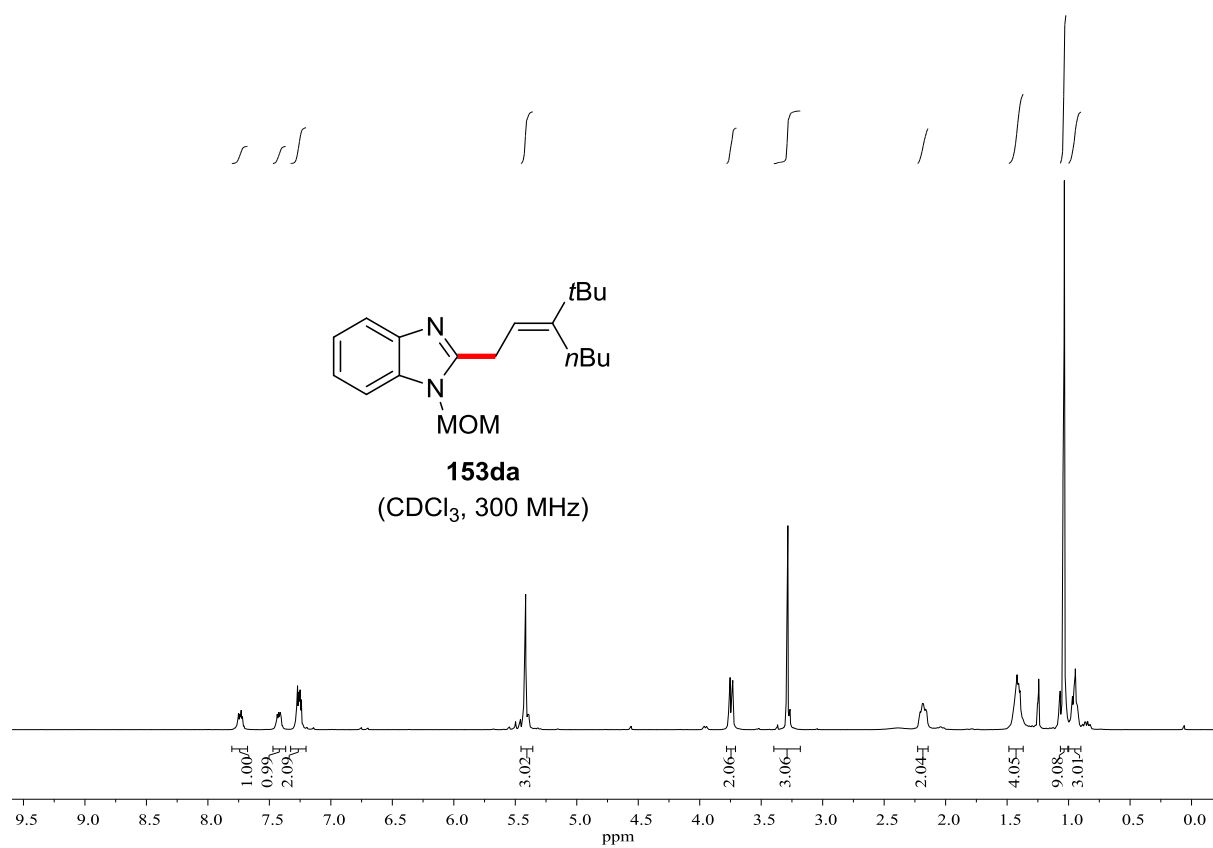


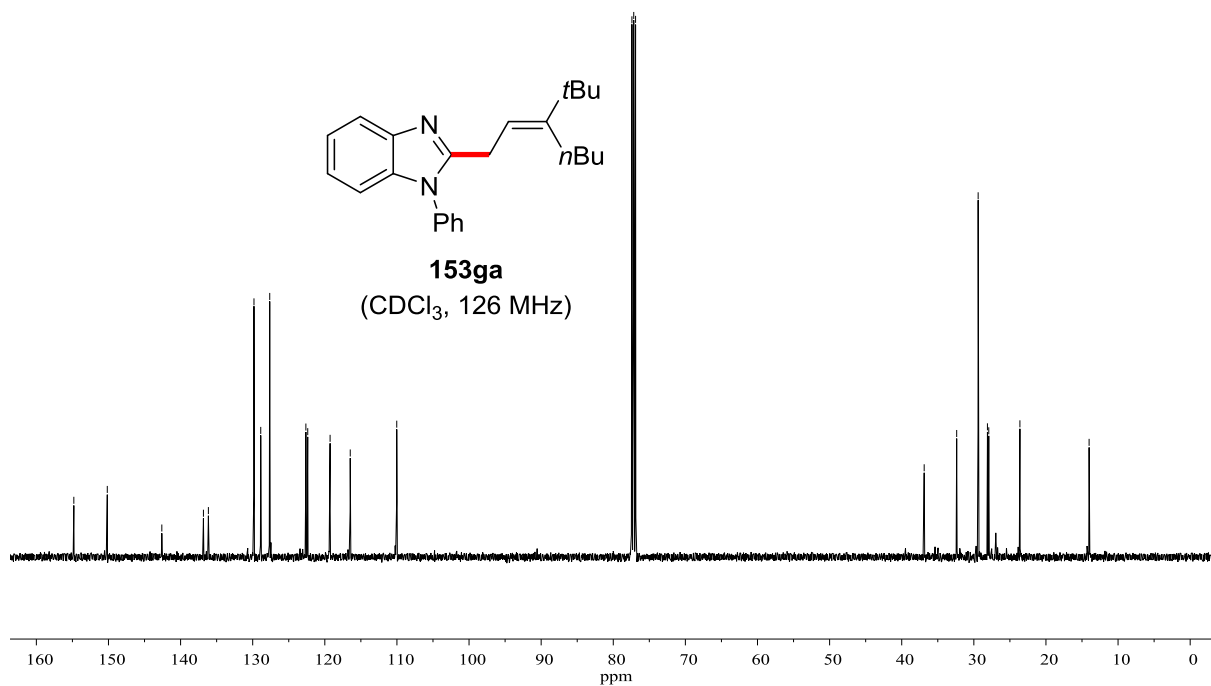
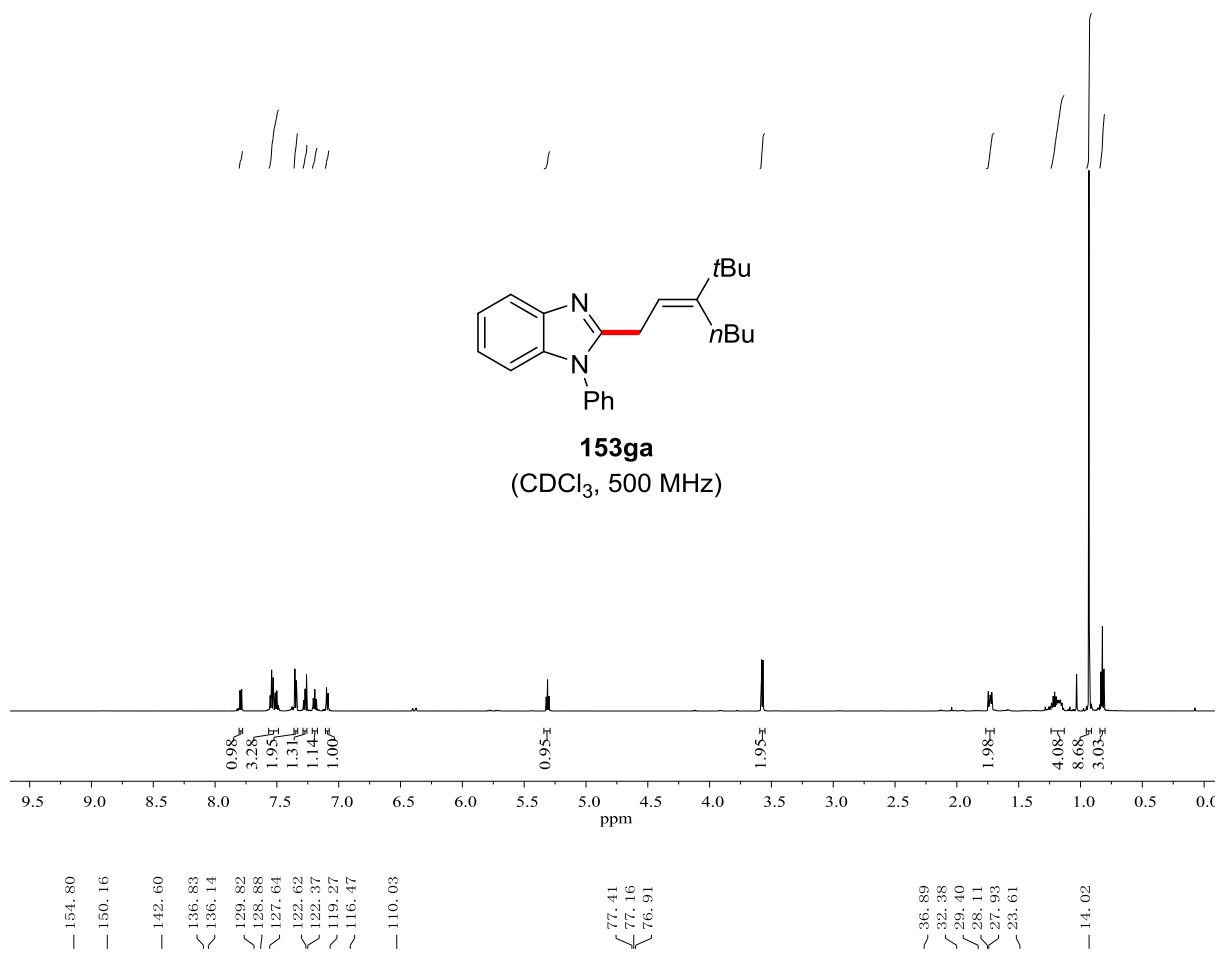


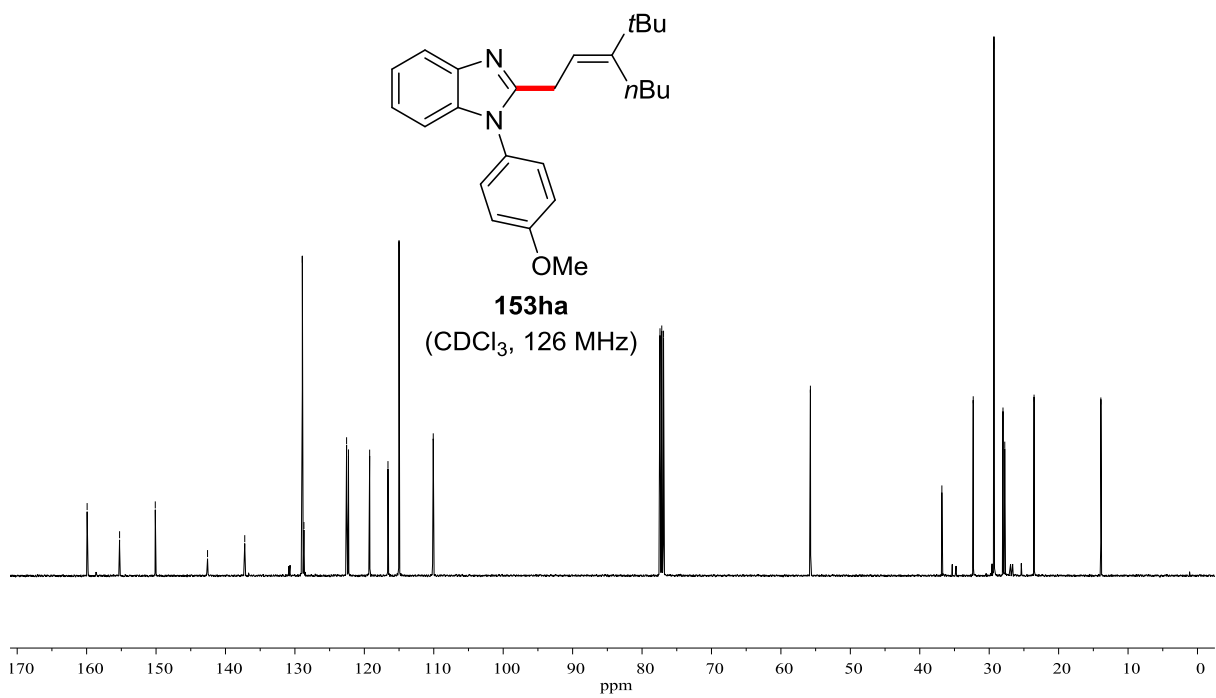
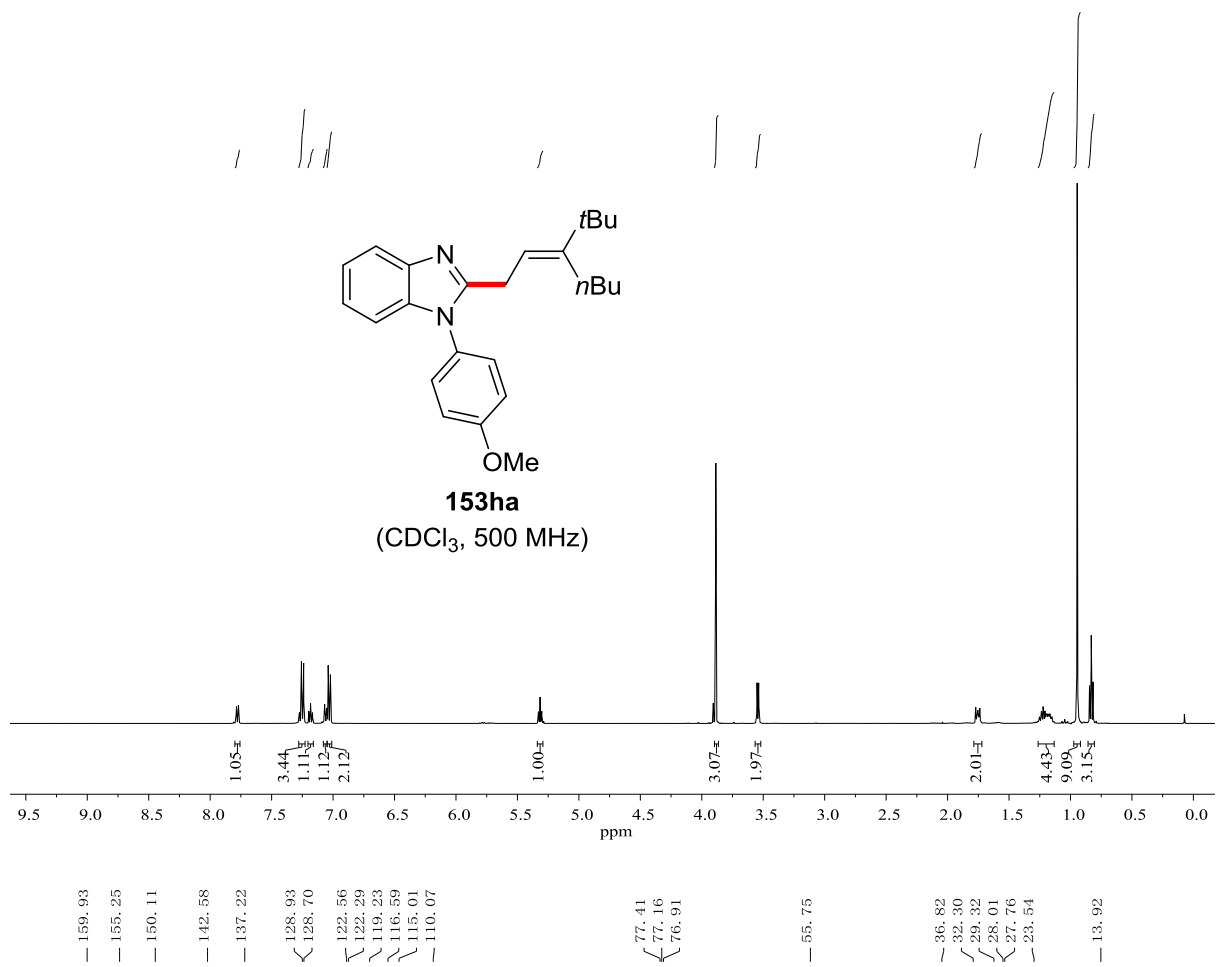


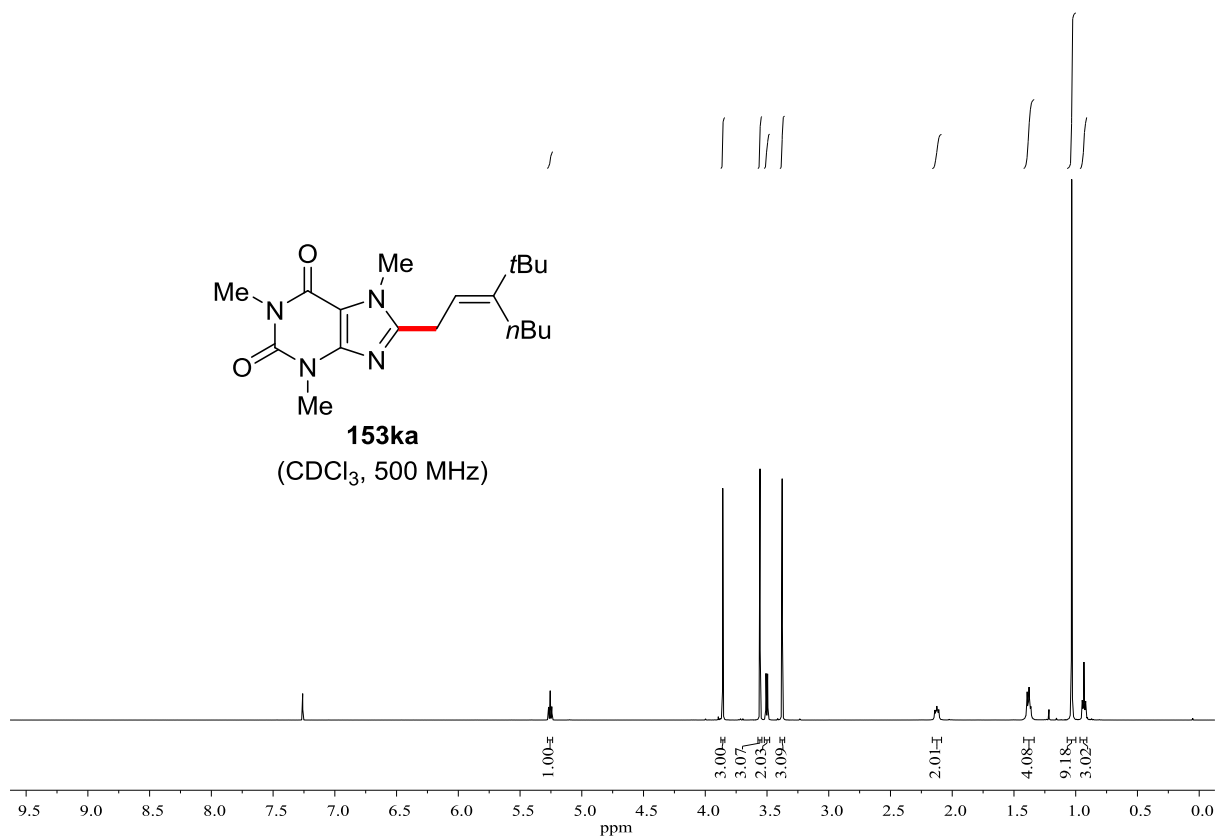










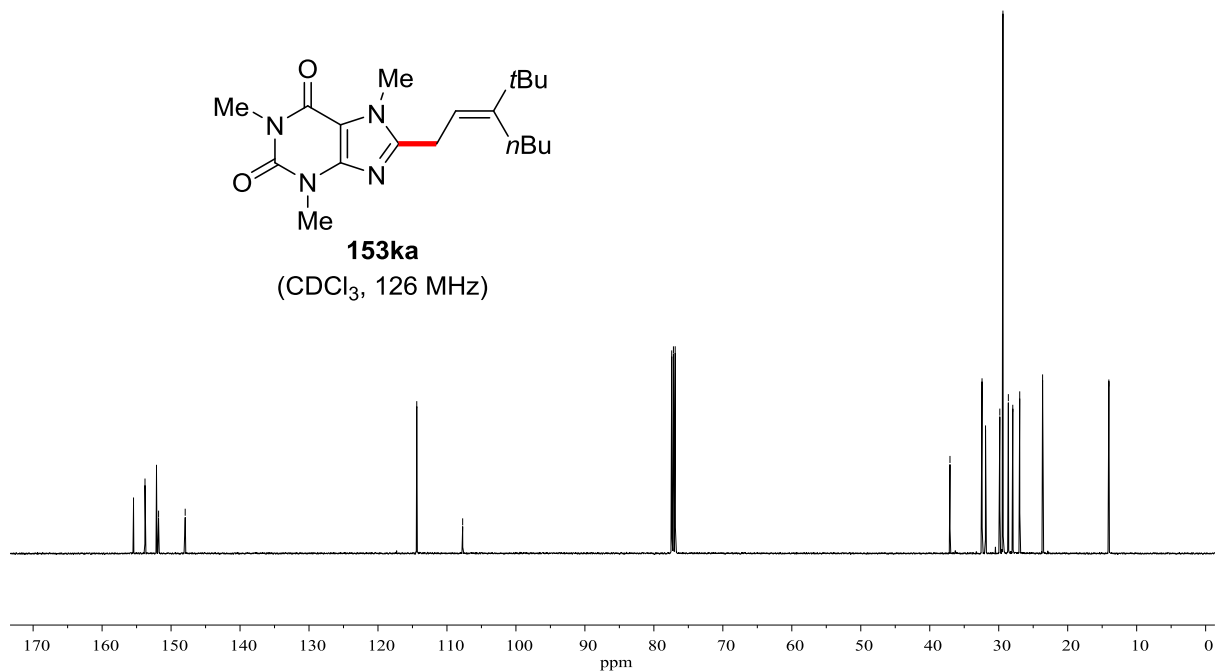


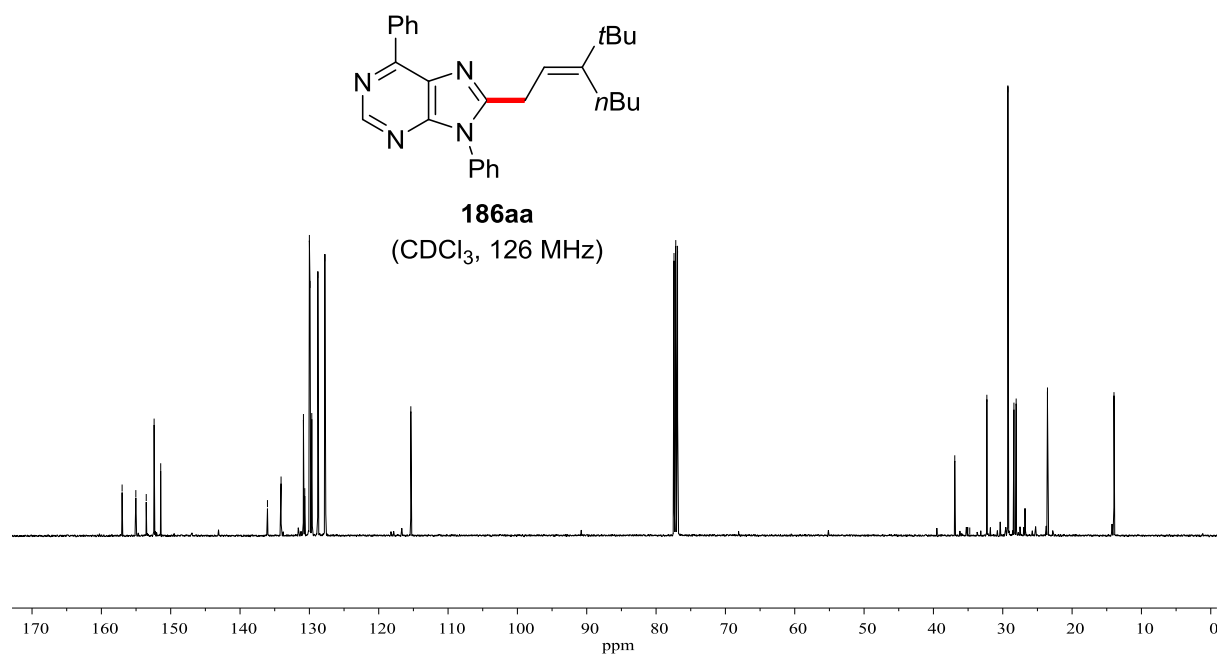
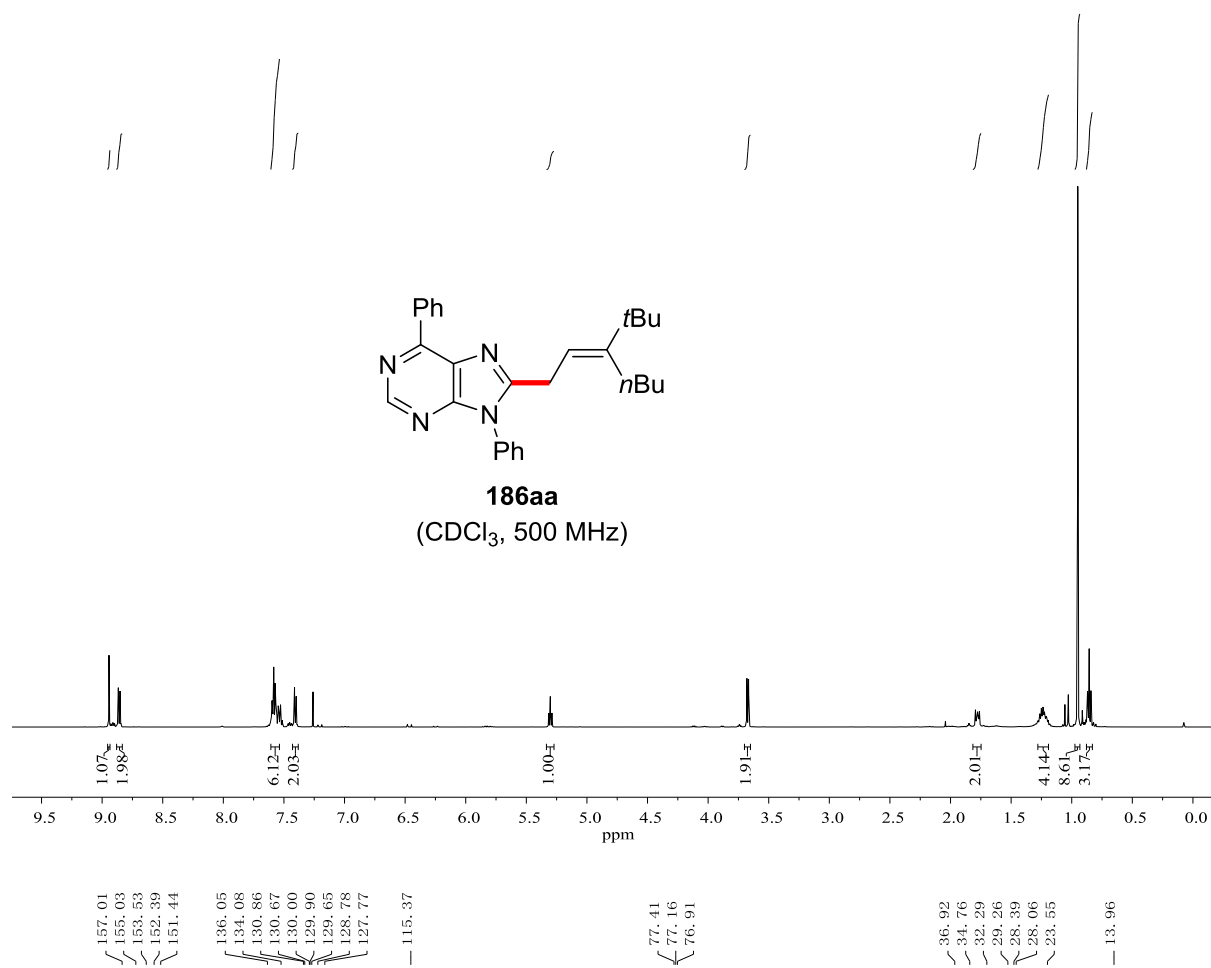
155.44
 153.78
 152.11
 151.81
 147.95

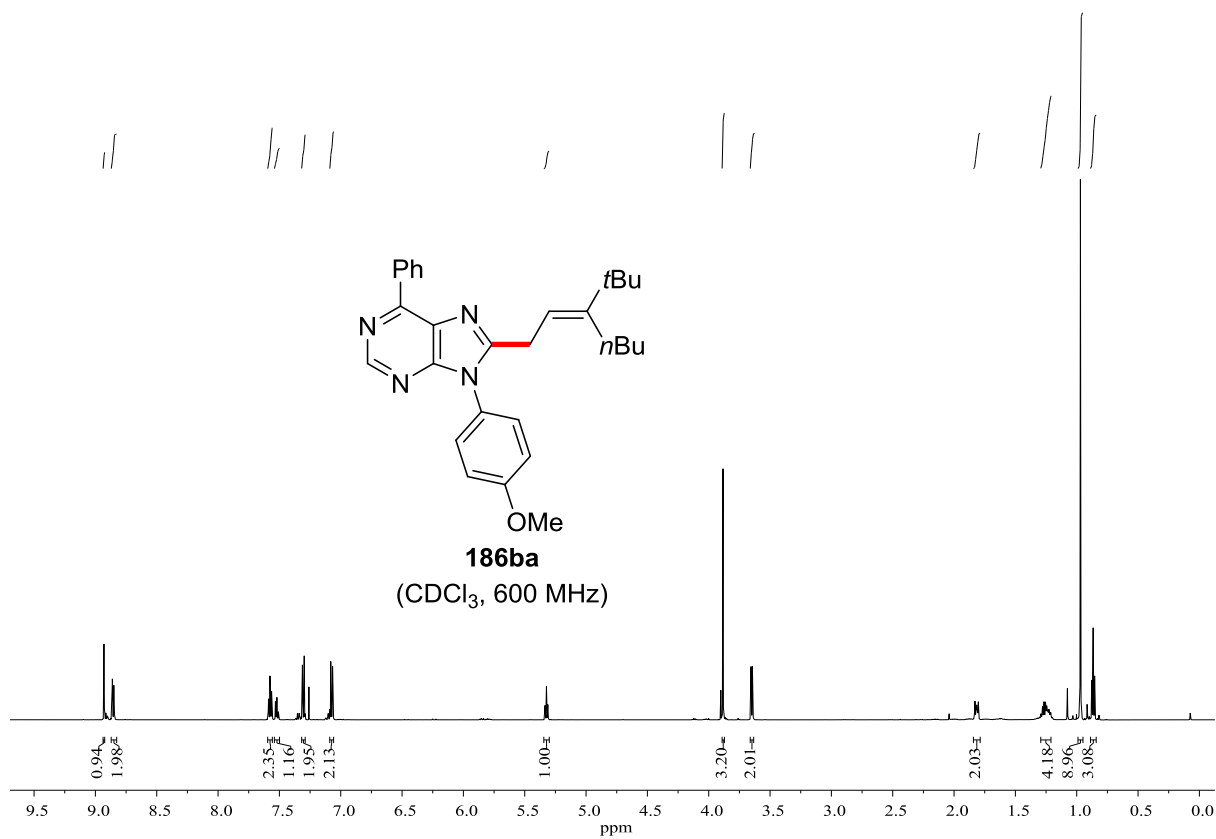
114.38
 107.72

77.41
 77.16
 76.91

37.07
 32.42
 31.91
 29.84
 29.39
 28.60
 27.96
 26.96
 23.64
 14.03







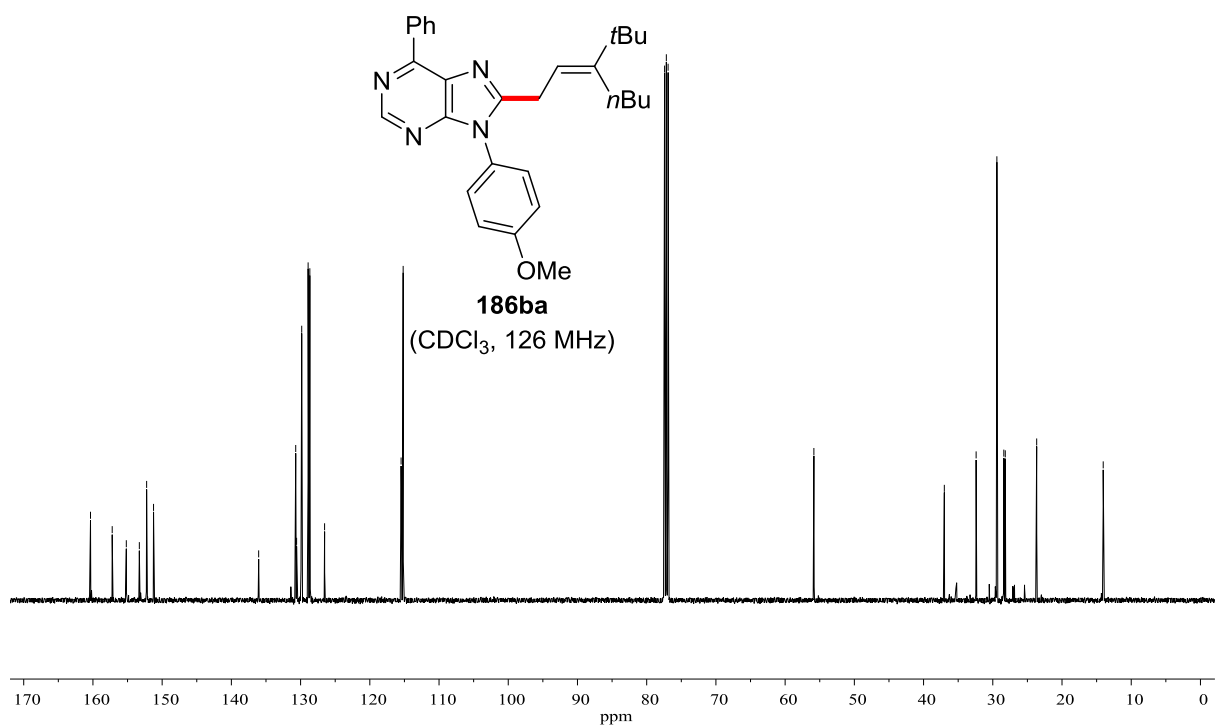
160.35
157.22
155.18
153.29
152.24
151.24

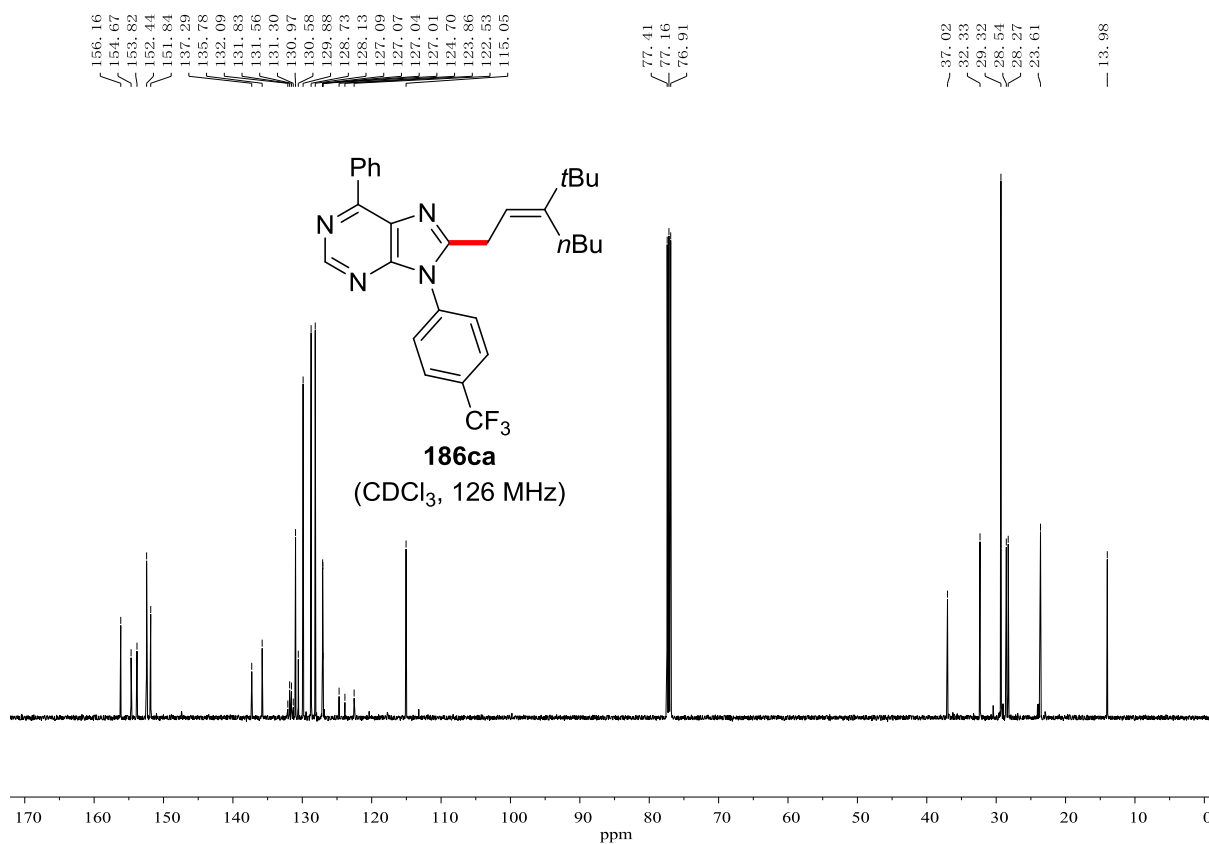
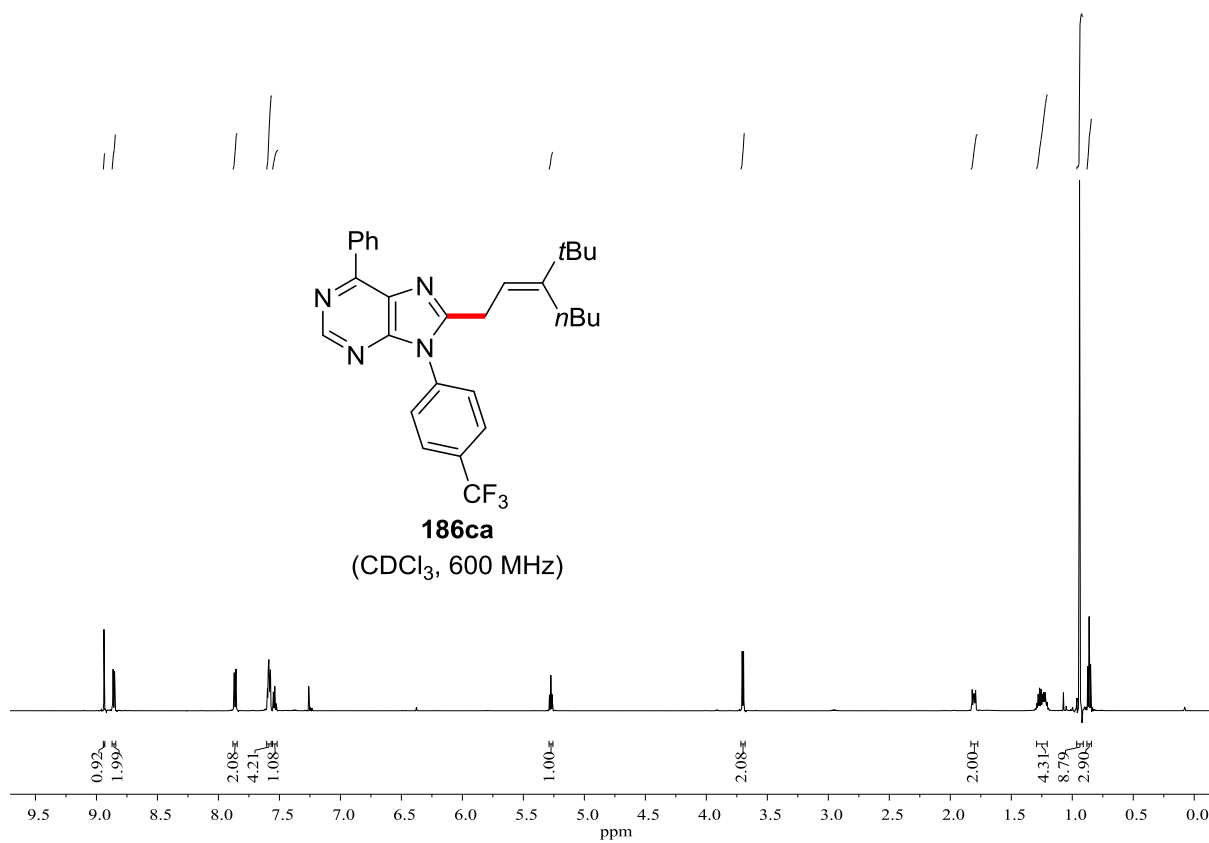
136.06
130.70
130.58
129.84
128.91
128.67
126.53
115.48
115.18

77.41
77.16
76.91

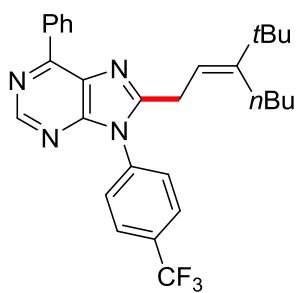
55.85

37.00
32.41
29.41
28.41
28.20
23.66
14.05



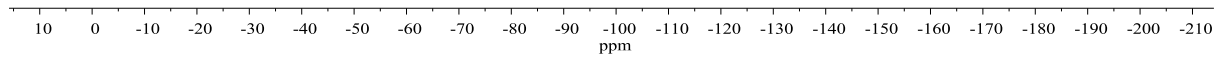


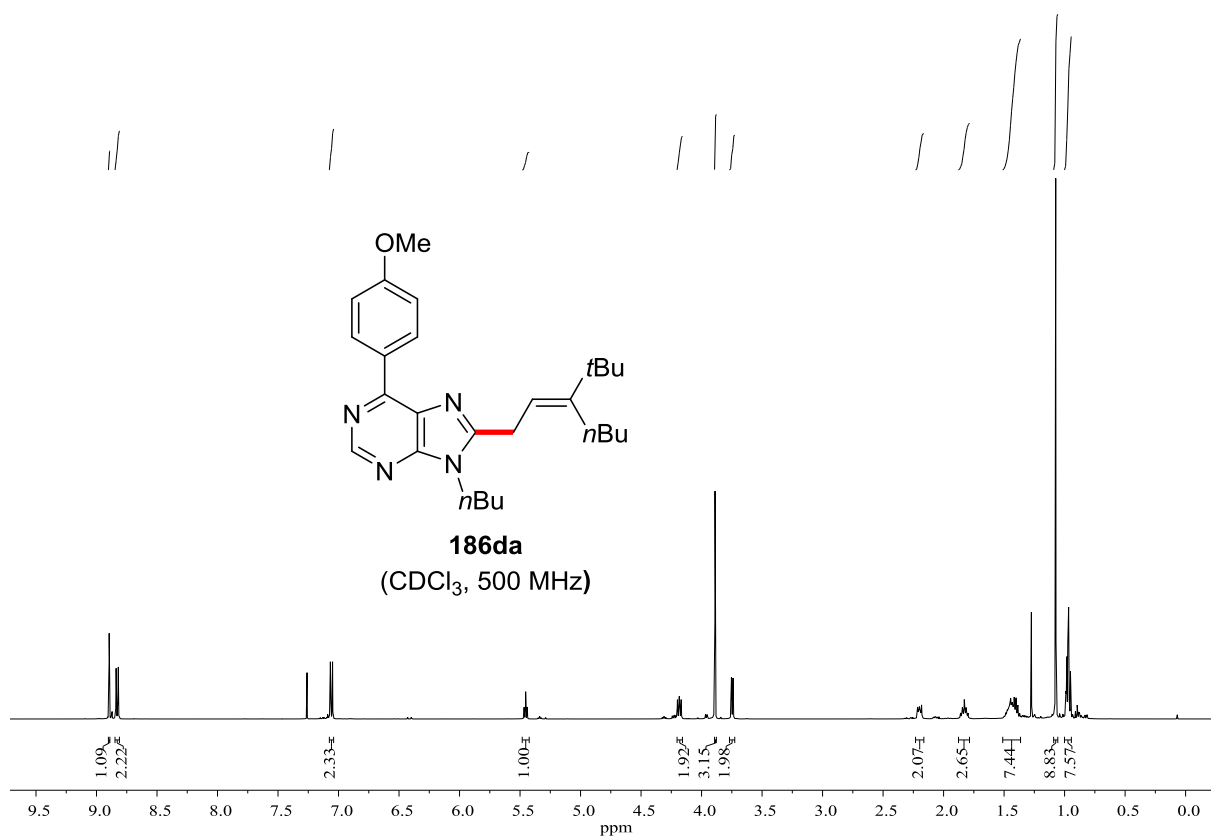
-62.84



186ca

(CDCl₃, 471 MHz)





161.79
156.25
153.95
152.73
151.72
151.51

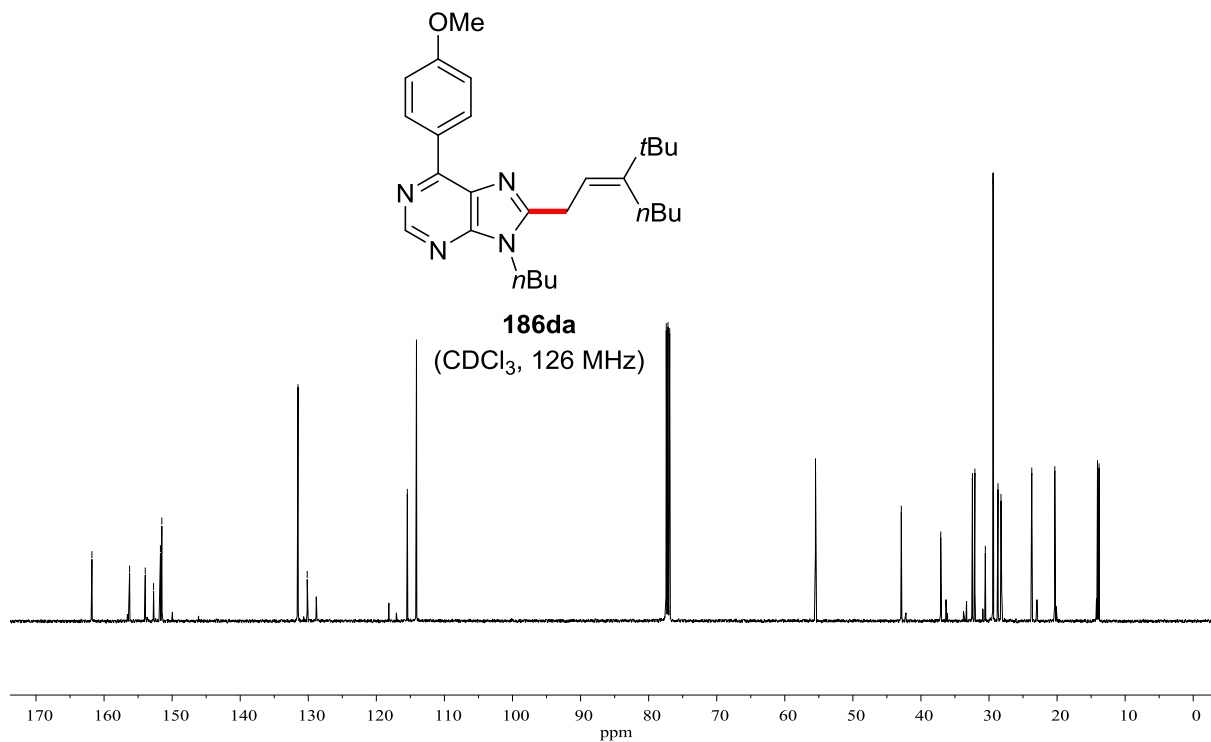
131.51
130.16

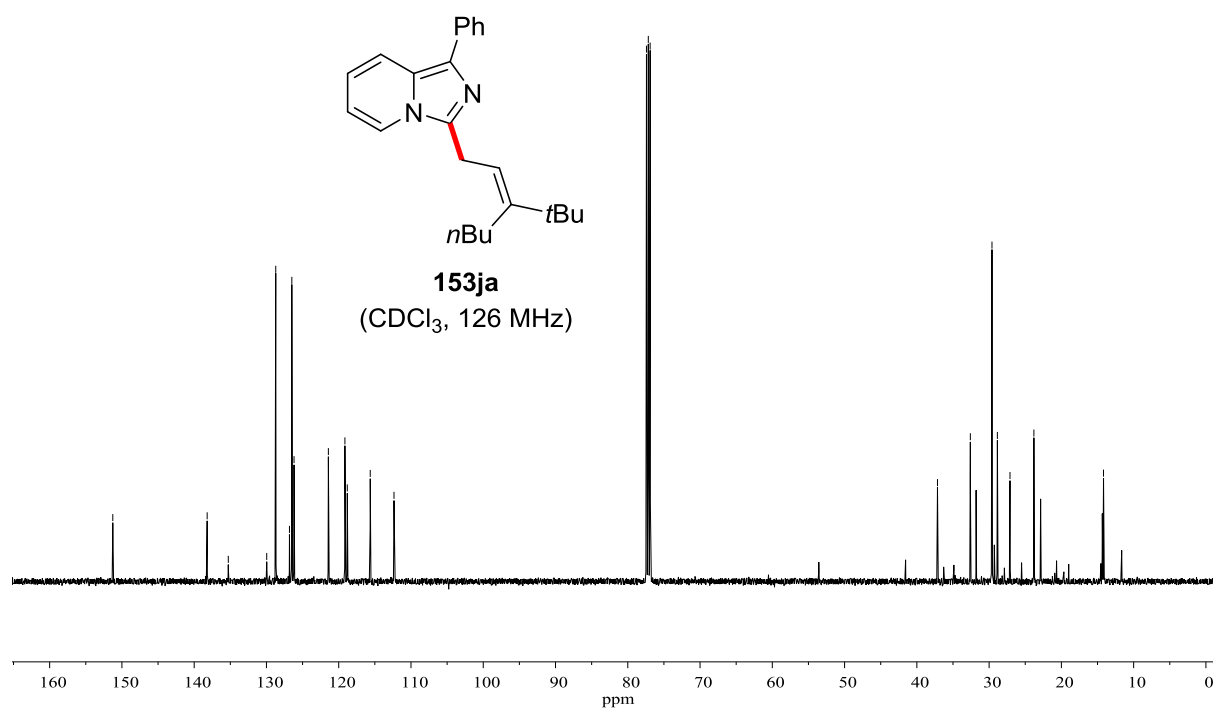
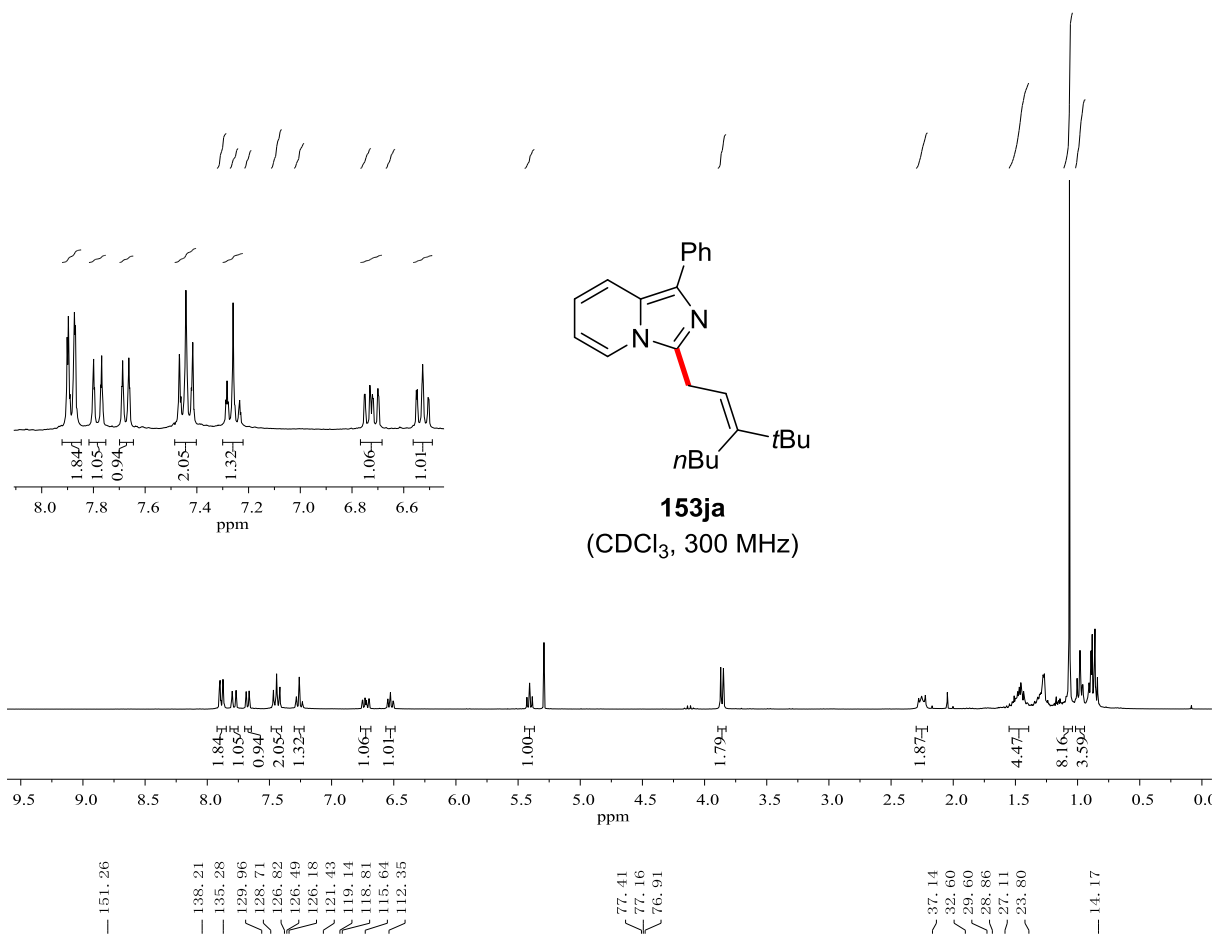
115.45
114.11

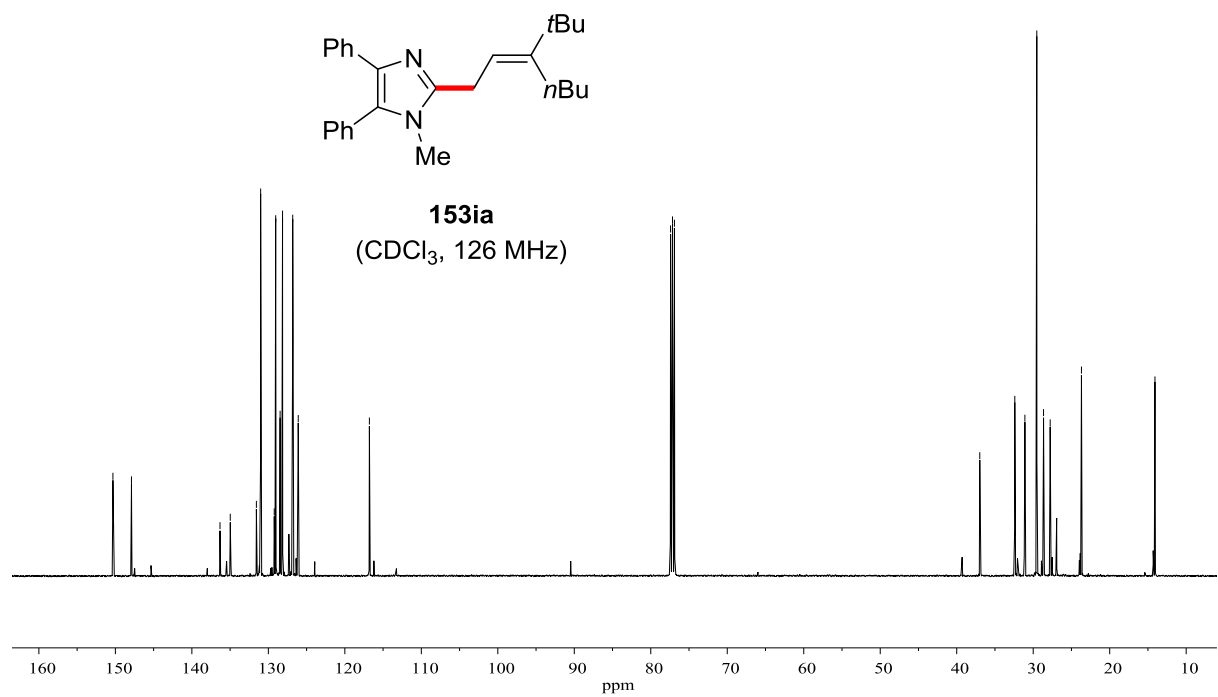
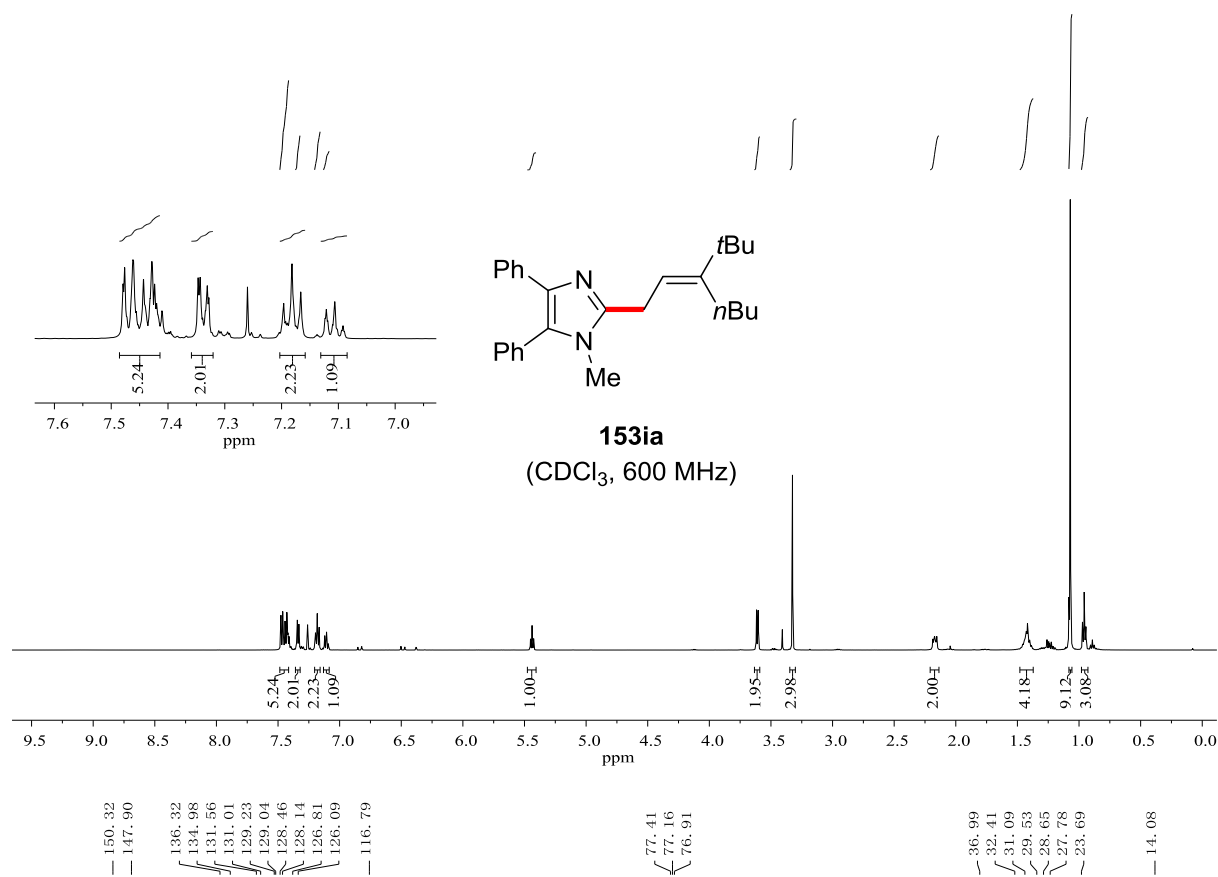
77.41
77.16
76.91

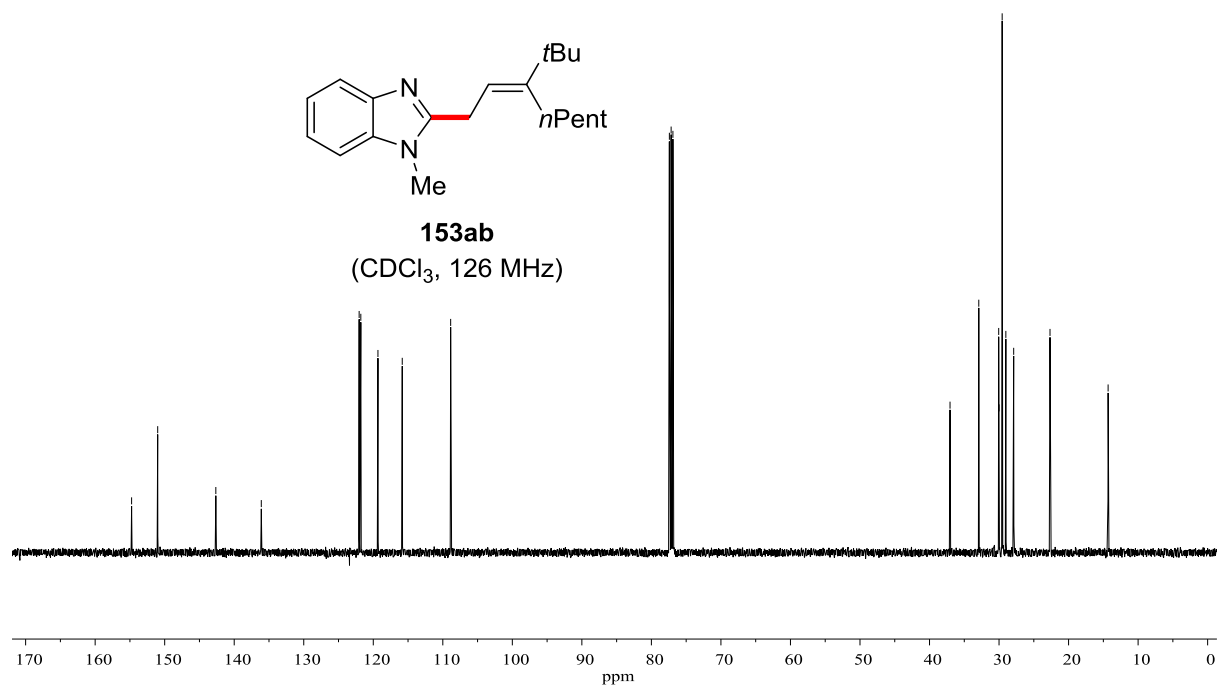
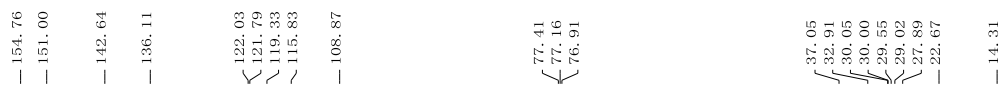
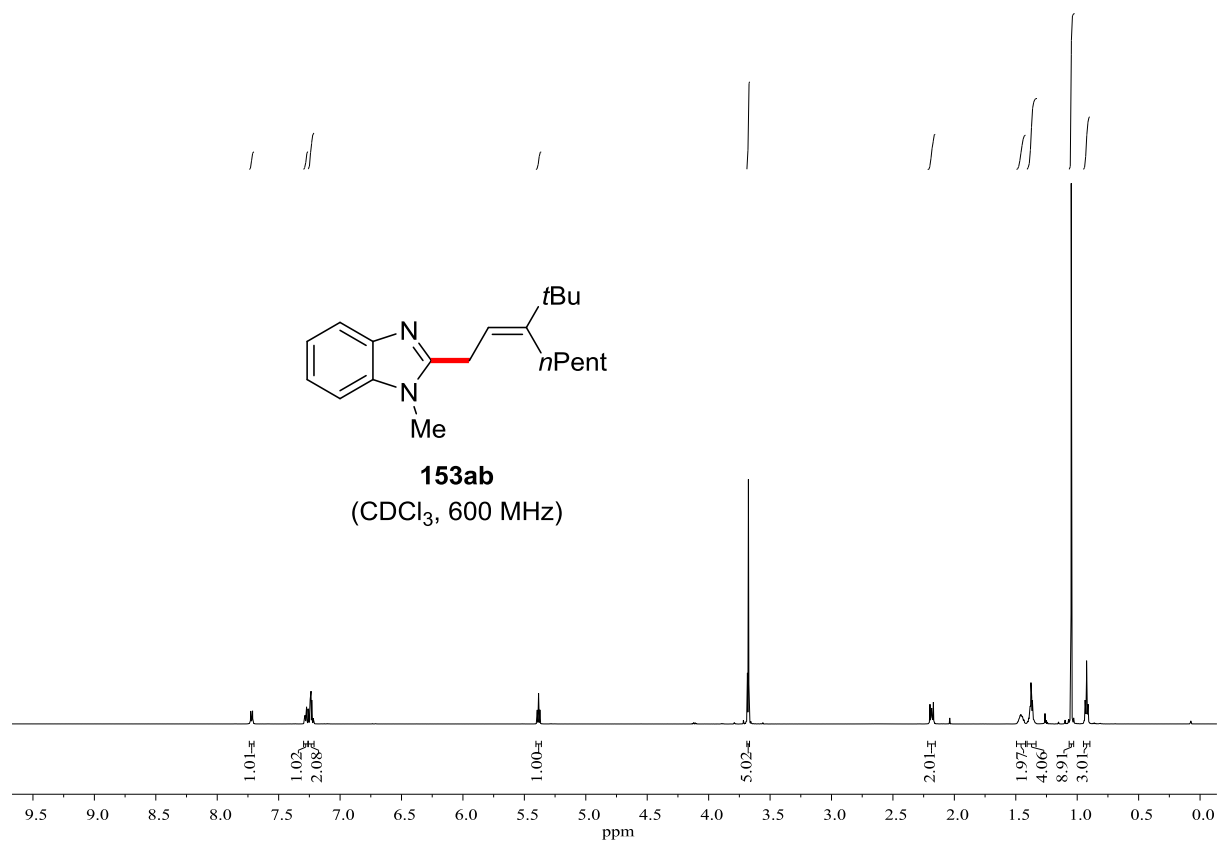
55.49

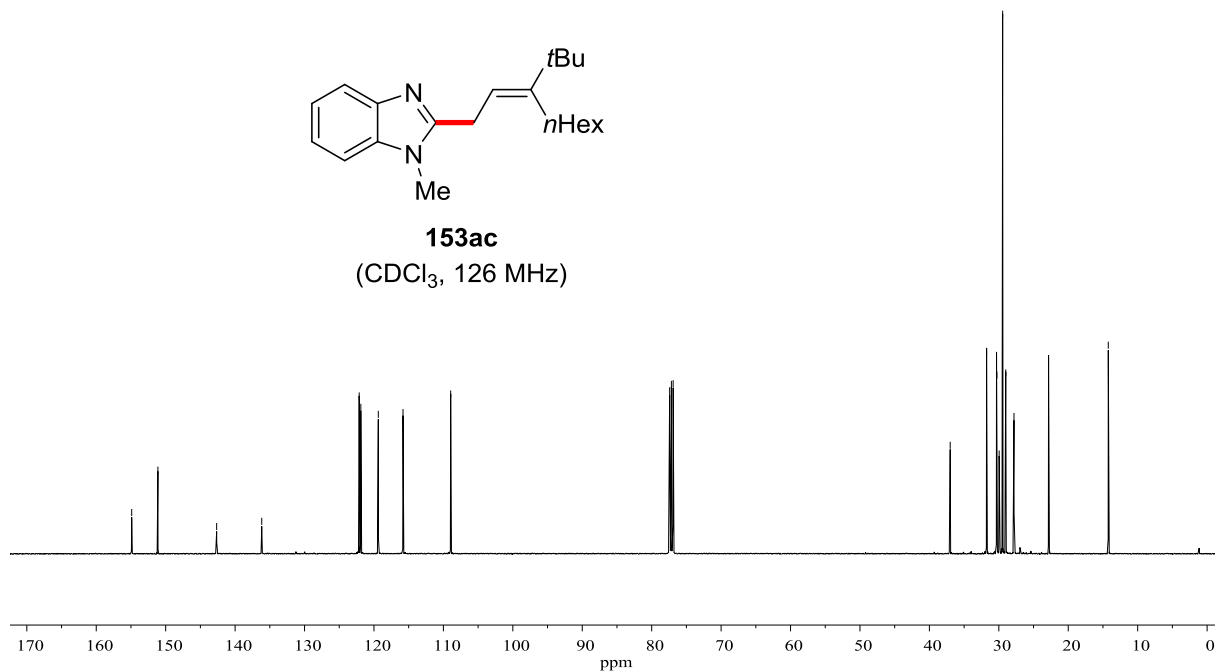
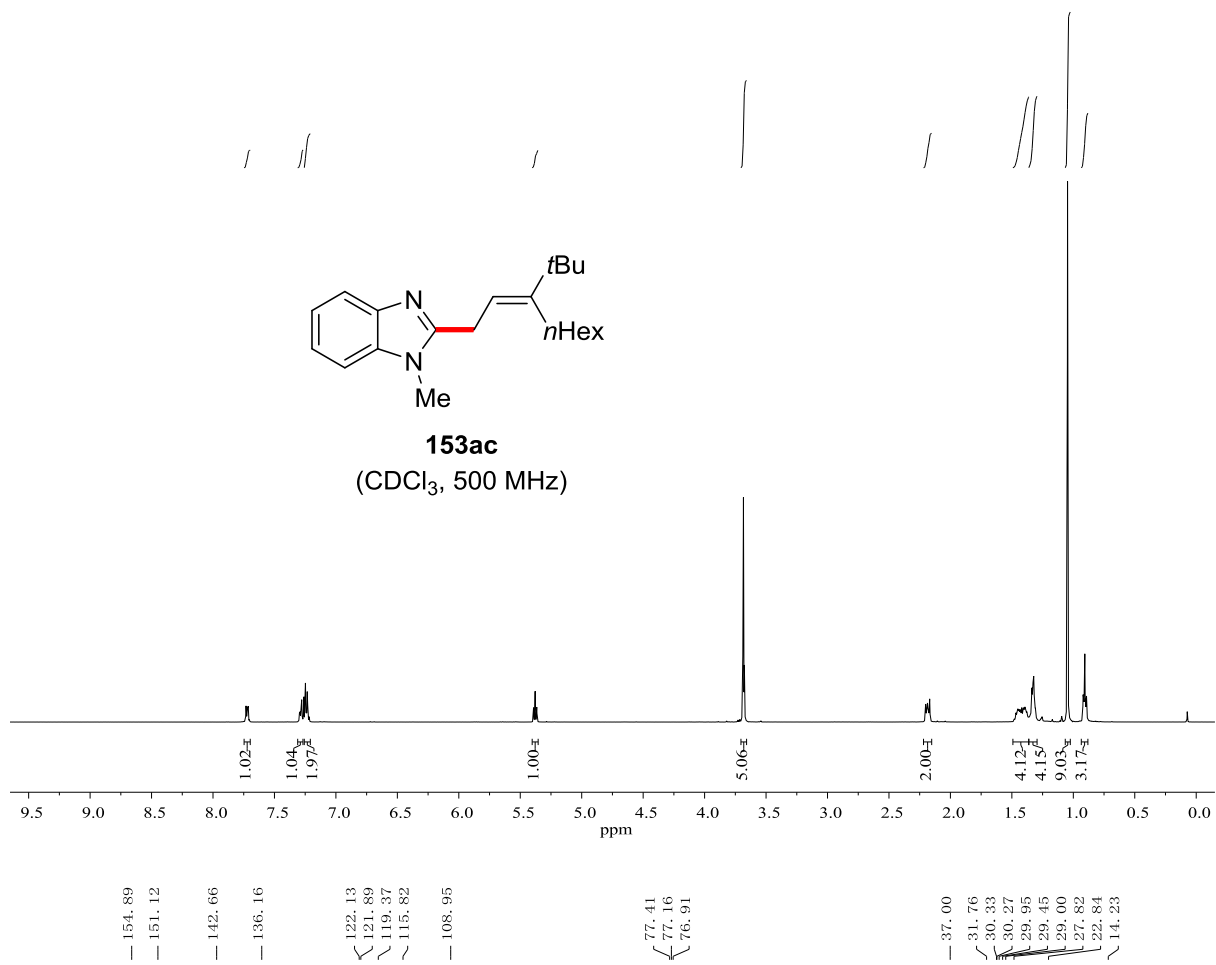
42.88
37.09
32.44
32.08
30.54
29.40
28.68
28.24
23.72
20.34
14.06
13.84

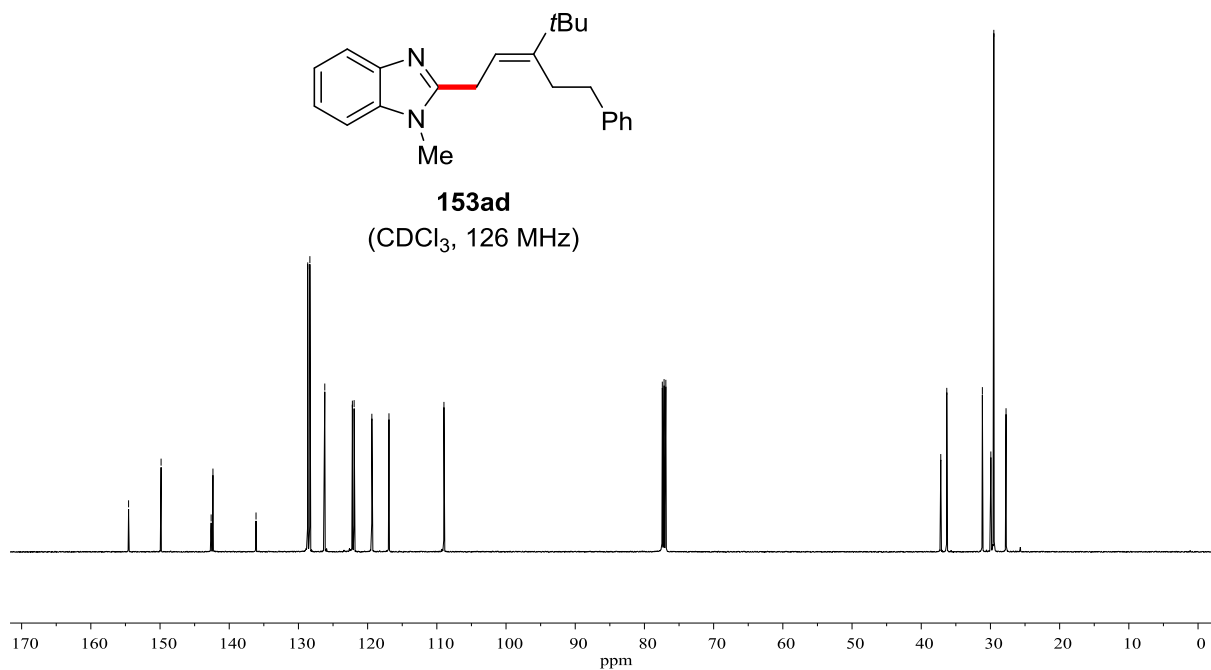
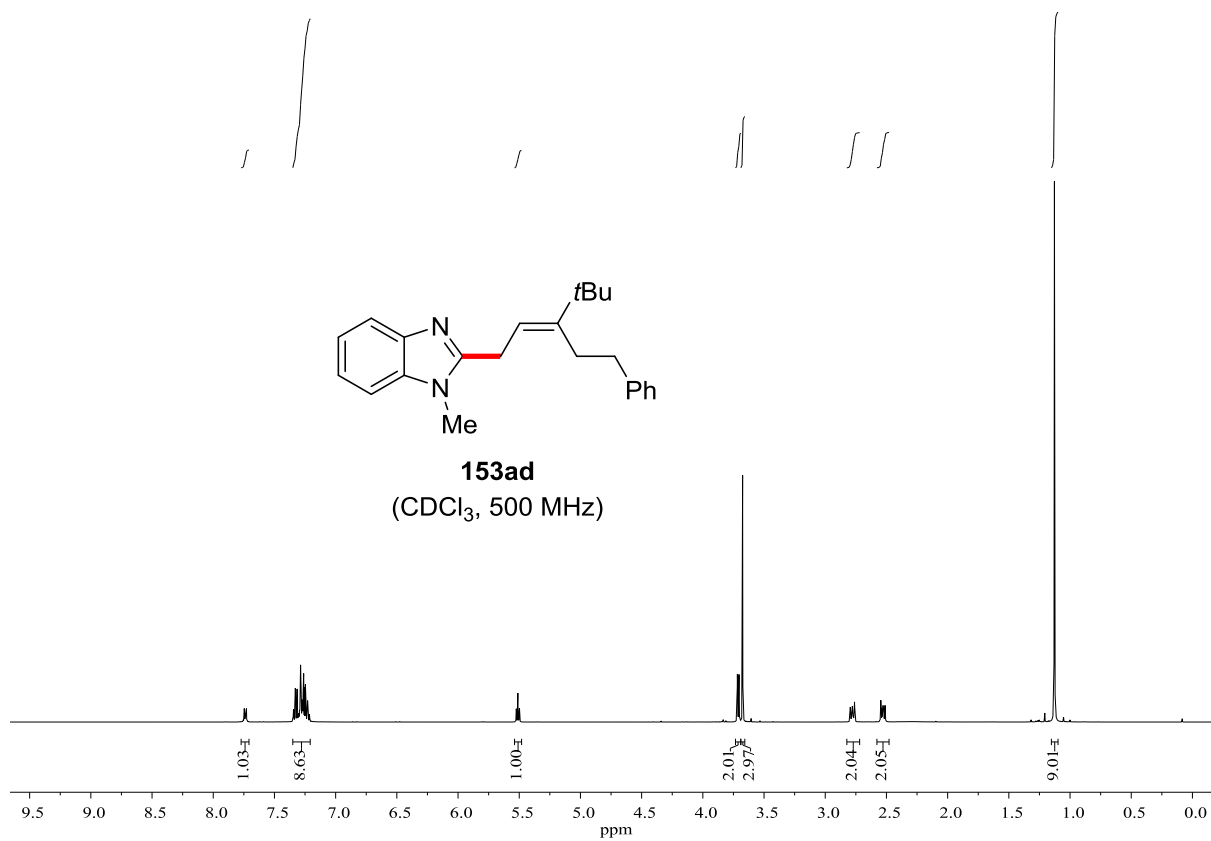


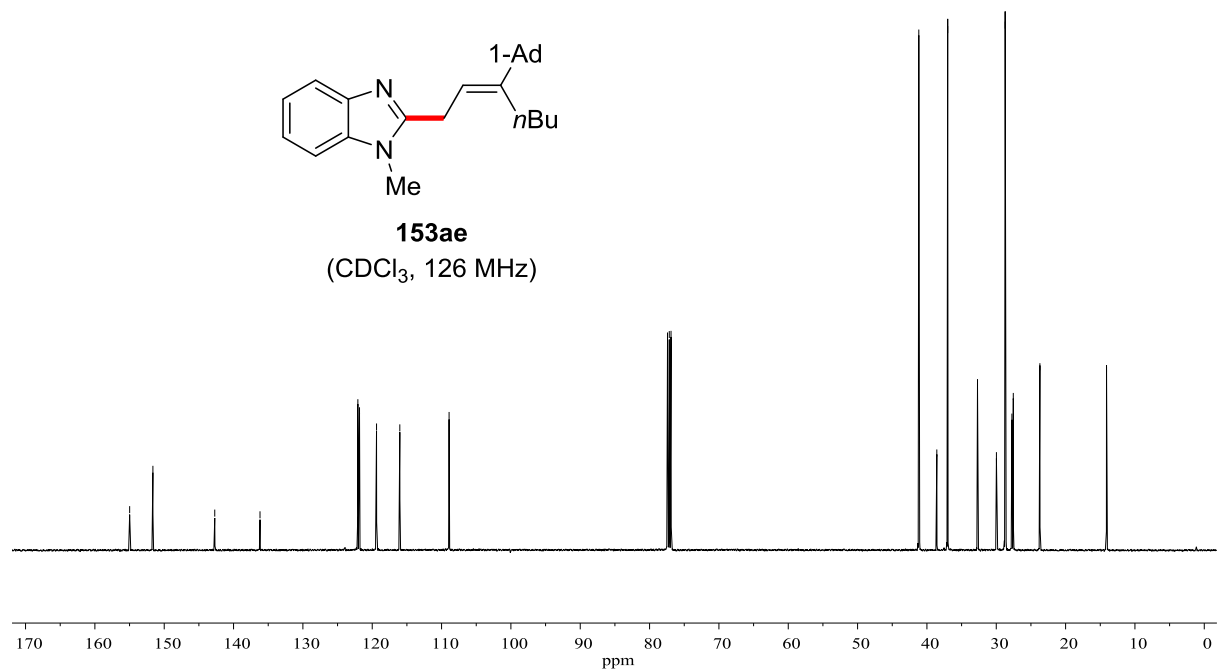
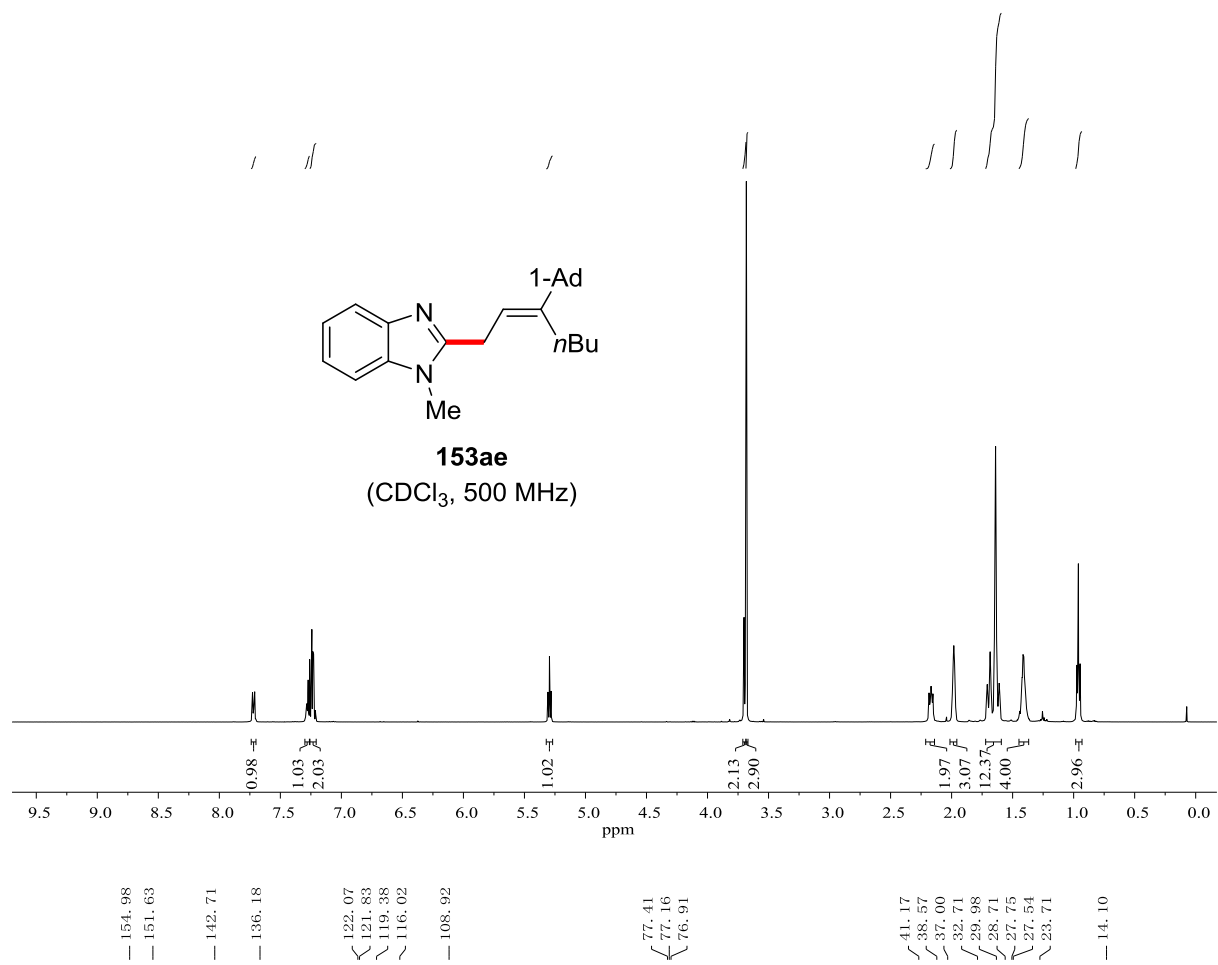


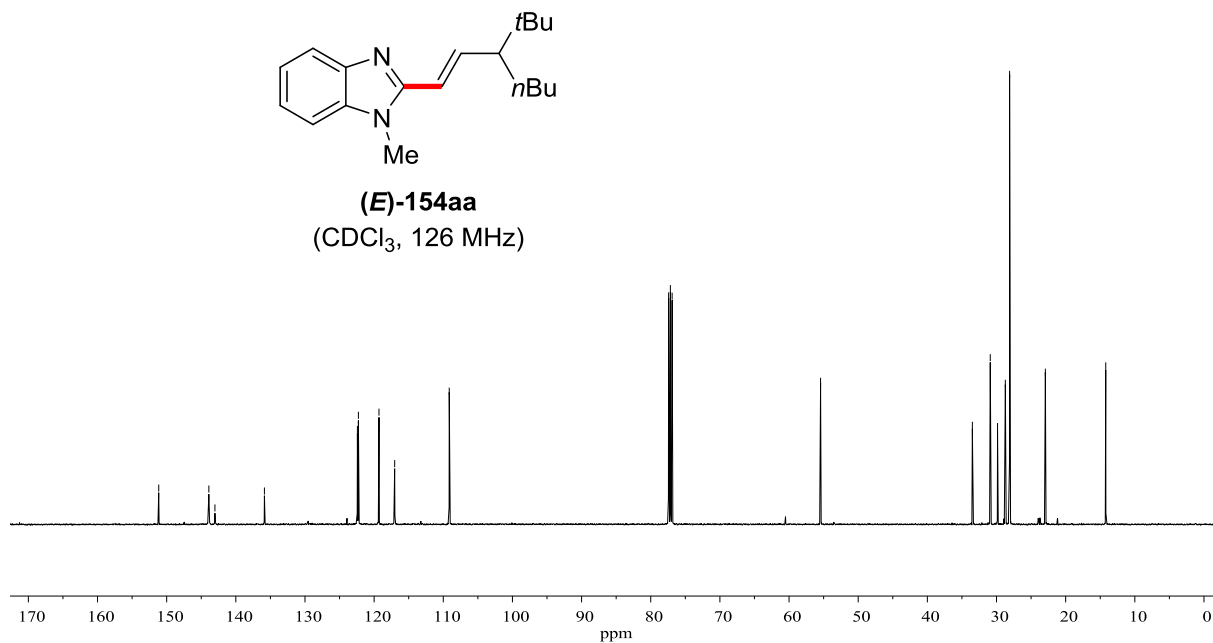
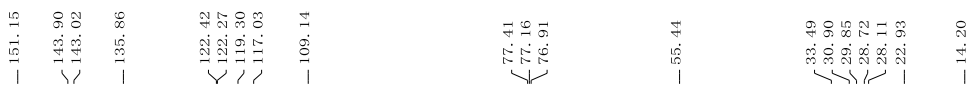
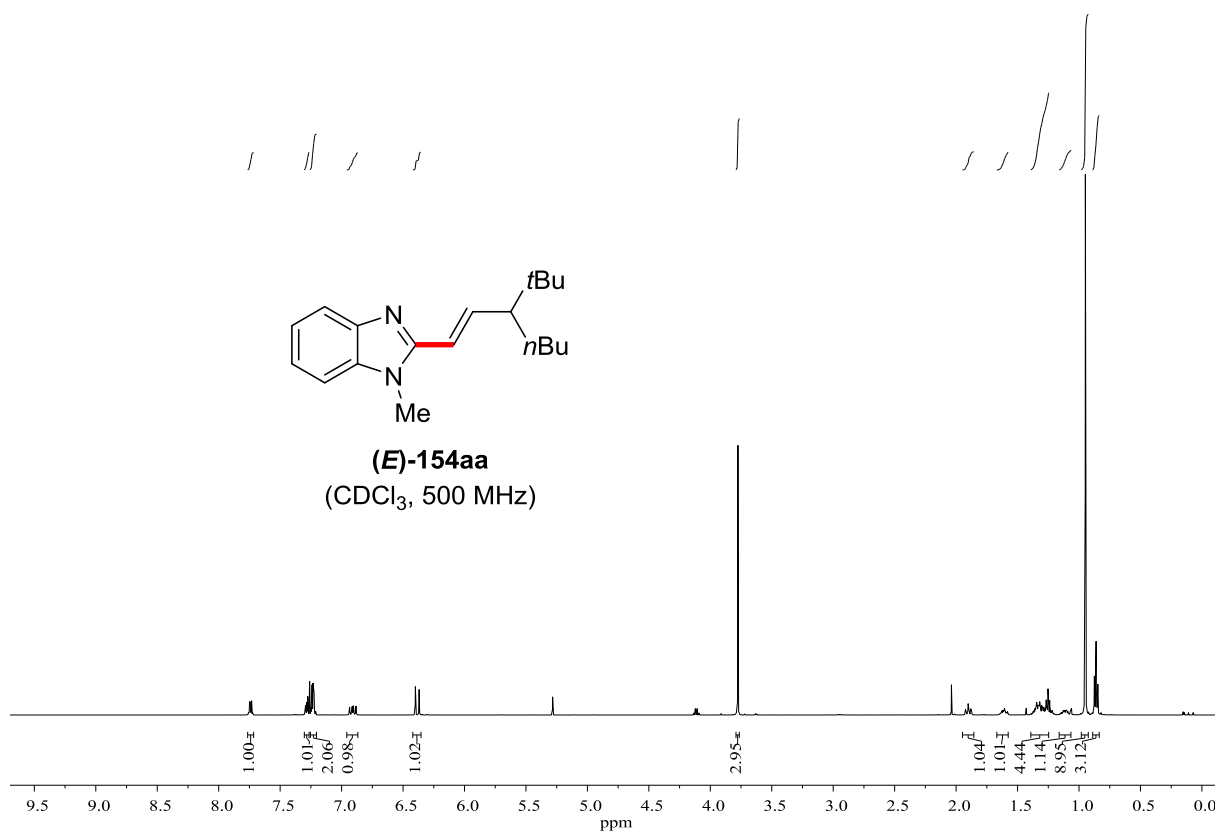


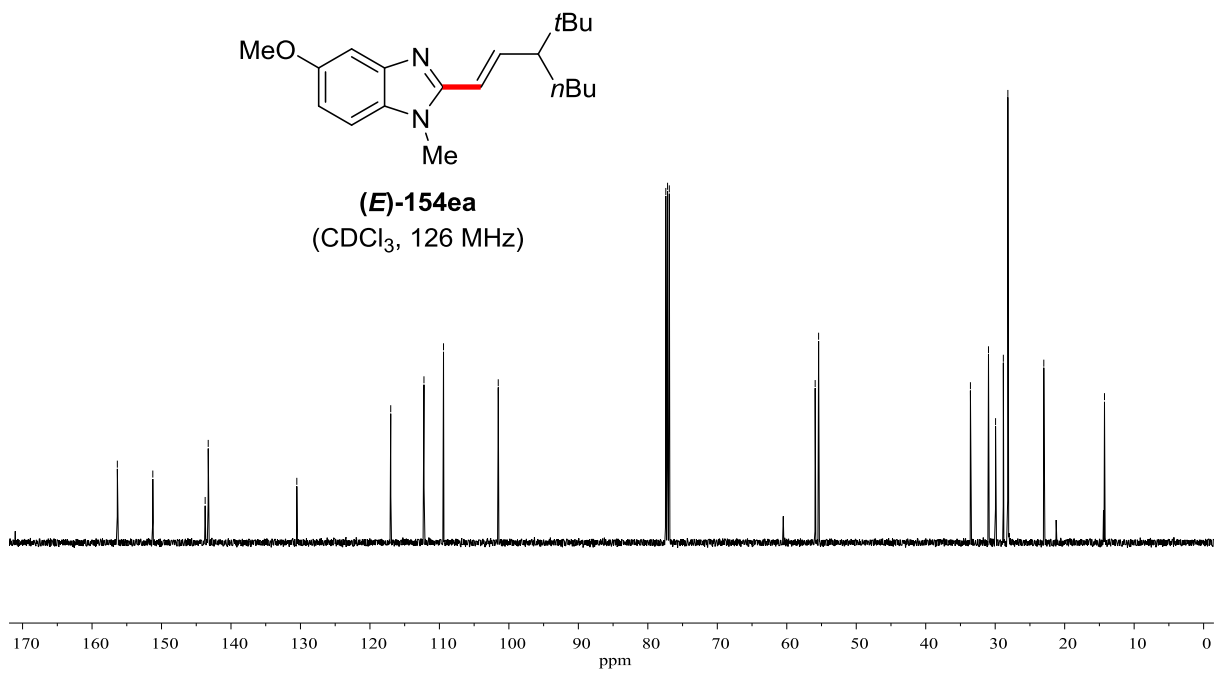
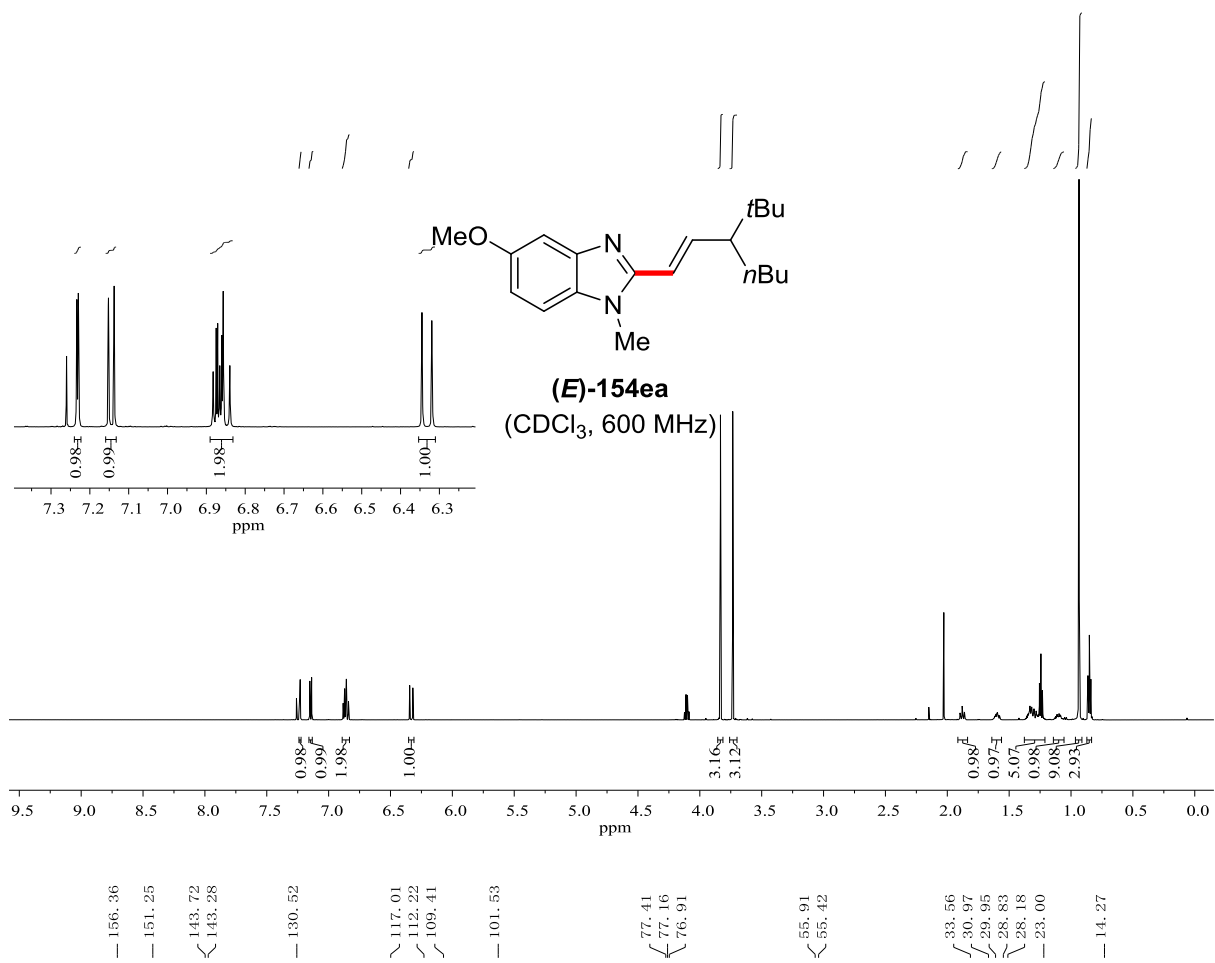


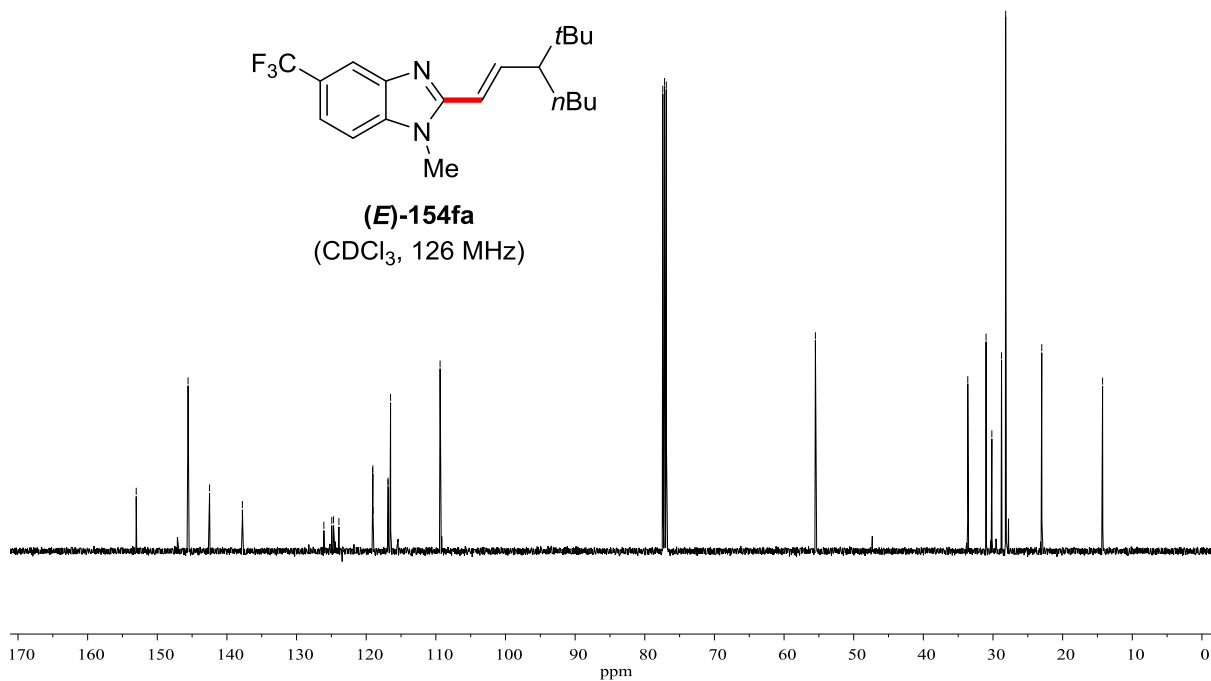
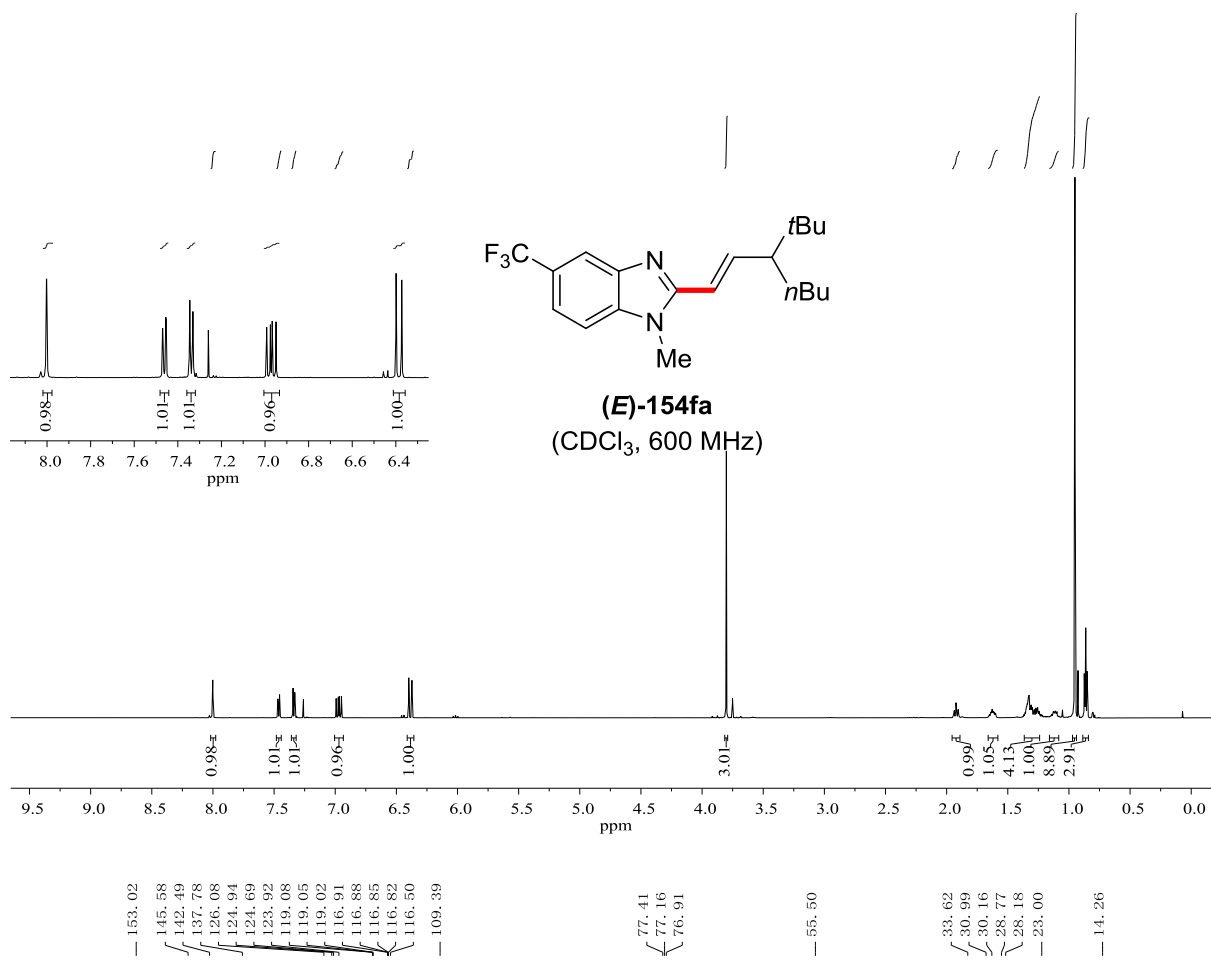




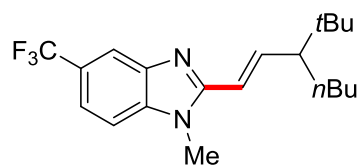




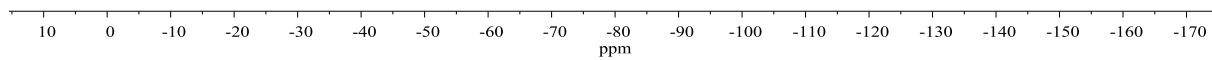


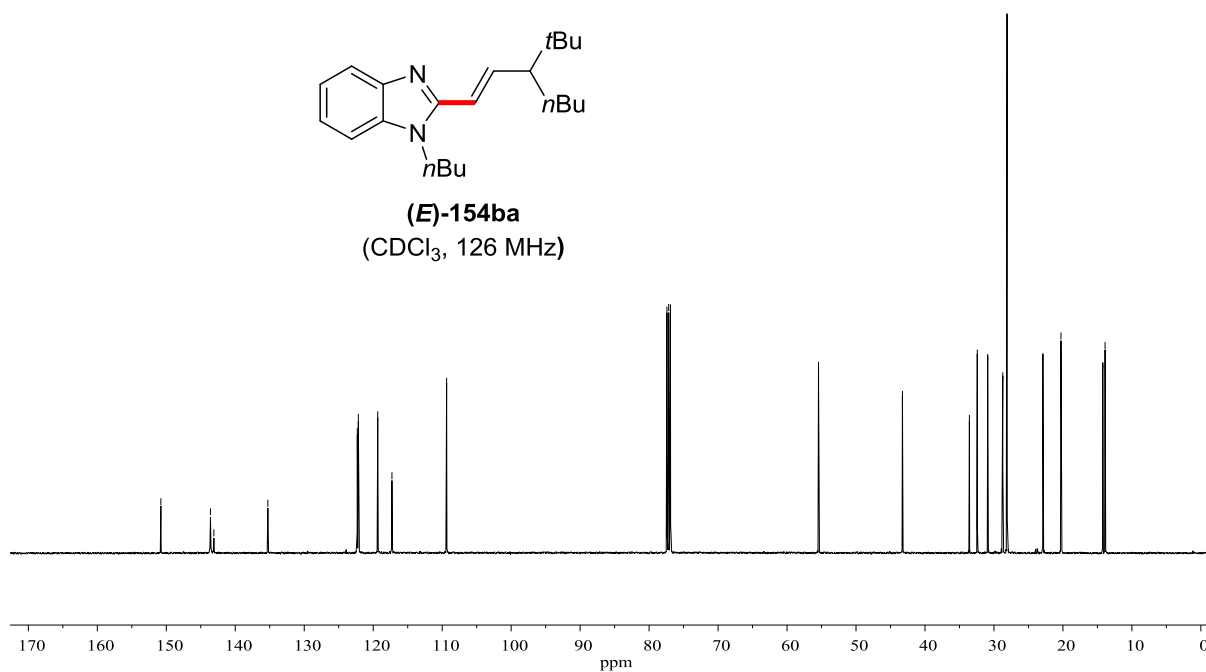
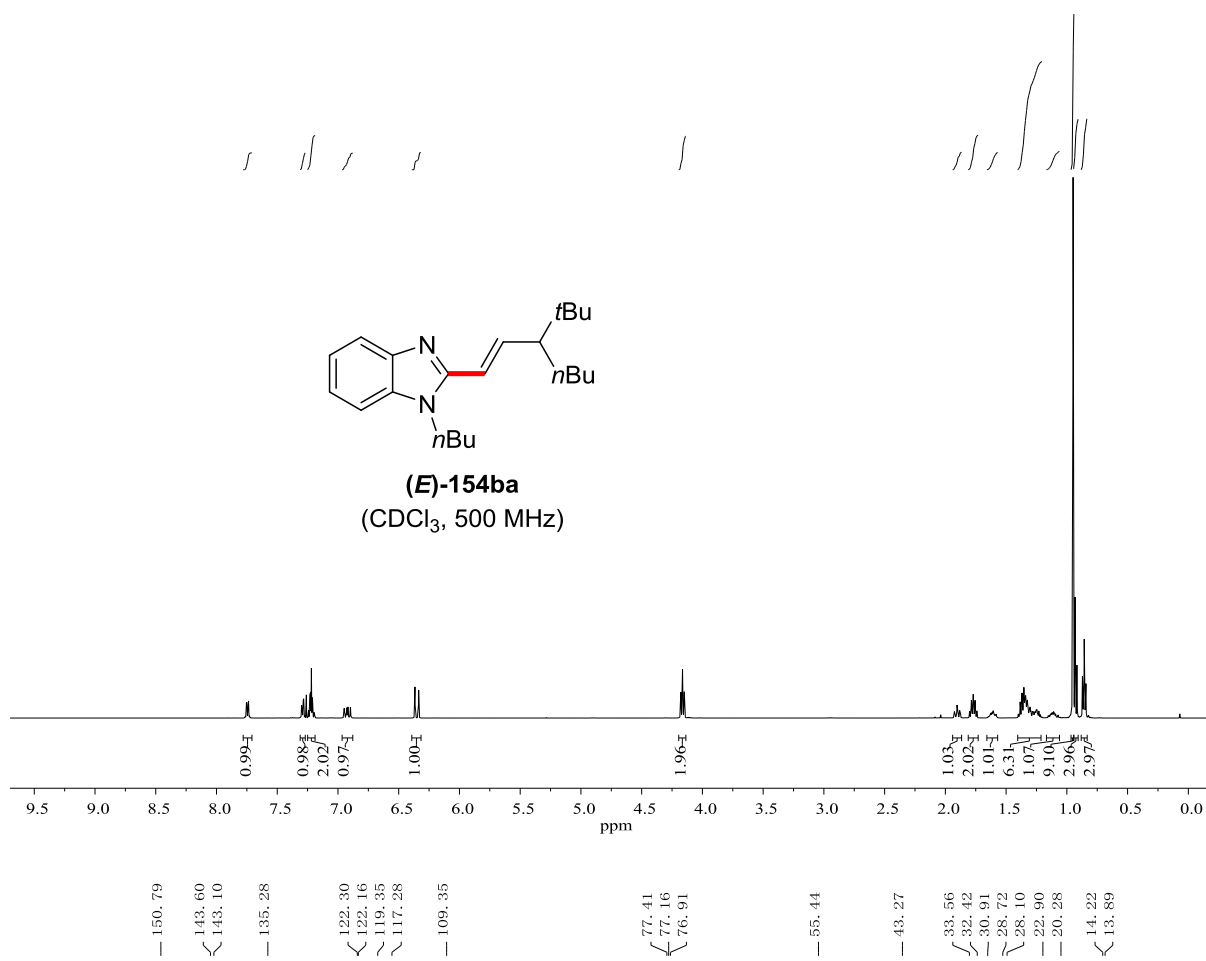


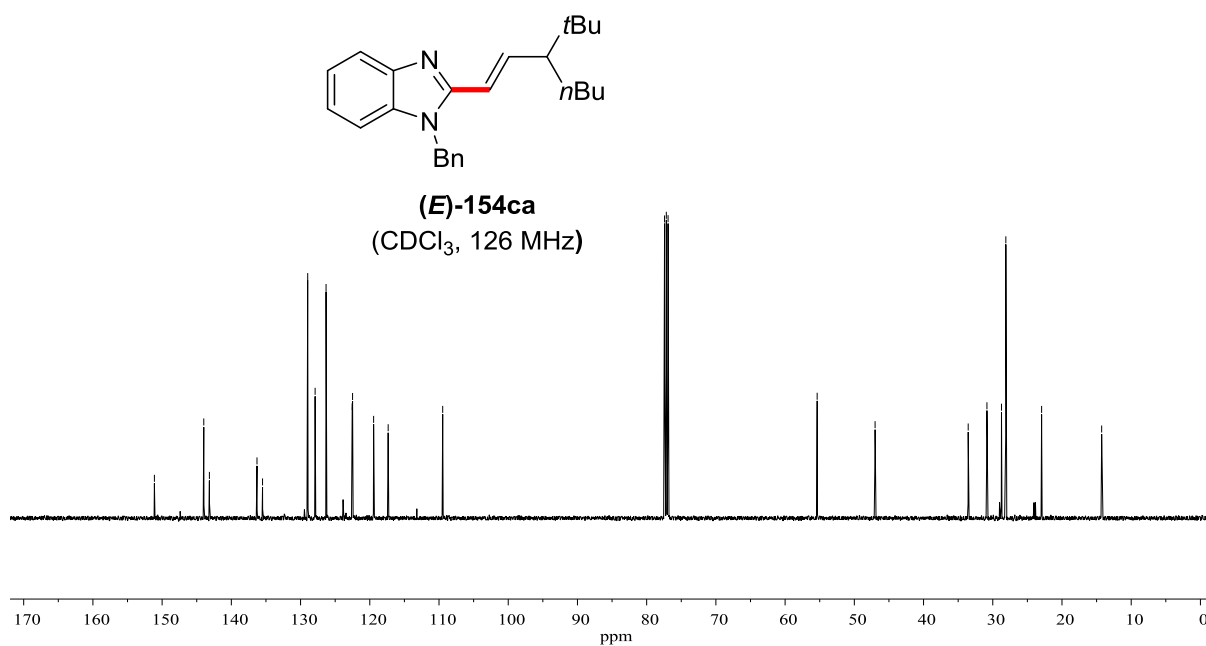
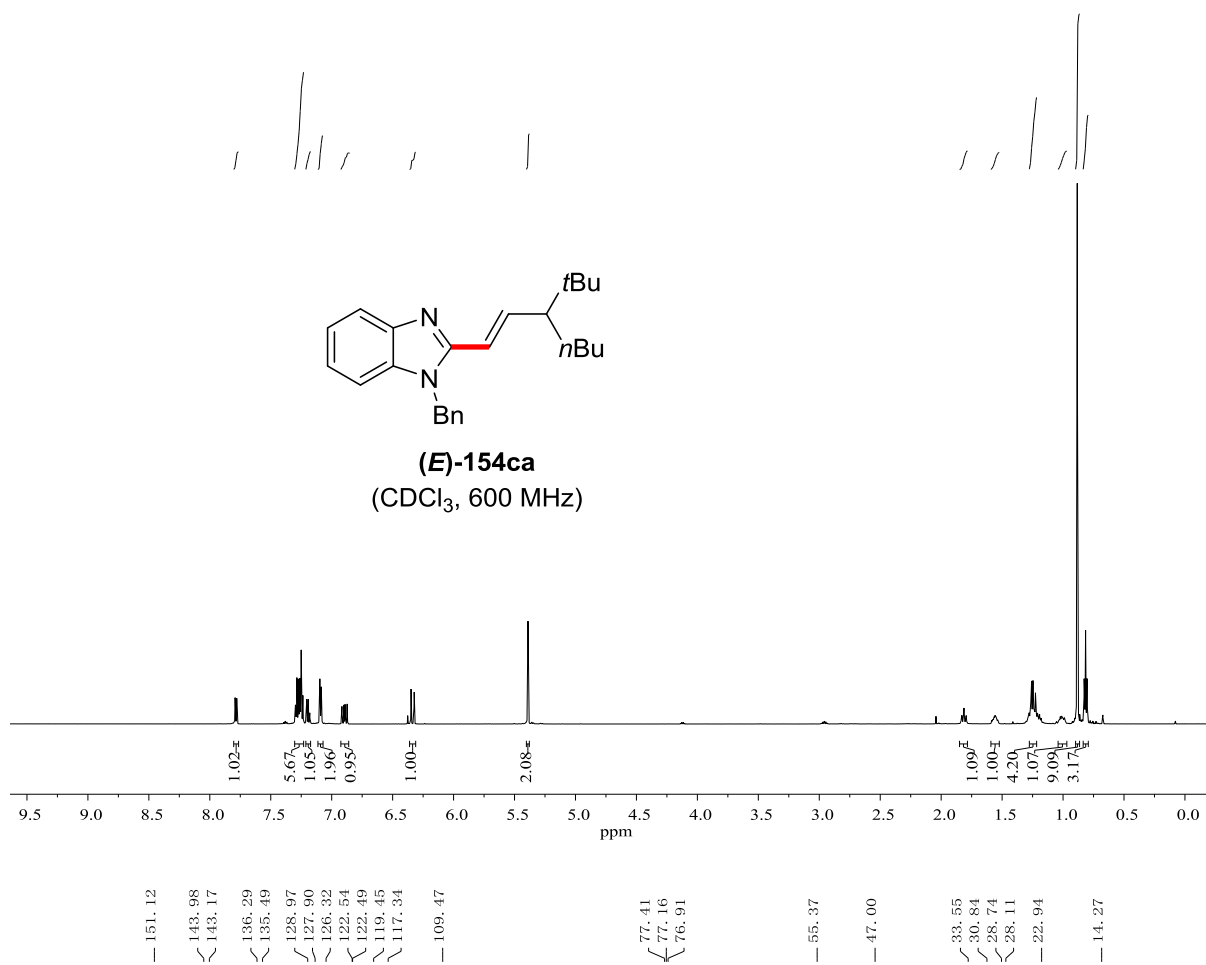
-60.63

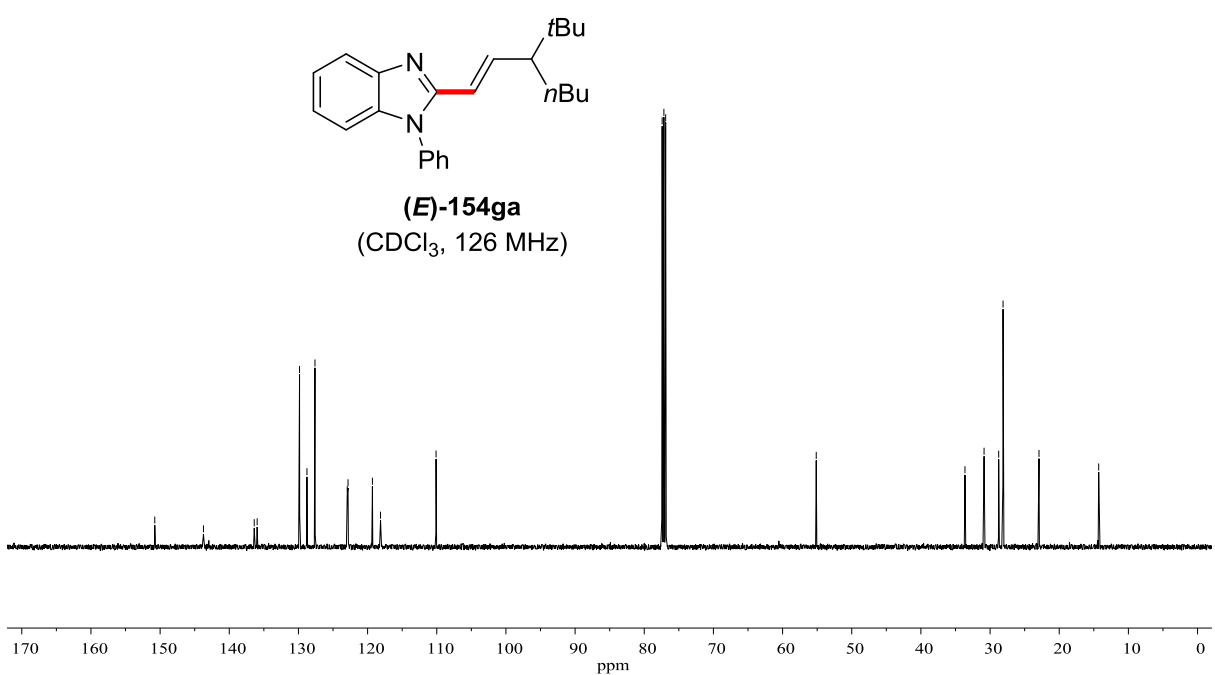
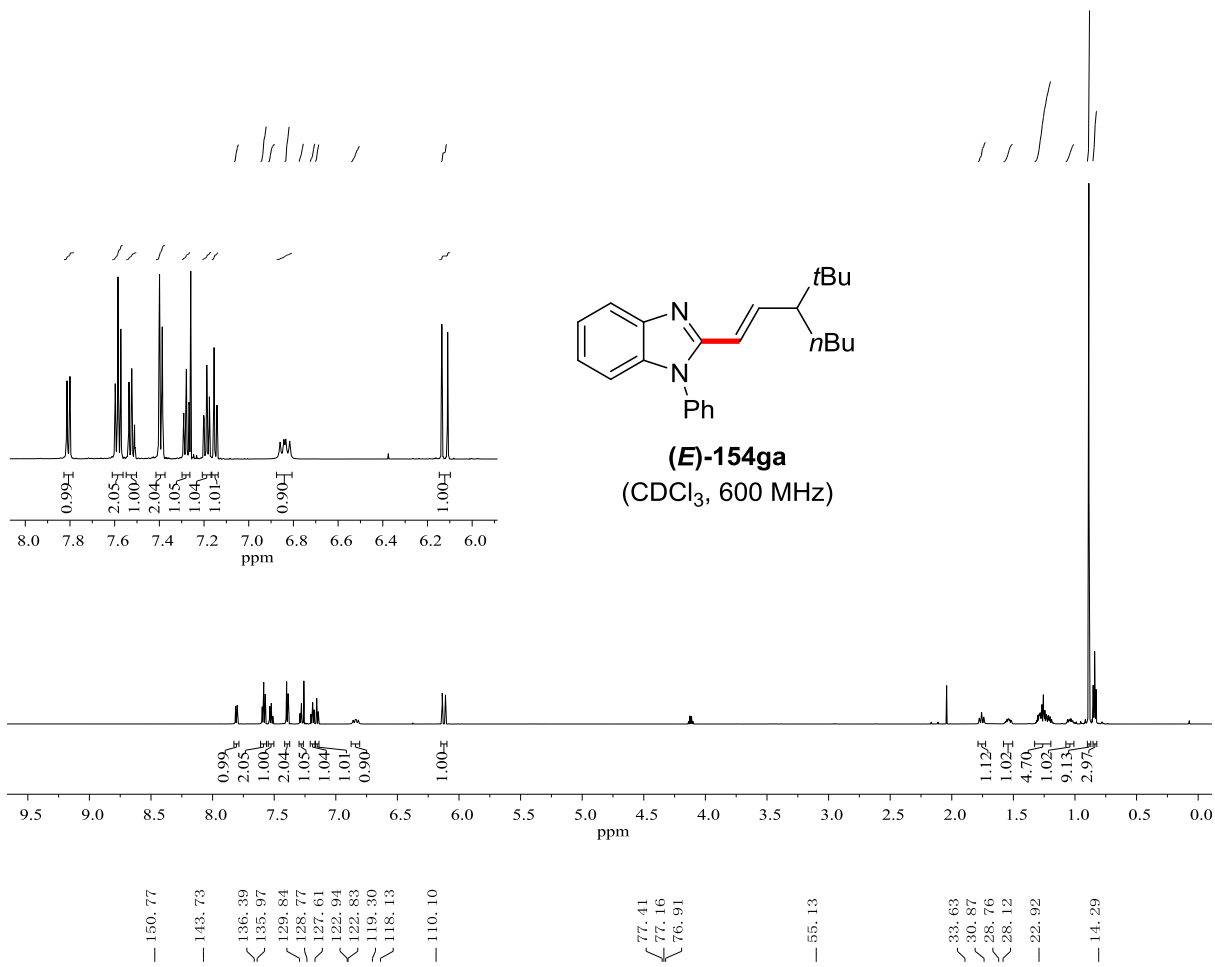


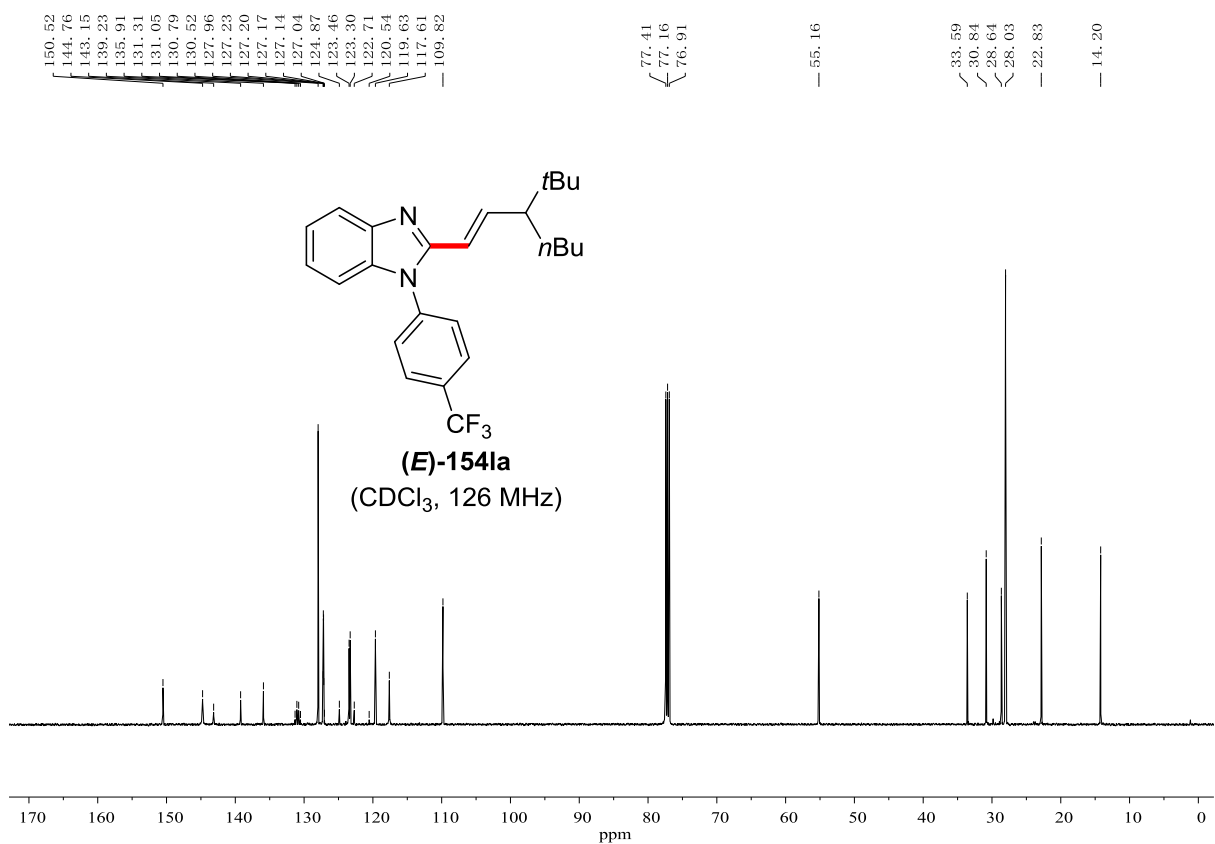
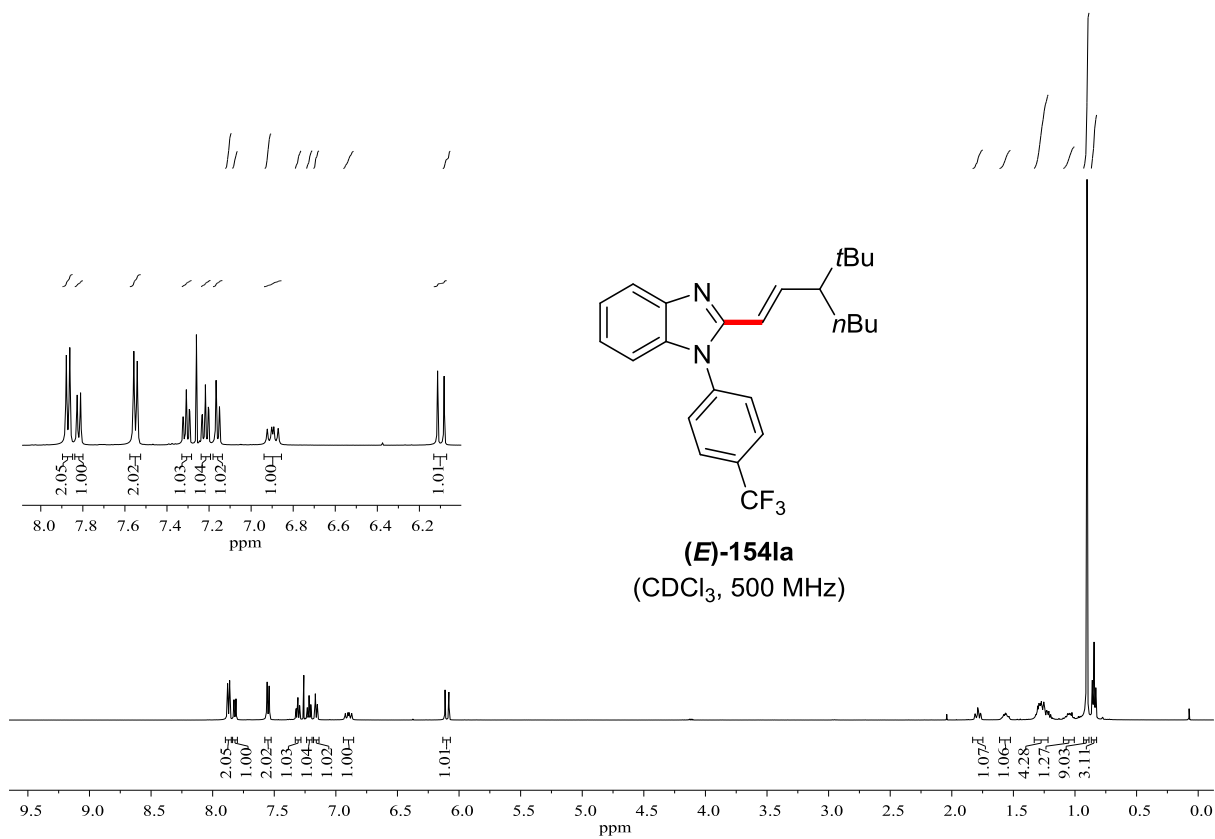
(E)-154fa
(CDCl₃, 471 MHz)

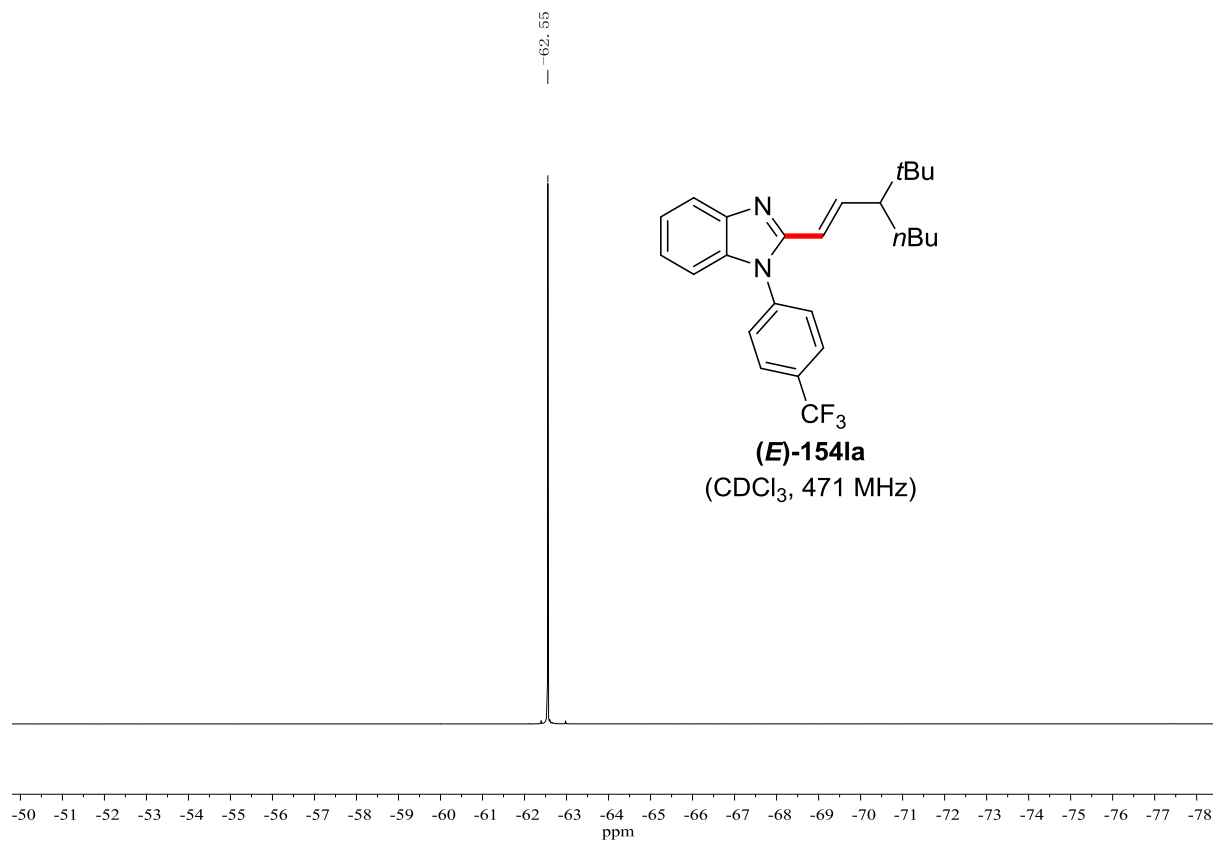


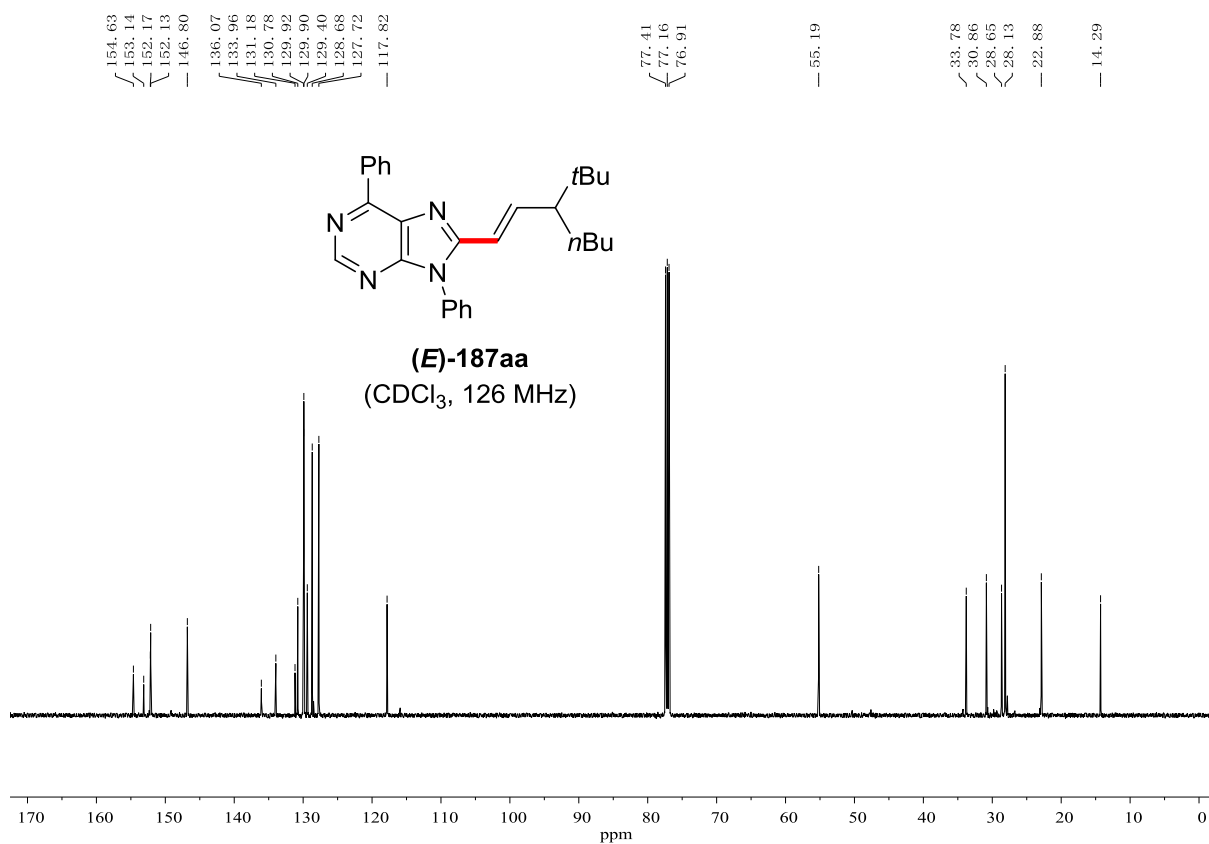
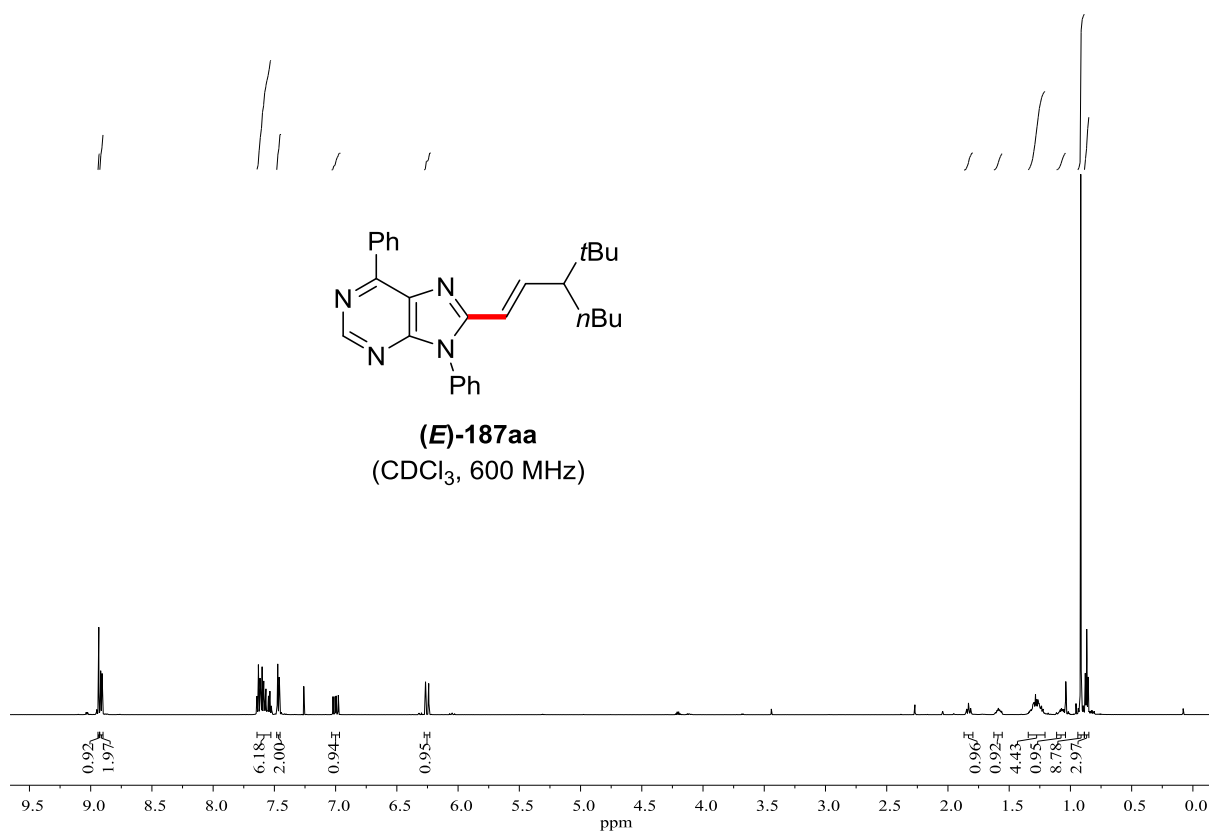


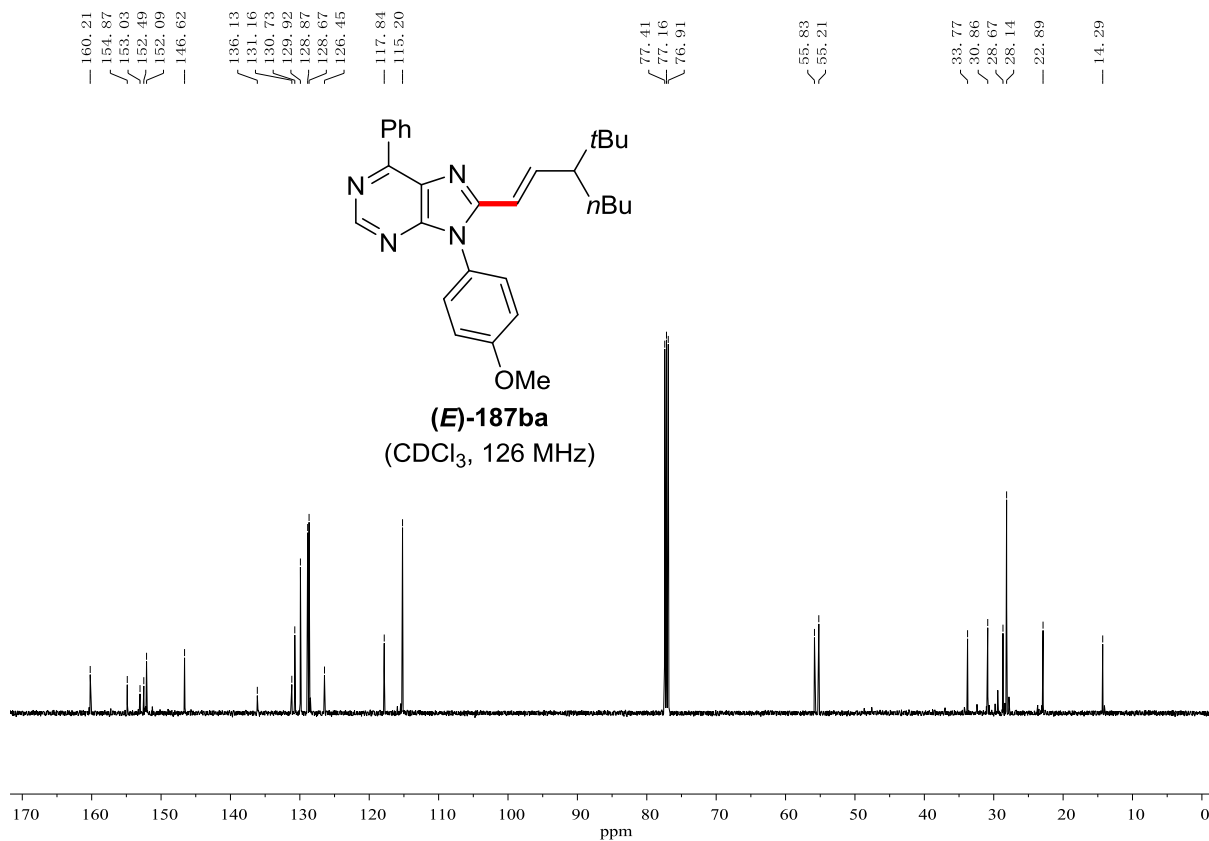
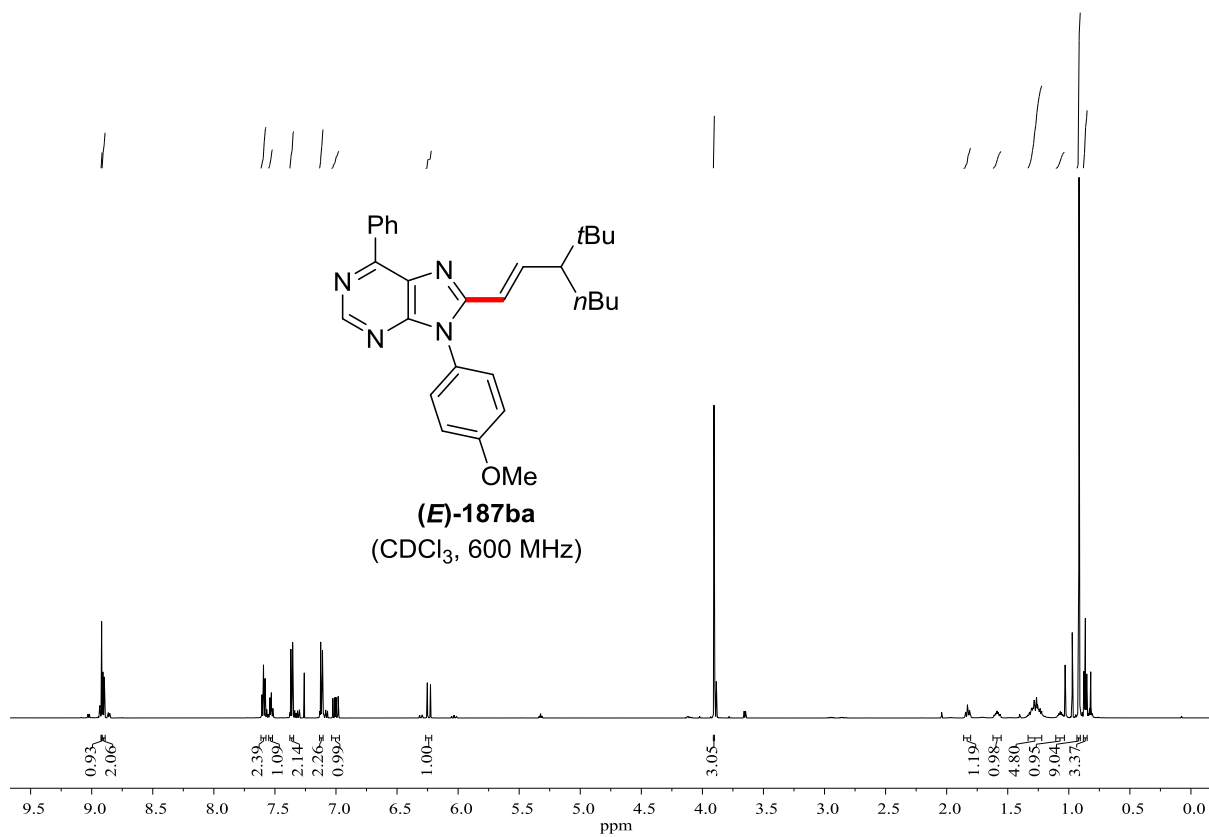


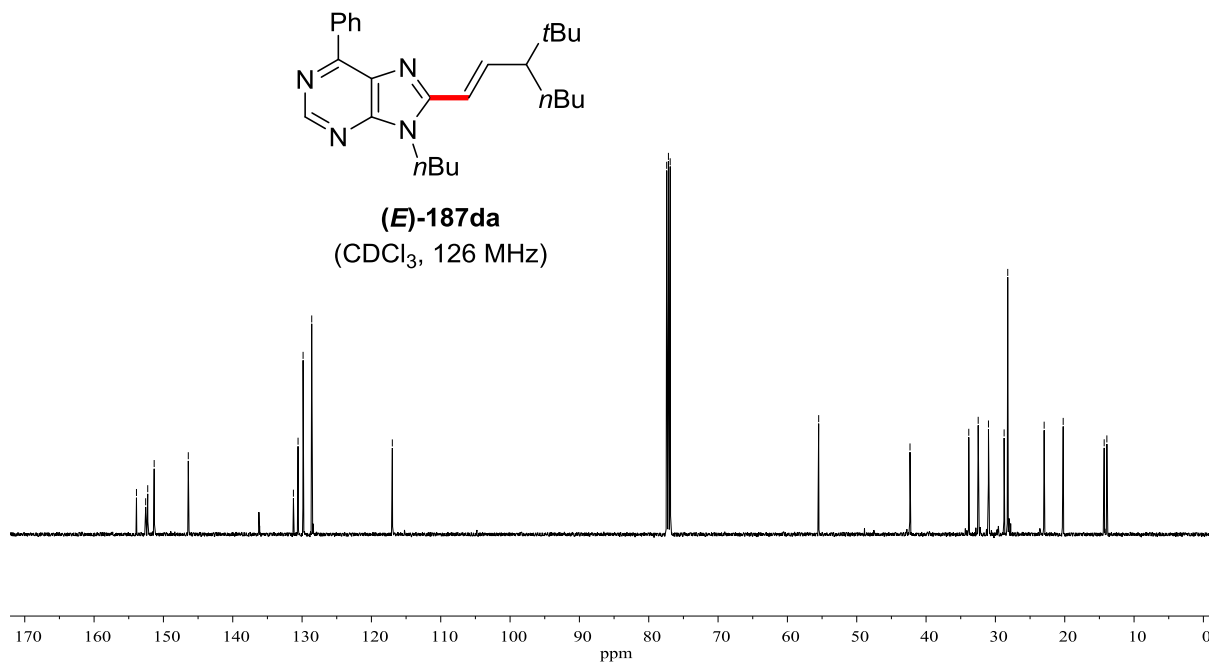
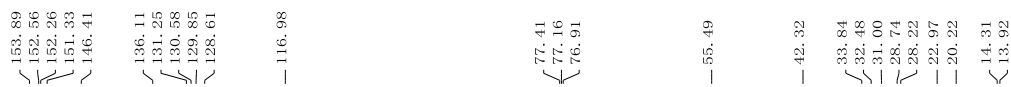
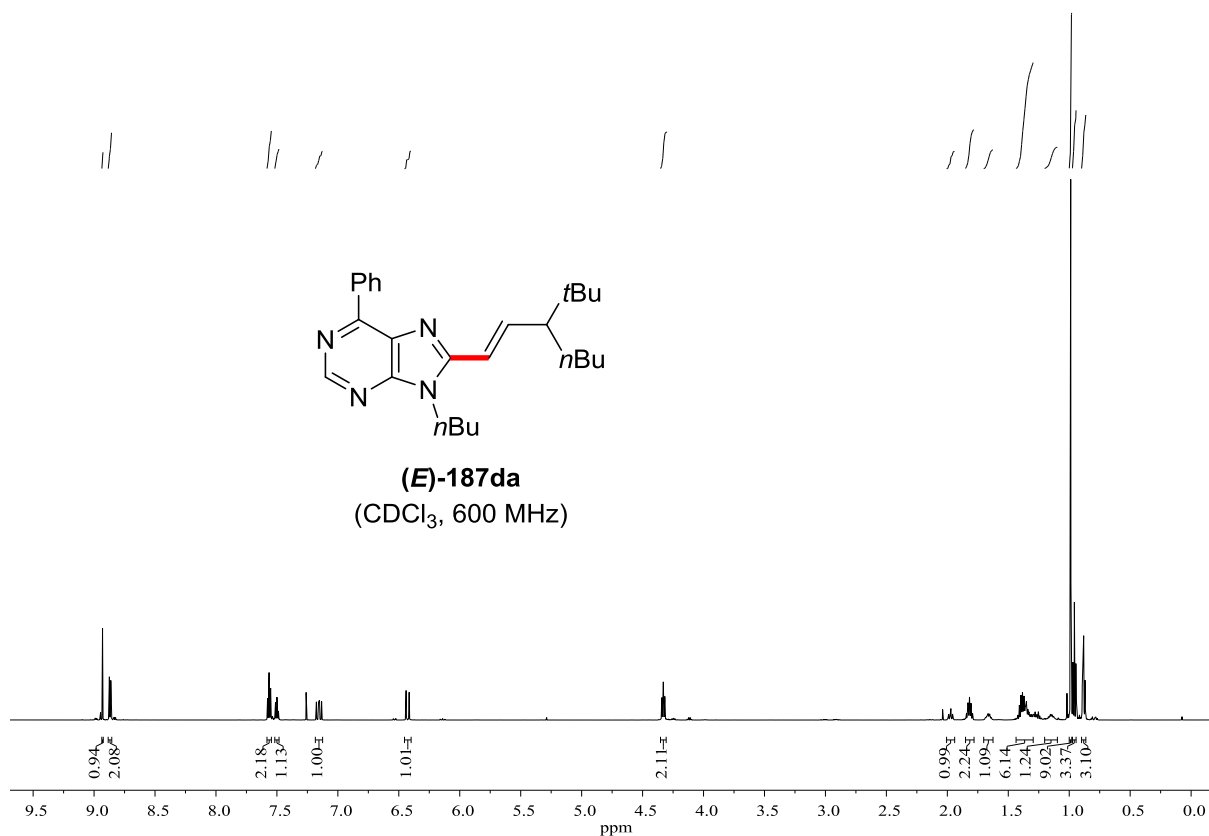


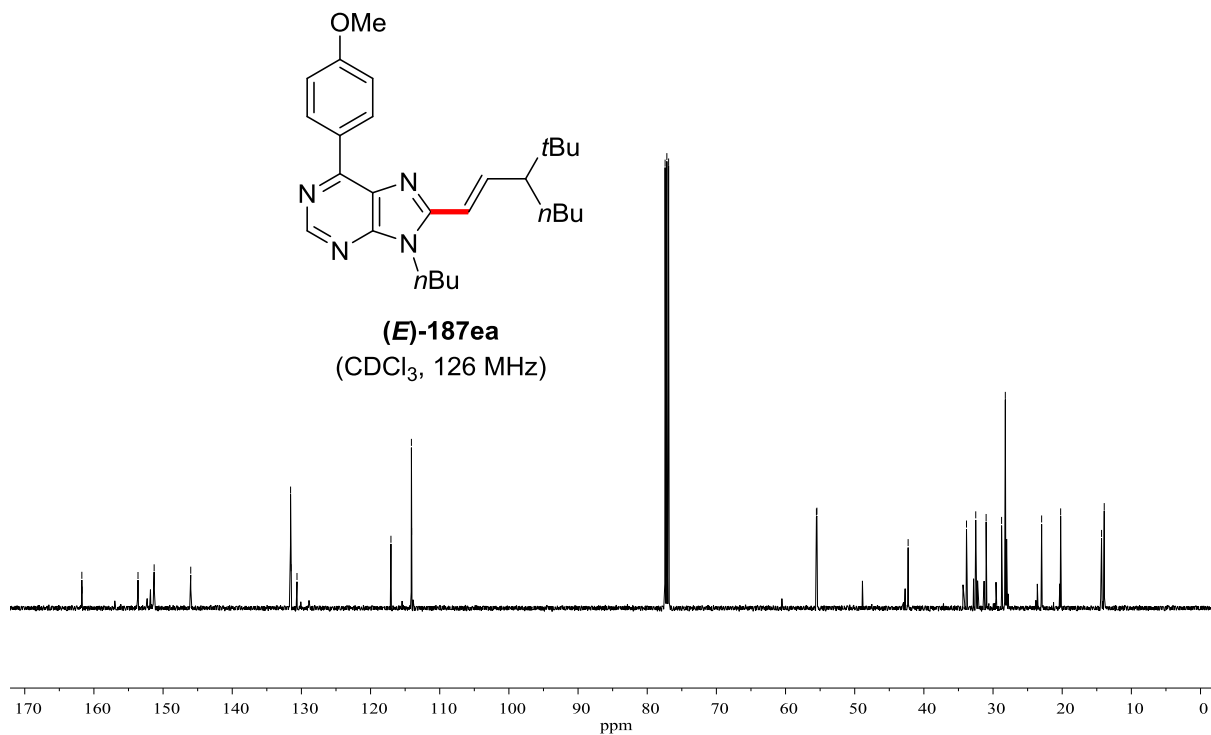
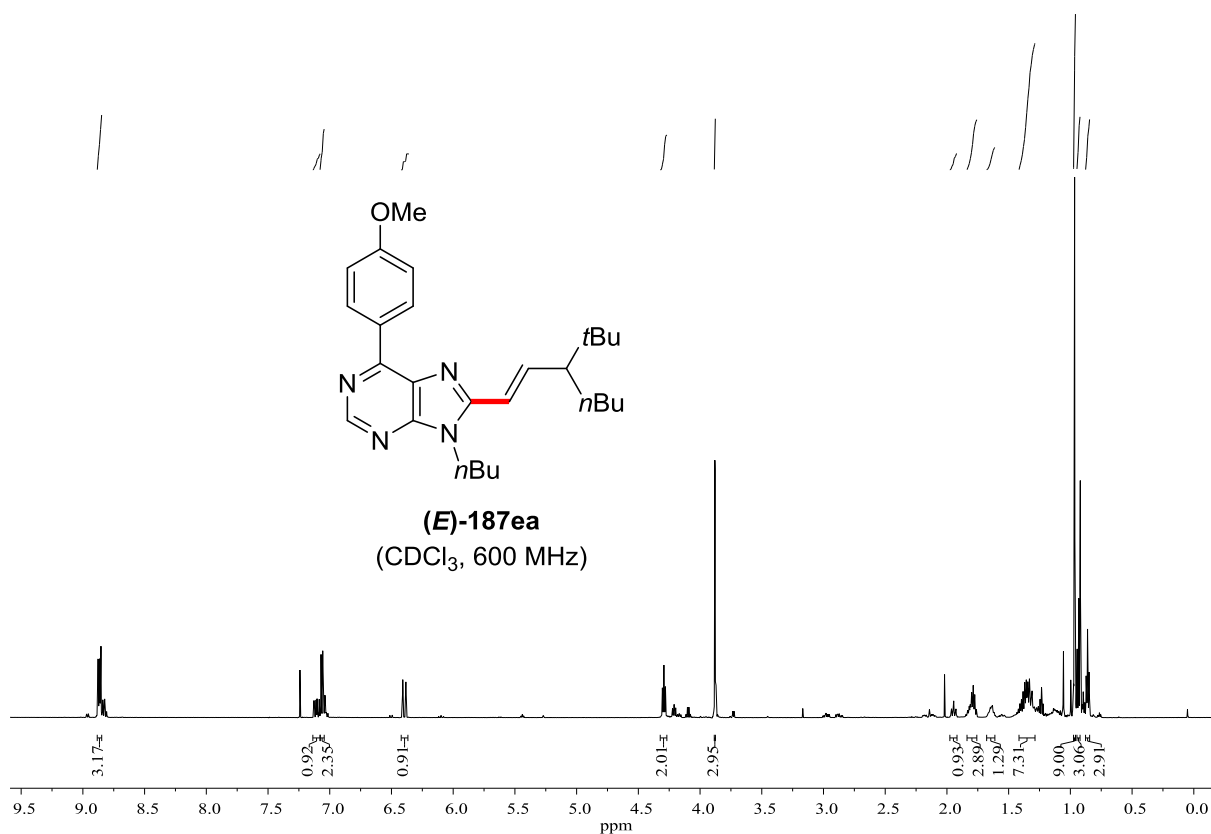


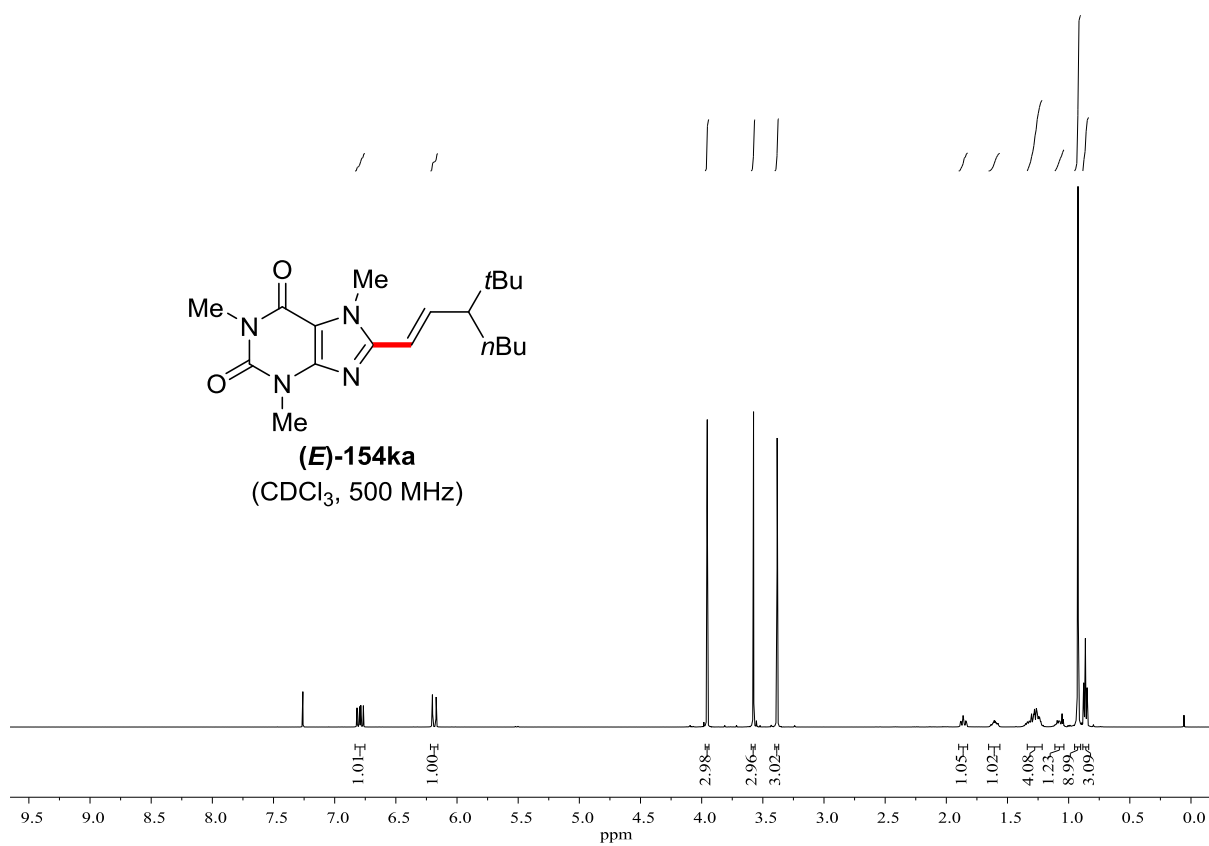












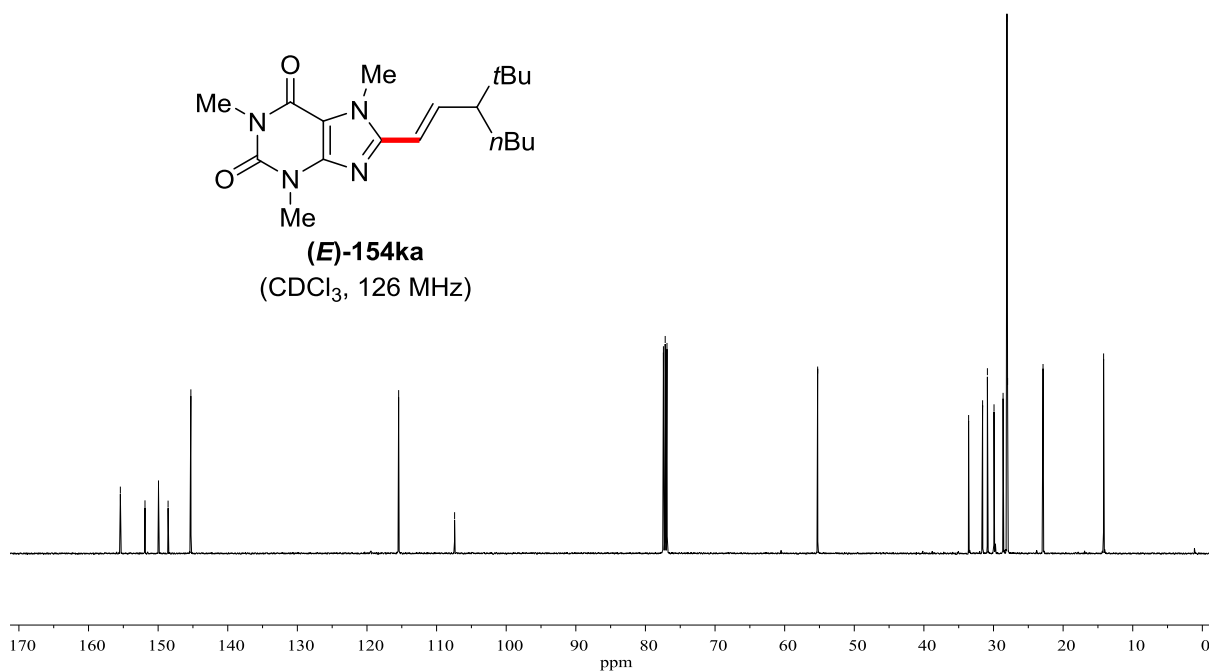
155.43
 151.89
 149.95
 148.57
 145.30

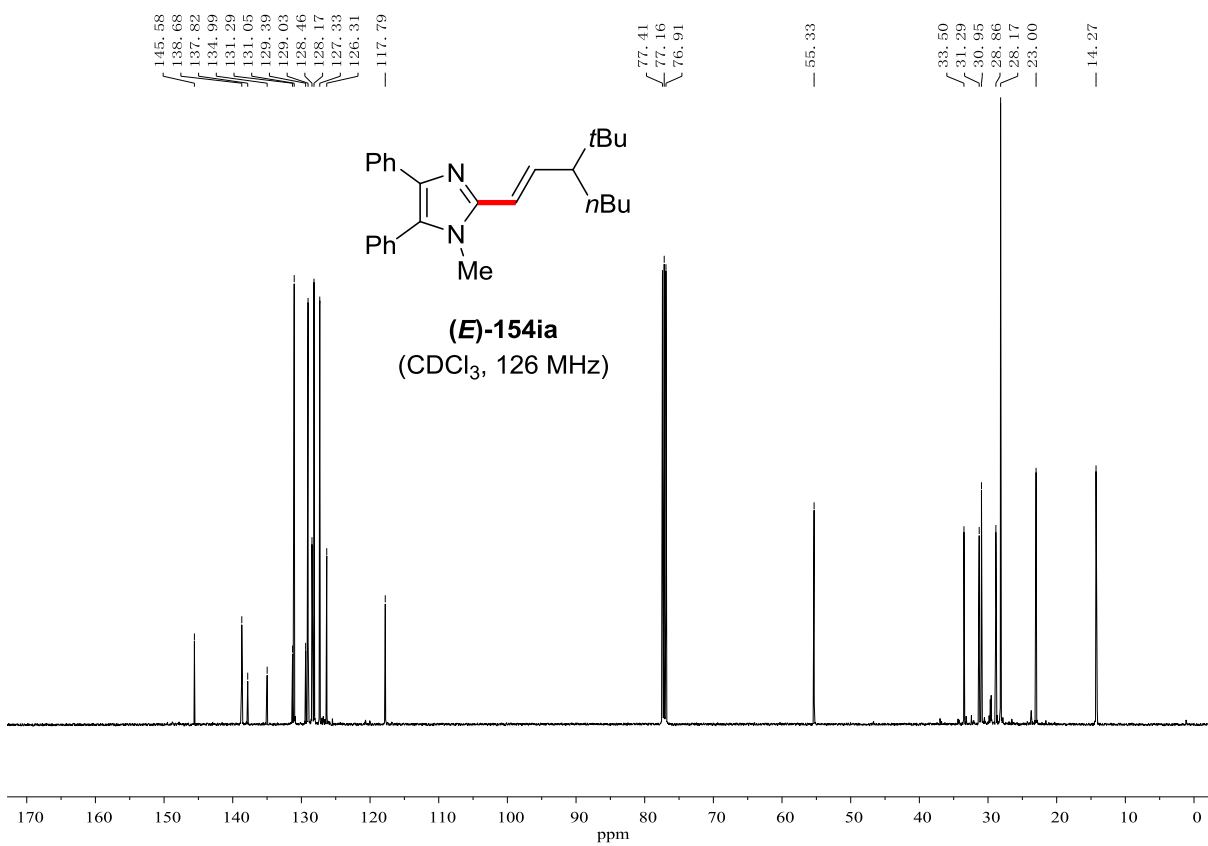
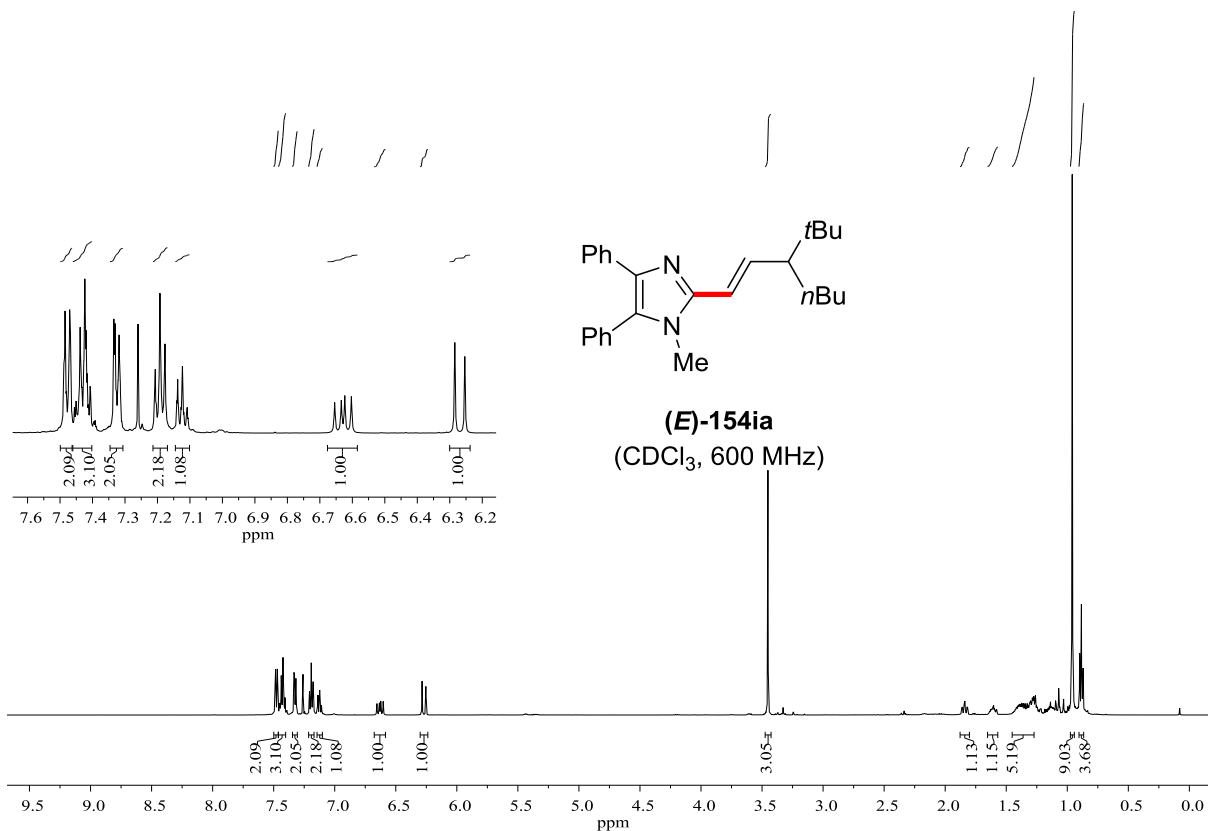
115.45
 107.41

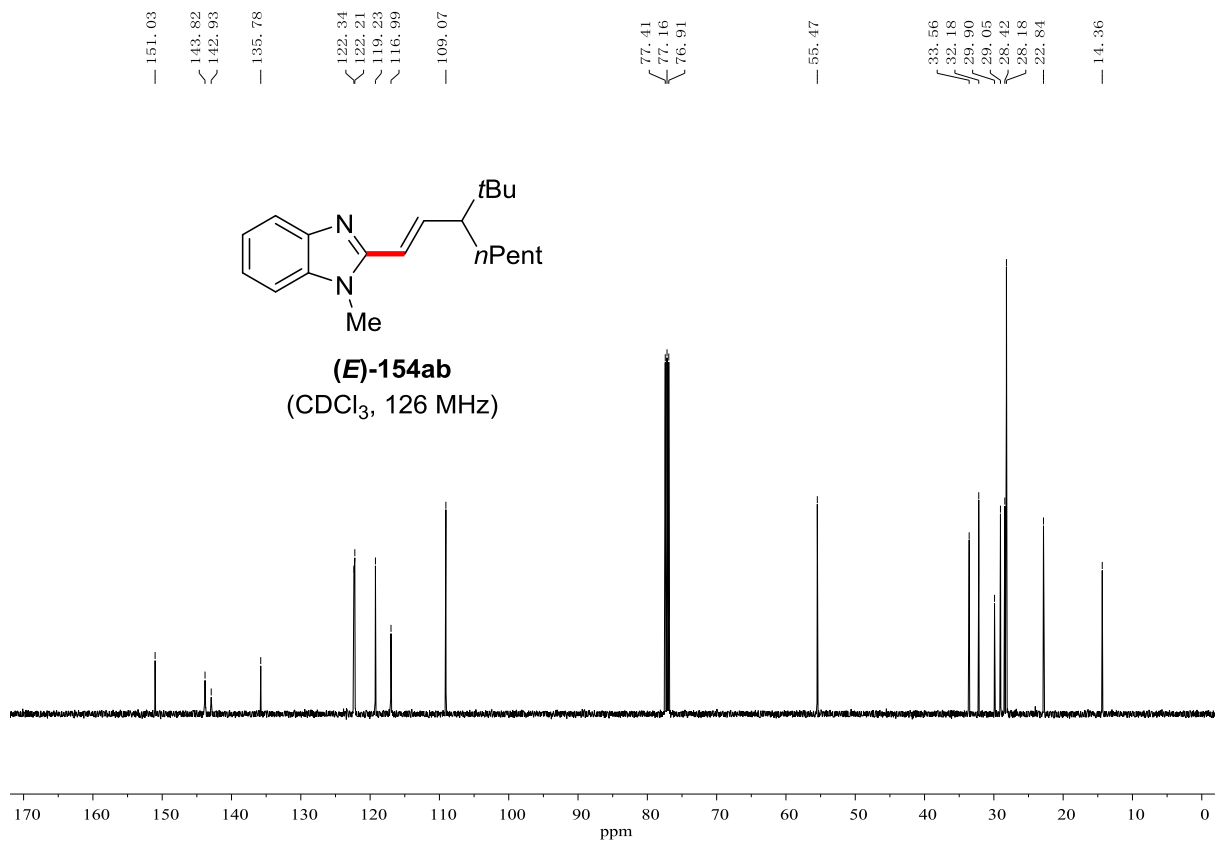
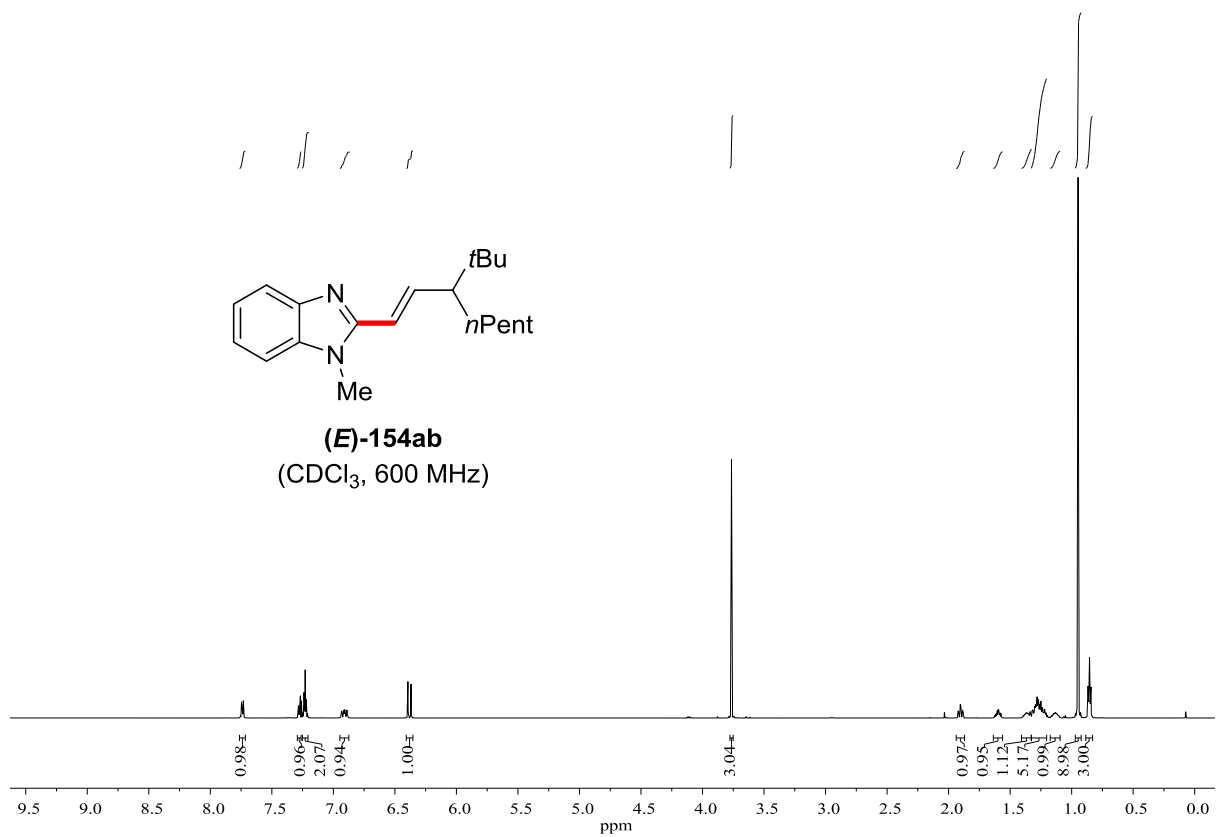
77.41
 77.16
 76.91

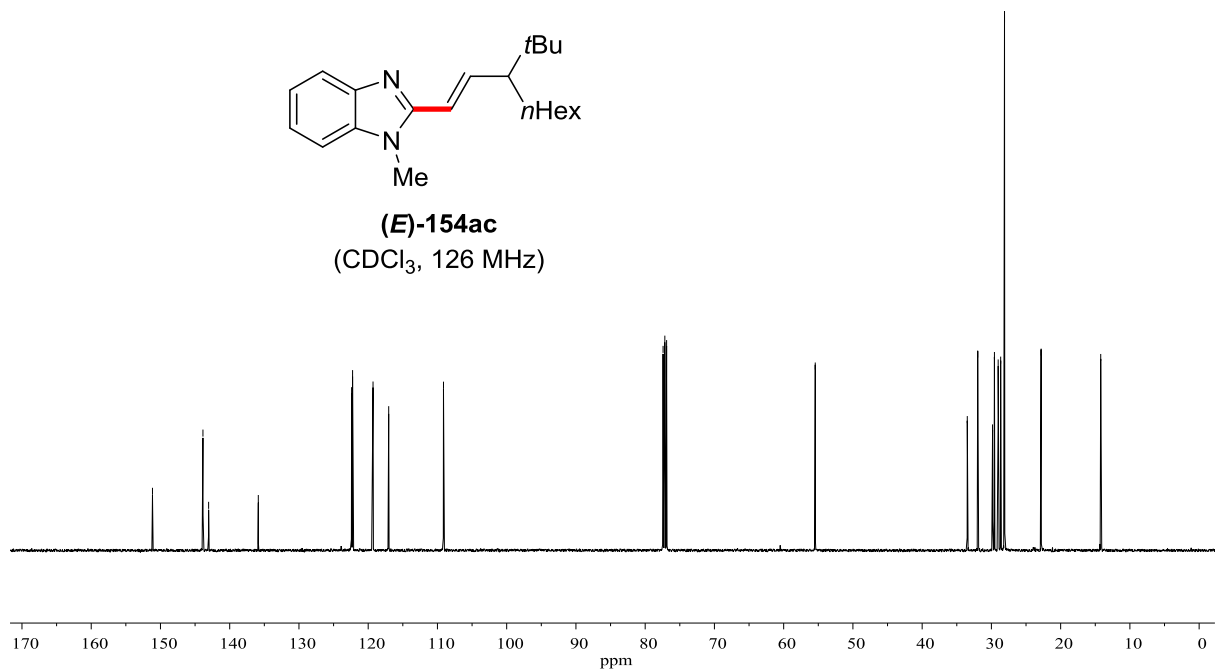
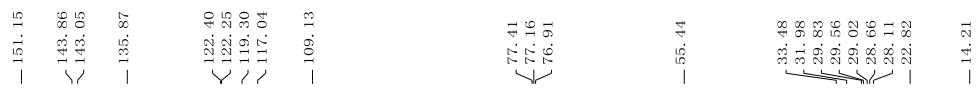
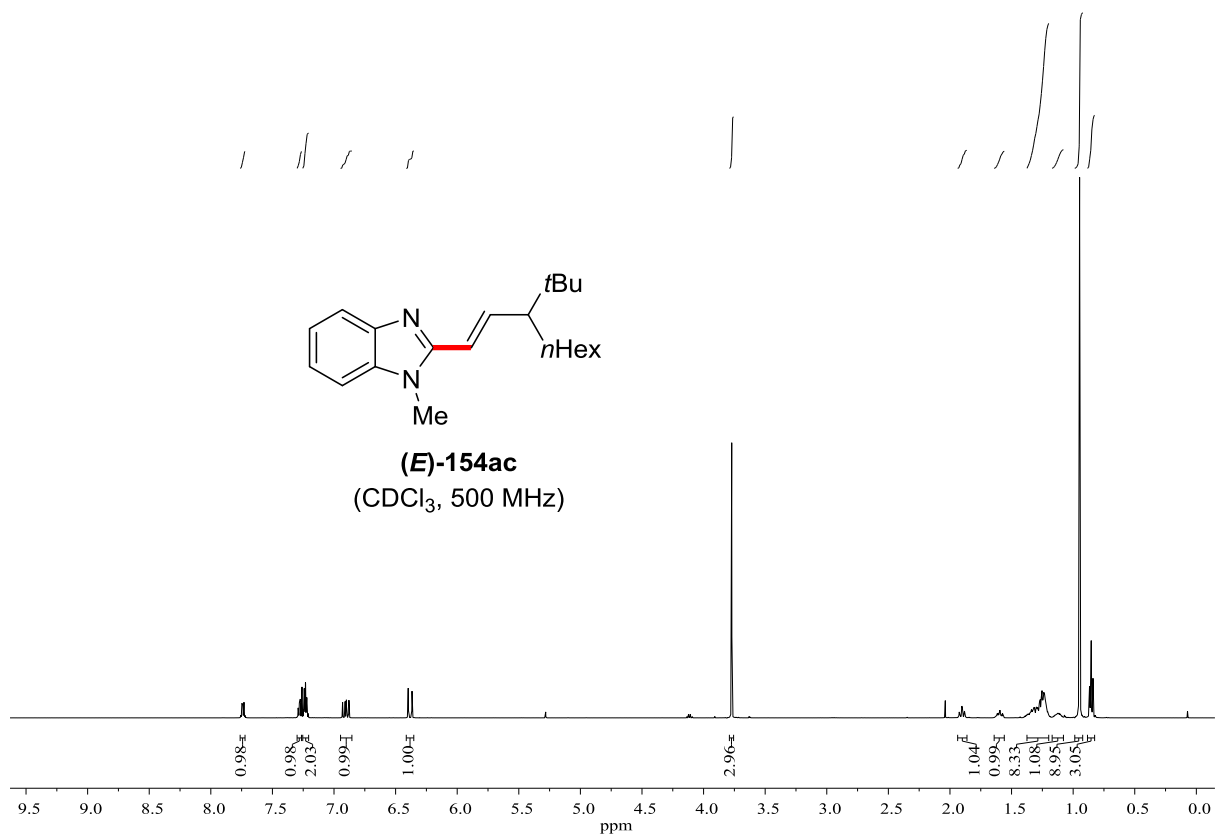
55.26

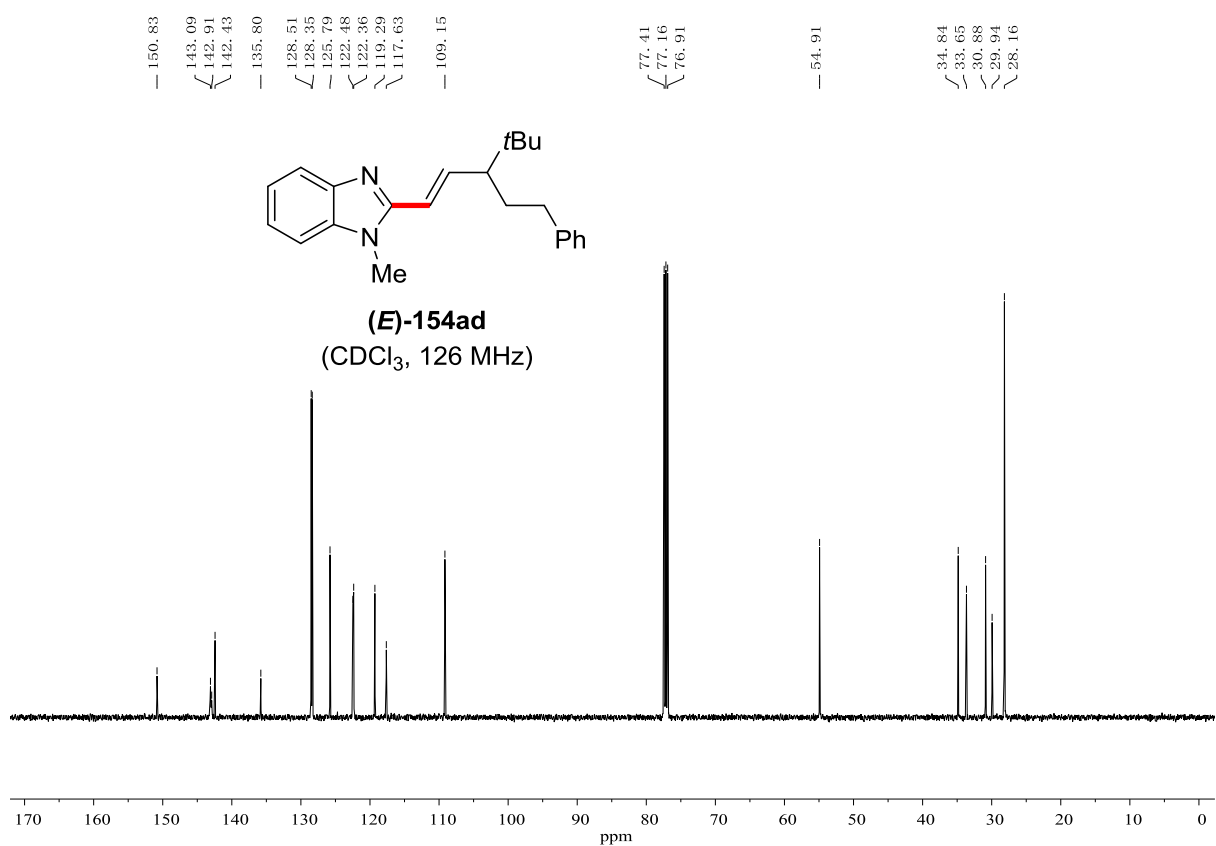
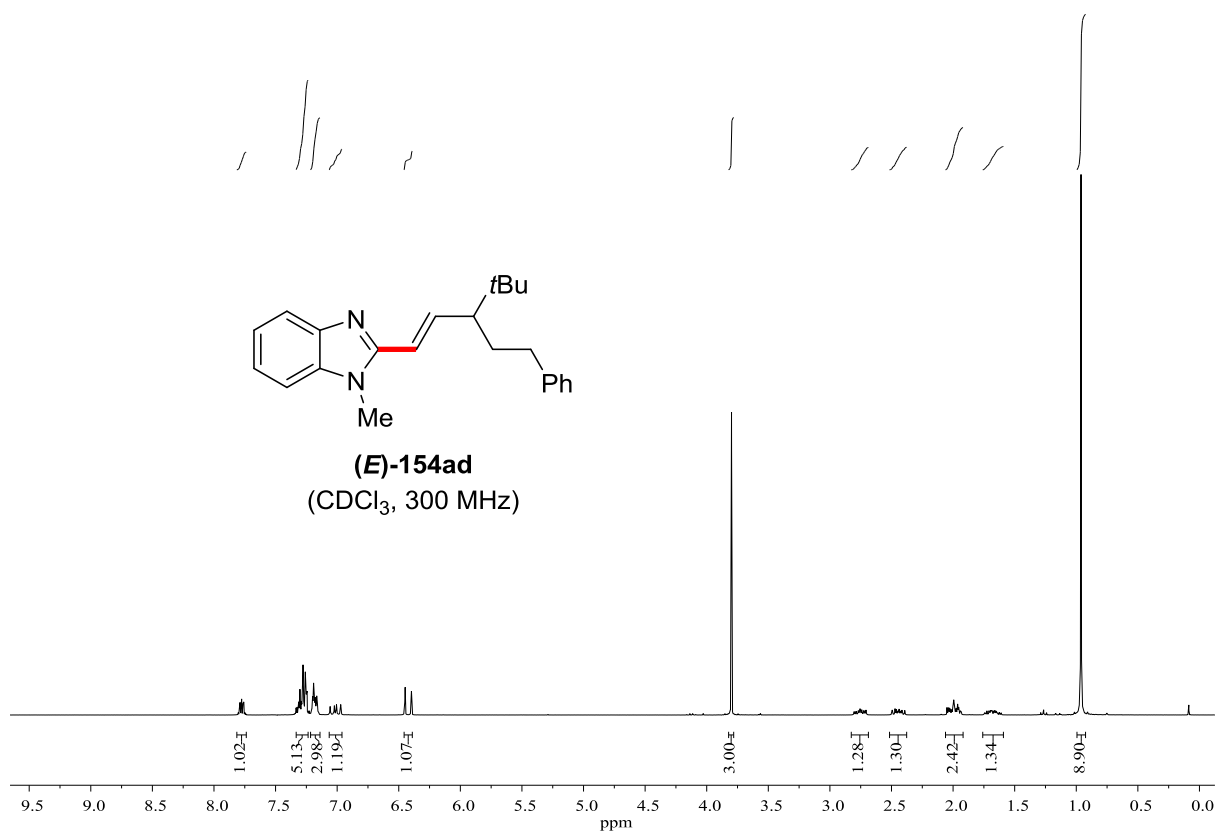
33.58
 31.57
 30.87
 29.93
 28.62
 28.07
 27.98
 22.89
 14.19

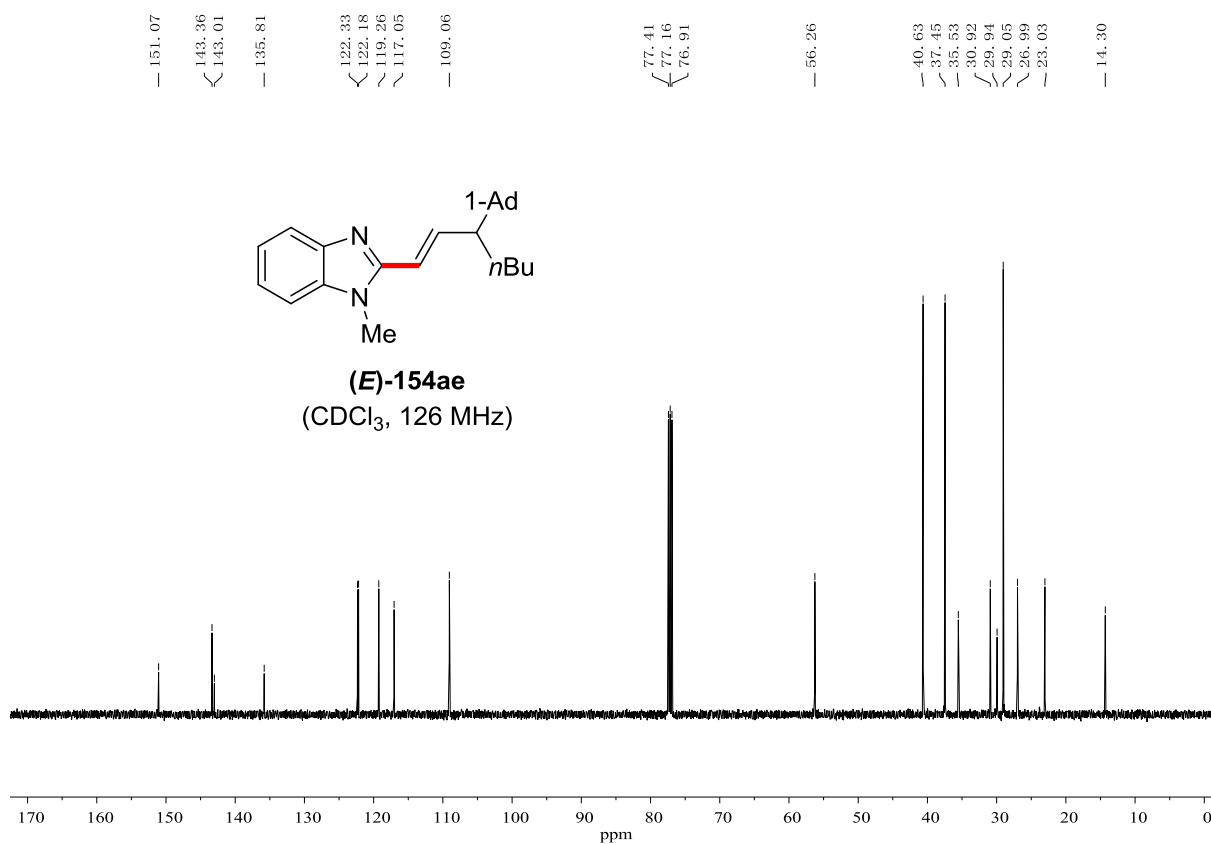
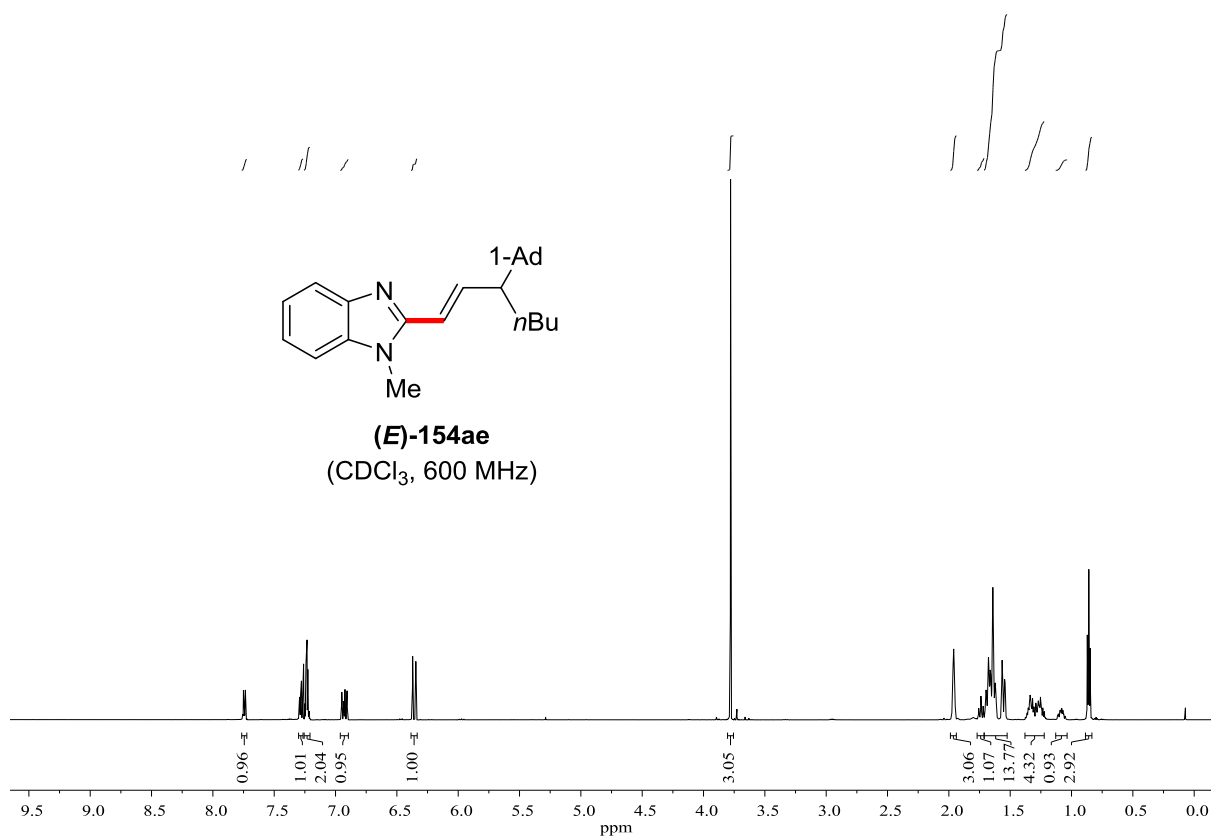


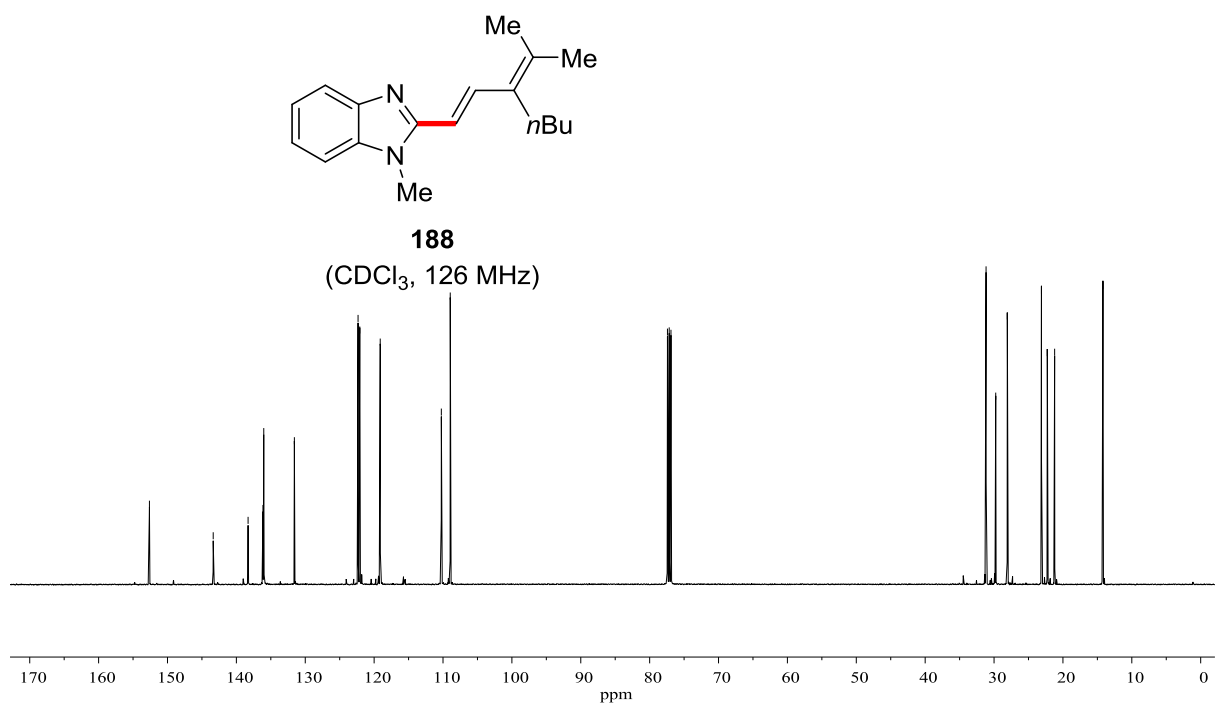
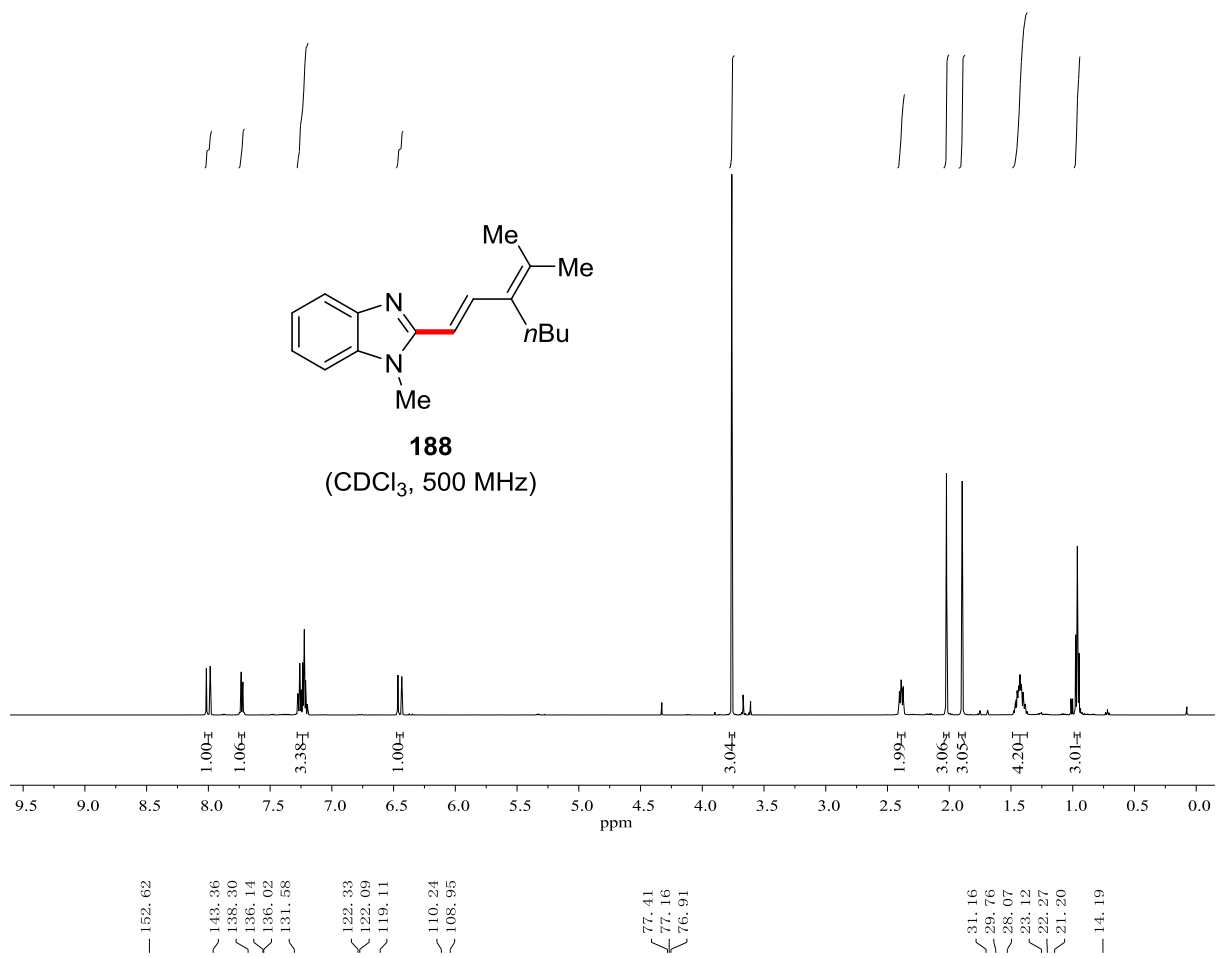


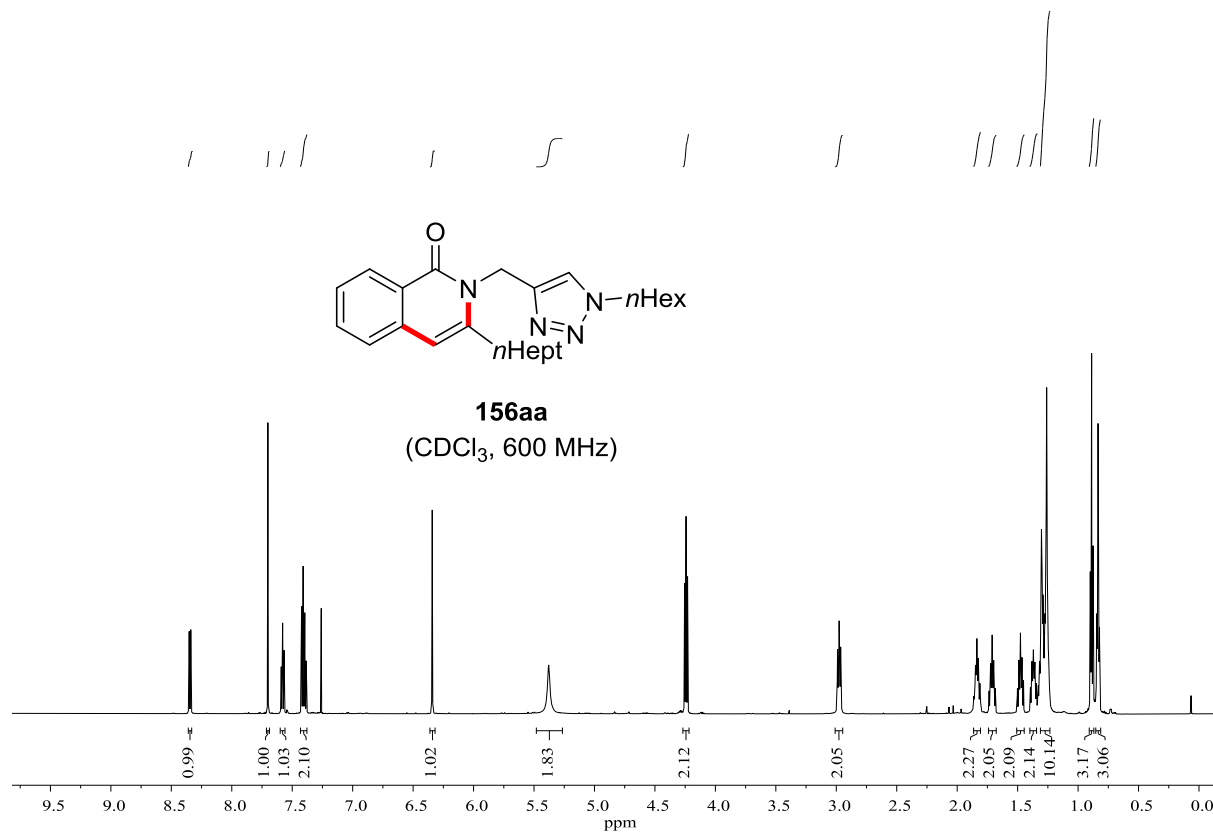




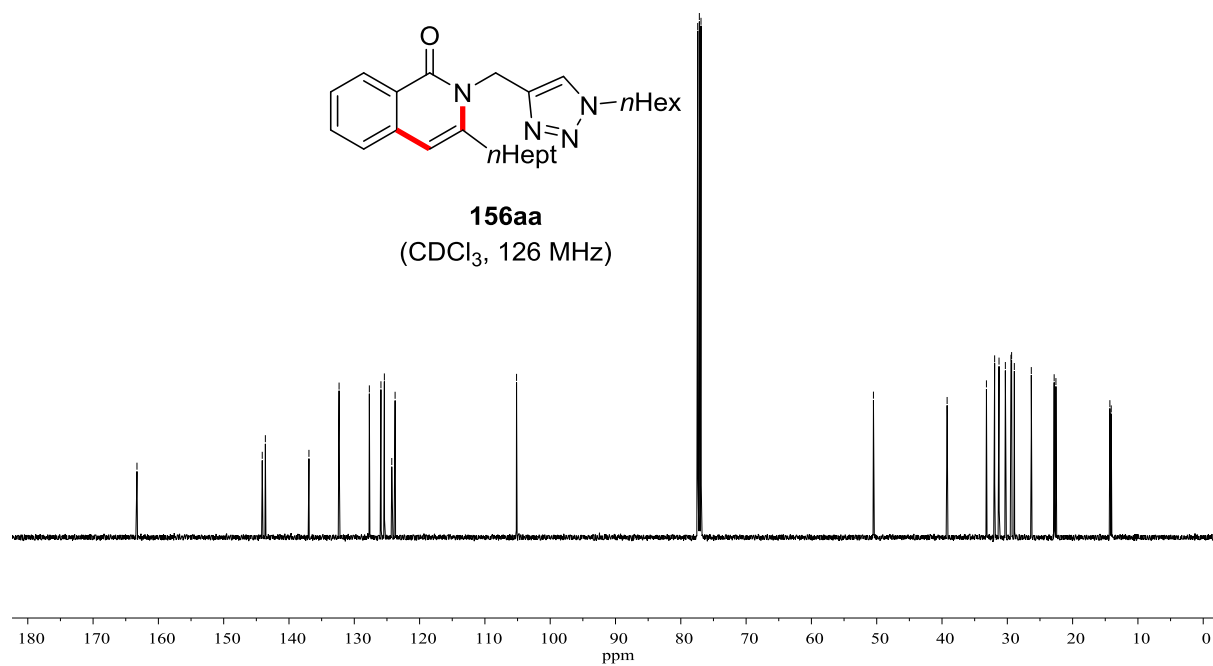


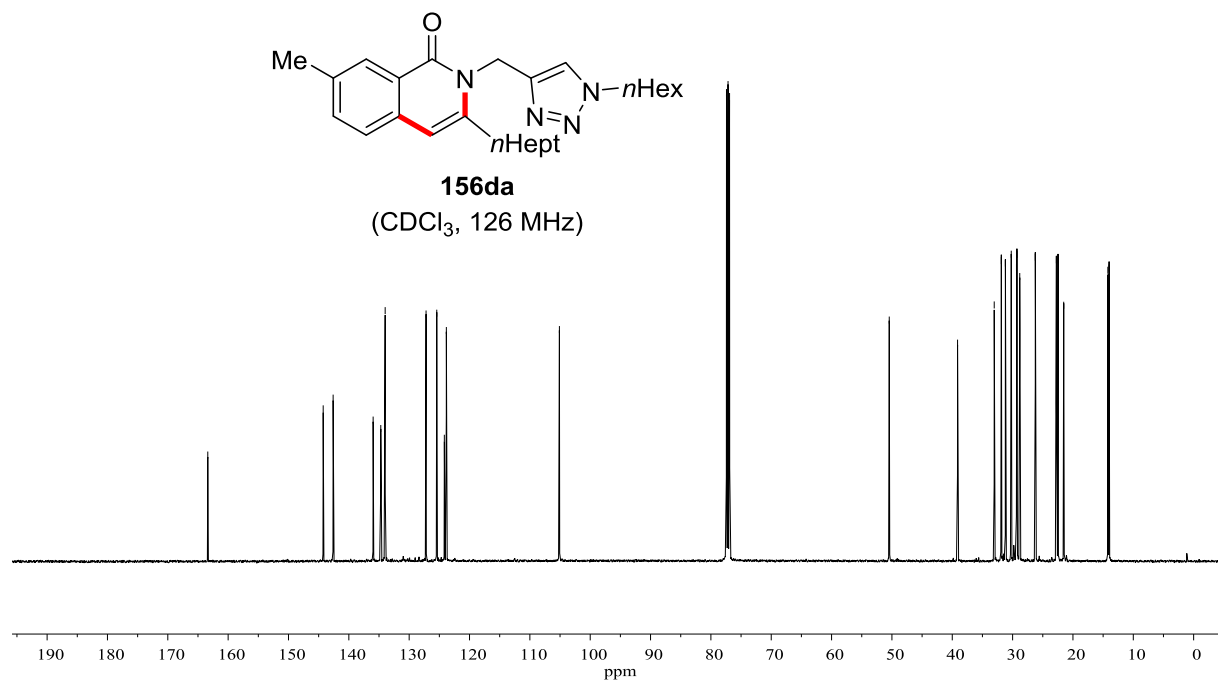
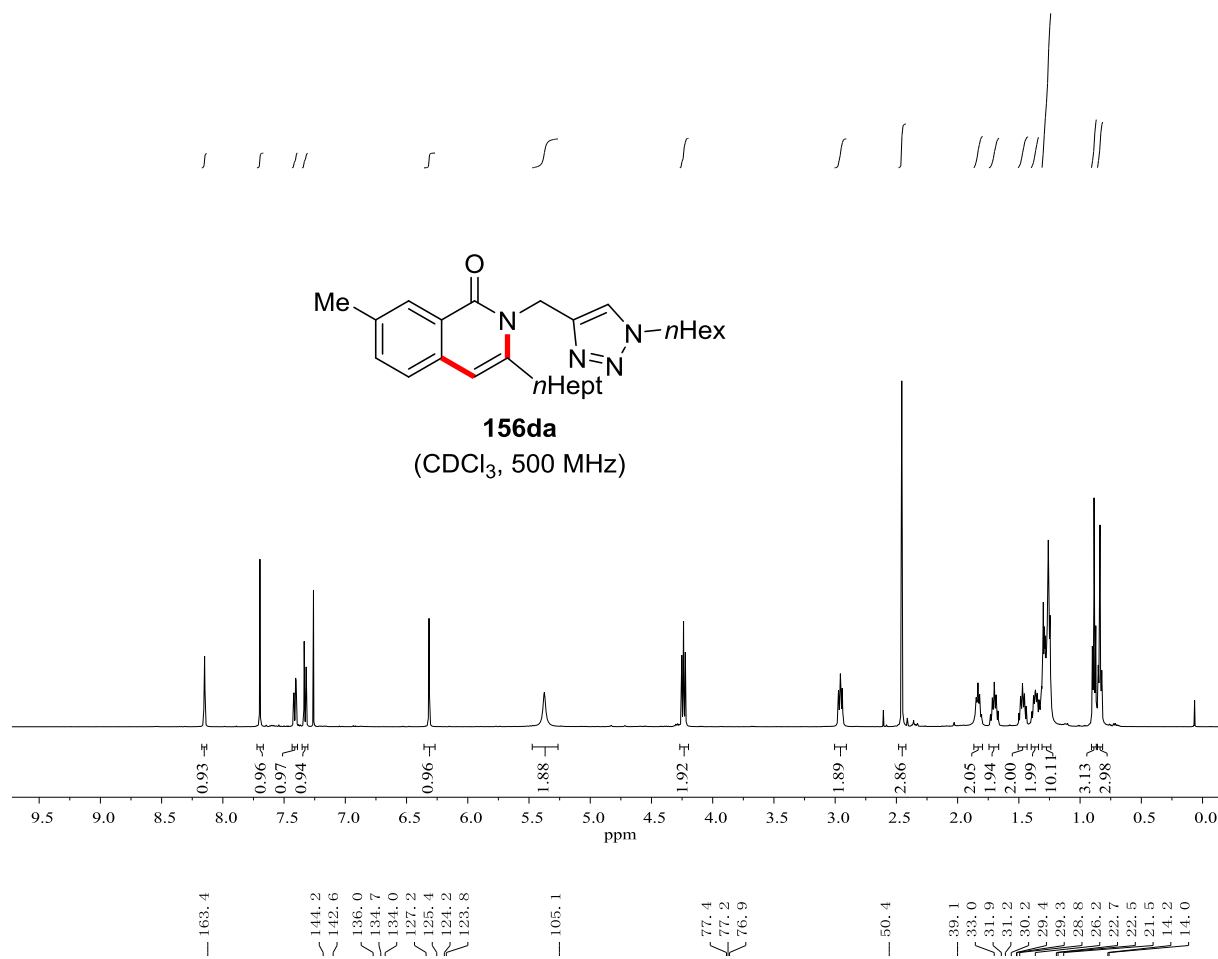


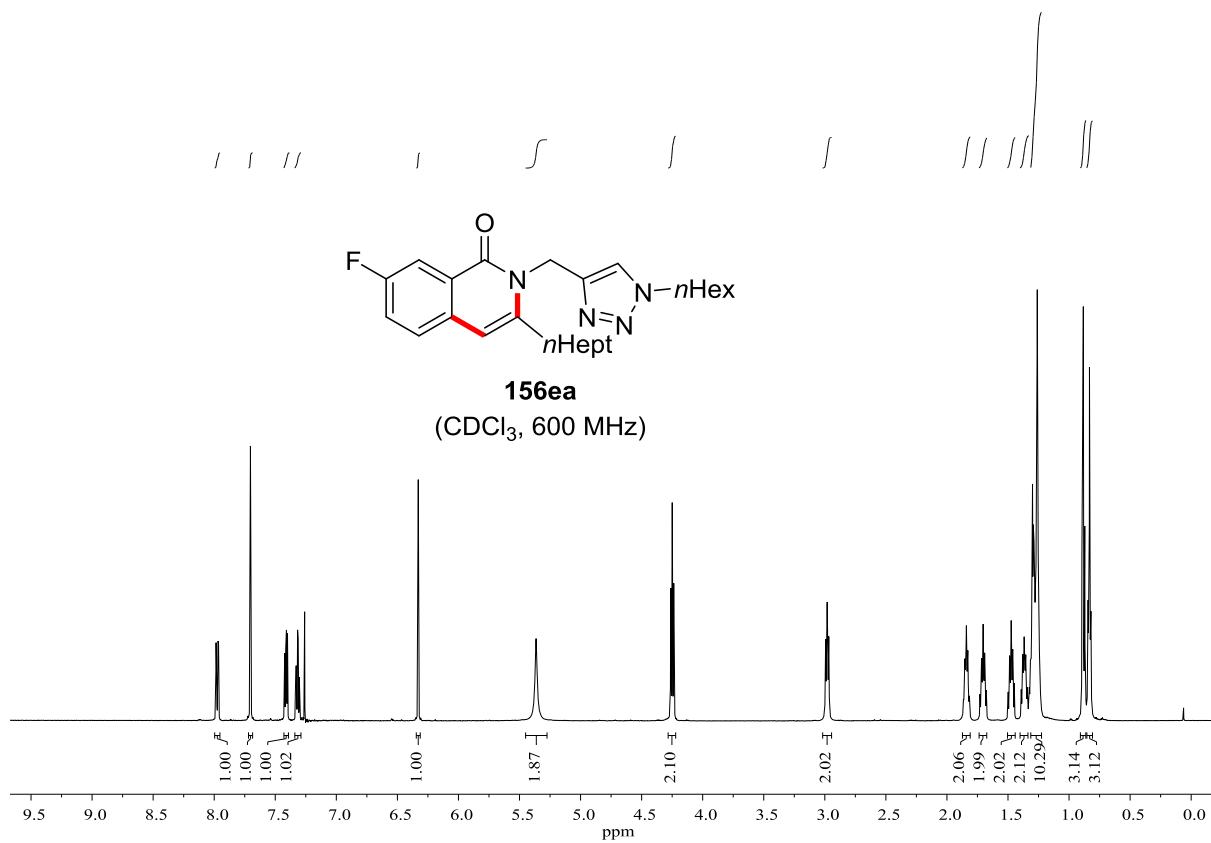




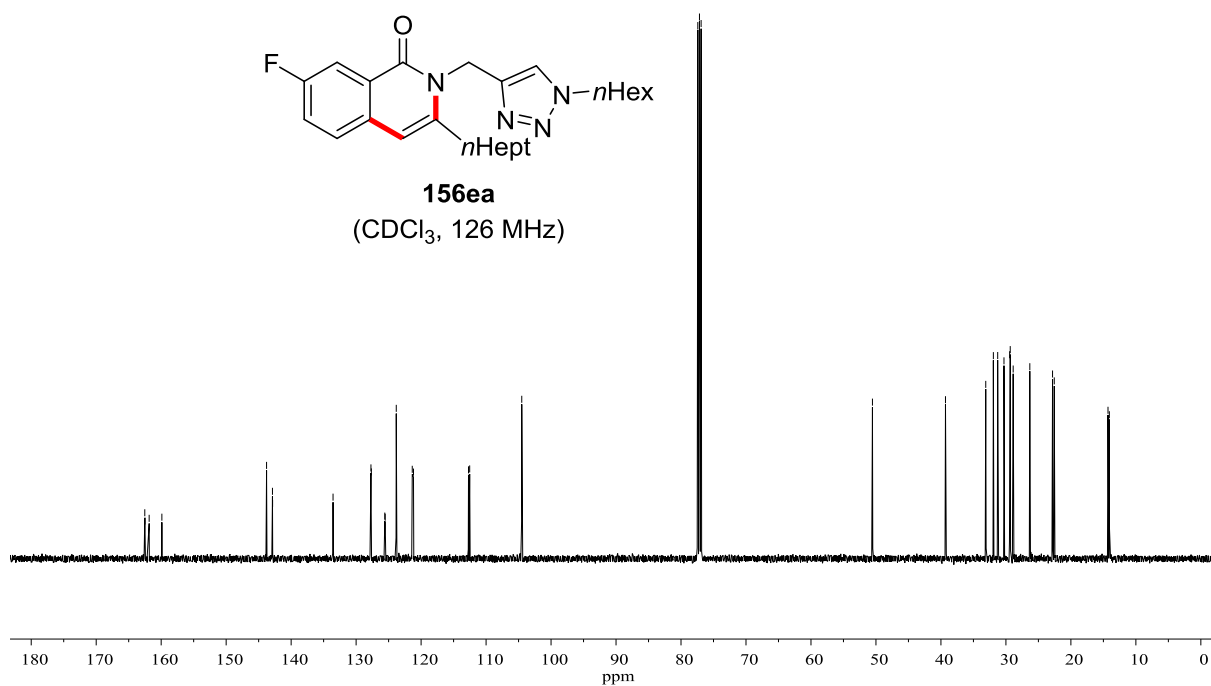
163.28
 144.09
 143.62
 136.94
 132.33
 127.70
 125.82
 125.39
 124.26
 123.75
 105.15
 77.41
 77.16
 76.91
 50.50
 39.22
 33.20
 31.94
 31.27
 30.30
 29.44
 29.34
 28.92
 26.33
 22.83
 22.56
 14.29
 14.09



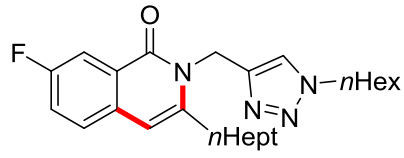




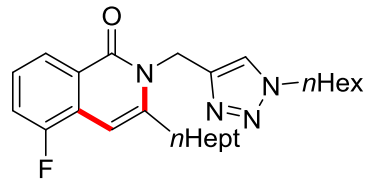
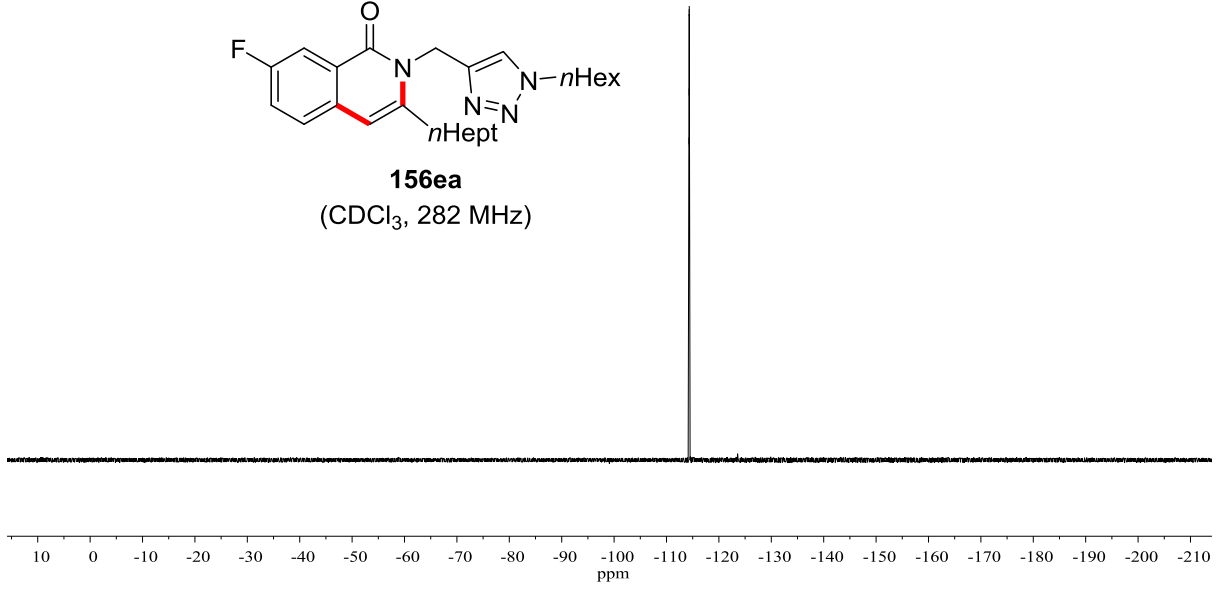
- 162.52
- 162.49
- 161.85
- 159.89
- 143.78
- 142.87
- 142.85
- 133.55
- 127.72
- 127.66
- 125.59
- 125.53
- 123.82
- 121.36
- 121.17
- 112.70
- 112.52
- 104.51
- 77.41
- 77.16
- 76.91
- 50.54
- 39.30
- 33.10
- 31.93
- 31.27
- 30.30
- 29.43
- 29.34
- 28.88
- 26.32
- 22.82
- 22.56
- 14.29
- 14.08



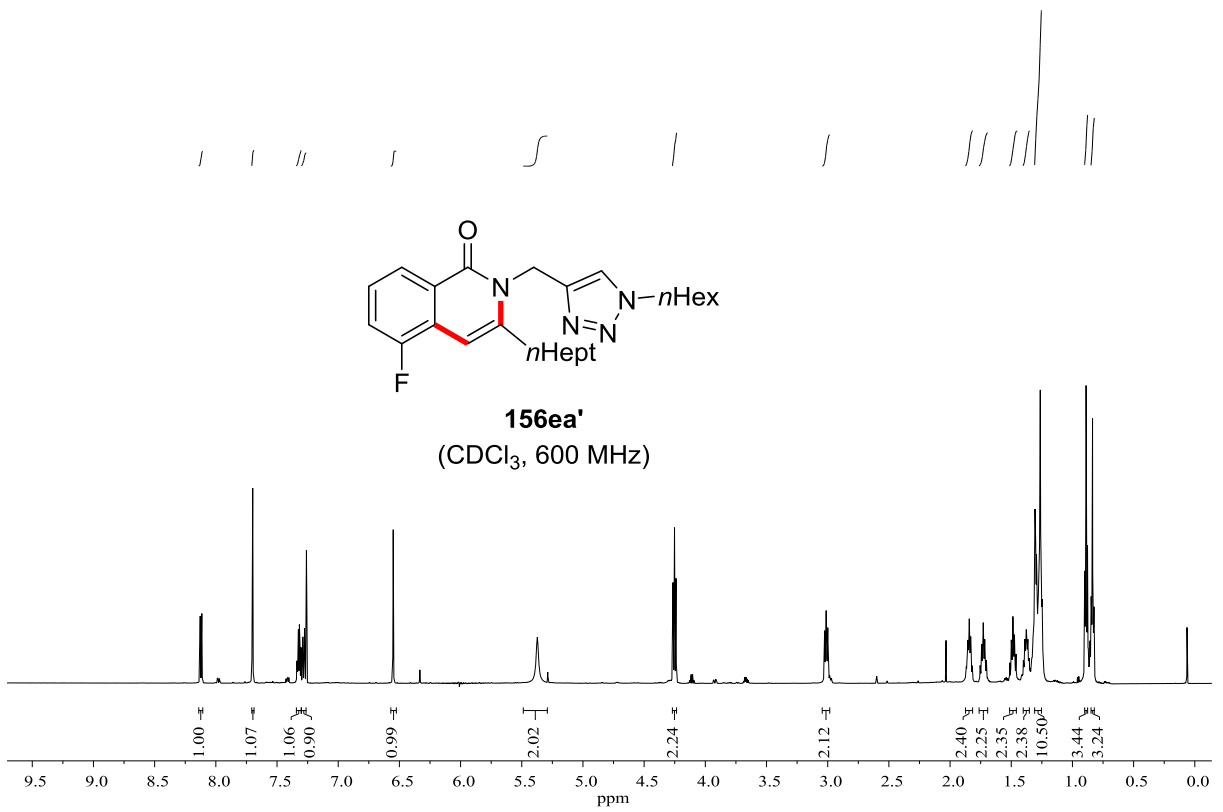
-114.30
-114.31
-114.33
-114.34
-114.36
-114.38

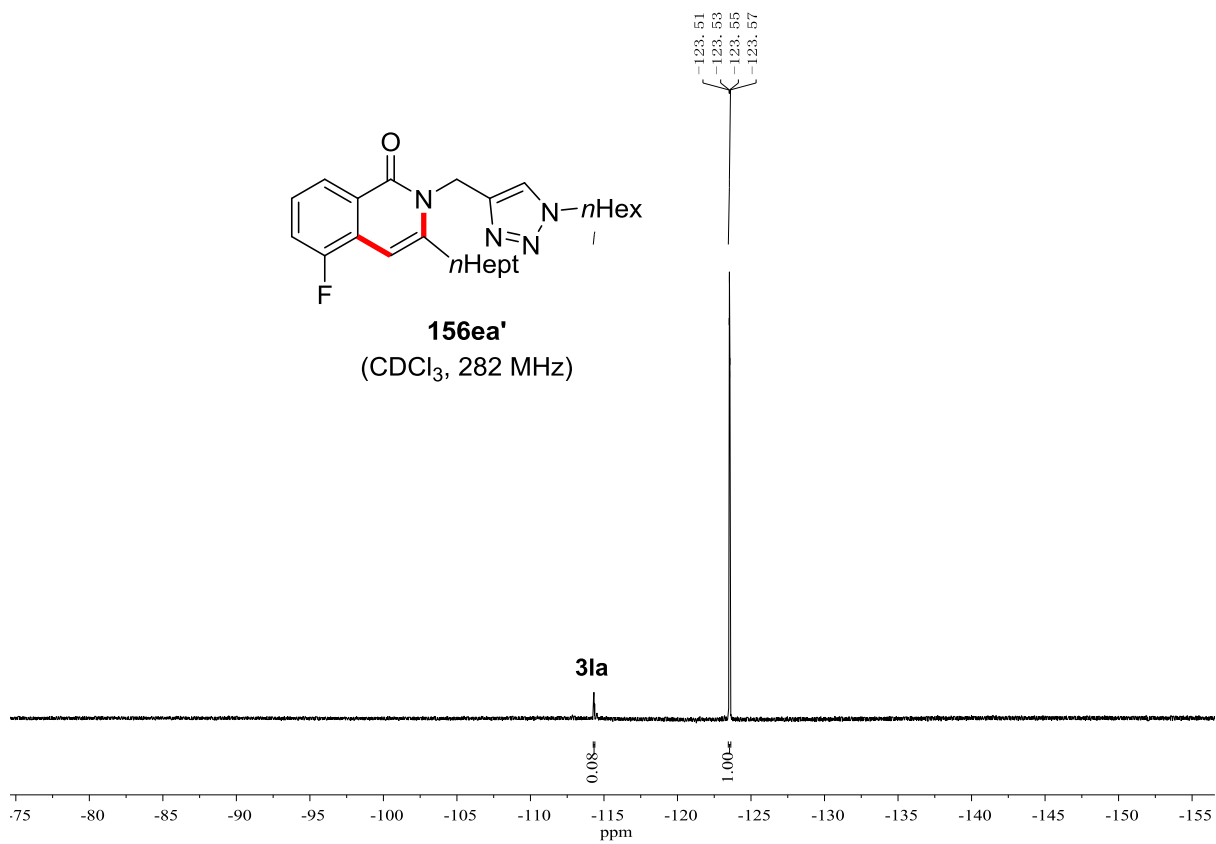
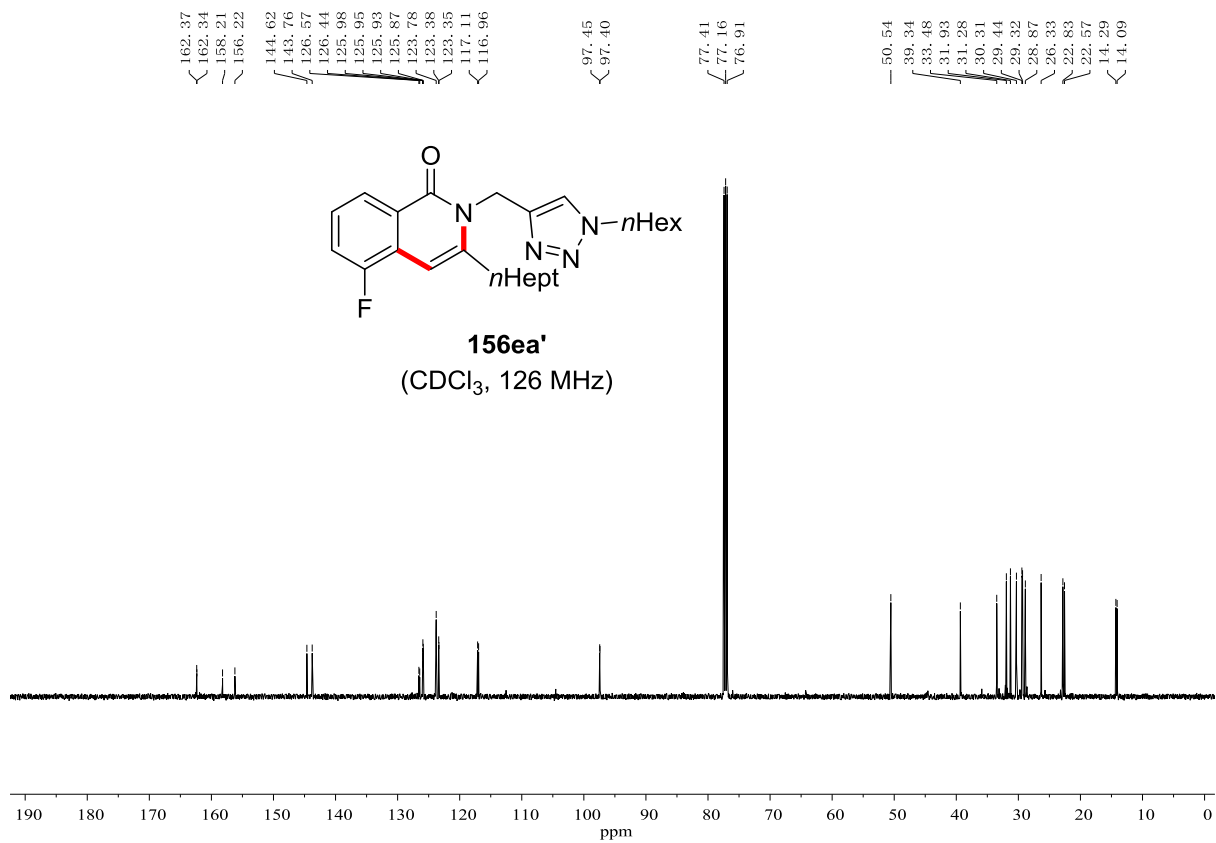


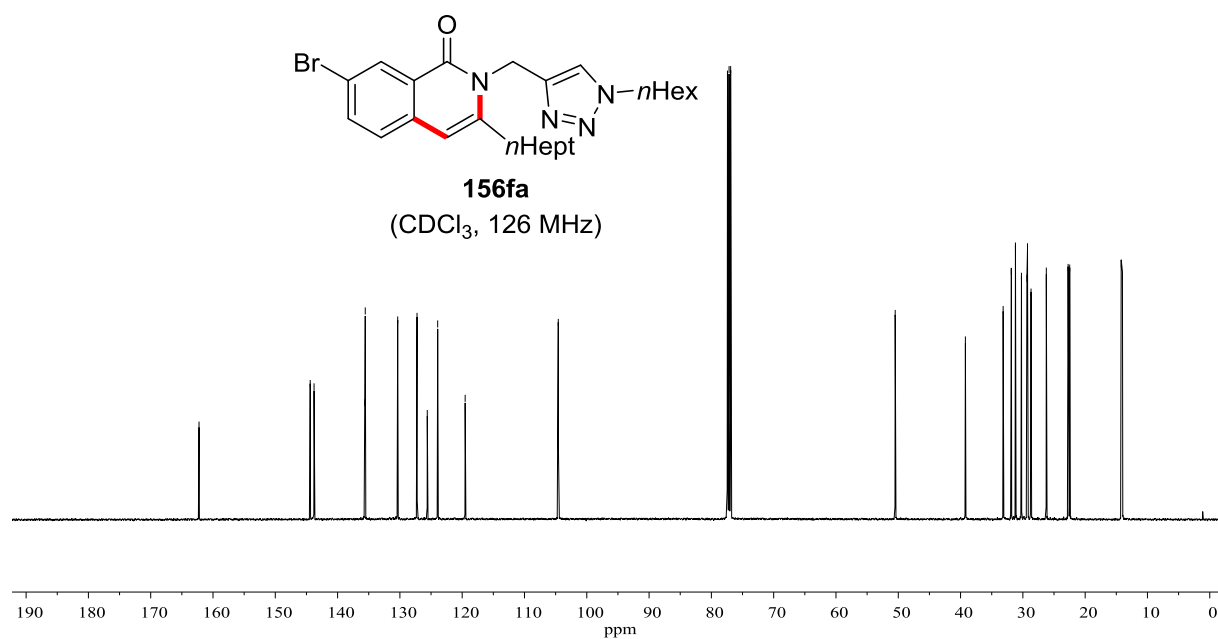
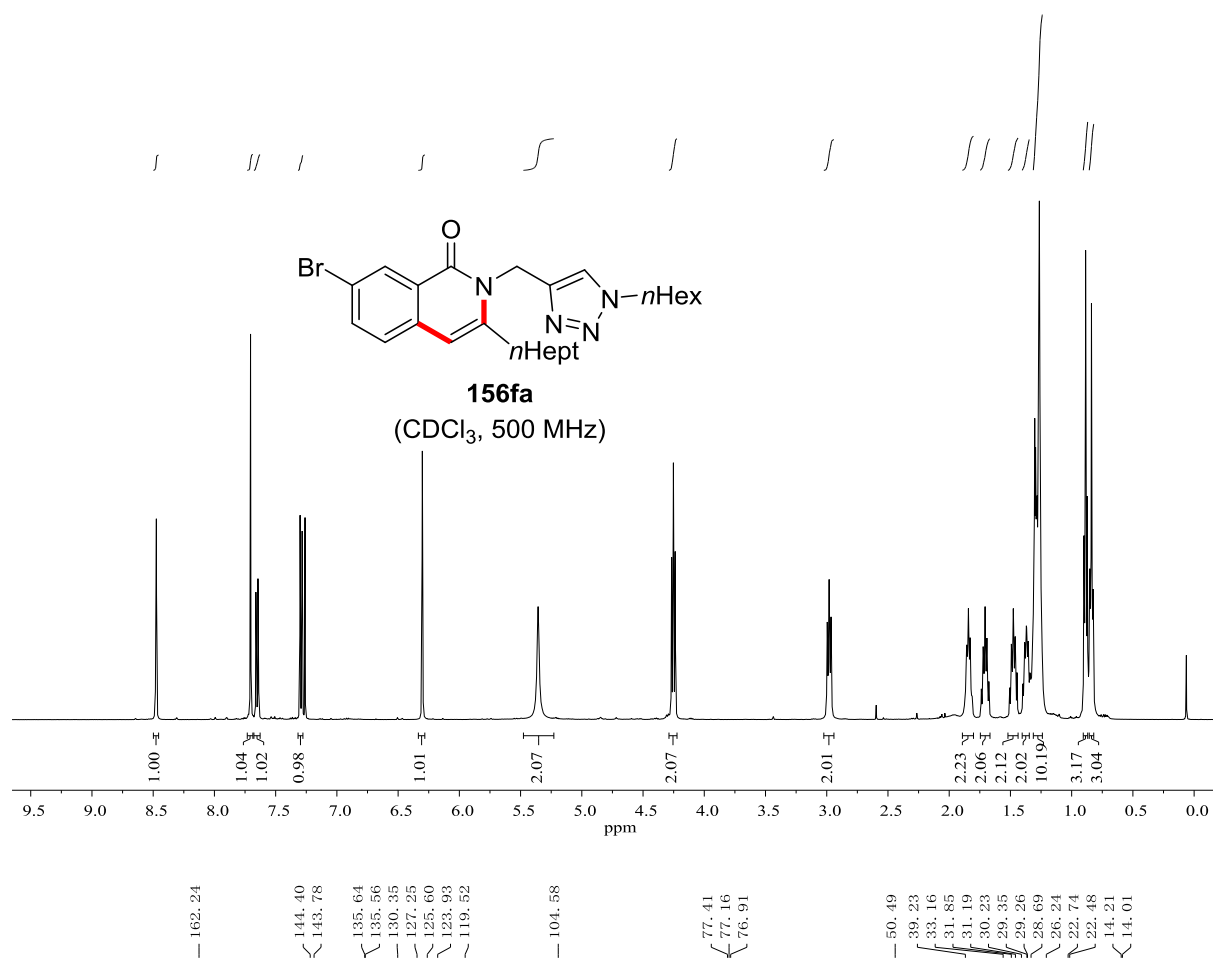
156ea
(CDCl₃, 282 MHz)

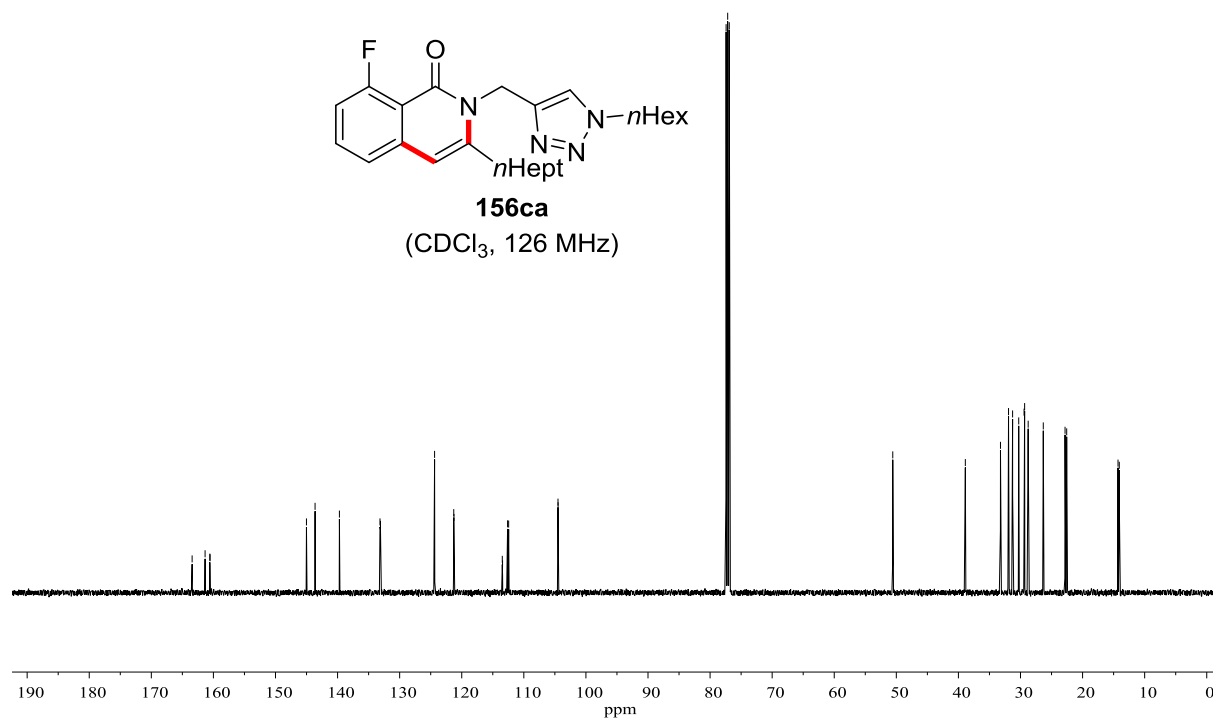
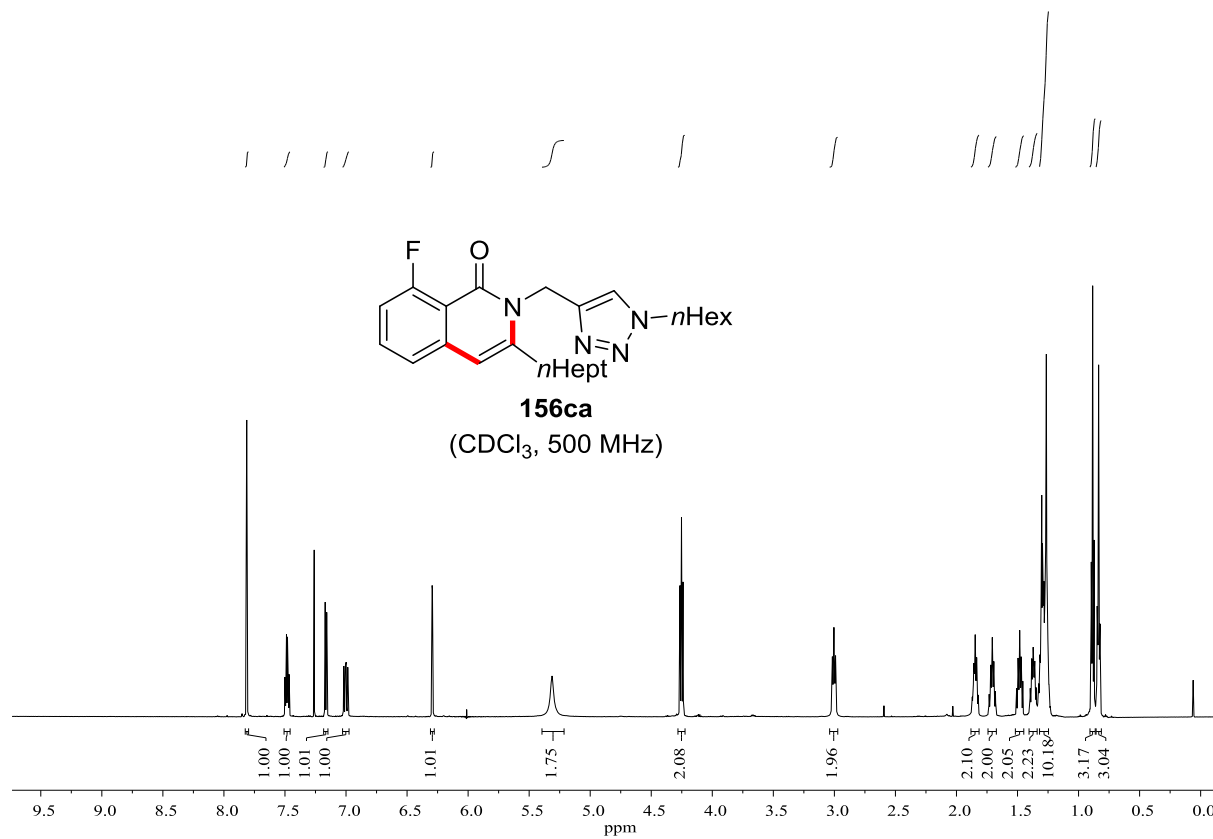


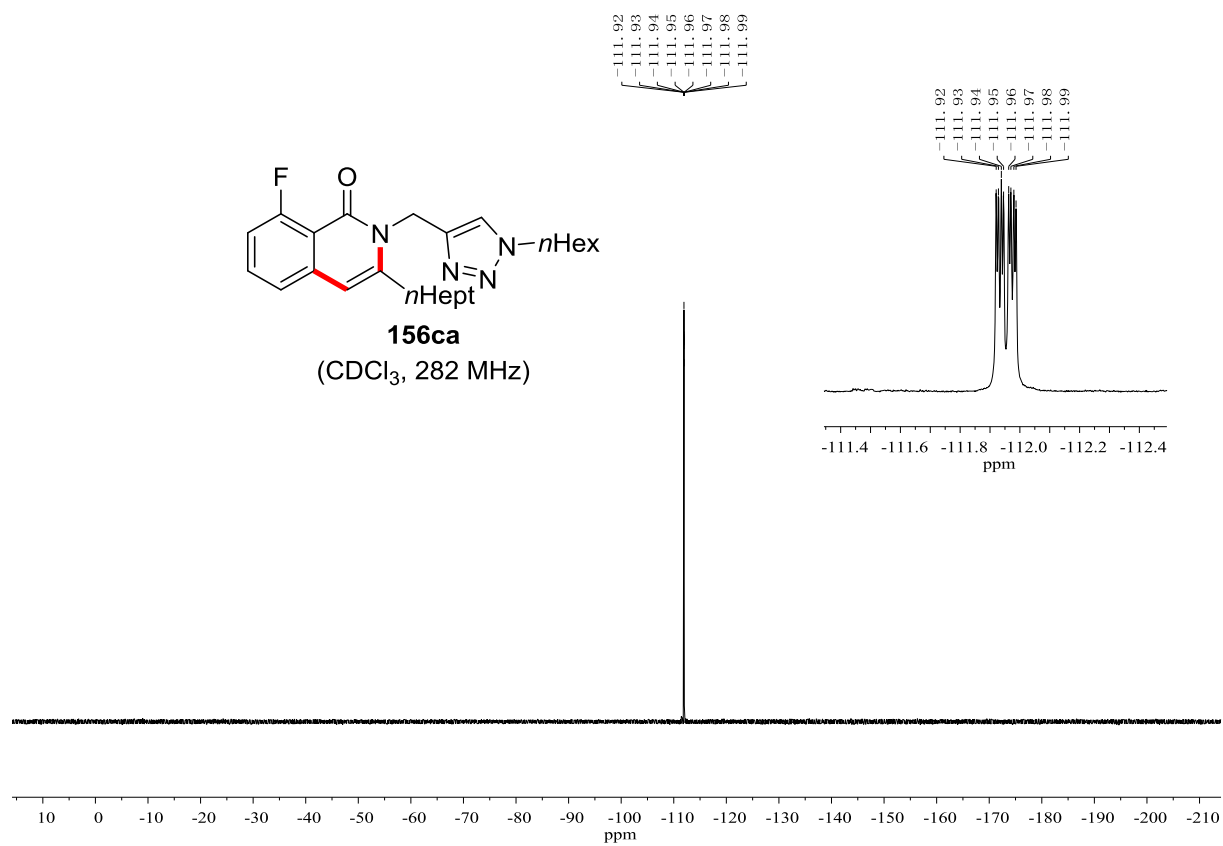
156ea'
(CDCl₃, 600 MHz)

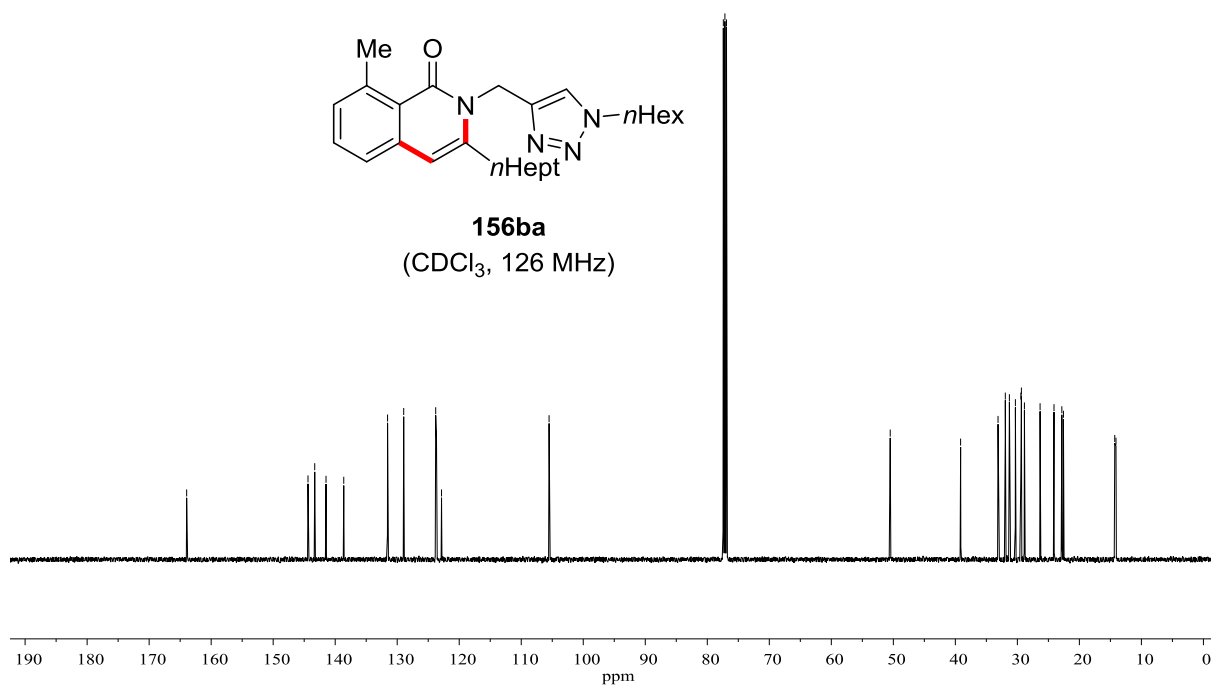
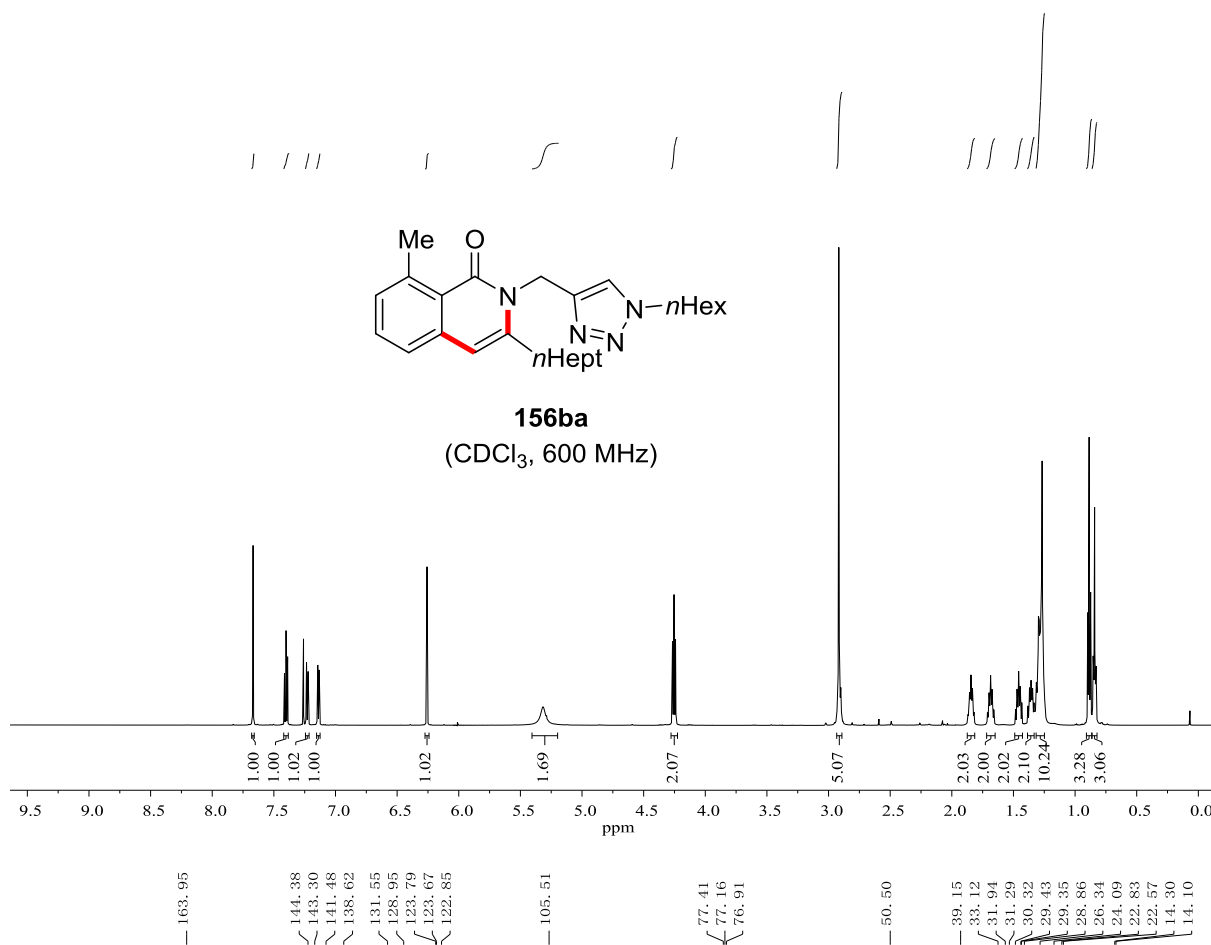


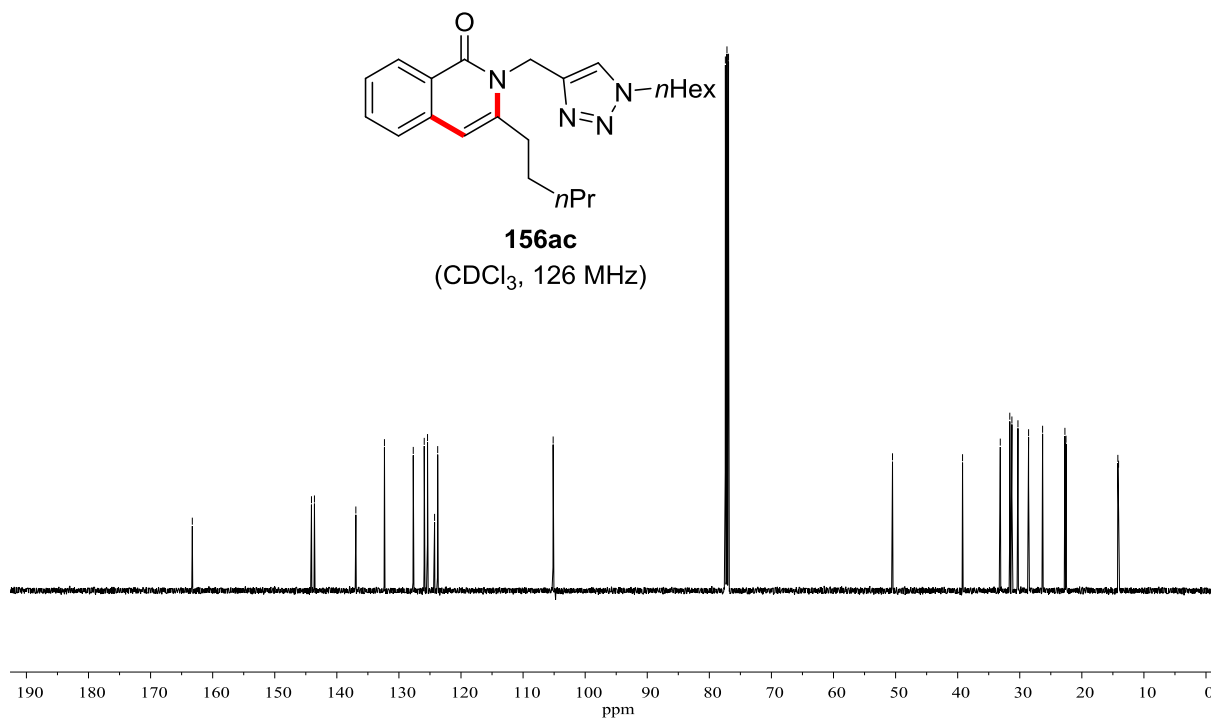
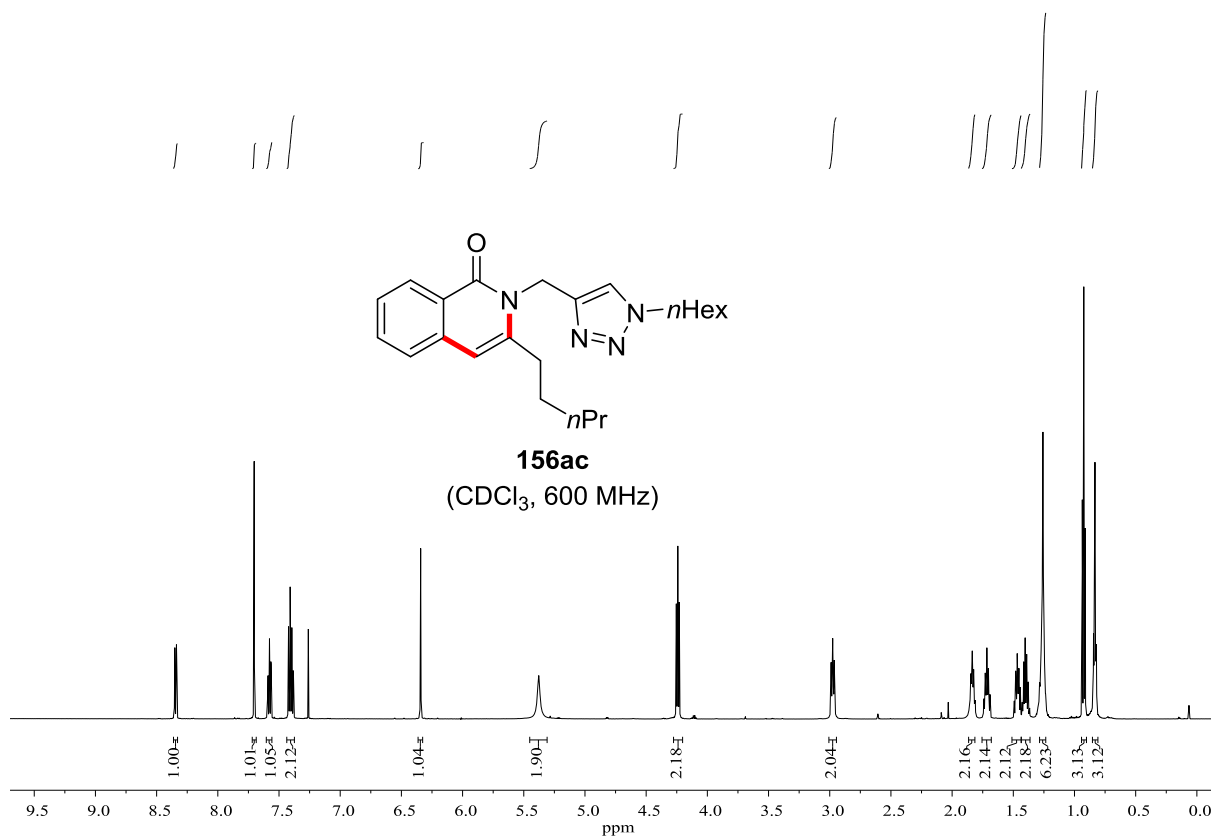


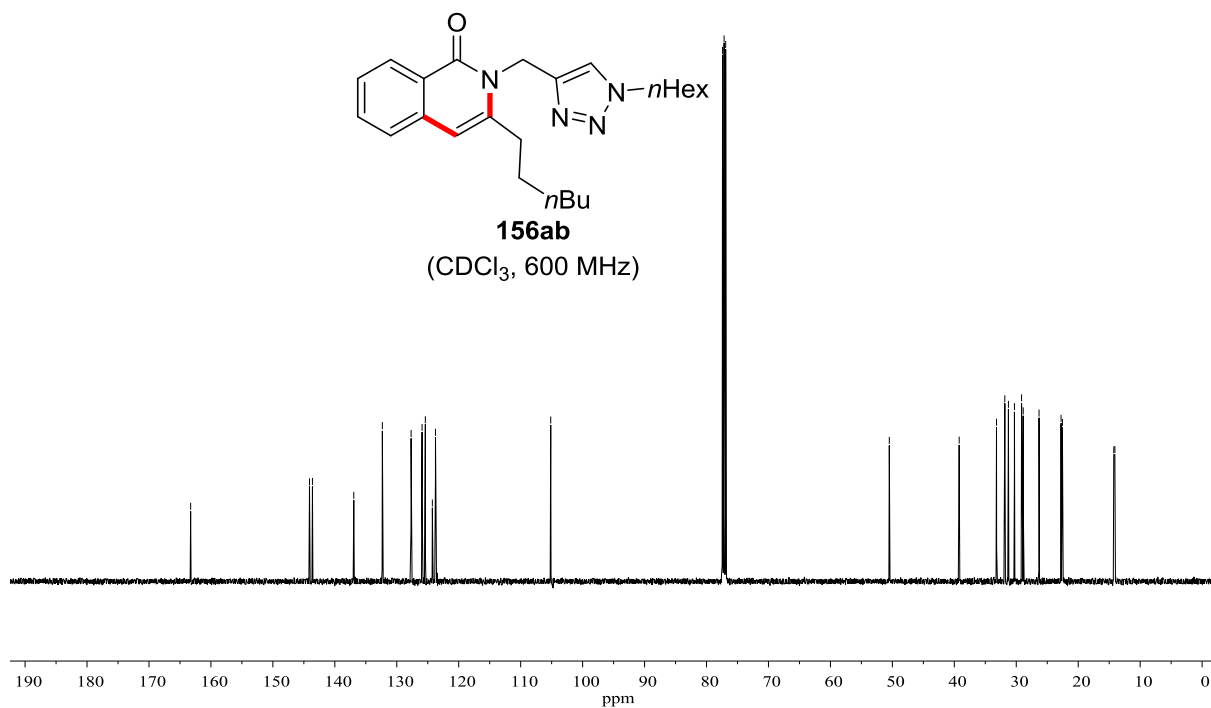
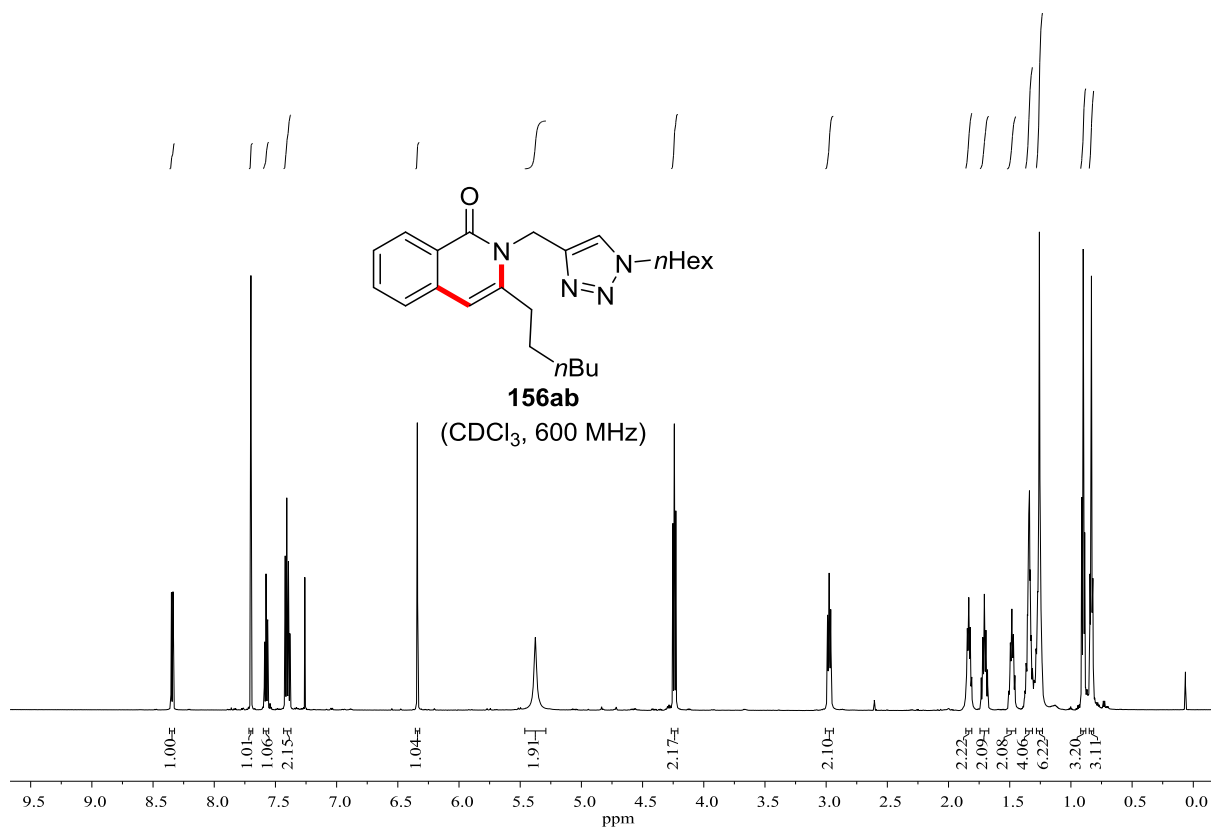


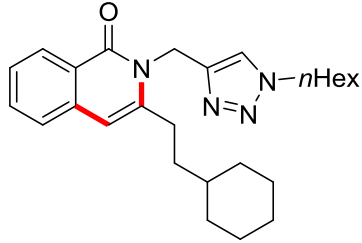




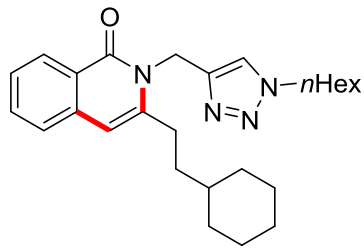
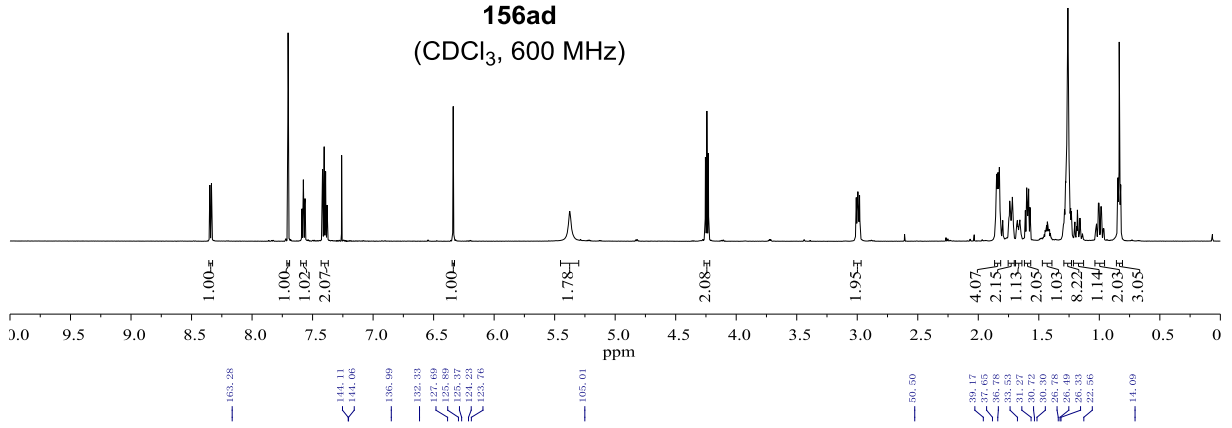




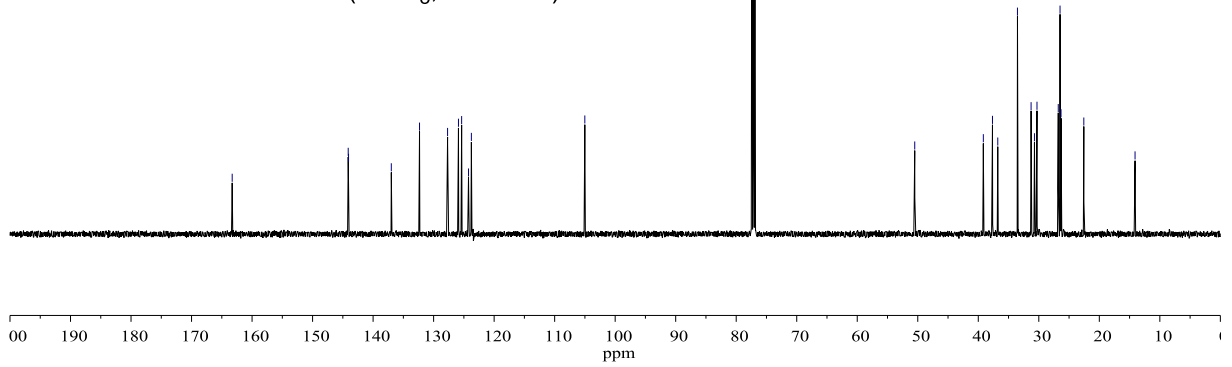


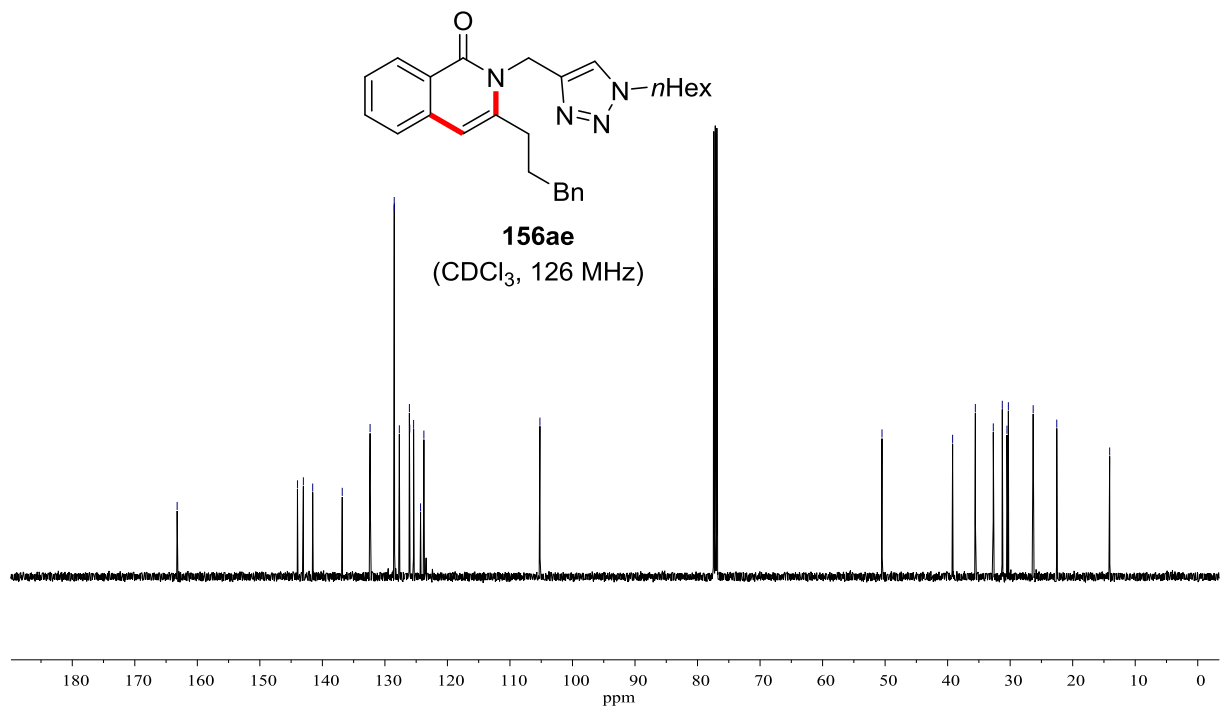
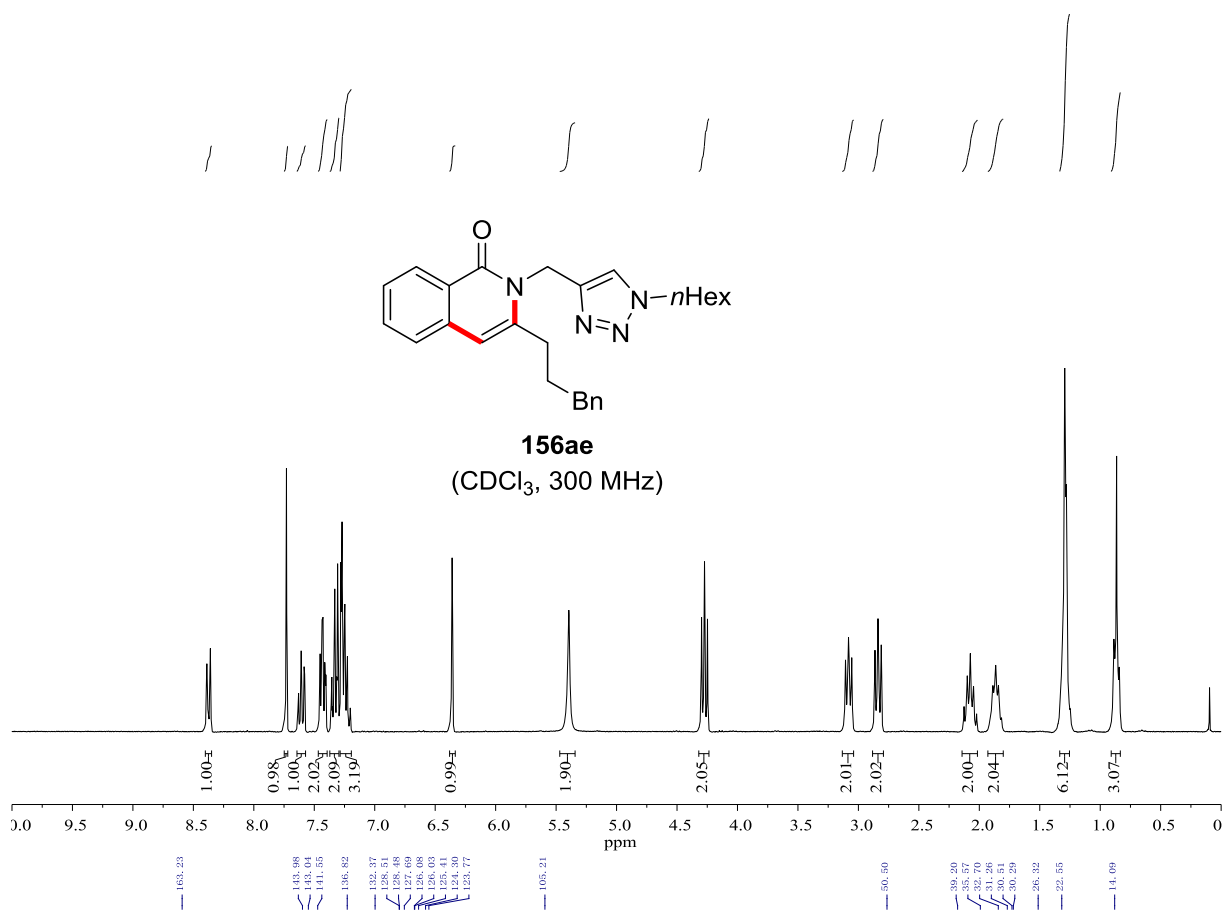


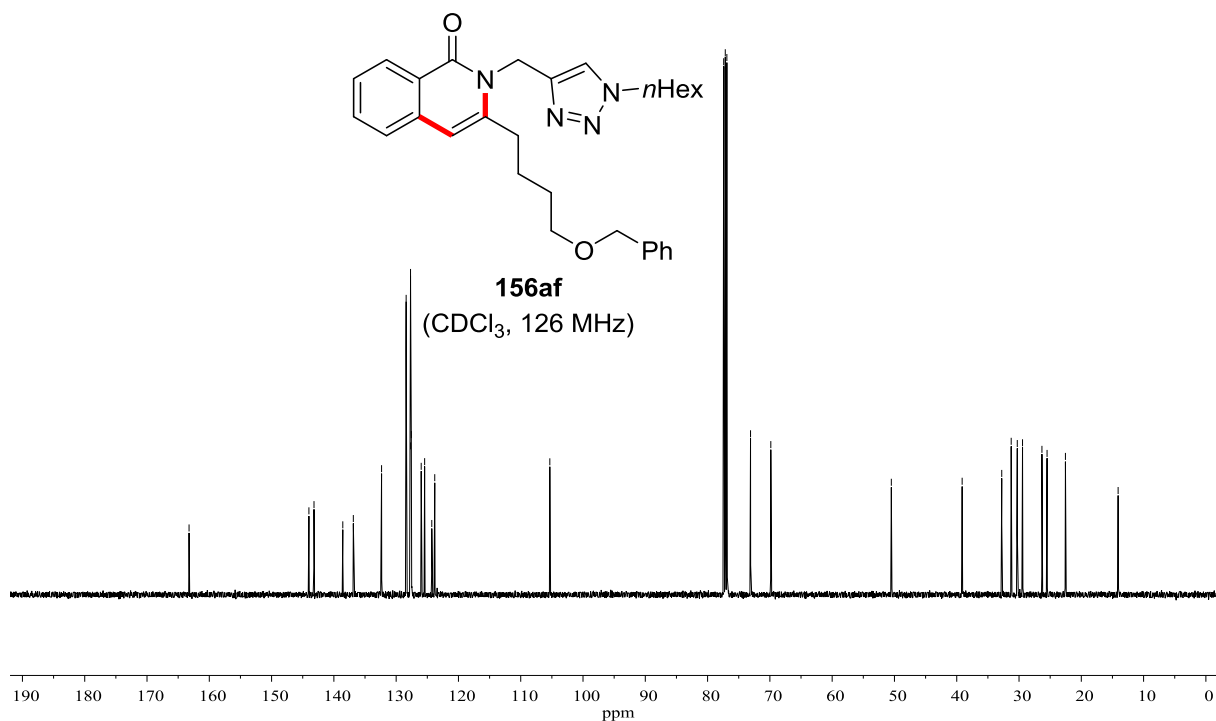
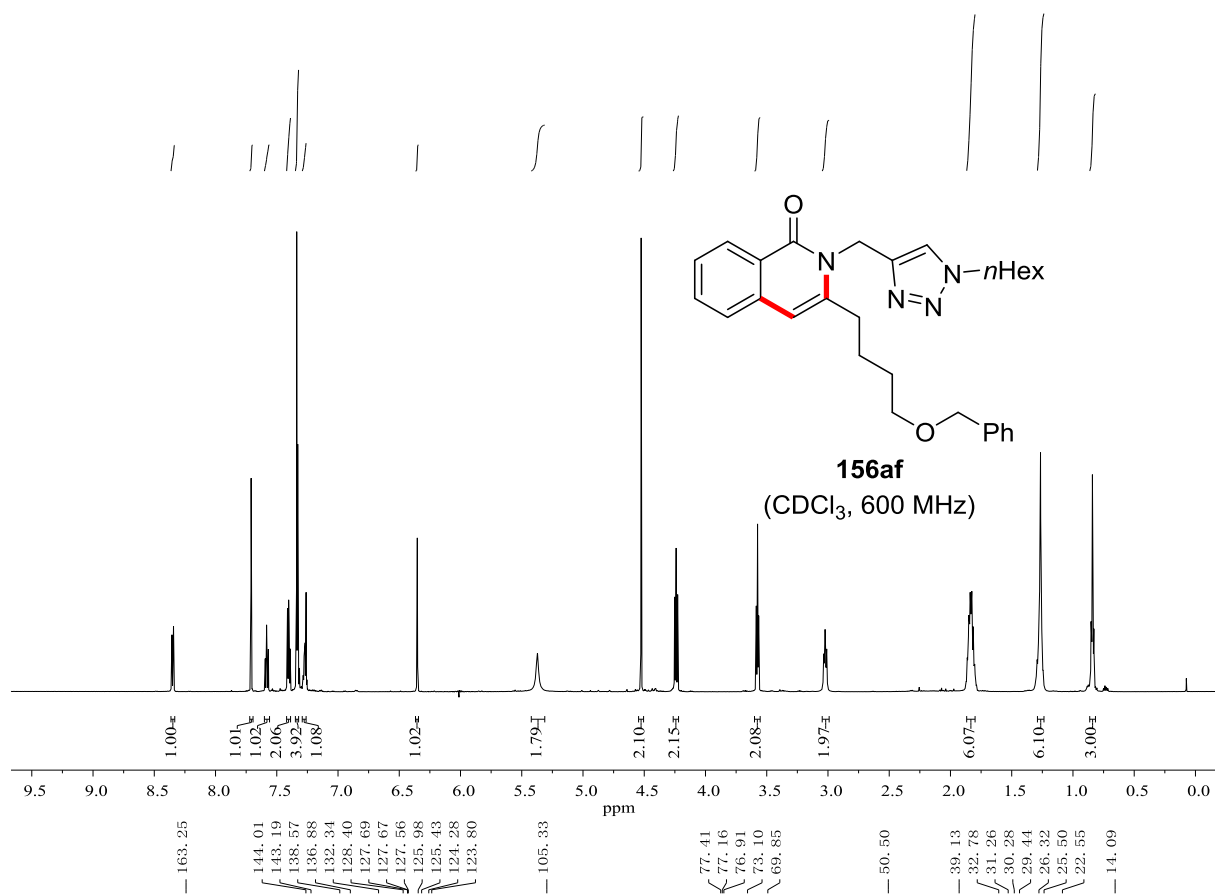
156ad
(CDCl₃, 600 MHz)

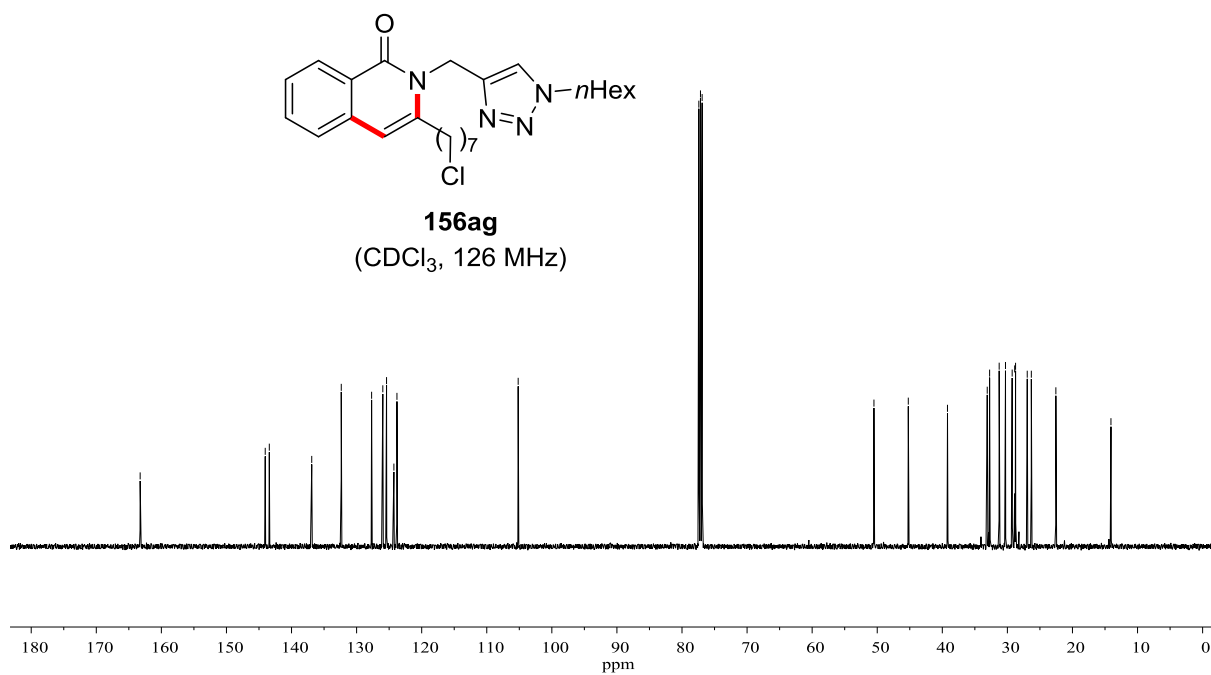
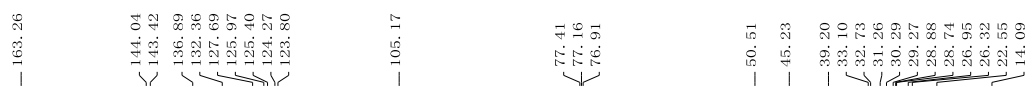
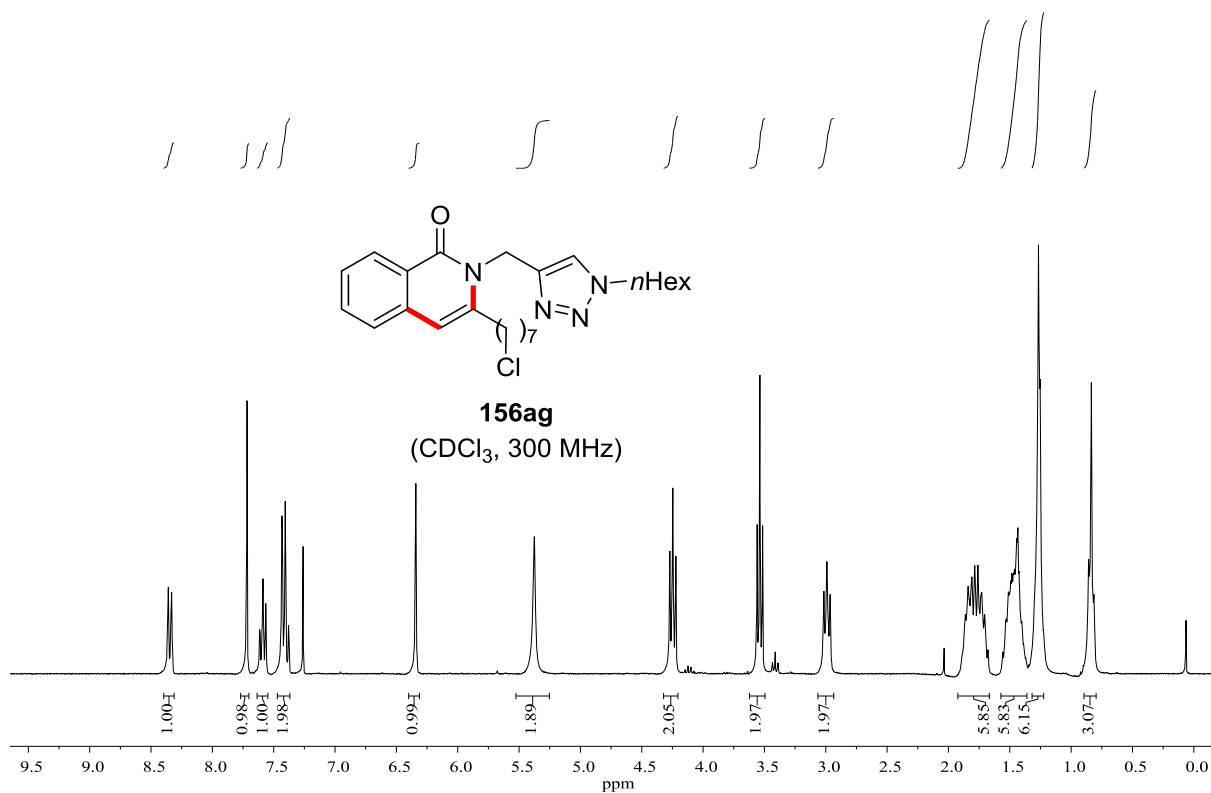


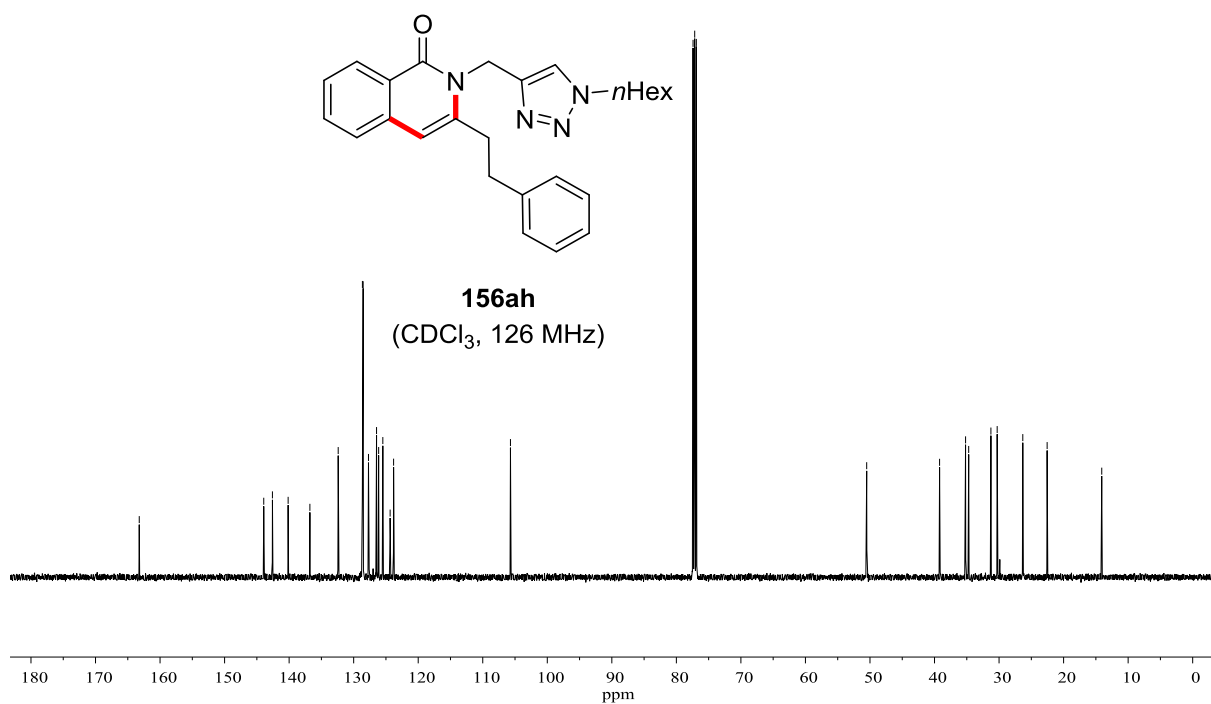
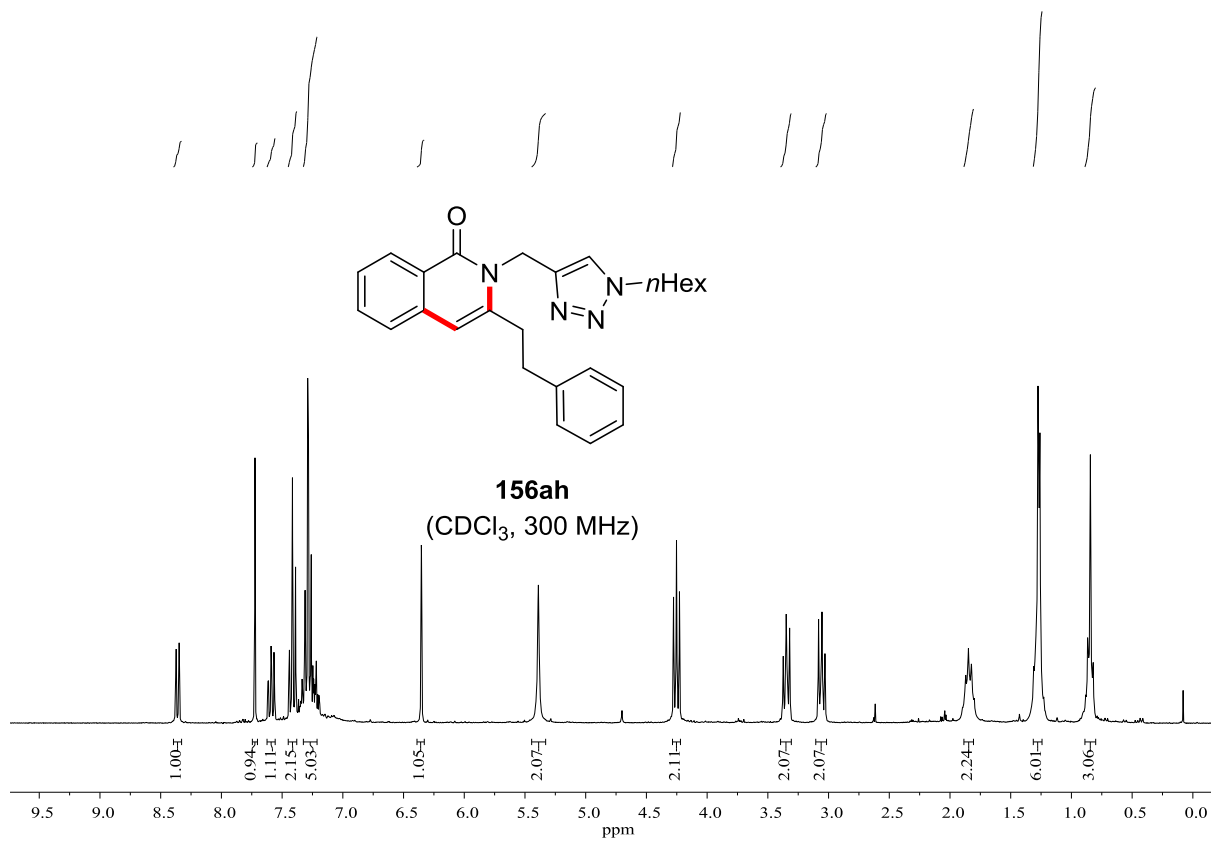
156ad
(CDCl₃, 126 MHz)

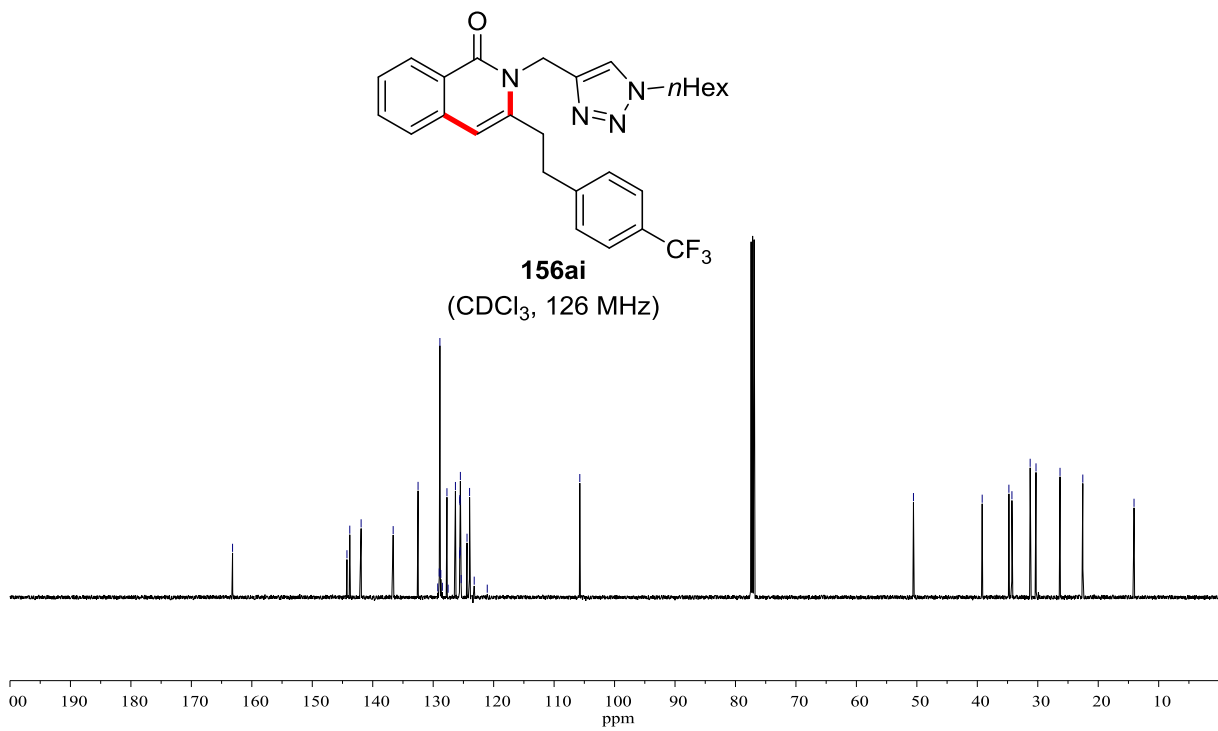
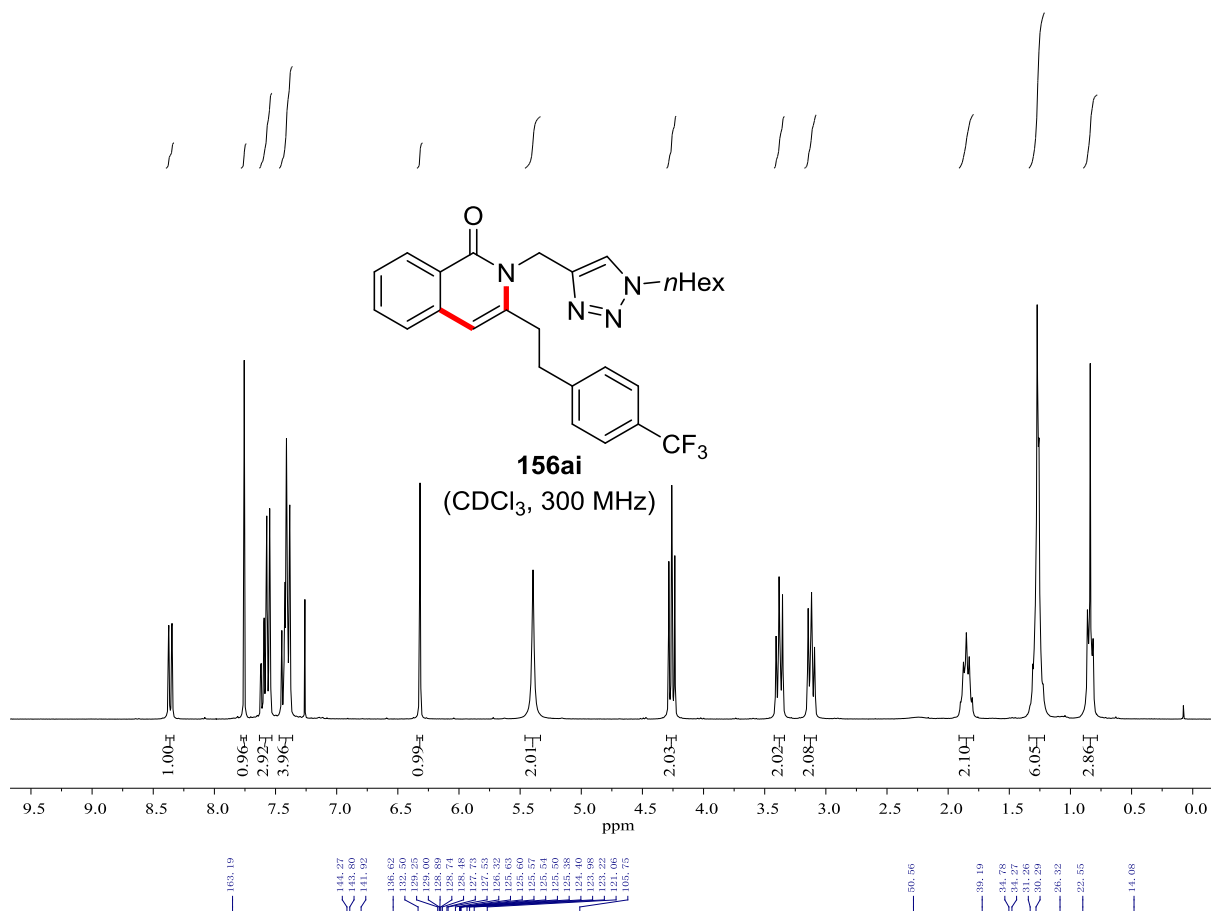




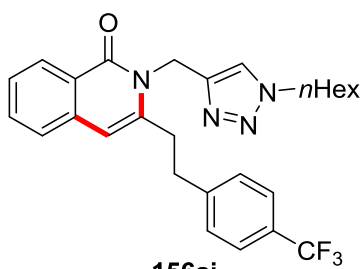




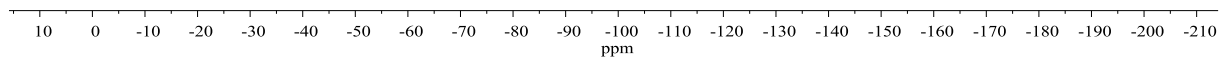


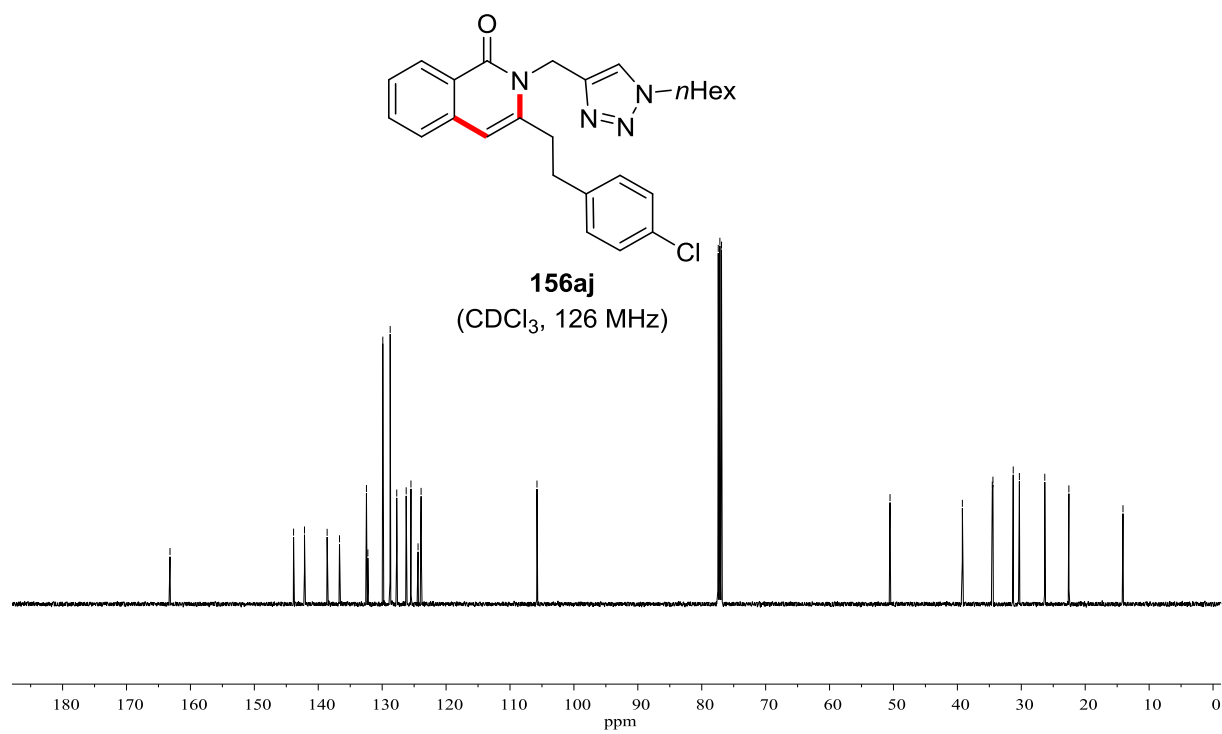
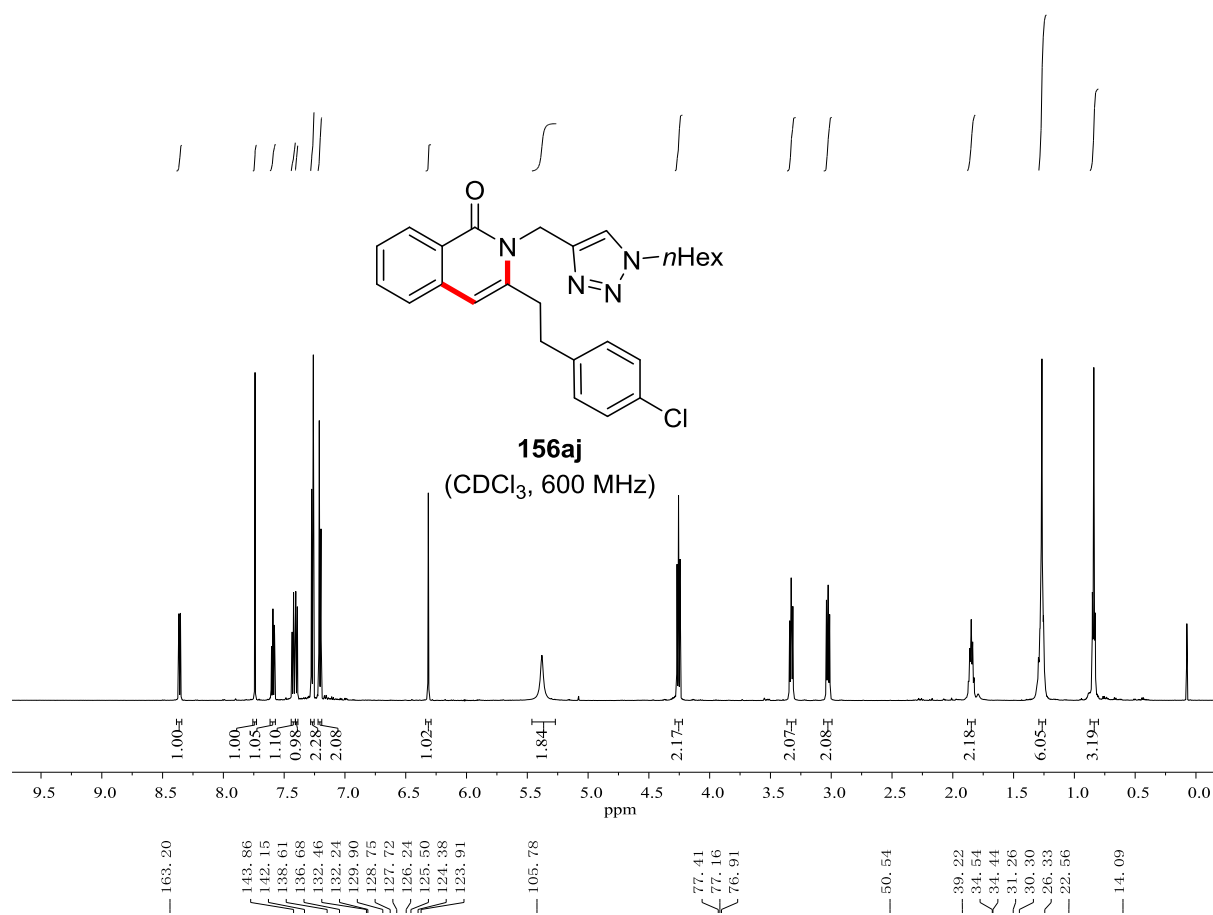


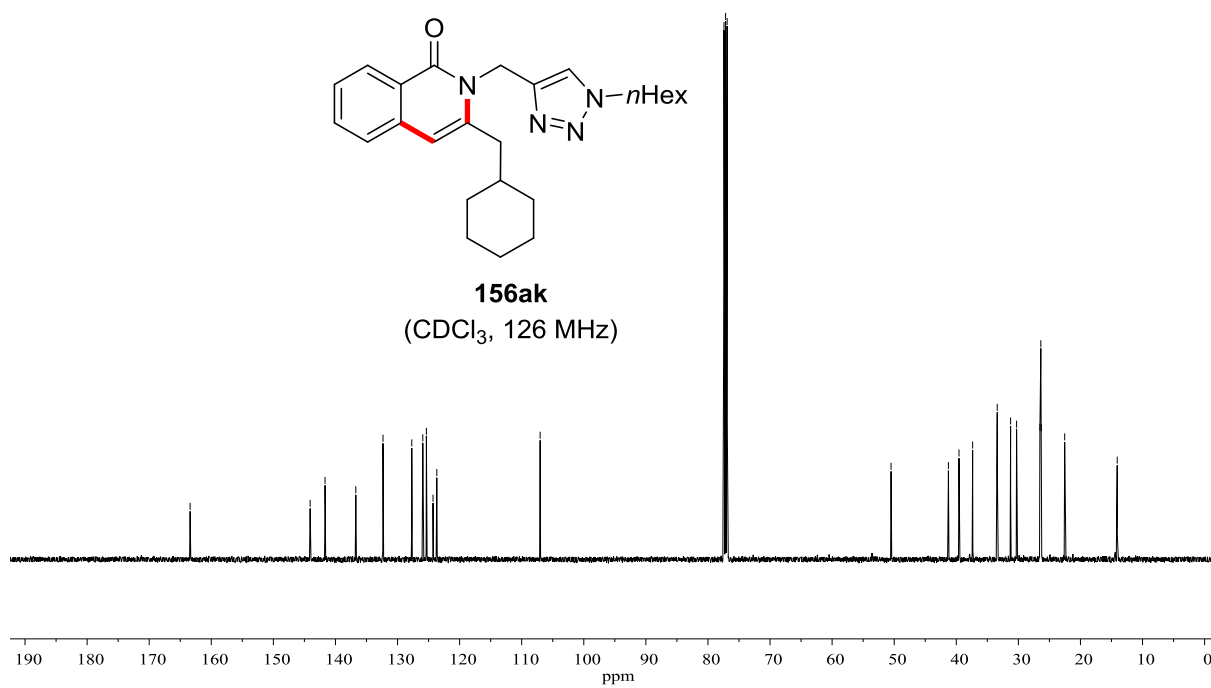
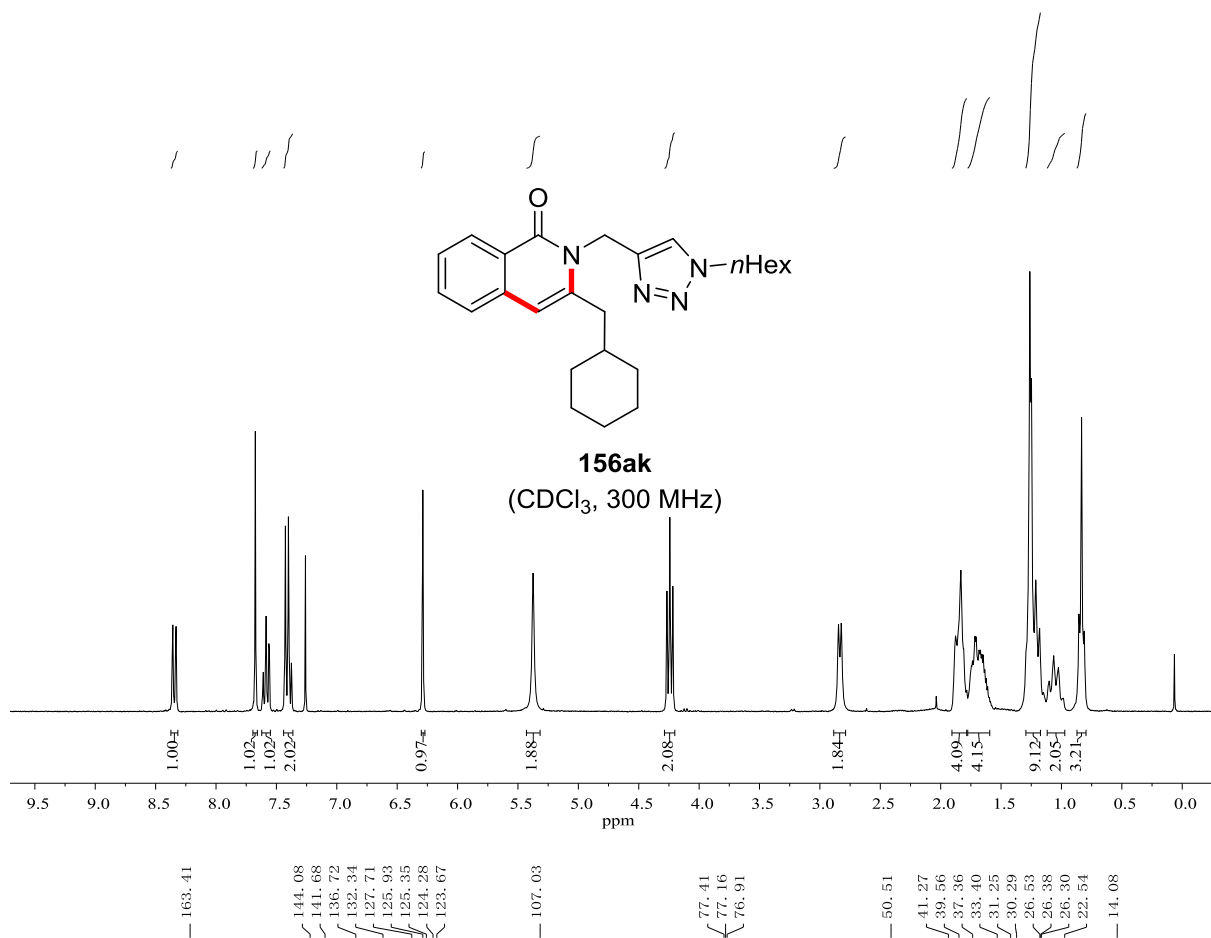
02.11

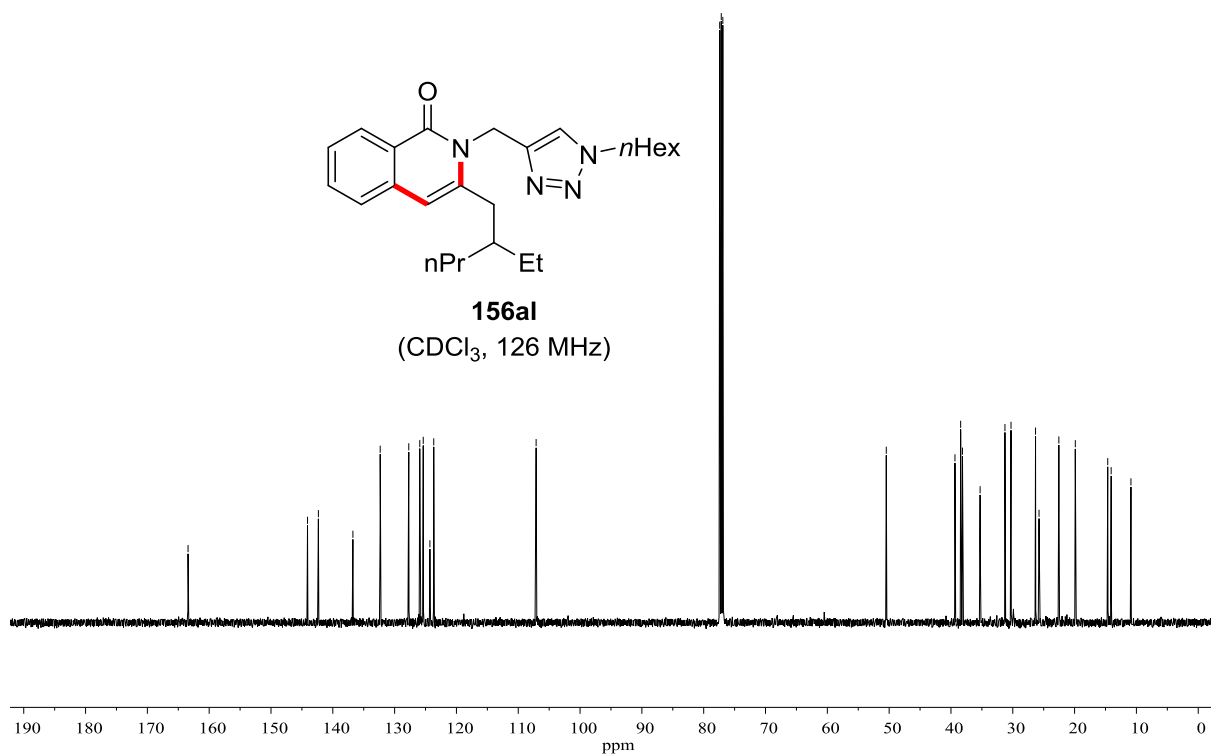
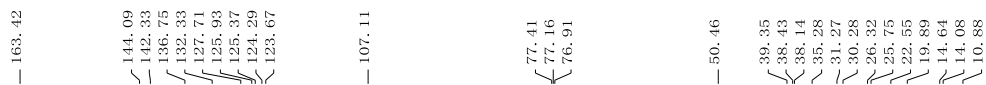
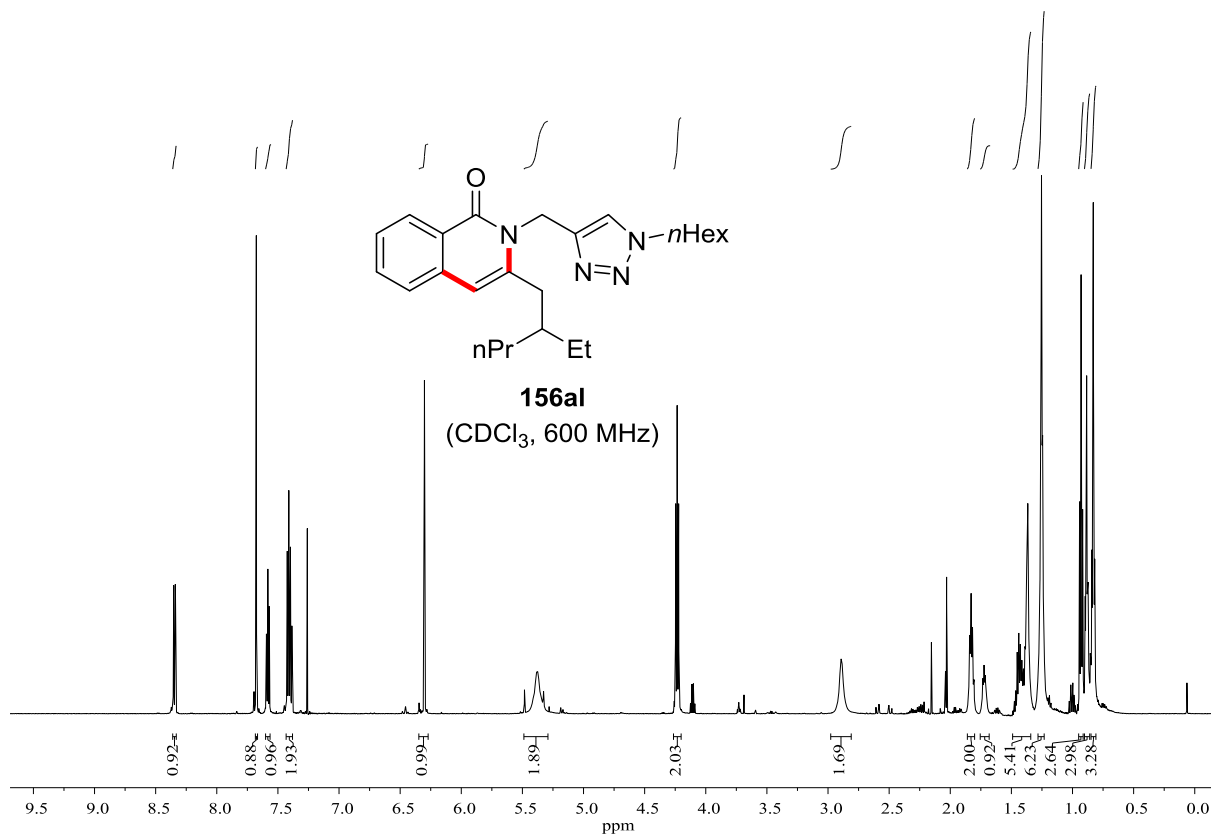


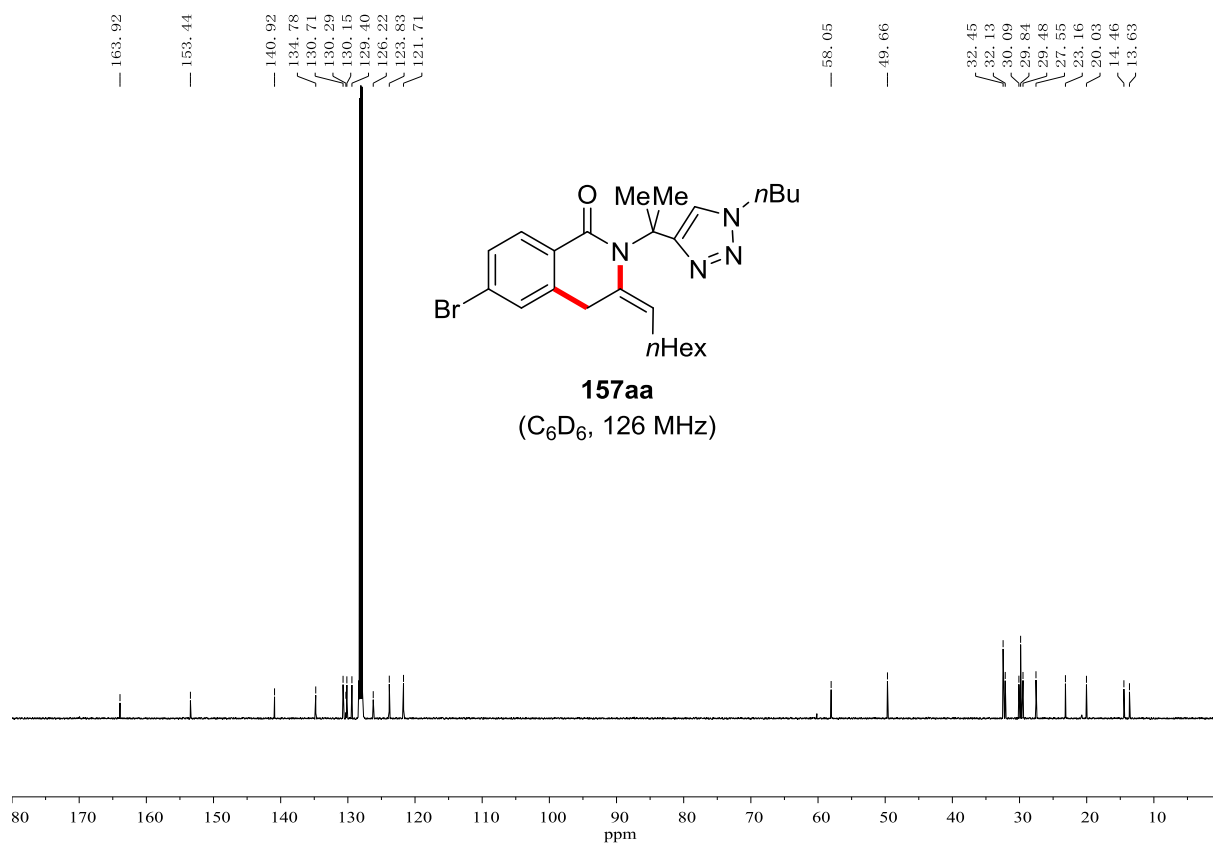
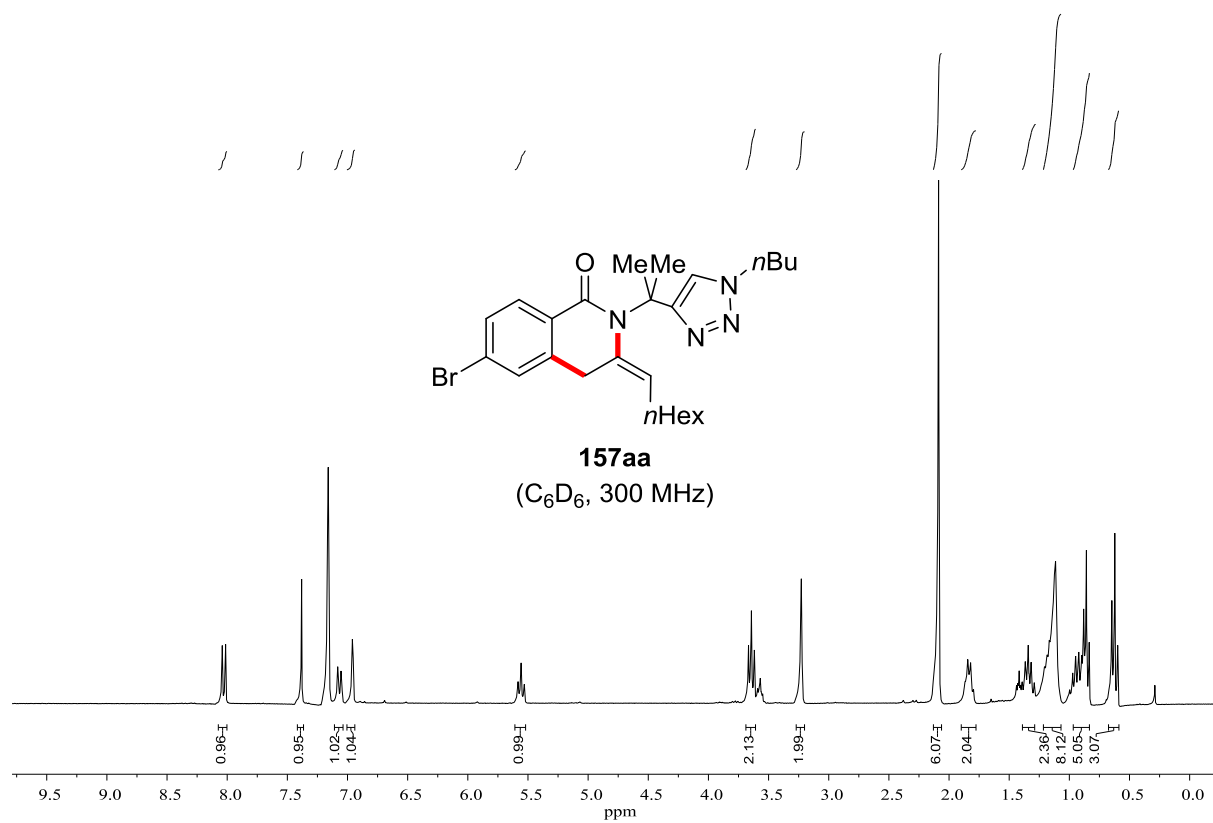
156ai
(CDCl₃, 282 MHz)

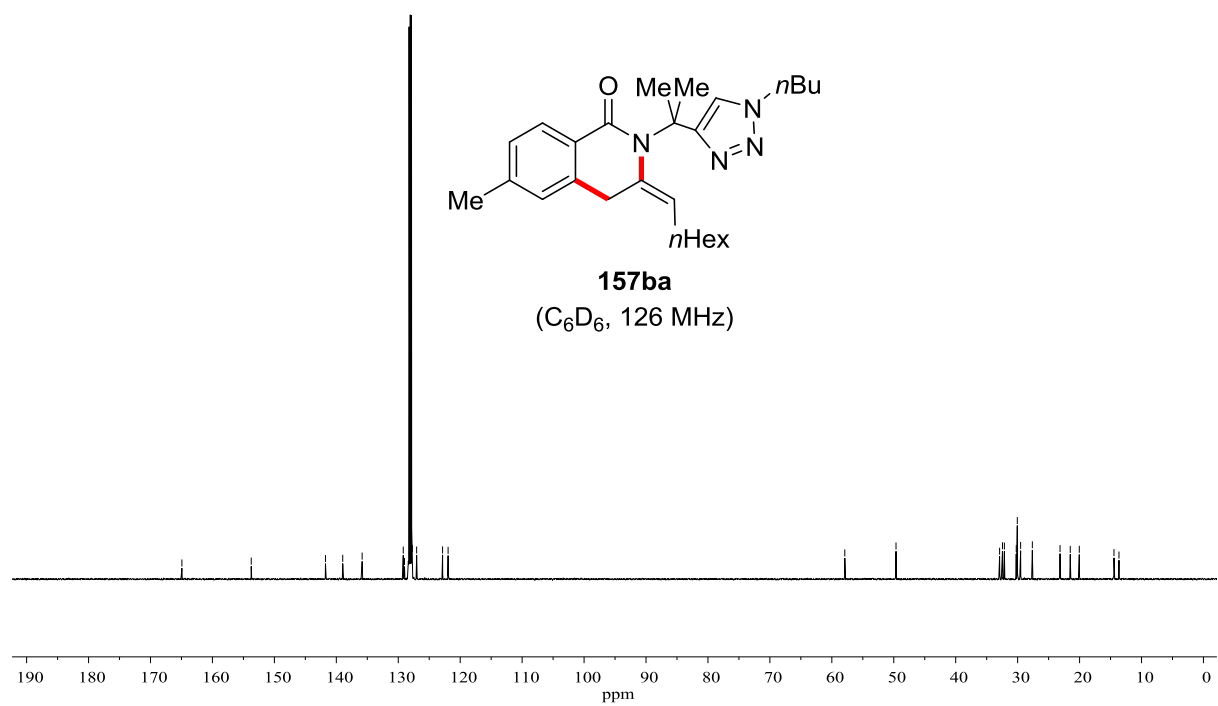
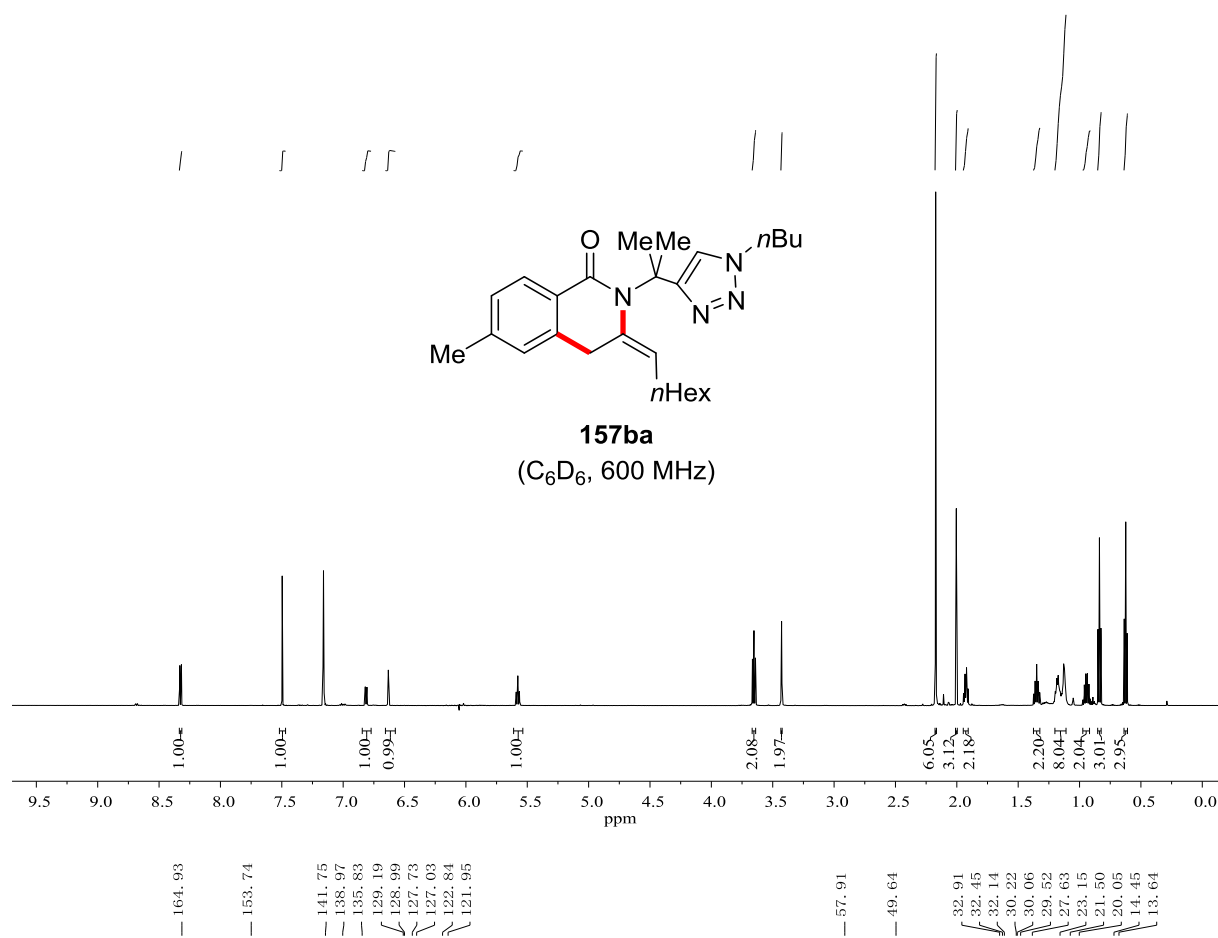


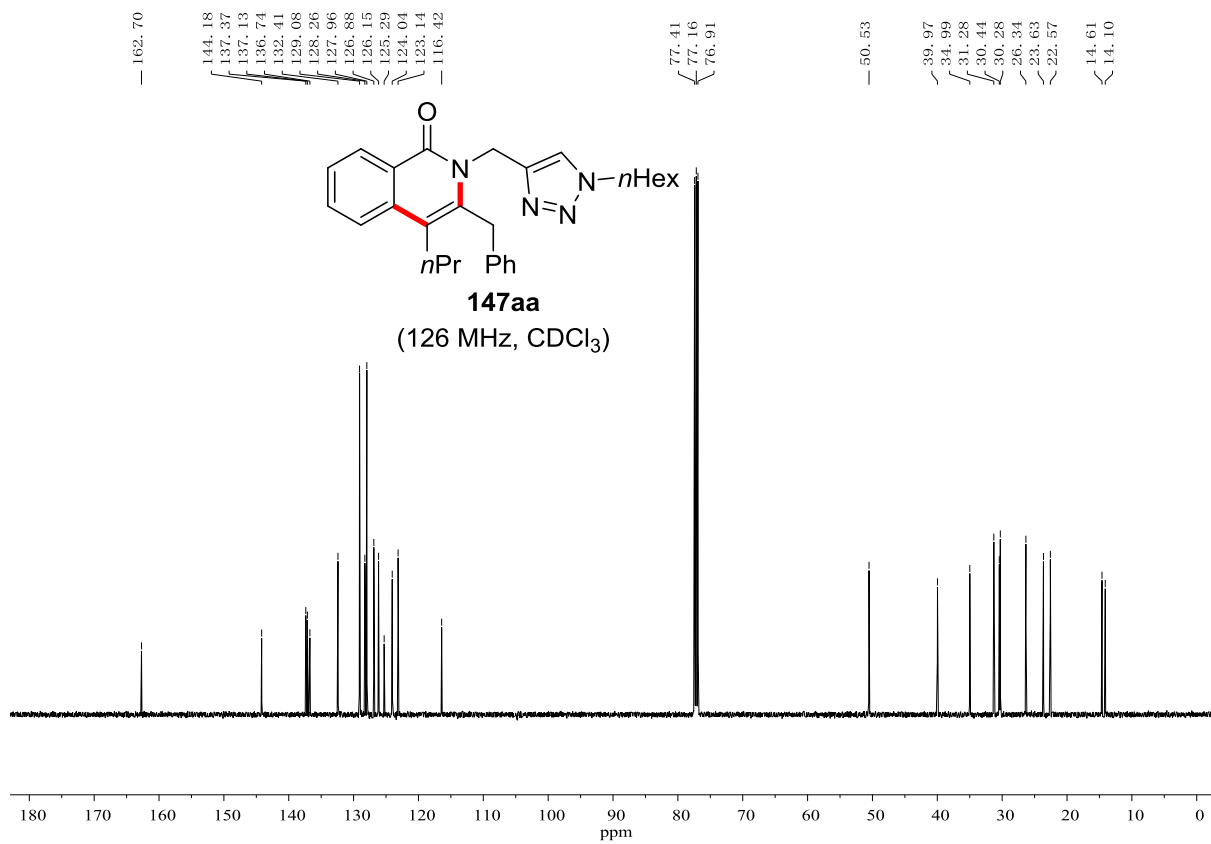
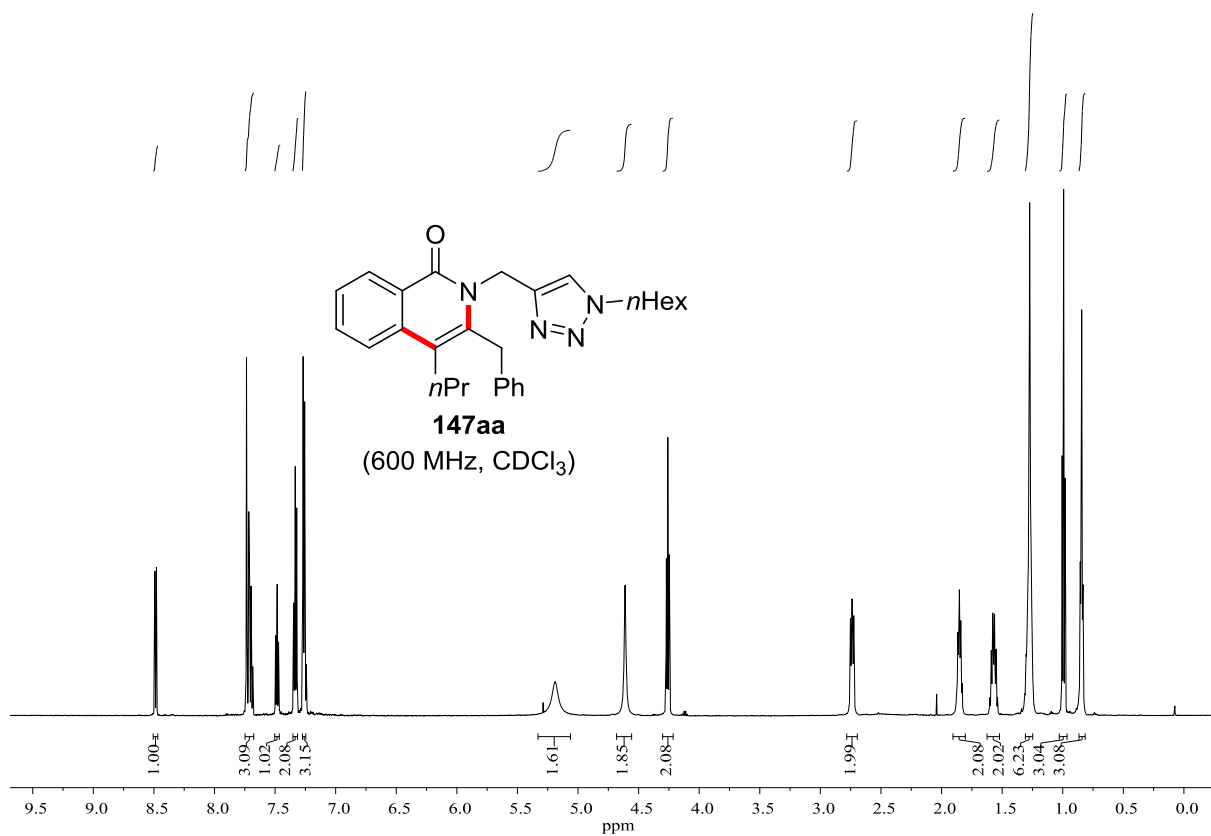


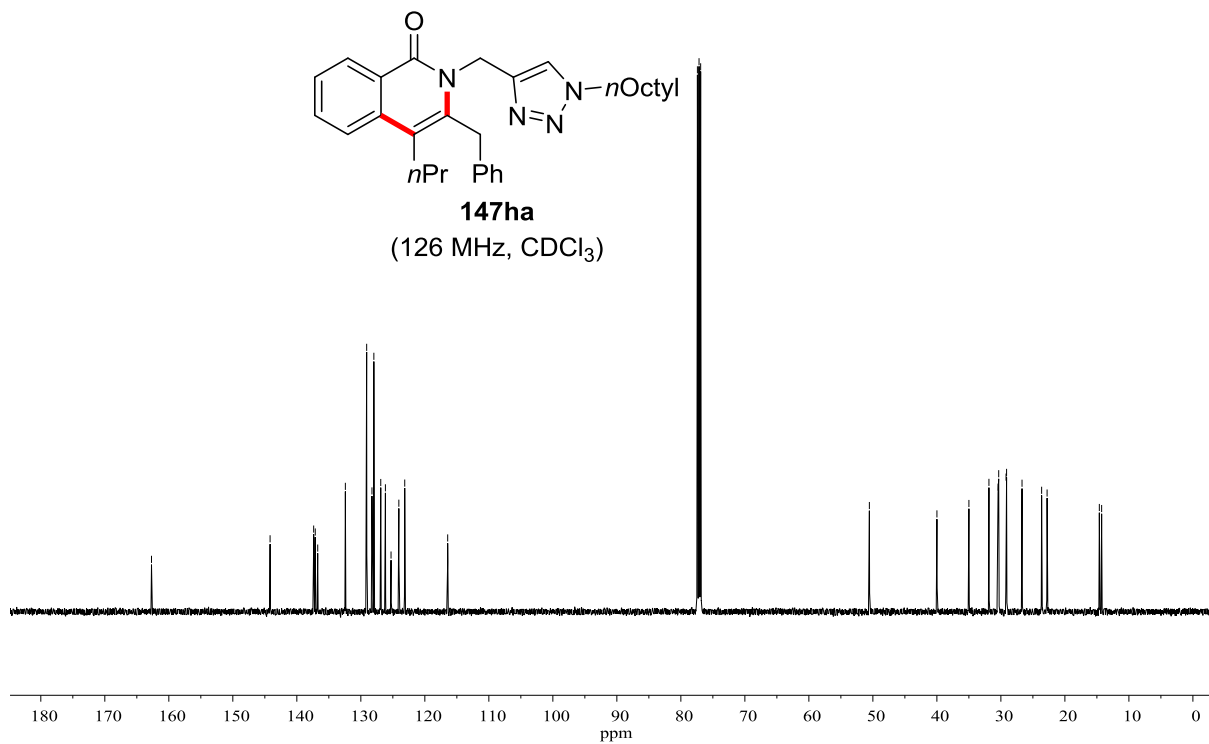
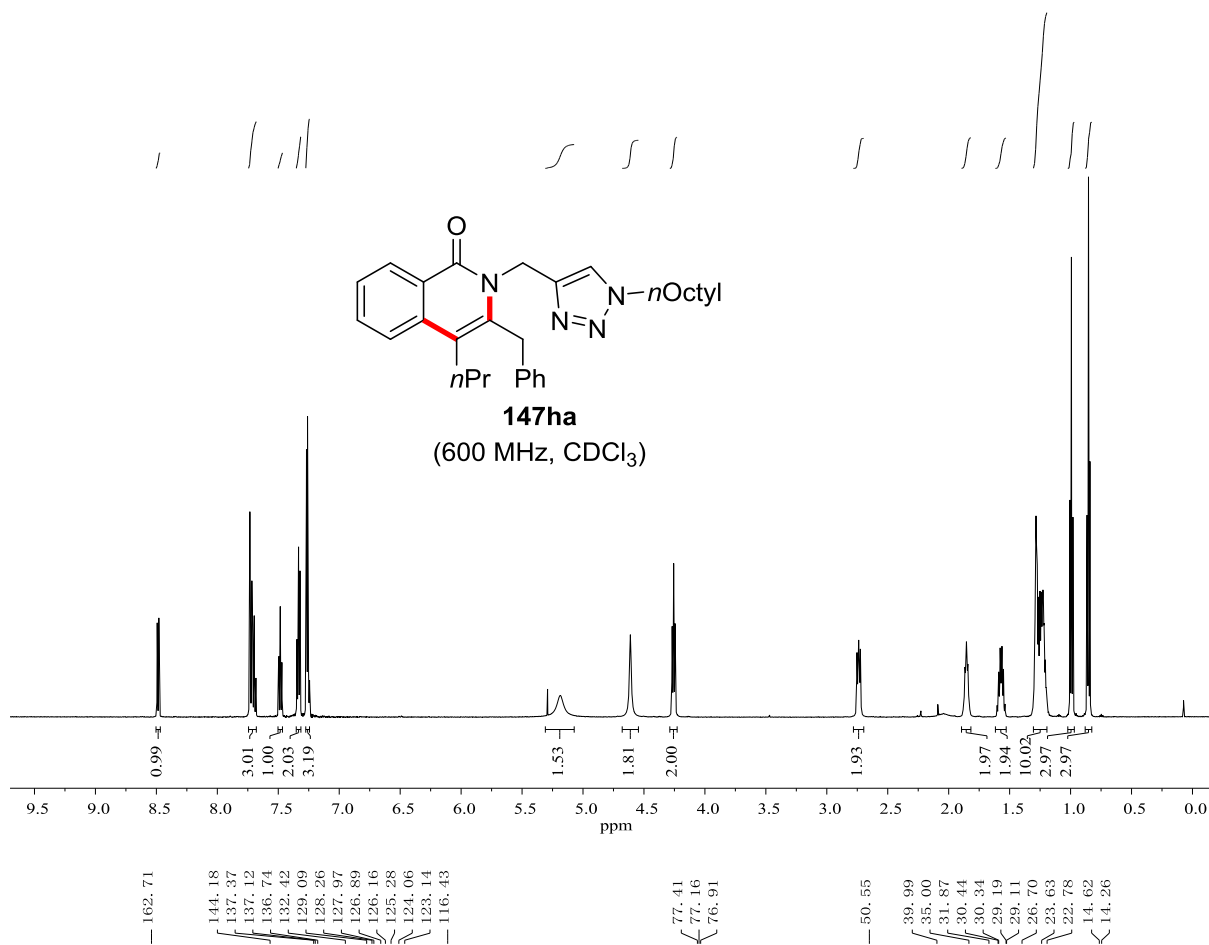


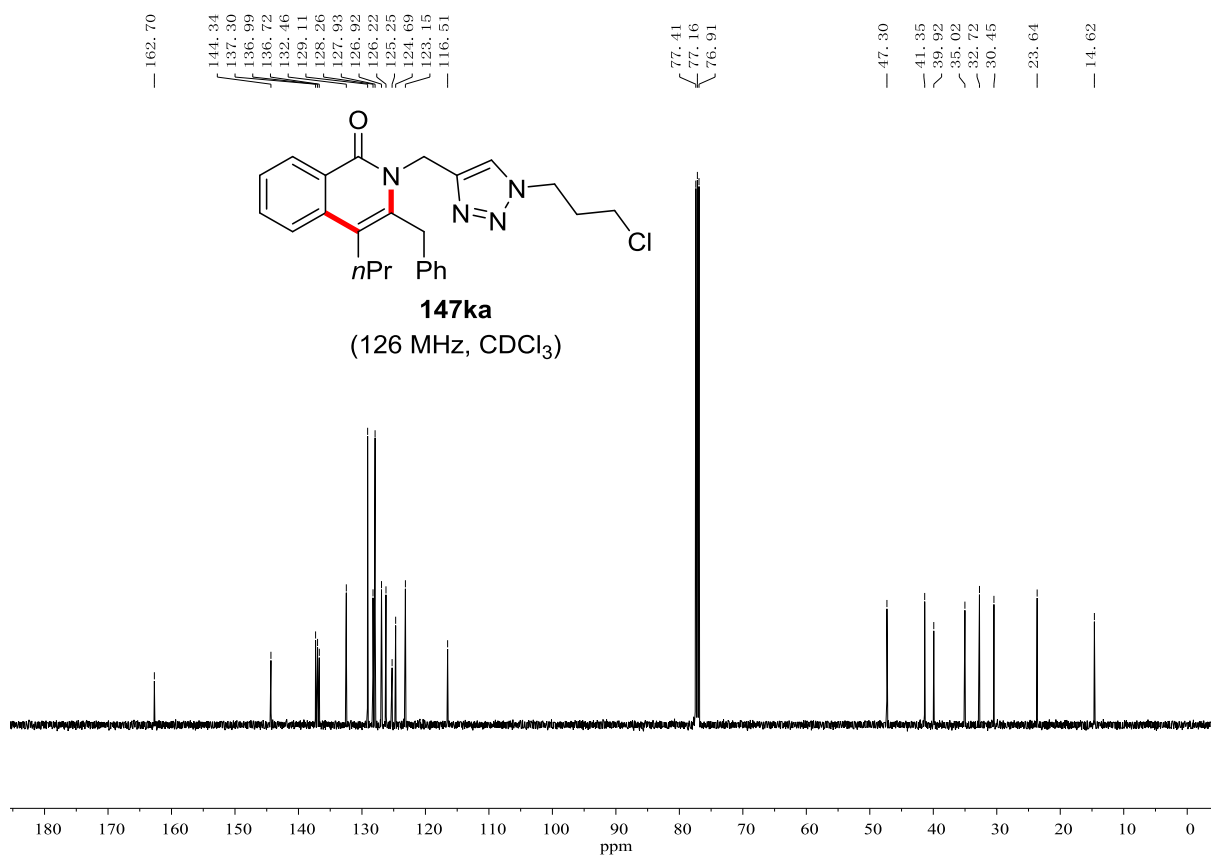
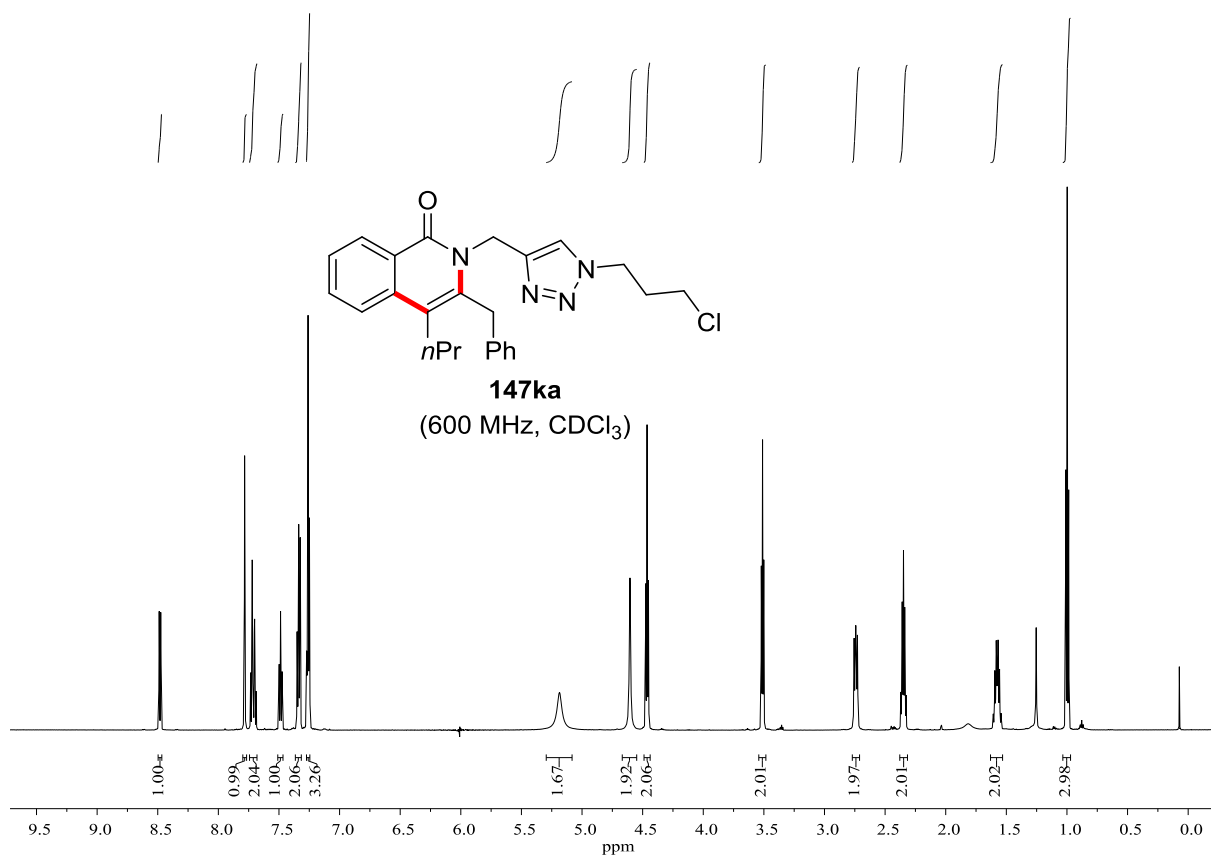


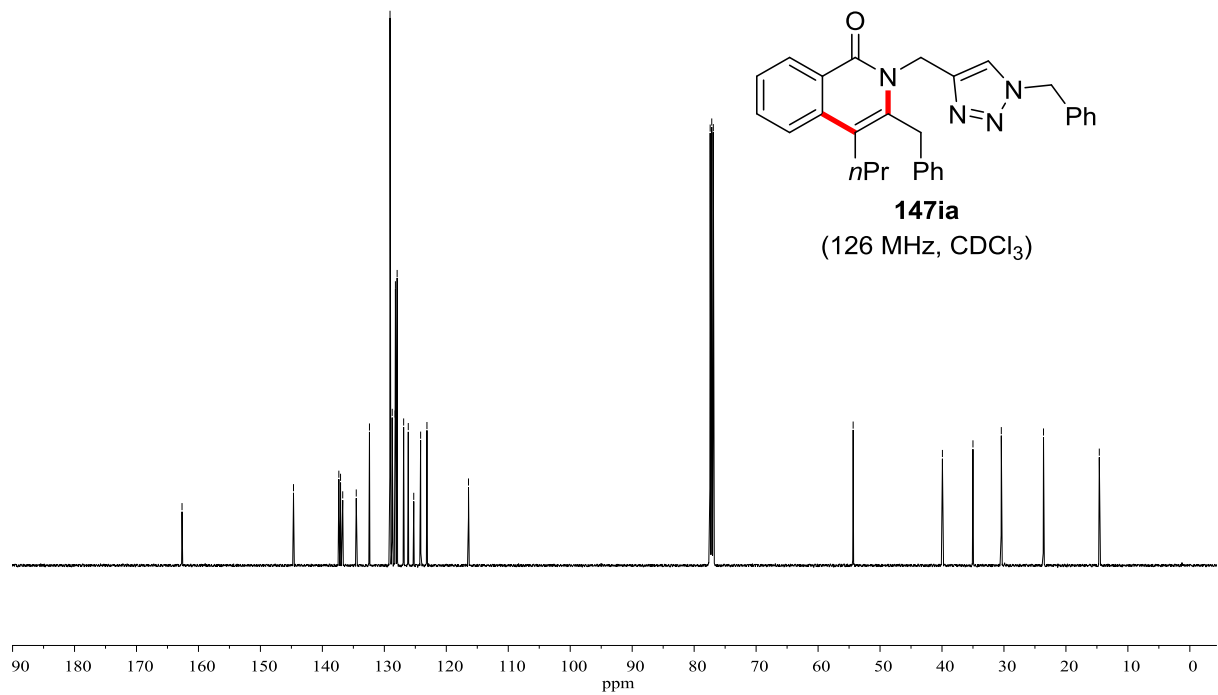
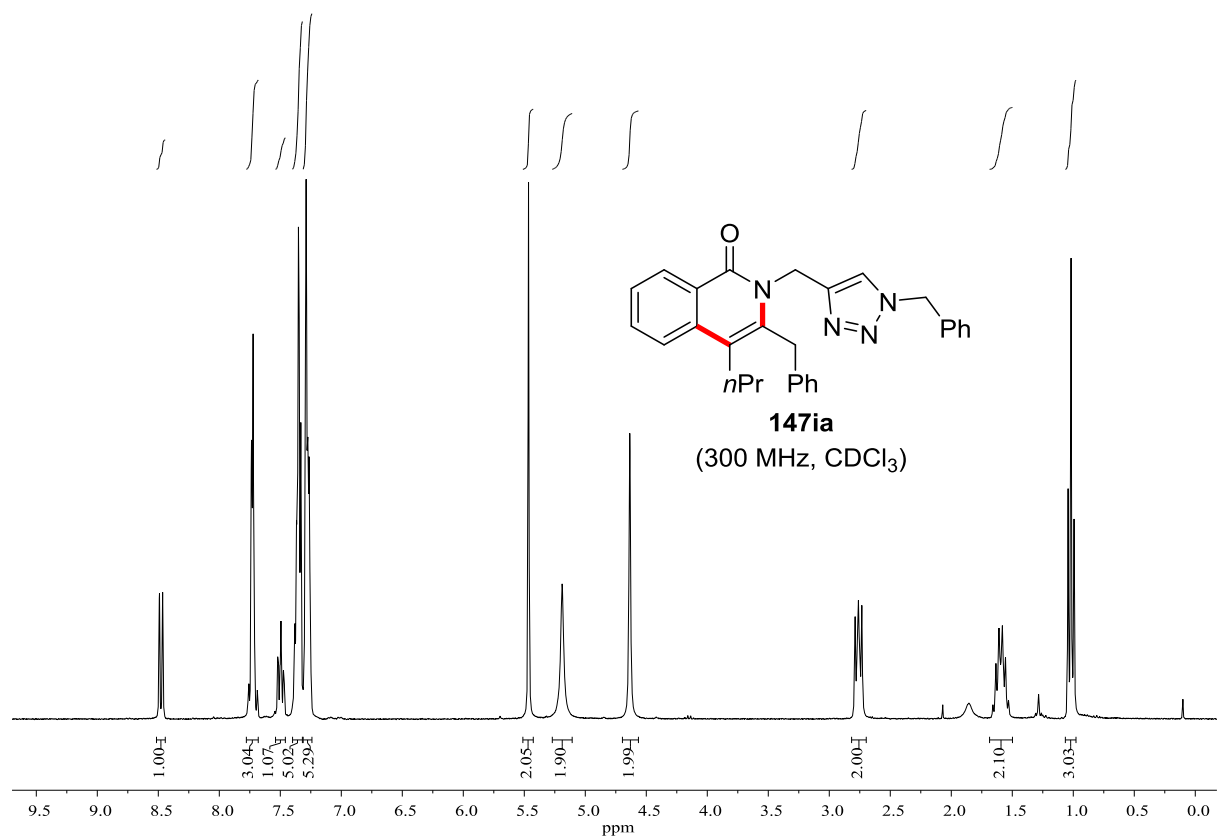


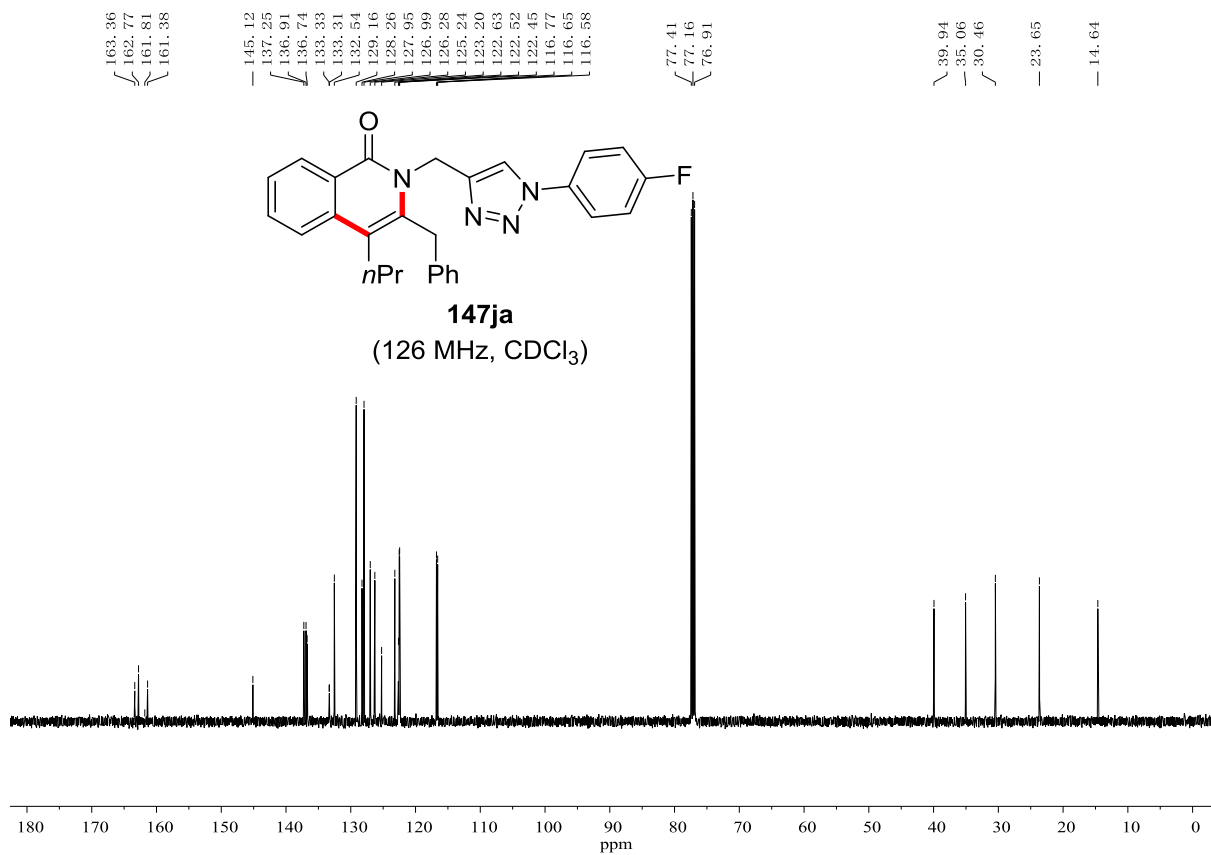
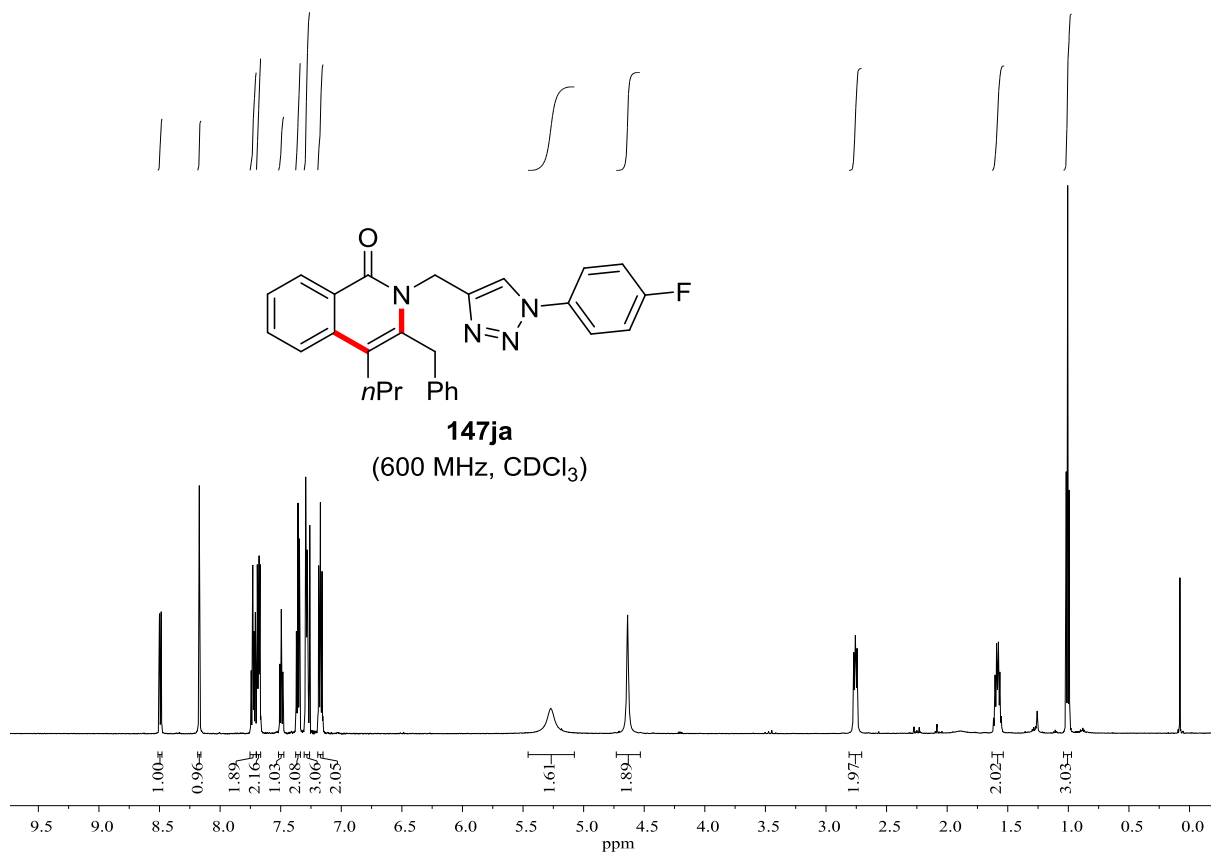


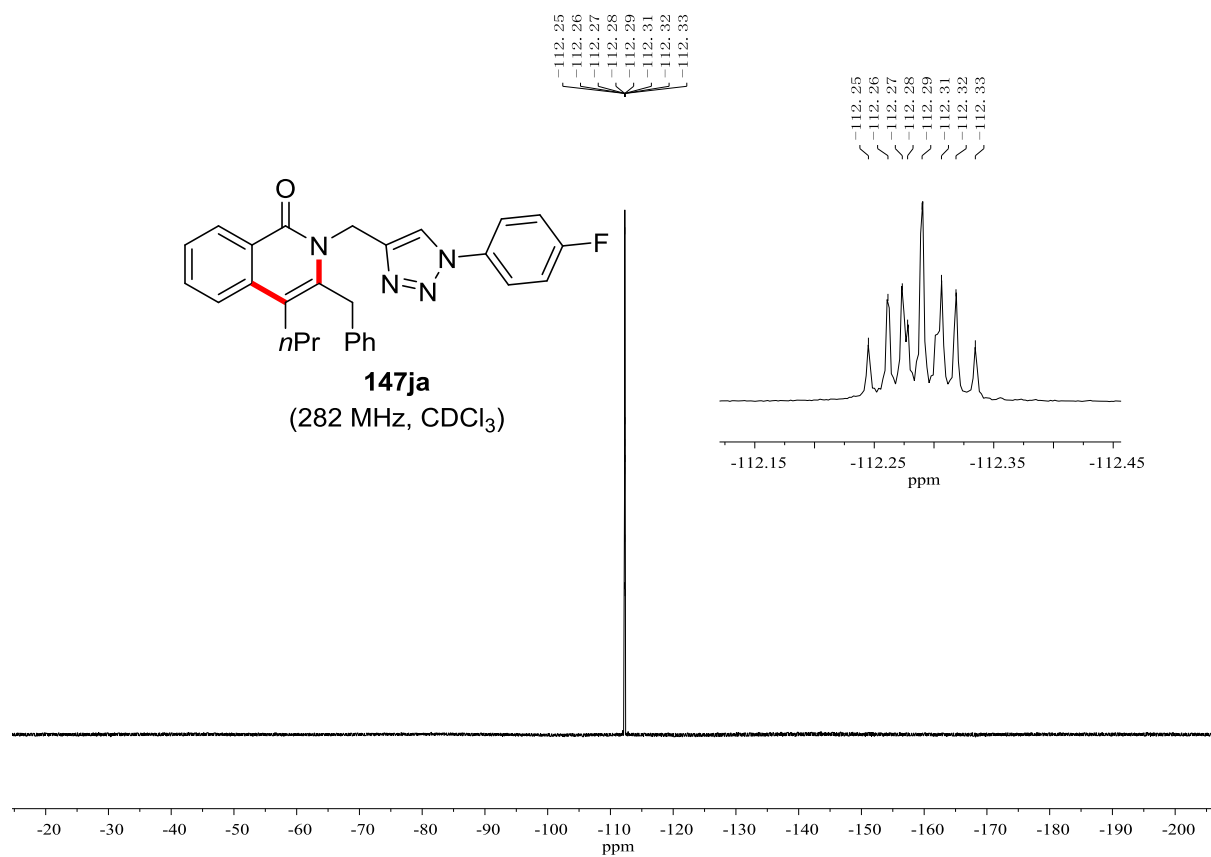


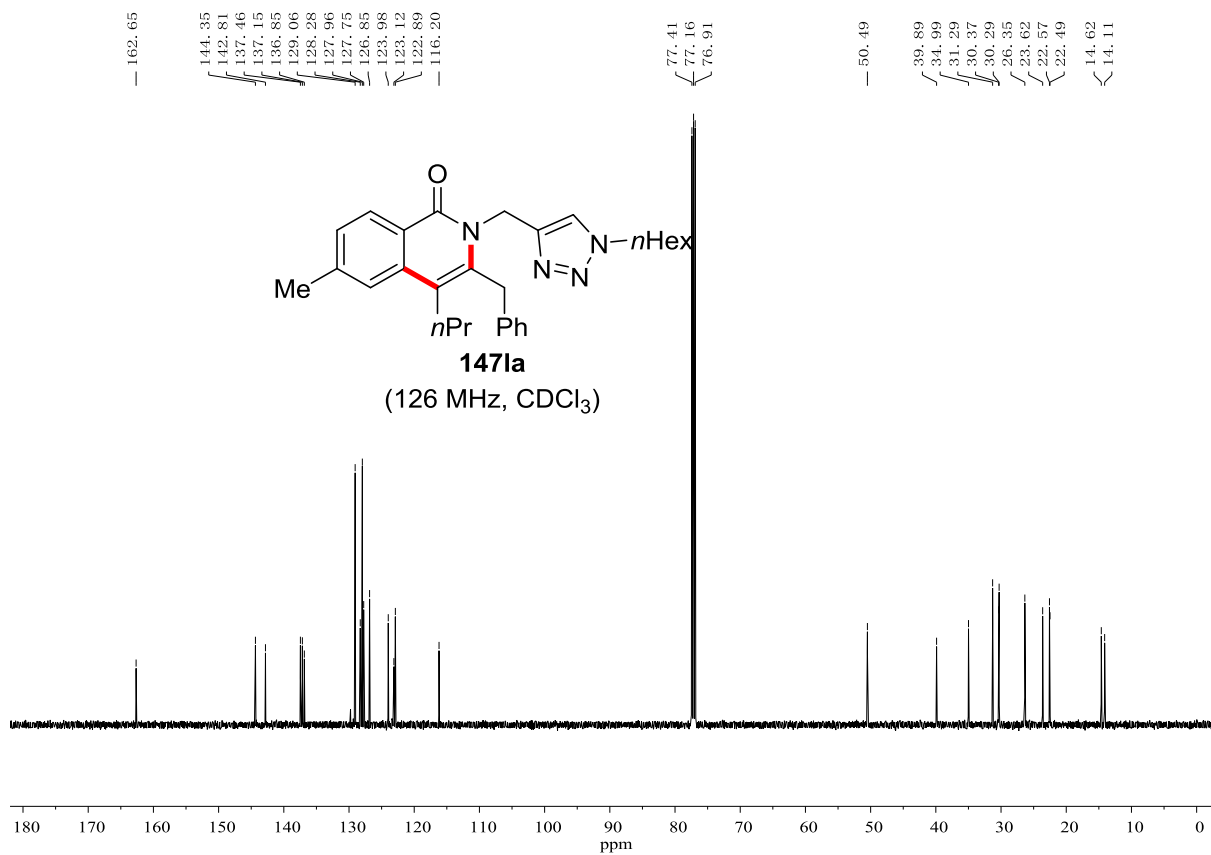
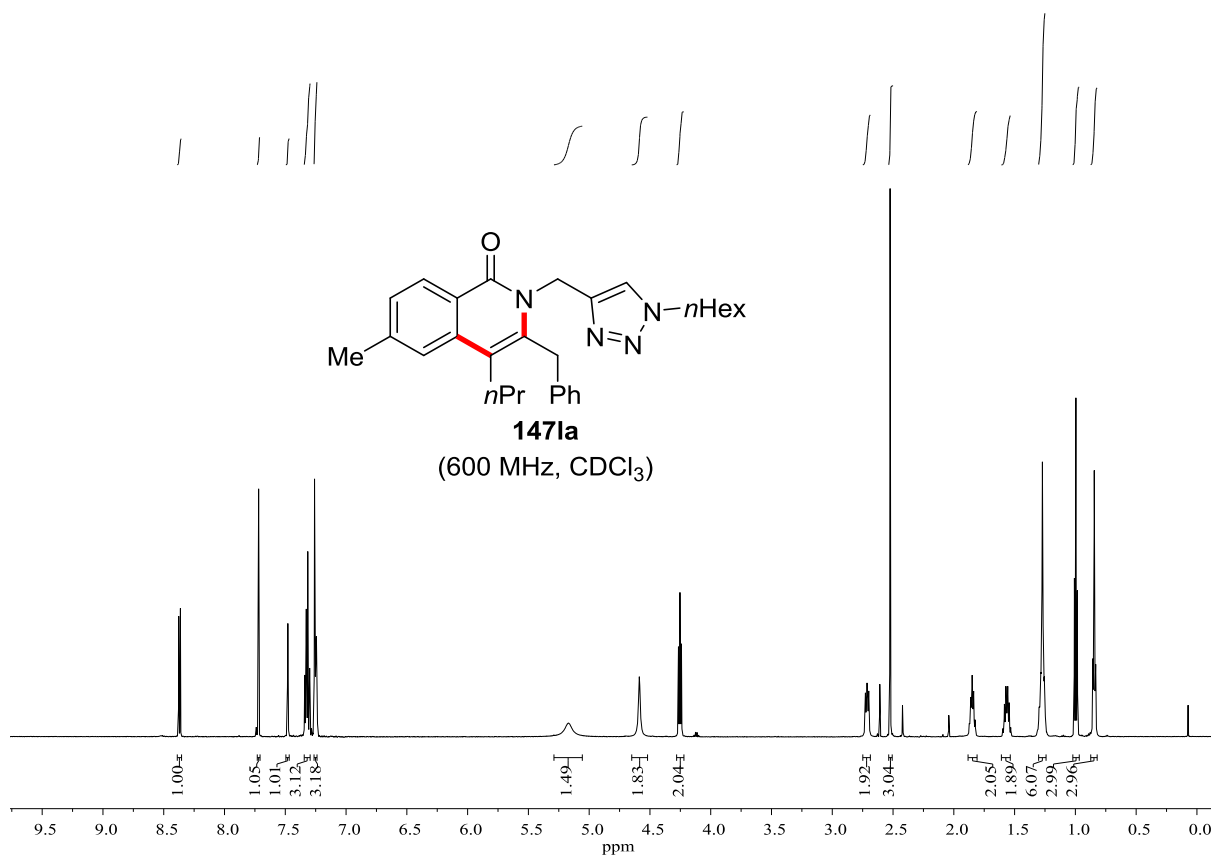


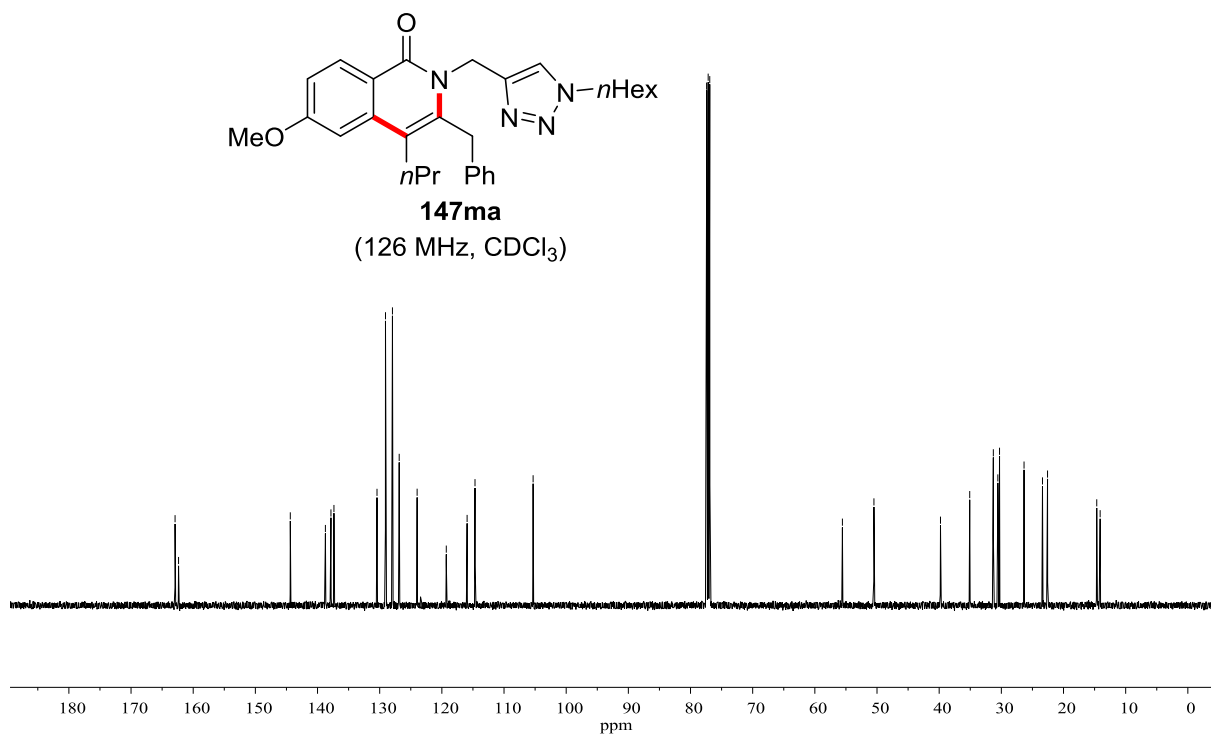
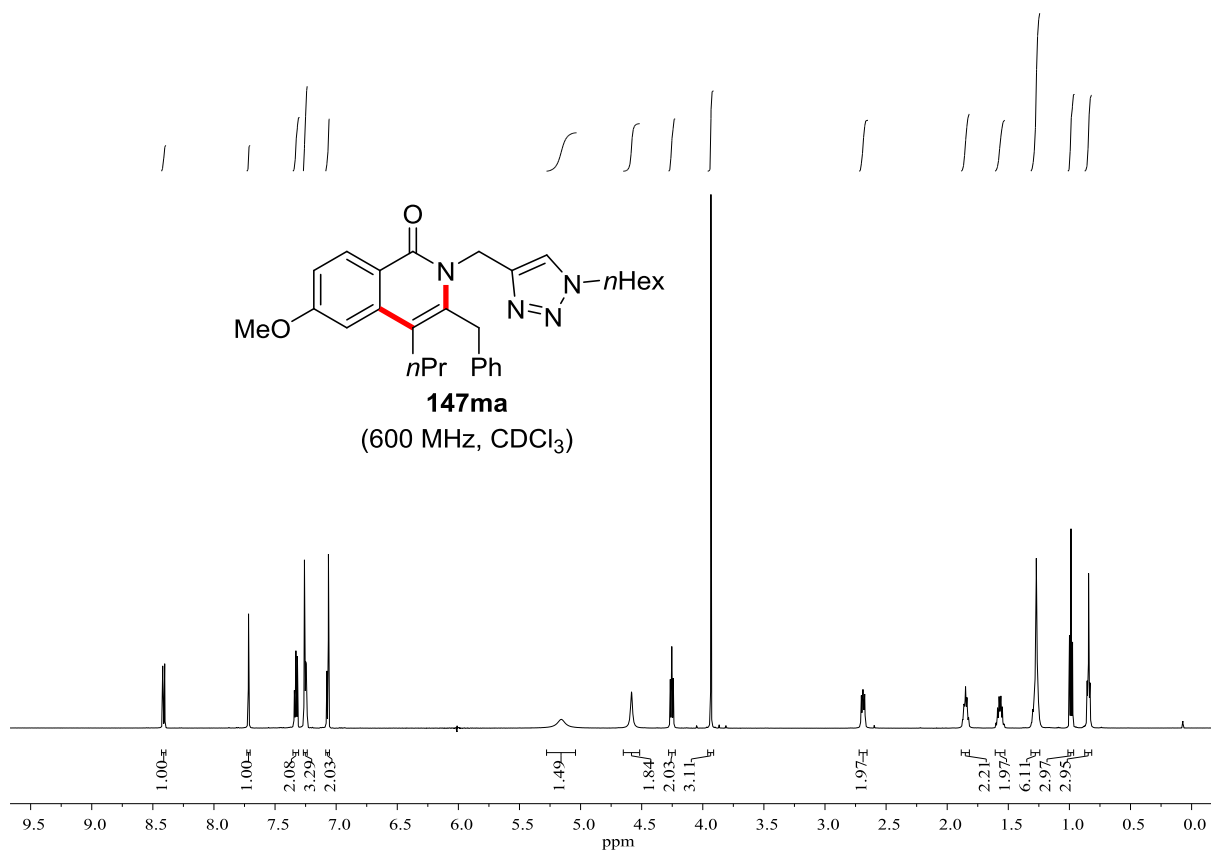


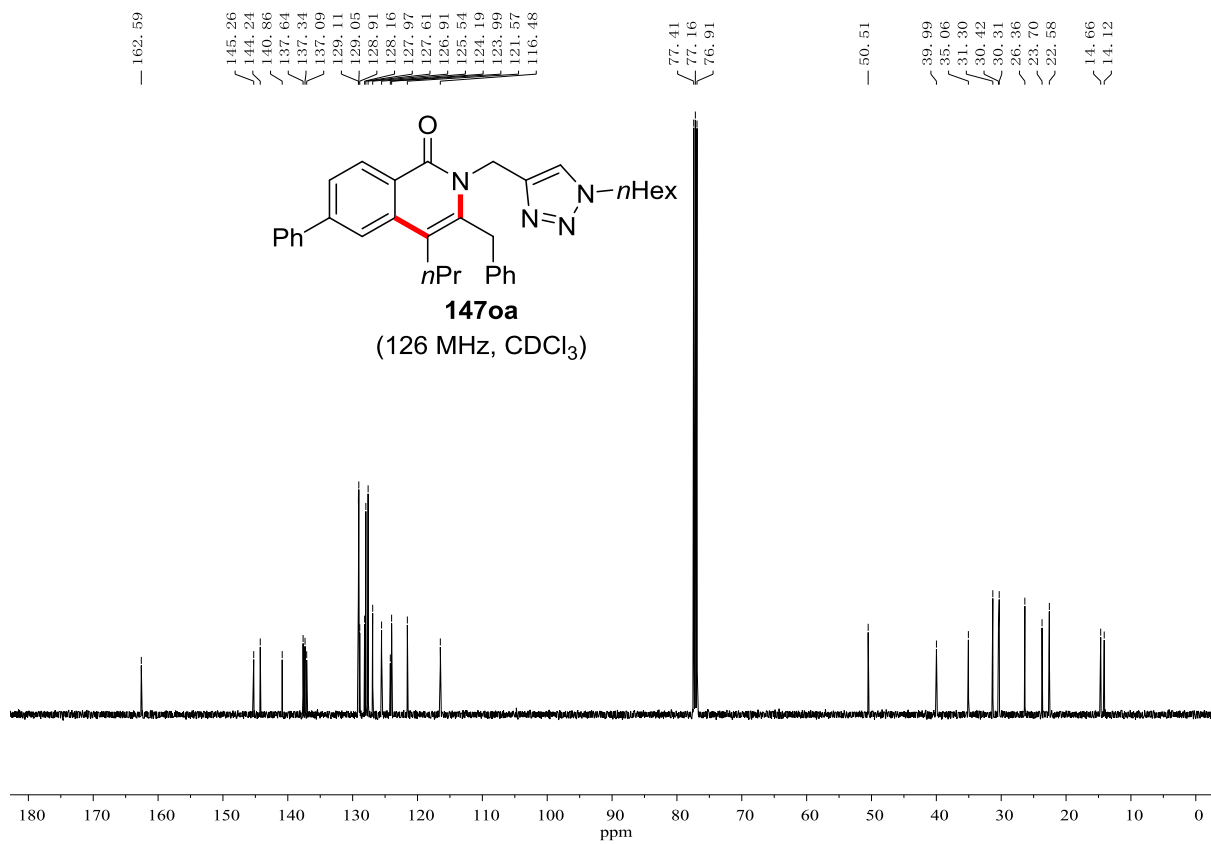
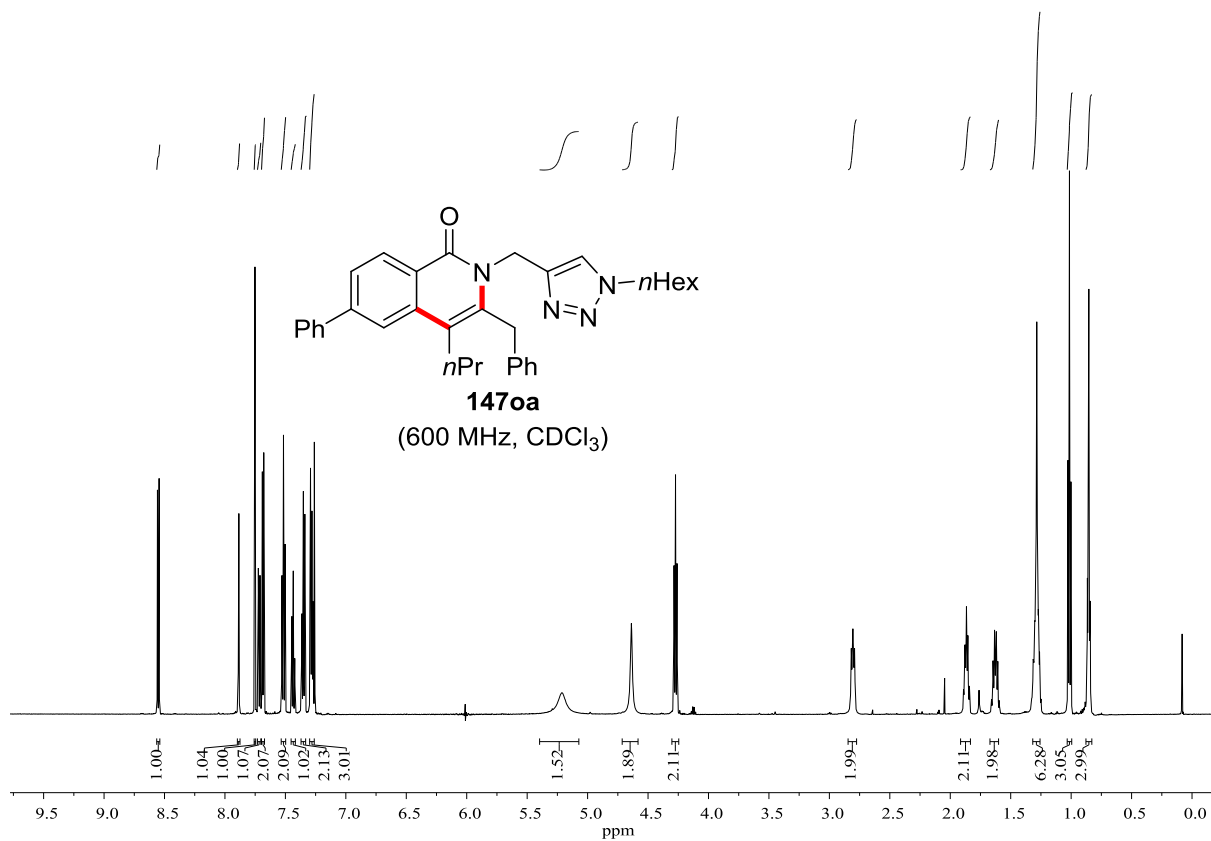


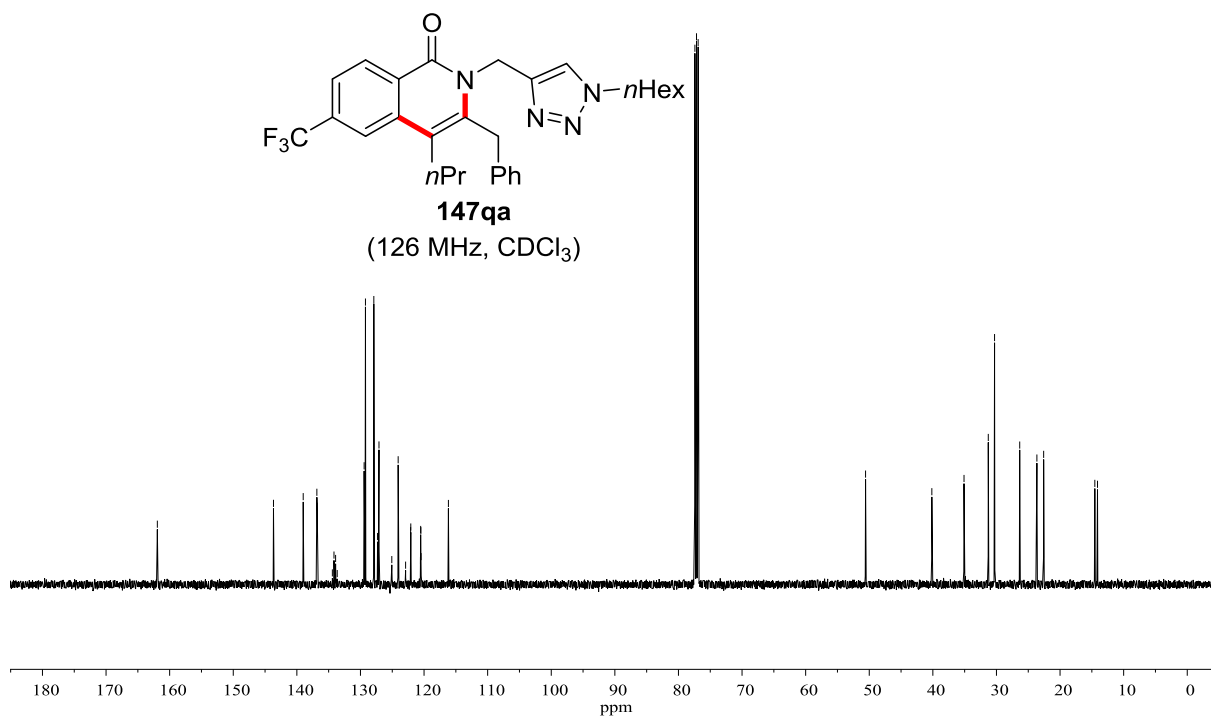
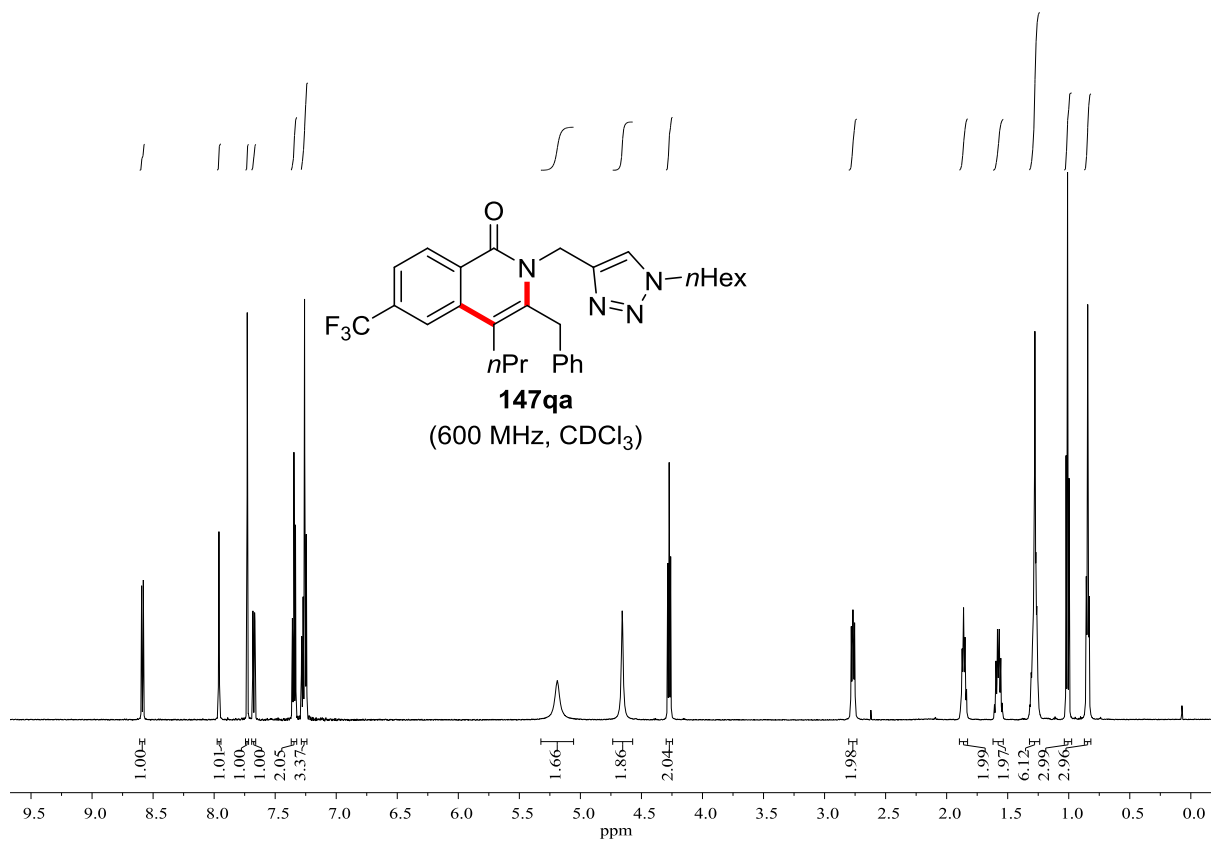




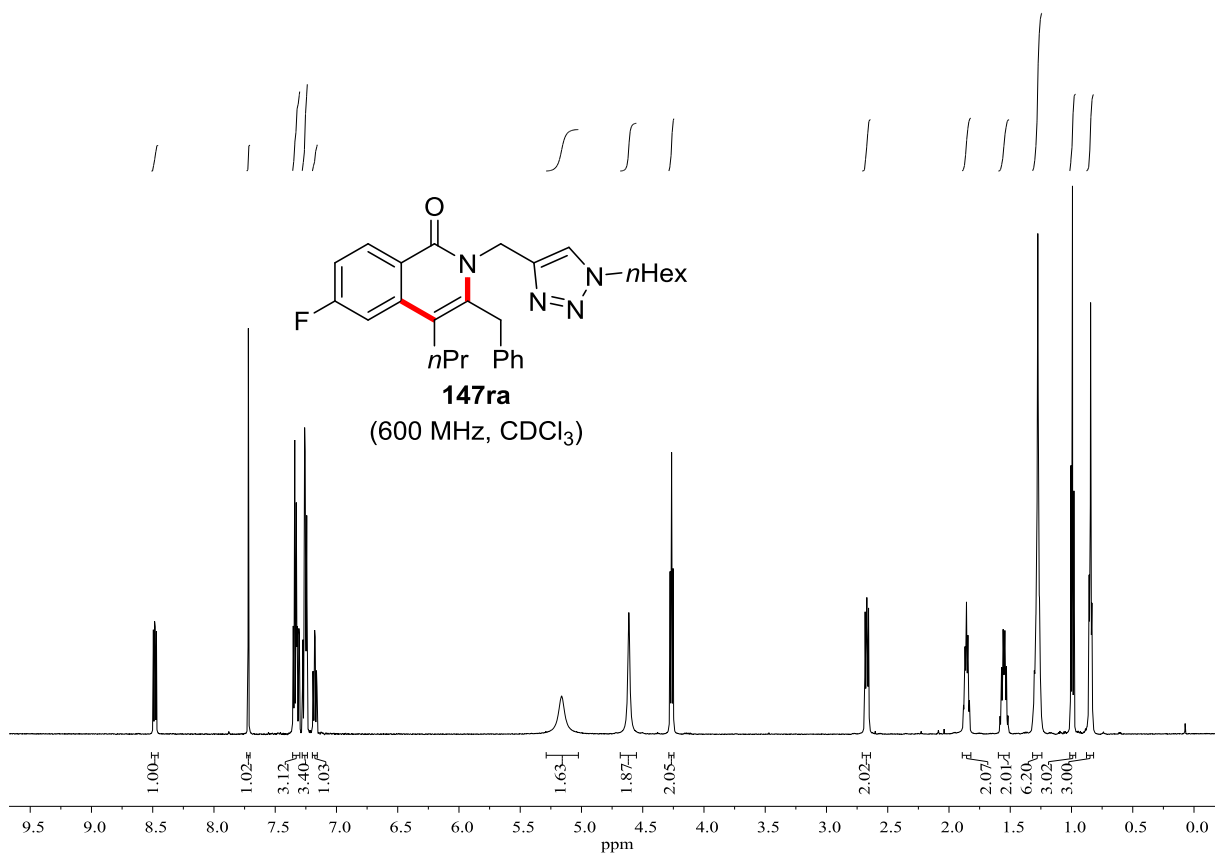
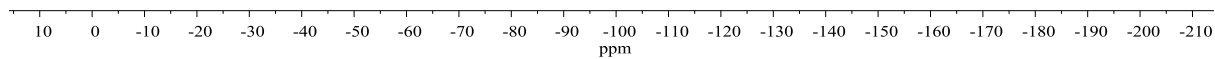
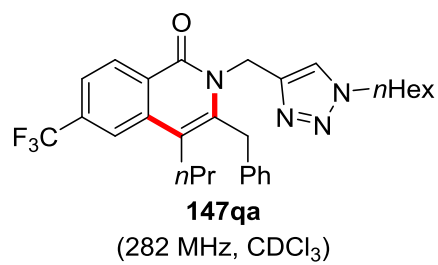


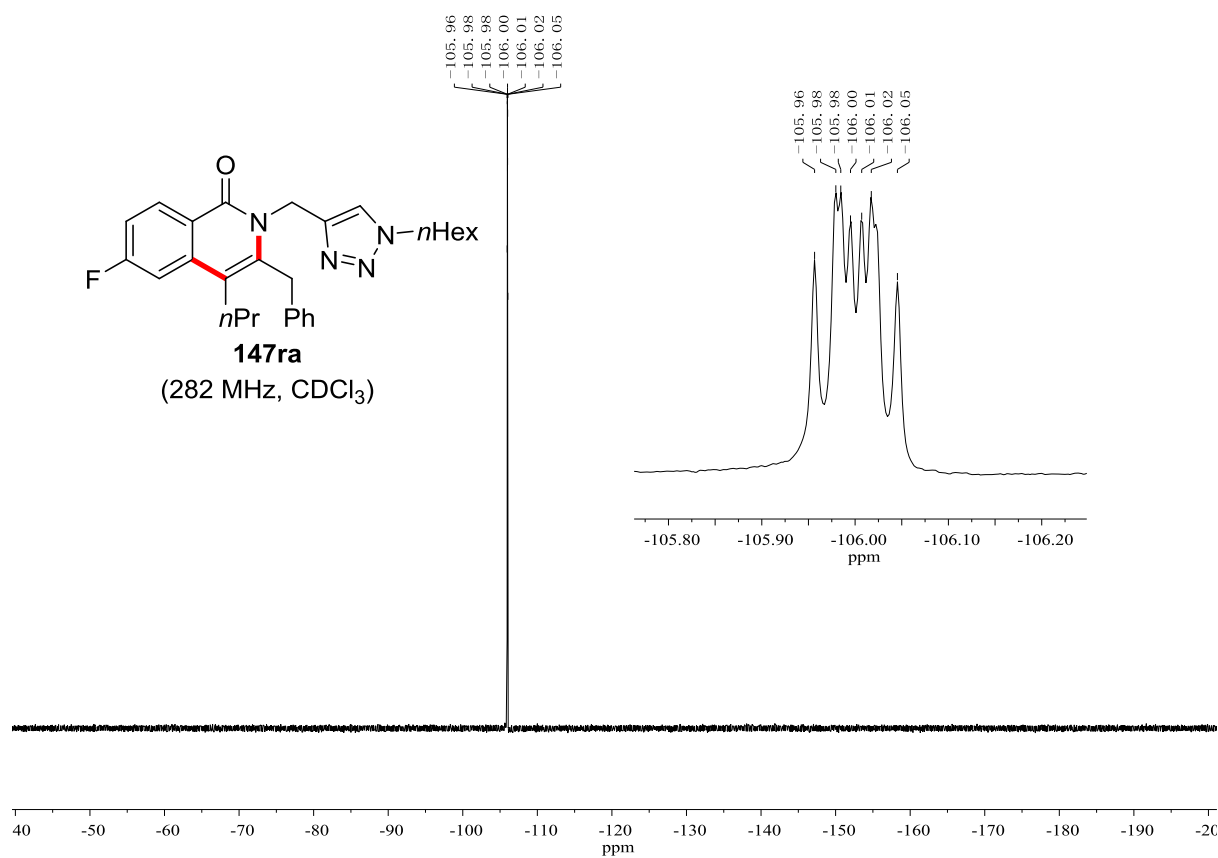
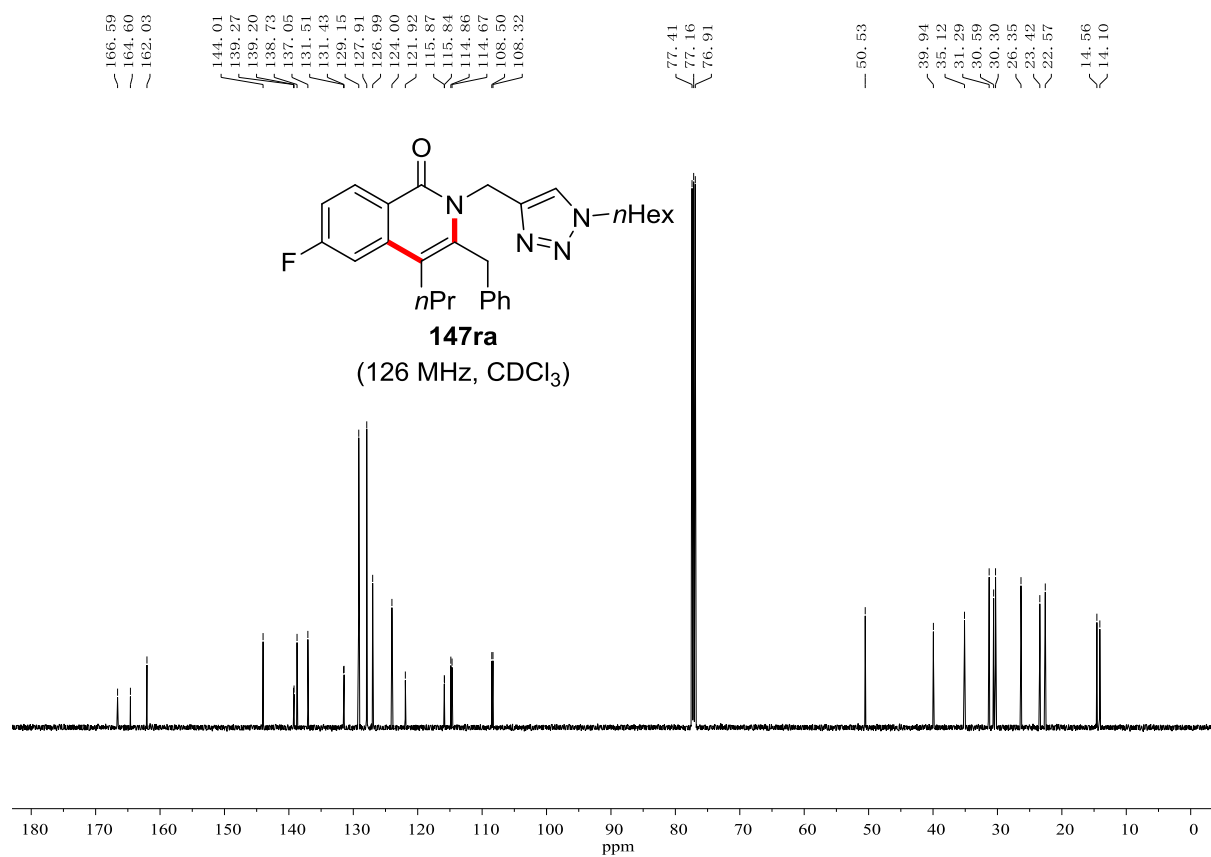


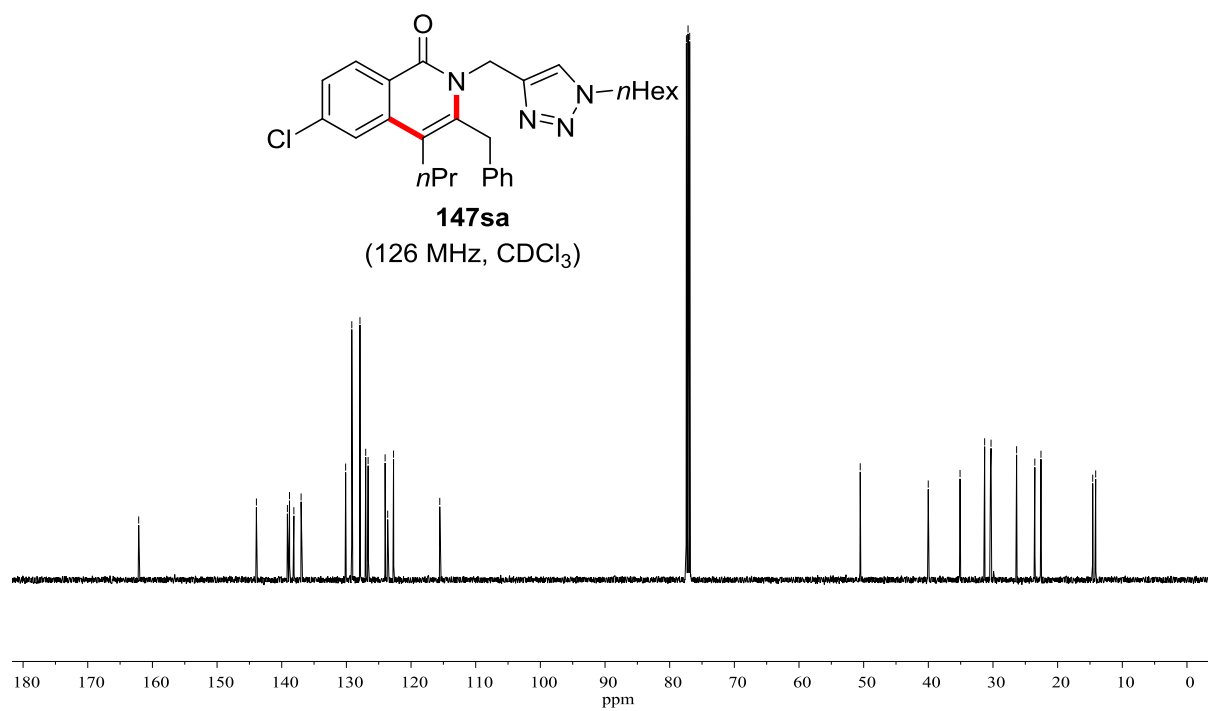
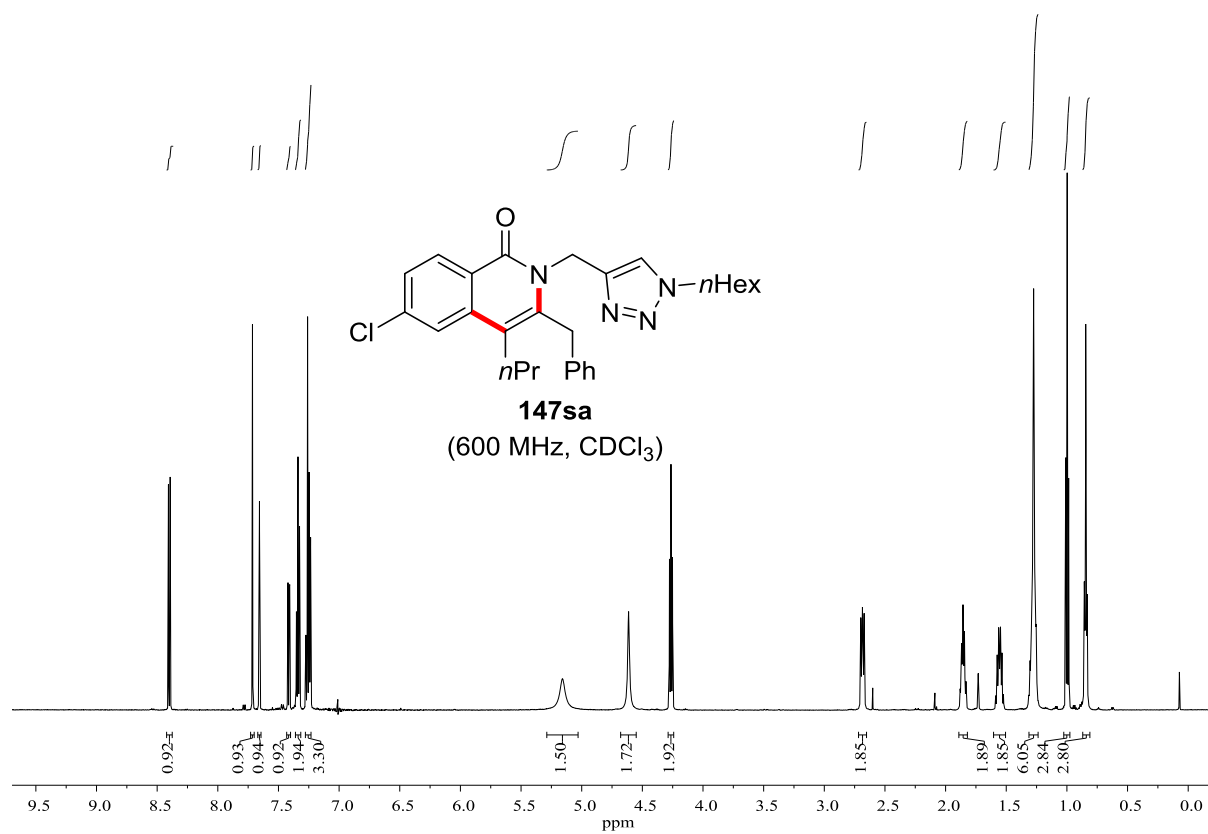


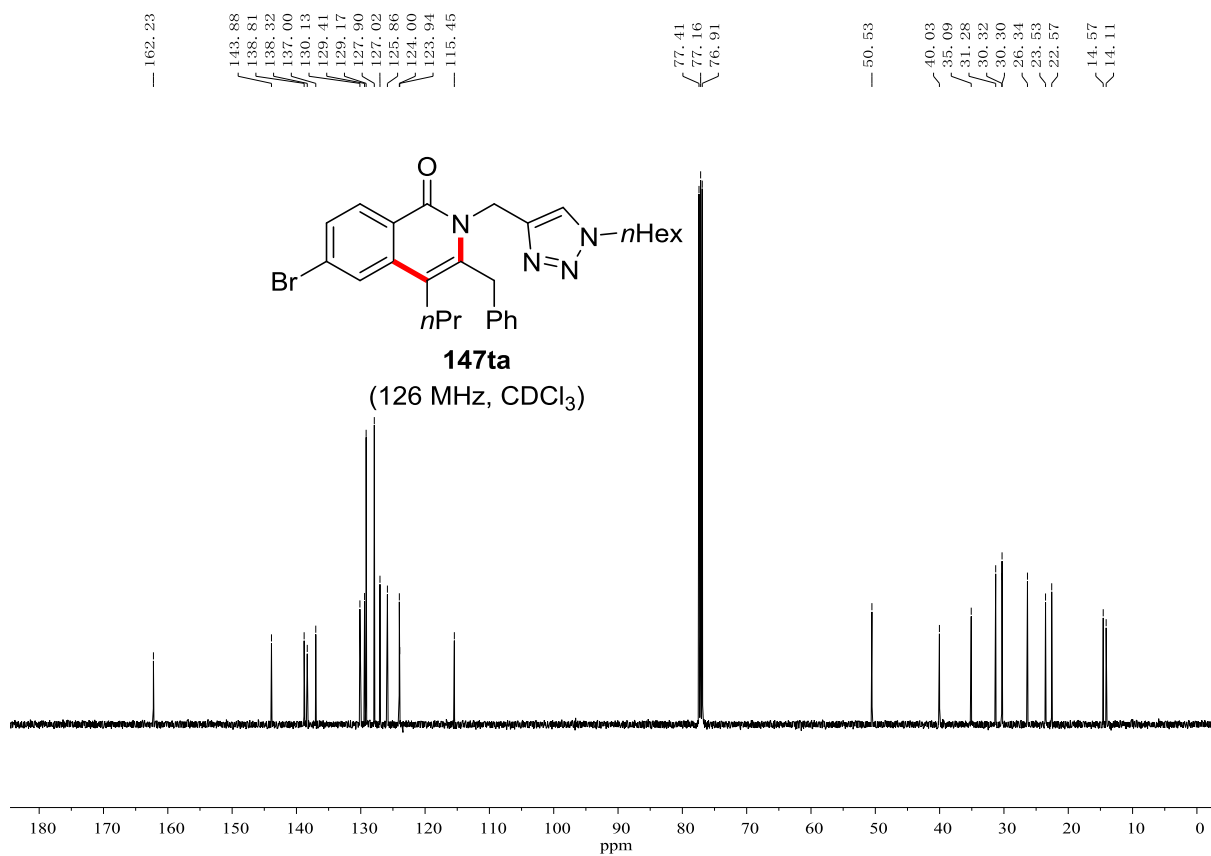
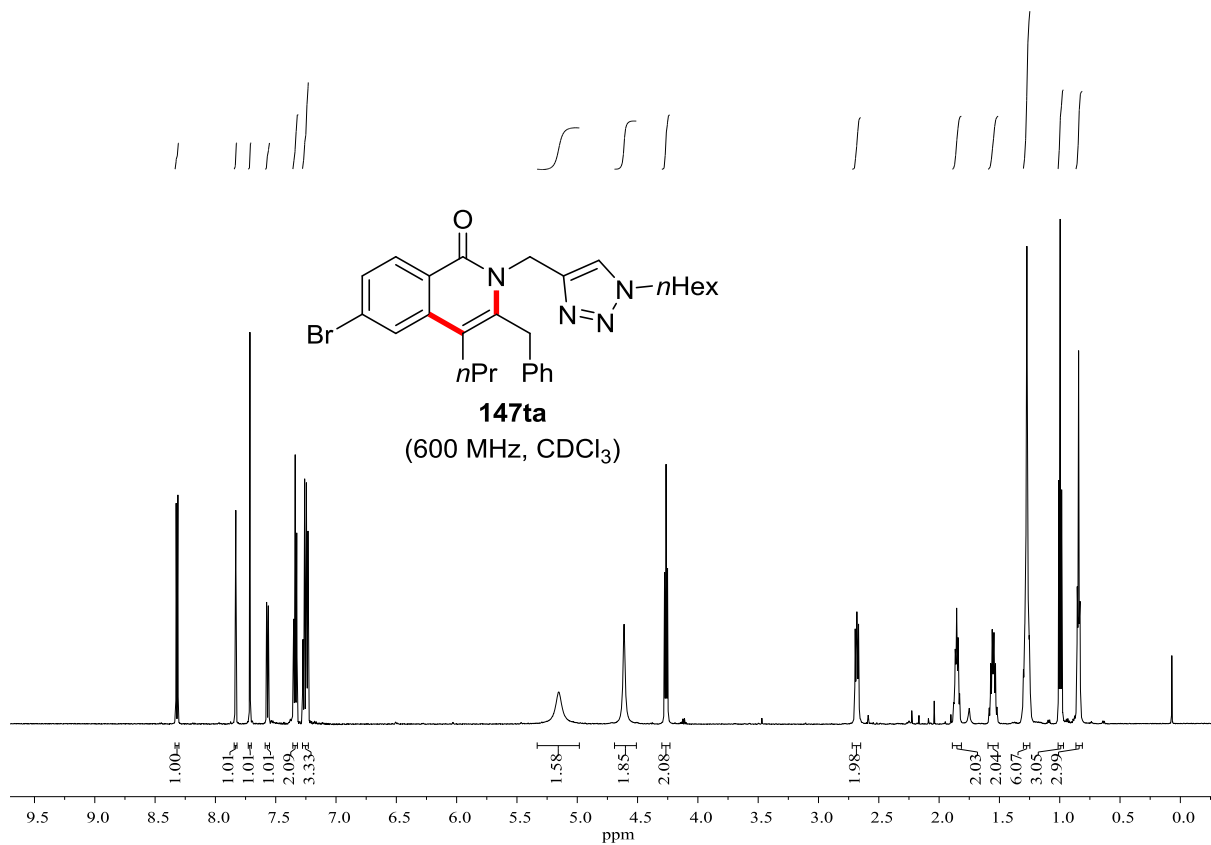


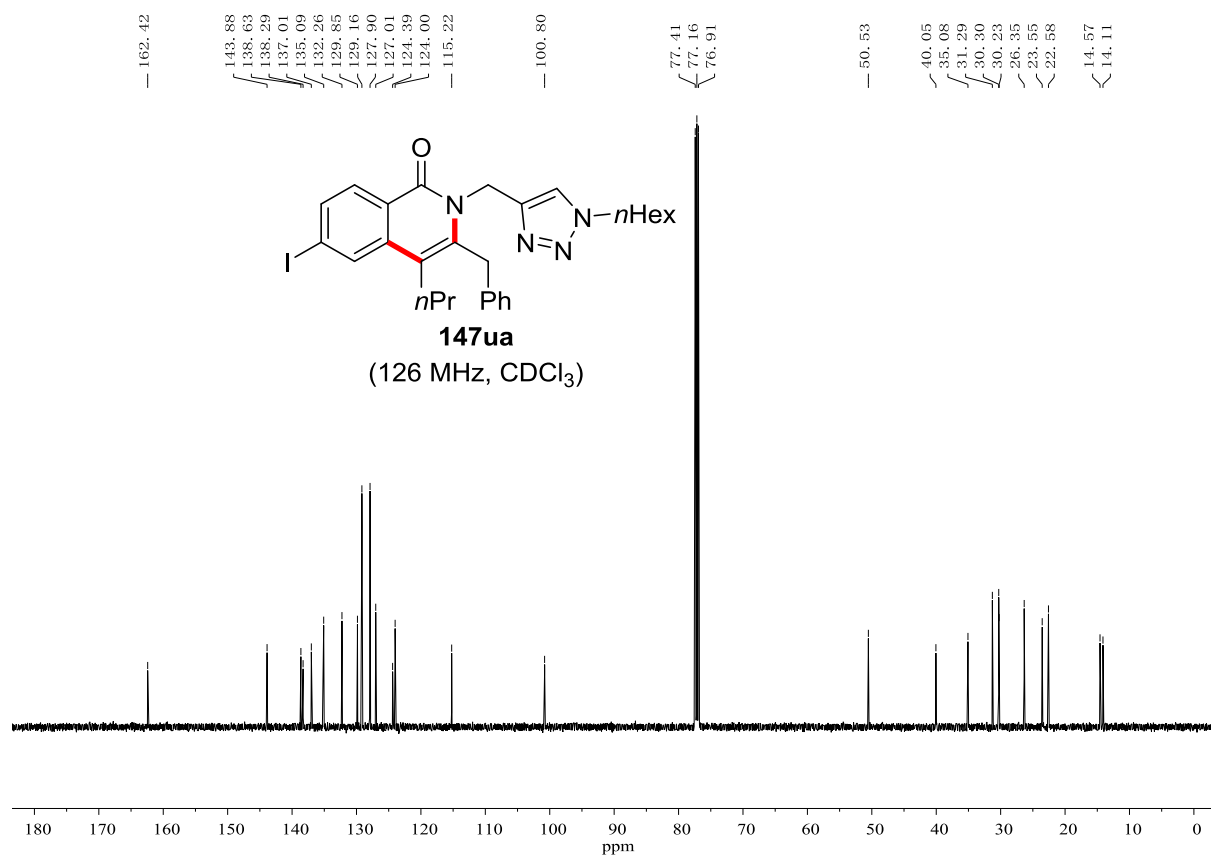
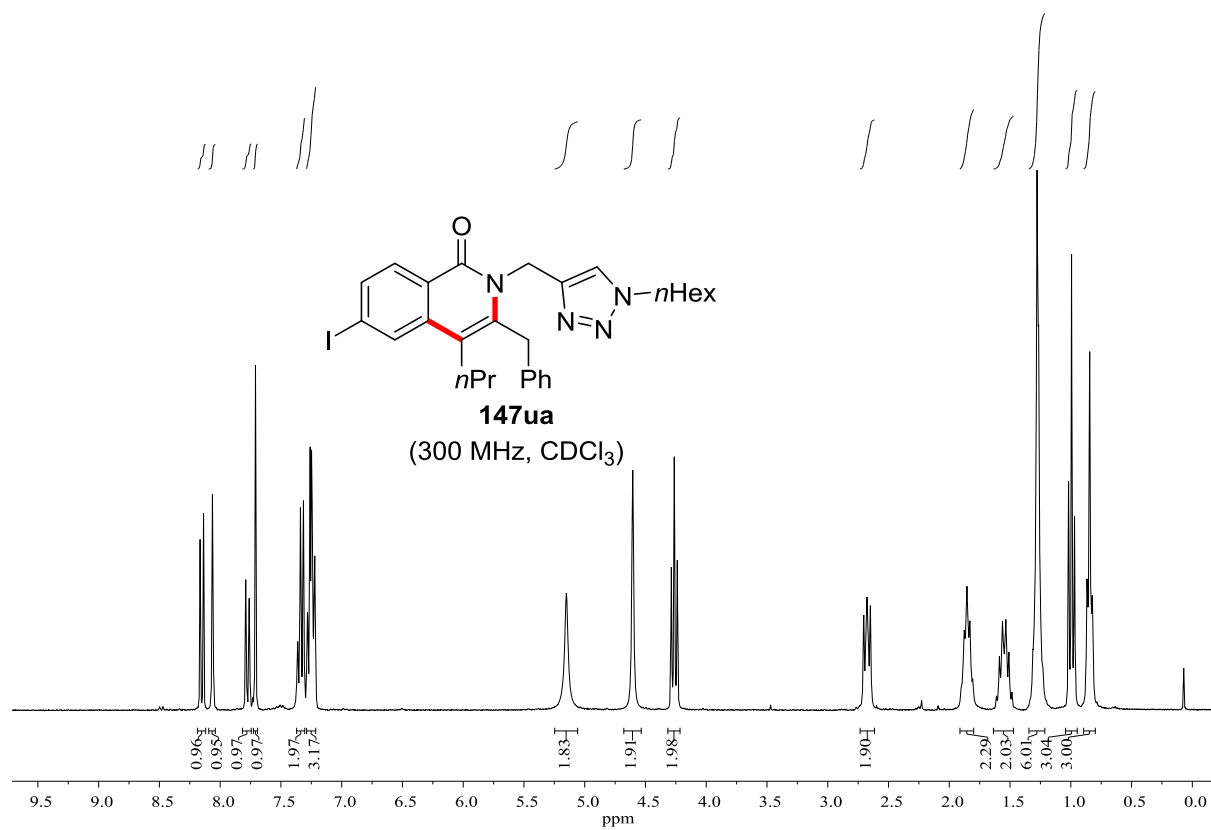
-62.93

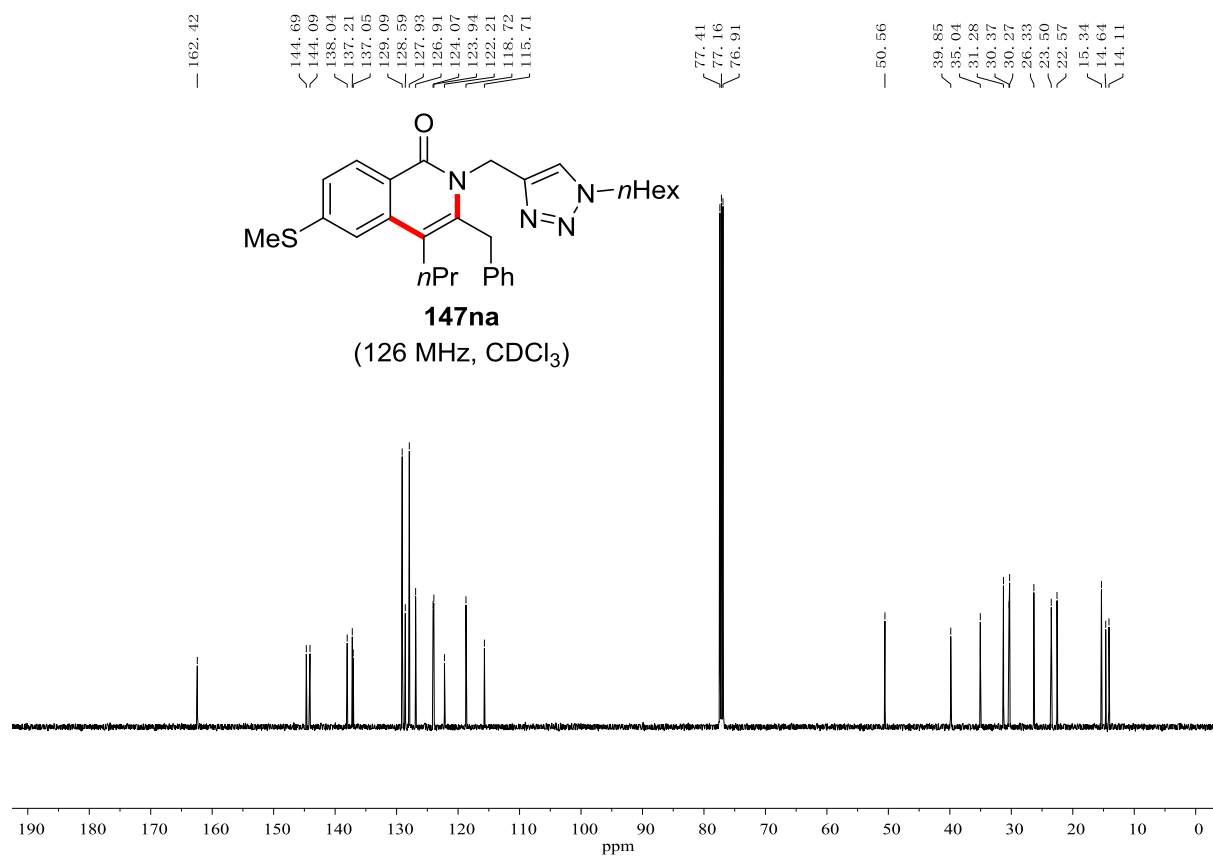
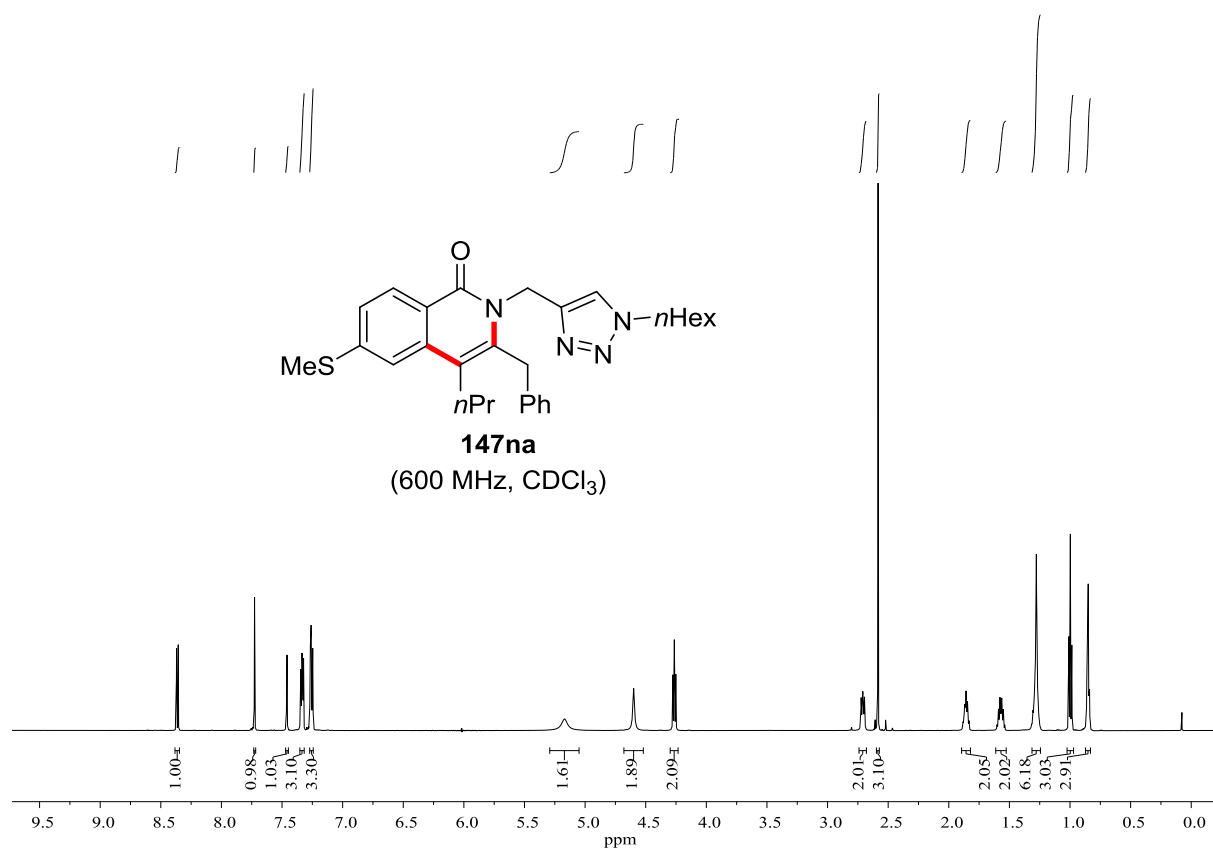


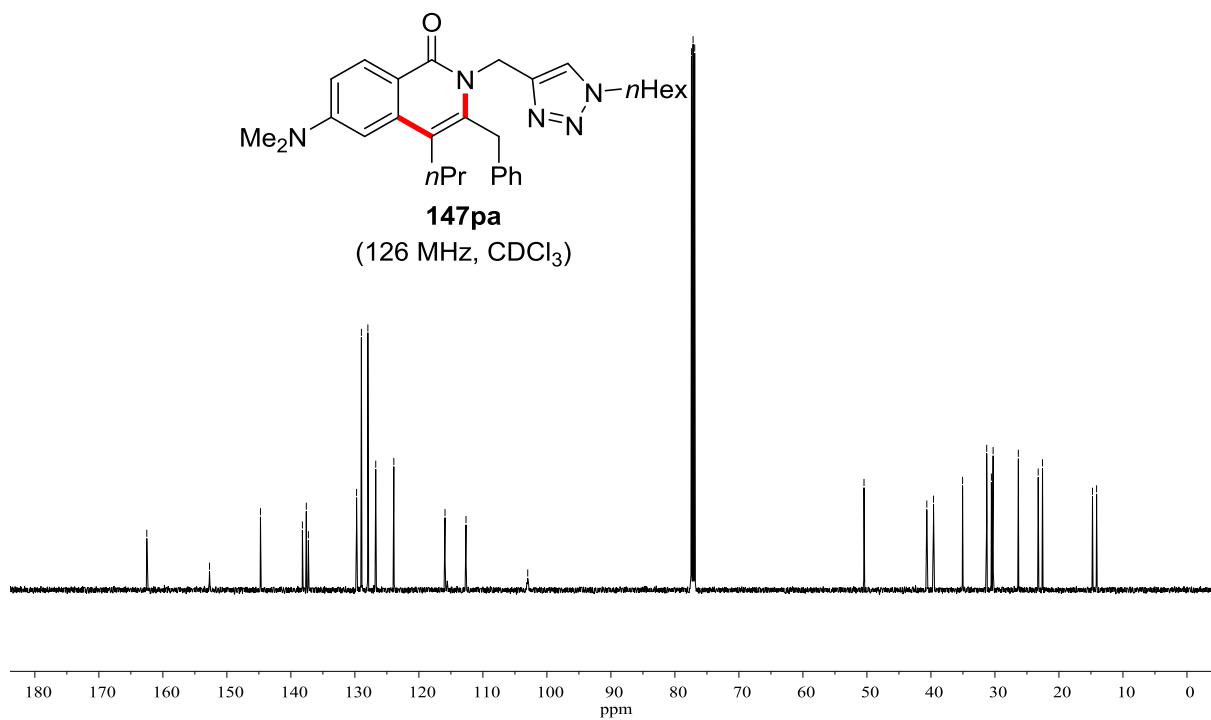
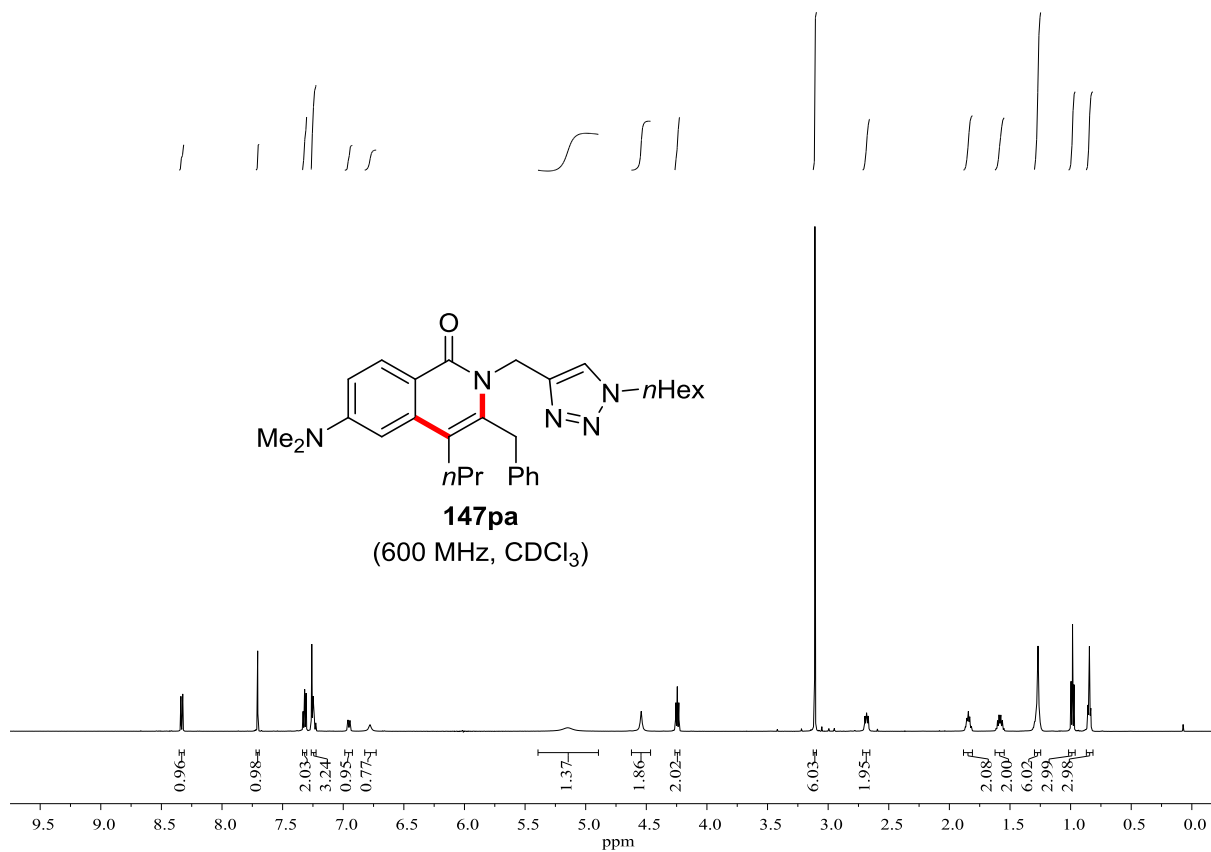


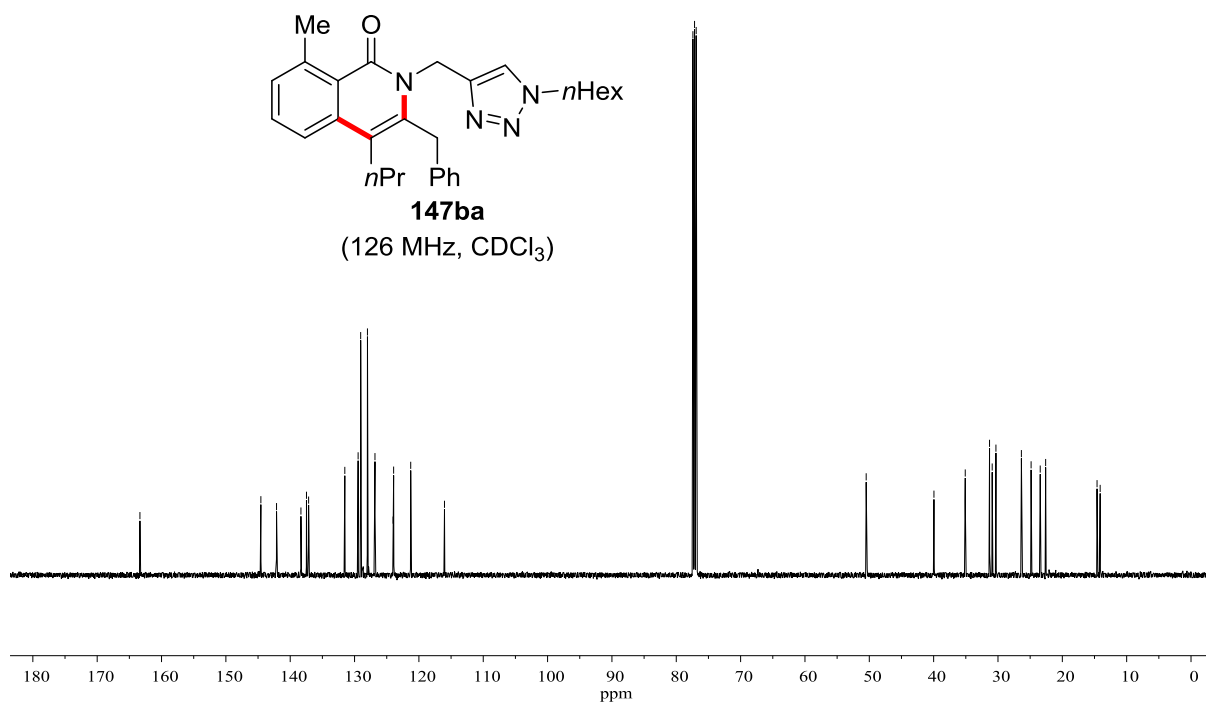
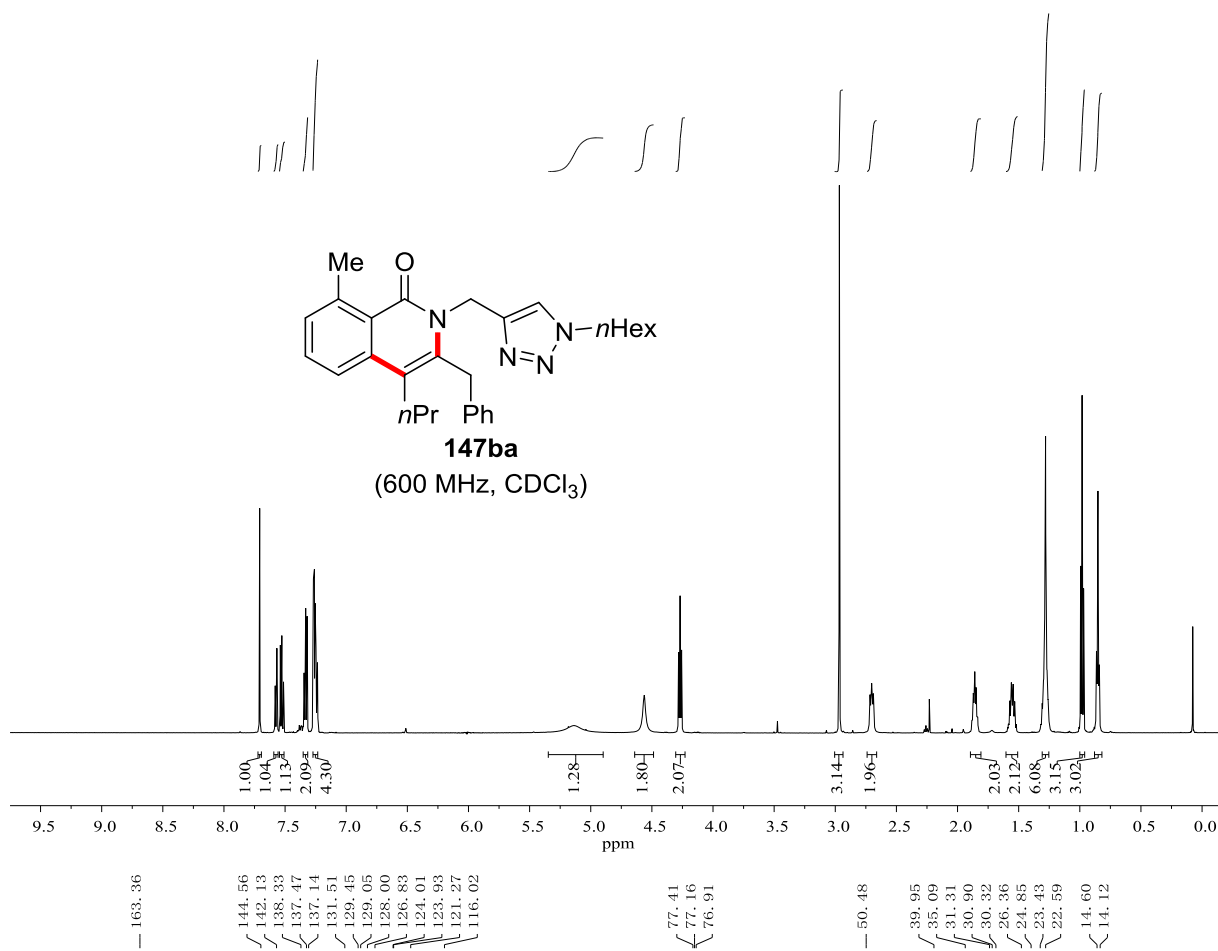


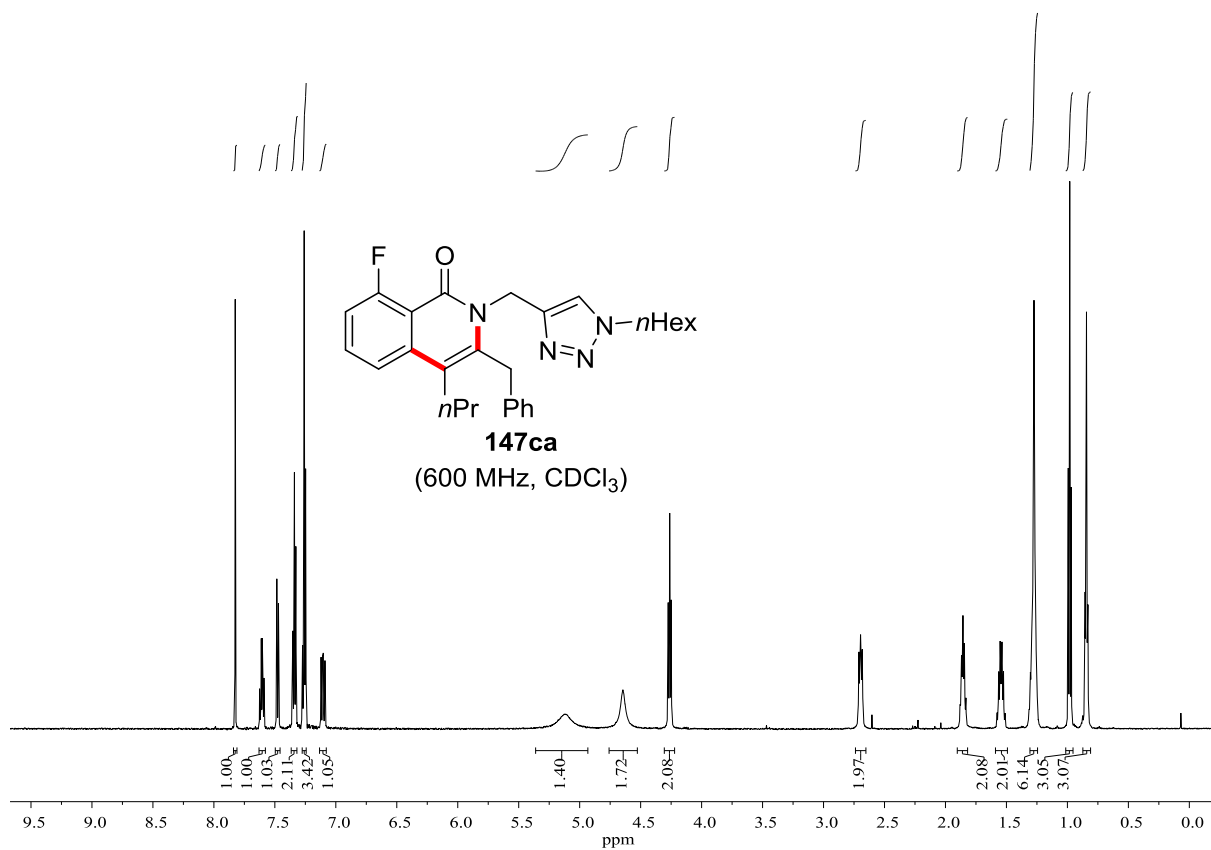


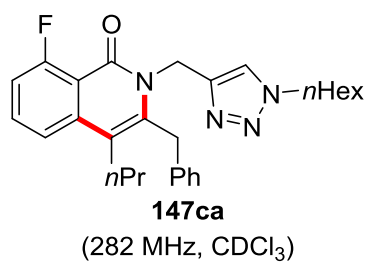




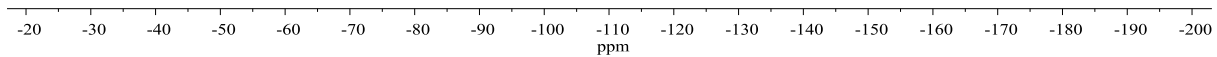
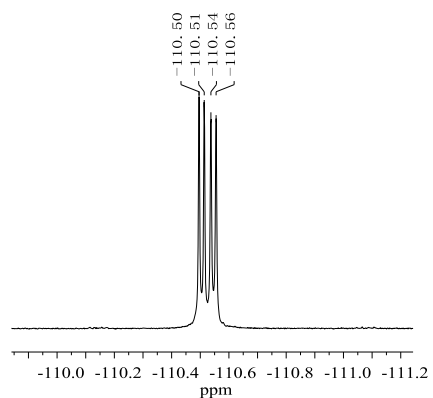


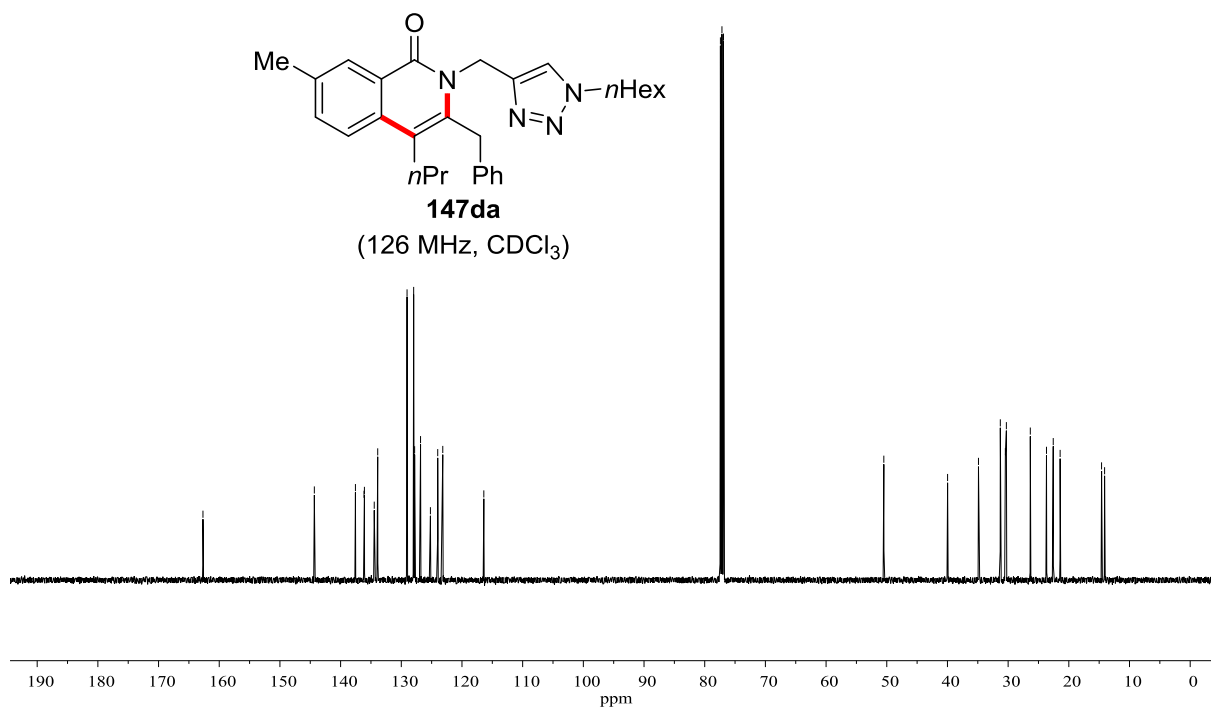
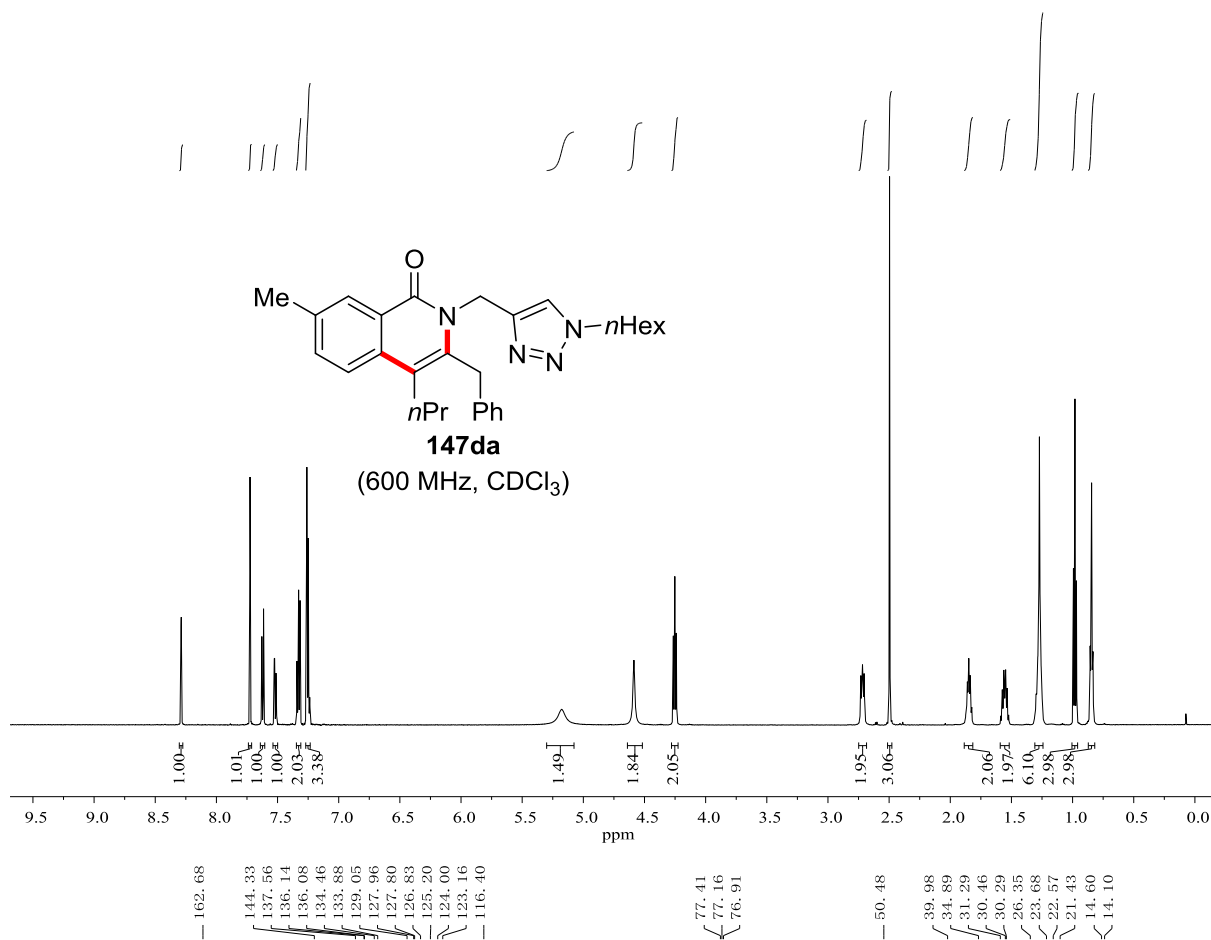


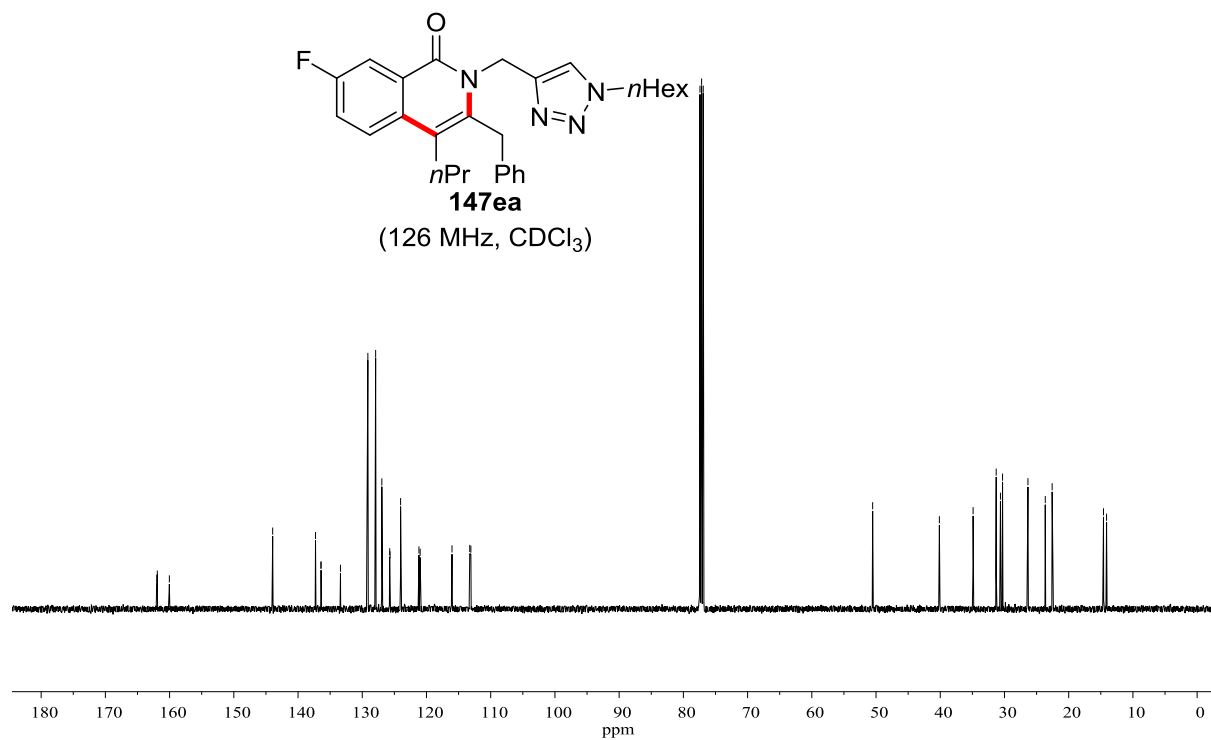
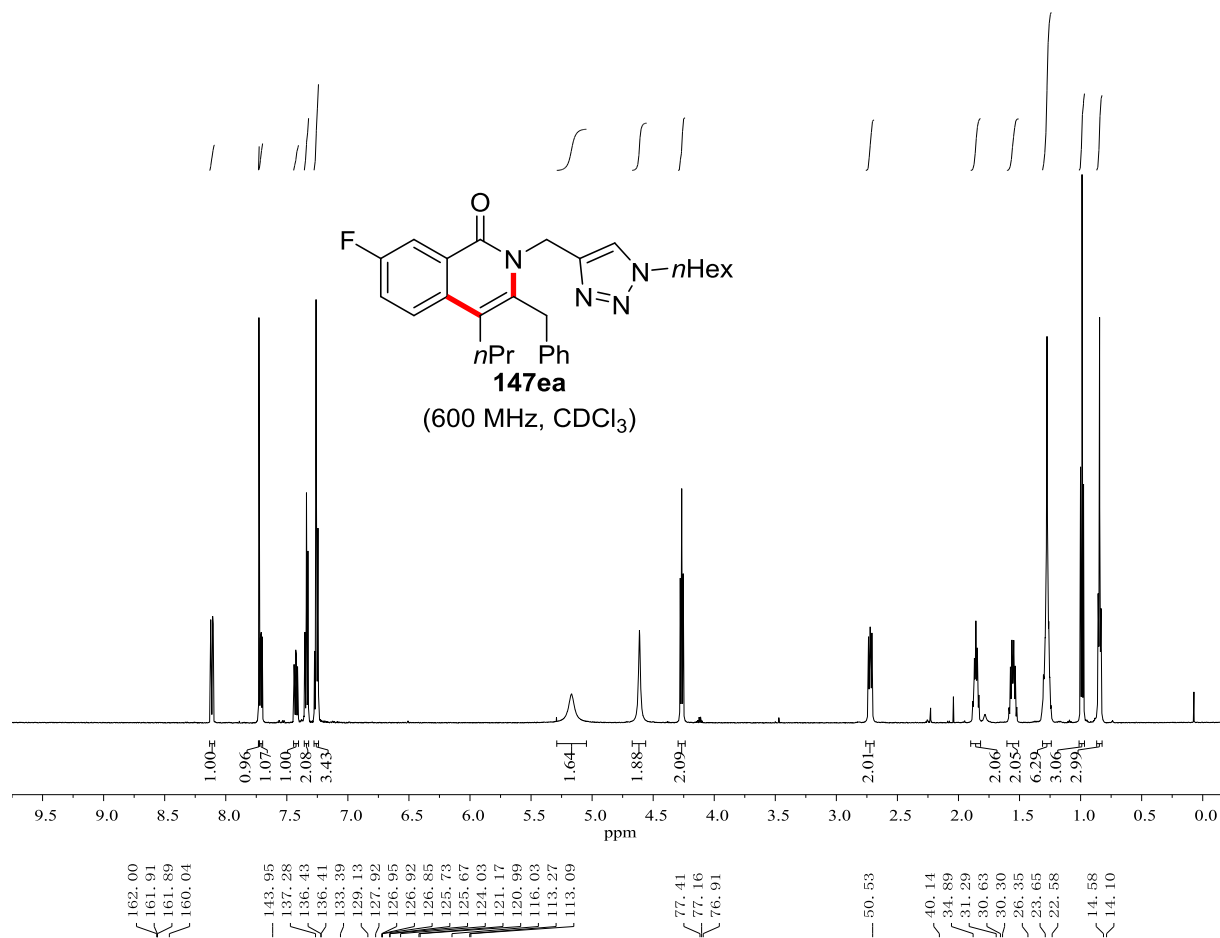


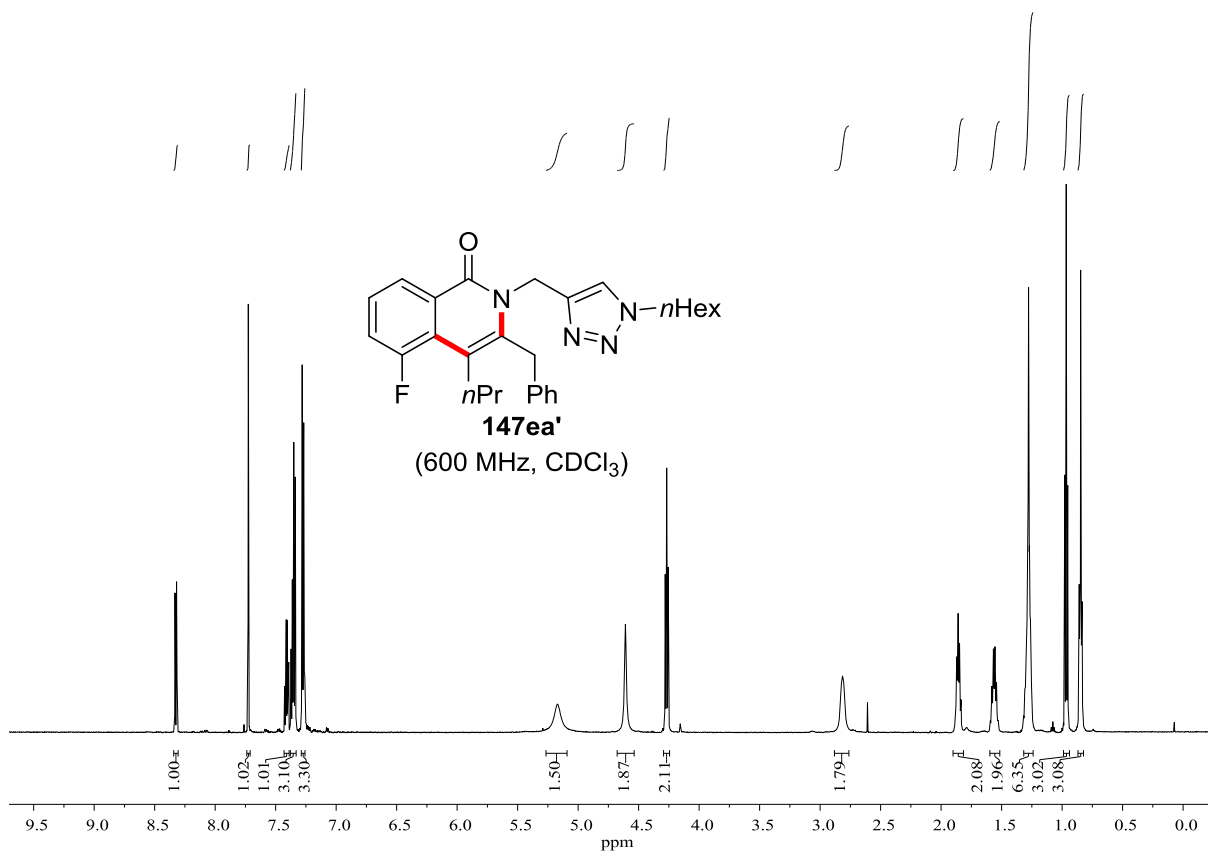
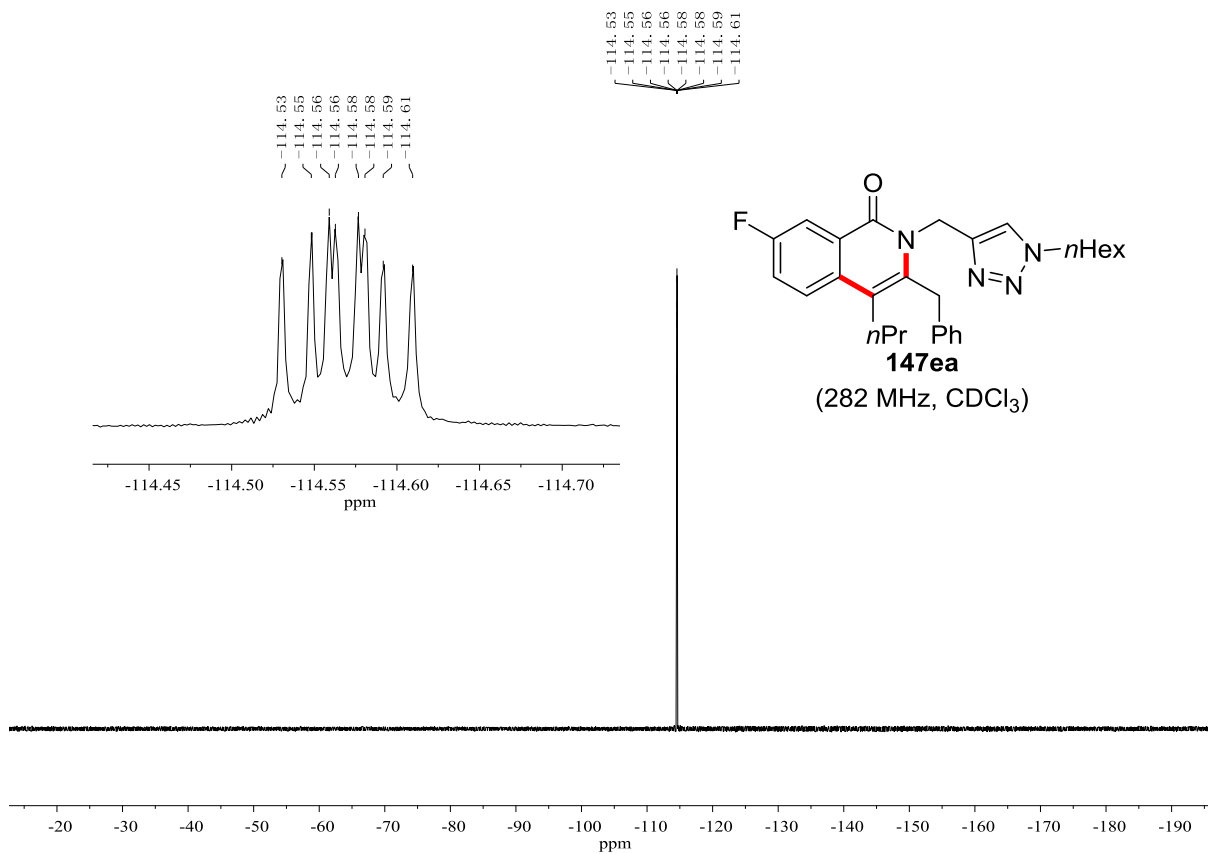


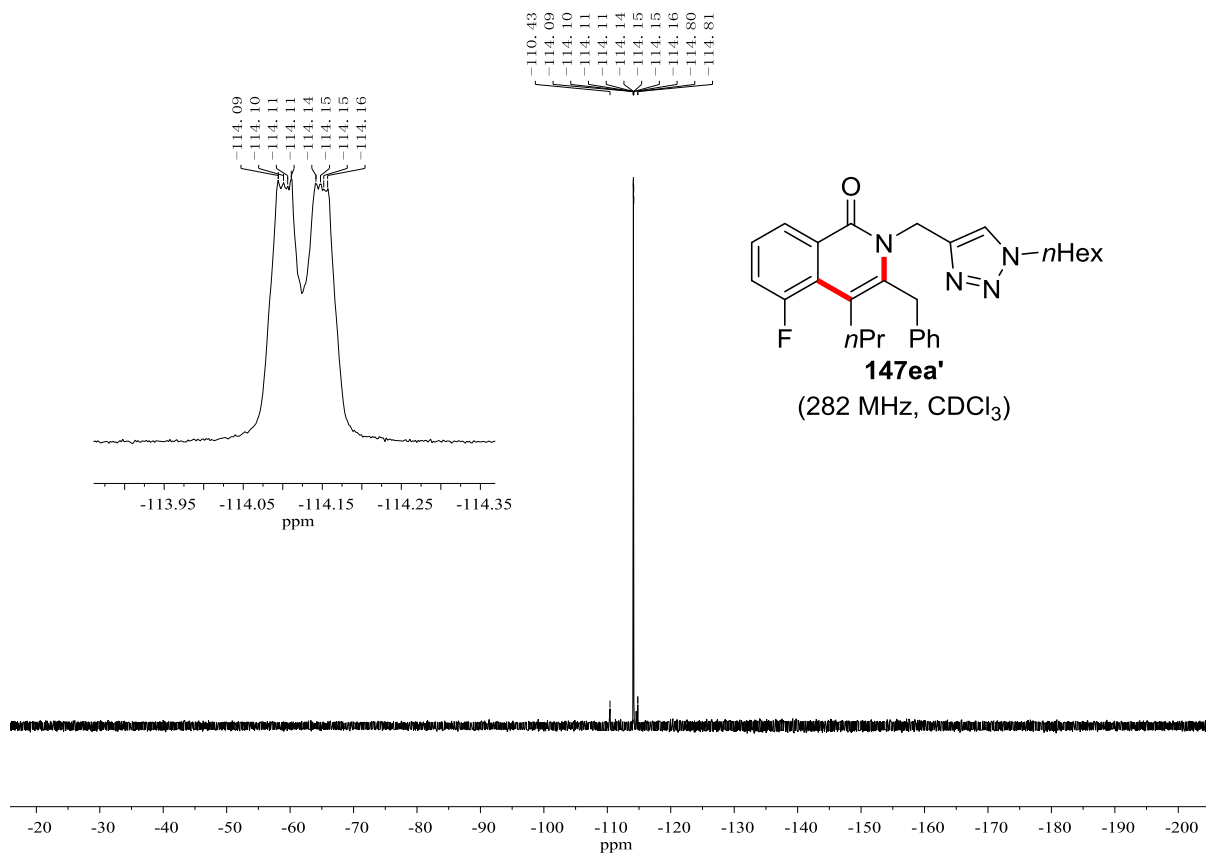
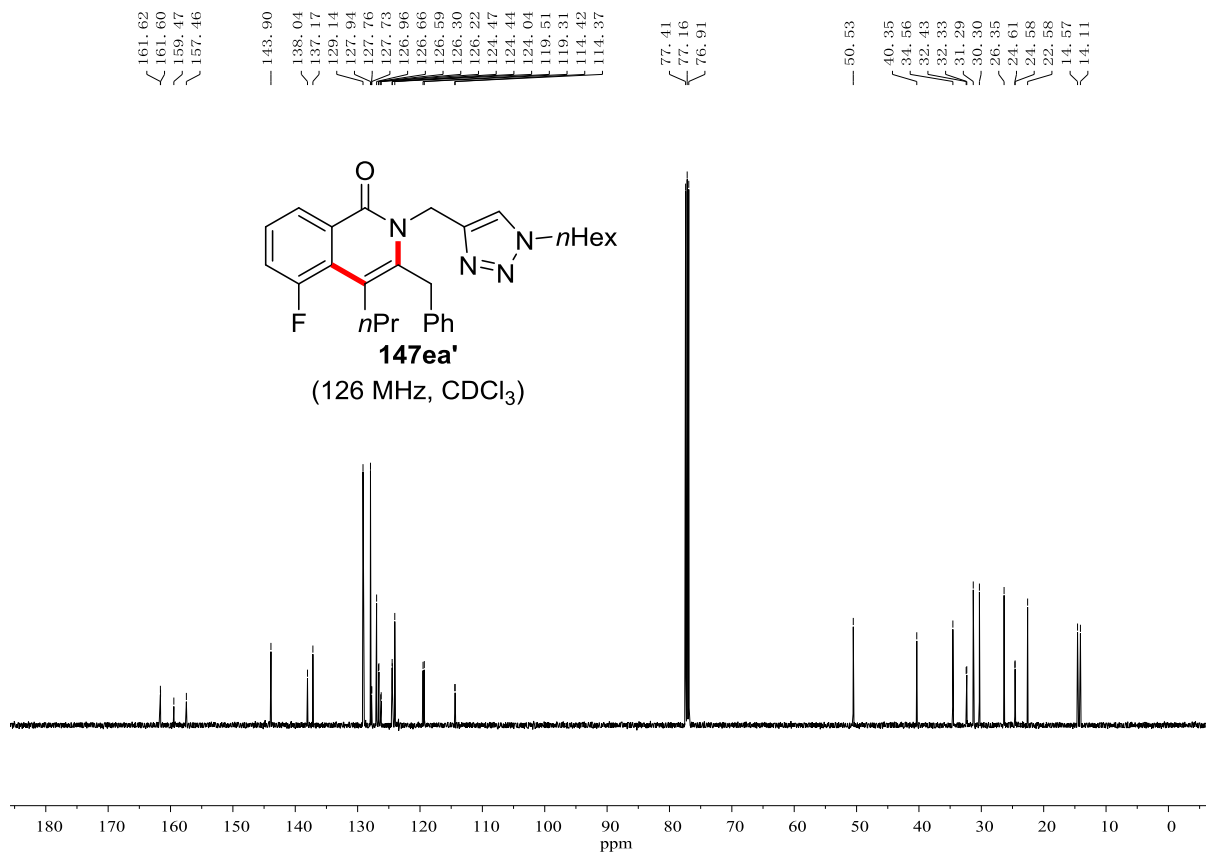
-110.50
-110.51
-110.54
-110.56

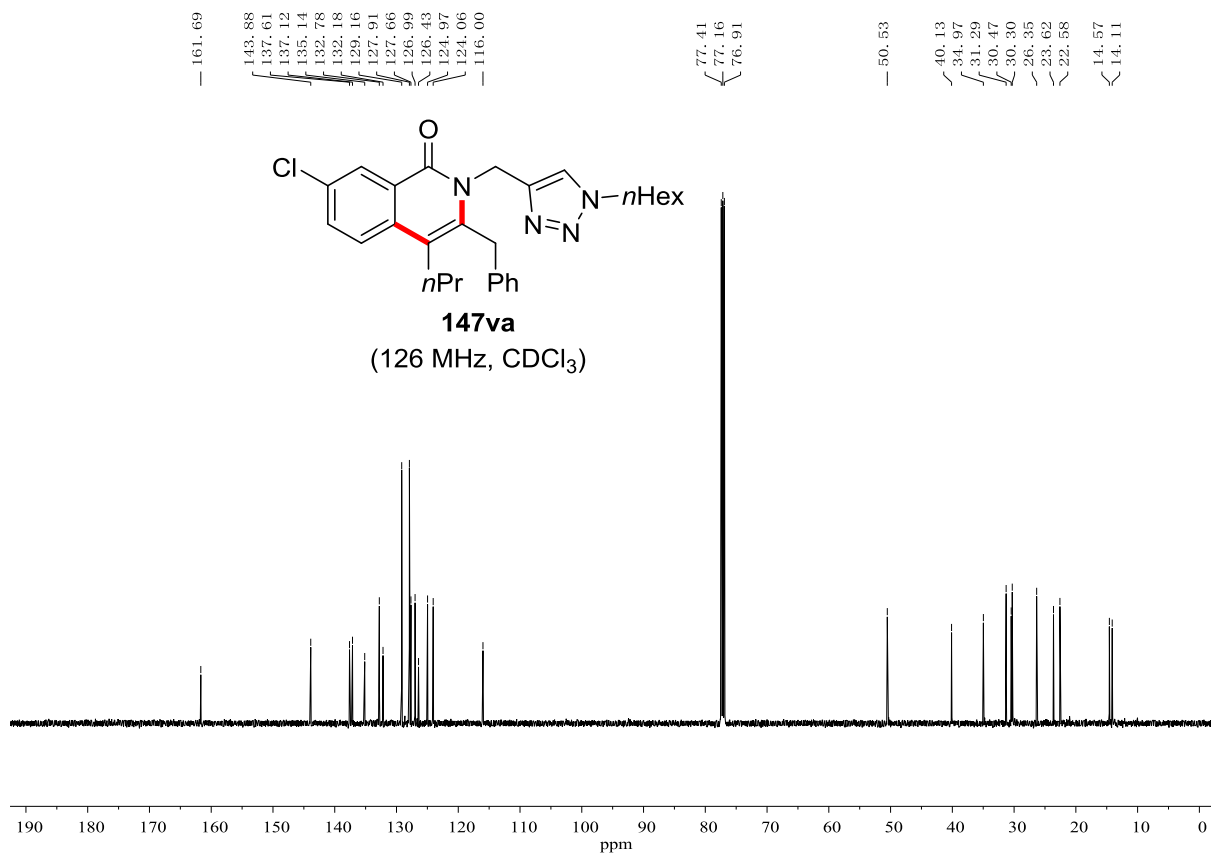
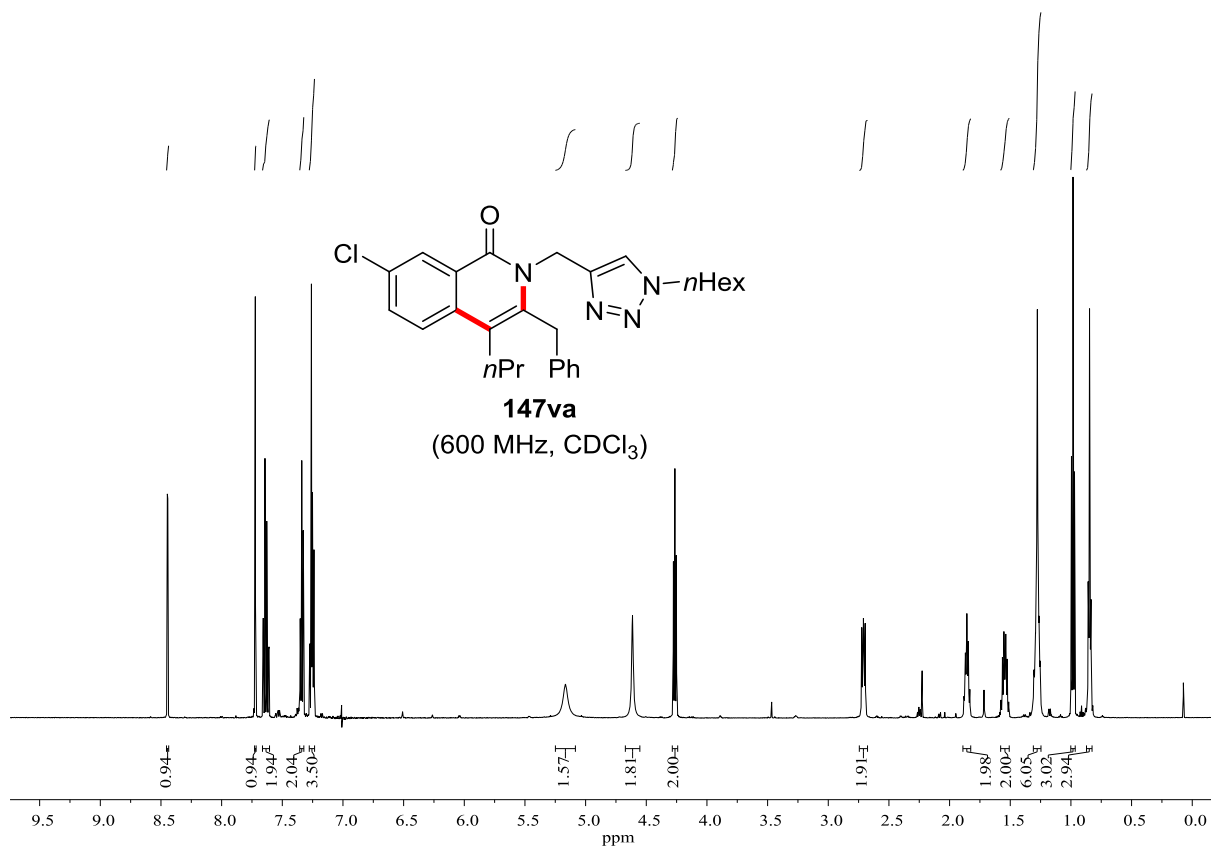


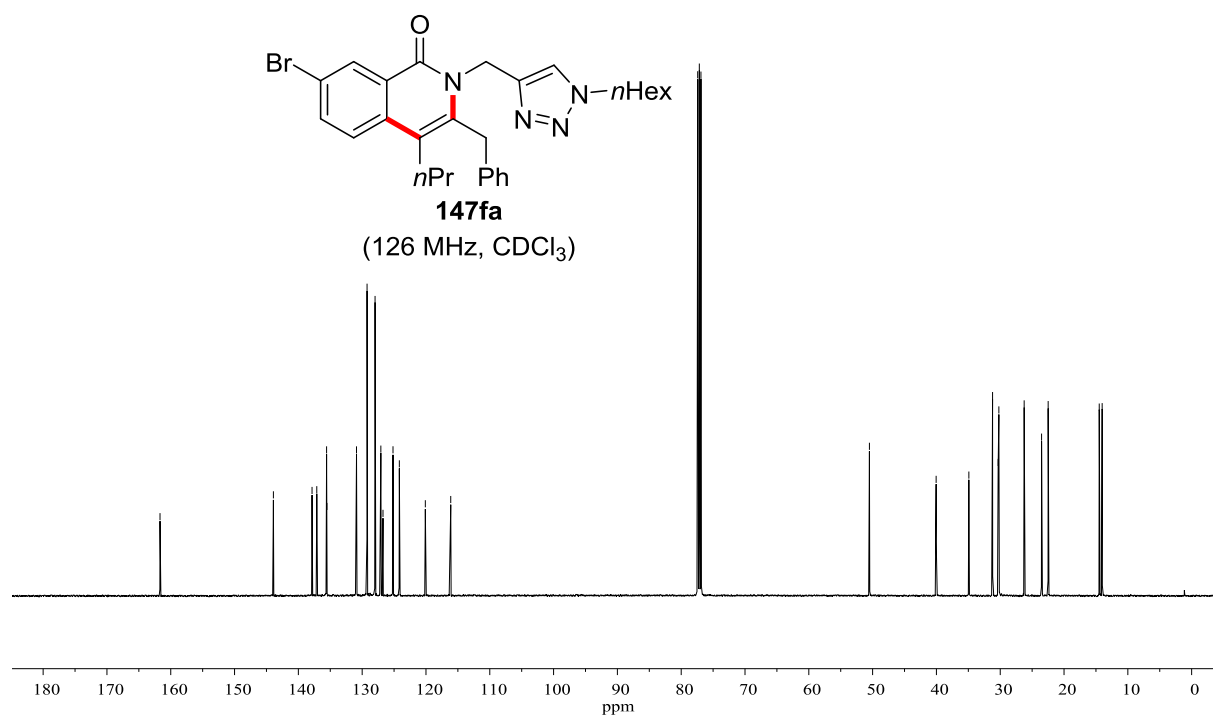
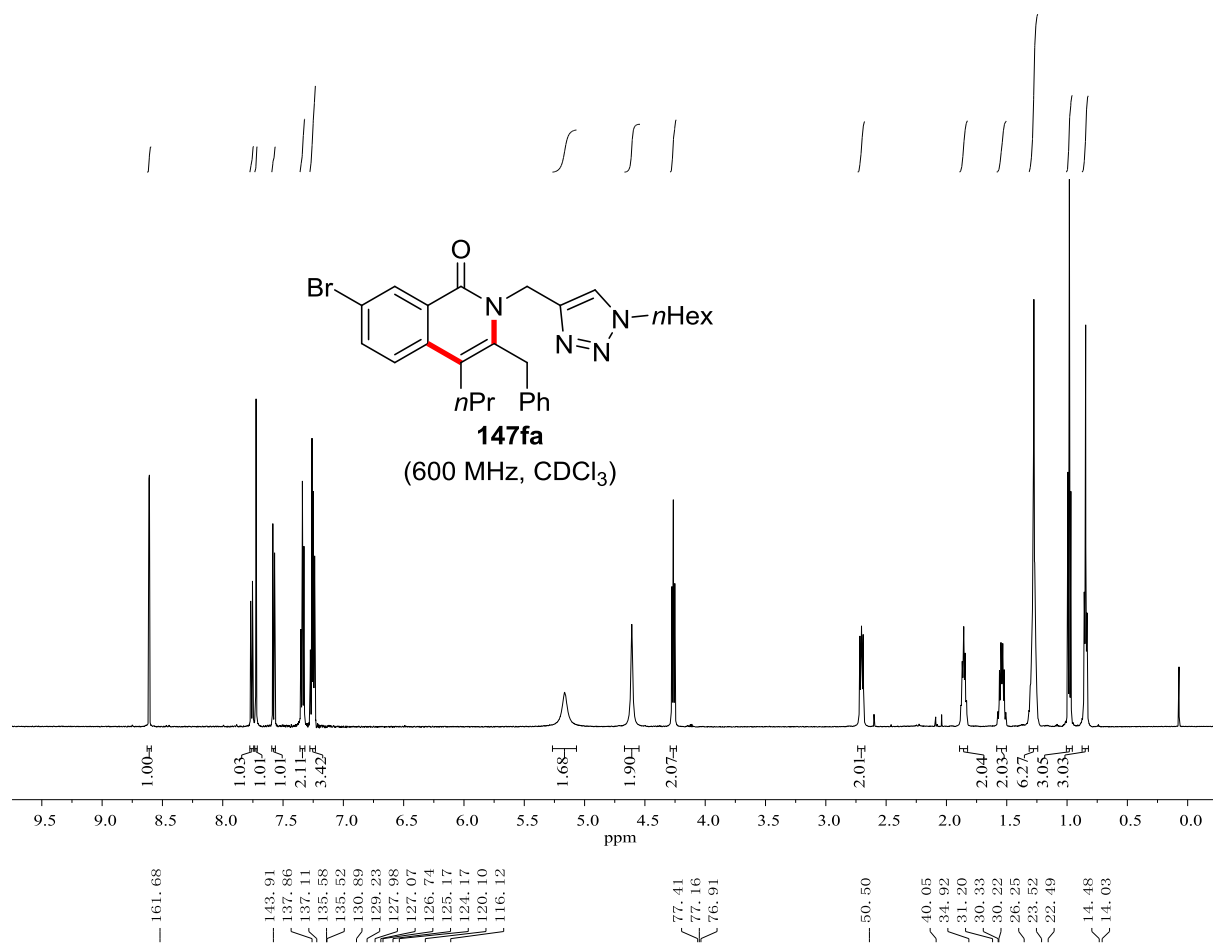


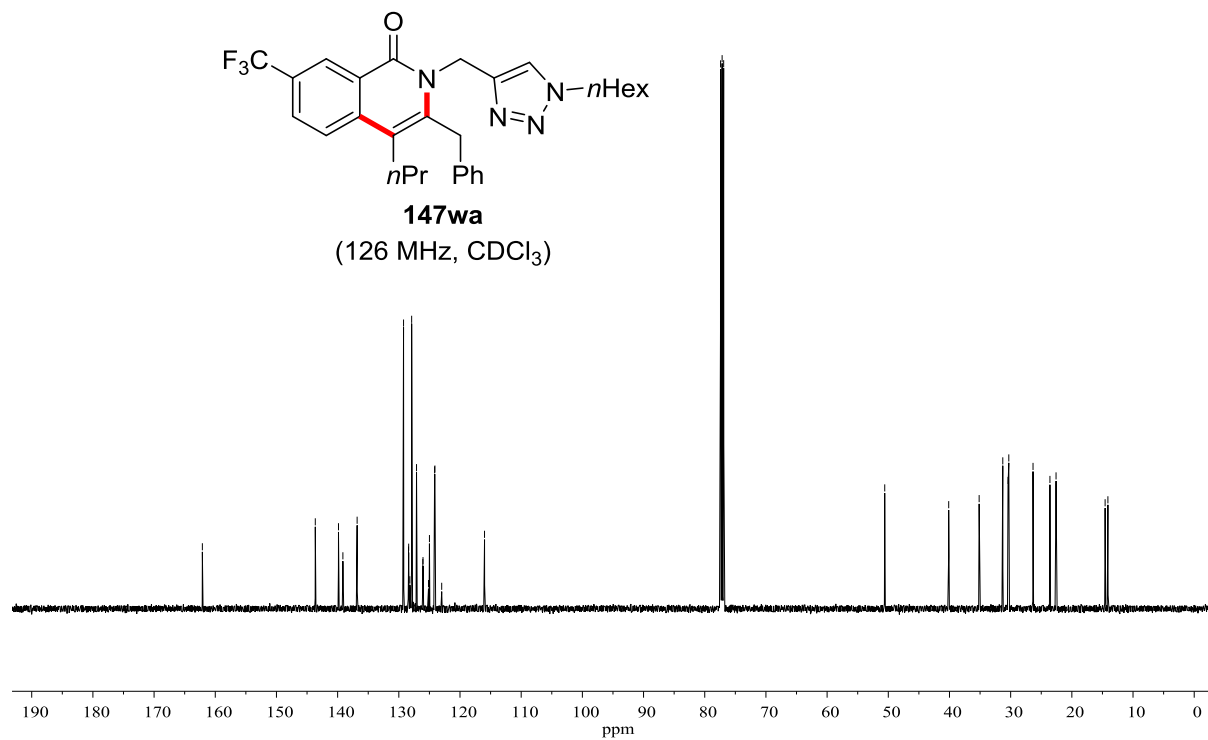
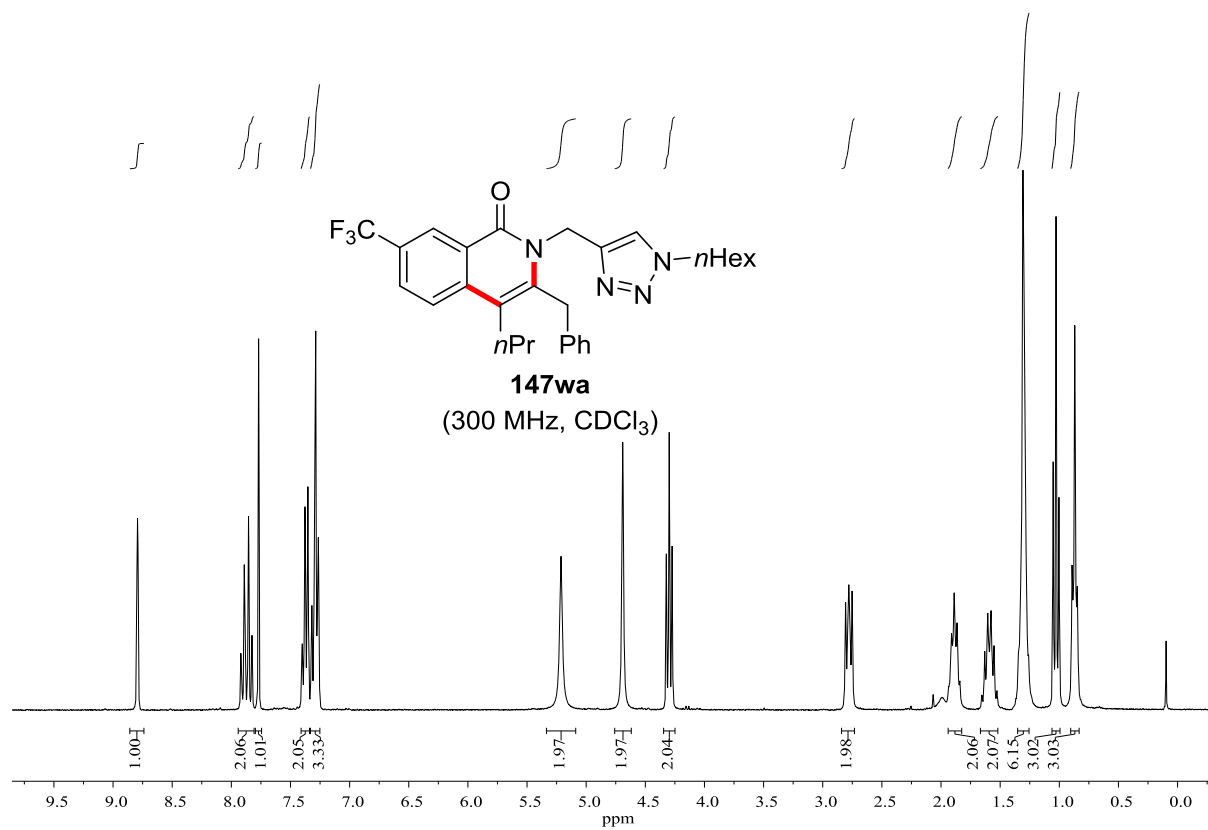




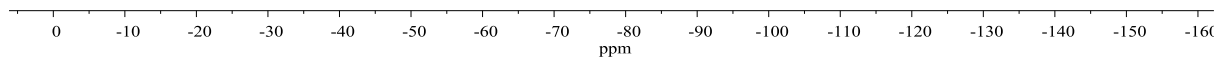
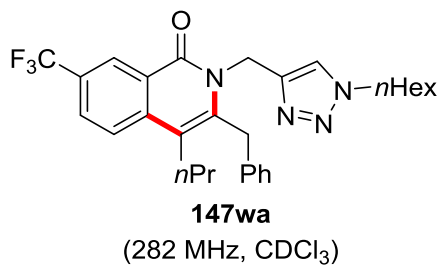


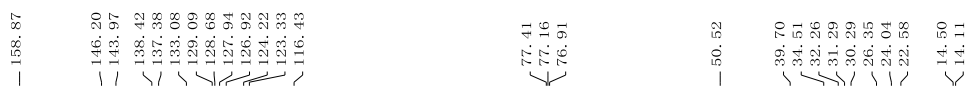
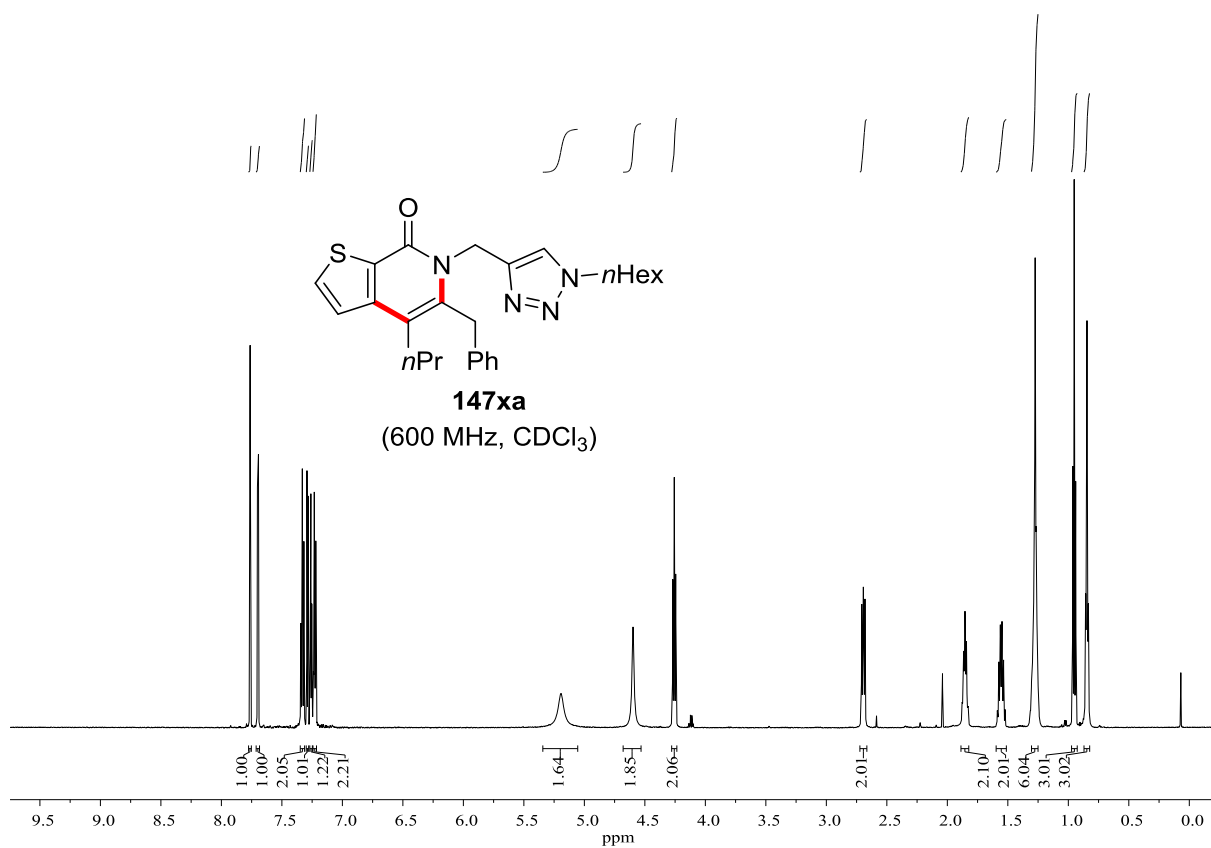


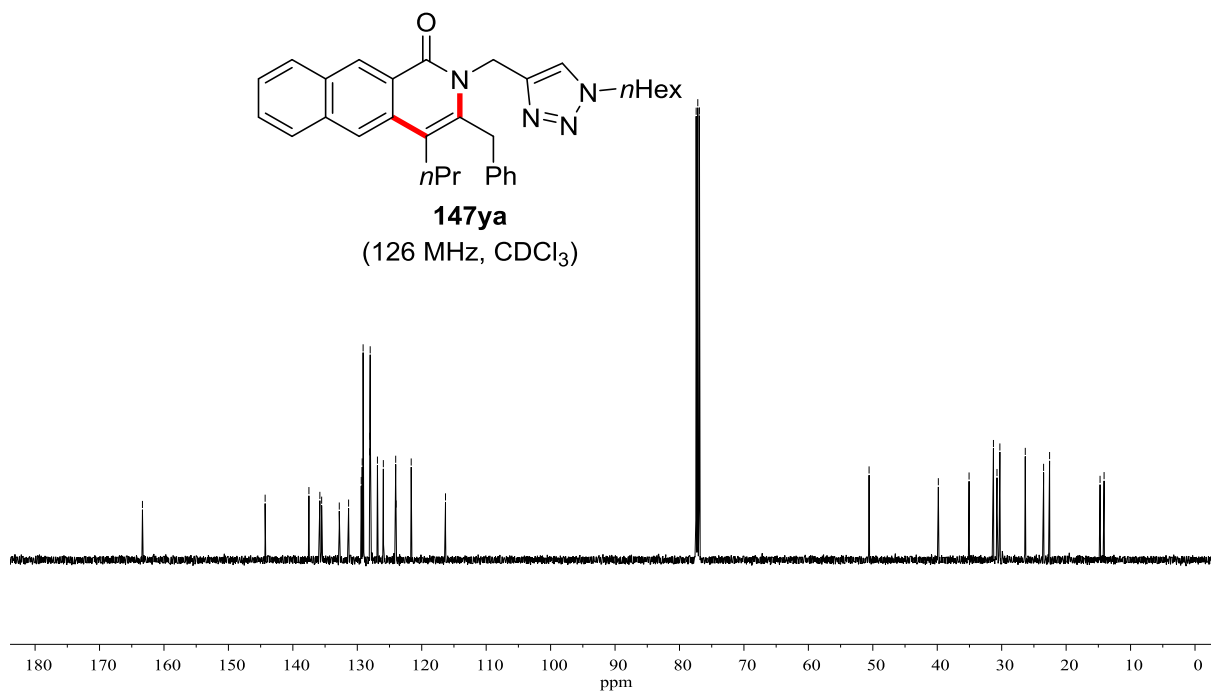
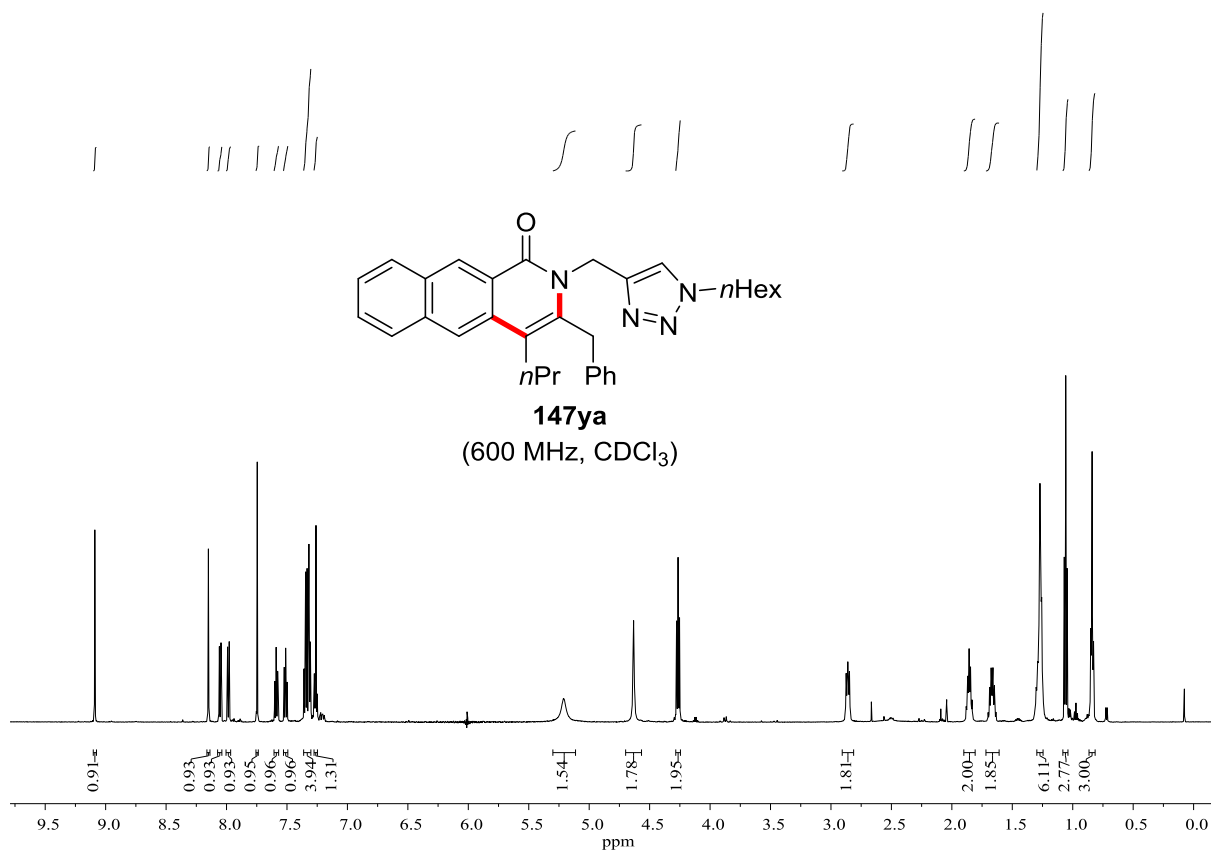


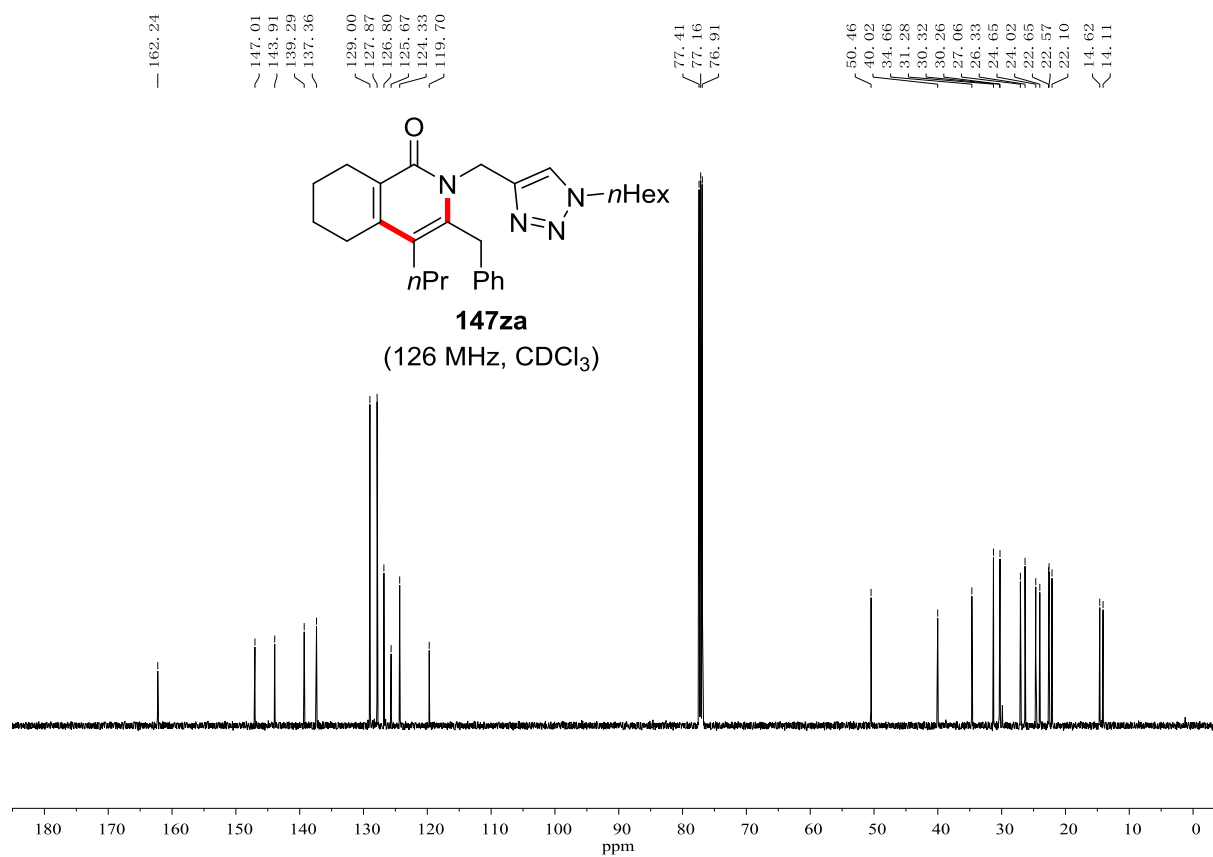
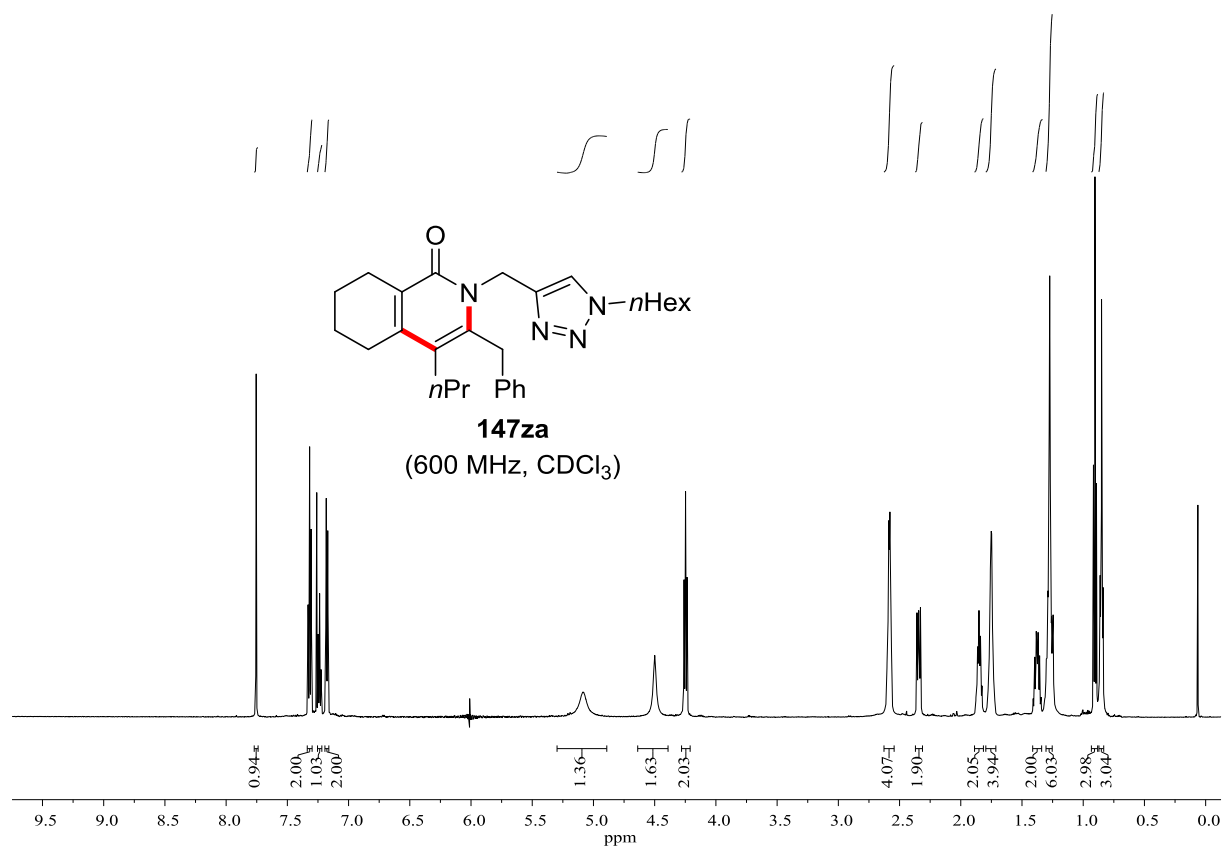


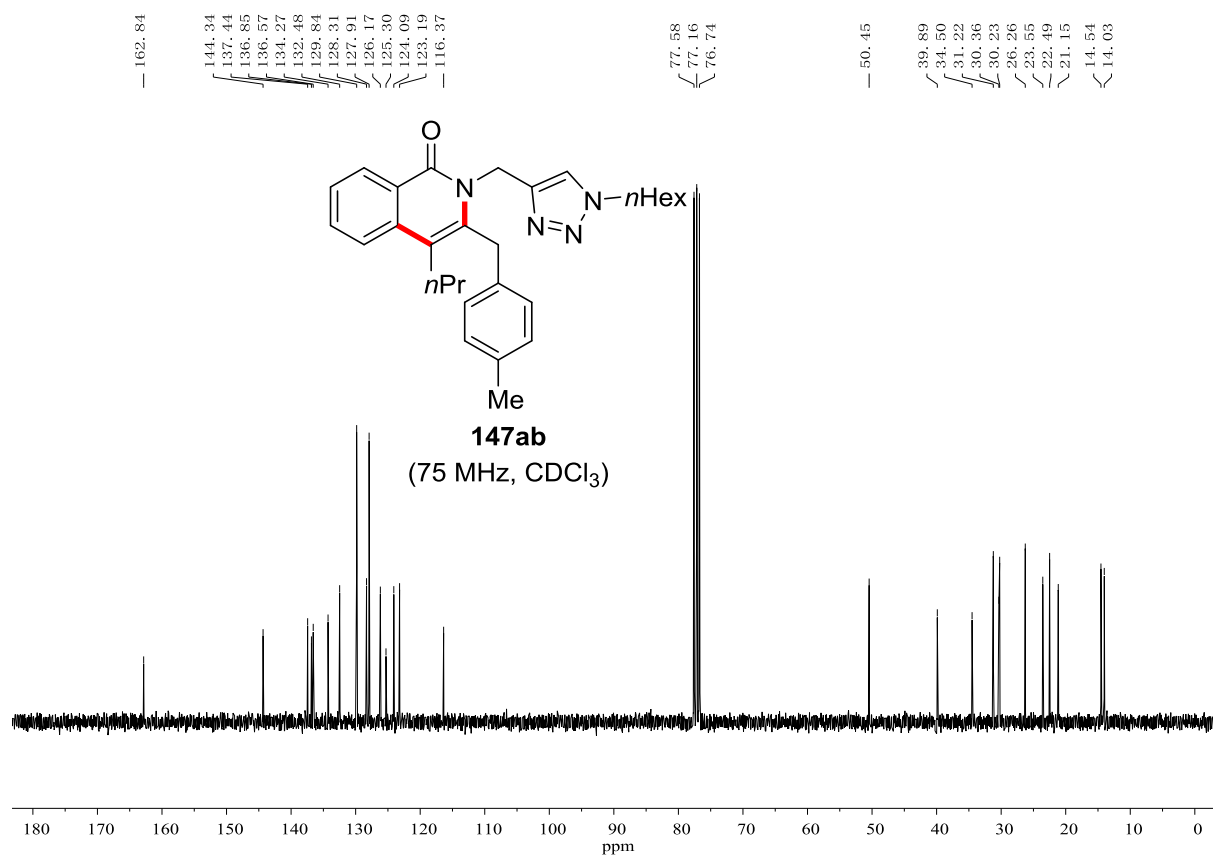
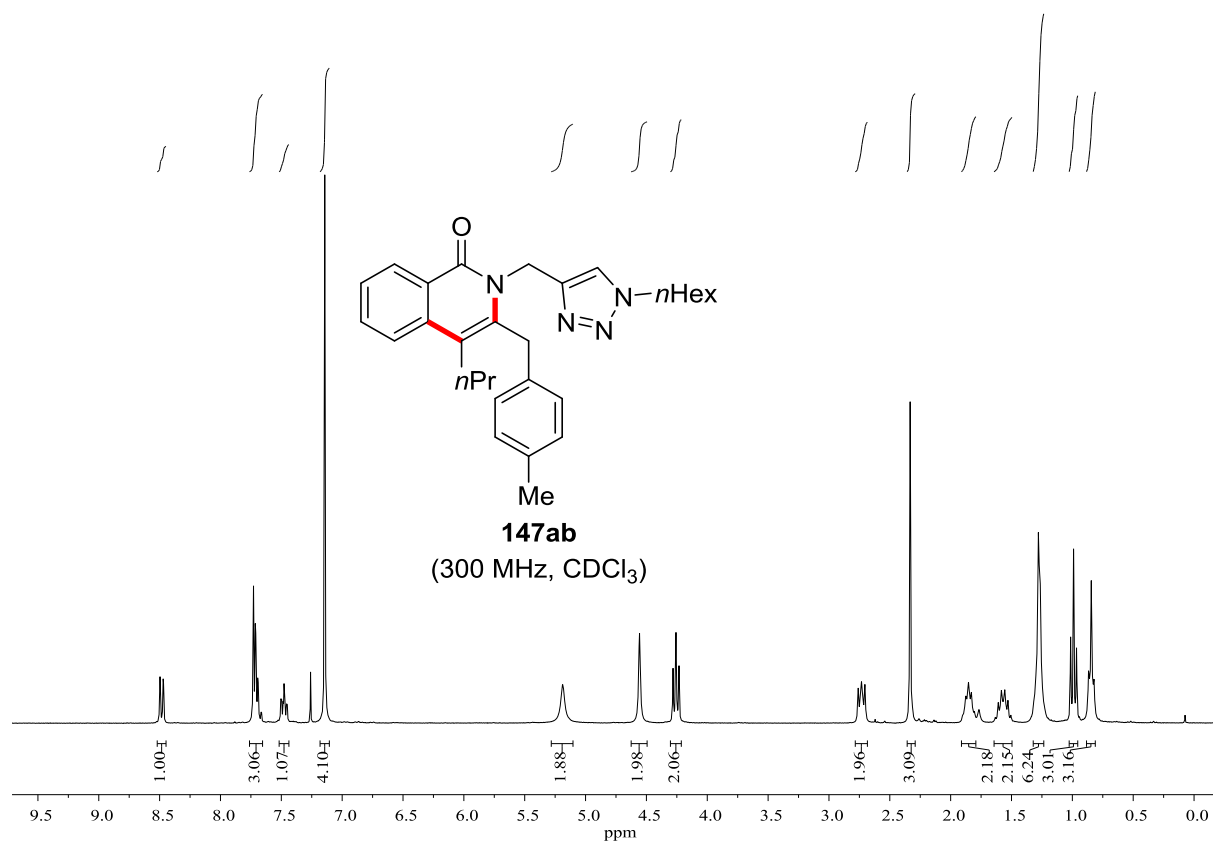
-62.38

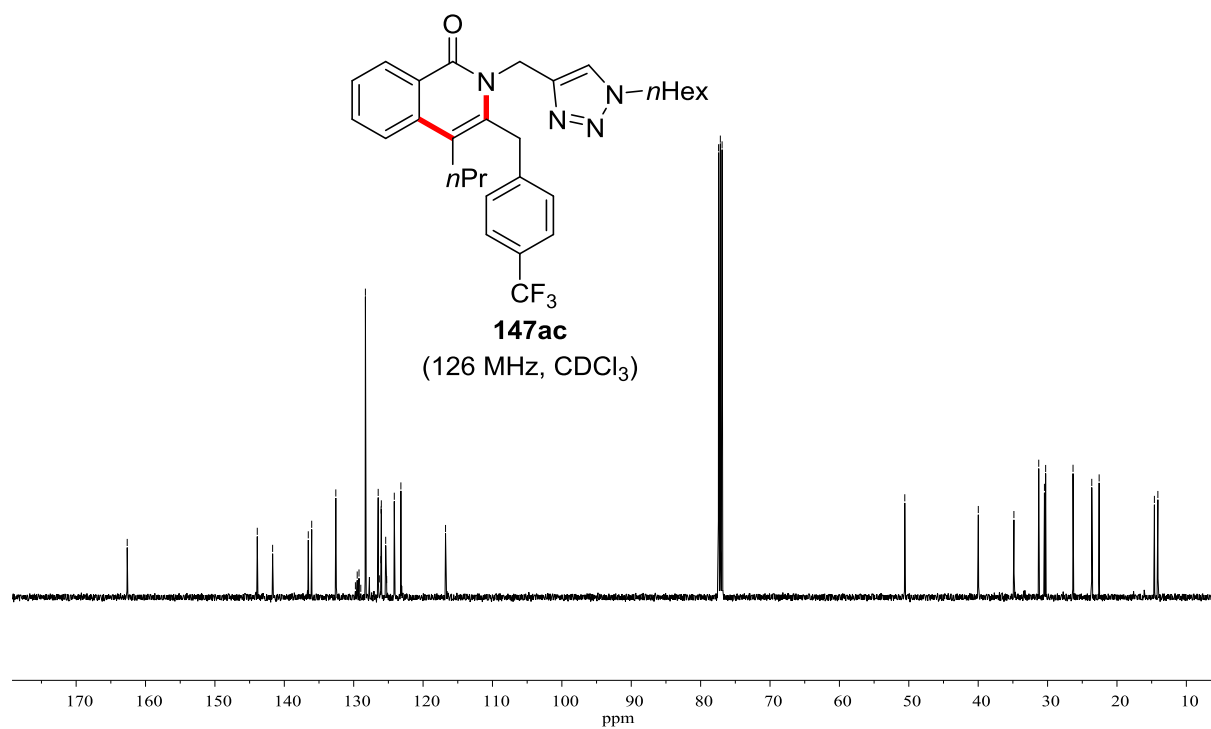
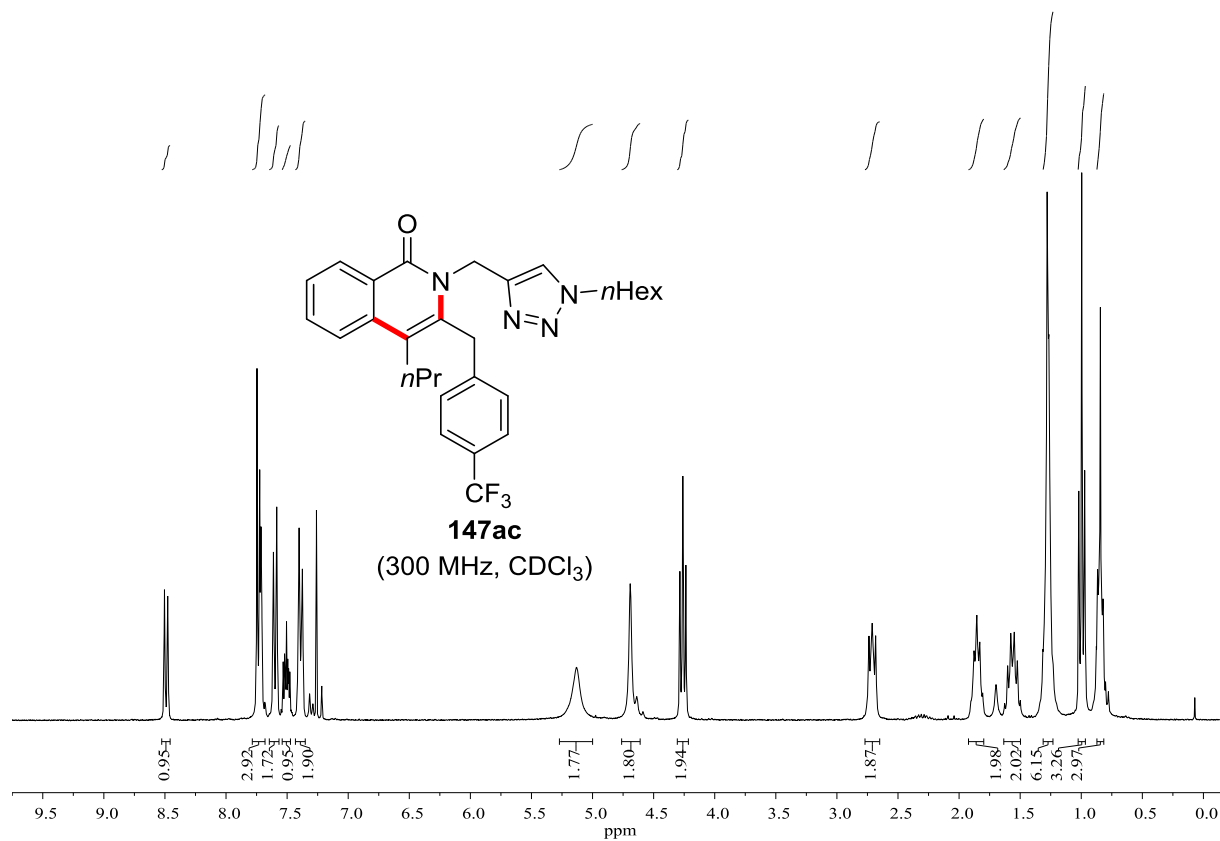


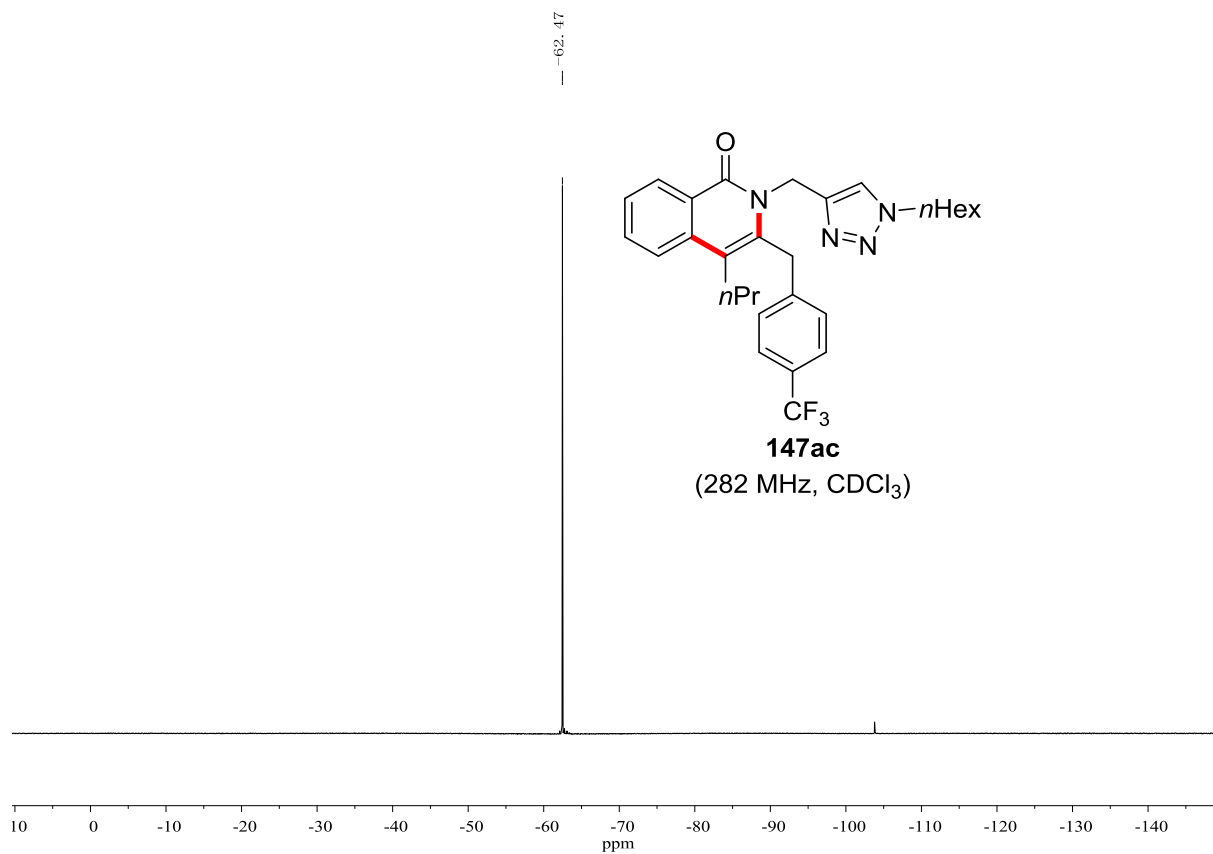


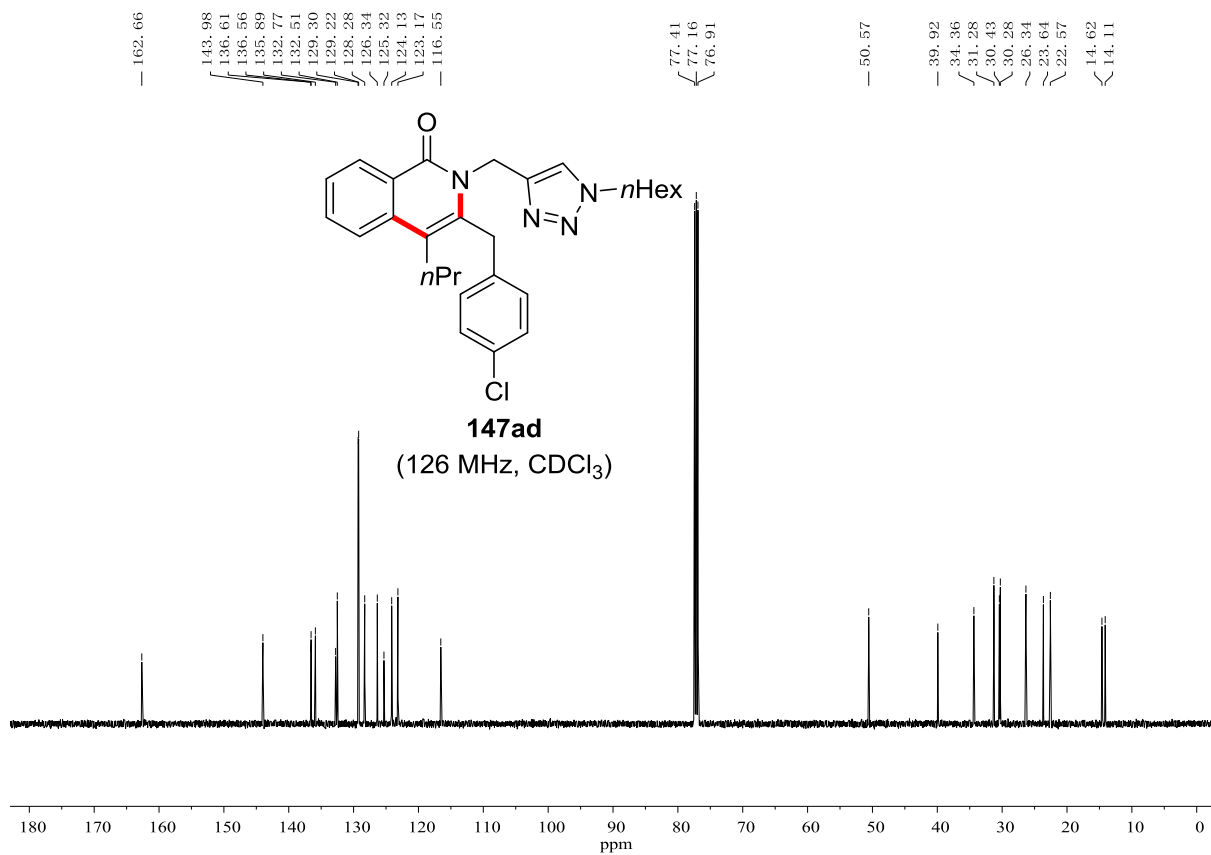
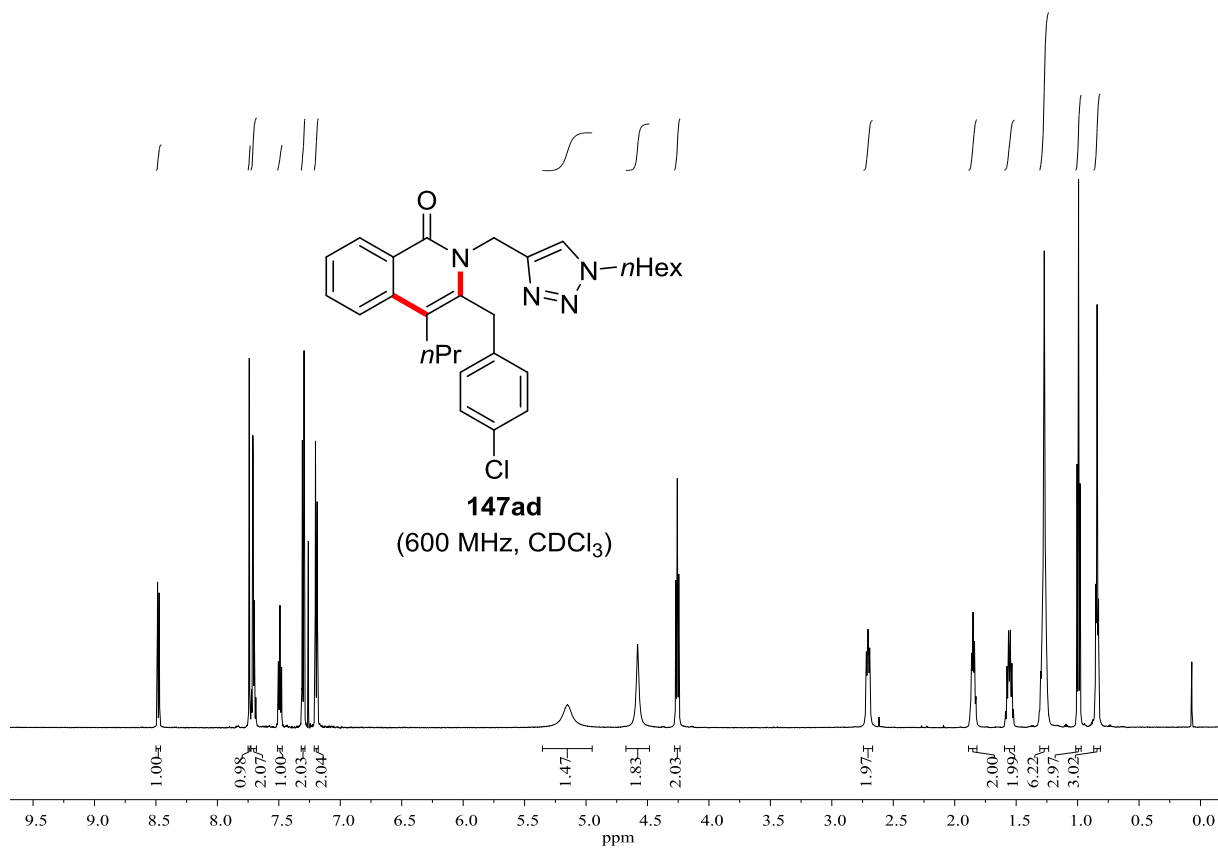


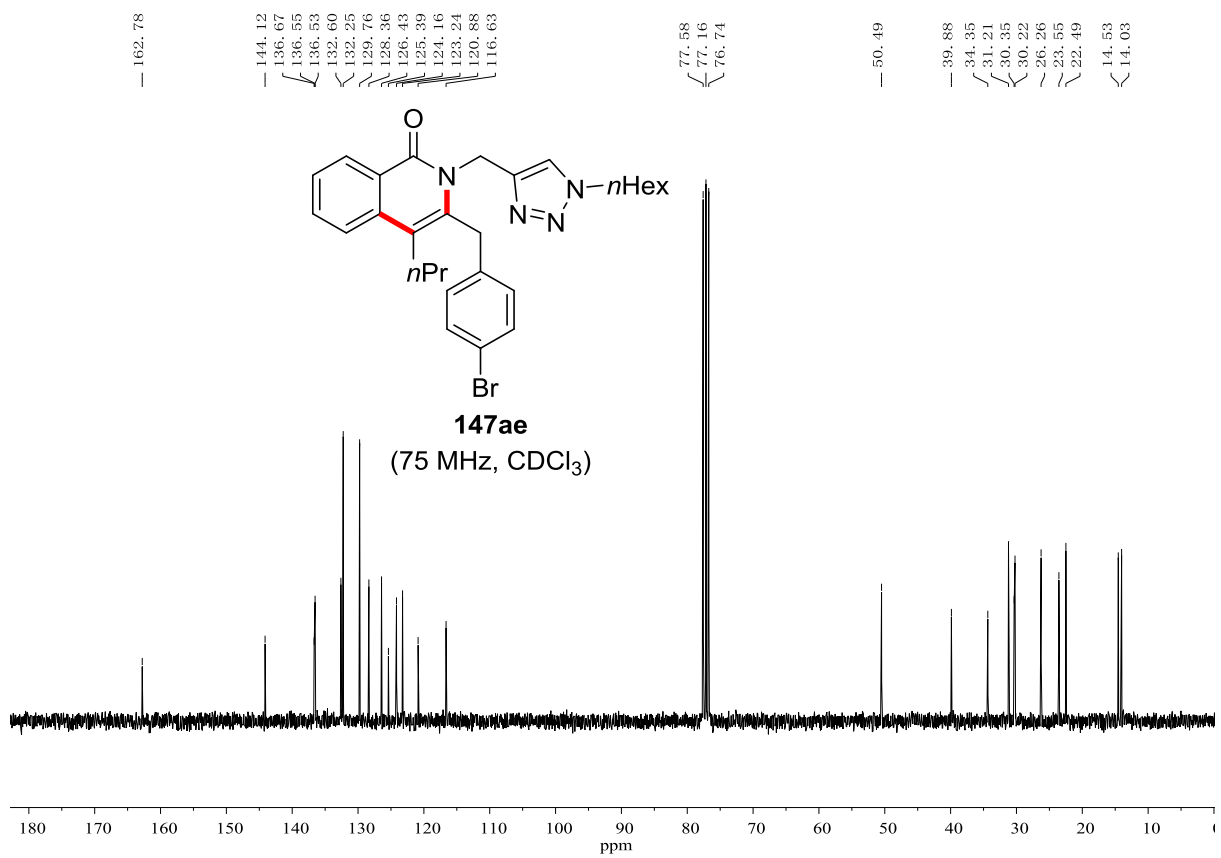
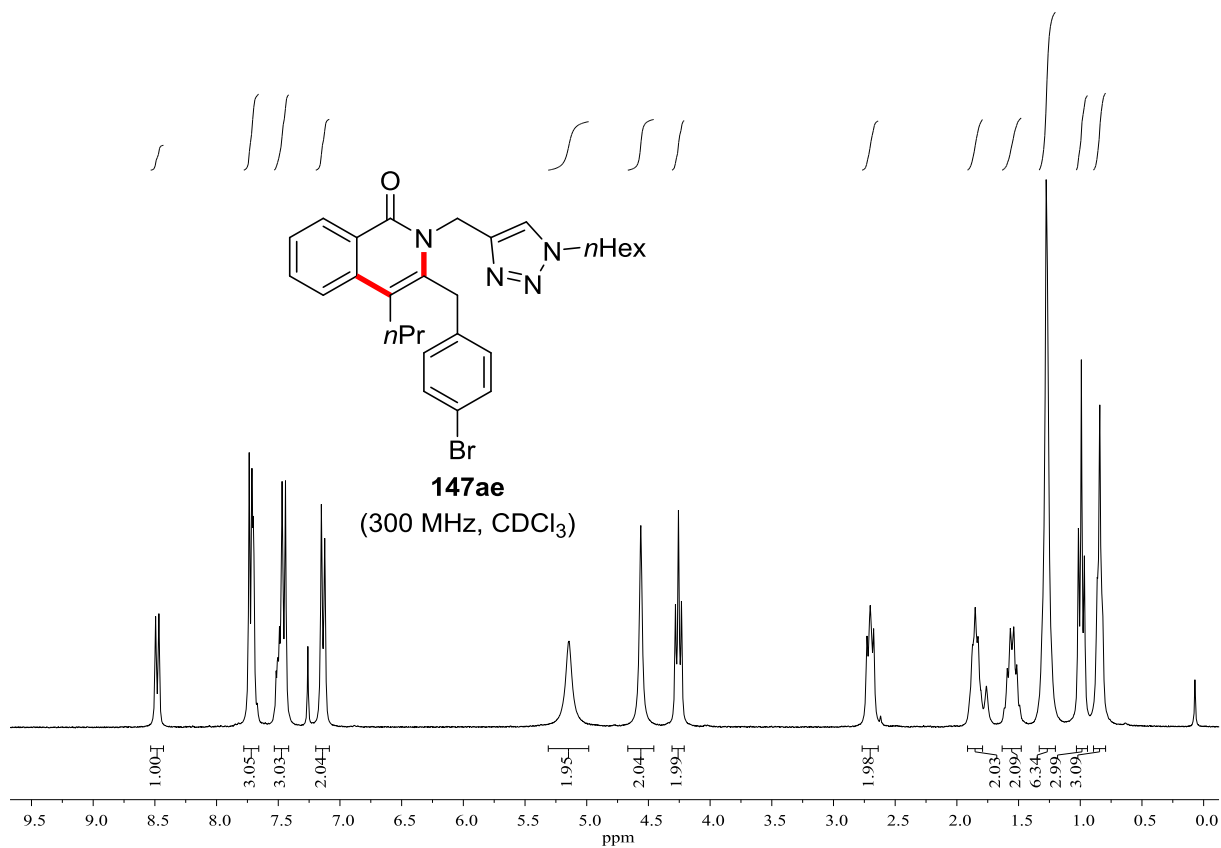


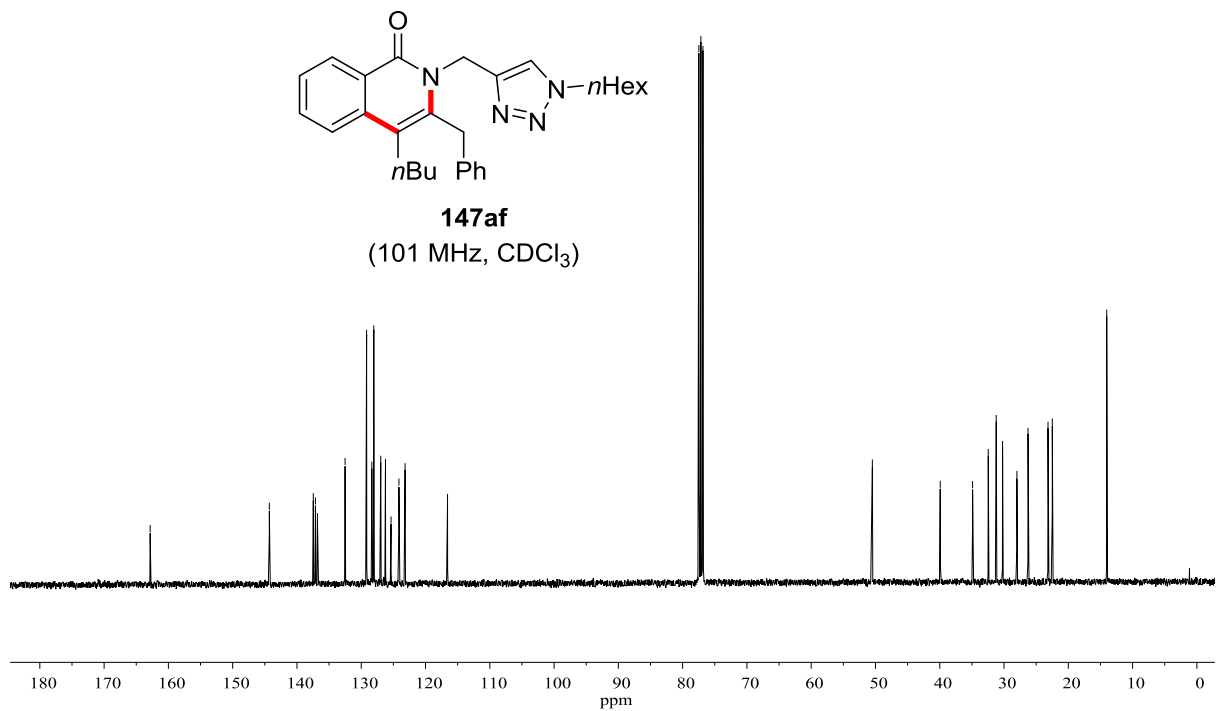
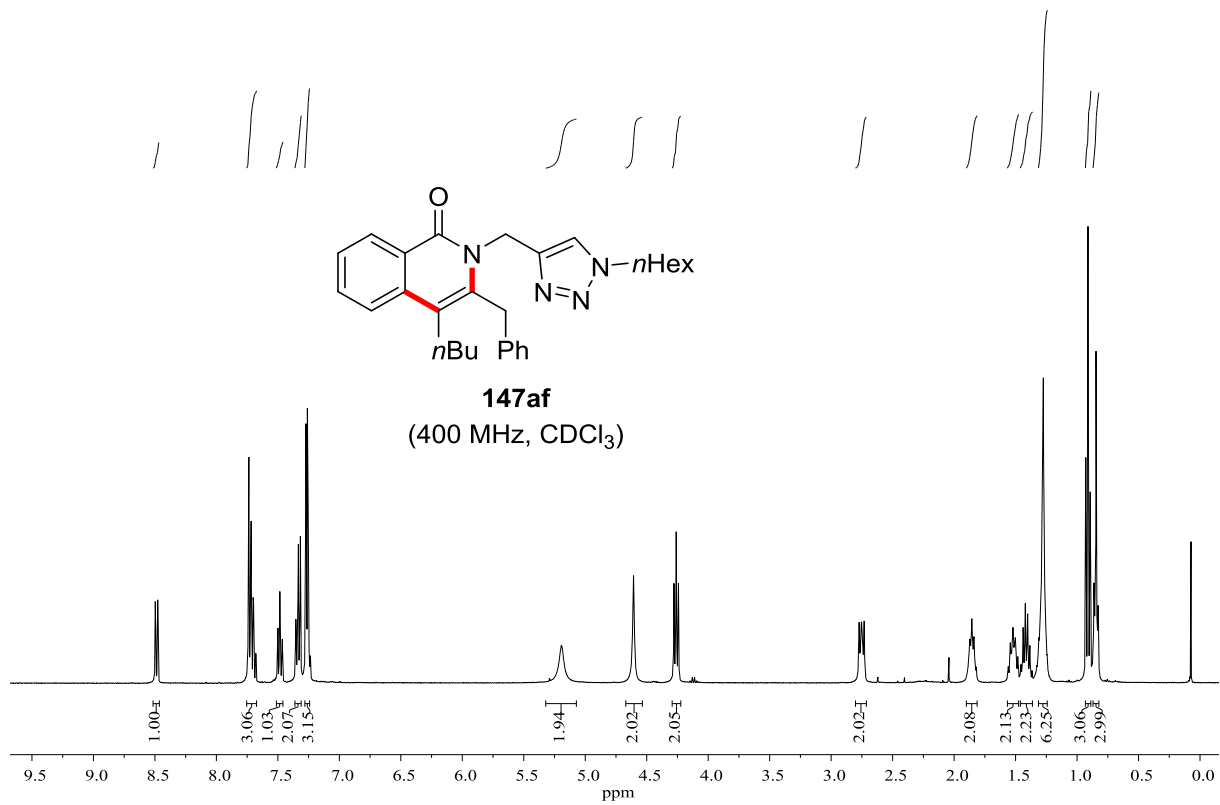


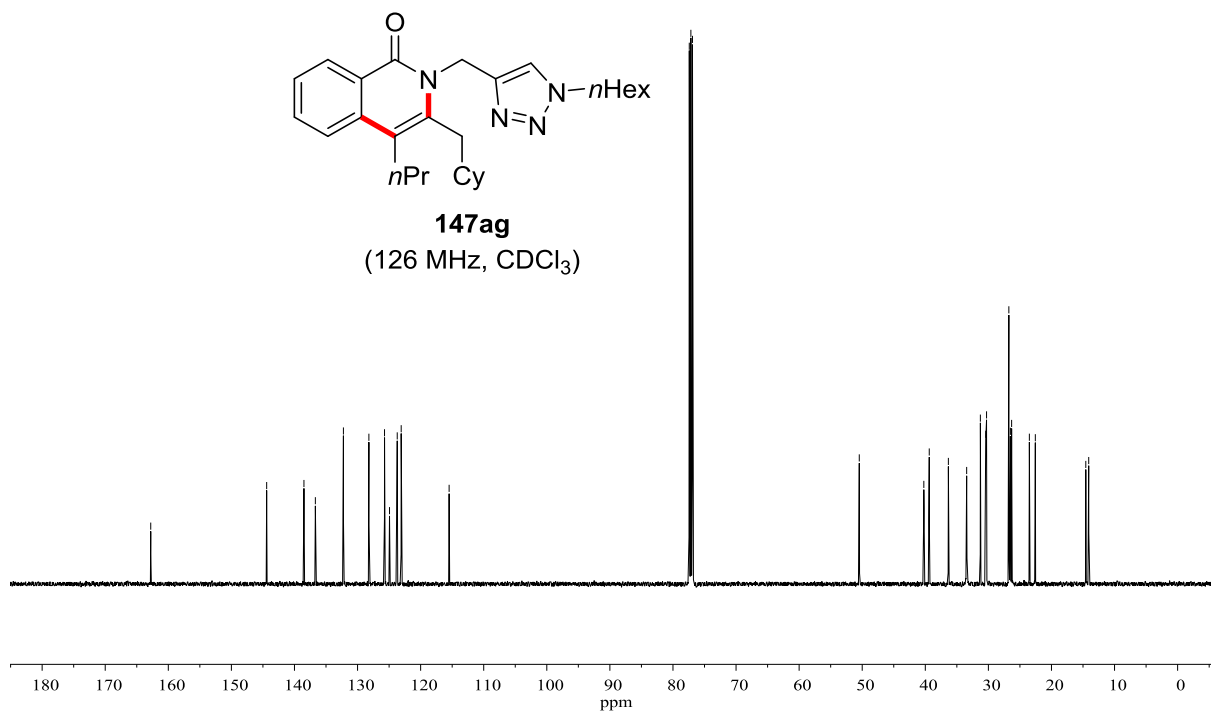
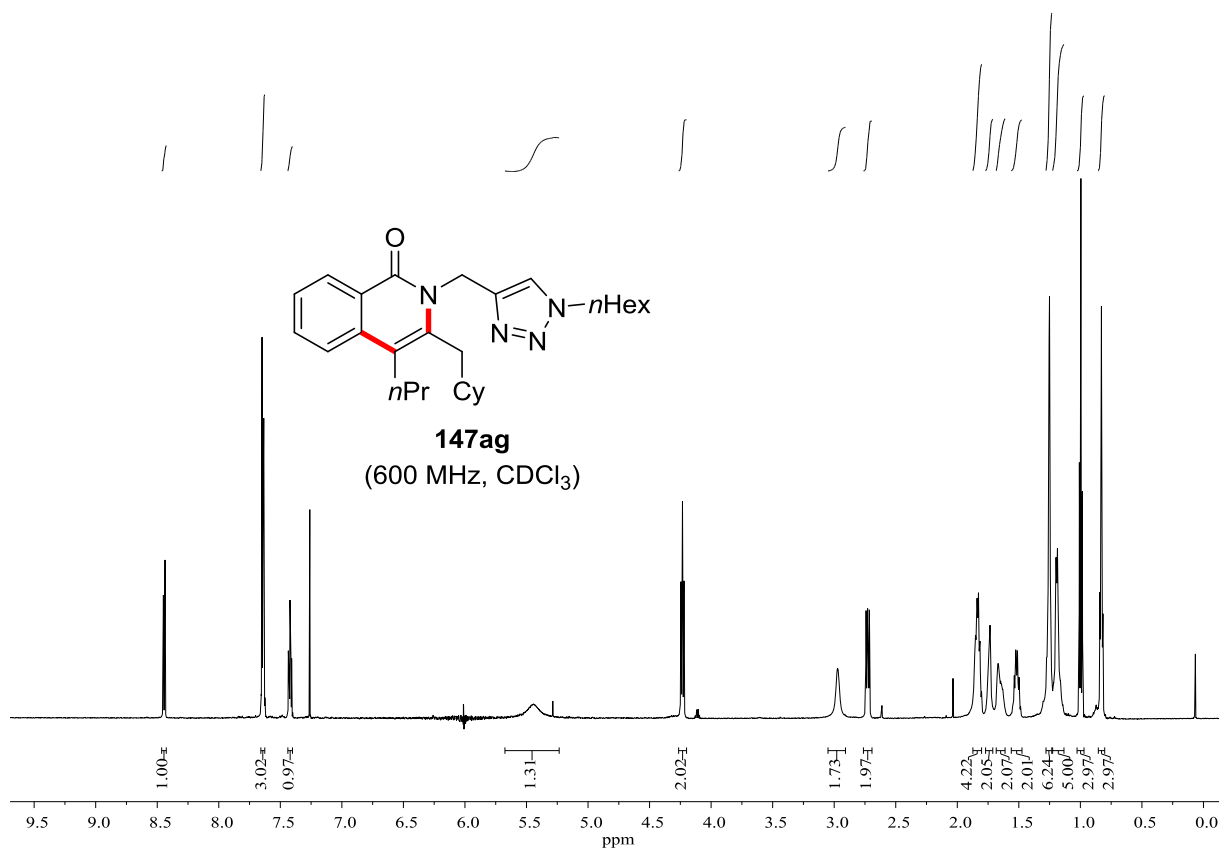


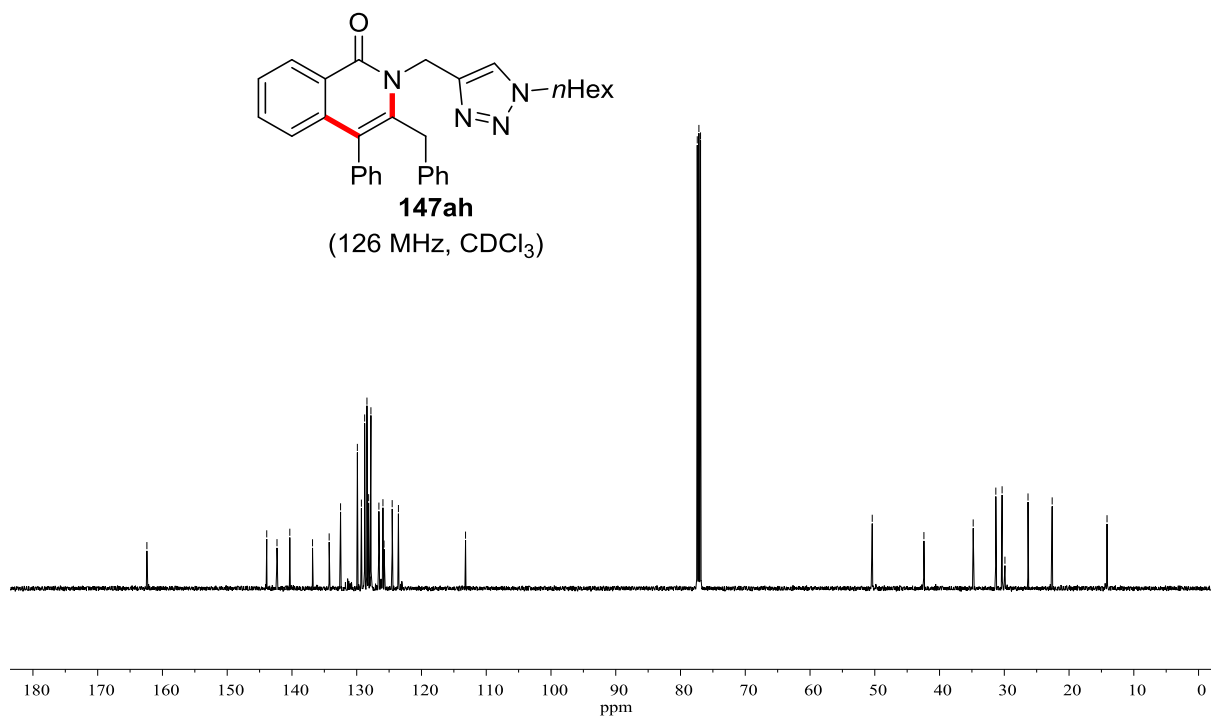
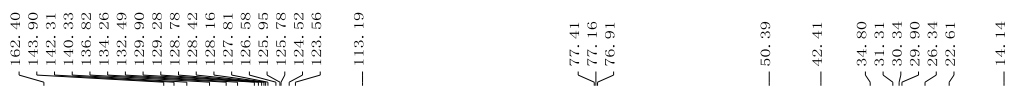
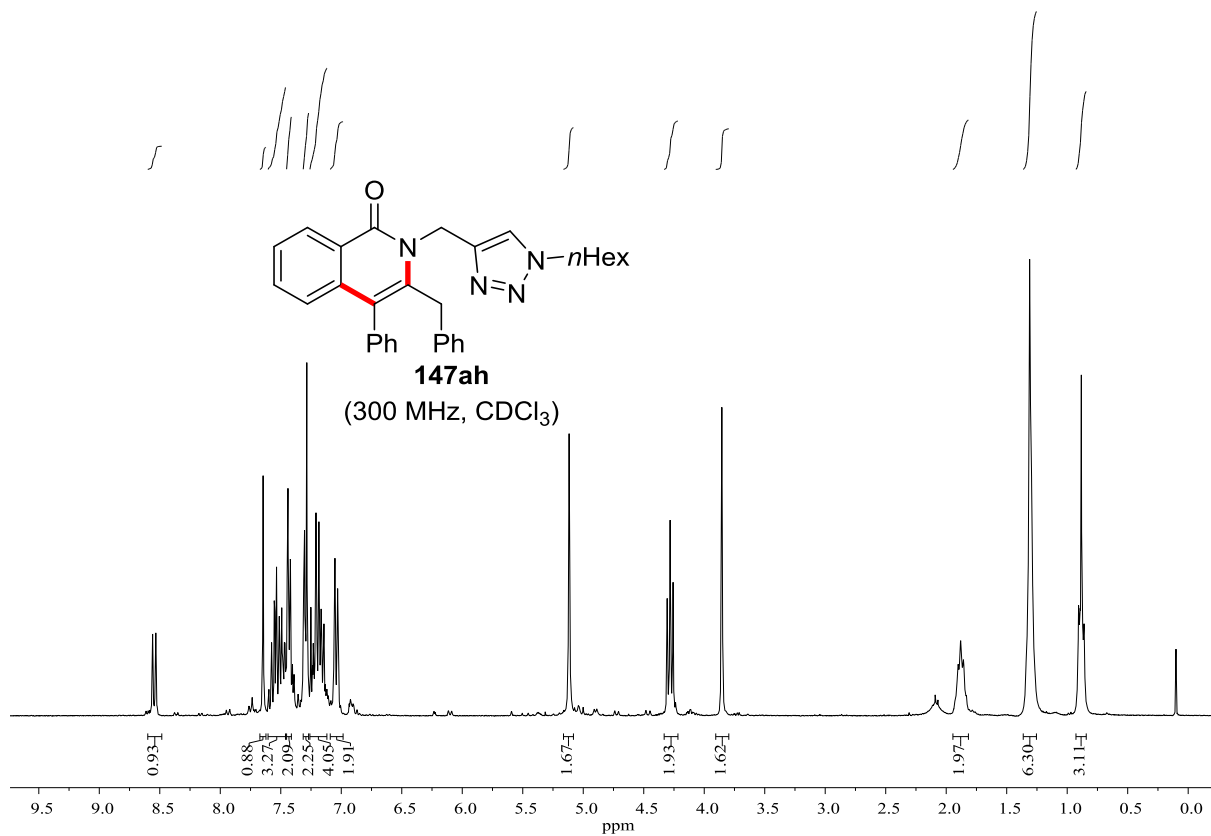


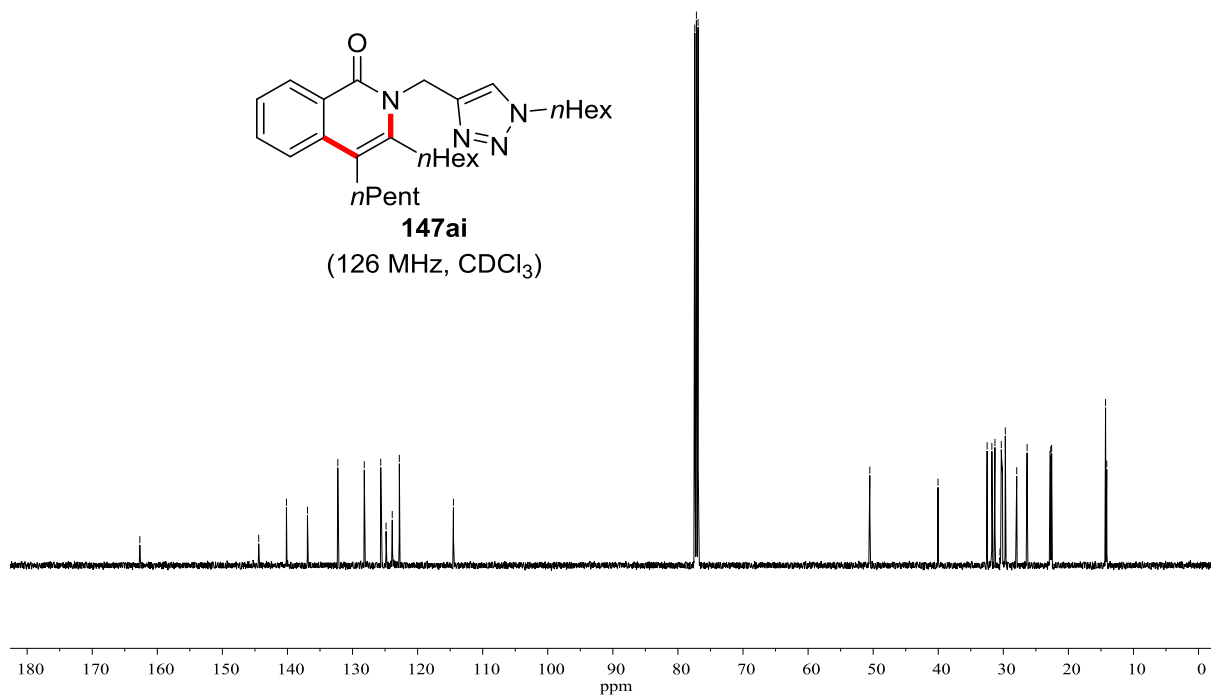
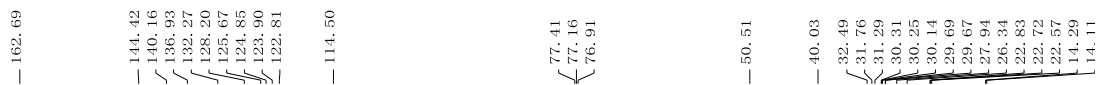
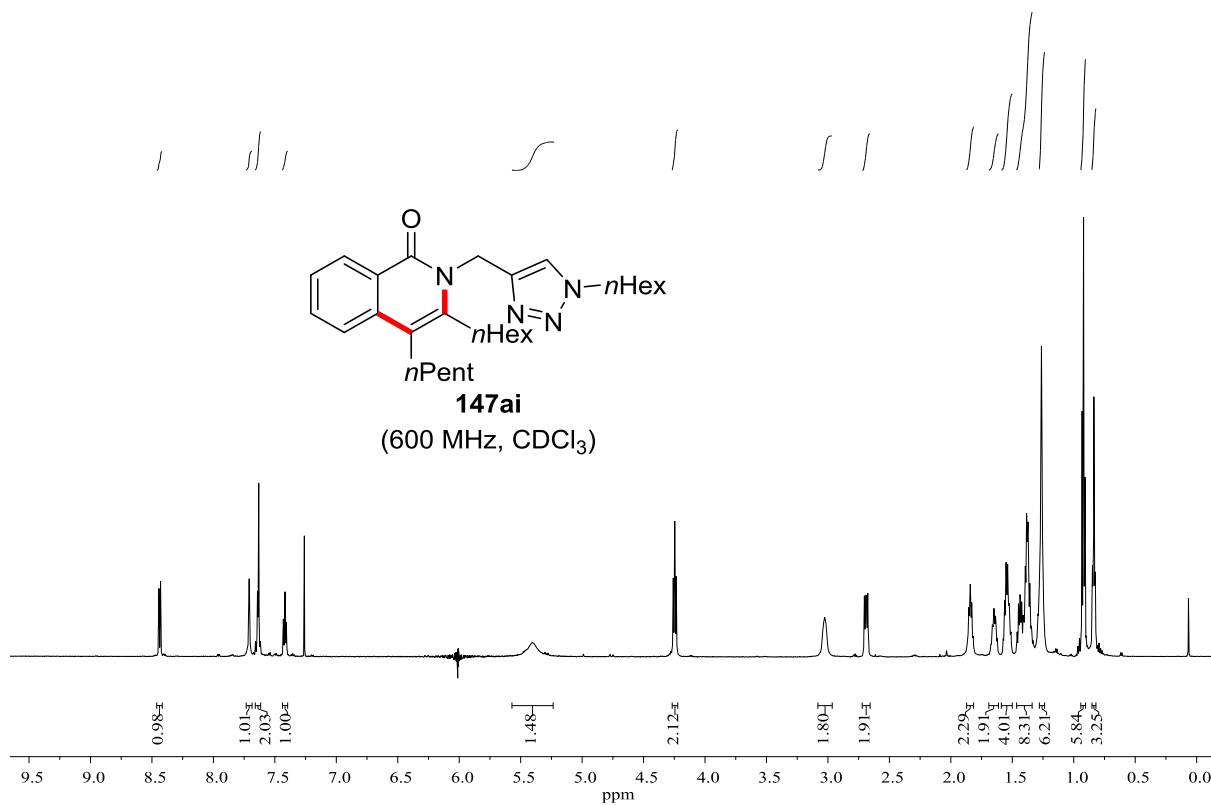


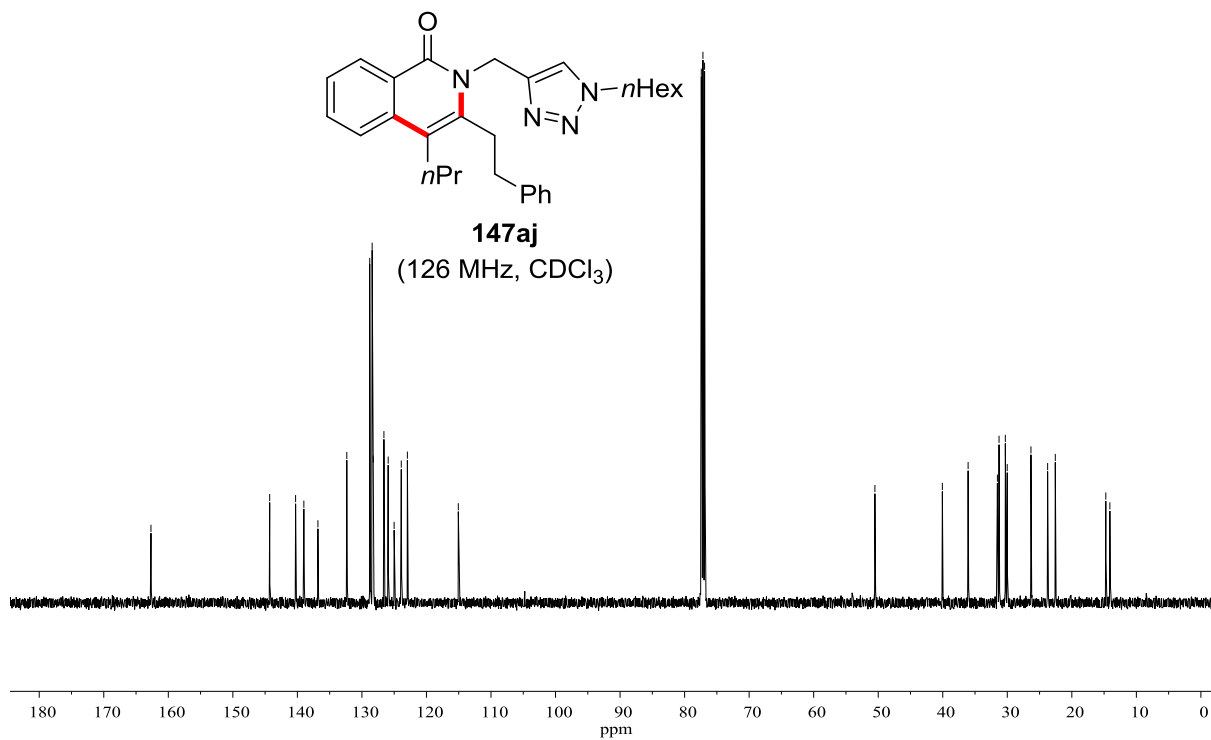
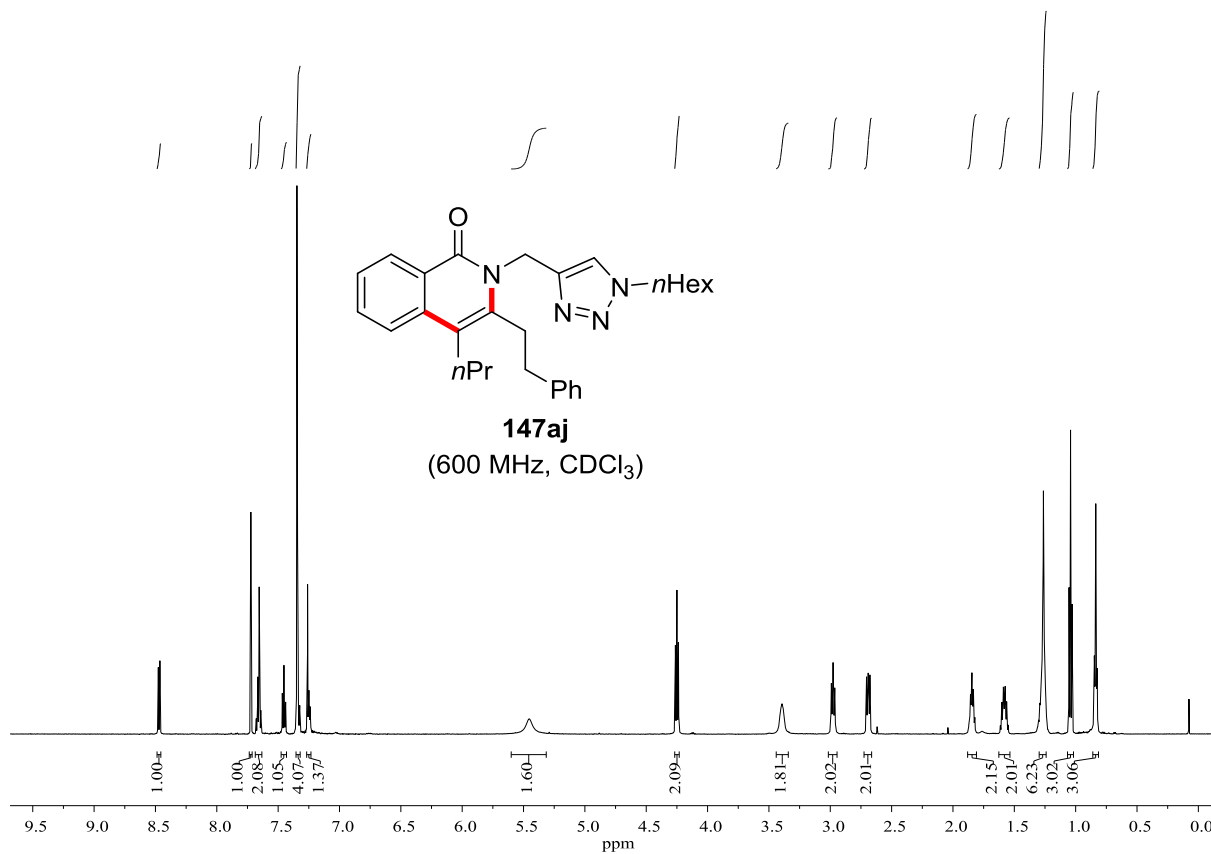












Erklärung

Ich versichere, dass ich die vorliegende Dissertation im Zeitraum von Januar 2015 bis Februar 2019 am Institut für Organische und Biomolekulare Chemie der Georg-August-Universität Göttingen

auf Anregung und und unter Anleitung von

Herrn Prof. Dr. Lutz Ackermann

selbstständig durchgeführt und keine anderen als die angegebenen Hilfsmittel und Quellen verwendet habe.

Göttingen, den 11.06.2019

Thomas Müller